Franz J. Dahlkamp

Uranium Ore Deposits

With 161 Figures and 55 Tables

Springer-Verlag Berlin Heidelberg GmbH

Prof. Dr. Franz J. Dahlkamp
Ölbergstraße 10
D-5307 Wachtberg
Germany

ISBN 978-3-642-08095-1

Library of Congress Cataloging in Publication Data

Dahlkamp, Franz J. Uranium ore deposits / Franz J. Dahlkamp.
Includes bibliographical references and index.
ISBN 978-3-642-08095-1 ISBN 978-3-662-02892-6 (eBook)
DOI 10.1007/978-3-662-02892-6
1. Uranium ores. I. Title
TN490.U7D28 1991
553.4'932 – dc20 91-9592 CIP

This work is subject to copyright. All rights are reserved, whether the whole or part of the material is concerned, specifically the rights of translation, reprinting, reuse of illustrations, recitation, broadcasting, reproduction on microfilm or in any other way, and storage in data banks. Duplication of this publication or parts thereof is permitted only under the provisions of the German Copyright Law of September 9, 1965, in its current version, and permission for use must always be obtained from Springer-Verlag Berlin Heidelberg GmbH.
Violations are liable for prosecution under the German Copyright Law.

© Springer-Verlag Berlin Heidelberg 1993
Originally published by Springer-Verlag Berlin Heidelberg New York in 1993
Softcover reprint of the hardcover 1st edition 1993

The use of general descriptive names, registered names, trademarks, etc. in the publication does not imply, even in the absence of a specific statement, that such names are exempt from the relevant protective laws and regulations and therefore free for general use.

Product Liability: The publishers cannot guarantee the accuracy of any information about dosage and application contained in this book. In every individual case the user must check such information by consulting the relevant literature.

Typesetting: Best-set Typesetter Ltd., Hong Kong

32/3145-5 4 3 2 1 0 – Printed on acid-free paper

Preface

An important prerequisite to the long-term use of nuclear energy is information on uranium ore deposits from which uranium can be economically exploited. Hence the basic purpose of this book is to present an overview of uranium geology, data characteristic for uranium deposits, and a synthesis of these data in the form of a typological classification of uranium deposits supported by more detailed descriptions of selected uranium districts and deposits. An additional goal is to provide access for the interested reader to the voluminous literature on uranium geology. Therefore a register of bibliography as global as possible, extending beyond the immediate need for this book, is provided.

The volume presented here was not originally designed as a product for its own sake. It evolved as a by-product during decades of active uranium exploration and was compiled thanks to a request by the Springer Publishing Company. Routine research work on identifying characteristic features and recognition criteria of uranium deposits, combined with associated modeling of types of deposits for reapplication in exploration, provided the data bank. The publisher originally asked for a book on uranium deposits structured as a combined text- and reference book. The efforts to condense all the text into a single publication were soon doomed. The material grew out of all feasible proportions for a book of acceptable size and price, a wealth of data on uranium geology and related geosciences having become available during the past decade, too vast for one volume. So the original idea had to be abandoned in favor of a two-volume publication. The contents of both volumes are arranged in such a way that each volume still represents, to an optimum degree, an entity.

This first volume deals primarily with geological principles of uranium deposits amended by descriptions of selected examples of deposits and districts. The companion volume contains presentations of individual deposits organized by different countries. For the sake of the comprehensiveness of each volume, not all the information could be distributed without some repetition. Nevertheless, the interested reader is recommended to use both books for cross-reference or as a guide for his own research and deposit modeling. Finally, it was the author's intention not only to present data and his own views on uranium geology and metallogenesis, but also theories and models of other geoscientists (Chap. 5), in order to stimulate and encourage further research to achieve continuous progress in the understanding of uranium deposits and their metallogenesis.

Franz J. Dahlkamp

P.S.: After finishing and proof printing of the manuscript, the opening of the former Eastern Block countries during 1990 and 1991 provided new and more precise information of uranium deposits in these countries. The available data have been added as far as feasable

in Chapter 4. Particularly one type of deposit characterized by strata-controlled, structure-bound uranium mineralization associated with black shales was an important uranium source in several East Block countries. This type was not considered economic by Western World standards and was therefore not designated as a special type in the original manuscript. It now has been included as Type 16 Strata-Controlled, Structure-Bound.

Acknowledgements

The author is indebted to the efforts of many geoscientists and colleagues in the uranium industry, national and international institutions, and universities for discussions and reading and correcting various parts of the manuscript and assisting in numerous other ways. Discussions with them date back many years and have contributed tremendously to the understanding of uranium geology, and the deciphering of recognition criteria of uranium mineralizations on a local (individual deposit) and regional scale (uranium province). Their ideas, observations, and data have directly or indirectly become a part of this report.

The author is most appreciative to James A. Rasmussen and Elmer Stewart for their endeavor to read and correct most parts of the manuscript.

He wishes to thank especially the following individuals for reviewing and improving descriptions of individual deposits or districts. (in brackets country, district, deposit reviewed): Adamek P. (Scandinavia), Adams S.S. (general), Arnaiz de Guezala J. (Spain), Barthel F. (general), Bernik J. (Yugoslavia), Brynard S.A. (South Africa, Namibia), Chenoweth W. (Colorado Plateau, USA), Coste A. (Limousin, France), Cuney M. (granites, France), Dardel J.R.M. (France), Ewers G. (Pine Creek Geosyncline, Australia), Fritsche R. (mineralogy), Föhse H. (general), Fuchs H. (Brazil), Grauch R. (western USA), Gautier A. (breccia pipe deposits, USA), Halladay Ch.R. (eastern USA), Harshman E.N. (Wyoming Basins, USA), Hruby J. (ČSFR), Kolb S. (Bavaria, W-Germany), Krol W. (Eastern Europe), Matos Dias J.H. (Portugal), McCarn D. (general), Ott G. (general), Ramdohr P. (mineralogy, metallogenesis), Robertson J.A. (Blind River-Elliot Lake, Canada), Ruhrmann G. (Saskatchewan, Canada), Ruzicka V. (ČSFR), Saucier A.E. (Grants Region, N.M., USA), Smith R.B. (South Texas, USA), Tan H.B. (Canada), Thamm J. (Colorado Plateau, USA), Tauchid M. (general), Vels B. (general), Voss C. (general), Wallace A.R. (Schwartzwalder, USA), Wutzler B. (Australia).

The numerous manuscripts were repeatedly typed by Ms. Bartelmus, Bonn, Reichl, Leoben, Vollmer and Weyer, Essen, and Boody, Denver.

Most drafts were prepared by Ms. Glässner. Drafting of cartoons of the types of deposits were performed by MRRD, Leoben, for which H. Kürzl and J. Wolfbauer deserve my gratitude.

Contents

Remarks, Definitions, Units 1

Organization of the Volume 1
Citing of Authors 2
Bibliography 2
Geological, Mineralogical, Mining and Related Terms 2
Conversion Factors 3
Abbreviations 3

1 Introduction 5

1.1 Brief History of Uranium 5
1.2 Types of Uranium Deposits and Occurrences and Their Economic Importance 8
1.3 Geographic Distribution of Uranium Deposits 10
1.4 Resources, Reserves, Grades and Production of Uranium 12
1.5 World Resources of Uranium 14
1.6 Uranium Production 15

2 Geochemistry and Minerochemistry of Uranium 17

2.1 Chemical Properties of Uranium 17
2.2 Global Geochemical Abundance of Uranium 17
2.3 Minerochemical Distribution and Abundance of Uranium in Minerals 18
2.3.1 Minerochemistry and Crystallography of Uranium 18
2.3.2 Minerogenic Distribution of Uranium 21
2.4 Geochemical Distribution and Abundance of Uranium in Rocks and Waters 23
2.4.1 Uranium in Magmatic/Anatectic Environments 23
2.4.2 Uranium in Sedimentary Environments 28
2.4.3 Uranium in Metamorphic Environments 30
2.4.4 Uranium in Metasomatic Environments 31
2.4.5 Uranium in Waters 33
2.4.6 Uranium in Living Organisms and Their Decay Products 33
2.4.7 Uranium in Exoterrestrial Rocks 34
2.5 Uranium Provinces and Districts 34

2.6 Crustal Evolution and Related Uranium Distribution 36

Selected References and Further Reading for Chapters 2 and 3 38

3 Principal Aspects of the Genesis of Uranium Deposits 41

3.1 The Global Metallogenic Cycle of Formation of Uranium Deposits 41

3.2 The Time-Related Occurrence of Uranium Deposits .. 48
3.2.1 Time-Stratigraphic Relationship of Uranium Deposits 49
3.2.2 Geochronological Distribution of Uranium Resources 50
3.2.3 Geochronologic-Metallotectonic Relationship of Uranium Deposits 50
3.2.4 Uranium Deposit Generations and Their Time-Stratigraphic Ranking 51

Selected References and Further Reading for Chapter 3.2 56

4 Typology of Uranium Deposits 57

4.1 Type 1: Unconformity-Contact 57
4.1.1 Subtype 1.1 Proterozoic unconformity-related 66
4.1.2 Subtype 1.2 Phanerozoic unconformity-related 68

4.2 Type 2: Subconformity-Epimetamorphic 69
4.2.1 Subtype 2.1 Not albitized sediments 72
4.2.2 Subtype 2.2 Albitized sediments 73

4.3 Type 3 Vein 74
4.3.1 Subtype 3.1 Granite-related 77
4.3.2 Subtype 3.2 Not granite-related 82

4.4 Type 4 Sandstone 84
4.4.1 Subtype 4.1 Tabular/peneconcordant 88
4.4.2 Subtype 4.2 Rollfront 92

4.5 Type 5 Collapse Breccia Pipe 94

4.6 Type 6 Surficial 96
4.6.1 Subtype 6.1 Duricrusted sediments 100
4.6.2 Subtype 6.2 Peat-bog 102
4.6.3 Subtype 6.3 Karst-cavern 103
4.6.4 Subtype 6.4 Surficial pedogenic and structure fill 103

4.7 Type 7 Quartz-pebble Conglomerate (Lower Proterozoic) 104
4.7.1 Subtype 7.1 U-dominated with REE 106
4.7.2 Subtype 7.2 Au over U-dominant 107

4.8 Type 8 Breccia Complex 108

4.9 Type 9 Intrusive 110
4.9.1 Subtype 9.1 Alaskite 112
4.9.2 Subtype 9.2 Quartz monzonite (Cu-porphyry) 112
4.9.3 Subtype 9.3 Carbonatite 113
4.9.4 Subtype 9.4 Peralkaline syenite 114
4.9.5 Subtype 9.5 Pegmatite 114

4.10 Type 10 Phosphorite 115
4.10.1 Subtype 10.1 Phosphoria 117
4.10.2 Subtype 10.2 Land pebble 118

4.11 Type 11 Volcanic 118
4.11.1 Subtype 11.1 Structure-bound 120
4.11.2 Subtype 11.2 Strata-bound 121

4.12 Type 12 Metasomatite 122
4.12.1 Subtype 12.1 Metasomatized granite 125
4.12.2 Subtype 12.2 Metasomatized metasediments 126

4.13 Type 13 Synmetamorphic 127

4.14 Type 14 Lignite 129
4.14.1 Subtype 14.1 Joint-fracture-related 130
4.14.2 Subtype 14.2 Stratiform 131

4.15 Type 15 Black Shale 131
4.15.1 Subtype 15.1 Bituminous-sapropelic black shale 132
4.15.2 Subtype 15.2 Humic/Kolm in alum shale 132

4.16 Type 16 Strata-Controlled, Structure-Bound 133

Selected References and Further Reading for Chapter 4 134

5 Selected Examples of Economically Significant Types of Uranium Deposits 137

5.1 Examples of Unconformity-Contact-Type Uranium Deposits (Type 1, Chap. 4): Athabasca Basin Region, Canada 137

5.2 Examples of Subunconformity-Epimetamorphic-Type Uranium Deposits (Type 2, Chap. 4) 168
5.2.1 Subunconformity-Epimetamorphic Uranium Deposits in Not-Albitized Metasediments: Alligator River Uranium Field, Australia 168
5.2.2 Subunconformity-Epimetamorphic Uranium Deposits in Albitized Metasediments: Uranium City Region, Canada 191

5.3 Examples of Vein-Type Uranium Deposits (Type 3, Chap. 4) 201
5.3.1 Intragranitic Vein Uranium Deposits: Limousin/La Crouzille District, France 201
5.3.2 Perigranitic Monometallic Vein Uranium Deposits: Příbram District, ČSFR 218

5.3.3 Perigranitic Polymetallic Vein Uranium Deposits: St. Joachimsthal/Jachymov District, ČSFR 224
5.3.4 Perigranitic Uranium Deposits in Contactmetamorphic Rocks: Iberian Meseta, Portugal-Spain 232
5.3.5 Metasediment-Hosted, Not Granite-Related Vein Uranium Deposits: Schwartzwalder Mine, Front Range, USA 237
5.3.6 Sediment-Hosted, Not Granite-Related Vein Uranium Deposits: Shinkolobwe, Katanga Copper Province, Zaïre 246

5.4 Examples of Sandstone-Type Uranium Deposits (Type 4, Chap. 4) 250
5.4.1 Extrinsic Carbon/Humate-Uranium Deposits in Phanerozoic Sandstones: Grants Uranium Region, USA 250
5.4.2 Vanadium-Uranium Deposits in Phanerozoic Sandstones: Colorado Plateau, USA 270
5.4.3 Channel/Basal Uranium Deposits in Phanerozoic Sandstones: Monument Valley-White Canyon Districts, USA 284
5.4.4 Roll-Type Detrital Carbon-Uranium Deposits in Phanerozoic Continental Basin Sandstones: Wyoming Basins, USA 290
5.4.5 Roll-Type Extrinsic Sulfide-Uranium Deposits in Phanerozoic Coast Plain Sandstones: South Texas Coastal Plain, USA 305
5.4.6 Uranium Deposits in Proterozoic Sandstones: Franceville Basin, Gabon 319

5.5 Examples of Collapse Breccia Pipe-Type Uranium Deposits (Type 5, Chap. 4): Arizona Strip Area, USA 324

5.6 Examples of Surficial-Type Uranium Deposits (Type 6, Chap. 4): Surficial Uranium Deposits in Duricrusted Sediments: Yilgarn Block, Australia 334

5.7 Examples of Quartz-Pebble Conglomerate-Type Uranium Deposits (Type 7, Chap. 4) 343
5.7.1 Uranium-Rare Earth Elements Deposits in Quartz-Pebble Conglomerate: Blind River-Elliot Lake, Canada 343
5.7.2 Gold-Uranium Deposits in Quartz-Pebble Conglomerates: Witwatersrand Basin, South Africa .. 353

5.8 Examples of Intrusive-Type Uranium Deposits (Type 9, Chap. 5): Alaskite Uranium Deposits: Rössing, Damara Orogenic Belt, Namibia 366

Appendix (Table of U-Minerals) 373

Bibliography 379

Locality Index 443

Subject Index 449

Remarks, Definitions, Units

Organization of the Volume

The emphasis of this volume is on the characterization of uranium deposits.

Chapter 1 includes an introductory note in the form of a brief summary of world uranium resources and their definitions with respect to confidence classes and cost categories. This was considered justified insofar as an understanding of an ore deposit cannot be achieved from purely geological parameters. Economic considerations have to be included. Demand for the commodity and, in the western world, related price/cost factors dictate and define whether a localized metal concentration is a deposit that can be profitably exploited presently or in the future, or whether it is a mineral occurrence of only scientific value.

Uranium geochemistry has been dealt with in a more general or subordinate way in *Chapter 2*, intended to provide only the sufficient basic information needed within the scope of the work. R.W. Boyle (1982) has published a comprehensive review on uranium (and thorium) geochemistry and the reader is referred to this publication for detailed information on the subject. Concerning uranium metallogenesis, its principles are at present sufficiently well understood only for some types of deposits, whereas other types are understood to a lesser extent and in varying degrees. For this reason and to avoid too much speculation or geofantasy, the principal aspects of the genesis of uranium deposits have been addressed only briefly in a separate chapter (*Chapter 3*) and summarized in the presentation of types of deposits (Chapter 4). Nevertheless, Chapter 5 includes more detailed views based on published information of the deposits or districts selected as representative examples for the important and economic types of deposits.

Chapter 4 forms the main part of the book and describes the principal recognition criteria, dimensions, and metallogenetic aspects of identified types of deposits.

In order to comprehend economic deposits and their parameters, it is equally important to recognize and understand criteria typical for subeconomic mineralizations ranging in size from small mineralogical showings to almost economic occurrences. For this reason, the classification chapter was not restricted to types of economic deposits but was amended to include types with not to marginal economic potential.

The views offered by the author in this and other chapters are his own interpretations, though strongly influenced by discussions with many colleagues, of data collected in the field and from pertinent literature study, and must not necessarily represent the final and correct version. The reader is therefore strongly encouraged to study the literature cited as references to form his own opinion, which may be contrary to the one presented here.

Chapter 5 contains abbreviated descriptions of selected major uranium districts or deposits considered to be representative examples for types of uranium deposits of established or potential future economic interest. This chapter was included for various reasons, (1) to support and complement the generalized descriptions in Chapter 4, (2) to provide the reader with more detailed data on important deposits and (3) to present data and views of geoscientists working on these deposits which are not necessarily congruent with those interpretations and hypotheses presented in Chapter 4.

Not all deposits are well researched. Some data are vague, if not biased or wrong. Others are presented ambiguously, being easily misinterpreted. Descriptions of the same deposit or specific features thereof by different authors are not necessarily unanimous. Interpretation of certain criteria may likewise be conflicting (see also introduction to Chap. 3). The attempt was made to reconcile the conflicting data and deviating hypotheses as far as possible; but it has to be admitted that this demanding task was not always satisfactorily achieved. In any event, the various views are presented and the reader is recommended to study the original literature and to come up with his own interpretation. For convenience, a *tabulation of uranium minerals* is added in the Appendix.

Graphic presentations and tables had to be limited to the extent considered necessary to

illustrate adequately the principles of geological setting and configuration of deposits. However, quantity and quality of illustrations are variable depending on the availability and reliability of data in the source material.

Citing of Authors

All the main chapters include a reference list of authors whose data have been used directly or indirectly or who have contributed work to the deposit or subject described in that particular chapter. This scheme was selected

a) to serve as reference index on literature pertaining to the respective deposit or subject. The list is restricted to respective principal uranium papers and to contributions to the general geology with relevant or possible implications on the uranium geology. Special publications not directly related to uranium geology, e.g., age datings of rocks, are cited in the text (titles of the papers can be found listed according to the author's name in the Bibliography);
b) to credit authors who have worked on the subject;
c) to reduce the immense repetition of authors' names to a bearable minimum within the text. In this kind of synoptical review, often using numerous papers on one single deposit or subject, a complete citation of all authors would in many instances have required a list of names after a couple of sentences or a short section. Alternatively, numbers referring to authors and their papers could have been used. My preference is, however, to see the name of an author and not a colorless number which requires additional search in the bibliography for the numbered individual. Although the selected system may not satisfy all authors who wish to see their names precisely repeated, for the sake of easier reading they may forgive me.

Bibliography

This section is organized in alphabetical order of authors providing complete coverage of papers cited in the text and reference lists. Papers published since the final revision of the manuscript have been added in the bibliography but, for technical reasons, could be incorporated into the standing manuscript only in exceptional cases.

The attempt was made to provide a bibliography as complete as possible, but some papers will still be missing. This deficiency does not reflect my disregard of the respective contribution, but should rather be excused as an imperfection on my side. Proceedings of workshops, symposia, etc. were in many instances not published until several years later. Meanwhile, some authors had published the workshop data elsewhere or the data had been disseminated otherwise and hence the material may have had influenced and may have found access to publications of other workers prior to the printing of the original presentation. Consequently, publication years of reference data do not necessarily reflect the first presentation of results.

Geological, Mineralogical, Mining, and Related Terms

Connotation and spelling of geological and mineral terms are in principle understood as and based on those given by: Thrush and the Staff of the Bureau of Mines (eds.), 1968, in *A Dictionary of Mining, Mineral, and Related Terms* US Dept. of the Interior Washington, DC.

Exceptions or additions to this are:

Uraninite/pitchblende: In this book "uraninite" is used for the macrocrystalline, more or less euhedral variety of UO_{2+x} which typically occurs in rocks of higher P–T metamorphic grades (amphibolite grade and higher, contactmetamorphic), igneous rocks such as granite and pegmatite but also in vein and veinlike-type deposits. "Pitchblende" is used for UO_{2+x} varieties of micro- or crypto-crystalline, colloform (collomorphous, botryoidal, spherulitic) habit which typically occur in low grade metamorphic and nonmetamorphic rocks such as greenschist facies metasediments and sandstone, and in most vein and veinlike-type uranium deposits. It is understood that both varieties crystallize in the same crystallographic system, the cubic system, but they have certain discriminating physico-

Table 1. Proposed terms for the alternative idiomatic equivalents of uranium oxides

Habit	Terminology		
	1		2
Idiomorphic (macrocrystalline)	Uraninite	or	Euhedral (subhedral) uraninite
Collomorphous, botryoidal (micro-, cryptocrystalline)	Pitchblende	or	Colloform uraninite
Sooty, earthy (amorphous)	Sooty pitchblende	or	Sooty uraninite

chemical properties (for details see Fritsche et al. in press; Ramdohr 1980, and Sect. 2.3.1).

The term pitchblende has been maintained for traditional reasons. It was the first name used for black uranium oxide minerals back in 1565 (see Chap. 1.1) and is widely used, particularly in Europe. Uraninite is a term commonly used for all kinds of uranium oxides in American literature. Worldwide, both terms are applied by a number of authors variably and in an overlapping way. The criteria used by various geoscientists to differentiate between uraninite and pitchblende are sometimes conflicting and can lead to confusion.

In order to avoid further misunderstanding, it is suggested that for the various oxide phases either the classical names are applied or alternatively the term uraninite is amended by a descriptive prefix to describe habit and/or physico-chemical properties of the uranium oxide in question (see Table 1).

Secondary uranium minerals: this term, commonly referring to colored U minerals, was abandoned in favor of "hexavalent U minerals" to avoid confusion. "Secondary minerals" are in several deposits, e.g., in surficial deposits, of primary origin. Both terms, primary and secondary, have been restricted in this book to their strict genetic sense denoting primary or secondary origin of a given mineral.

Mineralization, alteration, etc.: these terms are used in both connotations, to denote the process implied and the product of the process.

Ore: synonymous with minable mineralization.

Polymetallic mineralization/polymetallic mineralogy (corresponding to complex mineralization/mineralogy of some authors): mineralization containing at least two different metals including U in economic or potentially economic amounts.

Monometallic mineralization/mineralogy (simple mineralization/mineralogy): mineralization containing U only as recoverable element, although many other metals may be present but in trace or subeconomic quantities.

Granite/granitoid, pegmatite/pegmatoid, etc.: the terms are used synonymously and not in their strict genetic sense. Various authors apply both words differently and it is not always clear under which connotation.

Regolith: refers to saprolite/paleosol. It is not used in the sense often applied in Canada, where also weathered rocks are called regolith. In this case, the term regolithic rock is here preferred.

Reserves/resources, grades: calculated in metric tons (mt or tonnes) U_3O_8 and percent (%) U_3O_8 (respectively in ppm U for low grade mineralizations) except for data published by NEA/IAEA (presented in Chap. 1) which are in tonnes U met.

Costs, expenditures: in US $ unless otherwise stated.

Terminology, definitions and classifications of resources and production: see Sect. 1.4.–1.6.

Conversion Factors

1 mt	= 1.1023 sh.t. = 2200 lbs
1 mt U	= 1.18 mt U_3O_8
1 mt U	= 1.30 sh.t. U_3O_8 = 2600 lbs U_3O_8
1 mt U_3O_8	= 0.848 mt U
1 mt U_3O_8	= 1.1 sh.t. U_3O_8 = 2200 lbs U_3O_8
1 sh.t. U_3O_8	= 0.769 mt U
1 sh.t. U_3O_8	= 2000 lbs U_3O_8
\$1/lb U_3O_8	= \$2.6/kg U
\$1/kg U	= \$0.3824/lb U_3O_8

Abbreviations

a.o.	among others or and others
b.y.	billion years = 1000 m.y.

EAR	estimated additional resources
lb.	pound (7000 grains = 16 ounces = 451 grams)
mt	metric ton(s)
m.y.	million years
RAR	reasonably assured resources
redox	reduction-oxidation (boundary)
REE	rare earth elements
sh.t.	short ton
U met	metallic uranium or natural uranium
WOCA	World Outside Centrally Planned Economies Areas

1 Introduction

1.1 Brief History of Uranium

A comprehensive compilation of the historical knowledge about uranium including an extensive listing of uranium occurrences, known prior to about 1900 has been published by Kirchheimer (1963) in his book *Die Geschichte des Urans* (History of Uranium).

Discovery and first publications: Uranium was discovered in 1789 by Martin Heinrich Klaproth (1743–1817), pharmacist and professor for chemistry in Berlin. Klaproth detected the element when analyzing pitchblende from the George Wagsfort mine at Johanngeorgenstadt, Sächsisches Erzgebirge (Saxonian Ore Mountains). Uranit was the first name proposed, that was changed in 1790 to uranium, the name derived from the planet Uranus discovered in 1781 by Friedrich Wilhelm Herschel (1738–1822).

Although Klaproth discovered uranium he did not manage to produce the new element in its metallic state. Heating of the "gelben Urankalks" (yellow uranium lime) with reducing substances resulted only in black oxide. Other uranium compounds produced already in 1789 include nitrate, sulfate, phosphate, acetate and potassium- and sodium-diuranate. Klaproth established the important properties of uranium for commercial application, e.g., the coloring effect on a glassmelt.

Uranium minerals had been noticed by miners for a long time prior to their chemical identification, and had given rise to a variety of speculations on their composition. Pitchblende of the Saxonian Ore Mountains (Erzgebirge) was mentioned in 1565 as "Bechblende", a dialect version of the German "Pechblende". Other accounts of pitchblende date back to the years 1727 (Joachimsthal, Erzgebirge) and 1763 (Wittichen, Schwarzwald/Black Forest) where it was referred to as "schwarze bleyschwere Erzt-Arth" (black, lead-heavy ore type). Green and yellow micas and ochers, the relation of which to uranium was first suspected in 1778, could later be established as uranium minerals by Klaproth. The name "torbernite", named after the Swedish chemist To(r)bern Olof Bergman (1735–1784), was coined in 1786 by Abraham Gottlob Werner (1749–1817), i.e., prior to the discovery of uranium. Another strikingly colored uranium mineral, "autunite", although known from various locations in the early 18th century, was named in 1852 after a discovery locality near Autun in the north eastern Massif Central, where it was discovered in 1800 by Joseph-François de Champeaux de Saucy (1775–1845). Earliest colored pictures of uranium minerals date back to 1797, showing yellow and green crystals from Cornwall.

Early uranium mining: During the first decades of the 19th century, uranium ore was recovered as by-product in Saxony, Bohemia, and Cornwall. In about 1850, mining for uranium as a main product started in Joachimsthal now in the ČSFR. First recovery of uranium ore in North America was reported in 1871 from the Central City area, Colorado. In Cornwall, the South Terras mine opened for uranium production in 1873. During the past century, additional discontinuous or occasional mining of uranium ore has taken place in Autunois/Massif Central, in Oberpfalz (Upper Palatinate)/Bavaria, and at Billingen/Sweden.

In Saxony, approximately 110 t of uranium were recovered during 1825–1898, mainly from the Erzgebirge. Total sales price was about 525 000 Marks or the equivalent of 4.70 Marks/kg U met. In Bohemia between 1850 and 1898, Joachimsthal produced in excess of 620 t U of mainly high grade ore (Joachimsthal yielded a total of about 10 000 t U before it finally closed in 1968).

Cornwall, England, produced at least 300 t U in the 19th century, most of it coming from the South Terras mine near St. Stephen (ca. 275 t).

In Colorado, USA, mines of the Central City district yielded approximately 50 t high grade uranium ore until 1895. The Wood mine was the most productive one. Mining of carnotite ore started in 1898 in the Paradox Valley, Montrose County (now Uravan Mineral Belt), yielding annually about 10 t U metal.

Striking discoveries of uranium deposits in this century prior to World War II were in 1913

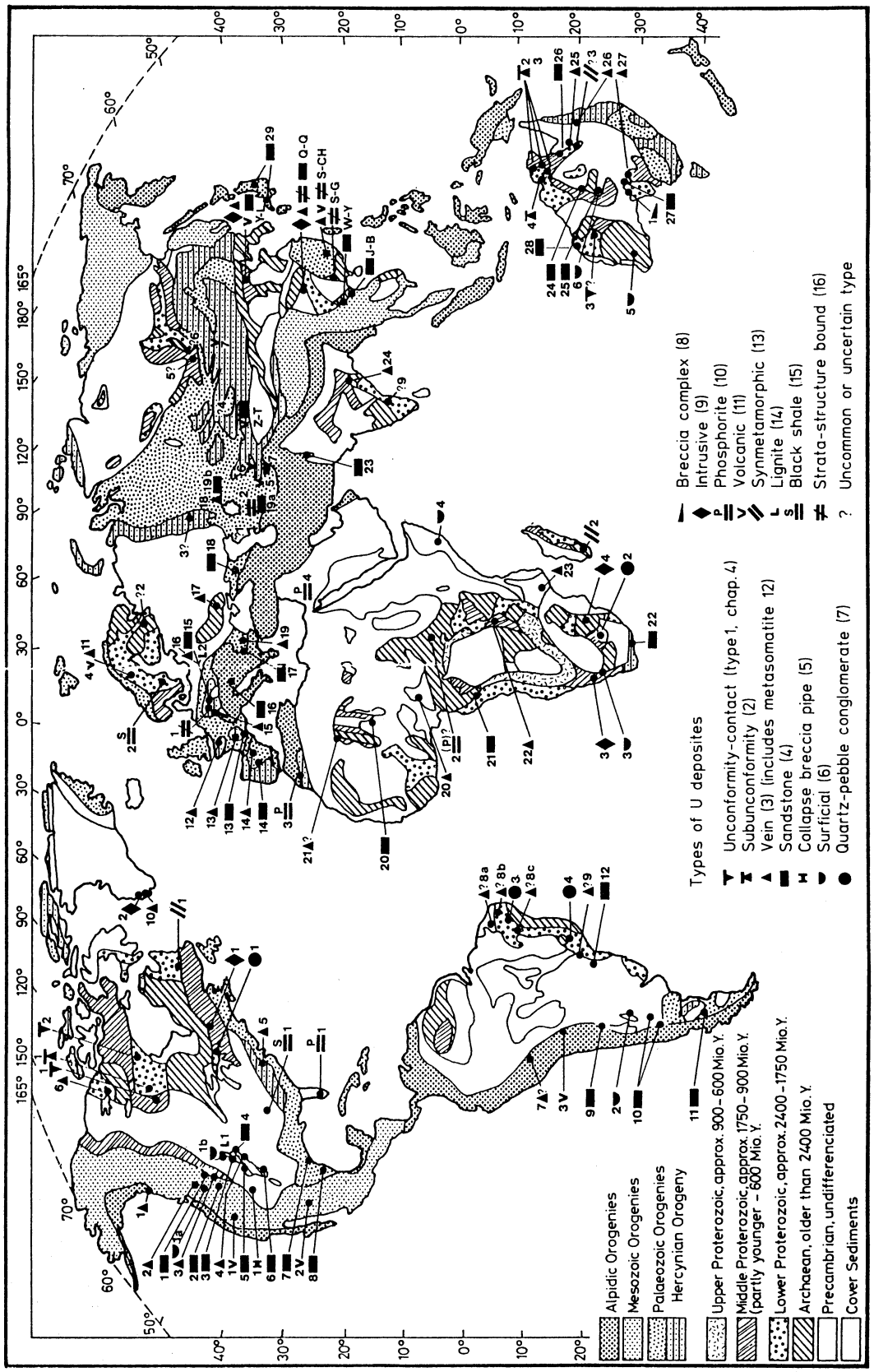

Fig. 1.1. World distribution of major uranium districts/deposits. (for attribution of shown deposits/districts to subtypes and classes see listing in Chap. 4; ? indicates questionable attribution to the selected type).

Unconformity-contact type (1); (▼)
1 Athabasca Basin, Canada
2 Kiggavik, Canada
3 Kintyre (?), Australia

Subunconformity-epimetamorphic type (2); (▼)
1 Uranium City/Beaverlodge, Canada;
2 Alligator Rivers, Australia;
3 South Alligator River, Australia;
4 Rum Jungle, Australia;
5 Kintyre (?), Australia.

Vein type (3); (▲)
(includes vein type deposits of metasomatite (m) (12) and partly of intrusive volcanic (v) (11) types)
1 Ross Adams, Bokan Mountain (m), USA;
2 Rexspar (v), Canada;
3 Midnite Mine, USA;
4 Colorado Front Range/Schwartzwalder, USA;
5 Coles Hill/Swanson, USA;
6 Port Radium, Canada;
7 Macusani (v), Peru;
8a Itataia, Brazil;
8b Espinharas (m), Brazil;
8c Lagõa Real (m), Brazil;
9 Poços de Caldas (v), Brazil;
10 Igaliko Fjord, Greenland;
11 Arjeplog-Arvidsjaur, Sweden;
12 Armorican Massif, France;
13 Massif Central, France;
14 Iberian Meseta, Spain-Portugal;
15 Black Forest, Germany;
16 Bohemian Massif-Erzgebirge, ČSFR-Germany;
17 Krivorozhsky-Kirovogradky (m), Ukraine;
18 Kokchetavsky (v ?), Kazakhstan;
19 Apuseni Mts., East Carpathians, Romania; East and West Balkan Mts., East and West Rhodope Mts., Bulgaria (includes v);
20 Kitongo (m), Cameroun;
21 Hoggar region (m?), Algeria;
22 Katanga Copper Province/Shinkolobwe, Zaïre;
23 Tete district, Mozambique;
24 Jaduguda, India;
25 Maureen (v), Australia;
26 Ben Lomond (v), Australia;
27 Radium Hill, Australia;
Z-T Zhungel-Tianshan uranium province/Balyanghe (v), China;
Y-L Yinshan-Liaohe uranium province/Lianshanguan (m), Quinlong-Daxing'anling volcanic belt (v,m), Langshan (v), China;
Q-Q Qilian-Qinling uranium province/West and East Longshoushan belts (m), North Qilian belt (m), Xi'an area, China;
S-CH Southeast China uranium province/Nanling granite U belt, Central-southern Jiangxi granite U belt, Lower Yangzi granite U belt, Gan-Hang volcanic U belt (v), South Jiangxi – North Guangdong volcanic U belt (v), China.

Sandstone type (4); (▬)
1 Blizzard, Canada;
2 Sherwood, USA;
3 Wyoming Basins, USA;
4 Black Hills – Crow Butte, USA;
5 Colorado Plateau/Chinle and Salt Wash districts, USA;
6 Colorado Plateau/Grants Uranium Region, USA;
7 South Texas, USA;
8 Burgos Basin, Mexico;
9 Tonco-Amblayo, Argentina;
10 Sierra Pintada, Malargue, Argentina;
11 Pichiñan, Argentina;
12 Paraná Basin/Figuera, Brazil;
13 Lodève, Pierre du Cantal, Lombre, Coutras, France;
14 Mazarete, Spain;
15 North Bohemian Basin – Elbsandsteingebirge, ČSFR-Germany;
16 Zirovski Vrh, Yugoslavia;
17 Mecsek Mts., Hungary; Apuseni Mts., Banat, Romania; Orranovo-Simitli Basin, West Rhodope Block/Eleshnitza, Tracian Basin/Momino, NW Balkan Mts., Bulgaria;
18 Caucasus region/Stavropol, Russia;
19a Kyzylkumsky/Navoi region, Uzbekistan;
19b Kokchetavsky/Semizbay, Kazakhstan;
20 Tim Mersoï Basin, Niger;
21 Franceville Basin, Gabon;
22 Beaufort-West, South Afrika;
23 Dera Ghazi Khan area, Pakistan;
24 Ngalia Basin, Australia;
25 Amadeus Basin, Australia;
26 Westmoreland, Australia;
27 Lake Frome Embayment, Australia;
28 Manyingee, Australia;
29 Tono, Ninyo-Toge, Japan;
Z-T Zhungel-Tianshan uranium province/Mengqiguer, Daladi, Kashi, China;
Y-L Yinshan-Liaohe uranium province/Jianchang area Quinlong-Daxing'anling-North Hebei region, Langshan area, China;
Q-Q Qilian-Qinling uranium province/Wudang-Huaiyong Massif, China;
W-Y West Yunnan uranium province/South Lancang and Gaoligang areas, China;
J-B Jingan Basin/Tunling, China.

Collapse Breccia Pipe type (5); ( )
1 Arizona Strip area, USA.

Surficial type (6); (▾)
1a Stevens County, USA – Okanagan Valley region, Canada;
1b Pryor Mts. (U in karst cavern), USA;
2 Achala Batholith/Schlagintweit, Argentina;
3 Namib Desert, Namibia – northern Cape Province, South Africa;
4 Dusa Mareb-El Bur, Somalia;
5 Yilgarn Block, Australia;
6 Arunta/Musgrave Block, Australia.
7 Ferghana Basin/Tyuya Muyun (U in karst cavern), Uzbekistan;

Quartz-Pebble Conglomerate type (7); (●)
1 Blind River – Elliot Lake, Canada;
2 Witwatersrand, South Africa;
3 Serra de Jacobina, Brazil:
4 Quadrilatero Ferrifero, Brazil.

Breccia Complex type (8); (▬)
1 Olympic Dam, Australia.

Intrusive type (9); (◆)
1 Madawaska/Bancroft, Canada;
2 Kvanefjeld/Illimaussaq, Greenland;
3 Rössing, Namibia;
4 Phalaborwa, South Africa;
Y-L Saima Massif, China;
Q-Q West and East Longshoushan belts, Danfeng-Zhuyangguan-Shangnan area, China.

Phosphorite type (10); (≡ᴾ)
1 Florida/Bone Valley – Land Pebble district, USA;
2 Bakouma, Central African Republic (perhaps surficial type);
3 Youssoufia – Khouribga, Morocco;
4 Zefa, Israel.

Volcanic type (11); (v) *(see also vein-type)*
1 McDermitt Caldera, USA;
2 Sierra de Peña Blanca, Mexico;
3 Cotaje, Bolivia;
4 Duobblon, Sweden;
5 Karamazarsky, Uzbekistan;
6 Pribalkhashky, Kazakhstan;
7 Streltsovsky, Transbaikal, Russia;
Z-T Zhungel-Tianshan uranium province/Balyanghe, China;
Y-L Yinshan-Liaohe uranium province/Quinlong-Daxing'anling volcanic belt, Langshan, China;
S-CH Southeast China uranium province/Gan-Hang volcanic belt, Yingtan and Xiangshan districts; South Jiangxi – North Guangdong volcanic belt, China.

Metasomatite type (12); (see under vein-type)

Synmetamorphic type (13); (//)
1 Kitts – Makkovik area, Canada;
2 Ambindrakemba, Madagascar;
3 Mary Kathleen, Australia.

Lignite type (14); (ι)
1 Williston Basin, USA;
2 Intermontane basins in Hercynian orogenic belt/Freital, Stockheim, Germany; Sokolov, Trutnov, Kladno, ČSFR;

Black Shale type (15); (≡ˢ)
1 Chatanooga, USA;
2 Ranstad, Sweden;

Strata controlled – structure-bound type (16); (≠)
1 Ronneburg, Germany;
2 Kyzylkumsky/Dzhantuar, Koscheka, Uzbekistan;
Q-Q Qilian-Qinling uranium province, S. Qinling area/Norgai, China;
S-CH Southeast China uranium province/Xuefong-Jiuling region; north and south side Jiangnan Block/Chanziping, Pukuitang; Guangxi-Hunan-N. Guangdong region/Chengxian, China;
S-G Southwest Guizhou uranium region/Chienxinan, China.

Uncommon and Uncertain types (?)
1 Zakaspiyisky, Melovoye Peninsula/Temakskoye, Tasmurun, Taybagar, Kazakhstan (U in Cretaceous-Paleogene-Neogene sediments associated with phosphatic bone detritus of fossil fish in pyritic clays);
2 Onezhsky/Kem, Chupa area, Russia (pegmatite?)
3 Zauralsky-Chelyebinsk/Vishnevogorsk, Novogorny, Russia (U associated with nepheline syenite);
4 Yeniseisky/Abokan, Vikhorevka, South-central Siberia, Russia (U fracture-bound in Archean metamorphics);
5 Vitimsky, Southeast Siberia, Russia;
6 Central-Transbaikalsky/Chita region, Russia;
7 Far East, Eastern Siberia, Russia;
8 Keberovsk, Southeastern Siberia, Russia.
9 Cuddapah Basin, India (U, V, Mo, Cu mineralization in Middle Proterozoic phosphorous dolomite).

Shinkolobwe/Katanga (now Shaba Province/Zaïre) and in 1931 Port Radium, Great Bear Lake/Canada. Others include Beira Province/Portugal, Tyuya Muyun, Ferghana/Uzbekistan, and Radium Hill/Australia.

Intensive exploration for uranium started at the end of World War II, initiated by the manufacture of atomic bombs. With the development of nuclear reactors for the peaceful use of nuclear energy, new incentives for searching for uranium arose. During three major exploration booms, in the second half of the 1950's, from about 1967 to 1971, and 1976 to 1982, most of the major deposits presently known were discovered.

1.2 Types of Uranium Deposits and Occurrences and Their Economic Importance

Fifteen principal types of uranium deposits and occurrences are recognized in WOCA and a sixteenth type in former East Block countries based in the first instance on host environment and/or geometry. The types are listed in Table 1.1. More than 40 subtypes and classes can be attributed to

Table 1.1. Types of uranium deposits and occurrences and their future and past economic ranking with respect to share of WOCA production (b = byproduct, c = coproduct; 1 = high (>20% of WOCA production), 2 = medium (>10%), 3 = low (<10%), ? = subeconomic) (for explanation see text)

Type of deposit	Economic ranking	
	Future	Past
In production		
1 Unconformity-contact	1	3
2 Subunconformity-epimetamorphic	1	2
3 Vein	2	3
4 Sandstone	2	1
5 Collapse breccia pipe	3	–
6 Surficial	3 (?)	–
Co- or by-product		
7 Quartz-pebble conglomerate (Au)	1 (b)	1
8 Breccia complex (Cu + Au)	3 (c)	–
9 Intrusive (Cu)	3 (b)	2
10 Phosphorite (P_2O_5)	3 (b)	3
Possible future or past production		
11 Volcanic	?	3
12 Metasomatite	?	3
13 Synmetamorphic	?	–
14 Lignite	?	3
15 Black shale	?	–

Table 1.2. WOCA, common grades and resources of major types of deposits

Type of deposit	Typical grade % U_3O_8	Resources		Product	
		1000 mt U_3O_8 Deposit	District	Main	Co-/By-
1 Unconformity-contact	0.3–4	<1–170	>400	U	Ni, Au
2 Subunconformity-epimetamorphic	0.1–0.4	<1–150	>300	U	Au
3 Vein	0.1–1	<0.1–25	<60	U	Ag, Co, Ni, Bi
4 Sandstone	0.1–0.4	<5–25	10–150	U	V, Cu, Mo, Se
5 Collapse-breccia-pipe	0.3–1	<2.5	<15	U	Au, Ag, Cu
6 Surficial	0.03–0.25	<0.1–30	<1–60	U	V
7 Quartz-pebble conglomerate[a]	0.03–0.15	<10 –100	>250	U Au	Y, REE U
8 Brecciia complex[b]	0.08	50 (360)	–	Cu, Au	U
9 Intrusive	0.03–0.1	<0.1–125	125	U Cu	U, Zr

[a] Minable as byproduct or due to favorable contracts.
[b] Only one deposit is known, Olympic Dam, Australia, containing total proven and possible resources of 360 000 mt U_3O_8 and unspecified additional resources of 840 000 mt U_3O_8 at 0.06% U_3O_8, (Battey et al. 1987); the listed 50 000 mt U_3O_8 correspond to the amount recoverable as co-product to Cu-Au production over about the next 20 years.

the 15 types. They are discussed in Chapter 4 subsequent to a review on principles of uranium geochemistry and metallogenesis. Figure 1.1 displays the worldwide distribution of major uranium deposits. Table 1.2 gives a summary of the size and resource magnitude of the various types of uranium deposits, and Fig. 1.2 shows the order of resources by type of deposits known in WOCA.

The 15 main types of uranium occurrence can be grouped in order of present and near future economic ranking as set out in Table 1.1. The primary economic parameters are grade (average >0.2% U_3O_8), contained uranium resources (>10 000 mt U_3O_8, or lower tonnage but higher grades, and the amenability to either conventional or unconventional (e.g., in situ leaching, heap leaching) mining and milling techniques.

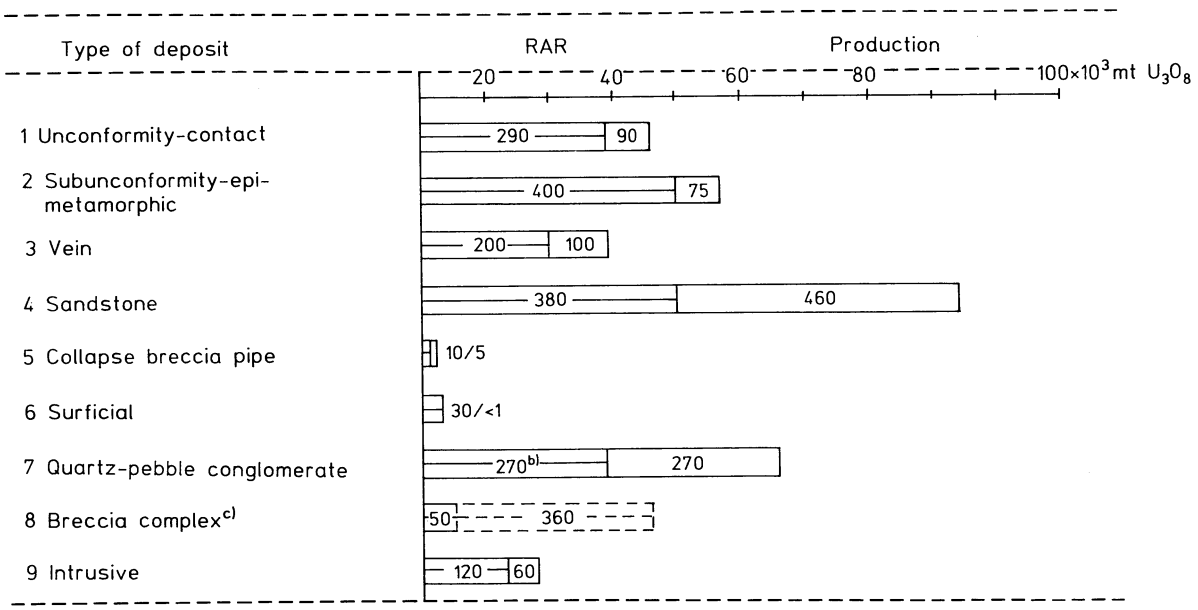

Fig. 1.2. Approximate uranium resources (category RAR <$30/lb U_3O_8) and past production by type of deposit[a] (status January 1990, former Eastern Block countries excluded). [a] U recovered from phosphoric acid amount to <5000 mt U_3O_8). [b] half of the amount recoverable as byproduct. [c] recoverable as coproduct, proven resources 360 000 mt U_3O_8, only one deposit known (Olympic Dam, Australia)

Locally, however, other factors may influence the economics but these are not considered here.

In terms of prices, deposits requiring total recovery costs of less than US$20 to 25/lb U_3O_8 are of economic interest. Basic prerequisites are free trade and normal marked conditions. For comparison, the economic ranking of deposits in the past (until the early 1980's) is added.

As can be seen from Table 1.1, for the opening of a new mine, at present and in the near future only four main types of deposits are economically attractive for uranium only (ranking 1 and 2) and consequently should constitute prime targets for exploration. Four more types contain uranium recoverable as a by- or coproduct. Their resources, although huge in some deposits (>0.5 mio. mt U_3O_8), are economically available only in limited quantity, i.e., to the amount achieved by the production of the main commodity, in most cases gold, copper, or phosphorous.

1.3 Geographic Distribution of Uranium Deposits

Although uranium is geologically a widespread commodity and numerous uranium showings and occurrences are known throughout many parts of the world, major uranium deposits have been discovered in relatively few countries, as illustrated in Fig. 1.1. Figures 1.3 and 1.4 document the striking accumulation of established conventional uranium resources of the RAR <$80/kg U category in seven countries of the WOCA each containing in excess of about 100 000 mt U (ca. 116 000 mt U_3O_8). Four of these countries are developed industrialized nations, Australia, Canada, South Africa, and the USA. Besides the wealth of uranium resources, these four countries account also for more than 80% of WOCA's uranium production of the past 30 to 40 years. Namibia and Niger, and to some extent Brazil,

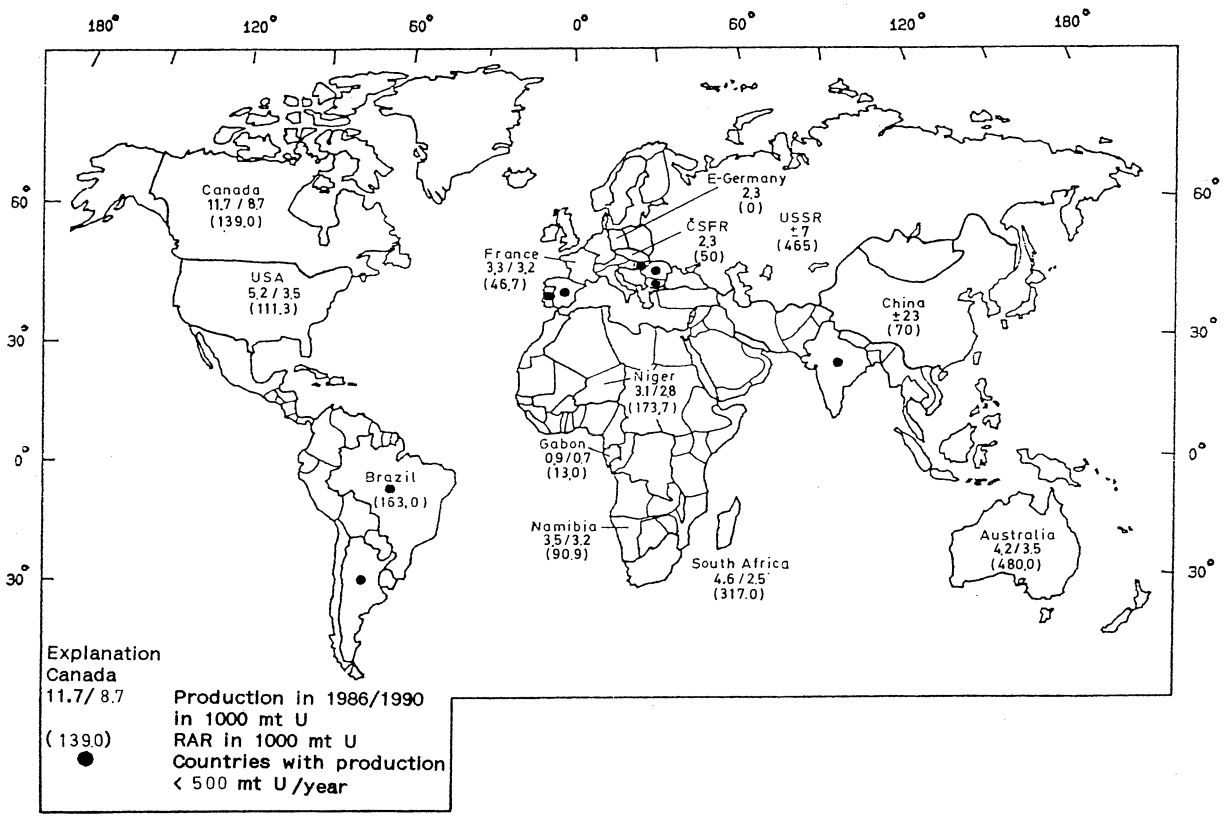

Fig. 1.3. Countries with significant uranium production and resources in the <$80/kg U RAR category. WOCA figures show the uranium production in 1986 and 1990 and their decline during this period resulting in a drop from a total of 37,200 mt U/year in 1986 to about 28,000 mt U/year in 1990. Shown production data of the former Eastern Block countries are for 1989. In the same year produced (estimated resources in the <$80/kg U RAR category in brackets) Bulgaria about 450 mt U (15,000 mt U), Hungary about 600 mt U (35,000 mt U) and Romania about 230 mt U (18,000 mt U). Since then production ceased in Eastern Germany and decreased to less than 800 mt U/year in ČSFR and to about 400 mt U/year in Hungary. WOCA resource and production data for 1986 from OECD (NEA)/IAEA 1990. Other data calculated from various sources.

achieved their high levels of uranium resources by the intense exploration activity of mining companies from industrialized nations.

To find the highest rates of uranium resources in developed countries is not fortuitous. Complementary to favorable geology and developed infrastructure, stable and reliable political and economic environments have encouraged intense exploration activity. The high domestic demand for uranium in the USA has added to the exploration efforts in this country.

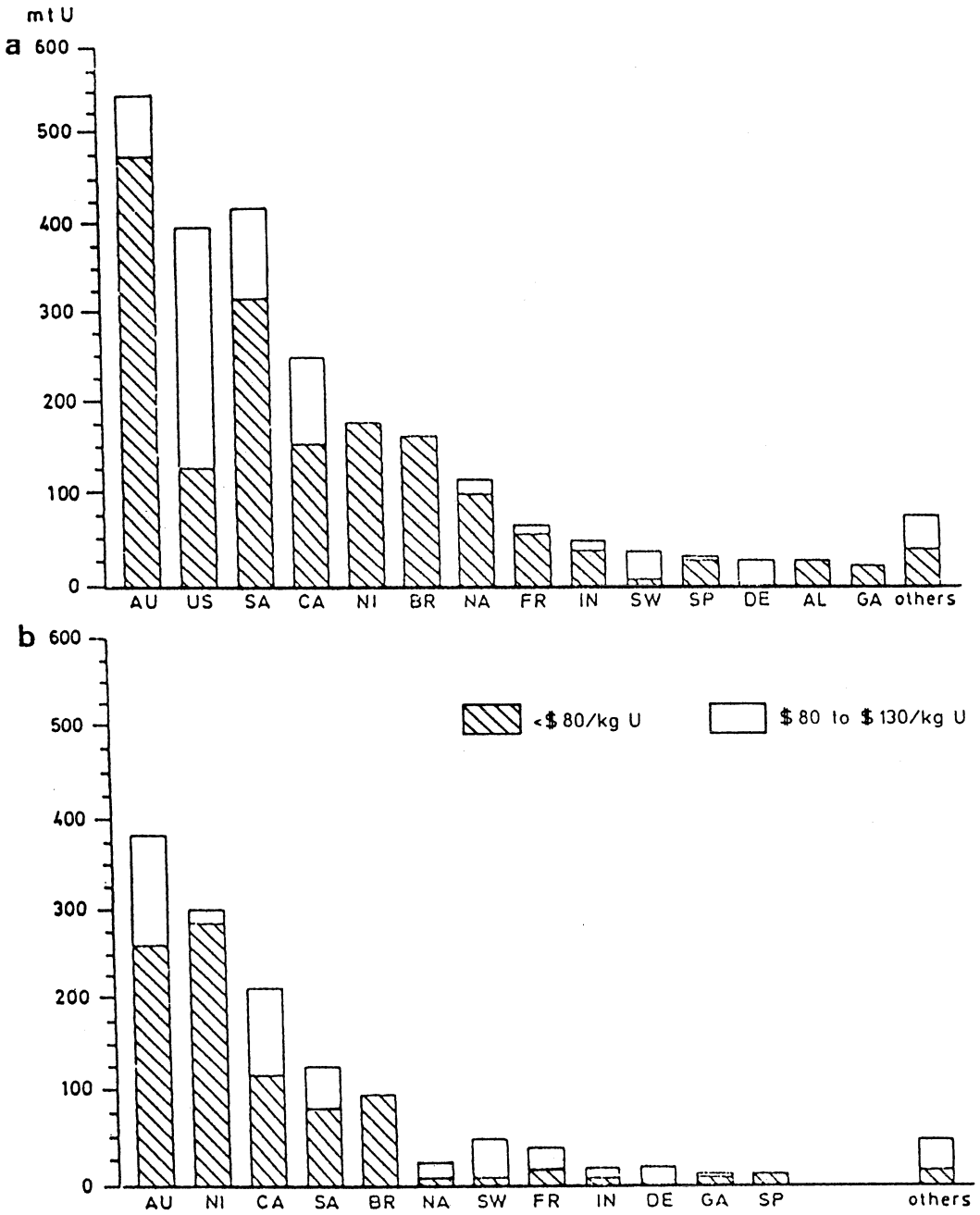

Fig. 1.4. Distribution of uranium resources among countries. **a** Reasonably Assured Resources. **b** Estimated Additional Resources – Category I. *AU* Australia; *AL* Algeria; *BR* Brazil; *CA* Canada; *DE* Denmark/Greenland; *FR* France; *GA* Gabon; *IN* India; *NA* Namibia; *NI* Niger; *SA* South Africa; *SP* Spain; *SW* Sweden; *US* United States. [OECD (NEA)/IAEA 1990]

1.4 Resources, Reserves, Grades, and Production of Uranium

The Nuclear Energy Agency (NEA) of OECD, together with the International Atomic Energy Agency (IAEA), have in the past published at approximately bi-annual intervals a volume entitled *Uranium Resources, Production and Demand* of WOCA countries, the so-called Red Book. In order to facilitate the categorization of uranium resources presented in the Red Book, the NEA/IAEA have established a classification scheme.

This scheme differs from resource classification systems of other countries. Table 1.3 provides, for comparison, approximate correlations of terms and categories used in uranium resource classification schemes by IAEA and the major uranium-producing countries.

Terminology and Definitions of NEA/IAEA Uranium Resource Categories (from NEA/IAEA 1988)

a) Definitions of Resource Categories

Reasonably Assured Resources (RAR) refers to uranium that occurs in known mineral deposits of such size, grade, and configuration that it could be recovered within the given production cost ranges, with currently proven mining and processing technology. Estimates of tonnage and grade are based on specific sample data and measurements of the deposits and on knowledge of deposit characteristics. Reasonably Assured Resources have a high assurance of existence.

Estimated Additional Resources – Category I (EAR-I) refers to uranium in addition to RAR that is expected to occur, mostly on the basis of direct geological evidence, in extensions of well-explored deposits, and in deposits in which geological continuity has been established but where specific data and measurements of the deposits and knowledge of the deposits' characteristics are considered to be inadequate to classify the resource as RAR.

Estimated Additional Resources – Category II (EAR-II) refers to uranium in addition to EAR-I that is expected to occur in deposits believed to exist in well-defined geological trends or areas of mineralization with known deposits. Estimates of tonnage and grade are based primarily on knowledge of deposit characteristics in known deposits within the respective trends or areas and on such sampling, geological, geophysical, or geochemical evidence as may be available.

Speculative Resources (SR) refers to uranium, in addition to Estimated Additional Resources – Category II, that is thought to exist mostly on the basis of indirect evidence and geological extrapolations, in deposits discoverable with existing exploration techniques. The location of deposits envisaged in this category could generally be specified only as being somewhere within a given region or geological trend.

Table 1.3. WOCA, approximate correlation of resource classification schemes used in major uranium producing countries. The terms illustrated are not strictly comparable as the criteria used in the various systems are not identical. "Gray zones" in correlation are therefore unavoidable, particularly as the resources become less assured. Nonetheless, the chart presents a reasonable approximation of the comparability of terms. (NEA/IAEA 1988)

NEA/IAEA	Reasonably assured		Estimated additional I		Estimated additional II	Speculative
Australia	Reasonably assured		Estimated additional		Undiscovered	
Canada (Energy, Mines and Resources)	Measured	Indicated	Inferred		Prognosticated	Speculative
France	Reserves I	Reserves II	Perspectives I	Perspectives II		
South Africa	Reasonably assured		Estimated additional I		Estimated additional II	Speculative
United States (DOE)	Reasonably assured		Estimated additional I + II			Speculative

Decreasing confidence in estimates →

b) Cost Categories
The resource categories are further separated into levels of exploitability based on the estimated cost of production. The cost brackets are:

Less than \$80/kg U (<\$30/lb U_3O_8)
\$80–130/kg U (\$30–50/lb U_3O_8)
\$130–260/kg U (\$50–100/lb U_3O_8)

When estimating the cost of production for assigning resources within these cost categories, account has been taken of the following costs:

- the direct costs of mining, transporting, and processing the uranium ore;
- the cost of associated environmental and waste management;
- the costs of maintaining nonoperating production units where applicable;
- in the case of ongoing projects, those capital costs which remain unamortized;
- the capital cost of providing new production units where applicable including the cost of financing;
- indirect costs such as office overheads, taxes, and royalties where applicable;
- future exploration and development costs wherever required for further ore delineation to the stage where it is ready to be mined.

Sunk costs were not normally taken into consideration.

c) Recoverable Resources
Resource estimates in the RAR and EAR-I categories are expressed in terms of recoverable tonnes of uranium, i.e., quantities of uranium *recoverable from* minable ore, as opposed to quantities *contained in* minable ore, or quantities in situ.

d) Conventional, Unconventional, and By-Product Resources
Conventional resources are those that have an established history of production where uranium is either a primary product, co-product or an important by-product, as in the case of gold production in South Africa's Witwatersrand or copper (-gold) production at Olympic Dam, Australia. The first nine deposit types listed in Table 1.1 are considered conventional resources. Very low grade resources, which under today's market condition (1992) are not economic or from which uranium is only recoverable as a minor by-product, are considered unconventional resources (e.g., phosphates, coal, lignites, black shales, etc.).

Note:

1. Estimates of resources within the various categories fluctuate with changes of economic conditions, with progress in exploration stages, and with improved extraction technology. Local production costs may vary in response to inflation or variations in exchange rates of currencies. The recovery costs of uranium in certain deposits may consequently cross the line between two cost categories, requiring a revision of the original estimates into a higher or lower cost class. With progressing exploration there is a shift of resources from EAR-I to RAR and as exploitation proceeds there is a corresponding depletion in RAR. Also, improvements in technology may result in better recovery rates and hence in upgrading of the resource estimate. It is not unusual that a particular deposit contains resources of several of the above listed categories.
2. National resource/reserve figures published by NEA/IAEA are provided in most cases by government agencies. Some of these national authorities occasionally underestimate the real mining costs. Therefore some of the national resource figures appear in, and consequently inflate to a certain extent, lower cost resource categories of the NEA/IAEA tables.
3. Based on present price levels of uranium, only deposits which can be mined for costs of less than about \$55 to 60/kg U (approximately \$20 to 25/lb U_3O_8) are of economic interest for the future.
4. A further restriction to cost categories is imposed by recovery costs of recycled uranium (and plutonium) from reactors, which put an upper bracket of approximately \$80 to 100/kg U (ca. \$30–40/lb U_3O_8) on production costs of natural uranium.
5. In this book, only national resource data are taken from the NEA/IAEA Red Book. Resource figures of individual deposits or districts discussed in later chapters do not necessarily correspond to the NEA/IAEA nomenclature and categories as outlined in the next paragraph.

Terminology of Resources of Individual Deposits (as used in Chap. 5)

The terminology suggested by NEA/IAEA has often not been applied by mining companies or their published figures are not attributed to one or the other category. Hence in many cases it remains unclear whether in situ (geological) or recoverable (mining) reserves/resources are given, i.e., whether mining dilution and milling losses are included or not, whether the numbers refer to RAR to EAR categories or any other equivalent category of reserves/resources (e.g., proven, probable, or possible reserves). Mining dilution can reduce recoverable reserves to less than 75% of the in situ tonnage and can downgrade the ore mined to 85% or less of the in situ grade.

For this reason reserve, resource, and grade figures given in Chapter 5 for individual deposits or districts are best estimates of, but not always, in situ tonnages and grades based on various, not necessarily published, information (particularly for figures of deposits in Eastern European countries). Also, the terms reserves and resources are not used in this volume in their strict sense but more synonymously. This means that no great distinction is made between the terms "resources" (except for being used in rather undefined or not clearly defined cases) and "reserves" (more restricted to better defined resources but independent of their status of confidence.

1.5 World Resources of Uranium

Conventional Uranium Resources

WOCA: As graphically displayed in Fig. 1.4, conventional resources of uranium in WOCA countries amount in the <$80/kg U class to a total of about 1.5 mio. mt U in the RAR category and to about 0.9 mio. mt U in the EAR-I category.

Uranium resources in former Eastern Block countries are estimated as follows:

Bulgaria: 15 000 mt U
China: >160 000 mt U
ČSFR: >50 000 mt U
East Germany: ca. 90 000 mt U
Hungary: >20 000 mt U
Kazakhstan: >90 000 mt U (<$80/kg U)
Romania: >10 000 mt U
Russia: >120 000 mt U (<$80/kg U)
Ukraine: >70 000 mt U (<$80/kg U)
Uzbekistan: >175 000 mt U (<$80/kg U)

These resources can be classified only as minable. No attribution to any western cost category (e.g., that applied by NEA/IAEA) is feasible because other economic or economic-political factors govern uranium mining in these countries.

Unconventional Uranium Resources

NEA/IAEA (1988) reports that in some countries unconventional and by-product sources of uranium are currently being exploited. With the possible exception of marine phosphates, none of these sources is expected to supply large tonnages in the foreseeable future. The more significant resources of this type are as follows:

Uranium in *marine phosphorite* is the most important source from this category. Morocco, which has the largest deposits of phosphorite, reported over 6 million tonnes of uranium in deposits with an average grade of 120 ppm. Egypt, Jordan, and Syria also report significant resources of uranium in phosphorite. Presently uranium is being recovered as a by-product of phosphoric acid production in Florida, USA, and from phosphoric acid produced from imported phosphates in Belgium and Canada. The grade of phosphorite treated ranges between 90 and 150 ppm U.

Uranium in marine *black shales* is reported by the Republic of Korea, Finland and Sweden. Sweden lists it as conventional RAR and EAR-I recoverable at costs between $80–130 kg U.

Unconventional resources associated with the *carbonatite* of Sokli are reported by Finland to total 2500 t U. In previous reports, South Africa estimated RAR below $80/kg U at 5500 and EAR-I at 1600 t U associated with the Palabora carbonatite complex, from which uranium is recovered as by-product from the extraction of copper and other metals. Brazil reported unconventional uranium resources in the Araxa carbonatite of about 13 000 t.

Uranium occurs also in *copper deposits*, and is being recovered as a by-product of copper leaching in India, which has significant resources of this type, totalling 23 000 tonnes U, and the USA,

with resources of approximately 2000 tonnes U in copper ores. Also Chile reports resources of this type, totalling approximately 5000 t U.

1.6 Uranium Production

Noteworthy uranium production started at the beginning of the 20th century, up to World War II chiefly in response to the demand for radium. The figures for radium production thus reflect the magnitude of uranium exploitation during this period, based on a recovery ratio of 1 g Ra per 3 mt U.

For 1937, mining statistics quote a world production of 40 g Ra, equivalent to slightly more than 120 mt U. Canada provided approximately 66% of the amount. Some 15% came from the Belgian Congo, now Zaïre. Eleven percent was produced in the ČSFR and the remaining 8% in the USA, Portugal, and other countries. Four production centers yielded the bulk of the ore, Port Radium on Great Bear Lake, NWT, Canada, Shinkolobwe in Katanga, Congo, St. Joachimsthal/Jachymov, Erzgebirge, ČSFR, and the Colorado Plateau, Colorado-Utah, USA. Additional producers include the uranium-mica mines of Portugal, which provided 35 g radium between 1911 and 1939, and the uranium-vanadium deposits of Tyuya-Muyun in Ferghana, Uzbekistan, which delivered 2.4 g radium from approximately 1000 mt uranium ore. After World War II and prior to 1992, almost 1 000 000 mt U were produced in WOCA countries, and an estimated 350 000 to 400 000 mt U in the former Eastern Block countries, with the largest contributions from the CIS, ČSFR, and East Germany.

2 Geochemistry and Minerochemistry of Uranium

In 1982 Boyle gave a comprehensive review of the geochemistry of uranium. Garrels and Christ (1965), Langmuir (1978) and Romberger (1984) among others provide data and diagrams of uranium solution – mineral equilibria. The other authors referenced (see end of chapter) discuss uranium behavior during processes active in the various geological environments. The reader is referred to this literature for detailed information and additional literature. More detailed information on uranium activity related to ore-forming events in individual deposits or districts is provided in Chapter 5.

2.1 Chemical Properties of Uranium

Physico-chemical data of uranium are atomic number 92, atomic weight 238, density 18.9 g/cm^3, melting point 1405°C, oxidation stages 6, 5, 4, and 3 (Table 2.1).

In Mendeleev's Periodic Table, uranium is placed in group VI below chromium, molybdenum, and tungsten. Uranium belongs to the actinides characterized by close chemical relationships and peculiar contraction behavior of ionic radius similar to the lanthanides.

Of the four *oxidation states*, stages 4 (U^{4+}) and 6 (U^{6+}) are geochemically and mineralogically important. Trivalent (U^{3+}) and pentavalent (U^{5+}) uranium constitute interim stages, being practically stable only under laboratory conditions.

Hexavalent uranium (U^{6+}) has an ionic radius of 0.80 Å, whereas that of tetravalent uranium (U^{4+}) is either 0.97 Å or 1.01 Å, depending on the coordination number 6 or 8 respectively.

Uranium is a distinctly *lithophile element* with a high affinity to oxygen. In nature, uranium occurs neither as native metal nor as sulfide, arsenide or telluride. In most subsurface environments uranium occurs as U^{4+}, while the hexavalent state (U^{6+}) is stable merely under oxidizing conditions prevailing at and near the surface.

Table 2.1. Physico-chemical data of uranium

Atomic number	Atomic weight	Natural isotopes	Percent fraction	Half-life time
92	238	U 234	0.0058%	2.6×10^5
		U 235	0.72%	7.3×10^8
		U 238	99.27%	4.5×10^9

Valencies (oxidation stages)	Ionic radii	Coordination number
U	1.43 Å	4
(U^{3+})	1.12 Å	6
	1.16 Å	8
U^{4+}	0.97 Å	6
	1.01 Å	8
(U^{5+})		
U^{6+}	0.80 Å	6

2.2 Global Geochemical Abundance of Uranium

The average *crustal abundance* of uranium is 2.7 ppm (Taylor 1964) but different lithologies have a wide range of U tenor, as will be discussed

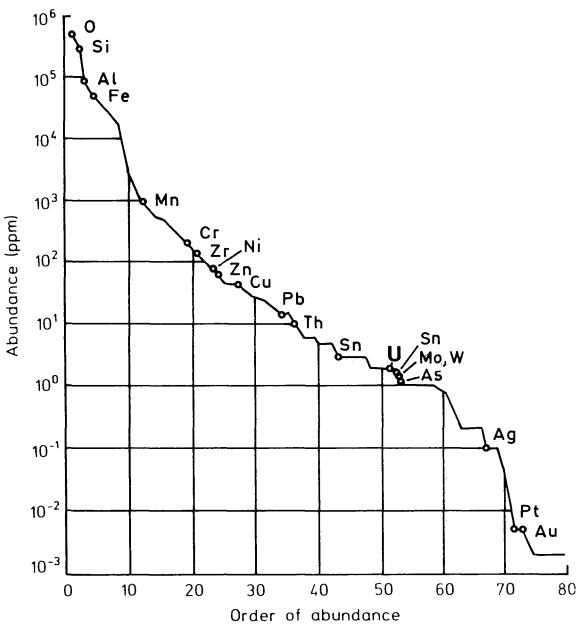

Fig. 2.1. Relative abundance of uranium in the continental crust compared to other selected elements. (After Dodd In: Robertson et al. 1978)

later. Although uranium is widely distributed in crustal rocks and minor accumulations are common, uranium is not an abundant element, as illustrated in Fig. 2.1, that displays the relative abundance of selected elements in the continental crust. Uranium is slightly more common than metals such as As, Mo, W, and Sn, but is much less abundant than Pb, Zn, Cu, or Ni, and it is about one-fourth as abundant as thorium. Table 2.2 shows a supplementary comparison of the order of enrichment factors of some metals required for formation of economic grade concentrations.

Table 2.2. Comparison of crustal abundance, order of payability grades, and respective enrichment factors of selected metals

Metal	Crustal abundance (ppm)	Payability grade (%)	Enrichment factor
Al	81,300	35	4.3
Fe	50,000	50	10
Cr	200	35	1750
Ni	80	1	125
Cu	70	1	143
Pb	16	5	3125
U	2.7	0.2	740
Sn	2.0	0.2	1000
Au	0.004	0.0005	1250
Pt	0.002	0.0005	2500

2.3 Minerochemical Distribution and Abundance of Uranium in Minerals

Boyle (1982), Dybek (1962), Langmuir (1978), Romberger (1984), Smith (1984), among others, have discussed in much detail the geochemical processes involved in uranium mineral formation. In essence, their findings may be briefly summarized as follows.

In nature, uranium interacts and associates with a number of elements and compounds in complex ways due to the following *properties and tendencies:*

a) variable oxidation states, mainly U^{4+} and U^{6+} as mentioned earlier;
b) variable cell units; all cell units are of large size, hence permit substitution for elements of similar ionic radii predominantly in rock constituting accessory minerals;
c) uranium phases hydrolyze in the presence of solutions;
d) uranium forms complexes or ion paws with a great variety of anions in aqueous environments;
e) uranium has to be reduced or complexed to precipitate as minerals from aqueous solutions, but also has a tendency to be adsorbed on clay, organic, and other particles or on certain hydroxides (Fe, Zr, Ti etc. hydroxides);
f) uranium forms a great variety of minerals of its own, the bulk of them based on hexavalent uranium, and only a few on tetravalent uranium (dominantly uraninite, pitchblende).

2.3.1 Minerochemistry and Crystallography of Uranium

In natural minerals uranium is present only in its hexavalent and tetravalent state of oxidation. Tetravalent uranium is by far the most important ion although only stable under reducing conditions. With increasing oxidation potential U^{4+} transforms into the hexavalent state.

Tetravalent uranium has in natural minerals predominantly the coordination number 8, i.e., it forms a central cation surrounded in equidistance by eight anions, normally oxygen ions. In this case, the ionic radius of U^{4+} is 1.01 Å. In addition, U^{4+} occurs with the coordination number 6, then having an ionic radius of 0.97 Å.

In magmatic and metamorphic environments including hypogene hydrothermal conditions the tetravalent uranium prevails. Principal ore minerals formed are *uraninite and pitchblende* also referred to as nasturan and uranpecherz (Ramdohr 1980; Sobolewa and Pudov Kina 1957). Both minerals crystallize in the isometric system and are of the formula UO_{2+x}. Pure U^{4+} O_2 phases do not exist in nature due to selfoxidation by radioactive decay. Uraninite commonly but not necessarily contains Th, REE, Pb and other elements, and has generally a higher lattice constant (a_0 > ca. 5.46 Å), and lower oxidation state than pitchblende (a_0 5.36 to ca. 5.465 Å). Pitchblende may contain Ca, Si, Ti, Pb, and other impurities but rarely Th and REE (Figs. 2.2, 2.3) The composition of both phases, however, relies strongly on the formational environment and conditions (for details see authors listed in Figs. 2.2 and 2.3).

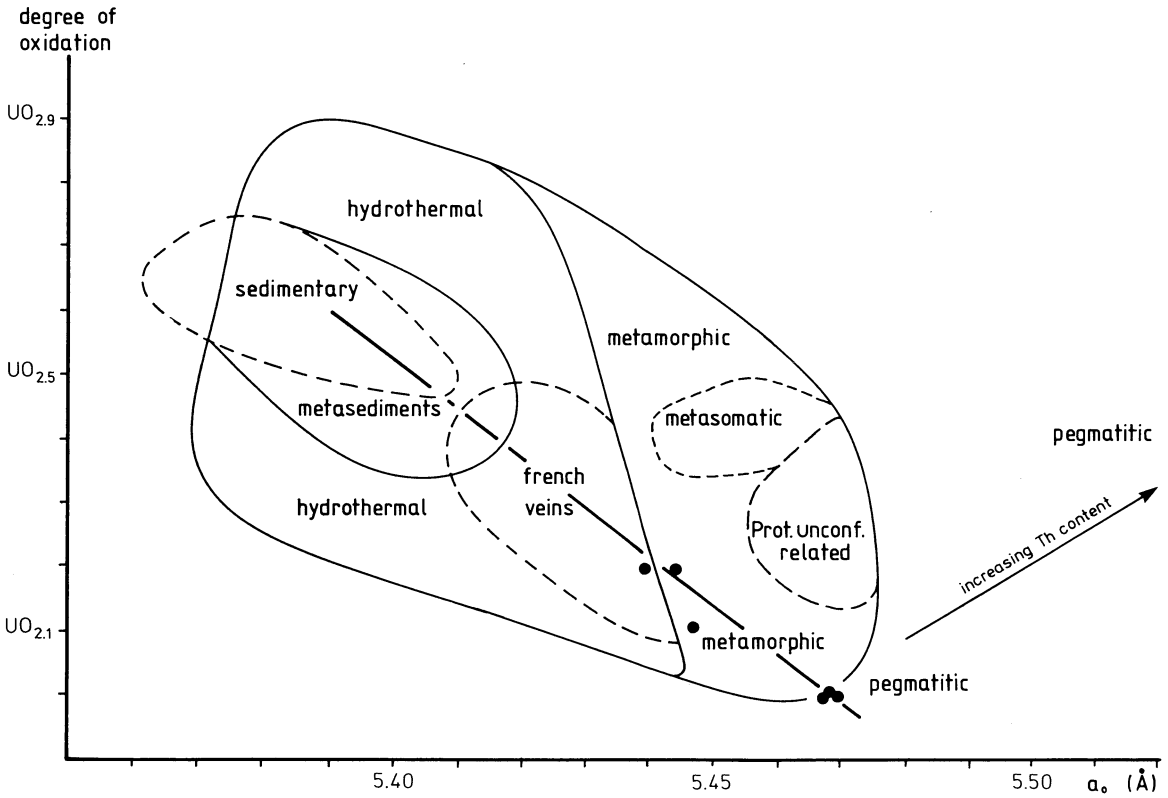

Fig. 2.2. Correlation diagram of oxidation degree-lattice constant for uranium oxide phases and their tentative attribution to genetic fields. (total of 120 samples). (Fritsche et al. in press, based on data from Brooker and Nuffield 1953 (*dots* and *extrapolated solid line*), Xu et al. 1981, Cathelineau et al. 1981, Fritsche et al. 1988)

In addition, the uranous ion *substitutes* for a variety of cations of similar size and charge in the lattice of accessory minerals in igneous rocks. Suitable elements include Th, Ce, Zr, Ti, Nb, Ta, Mo, W, Ca, and REE. The degree of substitution is a function of the size and charge of the replaced ion. Therefore the uranium tenor in the various host minerals varies in a large range from less than 1% U in rock constituting accessory minerals, up to about 10% U in many complex (Ta, Nb, Ti) oxides, to more than 20% in thorium oxide and thorium silicate (urano-thorianite and urano-thorite respectively).

Hexavalent uranium occurs as mineral constituent in two configurations, as an individual ion having the coordination number 6 and an ionic radius of 0.80 Å, and as a complex ion, the uranyl complex. The latter is the more frequent and forms many mineral species in oxidizing environments.

The *uranyl complex* $(UO_2)^{2+}$ develops in aqueous solution according to the formula

$$U^{4+} + 2H_2O \rightleftharpoons (U^{6+}\,O_2)^{2+} + 4H^+ + 2e$$

The uranyl complex displays a linear dumbbell shaped structure, 3.4 Å long and 1.4 Å wide, in which the hexavalent uranium is flanked by two oxygen ions. The uranyl complex is fairly stable and preferentially forms minerals with layered structures of the basic formulas

$$A(UO_2)(RO_4)^- \cdot xH_2O \text{ or } B(UO_2)(RO_4)^{2-} \cdot xH_2O,$$

where R is P^{5+}, V^{5+} or As^{5+}, A is K or Na, and B is Ba, Ca, Cu, Fe^{2+}, Mg, Pb.

Additionally, the uranyl ion forms hydrous minerals with MoO_4, SO_4, CO_3, SiO_3, SeO_3, and TeO_3 as anions and a variety of cations.

The cations are not strongly bonded and can be substituted easily. The H_2O component indicates the necessity of a hydrous environment for mineral formation and mineral instability when the water becomes expelled, for example at elevated temperatures. In contrast to the uranous ion (U^{4+}), a diadochic incorporation of the uranyl complex into other crystal structures is impossible for two reasons:

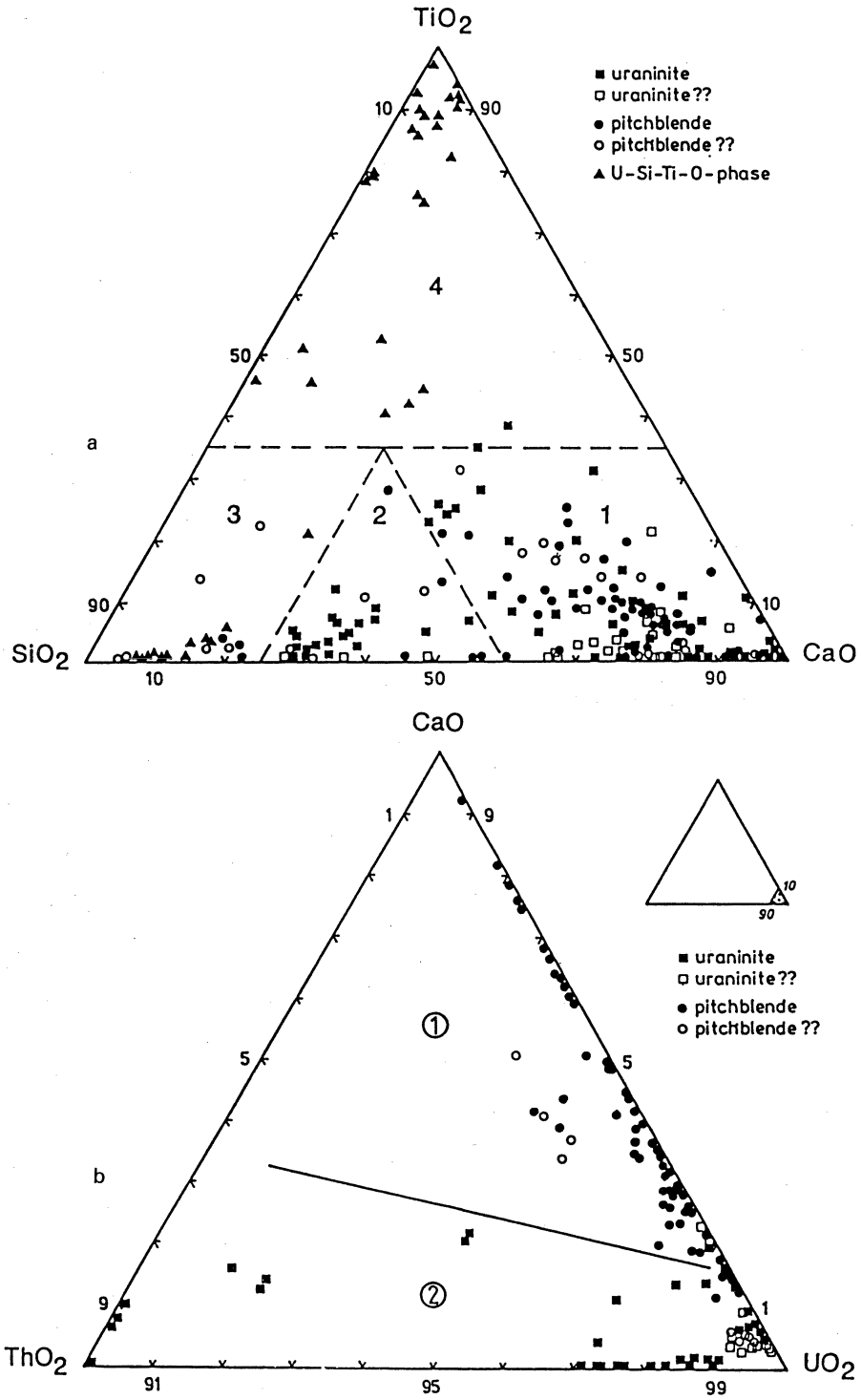

Fig. 2.3. **a** TiO_2-SiO_2-CaO triangle for uranium oxide phases showing the content variations of these compounds. Segment *1* corresponds to uraninite and pitchblende in sensu stricto which typically occur in igneous, metamorphic and sedimentary environments. Segment *2* corresponds to U-oxide phases with relative high Si-content, segment *3* to Si-rich U-oxide phases and coffinite, and segment *4* to Ti-rich U-oxide phases and brannerite. Mineral phases of segments 2 to 4 are often associated with redistributed and metasomatic mineralizations. (Fritsche et al. in press, including data from Äikäs and Sarikkola 1987; Cathelineau et al. 1982; Feather 1981; Feather and Glatthaar 1987; Fritsche et al. 1988; Hålenius et al. 1986; Li Tiangang and Huang Zhizhang 1986; Morton and Sassano 1972; Pagel and Ruhlmann 1985; von Pechmann and Hürter 1988; Ruhlmann 1985). **b** CaO-ThO_2-UO_2 triangle for U-oxide phases of segment 1 (**a**) showing the content of these compounds in pitchblendes (field 1) and uraninites (field 2). Uraninite has commonly lower Ca contents (<1.8 wt % CaO) and higher Th contents (0.1 to several percent ThO_2) than pitchblende (1–5% CaO, <1% ThO_2). Exceptions to these proportions exist, particularly in metasomatite U occurrences. (Fritsche et al. in press) *Open squares* and *circles* tentative identification.

a) the dumbbell-shaped morphology is incompatible with the structure of other minerals constituting complex ions;
b) the uranyl complex, as stated above, is instable at elevated temperatures as found in igneous and metamorphic environments.

Boyle (1982) points out that both uranium ions, U^{4+} and $(UO_2)^{2+}$, are strongly adsorbed by many inorganic and organic substances supposedly due to their large size and high charge density. *Adsorbing substances* include hydrous gels or hydroxides of Fe, Mn, Ti, Zr, Si, Al, Mo, further

zeolites, clay particles, clay-humic complexes, and humic substances. *Sorption capacities* of both inorganic and organic matter appear to rise with increasing pH values to approximately 8.5, with maximum adsorption in the pH range of 4.5 to 7.5 for inorganic material and 3.5 to 6.0 for humic substances. A general increase of adsorption on most substances tends to correlate also with increasing hydrolyzation and associated polymerization of uranyl ions. Adsorption processes of uranium in humic substances are highly variable and not well understood. They tend to depend essentially on type and origin of the humus, its degree of maturation or decomposition, perhaps involving ion exchange activities binding uranium through oxygen to carbonyl groups or uranium replacing hydrogen in carboxyl or other compounds.

Both substances, inorganic and organic, may also act as active transport media for uranium with optimum co-precipitation in a pH range of 5.5 to 7.5. Uranium may be desorbed from Fe and Mn hydroxides by alkali carbonate or sulfate solutions. Desorption by the former is almost complete at pH greater than 7 and, by the latter at pH below 5 (Boyle 1982).

Figure 2.4 illustrates the general cycle of U^{4+} and U^{6+} interconversions in nature.

2.3.2 Minerogenic Distribution of Uranium

Qualitative and quantitative distribution of uranium in minerals is governed at high temperatures such as in endogenic magmatic and metamorphic environments, by crystallization of uranous oxides (essentially uraninite or uranothorianite) and silicates (coffinite, uranothorite), and substitution of adequate cations in accessory minerals. *Principal rock-forming minerals* (Fig. 2.5) are diadochically entered by uranium only in limited extent due to coordination restrictions. But these minerals may contain some uranium concentrated in lattice defects, adsorbed along crystal inhomogeneities, grain margins and/or as inclusion of uraniferous microcrystals.

At low temperatures, such as in exogenic sedimentary regimes, the minerogenic behavior of uranium is dominated by changes in redox potential and/or adsorption. Therefore syngenetic uranium minerals are almost missing in sediments except for detrital species, urano-organic and urano-phosphatic complexes, and uranium adsorbed on sedimentary particles.

Petrogenic-geochemical distribution of uranium is primarily associated with three groups of uraniferous minerals, each characterized by rock-related mineral abundance and minerogenic uranium content (Fig. 2.5):

- rock constituting accessory minerals;
- complex ore minerals;

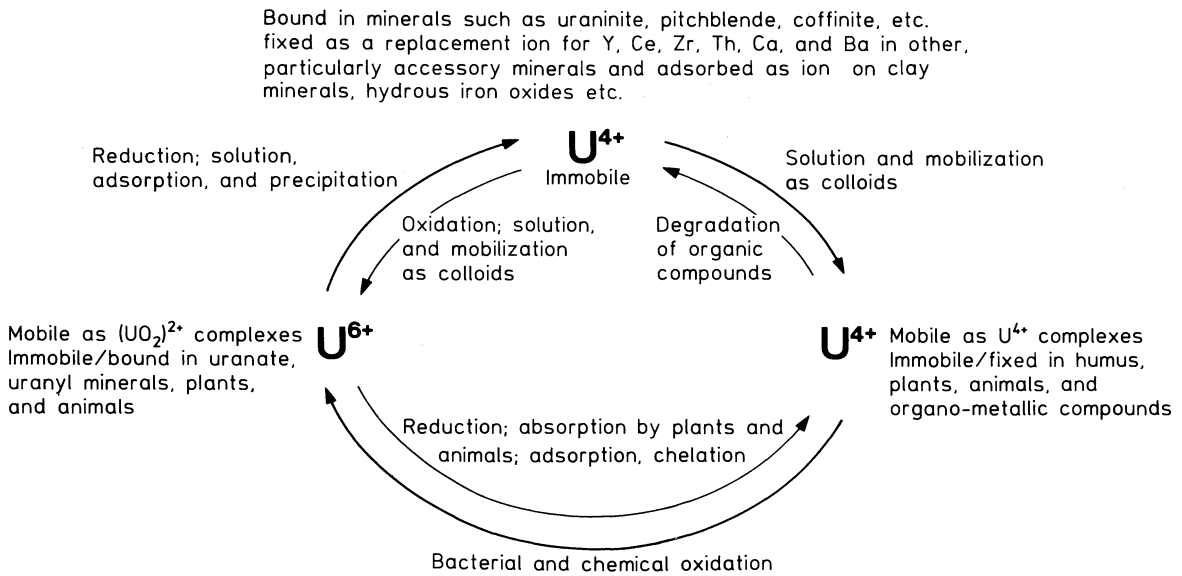

Fig. 2.4. Interconversion cycle of tetravalent (U^{4+}) and hexavalent (U^{6+}) uranium in nature. (After Boyle 1982)

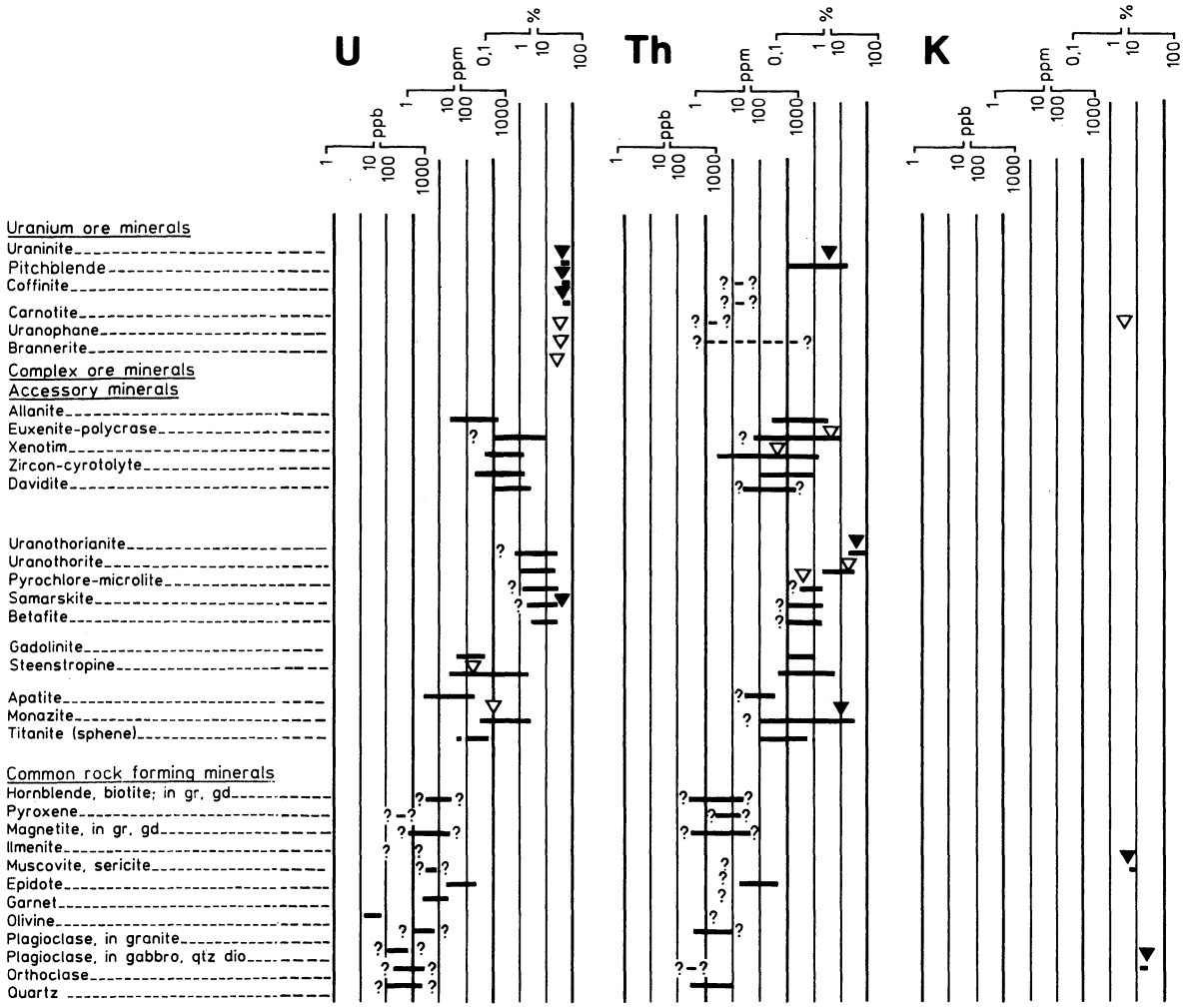

Fig. 2.5. Range and average content of uranium, thorium, and potassium of natural minerals. *Bars* indicate the range of concentration; *? ?* possible range of concentration; *solid triangle* average concentration; *open triangle* possible average concentration. (Based on Roylance J.G., in Van Blaricom ed. 1981, Adams et al. 1959; Bohse et al. 1974; Clark et al. 1966; Dybek 1962; Rogers and Adams 1969b)

- uranium ore minerals (predominantly U^{4+} minerals and subordinately U^{6+} minerals which are mostly derived from the forme(r).

For completeness, it should be noted that uranium may be present adsorbed as interstitial or intergranular films, along grain boundaries and on crystallographic or structural inhomogeneities and discontinuities in minerals and rocks.

Rock-constituting *accessory minerals* contain uranium only as a subordinate component. The ionic radius of U^{4+} of either 0.97 or 1.01 Å permits only a limited substitution in a variety of compounds by replacing other far more abundant elements. In such minerals as apatite, monazite, sphene, rutile, and eudyalite, uranium contents are generally below 1%. Alpha emission of the uranium may isotropize the minerals by destruction of the internal order of the originally crystalline structure (metamictization) but mostly only to a limited degree and very rarely completely. Although accessory minerals account for the bulk of uranium contained in rocks, they never achieve enrichment to economic magnitude except for apatite in phosphorites from which uranium is recovered as by-product.

Complex ore minerals are typical constituents of certain pegmatites, carbonatites, alkali syenites, etc. They also do not necessarily contain uranium as a major component. Uranium can

substitute for suitable elements up to 10% and more. U^{4+} preferentially replaces Th, REE, Ti, and Fe^{2+} in davidite, euxenite, samarskite etc. Most of these minerals are isotropized and, in contrast to accessory minerals, often to a complete metamict stage. Mineral color is mostly lustrous black and the original optical properties have been destroyed.

In the order of 200 complex minerals are recorded. Some of them, like euxenite and samarskite, or (urano)thorianite and (urano)thorite, occur in appreciable amounts typically but not exclusively in pegmatites, whereas others, such as those of the pyrochlore group, are more characteristic for carbonatites. Many complex minerals are resistive to weathering. They can accumulate in fluvial or beach placers together with other heavy minerals such as those of Sn, Nb, Ta, or Au with which they may be recovered as a by-product. Most complex minerals have little economic importance as a uranium resource, partially due to their refractory property.

Uranium ore minerals contain uranium as the main metallic component. They include, in order of economic importance, the uranium (U^{4+}) oxides uraninite and pitchblende (UO_{2+x}, mostly given as U_3O_8), the silicate coffinite ($USiO_4$), the U-Ti-oxide phases frequently referred to as brannerite (UTi_2O_6), and hexavalent uranium minerals often formed successively from the "primary" varieties. The U^{6+} mineral group predominantly consists of uranyl hydroxo-oxides, carbonates, phosphates, arsenates, vanadates, and silicates, which locally may accumulate in ore-forming quantities.

2.4 Geochemical Distribution and Abundance of Uranium in Rocks and Waters

Petrogenesis-related affiliations and tendencies of uranium can be outlined schematically in context with the three principal environments of the geological cycle of crustal evolution, namely:

a) Processes associated with magmatism or anatexis/palingenesis resulting in respective magmatic lithologies.
b) Processes associated with weathering, transport and redeposition of constituents of precursor rocks decomposed by chemical or physical attack at the earth's surface resulting in clastic, chemical or biogenic sediments.
c) Processes involving metamorphosis of preexisting rocks resulting in metamorphic rocks.

In summary, the geochemical behavior of uranium in *igneous environments* reflects its lithophile properties. It is affiliated with leucocratic rocks of the alkaline suites rather than with mafic rocks. Igneous facies which meet this criterion are primarily leucocratic peraluminous granites, granitic-alaskitic suites, sodium-rich intermediate rocks, and carbonatites. Their uranium tenor may range widely from about twice normal abundance to several hundreds of ppm. This feature applies equally to intrusive and extrusive suites and their late-stage derivates such as pegmatites and magmatic hydrothermal formations.

In *sedimentary environments*, uranium distribution falls into two basic categories, (a) of syngenetic and (b) of epigenetic emplacements. Synsedimentary accumulations typically occur in marine phosphorites and black shales. Epigenetic concentrations favor continental clastic inhomogenous sediments, deposited in intracratonic basins surrounded by or proximal to uraniferous crystalline rocks of dominantly Precambrian age.

In *metamorphic environments*, uranium distribution can be twofold, (a) in a closed system as fine disseminations, for example in stratiform mode in metasediments reflecting the original endowment of its protolith or in more ubiquitous distribution in metamorphosed igneous rocks; and (b) in an open system where uranium is redistributed and concentrated into sites of favorable deposition controlled by structures and locally in addition by certain rock facies. Figure 2.6 provides a summary of U contents in the various rock facies amended by tenors of Th and K which often, although not necessarily, show a geochemical relationship to the uranium.

2.4.1 Uranium in Magmatic/Anatectic Environments

Uranium occurs in trace amounts in practically all magmatic/anatectic rocks. Average tenor is commonly low, from fractions of 1 ppm to 15 ppm U, but may be augmented in certain lithologies, particularly in leucocratic facies to 100 ppm U and more. Igneous rocks of the

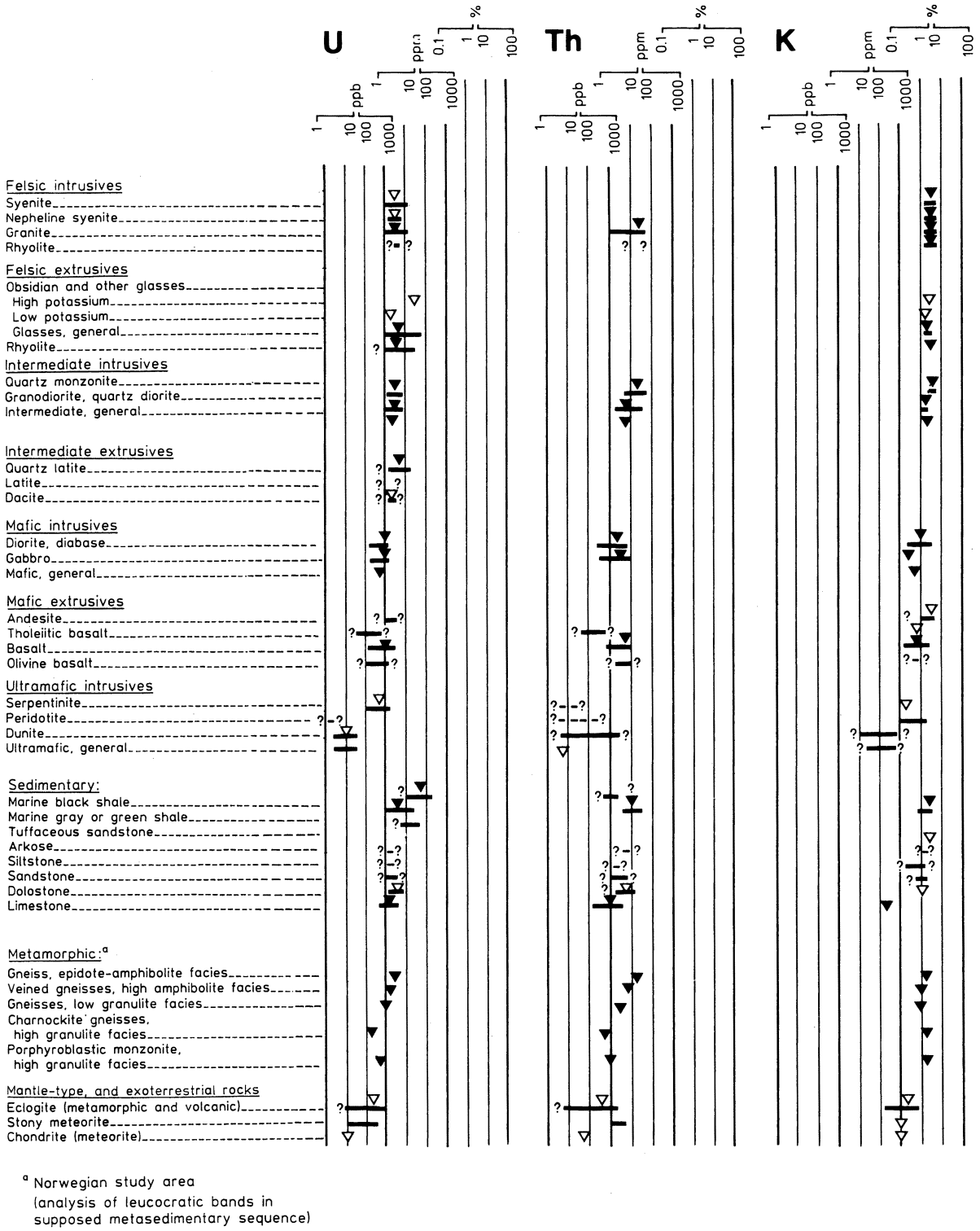

Fig. 2.6. Range and average content of uranium, thorium, and potassium of major rocks types. *Bars* indicate the range of concentration; *? ?* possible range of concentration; *solid triangles* average concentration; *open triangles* possible average concentration. (After Roylance J.G., in Van Blaricom ed. 1981)

oceanic crust average 0.5 ppm U (fresh seafloor basalts 0.02 to 0.08 ppm, island arc andesites 0.2 to 0.5 ppm U), whereas the continental crust has 2 to 3 ppm U (continental basalts and andesitic basalts 0.5 to 1.9 ppm U, andesite 1–4 ppm U, granite 2 to 15 ppm U).

Various rock types generally have highly variable contents of uranium with the general trend of higher values in more felsic, alkalic and late-stage members of igneous differentiation series than in mafic early-stage lithologies. Essential factors correlating with variations of uranium contents include:

- SiO_2, K or Na, or total alkali contents;
- type of rock-constituting minerals;
- relative age of facies in a cogenetic igneous suite;
- internal differentiation of a single batholith;
- orogenic or anorogenic emplacement of intrusion;
- postmagmatic processes (pneumatolytic alteration, metasomatism);
- rock derivation from crustal or mantle sources.

Individual magma series commonly display an increase of uranium tenor (a) from basic to acid members, i.e., (b) with increasing differentiation, expressed by increase of silica, and potassium or sodium or total alkali contents in successive facies (see below), and (c) to decreasing age from oldest to youngest facies. Rare elements such as Be, Hf, Nb, Ta, Th, Zr, and REE follow the same path, but correlate to only a limited extent with uranium. Reversals in these trends, however, are known from some cogenetic sequences of both intrusive and effusive rock suites.

Tables 2.3 to 2.5 present a compilation of uranium tenors in the principal *igneous* rock types. The values show an increase in uranium from gabbroid to granitic magmas by a factor of 3 to 4, and of more than 100 compared to

Table 2.3. Uranium contents of igneous rocks

	Intrusive			Extrusive	
	Average ppm U	Common range ppm U		Average ppm U	Common range ppm U
Ultrabasic	0.02	–			
Dunite, peridotite	0.02	0.003–0.05			
Pyroxenite	0.70	–			
Basic	0.90	0.20–3.40			
Gabbro	0.84	0.60–1.07	Basalt	0.60	0.10–2.30
			Trachydolerite	1.40	–
Intermediate	2.00	1.40–3.03			
Diorite, Quartz diorite	2.00	0.50–11.50	Andesite, Lamprophyre	0.90, 5.00	0.80–3.00
Granodiorite	2.60	1.00–9.00			
Felsic	4.60	2.20–21.00		5.00	2.50–15.00
Granite	3.50	2.20–15.00	Dacite	4.00	0.90–7.50
Monzo-granite	7.50	6.00–18.00	Rhyodacite	5.00	1.00–8.00
Leuco-granite	8.00	6.00–21.00	Rhyolite	8.00	3.00–25.00
Alaskite		10.00–500.00	Bostonite	11.00	3.00–18.00
Pegmatite	–	10.00–1000.00	Quartz bostonite		30.00–65.00
Alkaline-rich	–	0.04–>20			3.00–50.00
Alkali granite	–	10.00–200.00	Alkali trachyte		10.00–50.00
Alkali syenite	–	2.00–20.00	Phonolite	4.00	3.00–18.00
Nepheline syenite	–	3.00–60.00			
Lujavrite	–	10.00–1200.00			
Albitite	3.00	1.00–55.00			
Others					
Kimberlite	4.50	–			
Carbonatite	–	50.00–500.00			

From data and compilations by Belevtsev 1980; Boyle 1982; Clark et al. 1966; Dybek 1962; Goodell 1985a; Maucher 1962; Rogers and Adams 1969b; Roubault 1958; Wenrich 1985; Vinogradov 1963

ultrabasic rocks. Crust-derived felsic igneous rocks (peraluminous leucogranites) affected by late magmatic processes in particular exhibit increased uranium contents (10–25 ppm U in St. Sylvestre granite, Massif Central, France (see Chap. 5.3.1).

Effusive lithologies (Tables 2.3, 2.4) commonly exhibit a greater variance in uranium values. But here again uranium concentration increases analogous to progressing magmatic differentiation. Uranium averages 0.1–1 ppm in basaltic flows and 5–10 ppm in rhyolites, locally increasing to as high as 20–40 ppm U and more. Particularly, acid volcanics rich in vitreous matrix are strong uranium-collectors.

A comparison of *calc-alkaline* and *alkaline* igneous rock suites shows that the latter contain a higher uranium concentration than the corresponding calc-alkaline members. For example, alkali basalts have up to 2 ppm U compared to tholeiitic basalts, which average 0.1–0.5 ppm U. Calc-alkaline granites contain 3 to 6 ppm U, whereas high-alkali granites of the alkaline suite may contain two to ten times as much and more uranium. The K-Na-rich biotite granite of Conway/White Mountain Magma Series, New Hampshire, averages about 15 ppm U (Richardson 1964). Quartz bostonite dikes of the Central City district, Colorado, contain in the order of 100 ppm U (Phair 1952). Albite-riebeckite (-pyrochlore) granites of the Jos Plateau, Nigeria, have contents of 100 to 130 ppm U (Maucher 1962). In any event, highly differentiated granites and pegmatites have the largest amounts of uranium.

Volcanic equivalents may contain 1.5 to 2 times as much uranium as their plutonic counterparts.

Anorogenic alkaline intrusions of agpaitic composition often have higher uranium contents than their orogenic equivalents. For example, the nepheline syenite complex of Ilimaussaq/Greenland (Table 2.5) averages in total about 60 ppm U with concentrations of up to 200 ppm U in fine-grained black lujavrite members and 3000 ppm U in a second generation of coarse-grained black lujavrite (Bailey et al. 1981; Kunzendorf et al. 1982). Similarly, caldasite (baddeleyite and zircon) veins of the alkaline Poços de Caldas intrusion, Brazil, contain several hundred ppm U. Analogous to uranium, Th, Zr, Nb, and REE are also enriched in nepheline syenites. In both localities uranium is bound in refractory minerals except where redistributed by younger processes.

Carbonatite complexes contain concentrations of several 10 ppm U, mostly bound in refractory minerals such as pyrochlore but also in uranothorite as in Phalaborwa, South Africa. The Phalaborwa carbonatite averages 40 ppm U.

Crystallophysics and crystallochemistry control the selective behavior of uranium in the magmatic cycle. Magmatic differentiation progresses from low silica, mafic precipitates of the early crystallization stage through intermediate, and felsic varieties, to pneumatolytic and pegmatitic final crystallizates. Uranium and other elements of large ionic radius or inproper charge cannot substitute in most of the ferromagnesian minerals dominating the early stage, and in principal mineral constituents of the main stage of crystallization. Consequently, uranium, as well as the other incompatible elements, become progressively concentrated in the late felsic lithologies.

Typical minerals of early crystallization and incipient main crystallization such as olivine, pyroxene, amphibole, and basic plagioclase resist the incorporation of uranium, and because uraniferous accessorial minerals are lacking, the abundance of uranium in melanocratic rocks is low. This is consistent with the low tenor of uranium in the mantle (0.03 ppm) and in ultra-

Table 2.4 Uranium contents of selected volcanic complexes in unmineralized areas

San Juan Mts, Colorado, USA		
Hinsdale Lavas (Pliocene)		Larsen et al. (1956)
Basalt	1.0	
Trachydolerite	1.4	
Andesite-basalt	1.9	
Andesite	3.2	
Latite	2.9	
Rhyolite	9.2	
Japan (Tertiary)		Heier and Rogers (1963)
Tholeiitic basalt	0.15	
High alumina basalt	0.22	
Alkali-olivine basalt	0.53	
Carribbean Islands (Tertiary to Recent)		Rogers and Donnelly (1966)
Spilite	0.22	
Extrusive keratophyre	0.29	
Intrusive keratophyre	0.77	
Basaltic andesite	0.79	

Table 2.5. Uranium contents of selected igneous complexes and rocks in U mineralized districts

Intrusive	Average ppm U	Range ppm U	
Massif Central, France			Moreau et al. (1966)
Leucogranite, fertile, (Hercynian)			
– with assoc. U deposits	7.9–10.8	5.0–44.6	
– without U deposits	5.3–10.5	1.9–21.9	
– sterile	3.0–3.4	1.2–4.6	
Leucogranite of St. Sylvestre, (Hercynian)			Moreau (1977)
(peraluminous 2-mica granite)	8.7–21.0	–	
Biotite granites of Guéret	4.2–5.9		Moreau (1977)
Vendée, France			
Leucogranite of Mortagne (Hercynian)			Renard (1974)
– oriented, porphyritic, biotite dominance	12.3		
– albitized	13.4		
– muscovite dominance	20.4		
Granite Mountains, Wyoming, USA (Late Archean)			Stuckless et al. (1977)
Biotite alkali granite		12.9–56.4 (–1380.0) (eq. U)	
Leucocratic alkali granite		4.5–23.4 (eq. U)	
Albitized granite		7.3–11.2 (–107.5) (eq. U)	
Silicified and epidotized granite		15.4 (eq. U)	
Ilimaussag, Greenland (Middle Proterozoic)			Bohse et al. (1974)
Pulaskite	9.0		Bailey et al. (1981)
Heterogenous foyaite	10.0		Kunzendorf et al. (1982)
Sodalite foyaite	14.0		
Naujaite	–	6.0–12.0	
Lujavrite	–	20.0–67.0	
Kakortokite	–	19.0–23.0	
Fine-grained lujavrite	–	134.00–350.00	
Medium-grained lujavrite		190.00–310.00	
Steenstrupine lujavrite		<1200	
Coarse-grained black lujavrite		<3000	
Mc Dermitt Caldera, Nevada-Oregon, USA (Miocene)			Dayvault et al. (1985)
Aurora lava		2–86 (–2791)	
Aurora lava, altered		23–59 (–338)	
Rhyolite		11–40 (–103)	
Andesite		3–160	
Ash-flow tuff (rhyolitic, welded, or silicified)		3–77 (–163)	
Opalized shale		120–195	
Chalcedony bed		35	
Sierra de Peña Blanca, Mexico (Oligocene-Eocene)		mean ± SD.	Goodell (1985) (SD = standard deviation)
La Mesa Fm. (trachytic to rhyolitic ignimbrite)		3.00 1.00	
Peña Blanca Fm. (rhyolitic ignimbrite)		4.55 1.92	
Chontes Fm. (polymict volcanic conglomerate)		2.00 0.00	
Escuadra Fm. (rhyolitic ignimbrite)		11.15 32.95	
Vitrophyre		11.25 5.31	
Nopal Fm. (rhyolitic ignimbrite)		3.87 6.15	
Limestone		3.46 3.73	
Chalcedony		5.83 4.26	

mafic (0.01 ppm) and mafic facies (0.75 ppm U) (Nash et al. 1981). When ultrabasic or basic rocks display a somewhat higher uranium content, they commonly have been affected by later pneumatolytic or hydrothermal overprints with associated uranium introduction.

With increasing silica content uraniferous accessorial minerals such as allanite, anatase, rutile, apatite, zircon, sphene, monazite, xenotime, pyrochlore, and/or uraninite begin to crystallize, resulting in an increase in uranium content in the rock. In addition, rock-forming minerals such as

quartz, feldspar, amphibole, and micas may collect uranium. Although individual minerals accumulate only very minor amounts of uranium (felsic minerals up to 10 ppm U, mafic minerals particularly biotite up to 60 ppm U; Fig. 2.5), the large volume of principal rock constituents may cumulatively add substantially to any lithologic uranium background. Another trap for uranium is as adsorption or as minute grains of uraninite on cleavage planes, crystal faces, grain boundaries, intergranular films, or, in felsic volcanics, incorporated in the glassy matrix.

Accessorial refractory minerals account for from 50 to 60% of the uranium content in granitic rocks. The remainder may be present in the form of uraninite and/or adsorbed along cleavage planes in biotite or in intergranular space. The presence of this leachable uranium fraction is particularly typical for differentiated leucocratic peraluminous granites of the alkalic suite, which may have in the order of 5 to 20 ppm U (Table 2.5). They are considered fertile uranium source rocks for uranium deposits as discussed in Chapters 4 and 5.

For more details on uranium in magmatic/anatectic environments, the reader is referred to papers in IAEA, 1985 (Uranium Deposits in Volcanic Rocks); IAEA, 1988 (Recognition of Uranium Provinces); IAEA, 1989 (Uranium Deposits in Magmatic and Metamorphic Rocks); Maurice (ed.), 1982 (Uranium in Granites); Miller (ed.), 1983 (Evolution of the Damara Orogen).

2.4.2 Uranium in Sedimentary Environments

Uranium tenors in sediments average from 1 to 4 ppm, but range in individual facies over a wide span, from fractions of 1 ppm to ore grade concentrations (Table 2.6).

For supergene epigenetic or syngenetic redeposition in sediments, primarily dispersed and fixed uranium must be mobilized, transported and fixed again. Fundamental physico-chemical conditions and environments are provided particularly by climate, type of weathering, topographic relief, hydrology, hydrochemistry, and source and host rock. They control release, transport, and redeposition of uranium in either continental or marine sediments and by either syn- or epi-sedimentary processes.

Table 2.6. Uranium contents of sedimentary rocks

	Average ppm U	Common range ppm U
Arenites and rudites	1.50	0.45–3.25
Sandstone	–	0.45–3.21
Greywacke	–	0.50–2.10
Orthoquartzite	0.45	0.20–0.60
Bunter sandstone, argillaceous	2.20	–
Lutites and pelites	3.50	2.00–5.90
Common shale, argillite	3.70	1.00–13.00
Grey & green shales in N-America	3.20	1.20–12.00
Mancos shale (western USA)	3.70	0.90–12.00
Kupferschiefer (Germany)	39.00	–
Black shale, continental	–	2.00–4.80
Black shale, marine	–	10.00–1244.00
Mud, Pacific Ocean	–	1.50–4.00
Mud, Indian Ocean	–	0.20–0.50
Mud, Black Sea	3.7	–
Carbonates	2.20	0.01–9.00
Limestone, Florida	2.00	0.50–6.00
Limestone, California	1.30	0.03–4.90
Dolomite, dolomitic limestone	–	0.03–2.00
Evaporites	0.10	0.01–0.43
Anhydrite, gypsum	0.10	–
Halite, sylvite	0.10	–
Phosphorites		
Marine	–	8.50–300.00
Guano	?	
Fossil bones	–	50.00–300.00
Others		
Ferruginous laterite		10.00–100.00 (–1%)
Bauxite	11.40	3.00–27.00
Bentonite	5.00	1.00–21.00
Oceanic Mn nodules	–	3.00–6.50

From data and compilations by Boyle 1982; Clark et al. 1966; Dybek 1962; Rogers and Adams 1969b; Samama 1984

Favorable continental and marine *sediments* for uranium accumulation are:

- sediments rich in organic matter;
- sediments containing sulfides;
- sediments of phosphatic composition.

Principal reactions controlling the *precipitation and fixing* of dissolved uranium in sediments include:

- reduction of the uranyl ion to uranous ion, resulting in precipitation of uranium minerals (pitchblende etc.);

- precipitation of insoluble uranyl compounds (uranyl vanadates ect.);
- adsorption on clay particles, organic material and secondary oxides (limonite etc.);
- substitution for other elements of similar ionic radii and charge (for Ca in apatite, etc.).

The type of sediment and uranium-fixing mechanisms by themselves are not sufficient for uranium collection. Assuming that a potential uranium source is present, the other factors mentioned become to various degrees involved in any process of uranium *mobilization and distribution. Chemical weathering* and destruction of uraniferous rocks result in oxidation and release of uranium commonly as the soluble uranyl ion. In *humid climates* most of the uranium is transported by rivers into the ocean (average content of seawater 0.3–4 ppb U) and concentrated in organic ooze sediments (sapropel, black shale, coal), in phosphorites, and to a lesser extent in argillaceous sediments. Clean sandstones and pure calcareous rocks (limestone, dolomite) are usually poor in indigenous uranium.

In *arid and semi-arid climates* uranium becomes concentrated in solutions particularly in groundwater (the water table of which being relatively well below surface) and to a lesser extent in surface streams. Drainage is either intermittent to the sea or centripetal into intracratonic and intermontane basins, where uranium may precipitate in favorable environments (see subtype 6.1 and type 4, Chap. 4).

Where chemical weathering is incomplete or cannot keep up with erosion, uranium may remain in rock constituents, particularly in resistate accessories, and end up in immature clastic sediment such as arkose.

In environments dominated by *physical weathering*, under nonoxidizing conditions, which are essentially restricted to the early Proterozoic and earlier, all constituents of the precursor rocks including uraninite (unstable under oxygenated chemical weathering conditions) survive mechanical transport and form placer deposits. Such placers locally contain up to several hundred to a few thousand ppm U (see type 7, Chap. 4).

Continental sediments containing carbonaceous matter have a certain capability to precipitate uranium from percolating solutions by reduction of hexavalent (uranyl) ions to the tetravalent state. Such fluvial and lacustrine sediments range widely in their uranium tenor. Normally they contain 0.5 to 5 ppm U. In a uranium province, background values may increase to 10 or 20 ppm U and up to few hundred ppm in the vicinity of uranium deposits. Immature clastic sediments containing vegetal organic matter and/or acid volcanic components exhibit higher uranium contents to the extent of forming uranium mineralization composed in part of pitchblende.

Uranium in *fluvial sediments* is partly present in resistate minerals such as monazite, zircon, apatite, sphene, and others. The remainder occurs predominantly adsorbed on clay, silt, and vegetal particles, on various gels and microcrystalline substances; and/or as coprecipitate of hydrous substances such as limonite (10 to 7000 ppm U), wad, leucoxene, humic compounds, and other gelatinous and cryptocrystalline aluminiferous, phosphatic, titaniferous, zirconiferous and siliceous substances. Their uranium content varies over a large range, from 5 to 100 ppm, locally up to 7000 ppm U (Boyle 1982).

Peats, lignites and coals may also adsorb uranium from solutions with concentrations ranging from 1 to about 100 ppm U, although localized concentrations may be as high as 1% U (see subtype 6.2 and type 14, Chap. 4). Sediments containing hydrocarbon residues (asphaltite) average 100 to 500 ppm U but sometimes accumulate up to 4000 ppm U.

Sediments containing sulfides generally constitute a reducing environment. Anaerobic conditions may produce H_2S, a strong reductant capable of reducing large amounts of uranium (and other metals). Under favorable conditions uranium concentration may attain minable values in continental permeable, impure sulfidized sandstones (see type 4, Chap. 4).

Bituminous or black shales and alum shales characterized by reducing conditions during deposition reflected by abundant sulfides, finely dispersed organic material and/or distillable hydrocarbons sustained synsedimentary precipitation of uranium and other metals (Cu, Ni, Co, Mo, Ag, etc.) from seawater. Of the various marine black shales, in first instance, those of bituminous sapropelic composition are uraniferous (average 20 to 60 ppm U, rarely up to 400 ppm U as at Ranstad, Sweden), whereas those of humic composition contain lower uranium concentrations (see type 15, Chap. 4). Certain shales may have as much as 1000 ppm U, as the graptolite shale at Ronneburg, Germany (which

may have been caused, however, by overprinting processes).

Sediments of phosphatic composition and of marine origin range from some 10 ppm to about 300 ppm U and locally up to several 1000 ppm U as in Cabinda, Angola. Bedded phosphorites formed at the margin of a continental shelf (e.g., Phosphoria Formation, Idaho, USA) generally have higher uranium contents (average 100 to 200 ppm U, max. 6500 ppm U) than phosphorites of shallow marine near-shore deposition (e.g., Bone Valley Formation, Florida, average 20 to 80 ppm U). The latter, however, may by reworking have achieved secondary enrichments of up to 500 ppm U. In both cases it is assumed that uranium was more or less synsedimentary, extracted from sea-water and incorporated into apatite grains by substituting for calcium (see type 10, Chap. 4). In contrast to marine phosphorites, all continental phosphatic rocks are low in uranium, rarely exceeding 20 ppm U.

Soils have variable uranium contents averaging in the order of 1 to 5 ppm depending on the parent rock and soil composition. Higher concentrations of up to 100 ppm U or more are common in areas underlain by uraniferous lithologies. In this case enrichments are usually concentrated in the C-horizon, whereas commonly the A-horizon is the main uranium collector. Part of the uranium in soils is present in resistates such as monazite, xenotime, and zircon which, under favorable conditions, can form eluvial deposits of heavy minerals. Another part of the uranium is intimately bound to clayey, bauxitic, Ti hydroxide, Zr hydroxide, hydrous Fe and Mn oxide, and vegetal organic compounds of the soils.

Boyle (1982) designates as dominant parameters controlling uranium mobilization and fixation in soils: climate, parent rock and associated soil composition, pH, coprecipitation and adsorption of uranium ions by the various soil colloids, clay minerals and hydrous compounds mentioned above, further reactions with humic organic material and interaction of microorganisms. Uranium appears to be more mobile in soils of arid to semi-arid zones than in soils of tropical and temperate regions, supposedly due to the low abundance of organic substances in the former.

Surficial alteration products such as *bentonites* derived from tuffaceous material may have elevated uranium values of up to 20 ppm U which they inherited from their protolith. Likewise, *bauxite* formed from felsic igneous rocks may have cogenital uranium (<27 ppm U) from its parent rocks. *Ferruginous laterite* may accumulate 10 to 100 ppm U and locally up to 1% U. (Table 2.6)

Duricrusts (calcrete, gypcrete) may accumulate uranium up to several hundred ppm U and locally in excess of 1000 ppm U (see subtype 6.1, Chap. 4).

For more details on uranium in sedimentary environments the reader is referred to IAEA/Nininger et al., 1983, IAEA/Finch (ed.) 1985, IAEA/Grimbert et al., 1988, and papers in IAEA/Toens (ed.) 1984.

2.4.3 Uranium in Metamorphic Environments

Metamorphic rocks have rather variable uranium tenors (Table 2.7), in many instances comparable to those of their protoliths. It appears that uranium and some other trace elements are relatively insensitive to *epi- and mesozonal metamorphic* processes in closed systems (Getseva 1963; Cevales 1961). Under these conditions the main impact of regional metamorphism up to upper amphibolite facies seems to be more or less in situ remobilization (range of millimeters to perhaps meters) and, if no other effects interfere, recrystallization of uranium to pitchblende in low grade and to uraninite in medium to high grade metamorphic regimes (Ramdohr 1986). Other than some preferential concentrations in certain

Table 2.7. Uranium contents of metamorphic rocks

	Average ppm U	Common range ppm U
Quartzite, meta-greywacke	1.50	
Carbonaceous/graphitic quartzite		2.80–5.55
Slate	2.70	
Phyllite, meta-argillite	1.90	
Schist	2.00	0.10–10.00
Graphitic schist	3.50	1.00–100.00
Biotite schist	4.70	
Amphibolite	0.50	0.30–3.50
Gneiss	3.00	0.10–10.00
Granulite	1.00	0.2 –2.50
Eclogite	0.20	0.01–0.80

From data and compilations by Boyle 1982; Dybek 1962; Pagel and Svab 1985; Rogers and Adams 1974

mafic minerals, (particularly biotite, amphiboles etc.) and locally in fold noses, no significant transportation, introduction, or removal of uranium is apparent, as reflected by the commonly almost strata-concordant disseminated distribution.

In contrast, high grade *granulite facies* regimes may suffer uranium depletion compared to their unmetamorphosed igneous or sedimentary equivalents as reported by Dostal and Capredi (1978) and Heier (1979) (Table 2.8). This is explained by the possible upward migration of uranium in the crust during the very high grade metamorphism (Heier and Adams 1965). However, this appears not to be valid as a rule.

Adamson (1983) and Adamson and Parslow (1985) investigated cratonic granulite south of the Athabasca Basin, Saskatchewan, and found no evidence for depletion of uranium (and thorium) or, in addition, that reworked "linear belts" are enhanced in both elements, irrespective of the metamorphic grade.

Pagel and Svab (1985) researched granulite facies in the Carswell Structure within the Western Craton, located in Saskatchewan to the northwest of Adamson's (1983) area, and documented higher than average uranium values. The authors ascribed the enhanced U tenor to the presence of carbonaceous material (graphite) that maintained a low fO_2 during granulite-grade metamorphism and as such a low mobility of uranium, thereby retaining the original U content (see also Cuney 1981 and Barbey and Cuney 1982).

In some contrast to the above observations, Belevtsev (1980) notes that migration of elements becomes stronger with increasing metamorphic activity. Uranium-bearing sediments lose uranium and other metallic elements proportional to the intensity of metamorphism. During dynamic regional metamorphism, uranium migrates with maximum mobility in the amphibolite-granulite facies when practically all uranium is removed from its parent rock.

According to Yermolayev (1971), contact metamorphism of greenschist facies rocks results in depletion of uranium (Table 2.8).

Table 2.8. Uranium content changes during metamorphism

Regional metamorphism		ppm U
Gneiss, Longoy, Norway[1]		
Epidote-amphibolite facies		3.45
High grade amphibolite facies		1.22
Low grade granulite facies		0.88
High grade granulite facies		0.22
Schist and gneiss, Aldan Shield, CIS[2]	ppm U amphibolite facies	ppm U granulite facies (low grade)
Schist, gneiss	2.25	→1.72
↓	↓	↓
Granite gneiss, migmatite	1.29	1.02
Contact metamorphism[2]	Green schist facies	Hornfels facies
Carbonaceous quartzite (central Asia)	5.55	→2.87
Carbonaceous, siliceous and carbonaceous, micaceous schists (Erzgebirge, Germany)	5.48	→3.40
Albite, carbonate schist (Erzgebirge, Germany)	2.80	→2.23

[1] Heier and Adams 1965; [2] Yermolayev 1971

2.4.4 Uranium in Metasomatic Environments

Metasomatized rocks of both contact metasomatic and autometasomatic provenance resulted from migration of inherent or introduced elements which replace original rock constituents in igneous and (meta) sedimentary rocks. Na-metasomatized rocks appear to be the most important with respect to uranium accumulation. They include albitite and lithologies dominated by other Na-bearing minerals such as Na-amphiboles and Na-pyroxenes (aegirinites etc.).

Fritsche (1986) reviews albitite-related uranium mineralizations and discusses nomenclature and processes involved in metasomatism and albitization in general and of uranium albitites in particular. He attributes the various albitites into the following genetic groups.

A magmatic albitites
B autometasomatic albitites
C metasomatic albitites
Ca late-magmatic albitites

Cb albitites not associated with magmatites
- metamorphic albitites
- other albitites

Magmatic albitites (A) are primary crystallized rocks derived by magmatic differentiation. They include intrusive magmatic bodies or parts of them, veins, and volcanics. The latter include the so-called spilites of primary origin (Amstutz 1974).

Autometasomatic albitites (B) have originated from magmatic solutions and formed mainly in the roof- or contact zone of magmatic bodies. There has been no significant time interval between the intrusion of the magmatic body and the alteration. Autometasomatic albitites often grade towards depth into zones of potassium metasomatism reflected, e.g., by microclinization, until the unaltered magmatite is reached. Beus and Zalashkova (1964) call this alteration early albitization, which is often associated with greisens and fenites (Brögger 1920; Dukovsky 1980; Herzberg 1977; Smirnov 1970). This group includes in part the spilites of autohydrothermal origin (Amstutz, 1974).

Late-magmatic albitites (Ca) are the product of late-magmatic alkaline metasomatism defined by Borodin and Pavlenko (1974) as the displacement of rocks by alkali feldspar, alkaline mafics, and other alkali-rich minerals. Formation temperature is below the granite- and nepheline-syenite-eutectic. The late-magmatic metasomatism is controlled by post-intrusive faults. It is characterized by a distinct zonation of the affected rocks (Korshinsky 1965b). Beus and Zalashkova (1964) call this kind of alteration "late albitization".

Late-magmatic albitites occur preferentially within alkaline provinces. Various concepts as to the source of the solutions are presented. Derivation by magmatic differentiation as well as from deep-seated crust or even mantle-derived solutions are envisioned (Bonin 1982).

Metamorphic albitites (Cb) are thought to have formed subsequently to progressive metamorphism. They typically occur within metamorphic units affected by migmatization and granitization (Tugarninov and Smeyenkowa 1961; Kazansky et al. 1978b, Omelyanenko and Mineyeva 1982; Belevtsev et al. 1984) consider the Na-rich solutions metamorphic mobilisates. Mehnert (1960) shows the possible Na-enrichment during metamorphism and anatexis.

Metamorphic albitites typically display distinct zonations. But, in contrast to the late-magmatic albitites, the formation of secondary minerals depends largely on the original rock composition (Kazansky and Laverov 1977; Omelyanenko 1984). This group includes in part the spilites of autometasomatic origin (Amstutz 1974).

Other albitites (Cb) include albitites of possibly sedimentary or diagenetic origin and the spilites of so-called secondary origin (Amstutz 1974).

Uraniferous albitites.

Based on the above presented typology of albitites and taking into account earlier classification schemes by Kazansky and Laverov

Table 2.9. Uranium content of metasomatized rocks

	Average ppm U	Range ppm U	
Kitongo, Cameroun (Cambrian)			Fritsche (1986)
Diorite		<3–7	
Granodiorite	(av. of samples)	<3	
Granite	<5	3–8	
Arfvedsonite albitite	<5	<3–10	
Leucocratic arfvedsonite riebeckite albitite	14	4–40	
Melanocratic arfvedsonite riebeckite albitite	1924	50–1953 (–7647)	
Leucocratic riebeckite albitite	189	8–372	
Melanocratic riebeckite albitite	390	7–400 (–1756)	
Aegirin albitite	3502	7–260 (–4180)	
Mosquito Gulch, Nonacho, NWT, Canada (Proterozoic)			
Albitite	?	4–2400	Fritsche (1986)
Krivoj Rog, Ukraine (Proterozoic)			Belevtsev (1980)
Biotite gneiss	9	<50	
Granite and migmatite	17	<100	
Microclinite (syenite)	31	<550	
Coarse tabular albitite	35	<550	

(1977) and Sarcia (1980), Fritsche (written pers. commun.) distinguishes the following uraniferous albitite facies.

Uranium in *autometasomatic albitites* especially in association with alkaline intrusions. Na-metasomatism and ore mineral concentration takes place simultaneously with the magmatic intrusion or shortly afterwards. U tenors range from <10 ppm to several 100 ppm and locally up to a few 1000 ppm U. (Table 2.9)

Uranium in *late-magmatic albitites*. An obvious relationship to intrusion does not necessarily exist. Albitization and U distribution are controlled by brecciated and cataclastic fault systems within, at the contact with, or outside the magmatic body. The solutions causing the albitization are considered to be late intruding differentiates of a magmatic differentation process. U tenors are in the range of some 10 ppm U with local enrichments of several 1000 ppm U.

Uranium associated with *metamorphic albitites* formed in areas of anatexis, metamorphism and migmatism. These albitites are often associated with deap-seated fault systems and, therefore the sodium-rich solutions mobilized by anatectic or metamorphic processes may be mixed with meteoric water or mantle-derived fluids or with both (Belevtsev 1980; Kazanskiy et al. 1978). The source of sodium and uranium may or may not be identical. U tenors average 10 to 50 ppm U with local concentrations of a few 1000 ppm U.

Table 2.10. Uranium content in natural waters

	ppb U
Oceans	0.3–3.3 (average 1.3)
English Channel	3.3
Bay of Biscay	3.3
Baltic Sea	0.8–5.9
Black Sea	2.0
Caspian Sea	3.0–10.0
Gulf of Mexico	3.15
Rivers	0.03–5.9
Springs	0.20–40.0
Thermal springs	0.20–48.0
Groundwater (average)	<0.10–40.0
Groundwater[1] in	
Igneous silicic terrane	0.00–32.0 (average 4.5)
Igneous basic-intermediate terrane	0.00–9.2 (average 0.9)
Metamorphic terrane	0.00–37.0 (average 4.4)
Sedimentary terrane	
Sand, gravel	0.00–74.0 (average 2.5)
Sandstone, conglomerate	0.00–2100.0 (average 2.2–26.2)
Siltstone, shale	0.00–69.0 (average 10.6)
Limestone, dolomite	0.00–33.0 (average 2.0)
Mineralizing aquifers	10.0–400.0

From data and compilations by Arakel 1988; Culbert et al. 1984; Dybek 1962; Maucher 1962; Rogers and Adams 1969b;
[1] Scott and Barker 1962

2.4.5 Uranium in Waters

Sea and ocean waters contain 0.5 to 10 ppb U. Oceans average 1.3 ppb U (Table 2.10). *Terrestrial waters* although normally low in uranium have values ranging widely from less than 0.1 ppb to more than 1 ppm U. Surface waters usually contain little uranium (<1 ppb). Uranium in groundwaters is commonly one order of magnitude higher than in surface waters of the same region. Groundwaters average about 0.5 to 10 ppb U but may carry increased amounts up to 100 ppb U or more in terranes underlain by uraniferous lithologies hereby reflecting the lithologic uranium background. Waters rich in dissolved salts such as carbonate, chloride, sulfate, nitrate, and/or phosphate are particularly receptive for high uranium contents. Such chemically loaded groundwaters are typically encountered in arid to semi-arid regions. In the extreme case, such waters may condense to brines containing extraordinary high amounts of uranium and other elements, as for example in the Searles Lake, California, which contains as much as several hundred ppb U.

2.4.6 Uranium in Living Organisms and Their Decay Products

Table 2.11 gives the contents of uranium in plants and animals and their decomposition products.

Table 2.11. Uranium content in living organisms and their decomposition products (Boyle 1982).

Materials	Uranium content (ppm) (range)	Remarks
Flora		
Algae	0.5–50	In dry matter
Aquatic plants	1–15	In dry matter
Moss	0.5–5000	In the ash
Lichen	0.3–200+	In the ash
Land plants	0.005–0.1	In dry matter
Land plants	5–5000	In dry matter; vicinity of uraniferous deposits
Fauna		
Aquatic animals	0.2–0.5	In dry matter
Land animals	0.003–0.05	In dry matter
Land animals	0.01–0.08	In dry matter; vicinity of uraniferous deposits
Decomposition products		
Peat	0.05–3	In peat as found
Lignite	0.05–3	In lignite as found
Coal	0.05–3	In coal as found
Petroleum	0–5 ppb	In petroleum as found
Rock asphalt and bitumen	av. 1 ppb av. 1000 ppb	In asphalt as found
Peat and muck	5–4000	In dry material; vicinity of uraniferous deposits
Lignite	30–7000	In lignite as found; vicinity of uraniferous deposits
Sub-bituminous coal	30–1000	In coal as found; vicinity of uraniferous deposits
Bituminous residue, humate, etc.	up to 5000 (in ash)	In vicinity of and in uraniferous deposits
Thucholite, ucholite, etc.	up to 20% (in ash)	In vicinity of and in uraniferous deposits

2.4.7 Uranium in Exoterrestrial Rocks

Table 2.12 provides, for completeness, some published analyses on uranium tenors in meteorites, tectites, and exoterrestrial glass.

Table 2.12. Uranium content in exoterrestrial material

	ppb U
Meteorites	
Iron	0.003–21.9
Stony iron	0.005–19.0
Chondrite	8.0–240.0
Achondrite	1.5–198.5
Tectites	–
Average	$1.0–2.0 \cdot 10^3$
Range	$0.8–2.7 \cdot 10^3$
Glasses	$0.8–18.4 \cdot 10^3$

From data and compilations by Dybek 1962; Rogers and Adams 1969b

2.5 Uranium Provinces and Districts

Uranium occurrences are not distributed randomly throughout the earth's crust. Instead, uranium concentrations, like those of other metals, are found in restricted areas referred to as metallogenetic provinces. A *uranium province* may be defined as a broad, more or less contiguous domain of the continental crust, where successively younger rocks of variable lithologies and provenance contain uranium levels above normal crustal abundance. When metal values increase to concentrations of economic magnitude (deposit), they form an economic province.

The evolution of a uranium province begins with an initial concentration of uranium from igneous differentiation in the respective crustal section. Uranium continues to be lithologically enriched by successive redistribution or introduction over periods of time in some regions running to hundreds of millions of years. This applies equally to concentrations and deposits in sedimentary, metamorphic, and anatectic igneous rocks forming a province. Some evidence suggests that the episodic redistribution of the uranium may be related to orogenic or epeirogenic events and associated processes.

The oldest unit of such a cycle constitutes the factual initial source for the uranium in the younger rocks. Therefore, its uranium endowment must have been present, partly at least, in labile form, so that subsequent endogenic or exogenic processes could extract and redistribute it into the younger rocks of the province, under favorable conditions to grades and tonnages of deposit size.

In essence, an economic uranium province requires a favorable or fertile uranium-bearing source environment from where uranium can be mobilized to form economically viable deposits in younger host environments, provided that physico-chemical and/or thermodynamic conditions were adequate to promote the required concentration processes (for more details see e.g., in IAEA 1988, *Recognition of Uranium Provinces*, and Toens 1981).

Uranium districts (economic) may be defined as areas within uranium provinces containing clusters of deposits, perhaps with the restriction to deposits of the same type.

The accompanying listing of uranium provinces (for location see Fig. 1.1) marks most of them by discovered deposits or at least noteworthy occurrences. It should be noted that the tabling does not include all existing provinces but is restricted to presently known and prominent uranium provinces.

On a worldwide basis most of the prominent uranium provinces are associated directly or indirectly with Precambrian terrane, and in Europe additionally with the Hercynian orogenic belt.

North America
Canada
- Athabasca Basin – Uranium City region, Saskatchewan
- Elliot Lake – Quirke Lake – Blind River, Ontario
- Bancroft, Ontario
- Great Bear Lake, NWT
- Baker Lake – Thelon Basin, NWT
- Makkovik – Seal Lake, Newfoundland
- Kelowna – Beaverdell, British Columbia

United States
- Colorado Plateau
- Wyoming Basins – Black Hills
- South Texas Coastal Plains
- Colorado Rocky Mountains/Front Range, Colorado
- Northern Rocky Mountains/Mount Spokane Region, Washington-Idaho
- Appalachian-Piedmont, North Carolina-Virginia-Pennsylvania
- Alaska Panhandle/Bokan Mountain, Alaska

Latin America
Argentina
- Sub-Andean Zone

Brazil
- Atlantic Shield/Brazilian orogenic belt
- Paraná Basin

Bolivia – Peru
- Andean volcanic belt

Mexico
- Sierra de Peña Blanca, Chihuahua
- La Sierrita – Burgos Basin, Nuevo Leon

Africa
Algeria – Niger
- Hoggar – Aïr Massif – Agades Basin

Gabon
- Massif de Chaillu – Franceville Basin

Namibia
- Damara Belt

Sambia – Zaïre
- Katanga Synclinorium

South Africa
- Witwatersrand Basin – Kaapvaal Craton

Australia
- Pine Creek Geosyncline, Northern Territory
- Westmoreland – Pandanus Creek, Northern Territory – Queensland
- Mount Isa Geosyncline, Queensland
- Georgetown Inlier, Queensland
- Lachlan Fold Belt, Queensland
- Arunta Block – Ngalia Basin – Amadeus Basin, Northern Territory
- Lake Frome Embayment, South Australia
- Stuart Shelf, South Australia
- Yilgarn Block, Western Australia

Asia
China
- Zhungel – Tianshan, NW, China
- Yinshan – Liaohe, NE China
- Qilian – Qinling, Central China
- West Yunnan, S. China
- Southwest Guizhou, S. China
- Jiangnan Old Land, SE China

India
- Singhbhum Thrust Belt

Japan
- Central and western Honshu (Tono-Ningyo toge)

Kazakhstan
- Pribalkhashsky
- Kokchetavsky

Pakistan
- Eastern Baluchistan (Baghal Chur)

Russia
- Streltsovsky, Transbaikal

Uzbekistan
- Kyzylkumsky
- Karamazarsky

Europe

Poland – ČSFR – Germany – France – Spain – Portugal

Moldanubian and Saxo-Thuringian metallogenetic zone of the Hercynian orogenic belt and enclosed and adjacent continental sedimentary basins, including
- Bohemian Massif, Poland – ČSFR – Germany
- Black Forest – Voges, Germany – France
- Massif Central – Armorican Massif, France
- Cornwall, Great Britain
- Iberian Meseta, Spain – Portugal

Bulgaria
- Western and eastern Balkan metallogenetic zone

Russia
- Caucasus region

Sweden
- Svecofennian belt (Arjeplog-Arvidsjaur-Sorsele)
- Hotagen – Olden Window

Greenland
- Ketilidian Belt, south Greenland

Ukraine
- Krivorozhsky/Krivoj Rog region

2.6 Crustal Evolution and Related Uranium Distribution

Four prominent periods of the crustal evolution, partitioned at about 2.8, 2.2, and 0.4 b.y. ago may be distinguished with respect to a characteristic behavior of uranium.

After the initial cratonization of the earth and except for magmatic processes, the mode of mobilization and lithologic distribution of uranium during these periods is pronouncedly linked to distinct surface-related exogenic conditions and environments, namely anoxic atmosphere (prior to ca. 2.2 b.y.) oxygenated atmosphere (after approximately 2.2 b.y.), evolution of marine life forms (since ca. 3 b.y.) and later of land plants (since ca. 400 m.y.) (Fig. 2.7), development of early intracratonic basins (prior to 2.2 b.y.) and geosynclines and shallow water basins (after 2.2 b.y.).

Ferguson (1988), Nash et al. (1981), and IAEA (1986) reviewed the evolution of the earth's crust and related uranium distribution and arrived at the following conclusions:

1st Period – prior to about 2.8 b.y.: Characterized by protocrust development.

The early Archean crust of the earth was dominated by mafic and ultramafic, mainly komatiitic rocks and minor felsic rocks as reflected by the abundance of greenstone belts in old cratons. The original chemical composition of the greenstones is thought to have been comparable to modern oceanic basalts. The early Archean rocks have concentrated U and Th by a factor of five compared to chondritic abundances but average less U, Th, and K than younger rocks of equivalent facies. It seems that during this period of the earth, neither uranium concentrations nor recognizable uranium provinces developed. The first noticeable introduction of radioelements into the crust occurred with the generation of sodium-rich magmas, at about 3.8 to 3.3 b.y. ago (Ferguson 1988).

2nd Period – ca. 2.8–2.2 b.y.: Characterized by cratonization, granitization, development of intracratonic basins, appearance of marine organisms (algae), anoxic atmosphere.

This period is characterized by the evolution of two major regimes. (a) Development of potassium-rich salic magmas by subduction and recycling of crustal material at about 2.8 to 2.4 b.y. ago, by fractionation to a first noteworthy enrichment of the radioelements in granitic rocks and thereby to the initiation of uranium provinces (see later). These uraniferous granitic complexes constitute the source for subsequent uranium recycling in various geological environments. (Examples: Yilgarn Block, Australia; Superior Province, Canada; Kaapvaal/Kalahari Craton, South Africa; São Francisco Craton, Brazil). (b) Development of the first major intracratonic basins became possible after prerequisitory cratonization of the earth's crust during the late Archean–early Lower Proterozoic. The basins were filled with clastic sediments, mainly arenites, including oligomictic quartz-pebble conglomerates which accumulated significant amounts of detrital uraninite and other heavy minerals. Crucial for the mechanical trans-

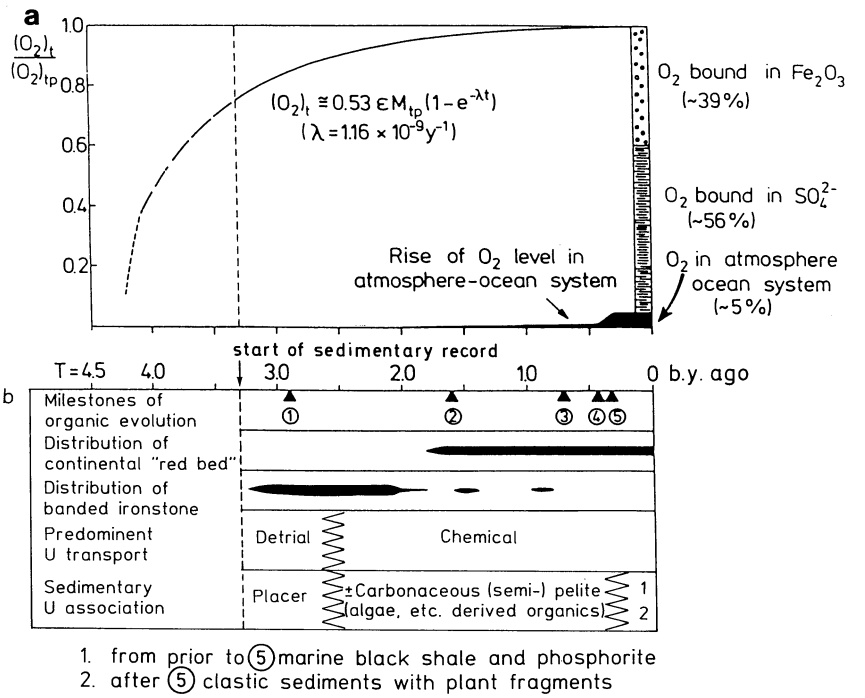

Fig. 2.7. Evolution of the Earth's atmosphere and organic life and associated conditions for uranium transport and most favorable depositional sedimentary environments. *Arrow* in **b** indicates the start of sedimentary record. **a** Evolution of the Earth's total budget of photosynthetic oxygen, based on the terrestrial ^{13}C balance and current concepts for the accumulation of the stationary sedimentary mass as a function of time (Schidlowski et al. 1975). Stationary oxygen reservoirs existing at times T are expressed as fractions of the present reservoir $(O_2)_{tp}$. M_{tp} is the present sedimentary mass with tp = 4.5 b.y. Column on the *right side* shows partitioning of oxygen between the "bound" and "free" reservoirs in the present budget (Li 1972), with molecular oxygen accounting for about 5% only. A disproportionation exists between bound and free reservoirs during the Precambrian and early Paleozoic, most probably due to a short circuit of the ancient oxygen cycle in the Precambrian seas. Tentative rise of free oxygen level in atmosphere-ocean system (*black field*) is inferred from paleontological and geological evidence shown. **b** Milestones of organic evolution indicated are *1* appearance of oldest algal bioherms (photoautotrophic blue-green algae), *2* appearance of eukaryotic biota, *3* appearance of oldest eumetazoan faunas; *4* life conquering continents (Upper Silurian); *5* appearance of exuberant continental floras (Upper Carboniferous). (After Schildlowski et al. 1975; Schildlowski 1981)

port of uraninite grains was a nonoxidizing atmosphere, which prevailed prior to about 2.2 b.y. (Examples: Huronian Blind River – Elliot Lake – Quirke Lake Basin, Canada; Witwatersrand Basin, South Africa; Serra de Jacobina and Quadrilatero Ferrifero, Brazil; Nullagine Conglomerate, Australia; Palimba Conglomerate, Jenissei province, Russia).

The presence of contemporaneous Lower Proterozoic banded iron formations has occasionally been cited as counter-evidence of an anoxic atmosphere at the time of uraniferous conglomerate deposition. However, as Schidlowski et al. (1974), and others point out, the first oxygen produced by photosynthesis of early life forms (green algae) was in seawaters. Over a long time span the oxygen was consumed for oxidation of reduced compounds abundant in all oceans, particularly ferrous iron. In restricted marine basins where oxygen generation was early or more advanced, oxidized iron could precipitate as banded iron formation, whereas in coeval intracratonic basins uraninite placers could accumulate.

3rd Period – ca. 2.2–0.4 b.y.: Characterized by a stabilized sialic crust, development of geosynclines and shallow water basins, marine microorganisms (algae), oxygenated atmosphere.

The early stage of this period (ca. 2.2 to 1.9 b.y.) is characterized by a rigid crust and development of the first geosynclines, and large intracratonic shallow water or lagoonal basins. Contemporaneously, a rapid spread of marine microorganisms is postulated coupled with a progressively increasing photosynthetic oxygen

generation to present-day oxygen levels in the atmosphere starting some time between 2.2 and 1.9 b.y. ago. Large-scale oxidizing conditions evolved and oxygenated meteoric waters began to dissolve uranium and transport it in solution in its hexavalent state, mainly as uranyl ion. Part of the liberated uranium traveled into shallow water basins, where it accumulated in carbonaceous pelite, psammite, and chemical (carbonate) sediments. Precipitation of the hexavalent uranium occurred primarily where marine microorganism (algae) generated a reducing environment.

Examples: Aphebian basins (Wollaston, Amer Lake, Hurwitz, Aillik groups), Canada; Pine Creek Geosyncline, Australia; Franceville Basin, Gabon.

In geosynclines phosphorites acted as uranium collectors (Example: Upper Jatulian Group, Finland).

These uraniferous sediments became the source for subsequent uranium enrichments in younger rocks or in deposits, either by endogenic magmatic-anatectic or metamorphic, or by exogenic including diagenetic processes.

Examples: Beaverlodge, Athabasca, Kaipokok Bay – Big River districts, Canada; Alligator Rivers, Rum Jungle districts, Australia; Pan-African and Brazilian mobile belts, Africa-South America; Singhbhum Thrust Belt, India; Arjeplog-Arvidsjaur province, Sweden; South Greenland province, Greenland; Krivoj Rog, Ukraine.

4th Period – 500/400–0 m.y.: Characterized by euxenic basins and development of land plants, and a crustal configuration as in the third period.

During the Cambrian to Silurian uranium accumulated in euxenic basins to form low grade uraniferous alum or black shales. Examples: Billingen – Ranstad, Sweden; Chattanooga Shale, USA; Ronneburg, Germany.

With the advent of land plants in the Devonian and their incorporation into continental and marginal marine sediments from then on, the previous geochemical-metallogenetic regime changed.

The vegetal organic matter was able to create reducing conditions in their host sediments capable of reducing and collecting uranium from circulating ground and surface waters.

Examples: Colorado Plateau, Wyoming Basins, South Texas Coastal Plains, USA; Lake Frome Embayment, Australia; Agades Basin, Niger; Paraná Basin, Brazil; North Bohemian Basin, ČSFR – Germany; Kyzylkumsky, Uzbekistan; Jingan Basin, China.

Uranium from uraniferous arkoses and similar rocks was further recycled by magmatic-anatectic processes into highly uraniferous leucogranites and related hydrothermal deposits.

Example: Hercynian orogenic belt, Europe.

References and Further Reading for Chapters 2 and 3

(for details of publication see Bibliography)

Adams 1954; Adams et al. 1959; Adamson 1983; Adamson and Parslow 1985; Adler 1977; Ahmad and Wilson 1981; Ahrens 1965; Alekseyev et al. 1981; Andreyev and Chumachenko 1964; Arribas 1986; Ashley 1984; Aumento 1979; Avital 1983; Ball and Basham 1979; Banas and Mochnacka 1989; Barbey and Cuney 1982; Barbier et al. 1967; Barbier and Ranchin 1969a, 1969b; Bell 1985; Barreto 1988; Barthel and Mehnert 1970; Basham et al. 1982a, 1982b, 1982c; Belevtsev 1980; Belevtsev et al. 1984; Berman 1957; Berthelin et al. 1984; Berzina et al. 1980; Betekhtin 1959; Binns et al. 1980; Bohse et al. 1974; Boyle 1982, 1984; Breger 1974; Briot 1982; Brooker and Nuffield 1952; Brookins 1980; Brynard and Andreoli 1988; Burt and Sheridan 1980, 1985; Burwash and Cumming 1976; Butler 1975; Butt 1988; Calas 1979; Carlisle et al. 1978; Cathelineau 1981a, 1982, 1987a; Cathelineau et al. 1982, 1985, 1987; Cevales 1961; Chen Zhaobo 1981; Chen Zhaobo et al. 1982; Chen Zhaobo and Xiheng Fang 1985; Chernokov 1982; Civetta and Gasparini 1972; Clark et al. 1966; Collot 1981; Cordfunke 1969; Cortini 1984; Cuney 1982, 1985; Cuney and Friedrich 1987; Cuney et al. 1981, 1984, 1989; Coppens and Bernard 1978; Dahlkamp 1982, 1985; Dall'Aglio et al. 1974; Darnley 1981; Darnley et al. 1977; Davidson and Cosgrove 1955; Davidson and Ponsford 1954; Dekkers et al. 1983b; Dill 1980, 1983a, 1983b, 1985; Dimroth and Kimberley 1976; Doi et al. 1975; Dostal and Capredi 1978; Dubessy et al. 1987; Dubinchuk and Siderenko 1978, 1980; Dybek 1962; Dyck 1978; Dyck and Tan 1978; Ethridge et al. 1980; Ewers et al. 1984; Fehn et al. 1978; Ferguson 1987, 1988; Ferguson et al. 1980a; Finch et al. 1980; Flehoc et al. 1989; Fowler and Doig 1979; Friedrich 1984, 1986; Friedrich et al. 1987; Fritsche et al. 1988; Frondel 1958; Frondel et al. 1967; Fuchs 1989; Fyfe 1979; Gabelman 1970, 1977; Galer and O'Nions 1985; Galloway 1978; Garrels and Christ 1959, 1965; Garrels and Larsen 1959; Geffroy and Sarcia 1955, 1958, 1960; George et al. 1986; George-Aniel et al. 1985; Gerasimovskiy 1957; Getseva 1963; Giere 1986; Goldhaber et al. 1979, 1987; Goodell 1985b; Goodell and Trentham 1980; Gorbunova 1974; Gosnold 1976; Grandstaff 1976; Granger 1976; Granger and Finch 1988; Granger and Warren 1969, 1974, 1978, 1979; Grauch 1978; Grauch and Zarinski 1976; Gruner 1956; Gruzder and Rubtsov 1972; Guineberteau 1986; Gustafson and Curtis 1983; Haack 1983; Hambleton-Jones 1976, 1978, 1984; Hambleton-Jones and Smit 1984; Harlass and Schützel 1965; Harshman 1974; Hedges et al. 1984; Heier 1979;

Heier and Adams 1965; Heier and Rhodes 1966; Heinrich 1958; Hoffmann 1943a, 1943b; Hostetler and Garrels 1962; Hsi and Langmuir 1985; Hunter and Michie 1988; Husmann 1956; Hutchinson and Blackwell 1984; Jennings 1976; Jurain and Renard 1970a, 1970b; Kazansky et al. 1968, 1974, 1975, 1976, 1978a, 1978b; Kaspar and Hejl 1970; Kazdan 1978; Kimberley (ed.), 1978; Klepper and Wyant 1957; Kochenov et al. 1965, 1978; Komarov and Shukolyukov 1966; Korolev and Rumyantseva 1976; Kostov 1977; Kryloy and Atrashenok 1959; Kuznetsov et al. 1975; Lambert and Heier 1967, 1968; Lambert et al. 1976; Landais 1989; Landais et al. 1987; Lang et al. 1962; Langmuir 1978; Larsen et al. 1956; Larsen and Gottfried 1961; Larsen and Phair 1954; Le 1975; Lemoine 1975; Leroy and Holliger 1984; Leventhal et al. 1986; Levinson 1980; Li et al. 1980; Liebenberg 1955; Little 1970; Little et al. 1972; Locardi 1977, 1988; Lyons 1961, 1964; Mahaderan 1988; Mahod 1983; Makarov et al. 1960; Malan 1972; Mann and Deutscher 1978; Marjaniemi and Basler 1972; Marlow 1983; Maruejol and Cuney 1985; Maucher 1962; Maurice (ed.), 1982; McKelvey et al. 1955; McMillan 1977a, 1977b; Mclennan et al. 1980; Melgunov et al. 1975; Mel'nikov and Berzina 1973; Meunier et al. 1987; Miller and Kulp 1963; Mineeva 1984; Mineeva and Tarkhanova 1964; Minter 1976; Modnikov et al. 1978; Mohagheghi 1985; Moore 1954, 1967; Moreau 1977; Moreau et al. 1966; Morton and Sassano 1972; Nakashima et al. 1984; Nash et al. 1981; Naumov 1959, 1961, 1973, 1978; Naumov and Mironova 1965, 1969a, 1969b; Naumov et al. 1971; Needham and Stuart-Smith 1984; Needham et al. 1988; Negga et al. 1986; Nekrasova 1958; Nininger 1977; Nguyen-Trung 1985; Omel'yanenko and Mineeva 1979, 1982; Orajaka 1981; Ostle 1982; Pagel 1979, 1981a, 1981b, 1982a, 1982b, 1983; Pagel and Pironon 1986; Pagel and Ruhlmann 1985; Pearce et al. 1984; Pertlik et al. 1969; Petrov et al. 1972; Phair 1952, 1975; Pironon 1986; Pliler 1956; Poty et al. 1986; Poty and Nguyen Trung 1989; Pretorius 1976; Rackley 1976; Rafal'skiy 1958, 1979; Rafal'skiy et al. 1979; Rafal'skiy and Odipov 1967; Ragland and Rogers 1980; Rakotondratsimba 1983; Ramdohr 1957, 1961, 1980; Ramaekers and Hartling 1979; Ranchin 1970, 1971; Renard 1974; Reynolds and Goldhaber 1978, 1983; Reynolds et al. 1977, 1982, 1986; Rich et al. 1977; Richardson 1964; Robb 1986; Robertson 1989; Robertson et al. 1978; Robinson and Spooner 1984; Rogers 1947; Rogers and Adams 1969a, 1969b; Rogers et al. 1965, 1978; Rogers and Ragland 1961; Romberger 1984; Rosholt 1983; Rosholt and Bartel 1969; Rosholt et al. 1971, 1973; Roubault 1958; Rouzoud et al. 1981; Rozhkova et al. 1958; Ruhlmann 1980, 1985; Rytuba and Glanzmann 1978; Saager and Strupp 1983; Samama 1984; Schidlowski 1976; Schmidt-Collerus 1979; Scott and Scott 1985; Sergeyeva et al. 1972; Shatkov et al. 1970; Sibbald 1988; Siderenko 1958; Silver et al. 1982; Simov 1988, 1989; Simpson and Hurdley 1988; Simpson et al. 1976, 1979, 1982a, 1982b; Simpson and Plant 1984; Simpson and Yu Shiqing 1989; Smellie 1982; Smellie et al. 1978; Smith et al. 1982; Smyslov 1974; Sobolewa and Pudow Kina 1957; Sorensen 1970; Starinsky et al. 1982; Steven et al. 1981; Stuckless 1979, 1987; Stuckless and Ferreira 1976; Stuckless and Nkomo 1978; Stuckless et al. 1977, 1981a, 1981b; Swanson 1960, 1961; Szalay 1964; Szalay and Samsoni 1969; Tarkhanov and Poluarshinov 1989; Tauson 1954; Theis 1979; Titov et al. 1975; Thomas 1983; Toens 1981; Toens and Andrews-Speed 1984; Trentham 1981; Treuil 1985; Treuil and Joron 1989; Tugarinov 1963, 1975; Tugarinov et al. 1964; Tugarinov and Naumov 1969, 1974; Turekian and Wedepohl 1961; Turpin et al. 1989; Tweedie 1979; von Borstel 1984; Voultsidis and Carsten 1978; Walton 1978; Walton et al. 1981; Wanty et al. 1987; Waters and Granger 1953; Watson and Plant 1979; Watson et al. 1982; Weber et al. 1985; Wedepohl 1974; Weeks and Thompson 1954; Wenrich 1985; Westrum and Gronvold 1962; White and Martin 1980; Whitfield et al. 1959; Woodmansee 1976; Wyllie 1979; Xu et al. 1981; Yhao Zenkai et al. 1986; Yeliseyeva 1977; Yermolayev 1971, 1973, 1975; Yermolayev and Zhidikova 1966; Yermolayev et al. 1965; Yeliseyeva and Omel'yanenko 1976; Yevseyeva et al. 1974; Zhuravleva et al. 1976; Ziegler 1978; Zielinski 1978, 1979, 1982, 1983, 1985; Zielinski et al. 1987; Zimmer 1986; (see also references in chapter 4) (for extensive references up to 1982 see Boyle 1982)

3 Principal Aspects of the Genesis of Uranium Deposits

Our knowledge of the metallogenesis of many uranium deposits, although believed to be globally or principally understood, is in many cases meager, dubious, or ambiguous. This becomes obvious when trying to reconcile conflicting data from various geoscientific disciplines on the same subject. Some deposits are well researched, others, including important ones, are not. In other cases, a complex, polyphase evolution of deposits greatly hampers the deciphering of the actual origin of the mineralization. Based on theoretical and empirical deductions and interpretations of the available data, interesting concepts and sound models on the metallogenesis of uranium deposits have been forwarded by many knowledgeable geologists. In spite of this, the factual origin of many deposits is still entirely or partially enigmatic.

The principles of metallogenesis are presently sufficiently well understood only for some types of deposits including Lower Proterozoic quartz-pebble conglomerate, rollfront sandstone, intrusive, phosphorite, and certain surficial deposits. In addition, the genesis of the Hercynian, Limousin-type vein deposits has been satisfactorily established. All other uranium ore deposits are understood to a lesser extent and in varying degrees.

This chapter provides a synopsis on the global and principal processes involved in deposit formation. Metallogenetic hypothesis on specific types of deposits and individual deposits are presented in Chapters 4 and 5 respectively. Selected References and Further Reading for Chapter 3 are included in those of Chapter 2.

3.1 The Global Metallogenetic Cycle of Formation of Uranium Deposits

In a global sense, formation of uranium deposits can be attributed schematically to three genetic categories, each related to one of the three dominant regimes of the geological cycle of crustal evolution. These categories are:

1. Primary uranium deposits formed by endogenic magmatogenic/anatectic processes.
2. Secondary uranium deposits formed by subsequent exogenic, i.e., supergene and/or sedimentary (including diagenetic) processes from the primary types.
3. Tertiary uranium deposits formed by endogenic metamorphic processes from primary and secondary deposits.

This cycle closes if deposits of the secondary and tertiary categories are retransformed by anatexis or palingenesis into those of the primary category. On the other hand, exogenic processes may liberate uranium from metamorphic environment and reconcentrate it to form secondary category deposits. Figure 3.1 gives an overview of the three categories of deposits and their genetic relationships. Figure 3.2 illustrates diagrammatically the geological position of uranium deposits and the presumed migration of U in deposit formation.

The formation of uranium deposits, however, is not restricted to these principal genetic regimes. Instead, complex polygenetic processes may be responsible for the genesis of many deposits. Some of the deposit types cannot be attributed either to the one or the other category. They will be dealt with under "*mixed category*" deposits.

The formation of uranium deposits and the implications involved in the various inferred metallogenetic processes may be summarized as follows:

1. Primary uranium deposits: The origin of the uranium in primary mineralizations is reasonably well established as either juvenile magmatic, prevailing in Early Precambrian, or anatectic/palingenetic, prevailing in younger times.

To the primary deposits belong sensu stricto only the syngenetic (intra)intrusive deposits (type 9, Chap. 4). (Examples: Rössing, Namibia; Palabora, S. Africa; Kvanefjeld, Greenland; Bancroft, Canada) and, sensu lato, epigenetic vein deposits (subtype 3.1, Chap. 4) which commonly are of polyphase origin (see Chap. 5.3).

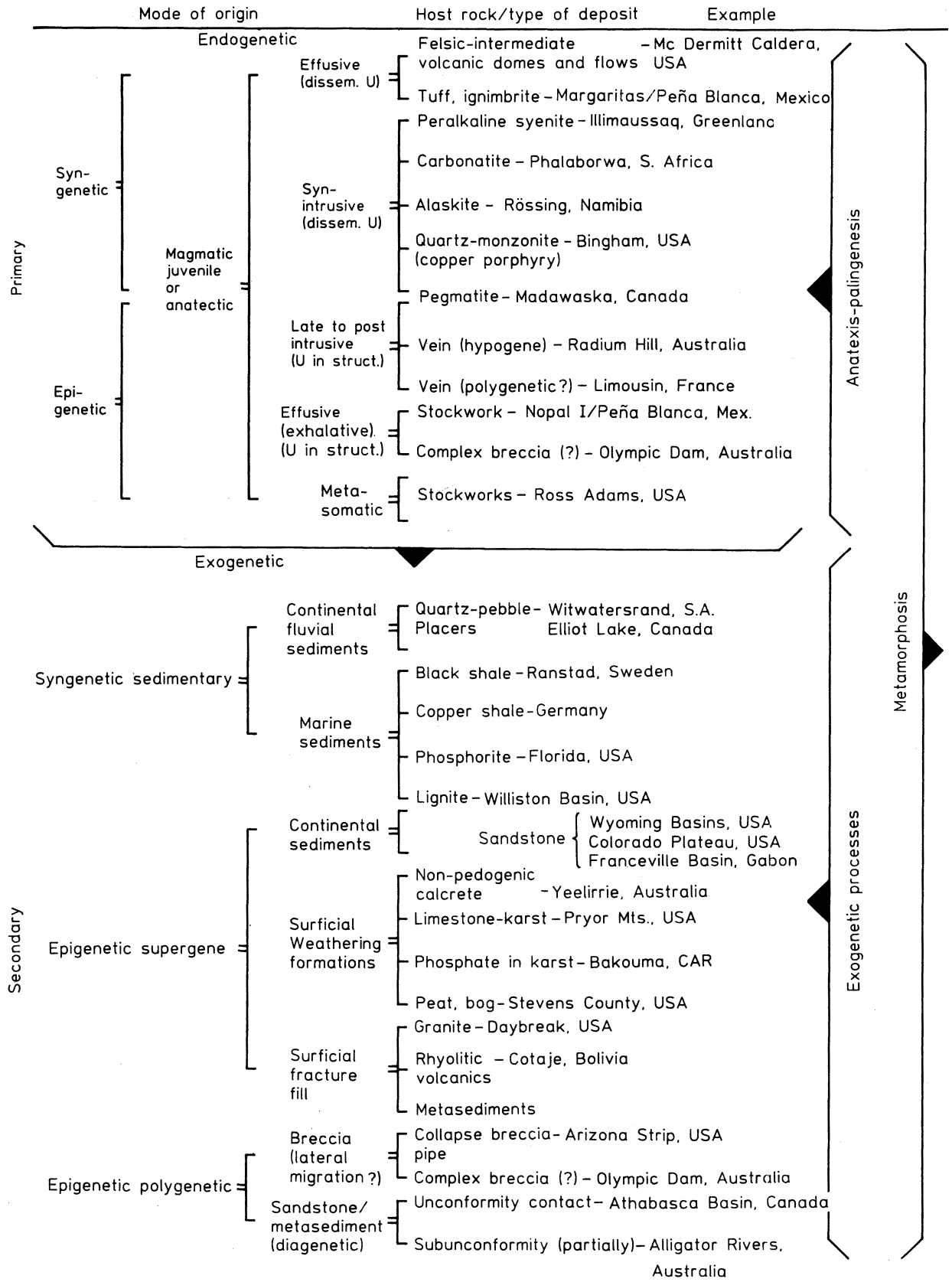
Mode of origin
Host rock/type of deposit
Example
Endogenetic
Primary
Syn-genetic
Epi-genetic
Magmatic juvenile or anatectic
Effusive (dissem. U)
Felsic-intermediate volcanic domes and flows – Mc Dermitt Caldera, USA
Tuff, ignimbrite – Margaritas/Peña Blanca, Mexico
Syn-intrusive (dissem. U)
Peralkaline syenite – Illimaussaq, Greenland
Carbonatite – Phalaborwa, S. Africa
Alaskite – Rössing, Namibia
Quartz-monzonite – Bingham, USA (copper porphyry)
Late to post intrusive (U in struct.)
Pegmatite – Madawaska, Canada
Vein (hypogene) – Radium Hill, Australia
Vein (polygenetic?) – Limousin, France
Effusive (exhalative) (U in struct.)
Stockwork – Nopal I/Peña Blanca, Mex.
Complex breccia (?) – Olympic Dam, Australia
Meta-somatic
Stockworks – Ross Adams, USA
Anatexis-palingenesis
Exogenetic
Secondary
Syngenetic sedimentary
Continental fluvial sediments
Quartz-pebble Placers – Witwatersrand, S.A. Elliot Lake, Canada
Marine sediments
Black shale – Ranstad, Sweden
Copper shale – Germany
Phosphorite – Florida, USA
Lignite – Williston Basin, USA
Epigenetic supergene
Continental sediments
Sandstone
Wyoming Basins, USA
Colorado Plateau, USA
Franceville Basin, Gabon
Surficial Weathering formations
Non-pedogenic calcrete – Yeelirrie, Australia
Limestone-karst – Pryor Mts., USA
Phosphate in karst – Bakouma, CAR
Peat, bog – Stevens County, USA
Surficial fracture fill
Granite – Daybreak, USA
Rhyolitic volcanics – Cotaje, Bolivia
Metasediments
Epigenetic polygenetic
Breccia (lateral migration ?)
Collapse breccia – Arizona Strip, USA pipe
Complex breccia (?) – Olympic Dam, Australia
Sandstone/ metasediment (diagenetic)
Unconformity contact – Athabasca Basin, Canada
Subunconformity (partially) – Alligator Rivers, Australia
Exogenetic processes
Metamorphosis

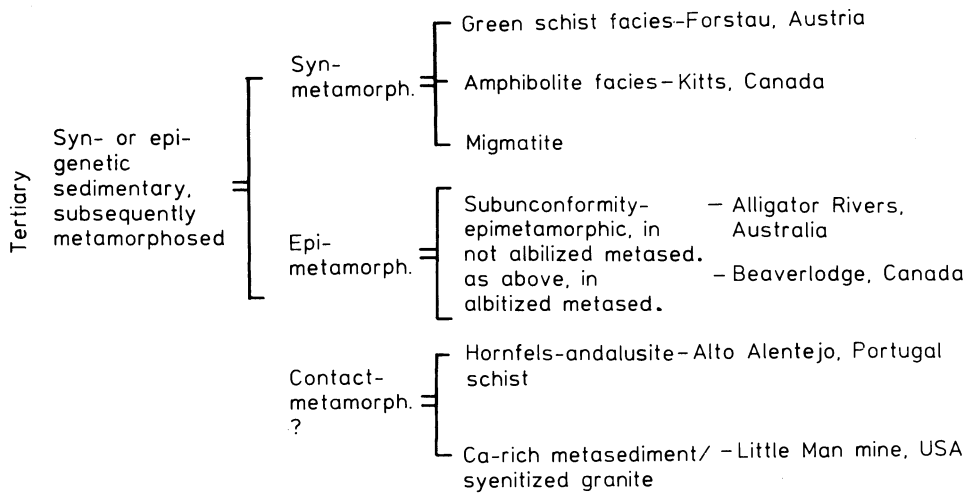

Fig. 3.1. Schematic metallogenetic correlation of uranium deposits and occurrences. Note: Some of the deposits are gradational into each other, others are of polyphase origin, and of a number of deposit types the provenance is uncertain. These deposits are here attributed to processes which supposedly generated the final stage of mineralization and/or deposit configuration

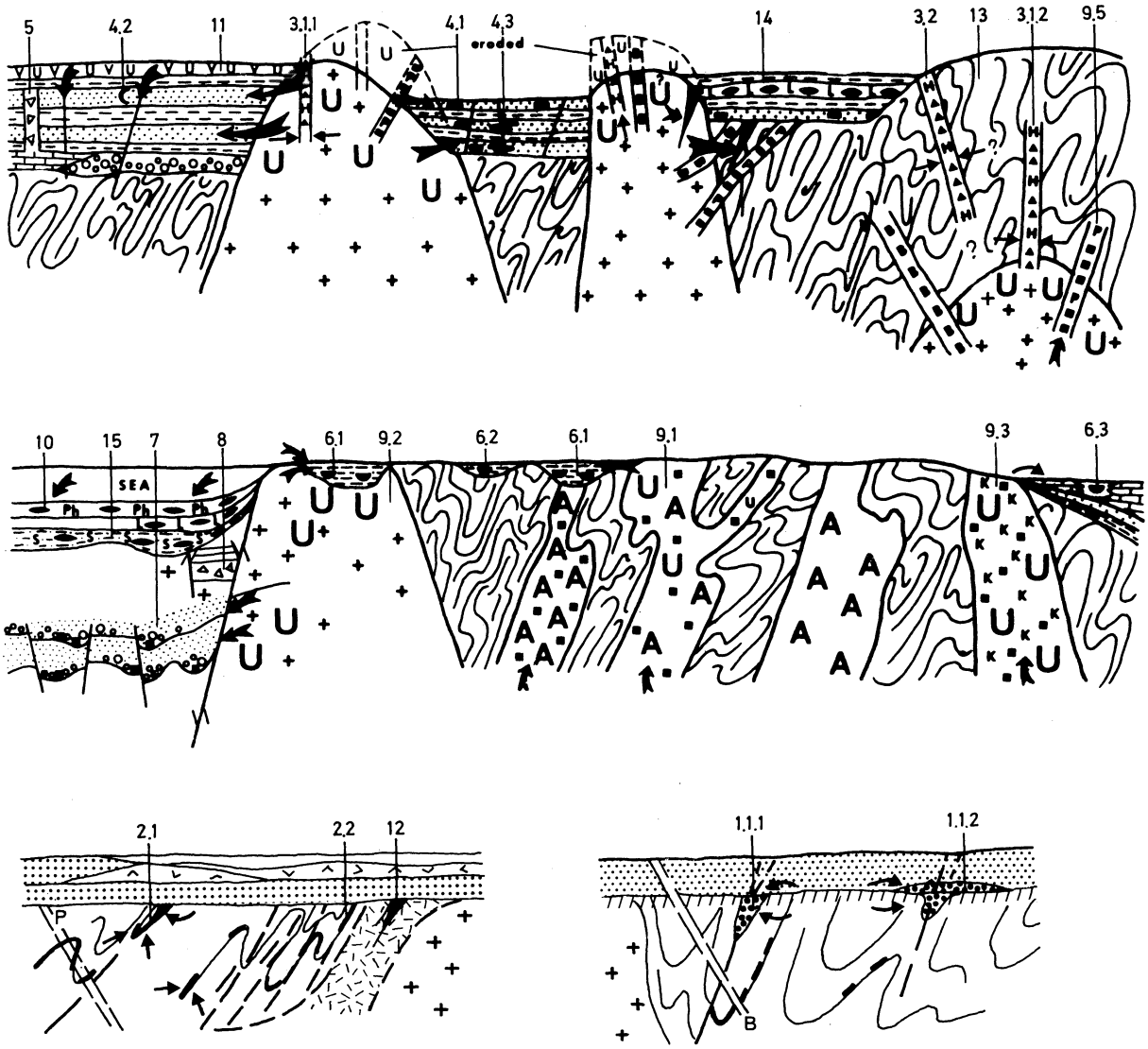

- Unconformity-contact deposit (type 1)
- Subunconformity-epimetam. (2)
- Vein (3)
- Sandstone (4), tabular (4.1)
- Sandstone, rollfront (4.2)
- Sandstone, tectonic-lithologic (4.3)
- Collapse breccia pipe (5)
- Surficial (6)
- Quartz-pebble conglomerate (7)
- Breccia complex (8)
- Intrusive, alaskite (9.1)
- Intrusive, carbonatite (9.2)
- Intrusive, pegmatite (9.5)
- Phosphorite (10)
- Volcanic (11)
- Metasomatite (12)
- Metasediment includes synmetamorphic (13)
- Lignite (14)
- Black shale (15)
- Igneous U source rock
- Uraninite, uranothorianite,
- U impregnation
- Presumed transport direction of U
- Dike, B=basic, P=pegmatitic
- Pelitic sediment
- Psammitic sediment
- Psephitic sediment
- Fault with displacement direction
- Regolith
- Intrusive
- Late or post-intrusive hydrothermal
- Metamorphic hydrothermal
- Exogenic
- Diagenetic hydrothermal

Fig. 3.2. Schematic diagram of regional structural and lithologic setting of uranium deposits and occurrences and the hypothetical migration paths of uranium to form the deposits

(Examples: Přibram, Jáchymov, ČSFR; Limousin and Vendée, France).

If magmatic/anatectic events generate metasomatism, some marginal or transitional styles of mineralization may develop. Some autometasomatic and contact-metasomatic deposits are probably of this nature (type 12, Chap. 4).

2. Secondary uranium deposits: These deposits owe their existence to exogenic processes. Two categories of deposits have formed, distinguished by syn- and epigenetic uranium emplacement (Table 3.1). The Lower Proterozoic conglomerate, the black shale, and the phosphorite deposits are of synsedimentary nature. The various mineralizations in sandstone, surficial, sedimentary breccias, and lignite types are epigenetic. A further division can be drawn by either detrital or chemical uranium transport.

Prior to the *oxygenation of the earth's atmosphere* (older than about 2.2 b.y.), mechanical weathering and sedimentation formed placer deposits with detrital uranium minerals in oligomictic quartz-pebble conglomerates (type 7, Chap. 4). (Examples: Witwatersrand, S. Africa; Elliot Lake, Blind River, Canada).

After the change to an oxidizing atmosphere, which occurred at the latest during the middle of the Lower Proterozoic (approximately 2.2 b.y. ago) (Roscoe 1969; Frarey and Roscoe 1970; Schidlowski et al. 1974, see also Chap. 2 and Fig. 2.7) chemical liberation of uranium from a variety of uraniferous source rocks (granites, felsic volcanics, metasediments etc.) led to concentrations of uranium mineralization in suitable litho-chemical environments. Dependent on climatic and transport conditions uranium was (a) either transported into the sea and concentrated *synsedimentary* in black shales and phosphorites (type 15 and 10, Chap. 4). (Examples: Ranstad, Sweden; Land Pebble district, Florida and Montpelier, Idaho, USA, respectively) or (b) concentrated *epigenetically* into terrestrial sediments in intracratonic and intermontane basins (type 4, Chap. 4) (Examples: Wyoming Basins and Colorado Plateau, USA), occasionally in littoral, marginal marine clastic sediments (Example: South Texas Coastal Plains) and in surficial deposits (type 6, Chap. 4) (Examples: Yeelirrie, Australia; Langer Heinrich, Namibia; Stevens County, USA). Part of the sediment-bound uranium, however, may also have been introduced by *geothermal systems* associated with volcanism (subaquatic volcanic metalliferous exhalations?) as suggested for the breccia complex type deposit Olympic Dam, Australia (type 8, Chap. 4).

Localization and formation of second category deposits require a combination of distinct regional and local metallogenetic conditions. Uraniferous source rocks combined with adequate paleotopography, paleoclimate, paleoweathering, paleobiology (evolving of life forms), paleohydrology, and tectonics are essential to produce favorable host environments and to put uranium into solution. The coincidence of these factors leads to suitable hydrodynamic and chemophysical regimes (solution/groundwater flow, redox interface etc.) and uranium precipitation. Deposits of economic magnitude formed only where the host provided sufficient open space to allow the precipitation of sizable concentrations of uranium.

3. Tertiary uranium deposits: The metallogenesis of tertiary uranium mineralizations is still vague. Relatively little is known about the behavior of uranium during metamorphism. In a generalized approach, two thermodynamic systems may be envisaged, the first a closed, the second an open system. A *closed system* refers to a crustal unit affected by a metamorphic event of more or less in situ mobilization and recrystallization without marked introduction or loss of elemental constituents. In contrast, an *open system* is reflected by brittle deformational ground preparation (dilation faulting) and internal and/or external mobilization and redistribution of sensitive elements by metamorphic hydrothermal fluids.

In a *closed system*, formation of mineralization relies on the intrinsic uranium inventory of the protolith. For example, if sandstone type deposits such as that of Oklo, Gabon, which is of the Lower to Middle Proterozoic age, undergo low to medium grade metamorphism (below upper amphibolite-granulite facies) in a closed system, one might expect to find a stratiform synmetamorphic mineralization (type 13, Chap. 4) such as at Forstau, Austria. Uranium tends to move only in the range of millimeters to perhaps meters, as indicated by its stratiform disseminated distribution with preferential but not exclusive affinities to mafic minerals and sometimes in fold noses. The only difference between greenschist facies and amphibolite facies grade of metamorphism tends to be in a general way the degree of crystal-

Table 3.1. Mode of origin of principal types of uranium deposits. The attribution of deposit types is tentative and reflects the prevalent opinion on, but not necessarily the factual genesis of, a deposit type not yet conclusively researched (for locations of examples see Fig. 1.1)

Type (numbers refer to types in Table 4.1)	Host Environment/U-Distribution (Subtype)	Mode of Origin	Example
Syngenetic Mineralization			
Quartz-pebble Conglomerate (7)	Stratiform in oligomictic quartz-pebble conglomerate of Lower Proterozoic age	Syn-sedimentary detrital	Witwatersrand, S.A.
Phosphorite (10)	Stratiform	Syn-sedimentary chemical	Florida, USA
Black Shale (15)	Stratiform	Syn-sedimentary chemical	Ranstad, Sweden
Lignite (14)	Stratiform (14.1), joint-fracture bound (14.2)	Syn-sedimentary chemical, redistributed	Williston Basin, USA
Intrusive (9)	Disseminations in		
	a) alaskite (9.1)	Syn-intrusive (granitization)	Rössing, Namibia
	b) quartz-monzonite/ copper-porphyry (9.2)	Syn-intrusive (granitization)	Bingham, USA
	c) carbonatite (9.3)	Syn-intrusive (orthomagmatic)	Phalaborwa, S.A.
	d) peralkaline syenite (9.4)	Syn-intrusive (orthomagmatic)	Ilimaussag, Greenland
	e) pegmatite (9.5)	Syn-intrusive (magm. differentiated)	Bancroft, Canada
Syn-metamorphic (13)	Strata-(pene)concordant disseminated in (graphitic) metasediments and metavolcaniclastics	Syn-metamorphic (in closed system)	Forstau, Austria, Kitts, Canada
Metasomatite (12)	Na-metasomatized granite and metasediment, albitite	Syn-autometasomatic (?)	Ross Adams, USA
Epigenetic Mineralization			
Unconformity-contact (1)	a) Fracture-bound in metasediments beneath unconformity	Polyphase; supergene (?) and diagenetic hydrothermal	Athabasca Basin, Rabbit Lake, Canada
	b) Clay – bound in argillaceous lenses on top of unconformity		Athabasca Basin, Cigar Lake, Canada
Subunconformity-epimetamorphic (2)	Structure – strata-bound ± peneconcordant to strata	Late to post-orogenic metamorphic-metasomatic-hydrothermal with (unconformity related) diagenetic-metasomatic overprint	
	a) In not albitized metasediments (2.1)		Alligator Rivers, Ranger, Australia
	b) In albitized metasediments (2.2)		Beaverlodge, Canada

Table 3.1. *Continued*

Type (numbers refer to types in Table 4.1)	Host Environment/U-Distribution (Subtype)	Mode of Origin	Example
Vein (3)	a) Granite-related (3.1) – intragranitic (Limousin-type) – perigranitic – in(meta) sediments (Bohemian & Erzgebirge types) – in contact-metamorphics (Iberian type)	Late to post-magmatic convective (hypogene?) hydrothermal	Massif Central, Limousin, France Bohemian Massif, ČSFR Iberian Meseta, Spain, Portugal
	b) Not granite-related (3.2) in(meta-) sediments	Late to post-orogenic convective hydrothermal	Schwartzwalder, USA
Sandstone (4)	a) Tabular/peneconcordant (4.1) b) Rollfront (4.2) c) Tectonic-lithologic (4.3)	Infiltration by groundwater migration and interaction with reductants either on a stationary (4.1) or dynamic (4.2) basis, and as above plus redistribution (4.3)	Grants, USA Wyoming Basins, USA, South Texas, USA Franceville Basin, Gabon
Collapse Breccia Pipe (5)	Fragments and matrix (sandy) within pipe and fractures surrounding pipe	Lateral infiltration along permeable sandstone beds or fractures	Arizona Strip, USA
Breccia Complex (8)	Granitic and polymict sedim. breccia filling graben structure	Infiltration by groundwater or volcanic exhalations	Olympic Dam, Australia
Volcanic (11)	a) Structure-bound (11.1) – intrusive vein – surficial fissure coating or filling	Volcanic hydrothermal Supergene accretion	Peña Blanca, Nopal I, Mexico Cotaje, Bolivia
	b) Strata-bound (11.2) – intracaldera (moat) – exocaldera volcaniclastic sediments	Supergene infiltration by groundwater migration partly perhaps volcanic exhalative	Mc Dermitt, Aurora, USA Peña Blanca, Margaritas, Mexico
Surficial (6)	a) Duricrust non-pedogenic (6.1) – fluvial/valley fill – lacustrine or playa	Supergene leaching, infiltration by groundwater migration and interaction/ evaporation	Yilgarn, Yeelirrie, Australia Yilgarn, Lake Maitland, Australia
	b) Peat and bog/organic-rich swamp (6.2)	Adsorption on organic matter by extraction from surface and groundwater	Stevens County, USA
	c) Floor cover in karst cavern (6.3)	Supergene infiltration and mixing of groundwaters	Pryor Mtns., USA
	d) Coatings + fillings of surface-related fissures in or adjacent to uraniferous igneous, metamorphic and sedimentary rocks (6.4)	Fracture fill by supergene redistribution and concentration	Daybreak, USA Cotaje, Bolivia
Epigenetic mineralization			

lization. Pitchblende occurs in the former and uraninite in the latter (see also Chap. 2).

In an *open system*, where metamorphic hydrogenic fluids can migrate, veinlike (metamorphic hydrothermal) deposits may be initiated such as type 2, (Chap. 4), perhaps in a late orogenic phase. The fluids may leach uranium and other elements/compounds (CO_2^{2+}, SO_3^{2+} etc.) by percolating through uraniferous metasediments or other fertile rocks and transport it to favorable structures. Here, uranium could be precipitated from the solutions by mechanisms comparable to those of vein generation (type 3, Chap. 4) (changes in P-T, eh, and/or pH conditions). These processes may or may not be associated with metasomatism, such as albitization etc., of host environments. If metasomatism is involved, deposit types transitional to those of the metasomatic deposits may evolve.

In many cases, processes, for instance triggered by epeirogenic movements associated with or without dike intrusions, or diagenesis of overlying sediments may generate remobilization regimes with addition or removal of uranium. Under these conditions, recrystallization of precursor mineral assemblages will occur and camouflage initial parageneses to a degree depending on the intensity of the overprint. In the extreme case it may result in a completely new mineral assemblage. As a consequence, the archetype of the deposit cannot be identified. Instead, these deposits may appear disconnected of metamorphism and related to the younger processes. Deposits of the subunconformity-epimetamorphic type (type 2, Chap. 4) belong to this category. (Examples: Beaverlodge district, Canada, Ranger One, Alligator Rivers district, Australia)

"*Mixed category*" deposits are of two modes. One group cannot be clearly assigned to any one of the main regimes of the geological cycle and constitutes a transitional category. It includes metasomatic, certain vein and volcanic type deposits (type 12, 3.2, and 11 respectively, Chap. 4).

The other group includes deposits evolved by ambiguous frequently multistage processes, the individual stages of which often being difficult to decipher. This group includes particularly unconformity-contact, certain subunconformity-epimetamorphic and collapse breccia pipe deposits (type 1, 2 and 5 respectively, Chap. 4). Mechanisms suggested for the formation of such deposits range from supergene concentration, diagenetic hydrothermal to hypogene hydrothermal and unknown hydrothermal processes. Either one or a combination of these processes is suggested by the various investigators, partly dependent on individual preference and observations.

Finally, it should be mentioned that metallogeny as related to plate tectonics has been applied to explain the creation of uranium provinces and the formation of certain types of uranium deposits. The regional location of these deposits and of uranium provinces as viewed in their total geological context appears to be connected with plate tectonics. Fyfe (1979), Gabelman (1977a, 1977b). Toens et al. (1980), and IAEA (1986) among others have reviewed this topic.

Gabelman (1977b) notes that regional mineralized zones are associated with tensional taphrogenic tectonics. He also expresses the opinion that a close spatial and genetic relationship exists between epigenetic uranium occurrences and circumcontinental mobile belts. Favorskaya (1977) obviously shares this view and puts forward a hypothesis according to which polystage magmatic complexes and mineral deposits had their origin at great depth.

3.2 The Time-Related Occurrence of Uranium Deposits

The time and formation relationship of certain metallogenetic parameters applying to the various types of uranium deposits indicates in general the following:

a) Restrictions in distribution of uranium deposits to distinct epochs in the earth's history.
b) Uranium-rich source rocks prevailed during distinct geological times.
c) Uranium deposits in sediments and metasediments show on numerous occasions a distinct spatial affinity to uraniferous source rocks which themselves are related to distinct geological times as indicated under (b).
d) The known uranium deposits can be grouped on the basis of time-stratigraphic and metallogenetic parameters into five principle generations.

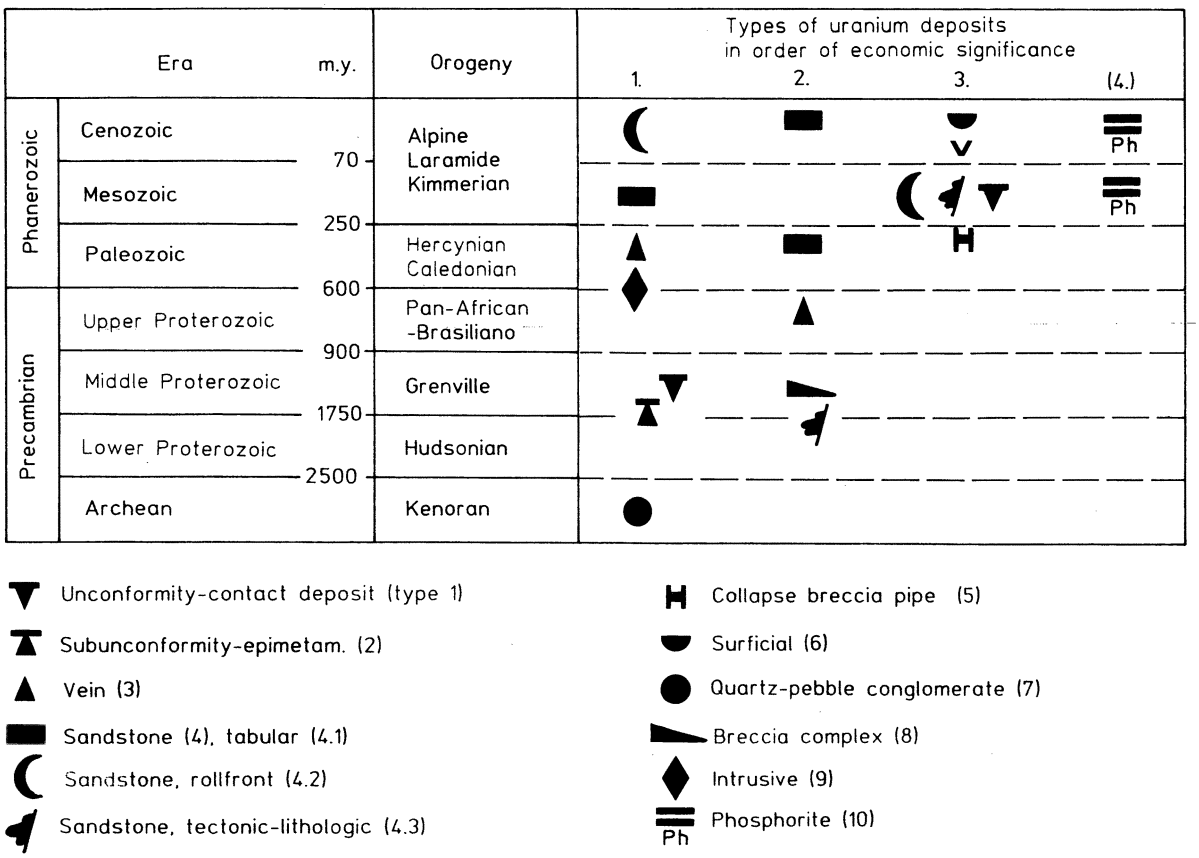

Fig. 3.3. Prevalent geochronologic-stratigraphic distribution of major types of uranium deposits

In any event, any time-bound ore forming process may constitute the final or an intermediate stage. This synthesis is based on the following data of both qualitative and quantitative nature.

3.2.1 Time-Stratigraphic Relationship of Uranium Deposits

Plotting of the main types of deposits in a geochronological stratigraphic column with simultaneous considerations of their economic significance (Fig. 3.3) reveals the following time-bound distribution:

a) During the Cenozoic, surficial deposits occur in Tertiary to Recent sediment-duricrusts; rollfront and some tabular deposits occur in Tertiary sandstones. Most volcanic type U occurrences have formed during this period.

b) During the *Mesozoic*, tabular and, to a lesser extent, rollfront type and tectonic-lithological sandstone deposits prevail. Some granite-unrelated veins are found in the Laramide orogenic belt.

c) During the *Paleozoic*, tabular sandstone deposits, particularly in post-Devonian strata, and granite-related vein type deposits restricted to the Hercynian Orogeny occur. A few unconformity-bound deposits are known at the Permian-Hercynian unconformity.

d) During the *Upper Proterozoic*, the (intra)intrusive Rössing deposit and few granite-unrelated vein deposits have formed.

e) During the *Lower to Middle Proterozoic*, subunconformity-epimetamorphic and unconformity-contact deposits, as well as the tectonic-lithologic sandstone deposits of Gabon prevail.

f) During the *Upper Archean to lowermost Lower Proterozoic*, the uraniferous quartz-pebble conglomerates have formed.

Table 3.2. Geochronologic-stratigraphic distribution of uranium resources (RAR < \$30/U_3O_8) and former production (status: January 1987) (in U_3O_8)

	RAR		Production		Total	
	1000 mt	%	1000 mt	%	1000 mt	%
Cenozoic-Mesozoic	ca. 390	22	420	43	810	29
Paleozoic (mainly Hercynian + Permian)	ca. 100	6	70	7	170	6
Upper Proterozoic	ca. 280	15	70	7	350	13
Lower-Middle Proterozoic	ca. 740	41	160	16	900	32
Lower Proterozoic	ca. 290	16	270	27	560	20
Total	ca.1800	100	990	100	2790	100
Total Precambrian	ca.1310	72	500	50	1810	65

3.2.2 Geochronological Distribution of Uranium Resources

Reasonably Assured Resources of the Western World recoverable for less than \$30/U_3O_8 (IAEA cost category \$80/kg U) amount to ca. 1.8 mio.mt U_3O_8 and production prior to 1987 to ca. 0.99 mio.mt U_3O_8 (OECD/IAEA 1988). Of the combined total of 2.79 mio.mt U_3O_8 about 65% is in or was produced from Precambrian rocks (RAR: ca. 72%, production: ca. 50%), and most of the remainder, ca. 25% of the total (RAR: 15–20, production: 35–40%) is or was mined from Phanerozoic lithologies adjacent to Precambrian basement. Table 3.2 provides respective data and a breakdown of the Precambrian-hosted resources and former production quantities.

3.2.3 Geochronologic-Metallotectonic Relationship of Uranium Deposits

The resource numbers (Table 3.2 and Figs. 3.4 and 3.5) already point to a quantitative prevalence of the uranium, and of certain types of deposits as well, to certain geological eras. More clearly, this is documented on a metallotectonic map (Fig. 1.1) showing individual deposits and/or ore districts combined with selected

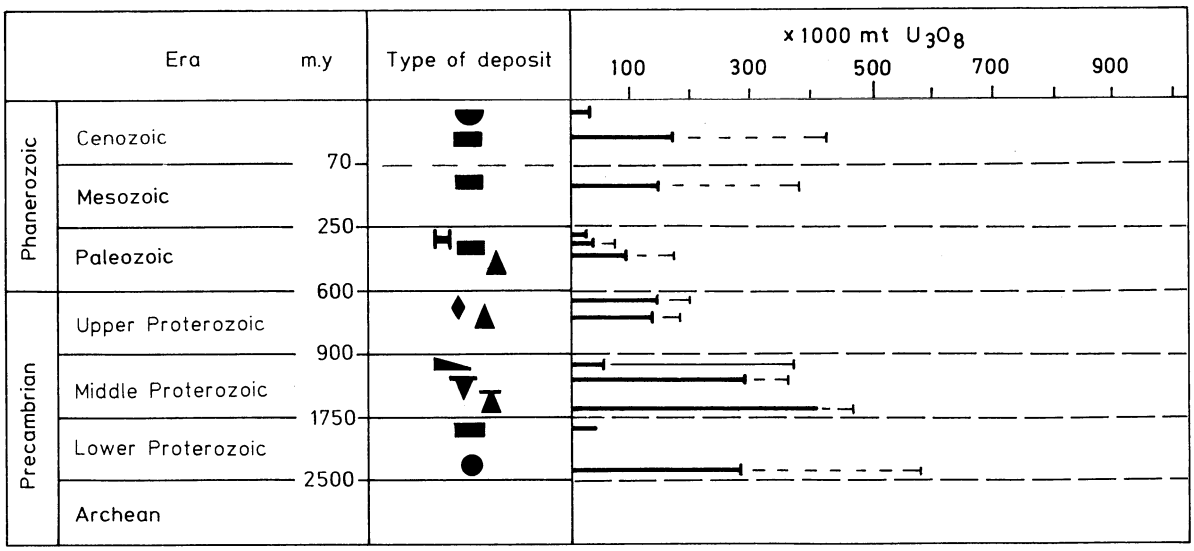

Fig. 3.4. Geochronologic-stratigraphic distribution of total uranium resources (RAR < \$30/lb U_3O_8, *solid line*) plus past production (*dashed line*) by type of deposit. (former Eastern Block countries and China not included)

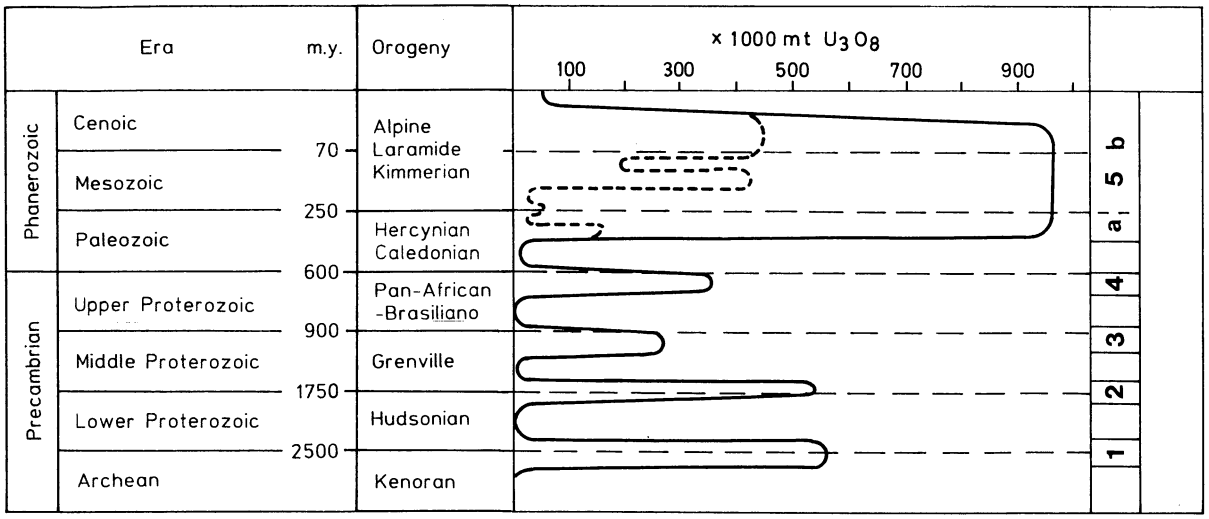

Fig. 3.5. Geochronologic-stratigraphic concentration of uranium and related deposit generations reflected by distribution of cumulative RAR (<$30/lb U_3O_8 category) and past production. (former Eastern Block countries and China not included) Numbers to the *right* denote U deposit generations

geochronological-tectonic units. The map illustrates that certain types of deposits display a distinct affinity and restriction to certain geological eras, namely to:

a) the Upper Archean to Lower Proterozoic;
b) the Hercynian;
c) the Upper Proterozoic, but less prominently.

In addition to these facts, epigenetic deposits in sandstones and calcretes occur remarkably close to granitic complexes of the above eras, as illustrated graphically by a selected example displaying the situation in the western USA (Fig. 3.6) and evidenced on a worldwide basis by the following pairs (the first location refers to the deposit or ore district, the second to the assumed source area of the uranium):

Australia: Lake Frome Embayment (Tertiary) – Mount Painter and Willyama Block (Lower Proterozoic);

Yeelirrie (Tertiary to Recent) – Yilgarn Block (Archean to Lower Proterozoic).

Africa: Agades Basin (Arlit, Akouta), Niger (Visé to Cretaceous) – Aïr Massif (Old Precambrian);

Franceville Basin (Mounana, Oklo), Gabon (Lower-Middle Proterozoic) – Massif de Chaillu (Lower Proterozoic);

Langer Heinrich, Namibia (Quaternary) – Damara mobile belt (Upper Proterozoic).

Europe: Lodève Basin, France (Permian) – Massif Central (Hercynian); Forstau, Austria (Permian) – Niedere Tauern (Hercynian); Müllenbach, Germany (Permo-Carboniferous) – Schwarzwald (Hercynian).

Almost all crystalline uraniferous source rocks in central and western Europe belong to Hercynian complexes which occur within or adjacent to Precambrian terrane and which in part at least are derived by anatexis from Precambrian rocks.

America: Gas Hills, Wyoming (Tertiary) – Granite Mountains (Lower Proterozoic); likewise all deposits in the basins of Wyoming as well as most of the deposits of the Colorado Plateau exhibit a spatial relationship to Precambrian crystalline complexes as shown in Fig. 3.6.

3.2.4 Uranium Deposit Generations and Their Time-Stratigraphic Ranking

The above listed situations and relationships lead to the question of how far the environments and mechanisms governing uranium ore formation can be delineated with respect to time and space. Investigations by means of paleogeography based on paleomagnetism, continental drift, orogenic and epeirogenic events, further by paleoclimates and paleobiology, as outlined earlier, assist in the

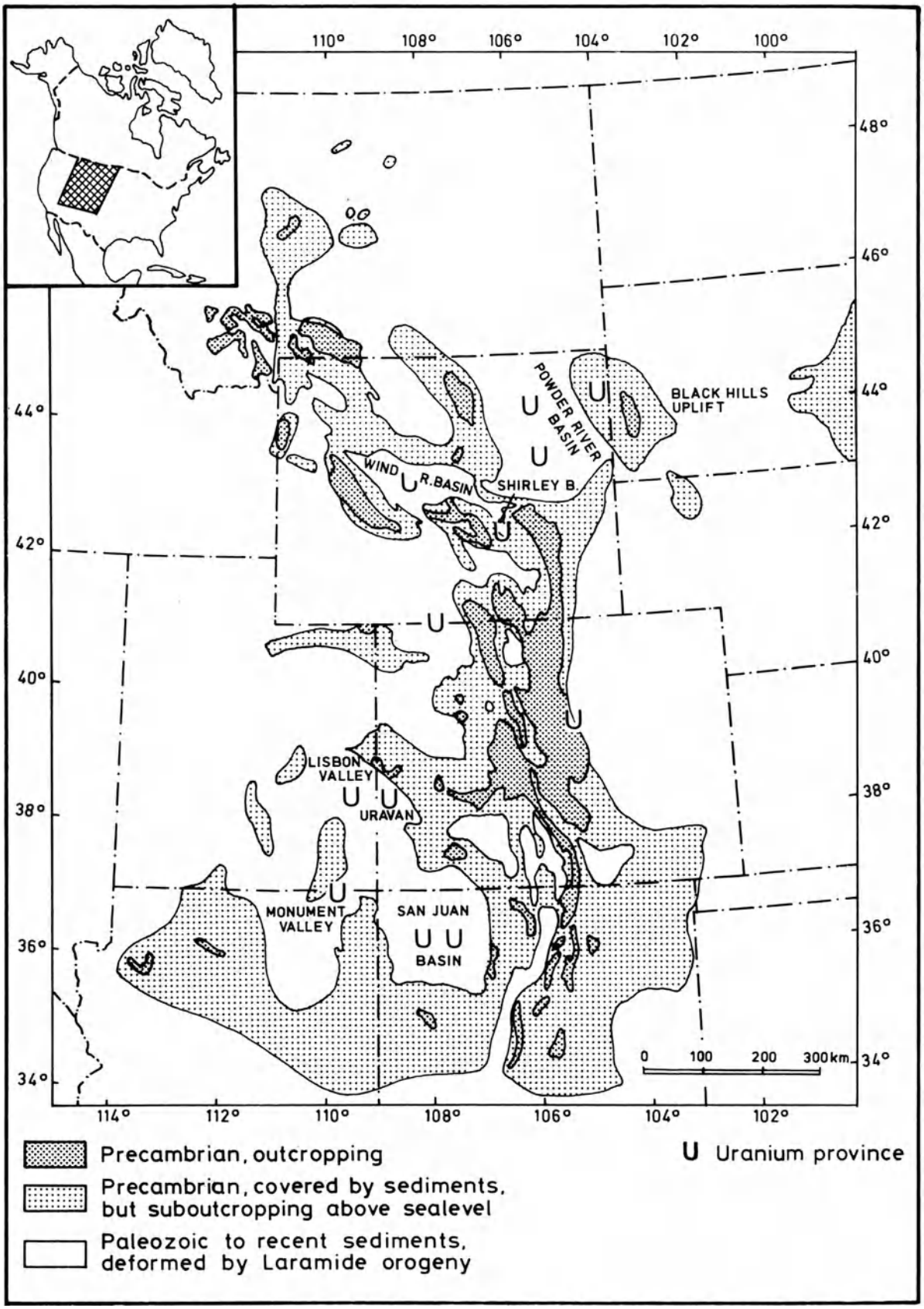

Fig. 3.6. Western USA, spatial relationship of uranium districts to Precambrian crystaline basement terrane. (After Mallery et al. 1972)

delineation of specific time related metallogenetic parameters that permit the identification of five principal generations of uranium deposits (Fig. 3.7) which fit into the overall evolution of the earth's crust.

Generation one (Upper Archean to lowermost Lower Proterozoic, 2800 to 2200 m.y. ago)

The oldest nonmagmatic uranium deposits occur in *oligomictic quartz-pebble conglomerates*. The primary mineralization is uraninite, uranothorianite, and uranothorite of detrital origin, as recognized by Ramdohr (1955). This type of uranium deposit remains restricted to the time in earth history when an oxidizing atmosphere was lacking, i.e., prior to the middle Lower Proterozoic (>2200 m.y. old).

Examples: Blind River-Elliot Lake, Canada; Witwatersrand, South Africa.

Generation two (Lower-Early Middle Proterozoic, 2200 to 1900 to 1700 m.y. ago)

During the middle Lower Proterozoic (2200 to 1900 m.y. ago), the oxidation potential of the atmosphere increased which effectively blocked the mechanical transport of uranium. During and from this period onwards, uranium travelled essentially in solution as either ion or uranyl-complex and accumulated in shallow water or lagoonal basins. Initially, uranium precipitated either syn- or postsedimentary in pelitic to psammitic sediments in or close to organic horizons.

Examples: the unmetamorphosed *sandstone* deposits of the Franceville Basin, Gabon (Oklo, Mounana etc.) dated ca. 2050 m.y.; metasediments of the Pine Creek Geosyncline, Australia, and the Tazin and Cree Lake Mobile Belt, Canada.

During the Hudsonian and time equivalent orogenies (1900 to 1700 m.y. ago) amphibolite to granulite grade metamorphism affected these sedimentary units, causing a more or less in situ crystallization, or limited late orogenic redistribution of the uranium by metamorphic-hydrothermal processes resulting in either *synmetamorphic stratiform* mineralizations (type 13, Chap. 4) or *epimetamorphic veinlike* deposits (type 2) respectively.

Examples: (a) synmetamorphic stratiform deposits: Forstau, Austria; Kitts, Canada; (b) subunconformity-epimetamorphic deposits: Beaverlodge (Ace-Fay-Verna mines), Canada; and perhaps a precursor type to the Alligator Rivers deposits, Australia. Other veinlike type deposits of this period are in the Singhbhum Thrust Belt, India, and at Krivoy Rog, Ukraine.

Generation three (Middle Proterozoic, 1500 to 900 m.y. ago)

During the middle and late Middle Proterozoic deposits of the *unconformity-contact* type (type 1) developed. They formed either by polygenetic evolution, including supergene preconcentration of uranium after a climate change from tropical humid to arid, followed by diagenetic-hydrothermal concentration of uranium to final deposit size after burial by sandstone, or alternatively by diagenesis-related hydrothermal processes alone. Similar diagenetic processes affected buried subunconformity-epimetamorphic deposits (type 2), generating a second generation of redistributed uranium. Where the redistributed uranium was reconcentrated immediately below the early Middle Proterozoic unconformity as in the Alligator Rivers area and locally in the Beaverlodge region the impression may arise of an original unconformity-related deposit.

Examples for type 1 deposits: Athabasca region (Cigar Lake, Key Lake etc.), Canada; for redistributed mineralizations in type 2: Ranger, Alligator Rivers, Australia, and Bolger, Beaverlodge, Canada. Other types of deposits of this time interval are *intrusive* varieties formed in mobile belts. They include the *pegmatite* deposits (subtype 9.5) of the Bancroft district, Canada, and the *peralkaline syenite* occurrence (subtype 9.4) of Kvanefjeld/Illimaussaq, Greenland.

Generation four (Upper Proterozoic, 700 to 500 m.y. ago)

Deposits of generation four appear to be restricted to orogenic belts and include *vein* (subtype 3.2) and *intrusive* (subtype 9.1) deposits. They are found in the Damara – Katanga Orogen (part of the Pan-African Orogeny) in Shaba, Zaïre, and in Namibia respectively, and in the Brazilian mobile belt, Brazil. The uraniferous *alaskites* of Rössing, Namibia, are interpreted as anatectic differentiates derived from uranium-bearing feldspar-rich clastic sediments of older units.

The origin of the *katathermal vein* deposits of Shaba is not yet resolved. One hypothesis assumes the derivation from an unknown granitic pluton, another speculates on the partly uraniferous sediments as found, for example, in the

"Série des Mines" as a source of the uranium mobilized during the Pan-African Orogeny and redeposited in favorable structural traps.

Metallogenetically this fourth generation is, in a limited sense, comparable to the Beaverlodge-Alligator Rivers (Ranger) deposits of the second generation, except that deposit formation seems to have been more synorogenic and in response to higher grade metamorphic processes of the palingenetic-anatectic phase. In a "closed system" these processes formed intrusive alaskite deposits and led in an "open system" to locally distinct mobilization and transportation of U and other metals, such as Co, Ni, etc., into higher levels resulting in vein deposits.

Examples: Shinkolobwe, Shaba, Zaïre; Mindola, Sambia; Rössing, Namibia; Lagõa Real, Itatia, Espinharas, Brazil.

Generation five [(Cambrian) Devonian to Recent, (500) 400 to 0 m.y. ago]

With the onset of the Phanerozoic, uranium metallogenesis changed to the formation of other types of deposits partly associated with the evolution of continental plant life.

In Proterozoic times more or less synsedimentary and structurally controlled deposits prevailed. During the Phanerozoic era, *epigenetic sandstone* deposits (type 4), *surficial deposits* (type 6) and, in orogenic belts, *vein* and some *unconformity – related* deposits (type 3 and 1 respectively), and to a lesser extent *volcanic* type deposits (type 11) became prominent.

Granite-related vein deposits are in Europe typical for the Hercynian (=Variscan) Orogen where they are associated with highly differentiated, late granites (330 to 300 m.y. old), which occur in or adjacent to Precambrian complexes. No economic uranium deposit of this type has been found in the Caledonian and Alpidic orogens in Eurasia. The resource potential of Elsonian, Appalachian and Laramide orogens in America is undetermined. A few deposits of the volcanic type have been discovered in the West American Cordillera. These mineralizations are associated with rhyolitic extrusives and volcaniclastics.

Epigenetic *sandstone* deposits are commonly relatively uniform with respect to host rock, geotectonic-morphologic position and metallogenesis. Their main genetic and ore-controlling parameters are (a) continental clastic sediments, often containing carbonaceous material, with changing redox conditions along chemical fronts or zones and (b) proximity to uranium source rocks which are predominently Upper Archean-Lower Proterozoic and, to a lesser extent, Upper Proterozoic and Hercynian granites and/or metasediments of pelitic to psammitic origin.

Rocks of the above-mentioned provenances and similar lithochemical character are found worldwide, whereas epigenetic uranium deposits of the sandstone type are of restricted distribution. Obviously, additional parameters and processes are necessary to concentrate uranium in economic quantities in these sandstones. Certain climatic conditions appear to be an important prerequisite, in particular periods of arid to semi-arid climates preceded by a tropical humid climate.

Examples: A time-related subdivision of generation five deposits displays the following distribution of selected type examples during the Phanerozoic (number of type, subtype, class referring to Chap. 4 are in brackets).

Early Paleozoic (500 to 320 m.y. ago): (a) black or alum shales (15): Ranstad, Sweden; Ronneburg, Germany; Tien-Shan and Altai Mountains, CIS; (b) alkaline granite/albitite (12): Ross Adams, USA.

Permo-Carboniferous (300 to 250 m.y. ago): (a) veins (3.1) associated with the Hercynian Orogeny in Europe: Massif Central and Vendée, France; Erzgebirge-Bohemian Massif, ČSFR – Germany; (b) sandstone (4): Lodève Basin, France; Sierra Pintada, Argentina; Agades Basin, Niger; Ngalia and Amadeus basins, Australia; (c) phosphorite (10.1): Idaho, USA.

Triassic-Jurassic (250 to 150 m.y. ago): tabular sandstone: Colorado Plateau, USA.

Cretaceous-Tertiary (100 to 5 m.y. ago): (a) rollfront sandstone (4.2): Wyoming Basins and South Texas Coastal Plains, USA; North Bohemian Basin, ČSFR; Königstein, Germany; (b) intrusive, carbonatite (9.3): Phalaborwa, South Africa; alkaline (9.4): Poços de Caldas, Brazil; (c) phosphorite (10.2): Florida, USA; Bakouma, CAR.

Tertiary-Recent: (a) surficial duricrust (6.1): Yilgarn Block, Australia; Namib Desert, Namibia; Mudugh, Somalia; (b) surficial organic (6.2): Stevens County, USA.

In summary, the various types of uranium deposits reveal a distinct direct or indirect affinity to certain geochronological intervals in earth history. While the Upper Archean-Lower

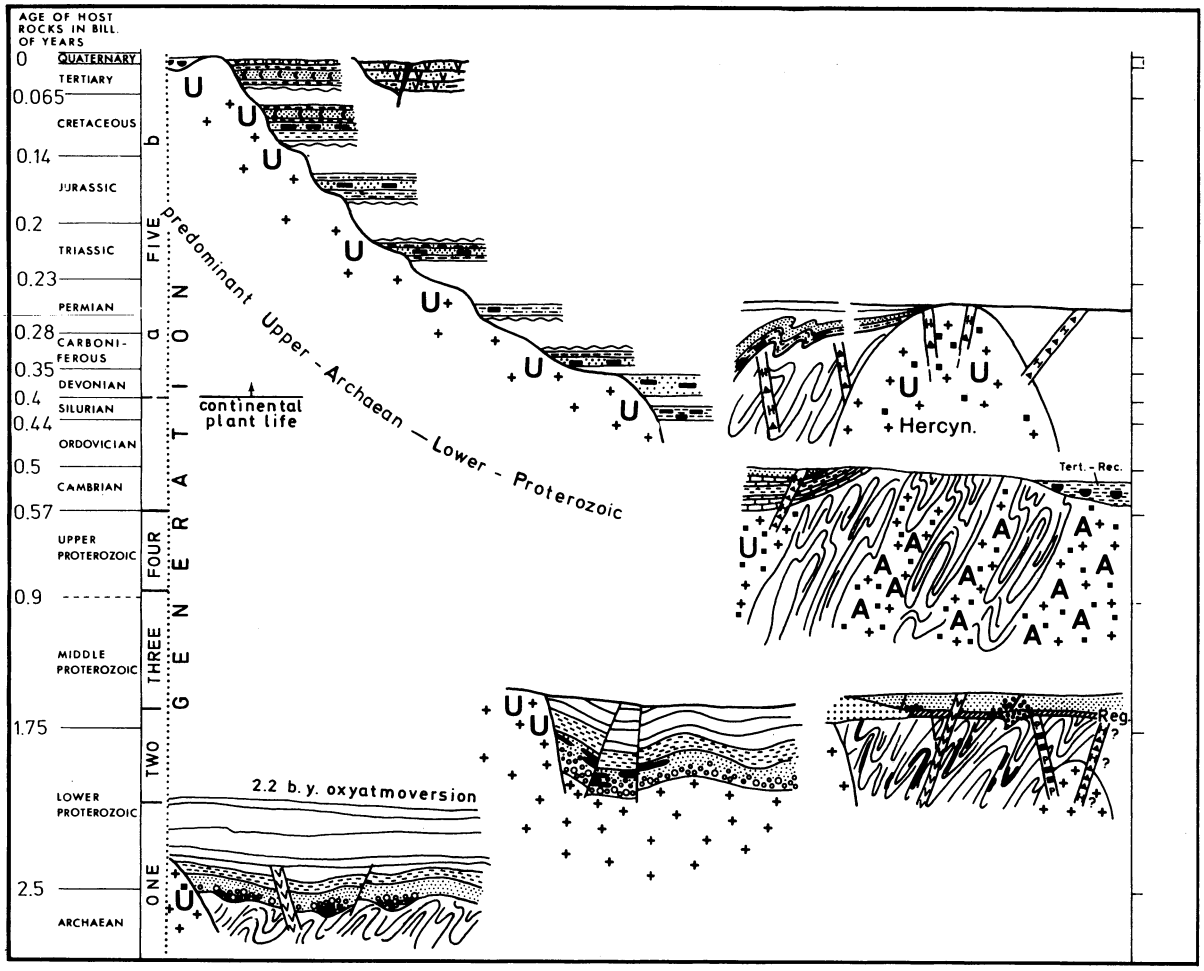

Fig. 3.7. Schematic diagram of geochronologic distribution and deposit generations of major uranium deposits. For legend see Fig. 3.2

Proterozoic is favored by deposits of the quartz-pebble conglomerate type, the subunconformity-epimetamorphic deposits prevail in the early Middle Proterozoic and unconformity-contact deposits in the middle to late Middle Proterozoic. Granite-related veins demonstrate a preference for the Hercynian. The position of the unconformity-epimetamorphic and vein deposits, however, may not be so much a time-bound restriction as a style of orogeny/metamorphism-related phenomenon.

Furthermore, certain uraniferous granites or granite-related intrusives and extrusives and metasediments of the mentioned geological time intervals represent prime uranium source rocks. Terrestrial sediments, especially of Phanerozoic age, enveloping these source terranes offer optimum locations for the formation of sandstone and surficial type deposits. However, provenance and time stratigraphic position of favorable host rocks in conjunction with fertile source rocks do not provide, on their own, the necessary metallogenetic environment and processes to produce substantial ore bodies. Epigenetic non-magmatic and non-metamorphic uranium deposits originated only in regions where distinct climatic conditions generated and controlled surface and groundwater regimes and thereby the qualitative and quantitative mobilization, range of transport, and concentration of the uranium. Where uraniferous (meta)-sediments have been incorporated into magmatic/anatectic processes, recycling of the uranium could result in vein or intra-intrusive types of deposits.

Selected References and Further Reading for Chapter 3.2

(for details of publication see Bibliography)

Anhaeusser 1973; Barbier 1974; Bowie 1979; Dahlkamp 1977, 1980; Ferguson 1987, 1988; Fiebiger 1976; Grandstaff 1973; Morosenko 1965; Robertson 1974; Robertson et al. 1978; Schidlowski 1976; Schidlowski et al. 1975; Seyfert and Sirkin 1973; Simov 1979; Toens 1981; Toens and Andrews-Speed 1984; Toens et al. 1985; Yevstrakhin 1967

4 Typology of Uranium Deposits

A number of global and regional classifications of uranium deposits have been proposed in the past by Heinrich (1958), Ruzicka (1971), Ziegler (1974), Kazansky and Laverov (1977), Mickle and Mathews (1978), Mathews et al. (1979), Dahlkamp (1980), Nash et al. (1981), Barthel et al. (1986), and others. Although they remain in principle valid, recently published descriptions of uranium deposits discovered during the past exploration boom, and new research data on earlier established and defined types of uranium deposits justify a rearrangement and refinement of the classification scheme. Many open questions still exist with respect to specific provenance of the ore forming uranium and solutions, the conditions of uranium mobilization, transport and redeposition, and repetitive redistribution in many cases. Therefore a classification scheme based purely on metallogenetic criteria does not appear feasible. Instead, for all practical purposes, a typology based more on descriptive data has been given preference here.

The principal recognition criteria used for the identification and definition of the individual types and subtypes of deposits include particularly lithologic and structural relationships, alteration, mineralogy, paragenesis, age constraints, and spatial geotectonic distribution of deposits. According to the chosen system, the terminology selected for types and subtypes refers primarily to the geotectonic setting or host environment of the discussed type.

On this basis sixteen principal types of uranium deposits are distinguished. They include almost forty subtypes and classes. All classes have certain principal parameters in common permitting their attribution to a specific type, but they also exhibit distinctive features justifying an individual status.

Each type is introduced by a type *Definition*, followed by *Principal Recognition Criteria* and *Metallogenetic Aspects* before presenting characteristics of subtypes. Inevitably, this kind of organization involves overlap and repetition, which is considered minor in order to achieve a better type- and subtype-related comprehension and precision and avoidance of confusion.

Complementing the selected type examples, a list of examples is added. The attribution of these examples is in many cases only tentative and the example may belong to another type, subtype or class than listed, or it may have characteristics of several subtypes or classes.

The description also includes selected references though not exclusively of authors who either reviewed comprehensively the given type of deposit or districts thereof and list extensive bibliographies for further reference, or of authors describing in detail a specific deposit taken as type example.

Those types of generally subeconomic order which are not complemented by a detailed deposit/district description in Chapter 5 are more extensively reviewed here to provide sufficient background for their understanding.

Cartoons (Figs. 4.1 to 4.15) are added to furnish a schematized presentation of the geological setting of the various types, subtypes, and classes of deposits.

Division and numbering of the presented typology corresponds to that of Table 1.1, which gives an overview and economic ranking of the types of deposits.

Table 4.1 summarizes the significant geological recognition criteria of the various types, subtypes, and classes of deposits.

4.1 Type 1: Unconformity-Contact

(Fig. 4.1)

Definition

Unconformity-contact deposits are associated with and occur immediately below and above an unconformable contact that separates a crystalline basement intensely altered by lateritic weathering from overlying clastic red bed type sediments of either Proterozoic or Phanerozoic age.

The unconformity-contact type includes the following subtypes and classes:

Table 4.1. Classification and principal geological recognition criteria of principal types of uranium deposits and occurrences (for location of type examples of deposits see Fig. 1.1)

Type Subtype	Class	Principal Recognition Criteria	Type Example	Selected References
1. Unconformity-contact *1.1 Proterozoic unconformity* *1.2 Phanerozoic unconformity (see text)*		Lower Proterozoic metasediments mantling Archean domes, overlain by Middle Proterozoic red bed sandstones, strong unconformity related alteration of metasediments and sandstone. Some small deposits associated with Phanerozoic unconformities		Dahlkamp and Adams 1981; Fogwill 1985; IAEA/Ferguson (ed.) 1984; Lainé et al. (eds.) 1985; Sibbald and Petruk (eds.) 1985; Sibbald 1988; Tremblay 1982
	1.1.1 Fracture-bound in altered metasediments immediately below unconformity	U disseminated to massive in structures within Lower Prot. metasediments containing graphitic horizons, vertical extension commonly less than 200 m below unconformity; ore often extends along fractures into overlying Middle Prot. sdst.; medium rarely very high grade; med. to large reserves, dominantly monometallic	Athabasca Basin, Rabbit Lake, Eagle Point, Canada	Heine 1986; Eldorado Resources Ltd 1987
	1.1.2 Clay-bound upon unconformity	U disseminated to often massive in tabular to lenticular horizontal ore bodies in clay and argillic sandstone of (mixed) pedogenic and/or early Athabasca diagenetic origin, resting on Lower Prot. metasediments; very high grade (>1% U_3O_8), large reserves, commonly polymetallic	Ath. Bas., Cigar Lake, Key Lake, Canada	Fouques et al. 1988; Ruhrmann 1986
2. Subunconformity-epimetamorphic		Deposits occur in same environment as subtype 1.1 but under early Middle Prot. unconformity, and basement shows only mild to moderate paleoweathering; type 2 deposits may be transitional into class 1.1.1		Dahlkamp and Adams 1981; Ferguson and Goleby (eds.) 1980; IAEA/ Ferguson (ed.) 1984; Needham et al. 1988
Metasediments *2.1 not albitized* *2.2 albitized*		U as fracture and breccia filling within distinct Lower Prot. metased. horizons, ± peneconcordant to strata attitude, strong wall rock alteration; nearby migmatitic-granitic complexes, cover by early Middle Prot. red bed sedim.; fairly continuous mineralization, med. (to high grade); often large reserves; all large deposits are monometallic, some small deposits polymetallic	Ex. 2.1 Alligator Rivers, Ranger, Australia Ex 2.2 Beaverlodge, Fay-Verna, Canada	Ewers and Ferguson 1980; Hegge et al. 1980 Beck 1986; Tremblay 1978
3. Vein		Vein deposits consist of U lodes in fractures, breccias, stockworks and occur spatially related or unrelated to a granitic pluton		IAEA/Fuchs (ed.) 1986; Kolektiv 1984; Poty et al. 1986; Rich et al. 1977

3.1 Granite-related		Granite-related veins occur inside or outside of late magmatically or autometamorphically altered peraluminous leucogranite; only restricted wall rock alteration; mostly discontinuous mineralization; low to high grade, small to medium reserves		
	3.1.1 Intragranitic (Limousin type) – in leucogranite	Veins, networks, stockworks of limited vertical extension within a 300 m segment below intrusion contact	Massif Central, Fanay/ Limousin, France	Leroy 1978a, 1978b
	– in episyenite	Open space filling in irregular pipe-like episyenite within leucogranite, often grading into veins in surrounding granite	Massif Central, Pierres Plantées, Margeride, France	Cariou 1964 Leroy and Cathelineau 1982
	3.1.2 Perigranitic			
	3.1.2.1 in (meta) sediments Monometallic (Bohemian type)	Veins, networks, stockworks in (meta-) sedimentary mantle rocks, extensive vertical persistence in Bohemian type (<2000 m); low to high grade, low to high reserves	Bohemian Massif, Příbram, ČSFR	Petroš et al. 1986
	3.1.2.2 in (meta) sediments Polymetallic (Jachymov type)	As above but U associated with Ag, Co, Ni, Bi, or Cu, Mo or other metals in noteworthy amounts	Erzgebirge, Jáchymov, ČSFR	Kominek and Veselý 1986
	3.1.2.3 in contact-metamorphics (Iberian type)	Disseminations and fracture fillings along shear and breccia zones in contact-metamorphic aureole	Iberian Meseta, Alto Alentejo, Portugal	Basham and Matos Dias 1986
3.2 Not granite-related		Not granite-related veins do not display any apparent link to granitic intrusions but occur in rocks within orogenic belts		
	3.2.1 Metasediment-hosted 3.2.2 Sediment-hosted	U as veins, stockworks discordant to strata but ore may spatially be restricted to sections within distinct strata (or to overprinted unconformities), restricted wall rock alteration; low to high grade, small to large reserves	Ex. 3.2.1 Schwartzwalder, USA Labe Lineament, ČSFR Ex. 3.2.2 Shinkolobwe, Zaire	Wallace 1986 Kolektiv 1984 Derriks and Vaes 1956
4. Sandstone		U as disseminations in dominantly continental fluvial (less commonly marginal marine) arkosic sandstone commonly interbedded with argillaceous horizons, and almost flat-lying (<5°) unless post-ore tilted. Frequently associated with tuffaceous sediments. A distinction is made between (a) Phanerozoic (post-Devonian) deposits associated with terrestrial plant derived organics and (b) Proterozoic deposits associated with marine derived organics		Crawley 1983; Grutt 1972; IAEA/Finch (ed.) 1985; Rackley 1976

Table 4.1. *Continued*

Type Subtype	Class	Principal Recognition Criteria	Type Example	Selected References
4.1 Tabular/ peneconcordant		Mineralization occurs generally in tabular zones of uranium matrix impregnations that are peneconcordant to but also crosscut sandstone bedding. The zones are irregular in shape up to several meters thick and are bounded on all sides by pyrite-bearing sandstone		
	4.1.1 Extrinsic carbon (Grants type)	U associated with redistributed carbonaceous matter (e.g., humate) disseminated in lenses within continental sandstone. The host sandstone has deposited in a mid-fan environment within an extensive fluvial-lacustrine sedimentary system. Moderate quantities of volcaniclastics are present. Sand-shale proportions are typically 60–80% sandstone. Alteration includes destruction of ilmenite-magnetite and significant pyritization. Feldspar is moderately to strongly altered; large reserves, medium grade	Grants Uranium Region, USA	Adams and Saucier 1981; Granger and Finch 1988; Turner-Peterson et al. (ed.) 1986
	4.1.2 Vanadium-uranium (Salt Wash type)	U associated with vanadium (V > U) within fluvial sandstone. Associated sediments are of continental origin "red-bed" type with thin but widespread units of reduced sandstone with interbeds of grey clay and carbonaceous debris. Most favourable sandstone parallels an adjacent contact of red oxidized sandstone and is overlain, underlain or interbedded with grey lacustrine clays. Altered, reduced sediments show ilmenite and magnetite destruction and significant concentrations of pyrite; small to medium reserves, low to high grade	Colorado Plat., Uravan Mineral Belt, USA	Thamm et al. 1981
	4.1.3 Basal channel (Chinle type)	U associated with plant fragments in basal part of fluvial channel. Deposits may occur in (a) distinct fluvial channels or (b) extensive blanket sands formed in braided fluvial systems that either unconformably overly or are eroded into unterlying sedimentary or crystalline rocks; mostly small reserves, low to medium grade	Colorado Plat., Monument Valley, USA Ningyo-Toge, Japan	Chenoweth and Malan 1973; Katayama et al. 1974
4.2 Rollfront (or Roll-type)		Mineralization occurs in arcuate zones of uranium matrix-impregnations that crosscut sandstone bedding. Zones extend from overlying to underlying less-permeable horizons. Zones are convex down hydrologic gradient and elongate and sinuous perpendicular to hydrologic gradient. Contacts of zones are sharp with hematite and/or limonite bearing sandstone on the up-gradient side (except in rereduced sands) and diffuse with carbon and/or pyrite-bearing sandstone on the down-gradient side		

	4.2.1 Continental basin, associated with detrital carbon (Wyoming type)	U as disseminations at redox boundary at contact with detrital carbonaceous (generally plant) debris on the down-gradient side in arkosic and subarkosic sandstones deposited in intracratonic or intermontane basins in spatial proximity to rocks containing anomalous U concentrations such as tuffs or granites. Most deposits occur within interbedded sequences of fluvial sandstones and volcanic rich sediments. Alteration is variable and includes hematitic alteration or bleaching. The shape of the deposit is strongly controlled by the hydrology of the host rocks. Some deposits have long tabular rollfront limbs against overlying and/or underlying carbonaceous-rich sediments; small to large reserves, medium grades	Wyoming Basins, USA Lake Frome Emb., Beverley, Australia	Crew 1981; Harshmann and Adams 1981
	4.2.2 Marginal marine, associated with extrinsic sulfide (South Texas type)	U is concentrated in roll-type deposits near faults and in contact with pyrite/marcasite bearing sandstone on their down-gradient side. Sandstone on the up-gradient side of deposits is hematite and/or limonite bearing except for some deposits which occur totally within reduced, pyrite bearing sandstone which probably reflects the post-ore introduction of H_2S along faults. H_2S introduced before ore formation prepared the host for rollfront development. Host environments include point bars, lateral bars and crevasse splays deposited in a fluvial environment and barrier bars and offshore bars in a marine environment; small to medium reserves, low to medium grades	South Texas Coastal Plains, USA Crow Butte (Wyoming Basins) USA	Adams and Smith 1981; Galloway 1985
4.3 Tectonic-lithologic		U (re)distributed into faults cutting through mineralized sandstone and permeating tongue-like into permeable sand horizons	Grants, USA Franceville Basin, Gabon	Diouly-Osso and Chauvet 1979; Gauthier-Lafaye et al. 1980
5. Collapse breccia Pipe		Circular collapse structure cutting through flatlying strata including permeable sandstone horizons. Pipes are filled with breccia fragments and matrix. U occurs predominantly as matrix impregnations and in annular ring structures; small reserves, high grade	Arizona Strip, USA	GSA/Wenrich and Billingsley (eds.) 1986; Wenrich and Sutphin 1987
6. Surficial		U almost exclusively as uranyl minerals as disseminations, void filling, coating, or adsorbed on host constituents (organics, clay, etc.) in surficial depressions, dissolution caverns, at near-surface fractures, joints within or near uraniferous source rocks		Carlisle 1983; IAEA Toens (ed.) 1984
6.1 Duricrust (nonpedogenic)	6.1.1 Valley fill	Fluvial valley fill cemented by nonpedogenic calcrete, silcrete, gypcrete of recent age in arid region, often incised into granitic basement, U principally as uranyl minerals or adsorbed; small to med., exceptionally large resources mostly low grade	Yilgarn/Yeelirrie, Australia Namib Desert, Langer Heinrich, Namibia	Cameron 1984; Butt et al. 1984; Hambleton-Jones 1984; Mann and Deutcher 1978

Table 4.1. *Continued*

Type Subtype	Class	Principal Recognition Criteria	Type Example	Selected References
	6.1.2. Lacustrine or playa	Similar to above but assoc. with shallow lake sediments; small resources, low grade	Yilgarn/Lake Maitland, Australia	Cavaney 1984
6.2 Peat and Bog		Organic-rich sediments/swamps, bogs filling shallow depressions, valleys; organic material often composed of sphagnum peat, U adsorbed on orgainc matter; small reserves, low grade	Stevens County, Washington, USA	Johnson et al. 1987
6.3 Karst cavern		Floor cover in caverns within limestone, dolomite by uranyl minerals; small reserves, low to med. grade	Pryor Mtns., USA	Bell 1983
6.4 Surficial Pedogenic and Structure Fill		U as dissemination, coating, filling of near surface permeable cataclastic zones (shears, fissures, joints) in igneous, metamorphic, sedimentary rocks, and soils, can be be found associated with all deposit types in and near their outcropping parts; small resources, low grade	Daybreak, USA	US-AEC 1959
7. Quartz-pebble Conglomerate		U as disseminations in fluvial to deltaic oligomictic, pyritic quartz-pebble conglomerate, typically trough cross-bedded, of lowermost Proterozoic age on or peripheral to Archean shields. 2.2 to 2.7 M.Y. appears to be the most favorable age. Generally low grade, but large reserves		Button and Adams 1981 Pretorius 1981; IAEA/Pretorius(ed.) 1987;
7.1 U-dominant with REE	Basal conglomeratic beds in single stratigraphic unit	U mineralization concentrated in the basal section of a clastic sequence	Blind River – Elliot Lake Lake, Canada	Robertson 1989; Ruzicka 1988;
7.2 Au > U dominant	Conglomerate beds in multi-stratigraphic units	Au > U mineralization concentrated in several successive conglomeratic horizons, commonly only few cm to some ten cm thick with partly redistributed ore; U is by-product of Au production	Witwatersrand, S. Africa	Hallbauer 1986; Pretorius 1976; Anhaeuser and Maske (eds.) 1986
8. Breccia Complex		Matrix-poor bedded granite breccia and matrix-rich polymict breccias mineralized with Cu, Au, Ag, REE and U ore minerals as disseminations and fracture and void fillings; low grade, large U reserves, U is by-product	Olympic Dam, Australia	Roberts and Hudson 1984; Roberts 1988
9. Intrusive		U disseminations, distributed regularly in mostly unaltered acidic or alkaline massive magmatic or anatectic intrusion; commonly very low grade but large resources in 9.1		
9.1 Alaskite		As above, in anatectic alaskite	Rössing, Namibia	Berning 1986; Berning et al. 1976; Brynard and Andreoli 1988

9.2 Granite, monzonite		As above, in granite or monzonite/copper porphyry	Bingham, USA	John 1978; Lanier 1978
9.3 Carbonatite		As above in carbonatite, associated with REE	Phalaborwa, S. Africa	Camisani-Calzolari et al. 1985; IAEA 1986a
9.4 Peralkaline syenite		As above, in alkaline intrusion	Kvanefjeld, Greaniand	Sørensen et al. 1974
9.5 Pegmatite		U as mainly uraninite in pockets and lenses, host rocks of similar origin as acidic magmatic stocks, but U distribution very erratic/limited in extension & resource; grade highly variable, generally low	Madawaska/Bancroft, Canada	Alexander 1986
10. Phosphorite		Syngenetic U in phosphatic sediments; large resources, very low grade, U is byproduct		Heinrich 1958
10.1 Phophoria		Oolitic marine phosphate beds	Idaho, USA	McKelvey et al. 1956
10.2 Land-Pebble (Florida type)		Uraniferous apatite within land-pebble phosphatic sandstone	Florida, USA	Altschuler et al. 1958
11. Volcanic		Felsic to intermediate volcanics mainly of rhyolitic composition and high U background; low grade and small resources		Chen Zhaobo 1981; Goodell and Waters 1981; IAEA 1985
11.1 Structure-bound	11.1.1 Intrusive vein in rhyolite intrusion	U as veins and fracture fillings associted with ring dike intrusions or resurgent domes	McDermitt, Moonlight USA Peña Blanca, Nopal I, Mexico	Dayvault et al. 1985; George-Aniel et al. 1985; Leroy et al. 1987
	11.1.2 Surficial fracture fill	U as disseminations in surface-near fractures and breccias	Cotaje; Bolivia	Leroy et al. 1985; Pardo-Leyton 1985
11.2 Strata-bound	11.2.1 Intracaldera	U as disseminations in volcaniclastic and lake bed (moat) facies	McDermitt, Aurora-Cottonwood, USA	Dayvault et al. 1985
	11.2.2 Exocaldera	U as disseminations in outflow volcaniclastics and lacustrine facies	Peña Blanca, Margaritas, Mexico Date Creek Basin, USA	Goodell 1985; Sherborne et al. 1979
12 Metasomatite *12.1 Metasomatized granite* *12.2 Metasomatized metasediments*		U as fissure filling, partially to totally Na-metasomatized (albitite) granitic and adjacent country rocks (albitization, Na-amphibole/pyroxen formation); mostly small resources, low to med. grade	Krivoj Rog, Ukraine, Ross Adams, Alaska, USA Espinharas, Brazil	Belevtsev et al. 1984; Fritsche 1988; Collot 1981; Fuchs et al. 1981; Kazansky and Laverov 1977; Mineeva 1984
13. Synmetamorphic		U as dissemination, (pene-)concordant to metamorphosed strata, minor to no alteration; commonly low to med. grade, small resources Dominantly (semi-)mafic metasediments with graphitic interbeds and in mixed sedimentary/volcanigenic rocks	Forstau, Austria	Dahlkamp and Scivetti 1981

Table 4.1. *Continued*

Type Subtype	Class	Principal Recognition Criteria	Type Example	Selected References
14. Lignite		Syn- epigenetic U in lignites often associated with adjacent tuffaceous sediments		Kolektiv 1984
14.1 Stratiform		U disseminations (mostly adsorbed) regularly through lignite sedm.; small to med. resources very low grade	Williston Basin, USA	Denson and Gill 1965
14.2 Fracture/Joint Fill		U filling fractures, joints within lignite seams underlying uraniferous strata (rhyolitic volcaniclastics, sandstones); small resources, low to medium (locally) grade	Williston Basin, USA	Denson and Gill 1965
15. Black Shale		Syngenetic U uniformly distributed in marine black shale. Sometimes with bentonite interbeds		Bell 1978
15.1 Bituminous sapropelic		U disseminations regularly distributed ubiquitously throughout black shale beds; large resources, very low grade	Chattanooga, USA	Mutschler et al. 1976
15.2 Humic/Kolm		As above but higher in grade in alum shale/kolm; med. to large resources	Ranstad, Sweden	Carlsson and Nojd 1977

Deposit size: small reserves = <5000 mt U308
medium –"– = 5000–20 000 mt U308
large –"– = >20 000 mt U308

Ore grades: low grade = <0.15% U308
med. –"– = 0.15% –0.5% U308
high –"– = >0.5% U308

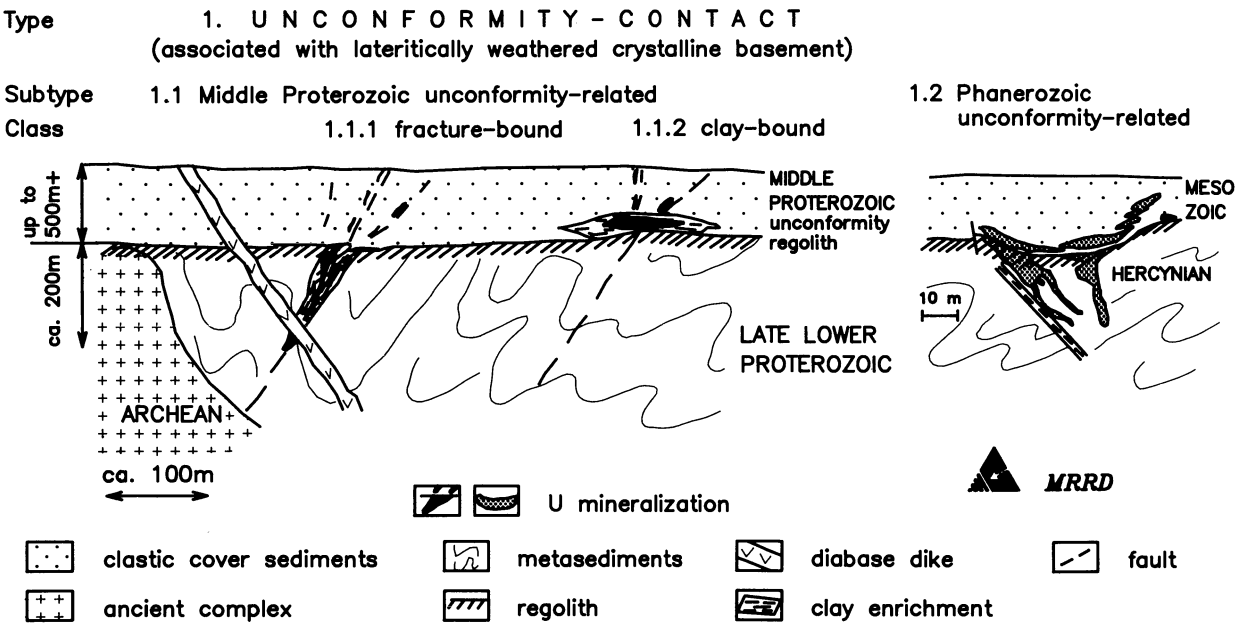

Fig. 4.1

Subtype 1.1: Proterozoic unconformity related

Class 1.1.1: Fracture-bound
Type Example: Rabbit Lake, Eagle Point, Athabasca Basin, Canada

Class 1.1.2: Clay-bound
Type Example: Cigar Lake, Athabasca Basin, Canada

Subtype 1.2: Phanerozoic unconformity related
Type Example: Bertholène, Aveyron, France

References: Dahlkamp and Adams 1981; Evans (ed.) 1986; Fogwill 1985; IAEA/Ferguson (ed.) 1984; Lainé et al. (eds.) 1985; Sibbald and Petruck (eds.) 1985; Tremblay 1982

The two classes of Proterozoic unconformity-contact deposits are defined by their setting with respect to the unconformity, host rock, paragenesis, and ore grade. *Fracture-bound deposits* (class 1.1.1) occur in metasediments immediately below the unconformity. Mineralization is commonly monometallic and of medium grade (0.3–1% U_3O_8). *Clay-bound deposits* (class 1.1.2) occur associated with clay at the base of the sedimentary cover directly above the unconformity. Mineralization is commonly polymetallic (U + Ni + Co + As) and associated with bitumen and of high to very high grade (1–14% U_3O_8). Principal uranium phases in both classes are pitchblende and uraninite.

Phanerozoic unconformity-contact deposits are of similar setting as Middle Proterozoic deposits but are small and of low grade.

Principal Recognition Criteria

Host Environment

- Basement is similar to type 2 subunconformity-epimetamorphic deposits and consists of middle to upper Lower Proterozoic metasediments including graphitic horizons and strata with elevated U content surrounding Archean granitic domes, cut by various pegmatites
- Cover of middle Middle Proterozoic continental red bed facies sandstone (Athabasca Group ca. 1500 m.y.) above markedly weathered crystalline rocks below an unconformity
- Diabase dikes, and sills cutting both basement and cover
- Ancient lineaments and mylonite zones in basement
- Tensional repeatedly reactivated structures in the basement with extensions into the sandstone

Alteration

- Intense regional paleoweathering of basement

- Intense alteration halos around deposits in basement and sandstone

Mineralization

- U present dominantly as pitchblende or uraninite in disseminated to often massive accumulations
- Mineralization of class 1.1.1 mostly monometallic, of class 1.1.2 polymetallic
- Mostly sharp ore-waste boundaries
- Redistribution of uranium and sulfides into fractures in the sandstone within the alteration halo above the deposits

Age Constraints

- Formation of major deposits of subtype 1.1 tends to be restricted to middle Middle Proterozoic (see following Remarks)
- U-Pb minimum ages of first generation pitchblende of Athabasca deposits: 1200 to 1400 m.y.

Metallogenetic Aspects

Processes leading to mineralization and related alteration are only partially established. The most obvious are products of diagenetic-hydrothermal activity indicating the critical role of these processes as the essential step in the formation of the deposits as they exist today. It remains unclear, however, whether or not polyphase processes have developed this type of deposit. The open question is whether (a) the diagenetic hydrotherms have also introduced the uranium (and other metals) or (b) have only finally concentrated and recrystallized (and redated) preexisting mineralization formed by supergene surficial (paleoweathering) or perhaps early diagenetic processes. A surficial type deposit (type 6) may be envisioned as a precursor stage transformed by diagenetic-hydrothermal overprinting to a Proterozoic unconformity type deposit.

Remarks

a) Middle Proterozoic unconformity deposits commonly are high-grade and have large resources constituting about one third of the western world's low-cost uranium reserves.

b) Although all large unconformity type deposits known are restricted to the above listed environment and belong to subtype 1.1, deposits of equivalent type also occur in comparable geological environments of younger age (subtype 1.2, Phanerozoic unconformity related) but are of smaller magnitude (see also Remarks in Section 4.1.2 subtype 1.2).
For more details see Chapter 5.1.

4.1.1 Subtype 1.1: Proterozoic-unconformity related

Class 1.1.1: Fracture-bound

Type Example: Rabbit Lake and Eagle Point, Saskatchewan, Canada
References: Heine 1986; Eldorado Resources Ltd. 1987

Host Rocks/Structures

Altered gneisses, schists, with intercalations of graphitic horizons, metacarbonates (dolomitic marble etc.) and calc-silicate rocks originally metamorphosed to amphibolite-granulite facies. Locally migmatites. Often abundant pegmatitic, microgranitic and/or granitic dikes or segregations (pegmatitic and granitic segregations constitute 15 to 20% of host rocks at Eagle Point). Diabase dikes. Host rocks are strongly fractured, sheared and/or brecciated along repeatedly reactivated faults including old mylonite zones. Deposits tend to occur in subsidiary structures in the hanging wall of major thrust faults.

Unmetamorphosed red bed arenites may overlie the basement.

Alteration

Three principal types of alteration are distinguished:

- early Na- and/or Mg-metasomatism (albitization, dolomitization) of the basement;
- pre-cover sandstone (Meso-Helikian in Saskatchewan) paleoweathering extending in excess of 50 m below the unconformity (hematitization, chloritization, sericitization, argillitization);
- post-sandstone early diagenetic, and later ore-related diagenetic hydrothermal alteration

overprinting the former alteration zones by illitization, chloritization, carbonatization, tourmalinization (dravite), silicification, sulfidization, destruction of graphite, and corrosion of quartz. This alteration is intensely developed within a deposit but forms only a narrow aureole around it.

Ore and Associated Minerals

Uraninite/pitchblende and alteration products thereof. Quartz and carbonates in minor amounts. Fe-chlorite, Mg-chlorite, illite-sericite, kaolinite, dravite and hematite. Base metal minerals in trace amounts. Ore and associated minerals are present in several generations.

Mode of Mineralization

Uranium minerals occur disseminated to massive and fairly continuous in moderate to steep dipping fractures and breccia zones in the basement. These zones are commonly best developed proximal below the unconformity but may extend to a depth exceeding 400 m. Mineralization may persist upward along fractures into the overlying sandstone. These deposits are commonly monometallic with moderate to high uranium grades and contain only traces of other metallic elements.

Age Constraints

Class 1.1.1 deposits are restricted to areas affected by early Middle Proterozoic orogeny (Hudsonian in Canada), followed by a warm-humid climate changing into an arid climate as reflected by lateritic paleosol (regolith) development, then succeeded by sedimentation of red bed arenites (Athabasca Group ca. 1500 m.y.). Minimum U/Pb ages of earliest uranium oxide generation are 1400 m.y. at Eagle Point (Eldorado Resources Ltd. 1987) and ca. 1280 m.y. at Rabbit Lake (Cumming and Rimsaite 1977).

Dimensions/Resources

Individual deposits may be up to 1000 m long, a few meters to several 10 m wide and several 10 m to more than 400 m deep, containing up to >50 000 mt U_3O_8 at grades ranging from 0.3 to 1.0%, rarely a few percent U_3O_8. Districts may contain up to 100 000 mt U_3O_8.

Remarks

Fracture-bound deposits of the Rabbit Lake area (Rabbit Lake, Eagle Point) display peculiar geological features resembling those of subunconformity-epimetamorphic deposits such as found in the Beaverlodge district (subtype 2.2), e.g., albitization, migmatitization, and essentially monometallic mineralization. An explanation may be that the class 1.1.1 deposits originated from preexisting Beaverlodge-type deposits by unconformity-type overprinting.

Examples of Middle Proterozoic Unconformity-contact, Class 1.1.1 Fracture-bound Deposits/Occurrences

Australia: ? Nabarlek/Alligator Rivers, Northern Territory, ? Kintyre, West Australia
Canada: Dominique-Janine, Dominique-Peter, Horseshoe, Raven/Athabasca Basin, Saskatchewan, Kiggavik/Thelon Basin, NWT
Guyana-Venezuela: Roraima region

Class 1.1.2: Clay-bound

Type Example: Cigar Lake and Key Lake, Saskatchewan, Canada
References: Fouques et al. 1986; Ruhrmann 1986

Host Rocks/Structures

Argillaceous facies (clay, mudstone, argillic sandstone), locally containing carbonaceous material (bitumen) resting along the unconformity upon paleoweathered crystalline basement. The clay is mostly concentrated at slight basement ridges and grades upwards and laterally into ubiquitously oxidized sandstone. Basement under or near overlying deposits is disturbed by faulting including ancient lineaments (mylonite zones). The clay may have originated from pedogenic or lacustrine deposits of outwashed lateritic paleosol, or from fault gouge or diagenetic alterations, or from a combination of several of these features.

Alteration

Paleoweathering, diagenetic and mineral-related alteration corresponds to that of class 1.1.1, but

the latter forms a far larger halo. In contrast to subtype 1.1.1, albitization of basement rocks is practically absent.

Ore and Associated Minerals

Uraninite/pitchblende and alteration products thereof. Al-, Mg- and Fe-chlorite, illite, kaolinite, dravite, quartz and hematite. Veinlets of quartz, carbonates, and dravite. Associated metallic minerals may include sulfides and arsenides of Ni, Co, Cu, Pb, Zn, Mo, Bi, Sb, and V, locally Te, Se, Au, Ag, and Pt-group elements, some in appreciable amounts (up to several percent). Ore and associated minerals are present in several generations.

Mode of Mineralization

U minerals occur in the clay envelop as disseminated to often massive, continuous mineralization forming linear, pipe or cigar-shaped, more or less horizontal deposits, composed of a high grade core surrounded by a lower grade halo. The deposits exhibit a rather sharp ore-wall rock boundary. Mineralization may extend along cataclastic zones higher up into sandstone and downward into the basement. These deposits consist almost always of polymetallic mineralization of high to very high grades (>1% U_3O_8). Ni is commonly the most notably enriched associated metal.

Age Constraints

Correspond to those of class 1.1.1.

Dimensions/Resources

Individual deposits are a few 10 m to ca. 1500 m long, a few meters to ca. 100 m wide and a few meters to 25 m thick, containing a few 100 to >125 000 mt U_3O_8 at grades ranging from ca. 1 to 14% U_3O_8. Districts may contain up to 200 000 mt U_3O_8 and more.

Examples of Middle Proterozoic Unconformity-contact, Class 1.1.2 Clay-Bound Deposits/ Occurrences

Canada: Cluff Lake "D", Collins Bay, Dawn Lake, Maurice Bay, Midwest, McClean, P2-North/Athabasca Basin, Saskatchewan

4.1.2 Subtype 1.2: Phanerozoic unconformity-related

Type Example: Bertholène and Le Roube/ Brousse Broquies, Aveyron, France
References: Schmitt et al. 1984; George 1985

Host Rocks/Structures

Permo-Carboniferous clastic sediments with some volcanic components resting along the post-Hercynian unconformity on altered Upper Proterozoic to Lower Paleozoic schists and gneisses containing minor graphitic horizons. Faults transect basement and sediments. Redox conditions in the cover sediments are variable.

Alteration

Two types of alteration are distinguished:

- pre-mineralization: albitization, Fe-chloritization, sideritization;
- syn- to post-mineralization: silicification, argillitization (smectite, illite, minor kaolinite), carbonatization, pyritization, hematitization.

Ore and Associated Minerals

Coffinite, minor pitchblende and tetragonal α-U_3O_7, and alteration products thereof (uranyl vanadates).

Gangue or similar minerals: Illite, smectite, dolomite, calcite, siderite.

Metallic minerals: Pyrite, minor marcasite, galena, sphalerite, hematite replacing pyrite.

Mode of Mineralization

U minerals occur as disseminations and fine veinlets forming small ore bodies. The ore bodies straddle along the post-Hercynian unconformity most commonly where the unconformity is transected by faults. Mineralization occurs either in the basement (Bertholène) or cover sandstone (Bennac) or in both (Le Roube).

Age Constraints

Mineralization in the type examples formed in Jurassic time, contemporaneously with intrusion of basic dikes and approximately time-equivalent to global tectonics marked by the incipient stage of the opening of the North Atlantic ocean.

Dimensions/Resources

Individual deposits may be up to 1000 m long, a few meters to 50 m wide and may extend up to ca. 30 m above and ca. 30 m below the unconformity. Resources are a few tens to ca. 2000 mt U_3O_8 at (average) grades of 0.1 to 0.15% U_3O_8.

Remarks

Differences between subtype 1.1 deposits in Saskatchewan and those of subtype 1.2 in Aveyron, France include (a) well-developed albitization in Aveyron attributed to diagenesis of cover sediments. Albitization is practically absent in class 1.1.2 deposits in Saskatchewan. (b) Clay minerals associated with mineralization are dominently illite and smectite in Aveyron, and illite and Al-, Mg-chlorite in Saskatchewan. (c) Metal association is more simple in Aveyron than in Saskatchewan. (d) Cover sediments have contrasting redox environments in Aveyron, whereas those in Saskatchewan are uniformly oxidized. (e) Graphite horizons are of only minor importance in Aveyron. (Pagel 1989).

4.2 Type 2: Subunconformity-Epimetamorphic (Fig. 4.2)

Definition

Subunconformity-epimetamorphic deposits are strata-structure-bound in metasediments below an unconformity on which clastic sediments rest. Type example deposits occur below an early Middle Proterozoic unconformity that is overlain by early Middle Proterozoic clastic sediments and volcanics.

Deposits consist of peneconcordant lenses or tabular mineralizations emplaced in fractures and breccias within distinct stratigraphic units. Host strata are predominantly pelitic (subtype 2.2 or carbonatic (2.1) sediments with intercalated carbonaceous horizons of late Lower Proterozoic age metamorphosed to amphibolite grade facies and superimposed by retrograde (greenschist) metamorphism. Granitic-migmatitic complexes occur discordantly in the metasediments. Paleoweathering of the crystalline rocks was only mild (in contrast to areas of "unconformity-contact"

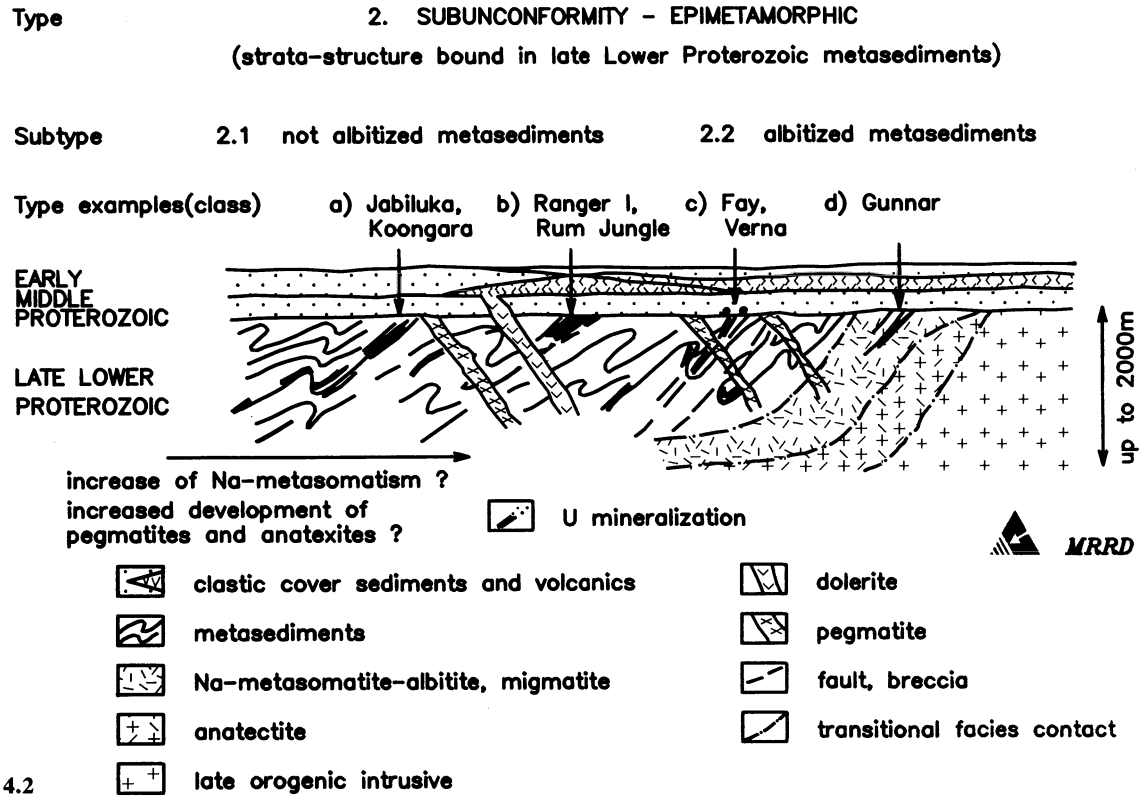

Fig. 4.2

deposits). Principal uranium phases are pitchblende and uraninite. Intense and extensive host rock alteration surrounds mineralization.

Two settings of mineralization are recognized on the base of Na-metasomatism of the host metasediments and other features:

Subtype 2.1: not albitized metasediments

Type Example: a) Jabiluka, Koongara,
b) Ranger,
Alligator Rivers district, Australia

Subtype 2.2: albitized metasediments

Type Example: c) Fay-Verna,
d) Gunnar,
Beaverlodge district, Canada

References: Beck 1986; Dahlkamp and Adams 1981; Ferguson and Goleby (eds.) 1980; IAEA/Ferguson (ed.) 1984; Needham et al. 1988; Tremblay 1978

a), b), c), and d) refer to type examples shown in Fig. 4.2.

Subtype 2.1 does not display albitization but extensive Mg-, Li-, and B-metasomatism of both host metasediments and overlying sediments. Subtype 2.2 exhibits albitization of host rocks partly of high intensity up to albitite formation and also shows a stronger structural control and contains relative abundant gangue minerals as compared to subtype 2.1.

Principal Recognition Criteria

Host Environment

- Orogenic belts
- Metasediments (schist, gneiss) with interbedded graphitic horizons of pelitic and psammitic eugeosynclinal or lacustrine origin
- Regional metamorphosed to amphibolite grade locally up to granulite grade facies
- Retrograde greenschist facies metamorphic overprint
- Presence of granitic-migmatitic complexes and pegmatite dikes in basement
- Cover by continental clastic sediments with intercalated and transgressive basic volcanics
- Post-sedimentary diabase/dolerite dikes
- Brittle deformation of host strata by intense faulting and brecciation often but not necessarily developed adjacent to and at intersections of major faults (particularly evident in Beaverlodge district)
- Host structures are faults, fractures, breccias, stockworks arranged more or less peneconcordant to attitude of strata

Alteration

- Mild paleoweathering-related alteration of basement (in Beaverlodge district of more physical than chemical nature)
- Pervasive diagenetic alteration including Mg-, Li- and B-metasomatism of several generations imposed on both basement and overlying sediments and reflected by tourmalinization (dravite), carbonatization (calcite, dolomite), argillitization, sericitization etc.
- Intense mineral-related wall rock alteration including argillitization, chloritization, desilicification, silicification, sulfidization and hematitization
- Widespread pre-ore albitization of basement rocks hosting subtype 2.2 deposits

Mineralization

- Principal uranium minerals are pitchblende, uraninite and alteration products thereof (coffinite, etc.). For associated minerals and metals, see Table 4.2
- Gangue minerals are associated with subtype 2.2 but rare or absent in subtype 2.1
- Most deposits, particularly all large ones are monometallic except for some containing locally Au; some smaller deposits are polymetallic (Rum Jungle: Cu, Pb, Zn)
- Several generations of mineralization exist, mainly derived by redistribution of primary mineralization (locally into cover sandstone)
- Ore distribution consists of U disseminations or massive veinlets within host structures
- Mineralized structures are arranged ± peneconcordant to attitude of host strata
- Type example (a) Jabiluka and Koongara display the most pronounced strata-bound structure correlation, whereas going from type examples (b) to (c) and (d) the strata-structure relationship becomes less evident
- Mineralization is fairly continuous
- Depth persistence is variable but can extend to great depth (>1600 m in Beaverlodge district)

Table 4.2. Associated minerals and metals

	Gangue minerals	Others (replacement, authigenic, etc.)		Metals
	Vein fillings	Basement	Overlying sandstone	
a)[a]	–	Chlorite Sericite/illite Kaolinite Silica Quartz	Locally Mg-chlorite, tourmaline (in Kombolgie sandstone and basement)	Au
b)	–	Carbonate Hematite		Cu, Pb, Zn
c)	Calcite, dolomite, quartz, chlorite (?)	Hematite Epidote		Co, Ni, Pb Cu, Pt, Au, Ag As, Se, S
d)	Quartz (?) Calcite (?) Chlorite (?)	Albite Calcite		

[a] a to d refer to type examples in Fig. 4.2

Age Constraints

- No age constraint except limitation to orogenies younger than late Lower Proterozoic
- All major deposits known are associated with upper Lower Proterozoic sediments metamorphosed during the Hudsonian or time equivalent orogenies (ca. 1900 to 1700 m.y. ago)

Metallogenetic Aspects

Subunconformity-epimetamorphic uranium deposits have a complex, polyphase evolution. Deposits in the Alligator Rivers and Beaverlodge districts most likely have their roots in late Lower Proterozoic time when pelitic-psammitic sediments interbedded with carbonaceous horizons collected anomalous amounts of uranium and other metals. It is possible that pre-metamorphic relocation of uranium led to the formation of sandstone-type deposits such as those in the Franceville Basin, Gabon. During Lower to Middle Proterozoic times these sediments were regionally metamorphosed to amphibolite and locally to granulite facies. In regions of open systems, i.e., in tectonically active terrane characterized by anatexis, migmatism, metasomatism, acidic and mafic intrusions, and brittle deformation, uranium was locally mobilized by late metamorphic and/or metasomatic hydrothermal processes and reconcentrated in structures which had opened within the uraniferous strata. In contrast, in areas of closed systems, i.e., those that lack the above listed criteria, uranium remained in situ and formed stratiform synmetamorphic mineralizations (Type 13). The position of more structurally dominated mineralization [type examples (c) and (d) at Beaverlodge] or more lithologically controlled mineralization [(a) and (b) in the Alligator Rivers district] may be related to zones influenced by Na-metasomatism, migmatization and/or palingenesis/anatexis. In regions where subunconformity-epimetamorphic deposits were covered by early Middle Proterozoic continental sediments, the cover protected the deposits against weathering and erosion. More or less intense diagenetically induced magnesium and boron metasomatism occurred in both crystalline basement and overlying sandstone as displayed in the Alligator Rivers district. These processes very probably created diagenetic modifications in the deposits including redistribution, partly into the overlying sandstone as at Beaverlodge, and recrystallization of the uranium and intense host rock alteration. Still younger processes led to further modifications, as reflected by several generations and isotope ages of uranium and associated minerals.

Remarks

a) Monometallic subunconformity-epimetamorphic U deposits particularly those of Lower to

Middle Proterozoic age, often have medium to large resources (up to >200 000 mt U_3O_8) at low to medium grade (0.2–0.4% U_3O_8) but may also contain sections of very high grade (several % U_3O_8). In contrast, polymetallic deposits except those with gold (e.g., Jabiluka) have small resources.

b) Although all large deposits of this category known are associated with Lower to Middle Proterozoic rocks, similar deposits may also occur in comparable geological environments associated with younger orogenic-metamorphic events.

4.2.1 Subtype 2.1: Not albitized metasediments

Type Example: Pine Creek Geosyncline, Australia
Monometallic (except for local Au concentration): a) Jabiluka, Koongara, Australia; b) Ranger One, Australia
Polymetallic: Rum Jungle
(a) and b) refer to Fig. 4.2)

References: Ewers et al. 1984; Ferguson and Goleby (eds.) 1980; IAEA/Ferguson (ed.) 1984; Needham et al. 1988

Host Rocks/Structures

Metasediments (schist, gneiss) with intercalated graphitic layers and carbonatic horizons derived from pelites and psammites of eugeosynclinal or lacustrine origin, regionally metamorphosed to amphibolite-granulite facies.

Migmatitic/anatectic complexes occur near deposits. Pegmatite and diabase/dolerite dikes intrude host sequences. Continental sandstone with intercalated and discordant basic volcanics, if not eroded, overlie mineralized areas.

Host rocks are deformed by intensive faulting and brecciation. Structures containing mineralization consist of fractures, breccias and stockworks arranged ± peneconcordant to attitude of strata. Type examples (a) Jabiluka and Koongara display the most distinct strata-bound structure correlation whereas that of examples (b), Ranger One and Rum Jungle is more structure prominent.

Alteration

Strong wallrock alteration and extensive metasomatism (Mg, B, Li) of several generations, The latter affected both basement and sandstone cover and includes tourmalinization (dravite), chloritization (Mg and/or Fe-rich), carbonatization (calcite, dolomite), sericitization, argillitization, desilicification, and silicification and hematitization. Alteration related to mineralization is commonly very intense and may extend to variable distance (m to 10's m) into wall rocks.

Ore and Associated Minerals

Principal uranium minerals are pitchblende, rarely uraninite and alteration products thereof (coffinite, brannerite, sooty pitchblende). Associated minerals/metals see under main heading, Type 2.

Mode of Mineralization

U occurs as disseminations or massive veins filling fractures, breccias and stockworks, ± peneconcordant to attitude of the strata. Mineralization is more or less continuous and may extend to more than 500 m below the unconformity. Most ore is monometallic except for some small deposits (Rum Jungle) and locally payable gold values (Jabiluka, Koongara). Several generations of uranium mainly derived by redistribution and recrystallization (rejuvenated U/Pb ages) of primary mineralization partly by diagenetic processes. Mineralization is controlled by both structure and lithology as reflected by emplacement in cataclastic zones ± peneconcordant to folded metamorphosed strata and often adjacent to graphitic horizons. Other recognition criteria include intense, partly pervasive chloritization, sericitization, argillitization, and hematitization of wallrocks; wide-spread halos into cover sediments of tourmalinization, carbonatization, silicification, etc.; (former) presence of continental cover sediments and volcanics; minor paleosol development prior to sedimentation and numerous pegmatite and diabase (dolerite) dikes.

Age Constraints

All examples known are associated with upper Lower Proterozoic sediments metamorphosed during an orogeny at about 1700 to 1900 m.y. ago.

Dimensions/Resources

Individual deposits may be up to >1000 m long, several tens to more than 400 m wide and in excess of 500 m deep, containing up to 200 000 mt U_3O_8 at (average) grades ranging from 0.1 to 0.4% U_3O_8 occasionally to >1% U_3O_8. Districts may contain up to 400 000 mt U_3O_8.

Remarks

For more details see Chapter 5.2.1.

Examples of Subunconformity-Epimetamorphic, Subtype 2.1 Not Albitized Metasediments Deposits/Occurrences

Australia: Alligator Rivers district, Rum Jungle district, ? South Alligator River district/Pine Creek Geosyncline, Northern Territory, ? Kintyre, West Australia

4.2.2 Subtype 2.2: Albitized metasediments

Type Example: Beaverlodge, Uranium City region, Canada
monometallic: c) Fay – Verna; d) Gunnar
polymetallic: c) Nicholson
(c) and d) refer to Fig. 4.2)
References: Beck 1986; Evans (ed.) 1986; Tremblay 1978; Ward 1984

Host Rocks/Structures

Metasediments (schist, gneiss) with intercalated graphitic layers derived from pelites and psammites of eugeosynclinal or lacustrine origin, regionally metamorphosed to amphibolite-granulite facies and partly Na-metasomatized to albitite rocks.

Migmatitic/anatectic complexes and/or granitic intrusions occur near deposits. Pegmatite and diabase/dolerite dikes cut the host rocks. Continental sandstone with intercalated and discordant basic volcanics, if not eroded, overlie mineralized areas and may carry (redistributed) mineralization.

Host rocks are deformed by intensive faulting and brecciation, often but not necessarily developed adjacent to and at the intersection of major faults. Structures containing mineralization consist of fractures, breccias, and stockworks arranged ± peneconcordant to the attitude of strata. Structural control is more prominent as in subtype 2.1.

Alteration

Extensive and locally intense Na-metasomatism and strong wall rock alteration of several generations modified the basement. Na-metasomatism is a pre-ore phenomena and locally achieved albitite formation. Host rock alteration of pre- to syn-mineralization age includes pervasive hematitization, chloritization, epidotization, carbonatization, and silicification.

Ore and Associated Minerals

Principle uranium minerals are pitchblende, rarely uraninite and alteration products thereof (coffinite, brannerite, sooty pitchblende).

Associated minerals/metals (see under main heading, Type 2).

Mode of Mineralization

U occurs as disseminations or massive veins filling fractures, breccias and stockworks, ± peneconcordant to attitude of the strata. Mineralization is more or less continuous and may extend to a considerable depth (>1600 m). Most ore is monometallic except for some small deposits (e.g., Nicholson). Several generations of uranium mainly derived by redistribution (locally into cataclastic cover sandstone) and recrystallization (rejuvenated U/Pb ages) of primary mineralization.

Mineralization is controlled by both structure and lithology as reflected by emplacement in structures ± peneconcordant to folded metamorphosed strata and often adjacent to graphitic horizons. Other recognition criteria include intense, partly pervasive chloritization, sericitization, argillitization, hematitization, carbonatization, silicification, etc. of the host rocks; (former) presence of continental cover sediments and volcanics; little or no paleosol (regolith) development prior to sedimentation and numerous pegmatite and diabase (dolerite) dikes.

Age Constraints

All major deposits known are associated with upper Lower Proterozoic sediments metamor-

phosed during the Hudsonian Orogeny (ca. 1700 to 1900 m.y.).

Dimensions/Resources

Individual deposits may be meters to 100 m long, several meters to more than 100 m wide and in excess of 1600 m deep, containing up to >15 000 mt U_3O_8 at (average) grades ranging from 0.1 to 0.4% U_3O_8. Districts may contain up to 25 000 mt U_3O_8.

Remarks

For more details see Chapter 5.2.2.

Examples of Subunconformity-Epimetamorphic, Subtype 2.2 Albitized Metasediments Deposits/ Occurrences

Canada: Bolger, Dubyna, Hab, Lake Cinch/ Beaverlodge, Saskatchewan

4.3 Type 3: Vein (Figs. 4.3a,b)

Definition

Vein deposits consist of uranium mineralization in lenses or sheets or disseminations filling joints, fissures, breccias and stockworks in deformed and fractured rocks. Size and complexity of vein sets are variable. Distribution and intensity of mineralization are irregular. Principal uranium phases are pitchblende, uraninite and coffinite. Gangue minerals are always present. Uranium may form monometallic mineralizations or polymetallic mineralizations. Associated metals include Co, Ni, Bi, Ag, Cu, Pb, Zn, Mo and/or Fe in form of sulfides, arsenides or sulfarsenides. Wall rock alteration is commonly restricted to a narrow margin (<1 m).

Two principal subtypes are recognized, veins spatially and genetically (?) related to granites (subtype 3.1) and veins not related to granites (subtype 3.2) which are further subdivided into the following classes:

Subtype 3.1: granite-related (Fig. 4.3a)

Class 3.1.1: intragranitic
(Limousin type)
Type Examples: 3.1.1.1 veins in granite: Fanay, France
3.1.1.2 disseminations in episyenite pipes: Pierres Plantées, France

Class 3.1.2: perigranitic
Type Examples: 3.1.2.1 veins in (meta)-sediments: monometallic (Bohemian type) Příbram, ČSFR
3.1.2.2 veins in metasediments: polymetallic (Erzgebirge type) St. Joachimsthal/ Jachymov, ČSFR
3.1.2.3 in contact-metamorphics: (Iberian type) Alto Alentejo, Portugal

Subtype 3.2: not granite-related (Fig. 4.3b)

Class 3.2.1: in metamorphic rocks
Type Example: Schwartzwalder, USA

Class 3.2.2: in sediments (polymetallic)
Type Example: Shinkolobwe, Zaire

References: IAEA/Fuchs (ed.) 1986; Basham and Matos Dias 1986; Derriks and Vaes 1956; Friedrich et al. 1987; Kolektiv ČSSR 1984; Poty et al. 1986; Rich et al. 1977; Ruzicka 1971; Wallace 1986

Granite-related deposits are associated with highly differentiated peraluminous leucogranites and form veins either within (intragranitic, class 3.1.1) or around (perigranitic, class 3.1.2) the intrusion.

Intragranitic deposits are commonly monometallic and occur either as (a) linear ore bodies in form of distinct veins or stockworks emplaced in fractured granite or (b) disseminations in pipes or chimneys of episyenite, a dequartzified, micaceous vuggy alteration product of granite. Depth extension of intragranitic veins is commonly less than 300 m.

Perigranitic deposits emplaced in (meta-)sediments are either monometallic consisting essentially of pitchblende and gangue minerals (3.1.2.1) or polymetallic (3.1.2.2) containing both U and Co, Ni, Bi and Ag minerals in economic quantities. The U and the other elements are not genetically related. Both monometallic and polymetallic veins can persist as much as 2000 m deep. Ore occupancy of host structures is generally low (in the order of 5 to 30%).

Perigranitic deposits emplaced in the contact-metamorphic aureole of the intrusion (3.1.2.3)

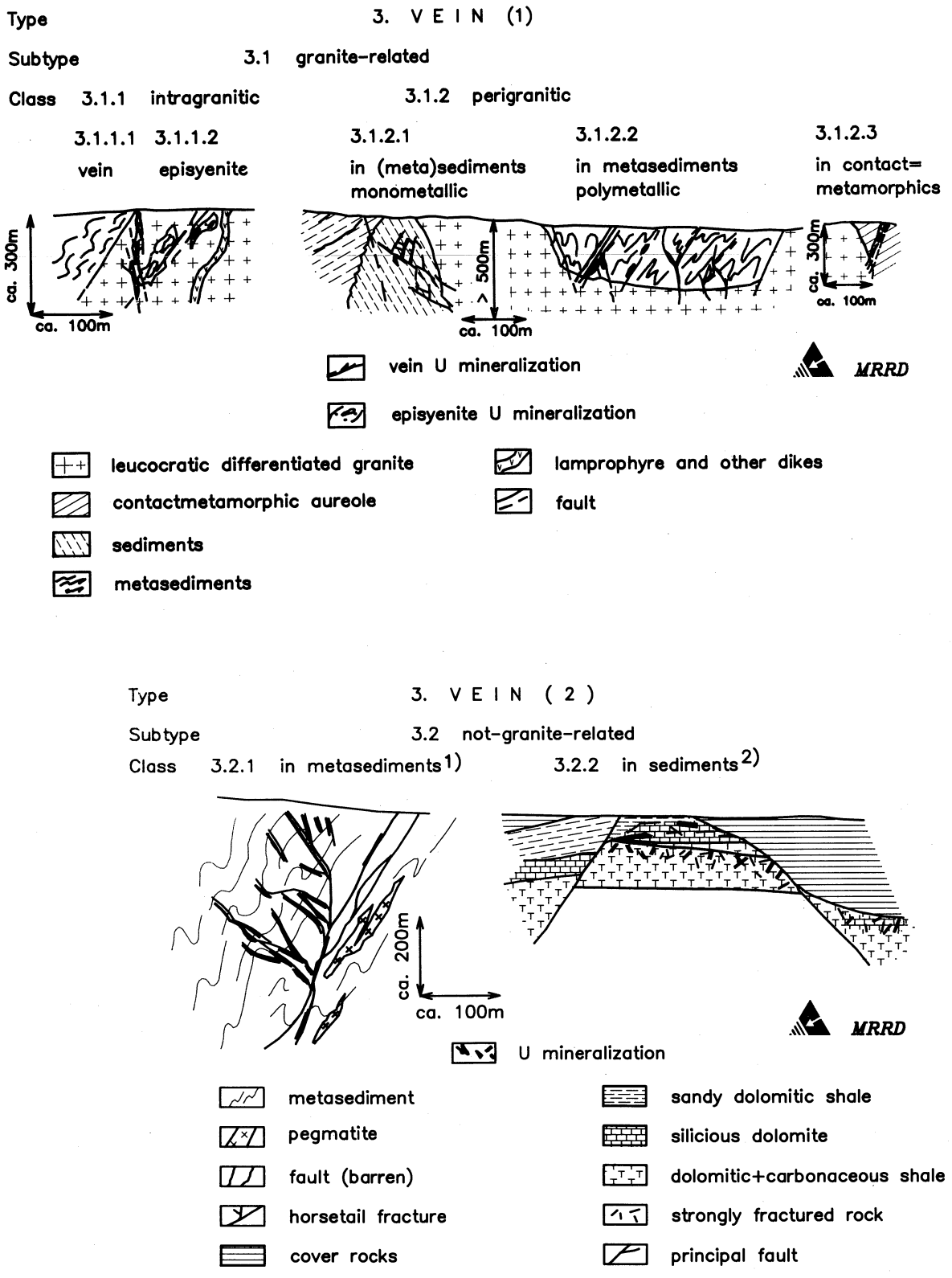

1) idealized after Schwartzwalder, USA/Wallace 1986

2) idealized after Shinkolobwe, Zaire/Derriks & Oosterbosch 1958

Fig. 4.3a, b

have monometallic mineralization in form of veinlets and disseminations in intensely fractured hornfels, speckled andalusite-cordierite schist and similar rocks up to approximately 2 km wide around the granite. Host rocks are severely altered.

Not granite-related deposits (subtype 3.2) are similar in mineral composition and wall rock alteration to perigranitic veins in (meta-)sediments but do not reveal any apparent link to granitic intrusions.

Principal Recognition Criteria

Host Environment of Granite-related Deposits

- Orogenic belt
- Presence of highly differentiated igneous complex including peraluminous leucocratic granite of crustal origin derived by multistage magmatic and deuteric processes
- Uranium content in granite above Clark standard (>5 ppm)
- Uranium fixed in leachable phases (uraninite)
- Sufficient size of pluton (outcrop extension at least 100 km^2)
- Presence of leucocratic (pegmatite, aplite) and mafic (lamprophyre) dikes
- Limited depth of erosion level (indicated by abundance of roof pendants in pluton, dikes, etc.)
- Structural vein control by commonly one, ± parallel oriented dilational fracture system

Host Environment of Not Granite-related Deposits

- Orogenic belt
- Absence of nearby granites or other igneous uranium source rocks
- Host rocks are folded sediments or metasediments, the latter often of mafic composition and metamorphosed up to amphibolite facies
- Intense brittle deformation by major faults associated with abundant subsidiary fractures and breccias which may form stockworks or horsetail patterns
- Emplacement of mineralization preferentially in subsidiary structures

Regional Alteration (Subtype 3.1)

- Albitization, muscovitization
- Feldspar and mica episyenitization

Ore-Related Alteration (Subtype 3.1 and 3.2)

- Spatially restricted wall rock alteration commonly persisting for less than 0.5 m, rarely to 3 m, from veins into wall rock
- Type of alteration depends to some degrees on host rock composition
- Alteration types may include carbonatization, chloritization, argillitization, silicification, hematitization, K-feldspathization

Mineralization (Subtype 3.1 and 3.2)

- Principal uranium minerals: pitchblende, locally uraninite, coffinite, and alteration products thereof
- Associated metallic minerals: dominantly pyrite, marcasite, and minor Cu, Pb, Zn, Mo sulfides
- In some deposits either arsenides or sulfides of Ag, Co, Ni, Bi accompany pitchblende but not paragenetically
- Gangue minerals: quartz, chalcedony, carbonates, fluorite, baryte (in class 3.1.1 present in minor amounts and sometimes almost absent, in class 3.1.2 abundant)
- U and associated minerals are mostly present in several generations
- U and gangue minerals form irregularly shaped and discontinuous ore shoots separated by barren intervals
- Low frequency of uranium ore occupancy of host structures commonly in the range from 5 to 30% in subtype 3.1, more continuous in subtype 3.2
- U mineralization is often associated with inhomogeneities of veins (change in trend, thickness) and wall rock lithologies

Age Constraints (Subtype 3.1 and 3.2)

- No stratigraphic age constraint
- Restriction to late orogenic stages
- In Europe the dominant association of subtype 3.1 is with the waning stage of the Hercynian Orogeny

Metallogenetic Aspects

Poty et al. (1986) suggest for *granite-related* pitchblende-vein deposits in the Hercynian orogenic belt in France (class 3.1.1) the following

metallogenetic model. Although largely based on research of intragranitic veins, the model appears, at least to some extent, to be also applicable to perigranitic vein deposits except for tectonic processes, creating the structural frame for vein emplacement, and, perhaps, incorporation of uranium from metasediments.

Evolution of granite-related vein uranium deposits started during the waning episode of the Hercynian Orogeny marked by general uplift, and intrusion of granite and a suite of leucocratic to mafic dikes. Certain peraluminous leucogranites contain uraninite as a primary magmatic rock constituent distributed in two modes (a) homogenously throughout the granite and (b) accumulated (up to 100 ppm U) along synmagmatic shear zones.

In zones of intense faulting, high heat flow, in response to tectonism (?) generated deep reaching convective circulation of mixed connate-meteoric waters in late to post-magmatic time. The fluids leached the uraninite and transported uranium as uranyl-carbonate complexes to the marginal zones of the pluton. Precipitation of pitchblende occurred in either dilational fractures (vein mineralization) or vesicular, vuggy episyenite bodies (disseminated mineralization). Precipitation supposedly resulted as a response to boiling of the hypogene convective hydrothermal fluids triggered by either a pressure drop, and/or by reactions with mafic rocks. Pitchblende crystallization was accompanied by deposition of pyrite and gangue minerals (mainly quartz, carbonate) and by K-metasomatism and muscovitization of wall rocks adjacent to veins. In several subsequent stages, hematite, coffinite, marcasite, and additional gangue minerals formed, most of them on account of the original ore generation. A supergene overprint redistributed part of the uranium.

Petroš et al. (1986) postulate a metasedimentary uranium origin with subsequent enrichment during magma differentiation and final hydrothermal redistribution into dilational structures, possibly with some contribution of uranium from residual magmatic fluids for perigranitic (Bohemian type) veins (class 3.1.2.1) in the Přibram district, ČSFR.

Metallogenetic hypotheses of Iberian type deposits (3.1.2.3) are contentious (perhaps due to limited exploration in depth) and include concepts such as supergene, lateral secretionary and hypogene origins.

Metallogenetic considerations for subtype 3.2, *not granite-related veins*, face in many cases the problem of an adequate uranium source and a mechanism for propelling the mineralizing fluids. Wallace (1986) suggests for the metamorphite hosted Schwartzwalder veins (class 3.2.1) that the source of uranium and all other vein components was the metamorphic terrane surrounding the deposit. Leaching of the elements occurred by evolved connate hydrothermal fluids. The fluids probably derived originally from meteoric waters and resided in deep cataclastic zones. Mobilization of the fluids was generated during the incipient uplift of the crystalline block of the Front Range in the course of the Laramide Orogeny. Migration occurred along permeable fault zones created by repeated deformation of brittle rocks. The connate hydrothermal solutions were carbonate-rich and produced successive wall rock alterations around fractures and several generations of vein mineralization during repeated major movement along faults. Mineral deposition resulted during episodic brecciation that reduced the confining pressure which simultaneously increased the pH and decreased $f(CO_2)$ and $f(O_2)$, Reduced sulfur species in solution reduced the uranium carried in solution.

Similar processes may have formed the sediment hosted Shinkolobwe deposit (class 3.2.2). In this case sediments with anomalous contents of uranium and other metals (Série de Mine) probably provided the vein forming elements.

Remarks

Vein deposits are often composed of small lodes and almost always occur in groups which cumulatively yield small to large resources. Grades are highly variable and many known deposits contain sections of very high grade ore.

4.3.1 Subtype 3.1: Granite-related

Class 3.1.1: Intragranitic (Limousin type)

3.1.1.1: veins in granite
Type Example: Fanay, Limousin, France
3.1.1.2: disseminations in episyenite pipes
Type Example: Pierres Plantées, Margeride, France
References: Cariou 1964; Cathelineau 1985; Friedrich et al. 1987; Leroy 1978a, 1978b; Leroy and Cathelineau 1982;

Host Rocks/Structures

Ziegler and Dardel (1984) define ore-hosting fertile granite as a highly differentiated two-mica leucogranite with an average composition of ca. 36% quartz, 27% orthoclase, 27% albite, 10% muscovite and biotite, enriched in Be, Li, F, Sn, W, Th and U. The main facies is medium to coarse-grained and has intercalations of a fine-grained facies. The granite is of peraluminous composition derived from crustal material (Friedrich et al. 1987). Lamprophyre, pegmatite, aplite and micro-granite dikes transect the complex.

Mineralized structures are dominantly controlled by a dilational system of a distinct direction (NW-SE in Limousin). Major faults are rarely or not mineralized. The most favorable host structures are those of secondary order, forming ± parallel fractures or complicated interwoven stockwork systems.

Alteration

Pre-mineralization alteration consists of albitization and episyenitization. Episyenitization is reflected by dissolution of quartz with destruction and neoformation of minerals leading to feldspar-episyenite (commonly barren of U) and mica-episyenite (Leroy and Cathelineau 1982).

Ore-related alteration extends usually for less than 0.5 m into wall rocks adjacent to veins and includes ± total muscovitization (phengitization) of K-feldspar, chloritization of mafic minerals and pyritization accompanying pitchblende emplacement. A second phase of alteration associated with coffinite formation after pitchblende consists of hematitization, montmorillonitization, adularia formation, and silicification partly by replacement of first stage alteration products.

Ore and Associated Minerals

Pitchblende, coffinite and the alteration products thereof are usually associated with pyrite, marcasite, melnicovite, quartz, chalcedony, fluorite, baryte, and calcite. Gangue minerals occur in minor amounts and locally are absent. Other sulfides (galena, bismuthinite, a.o.) are scarce, but occur in some deposits in significant amounts (e.g., Bois Noirs, Forez, France).

Mode of Mineralization/Dimensions

Veins in Granite. Veins, veinlets or stringers of pitchblende and associated minerals occur in simple linear configuration but more commonly occupy a complex network or stockwork of fractures or breccias particularly in proximity to lamprophyre dikes, roof pendants, and other inhomogeneities in the host granite. Individual veinlets/veins vary in thickness from a few mm to rarely more than 5 m. Lateral and vertical continuity is variable, averaging from less than 1 m to some 10 m, but may be as long as 1000 m and more. Depth extension is generally less than 300 m. Mineral distribution also varies considerably. Reserves range between less than 1 mt to some 100 mt U_3O_8 and grades between less than 0.1% and up to 40% U_3O_8 in some ore shoots (the Henriette deposit, France, yielded 120 mt U_3O_8 at an average mining grade of 37% U_3O_8 from a vein averaging 5 m long, 0.4 m thick and 250 m deep).

Disseminations in Episyenite. Mineralization is hosted in irregularly pipe- or lense-shaped bodies of mica episyenite developed at intersections of two structure systems. Vertical extensions range between 30 and 200 m, and diameters between few meters and several 10 m. Grades are generally high, up to 1% U_3O_8 and more. Where mineralized veins intersect episyenite pipes grades may increase to between 1 and 10% U_3O_8. Reserves vary between a few tonnes and several 100 mt U_3O_8, rarely 1000 mt U_3O_8 or more. The type example Pierres Plantées in the Margeride district, France, is an episyenite pipe measuring 35 to 50 m in diameter, 175 m deep and yielded 1300 mt U_3O_8 with an average mining grade of 0.3 to 0.5% U_3O_8. Mining districts may cover an area a few km to some 10 km long and wide (Limousin district France: ca. 15 km long, 5 km wide).

Resources

Individual vein systems contain reserves that range from some 10 mt to several 100 mt U_3O_8 but may be as large as 4000 mt U_3O_8 (La Commanderie, Vendée, France), at mining grades ranging from 0.15% U_3O_8 (La Commanderie) to 37% U_3O_8 (Henriette). Episyenite-hosted ore bodies have reserves of a few tonnes to 1300 mt U_3O_8 (Pierre Plantées) averaging 0.3 to 1% U_3O_8. Districts have resources in the order of 5000 mt U_3O_8 (Morvan, France, average grade

0.16% U_3O_8) to at least 35 000 mt U_3O_8 (Limousin, average grade 0.2% U_3O_8).

Remarks

For more details see Chapter 5.3.1.

Examples of Vein, Class 3.1.1 Intragranitic Deposits/Occurrences

Brazil: ? Itataia/Ceará
Canada: Millet Brook/Nova Scotia, ? Gunnar/Saskatchewan
China: Xiazhuang/Guidong Massif, Ruijin/Jiangxi, SE China, Xian/Central China
France: Limousin, Marche, Margeride, Millevaches, Morvan districts/Massif Central, Vendée district/Armorican Massif
Germany: Menzenschwand/Black Forest, Grosschloppen/Fichtelgebirge
Portugal: Alto Alentejo, Beiras districts
Spain: Los Ratones/Caceres

Class 3.1.2: Perigranitic
3.1.2.1: Veins in (meta)sediments, monometallic (Bohemian type)

Type Example: Příbram, Central Bohemian Pluton, ČSFR
Reference: Petroš et al. 1986

Host Rocks/Structures

Geology (at Příbram) consists of weakly metamorphosed Upper Proterozoic schists and Cambrian conglomerates and sandstones folded into a large NE-SW trending anticline. The SE limb of the anticline is occupied by granitic rocks of the differentiated Central Bohemian Pluton. Three dominant fault systems transect the region. Regional faults subparalleling the intrusive contact and anticlinal axis partition the anticline into longitudinal segments. The segment closest to the pluton hosts the mineralized veins. These veins mostly occupy second or third order faults trending preferentially perpendicular to oblique to both the anticlinal axis and intrusive contact. A wide variety of magmatic dikes occurs, including aplitic granite, granite-porphyry, aplite, pegmatite and lamprophyre.

Alteration

Pre-uranium host rock alteration includes silicification, sericitization, and carbonatization. Uranium mineralization related alteration commonly extend from 0.1 to 3 m, locally to several tens of meters (in zones of closely spaced or bifurcating veins) into the wall rocks and include sericitization, chloritization, and hydrohematitization.

Ore and Associated Minerals

Principal uranium minerals are pitchblende, coffinite, uranium-anthraxolite (high polymeric bitumen containing pitchblende, coffinite, calcite and other minerals), and the alteration products thereof. Associated metallic minerals include sulfides of Fe, Pb, Zn, Cu, a.o., which are present in minor to trace amounts. Gangue is abundant, and includes carbonates (dominantly calcite), quartz, and chlorite. Certain ore and gangue minerals form a characteristic paragenesis developed during consecutive stages.

Mode of Mineralization/Dimensions

Prominent types of mineralization are pitchblende-calcite veins, emplaced both inside and immediately outside of the intrusive contact and mixed uranium-anthraxolite-pitchblende veins occurring at some distance from the contact. Uranium and gangue minerals form stringers, veinlets, coatings, reniform accretions and pods, that range from mm to several 100 cm wide. This assemblage aggregates to irregularly shaped tabular or lense-like ore shoots that range from 1 to several tens of m long and deep, and a few cm to 5 m wide, interrupted by barren, gangue, or gouge-filled intervals within mineralized structures. Ore shoots commonly develop at inhomogeneities in the veins (change in strike or dip, thinning or widening, change of wall rock lithologies, splaying of structures). Ore-bearing structures may persist to as much as 2000 m deep containing irregularly distributed ore shoots at variable depth. Ore shoots usually occupy between 1 and 50% (average about 10 to 15%) of a structure with the remainder being barren. Mining districts may cover areas a few to some 10 km long and wide and may contain up to several tens of mineable veins (Přibram 1 to 2 km wide, 25 km long, about 30 shafts).

Resources

Individual vein systems contain from a few tonnes to a few 1000 mt U_3O_8 at grades varying between ca. 0.1% to some 10% U_3O_8. Districts may account for a few 100 mt to several 10 000 mt U_3O_8 (Příbram presumably yielded in the order of 50 000 to 60 000 mt U_3O_8, at grades of about 1 to 2% U_3O_8).

Remarks

For more details see Chapter 5.3.2.

Examples of Vein, Class 3.1.2.1, Perigranitic Monometallic Deposits/Occurrences

China: see class 3.1.1
ČSFR: Damětice/Central Bohemian Pluton, Brezinka/Zelezne Hory
France: ? Bois Noirs/Forez, Les Bondons/Lozére, Massif Central, La Dorgissière, Le Rousset/ Vendée, Pennaran, Materie Neuve/Guérande Peninsula, Armorican Massif
Greenland: ? Puissagtaq/Igaliko Fjord, SE Greenland
USA: ? Midnite/Washington [may belong to strata-structure type (16)]

Class 3.1.2: Perigranitic
3.1.2.2: In metasediments, polymetallic (Erzgebirge type)

Type Example: St. Joachimsthal/Jáchymov, Karlovy Vary/Eibenstock Massif, ČSFR
Reference: Komínek and Veselý 1986

Host Rocks/Structures

Geology at Joachimsthal consists of intensely folded Upper Proterozoic to Lower Paleozoic, partly pyritic or graphitic mica schists, phyllites and calc-silicate units, folded into an asymmetric anticline. The metasediments are intruded by the highly differentiated Eibenstock Massif which includes a younger deuterically (?) altered leucocratic granite facies characterized by high U/Th ratios. This facies underlies and partly surrounds the mineralized district in a form akin to a half-bowl at a depth of as much as 1000 m deep. A contact-metamorphic aureole (hornfels, more massive texture) up to 60 m wide surrounds the granite. Three dominant fault sets transect the district. Mineralized veins preferentially follow minor faults oriented perpendicular and oblique to the anticlinal axis.

A wide variety of magmatic dikes occurs, including aplitic granite, granitic porphyry, pegmatite, and lamprophyre.

Alteration

Pre-uranium host rock alteration is reflected by chloritization, phlogopitization, pyritization, and calcitization associated with destruction of mafic minerals. These alterations are overprinted by intense silicification with replacement of earlier formed minerals. Uranium mineralization related alteration rarely extends more than 10 cm into the wall rocks and is reflected by hematitization of pyrite, dolomitization of calcite and recrystallization of albite and adularia in calcite veins.

Ore and Associated Minerals

Principal uranium minerals are pitchblende, coffinite and alteration products thereof. Associated metallic minerals present in minable quantity are primarily sulfides and sulfarsenides of Ag, Co, Ni and Bi. Sulfides of other metals and hematite also occur. Gangue is abundant and includes carbonates (dominantly dolomite), quartz, albite, adularia, fluorite, and baryte. Certain ore and gangue minerals form characteristic parageneses developed during successive stages. Mineral phases occur in several generations.

Mode of Mineralization/Dimensions

Two principal varieties of vein forming mineral assemblages are distinguished. "*Simple veins*" are composed of pitchblende, carbonate, and gouge with mylonitized rocks, often selvaged by quartz, adularia, albite, and fluorite. These veins occupy structures of second or third order. Length commonly is 150 to 400 m and width 3 to 25 cm, rarely 50 cm. "*Complex veins*" are composed of several generations of pitchblende, carbonate, and younger carbonate-arsenide and quartz-sulfide assemblages, intermixed with breccias and gouge. These veins occupy higher order structures. Length of the veins may exceed 1000 m (max. 2200 m). Width is from 10 to 60 cm.

Mineralization occurs as erratically distributed ore shoots (a few m^2 to rarely 1000 m^2 in size) separated by barren intervals down to a depth

of about 700 m below surface. Cumulative occupancy of a structure by ore, although highly variable, averages less than 10%.

A vertical mineral zonation is reflected by predominance of arsenides and native Ag in the upper levels (down to 400 m), arsenides and native Bi in the medium to lower levels down to about 700 m below surface. The bulk of uranium occurs in the lower level. Near and within the contact-metamorphosed zone enveloping the granite, at distances of ca. 20 to 120 m from the contact ore structures tend to lose uranium mineralization except for a very few cases where wide veins contain some uranium down to the granite.

Structural ore control and distribution corresponds to that described under class 3.1.2.1.

Resources

Individual vein systems contain from a few tonnes to several hundred tonnes U_3O_8. Grades range from <0.1% to several percent U_3O_8. In addition, high grades of Ag, Co, and Ni may occur. Known districts account for a few 100 mt to 10 000 mt U_3O_8 and more (St. Joachimsthal presumably yielded 12 000 mt U_3O_8, ranging in grade from 0.1 to 1% U_3O_8).

Remarks

For more details see Chapter 5.3.3.

Examples of Vein, Class 3.1.2.2, Perigranitic Polymetallic Deposits/Occurrences

Canada: ? Port Radium, Echo Bay/Great Bear Lake, NWT
ČSFR: Javornik, Bila Voda, Rychlebske Hory (Glatzer Schneeberg)
Germany: Alberode-Niederschlema, Pöhla-Tellerhäuser, Schneeberg, Johanngeorgenstadt, Erzgebirge, Wittichen/Black Forest
Great Britain: Cornwall region
Poland: Kowary-Schmiedeberg/Riesengebirge, Kletno/Snieznik Klodzki (Glatzer Schneeberg)
USA: Black Hawk/New Mexico

Class 3.1.2: Perigranitic
3.1.2.3: In contact-metamorphics (Iberian type)

Type Example: Alto Alentejo, Portugal
Reference: Basham and Matos Dias (1986)

Host Rocks/Structures

Hosts rocks are pelitic-psammitic sediments that exhibit little or no effect of regional metamorphism (schist-greywacke complex of Proterozoic to Lower Paleozoic age on the Iberian Peninsula) but is contact-metamorphosed into hornfels, speckled andalusite-cordierite schist etc. up to approximately 2 km, from the granite intrusion. Granites and vein composition are similar to those in Limousin (see class 3.1.1). Zones of intense fracturing, brecciation and shearing disrupt the metasediments. Faults displace the granite contact. Dikes of microgranite and lamprophyre occur.

Alteration

Cordierite megacrysts may be completely altered to aggregates of sericite and muscovite. Chlorite-rich bands crystallized. Considerable hematitization occurs around mineralized zones.

Ore and Associated Minerals

Principal uranium minerals are hexavalent U species. Rare pitchblende and coffinite associated with quartz, pyrite, and chalcopyrite occur at depth.

Mode of Mineralization/Dimensions

Uranium minerals occur as disseminations mainly in the weathered or oxidized zone from 0 to 40 m deep, within intensely fractured slivers. The minerals impregnate and coat fracture and schistosity surfaces. Slivers extend laterally for tens to hundreds of meters. Mineralized zones composed of slivers with discontinuous mineralization have widths up to 2 km and may extend for a length up to several km along the granite contact (Nisa deposit Portugal: 5 km long, 1 to 1.5 km wide).

Resources

Individual deposits contain some 10 mt to about 2500 mt U_3O_8 (Nisa). Districts have a few 1000 mt to some 10 000 mt U_3O_8. Average grade is commonly low, about 0.1% U_3O_8 or less.

Remarks

For more details see Chapter 5.3.4.

Examples of Vein, Class 3.1.2.3, Perigranitic Deposits/Occurrences in Contact-metamophics

Italy: Alm Bos/Adamello Massif
Poland: Kowary-Schmiedeberg/Sudetes
Portugal: Beiras district
Spain: Don Benito/Badajóz, Ciudad Rodrigo district/Salamanca
USA: Little Man Mine/Wyoming

4.3.2 Subtype 3.2: Not granite-related

Class 3.2.1: In metamorphic rocks

Type Example: Schwartzwalder, Colorado, USA
Reference: Wallace 1986

Host Rocks/Structure

Host rocks include a variety of mafic metasediments often, but not necessarily, metamorphosed to amphibolite grade facies. Schwartzwalder ore is associated with large tensional structures (Illinois and Rogers faults) and their branching horsetail fractures that discordantly transect strata. They contain ore almost exclusively where they cut horizons of garnet-biotite-gneiss (protolith: iron and sulfur-rich pelitic sediment) and quartzite adjacent to hornblende gneiss (mafic volcanite). Regionally, the Schwartzwalder deposit is situated within the mobile belt of the Laramide Orogen a few tens of km away from the Colorado Mineral Belt.

Alteration

Several types of alteration may affect the host rocks. These are commonly restricted to a zone of less than 2 m into the walls from veins. Schwartzwalder veins are selvaged by early carbonatization and sericitization of the mafic wall rock constituents and later hematitization and K-feldspathization (adularia) replacing the earlier alteration products immediately proximal to a vein.

Ore and Associated Minerals

Principal uranium minerals are uraninite, pitchblende, coffinite, and in oxidized zones hexavalent U minerals. Associated minerals can include a variety of sulfides, arsenides, selenides mostly of Fe, Cu, Pb, Zn, Mo and trace amounts of Ag, Co, Ni, Hg, Sb, and others. Gangue minerals may be carbonates (calcite, dolomite, ankerite, rhodochrosite), quartz, chalcedony, adularia, albite, fluorite, baryte and chlorite. All minerals may be present in one or several generations.

Mode of Mineralization

Uranium and gangue minerals form stringers, veinlets, and veins within larger tensional structures and particularly in horsetail fractures which branch away from the main lodes. Mineralization is relatively continuous although grades are highly variable. Abrupt changes in strike and dip of host structures are associated with differences in width of veins and ore quality. Commonly wider structures correspond with lower grades. Sites of branching veins are often marked by high grade ore accumulation.

Age Constraints

There are no age constraints except the restriction to orogenic belts.

Dimensions/Resources

Individual veins (deposits in brackets) may be a few meters to 150 m (<200 m) long, several mm (50 m) to more than 15 m (150 m) wide and m to 150 m (in excess of 1000 m) deep, containing up to >10 000 mt U_3O_8 at (average) grades ranging from 0.2 to 0.4% U_3O_8 occasionally to several % U_3O_8. Districts may contain several 10 000 mt U_3O_8.

Remarks

Class 3.2.1 of vein deposits resembles very much perigranitic vein deposits (3.1.2.1) except for the noticeable absence of a granitic intrusion, and relative continuity of mineralization. Whether the continuity of mineralization is fortuitous and typical only for the Schwartzwalder deposit or whether it is a general rule has not been established.

For more details see Chapter 5.3.5.

Examples of Vein, Class 3.2.1 Not Granite-Related (Monometallic) Deposits/Occurrences in Metamorphic Rocks

Algeria: ? Hoggar region
ČSFR: Rožná, Olší/Moravia, Okrouhlá Radouň, S. Bohemia, Zadni Chodov, Dyleň/ W. Bohemia
France: Retail/Vendée
Mozambique: ?Tete district
Romania: Apuseni Mts., East Carpathians
Sweden: Arjeplog-Arvidsjaur districts
USA: Ascension, Mena/Front Range, Colorado, Coles Hill/Virginia
Russia: ?Vikhorevka/Lake Baykal region

Class 3.2.2: In sediments (polymetallic)

Type Example: Shinkolobwe, Shaba, Zaïre
Reference: Derriks and Vaes 1956

Host Rocks/Structures/Alteration

Host rocks may consist of various sedimentary lithologies. At Shinkolobwe host rocks are dominantly siliceous dolomite and dolomitic and carbonaceous shales, partly affected by Mg-metasomatism with magnesite replacing dolomite. Regionally, Shinkolobwe is located within a fold belt close to the hinge where the fold axis changes direction and the style of folding changes from open to tight overturned folds associated with thrusting. No granites or other intrusives are exposed in the area. At the deposit, host rocks are heavily fractured within a tectonic zone bound by two major faults about 200 m apart at the surface. Due to complex tectonics, flat-lying wedges of impermeable strata formed. They are underlain by more incompetent rocks in which numerous fissures, shears and joints opened, hosting the bulk of the mineralization.

Ore and Associated Minerals

Principal uranium minerals are uraninite (at Shinkolobwe) or pitchblende and alteration products thereof. Associated minerals may include Co-Ni sulfides and selenides, sulfides of Fe, Cu, Mo, Pb, Zn, a.o. and trace amounts of precious metals, phosphates (monazite) etc. Gangue minerals are carbonates (magnesite, dolomite), quartz, chlorite etc.

Mode of Mineralization

Uranium and gangue minerals occur in veins, stockworks, along bedding planes, as breccia matrix, replacement masses, nodules and as disseminated particles and aggregates in the host rocks. Major faults are barren. Mineralization is highly variable in grade and distribution but in general fairly continuous. At Shinkolobwe and other deposits in the Katanga copper belt of Zaïre and Zambia, uranium veins always occur in beds underlying the cupriferous strata, which locally contain anomalously U tenors, at the base of a thick pile of sediments of shallow marine origin.

Age Constraints

No age constraints appear to be valid except a very likely time correlation with regional tectonism associated with an orogeny (in the case of the Shaba copper district the core zone of the Lufilian Orogeny, reflected by granite intrusions and up to amphibolite grade metamorphism runs about 150 km S of Shinkolobwe).

Dimensions / Resources

Individual veins (deposits in brackets) may be m to 10 m (>200 m) long, mm to 1 m (more than 100 m) wide and m to several 10 m (>450 m) deep. Reserves are up to ca. 25 000 mt U_3O_8 at (average) grades ranging from 0.1 to >1% U_3O_8. Districts may contain up to several 10 000 mt U_3O_8.

Remarks

Shinkolobwe and other vein deposits of class 3.2.2 display a vein to stockwork type ore distribution discordant to strata, resembling in many aspects, notably in its ore and gangue mineral association and structural control granite-related vein deposits of class 3.1.2.2. Major differences include absence of granitic intrusions, a relative continuity of mineralization, and in the case of the Katanga copper belt, anomalously uraniferous sediments which may have provided the source for uranium and the associated elements.

For more details see Chapter 5.3.6.

Examples of Vein, Class 3.2.2 Not Granite-Related (Polymetallic) Deposits/Occurrences in Sediments

USA: ? Pitch Mine/Marshall Pass, Colorado
Zaïre: Kalongwe, Swambo/Shaba

4.4 Type 4: Sandstone (Fig. 4.4)

Definition

Sandstone uranium deposits occur in reduced continental fluvial and less commonly in mixed fluvial-marine (arkosic) sandstones that contain, are interbedded with and bounded by less permeable horizons. Primary uranium phases are generally of tetravalent state uranium and consist dominantly of pitchblende and coffinite.

Associated organic material in Phanerozoic (post-Devonian) deposits (type 4a) is of terrestrial plant origin as distinct to marine, algae (?) derived material in Proterozoic deposits (type 4b).

Based on configuration, spatial relation to the depositional and structural environment and/or elemental associations, sandstone uranium deposits may be divided into three overall subtypes and further into classes that can be gradational into each other:

Subtype 4.1: tabular/peneconcordant ((a) Phanerozoic, (b) Proterozoic)

Class 4.1.1: extrinsic carbon (a)
(Westwater Canyon type)
Type Example: Grants Uranium Region, USA

Class 4.1.2: vanadium-uranium (a, b)
Type Example: a) Uravan Mineral Belt, USA,
(Salt Wash type)
b) Mounana, Gabon
(Franceville type)

Class 4.1.3: basal channel (a)
(Chinle type)
Type Example: Monument Valley, USA

Subtype 4.2: rollfront (or roll-type) (Phanerozoic)

Class 4.2.1: continental basin assoc. with detrital carbon
(Wyoming type)
Type Example: Wyoming Basins, USA

Class 4.2.2: mixed fluvial marine assoc. with extrinsic sulfide (South Texas type)
Type Example: South Texas Coastal Plains, USA

Subtype 4.3: tectonic-lithologic

Type Example: a) Grants Uranium Region, USA
b) Mikouloungou, Gabon

[Description of subtype 4.3 is included in sections 4.1.1 and 4.1.2(b)]

References: (a) Adams and Saucier 1981; Adams and Smith 1981; Boyle 1986; Chenoweth and Malan 1973; Crew 1981; Crawley 1983; Grutt 1972; Galloway 1985; Granger and Finch 1988; Grutt 1972; Harshman and Adams 1981; Rackley 1976; Thamm et al. 1981; IAEA/Finch (ed.) 1985; Turner-Peterson et al. (eds) 1986 (b) Diouly-Osso and Chauvet 1979; Gauthier-Lafaye 1986

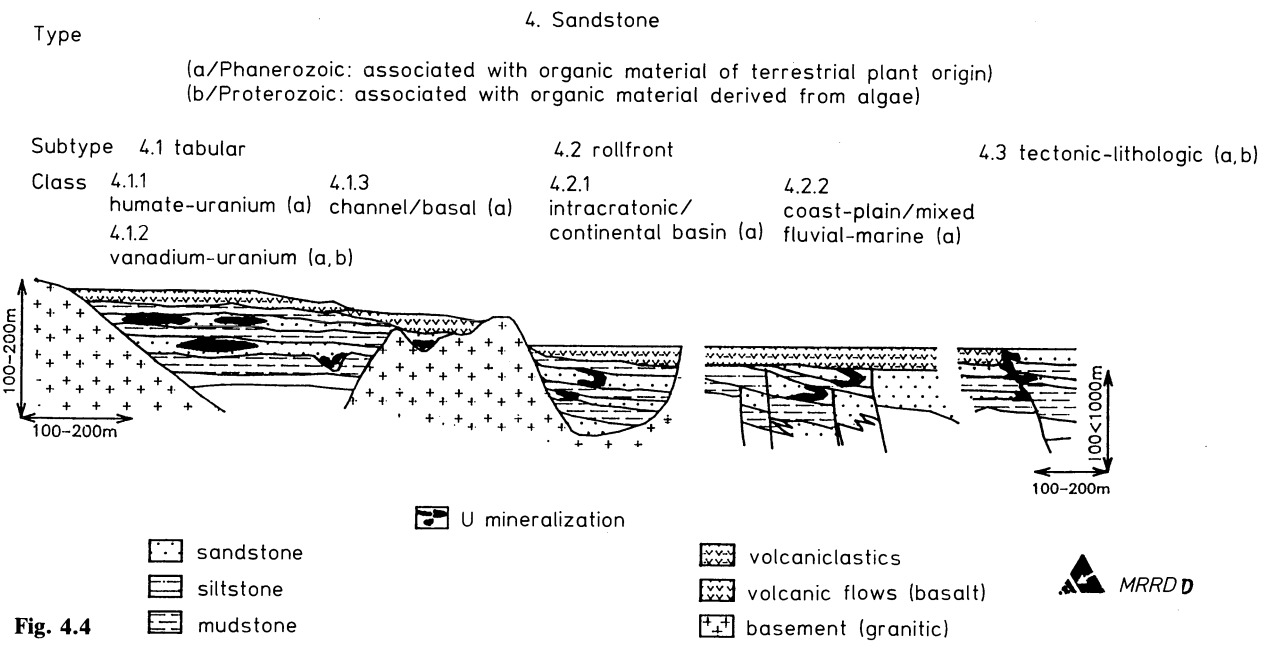

Fig. 4.4

Tabular deposits also referred to as peneconcordant deposits consist of uranium matrix impregnations that form irregularly shaped frequently elongated lenticular masses within selectively reduced sediments. The mineralized zones are, on a large scale, oriented parallel to the depositional trend but, on a small scale, they crosscut sedimentary features of the host fluvial sandstone.

Further subdivision into classes is based on uranium fixing agents such as amorphous organic material of extrinsic origin (e.g., humate), or detrital plant debris of intrinsic origin, or metallic associations (vanadium) that occur in fluvial systems. Deposits in sandstone channels incised into unconformably underlying sediments or crystalline rocks are referred to as basal channel deposits.

The primary mineralization may be redistributed into secondary uranium "stack" deposits in the host sandstone.

Rollfront deposits consist of arcuate zones of uranium matrix impregnations that crosscut sandstone bedding extending from overlying to underlying less-permeable horizons. The zones are convex down the hydrologic gradient. They display diffuse boundaries with reduced sandstone on the down-gradient side and sharp contacts with oxidized sandstone on the up-gradient side. The normally oxidized up-gradient sandstone can also be in a reduced state if it has been re-reduced through the influx or re-introduction of reductants as found in some deposits of class 4.2.2. The mineralized zones are elongate and sinuous approximately parallel to the strike, and perpendicular to the direction of deposition and groundwater flew.

Further subdivision of rollfront deposits is based on emplacement either in intracratonic basins filled with continental fluvial sediments and containing detrital carbon as a potential reductant, or in mixed fluvial-marine sediments of coastal plains containing pyrite and marcasite as potential reductant that originated from influx of H_2S into the host sands.

Tectonic-lithologic deposits are discordant to strata. They occur along permeable fault zones with linguiform impregnation of the adjacent clastic sediments where uranium may form rather thick ore bodies which are also referred to as stack deposits when derived from redistribution of uranium.

Principal Recognition Criteria

Host Environment

- Immature permeable sandstone, feldspathic or arkosic, more rarely quartzose and cherty sandstone, pebble conglomerates or marginal marine or eolean siltstone and sandstone
- Dominantly medium to coarse grain size, rarely fine or very coarse (pebble)-grained
- Mostly cross-stratified and with lenticular bedding
- Coefficient of permeability 75 to 350 l/m^2/day (Austin and D'Andrea 1978)
- Abundance of U precipitants/reductants, particularly carbonaceous material (fragments of woody material ± coalified, humic components, amorphous humate), hydrocarbons (petroleum, "dead oil") and/or sulfides (H_2S, pyrite)
- Tuffaceous material may be present as volcanic debris within host sands, interbedded tuff-rich layers or overlying bentonitic mudstone derived from tuffs
- Often interbedded with impermeable horizons (mudstone)

Mineralization

- Multiple mineralized horizons may exist
- Rollfront deposits are crescent-shaped in cross-section, transgressive to stratification of host sands, in planview they resemble an irregularly laid pipe; roll fronts can occur in multiple superjacent horizons
- Boundaries of mineralized bodies are in some deposits sharp and continuous whereas in other deposits they are highly irregular and diffuse
- Tectonic-lithologic ore bodies of stack type are multi-shaped, sometimes Christmas-tree like, depending on structural distribution and impregnation of permeable horizons adjacent to host structure
- Configuration, size and composition of subtypes seemingly are a function of (a) type and permissivity of aquifer/host sandstone, (b) stratigraphic interbedding of permeable with impermeable beds, (c) kind, mode, and distribution of reductants and/or complexing agents, (d) derivation, hydro-chemistry and flow rate of groundwater system

Age Constraints

- Principal distribution in sediments of middle Paleozoic to Tertiary age, i.e., after development of lush terrestrial vegetation
- Minor in Precambrian sandstones, particularly in those containing carbonaceous material supposedly of algae origin (e.g., Franceville Basin, Gabon)

Metallogenetic Aspects

Generally it is accepted that sandstone uranium deposits are of diagenetic-epigenetic low-temperature origin. Groundwater chemistry and migration are instrumental in uranium leaching from source rocks and its transportation to a chemical interface commonly provided by reducing or complexing agents where uranium is deposited. Essential parameters controlling these processes and localization of uranium mineralization are depositional environment, host rock lithology, permeability, adsorptive/reducing agents, adequate solutions, a uranium source, and apparently an arid to semi-arid climate.

Fluvial, first cycle feldspathic or arkosic sandstones of limited thickness (<10 m) interbedded with layers of fine-clastic sediments deposited in intracratonic basins provide the most favorable host for large and relatively high-grade uranium deposits. A marginal marine environment is also prospective, but to a lesser degree. The presence of uraniferous tuffaceous material either as a constituent of the host sandstone or in the overlying strata may enhance the favorability, due to its potential as a uranium source rock. The feldspar component of the host rock is probably of no direct importance in the mineralizing process, but indicates a granitic source from which the uranium may have originated and an environment of rapid erosion and sedimentation providing the required hydro-physical conditions, particularly permeability for adequate groundwater migration. Impermeable or less permeable strata or other barriers may be instrumental in channeling vertically and laterally uraniferous fluids to favorable sites of uranium deposition, at the same time prohibiting widespread flushing and dilution of fluids.

Uranium is soluble in large quantities only in its hexavalent state. Therefore, uranium-transporting fluids have to be sufficiently oxygenated to keep uranium in solution for transport, and limited to the point that reduction can take place in order to precipitate uranium in ore grade quality and quantity. Complexing agents such as carbonate ions are highly capable of enhancing the solubility and mobility of the uranyl ion in the form of carbonate or other complexes in groundwater that is neutral or alkaline and that may be oxidizing or reducing (Hostetler and Garrels 1962).

For precipitation, the hexavalent uranium in solution must be reduced to the tetravalent state to form pitchblende or coffinite, the principal uranium minerals in most reduced sandstone deposits. Under certain conditions uranium minerals may also crystallize in an oxidizing environment when complexing agents are present, for example vanadium compounds, to fix the uranyl-ion in form of uranyl vanadates which are fairly stable in oxidized rocks. To reduce the hexavalent uranium a reductant is required. Many substances have been invoked as uranyl reductants including ± coalified vegetal, woody fragments (coalification not higher than subbituminous), structureless organic matter (humate), petroleum, "dead" oil, "sour" natural gas, hydrogen sulfide, and pyrite or other sulfides. Bacterial activity is considered by some authors an important factor in producing a reducing environment.

The formation of either tabular or rollfront type deposits occurred in response to specific processes.

Tabular deposits presumably formed stationary in locally reduced zones within oxidized sandstones. Transport of uranium supposedly occurred by weakly alkaline, mildly reducing to oxidizing groundwater capable of keeping uranium in solution as uranyl-carbonate until it was locally precipitated by concentrated reductants, such as humate, plant remains or H_2S, and for chelation or complexing by which organic matter accreted uranium from the groundwater (Schmidt-Collerus 1979). Granger (1976) proposes that peneconcordant deposits remained stationary and accumulated their uranium from waters flowing mainly outside and not through the ore zones as in rollfront deposits. To permit such a mechanism, the author suggests diffusion of uranium ions in the groundwater to the site of deposition along a concentration gradient. The gradient develops by the extraction of uranium from the groundwater flowing marginal to the deposit.

Unlike tabular deposits, rollfront deposits are of dynamic nature. They form at the down-dip migration boundary of an active but short-lived oxidation interface ahead of a pervasive alteration tongue within originally reduced, pyrite-bearing sandstone. The spatial distribution of the altered tongue and unaltered sandstone suggests an oxidizing uraniferous groundwater of neutral to slightly alkaline nature that moved downdip in a confined aquifer in response to a hydraulic gradient. As the oxygenated solution moved downdip in the permeable horizon it penetrates the reduced facies. Organic material and sulfides, mainly pyrite, were destroyed, and ferric iron was produced until the water lost its potential for oxidation. In zones of abundant reductants, such as detrital carbon (commonly plant debris, class 4.2.1) or extrinsic sulfides (H_2S, pyrite, marcasite, class 4.2.2) a distinct geochemical front developed with an abrupt redox interface. At this site and for a short distance ahead of the ferrous/ferric iron interface, the uranium transported in the oxygenated solution is reduced and deposited as pitchblende.

Since the geochemical alteration system was of dynamic nature, the influx of oxidizing groundwater continued. The alteration front "rolled" downflow and spread laterally towards the boundaries of the transmissive host bed. Previously crystallized pitchblende became decomposed and the uranium redistributed across the front for renewed deposition as long as the system was operative. The crescent shape of a rollfront ore body (in cross-section) is considered evidence for the dynamic movement of the front which migrated more rapidly in the more permeable units mostly in the middle part of the sandstone layer.

Most of the rollfront deposits are considered the result of a single major cycle of uplift, erosion, sedimentation, and mineralization by fluids moving in response to the same hydraulic gradients which have been responsible for the sedimentation of the host sandstone. Another variety of rollfront deposits, although very similar to the type described above, are related only to the physical and chemical nature of the host sediments but not to the hydrologic system responsible for the host rock deposition. Instead they originated long after deposition of the host rocks by a second cycle of uplift, erosion, and deposition (Harshman and Adams 1981).

Tectonic-lithologic stack type deposits are in part considered the product of redistribution of primary uranium into permissive hosts such as structures by younger processes as typically found in the Grants Uranium Region, but likewise they may have originated by the introduction of primary uranium as interpreted for some deposits in Gabon (Mikouloungou).

The source of uranium and associated metals in sandstone deposits is considered to be either of uraniferous granitic provenance, or clastic granitic material or felsic volcaniclastics in the host sandstone, or felsic volcaniclastics (e.g., rhyolitic tuff) in overlying and/or underlying beds.

Remarks

Sandstone uranium deposits are commonly of low to medium grade (0.05–0.4% U_3O_8) and of small to large size, up to 50 000 mt U_3O_8 rarely more, but districts may have substantial resources of several 100 000 mt U_3O_8.

Examples of Sandstone, Subtype 4.1, Tabular Deposits/Occurrences (Not Differentiated)

(C = Cenozoic, M = Mesozoic, P = Paleozoic, PC = Precambrian)
Argentina: Tonco-Amblayo (M)/Jujuy-Bolivian Basin, Los Colorados (M)/Paganzo Basin, Sierra Pintada (P)/San Rafael Basin, Malargue (M)/Neuquén Basin, Pichiñan/Chubut (M)
Australia: Angela (P)/Amadeus Basin, Malbooma (P)/Drummond Basin, Mulga Rock (P)/Officer Basin, Westmoreland (PC)/Queensland, Manyingee W.A.
Brazil: Figueira (P)/Paraná Basin
Bulgaria: Orranovo-Simitli Basin (C), Eleshnitza district (C), W. Balkan Mts. (P)
China: Mengqiguer, Daladi, Kashi (M)/Zhungel-Tianshan U prov., Jianchang, Quinlong, Langshan areas (M)/Yinshan-Liaohe U prov., Wudang-Huaíyong Massif (M)/Qilian-Qinling U prov., South Lancang River, Gaoligong (C)/W. Yunnan U prov., Tunling (M)/Jingan Basin
ČSFR: Hamr-Stráz (M)/North Bohemian Basin
Germany: Königstein (M)/Elbsandsteingeb., Müllenbach (P)/Black Forest
Gabon: Oklo (PC)/Franceville Basin

France: Coutras (C)/Aquitaine Basin, Lombre (P)/Cerilly Basin
Hungary: Pecs (P)/Mecsek Mountains
Madagascar: Antsirabe Basin (C)
Niger: Akouta, Arlit, Ebala, Madaouela, (P), Azelik, Imouraren, Takardait, (M)/Agades Basin
Pakistan: Dera Ghazi Khan area (C)
Romania: Apuseni Mts (P), Banat (P)
South Africa: Beaufort West (P)/Karoo Basin
Spain: Mazarete (M)
USA: Colorado Plateau (P + M), Sherwood (C)/Washington, Tallahassee Creek (C)/Colorado, Anderson (C)/Date Creek Basin, Arizona
Slovenia: Zirovski vrh (P)
Russia: Stavropolsky, Pyatigorsk, Kislovodsky, Lermontovsky (P)/Caucasus

Examples of Sandstone, Subtype 4.2 Rollfront Deposits/Occurrences (Not Differentiated)

Australia: Beverley (C)/Lake Frome Basin, Manyingee (M)/Carnarvon Basin
Bulgaria: Tracien Basin (C)
Mexico: La Sierrita (C)/Burgos Basin
Niger: Akouta (P)/Agades Basin
USA: Wyoming Basins (C), Black Hills (C + M)/South Dakota, Crow Butte (M)/Nebraska, Weld County (M)/Colorado, Texas Coastal Plain (C)
Uzbekistan: Uchkuduk (M), Sugraly (M), Lyavlyakan (C), Beshkak (C), Bukinay (M), Kanimekh (M)/Navoi region, Kyzylkumsky

Examples of Sandstone, Subtype 4.3 Tectonic-Lithologic Deposits/Occurrences

Australia: Red Tree (PC)/Westmoreland
France: Mas Lavayre (P)/Lodéve Basin
Gabon: Mikouloungou, Mounana (PC)/Franceville Basin
USA: Ambrosia Lake district (M)/Grants region

4.4.1 Subtype 4.1: Tabular/peneconcordant

Class 4.1.1: Extrinsic carbon (Westwater Canyon type) (Phanerozoic)

Type Example: Grants Uranium Region, San Juan Basin, USA

References: Adams and Saucier 1981; Granger and Finch 1988; Turner-Peterson et al. (eds) 1986

The subsequent summary also addresses class 4.3.1, tectonic-lithologic stack deposits, as found in the Grants Uranium Region spatially associated with class 4.1.1 deposits.

Host Rocks/Structures

Type example is uranium mineralization in the Westwater Canyon Member of the Late Jurassic Morrison Formation, Grants Uranium Region, New Mexico, USA.

Host rock is fine- to coarse-grained, poorly sorted, cross-bedded mostly light yellow-brown to gray arkosic sandstone, containing small pebbles and cobbles and thin seams or beds of gray mudstone and siltstone. Sandstone consists of 50 to 90% quartz, 5 to 35% feldspar, up to 30% chert and less than 0.5% heavy minerals. White clusters of kaolinite are common. Other matrix materials are calcite, iron oxides, and clay. Amorphous carbonaceous material in the form of humate fills interstices and coats sand grains. Permeability ranges from low to high. Thickness of the host unit ranges from one to several tens of meters. The Westwater Canyon Member is overlain by a greenish-gray bentonitic (tuffaceous) siltmudstone of the Brushy Basin Member. Sand to mud/shale ratios are 1:1 to 2:1 for the Morrison Formation within the mineral belt. Depositional environment of the host sequences is an extensive coalescing alluvial fan system developed by aggrading braided streams within a continental basin (San Juan Basin). Source area of the host rocks is granitic terrane and volcanic air-fall ash and tuffaceous material.

Regional tilting associated with major N-S faulting developed during the Laramide Orogeny and caused redistribution of primary uranium mineralization into roll-type and, near structures, into class 4.3.1 "stack" deposits.

Alteration

Both oxidation and either a single or multiple episodes of reduction have altered the host rocks. Hematitization and weak limonitization characterize oxidized facies. Reduced facies display destruction of detrital feldspar, volcanic ash, magnetite and ilmenite associated with sulfidization (mainly pyrite), kaolinitization, chloritization, albitization, montmorillonitization, and

carbon (humate) formation. Calcitization and minor silicification cemented the units. The carbon with which the uranium is associated was introduced into the sandstone from adjacent silt-mudstones during compaction.

Ore and Associated Minerals

Principal ore minerals are pitchblende, coffinite and uraniferous humate present in reduced ore. Locally hexavalent U minerals occur in oxidized ore. Associated minerals of As, Ba, Fe, Mo, Sb, V, and others are commonly present in trace amounts. Pyrite is more abundant.

Mode of Mineralization

Class 4.1.1 mineralization is characterized by the association of uranium with humate in isolated and stacked peneconcordant lenses. Uranium minerals occur as disseminations coating sand grains, filling small interstices and partly replacing feldspar in the host sandstone. Primary mineralization occurs in multiple horizons commonly concomitant with humate. Mineralized zones are lenticular or tabular, peneconcordant elongated parallel with the paleochannel systems which are termed blanked or trend ore. Boundaries between mineralization and host rocks are irregularly shaped. Redistributed mineralization is within structures and also displays features of rollfront character developed proximal to fault and fracture zones that cut primary peneconcordant bodies. Redistributed uranium forms much thicker ore bodies than those of primary tabular mineralization and is therefore referred to as a stack deposit.

Dimensions/Resources (Grants Uranium Region)

Individual tabular deposits ("stack" deposits in brackets) may be several tens of meters to 2000 m (<100 m) long, several meters to several 100 m (a few m to 40 m) wide, a few centimeters to 5 m (few m to 50 m) and in excess of 1500 m deep, containing several tens and up to 50 000 mt U_3O_8 at (average) grades ranging from 0.1 to 0.4% U_3O_8 occasionally to >1% U_3O_8. Districts may contain up to 300 000 mt U_3O_8.

Remarks

The Grants Uranium Region is 175 km long and up to 80 km wide and includes five mining districts and other prospective districts. It constitutes the largest single known sandstone uranium region in the western world.

For more details see Chapter 5.4.1.

Examples of Sandstone, Class 4.1.1 Tabular, Extrinsic Carbon Deposits/Occurrences

France: Lodève Basin (P) ?, Aquitaine Basin (C) ?
South Africa: Beaufort West (P)/Karoo Basin

Class 4.1.2: (a) Vanadium-uranium (Salt Wash type) (Phanerozoic)

Type Example: Uravan Mineral Belt, Colorado Plateau, USA
Reference: Thamm et al. 1981

Host Rocks/Structures

Type example is V-U mineralization in the Salt Wash Member of the Late Jurassic Morrison Formation as present in the Uravan Mineral Belt, Utah-Colorado, USA.

Host rock is a fluvial fine- to medium- and coarse-grained feldspathic to quartzose sandstone. This unit ranges from 50 to 120 m thick, is red, brown or gray in color, and contains 5 to 25% tuffaceous material and abundant organic debris in the form of logs and fragments of vegetal trash. These materials accumulated particularly at sites where paleochannels change direction, in mud bars or changes in stream load carrying ability. Sandstone layers are interbedded with reddish and gray siltstones and bentonitic mudstones. The Salt Wash Member is part of a coalescing alluvial fan formed by a system of aggrading braided streams. The Uravan Mineral Belt occupies a transversal zone where grain size of the sandstone is transitional from medium to fine. Source area for Salt Wash sediments was the granitic Mogollon Highland.

Positive areas formed by salt diapirs and associated anticlines within the basement controlled river orientation and facies pinchouts during Salt Wash time.

Alteration

Reduction alteration is recognized chiefly by color changes and is most obvious in mudstones

turning from purplish or reddish to gray-green at contacts with mineralized sandstones which are stained light yellow-brown. Common authigenic transformations include pyritization, calcitization, and argillitization. Detrital ilmenite and magnetite are corroded.

Ore and Associated Minerals

Principal ore minerals in reduced zones are pitchblende, coffinite, and vanadium minerals. Oxidized zones are dominated by uranyl vanadates, commonly carnotite and tyuyamunite. Associated minerals are pyrite and marcasite. Mo, Cu and Se minerals occur in trace amounts. Vanadium-uranium ratio is 5:1 to 10:1 in the Uravan Mineral Belt and in other Salt Wash districts 1:1 to 15:1.

Mode of Mineralization

Class 4.1.2 mineralization is characterized by vanadium-uranium associated with plant debris. Mineralization occurs as disseminations filling pore spaces, coating sand grains and replacing interstitial clay, organic substances, and cementing material. U-V minerals have accumulated in commonly small pods which locally are highly mineralized tree trunks. The pods may display shapes ranging from tabular, concordant to bedding to roll-type. Deposits consist of clusters of pod-like bodies aligned parallel to the paleochannel, where they may occur in several superjacent sand horizons. Distribution of deposits is rather erratic.

Dimensions/Resources (Uravan Mineral Belt)

Individual deposits (ore trends in brackets) may be up to 200 m (up to a few km) long, <1 m to 100 m (several 100 to 1000 m) wide, several centimeters to 10 m thick, containing <1 to 2500 mt U_3O_8 at (average) grades ranging from 0.1 to 0.5% U_3O_8 occasionally to >1% U_3O_8. Districts may contain up to 50000 mt U_3O_8. Vanadium grades may range from <0.5 to >3% V_2O_5.

Remarks

The Uravan Mineral Belt is the largest known V-U district in the USA. Most other districts with similar mineralization associated with Salt Wash sandstone had resources of a few hundred to several thousand tonnes uranium.

For more details see Chapter 5.4.2.

Examples of Sandstone, Class 4.1.2(a), Tabular, Vanadium-Uranium Deposits/Occurrences

Argentina: Rodolfo (C)/Cosqin district
Australia: Bigrlyi (P)/Ngalia Basin
USA: La Sal-La Sal Creek (M), Lukachukai-Carrizo (M), Henry Mountains (M)/Colorado Plateau

Class 4.1.2: (b) Vanadium-uranium (Franceville type) (Proterozoic)

Type Examples: Franceville Basin, Gabon
4.1.2.1 tabular: Oklo, Gabon
4.1.2.2 tectonic-lithologic: Mounana and Mikouloungou, Gabon

References: Diouly-Osso and Chauvet 1979; Gauthier-Lafaye et al. 1980

Both type examples occur in the same stratigraphic horizon and show a number of similar features except for the structural component of mineralization and respective configuration of ore bodies. The subsequent synopsis addresses both subtypes together.

Host Rocks/Alteration/Structures

Continental sandstone and arkose containing redistributed marine carbonaceous matter. The uranium hosting unit is overlain by carbonaceous shales and rests on early Proterozoic granite and gneiss. Folding and faulting distorted the sediments. No apparent alteration except some silicification.

Ore and Associated Minerals

Pitchblende and coffinite in reduced zones, and uranyl vanadates and phosphates in oxidized zones. Associated minerals include in reduced mineralization karelianite, montroseite, roscoelite, and minor amounts of pyrite, marcasite, melnicovite, galena, sphalerite, chalcopyrite, baryte, and calcite as fissure fillings.

Mode of Mineralization

Uranium is in tabular deposits (Oklo) concentrated predominantly in fluvial sands in the form

of microcrystalline pitchblende within the organic matrix and occurs preferentially on the flanks or rims of paleochannels or where an intermediate thickness of sandstone is combined with high concentrations of organics. Mineralization of the tectonic-lithologic subtype occurs in the same organic-rich sedimentological environment but displays a strong affinity to cataclastic zones adjacent to uplifted crystalline basement (Mounana) or to an overthrust of carbonaceous shales (Mikouloungou).

Age Constraints

A certain age constraint is imposed by the required development of organic creatures (algae) in a continental environment.

Dimensions/Resources

Tabular deposits are up to 900 m long, 600 m wide, and several meters thick and contain as much as 13 000 mt U_3O_8 at a grade of ca. 0.4% U_3O_8. Tectonic-lithologic deposits range up to 100 m long, 40 m wide and 120 m deep, containing up to 6000 mt U_3O_8 at a grade of 0.2 to 0.6% U_3O_8. The Franceville district, Gabon, accounts for approximately 25 000 mt U_3O_8.

Remarks

Although uranium occurrences are not uncommon in Proterozoic sandstone displaying the above-listed features, the Franceville Basin is the only one known to contain minable U deposits.

For more details see Chapter 5.4.8.

Examples of Sandstone, Class 4.1.2(b), Proterozoic Deposits/Occurrences

Australia: Westmoreland/Queensland, Pandanus Creek/Northern Territory

Class 4.1.3: Basal-channel (Chinle type)

Type Example: Monument Valley, Colorado Plateau, USA
Reference: Chenoweth and Malan 1973

Host Rocks/Structures

Type example is uranium mineralization in the Shinarump Member of the Late Triassic Chinle Formation, as exposed in the Monument Valley, Utah, USA. Host rock is a fluvial medium- to coarse-grained conglomeratic, crossbedded, poorly sorted, lenticular arkosic sandstone. This unit ranges from 3 to 75 m thick, is gray-yellowish and red to brown in color and contains interbedded greenish-gray mudstone and siltstone. Carbonaceous material, logs, and fragments of vegetal trash are locally abundant, especially at bends, meanders of the paleochannels, in mud bars or where changes in stream load carrying ability occurred. The sediments deposited by degrading anastomosing streams incising distinct, relatively narrow channels into flood plains consisting of red siltstone of the Moenkopi Formation in the Monument Valley.

In other regions, deposits may occur in extensive blanket sands formed in braided fluvial systems that either unconformably overlie or are eroded into underlying sedimentary or crystalline rocks. Local areas of moderate relief controlled river flow and pinchouts during deposition of the Shinarump Member.

Alteration

Reduction reflected by bleaching of the originally red and brown sandstone to light gray, cream to yellowish and greenish colors is the most obvious alteration. Calcitization caused cementing of sandstone (up to 15% $CaCO_3$).

Ore and Associated Minerals

Principal ore minerals in reduced zones are pitchblende, coffinite and locally vanadium minerals (montroseite, corvusite). Oxidized zones are dominated by hexavalent U minerals and uranyl vanadates. Associated minerals can include sulfides of Cu, Fe, Mo, Pb, Zn, and minerals containing Ag, Cd, Cr, Co, Ni, Se, Sr. In several districts V_2O_5 contents exceed U_3O_8 contents (V:U ratio 1:2 to 7:1).

Mode of Mineralization

Class 4.1.3 mineralization is characterized by uranium associated with plant debris deposited in distinct channels preferentially in their basal parts or scours cut into underlying formations. This situation is in principle also valid for mineralization in all other members of the Chinle Formation. Uranium minerals impregnate sandstone

voids, coat sand grains, replace quartz grains, clay particles and particularly fossil plant debris, and fill vertical fissures beneath the scour base. Most deposits are of small size. They consist of closely spaced lenticular pods which are generally concordant with the bedding. Localization of deposits within channels is controlled by the abundance of carbonaceous trash which otherwise accumulated at inhomogeneities of paleochannels.

Dimensions/Resources

Individual deposits (ore trends in brackets) may be a few meters to 300 m (a few kilometers) long, <1 m to more than 100 m (several 100 m) wide and <0.2 to 3 m (<15 m) thick, containing 1 to several 100 mt U_3O_8 at (average) grades ranging from 0.1 to 0.35% U_3O_8 occasionally to 0.5% U_3O_8. Districts may contain up to 5000 mt U_3O_8.

Remarks

Class 4.1.3 deposits resemble those of class 4.1.2 except that the vanadium content is commonly lower and that the deposits are restricted to distinctly developed paleochannels and generally to only one horizon.

For more details see Chapter 5.4.3.

In some countries, e.g. Okanagan region (Blizzard deposit), British Columbia, Canada, and Central Honshu (Tono, Ninyo-Toge), Japan, U mineralization occurs in sand filled channels incised into a basement which includes uraniferous granites. U is thought to have been leached from the granites and redeposited in the channel sands. (For details see Boyle 1982b, 1985, 1986, Katayama et al. 1974, Katayama and Kamiyama 1977)

Examples of Sandstone, Class 4.1.3 Tabular, Basal Channel Deposits/Occurrences

Australia: ? Mulga Rock (P)/Officer Basin, Yarramba (C)/Lake Frome Basin, Manyingee (C)/Carnarvon Basin
Canada: Blizzard, Tyee (C)/Okanagan Highlands
France: St. Pierre du Cantal (C)/Massif Central
Japan: Ningyo-Toge (C), Tono (C)
USA: White Canyon, Lisbon Valley (M)/Colorado Plateau

4.4.2 Subtype 4.2: Rollfront

Class 4.2.1: Continental basin, associated with detrital carbon (Wyoming type)

Type Example: Wyoming Basins, USA
References: Crew 1981; Harshman and Adams 1981

Host Rocks/Structures

Host rocks are Upper Cretaceous and Tertiary poorly consolidated medium- to coarse-grained, poorly sorted arkoses to feldspathic sandstones that range from a fraction of 1 m to 100 m thick (av. less than 30 m). Thin discontinuous beds of mudstone, some pebbles of crystalline rocks or mudstone, and tuffaceous debris may be interstratified. Pyrite and carbonaceous matter in the form of woody remains and masses of humic components are abundant. In some basins natural gas and methane are present. The host sands are regionally transmissive, providing conduits for groundwater migration downdip. Mineralized sands are part of a stratigraphic sequence of alternating sandstone, siltstone and bentonitic mudstone deposited predominantly by braided streams in wedge-shaped coalescing alluvial fans with overbank flood plains. Sand/shale ratios range from 1:1 to 4:1 in the host formations. Provenance of the host sediments are granitic highlands surrounding the basins, and reworked pre-existing sediments. Volcanic air-fall ash and tuff contributed to the sedimentary pile and occurs either as constituent of the mineralized sands, interbedded tuffaceous rich layers or in superjacent bentonitic mudstone.

The attitude of the mineralized beds is commonly very shallow, usually dipping less than 5°. Steeper dips up to 25° exist locally. Minor faults dissect the mineralized horizons. Tilting of some basins subsequent to ore formation (Shirley Basin and Gas Hills) caused a reversal in the groundwater flow resulting in incipient destruction of mineralized zones. Regional controls for the mineralized paleodrainage system included regional tectonic movements which were instrumental in intracratonic downfaulting of basins of restricted dimensions in the foreland of fold belts. Graben structures have controlled paleodrainage systems. Intraformational unconformities appear to be influential on groundwater migration.

Alteration

Alteration effects vary to some degree from basin to basin depending on mineral constituents in host sands. The most conspicuous is hematitization and limonitization associated with decomposition of pyrite in some basins. In other basins pyrite corrosion, argillitization of feldspars and montmorillonitization of tuffaceous components may be more dominant. Normally, gray, tan, or pink sandstones are bleached by mineral forming solutions to cream or light gray hues. Formation of Fe-rich montmorillonite imparts greenish-yellowish colors to the rock.

Ore and Associated Minerals

Principal ore minerals are pitchblende and coffinite with associated pyrite, marcasite, hematite, ferroselite, native selenium and calcite. Minerals of Cu, As, P, and others may be present.

Mode of Mineralization

Uranium mineralization follows the redox front separating nonoxidized from oxidized sandstone. The mineralization transects the stratification of the host beds and is thus discordant with the strata. In cross-section, the form of a deposit resembles a crescent. In plan view, a deposit appears like a sinuous, irregularly laid pipe following the geochemical front of invading oxidation. The uranium minerals impregnate interstices of the sandstone and coat sand grains. Pitchblende and coffinite are concentrated in the front part of the redox zone, ferroselite has formed on the concave side, whereas native selenium, jordisite, and calcite typically occur on the convex side of the rollfront.

Dimensions/Resources

In the apex segment of the rollfront the thickness or height of mineralization ranges from a few tens of cm to 10 m and rarely 15 m, decreasing in the tails to zero. The width normal to strike (parallel to cross-section) varies between a few centimeters and several 100's m. The length along the strike may extend up to several kilometers.

Resources range from a few tonnes to several 1000's of mt U_3O_8 in individual deposits at grades averaging between 0.05 and 0.25% U_3O_8, rarely up to 0.5% U_3O_8 or more. Districts contain several 10 000 mt U_3O_8 (65 000 mt U_3O_8 in Gas Hills, Windriver Basin).

Remarks

For more details see Chapter 5.4.4.

Examples of Sandstone, Class 4.2.1 Rollfront, Continental Basin Associated with Detrital Carbon Deposits/Occurrences

Australia: Honeymoon, Beverley (C)/Lake Frome Basin, Manyingee (M)/Carnarvon Basin
USA: Gas Hills (C), Powder River Basin (C), Shirley basin (C), Red Desert (C)/Wyoming, Black Hills (M)/South Dakota, Weld County (M)/Denver-Julesburg Basin

Class 4.2.2: Mixed fluvial-marine, associated with extrinsic sulfide (South Texas type)

Type Example: South Texas Coastal Plain, USA
a) Fluvial-marine: Panna-Maria; b) Fluvial: Benavides
References: Adams and Smith 1981; Galloway 1985

Host Rocks/Structures

Host rocks consist of a variety of fluvial to marginal marine, poorly consolidated sandstones that range from 5 to 20 m thick. These units are interbedded with or overlain by volcanic ash or tuffaceous beds of several formations. Host rocks include

a) *fluvial-marine* fine-grained carbonaceous, tuffaceous, quartzose sandstone and greywacke interbedded with blackish shale and lignite deposited as lagoonal, deltaic and barrier bar sediments under shallow water, nearshore marine or brackish water conditions;

b) *fluvial* fine- to coarse-grained sands interbedded with bentonitic mudstone of an aggrading stream system and fine-grained feldspathic sands containing only minor vegetal debris, deposited in a fluvial-alluvial fan, stream and interchannel floodplain environment.

The sandbeds are locally along faults, invaded by hydrocarbons, methane and H_2S. Distribution of mineral trends is controlled by broad scale sedimentary features such as megachannel systems.

Faulting is extensive in the South Texas Coastal Plain. A series of growth faults trending parallel to the coast line permitted influx of hydrocarbons, H_2S and methane into the host sands. Likewise active salt domes, while creating favorable environments for petroleum reservoirs, also permitted migration of gases.

On a regional tectonic scale, all known uranium occurrences are confined to the Rio Grande Embayment.

Alteration

Several stages of reduction, oxidation, and re-reduction affected the host rocks, in part similar to the alterations in the Wyoming Basins (class 4.2.1). Processes include pyritization, marcasitization, hematitization, corrosion, and argillitization of feldspars, silicification, calcification, destruction of heavy minerals and montmorillonitization of pyroclastics. H_2S introduced along faults before ore formation reduced the host sands and prepared the hosts for rollfront development.

Ore and Associated Minerals

Principal ore minerals are pitchblende and coffinite commonly present as poorly crystalline, minute particles. Associated elements include Mo, Se, V, and P. In oxidized zones a variety of hexavalent U minerals have formed.

Mode of Mineralization

Uranium has accumulated in both peneconcordant blanket type, and rollfront deposits along paleochannels. Roll-type deposits greatly resemble those in the Wyoming Basins.

Dimensions/Resources

Rollfront deposits vary from 0.5 to 7.5 m in thickness, 10 to 100 m in width and are up to 10 km long. Individual deposits contain several 100 to 5000 mt U_3O_8, rarely up to 10 000 mt, at grades between 0.05 and 0.2% U_3O_8. Total resources of the South Texas Coastal Plain district are estimated at up to 80 000 mt U_3O_8 at an average grade of about 0.1 to 0.2% U_3O_8.

Remarks

For more details see Chapter 5.4.5.

Examples of Sandstone, Class 4.2.2 Rollfront, Mixed Fluvial-marine Associated with Extrinsic Sulfide Deposits/Occurrences

Karnes, Live Oak, Duval and Webb Counties districts (C)/Texas Coastal Plains, (?) Crow Butte (M)/Great Plains, Nebraska

4.5 Type 5: Collapse Breccia Pipe

(Fig. 4.5)

Definition

Collapse Breccia Pipe deposits occur in more or less circular (10–300 m in diameter) and vertical (up to 1000 m deep) collapse structures filled with down-dropped coarse fragments and fine matrix of the penetrated sediments. Uranium mineralization is predominantly confined to particular intervals of permeable (± sandy) matrix material and to arcuate bounding fractures (annular ring). Principal uranium phase is pitchblende, which is commonly accompanied by a variety of ore (Cu, Ag, etc.) and gangue minerals.

Type Example: Orphan Lode and Hack Canyon, Arizona Strip area, USA

References: GSA/Wenrich and Billingsley (eds.) 1986; Wenrich and Sutphin 1989

Principal Recognition Criteria

Host Environment

- Mineralized structures are roughly circular and vertical, extending from karst caverns in a basal limestone upward through flat-lying beds of alternating shales, siltstones, sandstones, and impure limestones occasionally as high as into uraniferous sandstones
- Pipes are filled with highly brecciated material composed of fragments and matrix material of the various penetrated lithologies
- Uranium mineralized pipes appear to be restricted to an area covered or formerly covered by sandstones that locally contain uranium deposits (Chinle Formation)
- Pipes are bounded by a set of concentric, circular fractures termed annular ring

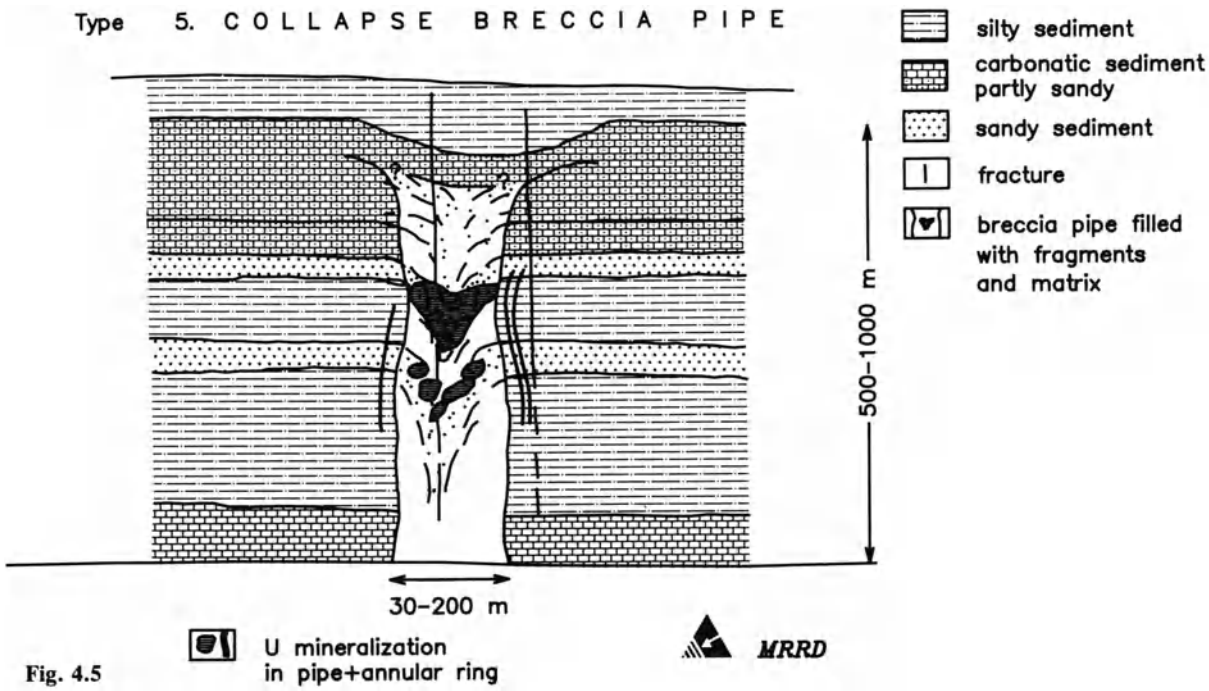

Fig. 4.5

Alteration

- Bleaching of red sediments, carbonatization, silicification, and some sulfidization of pipe infill and immediately adjacent wall rocks
- Alteration is commonly of weak intensity and little extension from pipe into wall rocks

Mineralization

- Principal U phases are pitchblende and coffinite and alteration products thereof
- Associated minerals include sulfides, arsenides, and locally oxides, carbonates and sulfates of Fe, Cu, Ni, Co, Mo, Pb, Zn, As and trace amounts of Ag, Au, Hg, Sb and V
- Gangue minerals include calcite, dolomite, siderite, baryte, collophane, chalcedony, quartz, gypsum, and anhydrite
- Uranium minerals occur (a) as veinlets and stringers in fractures within and surrounding the pipe, (b) as stratiform disseminations in porous sandstone blocks and irregular impregnations of the matrix within the pipe interior
- U mineralization is particularly associated with sand dominated pipe segments
- Sulfides are disseminated through most of the pipe
- Pyrite is enriched up to 15% in mineralized zones and often forms together with marcasite a sulfide cap (3–15 m thick, up to 80% sulfide) above the uppermost U mineralization

Age Constraints

No principal time constraint except that the type of sedimentation, hydraulic groundwater systems (karst development) and provision and transport of sufficient uranium require a coincidence of certain climatic conditions that prevail only during restricted periods in earth history.

Metallogenetic Aspects

The metallogenesis of uranium mineralization in collapse breccia pipes of the Arizona Strip type is still enigmatic. Uranium is thought to have entered a pipe either through sandstone aquifers interbedded with the sedimentary sequence or through structures extending upwards into overlying uraniferous sandstone horizons or perhaps through both. The pipe structure formed by stoping from a karst cavern upwards through the flat-lying sediments possibly along joint or fracture systems. Sulfur, organic material, and other elements may have derived from surrounding sediments or may have been introduced from basal lithologies by upward migration.

Dimensions/Resources

Pipe diameters range from 10 m to more than 300 m, averaging less than 100 m. Within the pipe, mineralization is restricted to variably wide sandy sections, and fissures. Vertical extension of mineralized intervals (commonly one rarely two) ranges from few meters to more than 100 m. Resources of individual pipes are few tonnes to about 2500 mt U_3O_8 at grades between 0.3 and 1% U_3O_8. Known reserves of the Arizona Strip area are about 15 000 mt U_3O_8. Au, Ag, and/or Cu have been recovered from some pipes.

Remarks

Although of small size, collapse breccia pipe deposits represent low cost uranium resources due to their high grades.

For more details see Chapter 5.5.

Examples of Type 5: Collapse Breccia Pipe Deposits/Occurrences

USA: Canyon, Easy 1, Kanab North, Mohawk, Pigeon, Pine Nut/Arizona Strip area

4.6 Type 6: Surficial (Fig. 4.6)

Definition

Surficial uranium mineralization may be defined as young near-surface uranium concentrations either stratabound in predominantly unconsolidated surficial formations/sediments proximal or superjacent to uraniferous source rocks or structure-bound within source rocks. Uranium occurs in mineral form almost exclusively as uranyl species or otherwise adsorbed on host constituents. Thorium is absent.

Based on host environment, four principal subtypes and some classes are recognized:

Subtype 6.1: duricrusted sediments

Class 6.1.1: fluvial/valley-fill
Type Example: Yeelirrie, Australia
Class 6.1.2: lacustrine/playa
Type Example: Lake Maitland, Australia

Subtype 6.2: peat-bog

Type Example: Stevens Co., Washington state, USA

Subtype 6.3: karst-cavern

Type Example: Pryor Mts, USA

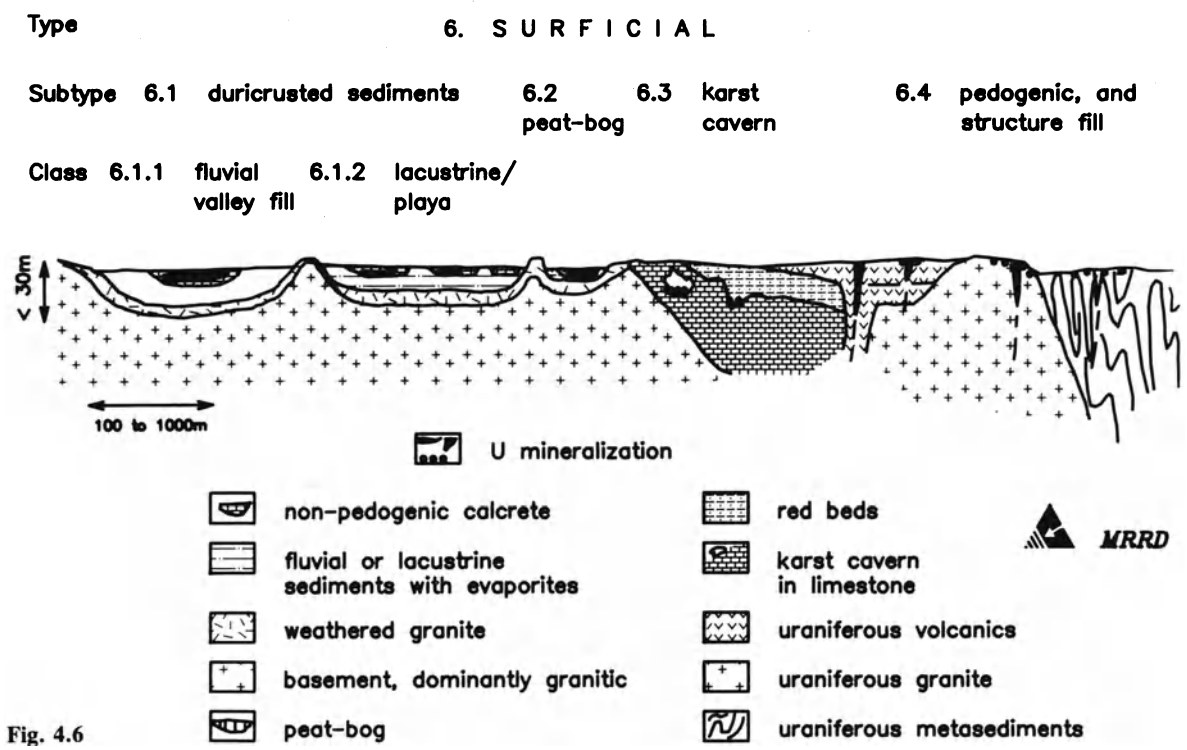

Fig. 4.6

Subtype 6.4: surficial pedogenic and structure fill

Type Example: Daybreak, USA; Cotaje, Bolivia

References: Bell 1963; Butt et al. 1984; Cameron 1984; Cavaney 1984; Carlisle 1983; Hambleton-Jones 1984; IAEA/Toens (ed) 1984; Johnson et al. 1987; Mann and Deutscher 1978; Pardo-Leyton 1985; U.S.-AEC 1959

The four subtypes are characterized by

1. *Duricrusted shallow sediments* in arid to semi-arid climates consisting of fluvial, alluvial and eolian channel fills and associated playa-marginal deltas, evaporative lacustrine basins, or alkaline and saline playas, cemented or replaced along the groundwater table by carbonates, silica and sulfates in form of nonpedogenic calcrete, dolocrete, silcrete, gypcrete. Organic matter is absent or occurs in insignificant amounts (subtype 6.1).
2. Highly *vegetal organic and clay-rich* shallow depressions in humid climates (6.2).
3. *Karst caverns* in limestone having a floor cover of fallen blocks, chert fragments and other insoluble residues of limestone embedded in a matrix of reddish-brown sand, silt and clay that may be loosely consolidated or cemented by silica (6.3).
4. *Surface-bound mineralization* (a) in pedogenic formations including soils and crustations such as pedogenic calcrete, silcrete, gypcrete, laterite/ferricrete etc. and (b) as joint and fracture filling (6.4).

Principal Recognition Criteria

Host Environment

- Variety of surface-bound settings (see above), capable of precipitating uranium and associated elements by reduction, complexing, adsorption, etc. from ground- or surface waters
- Hydrogeochemistry of ground- or surface waters enriched in U and other elements
- Zones of fluctuating groundwater table, and/or lateral groundwater migration within the host rocks
- Internal drainage, i.e., ± closed basins for subtype 6.1
- Absence of cover rocks
- Adequate nearby source for uranium and other elements (often but not necessarily uraniferous granitic complexes)
- Adequate humid climatic conditions for chemical weathering and liberation of ore-forming elements and arid enough to deposit the elements in intermontane or intracratonic environments and militating against flushing out of the newly formed minerals and as such preserving the mineralization (particularly important for subtype 6.1)

Mineralization

- Almost exclusively uranyl minerals, dominantly uranyl vanadates in subtypes 6.1 and 6.3; uranyl phosphates in subtype 6.4
- Much of the uranium adsorbed on host soil constituents (organic substances, clay minerals, etc. particularly in subtype 6.2)

Remarks

For details on mineralogy and petrography of surficial uranium occurrences see Pagel (1984).

Age Constraints

Restricted to recent times (estimated at less than 1 m.y. old).

Metallogenetic Aspects

Surficial uranium concentrations can generate in a wide range of geological and climatic environments provided

- an adequate source of ore forming elements is present,
- the climate promotes uranium mobilization and redeposition,
- adequate hydrologic and geomorphologic regimes exist for mobilization and transport of the ore-forming elements and their trapping in potential sites for ore formation such as ancient and recent valleys, basins, and structure zones,
- the lithology of potential hosts warrants precipitation and accumulation of uranium.

The source of uranium and other elements is only empirically deduced. Since essentially all surficial uranium deposits occur in regions containing uraniferous intermediate to felsic intrusive or extrusive rocks or uraniferous (meta) sediments it

is thought that these rocks provided the commodities required. For example, all duricrust type occurrences in the Yilgarn Block, Australia, occur in terrane dominated by late Archean granite containing partly 8–10 ppm U with maxima of 80 ppm U (Gamble 1984). A similar situation is given for the deposits in the Namib Desert that occur in regions with outcrops of Proterozoic granites, pegmatites, migmatites, many appreciably anomalous in uranium. Structure-controlled mineralizations on the Altiplano, Bolivia, are hosted by Tertiary rhyolitic ignimbrites containing up to 95 ppm U (Leroy et al. 1985). It is for this spatial relationship of surficial uranium occurrences to uraniferous complexes and the general high U content in groundwaters of the catchment area within these complexes that most authors consider them as the source of uranium and most other calcrete related elements. Vanadium poses a problem. No conclusive evidence for a source has been established as yet. Mafic minerals of greenstone belts or granitic rocks such as pyroxene, hornblende, and biotite have been suggested as a vanadium source for the Western Australian deposits by Mann and Deutscher (1978). Hambleton-Jones (1976) reports certain schists of the Damara Belt to be enriched in vanadium and a possible source for the Namib Desert surficial deposits.

Climate influence on the generation of the various types of surficial uranium deposits is reflected by the localization of (a) duricrust-related uranium deposits such as calcrete, dolocrete, silcrete, gypcrete in channels and playas, and of uranium accumulations in closed alkaline and saline basins as well in hot arid to semi-arid desert zones, and (b) organic matter-hosted deposits such as bogs and swamps in cold to moderate climates. Between these two extreme climatic cases there are a large number of organic and inorganic environments favorable for accumulation of uranium but, as mentioned earlier, almost all of them are of subordinate magnitude and of no economic importance. Boyle (1984) points out that the economic potential for surficial uranium deposits, relative to climatic zones, decreases from hot arid to semi-arid, cold-temperate, temperate and to tropical. This sequence also correlates with increasing dilution and precipitation of uranium in the hydrosphere.

Geomorphologic environments and hydrologic regimes required for ore formation include

- areas of lateral groundwater migration or discharge such as linear depressions in form of fluvial drainage systems;
- regions of internal drainage, i.e., closed or partially closed basins such as alkaline lakes, playas, deltas, swamps, bogs etc. supplied by surface or groundwaters which have traversed a source area;
- zones within source rock terrane characterized by faulting and fracturing and vertical groundwater movement and water table fluctuations.

Within the first two given areas localization of mineralization is often governed by local morphological features. (a) In linear depressions uranium precipitation may occur at constrictions laterally by narrowing of the channel or vertically by a basement rise. Throughflowing waters will stagnate or will suffer reduced flow rates at these barriers providing time for increased uranium precipitation as will be discussed later. (b) At internal drainage regimes, absence of outflow exits is a salient criteria for uranium accumulation in semi-arid and arid climates. In contrast, organic-rich depressions in humid environments require for concentrating uranium a relatively continuous percolation of groundwater through the organic material.

Lithology may exert a physico-chemical control on ore localization in various ways. Argillaceous layers commonly act as aquiclude. As such they may constitute both a barrier for groundwater flow, thereby enhancing the conditions for increased precipitation of uranium or, if present in multiple horizons, they may channel the waters into areas optimal for ore accumulation, for example in deltas, at bog-sediment interfaces, or in marl/clay-silt/sand-carbonaceous suites. Porosity and permeability are an additional lithologic prerequisite for mineral formation providing both, an aquifer for the mineralizing fluids and an ore mineral host such as the valley and delta calcretes-dolocretes in arid regions.

Mobilization, transport and redeposition of uranium and associated elements, particularly V for carnotite crystallization, and Mg, Ca, Ba, Sr, CO_2, SO_4 etc. for associated minerals in duricrust and karst deposits (subtype 6.1 and 6.3) and PO_4 for structure fill mineralizations (subtype 6.4), demand a coincidence of specific conditions, additionally to the above-discussed criteria. They are

- access to the required elements;
- adequate weathering conditions;
- hydrochemistry and complexing transport agents;
- physico-chemical precipitation mechanisms.

Access to elements and adequate weathering conditions is required to liberate, at least partially, the ore-forming elements from the source rocks. To achieve this purpose, the source terrane must be sufficiently exposed to and undergo intense chemical weathering under oxidizing conditions in a pre-mineralization period. Such weathering effects are reflected, in the Yilgarn Block for example, by deep-reaching regolithic profiles. For the formation of duricrust-type deposits, subsequent to the chemical weathering period a change into a hot, semi-arid or arid climate is mandatory to retain the uranium in an internal drainage system or, alternatively, to prohibit its flushing by streams and rivers into the seas, which is typical for humid moderate to tropical climates. Further on, under hot, arid conditions, the sporadic and mostly minor rain fall causes retardment of the groundwater flow, so that migration of the groundwaters transporting the ore-forming elements from the source to the site of deposition is slow. This situation, combined with a high rate of evaporation, provides also the hydrodynamic conditions favorable for the precipitation of the uraniferous nonpedogenic calcrete minerals such as calcite, dolomite, carnotite, etc. Another prerequisite for the availability of uranium in hot climates is the absence of certain saprolites such as pedogenic calcrete, ferricrete, ferralitic laterite, Fe-Mn oxides, and clays in the source areas. These surface constituents may seriously hamper the transport of uranium by its fixation in the regolith.

Hydrochemistry and complexing agents govern the mode of transport of the ore-forming elements. Uranium is commonly dissolved in natural waters as the uranyl ion which may complex as bi- or tri-carbonate, phosphate, sulfate, fluoride, chloride, or hydroxide. The nature of the complex is a function of the pH domain. Therefore, certain uranyl complexes are specific for certain environments of acidity.

Boyle (1984) lists the following pH ranges for the formation of various types of surficial deposits.

- In waters with pH > 7 uranyl bi-carbonate and tri-carbonate complexes are dominant and most important for the generation of subtype 6.1 (duricrust type) deposits such as Yeelirrie, Australia, and Langer Heinrich, Namibia.
- Waters with pH 4.5 to 7.5 provide stability for uranyl-phosphate complexes that may have been instrumental in the formation of subtype 6.4 deposits such as Daybreak, USA, and Cotaje, Bolivia.
- Waters with pH < 5 support uranyl sulfate and fluoride complexes which are important during the weathering of sulfide deposits such as Bondon, France, where pre-Liassic paleo-weathering processes contributed to mineral formation as reported by Eulry and Vargas (1980).

Physico-chemical mechanisms leading to precipitation of the ore-forming minerals from the transporting surface or groundwater include particularly destabilization of uranyl-complexes and sorption of uranium and, in some cases, reduction of uranium. Processes involved, individually or combined, are

- decrease in hydrostatic partial pressure due to loss of CO_2, for example by evaporation in near surface environment leading to dissociation of uranyl-carbonate complexes;
- change in pH either by loss of CO_2, oxidation of sulfides, interaction with soluble humic or fulvic particles or mixing of different solutions, affecting the solubility and stability of uranyl-complexes;
- change in redox conditions by carbonaceous matter, gases such as hydrocarbons and H_2S, anaerobic bacterial activity and oxidation of sulfides reducing hexavalent to tetravalent uranium;
- sorption processes resulting in adsorption of both uranous and uranyl-ions on carbonaceous particles, clays, phosphates, zeolites and hydrous oxides of Fe, Mn, Al, Ti and Si.

Other processes that also may have influenced directly or indirectly precipitation of U and/or U-V minerals include

- evaporation of surface and groundwaters, for example in arid climates by upwelling of groundwater in calcrete-dolocrete drainage channels that results in both increase of U, V, and K contents and release of CO_2 or, in alkaline and saline playas, leads to accumulation of U in final residues; evaporation of

soil moisture associated with capillary rise of groundwater may be the mechanism for U enrichments in pedogenic calcretes or ferricretes in hot climates and perhaps of the structurally controlled mineralizations in moderate climates such as the autunite deposits of Daybreak, USA;
- interaction of two or more groundwaters, for example mixing of separate uraniferous and vanadiferous groundwaters resulting in deposition of carnotite (Mann and Deutscher 1978).

For extensive discussions of the above summarized mineralization processes, the reader is referred, among others, to Arakel (1988), Boyle (1982, 1984), Briot (1978), Carlisle et al. (1978), Hambleton-Jones (1976), Mann and Deutscher (1978), Samama (1984).

For more details on the *metallogenesis of subtype 6.1* deposits see Chapter 5.6.

Additional details on the formation of subtype 6.2, 6.3, and 6.4 mineralizations are given below.

Subtype 6.2, peat – bog, metallogenetic aspects: Noteworthy mineralization has formed in glaciated terrane of cold to cool temperate climates of the northern hemisphere, and in recent times as indicated by strong radioactive disequilibrium. Prerequisite for optimal U accumulation are organic-rich channels or basins through which a relatively constant filtering of uraniferous surface or groundwaters occurs. The waters collect the uranium by weathering and leaching from uraniferous granites, volcanics, or other lithologies. For example, in the Flodelle Creek area, probable source rocks are provided by the Cretaceous Phillips Lake Granodiorite containing 4 to 80 ppm U (av. 16 ppm U), part of which must be present in leachable form as reflected by shear-controlled near-surface mineralizations grading as much as 500 ppm U. Uranium-transporting waters appear to be neutral to slightly acid and may carry several hundred ppm U. Otton and Zielinski (1985) report for the Flodelle Creek head waters a pH-range from 5.85 to 7.55, and contents of 17 to 318 ppm U associated with high covariation of Ca^{2+}, Na^{+}, Mg^{+}, and HCO_3^{-} ions.

A mechanism that is essential for the fixation of uranium is not so much reduction but ion exchange and adsorption on organic material as reflected by the high correlation coefficient of up to 0.8 for U to organic matter.

Subtype 6.3, karst-cavern, metallogenetic aspects: The most likely source of uranium is tuffaceous sediments formerly overlying the Madison Limestone. Uranium is thought to have been leached from the pyroclastics during the present erosion cycle by groundwaters which transported it downwards to be redeposited in the karst openings as uranyl vanadates.

Subtype 6.4, surficial pedogenic and structure fill, metallogenic aspects: The most appealing hypothesis on mineral formation at Daybreak, USA is supergene leaching of uranium from a uraniferous quartz-monzonite during a period of deep weathering since Tertiary times and subsequent redeposition of the uranium as open space fillings along a fluctuating water table. The actual cause for precipitation of the relative high grade uranium remains open for speculation. A similar type of near-surface structure-controlled deposit, with uranium derived from uraniferous rhyolitic volcanics and supposedly precipitated by H_2S or hydrocarbons, occurs at Mina Cotaje, Bolivia (ca. 100 mt U_3O_8, 0.1% U_3O_8).

Remarks

Surficial uranium deposits are commonly relatively small and of low grade except those deposits used as type examples. From the latter only Yeelirrie, Australia, is of large and potentially economic size. Mining of the small deposits mentioned was possible under exceptional favorable conditions (nearby mill, amenability to heap leaching, etc.).

4.6.1 Subtype 6.1: Duricrusted sediments

References: Butt et al. (1984); Hambleton-Jones (1984); Mann and Deutscher (1978)

Class 6.1.1: Fluvial valley-fill

(also referred to as calcrete, groundwater-calcrete or valley-calcrete type)

Type Example: Yeelirrie, Yilgarn Block, Australia
Reference: Cameron 1984

Host Rocks/Alteration/Structures

Mineralization is hosted by nonpedogenic earthy or porcellaneous, porous calcrete or highly carbonatized fluvial and alluvial sediments composed of dolomite, calcite, clays, feldspar and locally gypsum and celestite. The calcrete grades laterally and downward into clay-quartz and argillaceous grit sediments from which it has been derived by groundwater-related alteration. Calcretized sediments occupy the axial portion of shallow valleys up to a few km wide and up to 200 km long. Basement topography under valleys has locally strong relief with abrupt drops of up to some tens of meters. For example, at Yeelirrie a basement high chokes the channel section. Calcrete forms near-surface, semi-continuous highly elongated, tabular lenses which may be 20 to 150 km long, 0.5 to 4 km wide and 2 to 15 m thick. Longitudinal topographic gradient of channels is rather gentle, between 0.05 and 0.1%. Channel-filling alluvium and calcrete commonly broaden into wide flood plains and deltas in their lower course prior to terminating in playas.

In other regions (e.g., Namibia) instead of, or in addition to calcrete, channel sediments may have been transformed into silcrete or gypcrete providing the host for mineralization.

Ore and Associated Minerals/Mode of Mineralization

Principal ore mineral is carnotite and rarely other uranyl-minerals. Carnotite occurs as stringers, seams and disseminations in earthy calcrete, as fracture coating and vug lining in porcellaneous calcrete, and as grain coating in clay-quartz sediments immediately below the calcrete. Mineral distribution, although highly irregular in detail, displays a general continuity in form of flat-lying shallow elongated lenses up to a few meters thick. Most of the mineralization is emplaced immediately beneath the present water table and is best developed in the transition zone below the calcrete.

Pagel (1984) notes that in valley-fill and lacustrine/playa deposits in various countries, the uranium minerals are commonly associated with a variety of other minerals. Celestite is known from a number of deposits but is largely erratically distributed and confined to specific parts of a deposit. Its presence is reflected by Sr contents of as much as 6%. Fluorite and baryte are reported from a few deposits. Sepiolite occurs often and attapulgite is occasionally present. Barbier et al. (1980) estimate that in the Mudugh occurrence, Somalia, between 5 and 20% of mineralized samples contain attapulgite and sepiolite. This is also the case in the Hammadas, Ain Ben Tili area, Mauritania, from where Braun (1974) reports a clay mineral associations change within the sedimentary profile from bottom to top as follows: the basal conglomerate contains montmorillonite and illite, the mid section, montmorillonite and attapulgite; and in the top calcareous cap, montmorillonite decreases and sepiolite appears. Smectite is present in several deposits. Briot (1978) found in Yilgarn Block deposits an interlayered illite/smectite clay and suggests that smectite derived by alteration of illite. Smectite and illite are also present in the Tumas River occurrence, Namibia. Kaolinite and illite exist often in surficial uranium occurrences, but their relationships to mineralization is unclear in some cases whereas in others they are the only clay minerals present. At a short distance away from deposits other clay mineral assemblages may occur. Briot (1978) noticed chlorites with traces of illite and talc along the margins of the Yeelirrie deposit.

Dimensions/Resources

Nonpedogenic valley calcrete U deposits may extent several km long, a few tens of meters to ca. 2 km wide and <1 to 15 m thick, commonly containing from some <10 to about 5000 mt U_3O_8 at grades of 0.03 to 0.08% U_3O_8.

Yeelirrie, Australia, is an exception. It measures 9 km long, 0.5 to 1.5 km wide and 1 to 15 m, average 3 m thick, containing 52 500 mt U_3O_8 at an ore grade averaging 0.15% U_3O_8. Total resources of a district such as the northern Yilgarn Block may be in the order of 60,000 to 70 000 mt U_3O_8.

Examples of Surficial, Class 6.1.1 Valley Fill Duricrust Deposits/Occurrences

Australia: Lake Way, Lake Raeside, Hinkler-Centipede/Yilgarn Block
Namibia: Langer Heinrich, Aussinanis, Tumas/Namib Desert
Somalia: Dusa Mareb-El Bur region/Mudugh
South Africa: Brulkolk/Bushmanland Plateau, Cape Province

Class 6.1.2: Lacustrine/Playa

Type Example: Lake Maitland, Yilgarn Block, Australia
Reference: Cavaney 1984

Host Rocks/Alteration/Structures

Playa sediments are dominantly fine-grained clays and silts containing gypsum, halite, and carbonates, and are associated with hypersaline waters. Dolomite and calcite, together with clay minerals and quartz, form a discontinuous horizon, some dm to m thick, of calcrete/dolocrete. Intervening material consists of carbonatized clays. The calcrete is a major aquifer and the principal uranium host. It lies a few meters below the surface under a sequence of almost impermeable dolomitized clays and silt-clay sediments. Silts and sands underlie the calcrete and may be interbedded with more calcrete horizons.

Ore and Associated Minerals/Mode of Mineralization

Principal ore mineral is carnotite, present as disseminations, coating cracks and filling vugs within the harder calcrete beneath the dolomitized clay horizon. Most of the mineralization occurs in calcrete but extends into underlying silts and sands. Distribution of the mineralization is irregular although in overall continuity.

Dimensions/Resources

Individual deposits may be <1 km to 8 km long, <100 m to 1.5 km wide and 0.1 to 3 m thick containing <10 to ca. 4000 mt U_3O_8 at (average) grades ranging from 0.03 to 0.09% U_3O_8 occasionally to 0.15% U_3O_8. Districts may contain up to some 10 000 mt U_3O_8.

Remarks

For more details on subtype 6.1 deposits see Chapter 5.6.

Examples of Surficial, Class 6.1.2 Lacustrine or Playa Duricrust Deposits/Occurrences

Australia: Lake Maitland, Lake Austin/Yilgarn Block

South Africa: Abikwaskolk, Dirkskop/Bushmanland Plateau, Cape Province

4.6.2 Subtype 6.2: Peat-bog

Type Example: Flodelle Creek, Washington state, USA
Reference: Johnson et al. 1987

Host Rocks/Alteration/Structures

Swamps, bogs, muskegs, swampy meadows at the edge of lakes or ponds in flood plains or cutoff meanders composed of vegetal organic matter (up to 65% of rock), often peat mixed with and embedded in alluvial clay, marl, silt, and sand constitute the most favorable host environment. The organic sediments have accumulated in blanket-like lenses, 1 to 10 m thick, elongated along the axis of valleys tens to 100 m wide. Mineralized bogs or swamps commonly occur in clusters controlled by topography along drainages underlain by anomalously uraniferous granitic rocks (at Flodelle Creek, Cretaceous Phillips Lake Granodiorite containing 4 to 80 ppm, average ca. 16 ppm U).

Ore Minerals/Mode of Mineralization

No discrete U minerals occur. U is probably present as urano-organic complexes and/or adsorpt on organic material (correlation coefficient U-organic matter often 0.6 to 0.8), but also on clay, marl and gray to black silty sand particles. U distribution and tenors are highly variable apparently depending on mode of waters (surface, ground, upwelling waters), direction of water flow, and transmissivity of the peat and interbedded sediments. The highest concentrations (up to some 1000 ppm U, locally 1% over as much as 1 m) may occur in either the upper or lower part, at the upstream section of a peat lense but also as spotty mineralization throughout the unit.

Some uranium occurrences of this subtype contain molybdenum and selenium and/or other elements. Boyle (1982) reports local concentrations of, and positive correlations between Mo, Se, Cu, V, As, REE, and U in recent bogs and marshes.

Age Constrains

Mineralization is of Holocene age. All uranium is in disequilibrium. Daughter products are often almost absent, reflecting a recent age of uranium precipitation.

Dimensions/Resources

Individual deposits may be tens of meters to some 100 m long, few meters to more than 100 m wide and <1 m to few meters thick containing <1 to ca. 50 mt U_3O_8 at (average) grades of some 100 ppm U, rarely up to 0.2% U_3O_8. Districts may contain up to some 100 mt U_3O_8.

Examples of Surficial, Subtype 6.2 Peat and Bog Deposits/Occurrences

Canada: Prairie Flats/Okanagan Valley region
South Africa: Henkries, Kannikwa/northern Cape Province
USA: Flodell Creek/NE Washington

4.6.3 Subtype 6.3: Karst-cavern

Type Example: Pryor-Little Mountains, USA
Reference: Bell 1963

Host Rocks/Alteration/Structures

Karst caverns in limestone (Mississippian Madison Limestone) having a floor cover of fallen blocks, chert fragments and other insoluble residues of limestone embedded in a matrix of reddish-brown sand, silt and clay, that may be loosely consolidated or cemented by silica, constitute the host for this type of U deposit. The caverns developed in limestone units mainly in Tertiary time after uplift during the Laramide Orogeny.

Ore and Associated Minerals

Principal uranium minerals include tyuyamunite and metatyuyamunite associated with calcite, hematite, baryte, gypsum, opal, and locally fluorite and celestite.

Mode of Mineralization

Uranium minerals occur as fine-powdery coatings of fractures and solution voids, crusts on limestone blocks, calcite crystals, chert nodules, as fissure and vug fillings, and as disseminations in the matrix of the cavern fill. Distribution is restricted to major drainage routes cutting through the uplifted limestone unit.

Age Constraints

Radiometric disequilibrium indicates a relatively recent ore formation.

Dimensions/Resources

Uranium-hosting caverns vary widely in size and configuration between small cavities, a few meters or less across to openings up to 10 m high, 25 m wide and 50 m long. Mineralized floor fill ranges from a few centimeters to almost 3 m thick. The magnitude of ore bodies mined was highly variable containing mostly a few tonnes U_3O_8 with exceptions as large as 80 mt U_3O_8. Ore grade mined averaged 0.5 to 0.8% U_3O_8 and 0.6 to 1% V_2O_5. Some lodes were as rich as 1.27% U_3O_8 (Old Glory Mine). Resources of the district are estimated at several hundred tonnes U_3O_8.

Examples of Surficial, Subtype 6.3 Karst Cavern Deposits/Occurrences

Central African Republic: ? Bakouma
Uzbekistan: Tyuya-Myuyun/Ferghana Basin

4.6.4 Subtype 6.4: Surficial pedogenic and structure fill

Type Example: Daybreak mine, Washington state, USA
Reference: US-AEC 1959

This category comprises surface-bound mineralizations occurring widespread in pedogenic formations, including soils, pedogenic crustations such as laterite/ferricrete, calcrete, silcrete, gypcrete, etc., and structure-bound mineralizations. All occurrences are associated with uraniferous source rocks comparable to those associated with the other types of surficial deposits. All occurrences are of minute to small size and commonly of low grade. Only a very few have been mined. The Daybreak mine, Washington state,

USA, will be described as the type example of this style of minable mineralization.

Host Rocks/Alteration/Structures

At the Daybreak mine, quartz monzonite is the host rock for a shallow dipping mineralized shear zone. The shear is surrounded by intense bleaching and alteration including kaolinitization of feldspars, sericitization, and decomposition of biotite.

Ore Minerals/Mode of Mineralization

The only uranium mineral at the Daybreak mine is meta-autunite without any sulfides or gangue minerals. Uranium minerals, mainly uranyl phosphates and silicates, locally sooty pitchblende and/or coffinite, are reported from other occurrences.

At the Daybreak mine, meta-autunite lines open fractures and voids within a shear zone proximal to the water table, aggregating to pods and vuggy masses as much as 10 cm thick and 1 m long. The best mineralization occurs at intersections of the main shear with cross-fractures where lodes up to 1.5 m long, 1 m wide and 0.3 m thick may accumulate. Comparable mineralizations are known in rhyolitic environments, e.g., in the Peña Blanca district, Mexico, and at Cotaje, Bolivia.

Dimensions/Resources

At the Daybreak mine, mineralization is hosted in a shear zone in which it extends discontinuously for 600 m long, up to 25 m wide and 30 to 40 m deep with mineable ore limited to a section slightly below the water table. Total production was 25 mt U_3O_8 at an ore grade of 0.3% U_3O_8.

Examples of Surficial, Subtype 6.4 Pedogenic and Structure Fill Deposits/Occurrences

Argentina: Schlagintweit/Achala batholith, Sierras Pampeanas
Canada: Summerland area/British Columbia
Greece: Archontovouni/Paranesti
USA: Copper Mountain/Wyoming

4.7 Type 7: Quartz-pebble Conglomerate (Lower Proterozoic) (Fig. 4.7)

(also referred to as oligomictic conglomerate or Lower Proterozoic conglomerate or paleoconglomerate type)

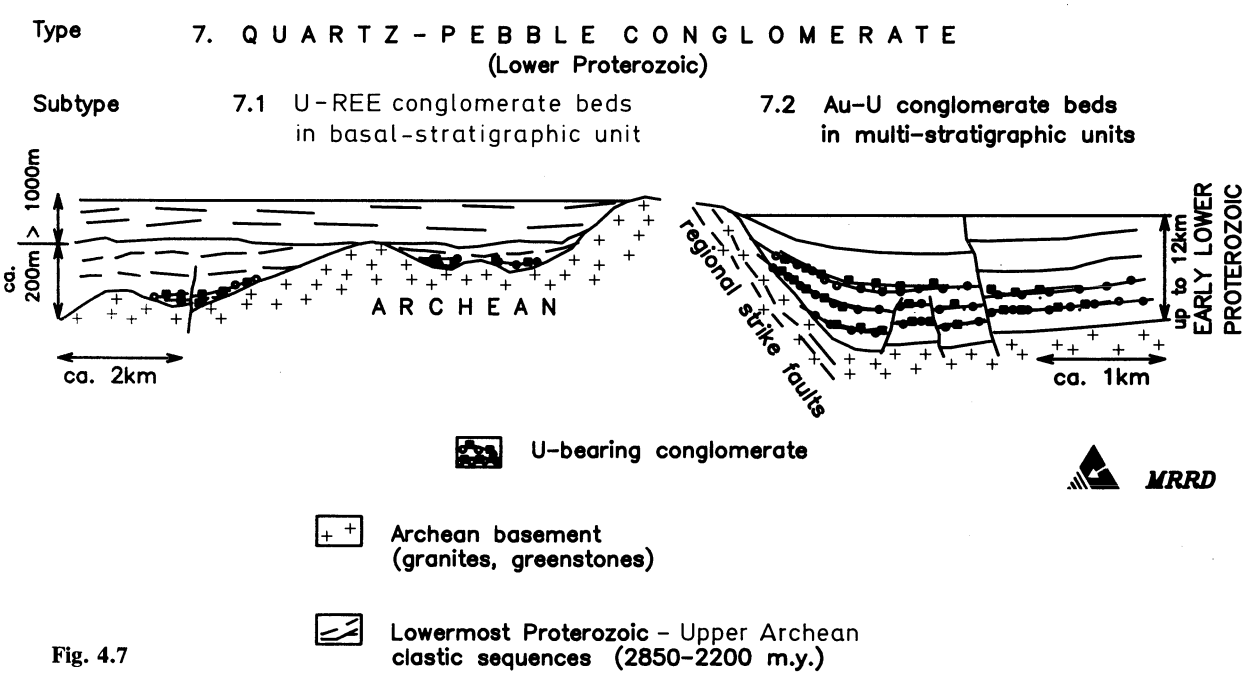

Fig. 4.7

Definition

Quartz-pebble conglomerate deposits consist of uranium and/or other metallic elements of syn-sedimentary detrital origin, modified by diagenetic processes (modified placers). The principal primary uranium phase is detrital uraninite. The conglomerates are interbedded with silicic clastic sequences containing layers of quartzite and argillite. Quartz-pebble conglomerate deposits are restricted to basal Lower Proterozoic units unconformably overlying Archean rocks which include granites.

Two varieties of mineralization can be in the conglomerates:

Subtype 7.1: U-dominant with REE

Type Example: Blind River-Elliot Lake, Canada

Subtype 7.2: Au > U-dominant

Type Example: Witwatersrand, South Africa

References: Button and Adams 1981; Hallbauer 1986; Pretorius 1976, 1981; IAEA/Pretorius (ed.) 1987; Robertson 1989, Roscoe 1969; Ruzicka 1988

In subtype 7.2 deposits, gold is the main product and uranium is by-product.

The time bracket "Lower Proterozoic" has been added to avoid confusion with younger, post-oxyatmoversion oligomictic conglomerates which also contain uranium but of epigenetic origin. Mineralization of both kinds requires different depositional environments, the first that for detrital ore mineral accumulation, the second that with reductants for precipitation of uranium dissolved in solutions; the latter corresponds to sandstone-type deposits.

Principal Recognition Criteria

Host Environment

- Oligomictic quartz-pebble conglomerate composed of well-rounded and well-sorted pebbles (mean diameter 5 to 7 cm) of predominantly quartz and lesser chert (10 to 20%) in highly pyritiferous siliceous matrix containing minor feldspar, sericite, chlorite, and heavy minerals; either submetamorphic or metamorphosed to lower greenschist facies
- Thin and lenticular conglomerate beds often coalescing into thin sheets of fluvial to deltaic sediments in braided-stream sedimentary regimes
- At or near the base of a clastic sequence within depressions possibly paleochannels incised into Archean basement (subtype 7.1) or in repeating conglomeratic beds (reefs) at or near (intraformational) unconformities, within several overlying stratigraphic units, the beds partly originating by reworking of precursor conglomerates (subtype 7.2)
- Lateral extension of payable conglomerate beds from a few km^2 to as much as 400 km^2
- Interbeds of terrestrial to marginal marine quartzite, arkose, siltstone, argillite, and polymict conglomerate, partly arranged in cyclic sequences of variable, sometimes great thickness (several 1000's of m); iron formations may occur higher up in the sequence
- High K/Na (20 to 100) and K/Ca ratios (>40) of host-related arenites indicating provenance from granitic source
- Basins flanked by Archean granites and greenstone belts
- no ore-related alteration, but physical weathering of Archean basement,
- no structural control except for proximity to major unconformities.

Mineralization

- Primary U minerals: uraninite partly thoriferous, uranothorite, perhaps U-Ti oxide phases, associated with secondary U-Ti oxide phases (brannerite), coffinite, thucholite, a.o.
- Associated minerals: wide variety of detrital heavy minerals, including locally native Au; and diagenetic authigenic minerals, locally carbon
- Associated trace elements possibly present: Au, Ag, REE (1 to 100 ppm); As, Co, Cr, Cu, Ni, Pb, Zn, Zr (10 to a few 100 ppm); TiO_2 (0.1 to 2%); S (>1%), and traces of Pt, Os, Ir, etc.
- Subtype 7.1 is monometallic except for occasionally recovered REE minerals, subtype 7.2 polymetallic, gold being the main product
- U/Th ratio of conglomerate matrix: 1 to 15
- Stratiform, matrix-bound dissemination of U and associated minerals
- Ore localization and concentration correlate with well-sorted and densely packed quartz-pebbles reflecting control by hydrodynamic

processes, abundance of pyrite and its predecessors, presence of internal partings of pyrite-rich arenite and occasionally argillite lenticular in shape and structured by trough or tabular crossbed sets, proximity to unconformities or disconformities.
- Geometry of uraniferous conglomerate ore bodies is highly variable, depending on the topography of pre-conglomerate unconformity, commonly by far longer than wide and rather thin

Age Constraints

- Restricted to early Lower Proterozoic time prior to oxyatmoversion, (ca. 2200 m.y. ago)

Metallogenetic Aspects

A modified placer metallogenesis is commonly forwarded for U mineralization in Lower Proterozoic quartz-pebble conglomerate deposits. The origin of uranium is generally accepted as synsedimentary detrital, uraninite, and other heavy minerals deposited as placers in fluvial or deltaic environments. The source of uranium is thought to be Archean granite. The other heavy minerals are considered to have derived from either granite or greenstones. Liberation of ore minerals occurred essentially by physical weathering and erosion. Prerequisite for such a proposition is an anaerobic atmosphere permitting fluvial transport of uraninite and other minerals which are instable and easily weathered in an oxidizing environment. An anaerobic atmosphere prevailed on earth during the Archeen and early Lower Proterozoic until oxyatmoversion in the middle Lower Proterozoic (ca. 2200 m.y. ago). Since then, the oxygenated atmosphere prohibits longer transport of uraninite, and hence excludes formation of this type of conglomerate deposit.

The diverse heavy minerals associations in the various districts primarily reflect petrologically different sources.

Post-depositional redistribution and mineral crystallization mainly by diagenetic processes led to the formation of a suite of authigenic ore and associated minerals such as brannerite, rutile and anatase by reaction of U with ilmenite, pyrite by sulfidization of magnetite, the sulfide supposedly derived from volcanism.

Remarks

Lower Proterozoic conglomerate deposits are of very low to low grades (0.01 to 0.15% U_3O_8) but contain large resources. Deposits mined primarily for gold yielding uranium as by-product appear to have a longer term economic perspective compared with strictly uranium producers.

Examples of Type 7 Quartz-Pebble Conglomerate Deposits/Occurrences (Undifferentiated)

Brazil: Serro do Corrego/Jacobina, Bahia, Quadrilatero Ferrifero
Canada: Agnew Lake/Ontario, Sakami Lake/Quebec
India: western Karnataka
USA: Phantom Lake/Medicine Bow – Sierra Madre, Wyoming, Black Hills/South Dakota
Russia: ? Noril'sk/northern Siberia

4.7.1 Subtype 7.1: U-dominant with REE

Type Example: Elliot Lake – Quirke Lake district, Canada
References: Robertson 1989; Ruzicka 1988

Host Rocks/Structures

Pyritic oligomictic quartz-pebble conglomerate (termed "reef") of fluvial origin, deposited in braided-stream channels, with lateral migration coalescing conglomerates into thin crossbedded sheets, interbedded with quartzite banks, chiefly in paleovalleys scoured into Archean greenstones mainly but also into granite. Three different channel systems (termed "trend") are recognized in the Elliot Lake-Quirke Lake district.

No structural control, except for concentration in channels and their abutment against basement highs, and post-ore displacements.

Alteration

No ore-related alteration, but deep essentially physical weathering and erosion of the Archean paleosurface. Granites are weathered to a quartz-microcline rock displaying a relic granite texture containing sericite derived from plagioclase destruction, and some chlorite. Ferromagnesian

minerals and ferric iron have been removed whereas ferrous iron minerals (pyrite) and tetravalent uranium (uraninite) are still present, reflecting weathering under anaerobic conditions. The weathering is geochemically expressed by Ca leaching indicated by high K/Ca ratios (>40) due to almost complete decay of plagioclase.

Ore and Associated Minerals

Uraninite, U-Ti oxyde phases (brannerite), coffinite, thucholite, uranothorite, uranothorianite, monazite, xenotime, locally gummite.

Pyrite (5 to 20 wt. %), allanite, ilmenite, chromite, cassiterite, magnetite, rutile, zircon, garnet, spinel, tourmaline, titanite, apatite, pyroxene.

Mode of Mineralization

Uranium is the primary commodity produced with occasional recovery of Th and some REE, particularly Y.

Several generations of ore and associated minerals occur as disseminated detrital and redistributed matrix components in at least seven conglomeratic horizons that range from 0.5 to >3.5 m thick. Three of the thicker reefs (1.5 to 3.6 m) have uranium grades of 0.05 to 0.15% U_3O_8. The conglomerate beds separated by quartzite banks (0.5 to 6 m thick) are within a sequence about 50 m thick immediately overlying the Archean unconformity. They cover areas, up to 20 km^2 in lateral extension, within three NW-SE oriented fluvial systems.

Age Constraints

Restricted to the early Lower Proterozoic (ca. 2200 to 2500 m.y. ago).

Dimensions/Resources

The Nordic Trend is 5700 m long and 1300 to 1800 m wide. The Quirke Trend is 9600 m long and 1800 to 2700 m wide. Minable reefs are 1.5 to 3.5 m thick. Total resources are 400 000 to 500 000 mt U_3O_8. Average grades are 0.07 to 0.1% U_3O_8.

Remarks

For more details see Chapter 5.7.1.

4.7.2 Subtype 7.2: Au over U dominant

Type Example: Witwatersrand, South Africa

References: Anhaeusser and Maske (eds) 1986; Pretorius 1976; Hallbauer 1986

Host Rocks/Alteration/Structures

Pyritic, oligomictic quartz-pebble conglomerate of fluvial origin interbedded with quartzite, arkose, shale and volcanics. Carbonaceous material occurs in several horizons. Deposition of conglomerates in several separate stratigraphic cycles within six large fluvial fans on the north and west side of the Witwatersrand Basin.

Ore and Associated Minerals/Metals

Uraninite (2 to 6% Th), uranothorite, brannerite, thucholite, native gold and platinoid (Os, Ir, Ru, Pt) minerals.

Pyrite, arsenopyrite, pyrrhotite, cobaltite, gersdorffite, galena, chromite, zircon in relative abundance and about 60 more minerals in extremely small quantities.

Mode of Mineralization

Gold is the main product (<1 to several 100 ppm Au, average 5 to 12 ppm Au) and uranium by-product (av. 0.015 to 0.03% U_3O_8) except in a few mines (e.g., Africander/Vaal Reefs: 0.15% U_3O_8, 1.1 ppm Au).

Several generations of ore and associated minerals occur as detrital and redistributed matrix components in several conglomerate horizons within large fluvial fans. Mineralized reefs occur in all four stratigraphic systems, but the most productive is the Bird Reef Stage in the Upper Witwatersrand System, which yielded ca. 80% of past production. Important concentrations of ore are restricted to distinct narrow zones occupying ca. 2% of the entire Upper Witwatersrand System within a belt running parallel to the former coastline.

On a more local scale, ore minerals tend to have preferentially concentrated (Von Backström 1975, 1976):

- in conglomerate beds less than 30 cm thick,
- immediately above stratigraphic and intraformational local disconformities or unconformities, particularly where conglomerates fill

depressions or scours in the footwall rocks, or about a slight rise or swell of underlying strata.
- in shallow depressions with gentle slopes,
- in peripheral zones of deep depressions with steep slopes (axial center zones are weakly mineralized probably due to poorly developed conglomerate),
- near the base of conglomerate beds along distinct, partly carbonaceous argillaceous/shaly footwall boundaries,
- in pay-streaks running generally parallel to each other characterized by densely packed, well-rounded and well-sorted pebbles predominantly of quartz, and larger accumulations of other heavy minerals,
- rare extensions into adjacent arenaceous sediments except by redistribution.

Age Constraints

Restricted to the late Archean – early Lower Proterozoic (ca. 2300 to 2800 m.y. ago).

Dimensions/Resources

The ore-hosting fluvial fan may be up to 40 km long and 90 km wide, across the distal fan base, and several 1000 m thick. Individual deposits are several 100 m to several 1000 m long, several 10 m to several 100 m wide and 5 to 200 cm thick containing up to several 10 000 mt U_3O_8 at (average) grades ranging from 0.015 to 0.03% U_3O_8 occasionally to 0.15% U_3O_8. Resources can be >600 000 mt U_3O_8. Gold values may range from <1 to 25 ppm.

Remarks

For more details see Chapter 5.7.2.

4.8 Type 8: Breccia Complex (Fig. 4.8)

Definition

The breccia complex deposit occurs in coarse breccias comprised largely of polymict granite- and hematite-dominated fragments in a hematitic-chloritic-sericitic-silicic matrix. Finer-grained layered rocks occur within the breccias. The breccias fill a large graben-like structure surrounded by alkaline granite. Mineralization consists of a polymetallic Cu-U-Au assemblage. Geological distribution, sulfide assemblage, rock association, and stratigraphic position permit a distinction between strata-bound and strata-transgressive mineralizations.

Type Example: Olympic Dam, South Australia
References: Roberts 1988; Roberts and Hudson 1984

Principal Recognition Criteria

Host Environment

- Host rocks are a thick pile (ca. 800 m) of matrix-rich polymict breccias (Olympic Dam Formation) with some intercalated finer-grained layers
- Fragments consist of altered granite; felsic, intermediate, mafic volcanics; banded iron formation, hematitic siltstone, carbonate, arenite; fluorite, baryte, sulfides (diameter mostly 1 to 3 cm, but up to 12 m)
- Matrix of several phases of hematite, sericite, chlorite, siderite and arkosic material
- Mineralized polymict breccias overlain and underlain by barren monomict granitic breccias
- Position within a large graben-like structure (>7 km long, <4 km wide)
- Surrounding rock is an anorogenic, A-type, K-feldspar rich biotite granite containing 25 to 40 ppm U, 30–50 ppm Th and locally as much as 500–1000 ppm REE
- Structural arches associated with displacement faults cut the graben
- Deposition of breccias in high energy environment under arid sub-aerial conditions
- Rapid facies changes, disconformable contacts between individual breccia units
- Intruded dolerite dikes

Alteration

Two episodes of alteration reflected by:

- Weak pervasive alteration of all lithologies by hematitization, sericitization, chloritization and locally silicification and carbonatization, replacing particularly feldspars and mafic minerals of granite clasts;
- Intense vertically zoned alteration by hematitization and chloritization, dominant in

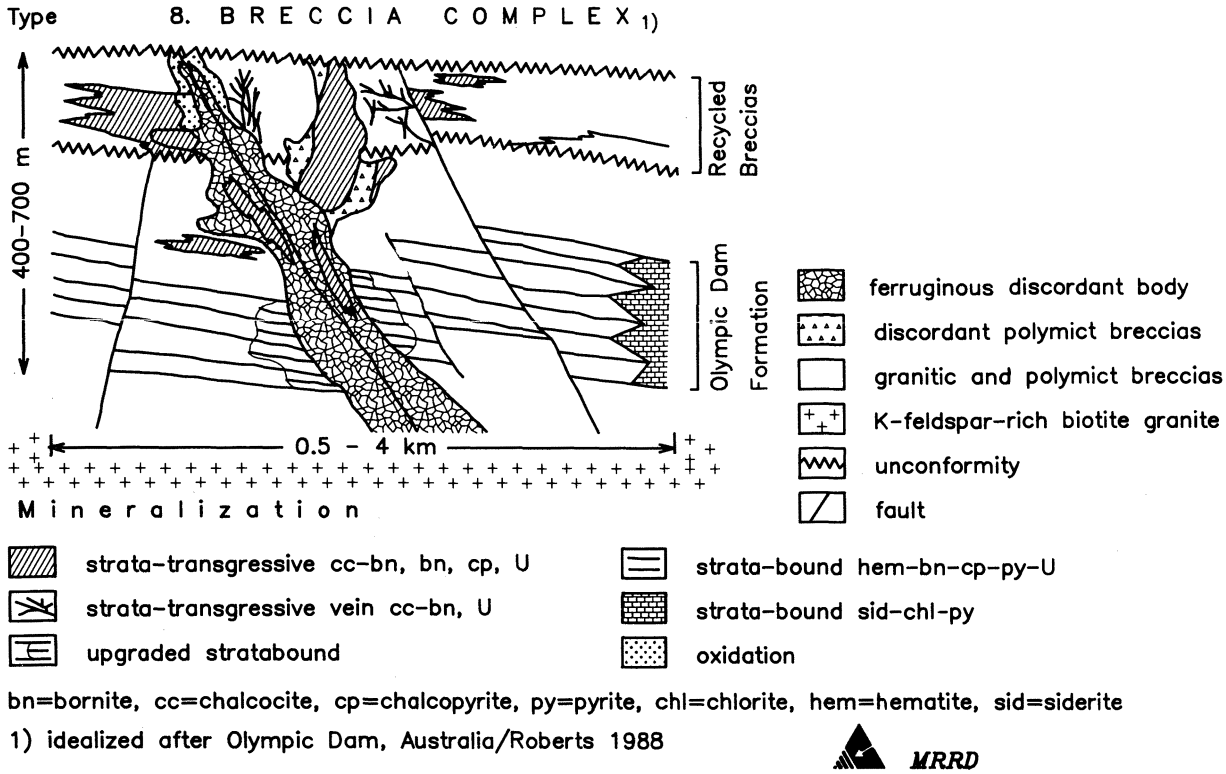

Fig. 4.8

the lower section of the mineralized sequence (Olympic Dam Formation), and silicification and sericitization in the upper section.

Mineralization

- Association of Fe, Cu, U, REE, Au, Ag, with trace amounts of other metals, abundant hematite, and a variety of gangue minerals dominantly quartz and fluorite
- Principal U minerals are pitchblende, subordinate coffinite, locally minor brannerite; Cu occurs mainly as sulfides, in basal part of the deposit associated with abundant pyrite
- Sulfide and associated minerals form two modes of mineralization: older strata-bound assemblages of dominantly Fe- and Cu-sulfides and younger strata-transgressive mineralization of predominantly Cu-sulfides
- Strata-bound mineral assemblage is bornite (chalcocite)-chalcopyrite-pyrite associated with subordinate to trace amounts of minerals of U, Au, Ag, REE, Co, Ni, and abundant hematite. Principal gangue minerals are quartz, sericite, fluorite, and minor siderite and baryte. Vertical zonation is reflected by sulfur-rich, copper-poor assemblage (pyrite-chalcopyrite) at the base grading upwards to a relative Cu-rich, S-poor assemblage (bornite-chalcopyrite). Ore and gangue minerals impregnate the hematite-rich matrix of polymict breccias but also occur in rock fragments. They constitute 5 to 20 vol. % of the matrix in the form of disseminations, replacements, void-fill, and occasionally as thin stratiform layers. The concentration of sulfides displays a consistent relationship to the amount of matrix
- Strata-transgressive mineral assemblage is chalcocite-bornite associated with subordinate U, minor amounts of other sulfides, arsenides/arsenates of Cu, Ni, Co, native Au, Ag, and Cu, and abundant hematite. Principal gangue minerals are fluorite, quartz, and subordinate sericite, chlorite. Ore and gangue minerals form veinlets, veins, irregular lenses restricted to structurally prepared linear zones paralleling the long axis of the graben
- Strata-bound mineralization characteristically displays simultaneous rhythmic precipitation of hematite and sulfides

- Strata-bound mineralization commonly is below strata-transgressive mineralization, but spatial overlapping exists

Age Constraints

Not established (host rocks at Olympic Dam are Middle Proterozoic, not older than ca. 1600 m.y. and sericite alteration is about 1320 m.y. old).

Metallogenetic Aspects

Roberts (1988) suggests for the Olympic Dam deposit that it originated from a large evolving hydrothermal system in an extensional continental environment. During an early, more or less synsedimentary episode, hydrothermal fluids containing ferrous iron are thought to have entered sulfate-rich sedimentary environments forming by rhythmic precipitation of sulfides and hematite strata-bound mineralization in coarse clastic sediments. Continuous modification of the mineralization occurred. In a final stage, extensive high level intrusive activity of probably alkaline nature interacted with and superimposed widespread structure controlled transgressive Cu-U-Au-mineralization on the older strata-bound mineralization.

Dimensions/Resources

Olympic Dam is large in size, extending over an area of up to 7 km long, 4 km wide and 300 m thick. Within this area, structurally controlled mineralization occurs in linear zones greater than 6 km long, up to 0.7 km wide, and more than 300 m thick.

Total resources of the deposit amount to ca. 32 mio. mt Cu, 1.2 mio. mt U_3O_8 and 1200 mt Au. Average grades are 1.6% Cu, 0.06% U_3O_8 and 0.6 g/mt Au. This amount includes higher grade sections with probable reserves of 450 mio. mt containing ca. 11 mio. mt Cu, 360 000 mt U_3O_8 and 270 mt Au, at grades averaging 2.5% Cu, 0.08% U_3O_8, 0.6 g/mt Au and 6 g/mt Ag (Roberts 1988).

Remarks

Olympic Dam and the nearby Acropolis prospect are the only known deposits of the tentatively named "Breccia Complex" type. Although of huge size, accessable U amounts are restricted to the quantities recoverable as coproduct to Cu-Au mining.

4.9 Type 9: Intrusive (Fig. 4.9)

Definition

Intrusive deposits consist of disseminated primary, non-refractory uranium minerals, dominantly uraninite, uranothorianite and/or uranothorite in rocks of intrusive magmatic or anatectic origin. Deposits are of low to very low grade (20–500 ppm U) but may contain substantial resources. Further subdivision is based on host rock petrology:

Subtype 9.1: alaskite

Type Example: Rössing, *Namibia*

Subtype 9.2: quartz-monzonite

Type Example: Bingham, USA

Subtype 9.3: carbonatite

Type Example: Phalaborwa, S. Africa

Subtype 9.4: peralkaline syenite

Type Example: Kvanefjeld, Greenland

Subtype 9.5: pegmatite

Type Example: Madawaska, Canada

References: Alexander 1986; Brynard and Andreoli 1988; Berning 1986; Camisani-Calzolari et al. 1985; Maurice (ed) 1982; Sørensen et al. 1974

Subtype 9.1 is in medium- to very coarse-grained alaskite bodies ranging in size from large stocks and domes to tabular dikes and small lenses discordantly to concordantly within isoclinally folded highly metamorphosed and migmatized metasediments. No uranium related alteration is present.

Subtype 9.2 consists of very low grade uranium disseminations in highly differentiated granitic to (cupriferous) quartz-monzonitic (copper porphyries) complexes.

Subtype 9.3 is associated with differentiated (cupriferous) carbonatite complexes.

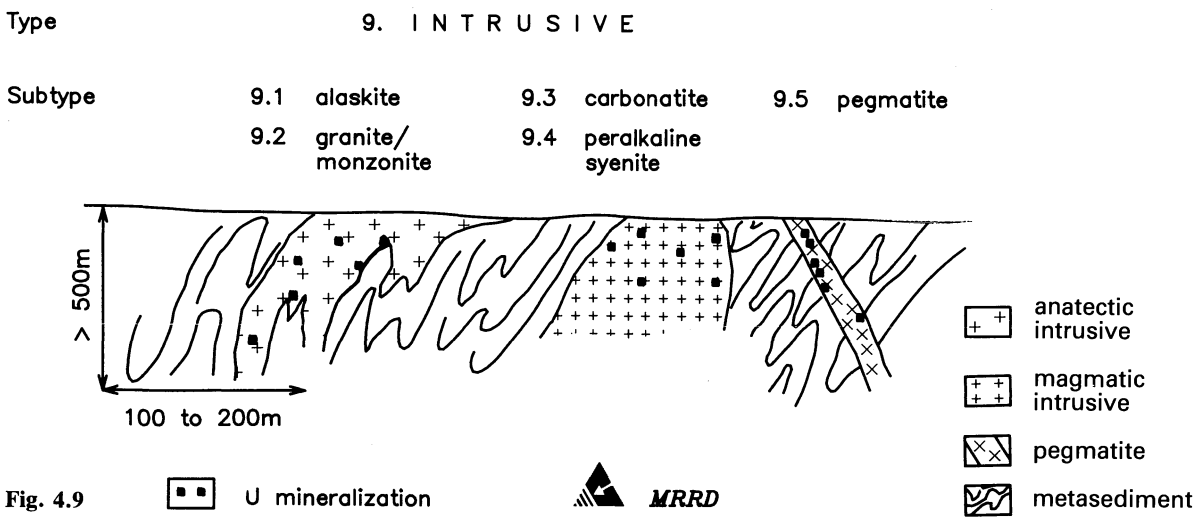

Fig. 4.9

Subtype 9.4 is in peralkaline syenitic domes or stocks. Uranium phases are commonly of more refractory nature.

Subtype 9.5 is in dikes of granitic, rarely syenitic unzoned pegmatite of silicious and mafic tendency (aegirine-augite).

Principal Recognition Criteria

Host Environment

- Syn- to post-orogenic intrusions within intracratonic mobile belts.
- Commonly sharp contacts and narrow contactmetamorphic aureoles around intrusions
- Subtypes 9.1 and 9.2 are late leucocratic peraluminous Si, Al and alkali rich facies in highly differentiated granitic or granitoid complexes, subtypes 9.3 and 9.4 are of basic and peralkaline tendency and occur in distinct stocks and domes
- Abundance of pegmatitic, aplitic and lamprophyric dikes
- Abundance of xenoliths and roof pendants
- Enrichment of volatile (F, Li, Be), RE and/or metallic elements (Cu, Mo, etc.)

Alteration

- No primary ore related alteration except hematitization in pegmatite
- Subtype 9.2 (granite) often affected by Na-metasomatism (albitization)

Age Constraints

No age constraints except for restriction to mobile belts.

Mineralization

- Principal U minerals: ± thoriferous uraninite, uranothorianite, uranothorite and/or uraniferous refractory minerals (typical for subtype 9.4), locally in weathered zones hexavalent U minerals
- U-minerals finely dispersed ubiquitously throughout host rock in subtypes 9.1 to 9.4; in pockets and clusters irregularly distributed in subtype 9.5 pegmatite
- Th/U ratio generally <1 to 3

Metallogenetic Aspects

Uranium-rich alaskite, quartz-monzonite, granite and associated pegmatites are supposedly the product of granitization of uraniferous crustal material as indicated by Sr isotopes. *Subtype 9.1* deposits, such as Rössing, are attributed more to ultrametamorphic-anatectic processes whereas for *subtype 9.2* magmatic differentiation with uranium retained in late-stage phases is favored. The content of U, Th, REE, and other metals in the various granitic facies presumably is a function of their original abundance in the precursor (meta)sediments. Prerequisite for the elemental retainment is a dry granitization process in a closed system.

The origin of both carbonatite *subtype 9.3* and peralkaline syenite *subtype 9.4* related deposits is interpreted as of orthomagmatic differention.

Remarks

Intrusive subtype 9.1 to 9.4 deposits are all of very low grade (ca. 20 to 400 ppm U) but may contain large resources. Subtype 9.5 pegmatite deposits may average up to 0.1% U_3O_8 but resources are generally low (a few tonnes to a few hundred tonnes U_3O_8). Uraniferous intrusive deposits in most cases provide good uranium source rocks rather than viable deposits. The only exceptions are the Rössing alaskite deposit and pegmatite deposits of the Bancroft district (Madawaska deposit). Uranium is extracted as by-product from subtype 9.2, e.g., from the Bingham porphyry copper deposit associated with quartz-monzonite, and from subtype 9.3, e.g., from the Phalaborwa carbonatite.

4.9.1 Subtype 9.1: Alaskite

Type Example: Rössing, Namibia
Reference: Berning 1986; Berning et al. 1976; Brynard and Andreoli 1988

Host Rocks/Alteration/Structures

Syntectonic medium- to very coarse-grained alaskite emplaced as bodies ranging from large stocks and domes to tabular dikes and small lenses discordantly to concordantly within isoclinally folded highly metamorphosed and migmatized metasediments. No uranium-related alteration.

Ore and Associated Minerals

Uraninite (U/Th ratio = 9), betafite and alteration products thereof, predominantly β-uranophane in near-surface zone.

Monazite, zircon, apatite, titanite, pyrite, chalcopyrite, bornite, molybdenite, arsenopyrite, magnetite, hematite, ilmenite, fluorite as accessorial rock constituents.

Mode of Mineralization

Uranium minerals of minute size occur as inclusions in quartz, feldspar, and biotite disseminated throughout the alaskite, in interstices and in microfractures. U in mineralized alaskite has particularly concentrated in zones rich in biotite, at constrictions of wide alaskite bodies passing into dikes or apophyses, in alaskites intruded along axial planes into metasediments and in alaskites replacing amphibolite.

Age Constraints

Although Rössing formed during the Damara Orogeny/Pan African Orogeny, 500 to 600 m.y. ago, similar deposits may have formed during any orogenic event of equivalent thermodynamic conditions provided adequate source lithologies were available.

Dimensions/Resources

Individual deposits (in brackets Rössing deposit) may be several tens of meters to several hundred meters (ca. 700 m) long, several tens to more than 500 m (ca. 600 m) wide and in excess of 700 m deep, containing up to ca. 125 000 mt U_3O_8 (Rössing) at (average) grades ranging from 0.002 to 0.04% U_3O_8, occasionally to 0.1% U_3O_8.

Remarks

For more details see Chapter 5.9.

Examples of Intrusive, Subtype 9.1 Alaskite Deposits/Occurrences

Canada: Johan Beetz/Quebec, ? Charlebois Lake/Saskatchewan
Namibia: Goanikontes, Ida Dome, Valencia-Trekkopje, SJ Claims/Damara Orogenic Belt

4.9.2 Subtype 9.2: Quartz monzonite (Cu-porphyry)

Type Example: Bingham, Utah, USA
References: John 1978; Lanier et al. 1978

Host Rocks/Alteration/Structures

Epizonal intrusion of several igneous phases ranging in composition from monzonitic to quartz monzonotic. In the Bingham stock six major igneous phases are recognized, from oldest to

youngest: Quartz-poor (<10 vol. % quartz) equigranular to porphyritic monzonite, porphyritic quartz monzonite and recrystallized monzonite; quartz-rich (>20 vol. % quartz), porphyritic latite, quartz monzonite porphyry and hybrid quartz monzonite porphyry; latite porphyry dikes and quartz latite porphyry dikes.

Hydrothermal alteration in and around the ore controlling quartz monzonite porphyry is reflected by Mg and K metasomatism forming an inner zone of quartz-orthoclase-phlogopite, an outer zone of actinolite-chlorite-epidote, and a late sericitic and argillic (montmorillonite mainly) overprint.

Ore and Associated Minerals/Mode of Mineralization

The ore minerals form overlapping sulfide mineral zones containing from the interior low grade core outward: molybdenite, bornite-chalcopyrite, chalcopyrite-pyrite, pyrite, and galena-sphalerite. Gold and silver is present in significant amounts. Pt, Pd, Re, Se, Bi, and U occur in recoverable traces. No uranium mineral is listed, but U may be present as uraninite or uranothorianite. Molybdenite and Cu-sulfides occur as disseminations, and galena-sphalerite with part of the pyrite as veins. The mineralization is concentrated on and drapes around and through the quartz monzonite porphyry facies. Distribution and zoning of mineralization and alteration is controlled by the location relative to the quartz monzonite porphyry facies within the intrusive complex, rock type, degree of fracturing, and permeability.

Age Constraints

Although the Bingham stock is of Eocene age, there should be no principal age constraint other than to periods of magmatic activity.

Dimensions/Resources

Cu- and Mo-mineralization at Bingham with which the recoverable U is associated extends over an area of about 1200 m by 2100 m around and through the quartz monzonite porphyry phase which measures laterally 420 m by 1000 m. Persistence of mineralization into depths is at least 1500 m. Uranium content in the Cu-Mo ore is 20 to 50 ppm. Uranium is extracted from leach containing 8 to 12 ppm U. Uranium resources recoverable as by-product to the year 2010 amount to ca. 1500 mt U_3O_8 (OECD/IAEA 1986).

Examples of Intrusive, Subtype 9.2, Granite/Monzonite Deposits/Occurrences

Australia: ? Crockers Well/Olary Province (REE + U)
Chile: Chuquicamata Norte (Cu + U)
USA: Twin Buttes/Arizona, Yerington/Nevada (Cu + U)
CIS: ? Akbabay, Aksuyek, Kiyakhty, Koktas/S of Lake Balkash (Cu + U)

4.9.3 Subtype 9.3: Carbonatite

Type Example: Phalaborwa, South Africa
References: Camisani-Calzolari et al. 1986; IAEA 1986a; Phalaborwa Mining Co, 1976

Host Rocks/Alteration/Structures

Carbonatite emplaced into the core of a differentiated alkaline intrusive complex. The carbonatite consists of a younger transgressive carbonatite core intruded into banded carbonatite. Fault systems apparently control the position of the transgressive carbonatite. Both facies are petrographically almost identical and consist of a magnetite-rich soevite. A rim facies of phoscorite has developed. It consists of serpentinized olivine, magnetite (ca. 30%), apatite (ca. 15%), phlogopite and calcite.

Ore and Associated Minerals

Recoverable ore minerals are chalcopyrite, bornite, titaniferous magnetite, baddeleyite, and uranothorianite. Other minerals and elements present in minor to trace amounts are pyrrhotite, pyrite, marcasite, pentlandite, millerite, bravoite, violarite, linnaeite, tetrahedrite, sphalerite, galena, covellite, chalcocite, cubanite, valleriite, as well as gold, silver, platinum, and palladium.

Mode of Mineralization

The transgressive carbonatite contains a high content of copper sulfides, mainly chalcopyrite

and less bornite, and accessory minerals, often in veinlets, up to 2 cm wide and less than 1 m long, horizontally and vertically. The banded carbonatite contains copper sulfides, mainly bornite as discreet grains widely disseminated throughout the rock. All ore minerals extend from the carbonatite into the phoscorite with bornite also prevailing in the phoscorite. Uranothorianite and baddeleyite are equivalent in all facies.

Age Constraints

No age constraints except to periods of magmatic activity.

Dimensions/Resources

Mineralized carbonatite and phoscorite at Phalaborwa form an elliptical, almost vertical dipping pipe. Diameters are 800 m and 1400 m. Drilled depth exceeds 1000 m. Average grade is ca. 0.004% U_3O_8 (0.51% Cu). Recoverable resources amount to several thousand tonnes uranium.

Examples of Intrusive, Subtype 9.3 Carbonatite Deposits/Occurrences

Brazil: Araxa
Finland: Sokli
India: Sevathur

4.9.4 Subtype 9.4: Peralkaline syenite

Type Example: Kvanefjeld, Illimaussaq, Greenland
References: Bohse et al. 1974; Sørensen et al. 1974

Host Rocks/Alteration/Structures

A differentiated agpaitic-peralkaline nepheline syenite complex includes as latest member lujavritic facies. The syenites have intruded into altered volcanic rocks and continental sediments.

Ore and Associated Minerals/Elements

Principal U-Th-bearing minerals are of refractory nature and include steenstrupine, eudialyte, and monazite. Associated elements include F, Li, Be, Zn, Zr, Y, Nb, and other REE.

Mode of Mineralization

U-Th minerals are disseminated in lujavrite. Highest but heterogeneously distributed U-Th concentrations occur at or near the contact of intrusive apophyses and sheet-like bodies of medium- to coarse-grained lujavrite in strongly deformed and metasomatically altered lavas. Analcime veinlets are often abundant in the contact zone. Mineralized zones containing in excess of 400 ppm U are rather small.

Age Constraints

The Illimaussaq syenite suite is about 1150 m.y. old but similar types of uranium occurrences may exist in comparable lithologic facies of any age from late Archean to Recent.

Dimensions/Resources

The Kvanefjeld deposit covers an area of about 700 m by 1500 m and extends for more than 100 m deep (investigated depth). Average grade is 0.03 to 0.04% U_3O_8. Resources amount to more than 30 000 mt U_3O_8.

Examples of Intrusive, Subtype 9.4 Peralkaline Syenite Deposits/Occurrences

Brazil: Catalão
Cameroun: Lolodorf
China: Saima Massif/NE China
Greenland: Motzfeldt Center/SE Greenland
South Africa: Pilanesberg/Bophuthatswana
Russia: Vishnevogorsk, Novogorny/Ural Mountains

4.9.5 Subtype 9.5: Pegmatite

Type Example: Madawaska/Bancroft, Canada
Reference: Alexander 1986

Host Rocks/Alteration/Structures

Granitic, rarely syenitic unzoned pegmatite of SiO_2 and mafic tendency (aegirine-augite), stained pink to brick-red by hematite, fine- to extremely coarse-grained emplaced as en-echelon dikes of tabular to flat lenticular shape with swells, offshoots, and apophyses transgressive or

paralleling metasediments and igneous rocks metamorphosed to amphibolite facies. Post-metamorphic deformation and metasomatism are common. Hematite is a characteristic alteration product.

Ore and Associated Minerals

Uraninite, uranothorite, and alteration products thereof mainly uranophane. Average U/Th ratio is 2.

Thorite, allanite, euxenite, davidite, spencite, magnetite, pyrite, marcasite, pyrrhotite, chalcopyrite, molybdenite, zircon, sphene, fluorite in accessorial amounts, and abundant hematite.

Mode of Mineralization

U is concentrated in discontinuous pods, shoots and bands, commonly controlled by mafic minerals and particularly by hematite and magnetite. Some mineralization is associated with late fractures. Although mineralization occurs randomly in the pegmatite in larger bodies, it is frequently proximal to the footwall and hanging wall side. Depth continuation is often more persistent than lateral continuity. U-tenors range from traces to 0.06% and rarely to 4% U_3O_8 over limited extent, changing within fractions of 1 m.

Age Constraints

The Bancroft pegmatites occur within the Grenville orogenic belt (950–970 m.y. old) but similar deposits may occur in any orogenic belt.

Dimensions/Resources

Individual deposits may be less than 1 m to several 100 m long, several centimeters to several 10 m wide and in excess of 400 m deep, containing up to 200 mt U_3O_8 at (average) grades ranging from 0.05 to 0.15% U_3O_8. Districts may contain up to 2000 mt U_3O_8.

Examples of Intrusive, Subtype 9.5 Pegmatite Deposits/Occurrences

Canada: Campbell Island/Ontario
Finland: Palmottu/Nummi-Pusula
Russia: ? Kem, Chupa area/Onezhsky

4.10 Type 10: Phosphorite (Fig. 4.10)

Definition

Phosphorite-related uranium mineralization consists of marine phosphorites of continental-shelf origin containing synsedimentary stratiform, disseminated uranium. The dominant uranium mineral is cryptocrystalline fluor-carbonate-apatite containing syngenetic uranium substituting for calcium. Two subtypes are recognized:

Subtype 10.1: phosphoria (Idaho Phosphoria type)

Type Example: Montpelier, Idaho, USA

Subtype 10.2: land pebble (Florida type)

Type Example: Land Pebble district, central Florida, USA

References: Altschuler et al. 1958; Heinrich 1958; McKelvey et al. 1956

Principal Recognition Criteria

Host Environment

- Phosphorites of marine origin deposited on continental shelf
- Subtype 10.1: bedded phosphorite with oolitic, pisolitic, pelletal and laminated textures associated with fine-grained miogeosynclinal facies (black shale, mudstone, chert, lesser carbonate beds) but noticeable absence of carbonates within uraniferous phosphorites
  Subtype 10.2: nodular phosphorite locally reworked to apatite pebbles interbedded with fine- to medium-grained shallow marine facies (sand, clay) and carbonate beds
- Widespread extension of phosphorite horizons, up to several 1000's of km^2
- Bedded phosphorites contain a higher uranium content and are formed distal to shore-line (subtype 10.1) as compared to nodular phosphorites which are proximal to shore line formation, except for the land pebble subtype (10.2) (partly due to reworking and secondary U enrichment)

Mineralization

- Either none or only rare discrete primary uranium minerals

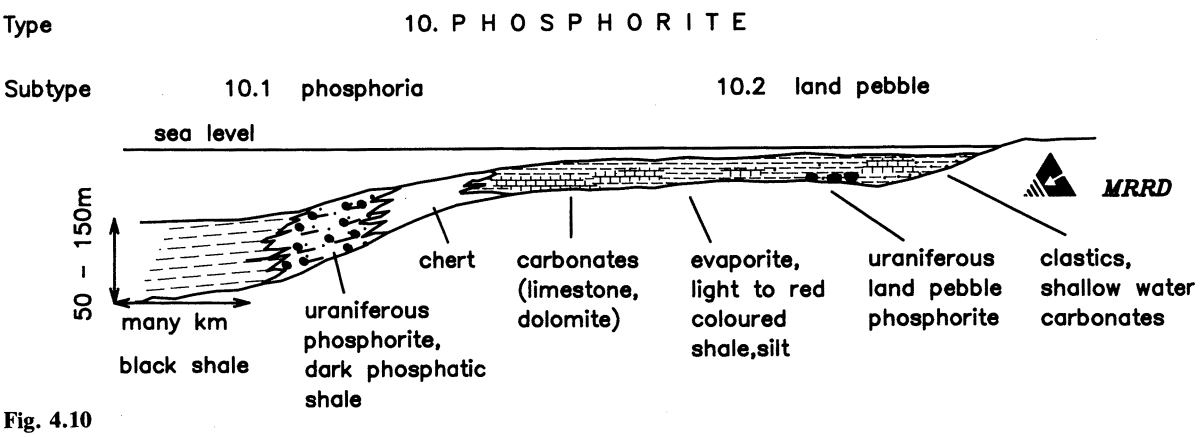

Fig. 4.10

- Principal uranium bearing mineral is cryptocrystalline fluor-carbonate apatite
- Unfavorable minerals for uranium accumulation are Al and Ca-Al phosphates (or other non-Ca phosphates)
- Positive correlation of U and P when concentration of both elements is relatively high
- Negative correlation of U and carbonate contents
- U exhibits a rather uniform distribution throughout a given bed
- No ore-related alteration except weathering
- No age constraints

Metallogenetic Aspects

Only phosphates of shallow marine origin contain appreciable amounts of uranium. Uranium accumulation is thought to be due to synsedimentary extraction of U from seawater and incorporation into phosphate minerals.

Two favorable environments of sedimentation are recognized.

The first, represented by the *Phosphoria Formation*, Idaho (subtype 10.1) has formed at the outer or distal shelf margin where thick layers of bedded phosphorite developed within a pile of very fine-grained miogeosynclinal sediments including black shale, more or less carbonaceous mudstone, chert beds, and only minor carbonates. Principal U-P mineral is cryptocrystalline fluor-carbonate apatite. Uranium is considered to have been syngenetically incorporated into the apatite lattice by replacing the Ca ion. The higher P (25 to 35% P_2O_5 over 1 to 3 m) and correlated higher U enrichment (up to 6500 ppm, average 60 to 200 ppm U) is attributed to the sedimentary environment of bedded phosphorite formation at the margin of a continental shelf, where (a) upwelling of P saturated deep marine waters provided a renewable P source, (b) slow rate of sedimentation caused longer exposure of apatite grains permitting extraction of U from the seawater to replace Ca in apatite, (c) absence of CO_2^{2+} ions in the waters which allows U to remain in solution. Variations in U content relative to P are interpreted to have resulted from either one or a combination of items (a) to (c) cited above.

The second environment is a shallow marine near-shore platform represented by lower grade phosphatic and uraniferous nodular phosphorites (average 10 to 20% P_2O_5, 20 to 80 ppm U) except for the land pebble mineralization. In this environment, fine- to medium-grained clastics (clay, sand, glauconite) and shallow-water carbonates precipitated contemporaneously with phosphate.

The *land pebble phosphorite* (subtype 10.2) as found in the Pliocene Bone Valley Formation, Land Pebble district, central Florida, contains pebbles and sand size grains of fluor-carbonate apatite enriched with up to 35% P_2O_5 and 500 ppm U and locally more. The enrichment is attributed to reworking and corresponding re-exposure of the apatite particles to uranium bearing seawater during repeated marine transgressions. Associated with this evolution is an irregular, up to a few meters thick, leached horizon developed within the Bone Valley Formation by weathering. Its upper section,

composed of Al-phosphates (wavellite), and its middle section, dominated by Ca-Al-phosphates (millisite, crandallite, referred to as aluminum phosphate zone), have released uranium supposedly by acid solution leaching. Altschuler et al. (1958) suggest U reconcentration at or near the base of the leached zone composed of incipiently leached residual apatite formed in response to neutralization of the acid fluids by the Ca-phosphate. Fixing of uranium resulted by adsorption on the porous, partially leached, residual apatite leading locally to concentrations of as much as several thousand ppm U. Principal U collectors are Ca-phosphates (apatite) and, to a lesser extent, Ca-Al-phosphates (crandallite), whereas Al-phosphates (wavellite) are unfavorable U collectors. Distribution of these minerals also reflect the U-grade zonation within the leached profile.

Remarks

Although uraniferous marine phosphorites constitute large U resources, their commonly very low average grade (<20 to 300 ppm U) and difficult metallurgical U extraction excludes them from being a primary U source. U is recovered, however, as a byproduct of phosphate production.

In contrast to marine phosphorites, all other phosphatic rocks contain lower concentrations of uranium. They include residual phosphorites derived by weathering of marine phosphatic limestone, phosphatized rocks resulting from solutioning of phosphates from rocks higher in the sequence and its redeposition as interstitial fillings or replacements in subjacent rocks, guano mainly composed of bird and bat excrements, and detrital weathering products thereof and of marine phosphorites such as fluvial pebble deposits.

Examples of Type 10 Phosphorite Deposits/ Occurrences (not Differentiated)

Central African Republic: ? Bakouma
Israel: Zefa/Negev
Morocco: Ganntour-Bahira/Youssoufia, Oulad Abdoun/Khouribga
USA: Bone Valley/Florida, Green River/Utah-Wyoming

4.10.1 Subtype 10.1: Phosphoria (Idaho type)

Type Example: Montpelier, Idaho, USA; Permian Phosphoria Formation
Reference: McKelvey et al. 1956

Host Rocks/Alteration/Structures

Phosphatic shales composed of bedded fluor-carbonate apatite as fine-grained oolites, pisolites, pellets or laminae and phosphatic fossil fragments (brachipod shells, fish scales, etc.) mixed with variable amounts of finest-grained detritus, mainly clay particles, carbonaceous matter and locally carbonate. Sedimentary environment is the distal part of a continental shelf, where uranium-bearing deep seawater could ascend and flood the phosphorite and where contribution of detrital clay and silt was minimal and accumulation rate was strongly retarded. Associated sediments include over- or underlying, often pyritic cherts, mudstone, black shale which laterally interfinger with sandy, carbonatic, red bed and evaporitic shallow water sediments.

Ore and Associated Elements/Mode of Mineralization

U occurs in rather uniform dissemination in phosphatic beds in dominantly bedded cryptocrystalline fluor-carbonate apatite of pelletal, oolitic etc. texture. Although present in almost all phosphorite beds U grades vary considerably from 10 to 6500 ppm U and to a large extent, but not necessarily, are correlative to the phosphate content. P_2O_5 enrichment is greatest in the top and/or basal segments of phosphatic layers as examplified by the Mead Peak Phosphatic Shale Member, the main phosphate member of the Phosphoria Formation. This member is 60 to 150 m thick and averages 11 to 12% P_2O_5, whereas the upper and lowermost 1 to 3 m contain from 25 to 35% P_2O_5 and also contain the highest uranium tenors.

Dimensions/Resources

The Phosphoria Formation stretches over many thousands of km^2, its phosphatic member ranges from 60 to 150 m thick. The best mineralizations occur over a thickness of 1 to 3 m. Total resources are several million tonnes U_3O_8. Uranium grades average 60 to 200 ppm.

4.10.2 Subtype 10.2: Land Pebble (Florida type)

Type Example: Land Pebble district, central Florida, USA; Pliocene Bone Valley Formation
Reference: Altschuler et al. 1958

Host Rocks/Alteration/Structures

Phosphatic pebbly argillaceous sandstones are crudely graded bedded, reworked and composed of nodules and sandsize grains of fluor-carbonate apatite mixed with clay minerals (smectite, montmorillonite) and quartz grains of shallow marine near-shore continental shelf origin. The phosphorite is interbedded with marine sands and shallow water limestone and dolomite. Black shales and cherts are noticeable absent. Where affected by weathering, apatite is replaced in the top zone by Al-phosphate (wavellite) and in the middle zone by Ca-Al-phosphate (crandallite, millisite). Smectite is transformed to kaolinite. Incipiently or incompletely leached residual apatite of the bottom zone is highly porous and enriched in U, whereas the secondary Al- and Ca-Al-phosphates contain only minor U.

Ore and Associated Minerals/Mode of Mineralization

U occurs in stratiform dissemination bound to Ca-phosphate (principally fluor-carbonate apatite) in the form of sandsize particles and nodules in beds mixed with quartz and clay minerals. Although apatite grains and nodules are often enriched up to 500 ppm U and locally up to several 1000 ppm at bottom of leached zone, the mineralized lower Bone Valley Formation averages ca. 150 ppm U: due to the quartz and clay matrix.

Dimensions/Resources

Lateral extension of the lower Bone Valley Formation is about 2500 km^2 in which deposits of the Land Pebble district occur. Mineralized beds range in thickness from less than a meter to 10 m averaging 5 to 7 m. Total U resources are in the order of 500 000 mt U_3O_8 or more. Grades of land pebble mineralization average ca. 150 ppm U.

4.11. Type 11 :Volcanic (Fig. 4.11)

(also referred to as volcanogenic type, or U-Mo type in Russian literature)

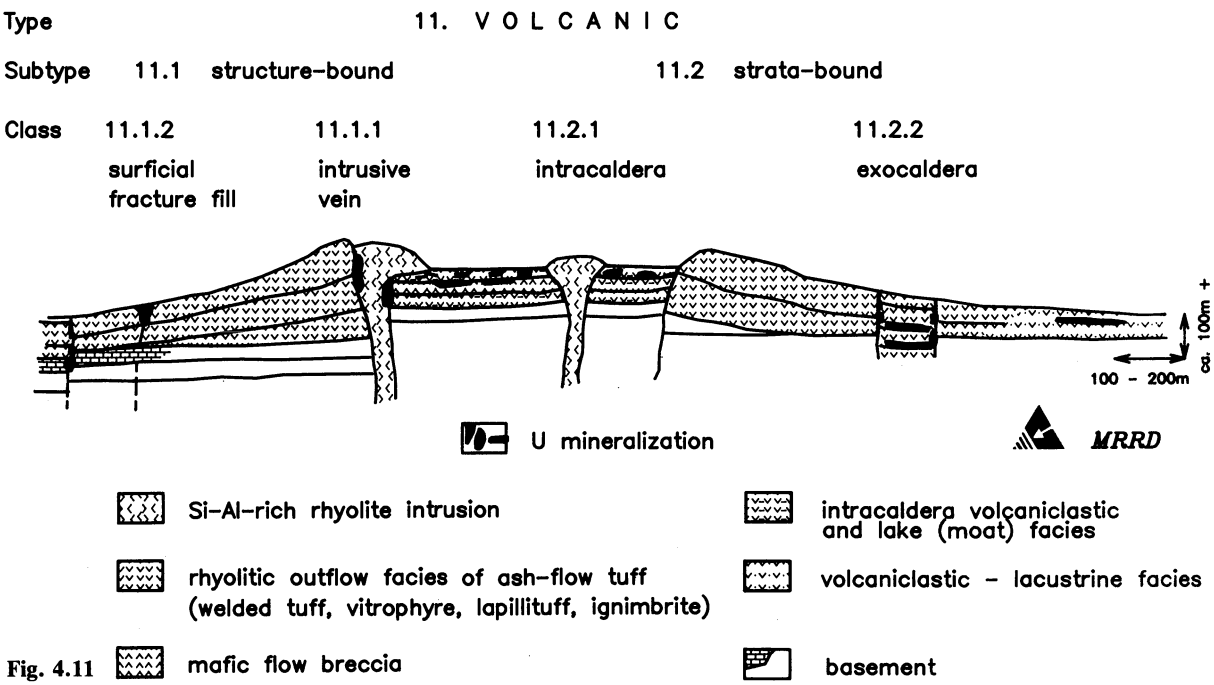

Fig. 4.11

Definition

Volcanic deposits are associated with felsic to intermediate volcanic rocks and their sedimentary derivates. Uranium occurs as structure-bound or strata-bound concentrations which can be separated into several classes:

Subtype 11.1: structure-bound

Class 11.1.1: intrusive veins
Type Example: Nopal I, Mexico

Class 11.1.2: surficial
Type Example: Cotaje, Bolivia

Subtype 11.2: strata-bound

Class 11.2.1: intracaldera
Type Example: Aurora, USA

Class 11.2.2: exocaldera
Type Example: Margaritas, Mexico

References: Chen Zaobo 1981; Dayvault et al. 1985; George-Aniel et al. 1985; Goodell 1985; Goodell and Waters 1981; IAEA 1985; Leroy et al. 1985, 1987; Pardo-Leyton 1985; Sherborne et al. 1979

Structure-bound mineralization include intrusive veins associated with volcanic intrusions, diatremes, flows or bedded pyroclastic units (class 11.1.1) and surficial fracture fills (class 11.1.2) in similar lithologies. *Strata-bound mineralization* consists of disseminations and impregnations in permeable and/or reactive flows, flow breccias, tuffs and other lithologies. Distinction of strata-bound classes is based on their intracaldera (class 11.2.1) or exocaldera (11.2.2) host environments, the latter is mixed with nonvolcanic clastic sediments.

Principal Recognition Criteria

Host Environment

- Volcanogenic intrusive and extrusive rocks of felsic to intermediate magmatism
- Preferentially leucocratic, rhyolitic facies high in silica and alumina, low in iron and calcium, rich in volatiles
- Abundance of fluorite, tourmaline, topaz reflecting volatile enrichments of F and B
- Enrichment in trace elements particularly U, Mo, Sn, W, Hg, As, Sb, Li
- Occurrence of volcanic domes, subvolcanic intrusives, ring dike intrusives, outflow facies of ash-flow tuffs, lavas, ignimbrites, pyroclastics, intracaldera volcaniclastic and lacustrine or moat facies
- Facies with major permeability variations due to welding or fracturing (vesicular flow zones, flow breccias, contacts between thick rhyolitic units and mafic lavas or limestones, ring dike faults, fault intersections, grabens, fracture zones proximal to domes, subvolcanic intrusions or major dikes)
- U source and U host rocks are often identical
- Glassy and unwelded volcanics are better sources than crystalline or welded rocks

Alteration

- Feldspathization
- Zeolitization
- Devitrification
- Advanced to complete argillitization
- Strong hematitization
- Intense silicification

Mineralization

- Principal uranium minerals are pitchblende, rarely coffinite, in many deposits uranyl minerals
- U adsorbed on or incorporated in various host minerals (U bearing clay minerals, uraniferous opal etc.)
- Associated metallic minerals include mainly pyrite, minor to traces of Mo, Pb, Sn, W, Li, Hg, Sb, W and other minerals
- Associated gangue minerals: fluorite, quartz, carbonates, baryte, jarosite
- Occurrence of U minerals predominantly as disseminations, very rarely as more massive concentrations (stringers, veinlets, pods)
- Higher grade mineralization always of erratic distribution

Age Constraints

No restrictions except to taphrogenic episodes

Metallogenetic Aspects

Prerequisite for mineralization are volcanic facies containing U in excess of average crustal

abundance and in leachable form. These parameters are provided mainly by rocks of rhyolitic composition that are unwelded and have a glassy groundmass. Matrix-bound uranium is easily liberated by devitrification in reaction to both volcanic hydrothermal (hot springs, fumaroles) and meteoric supergene waters, which then transported the U to sites of deposition either in porous volcanic beds or fractures. In addition, U may be introduced by volcanic hypogene fluids. U-transporting solutions are thought to be oxidized and slightly acidic, containing F, CO_2 or other ions, which facilitate transport of U. Suggested processes for fixing U include reduction and adsorption, associated with neutralization by wall rock interaction and boiling or evaporation of fluids. In near-surface deposits U precipitation often occurs along groundwater tables.

Remarks

Volcanic uranium occurrences have often been overprinted by strong hydrothermal or diagenetic processes, making it difficult to attribute them to a distinct class.

Most of the volcanic uranium occurrences also comply with criteria defining other types of deposits particularly of vein, surficial, fracture fill and tabular sandstone types except for their crucial volcanogenic relationship and subeconomic magnitude. Grades are low to very low (0.02 to 0.1% U_3O_8) and resources are commonly small (<1000 mt U_3O_8). Volcanic occurrences may be more important as potential sources for other types of deposits, particularly for those of sandstone type.

Examples of Type 11 Volcanic Deposits/ Occurrences (not Differentiated)

Australia: Maureen/Queensland
Brazil: Osamu Utsumi/Poços de Caldas
Bolivia: Cotaje/Altiplano
Bulgaria: East Rhodope Mts, East Balkan Mts
Canada: Michelin/Labrador
China: Quinlong-Daxing'anling volcanic belt, Langshan area/NE China, Balyanghe/NW China, Gan-Hang and S. Jiangxi-N. Guangdong volcanic belts/SE China
Kazakhstan: Pribalkhashky region
Romania: Apuseni Mts
Russia: Streltsovsky region/Transbaikal
Uzbekistan: Karamazarsky region

4.11.1 Subtype 11.1: Structure-bound

Reference: Leroy et al. (1987)

Class 11.1.1: Intrusive Veins

Type Examples: Nopal I, Peña Blanca, Mexico
Reference: George-Aniel et al. 1985;

Moonlight, Mc Dermitt, USA
Reference: Dayvault et al. 1985

Host Rocks/Alteration/Structures

Host lithologies are variable and include rhyolitic ignimbrite, rhyolitic breccias, dacite flows, granodiorite, a. o. Hydrothermal and/or diagenetic alteration is intense and may consist of devitrification, argillitization (kaolinite, montmorillonite), zeolitization and silicification. At Nopal I, host rocks are completely altered. Alteration increases with intensity and density of fracture systems and decreases with distance from the ore body (60 to 200 m away). Deposits occur in intensely fractured and brecciated zones caused either by crosscutting fault sets (Nopal I) or along ring fracture systems (Moonlight).

Ore and Associated Minerals

Principal uranium mineral in an unoxidized environment is pitchblende associated with minor pyrite, molybdenite, and traces of other sulfides. Gangue minerals may be fluorite, quartz, locally minor adularia, carbonate, apatite, jarosite, baryte, and Ti-minerals. Most mineralization is oxidized containing mainly uranyl-phosphates and -silicates and limonite. Mineralization commonly includes concentrations of Pb (<2000 ppm), Mo (<500 ppm) and anomalous amounts of As, Sb, Ag, Cu, Hg, Sn, W, Zr.

Mode of Mineralization/Dimensions/Resources

Uranium minerals occur as disseminations or coatings in a pipe-shaped deposit filled with silicified tectonic breccia at Nopal I (20 × 40 m wide, >100 m deep) or as disseminations, stringers

and veinlets within tectonic breccia and siliceous cement which form veins, 1 to 5 m wide, at least 50 m deep as at the Moonlight mine. Ore distribution is irregular changing from sections with little uranium to grades which locally reach 10% U_3O_8.

Deposits contain from less than 1 mt to a few 100 mt U_3O_8 at ore grades averaging from <0.1% to 0.5% U_3O_8 (Nopal I ca. 350 mt U_3O_8; 0.3% U_3O_8).

Examples of Volcanic, Class 11.1.1 Structure-Bound Intrusive Vein Deposits/Occurrences

Australia: ? Ben Lomond/Queensland
Canada: Rexspar/British Columbia
Kazakhstan: Pribalkhashsky region
Peru: Macusani
USA: Marysvale/Utah, White King Mine/Lakeview, Oregon
Russia: Streltsovsky/Transbaikal

Class 11.1.2: Surficial veinlike

Type Example: Cotaje, Sevaruyo, Bolivia
References: Leroy et al. 1985; Pardo-Leyton 1985

Host Rocks/Alteration/Structures

Host lithologies are rhyolitic to rhyodacitic ignimbrite and tuff layers with intercalated volcanic breccias and conglomerates. The tuffs have increased U, Th, Li, Sr, Ba, and REE tenors. Alteration is reflected by marked bleaching, argillitization, dominantly kaolinitization and silicification. Deposits occur near surface in zones of intense fracturing and brecciation.

Ore and Associated Minerals

Principal U minerals are (sooty) pitchblende, coffinite and uranyl phosphates associated with smoky quartz, baryte, siderite, gypsum, and minor Fe, Pb, Zn sulfides. Local enrichment of Mo and V also occur.

Mode of Mineralization

Uranium minerals are irregularly distributed in open fractures forming narrow veins and occur disseminated throughout zones of intense shearing or brecciation which are commonly oxidized.

Dimensions/Resources

Mineralized structures are commonly 10 to 60 m, rarely few 100 m long, 0.1 to 10 m wide and persist from surface to about 30 m deep. (Cotaje: 350 m long, 1 to 10 m wide, 30 m deep).

Deposits contain from less than 1 mt to some 10 mt U_3O_8. Grades average 0.05 to 0.07% U_3O_8, but may be as high as 2.5% U_3O_8. Cotaje accounts for ca. 40 mt U_3O_8, at an ore grade of 0.07% U_3O_8. Some districts may contain a few hundred, perhaps a few thousand tonnes U_3O_8.

Examples of Volcanic, Class 11.1.2 Structure-Bound Surficial Deposits/Occurrences

ČSFR: Novoveska Huta-Muran/Slovakia
USA: Lucky Lass Mine/Lakeview, Oregon

4.11.2 Subtype 11.2: Strata-bound

Reference: Orajaka (1981)

Class 11.2.1: Intracaldera

Type Example: Aurora-Cottonwood Creek, Mc Dermitt, USA
Reference: Dayvault et al. 1985

Host Rocks/Alteration/Structures

Host rocks are mafic to intermediate tuffs, flows, and flow breccias associated with domes and overlain by tuffaceous lacustrine (moat) sediments. Individual flows have massive central zones bordered by ± strongly altered vesicular to scoriaceous flow tops along intraformational unconformities. Alteration and mineralization in lavas is restricted to porous zones along flow tops, brecciated layers and fracture zones. Mineralized facies are almost completely altered to pyritic montmorillonite, chlorite, clinoptilolite, opal, leucoxene rocks with a groundmass of K-feldspar, clay, and quartz. Alteration of lacustrine sediments is reflected by sporadic zeolites, ubiquitous feldspar, and smectite, calcite and quartz crystallization.

Ore and Associated Minerals

Principal uranium minerals are pitchblende, coffinite, and locally hexavalent U minerals asso-

ciated with pyrite. Anomalous concentrations of Hg, Li, As, Sb, Mo, Zn, W, and F are associated with the mineralization.

Mode of Mineralization/Dimensions/Resources

Uranium minerals occur as fine coatings of pyrite and leucoxene mainly concentrated in highly altered porous layers along flow tops and in breccia layers up to a few meters thick. Tuffaceous lacustrine sediments contain minor amounts of U (up to 200 ppm U) predominantly concentrated in intercalated layers 0.5 to 2 m thick, composed of thinly bedded (mm to cm) opal, pyrite, ash, diatoms and minor carbonaceous matter.

Mineralization extends laterally for several 100 m to few 1000 m, and may penetrate upwards and downwards into fracture zones.

Deposits may contain a few tens and up to several 1000 mt U_3O_8, at grades ranging from 0.02 to rarely 0.1% U_3O_8. (Aurora: ca. 7500 mt U_3O_8, 0.05% U_3O_8). Districts, including other types of volcanogenic U deposits, may have potential resources of some 10 000 mt U_3O_8. (Mc Dermitt ca. 30 000 mt U_3O_8, 0.03% U_3O_8). No attempts are known to recover U as by-product of Hg, Li, or other metal mining.

Examples of Volcanic, Class 11.2.1 Strata-bound Intracaldera Deposits/Occurrences

Italy: Sabatini, Vulsini/Latium
Russia: Yubileynoye, Novogodneye/Streltsovsky, Transbaikal

Class 11.2.2: Exocaldera

Type Example: Margarites, Peña Blanca, Mexico
Reference: Goodell 1985

Host Rocks/Alteration/Structures

Host rocks are facies of ash-flow tuff (vitroclastic alkaline rhyolitic tuffs, etc.). At Margaritas the tuffs fill a graben, 500 m wide, bound on both sides by step faults with displacements of up to 100 m and more. Alteration includes extensive devitrification, partial argillitization, intense silicification and locally abundant hematitization.

If these volcanoclastics are interbedded with lacustrine sediments they form deposits such as those in the Date Creek Basin, Arizona.

Ore and Associated Minerals

Principal uranium minerals are hexavalent U species (uranyl silicates, vanadates, phosphates) associated with molybdenite, powellite, and locally with jarosite, pyrite, calcite and fluorite.

Mode of Mineralization/Dimensions/Resources

Uranium minerals occur as disseminations, encrustations, lamina occupying fractures, joints, and voids. Mineralization distribution is erratic. At Margaritas, higher-grade sections ranging from 0.1 to 0.4% U_3O_8 and 0.1 to 3% Mo are separated by low grade intervals. Mineralization occurs over intervals ranging from 1 to 7 m thick, 100 to 150 m wide and about 300 m long. In most cases, deposits of this type are smaller in dimensions.

Deposits may contain a few tonnes to some 1000 mt U_3O_8, at grades ranging from 0.02 to rarely 0.2% U_3O_8. (Margaritas: ca. 2000 mt U_3O_8, 0.1% U_3O_8). Districts may have resources of several 1000 mt U_3O_8 (Peña Blanca district: ca. 4000 mt U_3O_8).

Examples of Volcanic, Class 11.2.2 Strata-bound Exocaldera Deposits/Occurrences

Australia: ? Maureen/Queensland
Canada: Michelin/Labrador
Italy: Novazza/Val Seriana
Sweden: Duobblon/Sorsele
USA: Date Creek Basin/Arizona

4.12 Type 12: Metasomatite (Fig. 4.12)

Definition

Metasomatite deposits consist of unevenly disseminated uranium in structurally deformed rocks that were affected by alkali metasomatism of dominantly sodium tendency. Metasomatic facies include albitites, aegirinites and alkali-amphibole rocks. Principal uranium phases are uraninite ± Th rich and U-Th oxides and silicates.

Two subtypes are defined on the basis of the precursor rock facies:

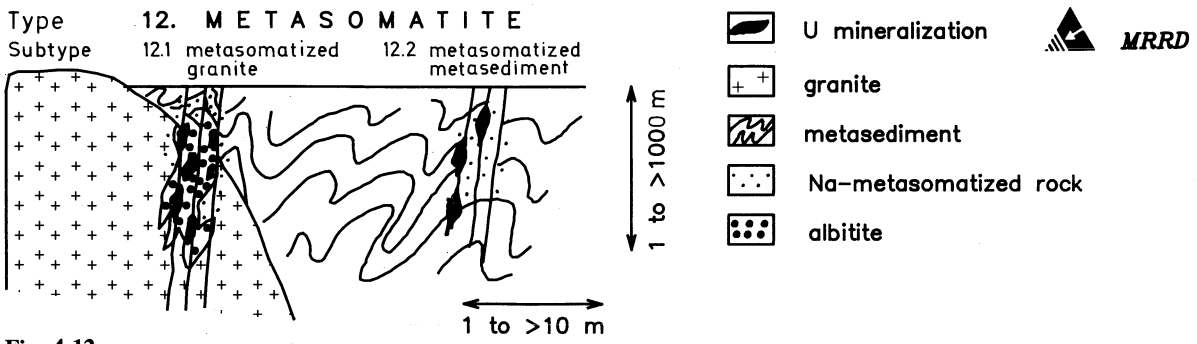

Fig. 4.12

Subtype 12.1: metasomatized granite

Type Example: Ross Adams/Bokan Mountain, USA

Subtype 12.2: metasomatized metasediments

Type Example: Krivorozhsky-Zheltye Vody, Ukraine

References: Avrashov/Bendix (ed.) 1980; Belevtsev et al. 1984; Collot 1981; Fritsche 1986; Fuchs et al. 1981; Kazanzky and Laverov 1977; Mineeva 1984

Principal Recognition Criteria

Host Environment

- Albitites and granites or metasediments with metasomatic albite-aegirine, albite-arfvedsonite-aegirine or other Na-silicates
- Distribution of metasomatites along cataclastic zones in parent rocks
- Transition margins between metasomatized facies and parent rocks are commonly narrow
- Emplacement of mineralization along micro- and macro-fractures confined to albitized facies
- Parent rocks have often but not necessarily anomalous uranium background values
- Intrusive granites are enriched in alkalis, Al_2O_3, U, Th, Nb, and REE
- Albitized metasediments are mostly found in middle to high rank, partly dynamothermally, metamorphosed rocks adjacent to leucocratic granite intrusions in mobile belt terranes

Alteration

- Na-metasomatism reflected by enrichment of Na_2O and depletion of SiO_2 and K_2O
- Argillitization (commonly weak)
- Hematitization (locally intense)
- Locally carbonatization

Mineralization

- Principal uranium minerals: uraninite ± Th rich, uranothorianite, uranothorite, thorite, nenadkevichite, U-Ti oxide phases (brannerite), pitchblende and coffinite
- Associated minerals: allanite, bastnaesite, monazite, xenotime, zircon, apatite, galena, pyrite, magnetite, and/or calcite in accessorial amounts; locally abundant hematite
- Occurrence of U minerals as disseminated anhedral to euhedral grains and in thin veinlets.

Belevtsev et al. (1984) provide the following additional features for Proterozoic albitite uranium deposits, presumably referring to the Zheltye Vody district, Ukraine:

- U mineralized albitites occur within sediments and volcanogenic rocks that have been metamorphosed to amphibolite grade facies or granitized and which contain elevated U backgrounds
- U hosting albitite occurs along cataclastic and mylonitic zones within metasomatic albitite
- U hosting albitite differs from ordinary U barren albitite by blastoclastic structures, better permeability and presence of hematite, aegirine, alkaline amphibole, chlorite, epidote, and carbonate
- U minerals occur as fine-grained impregnations associated with dark-colored minerals among albite grains

Kazanzky and Laverov (1977) und Kazanzky et al. (1978) distinguish iron-uranium deposits associated with Na- and CO_3^--metasomatites (Krivoi Rog) and uranium deposits associated with Na-metasomatites. For both types, a distinct zoning and the association with deep-seated multi-activated fault systems combined with

brecciation and mylonitization are said to be typical.

Age Constraints

No age constraints except restriction to periods of late or post-orogenic magmatic activity.

Metallogenetic Aspects

Metasomatite-bound uranium mineralizations appear to be the final result of a (Na-)metasomatic evolution during the waning stages of an orogeny. In the case of *subtype 12.1* deposits, metasomatism transformed during an early stage previously crystallized leucocratic igneous rocks, essentially granite, into Na-rich facies culminating in albitite in structurally deformed ground perhaps in the apex part of a pluton. Cathelineau (1986) points out that (a) the fluids responsible for albitization and associated desilicification are in composition similar to those of meteoric origin, (b) metasomatic alteration takes place several tens of m.y. after granite crystallization, and (c) there is no relation between late magmatic, pneumatolytic to deuteric processes which also can cause alkali enrichment and albitite-forming metasomatism.

Subsequent to albitization, introduction of U associated with Th and REE occurred on the same reactivated structures along which the albitizing fluids permeated the host granite. This spatial relationship also suggests a metasomatic origin of the U, Th, REE mineralization. Similar processes are assumed for the formation of *subtype 12.2* deposits. But instead of autometasomatism as in granite, metasediments were altered presumably by fluids derived from or mobilized by intruding granites or by late metamorphic events.

Mineeva (1984) comments on the metallogenesis of uranium albitites associated with deep rooted-lineaments which can be attributed to subtype 12.2 and states that:

- albitization and mineralization evolved through several stages ranging from ultrametamorphism to post-albitite events;
- polyphase processes imprinted primary and secondary lateral and vertical zoning on host rocks reflected by mineralogy and geochemistry. In contrast, unmineralized albitites are not zoned and REE mineralized albitites display only primary lateral and vertical zoning;
- post-albitite events superimposed a secondary zoning reflected by a hydrothermal mineral paragenesis of various phases which typically are associated with economic deposits. They include apatite, chlorite, carbonate, baryte, quartz, sulfides and hematite;
- spatial extension of U mineralization in albitites correlates with extension of carbonatization. This reflects the importance of CO_2. CO_2 controls the pH values in the fluid system and influences complexing of U and other elements in solution and their redeposition;
- U redistribution proceeds downwards and affects ubiquitously the host albitites thereby achieving U enrichments.

According to Belevtsev et al. (1984), uranium mineralization resulted from residual metamorphogenic fluids contained within cataclastic and mylonitic zones of protoactivation. The mineralizing activity progressed through the final stage of metamorphism. Fluid inclusion studies indicate that involved solutions contained carbonate, chloride, and sulfide with concentrations of 10 to 40%. Temperatures ranged during the albitization stage from 350 to 150°C and during the mineralizing stage from 200 to 120°C at pressures of 600 to 900 bar. According to Batashov et al. (1984), the temperature of mineralization was 300 to 200°C.

The source of the uranium for both subtypes remains debatable. Both lateral secretion by the metasomatic solutions leaching U from either uraniferous host granite or host (meta-) sediments or other rocks, or U concentrations in the residual magma are speculated. Size and grade of a deposit may be a function of availability of uranium, ground preparation and the duration of the metasomatic process. Pervasive metasomatism may cause wider distribution associated with dilution of the uranium throughout a large volume of rock. In contrast, narrow zones of metasomatism may have concentrated the uranium to form higher grade mineralization.

Remarks

The processes involved in metasomatism and related mineral formation are to some extent comparable with those leading to vein deposits.

The distinction between the two may be difficult. On the other hand, metasomatic deposits of subtype 12.1 commonly are within anomalously uraniferous granites which may be attributed to the intrusive type of deposits.

Both subtypes generally contain resources of small quantities (<1000 mt U_3O_8) and low grade (<0.2% U_3O_8). Known exceptions are the deposits of Ross Adams, USA, Gunnar, Canada and Zhelty Vody (= Yellow Waters), Ukraine.

Note

Uraniferous Na-metasomatized lithologies have drawn much attention in the former USSR for many decades but have been largely neglected in the Western World until recently. The term *albitite deposits* in connection with uranium mineralization was used first by Russian authors. Thorough investigations of this type of uranium deposits were carried out by many of them, e.g., Kazanzky et al. (1968) Smirnov (1977), Kalyaev (1980). Early work in Canada by Robinson (1955) hints to a uranium paragenesis within albitic vein rocks in the Goldfields-region (Beaverlodge district), Saskatchewan. Christie (1953) and Dawson (1951, 1956) describe there veins consisting of microcrystalline aggregates of albite and quartz, stained with hematite associated with calcite and chlorite.

Fritsche (1986) has reviewed pertinent literature and defined types of albitites and related uraniferous albitites (see Chap. 2).

Up to the present, albitites are defined as primary magmatic rock types in most geological nomenclatures, although Goldschmidt (1911) already explained albitite veins as of pneumatolytic contact metasomatic origin. Sørensen (1974) defined albitites as rocks of plutonic character with mainly albite, about 10 vol. % of more calcic plagioclase, 5 vol. % of quartz and with olivine, augite, amphibole, and biotite as minor components. Sørensen (1974) considered the possibility of a secondary metasomatic origin for albitites in addition to a magmatic genesis. Albitization, as defined by Schieferdecker (1959) universally, is "the production, in a rock of albite, as a secondary product". Other definitions restrict albitization to the autometasomatic alteration of plagioclases in magmatic rocks only (e.g., Holmes 1928).

According to Kalyaev (1980), albitization is found in almost every rock type. Mostly it occurs in magmatic rocks but likewise in metamorphic and sedimentary rocks and in porphyry copper deposits. In most cases these autometasomatic, metamorphic or diagenetic albitization processes do not cause a complete alteration of the rock and do not lead to the formation of albitites.

Sarcia (1980) gives a summary concerning uranium in albitites and classifies these deposits as:

- anorogenic deposits associated with deep faults, without direct relation to magmatic rocks. Example: Deposits of the Ukrainian Shield (Smirnov 1977) or Alio Ghelle, Somalia (Cameron 1970);
- deposits in orogenic zones associated with faults accompanied by granitization and magmatism. Examples: Pleutajokk/Sweden (Adamek and Wilson 1977). Espinharas/Brasil (Ballhorn et al. 1981), Kitongo/Cameroon (Fritsche 1986);
- deposits bound to postorogenic fault systems within the basement and the metamorphosed cover. Example: Brousse-Broquiés, Aveyron Rouerque, France (Yerle 1978).

Uranium occurrences associated with alkaline bodies especially in relation to autometasomatically albitized or hydrothermally altered zones or late magmatic fractures where later, post-magmatic hydrothermal processes have been in operation are described by Mackevett (1963) and Thompson et al. (1980, 1982) from the peralkaline intrusion of Bokan Mountain/Alaska and by Sørensen (1970) from Ilimaussaq (Greenland). Similar zones are known from the intrusive bodies of Poços de Caldas/Brazil and Seal Lake/Labrador (Group 1970) or from the CIS (Kozlova and Gurvich 1979), from China and the Mongolian Peoples Republic (Saima Deposit Research Group 1976; Boguslavsky et al. 1966).

4.12.1 Subtype 12.1: Metasomatized granite

Type Example: Ross Adams/Bokan Mountain, USA

References: Collot 1981; Thompson et al. 1980, 1982

Host Rocks

Albitic aegirine granite, albitic arfvedsonite-aegirine granite, albitite derived by epigenetic Na-metasomatism along cataclastic zones in anomalously uraniferous granite. Transitional aureoles between metasomatized facies and parent rocks are commonly narrow. Spatial distribution of metasomatism appears to be restricted to structurally prepared zones in the apical part of a postorogenic or anorogenic pluton.

Pluton-internal shear, fracture and breccia zones confined to albitized facies commonly provide the site for mineralization.

Alteration

Two principal types of alteration can be distinguished:

- Na-metasomatism is characterized by albitization associated with desilicification and in the case of insufficient Al to form albite, by the formation of aegirine and/or arfvedsonite. Geochemical changes are enrichment of Na_2O and depletion of K_2O and SiO_2 (replacement of K-feldspar, Ca-rich feldspar and quartz by albite).
- Weak argillitization of feldspars including secondary albite, and locally intense hematititization. At Ross Adams, hematite imposes a pervasive red staining on microfractured albite and coats uraninite grains indicating a post-albite, post-uranium formation.

Ore and Associated Minerals

Uraninite ± Th rich, uranothorianite, uranothorite, thorite, some brannerite, and coffinite.

Allanite, bastnaesite, monazite, xenotime, galena, pyrite, magnetite, zircon, apatite, fluorite, and calcite in accessorial amounts. Locally abundant hematite.

Mode of Mineralization

U minerals occur as disseminated anhedral to euhedral grains and in thin veinlets, with or without accessorial pyrite, galena, fluorite, and galena within zones of closely spaced jointing and shearing and some brecciation in a metasomatized albite and aegirine granite. At Ross Adams, the mineralized rocks are related to portions of the Bokan Mountain granite geochemically enriched, in Na_2O, Al_2O_3, U, Th, Nb and REE.

Age Constraints

No age constraints except restriction to periods of late- or post-orogenic magmatic activity.

Dimensions/Resources

Individual deposits (in brackets Ross Adams deposit) may be several meters to >100 m (ca. 110 m) long, several meters to more than 20 m (7.5–22 m) wide, and in excess of 100 m deep, containing few tens and up to ca. 1000 mt (850 mt) U_3O_8 at (average) grades ranging from <0.1 to >1% U_3O_8 occasionally to 3% U_3O_8. Districts may contain up to few 1000 mt U_3O_8.

Examples of Metasomatite, Subtype 12.1 Metasomatized Granite Deposits/Occurrences

Australia: ? Radium Hill/Willyama Block, South Australia
Canada: ? Gunnar/Saskatchewan
Brazil: Lagoa Real/Bahia
Cameroun: Kitongo

4.12.2. Subtype 12.2: Metasomatized metasediments

Type Example: Krivorozhsky-Zheltye Vody district/Krivoy Rog, Ukraine
References: Batashov et al. 1984; Kazansky and Laverov 1977

Host Rocks/Structures

Archean amphibolite and biotite gneiss intruded by quartz diorite and granodiorite form basement to Lower Proterozoic metasediments in the Zheltye Vody district. The Proterozoic suite includes three units, a lower schist-quartzite unit composed of micaceous quartzite, meta-arkose, uraniferous meta-conglomerate, schists and leptites; a middle taconite unit of amphibole-magnetite schist, biotite schist and Fe-rich (magnetite, hematite) quartzite; and an upper dolomite-leptite unit of dolomitic marble, quartzite, graphite-biotite and actinolite schist,

and metasomatic talc-carbonate rocks. Stocks and dikes of microcline granite have intruded along lineaments. Host rocks are folded into large isoclinal folds with steep axes and have repeatedly been strongly fractured.

Alteration

Intense metasomatism has altered metasediments and granites along lineaments. Four main phases of alteration are distinguished: Early Fe-Mg-metasomatism that generated stratiform iron ore bodies, Na-metasomatism, carbonate-metasomatism, and finally silicification that formed secondary quartzites. Products of Na- and carbonate-metasomatism are listed below.

Ore and Associated Minerals

U minerals include uraninite, pitchblende, coffinite, brannerite and nenadkevite. Four principal U-associated mineral assemblages are discerned: (1) apatite-malacon (uraniferous apatite, zircon/malacon, sphene); (2) amphibole-nenadkevite (nenadkevite, brannerite); (3) carbonate-uraninite (uraninite I) and amphibole-aegirine (regenerated uraninite I); and (4) sulfide-pitchblende (pitchblende, coffinite, uraninite II) (Zhukova 1980).

Mode of Mineralization

Economic U mineralization is restricted to Na- and carbonate-metasomatite zones in the middle and upper Proterozoic units. Mineralization occurs in fractured sections at flexures in limbs and in the axial zone of folds in form of lenses, shoots, stratiform bodies in which U minerals are finely disseminated and associated with dark-colored minerals, and as veins. Batashov et al. (1984) distinguish four lithologic mineral settings based on parental heritage,

a) albitites with alkaline amphibole, aegirine and uraninite, brannerite, and pitchblende derived from biotite, graphite-biotite schists, and granite dikes,
b) magnetite-riebeckite rocks, aegirinites, martite-carbonate-metasomatites with uraninite derived from iron ores, amphibole-magnetite schists and ferruginous quartzites,
c) talc-carbonate rocks containing uraniferous apatite-malacon with Th and REE,
d) pitchblende-coffinite veins.

Age Constraints

Age of U mineralization at Zheltye Vody is about 1770 m.y. but it can be assumed that mineralization can take place at any time of magmatic or metamorphic (?) activity.

Dimensions/Resources

U mineralization at Zheltorechenskoe/Zheltye Vody extends laterally along a large, steeply dipping fold for 1500 m on the W limb, 900 m on the E limb and 700 m in the keel of the fold. It persists to a depth of ca. 2000 m. U hosting metasomatites are tens of meters wide. They decrease at depth below about 1000 m associated with disappearance of uraninite which gives way to uraniferous malacon-apatite.

Examples of Metasomatite, Subtype 12.2 Metasomatized Metasediments Deposits/ Occurrences

Canada: Mosquito Gulch/Nonacho, NWT, parts of Pronto/Blind River-Elliot Lake, Ontario
Brazil: Espinharas/Paraiba
Finland: Kouvervaara/Kuusamo Schist Belt

4.13 Type 13: Synmetamorphic (Fig. 4.13)

Definition

Synmetamorphic uranium mineralization consists of disseminated uranium distributed strata-concordant in more or less continuous lenses or erratically scattered patches within metasediments and metavolcaniclastics. Principal uranium phases are uraninite typical for higher grade metamorphic facies and pitchblende prevailing in low-grade (greenschist) facies.

Type Example: Forstau, Austria
Reference: Dahlkamp and Scivetti 1981

Principal Recognition Criteria

Host Environment

- Metasediments: phyllites, schists, gneisses partly carbonaceous (graphitic), phosphatic or

Type 13. SYNMETAMORPHIC

(stratiform U disseminations in unaltered metasediments and metavolcaniclastics)

Fig. 4.13

pyroxenitic, derived from pelites, psammites and associated sediments with or without tuffaceous interbeds of eugeosynclinal or lacustrine origin, metamorphosed to from greenschist to amphibolite grade
- Metavolcaniclastics: metamorphosed felsic to intermediate, dominantly rhyolitic volcaniclastic horizons which may be interbedded with clastic sediments

Alteration

- No or only very minor alteration related to mineralization
- No or only minor metasomatism of host rocks

Mineralization

- Principal uranium minerals: uraninite and/or pitchblende
- Some U in lattice or on cleavage planes of various rock constituents such as apatite, biotite, amphibole
- Associated minerals: locally some Mo, Ni, Pb, Zn, a.o. as sulfides, sulfarsenides, etc.; metavolcaniclastics often with Mo enrichments
- U minerals occur disseminated in lenses or in minute to small pockets scattered in favorable lithologies
- Only lithologic, no structural control

Age Constraints

No age constraints other than to orogenies of Lower Proterozoic to recent age.

Metallogenetic Aspects

Synmetamorphic uranium occurrences appear to result from regional metamorphism of uraniferous sediments or volcanics within a closed system, remote from intrusions, anatectic centers, or metasomatic fronts. Depending on crystallization conditions, the sedimentary uranium became transformed in situ either to pitchblende, which is prevalent in lower grade metamorphic environments or uraninite prevailing in higher grade metamorphic lithologies.

Dimensions/Resources

Synmetamorphic uranium occurrences are most commonly of low grade (0.001–0.1% U_3O_8) and contain small resources of subeconomic magnitudes (kg to 1000 mt U_3O_8).

The most common occurrences are spotty mineralizations. These mineralizations are discontinuously spread over many km^2 in favorable horizons. They locally achieve high grade. The mineralizations are small in dimensions ranging from mm to m in lateral and vertical extension and exhibit erratic distribution.

Remarks

Synmetamorphic mineralizations make favorable uranium source rocks or protore for other types of deposits rather than feasible exploration targets.

Examples of Type 13 Synmetamorphic Deposits/Occurrences

Australia: ? Mary Kathleen/Queensland
Canada: Duddridge Lake/Saskatchewan, Amer Lake/NWT, Kitts/Makkovik, Labrador, Mont Laurier/Quebec
Finland: Nuottijärvi/Paltamo, Lampinsaari/Vihanti (Proterozoic metamorphosed phosphorite)
Germany: Höhenstein/Bavaria
Madagascar: Ambindrakemba/Fort Dauphin
Togo: Lama Kara/Niamtougou
USA: Kettle Falls Gneiss Dome/Orient, Washington state.

4.14. Type 14: Lignite (Fig. 4.14)

Definition

Lignite-related uranium mineralization consists of paludal material composed of a high percentage of land plant debris mixed with detritus coalified to not higher than subbituminous grade and containing either trace to minor amounts of syn-sedimentary, uniformly disseminated uranium or epigenetic, irregularly distributed structurally controlled uranium, the uranium being adsorbed in both cases on carbonaceous matter. Accordingly two subtypes are distinguished:

Subtype 14.1: joint-fracture-related

Subtype 14.2: stratiform

Type Example: southwestern Williston Basin, N and S Dakota, USA

Reference: Denson and Gill 1965

Principal Recognition Criteria

Host Environment

- Lignitic sediments of paludal, limnic or paralic origin
- Generally thin lignitic beds
- Coalification less than bituminous grade
- Pyrite and high ash content
- Intraformational unconformities
- Certain degree of jointing and fracturing
- Lignitic seams interbedded or overlain by acid pyroclastics (rhyolitic tuffs, etc.) containing anomalous contents of U
- Basins surrounded by granites or other rocks with anomalous U contents

Mineralization

- No discrete primary U minerals (locally secondary hexavalent U minerals)
- U adsorbed on carbonaceous matter or as uranyl-humate
- Syngenetic U stratiform and persistent but commonly of low values (few 10 ppm)
- Spotty and irregular epigenetic U mineralization of better grade (up to 0.4% U_3O_8) controlled by joints, fracture systems
- U often bound to upper section of the lignite below intraformational unconformities
- Host beds of mixed vegetal carbonaceous and mineral detritus (silt, clay) yielding high ash content
- Thin lignitic host beds (<2 m)
- Often associated with a variety of metallic trace elements

Age Constraints

- Time constraint by emergence of land plants, i.e., younger than Devonian

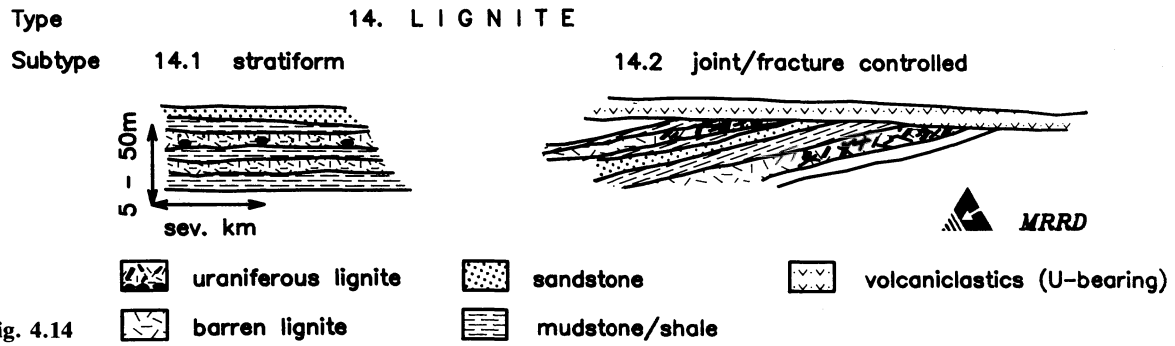

Fig. 4.14

- Lignites, particularly those of Late Cretaceous and younger origin are more favorable; older lignites may have suffered a higher degree of coalification, an apparently negative process hampering epigenetic U mineralization

Metallogenetic Aspects

Lignite, coal, and carbonaceous mud-siltstone are favorable sites for U accumulation when they originated from paludal, low-lying poorly drained shallow depressions with abundant vegetation located either on coastal plains (paralic lignite) or within land-locked basins (limnic lignite). U supposedly originated from either granites, volcanics or other rocks that border the depressions or from interbedded or overlying pyroclastics containing anomalous amounts of U. U is thought to have been leached from these sources. U transport into the basins has been (a) either by surficial waters with precipitation by synsedimentary adsorption on organic material (as today found in swamps and bogs in adequate environment, e.g., Stevens County, Washington) to form syngenetic mineralizations, or (b) postsedimentary by groundwater migration into buried basins to form epigenetic mineralization. Infiltration in the latter case occurred along permeable zones, dominantly joint and fracture systems, hence the irregular U distribution. Precipitation of U resulted from adsorption on organic material along dishomogeneities, mainly joints, fractures, more silty intercalations and intraformational unconformities.

Remarks

Uraniferous lignites constitute only potential U resources. Deposits are commonly either too small or of too low grade. The latter is particularly true for stratiform syngenetic deposits (type 10.1) whereas type 10.2 deposits may locally contain noteworthy U tenors.

In addition, uranium extraction is hampered by its binding in organic compounds creating an almost refractory nature for metallurgical extraction.

Examples of Type 14 Lignite Deposits (Not Differentiated)

ČSFR: Sokolov and Trutnov basins/Bohemia
Greece: Serres Basin, Kotili Basin
Germany: Stockheim/Bavaria, Freital/Saxony
South Africa: Springbok Flats-Karoo Subbasin/Transvaal

4.14.1 Subtype 14.1: Joint-fracture-related

Type Example: Slim Buttes, southwestern Williston Basin, S-Dakota, USA
Reference: Denson and Gill 1965

Host Rocks/Alteration/Structures

Pyritic, high-ash lignite, subbituminous coal and nonmarine carbonaceous mud-siltstone. The latter contains abundant plant debris, scattered throughout the rock but preferentially concentrated along bedding planes. Sulfides, dominantly pyrite, are typical, as is a high ash content. The carbonaceous sediments are often interbedded or overlain by uraniferous acid pyroclastic sediments (rhyolitic tuffs etc.) or sandstones. Jointing and fracturing is common. No alteration. Some of the mineralized lignites are in basins bordered by granites or other rocks containing anomalous amounts of U.

Ore and Associated Elements/Mode of Mineralization/Dimensions/Resources

No discrete primary U minerals have formed. Locally secondary hexavalent U minerals occur in joints and fractures. U is adsorbed on carbonaceous matter or bound in organic compounds (e.g., uranyl humate) particularly in cataclastic zones. Other metals present in anomalous amounts but not necessarily correlative with U may include As, Be, Cd, Co, Cu, Ge, Mo, Ni, Pb, Se, Ti, V, Y, Zr and/or REE. Mineralization is spotty and irregularly distributed with strong variations of tenor. Grades are commonly a few hundred ppm U and rarely 0.1% U_3O_8 or more. Thinner seams (cm to less than 1 m) may be mineralized ubiquitously, whereas in thicker seams only parts thereof are mineralized, often restricted to their top. Intraformation unconformities often control U accumulations. Resources vary between <1 mt U_3O_8 to few 100 mt U_3O_8.

4.14.2 Subtype 14.2: Stratiform

Type Example: Slim Buttes, southwestern Williston Basin, S-Dakota, USA
Reference: Denson and Gill 1965

Host Rocks/Mode of Mineralization

Host rocks and geological setting are more or less identical with those of subtype 14.1 except that interbedded uraniferous volcaniclastics or sandstones may not be present. Uranium is adsorbed on carbonaceous and clayey material and/or bound in organic ionic compounds, e.g., uranylhumate, and occurs stratiform disseminated throughout the carbonaceous/lignite horizon. Associated elements are similar to those of subtype 14.1. Uranium tenor is generally very low, amounting rarely to more than 50 ppm U.

4.15. Type 15: Black Shale (Fig. 4.15)

Definition

Black shale-related uranium mineralization consists of marine organic-rich shale or humic/coal-rich pyritic shale, containing synsedimentary stratiform, uniformly disseminated uranium adsorbed on organic material and clay minerals. Based on the organic substances two subtypes are distinguished:

Subtype 15.1: bituminous/sapropelic black shale

Type Example: Chattanooga, USA

Subtype 15.2: humic/kolm in alum shale

Type Example: Ranstad, Sweden

References: Bell 1978; Carlsson and Nojd 1977; Kim 1988; Mutschler et al. 1976

Principal Recognition Criteria

Host Environment

- Very fine-grained black shales with high contents of organic matter, pyrite and/or marcasite, evenly laminated, dense, may contain thin coalified, phosphatic and/or silty intercalations
- Interbedded with limestone, sand/siltstone and shale beds
- Fairly uniform shale thickness, commonly a few meters and up to some 10 m
- Widespread extension of black shale over several 100's to 10 000's km^2
- No ore-related alteration

Mineralization

- No discrete primary U minerals (except locally secondary hexavalent U minerals), instead U is adsorbed on organic and clay particles
- Very low grade mineralization ranging from 50 to 400 ppm U

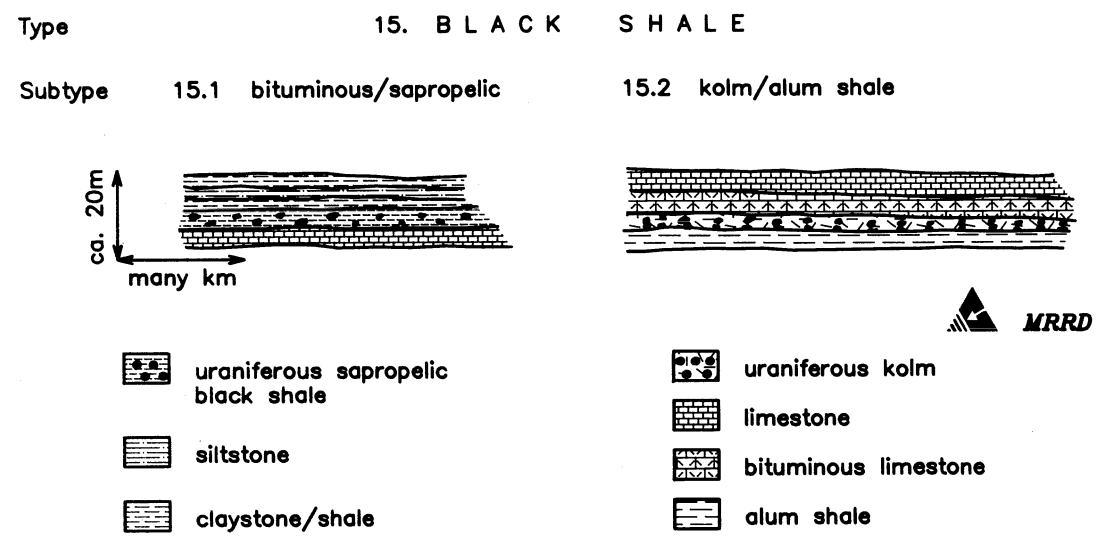

Fig. 4.15

- U disseminated uniformly throughout and coextensive with individual beds over large areas, with different beds commonly having different U tenors
- Better grades in certain beds (dm to m thick) either rich in organics, particularly of vegetal provenance, and/or sediments very fine-grained, or finely laminated or containing phosphatic minerals (e.g., kolm: 380 ppm U)
- Presence of small quantities of other metals (Cu, Cr, Mo, Mn, REE, V and P)

Age Constraints

No age constraints but deposits occur dominantly in Phanerozoic formations particularly of Paleozoic age.

Metallogenetic Aspects

Black shales of marine origin were deposited in shallow, partially closed epicontinental basins within continental terrane tectonically stable for a long period. The depositional environment is characterized by a low rate of sedimentation, brackish to normal marine salinities, anaerobic, strongly reducing conditions, formation of sapropelic-bituminous, and humic, coaly matter from planktonic marine algae and land plant (wood spores) debris.

Synsedimentary deposition of U from seawater by adsorption dominantly on organic matter with particular concentrations in humic-coaly material. If phosphate nodules are present, they normally collected more uranium than the surrounding shale.

Remarks

Black shales, although widespread in the world and hosting enormous quantities of uranium (many million tonnes) constitute only potential U resources. U is perhaps extractable as a by-product of oil, or other metals recovery.

Examples of Type 15 Black Shale Deposits (not differentiated)

China: Jiangnan Block/SE China
South Korea: Ogcheon Group
Russia: Lake Onega region

4.15.1 Subtype 15.1: Bituminous-sapropelic black shale

Type Example: Chattanooga, USA
References: Mutschler et al. 1976; MSR & D 1978

Host Rocks/Alteration/Structures

The Gassaway Member, the upper unit of the Devonian-Mississippian Chattanooga Shale is the main host for uranium. It consists of massive, grayish-black shale with paper-thin partings of silt and films or bands of pyrite and marcasite. About 20 wt. % of the shale is organic material (saprolite, vitrain, bituminous coal) derived mainly from planktonic marine algae and less from land plant debris. The organics fill interstices and coat the minute rock grains of the shale. No structures or alteration are present.

Ore and Associated Elements/Mode of Mineralization/Dimensions/Resources

U distribution is stratiform, adsorbed mainly on organic and to a lesser extent on clay particles. MSR & D (1978) report from a test area in Dekalb County, Tennessee: 55–65 ppm U, 230 ppm Co, 530 ppm Ni, 200 ppm Mo, 1360 ppm V_2O_5, 8600 ppm S and 9 gal/sh.t. of syncrude oil.

Lateral extension of Chattanooga Shale is in the order of 80 000 km^2, averaging about 10 m thick and a mean grade of 57 ppm U. Estimated resources are at least 4 to 5 million tonnes U (calculated for a restricted area of 12 counties in central Tennessee by Mutschler et al. (1976).

4.15.2 Subtype 15.2: Humic/kolm in alum shale

Type Example: Ranstad, Sweden
Reference: Carlsson and Nojd 1977

Host Rocks/Structures/Alteration

Principal U-host is the kolm horizon within black bituminous alum shale of Cambrian age. The flat-lying black shale unit rests on Cambrian sandstone and is covered by Ordovician Limestone.

Ore and Associated Elements/Mode of Mineralization/Dimensions/Resources

U distribution is stratiform, adsorbed on organic matter and in particular on kolm nodules. The kolm contains about 30% ash. Nodules may contain up to 80% organics and up to 0.4% U. Average values for the kolm horizon are: 300 to 380 ppm U (alum shale ca. 200 ppm U), 22% organic material, 13% pyrite, 6.5% S, 0.065% V, 0.03% Mo, 0.02% Ni, 0.4% Mg, 0.7% P, and high Al and K contents.

Lateral extension of the kolm-bearing alum shale is about 500 km^2. Thickness of the alum shale is 15 m and the kolm horizon varies from 2.5 to 4 m. Assuming an average grade of 200 to 300 ppm U_3O_8 the Ranstad occurrence is estimated to contain 300 000 mt U_3O_8, including 75 000 mt U_3O_8 averaging about 350 ppm U_3O_8.

4.16 Type 16: Strata-Controlled, Structure-Bound

Type Example: Ronneburg District, Thuringia, Germany

Reference: Lange, Schuster, Weise, Gradowski pers. commun.

Definition

Strata-controlled, structure-bound uranium deposits consist of uranium concentrations in minifractures which form stockworks within or immediately adjacent to carbonaceous, pyritic black shales.

Principal Recognition Criteria

Host environment

- Argillaceous and siliceous black shales with intercalations of dolomitic and phosphorite nodule beds (Graptolitenschiefer)
- High organic carbon (up to 9% C), sulfide (up to 3.5% S) and anomalous trace element (U, Mo, Ni, V, As, Sb) contents in the black shale
- Carbonaceous sandy and carbonatic shales (Lederschiefer) underlie, and limestone-dolomite (Ockerkalk) overlie the main black shale horizon
- Pre-orogenic diabase dikes and sills cut the sedimentary sequence
- Marked tectonic imprint reflected by complex folding, pronounced faulting and thrusting, and high density of minifractures (fissures, joints, cleavages)
- Sediments are not or only weakly metamorphosed

Alteration

- Silicification, chloritization, dolomitization
- Narrow aureoles of bleaching and hematitization (few centimeters wide) around mineralized structures
- Carbonatization and sulfatization in form of narrow fissure fillings
- Post-orogenic (post-Hercynian at Ronneburg) supergene oxygenation (reddening of rocks due to Fe-oxide, Fe-hydroxide formation) associated with partial mobilization of trace elements in subsurface (below Permian paleosurface) and further downwards along major faults
- Formation of cementation zone below the oxidation zone

Mineralization

- Older pitchblende associated with Mg-Fe-carbonates, chlorite, subordinate sulfides, rare coffinite, tennantite
- Younger pitchblende, bravoite, marcasite, Ni-Co-arsenides, hematite, calcite, dolomite
- (Sooty) pitchblende associated with pyrite (no gangue minerals)
- U minerals predominantly fill, coat and impregnate minifractures (joints, cleavages) which are arranged in a stockwork-like pattern within distinct lithologic units
- Porous wall rocks may contain disseminated mineralization for short distances from mineralized fractures
- Distribution and concentration of U in the fractures is highly variable
- Mineralized fractures group to stockwork-type ore bodies, which occur irregularly distributed within weakly mineralized zones
- Position, size and shape of ore bodies are controlled by faults, particularly by intersections of faults

- U mineralization occurs below the lower boundary of the oxidation zone from where mineralization can be found over a vertical interval of about 400 m

Age constraints

- No principal constraints with respect to the age of the host strata but known deposits occur in Eocambrian and Paleozoic sediments
- Geological evidence suggests that the principal ore formation coincided with periods of marked oxidizing climatic conditions (Rotliegend/Permian at Ronneburg, Cretaceous to Tertiary in South China)

Metallogenetic Aspects

Strata-controlled, structure-bound uranium deposits tend to be of polyphase origin involving the following stages:

1. Synsedimentary accumulation of uranium and other metals in favorable sediments such as black shales (at Ronneburg Middle Devonian Tentaculitenschiefer and Silurian Upper and Lower Graptolitenschiefer).
2. Perhaps but not necessarily limited redistribution of uranium by metamorphic processes (at Ronneburg during the Hercynian Orogeny reflected by elevated U concentrations of ca. 100 ppm U in certain anticlinal structures as compared to a synsedimentary inventory of about 50 to 60 ppm U).

These uraniferous (meta-) sediments provided the primary U source.

At Ronneburg, a supplement U source is present in form of pitchblende veinlets of supposedly late to post-orogenic hydrothermal origin.

3. Ore grade uranium concentration by a combination of
- structural ground preparation,
- deep reaching weathering in a semiarid to arid climate associated with liberation of uranium by infiltration of oxygenated meteoric waters into the U source rocks,
- fluid mobilization supposedly in response to tectonic activity and/or intrusion of igneous dikes (lamprophyres, porphyries) resulting in circulation of the U pregnant solutions downward along permeable structures into reduced sediments, and
- precipitation of uranium in form of pitchblende mainly in subsidiary minifractures within the cementation zone.

After this ore forming event, supergene processes may have remobilized the uranium again (at Ronneburg at about 210–190 m.y. and 120–90 m.y. which are consistent with redistribution or introduction episodes of uranium in other deposits in central and western Europe).

Typical Dimensions/Resources

At Ronneburg, mineralized zones are up to several hundred meters long and wide and up to several ten meters, rarely in excess of 100 m thick. They enclose irregularly shaped ore bodies that vary from 20 to 500 m long, from few meters to few hundred meters wide and from less than 2 m to 100 m thick. In situ U contents range from 0.085 to 0.17% U_3O_8. Resources are in the order of 200 000 mt U_3O_8 contained in an area of 164 km^2.

Examples of Type 16 Strata-Controlled, Structure-Bound Deposits/Occurrences

China: Chienxinan/SW Guizhou; Chanziping/N Guangxi; Pukuitang/Hunan, Chengxian/Guangxi-Hunan-Guangdong region, SE China; Norgai/S Qinling area, Central China
Uzbekistan: Koscheka, Dzhantuar/Kyzylkumsky, Navoi region

Selected References and Further Reading for Chapter 4 (for details of publication see Bibliography)

Adams et al. 1989; Adams and Saucier 1981; Adams and Smith 1981; Alexander 1986; Altschuler et al. 1958, 1980a; Andrade 1989; Aniel 1983; Antropov et al. 1978; Austin and D'Andrea 1978; Avrashov 1980; Bailey and Childers 1977; Bailey et al. 1981; Barthel et al. 1986; Barthel and Hahn 1986; Basham and Matos Dias 1986; Battey et al. 1984; Beck 1986; Belevtsev 1980; Belevtsev et al. 1984a, 1984b; Bell 1963, 1978, 1982; Berning 1986; Boitrov and Legierski 1977; Bowie 1979; Boyle 1984, 1985, 1986, 1989; Breit and Goldhaber 1987; Briot 1983; Butt et al. 1984; Button and Adams 1981; Byers 1978; Cameron 1984;

Cariou 1964; Carlisle 1983, 1984; Carlsson and Nojd 1977; Cathelineau 1984, 1986; Cavaney 1984; Chen Zhaobo and Fang Xibeng 1985; Chenoweth and Malan 1973; Collot 1981; Crawley 1983; Crawley et al. 1984; Crew 1981; Cumming and Rimsaite 1977; Dahlkamp 1980, 1989; Dahlkamp and Adams 1981; Danchev and Strelyanov 1978; Dayvault et al. 1985; de Kun 1965; Denson and Gill 1965; Derrick 1977; Derricks and Vaes 1956; de Voto 1978; de Voto and Stevens 1979; Evans (ed.) 1986; Ewers and Ferguson 1980; Ferguson and Goleby (eds.) 1980; Finch 1967; Fischer 1968; Fogwill 1985; Forman and Angeiras 1981; Fouques et al. 1986; Fraser 1980; Friedrich and Cuney 1989; Friedrich et al. 1987; Fritsche 1986; Fuchs and Hilger 1989; Fuchs et al. 1981; Gandhi 1986; Garrels and Larsen 1959; Gangloff 1970; George-Aniel et al. 1985; Goodell 1985a, 1985b; Goodell and Waters, eds., 1981; Gosnold 1976; Granger 1976; Granger and Finch 1988; Griffith 1986; Grutt 1972; GSA/Wenrich and Billingsley (eds) 1986; Halladay 1989; Hallbauer 1986; Hambleton-Jones 1984; Harshman and Adams 1981; Heine 1986; Hostetler and Garrels 1962; IAEA 1979, 1980, 1981, 1982, 1983, 1984, 1985, 1986a, 1986b, 1988a, 1988b, 1988c, 1989a, 1989b; IAEA/Ferguson (ed.) 1984; IAEA/Finch (ed.) 1985; IAEA/Fuchs (ed.) 1986; IAEA/Pretorius (ed.) 1987; IAEA/Toens (ed.) 1984; Jones 1978; Jiashu and Zehong 1984; Jiashu et al. 1989; Johnson et al. 1987; Kazansky et al. 1978; Kazansky and Laverov 1977; Kazdan, 1978; Kolektiv (ČSSR) 1984; Komenik and Veselý 1986; Kotlyar 1961; Kyser et al. 1989; Landais et al. 1987; Leroy 1978; Leroy and Cathelineau 1982; Leroy et al. 1987; Li Tiangang and Huang Zhizhang 1986; Mann and Deutscher 1978; Mathews et al. 1979; Mc Kelvey et al. 1956; Mellinger et al. 1987; Mickle and Mathews 1978; Mineeva 1984; Modnikov et al. 1978; MSR and D 1978; Mursky 1973; Mutschler et al. 1976; Nakoman 1979; Nash et al. 1981; Needham 1985; Nevskiy and Filonenko 1976; Nishimori et al. 1977; Orasaka 1981; Otton and Zielinski 1985; Page 1983; Pagel 1984; Pardo-Leyton 1985; Petroš et al. 1986; Petrov et al. 1969; Piirainen 1968; Poty et al. 1986; Poty and Pagel 1987; Pretorius 1976, 1981; Rackley 1976, 1980; Reeve et al. 1989; Rich et al. 1977; Roberts 1988; Roberts and Hudson 1984; Robertson 1989; Rundkwist and Nesheskij 1977; Ruzicka 1971, 1981, 1984, 1988, 1989; Saima Deposit Research Group 1976; Sakar 1982; Schmidt-Collerus 1979; Sherborne et al. 1979; Shiqing Yu 1989; Shtshurov and Timofeiev 1965; Sibbald 1988; Sibbald and Petruk (eds) 1985; Skinner 1981; Thamm et al. 1981; Tremblay 1978, 1982; Turner-Peterson et al. (eds) 1986; US-AEC 1959; Virag and Vincze 1967; Volfson et al. 1967; von Backström 1975, 1976; Wallace 1986; Wenrich 1986; Wenrich and Sutphin 1989; Yu 1986; Ziegler 1974; Zielinski et al. 1987.

5 Selected Examples of Economically Significant Types of Uranium Deposits

This chapter contains abbreviated descriptions of selected major uranium deposits or districts including metallogenetic concepts proposed by geoscientists who have worked on these deposits. The given deposits and districts are considered representative examples for the types of uranium deposits of established or potential future economic value. To provide an idea of the magnitude of the deposit or district described in the respective section, some figures on the resources and grades have been included in the introduction to this section. Related details on dimensions are provided under section Mineralogy in the deposit descriptions. For additional comments see Paragraph Remarks, Definitions, Units.

5.1 Examples of Unconformity-Contact-Type Uranium Deposits (Type 1, Chap. 4): Athabasca Basin region, Canada

The Athabasca Basin region is south of Lake Athabasca in northern Saskatchewan. Three major districts characterized by large and high-grade uranium deposits may be distinguished, the East Athabasca, Southeast Athabasca, and Carswell Structure districts. These districts are located in the eastern, southeastern, and central western part of the Athabasca Basin respectively. Small deposits occur at the northern edge of the basin in the North Rim and Northwest Rim Athabasca districts (Fig. 5.1).

Total resources of the Athabasca Basin region are in excess of 440 000 mt U_3O_8. Average ore grades of deposits vary between 0.14 and 14.4% U_3O_8, but most major deposits have grades of more than 1% U_3O_8. The district includes with Key Lake (89 000 mt U_3O_8, average grade ca. 3% U_3O_8) the largest high-grade, low cost uranium mine (open pit) in the world, and with Cigar Lake (128 000 mt U_3O_8, average grade 14.4% U_3O_8) the largest high-grade deposit discovered in the world.

The uranium deposits of the Athabasca Basin region are associated with a distinct Middle Proterozoic unconformity and are therefore defined as Proterozoic unconformity-contact deposits. Two classes of this type have been distinguished which are fracture-bound (class 1.1.1, Chap. 4) and clay-bound (class 1.1.2). In addition, Beaverlodge type mineralization of Hudsonian age (subtype 2.2, Chap. 4, and Chap. 5.2.2) has been identified. Both unconformity-contact classes exhibit many similarities, but also some distinct differences.

The following description of the regional geology is largely based on the comprehensive work by Lewry, Sibbald and Ramaekers. Ruzicka (1989), Sibbald (1988), Artru et al. (1986), Lainé (1986), Fogwill (1985) Tremblay (1982), Dahlkamp and Adams (1981), Hoeve et al. (1980), Pagel et al. (1980) and Voultsidis et al. (1980) provided concise reviews with conceptual genetic models. Evans (1986) and Lainé (1985) edited major volumes on the uranium deposits of the Athabasca Region. Information from these publications together with that from a great number of other authors who contributed extensive information on a regional or local (deposit) scale have been taken for the presentation of mineralization and alteration. All these authors cannot be listed here but are mentioned in the text and found in the reference list at the end of this chapter.

Geological Setting of Mineralization

The Athabasca Basin region lies near the southwestern edge of the Churchill structural province of the Canadian Precambrian Shield. Archean and Aphebian (Middle to Upper Proterozoic) crystalline rocks constitute a basement which is overlain by dominantly continental sediments of the Meso-Helikian (Middle Proterozoic) Athabasca Group.

The *Archean and Aphebian* rocks are arranged in distinct lithostructural domains, each characterized by structural style and metamorphic

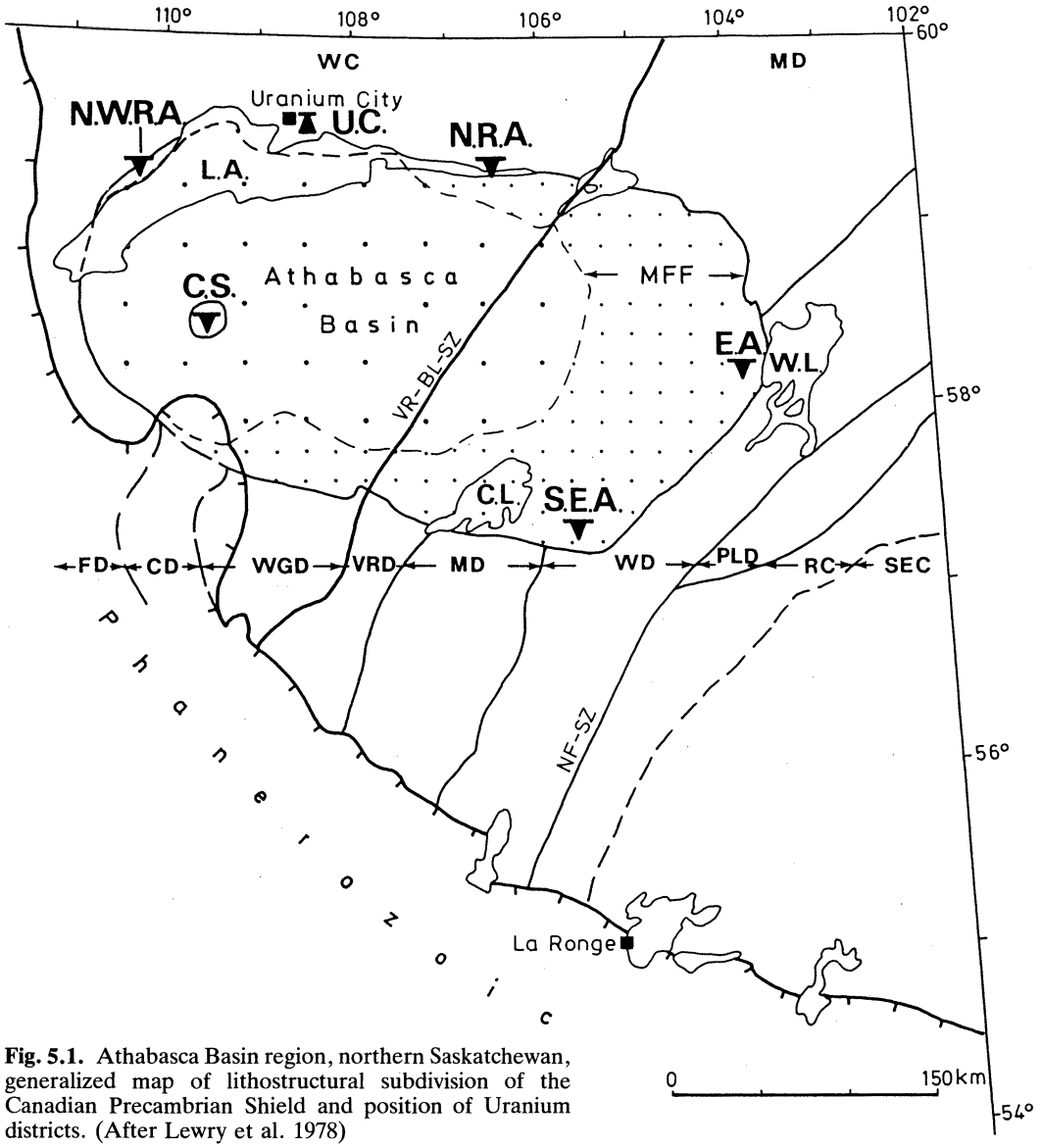

Fig. 5.1. Athabasca Basin region, northern Saskatchewan, generalized map of lithostructural subdivision of the Canadian Precambrian Shield and position of Uranium districts. (After Lewry et al. 1978)

Uramium districts:
E.A. East Athabasca district; *S.E.A.* Southeast Athabasca d.; *C.S.* Carswell Structure d.; *N.W.R.A.* Northwest Rim Athabasca d.; *N.R.A.* North Rim Athabasca d.; *U.C.* Uranium City region;
Lithostructural domains:
WC Western Cration; *FD* Firebag Domain; *CD* Clearwater d.; *WGD* Western Granulite d.; *VRD* Virgin River d.; *MD* Mudjatic d.; *WD* Wollaston d.; *PLD* Peter Lake d.; *RC* Rottenstone Complex; *SEC* Southeastern Complex; *L.A.* Lake Athabasca; *W.L.* Wollaston Lake; *C.L.* Cree Lake

grade (Fig. 5.1). Archean rocks are dominantly of granitic and minor monzonitic composition and form NE-SW elongated domes surrounded by Aphebian metasediments. The Aphebian metasediments include a variety of partly graphitic biotite to feldsphathic gneisses and schists, quartzites, calc-silicate rocks and impure marbles derived from a succession of pelitic to psammitic facies interbedded with carbonaceous layers (black shale) and calcareous to evaporitic units deposited in a miogeosynclinal shelf to lagoonal sedimentary environment in middle to upper Lower Proterozoic time. The metamorphic grade is predominantly middle to upper amphibolite and locally granulite facies with later retrogression to greenschist facies. Migmatites and anatectic segregations are common features. Late granitic and pegmatitic intrusions occur locally. Table 5.1 gives a summary of the Archean and Aphebian Lithologies.

Table 5.1. Northern Saskatchewan, Athabasca Basin region, generalized Archean-Aphebian stratigraphy-lithology of the Cree Lake zone. [Compiled by E. Stewart (pers. commun.) after Lewry and Sibbald 1978, 1980; Ray 1977; Ray and Wanless 1980]

Eon	Era	Group	Lithology
Lower Proterozoic	Late Aphebian		Pegmatite: many generations, three types: quartz-feldspar (Ap_1) biotite-quartz-feldspar (Ap_2) and with calc-silicate minerals (Ap_3) Granite: leucocratic nonfoliated (Aq_1) or foliated (Aq_2) form small intrusions less than 1 km in size Mafic intrusive rock: fine-grained to medium-grained, generally foliated. Composition varies from diabase (Ad_1) or gabbro (Ad_2) to diorite (Ad_3)
	Aphebian	Wollaston	Evaporitic metasediments (Hidden Bay Assemblage): medium-grained, foliated diopside quartz-plagioclase gneiss (calc-silicate, Ac_1) and impure dolomite or calcite marble (Ac_2). Often interlayered with graphitic gneiss/schist Psammitic metasediments (Upper Meta-Arkosic Unit): medium-grained, massive to well foliated quartz-feldspar gneiss (meta-arkose, Aq_1), diopsidic (calcareous) meta-arkose (Aq_2) and quartzite (Aq_3). Forms thick sequences above the basal meta-pelite horizon Pelitic metasediments (Lower Meta-Pelitic Unit): medium to coarse-grained, moderately to strongly foliated. Composed of biotite-plagioclase-quartz gneiss (Ab_1) interlayered with calc-silicate; biotite-K-feldspar -plagioclase-quartz gneiss (Ab_2) with garnet, cordierite, sillimanite and/or graphite; biotite-K-feldspar-quartz gneiss (Ab_3) with interlayered meta-psammite, banded iron formation, volcanics
	Late Archean Early Aphebian	Needle Falls	Metamorphosed sandstone, arkose, conglomerate, volcanics and volcanoclastics (Quartzite and Lower Arkosic Units).
Archean	Late Archean		Mafic gneiss: medium-grained, moderately foliated. Composed of hornblende-biotite-plagioclase gneiss with hypersthene (Am) Felsic gneiss: medium-grained, pink, moderately to strongly foliated. Syenogranite-monzogranite composition (Af). Lineation due to rodding of quartz often well developed

Regional predominantly NE-SW-trending pre-Athabasca fault and mylonite zones transect the Archean and Aphebian rocks.

North of Lake Athabasca, clastic sediments of the Paleo-Helikian Martin Formation deposited on the basement (see Chap. 5.2.2). South of Lake Athabasca, a thick (<2500 m) sequence of red bed type arenites overlain by marine sediments of the Meso-Helikian Athabasca Group rests on the crystalline basement. Table 5.2 shows the formations and respective lithologies of the group. A pronounced unconformity with gentle relief separates the two units.

Intense weathering of lateritic nature has altered the basement prior to the deposition of the Athabasca sediments.

Multiple episodes of both reverse and normal post-Athabasca faulting caused vertical displacements of the unconformity of up to several tens of meters. Diabase dikes and sills intruded both the basement and cover sediments (Fig. 5.2).

Host Rock Alterations

Since the waning phase of the Hudsonian Orogeny, seven principal episodes and types of alteration have imprinted their traces on rocks of northern Saskatchewan:

1. Late to post-Hudsonian Na-metasomatism with local development of albitites. Albitization is particularly typical for the Uranium City region (Chap. 5.2.2).
2. Late to post-Hudsonian retrograde metamorphism of the crystalline basement.
3. Pre-Martin Formation physical weathering of the basement surface.
4. Post-Martin Formation and pre-Athabasca Group lateritic weathering (regolithization) particularly evident and preserved on crystalline basement rocks below the Athabasca Group.
5. Syn-Athabasca diagenesis associated with deposition of the Meso-Helikian Athabasca Group.

Table 5.2. Northern Saskatchewan, generalized stratigraphy-lithology of the Athabasca Group. (Compiled by E. Stewart after Hoeve et al. 1981, 1982, 1985; Ramaekers 1979, 1980, 1981; Tapaninen 1976; Hendry and Wheatley 1985)

Eon	Era	Group	Formation	Lithology
Middle Proterozoic	Helikian	Athabasca	Carswell	Bedded dolomite; variable thickness of beds; stromatolitic, oolitic, and brecciated, more than 300 m thick
			Douglas	Interbedded siltstone, shale, and fine-grained sandstone
			(William River Subgroup)	Sandstones within Carswell Structure now correlated with other sandy formations of Athabasca Group
			Tuma Lake	Quartz-rich pebbly sandstone; maximum pebble size 34 mm, variable amounts of interstitial clay, planar and trough cross-bedding common, maximum thickness: 80 m
			Otherside	Quartz-rich sandstone; maximum grain size 2 mm, well sorted, variable amount of interstitial clay siltstone beds and interclasts common, planar, trough, low-angle cross-bedding and horizontal bedding common, typical clay: predominantly illite, maximum thickness: 350 m
			Locker Lake	Pebbly sandstone; maximum grain size 50 mm, pebbles of quartz, quartzite, and chert abundant, trough and planar cross-bedding, typical clay: predominantly illite, maximum thickness: 120 m
			Wolverine Point (Upper and Lower)	Interbedded sandstone, siltstone and mudstone; generally quartz-rich but arkosic sections common, clay-rich section present, siltstone and mudstone beds 5 to 150 cm thick form up to 10% of unit, patchy carbonate cement variably present, in upper portions zones with several percent P_2O_5 containing locally 200 ppm U, abundant and diverse sedimentary structures, typical clay: illite-chlorite, maximum thickness: 700 m
			Lazenby Lake	Marine sandstone; typical clay: predominantly illite, maximum thickness: 600 m
			Manitou Falls	Quartz sandstone; poorly sorted, variable amounts of interstitial clay, trough and planar cross-bedding common, thin (1 cm) silt or clay lenses a few meters in length common, locally interbedded with conglomerate at the base of unit, typical clay: 60% illite, 30% kaolinite, 10% chlorite, maximum thickness: 1400 m
			Fair Point	Conglomeratic quartz-rich sandstone; abundant clay matrix, quartz pebbles up to 10 cm abundant, planar, trough, hummocky, and low angle cross-bedding common, typical clay: chlorite, illite, kaolinite, maximum thickness: 300 m

6. Late Athabasca diagenetic hydrothermal alteration locally associated with mineralization/recrystallization of ore.
7. Post Athabasca alterations associated with uranium redistribution.

Alterations which may or may not be related to ore formation or uranium redistribution include a variety of syn- to post-Athabasca processes. Early diagenesis followed by diagenetic hydrothermal events have modified both the Athabasca sediments and the upper part of the crystalline basement.

Early, *pre-mineralization alteration* includes silicification, kaolinitization, tourmalinization, and finally illitization.

Diagenetic-hydrothermal alterations associated with or postdating the unconformity-bound mineralization are more complex, and different at the various deposits. The alteration products include several generations of dominantly phyllosilicates, carbonates, quartz, sulfides, tourmaline, hematite, and extensive bleaching (Hubregtse and Sopuck 1987). Illitization is always found, chloritization is very frequent but more restricted spatially, and sideritization is also common although varying in extent from one deposit to another. A later argillitization phase produced

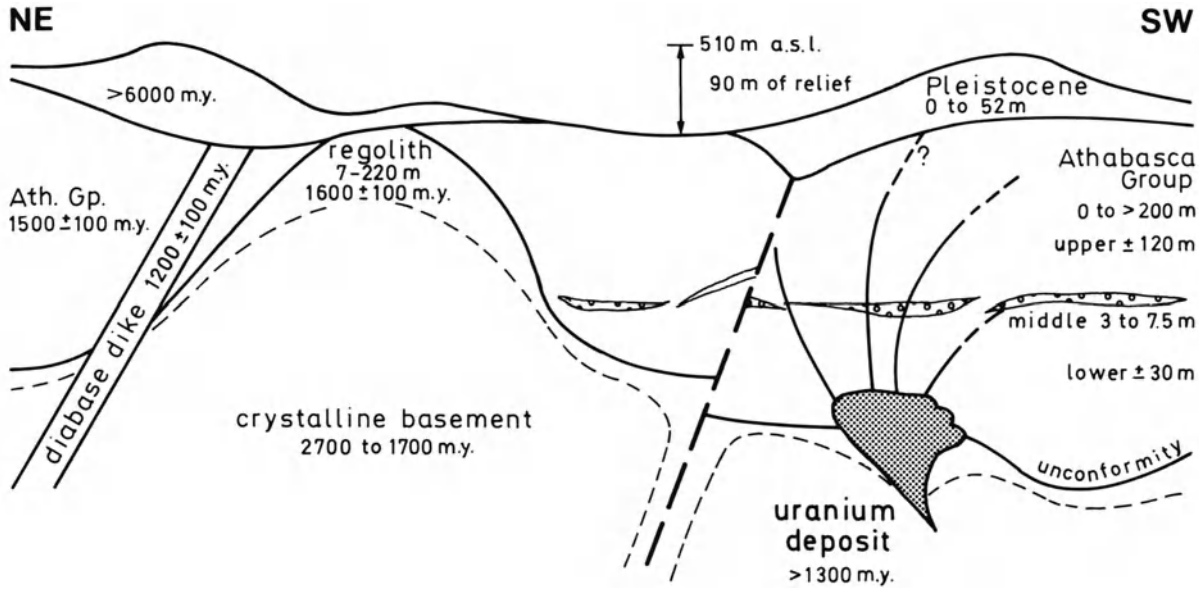

Fig. 5.2. East Athabasca district, schematic NE-SW section showing the principal stratigraphic units with thickness and approximate age, the pre-Athabasca unconformity relief, the zone of preserved regolithization, and the position of a clay-bound unconformity-contact type uranium deposit (example McClean). (After Wallis et al. 1986, age references see Table 5.9) (reprinted with permission from The Canadian Institute of Mining and Metallurgy)

chlorite, as reflected for example by an extensive overprint at Maurice Bay and kaolinite as observed at Key Lake. Hoeve (1984) remarks that argillitization (illitization and chloritization) and bleaching are largely congruent features but display crosscutting relationships, suggesting that argillitization predates the large-scale bleaching.

The various syn- to post-Athabasca Group alterations are diagrammatically illustrated in Fig. 5.3, and summarized with other data in Table 5.3 (see also Figs. 5.6, 5.7, 5.10, 5.11, and Table 5.12).

Principal Characteristics of Mineralization

The unconformity-contact type uranium deposits of the Athabasca Basin region include two principal classes: *Monometallic fracture-bound mineralization* in the basement (class 1.1.1, Chap. 4) (Fig. 5.4) and *polymetallic clay-bound mineralization* at the base of the Athabasca Group (class 1.1.2) (Figs. 5.5, 5.6). Both varieties have many features in common but also exhibit distinct differences.

The principal discriminating features include (class 1.1.1 first) emplacement of the bulk of the ore in either the crystalline basement below the unconformity or in a zone of argillic material capping the unconformity, quantitatively a more monometallic compared to a polymetallic mineralization, and often relatively narrow in contrast to a more extensive and pervasive alteration halo and moderate to high (0.3 to 1.5% U_3O_8) vs. very high average grades (1 to 14% U_3O_8) respectively. Mutual parameters are an intimate link to the Meso-Helikian unconformity, association with fault systems, often if not always related to old mylonite zones, alteration halos of similar mineralogical composition, and identical geochronological mineralization stages.

Most ore zones consist of a high grade core (>1% U_3O_8) surrounded by a halo of lower grade mineralization which can extend for a few meters to as much as ca. 50 m around the deposits (Figs. 5.4 to 5.7). Locally these halos persist in form of U coatings on quartz grains, as disseminated impregnations in the clay matrix and as veinlets for greater distances (>150 m) above the unconformity in grey to black and multicolored Athabasca sandstones and shales (Fig. 5.3). Below the unconformity, the mineralization of clay-bound deposits extends downward for rarely more than 150 m as fracture fillings and disseminations in crystalline basement rocks, whereas mineralization of the fracture-bound class may persist in excess of 300 m below the unconformity as at Eagle Point. All deposits may contain a variety of metallic elements but quantitatively in highly different proportions (Fig. 5.8) and with

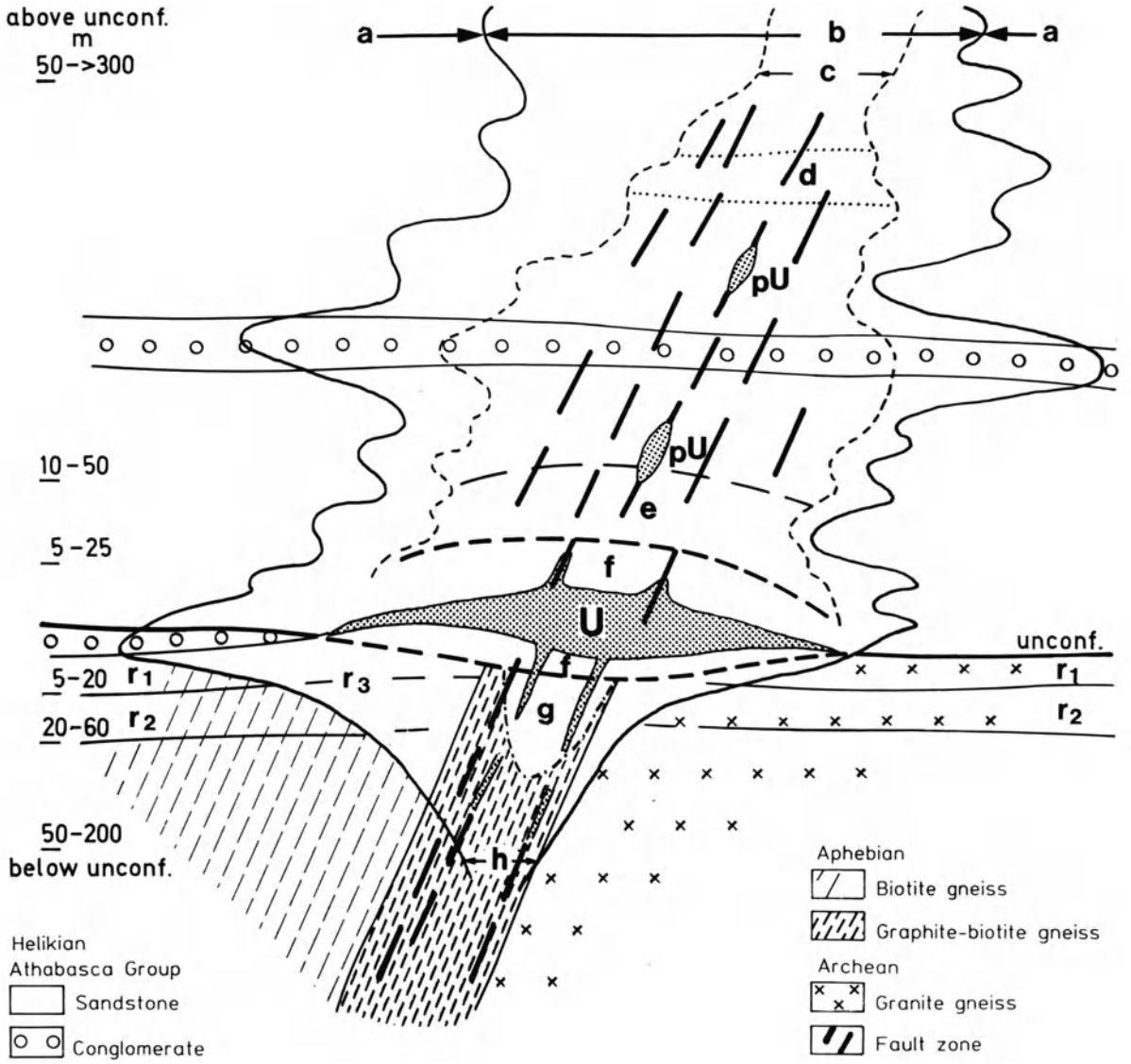

Fig. 5.3. Athabasca Basin region, diagramatic section of alteration features surrounding clay-bound unconformity-contact type (class 1.1.2) U deposits.
Sandstone (Athabasca Group)
a "Normal" pink sandstone with a clay fraction composed of ca.50% illite / 50% kaolinite; *b* clay alteration halo with illite > kaolinite; *c* fractured, friable sandstone, ± bleached; sulfides, carbonates, chlorite, dravite, clay along fractures, contains fracture controlled weak U mineralization, commonly <100 ppm U (perched U mineralization); *d* silicified intervals, quartz overgrowth, euhedral quartz along fractures; *e* clay-filled fractures, dominantly illite, minor kaolinite, Mg-chlorite, Fe-chlorite, locally secondary hematite, disseminated carbon "buttons"; *f* massive clay envelope surrounding and penetrating massive mineralization.
Basement (Aphebian and Archean)
g Graphite depletion; *h* clay alteration; *r* regolithic basement; r_1 red (hematitic) zone, r_2 green (chloritic) zone; r_3 bleached (hydrothermally altered) zone

compositional variations from one district to the other. For example, mineralizations in the eastern Athabasca Basin are dominated by a U-Ni-Co-Mo-As assemblage (Table 5.4) whereas in the Carswell Structure district a U-Te-Se-Bi-Au assemblage (Table 5.5) is found. These elemental inhomogeneities are thought to reflect local variations in geochemistry and metal endowment of lithostratigraphic units.

Principal *uranium minerals* in both classes of deposits are pitchblende, uraninite, coffinite,

Table 5.3. Athabasca Basin region, summary of characteristic features of uranium deposits and major uranium occurrences. (After Lainé 1985, based on references listed below, reproduced with permission from the Geological Association of Canada)

Deposit	Unconformity		Regolithic alteration		Basement rock		Host rocks		Organic matter	Alteration		Localization of ore			Basement fault control	Associated elements		References
	Well defined	Obscured by alteration	Strong	Weak	Type	Age	In basement	In Athabasca Group		Chlorite	Illite	At U/C	Below U/C	Above U/C		Major	Minor	
Class 1.1.1																		
Rabbit Lake	Eroded		x		M	Ap	Q, C, G, F		x	xMg			x		x		V, Mo, Cu, Ni	1
Eagle Point	Eroded			?	M, F	Ap, Ar?	F, C?, Q		x	xMg	x		x		x			3
Cluff Claude	Eroded			x	M	Ap	G, F		x	x	x		x		x		Mo, Pb	2
Cluff Dominique-Peter	Eroded in part		x		M	Ap	G, F		x	xMg	x		x		x	Te, Se	Au, Mo	2
Cluff N	Eroded		x		Gr	Ap	Q, F		x	x	x		x		x		Cu, Pb, Au	2
Cluff OP	Eroded in part		x		M	Ap	G, F		x		x		x		x		B, Mo, Cu	2
Class 1.1.2																		
Collins Bay A		x	x		M	Ap	F, G		x		x	x	x	x	x	Ni, As	Au, Ag, Pb	1, 8, 6
Collins Bay B	x			x	M, Gr	Ap, Ar	G, C	Sm	x		x	x		x	x	Ni, As		1, 8, 6
Midwest Lake		x	x		Gr	Ap, Ar	G, C, Q	Sm, Sb, P	x	xMg	x	x	x	x	x	Ni, As, Co	Ag, Pb	1, 8, 3
Dawn Lake	x			x	M	Ap	G, C	Sb	x	x		x	?	x	x	?	?	1
Mclean Lake	x	x		x	M, Gr	Ap, Ar	Q, C	Sm	x	x	x	x	x	x		Ni, Co, As	V, Mo, Cu	4
Cigar Lake	x	x	x		Gr	Ar	G	Sm, Sb, P	x	x	x	x	x	x	x	Ni, As, Co	Mo, Cu	8
Key Lake		x	x		Gr	Ap, Ar	G	Sb	x	x	x	x	x	x	x	Ni, Co, As		1, 8, 5
Cluff D	x		x		M	Ap	Q	P, Sm, Sb	x	xMg		x	x	x	x	Au, Te, Se	Co, Ni, Bi	2
Maurice Bay	x		x		Gr	Ar, Ap	F	Sm	x		?	x	x	x	x		Au, Cu	1, 8, 7
Stewart Island	x			x	T	Ar, Ap		Sb			?	?		x	?		Ni, Co, Cr	1, 8, 7
Fond du Lac	x		x		Gr	Ar, Ap		Sm	x					x	x			1, 8, 7

U/C – Unconformity
Q – Quartzite, feldspathic quartzite
C – Calc-silicate rocks
G – Gneiss, graphitic
F – Quartzofeldspar granitoid
M – Metasedimentary
Gr – Granitoid & metasedimentary
A – Aphebian
Ar – Archean
P – Mudstone
Sm – Sandstone (multicoloured)
Sb – Sandstone (black)

References
1 Tremblay (1982)
2 Tona et al. (1985)
3 Sopuck et al. (1983)
4 Wallis et al. (1983)
5 Dahlkamp and Adams (1981)
6 Jones (1980)
7 Homeniuk and Clark (1986)
8 Fouques et al. (1986)

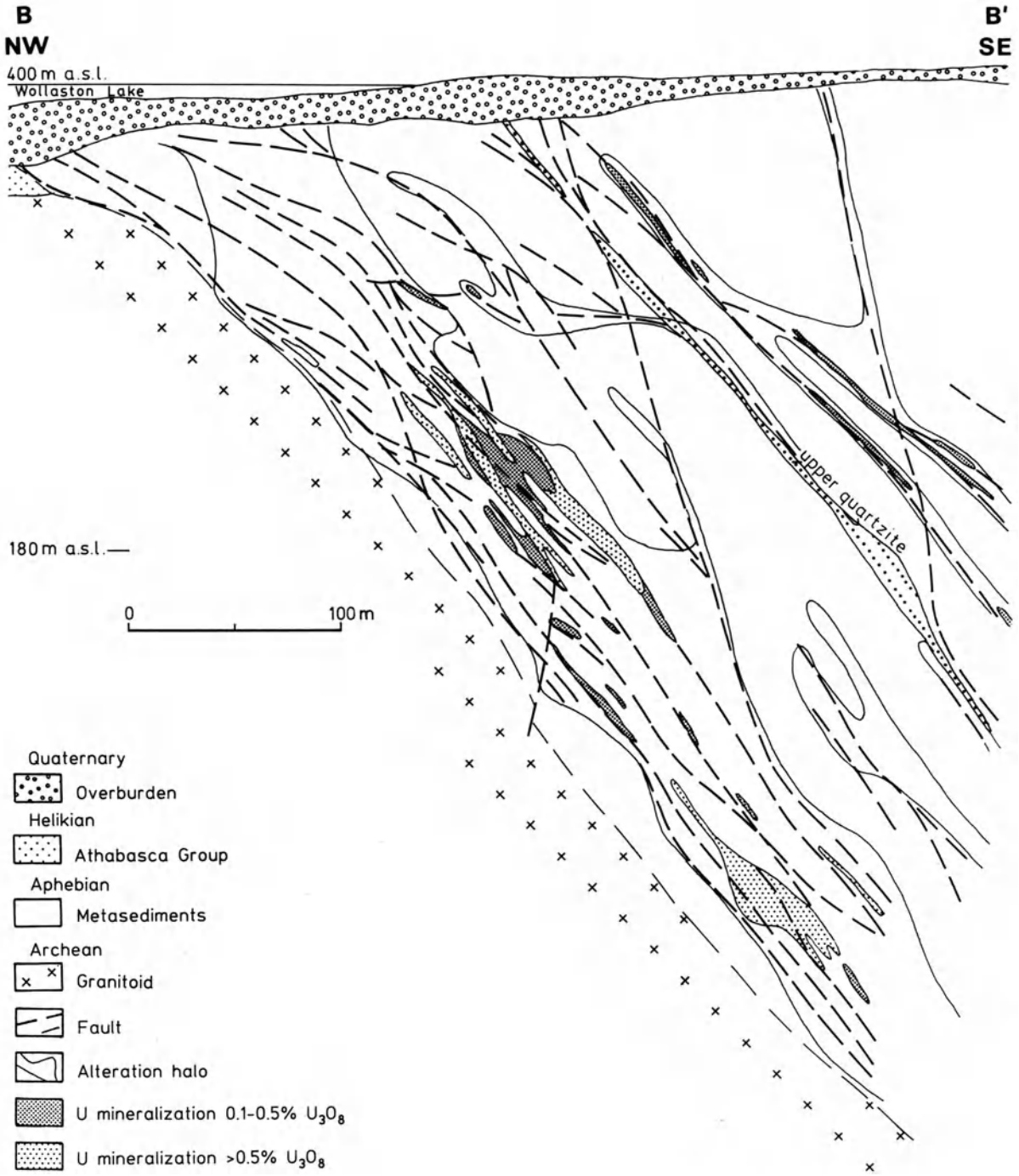

Fig. 5.4. Eagle Point, NW-SE cross-section across the Eagle South ore zone with distribution and grades of U mineralization and extension of associated alteration zones. The section demonstrates the persistence of pitchblende veins into great depth of at least 400 m below the surface. (After Eldorado Resources Ltd. 1987)

minor brannerite, and some amorphous uranium-carbon material (carburan) and in weathered zones hexavalent U minerals. Most of the uranium and associated minerals are present in several generations. Euhedral crystals of αU_3O_7 are described from several deposits, e.g., Key Lake (Voultsidis et al. 1982). Von Pechmann (1985) argues against this determination, and contends that the mineral phase is uraninite, at Key Lake at least. The misleading X-ray peaks

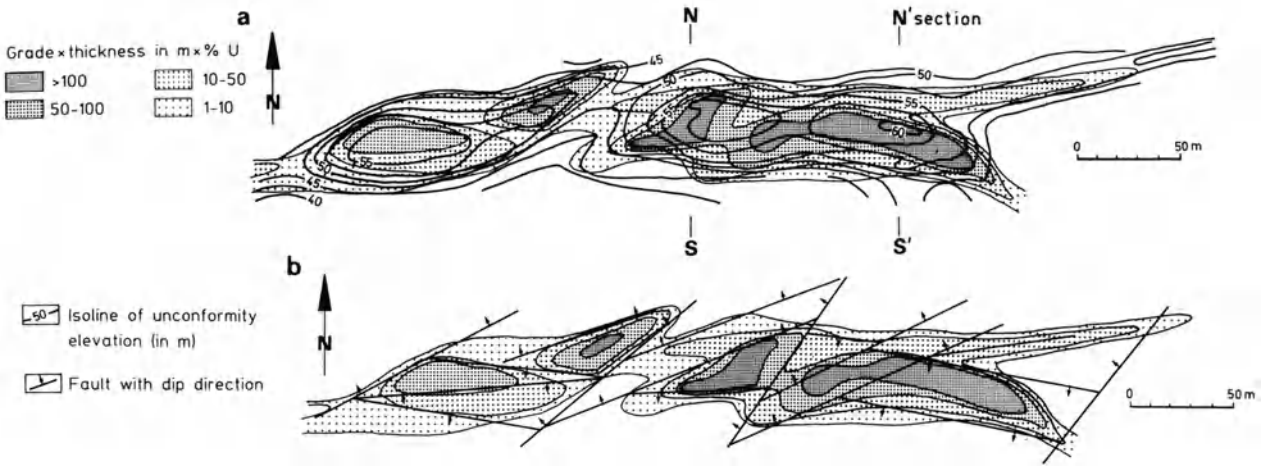

Fig. 5.5. East Athabasca district, Cigar Lake, isoline map of U accumulations (in grade thickness, *dotted*) combined with **a** isolines of unconformity elevation and **b** interpreted structure systems at the unconformity displaying the correlation between the three parameters. (After Fouques et al. 1986) (reprinted with permission of The Canadian Institute of Mining and Metallurgy)

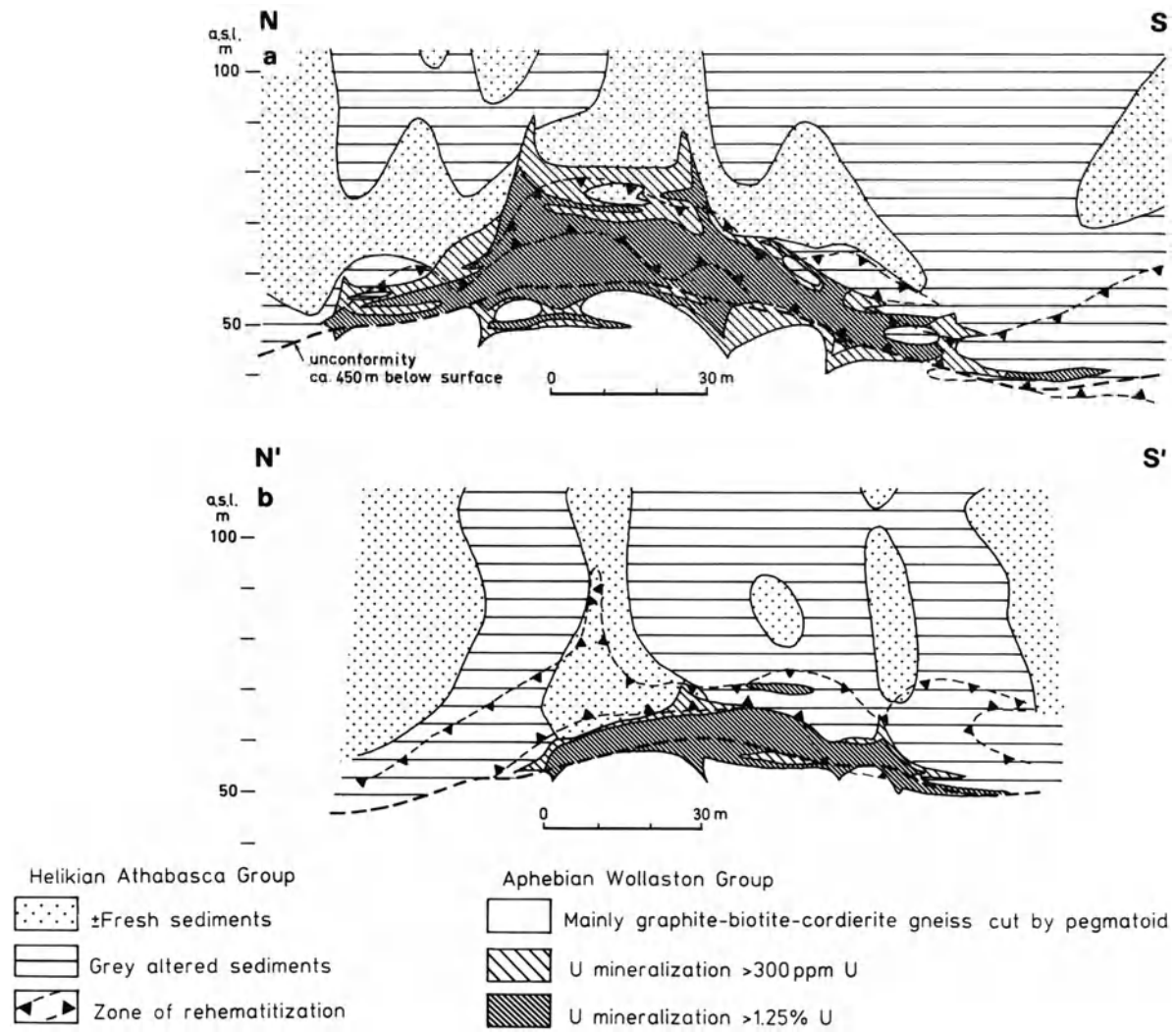

Fig. 5.6. East Athabasca district, Cigar Lake, cross-sections through the eastern part of the deposit showing distribution of low and high-grade U mineralization, and halos in the Athabasca Group of gray alteration (associated with Fe-sulfidization) and rehematitization. Note the relatively sharp boundaries of the high-grade U mineralization. (After Fouques et al. 1986) (reprinted with permission from The Canadian Institute of Mining and Metallurgy)

U contents

Pod	N-4	N-3	N-2	N-1	SW	SE	Candy Lake
% U_3O_8	0.79	0.69	2.43	2.56	2.10	0.73	0.35
mt U_3O_8	65	85	1180	3130	900	830	17

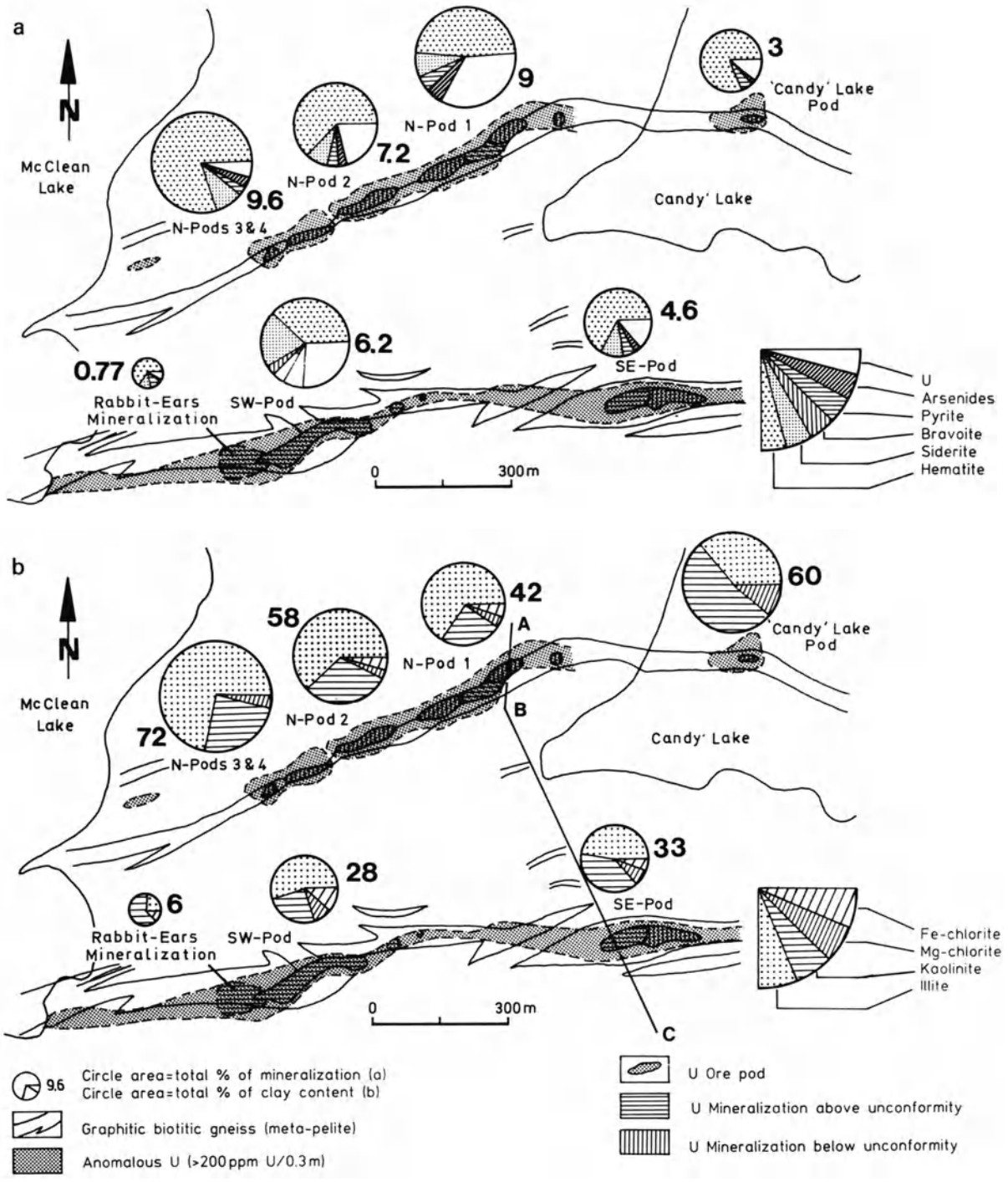

Fig. 5.7. East Athabasca district, McClean. Correlation of U mineralization with graphitic gneiss and the unconformity is displayed in the plans (graphitic units interpreted from EM and drill hole data). *Circles* show the percentages of **a** U and other metallic minerals and **b** clay minerals in the various ore pods (*numbers at circles* give total percentage of respective rock fraction). (After Wallis et al. 1985, 1986) (reprinted with permission from The Canadian Institute of Mining and Metallurgy)

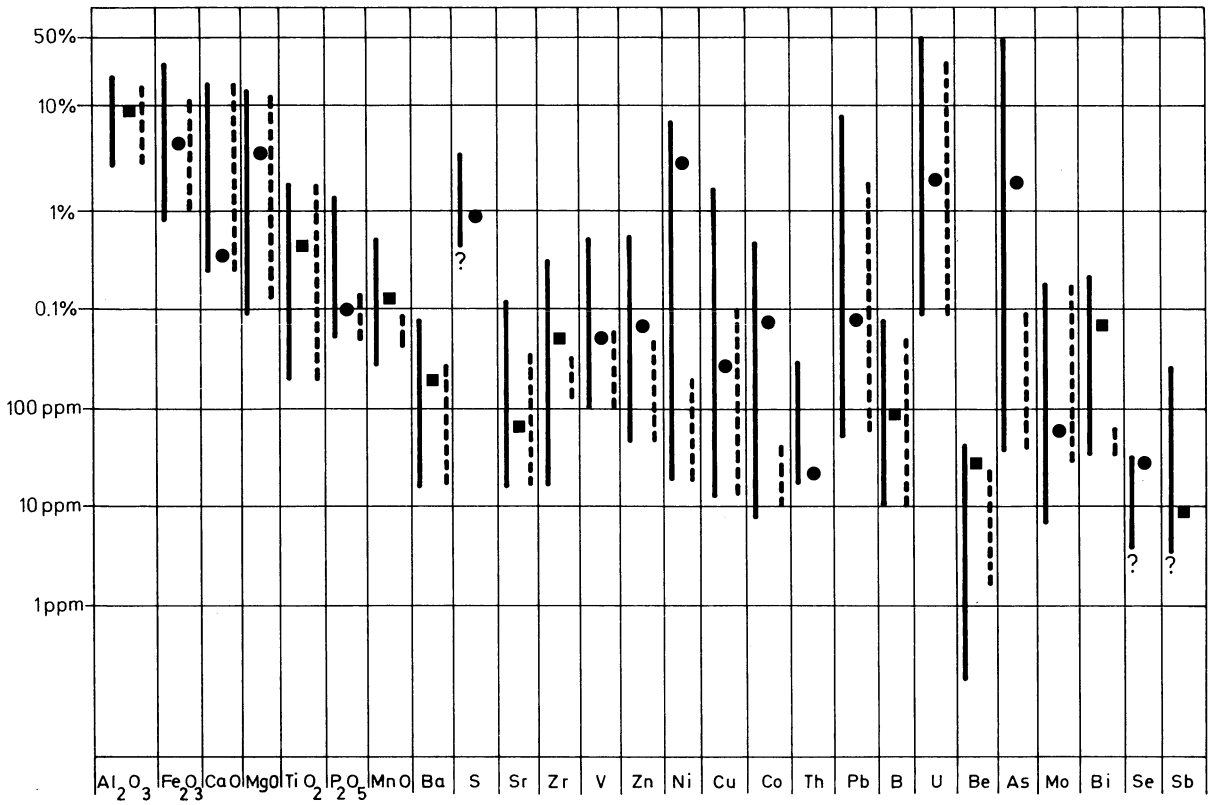

Fig. 5.8. Eastern Athabasca Basin region, range of contents of selected elements in unconformity-contact deposits in the Wollaston Belt. (*Heavy line* gives contents for both classes of deposits, *dashed line* only for fracture-bound type mineralization class 1.1.1, *dots* represent bulk and *squares* pit grab samples from the Gaertner ore body, Key Lake, only samples with >0.1% U_3O_8). (After G. Ruhrmann written pers. commun. based on data from Eldorado Resources Ltd. 1986; Fouques et al. 1986; Ruzicka 1986, 1988; Wray et al. 1985)

Table 5.4. Key Lake, Gaertner ore body, paragenetic assemblages of mineralization. (After Ruhrmann and von Pechmann 1989)

Assemblage	U	Ni, Fe, Cu, Co, U	U and Gangue		Ni, Fe, Cu, Pb, Zn, U			
Age m.y.	ca. 1400	ca. 900	ca. 300					
Minerals	Uraninite I	Rammelsbergite I Niccolite I Gersdorffite Bravoite I Covellite Hauchocornite Breithauptite Pyrite Bornite I Chalcopyrite I Coffinite I	Calcite Siderite Sericite Dolomite Rutile Apatite	Uraninite II Uraninite III Uraninite IV Uraninite V	Anatase Rammelsbergite II Kerogen Marcasite Bornite II Gersdorffite Bravoite II	Maucherite Millerite I Bismuthinite	Galena I Vaesite Millerite II Niccolite II	Sphalerite Millerite III Coffinite II Galena II Digenite Chalcopyrite II

Table 5.5. Carswell Structure district, summary of mineral parageneses, geological setting and age of mineralization in basement and overlying sediments. (After Ruhlmann 1985 and Lainé 1986, reprinted with permission from The Canadian Institute of Mining & Metallurgy and the Geological Association of Canada)

Stage	Subeconomic/pre-ore		Main ore		Redistribution/Late ore		
			I	II			
Assemblage	Monazite – uraninite	Pitchblende uraninite	Uraninite – selenide – sulfide	Uraninite – sulfide	Pitchblende – hematite	Pitchblende – carbonate	Coffinite – sulfide
Uraniferous phase	Monazite (th) Uraninite	Pitchblende Uraninite	Brannerite Uraninite	Uraninite	Pitchblende	Pitchblende	Coffinite
Non-uraniferous phase	Molybdenite Pyrite Galena	Pyrite Chalcopyrite Galena	Altaite – paraguanajuatite Guanajuatite – clausthalite Calaverite – trogtalite Freboldite – gersdorffite Nickeline – skutterudite Galena – chalcopyrite Molybdenum sulfides Gold – bismuth	Molybdenum – sulphide Galena – pyrite Chalcopyrite Sphalerite Tennantite	Hematite Magnetite Limonite Goethite Gold	Chalcopyrite Galena Pyrite	Pyrite Galena
Gangue	Garnet	Albite Chlorite	Chlorite (Mg/Al)	Quartz	–	Calcite	–
Host rock	Garnet – rich pegmatoid	Feldspar – rock	Basement & sandstone	Basement	Sandstone Basement	Basement	Sandstone Basement
Textural characteristics	Disseminated	Fractures	Coatings around the "zone à boules"	Fractures	Fractures	Fractures	Fractures
Characteristic element assoc.	U-Th	U	U-Mo-Bi-Se-S-(Te-Ni-Co)	U-Mo-Pb-Zn-Cu-S	U-Fe	U-Co-Pb-Cu	U-Si
Age, m.y.[a]	1928	1330?	1150–1050	820–890	380	All ages	All ages
Types of occurrences	Sophie	Numac	Claude – D-N Dominique – Peter	OP – Claude – Domin – Peter	Donna – D-N	All types	All types

[a] Reference see Geochronology.

Table 5.6. Eastern Athabasca Basin region, published analyses of selected elements of U mineralizetion in fracture-bound deposits (class 1.1.1). The ore typically contains high U grades and low values of the other metals except for Pb which is largely radiogenic. (values are in ppm except where noted). (After **a** Eldorado Resources Ltd. 1987, composite sample from 02 zone Eagle North; **b** Ruzicka 1986, nine drill core samples; **c** Ruzicka 1986, five grab samples from various parts of the deposit)

	Eagle Point		Rabbit Lake
	a	b	c
Ag	5	n.a.	n.f.
As	60	<1000	n.f.
Au	0.06	–	–
B	–	150–700	<10–500
Ba	–	200–500	20–500
Be	–	–	<2–50
Bi	60	–	–
Co	60	<10–15	<10–70
Cr	120	<10–30	50–70
Cu	370	15–1000	15–500
Fe	1.22%	0.3–7%	0.5–15%
La	–		n.f.–500
Mg	–	0.2–3%	0.5–10%
Mn	750	–	–
Mo	620	50–2000	n.f.–70
Nd	–	–	n.f.–700
Ni	90	20	50–200
P	200	–	n.f.–<1000
Pb	1570	500–50 000	70–15 000
Pt	<0.03	–	
S	–	–	–
Sc	–	–	3–150
Sb	<10	–	–
Se	<20	–	–
Sn	<10	–	–
Te	2.2	–	–
Th	–	–	n.f.
Ti	–	300–7000	–
U	1.865%	1.69–43.3%	0.13–17.9%
V	400	300–700	100–500
Y	–	30–1000	30–700
Yb	–	–	3–50
Zn	<50	–	50–700

leading to the αU_3O_7 identification are caused by coexisting uraninite and poorly crystallized "sooty" pitchblende. Ramdohr (pers. commun.) considers the αU_3O_7 possibly a distorted uraninite recrystallized after colloform pitchblende.

Additional features of the two classes (see also Chap. Ore Control) include:

a) *Fracture-bound class mineralization* (Fig. 5.4) is emplaced in highly fractured and altered crystalline basement rocks often associated with graphitic metasediments or calc-silicate rocks. U is accompanied by mainly Fe and Pb sulfides, and minor quantities of mainly Cu, Mo, V and traces of other elements (Table 5.6). Local variations in accessorial elements are apparently related to host rock lithologies. Principal gangue minerals are quartz, calcite, dolomite, minor siderite and ankerite. The deposits occur in an en-

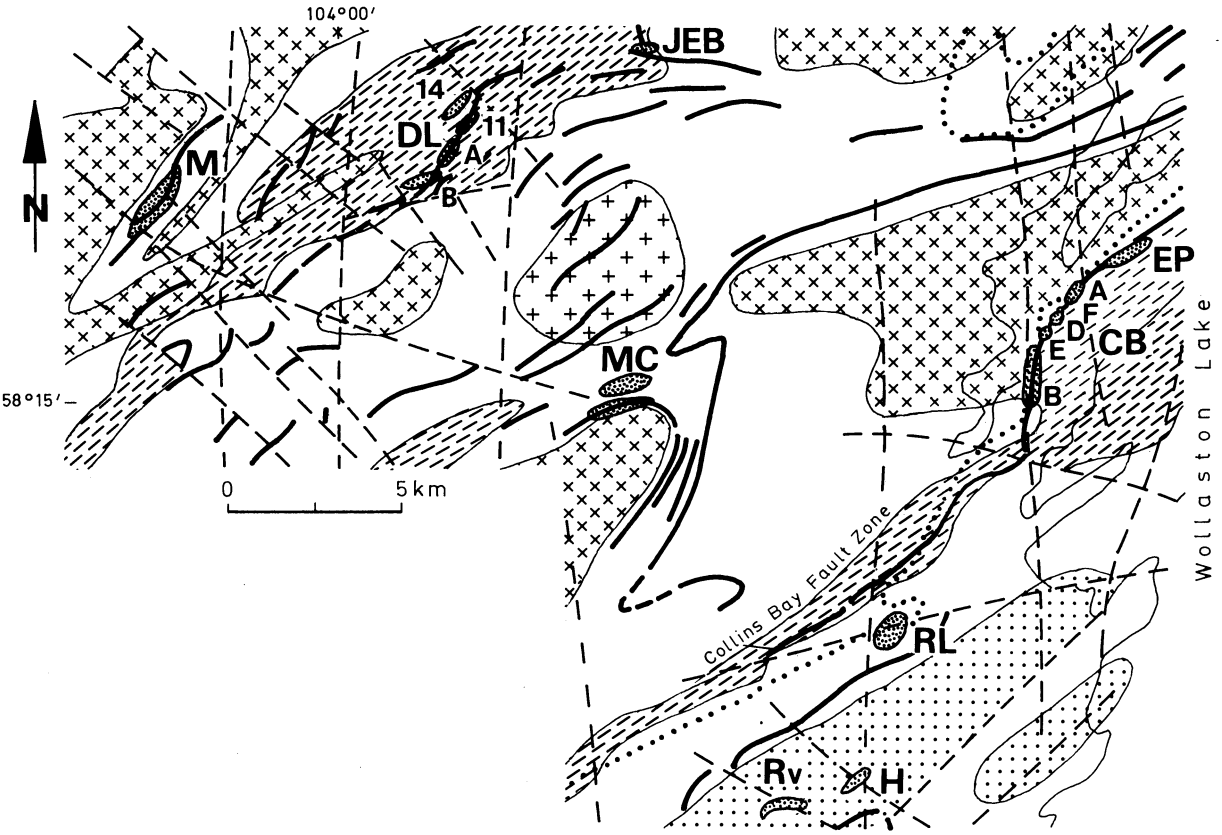

Aphebian
- Quartzite with feldspathic gneiss (meta-arkose)
- Biotitic gneiss (meta-semipelite) and feldspathic gneiss
- Biotitic gneiss (meta-pelite, -semipelite)
- Graphitic gneiss

Archean-Aphebian
- Aphebian feldspathic gneiss or Archean granite gneiss
- Granitoid of Torwalt Dome (below metasediments)
- Major fault
- Eastern limit of Athabasca Group
- U deposits (size exaggerated)

U deposits:
CB=Collins Bay (A,B,D,E,F zones), DL=Dawn Lake (11,11A,11B,14 zones),
EP=Eagle Point, H=Horseshoe, JEB=JEB, M=Midwest, MC=Mc Clean,
RL=Rabbit Lake, Rv=Raven

Fig. 5.9. Athabasca Basin region, East Athabasca U district, generalized geology of the crystalline basement interpreted from geophysical and drill hole data, and position of major uranium deposits. U deposits: *CB* Collins Bay (A, B, D, E, F zones); *DL* Dawn Lake (11, 11A, 11B, 14 zones); *EP* Eagle Point; *H* Horseshoe; *JEB* JEB; *M* Midwest; *MC* McClean; *RL* Rabbit Lake; *Rv* Raven (After McNutt 1980 In: Clarke and Fogwill 1986; Eldorado Resources Ltd. 1987; Sibbald 1983; Wallis et al. 1986)

vironment affected by marked Na-metasomatism, migmatitization, and the presence of often abundant pegmatite and microgranite dikes or segregations.

The deposits often occur in subsidiary structures located in the hanging wall of major reverse faults (e.g., Collins Bay Thrust Fault at Eagle Point, Rabbit Lake Fault at Rabbit Lake, Fig. 5.9). The Rabbit Lake, Eagle Point and other deposits of the East Athabasca district located to the east of the Collins Bay Shear Zone and some deposits in the Carswell Structure (Dominique-Peter, Claude, OP, N) represent this class of mineralization.

b) *Polymetallic clay-bound mineralization* (Figs. 5.3 and 5.5 to 5.7) occurs associated with argillaceous masses at the base of the arenaceous sedimentary cover (Manitou Falls Formation) directly above the unconformity and in the upper few tens of meters of highly altered basement.

Mineralization in these deposits exhibit a great chemical diversity. A suite of anomalous elements is commonly present in the form of sulfides,

Table 5.7. Eastern Athabasca Basin region, published analyses of selected elements of U mineralization in clay-bound deposits (class 1.1.2). The ore is characterized by high to very high U grades and high contents of other metals as well. Ni and As are particularly high. Values of almost all other metals are significantly higher than those in class 1.1.1 deposits. After *a* Ruzicka 1984, six selected drill core samples; *b* Ruzicka 1984, based on Ruzicka and Littlejohn 1982, and Canada Wide Mines Ltd. 1980, eight drill core samples; *c* Wray et al. 1985, five composite drill core samples; *d* Fouques et al. 1986, average metal contents of deposit; *e* Ruzicka 1984, seven selected drill core samples; *f* Ruzicka 1984, three drill core samples; *g* Ruzicka 1984, three drill core samples

	Key Lake Gaertner ore body	Midwest		Cigar Lake	Collins Bay		
					A-Zone	B-Zone	D-Zone
Ref.:	a	b	c	d	e	f	g
Ag	10–30	5–68	tr–68.3	–	3.77–1349.8	<5–150	50–150
As	0.7–>10%	0.23–>10%	1.68–9.62%	1.67%	0.03–33.46	>10%	50%
Au	–	–	0–0.34	–	–	–	–
B	–	–	–	–	–	–	–
Ba	–	–	–	–	–	–	100–300
Be	–	–	–	–	–	–	–
Bi	–	170–1500	130–640	–	–	–	–
Co	700–3000	<0.05–1.0%	360–6100	0.15%	–	50–1000	50–5000
Cr	<10–300	30–330	100–230	–	–	7–100	
Cu	200–2000	14–1500	580–4200	0.70%	–	700–>3000	
Fe	–	–	2.31–5.42%	–	–	–	
La	–	–	–	–	–	–	
Mg	–	–	–	–	–	–	
Mn	200–5000	–	–	–	–	–	
Mo	–	<50–1360	80–360	0.14%	–	50	<10–1000
Nd	–	–	–	–	–	–	
Ni	>7000	<0.005–>1.5%	0.94–4.8%	0.96%	0.56–5.09%	50–>7000	0.02–>10%
P	–	–	–	–	–	–	
Pb	1–5%	<0.04–3.0%	0.04–1.19%	1.16%	0.20–9.18%	0.15–5%	0.1–10%
Pt	–	–	<0.1	–	–	–	
S	–	–	0.55–3.18%	–	–	–	
Sc	–	–	–	–	–	–	
Sb	–	–	40–220	–	–	–	
Se	–	–	5– 20	–	–	–	
Sn	–	–	60–110	–	–	–	
Te	–	–	10–20	–	–	–	
Th	–	–	<50–330	–	–	–	
Ti	1500–2000	0.05–2.0%	–	–	–	100–2000	
U	20.4–32.1%	0.14–27.2%	0.25–11.8%	12.30%	2.33–64.8%	10.9–21.4%	0.09–32.2%
V	700–1500	0.01–0.49%	0.11–0.34%	–	–	100–500	150–3000
Y	–	–	–	–	–	–	70–2000
Yb	–	–	–	–	–	–	10–300
Zn	<1000	<0.02–0.11%	0.02–0.52%	0.04%	–	–	

Table 5.8. Athabasca Basin region, reserves and approximate dimensions of unconformity-contact uranium deposits (Status 1989: r = reserves, d = depleted, p = production)

District Deposit	Reserves mt U_3O_8		Grade % U_3O_8	Length m	Width m	Thickness m	Depth m	Athabasca Gp. Thickness, m	Main host unit	Type-Class
Carswell Structure										
D (9)	5100	(d)	4.0	120	<30	9	8 0–35	<20	Clay/sdst.	1.1.2
Claude (9)	2460	(p)	0.42	240	<120	<10	0–100	0	Basement	1.1.1
Dominique-Peter (9)	13600	(r)	0.77	700	<600	40–60	100–180	0	Basement	1.1.1
N (9)	2000	(r)	0.4	600	20	<60	<50–150	0	Basement	1.1.1
Dominique-Janine (9)	940	(r)	0.38	160	80		<65	0	Basement	1.1.1
OP (9)	180	(r)	0.33	150			<100	0	Basement	1.1.1
East Athabasca										
Eagle Point South (3)	33700	(r)	1.64	1000	100–240	18–37	35–>430	0	Basement	1.1.1
Eagle Point North (3)	26200	(r)	2.07			30–75	75–>360	0	Basement	1.1.1
Rabbit Lake (3,4)	18200	(d)	0.37	550	<250	0–200	0–200	0	Basement	1.1.1
Horseshoe (3,11)	5900	(r)	0.17	900			90–300	0	Basement	1.1.1
Raven (3,11)	4300	(r)	0.14	800			120–300	0	Basement	1.1.1
West Bear (3,11)	590	(r)	0.44	450	20	8	>20	<20	Clay/sdst.	1.1.2 (?)
Collins Bay A (3)	7600	(r)	5.68	50	45	<18	5–20	0–20	Clay/sdst.	1.1.2
Collins Bay B (3)	13900	(p)	0.63	1000	100	30	5–50	15–25	Clay/sdst.	1.1.2
Collins Bay D (3)	2500	(r)	2.19	200					Clay/sdst.	1.1.2
Dawn Lake (1,2) (several ore pods)	15800	(r)	1.9	300–700	15–100	20–50	30–200	100	Clay/sdst. Basement	1.1.2
McClean (12) (several ore pods)	6200	(r)	1.78	60–260	15–45	1.5–20	115–190	150	Clay/sdst.	1.1.2
Midwest (1,5)	15800	(r)	3.5	900	<50	<36	160–220	200	Clay/sdst.	1.1.2
Cigar Lake (1,6)	12800	(r)	14.4	1800	25–105	5–30	410–450	380–400	Clay/sdst.	1.1.2
(Cigar Lake, addit. est.) (1)	45000	(r)	4.0							
P2-North	?		±10	>600	?	?	500–600	>500	Clay/sdst.	1.1.2
Southeast Athabasca										
Key Lake-Gaertner (8)	28000	(p)	3.4	1500	10–40	4–50	50–80	10–50	Clay/sdst.	1.1.2
Key Lake-Deilmann (8)	54000	(r)	2.9	1200	10–200	10–70	65–140	5–80	Clay/sdst.	1.1.2
Key Lake-cobble ore (8)	7000	(r)	0.7						Glacial	
North Rim Athabasca										
Maurice Bay (10) (several ore zones)	550	(r)	<0.5	50–1500	50–450	20–50	15–150	0–120	Clay/sdst. basement	1.1.2 (?)
Fond-du-Lac (7)	450	(r)	0.25	390	<80	10–40	10–40	<30	Clay/sdst.	1.1.2 (?)
	>437900									

References: 1 Saskatchewan Geol. Surv./CIM Directory 1987, 2 Clarke and Fogwill 1986, 3 Eldorado Resources Ltd. 1987, 4 Eldor Mines Annual Report 1984, 5 Farstad and Ayers 1986, 6 Fouques et al. 1986, 7 Homeniuk and Clark 1986, 8 Kegel, K.E. pers. commun., 9 Lainé 1986, 10 Lehnert-Thiel et al. 1981, 11 Ruzicka 1986, 12 Wallis et al. 1986

Table 5.9. Athabasca Basin region, selected geochronologic data of uranium mineralization (pitchblende/uraninite) and associated (?) alteration of unconformity-contact deposits

Carswell Structure district		
m:	1330 ± 30	U-Pb Numac (10)
m:	1150 ± 25	U-Pb D (3)
m:	1095 ± 95	Pb-Pb Numac (2)
m:	1050 ± 30	U-Pb D (10)
m:	945 to 995	Pb-Pb Dominique-Peter (2)
m:	820 to 890	U-Pb OP (2)
m:	ca. 380	U-Pb Donna (2)
m:	ca. 250	U-Pb D (3)
a:	1293 ± 36	K-Ar hydroth. clays (5)
a:	1128 ± 450	K-Ar chl schist, D (23)
a:	988	K-Ar ser after cordierite (11)

North Rim Athabasca		
m:	400	U-Pb Maurice Bay (9)
m:	1196 ± 24	U-Pb Maurice Bay (11)
m:	415 – 240	U-Pb Maurice Bay (11)
m:	1100 to 1200	U-Pb Fond-du-Lac (15)
m:	215	U-Pb Fond-du-Lac (15)
m:	80	U-Pb Fond-du-Lac (15)
m:	318	U-Pb Stewart Island (15)
m:	24	U-Pb Stewart Island (15)

East Athabasca district			
m:	1400 ± 25	U-Pb	Eagle Point (7a)
m:	1000	U-Pb	Eagle Point (7b)
m:	450–700	U-Pb	Eagle Point (7b)
m:	5– 20	U-Pb	Eagle Point (7b)
m:	1320	U-Pb	Rabbit Lake (17)
m:	1281 ± 11	U-Pb	Rabbit Lake (6
m:	1075	U-Pb	Rabbit Lake (18)
m:	860	U-Pb	Rabbit Lake (17)
m:	494 ± 19	U-Pb	Rabbit Lake (6)
m:	200	U-Pb	Rabbit Lake (17)
m:	1238	U-Pb	Collins Bay B (16)
m:	450	U-Pb	Collins Bay B (16)
a:	1296 ± 34	K-Ar	Collins Bay music in bs (20)
a:	1266 ± 39	K-Ar	Collins Bay A, il in bs (20)
m:	1331 ± 8	U-Pb	Midwest (25)
m:	1328 ± 17	U-Pb	Midwest (1)
m:	1110 ± 28	U-Pb	Midwest (1)
m:	1094 ± 27	U-Pb	Midwest (25)
m:	338	U-Pb	Midwest (25)
a:	1411 ± 36	K-Ar	Midwest, clay musc 3 m below u/c (20)
a:	1332 ± 126	Rb-Sr	Midwest, ser assoc. with min. (25)
a:	1212 ± 33	K-Ar	Midwest, clay musc at u/c (20)
a:	1222 ± 28	Rb-Sr	Midwest, late ser (25)
a:	1249 ± 48	Rb-Sr	Midwest, late chl (25)
a:	1272 ± 42	K-Ar	McClean, mica, most alt. gn (22)
a:	1319 ± 3	K-Ar, Ar-Ar	McClean, il from alt. around high grade ore (4)
a:	1482 to 1453 ± 49	K-Ar, Ar-Ar	McClean, il at u/c (4)
m:	1300	U-Pb	Cigar Lake (19)

Southeast Athabasca district			
m:	1406 ± 45	U-Pb	Key Lake (14b)
m:	1350 ± 4	U-Pb	Key Lake (21)
m:	1328 ± 28	U-Pb	Key Lake (13)
m:	1224 ± 14	U-Pb	Key Lake (13)
m:	903 ± 40	U-Pb	Key Lake (12)
m:	286 ± 12	U-Pb	Key Lake (12)
a:	1189	K-Ar	Key Lake il from alt. sandstone
a:	1131	K-Ar	Key Lake above ore (24)
a:	765 ± 120	K-Ar	Key Lake chl from sheared clay 8 m below u/c (20)
m:	941 ± 16	U-Pb	Middle Lake (14a)

(m: mineralization, a: alteration, in m.y.; musc = muscovite, ser = sericite, il = illite, chl = chlorite, gn = gneiss, bs = basement, u/c = unconformity)

References:
1 Baadsgaard et al. 1984
2 Bell 1985
3 Bellon et al. 1976
4 Bray et al. 1987
5 Clauer et al. 1985
6 Cumming and Rimsaite 1979
7a Eldorado Resources Ltd. 1986/1987
7b Eldorado Resources Ltd. 1987b
8 Fahrig 1961
9 Gancarz 1979
10 Herring 1976
11 Hoehndorf et al. 1985a
12 Hoehndorf et al. 1985b
13 Hoehndorf et al. 1989
14a Hoehndorf and Carl, 1987
14b Carl et al. 1988
15 Homeniuk and Clark 1986
16 Jones 1980
17 Knipping 1974
18 Little 1974
19 Ruzicka and LeCheminant 1986
20 Stevens et al. 1982
21 Trocki et al. 1984
22 Wallis et al. 1986
23 Wanless et al. 1979
24 Wilson et al. 1987
25 Worden et al. 1985

arsenides, sulfarsenides, locally selenides and tellurides (the latter mainly in the Carswell district) (Table 5.7). However, the proportions of the elements vary considerably and in most cases show no economic concentrations. Principal gangue minerals include quartz and carbonates in minor quantities. Key Lake and most deposits of the East Athabsca district that are located to the west of and at the Collins Bay Shear Zone (Fig. 5.9), and some deposits of the Carswell Structure district (D-ore body) belong to this class.

Dimensions of the known deposits in the Athabasca Basin region are given in Table 5.8.

Isotope ages of ores from the Athabasca uranium deposits are provided in Table 5.9. The oldest uranium generation is dated about 1400 to 1250 m.y. Subsequent mineralization or remobilization events occurred about 1250 to 900 m.y. and 300 to 100 m.y. ago.

Stable Isotopes and Fluid Inclusions

Stable isotope (D, ^{18}O, ^{13}C, ^{34}S) and fluid inclusion data from different phases of phyllosilicates, quartz, carbonates, and sulfides reported by Bray et al. (1982, 1984, 1988) (McClean), Halter et al. (1987) (Carswell Structure), Pagel (1975a, 1975b, 1977), Pagel et al. (1980) (Carswell Structure and Rabbit Lake), Wallis et al. (1986) (McClean), Wilson (1987), Wilson and Kyser (1987) (Key Lake) among others document that several fluids of different composition had been repeatedly active in the Athabasca Group and the basement along the unconformity. Fluid inclusions in siliceous overgrowth on detrital quartz grains of Athabasca sandstone indicate that they derived from brines under oxidizing conditions during diagenesis (Pagel 1975a).

At McClean, hydrogen isotopes show two distinct populations in diagenetic illites from sandstone and regolith (D = −60 to −65) and in ore-related alteration illites (D = −100 to −155) demanding two different fluid compositions or sources (Wallis et al. 1986). Similar sulfur isotope values suggest that synmetamorphic sulfides ($\delta^{34}S$ = −32 to +21) provided the sulfur for ore sulfides ($\delta^{34}S$ = −24 to +17) (Bray et al. 1982).

At Rabbit Lake, stable isotopes (Pagel et al. 1980) and fluid inclusions (Pagel and Jaffrezic 1977) indicate that pale green chlorites and euhedral quartz veins, dolomite, and calcite have formed from different and not coeval fluids. At least two varieties of vein quartz can be identified by fluid inclusions. The first has inclusions with high and variable salinities and formed at a temperature of ca. 160°C. The other has low salinities and indicates a T of ca. 191°C. Dolomite crystallized at 130°C and later calcite at 120°C and from 127 to 150°C. Some of the vein quartz has isotopic compositions similar to dolomite and calcite, suggesting an origin from similar fluids. The Cl/Br ratios (55) in the fluid inclusions of vein quartz appear to be consistent with either a marine evaporitic environment or perhaps one with thermal degradation of organic matter or both.

At Key Lake, Wilson and Kyser (1987) interpret their data to indicate the presence of two fluids. One is indicated by Mg-chlorite in the basement and the other, a basinal brine, by the composition of illite. Mixing of these two fluids caused the concentration of uranium at the unconformity at temperatures postulated to be between 190 and 230°C (co-existing quartz-illite). Younger processes include kaolinitization by meteoric waters at low temperatures (50°C) and recent alteration of hydrothermal illite by modern meteoric waters. The latter is associated with hydration (increase of water content from ca. 4% to 7.7% in altered illites), lowering of δD values to as low as −170 and partial resetting of K-Ar ages (range from 1493 to 414 m.y.).

Potential Sources of Uranium

Certain metasediments, particularly more mafic gneisses, calc-silicate rocks, migmatites and pegmatites, and some granites contain elevated background values and localized concentrations of syngenetic uranium, often in form of uraninite, and other metallic elements in anomalous amounts. These uranium occurrences largely belong to the synmetamorphic type (for example, Yurchison Lake, Karin Lake, and Duddridge Lake, Wollaston Domain) but some also to the subunconformity-epimetamorphic/Beaverlogde type (Sophie and Laure, Carswell Structure, perhaps Way Lake, Wollaston Belt). They are documented for the Wollaston Group in the Cree Lake Mobile Belt by Dahlkamp 1978, Dahlkamp and Adams 1981, Kirchner et al. 1979, Lewry and Sibbald 1978, Parslow and Thomas 1982, Ruzicka 1984, Thomas 1979, Voultsidis et al. 1980 and others. Elevated uranium values are

likewise reported from the Carswell Structure area by Lainé 1986 and Pagel and Svab 1985.

The distribution of uranium deposits in the Athabasca region compared with the data supplied by the listed authors suggests that the uranium deposits are located in a region with seemingly more abundant anomalous uranium background values and local uranium concentrations and that a large part of this uranium was present in leachable form. This supports the hypothesis that the Aphebian metasediments in particular constituted a valid source of uranium for the formation of the unconformity-type deposits.

Geochronology

Significant ages of the Athabasca Basin region based on isotope datings of rocks in the Western Craton and in the Cree Lake Mobile Zone are presented in Table 5.11, and of uranium mineralization and associated alteration products in the main districts in Table 5.9. Figure 5.2 shows the geological setting of a deposit and approximate ages of ore-hosting units. A reconstruction of the geological events recorded by these data in the Athabasca Basin region can be found in Table 5.10 (see also Chap. 5.2.2, Uranium City region).

Table 5.10. Reconstruction of geological events in the Athabasca Basin region

1. Archean ending with Kenoran Orogeny >2500 m.y.	Formation of granites/granitic gneisses
2. Early Aphebian Blezardian Orogeny >2100 m.y.	Deposition of sediments, granitic and pelitic gneisses
3. Late Aphebian >1900 m.y.	Deposition of Wollaston Group sediments, formation of Peter River series, calc-alkaline magmatism, crystallization of uraninite and monazite
4. Hudsonian Orogeny 1900–1700 m.y.	Amphibolite to granulite grade metamorphism, migmatization, doming, generation of deep thrust faults and mylonite zones, late orogenic retrograde greenschist facies metamorphism, intrusion of granite and granodiorite and associated dikes, formation of subunconformity Beaverlodge-type U deposits
5. Paleo-Helikian >1500 m.y.	Lateritic weathering
6. Meso-Helikian >1500–1300 m.y.	Deposition of Athabasca Group, diagenetic and diagenetic-hydrothermal processes, crystallization of uraninite/pitchblende of unconformity-contact-type deposits
7. Neo-Helikian 1310–900 m.y.	Intrusion of diabase dikes, second generation of U mineralization, polymetallic mineralization
8. Hadrynian and younger 700–400 m.y.	Redistribution of uranium, Carswell Event
9. 300 m.y. to Recent	Erosion of Athabasca sediments, late remobilization of uranium

Ore Controls and Recognition Criteria

Significant ore controlling or recognition criteria of uranium deposits in the Athabasca Basin region include:

Host Environment

- All major deposits are grouped in three main districts, the East Athabasca, Southeast Athabasca, and Carswell Structure (Fig. 5.1).
- All three districts are characterized by a basement containing abundant Aphebian lower Wollaston Group partly graphitic metasediments wrapping around Archean granitic domes (deposit-type related details see next paragraphs).
- Red bed type arenites of the Athabasca Group rest unconformably on the crystalline basement.

Alteration

- Localized structurally controlled late Hudsonian (?) albitization (Na-metasomatism) and dolomitization (Mg-metasomatism) are noticed in the area of fracture-bound class deposits.

Table 5.11. Northern Saskatchewan, southwestern Churchill Province, selected geochronologic data

Age in m.y.	Western Craton	Age in m.y.	Cree Lake Zone
Archean-Kenoran Orogeny (>2500 m.y.)			
3070 (zircon) 3010 (zircon)	– Basement below Murmac Bay Group, Beaverlodge area (22a).	2680	– Rhyolite, Ennadai Group, Hattle Lake (8).
2864 (zircon)	– Quartz-feldspar gneiss/metaarkose, Fond-du-Lac.	2613 (Rb-Sr)	– Western granitic gneiss, Midwest (25).
2650 (Sm-Nd)	– Mountain Rapids granodiorite, Taltson Magmatic Zone, W of Western Craton (7)	2600 (zircon) 2600 (Rb-Sr)	– Granite gneiss, Zimmer Lake (13b). – Granite gneiss,
2630 (Rb-Sr)	– Hypersthene gneiss, Nevins Lake Block (2b).	2700 (Sm-Nd) 2490 (zircon)	Key Lake (12b). – Johnson River granite,
2580	– Megacrystic granite, Nolan Lake (7).		Bailey Lake (15).
2510 (zircon)	– Foot Bay gneiss, Beaverlodge area (20).		
Early Aphebian-Blezardian Orogeny (2500-2140 m.y.)			
ca: 2200–2100	– Deposition of middle and upper Tazin Group sediments and volcanics including Fay Complex and perhaps Donaldson Lake gneiss in Beaverlodge area (Tremblay 1978).	>2100 (?) 2338 (Rb-Sr) 2126 (Rb-Sr)	– Deposition of Needle Falls sediments. – Eastern granitic gneiss, – Pelitic gneiss, Midwest (25).
2360	– McIntosh granite,		
2333	– Anthona Mine granite,		
2180	– Gunnar granite, Beaverlodge area (22a).		
2315	– Garnetiferous felsic gneiss, Nevins Lake Block (2b).		
2320 (zircon) 2130 (zircon)	– Earl River Complex, Carswell Structure (1).		
2179 (zircon)	– Donaldson Lake gneiss, Beaverlodge area (20.3).		
2155 (Rb-Sr)	– Box, Frontier granites, Beaverlodge area (3).		
1999 (zircon)	– Box granite (22a).		
Late Aphebian-Hudsonian Orogeny (2100–1700 m.y.)			
ca. 2100–1900	– Deposition of Peter River Gneiss sediments in Carswell area (Lainé 1986)	>1900 1890	– Deposition of Wollaston Group sediments. – Junction granite (postdates Virgin River Shear Zone (4).
1990	– Slave monzogranite,		
1920	– Konth syenogranite, Taltzon Magmatic Zone, W of western Craton (5).	1830 (Rb-Sr) 1820 (Rb-Sr)	– Gneiss, – Granodiorite, Key Lake (12a).
1975 (Rb-Sr)	– Pegmatite, Beaverlodge area (17).	1765 (Rb-Sr) 1730 (K-Ar)	– Biotite granite (3) – Biotite and hornblende in Archean gneiss, dated 2600 m.y., Key Lake (12b).
1928 (U-Pb)	– Uraninite-monazite/Sophie,		
ca. 1880 (Rb-Sr)	– Feldspathic gneiss,		
ca. 1750 (Rb-Sr)	– Metapelitic Peter River Gneiss, Carswell Structure (1).	1711 (Rb-Sr)	– Biotite in gneiss, Midwest (25).
1930 (U-Pb)	– Uraninite in pegmatite, Beaverlodge area (Koeppel 1968, recalculated at 1860 m.y. by Bell 1981).	1735 (U-Pb)	– Uraninite vein, Way Lake (12c).
1835 (K-Ar)	– Gabbro dike, Beaverlodge area (24c).		
1815 (K-Ar)	– Pegmatite, Gunnar, Beaverlodge area (14)		
1780 (U-Pb)	– Pitchblende veins, Beaverlodge area (Koeppel 1968, recalulated at 1740 m.y. by Bell 1981)		

Table 5.11. *Continued*

Helikian-Hadrynian (<1700 m.y.)			
ca. 1740–>1490	– Deposition of Martin Formation.	? >1500	– Lateritic weathering.
1630 (K-Ar)	– Basalt sill in Martin Formation, Beaverlodge area (24a).	1632 (Rb-Sr)	– Deeply weathered basement (11b).
		1541 (K-Ar)	– Muscovite, highly altered basement, Maurice Bay (18).
		1523 (K-Ar)	– Least altered basement,
		1487 (K-Ar)	– Moderately altered basement, McClean (23).
		? >1500-1300	– Deposition of Athabasca Group.
		1700 (U-Pb)	– Apatite, Northern Alberta (10).
		1550	– Paleomagnetic data, Rumple Lake (11a).
		1513 (Rb-Sr)	– Wolverine Point Fm. (2a).
		1430 (Rb-Sr)	– Wolverine Point Fm. (0).
		1310-900	– Intrusion of diabase dikes.
		1310 (Rb-Sr)	– Diabase dike (0).
		1230 (K-Ar)	– Hornblende, Cree Lake (6).
		1094 (K-Ar)	– Diabase, Midwest (25).
		949 (K-Ar)	– Grab sample, Cluff Lake (24c)
		515-365 (Ar-Ar)	– Cluff Breccias, Carswell Structure (1)

References:

0 Armstrong and Ramaekers 1985
1 Bell 1985
2a Bell and Blenkinsop 1980
2b Bell and Blenkinsop 1982
3 Bell and McDonald 1982
4 Bickford et al. 1986
5 Bostock 1987
6 Burwash et al. 1962
7 Burwash et al. 1985
8 Chiaranzelli and McDonald 1986
9 Clauer et al. 1985
10 Cumming et al. 1987
11a Fahrig et al. 1987
11b Fahrig et al. 1978
12a Hoehndorf et al. 1985b
12b Hoehndorf et al. 1989
12c Hoehndorf and Carl 1987
13a Homeniuk and Clark 1986
13b Krogh and Clark 1987
14 Lowdon 1961
15 Ray and Wanless 1980
17 Sassano et al. 1972
18 Stevens et al. 1982
20 Tremblay et al. 1981
21 van Bremen et al. 1987
22a van Schmus et al. 1986
22b van Schmus et al. 1987
23 Wallis et al. 1986
24a Wanless et al. 1966
24b Wanless et al. 1968
24c Wanless et al. 1979
25 Worden et al. 1981

- Intense paleoweathering reflected by argillitization, chloritization, hematitization, etc. altered the basement to great depth (>50 m).
- Diagenesis of the Athabasca Group affected both the sediments and upper part of the weathered basement by silicification, kaolinitization, chloritization, illitization, bleaching, etc.
- Diagenetic hydrothermal alteration related to the various stages of mineralization and mineral redistribution generated halos of illite/sericite, chlorite, carbonate, sulfide, tourmaline, hematite, kaolinite, phosphate, bitumen/hydrocarbon, quartz dissolution, and often, but not everywhere, destruction of graphite around deposits (Fig. 5.3; for deposit-type related alteration features see next paragraph).
- Diabase dikes and sills affected by this alteration are serpentinized.
- Geochemical processes associated with the hydrothermal alteration include Mg and B metasomatism and/or mobility of Mg, K, Na, Ca, Al, Si, B, CO_2, locally F and P and local to widespread dispersion of trace amounts (few ppm) of metals including U.

Mineralization

Fracture-bound mineralization basement hosted (class 1.1.1) (Fig. 5.4):

- The primary ore control is by structure. Lithology plays a subordinate role in localization of these deposits.
- Mineralization occurs as breccia and fracture fillings partly as massive veins, veinlets, or stringers, and disseminations in adjacent cataclastic wall rocks.
- Preferential direction of mineralized structures fluctuates around NE-SW trending subparallel to the foliation and attitude of the host rocks.
- Host structures consist of a network of subparallel and anastomosing fractures often located in the hanging wall of major reverse and thrust fault zones.
- Position is at or adjacent to old, regional mylonite zones of supposedly Hudsonian origin that were reactivated in Athabasca time.
- Bulk of the ore is mainly within about 150 m below the Meso-Helikian unconformity (Rabbit Lake, Claude, Dominique-Peter) but can extend to a depth in excess of 400 m (Eagle Point).
- Lithologically and stratigraphically, the deposits in the eastern Athabasca Basin occur preferentially in Aphebian metasediments, but are apparently not restricted to particular rock facies or specific stratigraphic levels except for an overall association with graphitic horizons. The relationship of graphite to mineralization tends to be more spatial, since U minerals mostly occur along the margins of graphitic units and not within them.
- Deposits in the Carswell Structure district are positioned at or proximal above the Archean (?) Earl River Complex and Aphebian Peter River Gneiss contact (Aphebian unconformity ?). This contact correlates with the boundary of the anatexis that affected the Earl River Complex. A major mylonite zone follows the contact on the NE flank of the Dominique dome and apparently controls the location of several deposits (Tona et al. 1985).
- Host rock environments are marked by late Hudsonian (?) Na-metasomatism (albitization), Mg-metasomatism (dolomitization at Rabbit Lake), migmatization, and pegmatite and granite intrusions or segregations.
- Deposits are enveloped in a conspicuous alteration aureole characterized by moderately to strong decomposition of plagioclase, cordierite, sillimanite, ferromagnesian minerals, ilmenite, magnetite, and corrosion of quartz and replacement of these minerals by, or authigenic deposition of illite, chlorite, and locally mixed-layer clays of distinct crystal-chemistry, dravite, carbonate, quartz, sulfide, hematite, and locally kaolinite.
- The dimension of the ore-related alteration halo is variable but mostly narrow (at Eagle North restricted to within a few meters of mineralized structure systems, at Eagle South somewhat larger, supposedly due to more pervasive cataclasis).
- Phyllosilicate minerals may be zonally arranged. At Eagle Point (Fischer in Eldorado Resources 1986), magnesian chlorite (Mg/Fe ratio 7 to 20) apparently prevails in the upper 75 m below bedrock surface, whereas MgFe-chlorites (Mg/Fe ratio ca. 1) dominate further into depth. The highest grade sections of ore shoots contain predominantly illite with minor or no chlorite. Lower grade mineralization is associated with chlorite in comparable proportions with illite. In deposits of the Carswell deposits (Pagel and Svab 1985), peraluminous chlorites dominate over Al-Mg-chlorites within mineralization whereas marginal to these ore zones Al-Mg-chlorites prevail. The illite/sericite phases display a similar pattern.
- Later alteration or authigenic phases (dravite etc.) occur preferentially peripheral to mineralization.
- U is the dominant ore element. Associated elements are Pb and Fe, minor amounts of Cu, Mo and V, and traces of Ni, Co, etc. (Fig. 5.8, Table 5.6).
- Ore and associated minerals are present in several generations, including an early stage of mineral introduction and at least two stages of redistribution.
- The first stage of mineralization in the eastern Athabasca region is essentially a monometallic uranium-sulfide assemblage containing uraninite/pitchblende (Table 5.9) dated between ca. 1400 and 1300 m.y. A second stage of pitchblende is dated between ca. 1100 to 900 m.y.
- Deposits in the Carswell Structure are slightly different displaying a primary uraninite-selenide-sulfide stage followed by a uraninite-sulfide assemblage (Ruhlmann 1985).
- Subsequent rejuvenation episodes modified the earlier generations, at least between 300 and 100 m.y. ago.

Clay-bound mineralization topping unconformity (class 1.1.2) (Figs. 5.3 and 5.5 to 5.7):

- Ore controls are by lithology and structure.
- The bulk of the ore occurs in an elongated core of high grade pods, pockets, aggregates, and veins enveloped in lower grade material straddling the Meso-Helikian unconformity.
- Stringers, veinlets, and disseminations of mineralization penetrate from the high grade core along cataclastic/permeable zones upward into sandstones and downward into basement commonly for not more than ca. 30 m. Locally, low grade appendices may persist for ca. 150 m into the basement and upward into the sandstone for up to 200 m.
- Some mineralization can occur as perched pockets in the sandstone along fractures above deposits.
- The boundary between high grade ore and low grade mineralization or wall rock respectively is generally abrupt.
- The high grade core zone is often located at basement ridges that range from a few to as much as 30 m high (Cigar Lake). These are particularly prominent in the western part of the East Athabasca district (Cigar Lake, Midwest, McClean), whereas at other deposits they are presumably masked by later deformation (Key Lake).
- Host to the mineralization is soft or indurated silty or sandy clay/mudstone grading outwards into argillic sand of pre- or early Athabasca age.

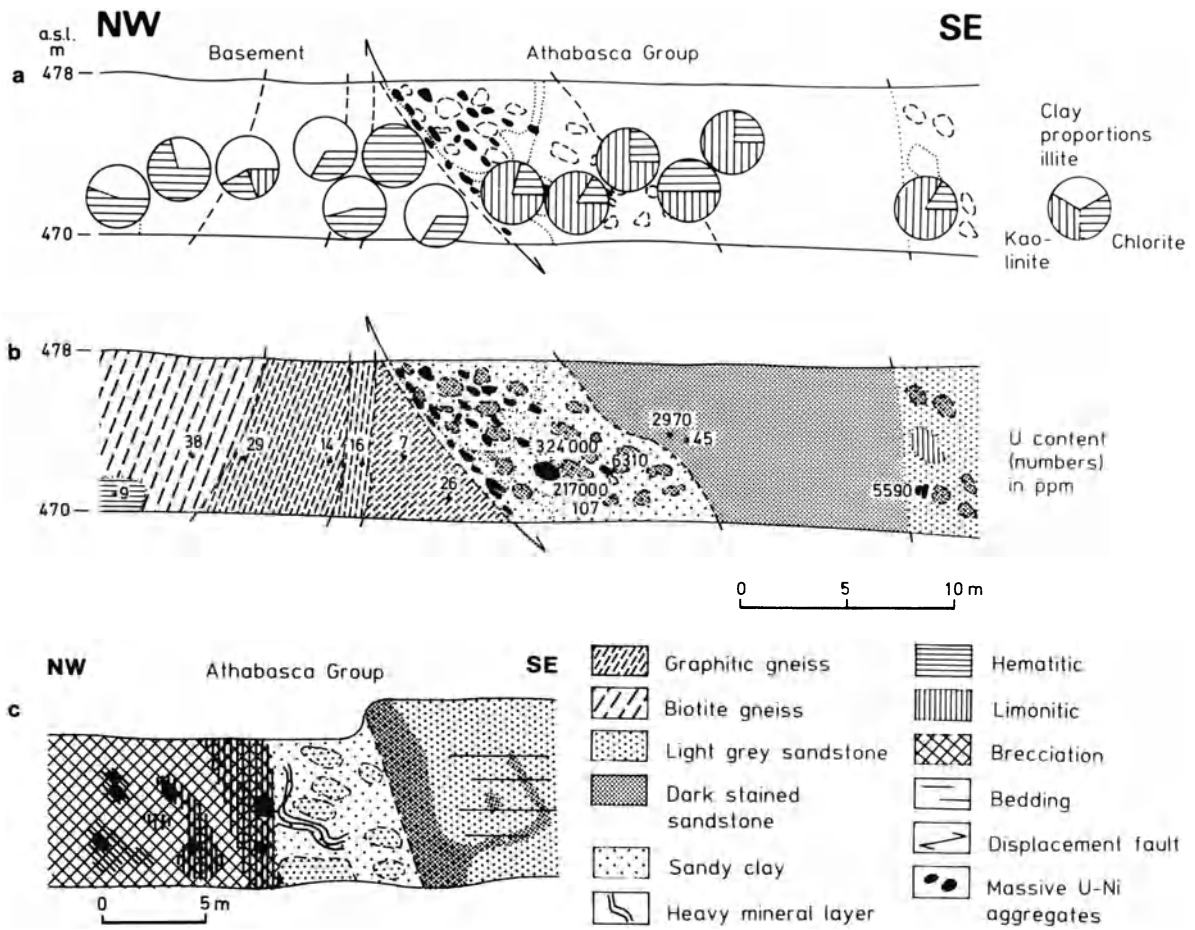

Fig. 5.10. Key Lake, Gaertner ore body, Face 470–6 (**a** and **b**) and 478–5 (**c**). **a** Distribution and proportions of alteration clay minerals displaying kaolinite-chlorite dominance in the downthrown southeastern sandstone block and illite-chlorite dominance in the uplifted basement block. **b** Lithology and distribution of U-Ni mineralization showing marked concentration of high-grade massive U-Ni aggregates embedded within clay matrix which also contains low-grade mineralized sandstone fragments in a narrow zone within the downthrown block. **c** Character of clay alteration in sandstone in the south-eastern part of the mineralized zone. Rounded sandstone fragments and distorted heavy mineral layers occur within the highly altered sandy clay zone. The adjacent north-westerly part is brecciated and locally limonitized. The deformation postdated the alteration. (After Ruhrmann 1986) (for index Fig. 5.1.1)

- Host sediments from the Carswell Structure are reported to include mudstones and siltstones that contain volcanic components and apparently have been deposited in scours or depressions incised into the basement (Pacqet and Namara 1985).
- Mineralized Athabasca sandstone can be dark gray to black mainly caused by sulfides and some carbonaceous material (Key Lake, north of Main Zone of Midwest Lake, Cigar Lake), or multicolored, ranging from dark green to brown and buff with shades of pink, gray and white (Collins Bay B, Main Zone at Midwest, McClean North Zone, Maurice Bay) (Tremblay 1982).
- Host material can consist of as much as 70% clay composed of illite/sericite and chlorite as matrix to corroded quartz grains and rounded sandstone fragments. Ratios of the phyllosilicates can be highly variable, as shown in Figs. 5.7 and 5.10.
- The phyllosilicates may display chemical zonation. In deposits of the Carswell Structure, Al-chlorite is dominant in the high grade and MgAl-chlorite occurs at the margins of the mineralization (Pagel and Svab 1985). At Cigar Lake Fe-bearing phyllosilicates prevail in high grade mineralization (see below).
- Carbon buttons (bitumen etc.), later tourmaline (dravite), carbonates, quartz, hematite,

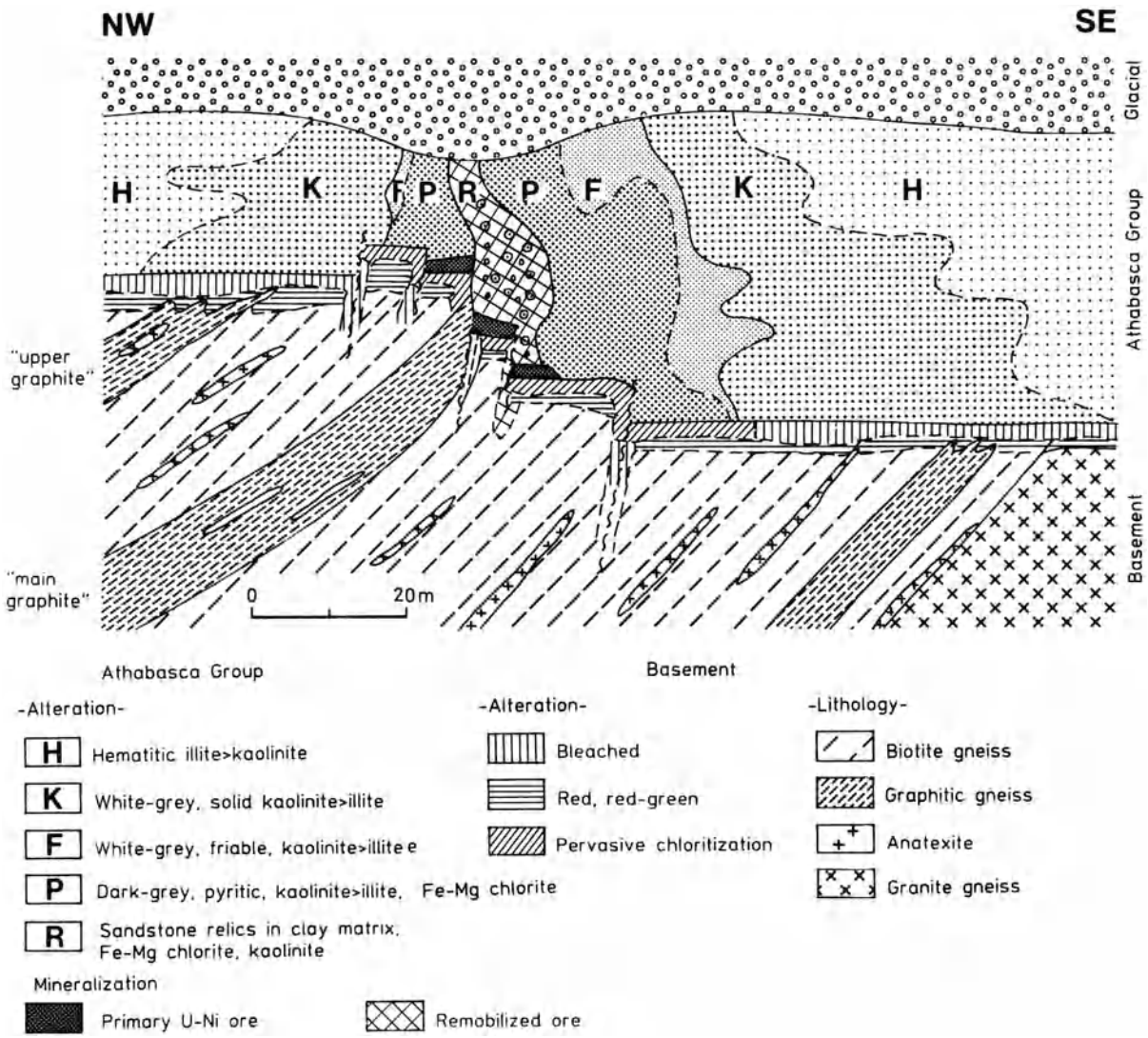

Fig. 5.11. Key Lake, Gaertner ore body, NW-SE section with schematic presentation of alteration zones and distribution of primary and remobilized U-Ni mineralization (see also Table 5.12). (After Ruhrmann 1986)

Table 5.12. Key Lake, Gaertner ore body, zonation and extension of alteration features in the Athabasca Group at a level of approximately 10 m above the unconformity (see also Fig. 5.11). (Ruhrmann 1986)

Alteration feature	Zone with hematite relicts (more than 80 m from ore)	Friable zone (ca. 40 m from ore)	Pyrite-carbonate zone (less than 40 m from ore)	Sandstone relicts in mineralized zone
Quartz overgrowth	•	•	•	•
Hematite	•			
Illite > (kaolinite and chlorite)	•			
Illite < (kaolinite and chlorite)		•	•	•
Kaolinite corroding quartz			•	•
Strong chloritization			•	•
Dravite corrodes quartz and impregnates kaolinite matrix	Rare		•	•
Microbrecciation	Rare	•		
Pyrite			•	•
Carbonates replace kaolinite, quartz and dravite		Rare	•	•
Hematite on siderite and Fe-hydroxides in pores		Rare	•	•
Illite replaces kaolinite and dravite				•
Uranium (ppm)	1 ppm (>10 rare)	3–15 ppm	5–5000 ppm	86–3000 ppm

and other alteration products are present in varying amounts, filling veinlets and as impregnations.

- Late kaolinitization overprinted locally the earlier clay assemblage (Key Lake, Ruhrmann 1986; Candy Lake Pod at McClean, Wallis et al. 1986) (Figs. 5.7, 5.10, 5.11).
- The alteration halo around deposits extends for several kilometers along strike of mineralized structures and laterally and vertically for tens to hundreds of meters distant within the Athabasca Group (500 m wide and 200 m high at Cigar Lake and Midwest). In the basement the alteration halo is less extensive (ca. 100 m deep at Cigar Lake).
- The geometry of an alteration halo exhibits in a generalized mode a zonation as shown for Key Lake in Fig. 5.11 and Table 5.12 and a dispersion pattern as documented for the Cigar Lake deposit (Fouques et al. 1986) as follows (from top to bottom):

Athabasca Sediments

- Gray altered zone: gray coloration of the normally pink to white sandstone due to reduction of ferric iron and formation of finely dispersed Fe-sulfides associated with dissolution of the siliceous matrix and simultaneous increase in clay content.
- Quartz zone: irregular, diffuse silicification and lining of fractures lined with euhedral quartz.
- Clay altered zone: increase in clay content of up to 30% of the rock, friabilization of sandstone resulting locally in loose sand.
- Massive clay zone at the unconformity that surrounds the main zone of mineralization: three distinct illitic facies are discerned, (a) soft gray to white clay dominantly composed of Mg-illite locally associated with siderite, (b) soft gray clay consisting of FeMg-illite and chlorite, and (c) indurated dark green clay composed of Fe-rich illite, FeMg-chlorite and Fe-rich kaolinite with siderite. Facies (c) forms the core and is surrounded by facies (a) and (b).

Crystalline Basement

- Massive clay zone (unconformity clay): gray-greenish MgAl-chlorite (sudoite) and Mg-illite, locally abundant calcite, siderite, and globules of organic material, occasionally dravite and phosphate (goyazite). All metamorphic textures have been destroyed.
- Altered basement with rock textures preserved: decrease of alteration with depth; near unconformity intense argillitization with illite/sericite-chlorite, destruction of graphite

within the upper few meters below the unconformity, widespread corrosion of quartz, zircon, and monazite. From 50 to 100 m below the unconformity the alteration is mainly reflected by more or less sericitization/illitization of feldspars and other amenable rock constituents.
- Basement immediately below the deposits consists essentially of Aphebian metasediments containing graphitic intercalations but other than that no preference to specific lithologic facies or particular stratigraphic levels is obvious.
- Most deposits are positioned above or near, and trend parallel to the intersection of a prominent basement fault, often a reverse fault, with the Meso-Helikian unconformity.
- These faults apparently follow ancient (Hudsonian?) mylonite zones.
- Orientation of the main structures vary around NE-SW.
- Oblique faults dissect and displace the main structures.
- Major ore bodies are cigar-shaped (Cigar Lake, Key Lake) elongated along NE-SW structures. Other deposits occur in similar shapes or form pods aligned along such structures (McClean, Dawn Lake).
- Mineralization is polymetallic and may include U, Ni, Co, Cu, Pb, Zn, Fe, Mn, Mo, Bi, Sb, V, As, Te, Se, Au, Ag, and Pt-group elements in varying but mostly subeconomic amounts. Some elements, notably Ni, Pb, and As are locally as abundant as U as at Key Lake. Co and Ni is frequent at Midwest, Ni, Pb, Ag, and Au in the Collins Bay A and D zones, Ni, Co, Pb, and Mo in Cigar Lake and Au, Te, Se in the D ore body, Carswell Structure (all except the precious metals in the range of permille to a few percent) (Fig. 5.8, Table 5.7).
- Uranium and associated minerals are present in several paragenetic assemblages including two early stages of mineral introduction and at least two more stages of redistribution (Tables 5.4, 5.5).
- The first stage is essentially a monometallic uranium-sulfide assemblage containing uraninite/pitchblende dated between 1400 and 1250 m.y. (ca. 1150 m.y. in Carswell Structure).
- The second stage is polymetallic. In the eastern Athabasca region, mineralization is composed of arsenides, sulfarsenides, and sulfides of various metals but dominated by Ni associated with pitchblende and/or coffinite. Deposits in the Carswell Structure contain in addition to the mineral assemblages of the East Athabasca district Te, Se, Bi, and some Au and Ag. This second stage supposedly formed between about 1250 and 900 m.y. ago.
- Episodes of rejuvenation between ca. 300 and 100 m.y. ago modified the earlier generations and redistributed metallic elements along cataclastic zones into Athabasca arenites.

Metallogenetic Concepts

Previous Models

Debate on the origin, nature, and channelways of metalliferous solutions, concentration processes, and their respective importance for the huge metal concentration in the Athabasca unconformity-contact deposits has ranged from supergene concepts to hypogene considerations. Three principal models have been forwarded for the initial U introduction and the formation of the mineralization

- diagenetic hydrothermal,
- hypogene hydrothermal, and
- supergene with diagenetic overprint.

Diagenetic hydrothermal model: The evidence supporting this model is the significant host rock alterations surrounding deposits that are considered to have been derived from solutions within the Athabasca Group based on fluid inclusions and stable isotope data. The salient components of this model are late diagenetic processes that have generated circulation of at least two fluids. One fluid was oxygenated, saline, and carried metalliferous ions, and migrated at the base of the Athabasca Group. The other fluid was reducing and ascended along fault zones from the basement. Precipitation of mineralization occurred where these two solutions interacted at the Meso-Helikian unconformity.

Pagel (1975) and Pagel and Jaffrezic (1977), based on fluid inclusion studies of gangue and associated minerals from Rabbit Lake and Carswell Structure deposits, assign to particular diagenetic solutions heated to temperatures of about 200°C the major role of deposit formation. These authors consider the basement rocks to be the uranium source. Pagel et al. (1980) propose a polyphase evolution for the mineralizing pro-

cesses. During an interim stage uranium must have been mobilized by pedogenic processes and part of it was trapped in organic matter in lagoons enriched in evaporitic elements (Mg, B, and Li). Subsequent diagenetic hydrothermal processes produced the deposits, deriving the uranium either from the lagoonal sediments or directly from the basement. Hoeve and Sibbald (1978) and Hoeve et al. (1980), based on their work at Rabbit Lake and basin-wide studies of alteration features, also propose a diagenetic hydrothermal model but they consider the Athabasca Group to be the principal source of metals (see discussion further below).

Hypogene hydrothermal model: Little (1974), Morton (1977), Kirchner et al. (1980), and more recently von Pechmann (1985) advocate a hypogene (magmatic or metamorphic ?) hydrothermal hypothesis. Von Pechmann (1985), based on his extensive mineralogical studies of the Key Lake deposit, argues that ore mineralogy, associated gangue minerals, and their intergrowth are identical to those of classical hypogene hydrothermal U-Co-Ni-Ag-Bi vein deposits, that the gangue in the deposits consists of true gangue minerals, and that the temperature of ore formation is relatively high. Consequently von Pechmann (1985) proposes that hydrothermal fluids produced the intense alteration supposedly during a period of cataclasis. Ore-forming elements were introduced by hypogene fluids at the time of alteration with deposition of collomorphous botryoidal pitchblende followed by Ni-arsenides and perhaps Ni-sulfarsenides. About 1400 to 1250 m.y. ago the original U-oxide phase recrystallized to uraninite and Ni was redistributed or perhaps introduced at this stage in response to either elevated temperatures due to the thick pile of Athabasca sediments or intrusion of diabase. Later events caused modification and redistribution of the original ore minerals.

The major shortcoming of a hypogene model is the lack of any magmatic or regional metamorphic event to provide a source of metals and generation of hypogene hydrothermal fluids at the time of suspected original ore emplacement. Diabase intrusions may constitute a driving power, but cannot be considered a source of uranium.

Supergene model: Knipping (1974), Langford (1977), Dahlkamp (1978, 1982), and Dahlkamp and Adams (1981) among others consider surficial processes during the pre-Athabasca weathering period to be a major impetus in the formation of mineralization. Dahlkamp assumes a multi-stage metallogenetic evolution starting with synsedimentary U accumulation in Aphebian time, succeeded by remobilization with local upgrading during the Hudsonian Orogeny, followed by supergene processes as a prominent interim stage in metal collection either to protore or ore grade. Certain diagenetic events subsequently remobilized and presumably further concentrated and finally recrystallized the early mineral assemblage to the now present primary uraninite/pitchblende generation. Critical parameters of a supergene model are (a) the presence of metasediments containing anomalous amounts of not refractory bound U and other metals, (b) a climate changing from subtropical to arid, as reflected by lateritic weathering profiles and transgressive red bed sequences, (c) liberation by weathering of leachable fractions of U, Ni, etc. and (d) collection, at least part thereof in surface depressions filled with argillaceous, evaporitic sediments or in near-surface structures perhaps comparable to surficial duricrust deposits such as Yeelirrie, Australia, and surficial structure fills such as Daybreak, USA, respectively. The principal problem with the supergene concept is the practically impossible proof for a pre-Athabasca preconcentration of U, Ni, and other metals. Only conditional evidence by analogy with presently known surficial deposits such as Yeelirrie, Australia, and the apparent lack of unconformity-contact deposits, elsewhere in the world in areas of geology similar to the Athabasca Basin region but devoid of lateritic paleoweathering of the basement can support a supergene hypothesis. The later overprint by diagenetic or other processes related to the Athabasca Group has masked all earlier signatures of paleo-surficial mineralization in the Athabasca region. In addition, the apparent radiometric ages of ore formation (1400 to 1250 m.y.) which post-date the Athabasca Group (ca. 1500 m.y.) can also be taken as an argument apparently contradicting a supergene pre-Athabasca metallogenetic event.

Proposed Model for a Polyphase Evolution of Unconformity-contact Uranium Deposits

Interpretation and synthesis of pertinent data leads to a state-of-the-art metallogenetic concept. This concept includes a complex, *polyphase evolution* of the geologic environment and its

uranium and metal endowment which ultimately culminated in the formation of unconformity-contact deposits in the Athabasca Basin region. A condensed version of the model with the principal uncertainties, ambiguities and remaining problems is discussed below. Critical factors that constrain such modelling include:

- source of uranium and associated metals;
- interim stages involved in mineralization;
- source, chemistry and redox potential of solutions for liberation and transport of U;
- conditions for precipitation of U;
- cause for restriction of deposits
  - to the Meso-Helikian unconformity;
  - to the intersection of basement faults/mylonite zones with the unconformity;
  - to selected sites at these structural features;
  - with respect to the clay-bound deposits their intimate association with argillaceous material topping the unconformity;
- source and/or nature of reducing agents or solutions;
- channelways for metalliferous fluids;
- energy resources for generating circulation of fluids involved in mineralizing processes;
- origin of the argillaceous mass hosting the clay-bound deposits;
- importance of evaporitic sediments and their constituents particularly K, Mg, B and Li;
- role of metasomatism of Na (albitization), Mg (dolomitization and phyllosilicate modification) and B (tourmalinization);
- role of paleoweathering;
- interrelationship of diagenetic, specific alteration and mineralization processes.

Uranium Mobilization During Aphebian Sedimentation and Metamorphism

Certain Archean granites in Northern Saskatchewan contain elevated U contents. It is postulated that in Middle to Upper Aphebian time part of this U was leached and redeposited in pelitic to psammitic sediments which now constitute the Wollaston Group.

Metamorphism of the Aphebian strata perhaps during the Blezardian but definitely during the Hudsonian Orogeny recrystallized and locally further concentrated the sedimentary uranium. Disseminations and narrow stringers of uraninite oriented more or less parallel to the bedding/schistosity of the metasediments, reflect this heritage. Anatexis or granitization concentrated uraninite and monazite aggregates in certain pegmatitic and granitic intrusions or segregations. (see section Potential Sources of Uranium).

Where late to post-orogenic cataclastic ground preparation opened pathways uranium and other metals may have been mobilized and expelled along with hydrothermal volatile fluids to form epimetamorphic veinlike deposits of the Beaverlodge type (see Subtype 2.2, Chap. 4 and next paragraph) which now may constitute the roots of the fracture-bound class of unconformity-contact type deposits as, for example, Eagle Point.

The Hudsonian event possibly ended in the formation of extensive, locally in excess of 50 m wide *mylonite zones*. Because many Athabasca deposits are located at or near these mylonites, it is speculated that the mylonite zones may have acted as channelways for metalliferous fluids or even as a preconcentration trap for uranium mobilized by retrograde metamorphic processes.

Pre-Athabasca Weathering and Surficial Preconcentration of Uranium

During Paleo- to Meso-Helikian time, approx. 1700 to 1500 m.y. ago, an extensive period of weathering and erosion affected the crystalline basement. During this period the region was located between latitudes 20° and 25°N (Fahrig and Jones 1969, Seyfert and Sirkin 1973) suggesting a semitropical climate. An extensive chemical weathering profile of lateritic nature more than 50 m deep in solid rocks and as much as 150 m along faults was imposed on the rocks as indicated by the present regolithic profile. Uranium and other metals must have been mobilized during this episode. Although the bulk of the liberated uranium was flushed into the sea, some of the uranium was probably caught and concentrated in pedogenic material or in cataclastic zones similar to that in present day surficial uranium occurrences (see Chap. 4.6). This concentration could have occurred particularly during the final stage of this episode when the climate changed to more arid conditions.

Such *pedogenic preconcentrations* of uranium are reported by Tremblay (1982). He analysed uranium concentrations ranging from close to zero to 0.05% U (average 0.033% U) in brown to red regolithic clay but noted that it is unknown how much of this uranium precipitated with the

regolith and how much was later. Similar anomalous U, Ni, Co, As etc. concentrations have been drill intersected in clayey material atop the unconformity in other properties distant from deposits. (E. Stewart, pers. commun.)

The common association of U with Ni and the often high grades of Ni in the clay-bound deposits poses the question for *Ni preconcentrations* by the existing Meso-Helikian climatic conditions. Circumstantial evidence for this is provided by the garnierite mineralization in New Caledonia where a subtropical climate like that postulated for the pre-Athabasca time in Saskatchewan has formed extensive supergene nickel deposits. This indicates that similar processes could also have been active during the paleo-weathering period in northern Saskatchewan.

Although circumstantial evidences suggest a surficial preconcentration of uranium and possibly nickel during the pre-Athabasca paleo-weathering period it remains uncertain whether such an interim stage is required in the metallogenesis of unconformity-contact deposits. Again, circumstantial considerations suggest their necessity, because elsewhere in the world, important unconformity-contact type deposits have not been discovered in terranes of comparable geology which are devoid of the regolithization typical for the Athabasca region.

Diagenesis and Related Ore Forming Processes in Meso-Helikian Time

During Meso-Helikian time, approx. 1500–1300 m.y. ago, the climate changed to a more arid one. Continental, arenaceous *red bed sediments* of the Athabasca Group were deposited on this surface. In some areas, for example in the Carswell Structure, an argillaceous facies, up to 50 m thick, of pre- or early Athabasca age was laid down in small, local depressions (Pacquet and McNamara 1985).

Uranium content is very low in Athabasca sandstones in the order of 1 ppm U, and that appears to be contained largely in refractory heavy minerals. (Earle and Sopuck 1987, report for the eastern Athabasca Basin an average of 0.37 ppm U determined by partial extraction = fluorimetry following HNO_3/HCl extraction). Accordingly, the Athabasca sandstones are rejected as a potential source of uranium.

Two principal alteration systems affected the Athabasca Group, between approx. 1500 to 900 m.y. ago, an early stage of true diagenesis succeeded by a later stage of hydrothermal activity. The latter coincided with the main mineralizing event. The two alteration systems involve oscillating oxydizing and reducing processes active in the Athabasca Group and in the crystalline basement along the unconformity. Both systems may have been interconnected.

a) Early diagenetic stage: Distinct clay mineral assemblages in each formation indicate that the flow of diagenetic solutions was confined to the various formations. Temperatures reached between 200–250°C at the base of the Athabasca Group. Physico-chemical conditions were oxydizing, as reflected by widespread specular hematite. Fluid inclusions diagnose brines as fluids responsible for the diagenetic alteration (Pagel 1975a, 1975b).

Fluids of this physico-chemical nature are capable of liberating uranium from uraninite or from other leachable positions in host minerals (U adsorbed on clays, etc.). As such, these early diagenetic solutions or descendants thereof may constitute a salient prerequisite for ore formation.

b) Hydrothermal event and associated main stage of ore formation (approx. >1400 to 1100 m.y.): Concurrent geological events that characterize this episode are brittle deformatiom, hydrothermal alteration, intrusion of diabase dikes (after ca. 1300 m.y.), and the main stage of mineralization.

Important *channelways* for the solutions responsible for alteration and mineralization were extensive fault zones in the basement and permeable arenite beds, in particular the locally present basal conglomeratic unit of the Athabasca Group. Other migration paths proposed are either the unconformity-regolith interface or paleotopographic features such as scours or depressions incised into the basement along fault zones.

Strong development of Mg- and Al-chlorites and illites, and Mg-tourmaline within and around mineralization attests to intense *hydrothermal activity* by Mg-, Al-, and B-bearing solutions. Stable isotope and fluid inclusion data (see section Stable Isotopes and Fluid Inclusions) suggest involvement of several fluids of varying composition. One fluid was a very saline but not always saturated brine (30% NaCl equiv.) of oxidizing nature, as indicated by hematite platelets in the inclusions (Pagel et al. 1980).

Evidence for circulation of reducing fluids is provided by destruction of hematite, bleaching, and sulfidization in the Athabasca Group. Consequently a reducing front must have invaded an otherwise oxygenated environment.

Mellinger et al. (1987) address the physico-chemical environment that prevailed during phyllosilicate alteration in the eastern Athabasca Basin. They noticed that the geochemical signature of this alteration is very similar at all unconformity deposits. Illitization is always observed. A chlorite trend occurs at Midwest, McClean and Dawn Lake. This indicates that illite or chlorite were stable during uranium mineralization which attests to a pronounced activity of K- and/or Mg-ions in the solutions. The solutions must also have contained CO_2 because siderite is a common constituent in the alteration suite. Ferrous iron was available from decomposition of hematite.

A later overprint of this alteration facies by chlorite is noticed at Maurice Bay (Mellinger et al. 1987) and by kaolinite at Key Lake (Ruhrmann 1986) and in the Candy Lake Pod at McClean (Wallis et al. 1986).

The above criteria and processes are consistent with the physico-chemical conditions required for uranium mobilization and redeposition within the given environment. Because the phyllosilicate alteration initially resulted from oxidizing solutions, as indicated by Pagel's work, it must have started prior to ore formation. On the other hand, these fluids were capable of leaching uranium from any accessible source.

Two alternatives for possible *uranium collection by fluids* residing in Athabasca sediments proximal to the unconformity can be contemplated. Uranium was either already collected by solutions during the early diagenetic stage when the environment was clearly oxygenated, as mentioned earlier, or accumulated at the onset of the later hydrothermal stage. Constraints on both scenarios are as follows.

Scenario 1: Access of fluids to a uranium source in the basement is thought to have been very limited due to insufficient structural pathways. Therefore solutions could collect uranium only from sites near the unconformity, i.e., essentially from uraniferous regolith. This conclusion is based on the assumption that relative stable tectonic conditions prevailed during this period and that therefore access to permeable structures required for water percolation in the basement was limited.

Scenario 2: With the change of this situation which occurred just before and at the time of the intrusion of diabase dikes, a prerequisite for the second scenario was accomplished. Structural preparation of the basement provided access for enough oxygenated fluids to buffer the reducing effect of the basement lithologies and to maintain sufficient oxidation potential to leach uranium from these lithologies.

Potential basement uranium sources could have been uraniferous rock constituents, for example synmetamorphic strata-bound uraninite, U-enriched mylonite zones, anatectic-pegmatitic mineralizations, and Beaverlodge type pitchblende veins. Uraniferous regolith could have also been a good complementary source of uranium.

In the case of an antecedant surficial deposit, as assumed in a supergene model, this deposit would have been largely destroyed by highly oxygenated fluids, but not if the fluids had an oxidation potential below the destruction level. In this case, modification of all pre-existing uranium mineralizations independent of type (surficial or basement hosted veins) was probably restricted to localized remobilization, disequilibration and recrystallization of the original uranium associated with a resetting of the U-Pb time clock.

The next step in the mineral accumulation requires a *reducing media* to reduce the hexavalent uranium for precipitation of pitchblende. Again, two scenarios and perhaps a third one can be envisaged. The first two are based on reductants provided from the basement and the third on postulated organic material contained in localized pre- or early Athabasca lacustrine (?) sediments. Basement reductants were very likely sulfides, as can be deduced from sulfur isotope ratios which are identical in both basement sulfides and ore assemblages (Wallis et al. 1986).

Although often proposed, graphite does not tend to be a valid reductant. Thermodynamic considerations prohibit a direct involvement. Destruction of graphite to form bitumen or other hydrocarbons which constitute effective reductants apparently post-dated the mineralization according to Landais and Dereppe (1985) (see later). The importance of graphite is most obviously on the structural side. Graphitic horizons provided the least competent rocks for structural stress hence becoming the site for faulting. The three possibilities of reducing agents and their impact on uranium precipitation are:

a) Reduction by fixed host rock constituents (mainly sulfides): Uraniferous fluids must have percolated along permeable structures below the sulfide-depleted regolithic section of the basement to interact with reductants such as sulfides. A mechanism like this cannot account for the formation of clay-bound deposits positioned at the unconformity. But it may at least theoretically explain the generation of fracture-bound deposits of class 1.1.1. A reason has to be found, however, for restriction of these deposits to a few sites when it has to be assumed that formation of the deposit should have taken place wherever adequate reducing conditions were provided by host lithologies unless such conditions were limited to the sites of presently known deposits, which is very unlikely.

b) Reduction by reducing solutions: Solutions of reducing capacity could have evolved from either connate basement waters or from Athabasca waters invading reducing basement environments. In the latter case the solutions should not have been enriched in uranium, because the uranium would have already precipitated in the basement, as discussed earlier. Whatever the origin of the reducing fluids may have been, position, configuration and mineral paragenesis of the clay-bound deposits straddling the pre-Athabasca unconformity demand solutions either and most likely, upwelling along fault zones from the basement, or migrating along channel-like morphologies/features at the unconformity. Only under these preconditions could the solutions arrive at the given sites to interact with uraniferous fluids. The uraniferous fluids were either stagnant in basal Athabasca arenite beds, or more probably, were migrating along the intersection of the unconformity with the structures from where reducing solutions were expelled.

c) Reduction by sediment hosted organics: A final possibility for a reductant is provided by organic matter that may have originated from algae formed in small lagoons, ponds, etc. which contained evaporitic and argillaceous sediments presumably derived from lateritic outwash material of the Meso-Helikian pediment. Sediments of this nature are reported, for example, from the Carswell Structure (Pagel et al. 1980, Lainé 1986).

Such an origin of the organic matter found in the argillaceous sediments is rejected by Landais and Dereppe (1985). They consider the bitumens found at the deposits to be derivative of graphite from the underlying basement. Perhaps new support for a nongraphitic origin has emerged from Leventhal et al. (1987). These authors report an "unusual uranium-organic matter association" in the Claude deposit, Carswell district, which encloses fragments of U minerals that crystallized prior to their incorporation in the organic material. The authors reject graphite as a source.

In summary, the above listed geochemical and mineralogical criteria combined with contemporaneous regional geological events may have contributed to the *evolution of the deposits* as follows.

A regional thermal/tectonic episode initiated perhaps by broad epeirogenic uplift partially coincident with the Grenville Orogeny coupled with late low-grade burial metamorphism/alteration in the basement and/or diagenesis in the Athabasca strata were fundamental for generating the processes for the formation of the deposits as we know them to day. Steepening of the geothermal gradient by regional intrusion of diabase dikes (Hoeve and Sibbald 1978) or, alternatively, by radiogenic heat generated from concentration of uranium in the basement (Fehn et al. 1978, Tilsley 1980), may have induced a large-scale convection of diagenetic pore solutions within the overlying Athabasca sediments and to some extent in the basement. Significant K- and Mg-ion activity and oxidation potential characterized these solutions. The elements in these solutions are assumed to have been derived from decomposition of evaporites at the base or within the Athabasca Group. Concurrent tectonism due to isostatic readjustment in response to successive periodic uplifting gave rise to thrust faulting and reactivation of old shear and mylonite zones which may have contained preconcentrations of uranium. This faulting increased secondary permeability and, consequently, allowed the oxygenated diagenetic solutions access to a number of sources of uranium and other metals in basement and regolith.

The crucial criterion for the next step of deposit formation is the oscillation of groundwaters between oxidizing and reducing conditions along the unconformity. During an initial stage when the solutions were sufficiently oxygenated, they leached and collected uranium, as mentioned above. Due to convective circulation these uraniferous solutions ascended, at least partially to the unconformity and into basal permeable

Athabasca beds forming a reservoir of uranium in solution. During the course of this process the oxidation potential of later invading fluids diminished by reaction with basement reductants and finally turned into reducing. It is debatable whether the solutions achieved their reducing nature in the basement level of previously uranium leached rocks due to renewed cataclasis permitting access to virgin ground, or at specific sites of significant enrichments of reductants such as sulfides, or by reaction with organic material in lacustrine sediments resting locally on the unconformity, or a combination of the one with the other.

In a scenario for the formation of *clay-bound deposits* where the reducing fluids originated in the basement and then migrated upward along fault zones to the unconformity, these fluids generated a redox front at the interface with the postulated oxygenated uranium-bearing fluids residing in basal Athabasca beds. Under these conditions, uranium should have been reduced and pitchblende precipitated along this redox interface at the intersection of the cataclastic channelway and the unconformity. In such a model, the ore-hosting clay masses may have derived from fault gouge sqeezed out at the unconformity. Such a clay origin poses a problem, however. Gouge normally seals fracture zones and hence would prohibit the postulated migration of the reducing fluids.

Under the assumption that lacustrine sediments containing organic material existed, precipitation of pitchblende took place where ascending or laterally migrating uraniferous solutions invaded these environments. Such a reducing matter combined with the adsorptive capability of the clays provided a highly favorable trap to capture and fix the uranium. This could explain the restriction of the clay-bound class of deposits to the argillaceous host rocks at the unconformity, and at the same time the origin of the clay masses without the negative impact of gouge derived clays.

With respect to the formation of the *fracture-bound deposits* which occur in the basement proximal to but below the unconformity, two scenarios of uranium precipitation can be envisioned. The same processes may have been active, as discussed earlier, but due to a lack of argillaceous beds topping the unconformity, the basement structures provided the only suitable site of uranium deposition. Or alternatively, if it is assumed that these deposits derived from deeper-seated Beaverlodge-type veins, the fluids involved caused only local remobilization and redistribution of the uranium along these fractures.

Fluid inclusion studies suggest that the *original mineral formation* of unconformity-contact deposits took place at temperatures of about 200°C. Stable isotope dating of phyllosilicates related to mineral accumulation yields ages of about 1400 to 1100 m.y. These ages concur with U-Pb ages of the oldest identifiable pitchblende/uraninite generation in all multimetallic clay-bound deposits in the Athabasca Basin.

Although the multimetallic mineral assemblage and associated phyllosilicates in clay-bound deposits tend to have formed by the same processes as proposed by Pagel et al. (1985), precipitation of uranium and other metals did not occur simultaneously as documented by Ruhrmann and von Pechmann (1987) for the Key Lake mineralization, and by Fouques et al. (1986) for Cigar Lake. Ruhrmann and von Pechmann (1987) note that the oldest pitchblende/uraninite generation formed at about 1255 m.y. ago (corrected to ca. 1400 m.y. by Carl et al. 1988), whereas the introduction of arsenides and sulfoarsenides occurred at about 900 m.y. ago.

Pagel et al. (1985) also report another episode at about 900 m.y. ago which introduced a multimetallic mineral assemblage different to the preceding one, and the formation of a distinct Mg-tourmaline. The nature and origin of the fluids involved in this second stage of mineralization remain open to debate. But in any case, they must have been of reducing character because otherwise they would have destroyed the older uranium ore.

Redistribution of Uranium in Hadrynian to Recent Time

Subsequent to the important Meso-Helikian event, periodic mild disturbances and reactivation of structures permitted influx of meteoric waters that caused local redistribution of the mineralization. This is reflected in younger ages of modified and new ore and gangue mineral assemblages, and the introduction of uranium up into the Athabasca sediments.

Three principal stages are documented by isotope dating: At about 900 m.y., as mentioned

above, at about 300 m.y. and at about 100 m.y. and younger.

At about 300 m.y., i.e. during the time of the Hercynian Orogeny elsewhere, it is proposed that renewed cataclasis of the older mineral assemblages occurred as a result of uplift of the Athabasca region. It was accompanied by multiple remobilization and redistribution of metals into wall rocks and up into sediments of the Athabasca Group, combined with hydrothermal carbonate and clay alteration. Ruhrmann and von Pechmann (1987) noticed that sphalerite appears during this stage, suggesting the introduction of new material, at least zinc.

Ruhrmann (1986) ascribes the kaolinite development within the Key Lake deposit also to the 300 m.y. event, which he attributes to a basin-wide event that overprinted the earlier illite aureole.

Stable isotope data are interpreted by Wilson and Kyser (1987) to indicate that the kaolinitization occurred at temperatures of about 50°C. In recent times, less than 100 m.y. ago, shallow structural adjustment resulted in vertical displacement of deposits. Processes due to modern meteoric waters caused hematitization, limonitization and altered and hydrated pre-existing hydrothermal illites and partially reset their K-Ar ages (Wilson and Kyser 1987).

References and Further Reading for Chapter 5.1 (for details of publications see Bibliography)

Alcock 1936; Artru et al. 1986; Beck 1986; Clark et al. 1982; Clarke and Fogwill 1985; Cramer and Vilks 1987; Dahlkamp 1978; Dahlkamp and Adams 1981; Dubessy et al. 1989; Earle and Sopuck 1989a, 1989b; Eldorado Resources Ltd 1986, 1987; Farstad and Ayers 1986; Fogwill 1985; Fouquet et al. 1986; Gatzweiler et al. 1979; Glackmeyer K., person. commun; Halter et al. 1989; Harper 1978; Harper et al. 1986; Heine 1986; Hoehndorf et al. 1987; Hoeve 1984; Hoeve and Quirt 1986, 1987; Hoeve and Sibbald 1978; Homeniuk and Clark 1986; Hubregtse and Sopuck 1989; Ibrahim and Woo 1985; Jones 1980; Knipping 1974; Lainé 1985, 1986; Lainé et al. (eds.), 1985; Langford 1978, 1986; Lehnert-Thiel K., person. commun;, Lewry and Sibbald 1980; Mac Donald 1980, 1985; Mazimhaka and Hendry 1987, 1989; McMillan 1977; Mellinger 1980, 1987; Mellinger et al. 1987; Money 1968; Money et al. 1970; Munday 1979; Pagel 1975a, 1975b; Pagel et al. 1980, 1985; Pagel and Jaffrezic 1977; Pagel and Svab 1985; Parslow 1989; Parslow and Adamson 1982; Parslow and Thomas 1982; Philippe and Lancelot 1988; Quirt 1985; Ramaekers 1983; Ramaekers and Dunn 1977; Ramaekers and Hartling 1978; Ruhrmann, G., person. commun; Ruhrmann 1987; Ruhrmann et al. 1987; Ruhrmann and von Pechmann 1989; Ruzicka 1984, 1985, 1986, 1987, 1988; Sibbald 1985, 1988; Sibbald et al. 1976, 1977, 1981; Sibbald and Quirt 1987; Sopuk et al. 1983; Stewart E., person. commun; Tan B., person. commun; Tremblay 1978, 1982, 1983; Wallis et al. 1986; Wilson and Kyser 1987; Wray 1985; References of workers on individual deposits see Evans (ed.), 1986; Lainé et al. (eds.), 1985; Tremblay 1982.

5.2 Examples of Subunconformity-Epimetamorphic-Type Uranium Deposits (Type 2, Chap. 4)

5.2.1 Subunconformity-Epimetamorphic Uranium Deposits in Not Albitized Metasediments: Alligator Rivers Uranium Field, Australia

The Alligator Rivers Uranium Field (A.R.U.F.) lies along the central stretch of the East Alligator River in northwestern Arnhem Land, N.T. The district covers an area of about 200 km long in NE-SW direction and is about 100 km wide (Fig. 5.12).

The major deposits in the district are Ranger One, Jabiluka, Koongarra, and Nabarlek. Jabiluka, Koongara, and Ranger One are composed of two or more ore bodies. Jabiluka is the largest single uranium deposit of the world by tonnage. It contains 204 000 mt U_3O_8 at an ore grade of 0.39% U_3O_8.

Total reserves of the Alligator Rivers Uranium Field including production amount to ca. 370 000 mt U_3O_8 (Battey et al. 1987).

All deposits are strata and structure controlled emplaced in metasediments below a distinct Middle Proterozoic unconformity. It is for this setting that they are here defined as sub-unconformity-epimetamorphic type uranium deposits (subtype 2.1, Chap. 4).

Ferguson and Goleby (1980) edited a major volume on Uranium in the Pine Creek Geosyncline with articles covering almost all geoscientific fields and giving a state of the art presentation of the ongoing research work. Ewers et al. (1984) published a concise and comprehensive compilation and synthesis on the Pine Creek Geosyncline and its uranium mineralization. Other

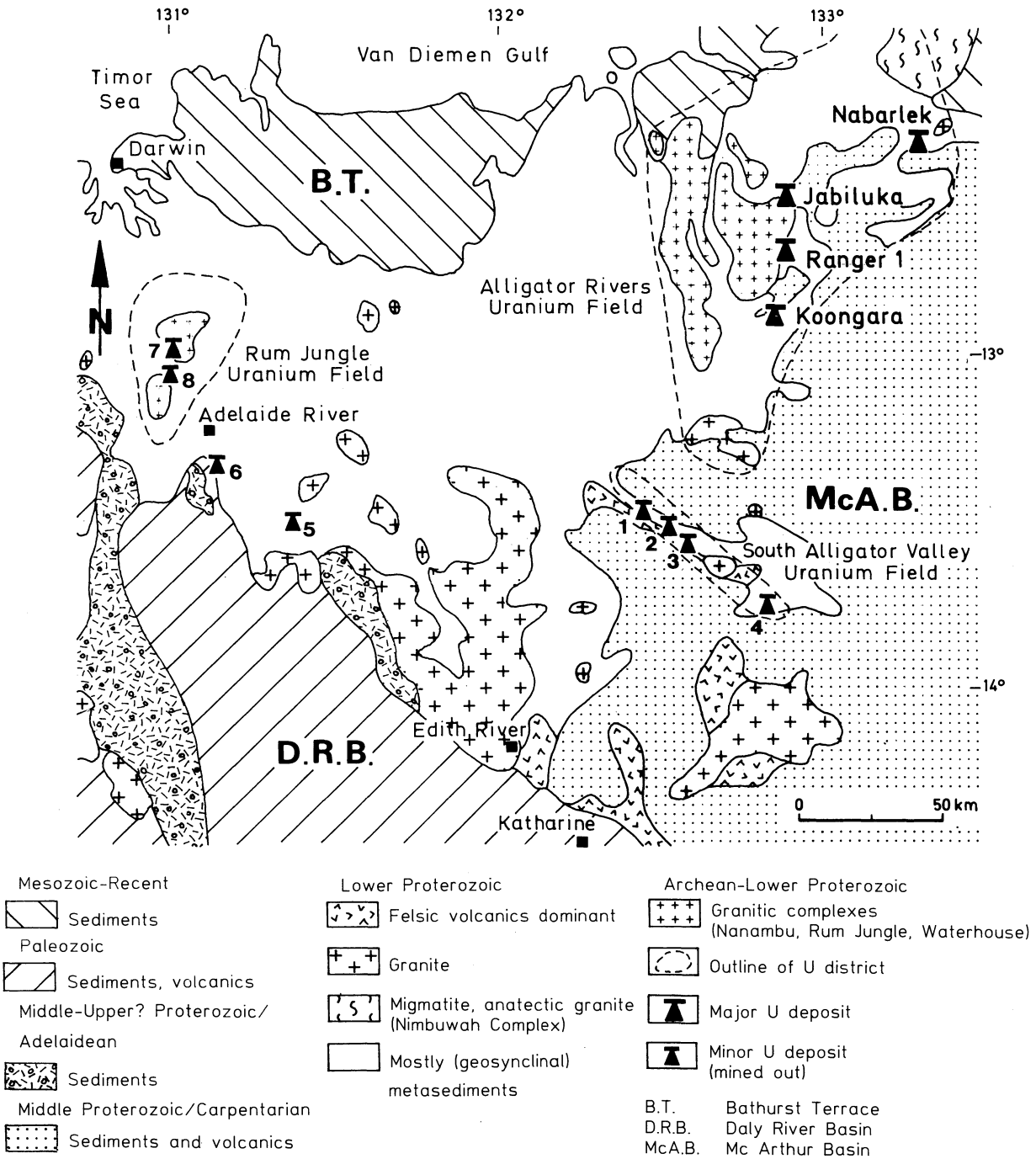

Fig. 5.12. Pine Creek Geosyncline, generalized geological map with situation of the three principal uranium districts (surrounded by *dashed line*) and minor uranium deposits. Former U mines: *1* Rockhole; *2* El Sherana and Palette; *3* Coronation Hill; *4* Sleisbeck; *5* Fleur de Lys; *6* Adelaide River and George Creek; *7* Rum Jungle Embayment area; *8* Rum Jungle Creek South (After Battey et al. 1987)

reviews have been provided by Battey et al. (1987), Needham (1985), Needham et al. (1980, 1988), and Stuart-Smith et al. (1980). The following description is primarily based upon the papers of these authors amended by data of the other authors listed.

Geological Setting of Mineralization

The Alligator Rivers Uranium Field is situated in the northeastern portion of the Pine Creek Geosyncline (Fig. 5.12). Principal stratigraphic units (Fig. 5.13, Table 5.13) are, from bottom to top, the Kakadu Group, the Cahill Formation, the lower member of which hosts all important uranium deposits, and the Nourlangie Schist. This sequence of Lower Proterozoic metasediments and intercalated metavolcanics occupies a folded, north to northwest-trending synclinorium lying between two prominent granitic and migmatitic highs. To the west is the Nanambu Complex of Archean/Lower Proterozoic age (ca. 2470 m.y., all age dates from Page et al. 1980) and to the northeast is the Lower Proterozoic or older Nimbuwah Complex.

At about 1870 to 1800 m.y. ago, a regional orogenic event affected the whole of the Pine Creek Geosyncline. Metamorphism associated with the orogeny was strongest in the Alligator Rivers region. Here it reached the staurolite-almandine grade of the amphibolite facies and resulted in polyphase deformation imprinting a regional NW-SE-oriented schistosity. The intensity of metamorphism decreased westwards to greenschist facies. The amphibolite/greenschist grade facies boundary roughly coincides with the western limit of the Alligator Rivers Uranium Field.

The orogeny was accompanied by a period of igneous activity stretching from about 1870 to 1690 m.y. During this period pre-orogenic (Zamu Dolerite) and post-orogenic tholeiitic dolerites (Oenpelli Dolerite), and numerous syn- and post-orogenic plutons of biotite granite, adamellite, granodiorite, and syenite such as the Nabarlek,

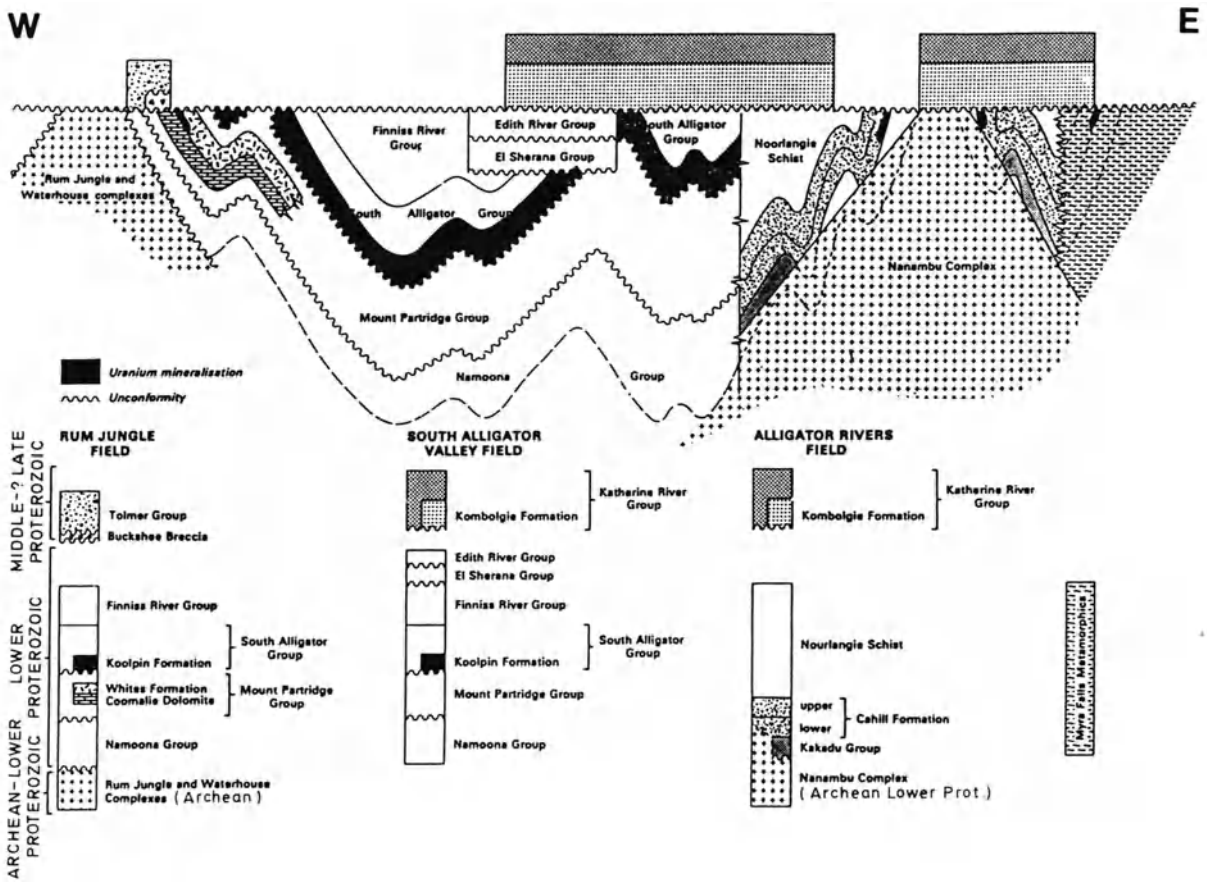

Fig. 5.13. Pine Creek Geosyncline, diagrammàtic section showing relationship between principal stratigraphic Archean to Middle Proterozoic units. Igneous intrusions other than of Archean age have been omitted. Principal setting of U mineralization is indicated. (After Battey et al. 1987)

Table 5.13. Alligator Rivers Uranium Field, synopsis of stratigraphy (for spatial correlation see Fig. 5.13) (After Needham 1985 amended by data from Ewers et al. 1984, reprinted with permission from The Canadian Institute of Mining & Metallurgy)

	Isotopic dates (Page et al. 1980)		Unit	Thickness (m)	Main rock types	Relationships
Quaternary			Marine sediments		Clay, silt, mud, sand and coquina	Intertidal muds, coastal and estuarine alluvium and beach ridges
			Continental sediments		Silt, sand, clay, sandy siltstone, black and brown humic soils	Creek and river alluvium transitional into estuarine deposits, outwash and colluvium, abandoned channel deposits in estuarine plains
Tertiary to Quaternary			Sand and colluvium	<75	Unconsolidated sand, ferruginous and clayey in places	Overlies Early Teritary laterite
			Laterite	<3	Nodular, concretionary, pisolitic and vermicular laterite	Developed mainly on deeply weathered Cretaceous and Early Proterozoic rocks. Minor pedogenic and transported types
Cretaceous	Neocomian to Aptian	Bathurst Island Formation	Marligur Member	<25	Poorly consolidated, well sorted and rounded fine to very coarse quartz sandstone, minor siltstone and conglomerate	Interfingering marginal marine members, north of Oenpelli
			Darwin Member	<35	Fine argillaceous sandstone, siltstone, micaceous mudstone, radiolarian shale, basal conglomerate	
	Late Jurassic to Early Cretaceous		Petrel Formation	<10	Sandstone, siltstone	Contemporaneous with and higher level continental equivalents of Bathurst Island Formation
	Regional unconformity					
Late Proterozoic	522 m.y.		Minor basaltic dikes	<0.3	Basaltic dike	Intrudes Kombolgie Formation volcanics east of Ranger 1
	1316 m.y.		Mudginberri Phonolite	<1	Phonolite dikes	Intrudes Nanambu Complex around Mudginberri homestead
	1316 m.y.		Maningkorrirr Phonolite	<1	Phonolite dikes	Intrudes Nimbuwah Complex in northeast
	1370–1200 m.y.		Dolerite dikes	<2	Quartz dolerite dikes	Widespread, poorly exposed, steep – occupy major fractures in Kombolgie Formation

Table 5.13. *Continued*

	Isotopic dates (Page et al. 1980)		Unit	Thickness (m)	Main rock types	Relationships
Middle Proterozoic (Carpentarian)		Katherine River Group Kombolgie Formation	Upper sandstone	350	Sandstone, minor conglomerate and siltstone	Markedly unconformable on older units except Edith River Volcanics; members generally conformable but upper sandstone unconformable on lower sandstone near Deaf Adder Gorge, with Nungbalgarri Volcanics absent
			Gilruth Volcanic Member	<5	Tuffaceous siltstone, vesicular basalt	
			Nungbalgarri Volcanic Member	0.170	Basalt, trachybasalt; rhyolite and ignimbrite at top; rare intercalated sediment	
			Lower sandstone	<300	Sandstone, pebbly and conglomeratic, locally ferruginous	
	Major unconformity					
	1688 m.y.		Oenpelli Dolerite	<250	Porphyritic and ophitic olivine dolerite, quartz dolerite, granophyric dolerite, minor serpentinite	Lopoliths forming basement ridges to Kombolgie Formation
			Edith River Group	1200	Tuff, tuffaceous siltstone, altered rhyolite, microgranite	Valley fill volcaniclastics
	Unconformity					
	ca. 1780 m.y.		Nabarlek Granite		Altered biotite granite cut by numerous quartz-filled shears	
	ca. 1755 m.y.		Tin Camp Granite		Altered biotite granite cut by numerous quartz-filled shears	Margins mostly faulted, post-orogenic
	ca. 1730 m.y.		Jim Jim Granite		Altered biotite granite	
			El Sherana Group		Rhyolite, greywacke, siltstone, sandstone, basalt	
		Myra Falls Metamorphics	Nourlangie Schist	Unknown	Quartz mica schist, quartz schist, commonly with garnet	Probable metamorphic equivalent of Wildman Siltstone ± parts of South Alligator Group and Fisher Creek Siltstone
	ca. 1800 m.y.		Transitional Zone		Quartz and quartz mica schist with minor quartz-feldspar bands	
			Lit-par-Lit Gneiss Zone		Quartz, biotite, garnet, and amphibole schist and gneiss with quartzofeldspathic layers and pods	Contain resisters of Cahill Formation and Kakadu Group – probable metamorphic equivalent of those formations
			Nimbuwah Complex		Granitic to tonalitic gneiss and migmatite, granite, pegmatite	Partly metamorphosed (granulite facies) 1870 m.y. granite

Table 5.13. *Continued*

	Isotopic dates (Page et al. 1980)		Unit	Thickness (m)	Main rock types	Relationships
	ca. 1800 m.y.		Regional metamorphism and deformation			
Early Proterozoic		Finniss River Group	Zamu Dolerite	<300	Ortho-amphibolite/ tholeiitic basalt	Sills folded and metamorphosed with enclosing sediments
			Burrell Creek Formation	1500 –5000	Siltstone, shale, slate, greywacke, arkosoquartzite, schist, minor interbedded volcanics	Conglomerate beds contain clasts of South Alligator River Group and Masson Formation
		South Alligator Group	Kapalga Formation	<5000	Chert-banded ferruginous siltstone, carbonaceous shale	Southwest only; conformable on Koolpin Formation
			Mount Bonnie Fm. Gerowie Tuff		Greywacke, shale, siltstone; felsic volcanics, volcanolithic greywacke	In center and west of geosyncline
			Koolpin Formation	1000	Chert-banded ferruginous siltstone, carbonaceous shale and dolomite in southwest. Banded ferruginous quartzite and garnet graphite schist in Cannon Hill area	Unconformable in southwest, contacts not seen in Cannon Hill area
		Mount Partridge Group	Wildman Siltstone	2000	Banded carbonaceous siltstone, minor sandstone, greywacke, phyllite	Conformable on Mundogie Sandstone; west only
			Mundogie Sandstone	<5000	Sandstone, quartzite, siltstone, phyllite, conglomerate	Probably unconformable on Masson Formation and Stag Creek Volcanics. Coarser and less metamorphosed equivalent of Cahill Formation upper member. Southwest only
	ca. 1870–2400	Namoona Group	Stag Creek Volcanics	1000	Mafic volcanic breccia, hawaiite, tuff, tuffaceous greywacke and shale	Conformable on Masson Formation, southwest only
			Masson Formation	3000	Carbonaceous siltstone, sandstone, dolomite	Lowest exposed Proterozoic unit in southwest. Less metamorphosed, open marine equivalent of Cahill Formation lower member

Table 5.13. *Continued*

	Isotopic dates (Page et al. 1980)		Unit	Thickness (m)	Main rock types	Relationships
Early Proterozoic		Kakadu Group	Cahill Formation	3000	Mica and quartz feldspar schist, quartzite; lower member (600 m) also contains carbonate, calcsilicate gneiss and carbonaceous schist	Apparently conformable on Kakadu Group, may overlap onto Archaean of Nanambu Complex
			Kudjumarndi Quartzite	150	Orthoquartzite ± mica, feldspar and hornblende; quartz gneiss	Confined to northeast. Equivalent of Munmarlary Quartzite. Conformable on Mount Howship Gneiss
			Mount Howship Gneiss	2000	Quartz feldspar gneiss	Confined to Myra Falls Inlier. Equivalent of Mount Basedow Gneiss. Lowest known Proterozoic unit in east
			Munmarlary Quartzite	2000	Muscovite and feldspar quartzite	Equivalent of Kudjumarndi Quartzite, transitional into Proterozoic component of Nanambu Complex
			Mount Basedow Gneiss	>1500	Meta-arkose, gneiss, minor schist	Equivalent to Mount Howship Gneissi marginal to and transitional with Proterozoic component of Nanambu Complex
Archaean – Early Proterozoic	1800–2500 m.y.		Nanambu Complex		Pegmatoid gneiss, muscovite-biotite granite, schist, pegmatite	Mantled gneiss dome – Archaean partly metamorphosed granite with accreted leucocratic Proterozoic metasediments (mainly from Kakadu Group)

Tin Camp, Jim Jim granites, and pegmatites were intruded.

Deposition of early Carpentarian/Middle Proterozoic platform cover sediments, mainly sandstone (<650 m thick) intercalated with basalt, trachybasalt, and rhyolite (ca. 1648 m.y.) of the Katherine River Group/Kombolgie Formation marked the beginning of the tectonic stability which has persisted to the present day except for the intrusion of some phonolite and quartz dolerite dikes in Adelaidean/early Upper Proterozoic time (1370–1200 m.y.). A major weathering period eroded 1 to 2 km of the basement forming a prominent unconformity prior to the sedimentation of the Katherine River Group (Ewers et al. 1984; see also Table 5.16).

Host Rock Alterations

Several episodes of alteration have altered the crystalline host rocks of the uranium deposits and to some extent the overlying Kombolgie Formation (Figs. 5.14 to 5.19). Prominent processes are chloritization, sericitization, hematitization, silicification, minor carbonatization, desilicification, and carbonate dissolution. Disruption and brecciation of certain strata accompanied some of the alteration stages and/or mineralization.

Ewers et al. (1984) recognized the following characteristic features of *alteration associated with deposits*.

Chloritization is most prominent and occurs in multiple generations in all deposits. It forms a

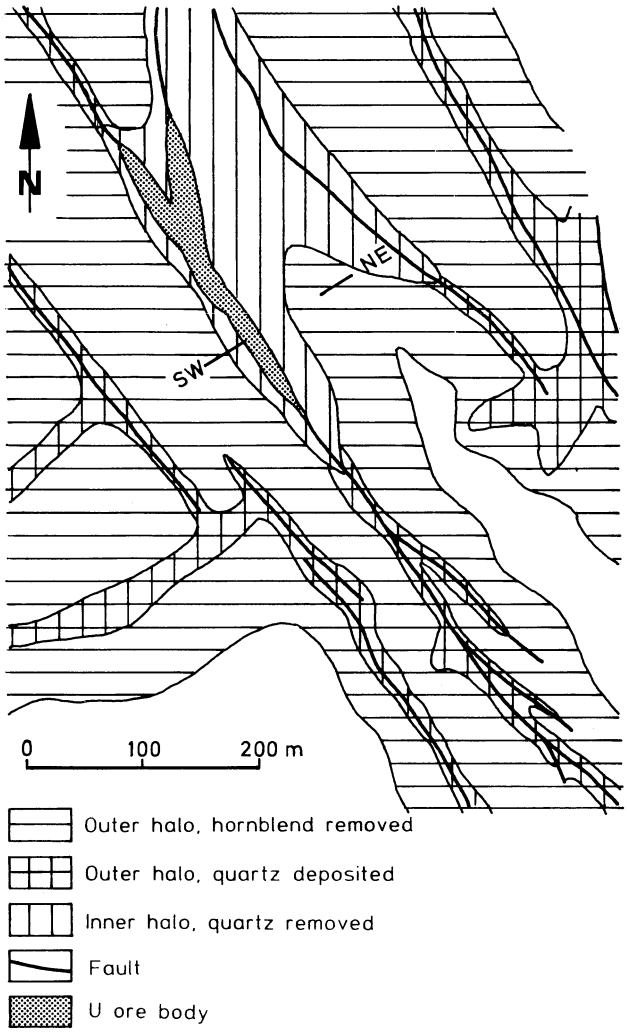

Fig. 5.14. Nabarlek, map showing the ore body (primary mineralization projected to surface) and distribution of associated alteration. (Strike of metasediments is ca. NE-SW) (After Wilde and Wall 1987) (reproduced from *Economic Geology*, 1987, v. 82, p. 1160)

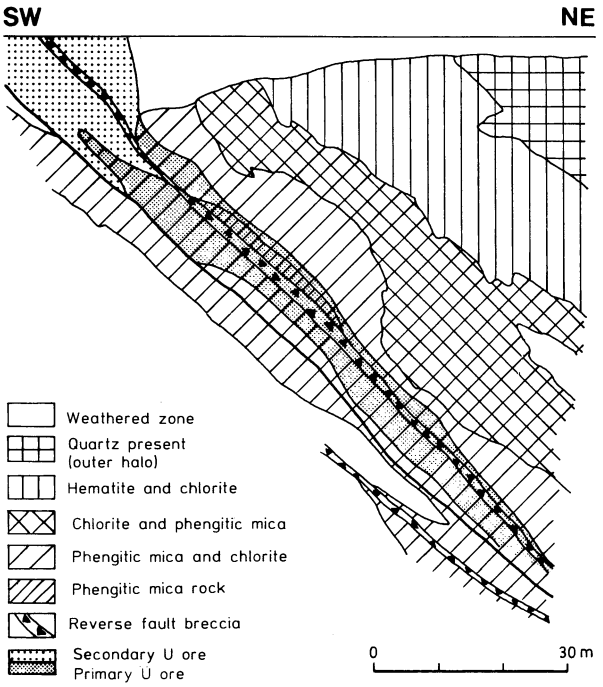

Fig. 5.15. Nabarlek, SW-NE cross-section through the southern end of the ore body displaying the distribution of primary (uraninite/pitchblende) and secondary (dominantly hexavalent U minerals) ore and alteration facies in the inner halo. (After Wilde and Wall 1987) (reproduced from *Economic Geology*, 1987, v. 82, p. 1161)

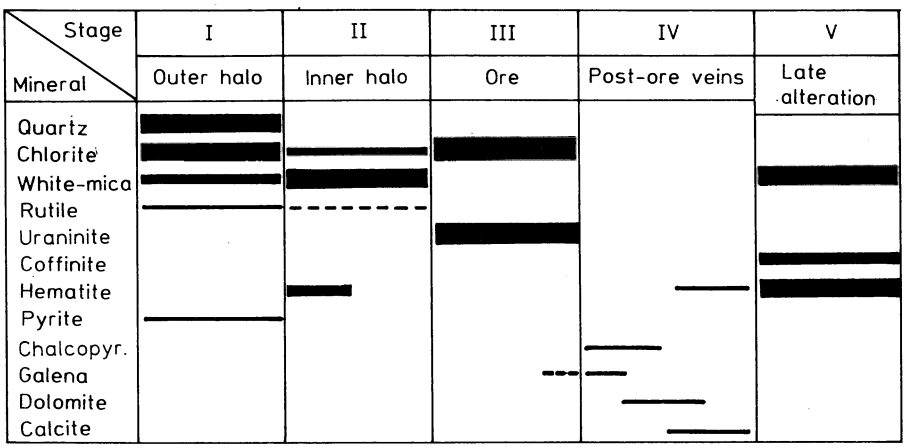

Fig. 5.16. Nabarlek, paragenetic scheme of ore and gangue/alteration minerals and their distribution in the outer and inner halos. (After Wilde and Wall 1987) (reproduced from *Economic Geology*, 1987, v. 82, p. 1165)

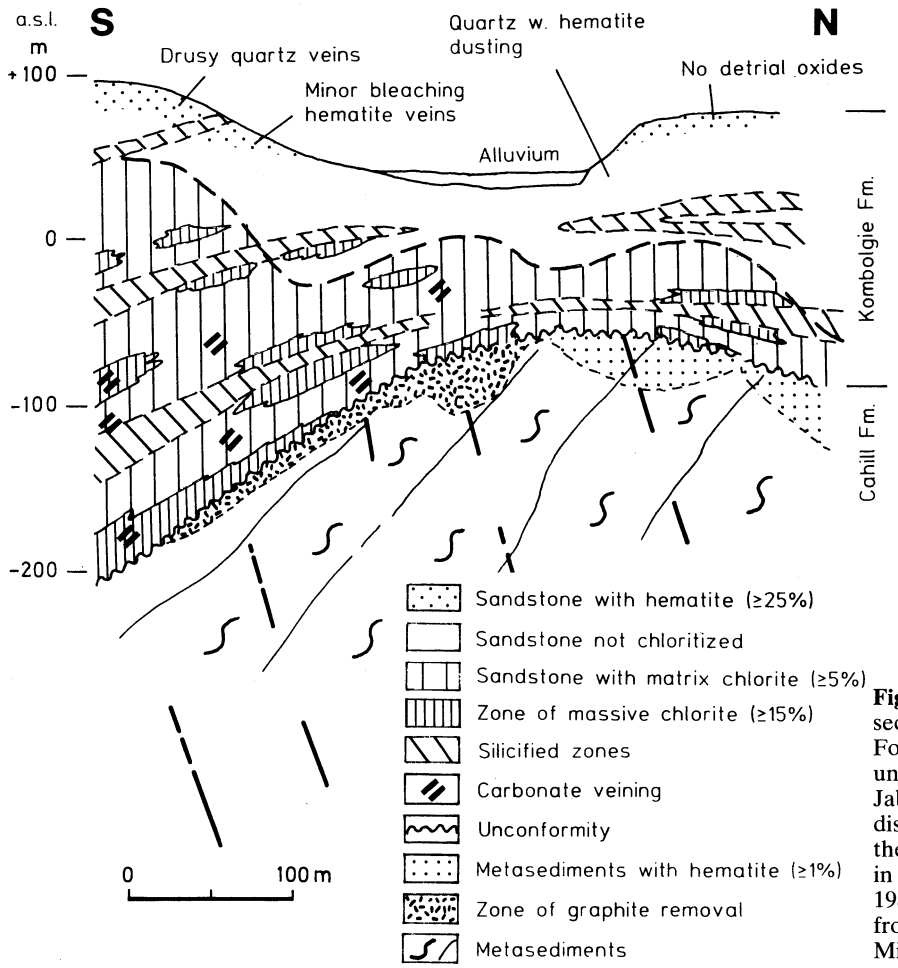

Fig. 5.17. Jabiluka, cross-section through the Kombolgie Formation and subjacent unconformity above the Jabiluka II deposit. The scheme displays in a simplified manner the various alteration signatures in the sandstone. (After Curtis 1985) (reprinted with permission from The Canadian Institute of Mining and Metallurgy)

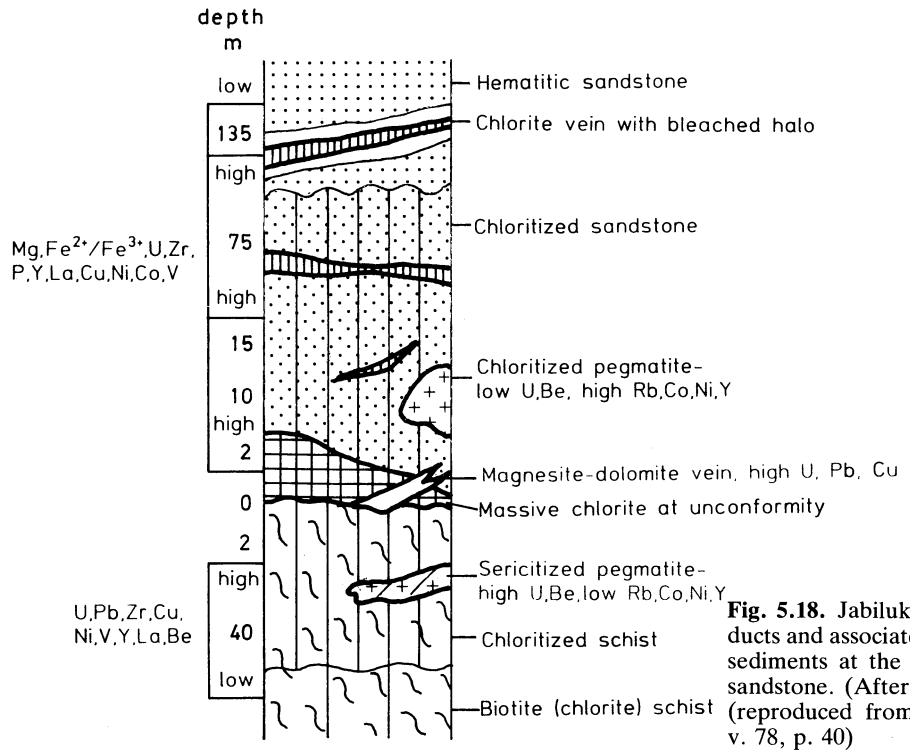

Fig. 5.18. Jabiluka, scheme of alteration products and associated chemical changes in metasediments at the unconformity and overlying sandstone. (After Gustafson and Curtis 1983) (reproduced from *Economic Geology*, 1983, v. 78, p. 40)

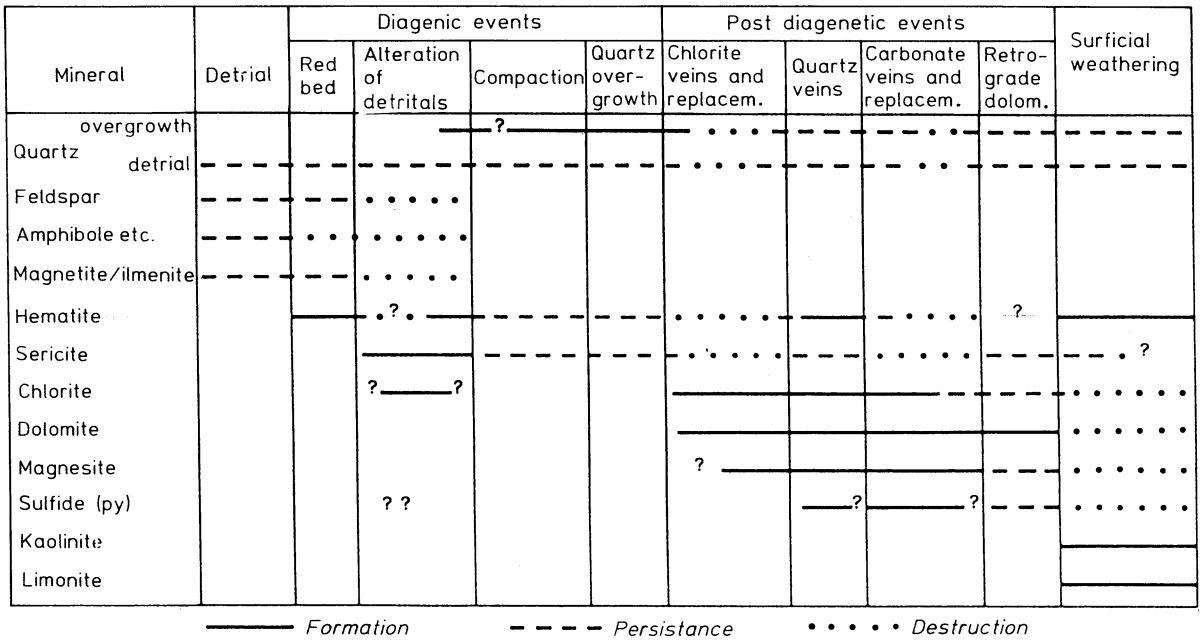

Fig. 5.19. Jabiluka, paragenetic scheme of alteration. (After Gustafson and Curtis 1983) (reproduced from *Economic Geology*, 1983, v. 78, p. 40)

pervasive halo but of variable intensity and spatial extent around the various deposits. Composition of chlorites within ore zones and adjacent host rocks overlap and are highly variable with respect to Al, Fe, Mg, and to a lesser extent Si, although in general Mg-rich phases prevail.

Sericitization (white mica, illite) is common in all deposits and replaces particularly feldspars. At Nabarlek, sericite is the dominant phyllosilicate in the ore zone derived by overprinting chlorite.

Hematitization is widespread and generally associated with chloritization particularly of ferromagnesian minerals. Hematite occurs disseminated, in veinlets, and as pseudomorphs after magnetite.

Silicification is a common feature in and around ore bodies. It produced chert replacing carbonates and euhedral quartz filling fractures and voids. At Nabarlek, silicification along fault planes, together with chloritization and sericitization, forms an outer halo around the deposit, whereas the ore zone itself was subjected to desilicification (Wilde and Wall 1987).

Carbonatization is a minor feature and reflected by local veinlets of dolomite, calcite and magnesite.

Decarbonatization is indicated by the presumed removal of bedded carbonates from mineralized zones. Because this decarbonatization is commonly associated with silicification, Eupene (1980) has postulated that silicification of carbonate resulted in reduction in volume and caused collapse and disruption, while Ferguson et al. (1980b) consider a solution of the massive carbonate, which led to excavation and collapse.

Age datings indicate that most pronounced intervals of alteration occurred at about 1650 to 1500 m.y., 1260 to 840 m.y. and 500 m.y. (Table 5.14). Fission track dating of zircon from basement rocks yields an additional age of ca. 1420 m.y. and a respective annealing temperature of ca. 175°C (Koul et al. 1984, 1987).

Principal Characteristics of Mineralization

Principal *ore minerals* are uraninite, pitchblende, minor coffinite, brannerite, locally thucholite, and in weathering zones hexavalent uranium minerals. Jabiluka II and Koongara contain economic gold and Ranger subeconomic gold.

Associated minerals and elements generally present in amounts of less than 1% include pyrite, pyrrhotite, chalcopyrite, and galena. Locally and mostly in traces occur bornite, chalcocite, covellite, digenite, arsenopyrite, cobaltite, marcasite,

cuprite, native copper, native gold, tellurides, mercury, and palladium. Hematite is relatively common. Principal *gangue minerals* include chlorite, quartz, white mica/sericite and lesser amounts of dolomite, magnesite, calcite, kaolinite, montmorillonite, apatite, tourmaline, sphene, anatase, leucoxene, and rutile. The various ore and associated minerals are present in several generations.

Table 5.14. Alligator Rivers Uranium Field, selected apparent ages of altered rocks from the major deposits.

Rock	Apparent age (m.y.)	Method	Reference
Jabiluka			
Chloritic-sericitic schist	1600± 80	Rb-Sr	2
Altered metasediments	1534 ± 90 to 1400	Rb-Sr	3
Pyrite in retrogressed graphitic schist few meters away from ore	1380 ± 110	Pb-Pb	1
Nabarlek			
Inner alteration halo: sericite-chlorite schist	1648 to 1512	Rb-Sr	2
Outer alteration halo: sericite-chlorite schist			
– muscovite separate	1781 ± 35	K-Ar	2
– biotite separate	1583 ± 32	K-Ar	2
Altered sericite-chlorite schist (mean model age)	1610 ± 40	Rb - Sr	2
Altered Nabarlek Granite	1561 ± 17	Rb-Sr	2
Mineralized sericite-chlorite schist	1260 to 842	Rb-Sr	2
	450	Rb-Sr	2
Sericite/illite	842	Rb-Sr	4
Jabiluka, Ranger One, Nabarlek areas			
Altered dikes (amphibolite)	1648 ± 17	K-Ar	2
Altered Oenpelli Dolerite (clinopyroxene)	1630 to 1600	K-Ar	2
Several altered granites (average)	1630	K-Ar	2
Zircon from basement	1420	Fission-track	2

Data from (1) Gulson and Mizon 1980; (2) Page et al. 1980; (3) Riley et al. 1980; (4) Wilde and Wall 1987; (5) Koul et al. 1984

Jabiluka contains up to 100 ppm palladium. Economic *gold* concentrations with values up to 695 ppm (average 10 ppm) as found locally in Jabiluka 2 (Fig. 5.20) occur independent of lithology and stratigraphic position. All observed gold accumulations are confined within uraninite veins. A few tiny gold grains (<3 μm) have been noticed in chlorite replacing uraninite, but there is no significant correlation between amounts of gold and uranium (Grauch 1984).

Sulfides are present in all deposits but in minor quantities (<1% to <5% Nabarlek).

Gangue minerals fill voids and fractures within the ore zones and wall rocks.

Most uranium deposits of the Alligator Rivers Uranium Field except Nabarlek are *structure-hosted, strata-bound* in multiply deformed quartz-muscovite-chlorite schists of the lower member of the Cahill Formation in close proximity (a few tens to a few thousand meters) to the Archean-Lower Proterozic Nanambu Complex (Figs. 5.12, 5.13). The majority of the ore is generally tabular or bowl-shaped (Figs. 5.20 to 5.22) located in more or less strata-concordant breccia zones within or close to graphitic pelitic schists and laterally adjacent to lenses of massive crystalline dolomite and/or magnesite. The carbonates disappear in the mineralized zones associated with a pronounced increase in fracturing and brecciation and grade into the ore-hosting schists. (Ewers et al. 1984).

Nabarlek (Figs. 5.14 to 5.16) is structure-hosted in schists of the Myra Falls Metamorphics which are considered a correlative of the Cahill Formation (Needham 1982). Table 5.15 provides a summary of *parameters of the principal U deposits* of the A.R.U.F.

Age dating yields several time intervals for ore formation and remobilization: ca. 1730 m.y., 1650 to 1600 (to 1440) m.y., 920 to 800 m.y. and ca. 500 m.y. (references see later).

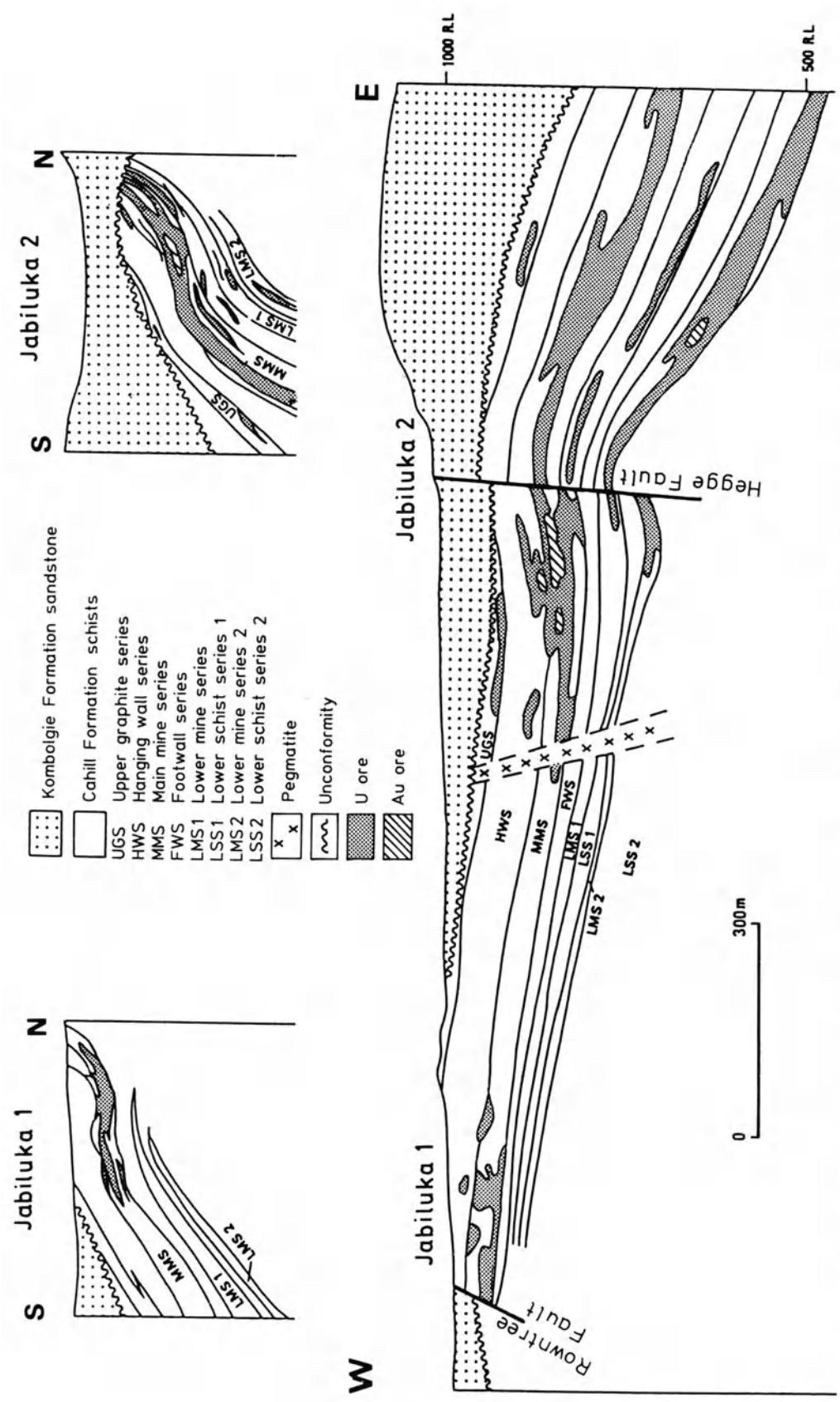

Fig. 5.20. Jabiluka, generalized S-N cross-sections and W-E longitudinal section of Jabiluka I and II. The breccia hosted mineralization diplays a discrete strata-bound control. The longitudinal section exhibits the position of the gold mineralization. (After Ewers et al. 1984, based on Pancontinental Mining Ltd)

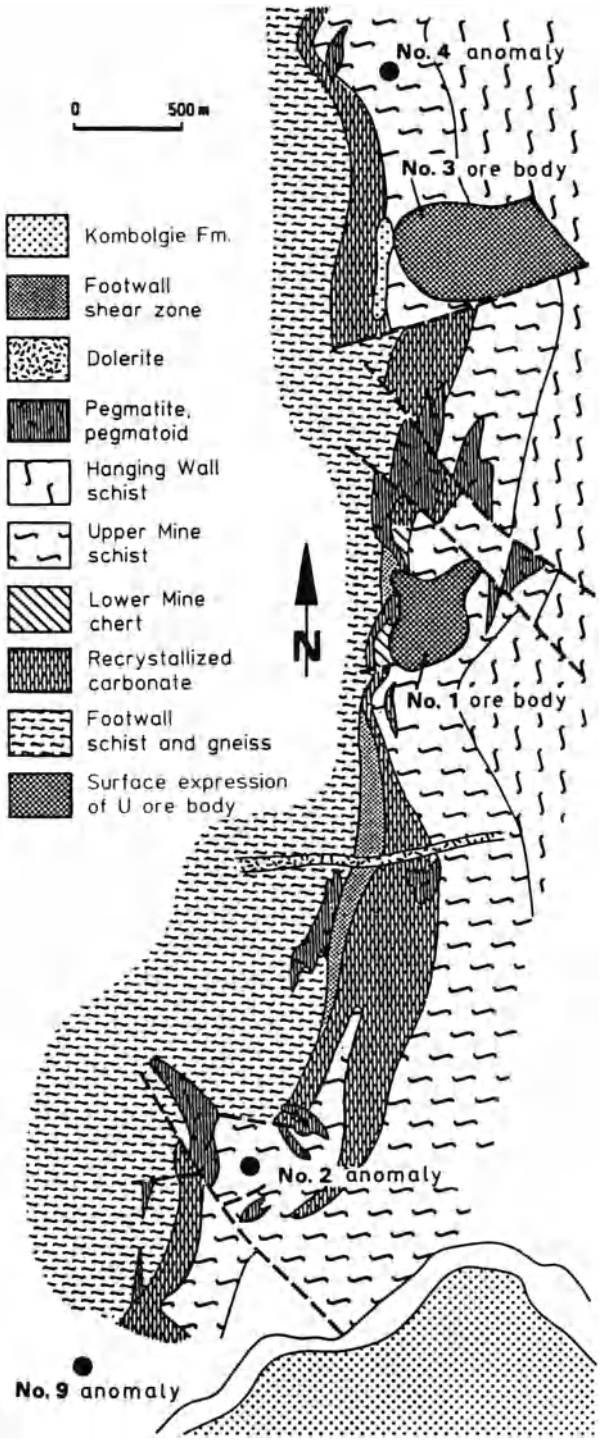

Fig. 5.21. Ranger One, generalized geological map with localization and surface expression of the two main ore bodies, *No. 1* and *No. 2* and adjacent uranium showings (anomalies). The Footwall schist and gneiss are supposedly part of the contact zone of the Nanambu Complex. (After Ewers et al. 1984, based on Eupene et al. 1975, Hegge et al. 1980)

Stable Isotopes and Fluid Inclusions

Fuzikawa (1982) and Ypma and Fuzikawa (1980) established two types of *fluid inclusions* in quartz and carbonate mainly of late stage veins of the Jabiluka and Nabarlek deposits. Type 1 contains a saline brine with dominant $CaCl_2$, $MgCl_2$, and NaCl, and yields homogenization temperatures between 100 and 160°C. Type 2 has low salinities and CO_2 in the vapor phase. Ypma and Fuzikawa (1980) interpret these data as suggesting a mixing of a very saline brine with a more CO_2-rich fluid, causing the deposition of uranium, possibly involving reduction by methane.

Wilde et al. (1988) confirmed these findings. In quartz from veins, breccias, and country rocks from Jabiluka, Koongarra, and Nabarlek, and from post-ore dolomite cementing breccias at Jabiluka, they established seven different types of inclusions which can be attributed to four cogenetic populations. The inclusions display an extreme variability in composition and associated physical properties. The variability is interpreted by the authors as resulting from trapping of varying proportions of two discrete Ca- and Mg-enriched end member solutions.

The first fluid is consistent with a *hypersaline brine* (salinity ca. 40 wt.% $CaCl_2$ equivalent) of relatively reduced nature which was trapped at high pressure of as much as 1.6 kbar and temperatures of 240°C or more. This fluid is assumed to have been saturated with respect to early Fe-rich chlorite and white mica in the altered host rocks. Solid inclusions of Fe-rich chlorite suggest that the fluid can be related to the early alteration stage present in the outer zone at Nabarlek, while solid inclusions of dolomite probably attest to a persistence of this fluid to the post-ore dolomite veining stage, or alternatively that minor dolomite formed during the early alteration stages.

The second fluid is a more *dilute brine* (ca. 7.5 wt.% $CaCl_2$ equivalent), more oxidized and CO_2 gas saturated. Recorded pressure is only 500 bar. Minimum temperature must have been at least 95°C according to the lowest vapor disappearance temperature. Wilde et al. (1988) postulate that this fluid may have caused the overprinting alteration halo including desilicification of the inner zone at Nabarlek because the chlorite of this zone is markedly magnesian, and hematite and anatase are the stable oxide phases as compared to magnetite and ilmenite, which are stable in the outer halo.

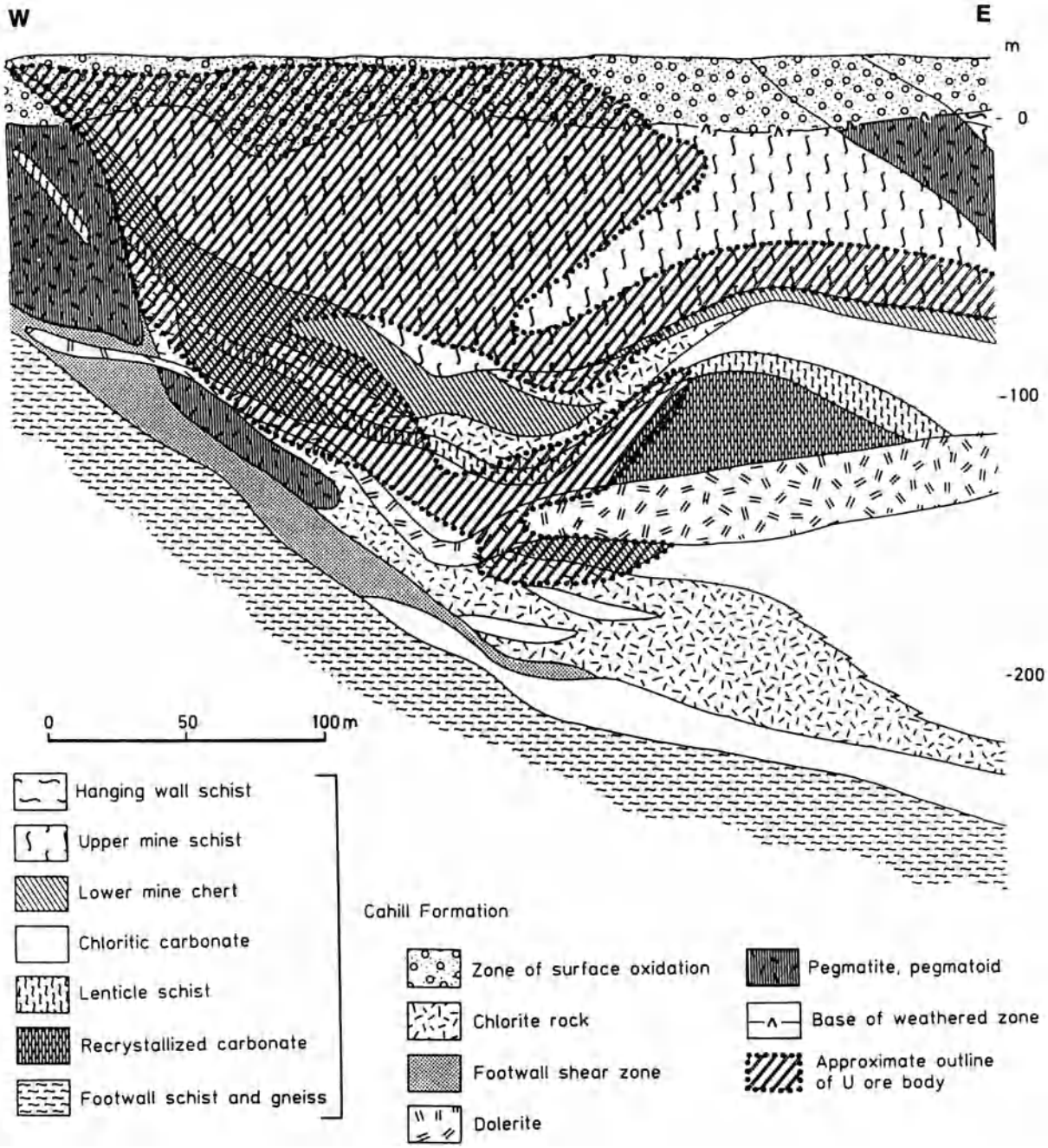

Fig. 5.22. Ranger One, No. 1 ore body, W-E cross-section showing distribution of mineralization and host lithologies. (After Ewers et al. 1984, based on Eupene et al. 1975, Hegge et al. 1980)

Ewers et al. (1984) review *stable isotope* studies performed on sulfides, carbonates, and organic matter from Jabiluka, Ranger One and Koongarra. Bedded *sulfides*, mainly pyrite, occurring in graphitic metasediments of the lower Cahill Formation adjacent to the deposits yield $\delta^{34}S$ values of $+2 \pm 1‰$, i.e., they are in accord with those of mantle sulfur and therefore presumably derived from volcanogenic hydrothermal fluids. Vein and vug filling sulfides from the deposits have a wide range of $\delta^{34}S$ values of between -6 and $+14‰$. This range indicates a probable metal sulfide crystallization in an organic-rich environment from sulfates by H_2S. The hydrogen

Table 5.15. Alligator Rivers Uranium Field, summary of characteristics and magnitudes of major U deposits.

Deposit	Grade % U_3O_8	Reserves mt U_3O_8	Geometry	Ore character	Host lithology	Host formation	Metamorphic grade	Ore control	Metallogenetic criteria
Nabarlek	1.84	9098+	Steep tabular to shallow cigar	Massive and disseminated pitchblende, near-surface oxidized halo	Chlorite mica quartz schist	Myra Falls Metamorphics	Retrograded m. amphibolite	Shear zone ?unconformity, ?chlorite alteration	Metamorphic hydrothermal, unconf. related, ?strata-bound (relict)
Ranger 1 ore body No. 1	0.32	53700++	Inverse cone with down-dip conformable lenses	Massive, disseminated and filmy pitchblende mainly in chlorite rock and chlorite schist, and carbonaceous schist, particularly in brecciated zones	Chlorite schist and microgneiss, silicified carbbonate, massive chlorite, graphite schist	Cahill Fm & Nanambu Complex	"	Strata-bound, brecciation, chlorite alteration, silicification, unconformity	Strata-bound + ?metamorphic hydrothermal + epigenetic – probably carbonate solution. Unconf. related?
No. 3	0.207 0.163	72800 (probable) 12200 (possible)	Shallow-dipping tabular to lensoid body with conformable base, and blind, down-dip lenses			"	"		
Jabiluka 1	0.25	3400	Folded layers and lenses 0–70°, in 4 main stratiform ore-bearing horizons	Disseminated and vein filling pitchblende, and selvages to chlorite and alteration zones. Minor coffinite and brannerite	Quartz sericite chlorite ± graphite schist	Cahill Formation	Retrograded m. amphibolite	Stratiform, unconformity, chlorite alteration, brecciation	Strata-bound, metamorphic hydrothermal and epigenetic; unconf. related?
Jabiluka 2	0.39 (15.3 g/t Au)	204000 (8.1 t Au)	"	"	"	"	"	"	"
Koongara ore body No. 1	0.269	13300	Coalesced stratiform lenses form elongate wedge, dip 55°	Disseminated pitchblende; secondary tail near surface	Quartz chlorite and graphite schists, garnet quartz muscovite chlorite schist	"	"	Strata-bound to stratiform chlorite alteration, brecciation; ?faulting, ?unconformity	Strata-bound + metamorphic hydrothermal + epigenetic, unconf. related?
No. 2		2300	"	"	"	"	"	"	"
Total		370798							

(Based on Ewers et al. 1984; Needham 1981; Battey et al. 1987) + mined out, ++ in operation, ca. 25000 mt U_3O_8 extracted prior to 1990

sulfide is thought to have been generated by anaerobic sulfate-reducing bacteria.

Donnelly and Ferguson (1980) applied sulfur isotope geothermometry and figured out that bedded and ore zone coexisting sulfides record the same temperature of (re-)crystallization of about 270°C.

Binns et al. (1980b) registered a similar temperature for one sulfide pair from Jabiluka and conclude that initial temperatures of the main mineralizing event were about 300 to 350°C.

Vein and vug *carbonate* from mineralized zones have variable $\delta^{13}C$ and $\delta^{18}O$ values ranging from −20 to 0‰ and +7 to +20‰ respectively. The $\delta^{13}C$ values suggest crystallization of the carbonate from organically derived CO_2, in part at least, whereas the $\delta^{18}O$ values indicate involvement of groundwater. The $\delta^{13}C$ and $\delta^{18}O$ values of vein and vug carbonates from Jabiluka and Koongarra plot on two reasonably defined correlation lines. Ewers et al. (1984) interpret these correlations as supporting the hypothesis calling for in situ reactions caused by influx of oxidizing groundwater whereby carbonate has been recrystallized and organic material oxidized. A greater groundwater involvement is indicated for the intensely altered ore zone at Koongarra by various studies and supported by $\delta^{13}C$ values of organic material. Stable isotope studies of carbonates from the Nabarlek mineralization by Ewers et al. (1983) show ^{18}O enrichment which suggests a low fluid/rock ratio. The isotope compositions of these carbonates also indicate higher temperature reactions than established for the other deposits mentioned above. ^{13}C depletion in the Nabarlek carbonates ($\delta^{13}C = -25$ to -15) are interpreted by the authors to indicate incorporation of CO_2 derived from organic matter. The low fluid/rock ratio is supported by $\delta^{18}O$ data from Oenpelli Dolerite at Nabarlek reported by Ypma and Fuzikawa (1980).

Potential Sources of Uranium

Data provided by Ewers et al. (1985), Ewers and Higgins (1985), and Needham (1985) indicate that Archean granite of the Nanambu Complex contains an average of 9 ppm U with uranium enrichments of up to 30 ppm, which is reported by McAndrew and Finlay (1980) to be readily leachable. Middle Proterozoic granites average 8 to 25 ppm U with values of as much as 47 ppm U. According to Ewers and Higgins (1985), all unaltered metasediments away from uranium occurrences contain U tenors which more or less compare with the average abundance for the given lithologies on a worldwide basis. For these reasons, these authors favor the Archean granitic rocks as the most likely source for uranium or perhaps felsic volcanics intercalated within the Lower Proterozoic metasedimentary sequence.

It has to be kept in mind, however, that Ferguson and Winer (1980) and Binns et al. (1980a) established significant U concentrations of up to 16 ppm U in graphite schists "away from the ore zones". It remains to be seen whether these concentrations represent only a distal uranium halo around a deposit, i.e., the ore-forming process distributed uranium far beyond the actual zone of mineralization, or the elevated values are perhaps associated with ancient uraniferous mylonite zones comparable to those found associated with unconformity-bound uranium deposits in the Athabasca Basin and vein deposits in the Hercynian Massifs in France. (see respective sections in Chaps. 5.1 and 5.3.1)

Geochronology

Table 5.16 provides a synopsis of geological and metallogenetic events in geochronological order as proposed by Needham (1985).

Mineralization/remobilization occurred during several periods but not all generations have been isotopically and/or mineralogically recorded in all deposits. Principal post-metamorphic mineralization/remobilization events are dated at about 1730 m.y., 1650 to 1600 (to 1440) m.y., 920 to 800 m.y. and 500 m.y.

Apparent ages of alteration products are given in Table 5.14. Reported ages of uranium minerals are as follows:

Hills and Richards (1976) identified by U/Pb isotope dating of pitchblende-uraninite an age of ca. 1855 m.y. corresponding to the time of the metamorphic event, an age of ca. 1700 m.y. for the oldest uranium mineralization at Ranger One and an age of 920 to 800 m.y. as the best-defined event of mineralization.

Ewers et al. (1984) report isotope ages of 1600 m.y., 900 m.y., and 500 m.y. for uraninite and galena, which reflect a time of mineralization and subsequent remobilization post-dating re-

Table 5.16. Alligator Rivers Uranium Field, synopsis of the geological evolution and metallogenetic events proposed by Needham (1985). (Ages of U mineralization after Hills and Richards 1976, other ages after Page et al. 1980; for additional ages see text). (Needham 1985)

Age	Deposition	Igneous events	Tectonic events	Metamorphism	Events relevant to ore genesis
Recent	Aggradation of swales, alluviation of major valleys		Coastal emergence – 7 m. Dissection of Koolpinyah Surface		Continued oxidation of orebodies near surface; minor precipitation of uranium in organically-rich black soils and possibly in pyritic black muds
Pleistocene	Aggradation of major valleys, formation of sand plains, minor deep weathering		Wide fluctuations of sea level, dissection of Koolpinyah Surface		
Miocene-Pliocene	Deposition of unconsolidated sands over lateritized lowlands to form Koolpinyah Surface				
	Lateritization of lowland areas, mechanical weathering, redeposition of sands from Kombolgie Formation				Continued oxidation of orebodies near-surface
			Further relative uplift and retreat of seas to beyond present coastline		Removal of Mesozoic to largely re-exhume pre-Kombolgie surface
Cretaceous	Deposition of Bathurst Island Formation: sandstone and siltstone in north		Retreat of Mesozoic seas suggesting relative uplift in south		Burial of pre-Kombolgie surface
			Regional unconformity		
		Intrusion of minor dolerite (522 m.y.)			Erosion of Kombolgie Formation mainly by scarp retreat to expose pre-Kombolgie surface, followed by partial oxidation of orebodies near surface. Apparent age of U mineralization (ca. 900 m.y. and ca. 500 m.y.)
Adelaidean		Intrusion of phonolites (1316 m.y.), dolerites (1370 and 1200 m.y.)		Minor alteration at Nabarlek (ca. 920 m.y.)	
Carpentarian 1610 m.y.				Low-grade metamorphism and metasomatism of the uranium deposits and surrounding rocks	Main mineralizing event, probably synchronous with faulting. Possible hydration of anhydrite
1650–1610 m.y.			Uplift. Extensive faulting and jointing of Kombolgie Formation and reactivation of some basement faults, displacements <600 m		
1650 m.y.	Deposition of Kombolgie Formation: quartz sandstone, minor conglomerate and siltstone; extrusion of basalt members				

Table 5.16. *Continued*

Age	Deposition	Igneous events	Tectonic events	Metamorphism	Events relevant to ore genesis
			Regional unconformity		
1688 m.y.		Intrusion of differentiated olivine dolerite lopoliths of Oenpelli Dolerite			Higher heat flow conditions. Continued erosion of Early Proterozoic rocks. Apparent age of U mineralization ca. 1700 m.y. at Ranger 1
1760 m.y.	Deposition of volcaniclastics, thickness unknown (<20 m?)	Effusive activity to S (Edith River Volcanics)			Possible introduction of U-enriched rocks. Erosion of Early Proterozoic rocks
1730–1870 m.y.		Intrusion of preorogenic granite (ca. 1870 m.y.) in NE. Post-orogenic (1780 · 1730 m.y.) in E and S	Period of complex deformation involving at least 4 fold episodes including 2 isoclinal events. Late near-vertical, mainly northerly faulting	Regional metamorphism to staurolite-almandine subfacies. Formation of Nimbuwah Complex by migmatization of 1870 m.y. granite. Formation of Nanambu Complex by metamorphism and accretion of Archaean granite and Kakadu Group	Possible transport of U by metamorphic hydrothermal fluids. Possible development of fault breccia zones. Period of major connate and groundwater movements. Apparent age of U mineratization ~1800 m.y. (minor occurrence)
Early Proterozoic		Intrusion of quartz-dolerite sills and minor dykes of Zamu Dolerite	Possible period of non-deposition		Higher heat flow conditions
	Koolpin Formation: siltstone, shale, pyritic carbonaceous chert, banded siltstone				Possible transport of U and precipitation in black shales
			Unconformity		
	Nourlangie Schist: sandstone, siltstone and shale		Probable mild folding at close of deposition		
			Possible local unconformity		
	Cahill Formation: clayey sandstone, siltstone with limestone and carbonaceous shale near base		Stable shelf surrounding moderately mature hinterland; quartz-rich upper member represents gradual transgression over shelf		Transport of U and precipitation in reduced environments and possibly in evaporites. Possible diagenetic alteration of clays to chlorite
			Possible disconformity		
	Kakadu Group: arkose, sandstone, minor shale		Juvenile hinterland		Possible transport of U – no known precipitation

Table 5.16. *Continued*

Age	Deposition	Igneous events	Tectonic events	Metamorphism	Events relevant to ore genesis
			Unconformity		
2200?–2500 m.y.			Erosion of granite basement, removal of Archaean cover rocks		Possible mechanical transport of U-reduced species
			Uplift		
Archaean 2500 m.y.			Crystallization of granite basement		Introduction of U-enriched rocks into crust

gional metamorphism and the deposition of the Kombolgie Formation. The 900 m.y. event was associated with widespread sericitization that may have erased evidence of an earlier uranium generation, as suggested by Ewers et al. (1983) for the Nabarlek deposit.

Maas and McCulloch (1988) provide Sm/Nd isotope data giving identical ages for primary uranium mineralization at Jabiluka II (1614 ± 132 m.y.) and Nabarlek (1616 ± 50 m.y.). Sm/Nd data for uraninites from Koongara are scattered, but indicate a model age of 1650 to 1600 m.y. Uraninites from Ranger do not form an isochron of Sm/Nd values, but indicate a possible age range of 1750 to 1600 m.y.

Ludwig et al. (1987) identified apparent U/Pb ages of 1732 ± 20 m.y. and 1437 ± 40 m.y. for the Ranger and Jabiluka mineralization respectively, and an episode 600 to 400 m.y. ago. The authors conclude from these data that a first (pre-Kombolgie Formation) high-grade concentration of uranium as established for Ranger occurred after the climax of regional metamorphism but at a time when early post-metamorphic plutons were still intruded. Later (post-Kombolgie) high-grade mineralization as typically found in Jabiluka, Koongara, and Nabarlek, probably originated by redistribution of the earlier uranium concentrations, although these earlier concentrations may have been of very low grade. $^{207}Pb/^{206}Pb$ ages older than ca. 1400 m.y. were not established at Jabiluka, which argues against an in situ remobilization in this deposit of high-grade pre-Kombolgie ore. The presence of relatively high contents of common Pb in many of the Jabiluka samples suggests that the 1437-m.y.-old mineralization event was not sufficiently effective to remove lead such as the radiogenic lead generated from the 1737 or 1437-m.y.-old generations from the site of ore formation. This implies that reworking in situ can be envisioned only for the case that the original uranium accumulation was of very low grade.

By far the most significant disturbance of the U-Pb isotope system occurred in a poorly defined interval about 600 to 400 m.y. ago. During this period, most of the post-1.4 b.y. radiogenic Pb of the high-grade ores of Jabiluka were removed. The ore at Ranger was similarly affected, but not as strongly. Some of the ores of both deposits also experienced a net loss of uranium or alternatively a gain in radiogenic lead during this interval.

Ore Controls and Recognition Criteria

Significant ore controlling or recognition criteria of the uranium deposits in the Alligator Rivers Uranium Field include:

Host Environment

- All deposits occur within the lower member of the Cahill Formation or a supposed correlative thereof.
- Host rocks are predominantly highly brecciated quartz-muscovite/sericite-chlorite schists which grade laterally into carbonate. Graphite is a constituant of these schists or adjacent layers at Jabiluka, Ranger One, and Koongarra but Ewers et al. (1984) do not find any apparent correlation between the presence of graphite and the concentration of uranium.
- The stratigraphic horizon hosting Jabiluka, Ranger One, and Koongarra is regionally a carbonate unit but almost devoid of carbonate at the deposits. Position of the ore hosting breccias-schists suggests, however, a close

correlation with the presumed original distribution of the bedded carbonate units.
- Most deposits occur in the proximity of an Archean complex (Nanambu) affected by younger migmatization.
- All large deposits are located immediately below the Middle Proterozoic unconformity covered by red bed type sandstone with intercalated volcanics (Kombolgie Fm.).

Alteration

- Alteration products include chlorite, white mica/sericite/illite, hematite, quartz, chert, dolomite, magnesite, and calcite.
- Mg-rich chlorites prevail in the immediate vicinity of the ore zones, suggesting Mg-metasomatism, whereas Fe-chlorite together with white mica is apparently more dominant in the outer halo (Wilde et al. 1988).
- Decarbonatization and locally variable desilicification modified the host lithologies, resulting in volume reduction.
- Extension and intensity of alteration halos around individual deposits is variable, ranging from few ten meters as at Ranger One and Koongarra to more than 200 m at Jabiluka and ca. 1000 m at Nabarlek.
- An inner alteration halo measuring a few meters to some tens of meters is overprinted on an outer halo (Fig. 5.14).
- Alteration follows primarily structures and is commonly most intense within the brecciated ore zones.

Mineralization

- Mineralization is monometallic except for local economic contents of gold.
- Principal U phases are uraninite and pitchblende.
- Associated metallic sulfide minerals, dominantly Fe, Cu, and Pb-sulfides are present in minor amounts only, as opposed to hematite, which is a common component in ore zones.
- Dominant gangue mineral is Mg-rich chlorite and, to a lesser extent, white mica.
- Ore and associated minerals cement breccias and form veins and veinlets within tabular, lenticular or bowl-shaped zones localized in more ore less strata-concordant breccia zones (Figs. 5.20 to 5.22), except for Nabarlek, which trends oblique to the host strata.
- Mineralization is practically absent from the cover rocks.
- Formation temperatures during mineralization are bracketed between 300 and 95°C. The upper limit is defined by relict metamorphic muscovite in altered host rock, retaining peak metamorphic K-Ar and Rb-Sr signatures characteristic for temperatures not exceeding 300°C (Page et al. 1980). The lower limit is concluded from CO_2-rich fluid inclusions (see below) demanding temperatures of at least 95°C (Wilde et al. 1988).

Metallogenetic Concepts

A variety of models have been put forward for the origin, transport, and fixation of the primary uranium generation. The two most recently published models are provided by Needham et al. (1988) and Wilde et al. (1988). The two models represent two end members of favored hypotheses with respect to the time of ore formation, viz. an origin in pre-Kombolgie Formation versus a post-Kombolgie Formation time. While these two models involve *supergene and diagenetic processes* and refute a hypogene genesis of the uranium deposits, Binns et al. (1980b) are proponents of a hypogene origin of the ore.

Model I: Pre-Kombolgie Ore Formation

Needham's et al. (1988) model follows to some extent that of Ferguson et al. (1980b) and Ewers et al. (1984). The authors state that subsequent to the regional metamorphism a period of weathering imposed a saprolitic profile as much as 100 m deep and peneplaned the Lower Proterozoic rocks. During this period, solution of the carbonate horizons resulted in solution collapse structures and brecciated zones which became the hosts for mineralization at Jabiluka, Ranger and Koongarra. Insoluble residue of breccia fragments accumulated in these breccia zones together with washed-in material such as clays, soil constituents, and perhaps organic material now represented by thucholite. The presence of biogenic carbonate and the postulated existence of sulfate-reducing bacteria within the breccia zones support the presence of organic substances (Donnelly and Ferguson 1980).

The great depth of solution cavity development to 600 m below the Middle Proterozoic

unconformity at Jabiluka is attributed by McArthur, G.A. (in Needham et al. 1988) to a paleotopographic high of at least 250 m, which presumably facilitated the percolation of waters.

In contrast to the deposits mentioned above, Nabarlek and deposits in other districts of the Pine Creek Geosyncline (Rum Jungle, South Alligator Valley) occur in tectonically generated fractures and breccias.

The *main mineralizing event* occurred after brecciation and fracturing and prior to the deposition of the Kombolgie Formation, which is deduced from the lack of mineralization in the cover rocks. The nature of the ore bodies indicates that they formed from downward percolation of mineralizing solutions. Criteria supporting such a mechanism include ponding effects causing uranium enrichments on the upper side of steeply dipping impermeable barriers in the mineralized zones, bottoming out of mineralization against impermeable mafic intrusives as at Jabiluka I and Nabarlek, and limited vertical continuity of the deposits. During the episode when clays and organic matter accumulated within the breccia zones, the plumbing system within these structures permitted migration of groundwater which was of low temperature, CO_2-rich, and contained uranium as uranyl carbonate complexes. These waters are thought to have probably also transported other elements characteristically enriched in the ore zones, viz. As, Au, B, Co, Cu, Li, Mo, Nb, W, and REE. Alternatively, the ore zones might have partly inherited these elements from the carbonaceous-rich residue produced during formation of the breccias.

Precipitation of uranium occurred in response to reduction in the anaerobic organic-rich environment in the breccias. Reduction may have further been facilitated by redox processes involving Fe^{2+} contained in phyllosilicates and other ferrous iron-bearing minerals as proposed earlier by Ewers and Ferguson (1980). Enrichment of uranium was possibly also enhanced by U adsorption on particulate substances.

Once the deposits were sealed either by compaction of the postulated regolith over topographic lows or by loading and dewatering of clay within the breccias, thereby reducing permeability, all subsequent processes recorded in the deposits occurred as in situ *modifications*. These modifications may have been triggered by high heat flow conditions generated by mafic magmatism of the pre-Kombolgie Oenpelli Dolerite and flows intercalated in the Kombolgie Formation.

Later igneous intrusions probably produced the temperature of about 270°C documented by stable isotope data by Donnelly and Ferguson (1980). During these events amorphous uranium oxides may have recrystallized to euhedral habits (uraninite) in disseminated distribution.

Very mild conditions, as forwarded by Binns et al. (1980b) and Ewers and Ferguson (1980), probably remobilized disseminated uraninite and redeposited the uranium as stringers and colloform aggregates of pitchblende subsequently, e.g., during the ca. 900 m.y. and ca. 500 m.y. episodes which may have been generated by epeirogenetic movements. The 900 m.y. event is contemporaneous with Upper Proterozoic sedimentation southwest of the Pine Creek Geosyncline and the 500 m.y. event correlates with the development of the Daly River Basin to the south (and with intrusion of basic dikes).

Preservation of the ore bodies was achieved by rapid deposition of cover rocks. The Middle Proterozoic Kombolgie Formation apparently fulfilled this protection request (Needham et al. 1988).

Model II: Post-Kombolgie Ore Formation

Wilde et al. (1988) studied fluid inclusions from Jabiluka, Koongarra, and Nabarlek. They endorse a post-Kombolgie Formation origin of the uranium mineralization and arrive at the following summarized hypothesis based on these *metallogenetic parameters*:

- All deposits occur within or adjacent to reverse fault zones which are of post-Kombolgie Formation age, as reported by Johnston (1984). (Note: Accepting this statement as valid does not exclude reactivation of pre-Kombolgie structures.)
- Quartz, pyrite, and/or hematite occur in pre-ore veins and breccias.
- Alteration associated with mineralization at Jabiluka postdates deposition of the Kombolgie Formation (see remarks below).
- Mineralization is associated with more restricted pervasive alteration manifested by growth of white mica, Mg-chlorite, anatase and locally hematite or apatite in the basement and along the sub-Kombolgie Formation uncon-

formity. This alteration overprinted earlier alterations.

- Ore formation postdates Mg-chlorite, the principle gangue mineral, and white mica. It is accompanied by desilicification which can be substantial, as documented by Wilde and Wall (1987) at Nabarlek, where up to 40% of SiO_2 were removed from the vicinity of the ore zone.
- Native gold is present as inclusions and veinlets in uraninite, reflecting gold deposition overlapping that of uraninite.
- Veinlets of dolomite and occasionally quartz, often with minor chalcopyrite and galena, represent the last stage of mineralization.
- An incongruent dissolution event overprinted the primary ore, resulting in formation of coffinite.
- Fluid inclusion data outlined earlier indicate two prominent fluids which were active during the time span of alteration and mineralization.

Wilde et al. (1988) conclude from these data that mineralization resulted from *interaction of two fluids* distinct in terms of oxidation state and salinity which derived from overlying sediments. The authors propose faulting as the mechanism to permit access of the fluids into the relatively impermeable basement and to facilitate mixing of the two fluids. They also attribute the extreme differences in pressure determined from halite dissolution to reflect variation from lithostatic to hydrostatic pressures at a depth of ca. 6 km due to faulting.

The alteration and assumed ore-forming solutions supposedly evolved (successively) from overlying terrestrial, evaporite-bearing sediments (McArthur Basin) during deposition and compaction of the cover sequence. The variations in salinity between the two fluids are explained as sedimentary brines tapped from various levels within the sedimentary pile.

An *early invading hypersaline brine* is thought to have become reduced by interaction with the basement rocks. Wilde et al. infer that the fluid, at a temperature in excess of 240°C, achieved saturation with respect to the relatively reduced Fe-chlorite and white mica in the alteration zone preserved in the outer alteration halo at Nabarlek. It developed into a high pressure (1.6 kbar) "resident" brine. The high pressure presumably reflects deep burial under a cover about 6500 m thick.

Continued brittle fracturing permitted influx of an originally cooler, more oxidized, *less saline, low pressure CO_2-bearing solution* from higher up, or laterally in the sedimentary sequence. The solution was very probably in equilibrium with hematite and possibly anhydrite in its provenance environment. Ingress of this solution to the site of ore precipitation was associated with heating to the ambient temperature at a depth of ca. 6 km. After the fluid achieved thermal equilibrium with the surrounding rock, it was consequently capable of dissolving and removing silica, and mixing of the two brines produced the alteration as observed, for example, in the inner halo at Nabarlek. Mixing of the two fluids is also proposed by Wilde et al. (1988) as the possible mechanism for ore formation.

The *problem* with applying fluid inclusion data as evidence for processes involved in actual uranium deposition is the lack of suitable gangue minerals which are unequivocally in paragenesis with uraninite. In the Alligator Rivers district, Mg-chlorite is the main gangue mineral, while quartz and carbonates appear to be earlier or later than the earliest ore mineral stage. The above discussed fluid inclusion data may thus not necessarily manifest ore formation but rather an early alteration and/or later modification/remobilization event.

Wilde et al. (1988) address this point. The analyzed hydrothermal quartz from veins and breccia cement predates mineralization. Most fluid inclusions are secondary, however, and thus may have trapped fluids which were coeval with or later than uranium precipitation. Another criterion is put forward by these authors in support of the metallogenetic validity of the presented fluid inclusion data. Accidental solid inclusions of primary alteration minerals have been found in fluid inclusions. They are believed to evidence a link between these fluid inclusions and ore formation. Fluid inclusions in post-ore dolomite are likely to be primary and represent a fluid present after mineralization, i.e., they are the final product of the mineralizing event.

Gustafson and Curtis (1983), based on their work at Jabiluka, arrive at the following genetic concept, which also postulates a post-Kombolgie Formation ore genesis.

Intense chloritization in and above the ore zones is the result of a metasomatic event(s) which followed diagenesis of the Kombolgie Formation. The fluids necessary for the alteration

were probably *meteoric-diagenetic groundwaters* derived from the Kombolgie Formation. Their movement, it can be speculated, was driven by a regional heating event which was also manifested by intrustion of the phonolite and/or diabase dikes.

The major *channelways* for movement of metasomatic fluids below the unconformity were bedded carbonates in the lower member of the Cahill Formation. The initial permeability, which led to the concentration of subsequent solution flow within these units, was probably the result of minor karst development at the profound pre-Kombolgie unconformity. The subsequent dissolution of magnesite and dolomite marbles by hydrothermal fluids produced large volumes of collapse breccias and markedly increased the Mg-content of the fluids. Highly fractured graphitic schists were stoped into the open spaces which were also channelways of major solution flow. In theory, this produced an opportunity for the interaction between uranium-bearing fluids and carbonaceous material that would have resulted in the *reduction and fixation* of uranium. (Since graphite itself is chemically inert, it remains unknown what actually caused the reduction except for the speculation of a reactive alteration product of graphite.)

In the overlying sandstones, practically no pitchblende was deposited, because no organic carbon was available for reduction, even though solutions may not have been exhausted of uranium. While reduction was essential for uranium fixation, this alone was not an adequate mechanism for the uranium precipitation from solutions which themselves were relatively reducing, as suggested by the Fe^{2+}/Fe^{3+} ratio of chlorite in the Kombolgie Formation.

The formation of chlorite, at least some of it apparently coprecipitated with minute inclusions of pitchblende, is a feature of the mineralization process closely linked to uranium fixation. But it can only be speculated on the processes involved in the paragenetic formation of pitchblende and chlorite. One of the critical parameters is the rather close correlation of mineralization with chlorite, more oxidized than chlorite in the surrounding metasediments and sandstone. Ferguson et al. (1980b) suggest that the oxidation of iron in the chlorites was completed with the precipitation of uranium, whereas Gustafson and Curtis (1983) suggest that this oxidation took place long after the mineralization. Based on these and other research data, Gustafson and Curtis (1983) propose that the high-grade uranium *ore formation* resulted from a relatively low-temperature (100–200°C) hydrogenic system of groundwater activated by a regional thermal event contemporaneous with the phonolite and/or diabase intrusions. The circulation of the fluids was largely through permeable carbonate units of the lower member of the Cahill Formation close to the unconformity and through fault-solution collapse breccias in the surrounding schists and overlying sandstone. The ore mineral deposition may have been coupled with precipitation of chlorite and a resultant drop of pH from alkaline approaching neutral. The drop would decomplex U^{6+} compounds and allow its reduction where organic material was available. Reduction could not occur in sandstone barren of organic material.

Sandstones of the Kombolgie Formation were an essential part of the ore-forming hydrologic system after the lithification of the lower thick clastic section, but possibly contemporaneous with diagenetic events in the upper part.

Gustafson and Curtis's (1983) model concurs in many respects with those of Eupene (1980) and Hegge et al. (1980), who ascribe the mineralization to post-Kombolgie metasomatism, guided largely by collapse brecciation following dissolution of carbonate sequences of the Cahill Formation. They both, however, stress the probability of lower grade pre-Kombolgie uranium concentrations possibly related to late-stage metamorphic events.

Differences between the above model and those of other geoscientists include:

Ferguson et al. (1980b), Ewers et al. (1984) and Needham et al. (1988) call primarily for a pre-Kombolgie Formation time of ore formation rather than post-Kombolgie.

Ypma and Fuzika (1980) and Wilde et al. (1988) consider a mixing of very saline brines with a more CO_2-rich meteoric fluid as a mechanism for mineralization.

Crick and Muir (1980) propose a *sabkha environment* in which uranium was enriched in evaporitic sediments. Expulsion of uranium-rich brines took place during diagenesis and deposition of uranium in deposits is postulated to have occurred during post-metamorphic replacement of evaporites by magnesite.

In contrast to the above models, Binns et al. (1980b) suggest that stable isotope data indicate a

deep-seated, *hypogene source* for the initial mineralizing fluids which were possibly modified by a mixture with surface water. They point out that the Jabiluka ores are enriched in elements such as Be, Sc, Y, Nb, Sn, Mo, Bi, and possibly B (Binns et al. 1980a; Ferguson and Winer 1980), as well as in Hg (Ryall and Binns 1980) and total REE (McLennan and Taylor 1980). Lithium is enriched in both ores and the retrogressed aureole, and thorium is low. Granitic gneisses which carry partly altered primary uraninite within the reactivated Archean Nanambu Complex underlying Jabiluka are considered a favorable source. Binns et al. postulate that Jabiluka is located in the upwelling discharge zone of a large fluid convection cell penetrating these source rocks. Fracturing due to epeirogenic movements associated with deposition of the Kombolgie Formation, or with its subsequent faulting, is suggested as a reason why the mineralization episode was deferred until the 1550–1440-m.y. age period indicated by geochronology.

References and Further Reading for Chapter 5.2.1
(for details of publications see Bibliography)

Battey et al. 1987; Berkman 1968; Berkman and Fraser 1980; Bone 1983; Compston and Arriens 1968; Condon and Walpole 1955; Crick and Muir 1980; Crick et al. 1980; Curtis 1985; Dodson 1972; Dodson et al. 1974; Dodson and Prichard 1975; Donnelly and Ferguson 1980; Dunn 1962; Durak 1983; Durak et al. 1983; Eupene 1980; Eupene et al. 1975; Ewers et al. 1983, 1984, 1985; Ewers G, pers commun.; Ewers and Ferguson 1980; Ewers and Higgins 1985; Ferguson 1980, 1984; Ferguson et al. 1980a, 1980b; Ferguson and Goleby (eds.) 1980; Ferguson and Winer 1980; Fraser 1980; Frishman et al. 1985; Fuzikawa 1982; Giblin and Snelling 1983; Goulevitch 1980; Gustafson and Curtis, 1983; Hegge and Rowntree 1978; Hills and Richards 1972, 1973, 1976; Hochman 1980; Ingram 1974; Johnston 1984; Koul et al. 1984, 1987; Ludwig et al. 1987; Maas 1989; McLennan and Taylor 1980; Mumme et al. 1979; Nash and Frishman 1982, 1983, 1985; Needham 1979, 1984, 1985; Needham et al. 1979, 1980, 1988; Needham and Roarty 1980; Needham and Stuart-Smith 1976, 1980, 1984, 1985; Noakes 1949; Nutt et al. 1984; Ojakangas 1986; Page 1976; Page et al. 1980; Pagel et al. 1984; Paterson et al. 1984; Plumb and Derrick 1975; Richards et al. 1977; Riley et al. 1980; Rossiter and Ferguson 1980; Ryan 1977; Smart et al. 1975; Stewart 1965; Stuart-Smith et al. 1980; Wall et al. 1985; Walpole and Crohn 1965; Walpole et al. 1968; Wilde and Wall 1987; Wilde et al. 1985, 1988; Ypma and Fuzikawa 1980.

Other authors have published papers on the individual deposits of the Alligator Rivers Uranium Field. They are listed in Battey et al. (1987) and the reader is referred to this publication.

5.2.2 Subunconformity-Epimetamorphic Uranium Deposits in Albitized Metasediments: Uranium City Region, Canada

The Uranium City region, located north of Lake Athabasca in northern Saskatchewan (Fig. 5.1), comprises the Beaverlodge district around Uranium City and the Gunnar mine situated about 25 km SW of Uranium City. All deposits are in an area some 25 km wide and 40 km long. Mineralization is of two varieties, monometallic and polymetallic. All major deposits are monometallic. They have yielded more than 90% of the uranium production of the region. The largest amount of uranium (19 200 mt U_3O_8, average ore grade 0.25% U_3O_8) came from the 1660 m deep Ace-Fay-Verna mining complex. Remaining reserves in this complex are estimated at 8600 mt U_3O_8. All other mines produced cumulatively 11 400 mt U_3O_8, giving a total of almost 40 000 mt U_3O_8 resources including past production.

All major deposits of the Beaverlodge district are essentially of veinlike configuration and may be best defined as structure-strata controlled uranium deposits of the subunconformity-epimetamorphic type (subtype 2.2, Chap. 4) hosted by more or less albitized crystalline rocks below a distinct unconformity on which continental sediments rest. An exception appears to be Gunnar, which has many characteristics of a metasomatite-type deposit.

The Beaverlodge deposits are to some extent similar to the deposits of the Alligator Rivers district in northern Australia (Chap. 5.2.1) except that the latter display a distinct strata control (e.g., Jabiluka), while in the Beaverlodge district the structure control is more prominent and strata control appears to be subordinate. In addition, at Beaverlodge the basement host rocks underwent Na-metasomatism (albitization) whereas at the Alligator Rivers both basement host rocks and overlying sediments (Kombolgie Formation) are Mg-metasomatized.

The following description focuses on the major deposits and is largely based on Beck (1969,

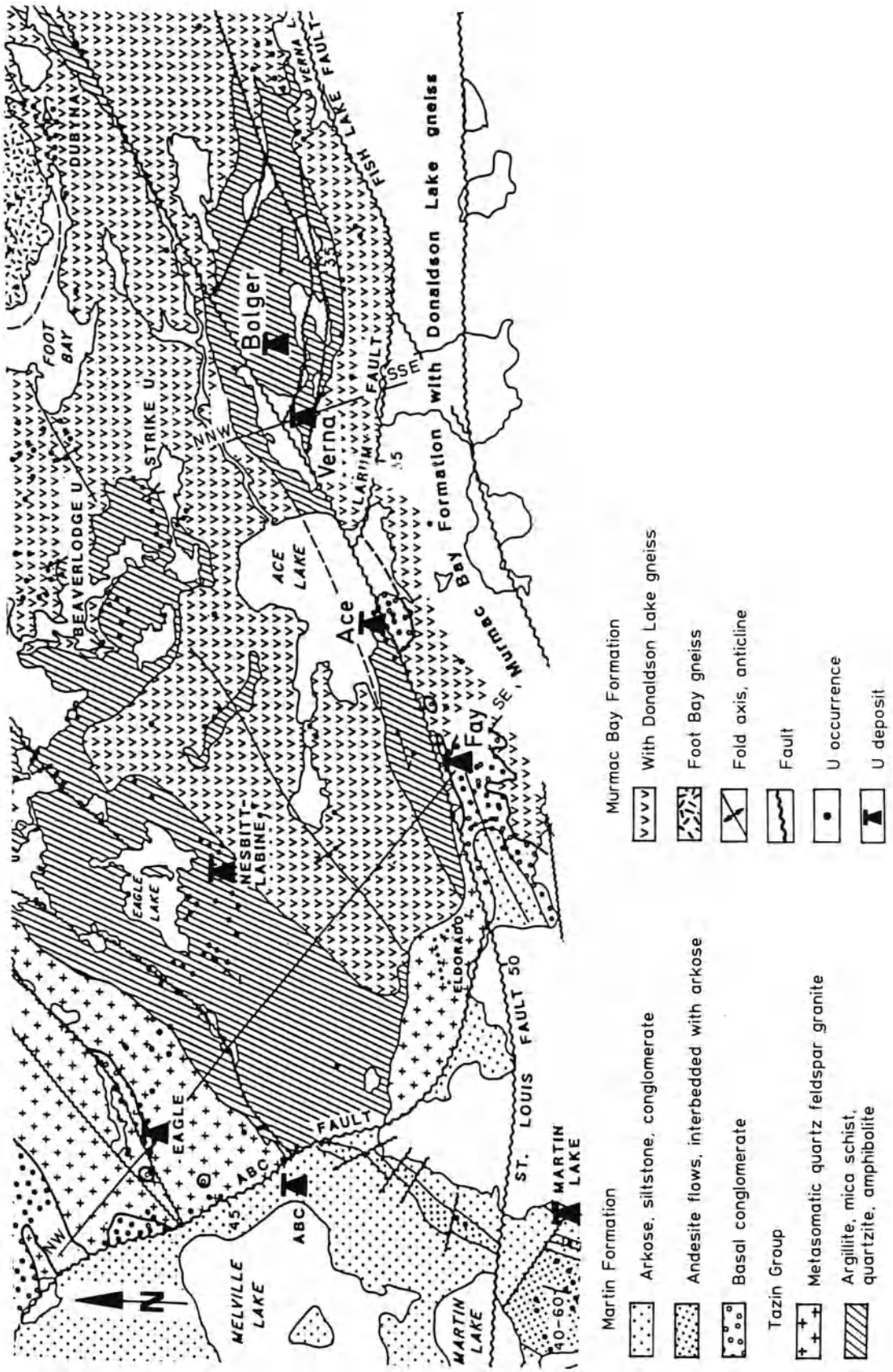

Fig. 5.23. Uranium City region, Beaverlodge district, geological map with location of U deposits. The major deposits Fay, Ace, and Verna are all located within Tazin metasediments along the St. Louis Fault. (After Smith 1986) (reprinted with permission from The Canadian Institute of Mining and Metallurgy)

1986), Kalliokoski et al. (1978), Smith (1986) and Tremblay (1972, 1978).

In several instances there are discrepancies in rock nomenclature, stratigraphic position of rock units, sequence of geological events, and other geological parameters among the various authors. Reconciliation of conflicting data has not been possible. This must be left to further research.

Geological Setting of Mineralization

Tremblay (1982) includes the geology of the Uranium City region in the Tazin Belt which is part of the Western Craton of the Churchill Structural Province in northern Saskatchewan.

The major deposits in the Beaverlodge area (Fay-Ace-Verna) (Fig. 5.23, Table 5.17) occur in the Fay Complex of the *Tazin Group*. These rocks were originally deposited as pelitic to psammitic, partly carbonaceous sediments of Middle to Upper Aphebian age (or late Archean according to Tremblay 1972, 1978) over a basement of Archean age. During the Hudsonian and earlier orogenies, the sediments were metamorphosed to an interbedded sequence of graphite-bearing quartzo-feldspathic gneisses, feldspathic quartzites, argillites, amphibolites, hornblende, and biotite schists. The metamorphic grade ranges from amphibolite to granulite facies with localized anatexis. The metasediments were tightly folded, and subsequently retrogressively metamorphosed to greenschist facies and affected by various alterations. Granites and pegmatites intruded during several stages.

The crystalline basement is unconformably overlain by the Paleo-Helikian *Martin Formation*, which consists of red bed sediments and locally interbedded volcanic flows. Deposition occurred in fault-bounded grabens. The Martin sediments were intruded by diabase dikes and sills and were slightly folded along NE-SW-trending axes during final Hudsonian deformation.

The basement paleosurface below the Martin Formation displays effects of mainly physical weathering.

Two major episodes of *faulting* have been recognized. The earlier phase occurred towards the end of or after the main period (D2) of Hudsonian folding and granitization. It is represented by E-W and NE-SW-striking mylonite and breccia zones a few meters to several hundred meters wide and up to 10 km long. The second phase of deformation produced faults which trend NE-SW, E-W, NNW-SSE, and NW-SE. This system created such major structures as the St. Louis, Black Bay, and ABC faults. Along some of the NE-SW-trending faults, major displacements took place producing either basins or grabens which were later filled with the Martin Formation.

Table 5.17. Uranium City region, Beaverlodge operations of Eldorado Resources Ltd., stratigraphic section and lithology. (After Ward 1984) (stars refer to the rock age dated)

Age (m.y.)	Stratigraphy/Lithology	
	Paleo-Helikian Martin Formation	
1490* 1630* 1799**	Diabase*, siltstone, shale Andesite, basalt*, porphyry** Arkose, sandstone, conglomerate	
	Aphebian Tazin Group	
	(Murmac Bay Formation and Fay Complex of Tremblay 1978)	
1975*	Pegmatite*, pegmatitic alaskite	
	Orange mylonite, feldspar rock, mylonitic alaskite	Mylonitic mica schist/paragneiss
	Argillite, paraschist	meta-argillite, migmatite
	Epidotic argillite, greenschist, phyllonitic amphibolite	Siliceous argillite, ultra-mylonite
	Quartzite	Silica, siliceous mylonite
	Diopside-calc-silicate rock	Dolomite
	Donaldson Lake Gneiss	
2100*	Alaskite*, leucocratic gneiss, (mafics <15%) amphibolite	Mylonite (<40% silica)
	Archean Foot Bay Gneiss	
2300* 3200**	Granitic crush rock Cataclasite*, augen-gneiss**, (mafics >15%), kakirite	Ultra-mylonite Amphibolite

Host Rock Alterations

Various alterations of metasomatic and hydrothermal nature affected the crystalline rocks of the Uranium City region during pre-, syn- and

post-ore episodes. Most prominent are albitization, epidotization, silicification, carbonatization, chloritization, and hematitization. At Gunnar, desilicification/episyenitization and carbonatization markedly altered the ore hosting zone within the albitized country rocks (albitic granite-albitite). Albite occurs in some veins intimately associated with pitchblende (Robinson 1955) suggesting a partial overlapping of Na-metasomatism and pitchblende deposition.

Principal Characteristics of Mineralization

Epigenetic mineralizations can be subdivided into those of simple (or monometallic) and complex (polymetallic) mineralogy. Over 90% of the deposits are monometallic, including all major ore bodies such as the Ace-Fay and Verna. Their distribution is restricted to the Tazin Group, whereas polymetallic deposits have been found both in the Tazin and the overlying Martin Formation. *Monometallic deposits* have pitchblende as the principal ore mineral and locally brannerite and coffinite. Associated metallic minerals include hematite, pyrite, and minor amounts of chalcopyrite, bornite, clausthalite, and galena. Calcite is the dominant gangue mineral but dolomite, quartz, chlorite, and locally albite are also present (Fig. 5.24).

Polymetallic mineralization consists of pitchblende accompanied by Co-Ni-arsenides and sulfides, Co-Ni-Pb-Cu-selenides and native Pt, Au, Ag, and Cu. Associated gangue minerals are calcite, dolomite, ankerite, siderite, quartz, chlorite, and abundant hematite. Polymetallic deposits are small in size (<60 mt U_3O_8).

The *basement hosted mineralization* occurs in subsidiary structures on both sides and within 200 to 300 m of major faults in the form of massive veins and veinlets (cm to m thick), and as disseminations in breccia zones (<15 m wide). Ore bodies may suboutcrop at the Paleo-Helikian unconformity or may be blind. The length of individual veins ranges from meters to tens of meters, rarely hundreds of meters. Depth extension, which is often intermittent, varies commonly between 100 to 300 m but persists for up to 1660 m in the Ace-Fay mine.

Large ore bodies are of two principal *configurations* characterized by different internal structural preparation and distinct host rocks as exemplified by the "01" and "09" ore bodies of Fay described by Smith (1986) (Figs. 5.25, 5.26). The first one, "01", is a highly elongated and steeply plunging breccia stockwork cemented

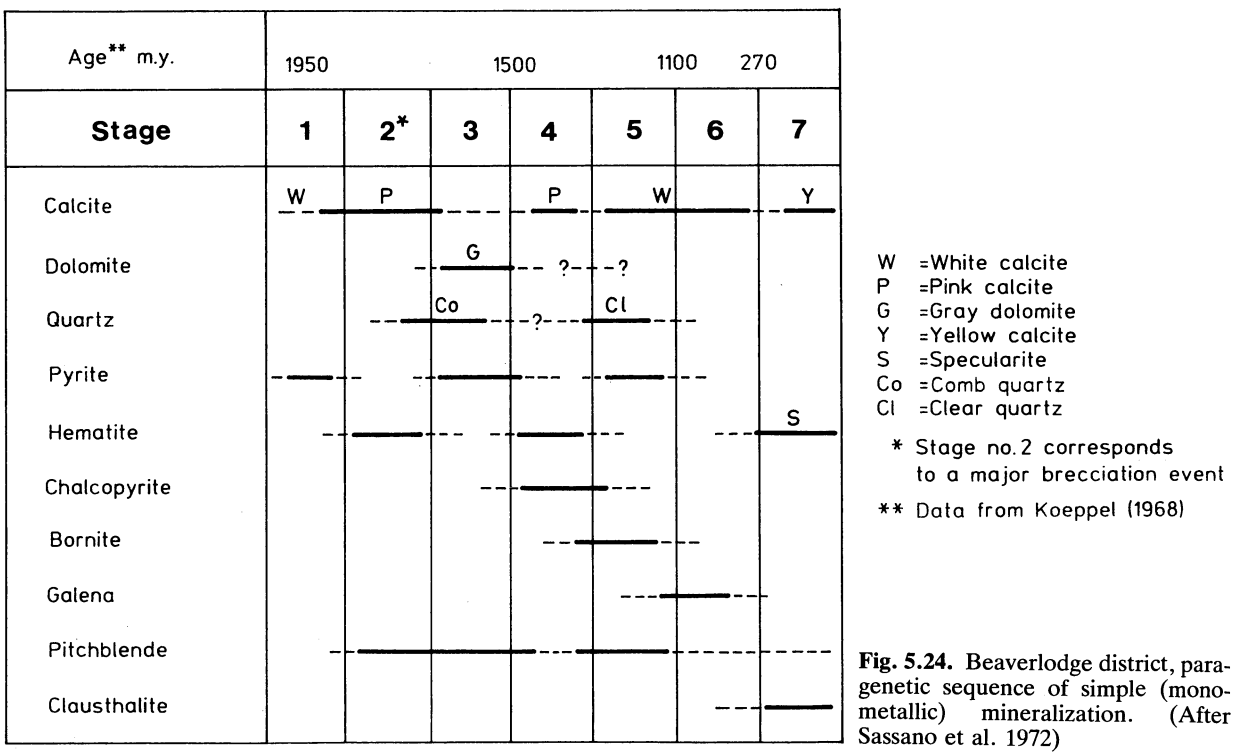

Fig. 5.24. Beaverlodge district, paragenetic sequence of simple (monometallic) mineralization. (After Sassano et al. 1972)

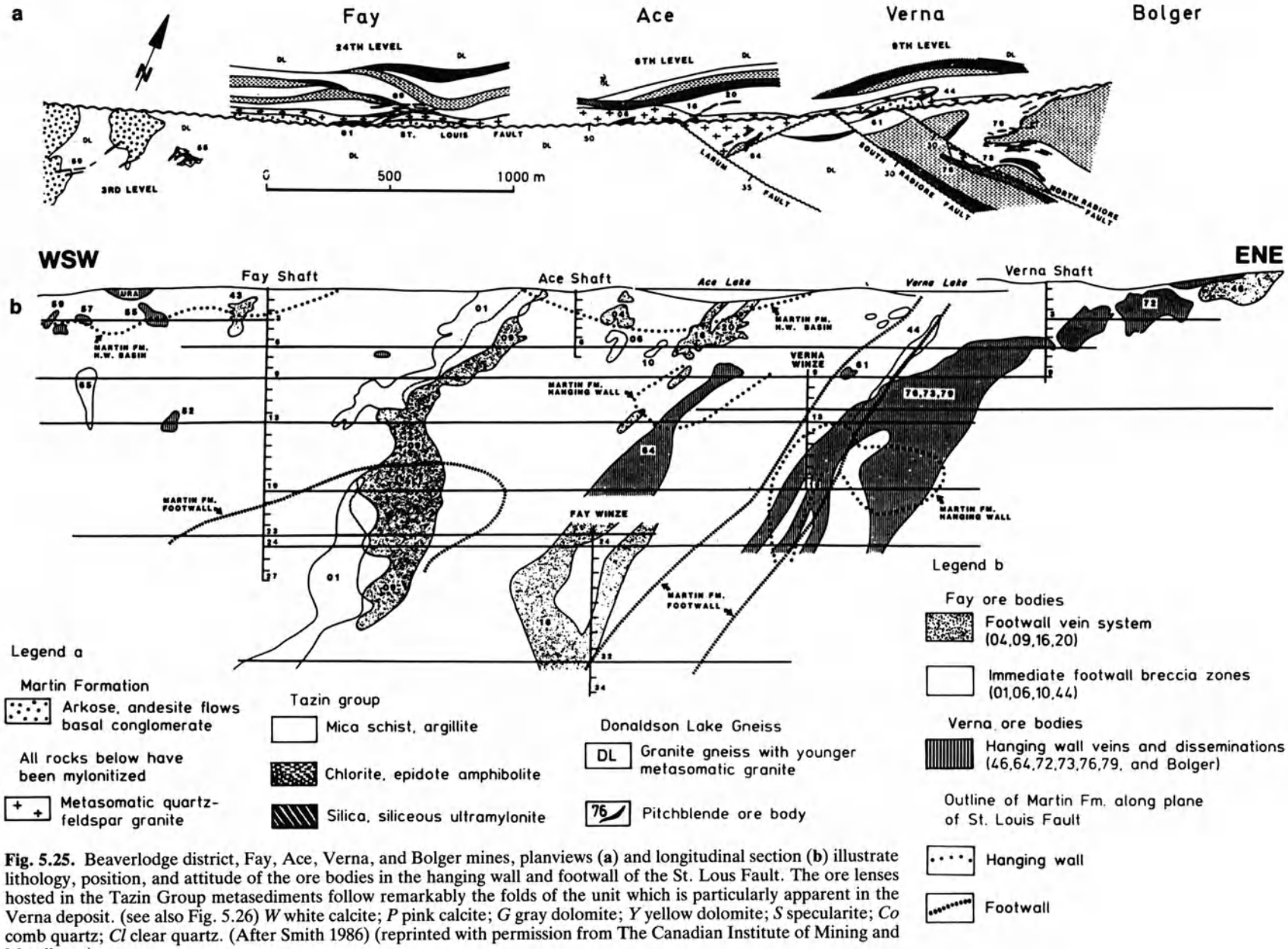

Fig. 5.25. Beaverlodge district, Fay, Ace, Verna, and Bolger mines, planviews (**a**) and longitudinal section (**b**) illustrate lithology, position, and attitude of the ore bodies in the hanging wall and footwall of the St. Lous Fault. The ore lenses hosted in the Tazin Group metasediments follow remarkably the folds of the unit which is particularly apparent in the Verna deposit. (see also Fig. 5.26) *W* white calcite; *P* pink calcite; *G* gray dolomite; *Y* yellow dolomite; *S* specularite; *Co* comb quartz; *Cl* clear quartz. (After Smith 1986) (reprinted with permission from The Canadian Institute of Mining and Metallurgy)

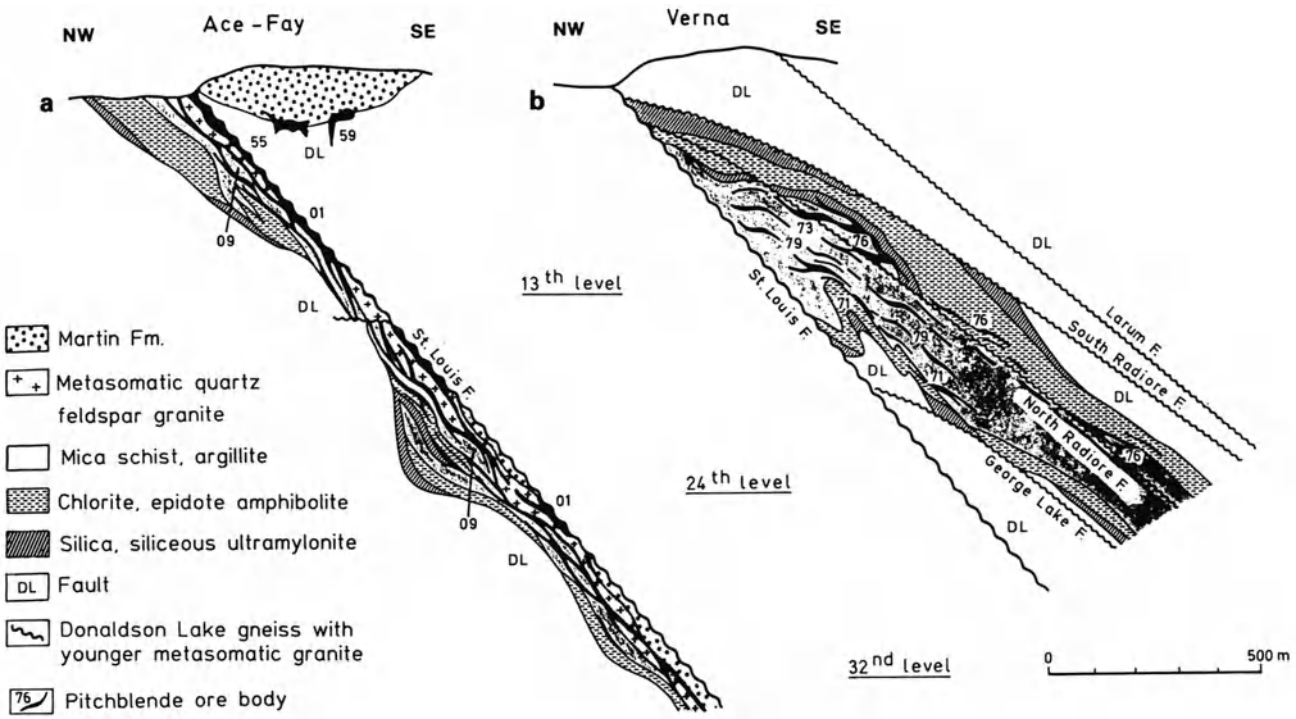

Fig. 5.26. Beaverlodge district, Ace-Fay and Verna deposits, generalized cross-sections displaying the attitude of ore lenses, their position in the hanging wall (**a**) and footwall (**b**) of the St. Louis Fault, and host rock lithologies. Smith (1986) shows Martin sediments down-faulted on the St. Louis Fault (**a**). Tremblay (1978) attributes these rocks to the Lower Proterozoic units. (After Smith 1986) (reprinted with permission from The Canadian Institute of Mining and Metallurgy)

by pitchblende and associated minerals. It is restricted to the immediate footwall of the St. Louis Fault in mylonitized quartz-feldspar metasomatic granite (quartz albitite or albitite according to Hoeve 1982) and parallel to that rock's contact with the underlying Tazin strata hosting the "09" ore body. The second variety, "09" is a highly elongated, steeply plunging network of veins emplaced in mica schist, argillite and amphibolite of the Tazin Group.

At least four generations of pitchblende have been established, with ages dated at about 1780–1740, 1110, 270, and 100 m.y. and less (Köppel 1968; Bell 1981, Table 5.18).

Potential Sources of Uranium

Although no distinct uranium source has been established various rock types have anomalous uranium background values indicating the presence of a uranium province and the availability of uranium for ore formation. Beck (1969) noticed three varieties of uraninite-bearing pegmatites which have contents of up to 0.08% U_3O_8. Within the metasediments, Beck found gneissic bands in zones of metamorphic and migmatitic rocks which contain uraninite, most commonly associated with biotite. Some uraninite-bearing granites and gneisses contain local concentrations of up to 0.07% U_3O_8. Tremblay (1978) reports contents of 0.3 to 6.8 ppm U for the main metasediments and up to 13 ppm U (average 5.4 ppm) in granites.

Ore Controls and Recognition Criteria

Significant ore controlling parameters or recognition criteria of the major deposits include:

Host Environment

- Deposits are emplaced in Archean-Lower Proterozoic crystalline rocks affected by regional metamorphism, retrograde metamorphism, and strong alteration.
- The basement is covered by red bed sediments and volcanics of Paleo-Helikian age (Martin Formation).

Table 5.18. Uranium City Region, selected geochronological data

Rock/Ore	Age in m.y.		Reference
Foot Bay Gneiss	2510	(U-Pb zircon)	Tremblay et al. 1981
Donaldson Lake Gneiss	2179	(U-Pb zircon)	Tremblay et al. 1981
Box, Frontier granites	2155 ± 40	(Rb-Sr whole rock)	Bell & McDonald 1982
Pegmatite (Ace-Fay area)	1975 ± 20	(Rb-Sr whole rock)	Sassano et al. 1972a
Gabbro dike	1835 ± 50	(K-Ar whole rock)	Wanless et al. 1967
Gabbro dike	1735 ± 40		Wanless ct. Tremblay 1978
Gabbro dike, chloritized	1721 ± 51		Tremblay 1972
Quartz-biotite-feldspar gneiss (8 km E of Uranium City)	1795	(K-Ar mica)	Lowdon et al. 1963
Martin Fm. basalt	1630 ± 180	(K-Ar whole rock)	Wanless et al. 1966
Martin Fm. gabbro sill	1410 ± 100	(K-Ar whole rock)	Wanless et al. 1966
Uraninite in pegmatite	(1) 1930 ± 40, (2) 1860	(U-Pb)	Köppel 1968 (1), recalculated by Bell 1981 (2)
Pitchblende	(1) 1780 ± 20, (2) 1740	(U-Pb)	Köppel 1968 (1), recalculated by Bell 1981 (2)
Pitchblende	(1) 1110 ± 50, (2) 1100	(U-Pb)	Köppel 1968 (1), recalculated by Bell 1981 (2)
Pitchblende	(1) 270 ± 15, (2) 270	(U-Pb)	Köppel 1968 (1), recalculated by Bell 1981 (2)
Pitchblende	100 to recent 270		Köppel 1968 (1), recalculated by Bell 1981 (2)

- Paleoweathering of the basement at the Paleo-Helikian unconformity was mainly of physical nature, which is in contrast to the chemically weathered Meso-Helikian paleosurface as preserved under the Athabasca Group further south (see Athabasca Basin Region, Chap. 5.1).
- Crystalline rocks, particularly in mineralized areas, exhibit an intense mylonitization of early age being rehealed prior to uranium emplacement.
- Most deposits occur at a specific stratigraphic level within the Tazin Group.
- Major deposits are hosted by or occur proximal to mainly mafic rocks (amphibolite, chlorite-epidote rock, chlorite schists, argillite).
- Few deposits are in granitoid rocks (Dubyna: quartz-feldspar granite adjacent to mafic Foot Bay Gneiss, Gunnar: albitized and carbonatized granite).
- Some small deposits, in particular complex-type mineralization, are in sediments and diabase of the Martin Formation.
- Secondary faults, fractures and breccia zones in proximity to regional or major faults (e.g., St. Louis, Black Bay, and Boom Lake faults) host most deposits.
- Structures of NW-SE, NE-SW, and E-W strike appear to be equally favorable for uranium emplacement.
- Uranium mineralization commonly occurs in a zone proximal to a major fault extending to a maximum of 200 to 300 m away from that fault.

Alteration

- Ore related wall rock alteration includes hematitization (dusty red hematite), chloritization (Mg and Fe chlorites) and carbonatization (mainly calcite) commonly extending for only a few centimeters and rarely up to 4 m into the walls of mineralized structures.
- Pre-ore alteration includes widespread hematitization reflected by disseminated hematite in breccia and mylonite zones and pink to red colored feldspars. Silicification, chloritization, epidotization, and carbonatization may be in part prior to or contemporaneous with early stages of mineralization.
- Widespread Na-metasomatism resulted in albitization, locally leading to albitite. Hoeve (1982) suggests an intimate connection between Na-metasomatism and pitchblende formation.

Mineralization

- Ore bearing structures may be simple veins, networks of interconnected veins and veinlets, and breccia zones.

- Tabular or planar ore shoots are elongated parallel to subparallel along the plunge of fold axes in host rocks.
- Host structures are only partially filled with mineralization.
- Ore zones may or may not outcrop on surface, e.g., at Verna all larger ore bodies are blind.
- Individual ore shoots preferentially follow specific horizons. In the Verna mine individual mineralized structures are arranged in a series of irregular lenses and tabular veins stacked above each other. They follow drag folds and contortions of the strata within the limits of the overturned syncline. For example, ore shoots of the "79" zone follow in cummulation the fold axis of the Tazin syncline staying within a horizon of argillaceous mica schist.
- Grade of the ore bodies may vary depending on the dip of the enclosing strate. For example, in the Verna deposit, at a steep to vertical dip in the plane of shearing, ore bodies quite commonly have higher grades and are narrower compared to those which are horizontally flattened by folds. Here the ore bodies are thicker but of lower grade.
- Two kinds of mineral associations exist, one of simple (monometallic) and one of complex (polymetallic) mineralogy.
- Deposits with simple mineralogy are restricted to the basement and contain several phases of pitchblende associated with calcite, chlorite, and quartz as paragenetic gangue minerals, and minor sulfides. Age of the first generation of pitchblende of this type is 1780 to 1740 m.y. (Köppel 1968; Bell 1981).
- Deposits of complex mineralogy have a similar mineral assemblage but have additionally Co-Ni-arsenides, sulfides and selenides, and native precious metals. Pitchblende of the complex ore assemblage is dated 1110 to 1125 m.y. (Köppel 1968; Bell 1981) which corresponds to the second generation of the simple type, and typically is hosted in structures cutting both Tazin metamorphics and overlying Martin sediments and volcanics.
- Initial temperature of ore formation is about 440 ± 30°C (Sassano et al. 1972b).

Metallogenetic Concepts

Most of the early investigators of the Beaverlodge uranium deposits postulated a magmatic hydrothermal origin, although some considered uraniferous Aphebian sediments as the source for the uranium. Sullivan (1957), Smith (1974), Langford (1977), and Tortosa and Langford (1986) have argued in favor of a supergene origin. Tremblay (1968, 1972) and Beck (1969) have proposed a metamorphic-hydrothermal model which was supported by Sassano et al. (1972b).

Ore formation in sensu stricto and the composition of the ore forming solutions have been discussed by Beck (1969, 1986). Based on mineralogical studies, Beck concludes that the paragenetic mineral sequences indicate a considerable change in the *chemistry of solutions* throughout a long and complex evolution of the mineralization. Sulfide minerals, in a general way, increased in variety and amount with time which suggests that the early uraniferous fluids were relatively free of other metal ions while later fluids must have been more enriched in metals. On a local scale, however, there are many diversions from or reversals of this sequence. In spite of the variations in content and quantity of various metals, the mineralizing fluids must have contained both calcium and CO_2 ions, as reflected by ubiquitous calcite associated with all pitchblende generations. Consequently, it may be deduced that uranium has been transported as carbonate complex. Initially, uranium may have been precipitated from a colloidal solution, as suggested by the colloform habit of early pitchblende. The later pitchblende, which is chiefly massive, has probably deposited from noncolloidal solutions.

With respect to the mechanisms of *ore mineral deposition*, Beck states that loss of pressure and catalytic reaction with iron were the crucial factors in causing precipitation and that the structural environment has determined which of the two factors was dominant in the formation of a specific ore zone.

Breccia zones and other open-space fractures provided the site for most of the large botryoidal masses and massive veins of pitchblende. Because these structures develop open spaces it has to be assumed that a loss in pressure occurred. On the other hand hematite is here not ubiquitous and therefore iron involvement cannot be considered significant for the precipitation of colloform and massive pitchblende. Beck therefore concludes that a drop in pressure has been the dominant factor in precipitating this pitchblende.

In contrast, fine-grained pitchblende disseminations are restricted to strongly hematitic

mylonite, and shear zones. In this environment confining pressures were probably high and the primary mechanism of pitchblende precipitation was most likely catalytic reaction of the uraniferous solutions with ferrous iron in the wall rocks.

Since their initial emplacement, the pitchblende accumulations have had a long history of *reworking and rejuvenation*.

Rejuvenation of pitchblende is believed to have been caused by localized tectonic-thermal events, including downwarping of the basement prior to deposition of the cover rocks, subsequent uplift and folding of the cover rocks, intrusion of diabase dikes and gabbro sills, and intermittent movements along the major faults related to epeirogenic movements in the Canadian Shield.

Beck (1986) addresses the *problematics* of interpreting relevant geological parameters with respect to their impact on ore formation. He points in particular to the following three criteria.

a) Does there exist a spatial relationship of the deposits to (pre-Martin) faults only or to the Paleo–Helikian unconformity as well on which the Martin Formation was deposited?
b) Is a chemical paleosol developed along the basement surface below the Martin Formation?
c) Is initial pitchblende formation related in time to a Hudsonian process, for example granitization, metasomatism (albitization) or perhaps to late orogenic retrograde metamorphism?

Beck (1986) notes to point a: that the deposits are more closely related to major faults and their subsidiary structures than to the *pre-Martin unconformity* although there appears to be a spatial relationship to both structures and unconformity. Smith (1974) argues for an unconformity relationship. He contends that all deposits are within 200 m of the unconformity. Smith explains the deep extension of the Ace-Fay veins (>1700 m), which is by far in excess of that of unconformity-contact deposits by suggesting that the St. Louis Fault closely follows the plane of the unconformity. The basis for this contention are slices and lenses of rocks defined by Smith as Martin Formation found down to a depth in excess of 2100 m along the trace of the St. Louis Fault. In contrast, Tremblay (1978) considers these rocks to be brecciated Tazin Group strata.

To point b: There is no chemical weathering profile developed on the basement surface. The Martin Formation rests directly on almost fresh Archean-Aphebian rocks except for a thin layer of detrital/*physical weathering* products.

To point c: *Initial pitchblende deposition* can most likely be attributed to a *Hudsonian event* as suggested by the coinciding parameters of geochronology giving an age of 1780 to 1740 m.y. for primary pitchblende, a K-Ar age for mica in metasediments of 1795 m.y. (Lowdon et al. 1963) and the structural relationship of deposits to Hudsonian faults which have been reactivated in later periods.

The *influence of the Martin Formation* could theoretically have been twofold. Its thickness, composition, and associated diagenetic processes may have had an impact on the original ore formation similar to that assumed for unconformity-contact type deposits in the Athabasca Basin. There is, however, no visible evidence of such an involvement. Also in order to exert any influence, the Martin sediments would have to be at least 1780 to 1740 m.y. old.

Another, more valid aspect is the role of the Martin Formation as a protective cover prohibiting leaching and destruction of near surface deposits by weathering. The postulated intense wet tropical period preceding the deposition of the Meso-Helikian Athabasca Group (see Chap. 5.1, Athabasca Basin Region) must also have been active in the Uranium City Region. Below the Athabasca Group lateritic type weathering extends to depths exceeding 100 m along structurally weakened zones. If not protected, near surface deposits would have been destroyed by these processes.

In conclusion, presently known data, which are rather limited particularly in the minerochemical and geochemical field (fluid inclusions, stable isotopes, geochemistry of metasomatites, U-Clarke figures), suggest with certain reservations a metamorphic-hydrothermal origin for the first pitchblende generation of the Beaverlodge deposits.

Tremblay (1978) presented a comprehensive model for the geological evolution of the Uranium City region which appears in principle still valid, and within this frame a *metamorphic-hydrothermal origin* of the Beaverlodge uranium deposits. His concept is as follows.

1. The *accumulation of sediments and volcanics* of the Tazin rocks started in Late Archean

time (this, however, is rejected by other authors, who propose a Lower Proterozoic age). The Fay Complex, regarded as the possible uranium source for the various uranium deposits of the Beaverlodge area, is near the base of the known Tazin succession, and is composed of interbedded metasediments and metavolcanics.

Some of these rocks have relatively high background uranium concentrations which are regarded as syngenetic accumulations.

2. The sediments and volcanics of the Tazin Group were folded, metamorphosed to the amphibolite facies, and locally granitized between 2300 and 2000 m.y., leading to the formation of granite, granite gneiss, and pegmatite dikes (approximately 2000 m.y. ago). This *orogenic activity* mobilized the uranium in the Tazin rocks into specialized granites and pegmatites while syngenetic uranium accumulations in the metasediments are now preserved in xenoliths within granite and gneiss. Some epigenetic (vein) deposits may have formed during these events, but no vein deposits of that age have been identified.

3. Toward the end of the Hudsonian orogenic activity (about 1800 m.y.), the Tazin rocks were cataclastically deformed. Wide mylonite and breccia zones developed accompanied by low-temperature retrograde metamorphism and the circulation of metamorphic-hydrothermal solutions. Tremblay suggests that uranium became mobilized during one of these last stages of metamorphism that affected the Tazin rocks and that the *original formation of the vein deposits* of the Uranium City Region occurred at this time by metamorphic-hydrothermal processes.

4. The *second main period* of faulting and formation of epigenetic (vein) deposits took place at about 1110 ± 50 m.y. The second generation of vein development corresponds to a period of uranium mobilization and concentration in the Beaverlodge area and in all of northern Saskatchewan. Faulting and uranium redistribution continued after this event, as evidenced by younger pitchblende ages. However, Tremblay (1978) notes, "it is possible that there was only one period of uranium mineralization at 1780 ± 20 m.y., and that all the other pitchblende dates represent merely periods of uranium remobilization and not new mineralization periods."

5. At a much later time, due to weathering and groundwater transport, uranium may have moved again with precipitation in breccias, along fractures, and at the unconformity to form supergene deposits. The Bolger deposit may be of this type.

This model is supported by Sassano et al. (1972b), who propose that the deposits were generated by metamorphic-hydrothermal fluids with some possible contribution of surface waters during the final stages of mineralization to an otherwise "closed" system. This hypothesis was suggested as a result of fluid inclusion and stable isotope ($\delta^{13}C$, $\delta^{18}O$) studies on dolomite, calcite, and quartz from ore of the Fay and Bolger mines. The studies identified five generations of carbonates and a cooling history from the initial phase of mineralization at 440 ± 30°C down to the final stages at about 80 ± 10°C.

Objections to any kind of ore-forming event related to granitization are expressed by Beck (1986). Rb-Sr dates for the pegmatites from the Box and Frontier granites (1975 m.y. and 2155 m.y.) are too old to link this episode to that of initial pitchblende emplacement (1780 to 1740 m.y.). This, of course, does not contradict ore formation related to a late metamorphic/orogenic event. By comparison with the Hercynian terrane in Europe, which also evolved through several orogenic episodes, all major uranium deposits formed during the latest orogenic events. This tends to be consistent with the Beaverlodge deposits, because initial pitchblende precipitation coincides roughly with a late metamorphic event dated about 1790 m.y. which may have been the motor for the generation and circulation of the ore solutions.

The second problem addressed by Beck (1986) is the dilemma of the spatial coexistence of the two diverse types of ore, monometallic and polymetallic. Hoeve and Sibbald (1978) and Hoeve (1978, 1982) contend, however, that the two paragenetic assemblages are not cogenetic; instead they have formed during subsequent stages.

This is indicated by different radiometric ages, stratigraphic setting, and wall rock alterations. Deposits of simple mineralogy are restricted to Tazin lithologies, and yield a pitchblende age of 1780 to 1740 m.y. Deposits of complex mineralogy are hosted by fractures in Tazin metamorphics and overlying unmetamorphosed Martin strata as well, yield an age of about 1125 m.y., and host rock alteration is similar to that of unconformity-contact type deposits in the Athabasca Basin. Hoeve and Sibbald conclude

that monometallic (simple) deposits are of Hudsonian metamorphic-hydrothermal origin and polymetallic deposits belong to a second generation of mineralization corresponding to the first remobilization episode at about 1100 m.y. established by Köppel (1968). They also compare the polymetallic deposits with the unconformity-contact type deposits of the Athabasca Basin and consider both to have formed as a result of the same metallogenetic event.

References and Further Reading for Chapter 5.2.2
(for details of publications see Bibliography)

Alcock 1936; Beck 1969, 1970, 1986; Christie and Kesten 1949; Dawson 1956; Eldorado 1964; Evoy 1961, 1986; Gandhi 1983; Griffith 1967; Hoeve 1982; Kalliokoski et al. 1978; Krupicka and Sassano 1972; Lang et al. 1962; Murphy 1948; Robinson 1955a, 1955b; Sassano 1972; Sassano et al. 1972a, 1972b; Smith 1974, 1986; Thomas 1982; Tortosa and Langford 1986; Tremblay 1958, 1970, 1972, 1978; Trueman and Fortuna 1976; Turek 1965; Ward 1984.

5.3 Examples of Vein-Type Uranium Deposits (Type 3: Chap. 4)

5.3.1 Intragranitic Vein Uranium Deposits: Limousin/La Crouzille District, France

The Limousin region is located in the northwestern Massif Central and includes the La Crouzille uranium district, the most important uranium district of France. Although most of the deposits are small, (some tens to few thousand tonnes U_3O_8) the entire district cumulatively contained estimated reserves including production in excess of 40 000 mt U_3O_8. Ore grades range in average between 0.1 and 0.6% U_3O_8.

Most deposits are centered in an area, 15 km in N-S length and 5 km in E-W width, within the Saint Sylvestre granitic massif (Fig. 5.27). The deposits are structurally controlled within a distinct leucogranite considered the parent rock of the uranium and are therefore classified as granite-related, intragranitic vein uranium deposits (class 3.1.1., Chap. 4). Two varieties are distinguished, classical veins and disseminations in episyenite bodies.

The following description is largely based on Leroy (1978a,b) who presents a comprehensive study on the Limousin deposits (Margnac and Fanay). Additional information is taken from Geffroy 1971, Moreau and Ranchin (1971), Ranchin (1971), Sarcia and Sarcia (1956), and other geoscientists cited later under References.

Geological Setting of Mineralization

The Limousin uranium region is within the Moldanubian Zone, i.e., the core zone of the Hercynian orogenic belt (380–300 m.y.) and located at the junction of two regional structural belts. The region is underlain by Proterozoic to Lower Paleozoic metamorphics which were intruded by granites and regionally metamorphosed, locally attaining anatexis, during the early Paleozoic. During the Hercynian Orogeny, a variety of granites invaded the ancient metamorphic basement. In the Crouzille uranium district (Fig. 5.27) the *Saint-Sylvestre leucogranitic complex* intruded ca. 325 m.y. ago (Holliger et al. 1986). It includes two principal genetically related granitic facies, the Brâme and the St. Sylvestre (-St. Goussaud) facies. Both are transected by dikes and stocks of younger fine-grained granite and other magmatites (lamprophyre, pegmatite, aplite, quartz veins). Intrusion of the lamprophyres occurred ca. 285 m.y. ago (Leroy and Sonet 1976).

The *Brâme facies* occupies the western part of the massif and constitutes the basal part of the granitic complex. It consists of migmatites and foliated porphyritic to medium-grained granites, is less differentiated than the St. Sylvestre facies and contains large xenoliths of partly transformed gneisses. Only minor U deposits (e.g., Montulat) are present.

The *St. Sylvestre facies*, which hosts all major U deposits is highly differentiated and contains no xenoliths of gneiss except at the periphery adjacent to surrounding metamorphics. It occupies the central and eastern section of the massif.

Major rock constituents of the St. Sylvestre facies are in average some 36% quartz, 27% orthoclase, 27% albite, and 10% muscovite-biotite (Ziegler and Dardel 1984). The average chemical composition is given by Dardel/Peinador Fernandes et al. (1979) as 71–74% SiO_2, 14–15% Al_2O_3, 1.3–1.6% FeO + Fe_2O_3,

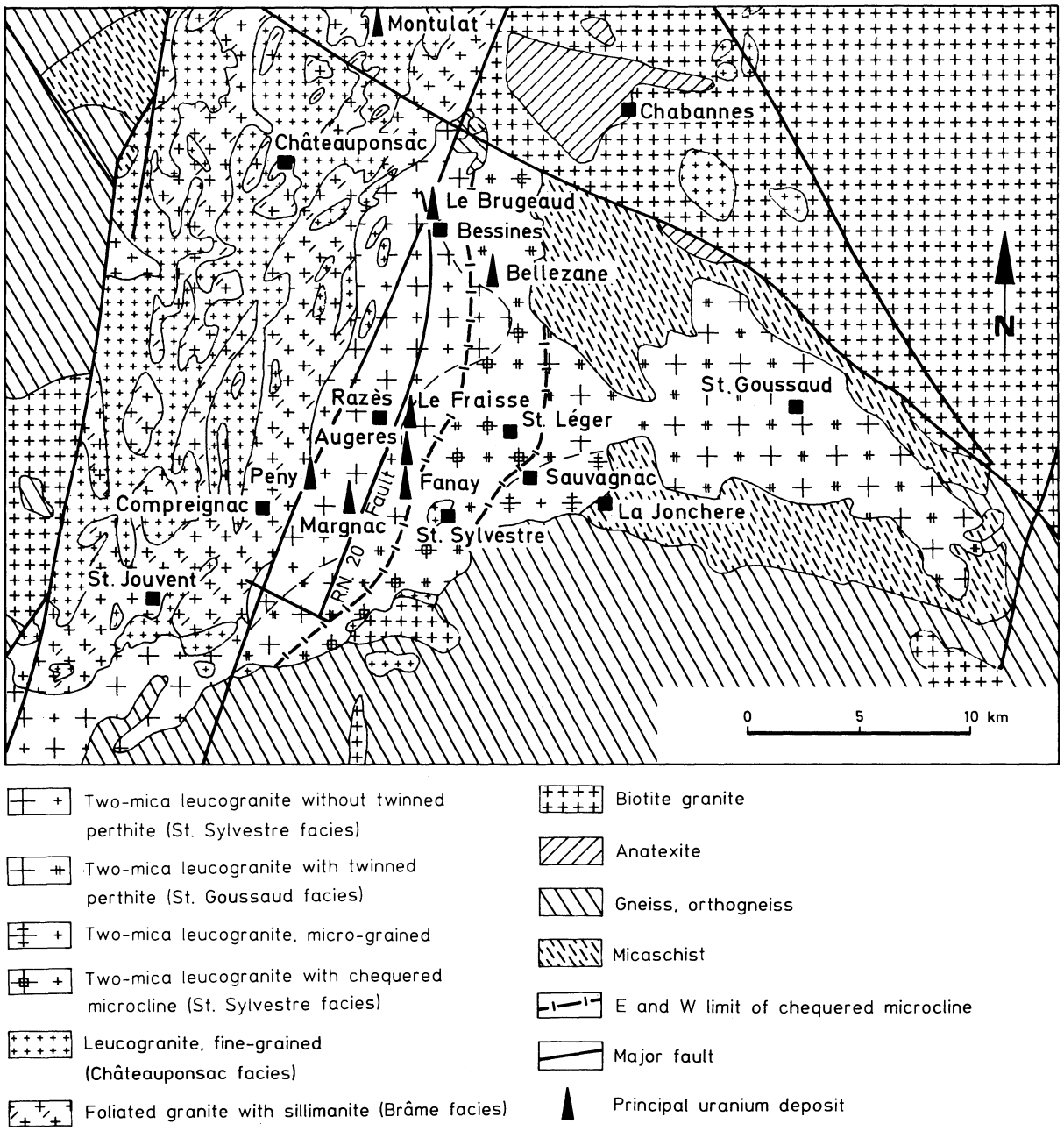

Fig. 5.27. Limousin, La Crouzille district, generalized map of petrographic facies distribution and location of principal uranium deposits. (After Barbier and Ranchin 1969a; Marquaire and Moreau 1969; Ranchin 1971; Ziegler and Dardel 1984)

0.2–0.5% MgO, 0.6–1.0% CaO, 3.3–3.8% Na_2O, 4.8–5.8% K_2O, 0.2–0.25% TiO_2, 0.3–0.4% P_2O_5, 1% loss of ignition.

Mineralogical and chemical composition, however, vary strongly but follow a coherent and continuous evolution of the massif as a whole. The dominant facies is *coarse- to medium-grained, often porphyritic granite* characterized by an abundance of Al-K phases, mainly Al-rich biotite, sillimanite, andalusite, cordierite, and muscovite over quartz, an acidic plagioclase with commonly less than An_{20} and anomalous concentrations of lithophile elements such as U, Th, Be, Li, F, Sn, and W (Friedrich and Cuney, 1986).

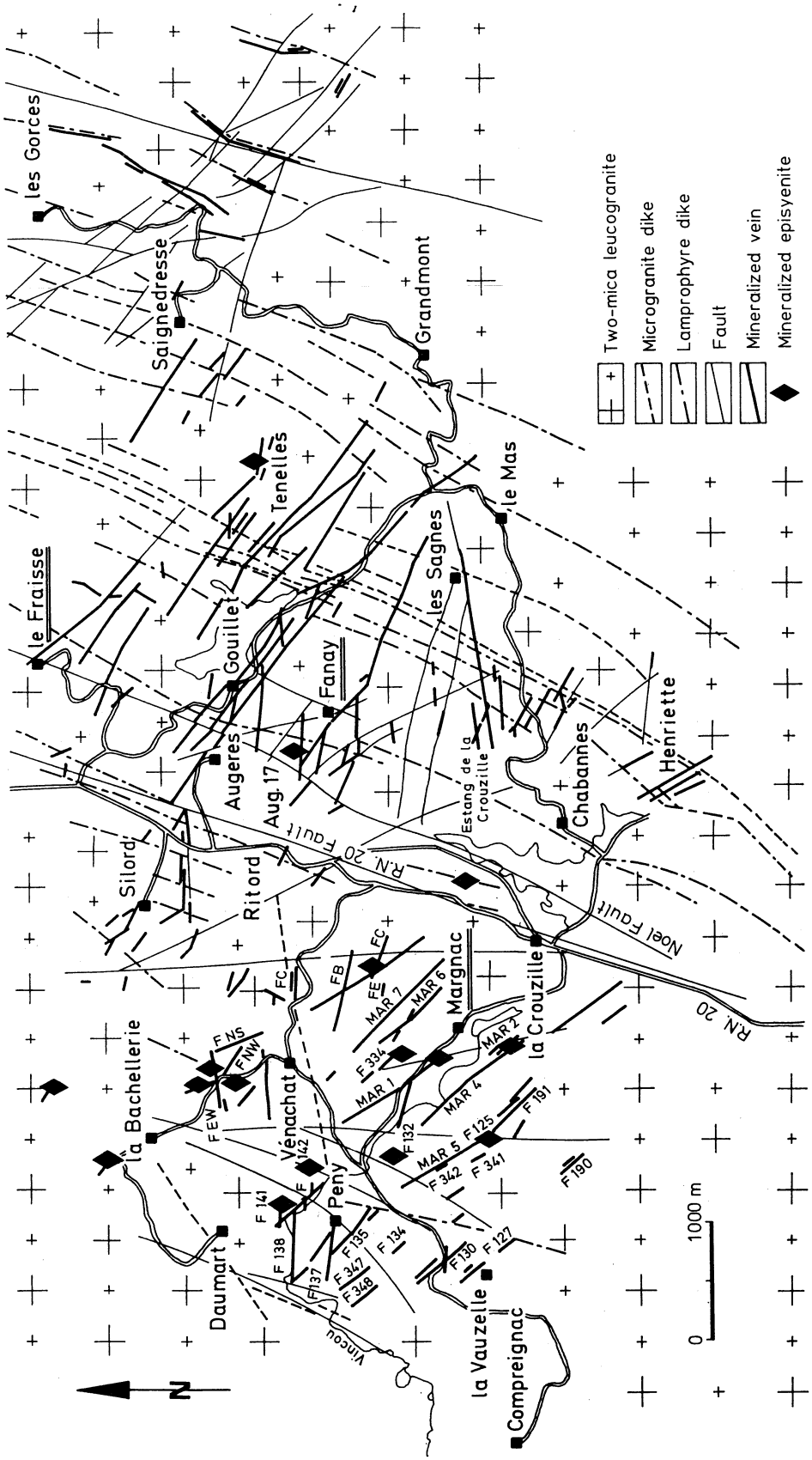

Fig. 5.28. Limousin, La Crouzille, uranium vein systems and episyenite bodies of Margnac-Fanay-Le Fraisse areas. (After de Fraipont et al. 1982; Moreau and Ranchin 1971; Dardel/Peinador Fernandes et al. 1979)

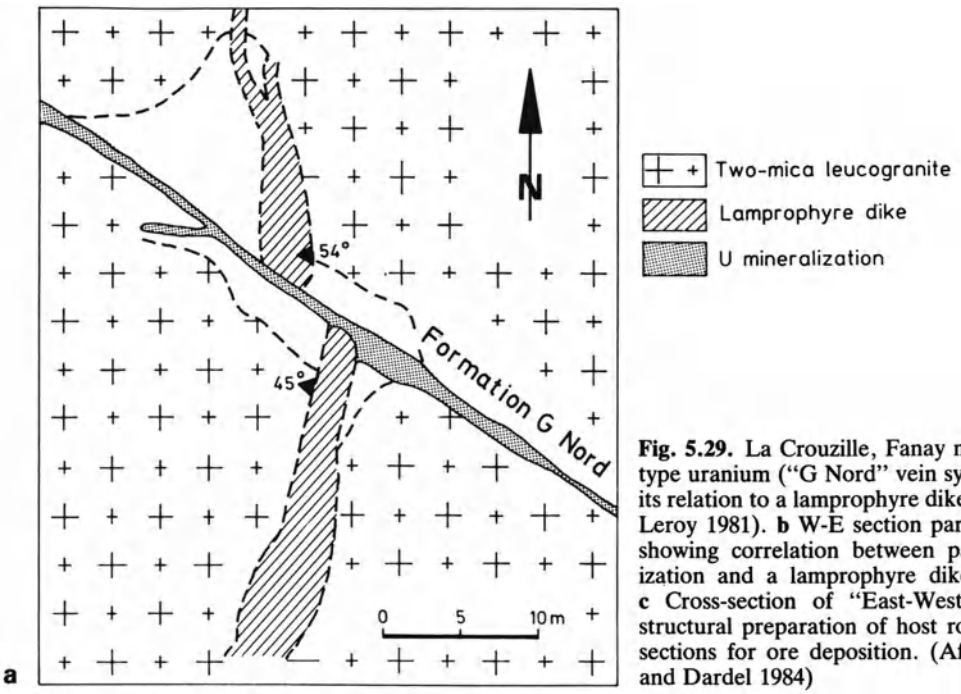

Fig. 5.29. La Crouzille, Fanay mine. **a** Planview of vein-type uranium ("G Nord" vein system) mineralization and its relation to a lamprophyre dike. (After Cathelineau and Leroy 1981). **b** W-E section parallel to "D" vein system showing correlation between part of uranium mineralization and a lamprophyre dike. (After Leroy 1978b). **c** Cross-section of "East-West" vein system showing structural preparation of host rock and preferential vein sections for ore deposition. (After Gagnadre in Ziegler and Dardel 1984)

Highly evolved phases are sodic with decreased K, Ca, Mg, Fe, Ti contents, and enrichments in incompatible elements such as Sn, Li, Bi, As, Cu, Cs, and F. They typically contain albite, muscovite phenocrysts, Li, Fe and Al rich (XFe = 0.9, Al^{6+} = 2.2) biotite, highly perthitic orthoclase, Th-poor uraninite, anatase, apatite, rare zircon, and monazite.

The least differentiated facies are potassic with enrichments of Ca, Mg, Fe, Ti, and either Cr, Co, Ni, Ba, Sr or Zr, Hf, Th, LREE, typical compatible elements in peraluminous melts. Characteristic rock constituents are biotite (XFe = 0.6, Al^{6+} = 0.8), less common muscovite phenocrysts, prismatic sillimanite, abundant ilmenite, monazite, zircon, apatite, and rare uraninite. Migmatites occur locally in the lesser evolved phase (Cuney et al. 1985; Friedrich 1984).

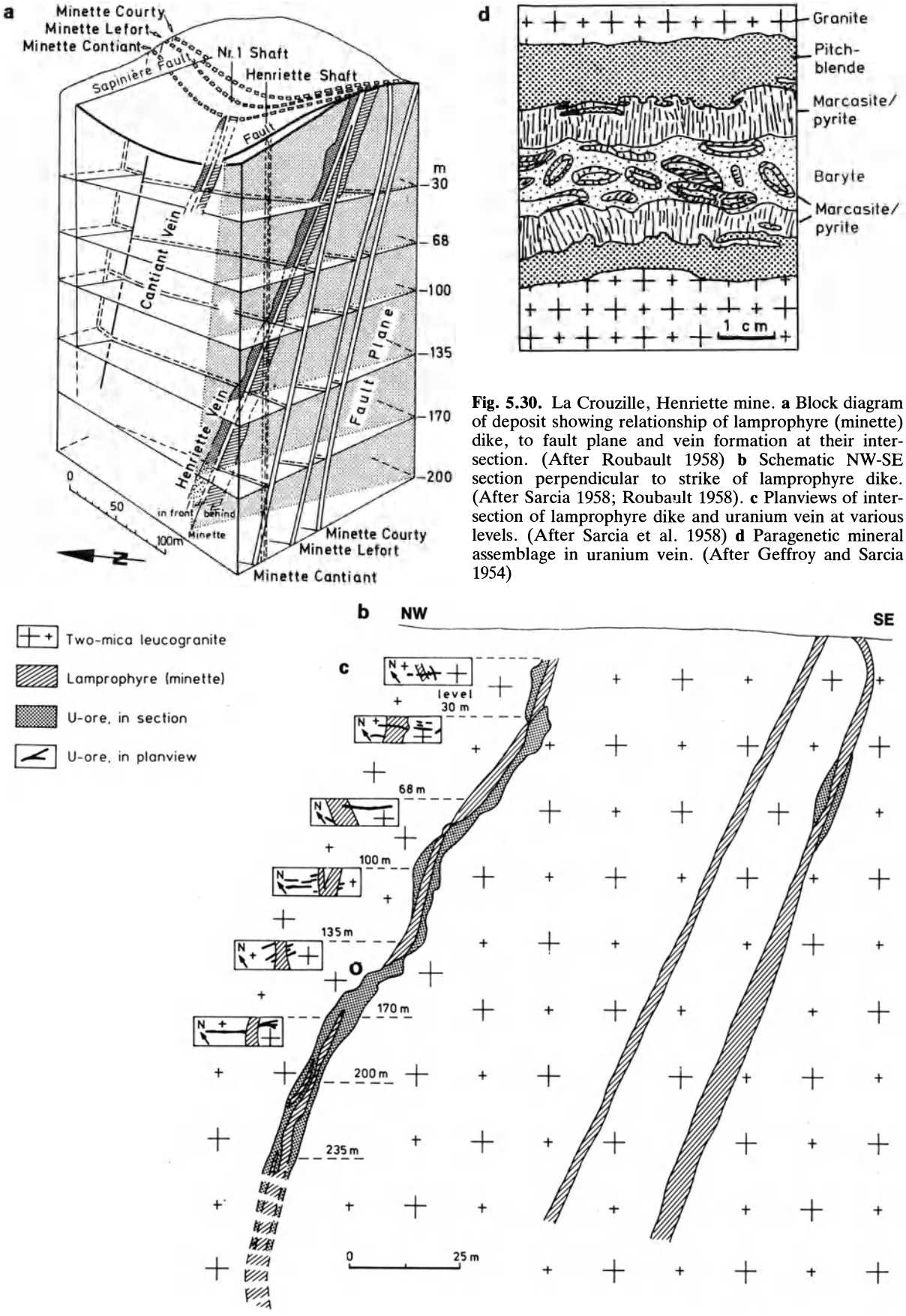

Fig. 5.30. La Crouzille, Henriette mine. **a** Block diagram of deposit showing relationship of lamprophyre (minette) dike, to fault plane and vein formation at their intersection. (After Roubault 1958) **b** Schematic NW-SE section perpendicular to strike of lamprophyre dike. (After Sarcia 1958; Roubault 1958). **c** Planviews of intersection of lamprophyre dike and uranium vein at various levels. (After Sarcia et al. 1958) **d** Paragenetic mineral assemblage in uranium vein. (After Geffroy and Sarcia 1954)

Numerous dikes and stocks of peraluminous *fine-grained granites* geochemically of highly variable composition intruded the coarse- to medium-grained facies prior to its final consolidation. A particular group of fine-grained granites intruded near or into regional synmagmatic mylonite zones. These intrusions have higher concentrations of both incompatible (U, Sn, Li, F) and compatible elements (Th, Ce, Zr, Ba, Sr, etc.) than the surrounding coarse-grained granites (Friedrich et al. 1987). Trace element patterns within the mylonite zones correspond to those of associated fine-grained granites (Friedrich and Cuney 1983).

Duthou (1977) reports elevated initial Sr isotope ratios (0.706 to 0.711) and Turpin (1984) high $\delta^{18}O$ values (+11‰) for the peraluminous leucogranites suggesting an anatectic, partial melting *origin* of the granites from metasedimentary sialic crustal material, very probably of Cambro-Ordovician age as proposed by Cuney and Peyrel (1984).

Principal *faults* trend N-S, NW-SE, NNE-SSW and E-W to ESE-WNW (Fig. 5.28).

Host Rock Alterations

Pre-ore granite alterations include albitization, muscovitization, greisenization, dequartzification, chloritization, and argillitization. Pre-ore alterations of hydrothermal nature resulted in localized quartz dissolution associated with destruction and neoformation of minerals, a process termed *episyenitization* by French geoscientists. Two types of episyenites are distinguished, earlier feldspar dominant episyenites (commonly barren of uranium) and later formed mica (muscovite) dominant episyenites (which often – but not necessarily – contain uranium deposits). Turpin (1985) gives an age of episyenite formation at ca. 300 m.y. ago.

Ore-related wall rock alterations extend into country rocks for commonly less than 0.5 m from a pitchblende bearing vein. The character of alteration depends to some extent on the host rock. Leroy (1978a,b) notes for the La Crouzille district, a first stage, synchronous with pitchblende deposition, of more or less total muscovitization (commonly phengitization) of potassic feldspars in leucogranites and mica episyenites and of the feldspathic matrix, and chloritization of pyroxenes and biotite, associated with pyritization in lamprophyre. This first stage alteration chemically corresponds to potassium metasomatism associated with decrease of Si, Na, and Ca in granitic wall rock, and increase in SiO_2 and decrease of Na, Ca, Mg and occasionally Fe in lamprophyres. Trace elements in pitchblende reflect these chemical processes (Cathelineau et al. 1979). In a second stage, contemporaneous with development of coffinite from pitchblende occurred hematitization, montmorillonitization, formation of some adularia, and silicification of wall rocks.

Principal Characteristics of Mineralization

Two settings of mineralization are recognized within the host granite, veins cutting the granite (Figs. 5.29, 5.30, 5.31) and disseminations in episyenite (Fig. 5.31). The mineralogy is very similar in both settings.

Primary mineralization is characterized by a *simple mineral association*. Pitchblende is the dominant uranium mineral and is mainly accompanied by iron sulfides. Other sulfides of Cu, Pb, Zn, and Mo are scarce. Gangue is present in minor amounts and consists of chalcedonic silica, fluorite, and locally baryte and calcite.

The following principal paragenetic sequence for *vein-type mineralization* is established by Geffroy 1971, Leroy 1978a,b, Poty et al. 1986:

1. Nonhematitic, transparent quartz deposited comb-like on vein walls,
2. spherulitic pitchblende associated with pyrite,
3. microcrystalline quartz, at first chalcedonic passing into combs and into large zoned crystals containing pyrite and hematite; hematitization immediately follows pyrite during quartz deposition; locally ankerite and hematite occurs instead of hematitic quartz,
4. brecciation,
5. transparent quartz associated with pyrite, marcasite; coffinite by alteration of stage 2 pitchblende,
6. banded purple fluorite, white calcite, and pink baryte.

Disseminated type mineralization is mainly located in mica episyenitic pipes, some is in brecciated leucogranite and rarely in feldspar episyenite. Pitchblende and pyrite are the first minerals to form. Pitchblende coats rock faces and penetrates into fractures and/or cleavages.

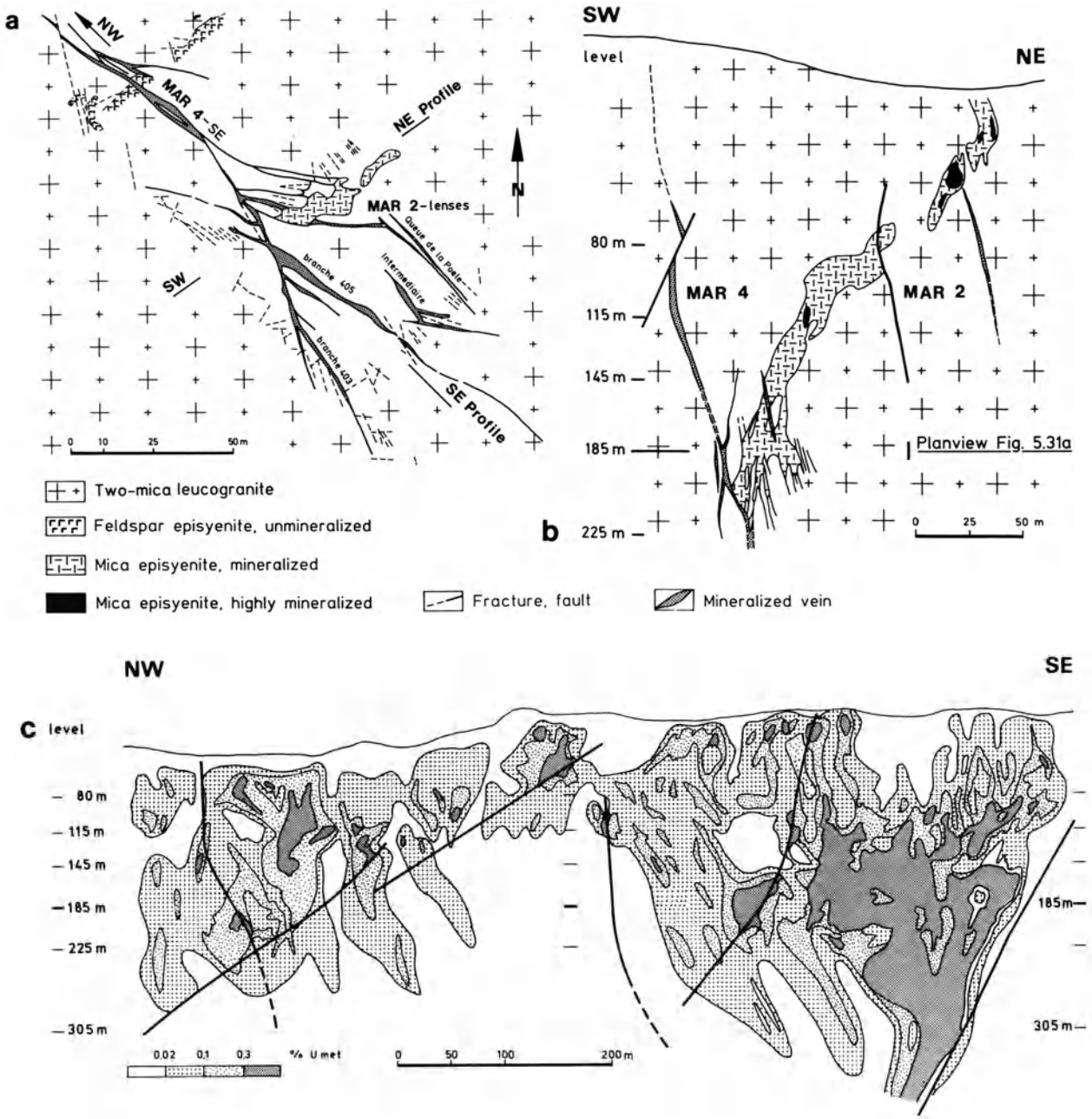

Fig. 5.31. La Crouzille, Margnac mine. **a** Planview of mineralization at intersection of Margnac 4 veins with Margnac 2 mica-episyenite. (After de Fraipont et al. 1982). **b** Cross-section through mineralized micaepisyenite of Margnac 2 cut by the uranium vein system of Margnac 4 (After Dardel/Peinador Fernandes et al. 1979; Leroy 1978b) **c** Zonation of uranium grades along Margnac 4 veins. (After Chapot 1979)

Quartz, more rare than in veins, grows as very tiny crystals with marcasite and rare prismatic coffinite at its base. This quartz is overgrown by concretionary coffinite. Fluorite and subsequently calcite are the last minerals to form.

Mineralized veins commonly trend about NW-SE and to a minor degree E-W, and have a steep dip (Figs. 5.28 to 5.31). The veins have *dimensions* from a few meters to several hundred meters but may extend for up to a kilometer long. Thickness of mineralized veins is frequently <1 to 2 m but can range from few centimeters up to 15 m in highly cataclastic zones. Vertical extension of the ore shoots varies between some meters

and >300 m. The grade is highly variable, ranging between several hundred ppm to >0.25% U_3O_8 (Fig. 5.31c) but may be as much as several percent U_3O_8 particularly when veins intersect or follow mafic dikes such as lamprophyres (Figs. 5.29, 5.30).

Episyenite-hosted mineralization, may have dimensions between several tens to several hundreds of square meters in plan-view and vertical extensions between about 10 and 300 m (Fig. 5.31). The average grade is generally high, ranging up to 1% U_3O_8 and more. At some locations, where mineralized veins enter into episyenite, the ore grade may range from 1 to 10% U_3O_8.

Weathering-related processes caused *remobilization* of original mineralization and redeposition of uranium as "black products" (neo-pitchblende, para-pitchblende, sooty pitchblende) below the water table and in the cementation zone, and as colored hexavalent uranium minerals in the oxidized near surface zone commonly extending to a depth of 20 to 30 m and locally to 80 m in most of the Hercynian granitic massifs in France. Strong radiometric disequilibrium is typical for this phreatic zone of meteoric water circulation and mineral redistribution. Where the remobilization occurred in complexely fractured zones, as at Brugeaud, it resulted in an enlargement of ore bodies but also in dilution of the ore grades.

Isotope *ages* of primary pitchblende are ca. 275 to 270 m.y. (Leroy and Holliger 1984).

Ore Controls and Recognition Criteria

Significant ore controlling or recognition criteria of vein uranium deposits in the Limousin district include:

Host Environment

- Deposits occur structurally controlled peripheral within a highly differentiated peraluminous leucogranite transected by synmagmatic mylonite zones and dikes and stocks of variable lithologies (details of petrology and geochemistry see later).

Alteration

- Pre-ore alteration includes albitization, muscovitization, dequartzification/episyenitization (feldspar- and mica-episyenite), chloritization, and argillitization.
- Ore-related alteration includes muscovitization, chloritization, and locally pyritization. A second-stage alteration associated with uranium redistribution includes hematitization, montmorillonitization, silicification, and adularia formation.

Mineralization

- The primary ore control is by structure, secondly by lithology.
- Two principal ore settings are recognized, veins which predominantly trend NW-SE and disseminations in mica-episyenite. Mica-episyenites are commonly only mineralized when intersected by or adjacent to pitchblende veins.
- Ore is monometallic and of simple mineralogy, consisting of pitchblende and alteration products thereof.
- Associated minerals are dominantly pyrite, marcasite and traces of Cu, Pb, Zn, and Mo sulfides. Gangue minerals include quartz, chalcedony, fluorite, baryte, and calcite.

Metallogenetic Concepts

The following synopsis reviews the evolution of uranium-fertile leucogranites and the metallogenetic principles of related vein uranium deposits on a broader scale. The documentation is not restricted to the Limousin uranium region, although this region serves as the main example. Many geoscientists contributed fundamental data to the understanding of these vein deposits and their parent granites. The most recent and comprehensive research is published by Cathelineau, Cuney, Friedrich, Poty and their coworkers. In essence, their results, amended by data of the other authors listed, may be summarized as follows.

Characteristics of Uraniferous Leucogranites

As defined by French geologists, a *fertile leucogranite* is a highly differentiated acid peraluminous ($A_2O_3/(CaO + Na_2O + K_2O) > 1$ in molecular proportions) granite of crustal origin which evolved by multistage magmatic processes and was subsequently affected by deuteric and/or

hydrothermal processes. It contains uranium in values above the Clarke figure and in form of uraninite as primary constituent. The Th/U ratios are low ranging from <3 to ca. 0.1 (Clarke = ca. 4).

Several types of leucogranites, also termed two-mica granites, exist. Some have related uranium deposits (fertile granites) others are devoid of them (sterile granites).

Stussi (1985) and La Roche et al. (1980) divide Hercynian granites into *petrochemical facies*, viz. calc-alkaline, subalkaline and alumino-potassic, the latter leucogranites further into those of alumino-silico-potassic and alumino-silico-sodic tendency and attribute *consanguine metal deposits* to the various facies:

a) U deposits and W, Be, and Au mineralizations are typically associated with alumino-silico-potassic two-mica leucogranites;
b) Sn, W, Li, Nb, Ta mineralizations with alumino-silico-sodic two-mica leucogranites.

Distribution of type a and b deposits and provinces coincides regionally, but is separated on a local scale. The deposits formed from solutions of different chemical and physical properties (Dubessy et al. 1987).

c) Some U deposits/domains are associated with subalkaline granites locally in relation with late alumino-potassic magmatism. This type produced also Mo and Cu mineralizations.
d) Calc-alkaline granite appears to be sterile for any specific metal potential.

Geotectonically, favorable leucogranites appear to have intruded preferentially along regional lineaments narrow in width but several hundred kilometers long, geophysically marked by elongated gravimetric lows. (Dardel/Peinador Fernandes et al. 1979).

Uranium deposits are restricted to leucogranites of a slab-shaped or laccolith-type intrusion (St. Sylvestre granite: 2–4 km thick, 50 km wide) emplaced during the last stage of an intense regional thrusting event and at a structural level corresponding to the sillimanite isograde.

Major synmagmatic ductile deformation zones transect the batholith. They are meters to some hundred meters wide and persist for tens of kilometers long and apparently formed in an early magmatic stage. The zones display foliation reflected by orientation of K-feldspar megacrysts and biotite laths and are occupied by numerous aplitic veinlets and dikes of fine-grained granite and pegmatite (Friedrich et al. 1987). Mollier et al. (1985) figured out that the mylonite zones are dominantly confined to proximities of fine-grained granitic intrusions and when they occur within coarse-grained granite they are within a few hundred meters of those.

Petrographic-geochemical features of the main facies of the St. Sylvestre granite have been presented earlier in the section "Geological Setting . . .". In essence, the petrochemical composition of a fertile granite is characterized by an abundance of Al-K phases and anomalous concentrations of lithophile elements such as U, Th, Be, Li, F, Sn, and W but in varying quantities and mineralogical distribution in the varies granitic facies. U and Th values are given in Table 5.19.

Table 5.19. St. Sylvestre Massif, U and Th values of various leucogranite facies. (Ziegler and Dardel 1984; Ranchin 1971)

Leucogranite facies	U (ppm)	Th (ppm)	Th/U
La Brâme	8.7 –14.8	?–12.67	?–0.86
Chateauponsac[a]	18.2	8.71	0.47
St. Sylvestre	16.0 –22.0	23.37–34.67	1.13–2.17
northern part (Brugeauds)	17.4	?	
western part (Margnac)	20.1 –22.0	23.37–30.99	
eastern part (St. Léger)	16.0	34.67	
St. Goussaud	14.9 –21.2	18.11–26.27	0.85–1.75

[a] Fine-grained facies intrusive in La Brâme leucogranite.

U and Th occur predominantly in two minerals, uraninite and monazite. Both have characteristic chemical compositions and are typically associated with other accessory minerals in the two principal stages of the St. Sylvestre granite. The main stage is characterized by ubiquitous distribution of both minerals, whereas uraninite prevails in the late stage, with particular concentrations along synmagmatic shear zones.

Distribution of *U and Th in the main stage* is as follows. Uranium is predominantly (50 to 79%, average 60% of the whole rock U endowment) incorporated in minute crystals of Th-poor uraninite. Zircon, monazite, and apatite account for 25–35%, and 5–6% of the whole rock U is attributed to U adsorbed on mineral faces and

microfractures. Uraninite in its diverse dispositions is commonly associated with apatite, zircon, and monazite of specific composition. (Ranchin 1971; Pagel 1981, 1982a)

Thorium is bound in refractory accessory minerals, predominantly in monazite. Early magmatic monazite in coarse-grained granite contains a variety of trace elements, but lacks the elemental enrichments noticed in late magmatic monazites (see later). Principally all varieties of monazite of the St. Sylvestre granites are unusually high in ThO_2 (6–14%) and also in UO_2 (0.4–7%). Early monazite typically associates with apatite and zircon (Cuney and Friedrich 1987; Pagel 1982a).

Late magmatic stage U and Th occur in two host varieties synmagmatic shear zones and dikes of fine-grained granites.

Synmagmatic shear zones display increased background values of up to 100 ppm U, with an average of 35 ppm U and 40 ppm Th, vs. an average of 8 ppm U and 10 ppm Th in surrounding undeformed porphyritic granite (Fig. 5.32a). U is predominantly present in form of uraninite which typically associates with monazite, elongated zircon, apatite, anatase, and ilmenite. The high values of U and Ca in monazite attest to its equilibrium crystallization with uraninite, which contrasts to the early magmatic monazite.

Dikes of *fine-grained granites* transecting porphyritic biotite granite (av. 6 ppm U) contain up to 40 ppm U (Fig. 5.32b). The dikes contain disseminated uraninite associated with apatite, zircon, and U, Th, Ca, Y-enriched monazite. In gneissose sections, these minerals are preferentially emplaced along shear planes.

The *late magmatic monazite* associated with uraninite in mylonites display characteristic crystal-chemical features. It contains high contents of U, Y, Ca, Th, and LREE (Table 5.20). These elements are incorporated into monazite by progressive zonal recrystallization. Monazites of fine-grained granites are likewise enriched with these elements but lack zonation. Consequently, monazites enriched in the above listed elements and displaying marked zonation are suggestive for uraninite bearing, highly leucocratic and hygromagmaphile element-rich (Li, Sn, Rb, F, Be, etc.) granites which constitute the source rocks for later formed pitchblende veins (Cuney and Friedrich 1987; Friedrich et al. 1987; Ranchin 1968, 1971).

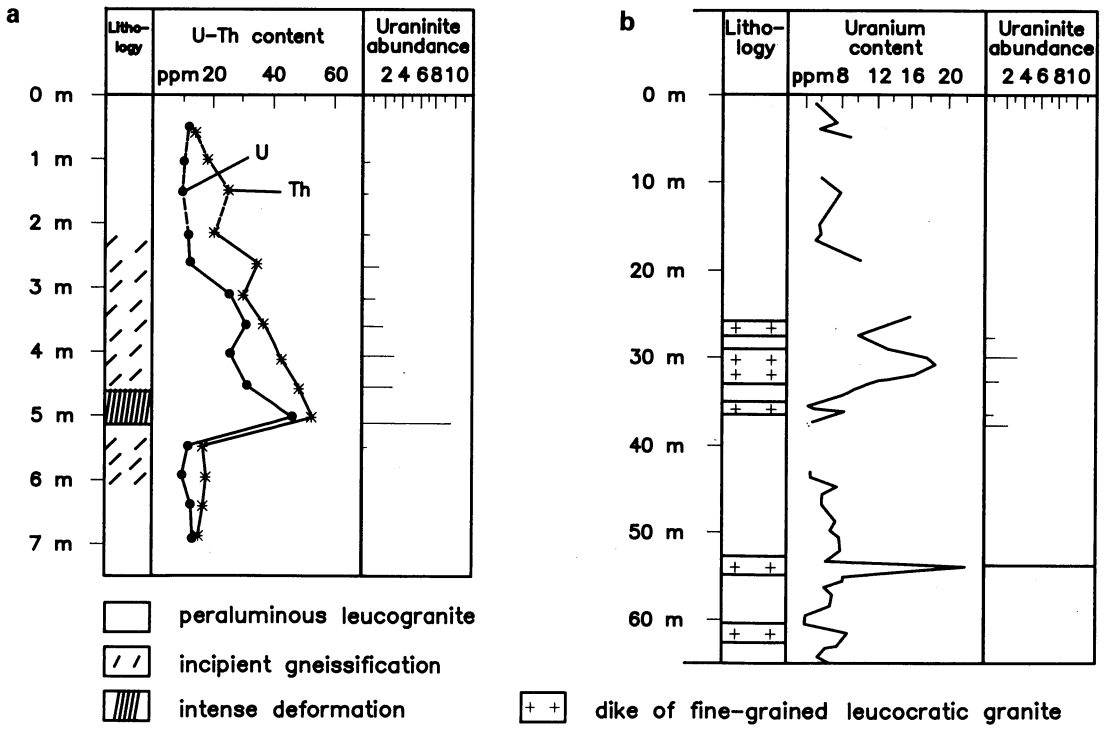

Fig. 5.32. St. Sylvestre Massif, uranium content and uraninite abundance associated with **a** a several meters wide shear zone within peraluminous granite, **b** dikes of leucocratic fine-grained granite transecting biotitic porphyritic granite. (After Friedrich et al. 1987, based on Ranchin 1968, 1971)

Table 5.20. St. Sylvestre Massif, chemical characteristics of main magmatic (1) and late magmatic (2) monazites (in wt.%). (Friedrich et al. 1987)

Sample		Y_2O_3	Ce_2O_3	SiO_2	CaO	UO_2	ThO_2	P_2O_5
Coarse-grained granite								
Th-rich (1)		2.30	25.38	–	2.74	1.73	12.75	29.28
		2.01	25.14	–	2.76	1.76	11.61	28.38
Th-poor zoned single crystal	core	1.37	26.08	–	2.37	0.39	10.79	24.60
	↓	1.65	24.48	–	3.24	2.01	10.99	24.63
	rim	2.82	22.70	–	3.11	3.85	10.64	26.11
U-rich (Th-poor) (2)		2.52	24.96	0.12	3.13	6.36	7.39	30.82
		3.01	25.41	0.01	3.34	7.09	7.38	32.19
Fine-grained granite (2)		2.29	23.46	0.14	4.57	6.00	9.64	28.54
		1.88	26.95	0.04	3.19	5.89	6.47	30.45
Late-magmatic ductile shear zone (2)		1.25	24.79	0.21	3.47	4.31	13.31	28.08
		1.80	26.05	0.02	3.24	3.03	10.85	27.15
Coarse-grained granite zoned single crystal (vicinity of a shear zone) (1 → 2)	core	0.55	31.5	0.08	1.66	0.65	6.32	31.53
	↓	1.81	26.83	0.00	2.01	1.64	5.36	31.95
	rim	0.36	25.86	0.17	3.99	3.62	14.15	31.90

Granite Petrogenesis and Related Uranium-Concentrating Processes

A number of differing hypotheses on the evolution of fertile leucogranites and associated modes of uranium concentration, particularly of those of the St. Sylvestre Massif/Limousin, have been forwarded in the past. The most recent and well-documented concept has been published in various papers by Cuney, Friedrich, Poty and their coworkers.

Friedrich et al. (1987) distinguish five principal modes of uranium mobilization and related uranium-concentrating processes associated with the evolution of a peraluminous granite:

- partial melting of uraniferous protoliths,
- magmatic differentiation,
- late magmatic activity,
- hydrothermal processes and
- supergene meteoric processes.

The five modes may be separated into two groups. The first three account for continuous and selective uranium accumulations in course of the petrogenesis of the parent granite to generate a highly fertile U source rock with uraninite the dominant U captor. The last two stages, particularly hydrothermal processes, are instrumental in liberation, transport, and redeposition of the uranium in the form of pitchblende veins. Adequate structural source and host rock preparations are mandatory interludes for the latter.

Partial melting achieves concentration of leachable U in peraluminous silicate liquids only under two conditions, anomalous, above Clarke value uranium contents in the protolith and sufficient in quantity to form uraninite. Consequently, Friedrich et al. conclude that a highly peraluminous uraniferous leucogranite is the product of variable intense partial melting of upper crustal rocks and strong differentiation during its evolution. High initial $\delta^{18}O$ and $^{87}Sr/^{86}Sr$ ratios suggest shales variably enriched in organic matter and uranium to be the precursor rock. Such shales would provide the adequate composition for the peraluminous nature, low oxygen fugacity, and high U content of the granite.

During *magmatic differentiation* U is first incorporated into common accessory minerals of usually refractory nature such as monazite, zircon, apatite, xenotime etc. Only if excessive U is available will it fractionate as a pronounced incompatible element in favor of the anatectic melt, from where it can crystallize as uraninite. The proportion of U precipitating as uraninite and the quantity of U in the silicate liquids increases with the differentiation of the melt. Such an incompatible attitude of U occurs in magmas of reducing nature, which mostly derived by partial melting of metasediments (Ishihara 1977), as distinct to magmas of oxidizing capacity, where U will strongly fractionate into the fluids when an oversaturation of the melts exists.

In the St. Sylvestre massif, progressive magmatic differentiation produced petrologic facies with two distinct end members and a subsequent member, as described by Friedrich et al. (1987). The least differentiated or front-end member is cafemic and enriched in elements compatible in peraluminous melts and has an accessorial mineral suite dominated by Th-rich (ca. 12% ThO_2, Table 5.20) monazite, zircon, apatite, and ilmenite. In contrast, highly evolved members are highly leucocratic and enriched in hygromagmaphile, incompatible elements (U, Sn, Li, Rb, Be, F, etc.) and have an accessory suite typically dominated by Th-poor uraninite and minor U-enriched, zonal monazite and zircon and as characteristic rock constituents albite and muscovite phenocrysts.

Late magmatic activity prior to the final consolidation of the main granite body, may expell highly uraniferous fluids and melts from syntectonic oversaturated specialized intrusions into synmagmatic ductile shear zones where anomalous quantities of uraninite crystallize. In the St. Sylvestre granite, the ductile deformation reflected by mylonite zones was followed or accompanied by intrusion of dikes and stocks of fine-grained peraluminous granites. These granites are of highly variable geochemical composition. A particular group of them, emplaced along major synmagmatic deformation zones, is characterized by marked enrichments of compatible (Th, Ce, Zr, Ba, Sr, etc.) and incompatible (U, Sn, Li, F, Rb, Cs, etc.) elements compared to the surrounding coarse-grained granite. Concentration of U and other incompatible elements is mostly restricted to the margins of the dikes and stocks although some fine-grained granites rich in SiO_2 and Na_2O are ubiquitously enriched. In this group of fine-grained granites U displays the best correlation coefficient with Sn, Cs, and Rb and is distinctly independent of Th, Zr, and Ce and as such indicates U concentration processes distinct from the main magmatic phase. The other elements that correlate with U are of highly mobile nature and typically represent a late magmatic phase of coexisting crystallized minerals, silicate liquid, and a fluid phase.

Subsequent to these magmatic processes, a variety of dikes (microgranite, lamprophyre, pegmatite) intruded and, after cooling below 400°C, the leucogranite underwent, cataclasis and hydrothermal modifications.

Post-magmatic hydrothermal processes reflected by their alteration imprints in the source rocks constitute the critical prerequisite for mobilization and redistribution of the primary magmatic uranium into pitchblende veins.

Friedrich et al. (1987) discuss the various modes of hydrothermal source rock alteration in the light of its efficiency in mobilization of uranium.

Solution-controlled *uranium liberation* takes place essentially along zones of fracturing and cataclasis that provide the transmissivity needed as pathways for the fluids. The nature of the fluids may vary between hypogene hydrothermal and supergene meteoric. Favorable sites of adequate permeability are restricted to brittle structures, transcurrent ductile mylonite zones, and gneissose segments marginal of granitic facies as documented by oriented trails of fluid inclusions, microthermometry, and structural patterns (Lespinasse and Pecher 1985).

The liberation of uranium from most accessory minerals by alteration fluids is very limited except for uraninite. Most accessories are refractory and demand either intense metamictization or extremely aggressive fluids to release their uranium. The dissolution of uraninite is a function of the physico-chemical nature of the solutions, in the first instance oxidation and complexing capacity (Dubessy et al. 1987). Easy destruction of uraninite may result from oxidizing and CO_2-rich solutions even without any significant host rock alteration if only minor quantities of solutions are involved. In contrast, reducing fluids, even in large quantities, may induce intense alteration but without liberating any significant quantity of uranium.

Alteration effects with respect to the behavior and mobilization of uranium by the common types of alteration observed in peraluminous leucogranites are as follows:

Albitization, a common, ubiquitous feature in many peraluminous granites, is considered a late magmatic process by Friedrich et al. (1987), whereas other authors favor a hydrous metasomatic origin, e.g., Ranchin (1971). Uranium, together with other incompatible elements such as F, Li, Be, and Sn, became enriched during albitization (Cuney et al. 1985).

Muscovitization, reflected by authigenic growth of muscovite phenocrysts is a typical and pervasive phenomenon for leucogranites (therefore also referred to as two-mica granite).

Ranchin (1971) suggests that uraninite crystallization occurred in a subsolidus (hydrous) phase related to muscovitization. This view is opposed by Friedrich et al. (1987), who provide evidence that uraninite is a magmatic product formed independently of this type of muscovitization. Another type of muscovitization formed by hydrothermal alteration is of only very limited extent.

During *greisenization* as documented by Pagel (1981), the original uranium concentration in various leucogranites in Bretagne, France, and Cornwall, Great Britain. remained stable. This would be in agreement with the reducing nature of the solutions involved in Sn-W greisen formation (Dubessy et al. 1987). In contrast, Simpson et al. (1979) report a loss of U in the greisens of Cligga Head, Cornwall.

Chloritization affected to various extent and intensity peraluminous granites. Some leucogranite massifs such as Guérande, Bretagne (Ouddou 1984), and Grandrieu, Margeride district (Peyrou 1981), display almost pervasive chloritization as distinct from the St. Sylvestre Massif, where intense chlorite alteration is limited to restricted areas. Uranium removal in response to chloritization appears to be related directly to water/rock ratios. Small ratios are associated with minor U loss, as demonstrated by Turpin (1984). His oxygen isotope data indicate only small amounts of meteoric waters and low water/rock ratios respectively to be involved in pervasive generation of chlorite in rocks which suffered only insignificant uranium losses. For an efficient U mobilization one would expect higher water/rock ratios and solutions of different chemistry. On the other hand, this kind of chloritization results in a more or less in situ redistribution of uranium. Le (1975) and Renard (1974) established that chlorites may contain much higher U concentrations than unaltered biotites. This is due to redeposition of remobilized uranium in microfractures and on grain boundaries and by adsorption on Fe- and Ti-oxides which derived from the chloritization process. Presence of hematite attests to oxygenated solutions involved in this process.

Dequartzification with progress into *episyenitization* is a common feature in many peraluminous granites and markedly efficient in destruction of uraninite and mobilization of uranium. Two varieties of episyenite are distinguished. They reveal the following characteristics in the La Crouzille and adjacent Marche districts. (Moreau and Ranchin 1971; Leroy 1978a, 1984; Leroy and Cathelineau 1982)

Feldspar-dominant episyenitization (Table 5.21A) is characterized by gradual dissolution of quartz, neoformation of albite, microcline and adularia, alteration of muscovite to feldspar, biotite to chlorite (ripidolite) and potassic feldspar, and intense increase of perthitic intergrowth (>50 vol. %) of original orthoclase while plagioclase becomes Na-enriched. Sites of feldspar episyenitization have apparently been prepared by microfracturing now largely overprinted by recrystallization.

Mica-dominant episyenitization (Table 5.21B,C) is recognized by quartz dissolution, and partial to total muscovitization replacing almost all pre-existing rock constituents of the host granite except orthoclase, which commonly is incompletely transformed. Some hematite crystallized in such white micas formed after biotite. Leroy (1984) notes for the Bernardan deposit/Marche district that the newly formed muscovite is of phengite type. Mica episyenitization is clearly related to intersecting fracture systems, where it forms irregularly shaped pipe-like bodies of up to 30–40 m in diameter and 30–300 m vertical extension. Intensity and dimension of episyenitization are direct functions of local fracturing and microcataclasis. Formation appears to be contemporaneous with lamprophyre emplacement but may also be related to the late fine-grained granite intrusions. Leroy (1984), based on fluid inclusion studies calculated for the Bernardan deposit fluid temperatures of 260 to 370°C and reports for that deposite a chemical change by loss of SiO_2 (−32%) and NaO_2 (−1.2 to −2.5%) and increase of K_2O (+0.5 to +3.2%) and changes in Rb (positive) and Sr (negative).

Kaolinitization affected widespread the peraluminous granites but is most intense within the most evolved parts of the massifs. This phenomenon suggests that early subsolidus (hydrous) activities must have occurred in large volumes of granite. Compared to the fresh parent granite, kaolinized granite always has very low U contents (Allman-Ward 1985; Simpson et al. 1979).

Supergene alterations by meteoric oxygenated solutions are very effective in dissolving uraninite. Barbier and his coworkers noticed a U loss of 30 to 50% from the leucogranite. The re-

Table 5.21. St. Sylvestre Massif, changes in mineral composition (in % volume) during alteration of leucogranite into **(A)** feldspar episyenite, **(B)** mica episyenite and **(C)** highly mineralized mica episyenite

A Feldspar episyenite

Facies / Minerals in vol %	Surrounding granite		F.-Episyenite		Fissure in F. episyenite	
	1 normal	2 fine-grained	1	2	1	2
K-feldspar	41	42	50	40	55	40
Na-Ca feldspar	20	23	34	49	32	49
Σ Feldspars	61	65	84	89	87	89
Biotite-chlorite (ch)	7	8.5	7 (ch)	5 (ch)	7 (ch)	6 (ch)
Muscovite	7	6.5	0	0	0	0
Quartz, granitic	25	20	0	0	0	0
Quartz, secondary	0	0	5	3	2	1
Σ Quartz	25	20	5	3	2	1
Voids	0	0	4	3	4	4
Total in volume	100	100	100	100	100	100

B Mica Episyenite

Facies / Minerals in vol %	Surrounding granite	Wall rock granite	Compact episyenite	Vesicular mica episyenite
Orthoclase	28.5	28.5	28.5	28.5
Plagioclase	37.0	32.0	25.0	11.0
Σ Feldspars	65.5	60.5	53.5	39.5
Micas Muscovite	6.0	15.0	7.5	10.0
Micas Biotite	6.0			8.0
Quartz granitic	22.5	24.5	0	0
Quartz secondary	0	0	25.0	5.0
Σ Quartz	22.5	24.5	25.0	5.0
Carbonates	0	0	1.5	4.0
Voids	0	0	12.5	33.5
Total in volume	100	100	100	100

C Highly mineralized mica episyenite

Facies / Minerals in vol %	Surrounding granite	Vesicular mica episyenite	Mineralized mica episyenite
Orthoclase	28.5	28.5	46.5
Plagioclase	37.0	11.0	0
Σ Feldspars	65.5	39.5	46.5
Micas Muscovite	4.5	12.0	21.5
Micas Biotite	6.5	6.0	5.0 (include chlorite)
Apatite	1.0	1.0	2.0
Quartz granitic	22.5	0	0
Quartz secondary	0	5.0	10.4
Σ Quartz	22.5	5.0	10.4
Carbonates	0	4.0	0
Voids	0	32.5	6.2
Pitchblende	–	–	8.9
Total in volume	100	100	100

Data from Margnac 1(A), Vincou (B), Vincou and Column 125, Margnac (C). (Moreau and Ranchin 1971)

maining U is partly bound in uraninite relicts contained mainly in quartz, monazite, and zircon, and partly occurs redistributed along microfractures and grain boundaries. Intensity of uraninite decomposition is a function of the rock permeability and the rate of uplift of the area. In the first case microfracturing is the critical factor. It is commonly better developed in the most evolved parts of a granitic complex, where fluid oversaturation prevails. There sections provide the sites for easy leaching of the uranium. Also, coarse-grained granites are commonly more easily attacked than the denser fine-grained facies.

Granitic complexes such as that of St. Sylvestre, which have been uplifted and exposed to erosion in recent times, still contain fairly fresh uraninite grains in near-surface sections. In contrast, granitic massifs with a smooth relief and subjected to only limited erosion such as those of Guérande and Grandrieu, France, display deep penetrating weathering effects. Practically no uraninite can be found to a depth of 100 m and more. All uranium present occurs in microfractures and adsorbed on Fe- and Ti-oxides and clayey material. It supposedly derived from dissolution of original uraninite.

In summary, Friedrich et al. (1987) conclude that a superimposition of uraninite concentrations along synmagmatic mylonite zones associated with emplacement of fluid-oversaturated highly evolved endogranitic intrusions enhances the U fertility of peraluminous granites. Pervasive alterations such as albitization, muscovitization, or chloritization do not provoke significant U mobilization at least as long as water/rock ratios are low. Of prime importance for U redistribution are, instead, several overlapping criteria, viz. brittle deformation of zones with late magmatic uraninite enrichments permitting subsequently intense source rock alteration by oxygenated and CO_2-enriched hydrothermal solutions of sufficient quantity, i.e., the process of efficient U mobilization is restricted to very limited favorable zones.

Proposed Models for the Evolution of Limousin-type Vein Uranium Deposits

A number of metallogenetic models have been forwarded for the final formation of Hercynian pitchblende veins in leucogranite. Geffroy and Sarcia (1955) propose an epithermal origin. Roubault and Coppens (1955, 1958) suggest a lateral secretion process but do not elaborate on the nature of fluids, whether hypogene or supergene. For Geffroy (1971), an ascendant hydrothermal lithogenetic origin is the least unlikely compared to other hypotheses. Moreau et al. (1966) and Barbier (1974) favor supergene processes. In their model, during certain climatic conditions described as biorhexistasis, leachable uranium of the leucogranites has been dissolved from the granite and redeposited in favorable structural traps forming pitchblende veins. Favorable periods for these processes have presumably prevailed during Permian and Tertiary time.

Leroy and Poty (1969), Leroy (1978a,b), Ziegler and Dardel (1984), and Poty et al. (1986) suggest a kind of hypogene convective hydrothermal ore genesis. In their model, a fluid of mixed connate and meteoric waters started circulation in response to tectonic movements and leached uranium for primary pitchblende formation from uraninite of enclosing leucogranites. Leroy, Poty and their coworkers document their reasoning with extensive data, particularly from minero-chemical, fluid inclusion, and mineralogical research work, data which contradict a supergene primary ore formation. Later weathering processes only overprinted the original mineral assemblage, probably in Permian but definitely in Tertiary to recent times.

Poty et al. (1986) provide the following genetic model for pitchblende vein deposits associated with leucogranites in the Limousin and other districts in the French Hercynian massifs. (see also Table 5.22)

a) The evolution of vein-type uranium deposits started during the final stage of the Hercynian Orogeny, 325 to 300 m.y. ago which was marked by general uplift associated with intensive magmatic activity in form of granite, microgranite and lamprophyre dike emplacement.
b) In distinct crustally derived peraluminous leucogranites uraninite crystallized as a primary magmatic rock constituent (Cuney et al. 1979; Pagel 1981, 1982a; Friedrich et al. 1987).
c) Uraninite, in the Saint Sylvestre granitic complex, shows two modes of distribution (Cuney et al. 1985; Friedrich 1984; Friedrich et al. 1987):

Table 5.22. Limousin, summary of evolution and principal geological events of the Saint-Sylvestre Massif since Devonian time. (After Leroy 1978a amended by more recent data as referenced)

Age m.y.	Period	Epoch	Principal geological events m.y.	
— 20	Tertiary	Miocene		
— 30		Oligocene	30	Cementation U-redistribution, loss of radiogenic Pb
— 40		Eocene		
	Permian	Saxonian		
—260		Autunian	270–280	Minimum apparent age for primary pitchblende-pyrite mineralization
—270		Stephanian	285 ± 10	Intrusion of lamprophyre, microgranite mica episyenitization, reactivation of brittle deformation
			ca. 295	Lamprophyre (Leroy & Sonet 1976)
—280	Carboniferous	Westphalian	300 ± 11	Closure of biotite cell (Rb-Sr)
			ca. 300	Feldspar episyenitization (tectonic phase P4) (Turpin 1985)
—290		Namurian	315 ± 18	Apparent age obtained for the Saint Sylvestre 'superstructure' in course of incomplete isotopic homogenization by late magmatic processes (muscovitization, albitization)
—300				
—310		Visean	324 ± 4	Emplacement of Brâme granite (Holliger 1984)
			325 ± 14	Emplacement St. Sylvestre granite (Holliger et al. 1986)
—320			336 ± 6	Emplacement of Châteauponsac granite
—330		Tournaisian	ca. 10 film	
—340	Devonian	Upper		
—350		Middle		
—360			360–380	Culmination of regional metamorphism

- Homogeneous distribution with abundance of uraninite correlated to magmatic differentiation,
- Uraninite accumulations along synmagmatic shear zones, derived from fluids expelled from highly uraniferous fine-grained granitic bodies. The fine-grained facies contains locally up to 100 ppm U. The fine-grained granites were emplaced along the synmagmatic fault zones almost contemporaneously with the enclosing coarse-grained leucogranites (Mollier 1984).

d) Subsequent to this magmatic stage tectonic movements created zones of intense faulting and high heat flow permitting deep reaching convective circulations of meteoric waters that caused local episyenitization. Leroy (1978a,b) relates this or an additional event to a period of lamprophyre and/or microgranite intrusion during the P 3 and P 4 tectonic phases in the Limousin district. (Lamprophyre: ca. 295 m.y.; Leroy and Sonet 1976) The fluids, heated to 370 to 260°C, migrated along early faults, trending N-S and E-W in Limousin, and formed mica episyenite.

e) Mixtures of these hot meteoric solutions with connate "heavy" fluids chemically of C-H-O character (CO_2, hydrocarbons, H_2S enrichments: Turpin 1984) derived from diagenetic or metamorphic rocks collected uranium by leaching uraninite and transported it as uranyl

carbonate complexes to the outer, marginal zone of the pluton.

f) Deposition of pitchblende presumably resulted in response to boiling of fluids triggered by pressure drop, and/or by reactions with mafic rocks such as lamprophyres. It was associated by K-metasomatism and muscovitization of the wall rocks. The pitchblende crystallization occurred about 275 m.y. ago, as indicated by apparent U/Pb ages (Leroy and Holliger 1984).

g) Sites of pitchblende deposition were either active dilational fractures (vein mineralization) or vesicular, vuggy mica episyenite bodies (disseminated mineralization). The latter experienced strong and extensive alteration, whereas fissures and breccia zones trending mostly about NW-SE in Limousin, underwent less extensive wall rock alteration.

h) Primary pitchblende accompanied or pre-dated by small amounts of quartz is associated exclusively with sulfides of iron (pyrite, marcasite) if iron is present. Hematite or other ferric minerals always post-date primary pitchblende, a criterion excluding reduction of hexavalent uranium by ferrous iron oxidation. This raises the question of a valid reductant, since reduction of U^{6+} to U^{4+} is required for pitchblende deposition. Several reducing agents are proposed, such as hydrocarbons found in fluid inclusions or sulfur species, since pitchblende co-precipitated with pyrite. The iron of lamprophyres has been suggested as reductant to explain the enrichment of pitchblende near lamprophyres, but this is contradicted by hematite formation well after pitchblende, as stated by Poty et al. In addition, lamprophyres in contact with uranium mineralization show changes in mineralogy and chemistry, but Leroy (1978b) points out that their iron content does not vary and occurs more in a reduced state in form of pyrite instead of being in the mafic rock constituents (biotite, pyroxene). Ca and Mg decrease in the lamprophyres near pitchblende veins. This may be explained by reactions of the CO_2-rich fluids with dike minerals, resulting in the formation of Ca-Mg-HCO_3 complexes. The related lowering of the HCO_3^- content, may cause the release of $(UO_2)^{2+}$, and as such may add to the boiling factor and to increased accumulation of pitchblende at the intersection of veins with lamprophyre dikes.

i) Fluid inclusion chemistry and isotope data suggest pitchblende deposition at 340 to 350°C from fluids containing CO_2 enrichments, N_2, H_2S, and traces of hydrocarbons. Isotopic values of $\delta^{13}C = -17.6‰$ contradict a mantel origin of this CO_2, whereas high values of $\delta^{18}O = +8$ to $+15‰$ and $\delta D = -45$ to $-30‰$ may indicate involvement of connate, perhaps metamorphic waters in the ore depositing hydrothermal systems.

j) During a second stage of still early hydrothermal activity but subsequent to pitchblende deposition, the CO_2 content of fluids decreased to a level that solutions became purely aqueous and temperatures dropped from 350° (pitchblende) to 140°C. At 130 to 150°C coffinite formed from pitchblende associated with Fe-sulfides and rare galena and quartz. Muscovites of first stage alteration were widely replaced by montmorillonite and adularia.

k) In a last hydrothermal stage, at about 100°C or less, calcite, baryte, and fluorite crystallized.

l) The mixed hypogene convective hydrothermal activity lasted over a period of 20 to 30 m.y., as indicated by age dating.

m) In Jurassic time, local remobilization of primary mineralization occurred in some veins of La Crouzille, or new mineralization from an unknown source may have been introduced, as indicated by data from Pierre Plantées, Margeride district (Respaut 1984).

n) Latest uranium remobilization is more or less recent, triggered by supergene processes.

Although Poty and his coworkers provide convincing evidence for their metallogenetic concept, other French geologists argue against at least part of it. In some deposits, e.g., Margnac in Limousin, pitchblende veins have been discovered in E-W trending structures in the bottom part of the deposit. A. Coste and I. Lozach (pers. commun. 1989) consider these veins to be of hypogene origin. Redistribution of uranium from these E-W veins, perhaps together with indigenous uranium from the granite, may have contributed to the formation of the NW-SE oriented veins, possibly by the processes suggested by Poty et al. (1986).

References and Further Reading for Chapter 5.3.1
(for details of publications see Bibliography)

Autran and Guillot 1974; Autran and Lameyre 1980; Barbier 1968, 1970; Barbier et al. 1967, 1970; Barbier and Ranchin 1969a, 1969b; Bernard-Griffith et al. 1985; Calas 1979; Carrat 1974; Cathelineau 1981, 1983a, 1983b, 1985, 1987; Cathelineau and Leroy 1981; Cathelineau et al. 1982; Chenevoy 1958; Coppens and Bernard 1978; Coppens et al. 1969; Coste, A., pers. commun.; Cuney 1978, 1981, 1982; Cuney and Friedrich 1987; Cuney and Peyrel 1984; Cuney et al. 1979, 1984, 1985; Dardel/ Peinador Fernandes et al. 1979; de Fraipont et al. 1982; Drin et al. 1985; Dubessy et al. 1987; Duthou 1977; Duthou et al. 1984; Friedrich 1981, 1984; Friedrich and Cuney 1983, 1989; Friedrich et al. 1987, 1989; Geffroy 1971, 1973; Geffroy and Sarcia 1958; Holliger and Cathelineau 1986; Holliger et al. 1986; Jiashu and Zehong 1984; Jurain and Renard 1970; Lameyre 1966; La Roche et al. 1980; Leroy 1971, 1978a, 1978b, 1982, 1984; Leroy and Cathelineau 1982; Leroy and Poty 1969; Leroy and Holliger 1984; Leroy and Sonet 1976; Lespinasse 1984; Marignac and Leroy 1979; Marquaire and Moreau 1969; Martin 1981; Michel 1983; Mollier 1984; Mollier and Bouchez 1982; Moreau 1977; Moreau and Ranchin 1971; Moreau et al. 1966; Ouddou 1984; Pagel 1981, 1982a, 1982b; Pecher et al. 1985; Poty et al. 1974, 1986; Ranchin 1968, 1971; Renard 1974; Respaut 1984; Sarcia 1958; Sarcia et al. 1958; Sarcia and Sarcia 1956, 1962; Stussi 1985; Turpin 1984, 1985; Vidal et al. 1984; Weber et al. 1985; Ziegler and Dardel 1984.

5.3.2 Perigranitic Monometallic Vein Uranium Deposits: Příbram District, ČSFR

Příbram is located about 60 km SW of Prague. The district contains perigranitic vein uranium deposits in a NE-SW elongated strip about 25 km long and 1 to 2 km wide (Fig. 5.33). 68 shafts, as much as 1800 m deep, had been sunk to exploit the various vein uranium deposits. Pb-Zn-Ag

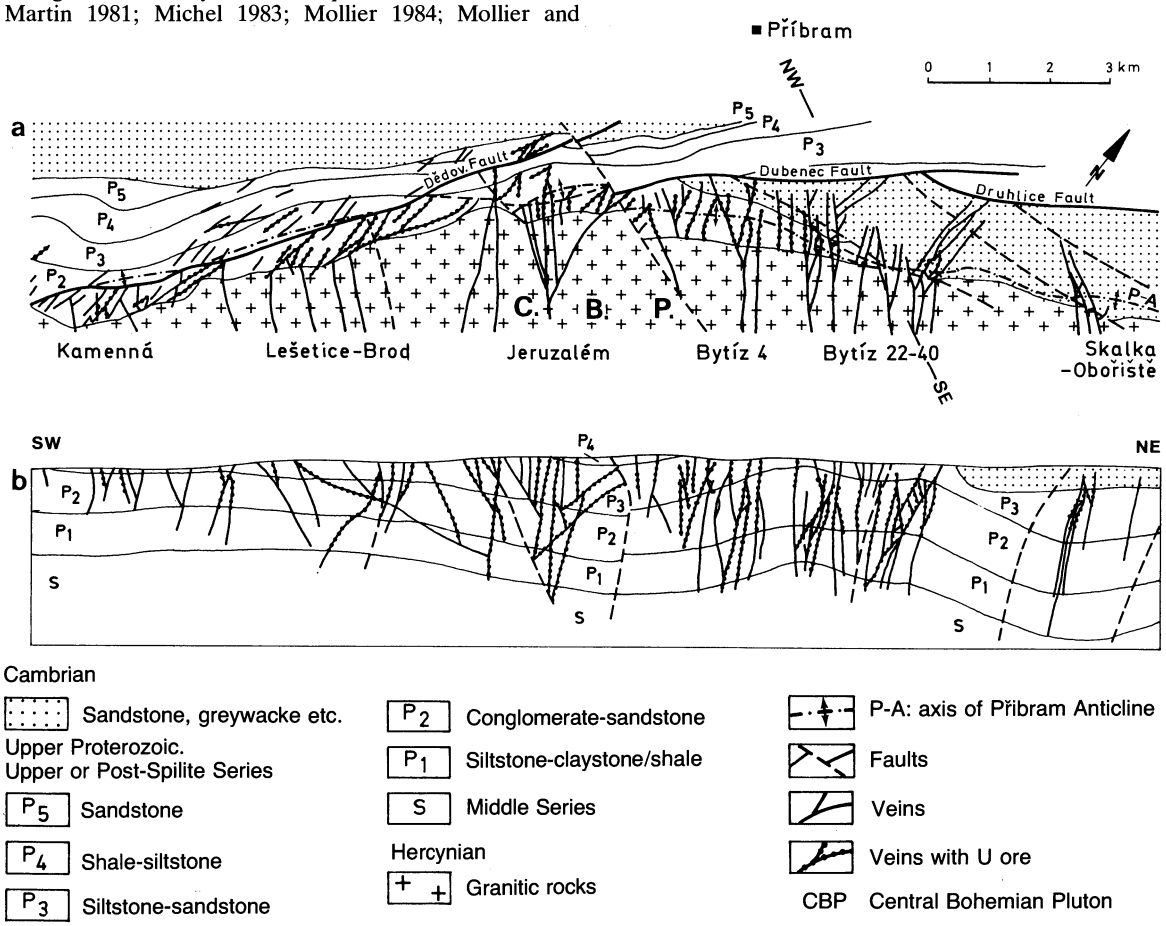

Fig. 5.33. Příbram district. **a** Geological map with the distribution of the most important vein systems/deposits; **b** curvilinear SW-NE section off the Central Bohemian Pluton (*CBP*) contact; **c** NW-SE section across the regional structural grain. **a** and **b** show the restriction of U veins to a narrow zone along the pluton contact and the attitude of principal veins. **c** illustrates in a schematic mode the location of Pb-Zn-Ag, U and Au veins with respect to the overhanging pluton contact. Structures of the Central Bohemian Lineament trend NE-SW, those of Jáchymov Lineament NW-SE. (After: Petroš et al. 1986 (**a** and **b**); Ruzicka 1971 (**c**) based on Kattner 1926)

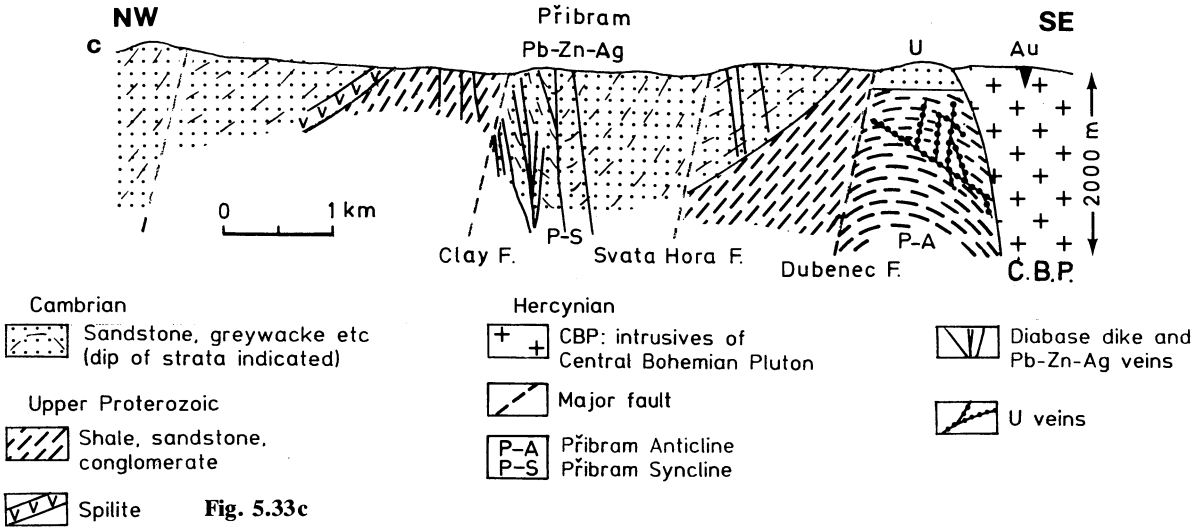

Fig. 5.33c

vein deposits, locally containing uranium, occur in the separate Příbram-Březové Hory and Bohutín districts, ca. 2–4 km NW of the uranium district.

The deposits are structurally controlled and located immediately adjacent to a differentiated granitic complex. The ore composition is practically monometallic. The deposits are therefore classified as perigranitic monometallic vein uranium deposits (class 3.2.2.1, Chap. 4).

Total reserves of the Příbram district are estimated in the order of 65 000 mt U_3O_8, at ore grades ranging from 0.1 to 1.8% U_3O_8.

The following geological description is based on the authors listed, particularly on Kolektiv (1984) and Petros et al., (1986). All figures on reserves and grades are best estimates derived from a variety of other sources.

Geological Setting of Mineralization

Host rocks are predominantly Upper Proterozoic flyschoid schists of the Post-Spilite Series and locally Cambrian clastic sediments which rest unconformably on the Proterozoic. The sediments are mildly regionally and contact-metamorphosed, complexely faulted, and folded into an asymmetric anticline and westerly adjacent syncline (Příbram anticline and syncline Fig. 5.33). A great abundance and variety of dikes, sills, apophyses, and stocks cut the sequences.

The sediments are intruded by the heterogenous granitic *Central Bohemian Pluton*. Its NW contact to the sediments is overturned and dips 35° to 85° SE to a depth in excess of 2000 m (Fig. 5.33c, 5.34b). Rock facies bordering the uranium district to the SE include a border facies consisting of dominantly adamellite which is followed inwards by biotite and two-mica granodiorites. Granitic apophyses extending for up to 300 m along bedding into the sediments are relatively frequent. Isotope dating yield ages of 417 m.y. for the oldest facies (amphibole-biotite granodiorite) to 285 m.y. (amphibole-biotite granite) for the various magmatic rocks of the pluton.

The district is at the junction of the NE-SW trending Central Bohemian Lineament and the NW-SE oriented Jachymov Lineament.

Displacement *structures* within the district are grouped by Petros et al. (1986) into two main systems with respect to their importance and position to the Příbram anticline viz. (a) regional and (b) local longitudinal ± NE-SW, diagonal ± N-S, and ca. NW-SE-oriented cross faults.

Host Rock Alteration

Wall rocks along veins are modified by a variety of alterations. Kolektiv (1984) attributes the alterations to the various stages of mineralization (see below) as follows:

- Siderite-sulfide stage: Sericitization of plagioclase and biotite.
- Early calcite stage: Illitization and sericitization as above but less intense associated with chloritization, carbonatization, and hematitization. Hematite and goethite replace sulfides

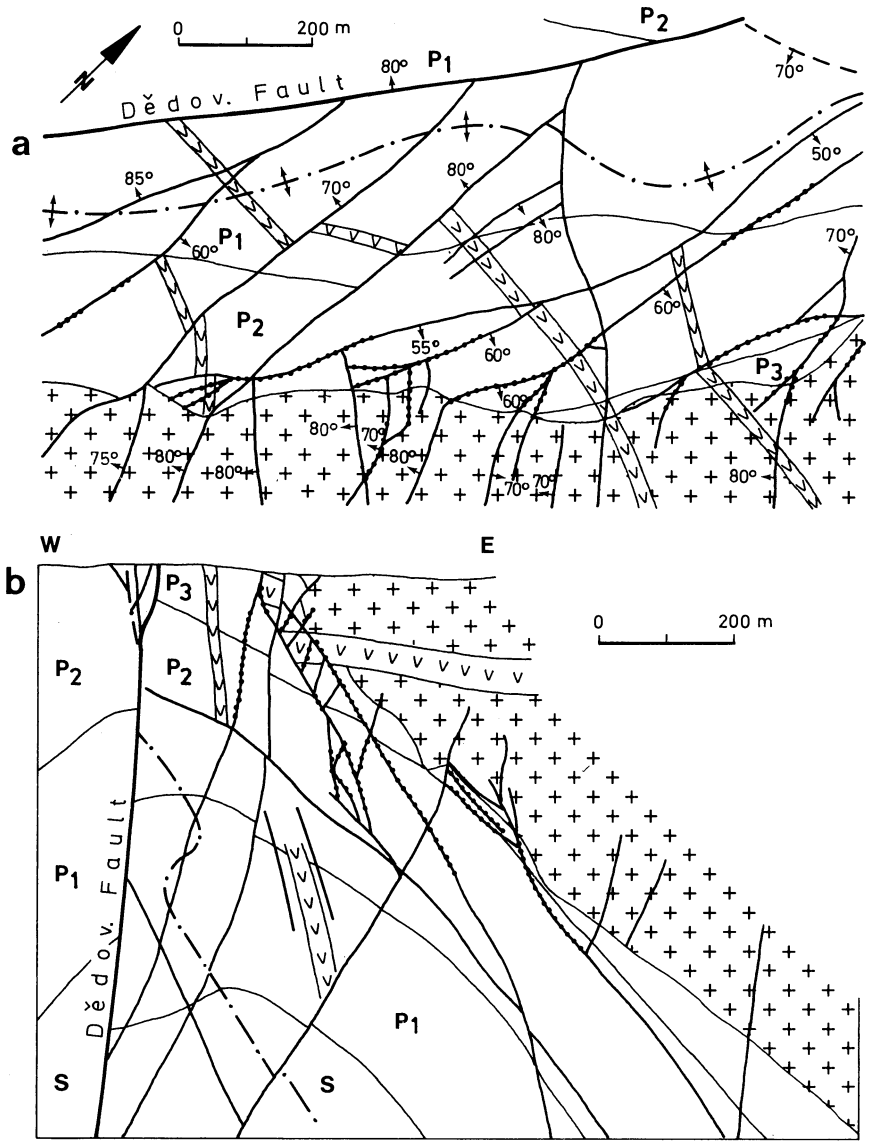

Fig. 5.34. Příbram district, S part (Lešetice-Brod area). **a** Plan of underground level; **b** W-E section approximately perpendicular to the Central Bohemian Pluton contact and fold trend. The figure illustrates the interrelationship of U mineralized vein clusters, N-S and NE-SW structures joining with the Dědovsky Fault and the overhanging pluton contact. (Legend see Fig. 5.33a,b; vvv = diabase) (After Petroš et al. 1986; Kolektiv 1984)

and impose a pink hue on the wall rocks for up to 2 m from veins.

- Calcite-pitchblende stage: Continued sericitization and hematitization at the initial phase of this stage followed by chloritization (without hematite) in up to 5-cm-wide rims during pitchblende deposition.
- Calcite-sulfide stage: Similar to previous stage.

Alteration aureoles in sediments commonly persist for 0.1 to 3 m from veins. Alteration is more extensive in intrusive rocks. In segments of multiple veins where the zones of cataclasis and vein infilling overlap, alteration may spread over intervals to several tens of meters width.

Principal Characteristics of Mineralization

Principal *uranium minerals* are pitchblende and minor coffinite and uraniferous anthraxolite. Sulfides are present but in minor quantities. Dominant *gangue mineral* is calcite. Others are quartz, baryte, chlorite and Fe-, Mg-carbonates. In total, more than 50 minerals including 35 ore minerals have been identified in the Příbram uranium ores (Fig. 5.35).

Four principal mineral parageneses/stages are distinguished by Komínek and Prokeš (in Petroš et al. 1986) as presented in Table 5.23. These mineral assemblages may form veins of its own or hybrid veins.

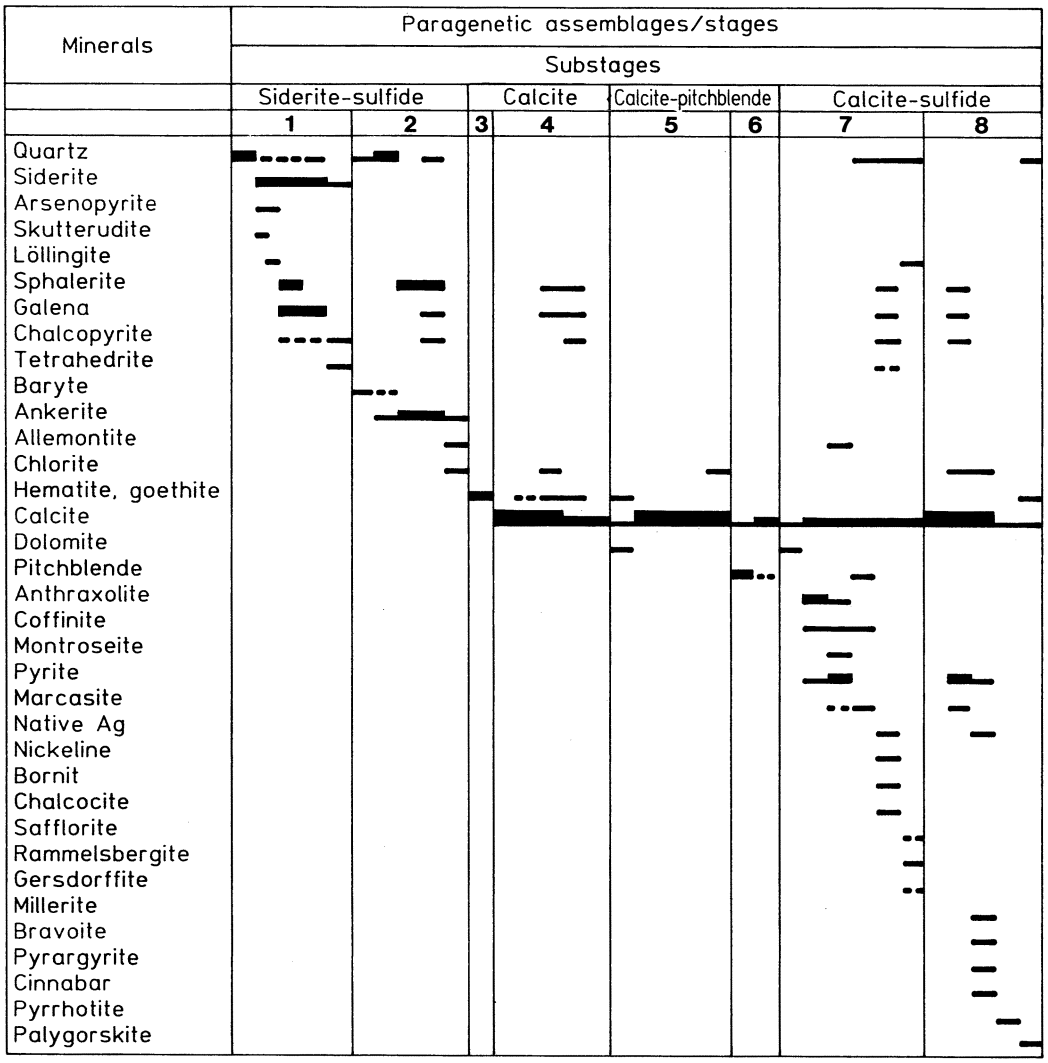

Fig. 5.35. Příbram district, paragenetic scheme of uraniferous veins. (After Kolektiv 1984)

Kolektiv (1984) recognizes *four types of vein infillings* based on the quantitative presence of the respective assemblages:

- siderite-sulfide veins containing 60–90 vol % of the stage 1 siderite-sulfide assemblage,
- calcite-pitchblende veins containing 90 vol % of minerals of stages 2 to 4,
- calcite veins containing 100 vol % of minerals of the stage 4 calcite-sulfide assemblage,
- mixed veins containing minerals of all stages.

Three types of *recoverable ore composition* are distinguished based on the predominance of distinct ore minerals: Pitchblende ore, uraniferous anthraxolite ore and sphalerite-galena-Ag ore.

The various mineral associations, as demonstrated by Kolektiv (1984) display preferences for different *structure systems* and some *zonation* in lateral and vertical directions.

a) Diagonal and cross veins of N-S orientation associated with major faults are of mixed type. Thickness of the mineralized section of these veins averages ca. 150 cm. Siderite-sulfide and calcite-sulfide assemblages are almost ubiquitously distributed throughout a vein whereas the calcite-pitchblende association occupies only vein intervals of greater thickness. The thickness of these veins decreases gradually with depth.
b) Longitudinal veins of NE-SW direction are of the calcite-pitchblende type. Average thick-

Table 5.23. Příbram district, paragenetic mineral assemblages/generations in uranium-bearing veins (from oldest to youngest) (see also Fig. 5.35) (After Komínek and Prokeš in Petroš et al. 1986 and Kolektiv 1984)

Stage	Mineral association	Remarks
1. Siderite-sulfide	Siderite, dolomite-ankerite, quartz, baryte, chlorite; galena, sphalerite, some chalcopyrite, tetrahedrite and probably allemontite, skutterudite, löllingite and others	Minerals mostly as marginal bands of vein; ca. 5–10 vol. % of vein fill, locally up to 90%, then forming minable 'polymetallic formation',
2. Early calcite	Calcite DK and K 1 with elevated Mn contents, chlorite; hematite and goethite, some galena, sphalerite, chalcopyrite, sometimes native Ag	Constitute 25–30 vol. % of vein fill; Fe-oxides derived from decomposition of siderite-ankerite,
3. Calcite-pitchblende	Calcite K 2, K 3, and K 4, dolomite, chlorite; pitchblende 1, hematite	Constitute 25–30 vol. % of vein fill; pitchblende 1 formed between K 3 and K 4,
4. Calcite-sulfide	Calcite K 5 in several varieties/generations, minor quartz, chlorite and palygorskite; some uraniferous anthraxolite[a], coffinite, pitchblende 2, commonly restricted to zones with pitchblende 1; several generations of pyrite; minor marcasite, pyrrhotite, sphalerite, montroseite, chalcopyrite, bornite, chalcocite, tetrahedrite, pyrargyrite, native Ag, millerite, nickeline, rammelsbergite, safflorite, allemontite, native As and Sb, and others	Constitute up to 40 vol. % of vein fill, formed by repeated replacement, dissolution and recrystallization of earlier minerals

[a] Uraniferous anthraxolite is a highly polymeric bitumen containing pitchblende, coffinite, calcite and sulfides.

ness of mineral fill is 20–25 cm. The average thickness of all mineral associations increases to a depth of 700 m from where it decreases.

c) NW-SE and more rarely N-S veins associated with the NW-SE tectonic zones and the Příbram anticline preferentially belong to the calcite-pitchblende type. A few veins of this system can be attributed to the mixed or siderite-sulfide type. Thickness of the siderite-sulfide association does not much change with increasing depth, but the thickness of the other assemblages increases to a certain depth and then decreases.

Mineralized veins commonly aggregate in groups or *vein clusters* or *vein knots* by multiple veins closely paralleling, approaching, or intersecting each other.

Mineralized veins can be separated into three groups based on their *dimensions*: Large veins extend laterally and vertically for 500–1000 m and some even more (some veins persist to >2000 m deep). Thickness is 5–100 cm, in extreme cases up to 12 m. These veins constitute the principal elements of vein clusters and account for ca. 5% of all veins of the district. Medium veins are 100 to 500 m in extension. Thicknesses are 1–50 cm and only exceptionally more. They commonly occur as subsidiary veins to the large veins and account for 45% of all veins.

Small veins are up to 100 m in extension and less than 50 cm wide. They occur subsidiary to the larger veins and constitute ca. 50% of all veins.

Oldest mineralization (pitchblende 1) yield a U/Pb *age* of 265 ± 15 m.y. (Legierski in Kolektiv 1984).

Ore Controls and Recognition Criteria

Principal ore controlling or recognition criteria include:

Host Environment

- Localization of the district is (a) at the intersection of two lineaments; (b) proximal to and between the Central Bohemian Pluton and major regional faults, a zone 1 to 2 km wide, and (c) along the axial zone of the Příbram anticline (Fig. 5.33a,c).
- Lodes are most numerous in the apex part of the Příbram anticline and in its SE limb close to the pluton contact. NW-SE cross

veins in the NE and central section of the district are richest near the anticlinal axis. They developed particularly where undulations, local brachyanticlinal folds, or closures and virgation modify the main axis. Here, tensional strain has generated a large width of cataclasis along open fractures and wide subsidiary fissures.
- Remarkable concentrations of ore pods and lenses within the veins, often of high grade occur at sites where the pluton contact forms a roof overhanging the (meta-) sediments for as much as 2 km wide (Fig. 5.34b).
- Host rocks are pelitic and psammitic sediments regionally metamorphosed up to greenschist facies, folded into major anticlines and synclines, and overprinted by contact-metamorphism.
- Lithology imposed a twofold control on the deposits by physical-mechanical properties influencing location and development of structures and by chemical composition affecting the chemistry of mineralizing fluids.
- Most of the uranium mineralization is emplaced within the Post-Spilite Series (97%) whereas Cambrian sediments, tuffites of the Spilite Series and granites only contain 3% of the lodes. Richest intervals developed where host rocks corresponded to tectonic stress by more brittle deformation. Intraformational conglomerate beds created a barrier effect in their footwall reflected by deviation of the dip of veins and, associated with movements during mineralization, a thickening and enrichment of veins, particularly in longitudinal veins. Similar barrier effects are found below Cambrian sediments, granites, and thicker intrusive dikes.

Alteration

- Ore-related alteration includes illitization/sericitization, chloritization, carbonatization, and hematitization which penetrated the wall rocks for commonly less than 3 m from a vein.

Mineralization

- The ore is essentially monometallic but composed of a great variety of minerals formed during several stages.
- Principal ore minerals are pitchblende, coffinite, and uraniferous anthraxolite.
- Associated minerals are mainly pyrite and minor sulfides and arsenides of Fe, Cu, Pb, Zn, Ag, Ni, Co, and other elements. Hematite can be abundant. Calcite is the dominant gangue mineral; others are other carbonates, quartz, baryte, and chlorite.
- Mineralogically the amount of ore-related calcite correlates with the amount of uranium in any given lode (coefficient factor 0.68), and individual ore lodes are principally associated with the older calcite generation.
- Younger post-ore solutions caused replacement of pitchblende and older calcite and dilution of the ore.
- Major ore bodies are restricted to large veins but the bulk of ore shoots is in subsidiary structures.
- Rich lodes, lenses, pods occur preferentially at a distinct bending of veins, ramification of veins, junction of subsidiary and horsetail fractures with major faults, intersection of major veins with intrusive dikes, intervals immediately below shallow dipping pluton contact, or below Cambrian sediments and intraformational conglomerates associated with a complication of the vein morphology, and above a level of 600–700 m under surface.
- Below a level of 600–700 m begins a reduction of size and intensity of veins (more barren ground between veins), length of veins (averaging 450–500 m above this level), decrease of bifurcation and ramification of veins and payload material.

Metallogenetic Concepts

Petroš et al. (1986) propose a close relationship of ore formation and the granites/granitoids of the Central Bohemian Pluton. Transport of uranium occurred in the form of carbonate complexes in alkaline solutions of medium to low temperatures. Precipitation of pitchblende resulted from degassing and decarbonation of the fluids and changes in pH and Eh.

The uranium is postulated to have originated from sediments with subsequent enrichment during magma differentiation. Leaching of uranium from the granitic rocks occurred by fluids migrating along NW-SE-oriented faults. Isotope studies suggest that a certain supply of uranium may have derived from residual magmatic solutions. Contact-metamorphism may also have

mobilized uranium within the metasediments. A direct relationship of ore formation and granite intrusion is disputed by the large time gap of at least 20 m.y. separating both (for references of the various aspects see Petroš et al. 1986).

Strnad (1986) refuses the (meta-) sediments and obviously also the granites as a uranium source because their uranium content is only in the order of Clarke values or less. Strnad argues that the district is located at the intersection of deep-seated lineaments and that this situation conditioned the development of the Hercynian uraniferous vein accumulations from Proterozoic precursors.

References and Further Reading for Chapter 5.3.2
(for details of publications see Bibliography)

Hruby, J., pers. commun.; Kolektiv 1984 (German translation by J. Hruby); Petroš et al. 1986; Ruzicka 1971; Ruzicka V, pers. commun.;

5.3.3 Perigranitic Polymetallic Vein Uranium Deposits: St. Joachimsthal/Jáchymov District, ČSFR

St. Joachimsthal (German) or Jáchymov (Czech) is located in the western Erzgebirge, 20 km N of Karlovy Vary (Karlsbad). More than 200 mineralized veins are known from the district about 45 km^2 in size. Seven major vein systems (Fig. 5.36) were subject to uranium mining exploited by shafts between 300 and 1000 m deep. Mining ceased in 1963. Total uranium reserves amount to about 10000 mt U_3O_8 at ore grades (mill feed) averaging between 0.1 and 1% U_3O_8 in addition to other metals.

The deposits are structurally controlled and located in the vicinity of a differentiated granite. Mineralization is characteristically polymetallic composed of Ag, Co, Ni, Bi, and U. The deposits are therefore classified as perigranitic polymetallic vein uranium deposits (class 3.1.2.2, Chap. 4).

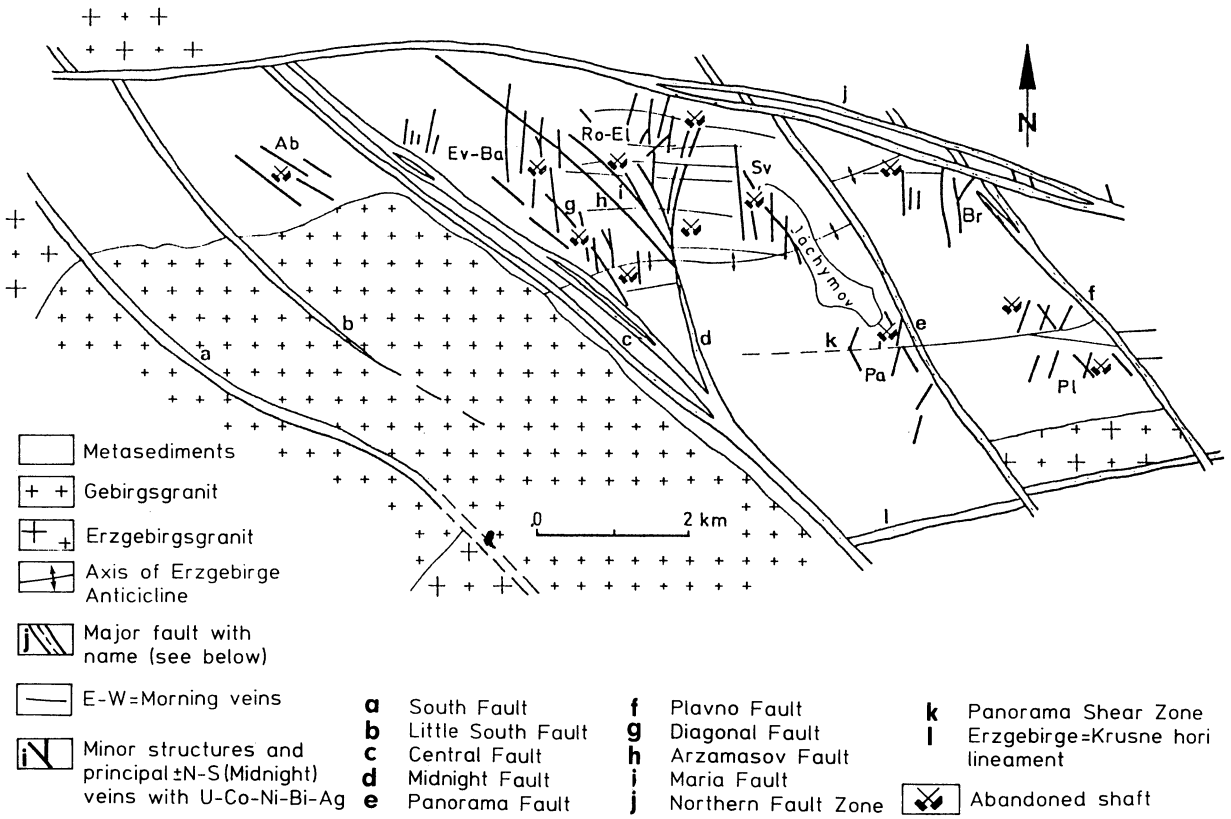

Fig. 5.36. Jáchymov district, generalized structural map projected into the Daniel horizon level (630–640 m a.s.l.). The map shows major faults/lineaments, the clusters of the NE to NW oriented U-Co-Ni-Bi-Ag "Midnight veins" and the E-W trending "Morning veins," and the position of the district with respect to the autometamorphic "Erzgebirgsgranit." Vein clusters: *Ab* Abertamy; *Br* Bratrství; *Ev-Ba* Eva-Barbora; *Pa* Panorana; *Pl* Plavno; *Ro-El* Rovnost-Eliáš; *Sv* Svornost. (After Komínek and Veselý 1986; Kolektiv 1984; Bernard et al. 1967)

The discovery of the district goes back to 1516. It was one of the leading silver producers of central Europe in its early days. Later, cobalt, nickel, and bismuth were recovered. Uranium mining started at the end of the last century. It was used for paints and the extraction of radium. Two railroadcars of concentrate of residues from paint production were shipped to Madame Curie in Paris, who discovered radium in these ores. Another historical aspect of Joachimsthal is the naming of currency. Its medieval silver mint produced coins called Thaler or Taler which, in later centuries, provided in the USA the root for the dollar.

Kolektiv (1984), Komínek and Veselý (1986) and Ruzicka (1971) published concise reviews on the Jáchymov deposits. Their data provided the base for the following compilation. Figures on grades and reserves are best estimates derived from other sources.

Geological Setting of Mineralization

The Jáchymov district is located at the southeastern margin of the Eibenstock Massif in the western Erzgebirge, a segment of the Saxo-Thuringian metallotectonic zone of the Hercynian orogenic belt. Host rocks are metasediments of the Barbora and Jáchymov series of the Mica Schist Formation.

The metasedimentary complex was intruded by early Hercynian diorite and gabbrodiorite stocks and late Hercynian granitic massifs followed by dikes of variable composition. Tertiary alkaline volcanics are the youngest igneous rocks (Ruzicka 1971).

The large *Eibenstock Massif* (ca. 600 km^2 in outcrop) is composed of late Hercynian granites. They outcrop on the southwestern side and in cupolas on the NW and SE margins of the Jáchymov district. The granites underlie the metasediments of the district at a depth of 300 to 1000 m. The granites generated a contact-metamorphic aureole 10 to 60 m wide (Figs. 5.36, 5.37).

Two principal types of late Hercynian granites are recognized (ages from Smeykal in Kolektiv 1984). The older "*Gebirgsgranit*" (340–320 m.y.) (or "normal granite") predominantly consists of porphyritic biotite granite.

The younger "*Erzgebirgsgranit*" (310–300 m.y.) (or "autometamorphic granite") is

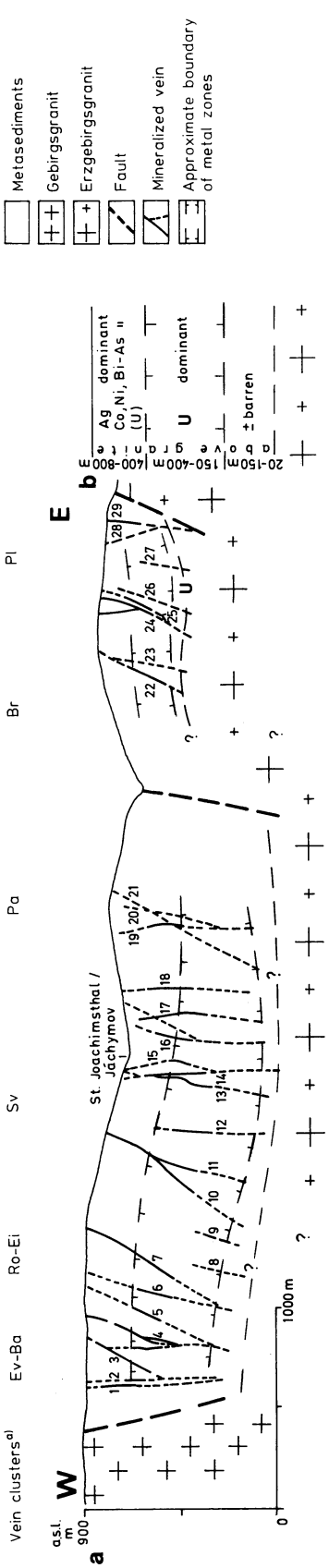

Fig. 5.37. Jáchymov district. **a** Generalized W-E section showing the principal vein systems/clusters and vertical zonation of metal distribution. **b** Schematic diagram of metal zoning. In the upper zone, approximately 400 to 800 m above the granite contact prevails Ag in the uppermost levels followed downwards by Co, Ni, Bi and As dominance with minor (redistributed) U. In the medium zone, ca. 150 to 400 m above the granite is U dominant with more or less Co and Ni and rare Ag. Veins of the lowest zone are almost barren of metals except for very wide veins. Veins: *1* Neuhoffnungs Gang (Gang = vein); *2* Fluder G., *3* Putzen Wacke; *4* Geister G.; *5* Hieronymus G.; *6* Bergkittler G.; *7* Schweizer G.; *8* Christof G.; *9* Josefi G.; *10* Rose von Jericho G.; *11* Johannes Evangelisten G.; *12* Häuerzecher G.; *13* Hildebrand G.; *14* Geschieber G.; *15* Becken G.; *16* Clementi G.; *17* Prokopi G.; *18* Marien G.; *19* Kaiser Josef G.; *20* Goldene Rose G.; *21* Lettenfäule (shear zone); *22* Glückauf G.; *23* Zufalls G.; *24* Franziszi G.; *25* Zeidler G.; *26* Lettenfäule; *27* Hilfe Gottes G.; *28* Bleiglanz G.; *29* Magareten G. *a)* approximate location of vein clusters as shown in Fig. 5.36. (After Kohl 1953, Kraus 1916, Petrascheck 1950)

leucocratic and typically contains higher amounts of accessory minerals and elevated Clarke uranium values. (Gebirgsgranit/biotite granodiorite 6.8 ppm U, 17–24 ppm Th, Erzgebirgsgranit/autometamorphic biotite granite 10.4–11.6 ppm U, 12.2–12.5 ppm Th, Škubal and Vachuška 1973 and Absolonová and Matoulek 1975 in Kolektiv 1984). Uranium occurs, among others, in form of minute uraninite crystals (Kohl 1954).

The Erzgebirgsgranit exhibits strong autometamorphic modifications comparable to a large extent with the late magmatic phenomena described by Poty and coworkers for granite related uranium districts in France. (see Chap. 5.3.1) Modifications include albitization, muscovitization, and greisenization (Sn-W greisens 280 m.y.).

A variety of *dikes* including granite porphyry (290–280 m.y.), quartz porphyry, pegmatite, and aplite intruded subsequent to the emplacement of the pluton.

Brittle *deformation* produced four fault systems oriented ENE-WSW, NW-SE, N-S, and E-W (Fig. 5.36). The NW-SE with associated N-S and the E-W structures are the principal hosts for mineralization.

Table 5.24. Erzgebirge, alteration features in metasediments and granitic rocks hosting vein-type uranium deposits. (After Dymkoff 1960 and Ruzicka 1971)

In metasediments
Pre-uranium alterations
Initial stage: formation of skarns and biotitization
Scapolitization of gneisses
Pyritization, chloritization of amphibolites, tuffs, gneisses etc.
Graphitization along shear zones
Syn ? to post-uranium alterations
Silicification, carbonatization, hematitization
Post-uranium alterations
Sericitization, silicification, kaolinitization
In granitic rocks
Pre-uranium alteration
Greisenization, albitization, muscovitization, silicification
Syn-uranium alteration
Sericitization
Post-uranium alteration
Sericitization, kaolinitization

Host Rock Alteration

General alteration features in rocks surrounding uranium deposits in the Erzgebirge are given in Table 5.24. Kolektiv (1984) recognizes two stages of wall rock alteration, a pre- and a syn-uranium stage.

The *pre-uranium stage alteration* affected wall rocks 0.5 to 3 m wide from veins. An early alteration phase begins with disintegration of mafic minerals and recrystallization of chlorite, phlogopite, rutile and, in immediate proximity to veins, pyrite and larger quantities of calcite. In a final phase, intense silicification replaced many minerals including calcite, and produced a wide zone of quartzification.

The *syn-uranium stage alteration* extends for only centimeters to several tens of centimeters away from the vein contact where it overprinted the older alteration zone. Principal recrystallization products are albite and adularia. Pyrite was replaced by hematite, and calcite by dolomite.

Principal Characteristics of Mineralization

Kolektiv (1984) and Komínek and Veselý (1986) separate the Jáchymov mineralization into seven *mineral associations/stages* (in sequential order) (Fig. 5.38):

1. Garnet-pyroxene-magnetite.
2. Quartz-wolframite-cassiterite.
3. Quartz-sulfide.
4. Carbonate-pitchblende.
5. Carbonate-arsenides.
6. Sulfarsenides.
7. Quartz-hematite-manganite.

The first two associations are of more regional distribution and the last five constitute the actual vein fillings of the district.

Ruzicka (1971) provides the following elemental suite and ranges of percentages of *metallic elements* in lodes of the Jáchymov veins: 1.00% U, Fe; 1.00–0.10% V, Y, Cu, Pb, Zn, Sb, As, Se; 1.00–0.01% Mn, Bi; 0.10–0.01% Ti, Th, Ag, Au, W, Y, Sc, P; <0.01% Mo, Sn, Li, Be, Co, Ni, Ba, Sr, Tl, Ce.

Primary *uranium* in form of colloform pitchblende is essentially restricted to the carbonate-pitchblende stage. Redistributed uranium occurs

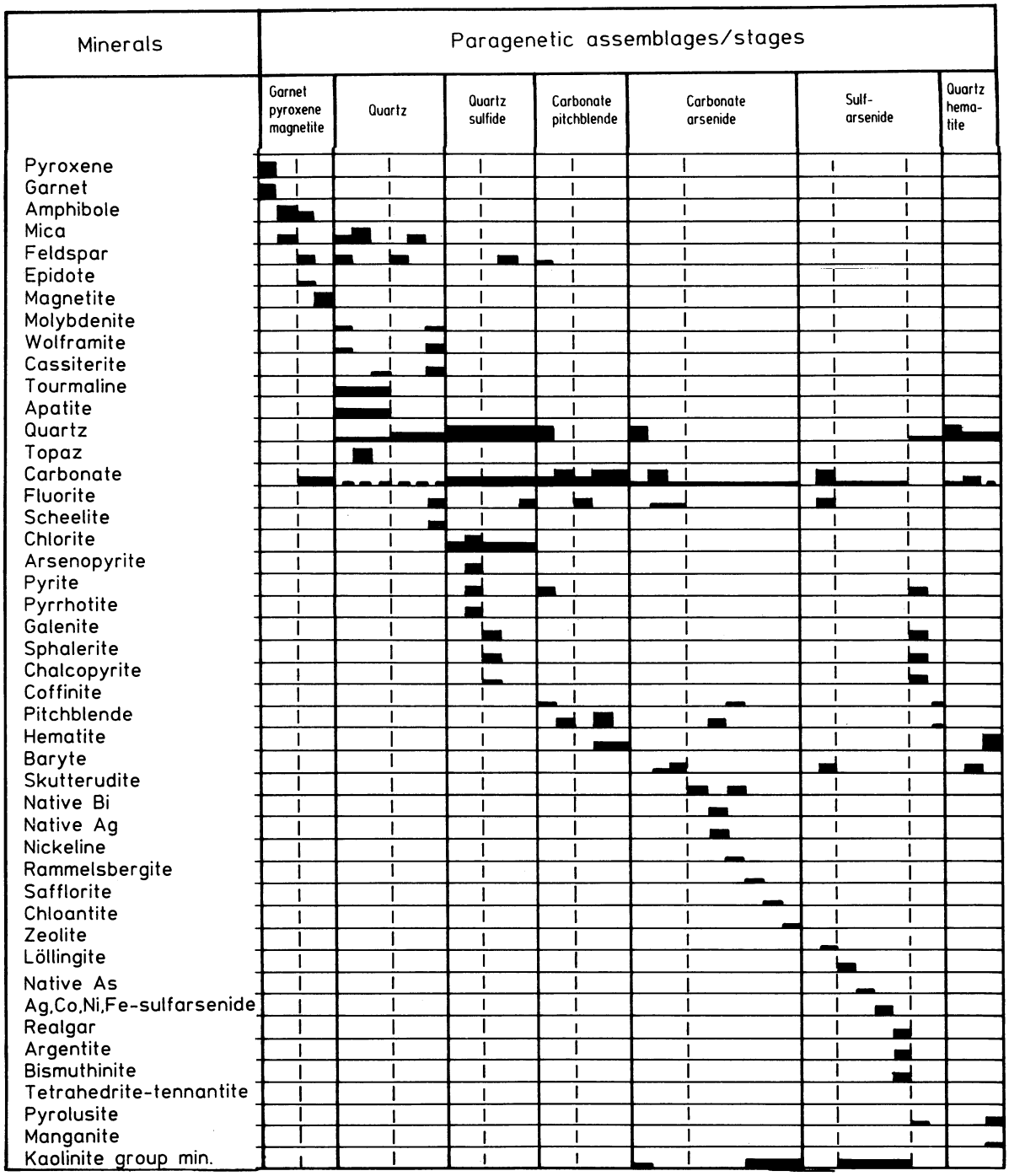

Fig. 5.38. Jáchymov district, paragenetic scheme of mineralization of U, Co, Ni, Ag-bearing veins. (After Kolektiv 1984)

mostly in the form of sooty pitchblende and coffinite which are the main uranium minerals in the arsenide and sulfarsenide stages, i.e., the original uranium phase is of monometallic nature and it only became polymetallic by a younger, uranium-unrelated, introduction of other metals.

Younger hydrothermal solutions caused ore modifications which in part occurred after the extrusion of the Tertiary volcanics.

Two varieties of veins containing uranium, the simple and the complex veins, are recognized by Kolektiv (1984) and Komínek and Veselý (1986).

Veins of *simple composition* contain the carbonate-pitchblende assemblage emplaced within gouge and brecciated wall rock material. Fractures hosting simple mineralization are mostly those of fifth and sixth order. Veins are 150 to 400 m long and 3 to 25, rarely 50 cm wide.

Two substages are present. Principal minerals of the older substage are pitchblende 1 and coffinite 1 associated with comb-textured aggregates of quartz, albite or adularia and fluorite. Minerals of the younger substage are pitchblende 2, dolomite and hematite.

Veins containing primary pitchblende are only preserved in structures that had been sealed early.

Veins of *complex composition* contain additional to minerals of the carbonate-pitchblende assemblage those of the younger carbonate-arsenide and quartz-sulfide stages. Fractures hosting complex veins predominantly are fourth order structures that had been reactivated and are now characterized by breccias and deformed gouge. Veins are more than 1000 m long and 10 to 60 cm wide.

Characteristic mineral components of complex veins are tri- and di-arsenides of Co and Ni together with native Ag, Bi and As. Gangue minerals include dolomite, ankerite, quartz, minor baryte and fluorite. U is present in several generations of pitchblende and coffinite largely derived by remobilization of pitchblende 1.

Figure 5.38 shows some examples of the composition and texture of different veins hosted by mica schist.

The composition of the veins shows a *vertical zonation* (Fig. 5.37).

- Upper levels, more than 600 to 800 m above the granite basement or from surface to 400 m deep respectively are dominated by native silver, arsenides and redistributed pitchblende.
- Lower levels extending 200 to 300 m upwards from the granite basement are dominated by native bismuth, arsenides and primary pitchblende.

Smeykal in Kolektiv (1984) established isotope *ages* of 270–230 m.y. (247 ± 7 m.y.) for 1st generation pitchblende and 150–100 m.y. for 2nd generation pitchblende, that is associated with quartz, dolomite and the Co, Ni, Bi, As stage. Ruzicka (1971) reports 30–5 m.y. for a 3rd generation of pitchblende supposedly associated with a young generation of Co-Ni minerals formed during Tertiary tectonism.

Ore Control and Recognition Criteria

Principal ore controlling parameters or recognition criteria include:

Host Environment

- On a regional basis, most of the polymetallic Ag, Co, Ni, Bi, U vein deposits have been found in the Saxo-Thuringian metallotectonic zone or southerly adjacent in the northern part of the Moldanubian Zone of the Hercynian belt. Whether this reflects geochemical-sedimentary zoning in the pre-Hercynian geosyncline along the northern margins of the now Moldanubian Zone or distinct geotectonic/hydrothermal processes different to those forming the Bohemian-type veins, or other causes remains open to debate.
- The district is associated with a highly differentiated uraniferous leucogranite located at the junction of two lineaments.
- Mineralization is essentially restricted to metasediments.
- Uranium distribution exhibits a pronounced spatial relationship to the intrusive surface of the granite in depth. Uranium mineralization prevails in a zone between (20-) 150 m and 400 m above and paralleling the granite contact which is 300 to 1000 m deep (Fig. 5.39).
- Uranium pinches out with very few exceptions within 20 to 150 m above the granite, i.e., at the margin within the hornfels zone of contact-metamorphism.

Alteration

- Pre-uranium stage alteration reflected by growth of chlorite, phlogopite, rutile, and abundant calcite penetrates wall rocks for up to 3 m. Subsequent pervasive silicification generated a wide silicified zone.
- Syn-uranium stage alteration reflected by albite, adularia, dolomite, and hematite development overprinted in a narrower halo the former alteration zone.

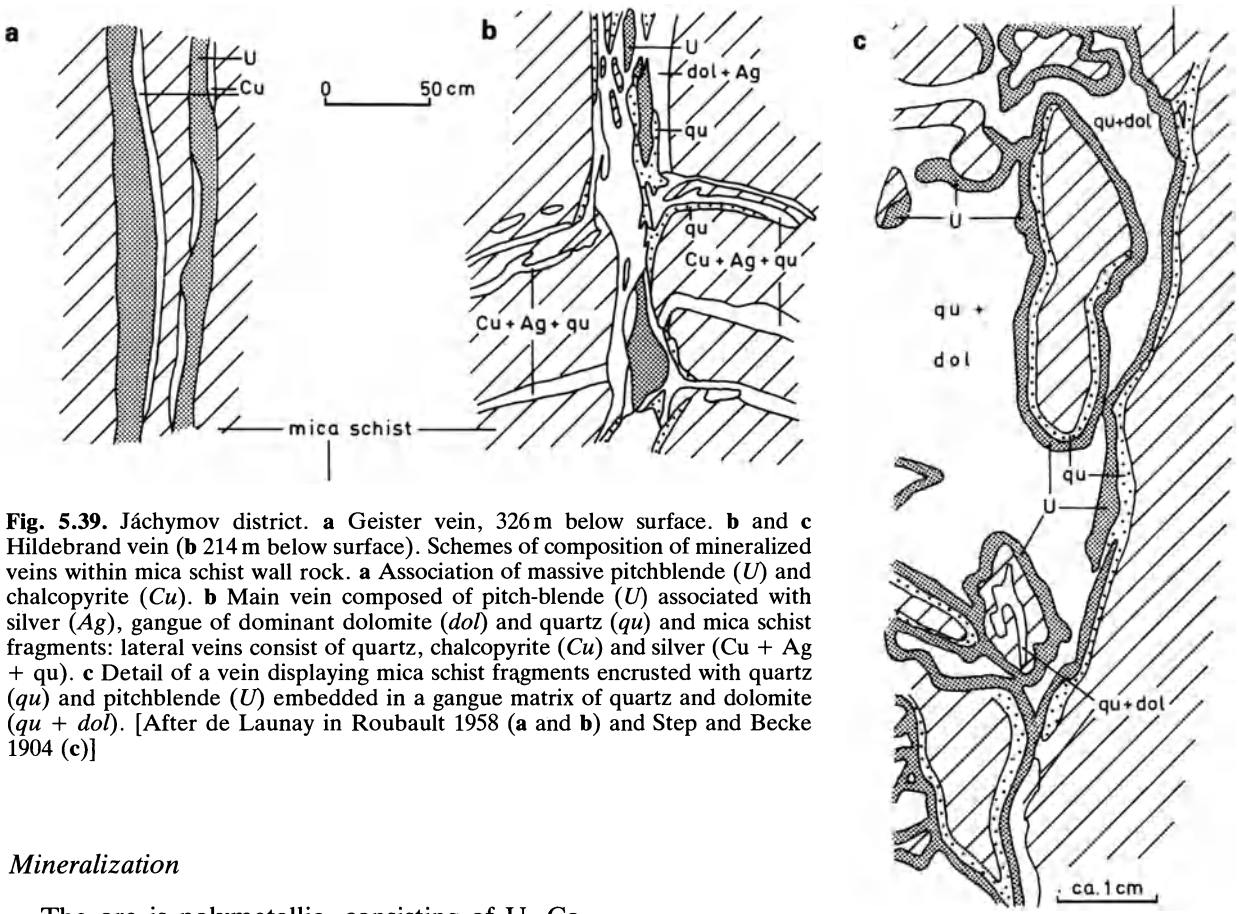

Fig. 5.39. Jáchymov district. **a** Geister vein, 326 m below surface. **b** and **c** Hildebrand vein (**b** 214 m below surface). Schemes of composition of mineralized veins within mica schist wall rock. **a** Association of massive pitchblende (*U*) and chalcopyrite (*Cu*). **b** Main vein composed of pitch-blende (*U*) associated with silver (*Ag*), gangue of dominant dolomite (*dol*) and quartz (*qu*) and mica schist fragments: lateral veins consist of quartz, chalcopyrite (*Cu*) and silver (Cu + Ag + qu). **c** Detail of a vein displaying mica schist fragments encrusted with quartz (*qu*) and pitchblende (*U*) embedded in a gangue matrix of quartz and dolomite (*qu* + *dol*). [After de Launay in Roubault 1958 (**a** and **b**) and Step and Becke 1904 (**c**)]

Mineralization

- The ore is polymetallic, consisting of U, Co, Ni, Ag, and Bi, but uranium is not paragenetically related to the other metals.
- Various mineral assemblages have formed during several stages.
- Veins of simple composition contain pitchblende and coffinite associated with quartz, albite or adularia, fluorite, and hematite.
- Veins of complex composition contain arsenides, sulfarsenides, and native forms of the other metals and redistributed uranium often as coffinite associated with dolomite, ankerite, quartz, minor baryte, and fluorite.
- The mineralized veins of the Joachimsthal/ Jáchymov district group in clusters. Seven of the clusters contained most of the uranium mined (Fig. 5.36).
- Vein clusters often consist of tree-like asymmetric geometry, the variably trending branches or fault systems filled with different mineral associations.
- Emplacement of the carbonate-pitchblende association occurred in structures of a distinct system trending about NW-SE to N-S with richest ore concentrations at sites of structural complication of veins such as (a) marked changes in strike and dip direction of veins, (b) sites of interjunction, branching or ramification of veins, (c) sites of splaying or horse-tailing, (d) intersections with faults or dikes providing structurel barriers (particularly E-W faults and granite porphyry dikes), (e) thickening of veins, and (f) moderately inclined sections.
- All intervals with above listed structural features display intense cataclasis of wall rocks, development of a series of microjoints and relatively wide aureoles of host rock alteration.
- Uraniferous intervals in veins are generally restricted to vein transections with mafic or semi-mafic schists. Best grades and the bulk of the ore occurs at intersections with strongly pyritic biotite and biotite-phlogopite schists of the Jáchymov Series. Similarly well mineralized are sections cutting through lithologic boundaries between chlorite-sericite phyllites and pyritic amphibolites and biotite schists. Other favorable sites are proximal to dikes and zones of abundant dikes. At intersections of veins with red granite porphyry dikes ore

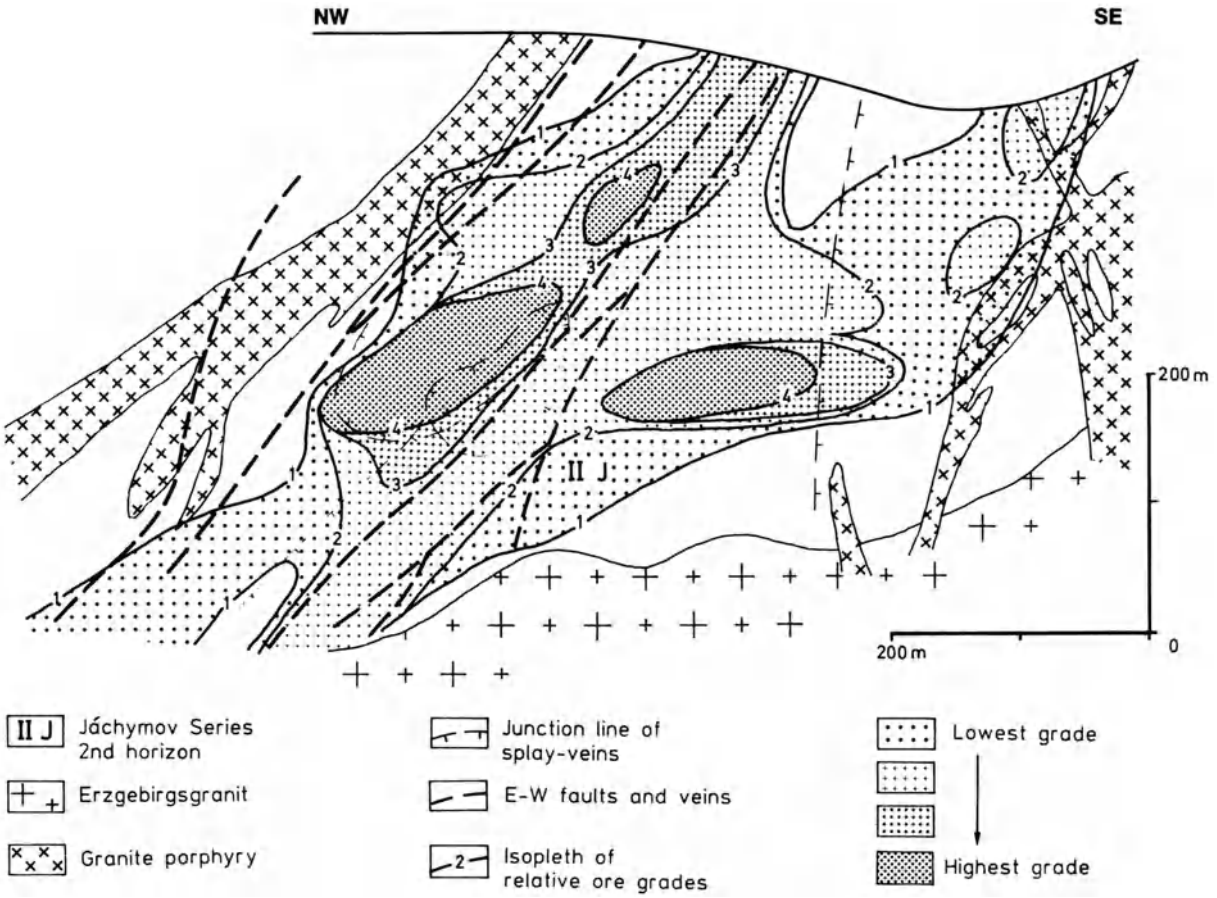

Fig. 5.40. Jáchymov district, A2 vein of the Abertamy vein cluster, (Ab in Fig. 5.36) longitudinal section (vertical projection) with isopleth of relative U ore grades. Mineralization of variable grades and extension forms a lode between and controlled by granite porphyry dikes. (After Komínek and Veselý 1986)

shoots are often accumulated below the dikes (Fig. 5.40).

- The carbonate-pitchblende stage occurs in variably shaped and extensive concentrations, in form of thin stringers, streaks, and patches. Thick veins commonly contain the richest lodes.
- The uranium accumulations are irregularly distributed throughout the vein system and separated by barren ground (Fig. 5.41). Uranium ore occupies only 4 to 6% of the total plane of a vein.
- Lodes are several square meters to some hundred, rarely more than thousand square meters in tabular size composed of sections of different grade (Fig. 5.40). Richest lodes attain dimensions of 100 × 300 m.
- Ore lodes most frequently occur in moderately dipping and only occasionally in flat or vertical dipping sections of the host structure.

Metallogenetic Concepts

The various mineral associations of the Jachymov veins are thought to have formed by discontinuous multistage hydrothermal processes spanning over a time interval from Permian to Cretaceous/Tertiary (Mrňa 1967).

Geochemically different fluids introduced the various metals to form five or six mineral associations of monometallic and polymetallic composition. Two principal periods of ore formation have been deciphered for the Erzgebirge in general by Baumann (1967). The first, which includes the carbonate-pitchblende stage, occurred during late Hercynian time and the second, with formation of Co-Ni arsenides/sulfarsenides etc., some time between late Triassic and Tertiary and probably is associated with the Saxonian/Alpidic tectonic event.

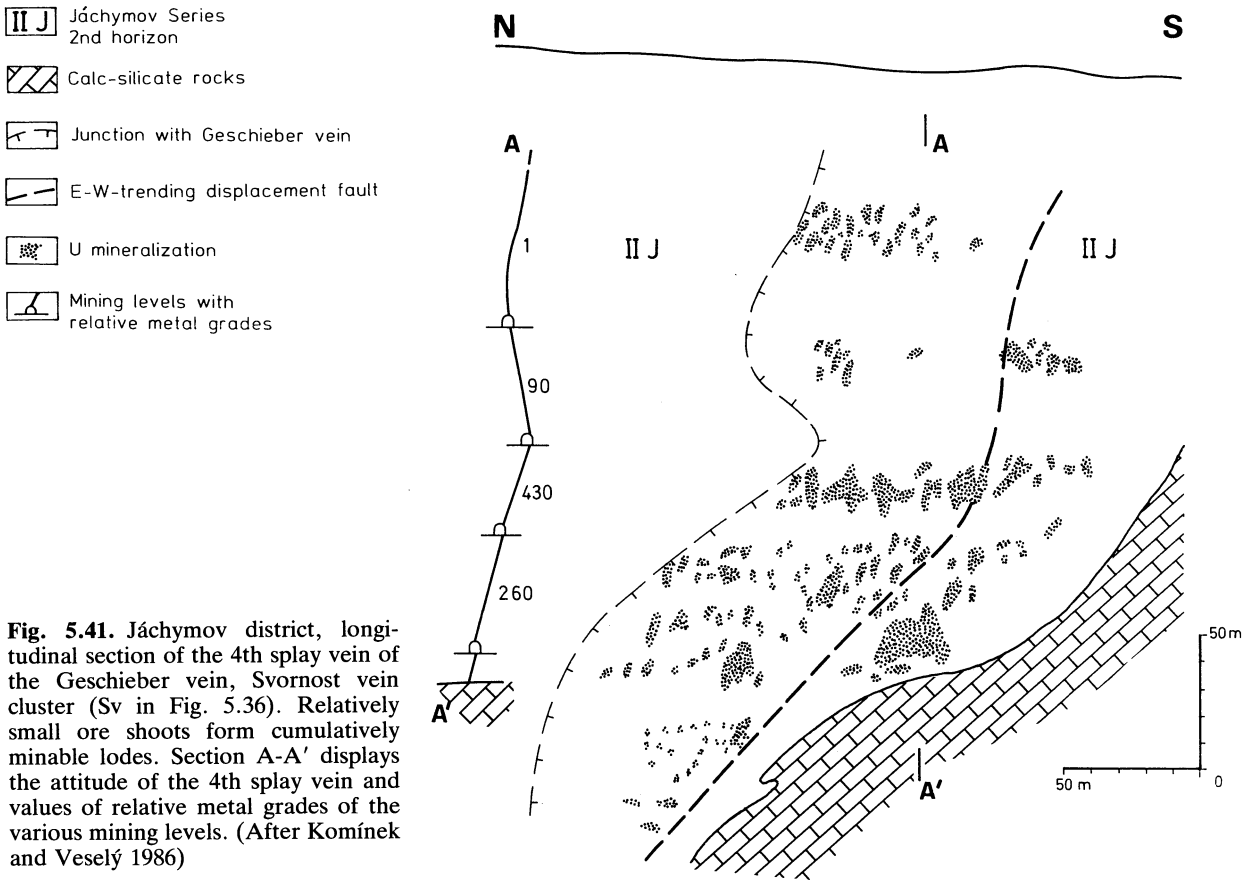

Fig. 5.41. Jáchymov district, longitudinal section of the 4th splay vein of the Geschieber vein, Svornost vein cluster (Sv in Fig. 5.36). Relatively small ore shoots form cumulatively minable lodes. Section A-A′ displays the attitude of the 4th splay vein and values of relative metal grades of the various mining levels. (After Komínek and Veselý 1986)

The carbonate-pitchblende association is the oldest ore generation introduced by mesothermal fluids. Decrepitation tests by Mrna and Pavlu (1967) indicate temperatures of 370 to 470°C.

The uranium-bearing solutions supposedly carried larger amounts of U, Fe, Mg, Ca, and CO_2, minor amounts of SiO_2 and F and traces of V and REE (Ruzicka 1971). Dymkov (1960) proposes that most of the pitchblende precipitated together with carbonates within a geochemical environment of pH 8 to 9. Kolektiv (1984) remarks that rocks with high Ca and Fe contents in form of pyrite and calcite influenced the precipitation of ore minerals and therefore served as host rocks. Pyrite acted as reductant and calcite maintained the alkalinity required for the redox reactions between Fe^{2+} of pyrite and U^{6+} to deposit pitchblende.

The time gap between Erzgebirgsgranit crystallization, 310–300 m.y. ago and pitchblende deposition, 270–230 m.y. ago puts restrictions on magmatic hydrothermal models.

Ruzicka (1971) favors the idea that lateral secretion was instrumental in the formation of the Jáchymov deposits and suggests that both metasediments and autometamorphic granites played significant roles. Both have anomalous contents of leachable uranium and hence may be considered potential source rocks.

Since the Erzgebirgsgranit resembles in composition and evolution, as far as is known, the St. Sylvestre granite in Limousin, France, (see Sect. 5.3.1) it would be of much interest to see whether the processes suggested for the formation of the French vein uranium deposits are also applicable for the Jáchymov and other pitchblende veins of the Erzgebirge.

The various processes and results of redistribution (150 to 100 m.y. and 30 to 5 m.y. ago) are addressed by Kolektiv (1984). Carbonate-pitchblende of the early stage only survived in subsidiary structures of the fifth and sixth order. These structures were activated only initially and for only a short time interval and then remained sealed against attack by younger solutions. In mineralized structures of fourth order, which were reactivated and opened to circulation of younger solutions, pitchblende and carbonate

were partially replaced by quartz associated with impoverishment of the ore and changes in the shape of lodes. This dissolution and subsequent redeposition of pitchblende 2 and coffinite occurred coeval with the precipitation of arsenides and locally baryte.

In third order structures that experienced relative long periods of activation, the uranium mineralization was attacked more heavily, and down-graded. The structures were reopened simultaneously with those of second order and prior to the introduction of sulfarsenides and sulfides. This provided time for infiltration of oxygenated fluids that leached the uranium and reacted contemporaneously with arsenides to form sulfarsenides.

In first order structures which were after emplacement of early pitchblende repeatedly and for long periods reactivated solutions destroyed pitchblende, carbonate, baryte, fluorite, and other minerals and replaced them by minerals of the young quartz-hematite stage and also formed magnetite-hematite-bearing veins.

References and Further Reading for Chapter 5.3.3
(for details of publications see Bibliography)

Bernard et al. 1967; Dymkov 1961; Kolektiv 1984; Komínek and Veselý 1986; Kraus 1916; Leutwein 1957; Mrňa 1963a, 1963b, 1967; Oelsner 1958; Ruzicka 1971; Ruzicka V, pers. commun.; Schumacher 1933; Vogl 1856; Zückert 1926

5.3.4 Perigranitic Uranium Deposits in Contact-Metamorphic Rocks: Iberian Meseta, Portugal-Spain

The Iberian Meseta, located in the western part of the Iberian Peninsula, hosts uranium deposits which are globally similar to vein deposits elsewhere in the Hercynian chain of Europe. But there are also vein-type deposits with different features, viz. the "Iberian type" deposits positioned in the contact-metamorphic aureole of plutons (class 3.1.2.3, Chap. 4).

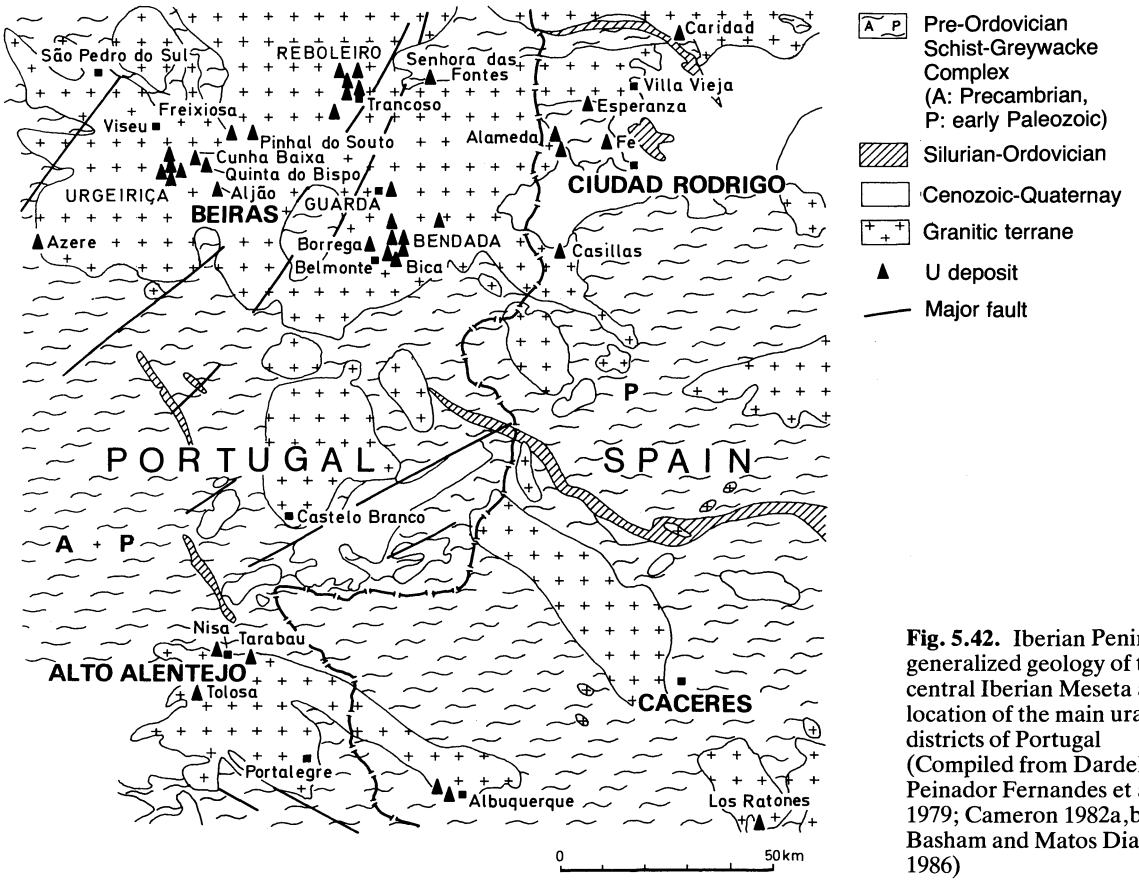

Fig. 5.42. Iberian Peninsula, generalized geology of the central Iberian Meseta and location of the main uranium districts of Portugal (Compiled from Dardel/Peinador Fernandes et al. 1979; Cameron 1982a,b; Basham and Matos Dias 1986)

Seven districts with vein-type mineralization have been established in the Iberian Meseta, five in Spain and two in Portugal (Fig. 5.42). They contain a total of approximately 50 000 mt U_3O_8 at commonly low grades of <0.1% U_3O_8.

The following synopsis is essentially based on papers by the authors listed in the References unless otherwise stated.

Geological Setting of Mineralization

The Iberian Meseta, a southwestern extension of the European Hercynian orogenic belt, consists of a Precambrian to Hercynian block, surrounded or covered by Phanerozoic sediments. Prevailing rocks of the Meseta are quartzites, schists, gneisses, and granites of Precambrian to lower Paleozoic age forming the *Schist-Greywacke Complex*. The complex was intruded by granites including uraniferous leucogranites and folded during the Hercynian Orogeny, but only slightly regionally metamorphosed to mostly greenschist facies grade, and contact-metamorphosed around the granite intrusions.

The Meseta can be divided into five structural zones (Capdevila et al. 1973) comparable to those of the Hercynian belt elsewhere in central and western Europe. All important uranium mineralizations occur in the Central Iberian Zone (comparable to the Moldanubian Zone) and some in the adjacent zones, but always close to the contact with the Central Zone.

Host Rock Alteration

Two time-related alterations can be distinguished. *Pre-ore alteration* of regional extent includes sericitization, chloritization, and tourmalinization of variable intensity. *Ore-related alteration* is of limited extent around mineralized zones and consists of intense chloritization, argillitization, silicification, and hematitization. The latter is particularly noticeable around disseminated type mineralization.

Principal Characteristics of Mineralization

Peribatholitic (perigranitic) disseminations, termed *Iberian type deposits*, are emplaced in rocks within the up to 2 km wide contact-metamorphic aureole of Hercynian granites, which often host pitchblende veinlets, and in schists distant from the granite.

Principal *ore minerals* at depth are pitchblende and coffinite. Hexavalent uranium minerals, predominantly autunite, occur above the water table in the oxidation zone, which extends from surface 15 to 40 m deep. The uranium minerals impregnate fracture zones, schistosity planes, or other heterogeneities of the host shale. Some pitchblende veinlets have been drill intersected up to 200 m deep. *Associated minerals* are sulfides, mainly pyrite, marcasite, galena, sphalerite, and chalcopyrite. *Gangue minerals* may include carbonates, fluorite, quartz, chlorite, and adularia. Associated and gangue mineral are present in only minor amounts.

Three characteristic *distributions* of perigranitic mineralization are recognized: (Dardel/Peinador Fernandes et al. 1979; Ziegler and Dardel 1984)

a) Disseminated mineralization within a 1000–1500-m-wide contact-metamorphed zone immediately along the granite contact. In zones of mineralization, the contact is often offset by orthogonal faulting causing embayments of shales displaced into the granite. Typical deposits of this setting include Alameda, Esperanza, and Caridad, Ciudad Rodrigo district, Spain; Nisa, Tarabau, Palheiros de Tolosa, Alto Alentejo district, and Azere, Beiras district, Portugal (reserves commonly some ten to a few thousand mt U_3O_8).
b) Veinlike mineralization within roof pendants of shales in granite. (e.g., Senhora das Fontes, Beiras district, Portugal, 100 mt U_3O_8, some 100 m deep).
c) Disseminated, fracture and joint filling mineralization in basins bordered by granites and filled with clastic sediments of the Schist-Greywacke Complex. Deposits can occur up to several kilometers from the nearest granite outcrop. A typical deposit of this setting is Mina Fe in the Ciuded Rodrigo district, Spain (Figs. 5.43, 5.44, Table 5.25).

Age datings on perigranitic pitchblende yield 100 to 60 m.y. (Stieff and Stern 1960; Horne 1960) and 57 to 37 m.y. (Ludwig in Arribas 1986).

Beside disseminated Iberian type mineralization, *intragranitic veins* associated with less differentiated granites occur in the Iberian

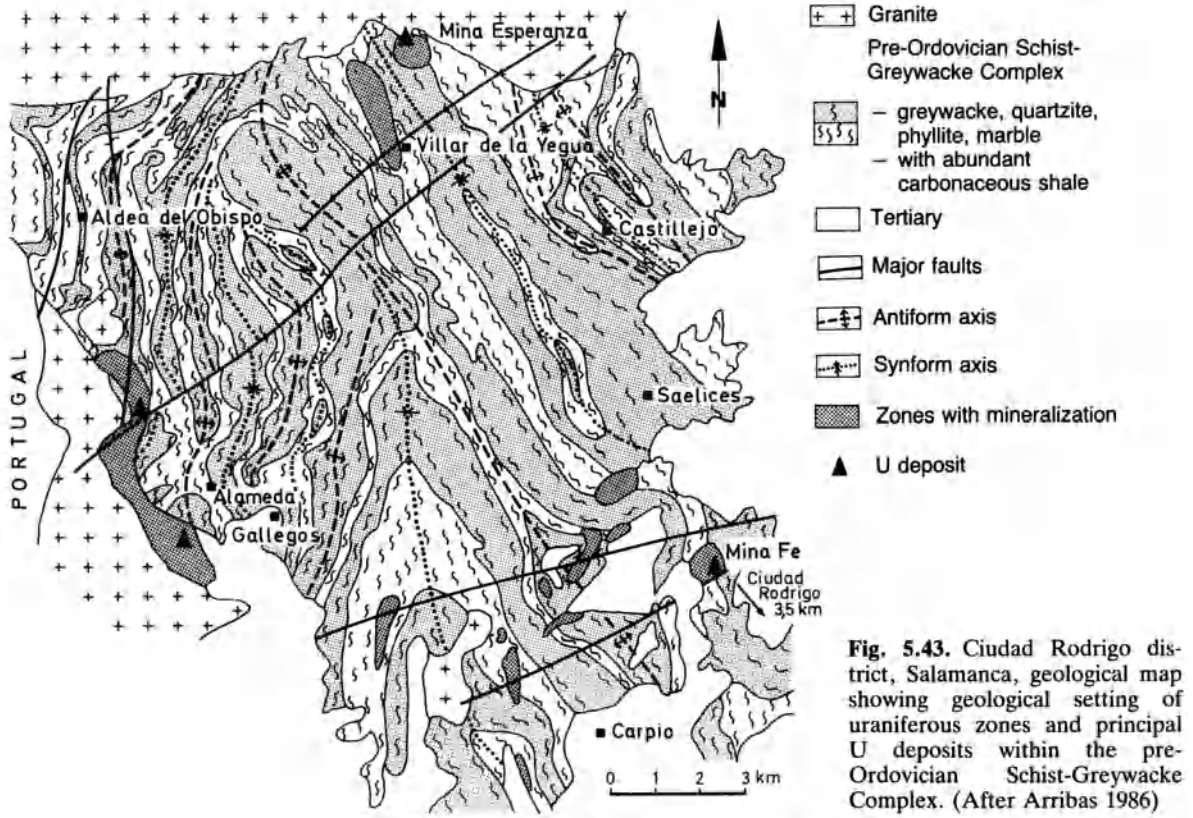

Fig. 5.43. Ciudad Rodrigo district, Salamanca, geological map showing geological setting of uraniferous zones and principal U deposits within the pre-Ordovician Schist-Greywacke Complex. (After Arribas 1986)

Table 5.25. Ciudad Rodrigo district, petrography of host rocks and ore-forming minerals of major deposits (localities see Figs. 5.42 and 5.43). (After Dardel/Peinador Fernandes et al. 1979)

Deposit	Host rocks	Uranium minerals		Gangue	Associated
		Primary	Secondary	minerals	
Fe, Zone D Rio Agueda south of Saelices	Argillaceous schist Micaschist Hornfels	Pitchblende Coffinite	Coracite, Gummites Uranotile Autunite, Torbernite Uranopilite, Ianthinite Black oxides	Quartz Carbonate Fluorite Adularia (?) Chlorite	Fe-sulfides Sphalerite Galena Chalcopyrite
Esperanza Villar de la Yegua	Micaschist Hornfels Microgranite dike Quartz vein	Pitchblende Coffinite	Coracite, Gummites Uranotile, Renardite Kasolite, Torbernite Saleeite, Ianthinite	Quartz	Galena Marcasite Cerussite Pyrite
Caridad Villa Vieja de Yeltes	Micaschist Hornfels	Coffinite	Autunite Torbernite Saleeite	Quartz	Pyrite
Zones 21, 23, 24 Alameda de Gardon	Micaschist, feldspathic Hornfels Granodiorite dike		Autunite, Renardite Uranotile Sabugalite Phosphuranylite		Pyrite

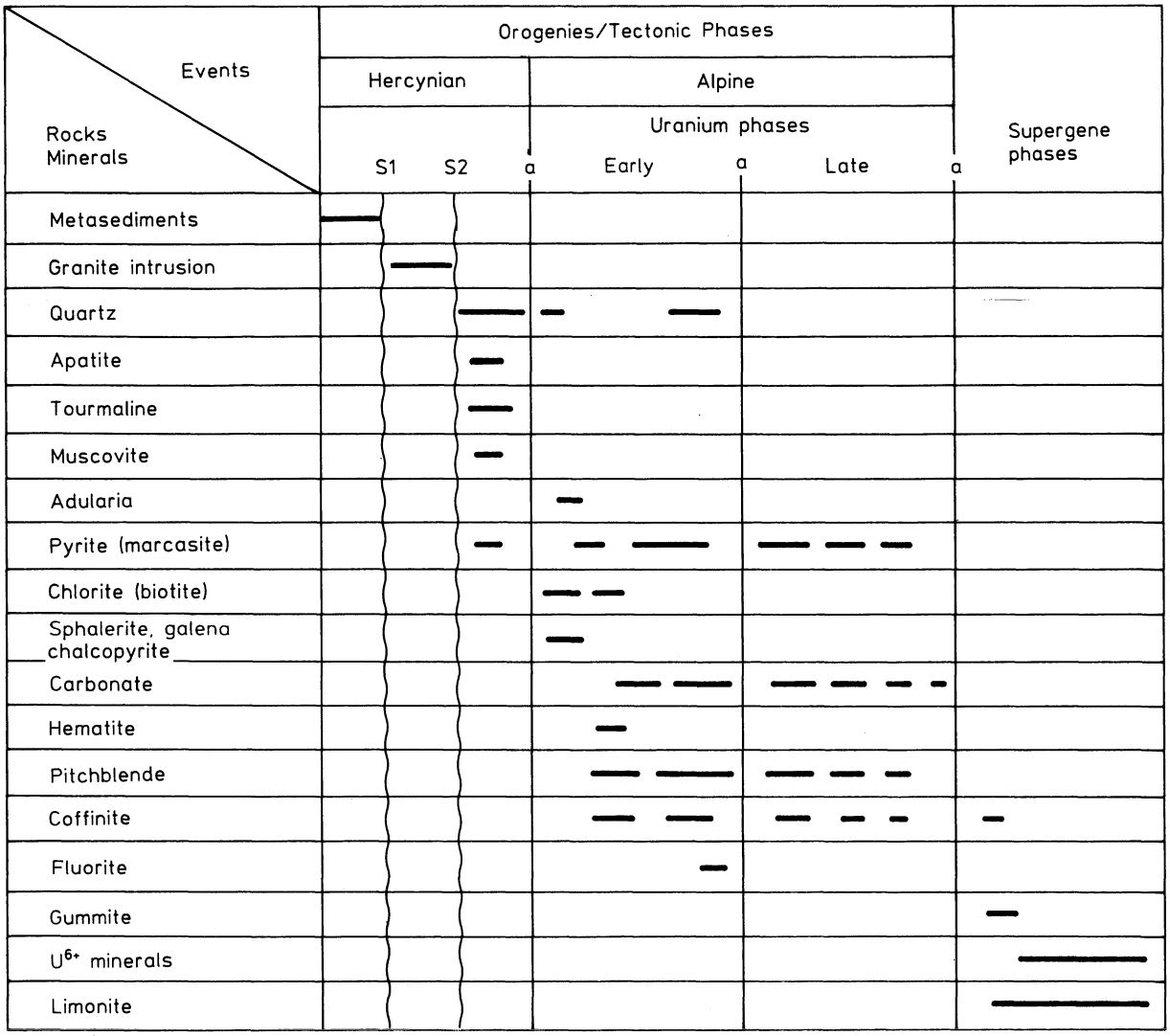

Fig. 5.44. Ciudad Rodrigo district, Mina Fe, tectonic events and metallogenetic succession of U mineralization. *S1* plastic deformation; *S2* crenulation; *a* brittle deformation. (After Arribas 1986)

Meseta, both often in the same district. Typical deposits are Urgeiriça and Cunha Baixa in the Beiras district, Portugal (order of reserves: about 1000 mt U_3O_8).

Principal *ore minerals* in the veins are pitchblende and coffinite which are often, particularly near the surface, altered to hexavalent uranium minerals. *Associated minerals* include pyrite, galena, sphalerite, chalcopyrite, fluorite, carbonates, and a variety of quartz-silica species. (Dardel/Peinador Fernandes 1979)

Potential Sources of Uranium

Two favorabe uranium sources are proposed, differentiated leucogranites and metasediments. "Younger" *granites* of the São Pedro do Sul pluton, northwestern Beiras district, Portugal, average 8 to 20 ppm U, 50 to 70% of which is contained in easily leachable, low-thorian uraninite and submicroscopic, intergranular form. Thorium content averages 38 ppm, (Basham et al. 1982a). Host granites to the Urgeiriça, Bica and Cunha Baixa deposits, Beiras district, have tenors of 4 to 17 ppm U and 20 to 37 ppm Th in surface samples (Pagel 1982c). The "younger" granites

characteristically contain a suite of accessory minerals comprising apatite, monazite, zircon, rare xenotime, very rare sphene, and low-thorian (less than 2%), low REE uraninite. This suite of accessories exhibits a strong contrast to uraniferous but infertile hornblende granites of Hercynian and Caledonian age, which typically contain a suite of high-thorian uraninite, thorite, sphene, allanite, and zircon.

Dekkers et al. (1983) note that present-day streamwaters draining the fertile granites of the Nisa-Tolosa-Castelo de Vide batholith contain elevated amounts of uranium, whereas those streams draining granites containing an accessory mineral suite dominated by high thorian uraninite and thorite have low uranium concentrations.

Sediments-metasediments: Basham and Matos Dias (1986) report uranium concentrations from 1 to 13 ppm for unweathered host metasediments of the Azere and Nisa deposits area, Portugal. These values are typical averages for shales. No evidence of synsedimentary enrichment has been found. Only minor redistribution and concentration of uranium occurred during regional and thermal contact-metamorphism, reflected by local redistribution of uranium into quartz veinlets, and cordierite knots or recrystallized chloritic bands within the contact haloes. No indication of a marked change of the whole-rock uranium content by these processes could be detected by the authors.

Arribas et al. (1984) report that carbonaceous shales/phyllites of the Schist-Greywacke Complex located W and N of Ciudad Rodrigo, Spain, contain from few ppm to 30 ppm U, with some values up to almost 200 ppm U. The uraniferous shales constitute ca. 40% of the stratigraphic sequence in the complex.

Ore Controls and Recognition Criteria

Significant ore controlling or recognition criteria of Iberian type mineralization include:

Host Environment

- Localization of districts is within the Central Iberian Zone.
- Country rocks are low-grade metamorphosed partly carbonaceous pelites and psammites intruded by a variety of granites including a late stage uraniferous leucogranite.
- Host rocks are intensely fractured.

Alteration

- Contact-metamorphism transformed the metasediments along granite contacts into andalusite speckled rocks and hornfels.
- Pre-ore alteration is reflected by sericitization, chloritization, and tourmalinization.
- Ore-related alteration includes chloritization, argillitization, silicification, and often intense hematitization.

Mineralization

- Ore minerals impregnate and coat schistosity and fracture planes and as such appear primarily structurally controlled. A certain lithologic control may be envisioned by the position of most deposits in the contact-metamorphic aureole surrounding uraniferous leucogranites (except Mina Fe in the Ciudad Rodrigo district).
- Ore mineralogy is commonly monometallic consisting predominantly of hexavalent U minerals (autunite etc.) and locally sooty pitchblende. Solid pitchblende is rare.
- Associated minerals are present in minor amounts and may include sulfides of Fe, Pb and Cu, carbonates, fluorite, and adularia.
- The distribution of mineralization is of limited depth commonly less than 40 m deep.
- Nearby granites often contain intragranitic pitchblende vein deposits.

Metallogenetic Concepts

Genetic models for peribatholitic Iberian type uranium deposits are contentious, perhaps due to restricted exploration in depth and limited research work. Hypotheses include *supergene models*, which contemplate leaching of uranium by weathering and erosion of uraniferous granites and superficial redeposition of uranium in topographic lows and fractured or brecciated zones adjacent to the source granites (Fernandes Polo 1970; Cameron 1982b).

Ziegler and Dardel (1984) propose a *lateral secretionary process* provoked by high-temperature isotherms accompanying granite intrusions. Temperature increase would create convective cells of heated surface waters extracting uranium from sedimentary source rocks such as black shales and reprecipitating it in favorable environments (structures, heterogeneities).

Pagel (1982c) presents supporting evidence for a split in the formation of veins and Iberian type mineralization. He suggests that (hypogene?) hydrothermal activity and earliest pitchblende crystallization can be linked probably to late Hercynian events whereas supergene processes involved in the formation of disseminated type mineralization have been strongly active from Tertiary to recent times.

Basham and Matos Dias (1986) propose an *interrelated metallogenetic evolution* for the broad spectrum of vein-type uranium deposits in Portugal. Their genetic scheme spans from post-granite hydrothermal formation of moderately high temperature jasper-pitchblende veins through lower temperature quartz veins and peribatholitic Iberian type uranium disseminations, to supergene ore formations in near surface structures (15 to 40 m below surface) by redistribution of earlier mineralization, and uranium leached from granites. The authors, argue in favor of a continuum between the various primary mineralizations, in principle intragranitic and perigranitic pitchblende ores. They suggest that initial uraniferous, oxidizing solution which introduced uranium and minor quantities of other metals to form intragranitic veins may have continued to move outwards and upwards by convective circulation into the contact-metamorphic aureole. Here, the uraniferous solutions encountered a strongly reducing environment in pyrite-bearing schists causing precipitation of uranium in the network of microfractures to form the Iberian type deposits. Basham and Matos Dias (1986) rule out a metasedimentary uranium source at least for the Azere, Beiras and Nisa, Alto Alentejo regions, Portugal, which contrasts to the presentation by Arribas (1985) on the nearby Ciudad Rodrigo district in Spain. Arribas (1986) proposes for the Ciudad Rodrigo district, Spain, leaching of uranium from uraniferous carbonaceous phyllites of the Schist-Greywacke Complex, and uranium transport as uranyl carbonate in hydrothermal fluids generated by *seismic pumping*. This model implies a hydrothermal fluid transport mechanism triggered by tangential deformation. Deposition of pitchblende occurred in near-surface dilation zones created by hydraulic fracturing in the course of shallow tectonic activity during Tertiary time. Strains developed within the Hercynian basement around shear zones in response to Alpine orogenic activity during lower to middle Tertiary time could have initiated episodic remobilization of uranium by hydrothermal solutions. These U mobilizations are documented by the apparent U/Pb ages of pitchblende in the Ciudad Rodrigo district, 57 to 37 m.y., which correlate with the Pyrenean phase of the Alpine Orogeny.

References and Further Reading for Chapter 5.3.4
(for details of publications see Bibliography)

Arnáiz J, pers. commun.; Arribas 1962, 1970, 1975, 1978, 1986; Arribas et al. 1983, 1984; Barros 1966; Basham and Matos Dias 1986; Basham et al. 1982a, 1982b; Cameron 1959, 1982a, 1982b; Cameron et al./IUREP 1980; Cerveira 1956; Coma 1983; Corretge and Lopez Plaza 1976; Dardel/Peinador Fernandes et al. 1979; Dekkers et al. 1983; Fernandes Polo 1970; Gómez Jaén et al. 1977; Limpo de Faria 1966; Mangas and Arribas 1984; Martin Izard and Arribas 1984; Matos Dias and Soares de Andrade 1970; Pagel 1982c; Pilar 1966; Portugal Ferreira and Matos Dias 1982

5.3.5 Metasediment-Hosted, Not Granite-Related Vein Uranium Deposits: Schwartzwalder Mine, Front Range, USA

The Schwartzwalder vein deposit is located in the Front Range, approximately 20 km NW of Golden, Colorado (Fig. 5.45). Production from the 750 m deep mine has been almost 9000 mt U_3O_8. Remaining reserves are unknown but thought to be at least in the order of 3000 to 5000 mt U_3O_8, occurring in a drill-indicated depth down to 900 m. Ore mined until 1979 averaged 0.5 to 0.6% U_3O_8, then dropped to 0.2 to 0.25% U_3O_8 at a cut-off grade of 0.09% (Wright 1980).

The deposit consists of veins hosted by metasediments several kilometers distant from the nearest known granite. It is therefore classified as metasediment-hosted not granite-related vein uranium deposit. (class 3.2.1, Chap. 4)

The most recent publications on the Schwartzwalder deposit are by Wallace and coworkers, who comprehensively and thoroughly researched both mineralization and alteration. These publications provided the prime source for the following description amended by data from the other listed investigators, particularly by De Voto and Paschis (1980), Wright (1980), and Young (1979a).

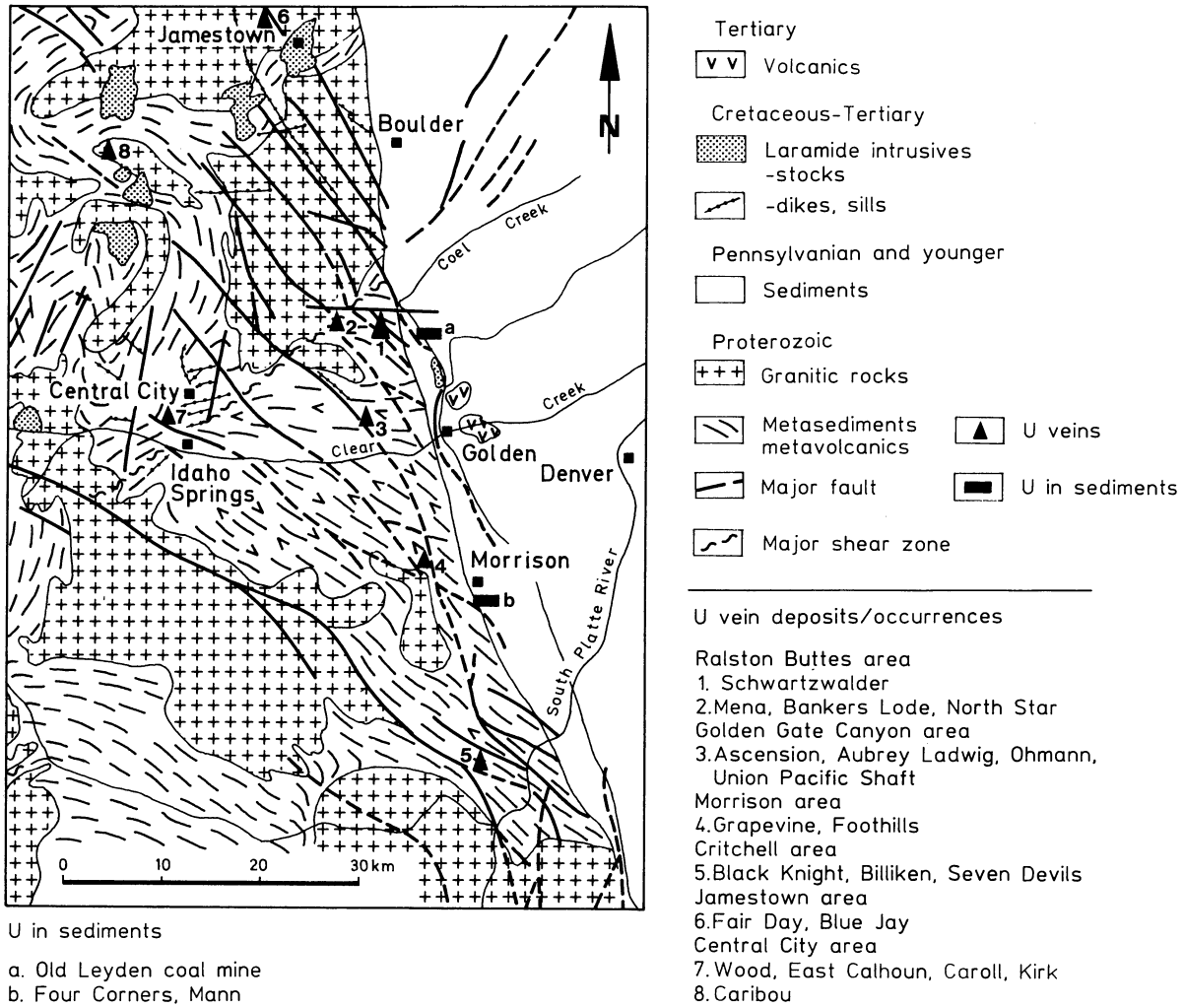

Fig. 5.45. Colorado Front Range, generalized geological map of the east-central part with location of the Schwartzwalder Mine and other uranium deposits and major occurrences. (After Sims and Sheridan 1964; Tweto 1979; Wallace 1983a)

Geological Setting of Mineralization

The Schwartzwalder uranium deposit is localized in an area with a complex array of structural dilation zones, fault branchings, deflections, or junctions between the E and W branches of the NW-SE-trending Rogers fault system, and is hosted by specific metamorphic lithologic units of Lower Proterozoic age, formerly named the Idaho Springs Formation. The country rocks were subjected to regional amphibolite-grade metamorphism at about 1.7 to 1.75 b.y. ago (Peterman and Hedge 1968) and to tight isoclinal folding. Retrograde metamorphism is very minor. Dikes of aplite and tourmaline-garnet-bearing pegmatite of Silver Plume age (±1400 m.y.) cut the metamorphic rocks.

Phanerozoic sedimentary rocks occur to the east of the deposit. The nearest outcrop is about 500 m from the mine. Red bed facies of Pennsylvanian age form the basal sedimentary unit. It is overlain by marine and continental sediments of Permian to Cretaceous age. Regolithization of the crystalline rocks extends from the Pennsylvanian unconformity for about 30 m downward.

The *petrographic-stratigraphic position* of the Schwartzwalder deposit (Fig. 5.46) is dominated by Lower Proterozoic foliated and layered metasedimentary and metavolcanic rocks which

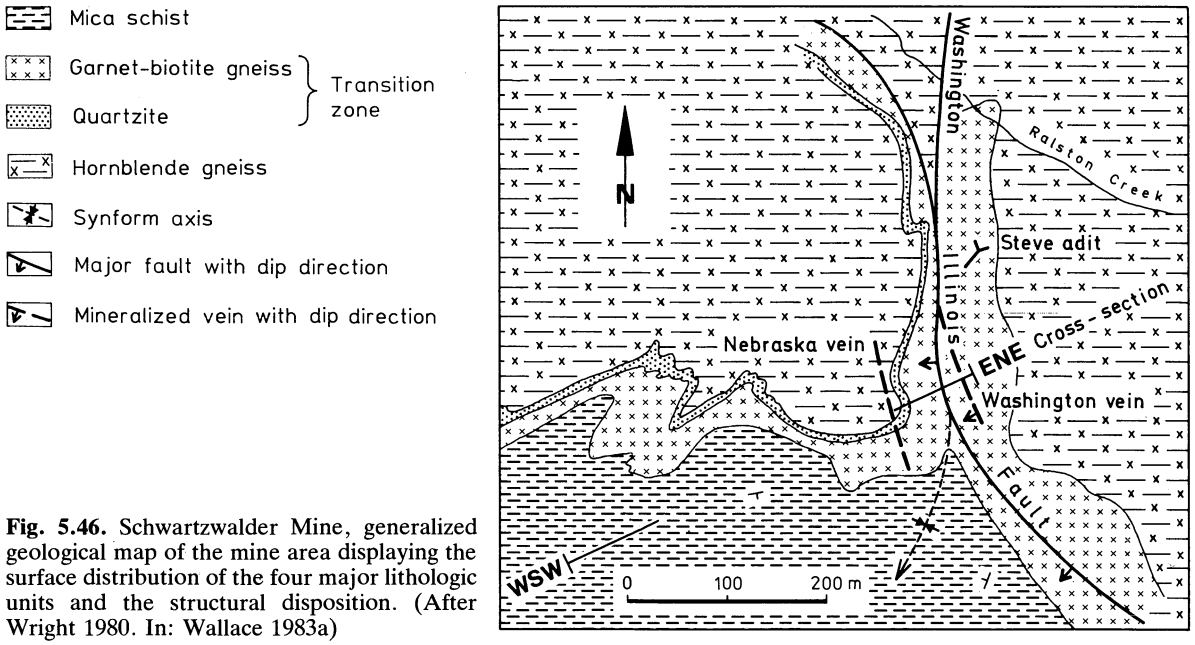

Fig. 5.46. Schwartzwalder Mine, generalized geological map of the mine area displaying the surface distribution of the four major lithologic units and the structural disposition. (After Wright 1980. In: Wallace 1983a)

can be grouped into four major units: Mica schist, garnet-biotite gneiss, quartzite and hornblende gneiss.

Hornblende gneiss and mica schist are thick and regionally extensive. Garnet-biotite gneiss and quartzite form a narrow 50 to 100 m thick transitional sequence between hornblende gneiss and mica schist.

The *structural position* of the Schwartzwalder deposit is dominated by two distinct elements of folding and faulting (Fig. 5.46).

a) A tightly isoclinally folded *synform* with a nearly vertical NNE-SSW-striking axial plane and a steeply SSW-plunging fold axis. In the nose of the synform the original thickness of the ore-hosting garnet-biotite gneiss and quartzite units of the transition zone is almost doubled to more than 100 m, whereas elsewhere mica schists occupy the core of the fold, bounded successively by garnet-biotite gneiss, quartzite, and hornblende gneiss.
b) A set of two major approximately parallel NW-SE-striking, 60 to 70° NE-dipping faults (E- and W-*Rogers faults*). The faults are ca. 1000 m apart and interconnected by diagonal cymoid faults trending NNW to WNW (Illinois Fault) with a stacked series of tensional horsetail-type fractures off-branching into the hanging wall of the Illinois Fault (Fig. 5.47).

The *Illinois Fault system*, which hosts the Schwartzwalder U veins, evolved through multiple repetitions of tectonic activity. As a result, a number of pre-ore and subparallel post-ore faults trending between NNW and NNE developed. Pre-ore faults dip 70 to 75° W and post-ore faults 60° W (Figs. 5.47, 5.48).

Horsetail fractures developed in a stacked fashion in competent rocks on the hanging wall side of, and apparently root in the pre-ore Illinois Fault. Wright (1980) considers the horsetail fractures as of Laramide age.

A characteristic feature of the Schwartzwalder deposit are dikes of altered clastic material a few centimeters to a meter wide, which invaded many of the structures and veins except the post-ore Illinois Fault.

Host Rock Alterations

Altered wall rocks typically display bleached and overprinted reddish coloration along veins, regardless of the presence or grade of mineralization. The alteration is mineralogically uniform throughout the 900 m vertical mine interval, but it nowhere had an extensive effect, or invaded far into the wall rock. It may locally even be absent, even adjacent to pitchblende-bearing veins.

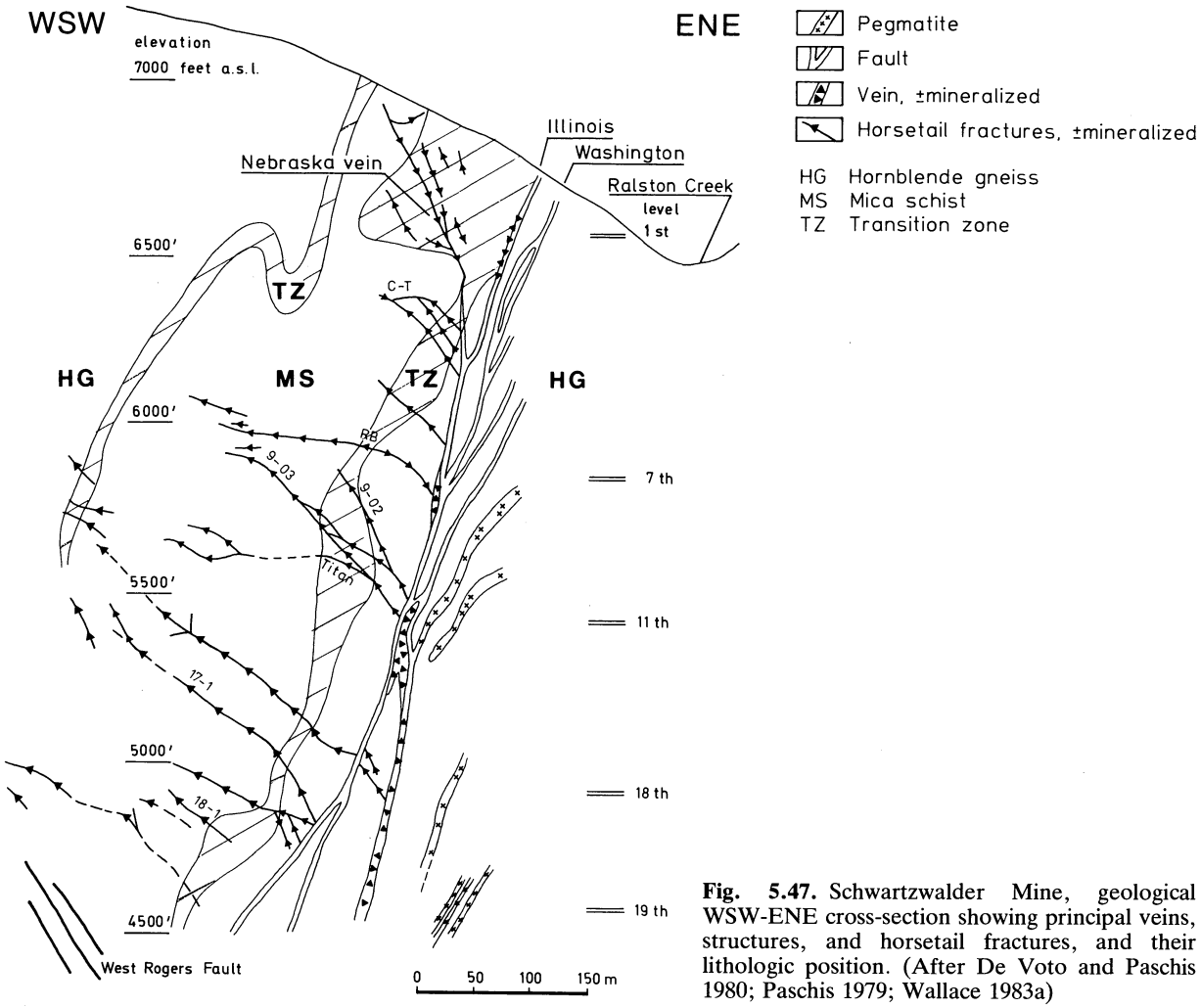

Fig. 5.47. Schwartzwalder Mine, geological WSW-ENE cross-section showing principal veins, structures, and horsetail fractures, and their lithologic position. (After De Voto and Paschis 1980; Paschis 1979; Wallace 1983a)

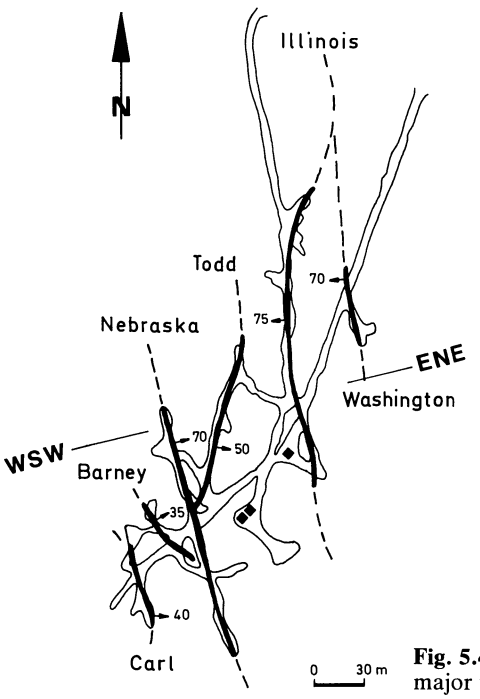

Fig. 5.48. Schwartzwalder Mine, planview of the first level with distribution of major veins and mine workings. (After Paschis 1979)

Two successive assemblages of wall rock alteration (Fig. 5.49) are distinguished (Wallace 1983a).

a) Early carbonatization and sericitization pseudomorphically replacing all mafic minerals of the host rocks within 2 m of the veins, indicating a large influx of CO_2 and concomitant loss of SiO_2;
b) subsequent hematitization and potassium feldspathization (adularia) replacing pre-existing alteration minerals immediately adjacent to the veins.

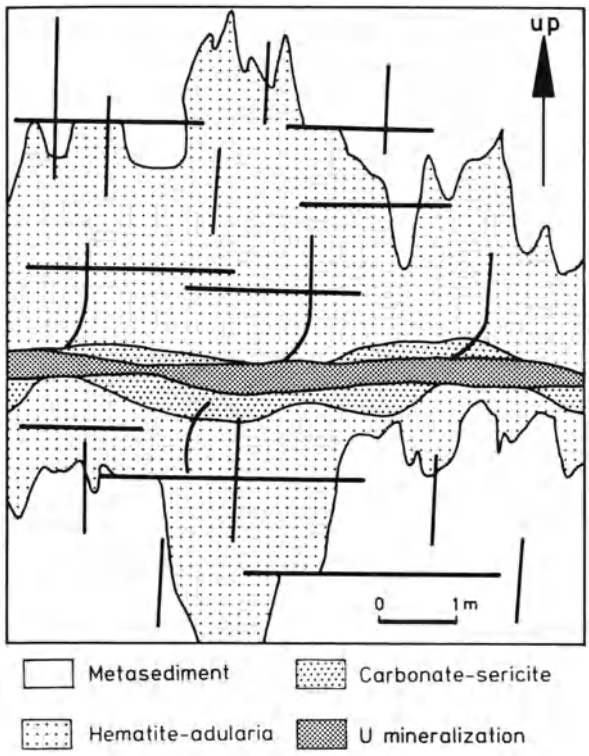

Fig. 5.49. Schwartzwalder Mine, schematic illustration of the relative distribution of the early carbonate-sericite and later hematite-adularia alteration zones along a vein. Vertical foliation is shown by *vertical lines*. Some of the foliation exhibits drag along the vein hosting fault. (After Wallace 1983a)

Principal Characteristics of Mineralization

Schwartzwalder vein mineralization occurs predominantly in the Illinois, West Rogers, and associated horsetail structures. The *ore* essentially consists of pitchblende accompanied by a number of trace elements of which As, Ba, Cu, Sb, Sr, V, and Zn can be greater than 100 ppm, and Mo, Pb, and Th several 1000 ppm. (Wallace 1983a).

Wallace distinguishes three main successive *paragenetic stages* including several substages of hypogene uranium and base metal mineralization:

I: Sulfide-carbonate-adularia
II: pitchblende-coffinite-carbonate-adularia-sulfide
III: calcite-sulfide

Stage I mineralization is sparsely represented. It includes two assemblages:

Ia) hematite-chalcedony-carbonate which formed contemporaneously with the second stage of alteration;
Ib) carbonates, mainly dolomite, non- to slightly hematitic adularia and base metal sulfides including zoned yellow sphalerite, pyrite, galena, chalcopyrite, and chalcocite.

Stage II is the principal uranium phase and produced the bulk of the vein fillings. Earlier workers (Heyse 1972; Rich and Barabas 1976) describe only one major uranium generation. In contrast, Wallace (1983a) subdivides stage II into three substages, as presented in Fig. 5.50.

Pitchblende and coffinite are the only uranium minerals. Pitchblende is paragenetically intergrown with an unnamed Fe-Mo-As-sulfide mineral with variable Mo/As ratios as determined by Wallace (1983a). The mineral, formerly referred to as jordisite or molybdenite, is characteristic for horsetail ore, whereas it is markedly rare in fractured ores along the Illinois and West Rogers faults.

Stage III mineralization comprises a coarse-grained assemblage of calcite-sulfide, predominantly pyrite and marcasite with minor chalcopyrite. The minerals fill vugs and fissures in uranium veins and in post-ore structures such as the post-ore Illinois Fault.

Chemical investigations show distinct *trace element associations* for the horsetail vein system, and different and less distinct correlations for the Illinois and West Rogers veins. Mineralization of horsetail veins exhibits two associations of elements: a) U, Mo, As, Hg and Sb, b) Ag, Co, and Ni.

Uranium is also closely associated with Pb, S, and Zr. The strong U, Mo, and As correlation reflects the paragenetic relationship of pitchblende and the Fe-Mo-As sulfide mineral in the horsetail veins which survived fault movements. (Wallace 1983a)

Distribution of uranium ore is intermittent, mainly in the steeply SW-dipping Illinois vein and in associated horsetail structures in its hanging wall (Fig. 5.47). Some ore is in the Washington vein which parallels on the footwall side and joins in depth the Illinois vein (Figs. 5.47, 5.48). The mineralized vein system extends laterally for approximately 150 to 200 m in NNW-SSE strike direction along the Illinois vein, and for 50 to 150 m in width perpendicular to and mainly on the western horsetail side of the Illinois vein. Depth

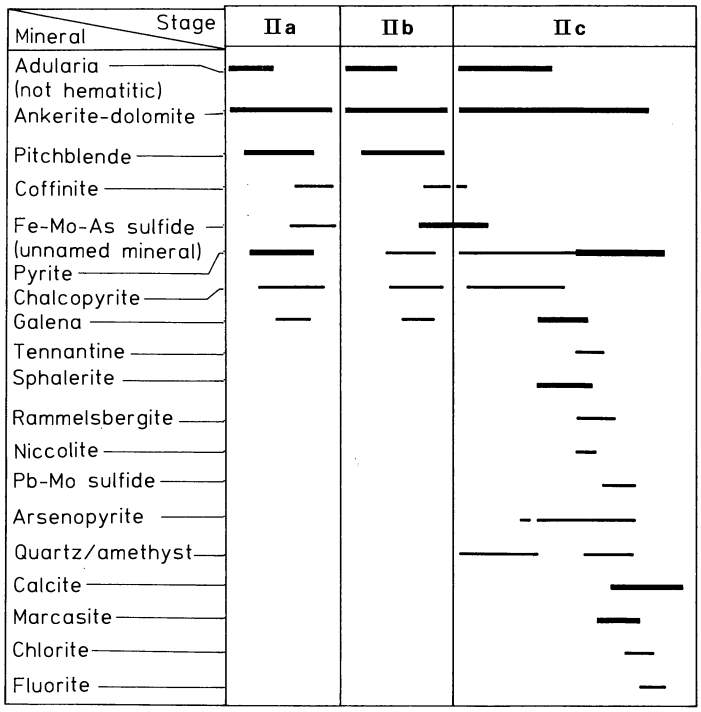

Fig. 5.50. Schwartzwalder Mine, paragenetic diagram of mineralization of stage II. The *thickness of lines* indicates the relative abundance of minerals. (After Wallace 1983a)

extension is more than 700 m along the dip of the Illinois vein. Wallace attributes this deep penetration to down-faulting of some vein sections.

Drilling has intersected additional mineralization in a depth of about 900 m within the West Rogers Fault approximately 200 to 250 m W of the Illinois vein.

The width of mineralized veins varies from millimeters to several meters. Horsetail veins average about 0.5 m and commonly contain high grade ore. The Illinois vein has a width up to 15 m, but ore, although of large minable tonnage, is of relatively low grade. The length of ore shoots may be as much as 100 to 200 m, as within the cymoid loops of the Illinois vein. Horsetail veins which root on the cymoid can have corresponding economic strike lengths, and dip extensions of 150 m and more (Wright 1980).

U/Pb *ages* of 69.3 ± 1.1 m.y. are established for ore from the Titan vein, a structure in the horsetail section of the Schwartzwalder deposit. The U/Pb isochron intercepts suggest that the mineral components derived from a source 1.6 to 1.9 b.y. old, which is equivalent to the age of the metamorphic host rocks (Ludwig et al. 1985).

Stable Isotopes and Fluid Inclusions

Stable isotope and fluid inclusion studies by Wallace and Whelan (1986) permit the following genetic interpretations.

Carbon of vein dolomite ($\delta^{13}C = -2.4$ to $-7.3‰$) and oxygen of minerals of early alteration and mineral stage I ($\delta^{18}O = +4.6$ to $+8.6‰$) yield inconclusive information because they can be interpreted as of both magmatic and metamorphic origin.

Oxygen in stage II minerals have $\delta^{18}O$ values ranging largely from 0 to $-5‰$. This lighter composition may suggest an influx of meteoric water mixing with the original fluids or less evolved connate water from the overlying sediments. $\delta^{18}O$ values of stage III average $-5.6‰$, implying an entirely meteoric origin which is compatible with the supposedly supergene provenance of paragenetically precipitated sulfides.

Sulfur isotopes (Wallace/Whelan and Heyse 1972) of stage II sulfides yield $\delta^{34}S = +1.6$ to $-17.1‰$ but are scanty. These values compare with those of metamorphic sulfides. Thus Wallace and Whelan (1986) consider these vein sulfides to be derived from metamorphic progenitors. Sulfides of stage III have $\delta^{34}S = -18$ to $-41‰$, which suggests that they possibly originated from

late iron sulfides deposited from a sulfate-rich solution.

Vein galena has $^{207}Pb/^{206}Pb$ *ratios* reflecting an age of the source of 1.9 to 1.6 b.y. old, i.e., time-equivalent to the metamorphism of the country rocks. This result excludes any magmatic source younger than the Boulder Creek granodiorite dated at 1750 to 1700 m.y. (ages from Peterman and Hedge 1968), thereby refuting models using Silver Plume (±1400 m.y.) or younger intrusions as sources for the ore-forming metals including uranium.

Research on alteration mineralogy, fluid inclusion micro-thermometry and sulfur fractionation by Wallace (1983a) suggest that *temperatures* of mineral formation were approximately 175 to 225°C during the alteration, 225°C in mineral stage I, decreasing to 100–125°C in stage II c (fluid inclusions in stage I sphalerite, trapping temperature: 225°C, in stage II c (?) amethyst and dolomite: 168–205°C; sulfur isotope fractionation of coexisting sphalerite and galena of stage II c: 68 and 120°C).

The bulk of pitchblende formed between stages I and II c together with certain sulfides (pyrite, chalcopyrite, Fe-Mo-As-sulfide) and large quantities of carbonate, mainly ankerite, and adularia, whereas bornite, iron oxides, sericite, and graphite are notably absent. The assemblage is suggestive for a *solution* of a pH of 5 to 8, a dissolved CO_2 concentration of 4 to 10%, and a likely uranium transport as a uranyl carbonate or bicarbonate complex.

Potential Sources of Uranium

Uranium and the other metals are thought to have derived from the ore hosting *metamorphics*. Uranium background in the hornblende gneiss averages 1 to 4 ppm U (max. 52 ppm), garnet-biotite gneiss 5 to 10 ppm (max. 88 ppm), quartzite unit 1.7 to 26.8 ppm and the mica schist unit 2.2 to 5.8 ppm U (Wallace 1983a). Wallace favors the extensive honblende gneiss unit as the most likely source of uranium.

Indirect evidence such as isotope composition and no detected magmatic source also support the assumption that the vein-hosting metavolcanics and metasediments were the source of uranium and other ore-related elements.

Ore Controls and Recognition Criteria

The Schwartzwalder veins show a distinct structural and lithological control as reflected by the following ore controls and recognition criteria.

Host Environment

- Ore veins occupy tensional structures such as the large Illinois and Rogers faults and associated horsetail fractures.
- The distribution of ore veins is restricted to distinct lithologies, particularly to garnet-biotite gneiss, a former iron (and sulfur?)-rich pelitic sediment, and quartizite. These rocks reacted to faulting by dilational fractures creating adequate transmissivity and space for minable ore shoots.
- Hornblende gneiss, a former mafic volcanic rock, and mica schist are unfavorable hosts, probably due to more ductile reaction to faulting that resulted in discontinuous openings and impermeable gouge fillings.
- Folding tectonically increased the thickness of the favorable host rocks, particularly in the nose of the Schwartzwalder synform, where the section of the transitional rock unit is approximately doubled in width.
- The structural combination of steeply dipping horizons of the brittle transition zone rocks and their disrupture by the steeply dipping Illinois and Rogers fault systems generated the favorable laterally narrow but very deep (at least 1000 m) system of continuous and interconnected permeable faults and breccias for ore emplacement.

Alteration

- Early alteration of wall rocks includes carbonatization and sericitization, and later alteration K-metasomatism and hematitization.

Mineralization

- Mineralization includes three stages. Stage II is the principal U phase. Stages I and III consist essentially of sulfides associated with mainly carbonates.
- U minerals are pitchblende and coffinite paragenetically associated with a Fe-Mo-As sulfide mineral, and minor sulfides and ar-

senides. Gangue minerals are Ca-, Fe-, Mg-carbonates and late chlorite and fluorite.
- Mineralization is intermittently distributed in few, steep-dipping major veins and in a great number of tributary horsetail fractures.
- Preferential sites for ore accumulation are at pronounced changes in the width of structures commonly derived by branchings of veins, and abrupt shiftings in strike and dip of horsetail fractures and major structures such as the Illinois and West Rogers faults.
- Repeated reactivation of major structures such as the Illinois vein probably caused dilution of ore grade in heavily affected zones, as indicated by trace element disparities compared to horsetail veins.

Metallogenetic Concepts

Models on the formation of the Schwartzwalder pitchblende veins have been put forward by a number of authors, e.g., Fisher (1976). Maslyn (1978). De Voto and Paschis (1980), Nelson and Gallagher (1982), Rich and Barabas (1982). These models range from ore emplacement in Proterozoic/Silver Plume time to Mesozoic/Laramide time, and from ore-forming processes initiated by magmatic centers such as the Silver Plume and Laramide intrusives of the nearby Colorado Mineral Belt, to hypogene processes that generated convective cells leaching uranium and the other metals from the Proterozoic country rocks, and to supergene processes active along the Phanerozoic unconformity and deriving U from perhaps the red beds of the Pennsylvanian Fountain Formation or other sources.

Thorough research work by Wallace and coworkers narrowed the conceivable frame of ore formation to *convective hypogene hydrotherms* extracting the ore elements from surrounding Proterozoic rocks and depositing the elements in distinct structurally prepared rock units during early Laramide time.

Wallace and his coworkers' concept may be summarized as follows:

1. Intense *faulting* along the frontal zone of the developing eastern Front Range in early Laramide time by interaction of NW-SE-trending major faults and the reverse faults along the eastern uplift boundary resulted in a dilation of the frontal zone.

2. Sites for optimal and extensive ore emplacement in the Schwartzwalder area were prepared in pre- and early Laramide time by *tensional tectonism* in a segment of structural coincidence of steeply dipping layers of brittle garnet-biotite gneiss and quartzite of the lithologic transition zone and its transection by a steeply dipping fault system. As a result, a laterally narrow but extremely deep stockwork of continuous and interconnected breccias, faults, and fractures was established (Illinois, Rogers faults, horsetail fractures). Repeated cataclastic reactivation was instrumental in the formation of the various successive stages of alteration and mineralization by producing abrupt releases of confining pressure and related increase in permeability.

3. Uranium mineralization began 69–70 m.y. ago during the incipient stages of Laramide uplift of the eastern Front Range and beneath a cover of Phanerozoic sediments approximately 3000 m thick. Fission track investigations of apatite (Naeser 1978; Marvin and Dobson 1979) indicate a relatively high *heat flow* at this time. The heat was supplied through an increased regional thermogradient due to igneous activity in the Colorado Mineral Belt.

4. Initial *hydrothermal solutions* originated from connate/metamorphic water that possibly resided in deep storage reservoirs along the major fault zones of Proterozoic ancestry which possibly became reactivated during the Pennsylvanian uplift. These connate fluids contained abundant CO_2 and were in isotopic equilibrium with the enclosing metamorphic rocks, but became mixed with some meteoric water from Mineral Stage II c onward. Rich and Barabas (1982) suggest that the mineralizing fluids were of organic or organo-aqueous character during Stage I (early) adularia and Stage II (late) ankerite formation and thus probably also during the pitchblende deposition.

The fluids probably started a convective circulation in response to early Laramide tectonic movements. On their structurally prepared paths they collected the elements needed for the ore formation from the metamorphic country rocks. This was possible because many of the major pre-ore faults consisted of relative wide cataclastic zones composed of abundant anastomosing fractures which provided large access and surface areas for element leaching in relation to the rock volume within the zones. As a result of the interaction with the rocks, the fluids could acquire

proportionately large quantities of CO_2, Ca, K, and other metals including uranium. The uranium was very probably mobilized as a soluble carbonate complex similar to reactions as described by Yermolayev (1971) and Dickson et al. (1979). The pregnant solutions which migrated into the most permeable sections of the fault zones and sites of ore deposition, had at the start of the alteration and ore formation phase a pH of 5 to 8.

5. Two successive *wall rock alteration* assemblages were produced by the hydrothermal fluids in virtually all existing faults and fractures except in late Laramide faults such as the post-ore Illinois fault, at a temperature of about 225°C and a pressure of 750 to 1000 bar. Early alteration formed sericite and carbonate by CO_2 metasomatism and SiO_2 removal at relatively slow flow rates of the solutions. Intermediate stages of brecciation increased the transmissivity and thereby the flow rate at contemporaneous CO_2 effervescence and pressure release. In consequence, the pH rose and oxygen fugacity dropped, and the second alteration assemblage of hematite and adularia replaced minerals of the early alteration stage.

6. *Ore emplacement* occurred in three successive stages from hypogene hydrothermal fluids, except in stage III when supergene fluids entered the system. Early vein mineralization formed at about 225°C and 750 to 1000 bar similar to the P-T conditions of the alteration stage. During stage II c the temperature decreased to about 125°C and the pressure dropped somewhat. Uranium was emplaced in virtually all accessible faults and horsetail fractures over a vertical interval of ca. 700 m below surface in the pre-ore Illinois Fault system, and in the bottom part of the western strand of the Rogers Fault, where mineralization occurred at a depth extending below 900 m under the present surface. Depth limitation of the mineralization may have been controlled by the threshold level of local pressure gradients which extended deeper in larger and more open faults and at which ascending fluids started to effervesce CO_2 and consequently precipitated the ore minerals. Uranium distribution and emplacement must have been rather uniform, as indicated by the paragenesis and ore textures.

7. The *mineralization events* started with stage I base metals, adularia and carbonate. This event was only of minor magnitude. Stage II was the principal ore-forming period. It included three substages. The first two produced the uranium ores together with volatile elements which strongly correlate with uranium. Other minerals include base metal sulfides and sulfosalts, as well as ankerite and adularia. Uranium *transport* was in solution as uranyl carbonate or bicarbonate, and its *deposition* occurred when abrupt release of confining pressure due to revived tectonic movements caused effervescence of CO_2, increase of pH, and a corresponding break-up of the uranyl complex. Subsequent *reduction* of hexavalent to tetravalent uranium by aqueous sulfur species then precipitated pitchblende.

The original sulfur compounds were predominantly sulfates, but may have included also significant amounts of intermediate sulfur. Through complex mechanisms and intermediate sulfate-thiosulfate and sulfate steps by sulfate reduction, as outlined by Spirakis (1981), a progressively more reducing fluid can evolve with an associated temperature and pressure decrease caused by tectonic brecciation. This process may produce and allow H_2S or HS^- to reduce the hexavalent uranium and precipitate it together with sulfides in a rapid process, as documented by the pitchblende-sulfide assemblages and textures in the Schwartzwalder ore.

Wallace excludes any involvement of external reductants such as ferrous iron, methane, or organic matter as suggested by other authors (e.g., Adams and Stugard 1956; Rich and Barabas 1982). Wallace's arguments against these kinds of reductants are: (a) Hematite is locally absent, (b) uranium also precipitated in fractures within iron-deficient quartzites, (c) hematite formed as an alteration product prior to pitchblende from which it was separated by unhematitized adularia, (d) iron sulfides and ankerite, not hematite, are the iron-bearing minerals paragenetically deposited with pitchblende, (e) carbonaceous material associated with pitchblende is not observed and chemical analyses indicate only small amounts (0.06 to 0.13% in weight) of organic carbon and no correlation of the carbon with the uranium.

8. During the later part of stage II c and III, supergene fluids intermixed with the hypogene solutions precipitated predominantly carbonate, pyrite, and marcasite.

9. Supergene overprinting of primary uranium minerals is restricted to within approximately 100 m below the present surface.

References and Further Reading for Chapter 5.3.5
(for details of publications see Bibliography)

Adams and Stugard 1956; Bird 1958, 1979; De Voto and Paschis 1980; Downs and Bird 1965; Heyse 1972; Karlson and Krokosz 1983; Maslyn 1978; Nelson and Gallagher 1982; Paschis 1979; Rich and Barabas 1982; Sheridan et al. 1967; Walker et al. 1963; Wallace AR, pers. commun.; Wallace 1983a, 1983b, 1986; Wallace and Karlson 1982, 1985; Wallace and Whelan 1986; Wallace et al. 1983; Wright 1980; Wright et al. 1981; Young 1977, 1979a, 1979b, 1985

5.3.6 Sediment-Hosted, Not Granite-Related Vein Uranium Deposits: Shinkolobwe, Katanga Copper Province, Zaïre

Shinkolobwe is situated near Likasi, in the Shaba part of the Katanga Copper Belt. The deposit, discovered in 1915, was mined for radium in an open pit down to almost 60 m between 1921 and 1936, producing a total of ca. 500 000 m^3 of ore yielding about 100 000 mt radioactive material (Derriks and Vaes 1956). It is guessed that this material graded several percent of uranium. In 1944 mining was resumed by underground methods, reaching a depth of 255 m. Operations were suspended in 1960 after production of annually 1200 to 2200 mt U_3O_8, or cumulatively ca. 22 500 mt U_3O_8 (CEA 1969). Adding production and remaining reserves, the deposit contained a total of at least 30 000 mt U_3O_8 at an estimated ore grade of 0.1 to 1% U_3O_8 and more.

The deposit consists of a vein stockwork in sediments distant from any known granite and is therefore classified as sediment-hosted, not granite-related vein uranium deposit (class 3.2.2, Chap. 4).

The subsequent summary is largely from the two comprehensive contributions on the geology of the uranium deposit by Derriks and coworkers (1956, 1958) updated by information from more recent publications.

Geological Setting of Mineralization

Shinkolobwe is in the median part of the *Katanga Synclinorium*, an arcuate fold belt ca. 300 km long extending from Zambia into Zaïre. Regional stratigraphic units are the Kibara Group (Precambrian III) overlain by the Upper Proterozoic Katanga Group (Precambrian IV).The sediments were deposited 1300 to 620 m.y. ago, and folded and faulted during three phases of the Lufilian Orogeny dated at 840 to 710 ± 40, 670 ± 20 and 670 to 620 ± 20 m.y. (Cahen 1970). The *Katanga Group* includes, in descending order, the Kundelungu, Grand Conglomerate and Shale-Dolomite (= Roan Group) Systems. The latter includes the Mwashya Series and the ore hosting *Mines Series* (Série des Mines) (600 to 1000 m thick).

Principal *host rocks* at Shinkolobwe are siliceous dolomites, and dolomitic and carbonaceous shales of the RSF, RSC, and SD units of the Mines Series. (Derriks and Oosterbosch 1958)

Shinkolobwe is located in a structurally complex deformed area due to folding, overturning, faulting and overthrusting. A dominant structure is here the *Shinkolobwe Fault Zone* trending between E and NE, dipping ca. 60° S. Thrusting pushed Kundelungu strata over each other, sqeezing beds of the Mines Series into an irregular NE-SW-oriented fold-fault wedge 150 to 250 m wide and several kilometers long on the surface.

NE-SW-trending longitudinal faults and commonly NW-SE and NNE-SSW cross faults segment the Mines Series wedge into three *displaced blocks* or spurs (Fig. 5.51). A fourth spur (IV) exists in depth, east of the mine, under a 350 m thick cover of Kundelungu sediments. Two pronounced cross-faults, the eastern and western boundary faults, delimit the main deposit laterally. The three main spurs persist from the surface downward to 100 to 150 m where they abut against the shallow inclined contact of the RAT nappe (Fig. 5.52). The RAT nappe consists of overturned thick beds of a variety of shales and dolomites of the RAT unit, the lowest unit of the Mines Series. The boundary between the three blocks is marked by breccia zones. (Derriks and Vaes 1956) Ore lodes occur in the Mines Series of the Massif Principal, and in the lower block IV in a crushed zone of the Mines Series pinched between the downdropped Kundelungu wedge and the Massif Principal.

De Magnée and François (1985) interpret the geological setting of Shinkolobwe as being on the flank of an anticlinal, breccia-filled diapir (termed "extrusion fault"). The breccia is composed of numerous, partly very large, fragments derived to

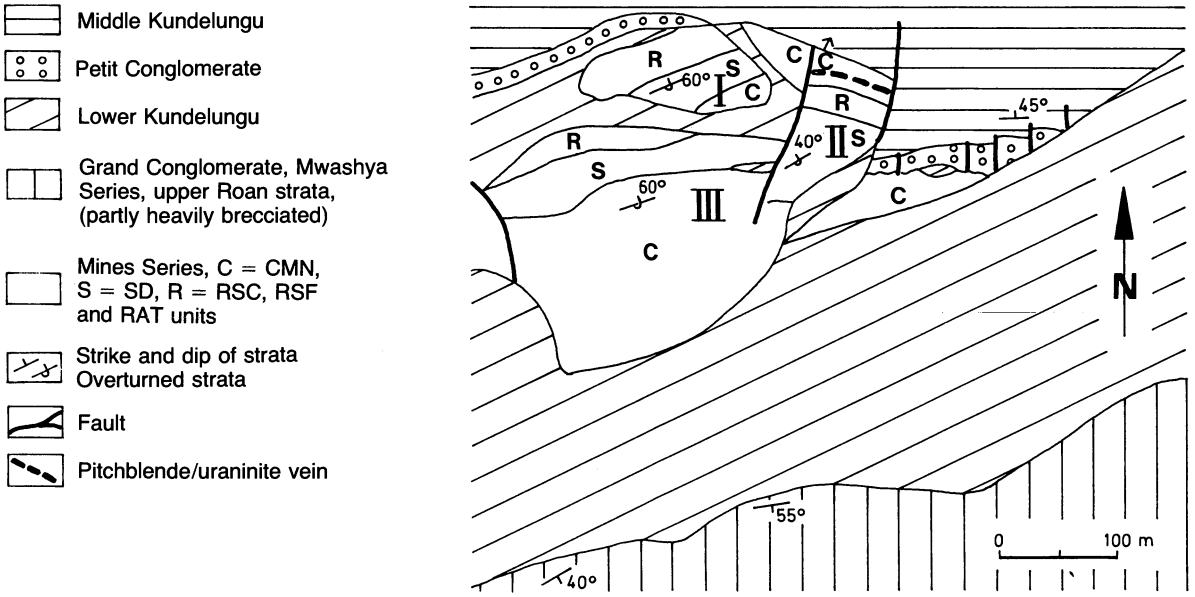

Fig. 5.51. Shinkolobwe, generalized geological map showing the complex structural setting of the deposit which is hosted in the overturned Mines Series. *I*, *II*, *III* tectonic blocks of the Massif Principal. (After Derriks and Vaes 1956; Ngongo-Kashisha 1975)

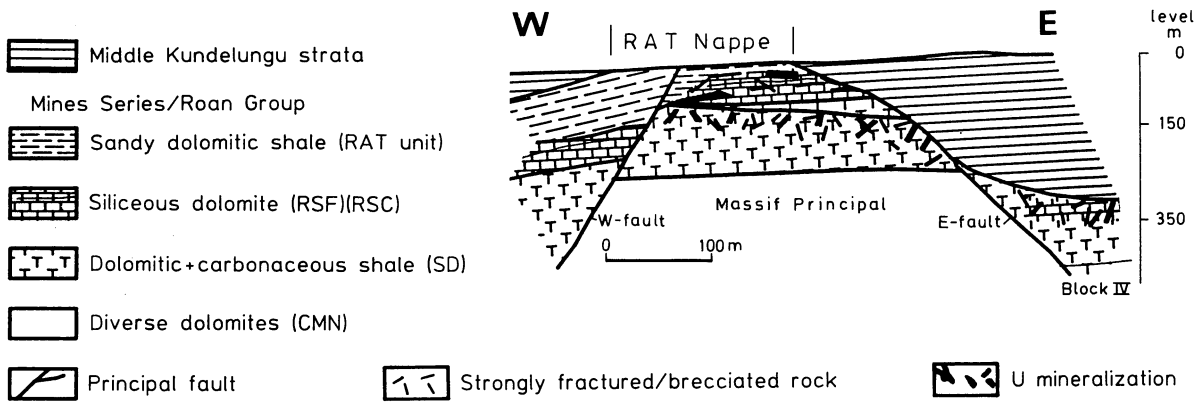

Fig. 5.52. Shinkolobwe, schematic W-E longitudinal section displaying the distribution of uranium veins associated with cataclastic zones in the RAT nappe. Host rocks are overturned strata of the Mines Series. (After Derriks and Vaes 1956)

a large extent from Mines Series facies. Many of these clasts contain "rich Cu-Co mineralization of the syndiagenetic Kupferschiefer type". Dolomitic marl with a variable component of silt, authigenic quartz, and hyper-magnesian chlorite (corresponding to Derriks's and Oosterbosch's (1958) RAT unit) provided the matrix material. Gypsum, anhydrite, and pyrolcastic constituents are common in this RAT unit.

Host Rock Alterations

Dominant host rock alterations are *pre-ore* silicification and Mg-metasomatism, resulting in siliceous dolomite etc., and magnesite replacing dolomite and forming veins, particularly in deeper sections of the deposit. *Ore-related alteration* includes chloritization, dolomitization, and weak silicification.

Principal Characteristics of Mineralization

Principal *ore minerals* (Table 5.26) are uraninite present in cubes up to 1 cm, occasionally 4 cm long, and, in oxidized sections, a large variety of hexavalent U minerals. Remarkably, no pitchblende has been formed. *Associated minerals* are chiefly Co-Ni-sulfides and selenides, minor pyrite, molybdenite, galena, Cu-sulfides, monazite, and traces of Au, Ag, Pd, and other elements. *Gangue minerals* include abundant magnesite, chlorite, quartz, dolomite, and rare aragonite.

Uraninite forms massive aggregates and associations with Co-Ni minerals. Co-Ni mineralization extends beyond uranium zones but Ni-values drop rapidly, as reflected by Ni/Co ratios being 3:1 in uraniferous ore dropping to 1:3 outside thereof.

The ore and associated minerals occur as discontinuous veins, veinlets, or stringers along fissures, joints, bedding planes, and minor faults, as breccia matrix, replacement masses and nodules, and as disseminated particles and aggregates in the host rocks (Fig. 5.53). Major faults are never mineralized but filled with clay-talc breccias.

A succession of *six mineral stages* is distinguished (Derriks and Vaes 1956):

1. Mg-metasomatism transforming the dolomites of the Mines Series into highly magnesian lithologies, mainly magnesite,
2. uraninite and pyrite deposition in open structures,

Table 5.26. Shinkolobwe, primary ore and gangue minerals. (After Derriks and Vaes 1956; [a]Kon 1945 in Derriks and Vaes 1956)

Uranium		
Uraninite		
Urano-molybdenite (molybdate?)		
Th-rare earth		
Monazite		
Sulfides-selenides-tellurides		
Cattierite[a]	Chalcopyrite	Molybdenite
Vaesite[a]	Bornite	Se-molybdenite
Ni-cattierite	Digenite	Pyrite
Co-vaesite	Covellite	Galena
Se-vaesite	Umangite	Pd-sulfide (?)
Se-siegenite		Pentlandite (reported)
Millerite		
Melonite		
Native elements:		
Gold		
Copper (very rare)		
Gangue:		
Silicates	Carbonates	
Quartz (not common)	Calcite	Apatite (minor)
Chlorite	Dolomite	
Tourmaline (minor)	Magnesite	

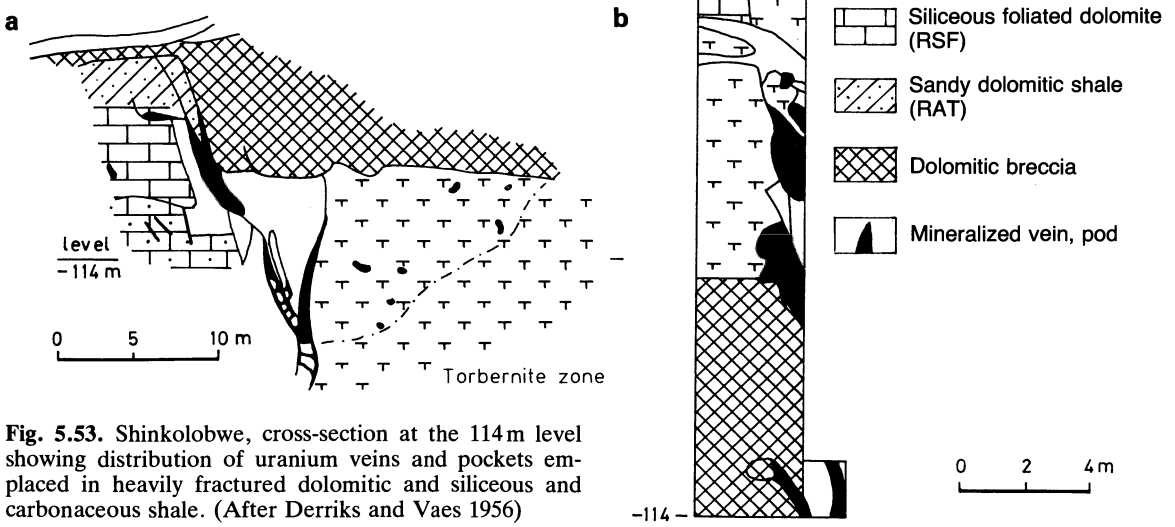

Fig. 5.53. Shinkolobwe, cross-section at the 114 m level showing distribution of uranium veins and pockets emplaced in heavily fractured dolomitic and siliceous and carbonaceous shale. (After Derriks and Vaes 1956)

3. crystallization of molybdenite, monazite, and chlorite; chlorite is coeval with monazite but later than molybdenite,
4. weak quartzification succeeded by deposition of sulfides of Ni and Co and selenides,
5. weak brecciation and dolomitization,
6. formation of chalcopyrite.

Subsequent *modification* resulted in formation of a large variety of hexavalent U minerals and secondary minerals of other metals. In a general way, the altered U minerals developed through four stages: (1) *hydrous stage*: (a) ianthinite, (b) becquerelite, curite, schoepite; (2) *silicate stage*: kasolite, soddyite, sklodowskite, uranophane; (3) *phosphate stage*: (a) parsonsite, (b) dewindtite, (c) torbernite; (4) *minor recrystallization stage*: hydrous oxides, especially curite.

Uranium ore within the *main ore zone* extends for more than 200 m in E-W direction, 100 m wide and at least 255 m deep. More ore is drill-indicated at depth in an easterly extension 300 to 450 m deep (block IV).

Dimensions of individual veins vary between a few centimeters to a meter thick. They commonly lack continuity, being only a meter or two, less often as much as 10 m long. Locally, veins and veinlets are numerous enough to form stockworks.

Mineralization occurs in the three blocks within the nappe mentioned earlier (Fig. 5.52). Ore has accumulated particularly in the numerous fissures, shears, and joints developed in dolomitic shale beneath the domelike structure formed by the impermeable front of the RAT nappe. Below about the 180 m level, uranium mineralization apparently shifts eastwards, whereas Co-Ni minerals still display ubiquitous persistance. Beneath the 220 m level, uranium tenors diminish in the central segment of the wedge, whereas along the western boundary fault and on both sides proximal to the eastern boundary fault, uranium is still present in appreciable amounts. (Derriks and Oosterbosch 1958).

Age dating of uraninite yield ages of $\geq$706, 670 $\pm$ 20, and 620 $\pm$ 10 m.y. (Cahen et al. 1971).

Potential Sources of Uranium

The most likely source of uranium and other metals appears to be the cupriferous horizon of the lower Mines Series. It contains throughout the Katanga Copper Belt elevated Clarke values of the ore-forming metals although of locally variable amounts. Maucher (1962) reports values of up to 50 and 100 ppm U.

Ngongo-Kashisha (1975) established a regional N-S-oriented mineral zoning in the Katanga belt in Shaba. U, Cu, Ni, Co, Mo associated with magnesite and monazite prevail in the southern segment of the arc where also Shinkolobwe and other uranium deposits are located. Further to the north U, Ni, magnesite and monazite decrease whereas Cu and Co increase.

Ore Controls and Recognition Criteria

Principal ore controlling or recognition criteria include:

Host Environment

- Regional structural setting is (a) within a fold belt, (b) in or near a hinge zone along which the tectonic style and direction of the Katanga fold belt change.
- Local structural setting is very complex due to complicated rock dislocations which lead, however, to favorable structural ground preparation. Tectonism generated fissures, breccias, stockworks etc. in more brittle rocks (siliceous dolomite) and displacements of more ductile lithologies (shales etc.) moving them into positions (RAT nappe) to act as impermeable barriers for migrating ore-forming fluids.
- Position of host and potential source rocks (lower Mines Series) is at the base of a several 1000 m thick marine sequence (Katanga Group) deposited in a large, though restricted, intracratonic basin.
- The ore-hosting strata, predominantly dolomitic rocks and shales, occur below the horizon of the Mines Series, which contains a variety of synsedimentary metals including anomalous uranium tenors and the stratiform copper deposits.
- Granitic or other intrusions are apparently absent.

Alteration

- Pre-ore alteration includes Mg-metasomatism and silicification.

- Ore-related alteration includes chloritization, dolomitization, and weak silicification.

Mineralization

- The ore is polymetallic, composed of U, Ni, Co, Cu, and minor other metals but U is only with Ni in apparent paragenesis.
- Gangue minerals include magnesite, chlorite, quartz, dolomite and aragonite.
- U is present as euhedral uraninite, a habit typical for high temperature crystallization.
- Ore and gangue mineral assemblages are comparable with those of hypogene deposits.
- The mineralization is structurally controlled, forming an irregular stockwork of fracture, fissure, and joint fillings and breccia impregnations.

Metallogenetic Concepts

Mineralization at Shinkolobwe is epigenetic hydrothermal. The actual processes involved are, however, still enigmatic. A granitic source can be discarded.

Hypotheses on ore formation at Shinkolobwe, and of vein deposits in general in the Katanga Group of Zaïre and northern Zambia range over a wide spectrum from magmatic hypogene hydrothermal to synsedimentary with subsequent redistribution. Most early workers, including Derriks and co-authors (1956/1958), favor a magmatic hydrothermal origin involving several pulses. Meneghel (1979) suggests a synsedimentary origin of the uranium which was later redistributed into structures to form veins by various processes related to tectonism, metamorphism, thermal events associated with post-tectonic metamorphism, and supergene enrichments. Stipanicic (in Meneghel 1981) arrives at the conclusion that Shinkolobwe, Swambo, Kalongwe in Shaba, and Nkana, Nchanga etc. in the Copperbelt "show a dominant stratiform pattern, to which pseudo-vein sectors are sometimes connected."

Most intriguing appears a concept mobilizing U and associated metals from synsedimentary or syndiagenetic protore inherent in the Mines Series strata and redistribution of the metals into favorable structures by convective circulation of fluids corresponding to the model proposed by de Magnée and François (1985). These authors consider circulating pressurized hot brines comparable to those known from certain active geothermal fields as instrumental in the formation of the Shinkolobwe ore and for other deposits as well, e.g., the Cu, Zn deposit Kipushi.

Isotope ages of uraninite (ca. 706 and 670 m.y., Cahen et al. 1971) correlate with the first three tectonic phases of the Lufilian Orogeny (ca. 840 to 710 m.y. and 670 m.y., Cahen 1970). This may support a convective hydrothermal model in which tectonic activity generated circulation of connate waters/brines and the associated processes mentioned above.

References and Further Reading for Chapter 5.3.6
(for details of publications see Bibliography)

Bell 1987; Cahen 1970; Cahen et al. 1961, 1971; Cluzel 1986; Deliens et al. 1981; de Magnee and François 1985; Derriks and Oosterbosch 1958; Derriks and Vaes 1956; Dibobol and Malu 1979; François 1974; Gerasimovsky 1956; Lefebvre and Tsauka 1986; Meneghel 1979, 1981, 1984; Ngongo-Kashisha 1975; Oosterbosch 1962, 1970; Roubault 1958; Schoep 1930; Thoreau and du Trieu de Terdonck 1933, 1936; Unrug, 1988

5.4 Examples of Sandstone-Type Uranium Deposits (Type 4, Chap. 4)

5.4.1 Extrinsic Carbon/Humate-Uranium Deposits in Phanerozoic Sandstones: Grants Uranium Region, USA

The Grants Uranium Region is located on the southeastern Colorado Plateau in northwestern New Mexico. It includes five major uranium districts distributed over an area of ca. 150 km in ESE-WSW length and up to ca. 30 Km in N-S width (Fig. 5.54).

The deposits occur at variable depths ranging from outcrop at the southern boundary to more than 1200 m downdip to the north.

The Grants Uranium Region which includes the Ambrosia Lake district, the single largest uranium-producing area in the USA, has at least 280 000 mt U_3O_8 estimated total resources in the \$80/kg U production category. Production until 1990 was almost 160 000 mt U_3O_8. The average grade of ore mined ranged from 0.1 to 0.25% U_3O_8.

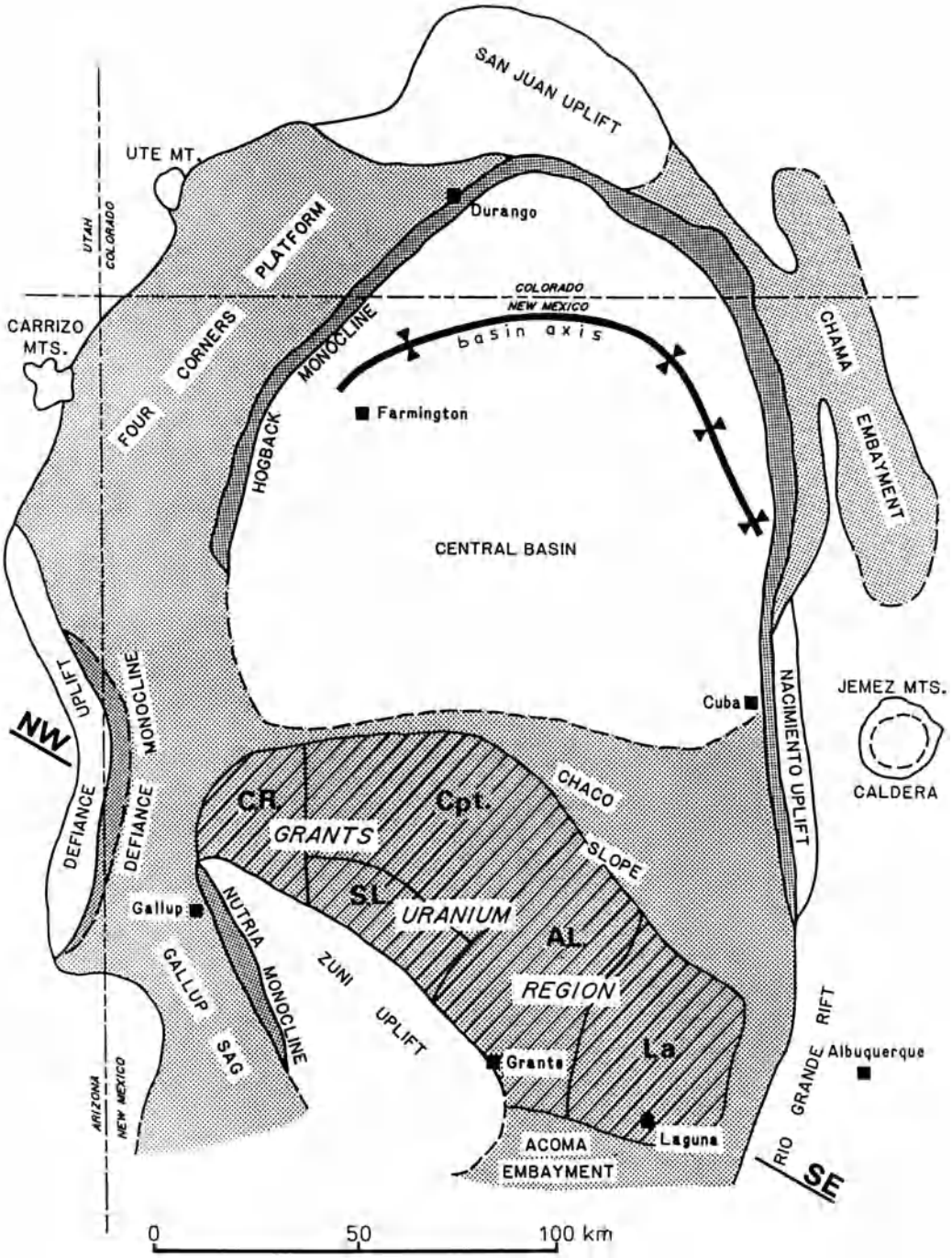

Fig. 5.54. Southeastern Colorado Plateau, San Juan Basin. The figure shows major structural elements, the extend of the basin and the situation of the Grants Uranium Region between the Zuni Uplift of Proterozoic crystalline rocks and the Chaco Slope. Individual districts of the uranium region are outlined. Principal districts: *C.R.* Church Rock; *Cpt.* Crownpoint; *S.L.* Smith Lake – Mariano Lake; *A.L.* Ambrosia Lake; *La.* Laguna. (After Santos and Turner-Peterson 1986 based on Kelley 1951) (reprinted by permission of AAPG)

Mineralization is primarily of tabular sandstone type in which the uranium is associated with redistributed carbonaceous material such as humate. The deposits are therefore classified as Phanerozoic tabular/peneconcordant extrinsic carbon/humate-uranium deposits.

The region has been the subject of numerous geoscientific investigations. Adams and Saucier

(1981) have compiled a geological model study on "uraniferous humate deposits," as they call the uranium mineralization in the Grants region. Adams and Saucier's (1981) documentation describes the known geology of the Grants region adequately and presents a comprehensive synopsis of the regional setting and local characteristics of the uranium deposits, their recognition criteria and the fundamental principles of ore formation. The subsequent description has drawn extensively from Adams and Saucier's (1981) report, and in many cases specific text has been quoted but with some modifications (therefore not set in quotation marks). Updates are taken from more recent publications, in particular from Granger and Santos (1982), Holen (1982), and Crawley et al. (1984).

Meanwhile a new memoir edited by Turner-Peterson et al. (1986) has been published providing extensive multidisciplinary research data, and the reader is referred to this excellent publication for more information.

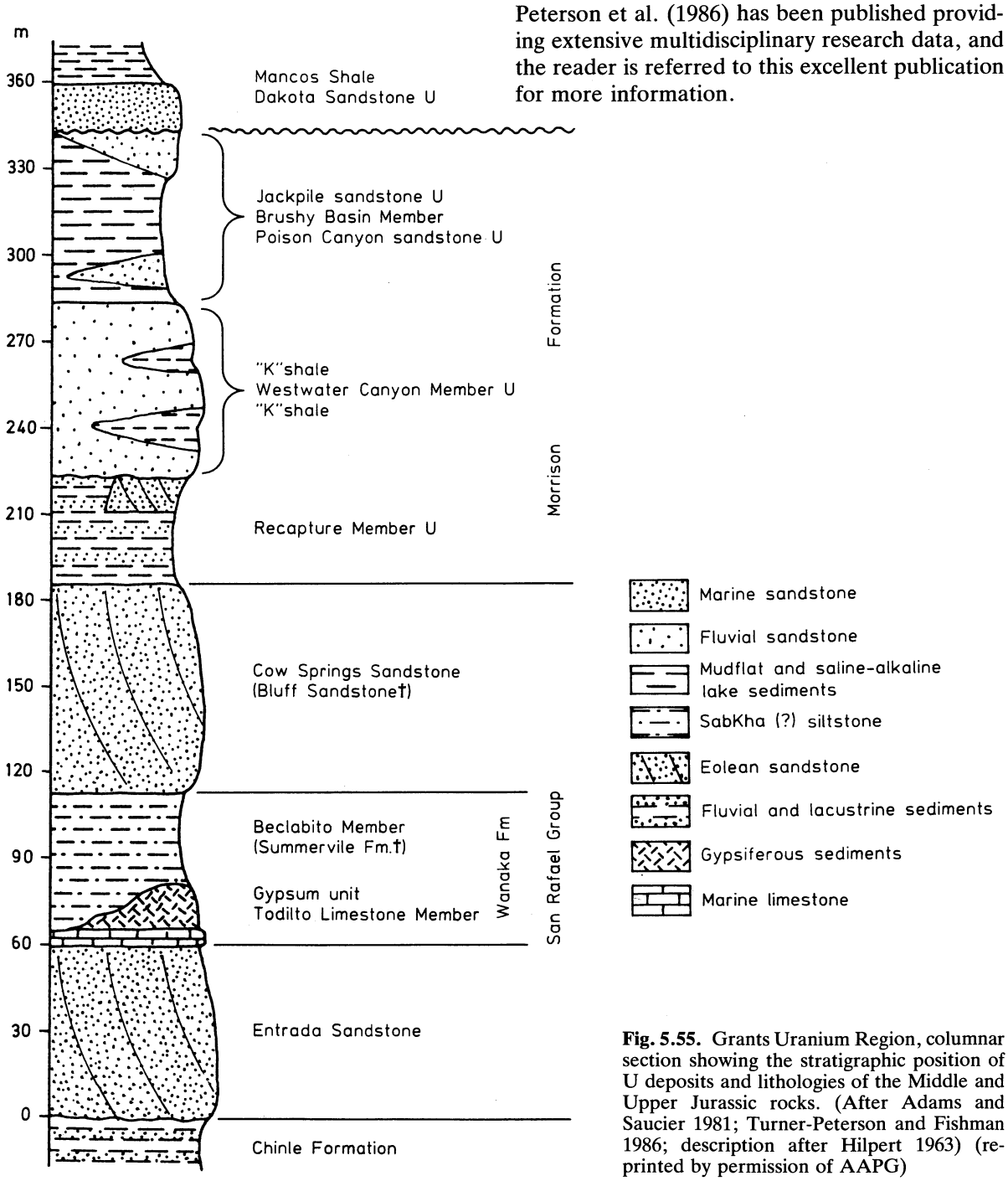

Fig. 5.55. Grants Uranium Region, columnar section showing the stratigraphic position of U deposits and lithologies of the Middle and Upper Jurassic rocks. (After Adams and Saucier 1981; Turner-Peterson and Fishman 1986; description after Hilpert 1963) (reprinted by permission of AAPG)

Geological Setting of Mineralization

The Grants Uranium Region extends inside and along the southern border of the *San Juan Basin*, north of the Zuni Uplift (Fig. 5.54). During late Jurassic time, three broad alluvial fans were deposited in the basin upon Middle Jurassic sediments. The fans constitute the major part of the Morrison Formation and correspond, from oldest to youngest, to the Salt Wash Member in the north, the Recapture, and the Westwater Canyon-Brushy Basin members in the south.

In Upper Cretaceous time, southern outcrops of the Morrison Formation were partly eroded before they were unconformably transgressed by the Dakota Sandstone and Mancos Shale.

Younger tectonic movements of presumably Laramide age (Cretaceous/Tertiary) resulted in the formation of the present Zuni Mountains in the southern part of the San Juan Basin and caused a slightly northward tilt of the Morrison strata. Fracture tectonics at the same time caused displacements of generally minor magnitude.

Tertiary volcanics of Mt. Taylor cover the Mesozoic sediments between Laguna and Ambrosia Lake.

Most of the uranium deposits of the Grants region are in sandstones of the Westwater Canyon-Brushy Basin members, Morrison Formation (Figs. 5.55, 5.56). The Morrison sediments have a shallow dip (<5°) to the N and NE except where locally disrupted by faulting or folding. The formation is up to 180 m thick and comprises, from top to bottom, the

- *Brushy Basin Member*, 6 to 90 m thick, which mainly consists of lacustrine greenish-gray mudstone with widespread, in part rather thick, intercalations of cross-bedded feldspathic sandstone. The predominant clay mineral is montmorillonite derived by devitrification of volcanic ash.

  Turner-Peterson (1985) separates the member into four lateral depositional facies. Going from the southern margins of the former Brushy Basin lake, the facies are: Alluvial plain-mudflat-playa margin-central playa (Fig. 5.57).

  Assigned to the Brushy Basin Member are two mineralized sandstone units:
  - *Jackpile sandstone*, up to 70 m thick, located in the eastern and topmost section of the Brushy Basin Member. It hosts U deposits in the Laguna district.
  - *Poison Canyon sandstone*, up to 25 m thick hosting deposits in the Mt. Taylor and some in the Ambrosia Lake districts.
- *Westwater Canyon Member* is the host for ore bodies in the Ambrosia Lake and in most of the other districts of the Grants region. The Westwater Canyon Member is 15 m thick in the Laguna district and thickens to 80 m in the Ambrosia Lake district. It is composed of buff to gray, badly sorted, cross-bedded, fine- to very coarse-grained arkose to feldspathic sandstone with local intercalations of gray, often montmorillonitic mudstone. It contains variable amounts of humate and organic plant material. Minor amounts of heavy minerals are

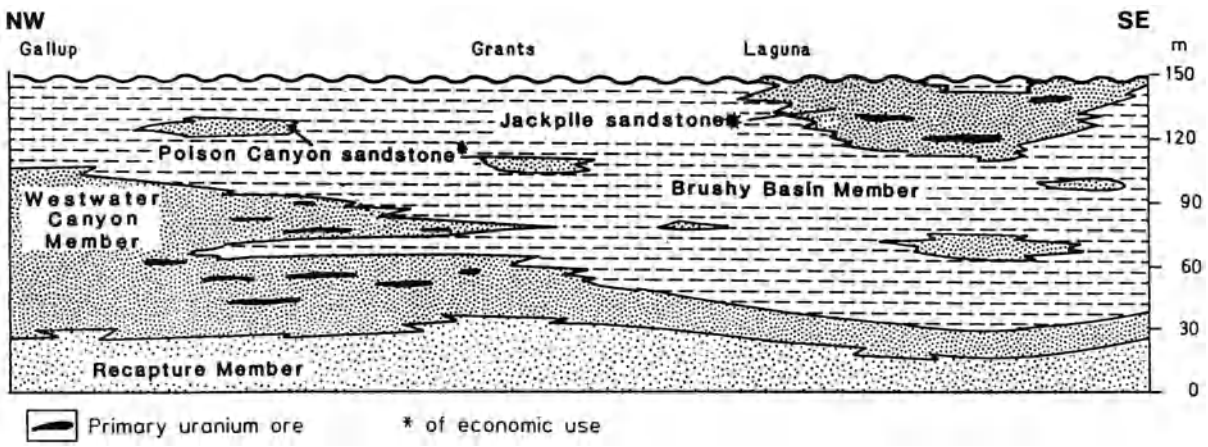

Fig. 5.56. Grants Uranium Region, schematic NW-SE stratigraphic section of the Morrison Formation along the southern part of the mineral belt displaying the distribution of the uranium mineralization within and the interrelationship of the host sandstone units. (After Turner-Peterson and Frishman 1986, based on Hilpert 1963) (reprinted by permission of AAPG)

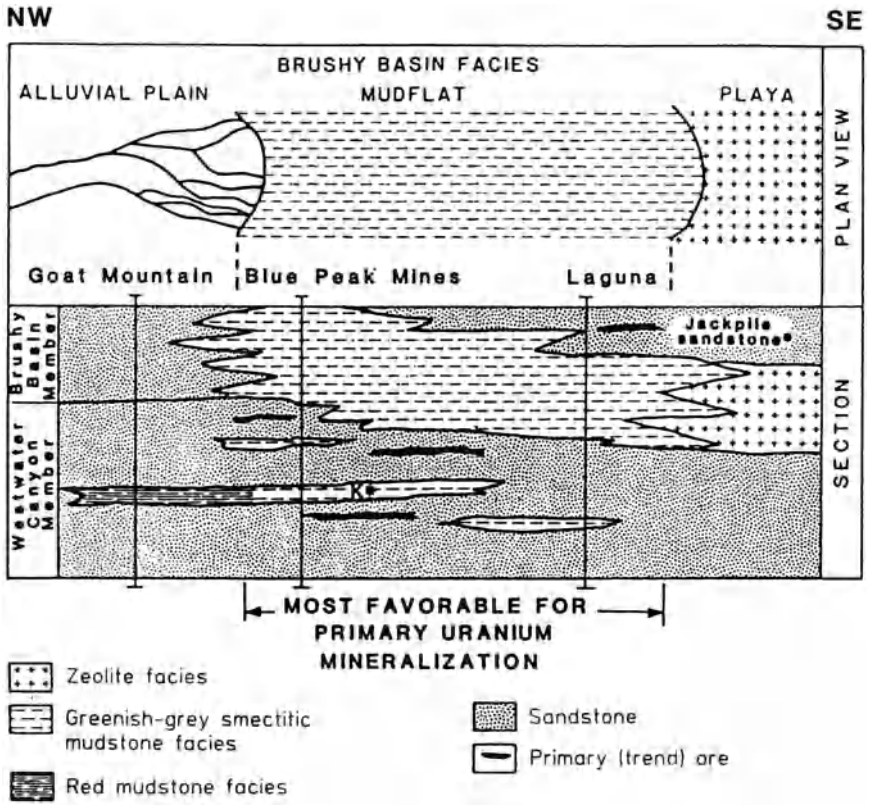

Fig. 5.57. Grants Uranium Region, diagrammatic section extending from the Laguna district in the SE to the southern part of the Ambrosia Lake district in the NW and displaying the relationship of U mineralized sandstone in the Westwater Canyon Member and Jackpile sandstone to sedimentary facies in the Brushy Basin Member and "K" shales. The zone overlain by greenish-gray mudstone/mudflat facies is supposedly the most favorable for U mineralization in the Morrison Formation sandstone. Similarly, facies changes in the "K" shale appear to be also important as suggested by the position of mineralization in the Goat Mountain-Blue Peak mines area. (Turner-Peterson 1985) (reprinted by permission of AAPG)

common (Cadigan 1967; Adams et al. 1974). The Westwater interfingers with the Brushy Basin sediments. A thin pelitic horizon, designated K-Shale, is locally intercalated in the Westwater Canyon Member.

- *Recapture Member*, 10 to 60 m thick, consists of alternating beds of gray sandstone and gray to maroon silt- and mudstones which interfinger with the Westwater Canyon sandstones.

The *Westwater Canyon and Brushy Basin sandstones* contain trace to 0.5% heavy minerals and widespread but irregularly distributed plant remains. Humate impregnates the sandstones in large, blanket-like masses and averages about 0.1 to 0.25% in weight (Adams and Saucier 1981). The sandstones have variable amounts (up to 5%) of pyrite when reduced, and hematite and/or limonite when oxidized (Knox and Gruner 1957). The Westwater Canyon sandstone contains 5 to 15 ppm uranium when reduced and 1 to 2 ppm uranium when oxidized (Brookins 1979).

Galloway (1980) interprets the *Westwater Canyon depositional environment* as a wet alluvial fan derived by rivers flowing between NE and SE from a source in the SW. This is indicated by the occurrence of coarsest sandstone and the thickest part of the fan near the SW margin of the San Juan Basin. Their source was very probably the ancient Zuni or Mogollon highlands, which provided the igneous and metamorphic fraction complemented by widespread volcanic ash-fall material. The more proximal part of the fan has been truncated by late Jurassic to late (?) Cretaceous pre-Dakota erosion. The proximal to mid-section of the fan consists of braided bed-load channel facies which grades down-fan into straight bed-load, sinuous mixed-load, and finally distributary mixed-load channel facies at the distal front system. All major uranium deposits occur in the mid-fan facies.

Host Rock Alterations

The bulk of the Westwater Canyon sandstones and the Brushy Basin sandstone lenses are reduced due to diagenesis under reducing conditions. Geological evidence suggests that the sandstones, at least some of them, experienced oxidation and re-reduction in pre-Dakota time. The reduction or re-reduction presumably occurred in conjunction with humate formation

from formerly water-soluble organic substances, very probably of plant origin.

Early alteration of volcaniclastic material produced montmorillonite, smectite, illite, and mixed layer clays. The process overlapped in part with the reduction of portions of the ore hosts, in particular of the upper part of the Westwater Canyon sandstones and of the entire Jackpile sandstone. The reduction destroyed the detrital magnetite and ilmenite with local replacements by pyrite.

In a subsequent stage, but partly overlapping the ilmenite-magnetite destruction, humic material together with uranium precipitated in the Westwater Canyon sands, where they are overlain by the above-mentioned Brushy Basin mudflat facies.

Alteration and replacement of feldspars, including albitization and probably replacement of sodium by potassium in an outer shell of sanidine grains (Austin 1980), developed locally within the Jackpile sandstone, and in a wider range within the Westwater Canyon sandstones. Clay coatings of various compositions formed within the sandstones in proximity to the uraniferous carbonaceous material. Subsequent to the formation of the primary ore lenses, baryte and calcite precipitated and kaolinite crystallized as nests within the sands. Figure 5.58 shows the paragenetic sequence of the varies alteration events.

In a later *post-Laramide alteration* stage, the Morrison sandstones were affected by a regional oxidation front which advanced from the southern outcrop zone of the Morrison Formation into the San Juan Basin. The oxidation zone extends from the outcrop for a few to 25 km and perhaps more downdip, as indicated by red hematitization of the sandstone, but left unoxidized islands behind. At its distal front it grades into a zone of brown limonitic sandstones, less than a kilometer to several kilometers wide, which border downdip-reduced gray sandstones.

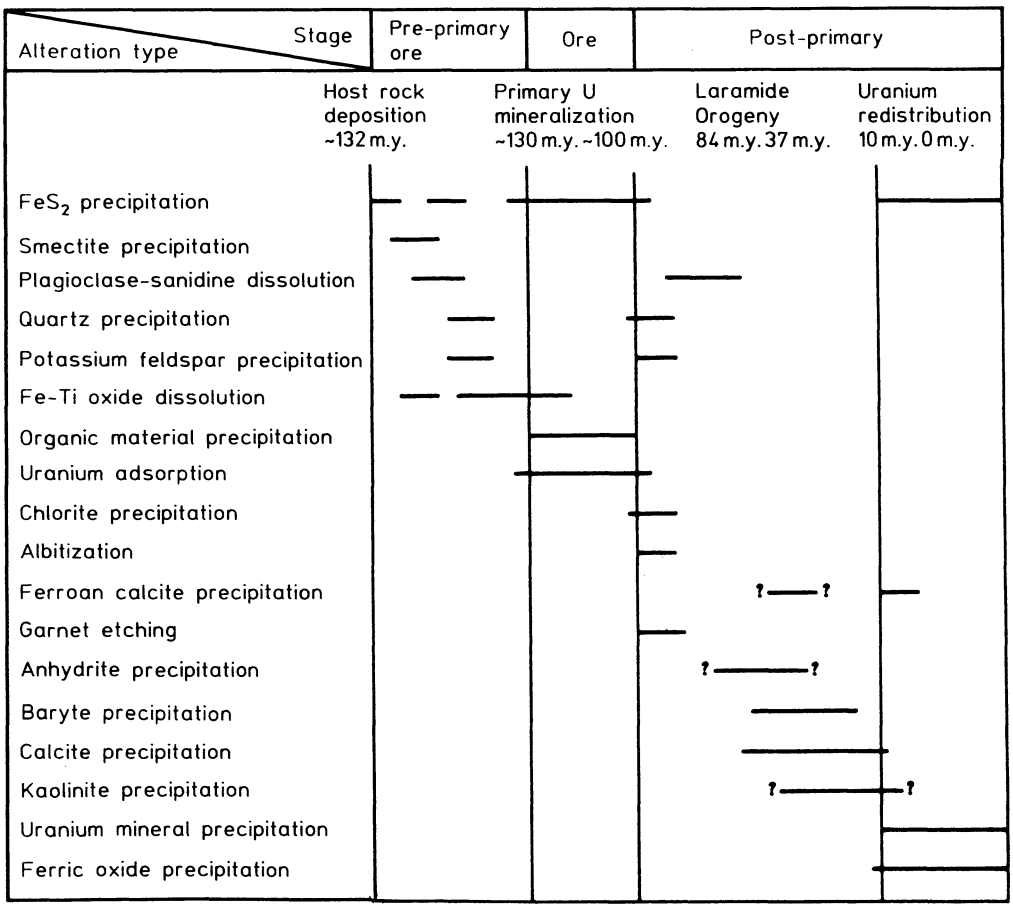

Fig. 5.58. Grants Uranium Region, paragenetic sequence of diagenetic alteration and mineralization events in sandstones of the Morrison Formation. (Turner-Peterson and Fishman 1986) (reprinted by permission of AAPG)

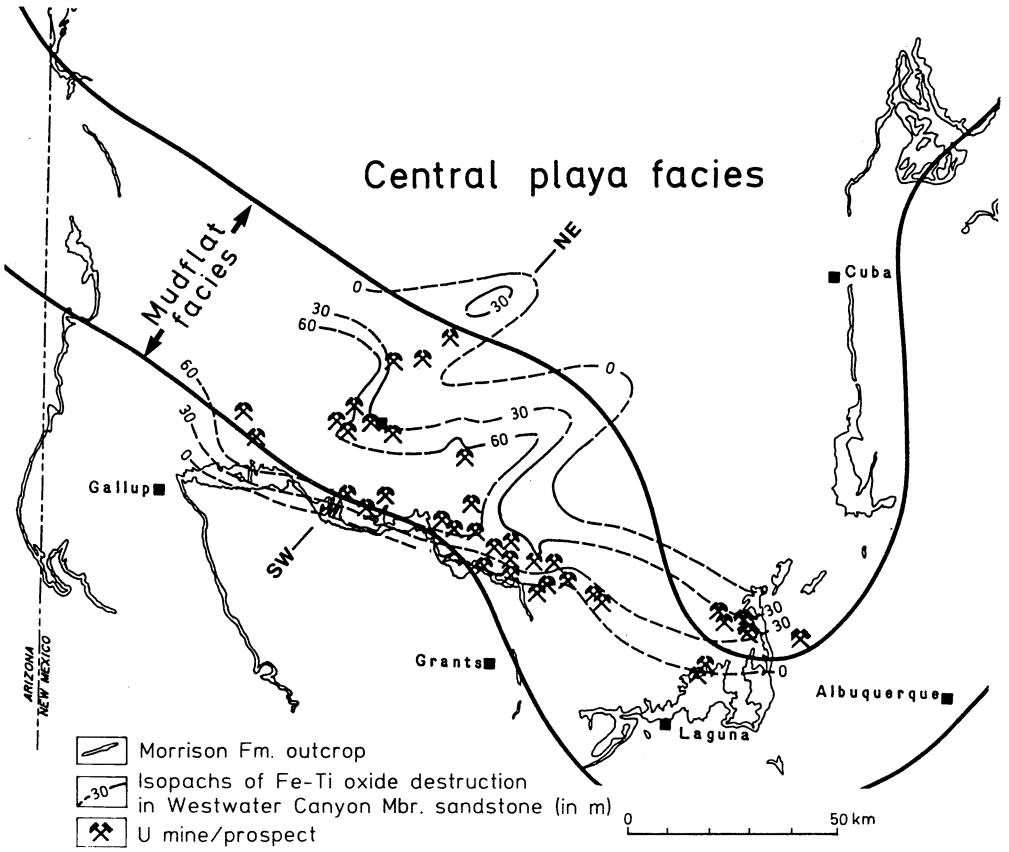

Fig. 5.59. Grants Uranium Region, compository map of isopachs of Fe-Ti-oxide destruction in sandstone beds of the Westwater Canyon Member and main facies of the Brushy Basin Member. Most of the U ore bodies are positioned in the zone of greatest Fe-Ti-oxide destruction which largely extends below the mudflat facies. (After Turner-Peterson and Fishman 1986) (reprinted by permission of AAPG)

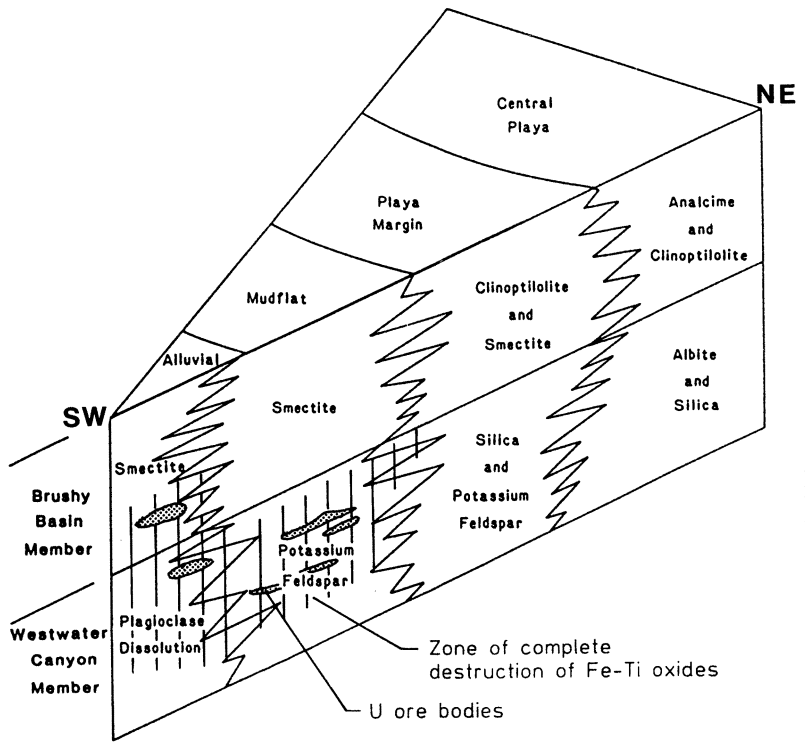

Fig. 5.60. Grants Uranium Region, block diagram illustrating the distribution and relationship of diagenetic alteration minerals/patterns in the Westwater Canyon Member (colluvial plain sandstone) and depositional facies and alteration minerals in the overlying Brushy Basin Member. (After Hansley 1986; Turner-Peterson and Fishman 1986) (reprinted by permission of AAPG)

The various alteration-derived minerals display certain lateral and vertical *distribution patterns* including rock facies-related zonation (Bell 1986; Turner-Peterson and Fishman 1986; Whitney 1986; Riese et al. 1980).

Distinct alteration patterns of feldspars and Fe-Ti-oxides are noticed in Westwater Canyon sandstones. Strongest alteration of these minerals is proximal to Brushy Basin pelites and limited to those of the mudflat facies. The mudflat facies characteristically contains smectite formed in response to alteration in an environment of pH 7 to 8.5 (Bell 1986) (Figs. 5.59, 5.60).

Principal Characteristics of Mineralization

The bulk of the uranium ore in the Grants region is in unoxidized deposits. Some minor occurrences consist of oxidized ore. Reduced deposits are differentiated into primary and redistributed mineralization. In principal, all ore of pre-Dakota age, which is offset by Laramide faults and associated uniformly with humate, has been attributed to primary mineralization (also termed prefault, blanket, trend, black band, and uraniferous humate mineralization). All ore of post-Laramide age, which is randomly associated with humate, is termed redistributed mineralization (also named post-fault and stack ore, explanations see later). Figure 5.61 provides a summary of the characteristics of the various types of ore and their lithostratigraphic distribution.

Adams and Saucier (1981) summarize the characteristics of mineralization as follows. Their data are updated by information mainly from Granger and Santos (1982, 1986), Holen (1982), and Crawley et al. (1984).

Reduced Mineralization: Principal uranium minerals are coffinite, pitchblende, sooty pitchblende, and black amorphous urano-organic complexes/uraniferous humate. The ore minerals impregnate the host sandstone by coating and being distributed interstitially to the sand grains.

Primary reduced mineralization: Much of the uranium is present in urano-organic compounds/uraniferous humate. Associated minerals include pyrite, marcasite, jordisite, ferroselite, chalcopyrite, galena, wurtzite, calcite, baryte, and kaolinite. Spirakis and Pierson (1986) report elemental enrichments of Cu, Fe, Mn, Mo, Se, V, Y, As, S and organic carbon along with U. Most of these elements occur rarely in form of ore minerals in the primary mineralization. They appear to be dominantly fixed by humate. Mo and commonly Se form halos around primary ore zones. V prevails in the western section of the mineral belt.

Primary mineralization (Figs. 5.62 to 5.65) occurs as peneconcordant blanket and channel ore bodies, roll-type ore bodies and partly in breccia pipes. Blanket and channel ores generally form relatively thin peneconcordant lenses suspended subparallel to the sandstone stratification. Boundaries between ore and barren ground are sharp. *Channel ore* is more tabular and elongated, sometimes following individual fluvial sand channels for as much as 2000 m. *Blanket ore* displays more an undulating sheet-like shape with WNW-ESE trending "roll"-like thickenings. These "*rolls*" occur where the mineralized blanket cuts sharply across sandstone bedding to a different elevation. In cross-section, the step up resembles a flattened S, where the mineralization in the sandstone is not only thicker but is often higher in grade. Other roll-type ore bodies exhibit C-shapes in cross-section similar to the Wyoming rollfront deposits. But, the upper and lower limits are generally wide and the host rock on the convex updip side has been reduced again.

In many cases, both the tabular and roll-type mineralization is WNW-ESE-trending more or less parallel to the orientation of the sedimentary transport direction (Fig. 5.66).

Dimensions of individual ore lenses range in length from several tens of meters up to about 2000 m, and in width from several meters up to some hundreds of meters. Their thickness is usually less than 2.5 m but ranges from a few centimeters to over 5 m. Exceptional thicknesses of up to 18 m are found where several channels converge as at Mount Taylor (Fig. 5.67).

Redistributed reduced mineralization contains coffinite as the dominent U mineral. Pitchblende is very rare. Associated minerals include montroseite, paramontroseite, häggite, ferroselite, native selenium, pyrite, marcasite and calcite (Granger and Santos 1986). Mo is practically missing.

In contrast to the primary ore, where humate is an essential constituent and coextensive with uranium at a ratio of approximately 1:1 by weight (Granger et al. 1961), the ratio is highly variable in redistributed unoxidized mineralization, probably due to discriminative separation of the

PRIMARY ORE
(Also called prefault ore, trend ore, black band ore)

- Thin—generally < 2.5m.
- Higher grade—generally averages >0.20% U_3O_8.
- Offset by Laramide-Tertiary faults.
- Sharp ore to waste boundary.
- Coextensive with humate and/or carbonized vegetal material.
- Color—dark gray to black.
- Age—Pre-Dakota; field relationships indicate that at least some primary ore is immediate post-depositional in age.

REDISTRIBUTED ORE
(Also called postfault ore, stack ore, secondary ore)

- Thick—generally > 3m up to 46m.
- Lower grade—generally < 0.20% U_3O_8.
- Sometimes localized by Laramide-Tertiary faults and fractures.
- Diffuse ore to waste boundary.
- May or may not be associated with humate or carbonized vegetal material.
- Color varies from dark brownish gray to light gray, probably depending on amount of humic material present.
- Age—oxidation that resulted in the redistribution of primary ore started after regional uplift and erosion in late Miocene or early Pliocene time and continues to the present.

TYPES OF PRIMARY ORE

A variety of orebody characteristics has resulted in different interpretations of ore habit and genesis. At least three types of primary ore are described in the literature.

1. Blanket Ore: Undulating blanket with pronounced, ESE-trending thickenings or "rolls"; coextensive with humate; very little vegetal material.
2. Channel Ore: Stronger facies control than blanket type; sometimes follows indiviual channels from tens of meters to as much as 2 kilometers; associated with more carbonized and silicified vegetal material (plus humate) than blanket ore.
3. Wyoming Roll-Type Ore: Pre-Dakota age; geometry in plan and cross section is similar to Wyoming rolls, but upper and lower limbs are generally wider; oxidized interior has been rereduced. Note: Not to be confused with redistributed ore which is also thought to be genetically similar to Wyoming roll ore.

A: "Ghost orebodies"; oxidized environment
B: Remnant primary orebodies; oxidized environment
C: Redistributed orebodies at advancing Tertiary-Quaternary oxidation front
D: Primary orebodies; reduced environment
E: Primary orebodies in Brushy Basin sand bodies; reduced environment except near outcrop
F: Orebodies in the Todilto Limestone
G: Small orebodies in fluvial sandstone, or associated with lignitic material, at the base of the Dakota Ss.

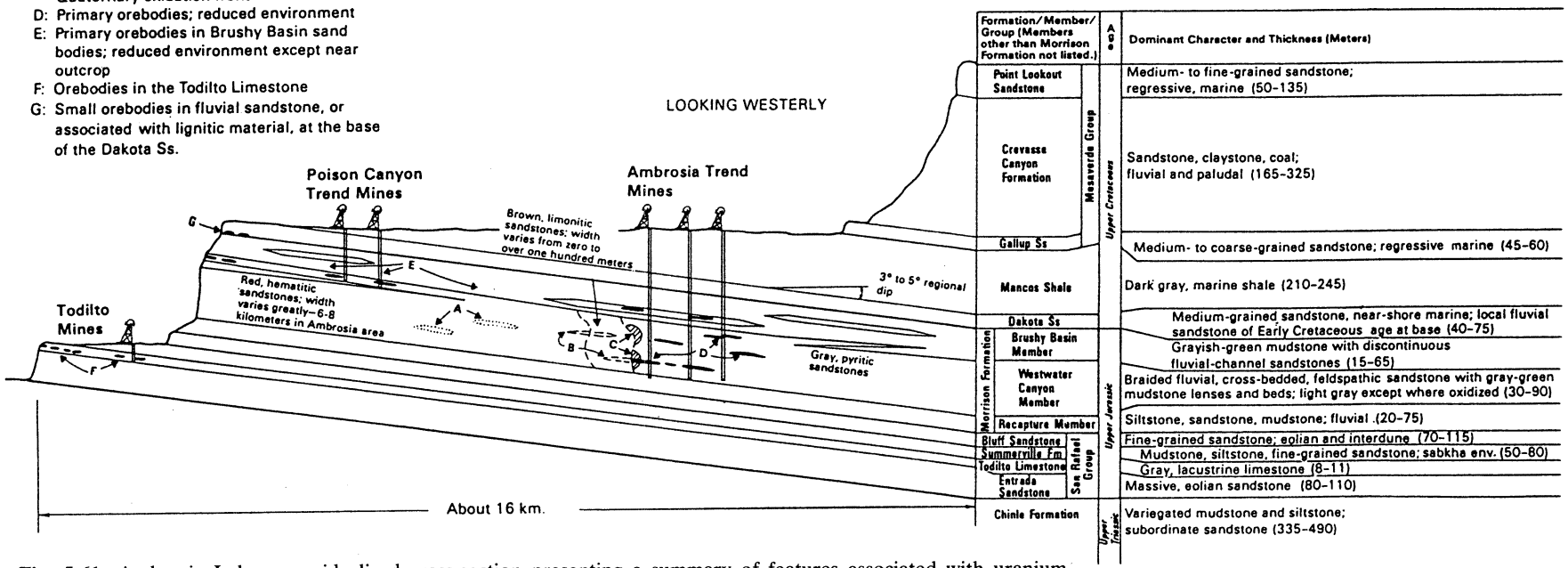

Fig. 5.61. Ambrosia Lake area, idealized cross-section presenting a summary of features associated with uranium mineralization. (Crawley et al. 1984 based on Holen 1982)

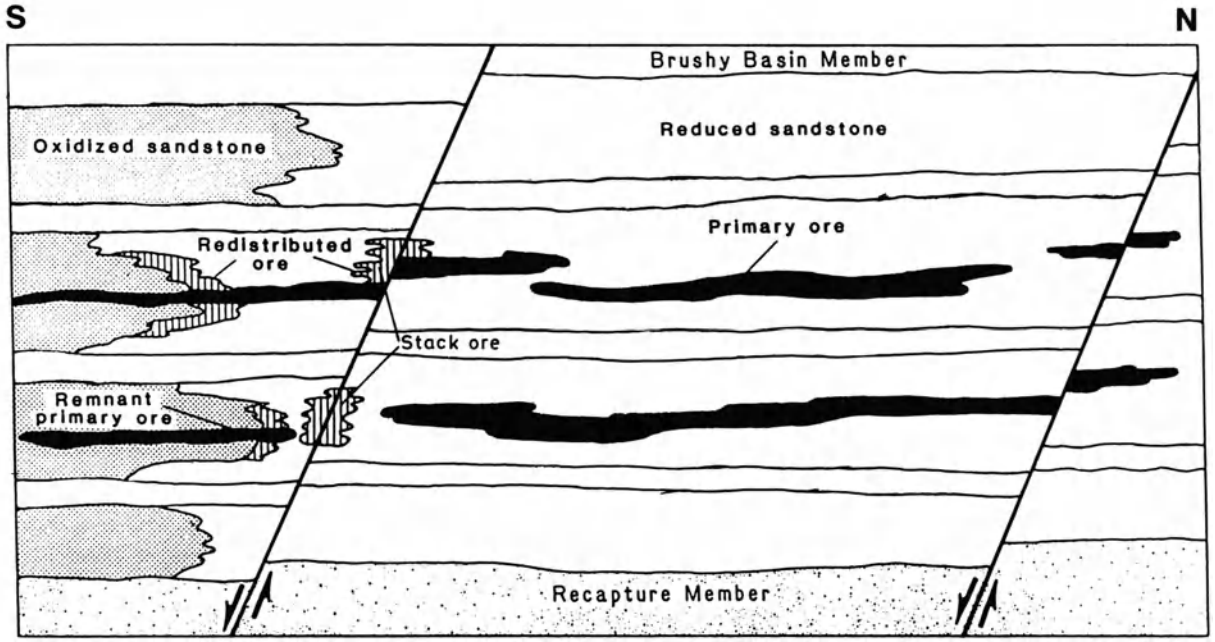

Fig. 5.62. Grants Uranium Region, diagrammatic S-N section illustrating the structural position and configuration of primary and redistributed U mineralization in Morrison Formation sandstones. Primary mineralization forms elongated tabular ore lenses suspended within reduced sandstone, while redistributed mineralization has accumulated along faults and at the contact between oxidized and reduced sandstone. Remnant primary mineralization occurs as islands within oxidized sandstone. (After Turner-Peterson and Fishman 1986) (reprinted by permission of AAPG)

uranium from humate. Some redistributed ore is virtually barren of organic complexes.

Redistributed mineralization, also named *stack ore* and post-fault ore, is essentially tectonically and lithologically controlled, but, in some cases, may be also of *rollfront* character (Figs. 5.62, 5.64, 5.65). The ore is considered to have been formed by redistribution of primary mineralization. The uranium in stack ore bodies commonly concentrates in or along steeply dipping faults of Tertiary age or younger, primarily where oxidized sandstones are in contact with unoxidized. The redistributed ore usually has a relatively sharp updip contact against thick oxidized sandstone. It engulfs the primary blanket ore in the reduced strata by impregnating the sandstone above and below the primary blankets. Redistributed ore is darker and richer close to the oxidation front and gradually fades into the reduced ground across the fracture zone. Where several ore blankets with primary uranium existed, the redistributed ore can mineralize intervening barren ground, creating thick sections of fairly continuous ore.

Stack ore is surrounded by a zone of limonitic and locally bleached rock, which evidently is transitional into red, hematitic sandstones (Fig. 5.64). The width of the limonite zone varies from a few meters (e.g., at Ambrosia Lake) to many tens of meters (e.g., at Church Rock).

Stack deposits are variable in shape and may resemble a tree in cross-section.

Dimensions of individual ore bodies range in length to 100 m and more, and in width and thickness from a few meters to more than 40 m. Average width is approximately 3 m. The grades are generally lower than in primary ore, averaging between 0.1 and 0.2% U_3O_8.

Breccia pipe hosted mineralization is restricted to those pipes that cut primary ore. Only three of such ore-bearing pipes have been found. The pipes are chimney-like collapse structures which cut Westwater Canyon and Brushy Basin sediments. They range in diameter from a few decimeters to more than 25 m. Their vertical extension can be up to 70 m (Woodrow pipe, Laguna district). Mineralization with grades locally in excess of 1% U_3O_8 is predominantly concentrated in the upper portion of the pipe. It consists of downfaulted blocks of strata-controlled primary ore or redistributed ore as in the Woodrow pipe. Remobilized uranium impregnates the breccia matrix.

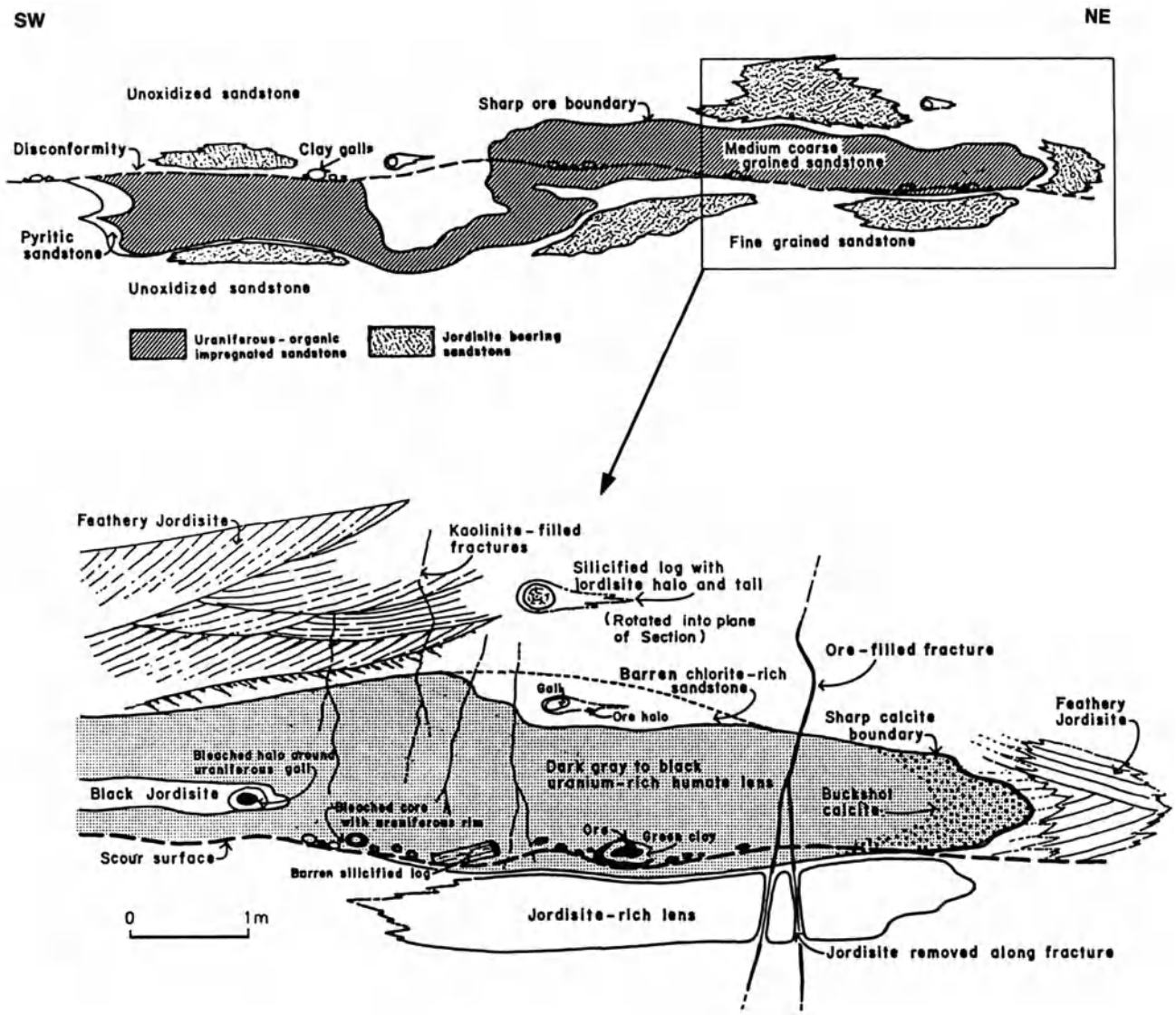

Fig. 5.63. Ambrosia Lake district, Ann Lee and Section 27 mines, composite diagram of features associated with mineralization. (After Adams and Saucier 1981 based on Squyres 1970, Kendall 1971)

McCammon et al. (1986) calculated statistical averages of *reserves* for the various configuration types of primary deposits. At a cutoff grade of 0.1% U_3O_8 trend-type deposits average an ore grade of 0.22% U_3O_8 and a reserve of 7250 mt U_3O_8. Corresponding figures for roll-type deposits are 0.16% U_3O_8 and 9400 mt U_3O_8, and for remnant ore bodies 0.2% U_3O_8 and 1350 mt U_3O_8. The authors also calculated an amount of 422 272 mt U_3O_8 discovered resources for the whole region based on a cutoff grade of 0.1% U_3O_8.

Age dating of uranium ores and associated clay minerals from various districts indicate several generations of mineralization and uranium redistribution respectively. Primary mineralization apparently is at least 140 to 130 m.y. old (Brookins 1980b; Rosenberger and Harper 1981, 1982). Apparent ages of ca. 115 to 110 m.y. (Brookins 1980b; Lee and Brookins 1978), supposedly reflect a remobilization event perhaps associated with a first roll-type ore formation. Redistributed ore associated with hematitic and limonitic alteration zones yield apparent ages of ca. 13 to 10 m.y. and ca. 4 to 3 m.y. respectively (Ludwig et al. 1984). Relatively young U/Pb ages of <1 m.y. have been established for some rollfront ore in the Church Rock district (Ludwig et al. 1982).

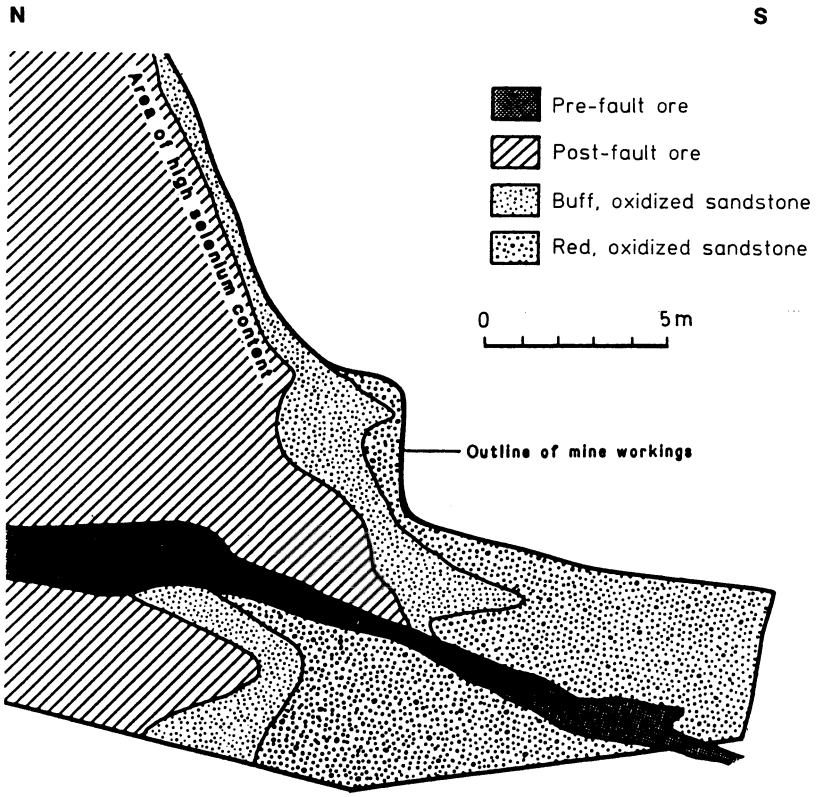

Fig. 5.64. Ambrosia Lake district, Section 23 mine, generalized cross-section through a variably oxidized sandstone zone illustrating the relationship of post-fault roll- or stack-type mineralization and remnant pre-fault trend mineralization. (After Granger and Santos 1986) (reprinted by permission of AAPG)

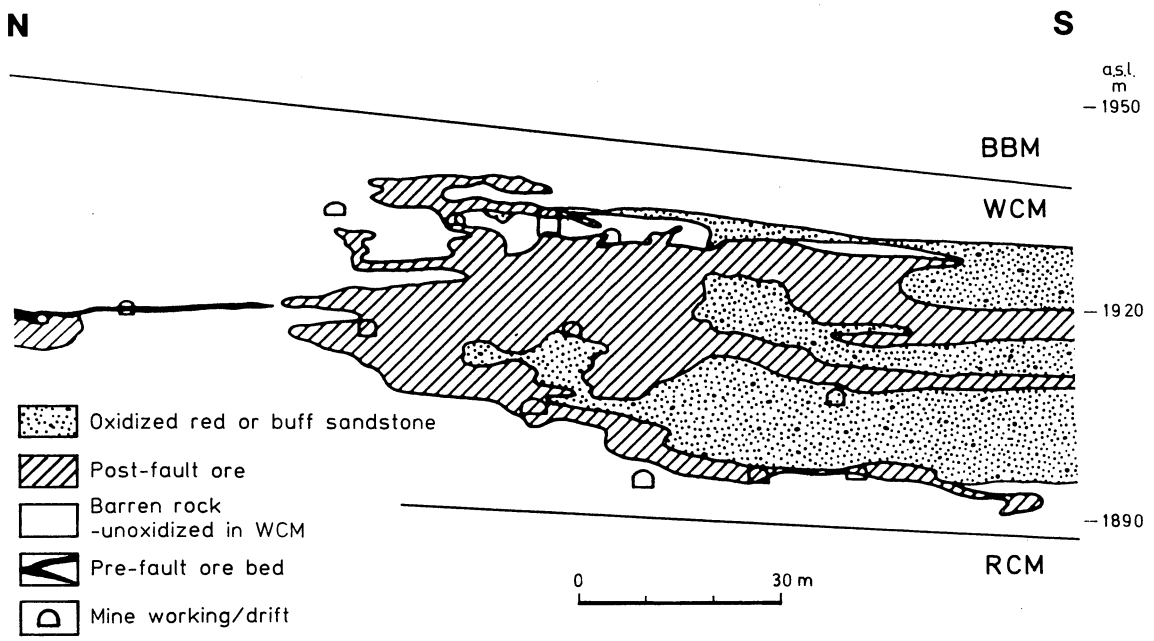

Fig. 5.65. Ambrosia Lake district, Section 23 mine, N-S cross-section showing post-fault roll-type U mineralization associated with the contact zone of oxidized sandstone. (After Granger and Santos 1986) (reprinted by permission of AAPG)

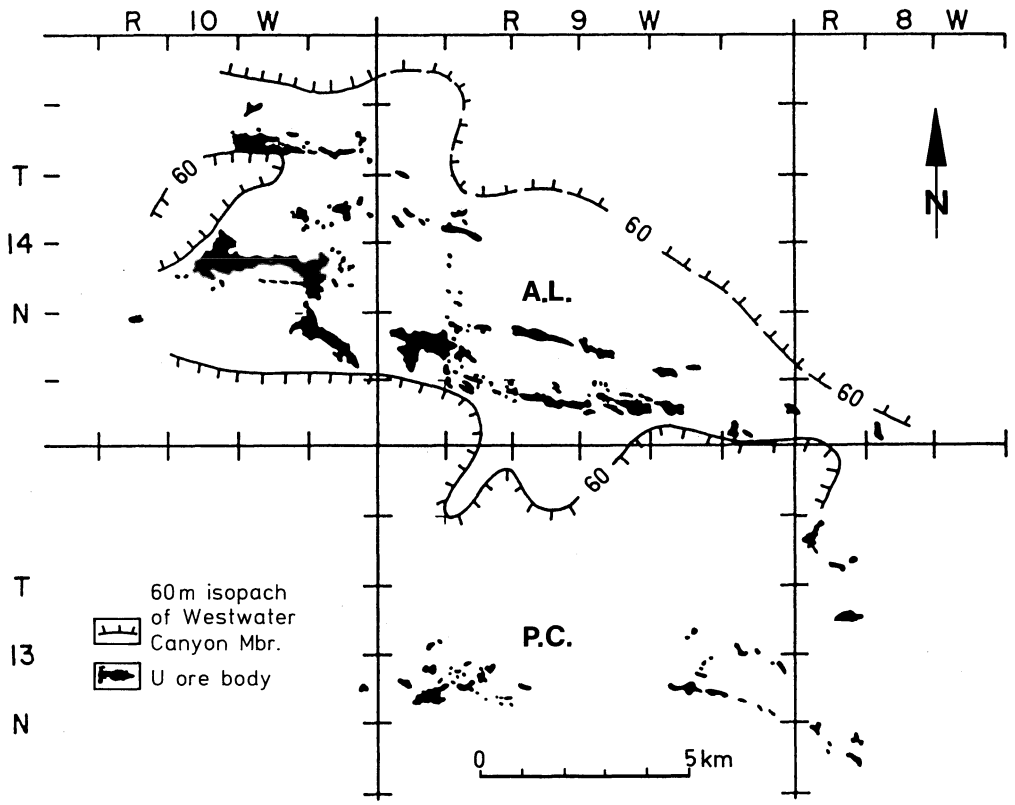

Fig. 5.66. Ambrosia Lake district, map of distribution of uranium ore bodies. Two ore zones occur in Westwater Canyon Member sandstones in the Ambrosia Lake trend (*A.L.*) to the north and a third zone in Poison Canyon sandstone/ Brushy Basin Member in the Poison Canyon trend (*P.C.*) to the south. (After Santos 1963)

Potential Sources of Uranium

The source of the uranium is still in dispute. Intraformational acid *volcanic* material either within the host sands themselves or in the adjacent Brushy Basin mudstones are favored by many workers as a probable source of uranium. This postulation, however, is derived mainly from circumstantial evidence provided by the frequent association of uranium deposits with tuffaceous sedimentary sequencs.

Much of the uranium and associated elements may also have derived from altered *igneous* material within the sandstones at some distance up the hydrologic gradient from where the deposits are presently located. Especially the coarse facies proximal to the sedimentary source that was later removed by erosion is considered a favorable source for the ore elements.

The Brushy Basin Member can probably be discarded as a valid source of uranium. Brookins (1979) and Della Valle (pers. commun. in Adams and Saucier 1981) report a Th/U ratio of about 1.5 for the member and interpret this as one point of evidence that uranium has not been released from the member. Another point may be given by Della Valle's findings that REE have apparently been depleted in the Brushy Basin pelites. Such a process requires a reducing, probably organic-bearing groundwater capable of complexing or chelating the REE (Della Valle in Adams and Saucier 1981; McLennan and Taylor 1979) while depressing the solubility of uranium. On the other hand, Th/U ratios are higher in the Westwater Canyon Member, than in the Brushy Basin Member, particularly in the lower part of the member as reported by Brookins (1979), suggesting that the Westwater Canyon has most likely provided the uranium for the ore formation. This is compatible with the generally reduced state of the Brushy Basin sediments implying low uranium solubility, whereas pervasive mild oxidation prevailed in the lower Westwater Canyon sandstone as reflected by the state of ilmenite and magnetite

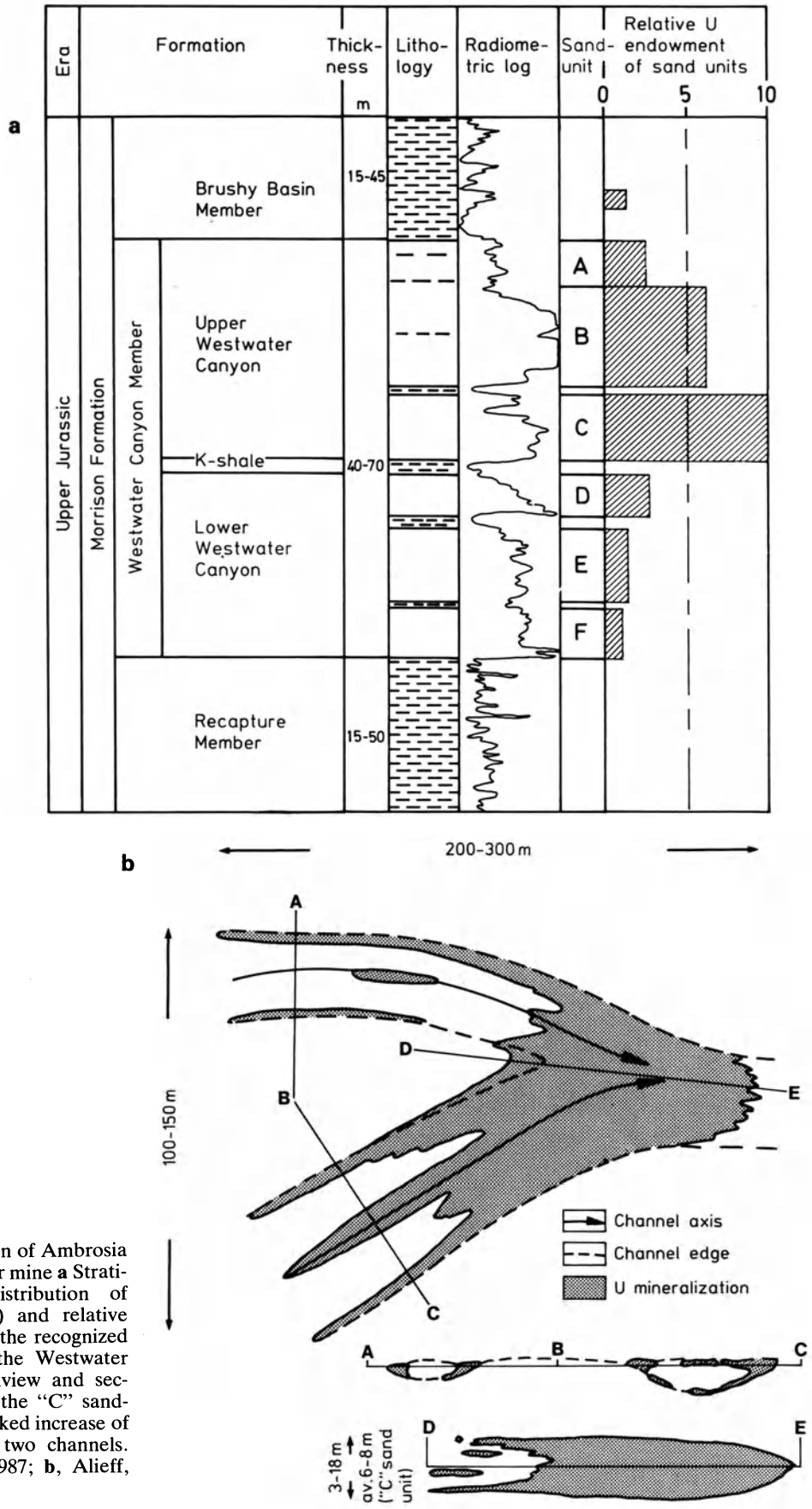

Fig. 5.67. Eastern extension of Ambrosia Lake district, Mount Taylor mine **a** Stratigraphic column with distribution of uranium (radiometric log) and relative endowment of uranium in the recognized sand units (*A* to *F*) of the Westwater Canyon Member. **b**. Planview and sections of mineralization in the "C" sandstone unit showing the marked increase of ore at the confluence of two channels. (After **a** Burgess et al. 1987; **b**, Alieff, pers. commun. 1987)

which are not destroyed by reduction and carry hematite rims.

Uraniferous Humate

Humate is a term defined by Granger et al. (1961) to describe the particular carbonaceous substance associated with the U mineralization of the Grants region.

Humate constitutes 0.05 to 0.5% by weight of the host sandstone. Its dominant characteristic is its ubiquitous and coextensive association with uranium in primary trend and channel ores. Although unmineralized humic material has reportedly been found, no completely uranium-barren humate has been confirmed in the Westwater Canyon sandstone.

Two principal hypotheses are forwarded on the *origin* of the humate in the Grants Uranium Region, an extrinsic and an intrinsic one with respect to the uranium mineralized sandstones. Both models envisage a Morrison-internal source. The extrinsic model derives the humate from plant debris in the Brushy Basin pelites, the intrinsic model from that in the Westwater Canyon sandstones. A third concept envisaging an external, non-Morrison source in form of surface vegetation or swamps, has been discussed by Granger et al. (1961) and, in modified form, by Turner-Peterson and Fishman (1986). The two internal source models comply best with the established geochemical and geological parameters of the region and will be discussed later.

Ore Controls and Recognition Criteria

Significant ore controlling or recognition criteria of the carbon-uranium deposits in the Grants Uranium Region as listed by Adams and Saucier (1981) and others are as follows.

Host Environment

- The largest ore bodies occur in reduced, pyrite, plant debris and humate-bearing continental fluvial sandstones of bed-load-dominated facies deposited in straight to sinuous stream systems of the mid- to distal section of the alluvial fans of the Morrison Formation as pointed out by Galloway (1980).
- Favorable host units have a high sandstone to mudstone ratio of 4:1 to 1:1, a gross thickness of the host sandstones above average, and a good continuity of the sandstone beds.
- Thicknesses of Westwater Canyon sandstone units of up to 100 m are especially favorable, as are Jackpile sandstone thicknesses of as much as 70 m.
- Sandstones with poor sorting and a wide range in grain size appear to make better hosts than sandstones of moderate to good sorting and finer-grained constituents.
- The Brushy Basin shale, which is in depositional continuity with the two principal host sands, the Westwater Canyon and Jackpile sandstone is generally not oxidized.
- Tuff-derived bentonitic clays are abundant in the sediments, particularly in the interbedded mudstones.

Alteration

- The host rocks along mineralized trends have been strongly altered. Reduction is indicated by destruction of detrital magnetite and ilmenite, and local formation of authigenic pyrite. Quartz is corroded and silica has been redeposited. Detrital feldspar is partly in a stage of dissolution, partly coated by an albite replacement rim. Ferric iron has been removed from mudstones. In the eastern central part of the San Juan Basin authigenic K-feldspar has crystallized, and various clay minerals have derived from tuffaceous material.
- Authigenic clay rims precipitated on detrital clasts within and immediately adjacent to uraniferous humate lenses are in the Jackpile sandstone predominantly illite-montmorillonite, in Westwater Canyon sands at Ambrosia Lake they are predominantly chlorite or a mixed-layer phase. Montmorillonite clay rims and clasts are altered to Mg-chlorite.
- Compositional variations exist within and adjacent to uranium mineralization: montmorillonite is the dominant clay mineral formed downdip of an ore body, chlorite is enriched in the ore zone, and kaolinite and altered montmorillonite are enriched updip of the ore. (Riese et al. 1980)
- Characteristically the most intense decomposition of Fe-Ti-oxides and feldspars in Westwater Canyon and Jackpile sandstones is restricted to the proximity of the mudflat facies

of intervening Brushy Basin pelites where also the bulk of mineralization occurs (Figs. 5.59, 5.60). (Turner-Peterson et al. 1986)

Mineralization

- *Primary peneconcordant ore* in blankets, pods, and channels is controlled by lithology-stratigraphy and by minero-geochemistry. The principal characteristics and controls of mineralization include:
- uranium minerals are in most deposits coextensive with the humate,
- uranium is associated with enrichments of Cu, Mo, Se, V, Y, Fe, Mn, As, and S,
- tabular ore generally occurs at several stratigraphic levels along linear trends of thickened sandstone (Figs. 5.56, 5.62, 5.66) which appear to be controlled by paleo-morphological sedimentary conditions,
- blanket ore is more sheet-like, is coextensive with humate, and contains very little detrital vegetal material,
- channel ore has a stronger facies control than blanket ore, sometimes following individual channels (Fig. 5.67b). While containing humates, it is also associated with more carbonized or coalified and silicified detrital vegetal matter than blanket ore.
- *Early roll-type* mineralization associated with peneconcordant ore horizons are similar in character to Wyoming rolls except that the oxidized sandstone on the convex, updip side of the roll has been re-reduced. The roll-type ore is apparently caused by an early oxidation event resulting in the remodeling of primary peneconcordant uranium into C-shaped bodies.
- *Redistributed post-fault ore* is typically found in stack deposits (Fig. 5.62) and controlled by structure, lithology, and redox boundaries including:
- presence of faults and fractures (of Laramide-Tertiary age) cutting primary mineralized rock,
- presence of reduced and oxidized sandstones along an oxidation front at or near the structures,
- humate and detrital plant material may or may not be associated with the uranium,
- probable chemical separation of Cu, Mo, Se, V, Pb, Y, Fe, Mn, Ca, and Sr, from uranium,
- Redistributed type, *late rollfront* mineralization is similar to that in Wyoming. The ore may be localized at nose and limb zones of vertically stacked rolls, marking the contact between oxidized and reduced sandstone. The oxidized sandstone generally seems to be limonitic near the redox-front but becomes hematitic within tens to hundreds of meters updip, as described by Ludwig et al. (1982) from the UNC Church Rock Mine.

Metallogenetic Concepts

The genesis of the primary ore in the Grants Uranium Region is still controversial. The peneconcordant, humate-associated trend and channel uranium mineralizations most obviously represent the first accumulation of ore grade uranium. All other types of mineralization, ranging from pre-Dakota roll-type to Tertiary and recent redistributed ore bodies, appear to have been formed subsequent to and probably from the tabular ore.

The *primary peneconcordant ore* is considered to have formed by diagenesis-related processes immediately after sedimentation in late Jurassic-Morrison time. Isotope studies indicate that the ore is at least about 140 to 130 m.y. old. Geological evidence documents that the ore formation occurred prior to the Laramide Orogeny because faults of Laramide age offset ore blankets, and prior to the deposition of the late Cretaceous Dakota Sandstone because an ore pod or roll in the Jackpile sandstone in the Paguate Mine, Laguna district, was truncated by the pre-Dakota erosion surface.

The peneconcordant primary ore is characterized by an *intimate association of uranium with humate*. This suggests that humic acids exerted a critical influence on the formation and the site of deposition of the primary ore. Therefore, the identification of the source of the humic acids and the processes involved in their formation, mobilization, and finally precipitation as humate are critical for any metallogenic modeling.

The *humic acids* are considered to have derived either from the ore-hosting sandstones themselves or from the Brushy Basin pelites and probably from a particular facies of the latter, namely the mudflat facies as proposed by Turner-Peterson et al. (1986). Accordingly, Adams and Saucier (1981) and later Turner-Peterson et al. (1986) have elaborated two alternative genetic models for the primary ore which are presented further below.

Additional parameters and mechanisms possibly instrumental in the accumulation of the large quantity of humate as found, for example, in the Ambrosia Lake district, and consequently in the metallogenesis of the uraniferous humate type of uranium deposits are given by Adams and Saucier (1981) as follows.

A *concentration* of transported organic debris appears to be located adjacent to the Zuni Uplift area in sedimentary trends that possibly are down-warps controlled by pre- to syn-Morrison basement displacements which channeled and caused the superposition of high energy fluvial systems. These shallow elongated depressions also funneled the groundwaters which transported dissolved humic substances and uranium along the same trends. In result, the very subtle structural influences controlled the accumulation of unusually large quantities of uraniferous humate and its deposition in relatively thin, sheet-like lenses elongated in the down-stream direction along the axes of the down-warps.

Assuming that the humate precipitated as tabular bodies along a shallow, horizontal chemical interface below the water table, it can be hypothesized that the earlier described distribution of uranium, selenium, and molybdenum may suggest that the humate body developed at an oxidation-reduction front separating surface-derived oxidizing waters from deeper perhaps H_2S-rich, reducing groundwaters (Saucier 1980) or from reducing fluids expelled from the Brushy Basin Member. The *chemical system* may have been in principle similar to that producing the redox fronts in the Tertiary Wyoming Basins. The marked difference is in the time of introduction of the oxidizing solutions. Oxygenated water migrated in the Wyoming Basins long after the sediment deposition and progressed as large tongues downdip in the slightly tilted sandstone horizons (see Chap. 5.4.4). In contrast, as suggested by Adams and Saucier (1981), the redox fronts in the Morrison Formation were active penesynsedimentary migrating as a horizontal interface vertically down into the fresh sediments from the depositional surface.

Mobilization and transport of uranium in the sedimentological environment outlined above was strongly influenced by the hydrolysis of the volcanic components in the Morrison sediments. It may be deduced that due to this hydrolysis the surface and shallow groundwaters in late Jurassic time were alkaline (pH of about 8), oxidizing, and had a concentration of dissolved substances in the range of 1000 ppm or less with sodium in excess over calcium (Squires 1970). It seems further probable that if uranium and associated elements were derived mainly from acid volcanic tuff either in the area of provenance or from the volcanics deposited within the sediment or both, then the uranium and its associated elements should also have been present in the late Jurassic groundwaters perhaps as uranyl carbonate complexes, as suggested by Gruner (1958) and/or fulvic acid complexes, as suggested by Schmidt-Collerus (1979).

Once the peneconcordant primary deposits had been established, *remobilization* destroyed part of the deposits and resulted in the formation of the younger types of uranium deposits. This may have occurred during at least three periods when oxygenated meteoric waters could have entered the Morrison aquifer:

1. In late Jurassic time, during and soon after the sedimentation of the Morrison host sandstones,
2. in late Jurassic to late Cretaceous time during the erosional interval prior to the deposition of the Dakota Sandstone,
3. in Miocene to recent time, i.e., during the present erosional period.

An *early remobilization* of primary ore in probably late Jurassic to mid-Cretaceous time is considered for some of the breccia pipe ore, e.g., in the Cliffside mine, Ambrosia Lake, where ore within the pipe is controlled by NE-striking joints and is thick and of higher grade than correlative ore outside the pipe. Roll-type ore as found at the Mariano Lake and Ruby mines, Smith Lake district, may also have formed during this remobilization event because geological evidence suggests a post-trend, post-Jurassic but pre-Dakota formation. This event must have been followed by subsequent alteration processes, since the ore rolls are enclosed in reduced sandstone.

Stack and post-Laramide rollfront ore bodies are assumed to have formed by *later redistribution* of uranium in Tertiary to recent time. This mineralization is tied to a broad tongue of hematitic oxidation believed to be Miocene or younger which migrated down the north slope of the Zuni Uplift. The oxygenated solutions that generated this tongue probably removed uranium in its path through the Grants Uranium Region

except locally where the oxidation was encountered or has been retarded in its basinward advance by organic-rich primary trend deposits. Between such ore deposits, the oxidation has advanced farther north leaving some of these deposits as remnant ore bodies behind, e.g., the Blackjack No.1 in the Smith Lake district, which is more than 10 km behind the regional redox front.

There are generally no uranium accumulations along these interfaces, as found, for instance, on similar oxidation fronts in the Wyoming Basins. An exception is the Church Rock district from where younger rollfront ore bodies are described.

Age dates on redistributed ores of the Church Rock district as of the Ambrosia Lake district give apparent *ages* around 8 to 10 m.y. Ore from a rollfront in the Northeast Church Rock mine and from other mines in the Church Rock district is 1 m.y. and younger (Ludwig et al. 1982). The authors interpret the <1 m.y. ages as being related to a rollfront type distribution of earlier formed ores by Pleistocene groundwater, perhaps to those that created the presentday limonitic zone within the Westwater Canyon sandstones. They attribute the 10 m.y. age to an earlier phase of redistributed ore formation, perhaps related to the Tertiary oxidation front that formed the hematitic zone in the Westwater Canyon sandstones.

Alternative Models

The previously mentioned two alternative models on the formation of the humate-uranium deposits of the Grants region presented by Adams and Saucier read in abbreviated form as follows.

Model I of Adams and Saucier (1981).
Essential criterion for this model is the assumption that the regional, early alteration symptoms, reflected by the ilmenite-magnetite reduction and destruction, and the feldspar alteration, resulted from organic-rich reducing solutions derived from a *Brushy Basin Member source*. The proposed ore-forming process then relies on the juxtaposition of the Brushy Basin Member and the underlying and overlying sandstones of the Westwater Canyon and Jackpile units.

Sedimentation: The thick sands of the Westwater Canyon below and the Jackpile sandstone above were laid down as a continuous sedimentary sequence with the intervening Brushy Basin Member under an arid or semi-arid climate. The thickness of the sands (50 to 100 m) and the shales (60 to 120 m) permitted the development of a major hydrologic system with high transmissivity and an integrated hydrochemical system that was active from the moment of sedimentation and early diagenesis.

The sediment pile provided an extraordinary "chemical potential" due to the juxtaposition of two inherently unstable components, organic material in the form of plant debris and volcanic glass within the tuffaceous intercalations. The diagenesis and alteration of these constituents are known to independently produce widespread alteration assemblages.

Both the sands and the muds received substantial amounts of organic debris during their deposition. In the sands, a larger component of logs and smaller fragments accumulated and in the muds fine carbonaceous material accumulated. Silicified logs and occasional carbonized logs, or trash pockets, attest to the organic debris deposited with the sands, whereas fine carbonaceous matter is essentially absent in the sands, presumably due to its destruction. No organic debris is found in the shales. Therefore, its former presence is speculative. Strong circumstantial evidence suggests, however, that it was originally present.

In conclusion, the pile of argillaceous and arenaceous sediments of the Brushy Basin and Westwater Canyon members contained all the ingredients necessary for the formation of the uranium humate mineralization, and also provided the hydrologic conditions during diagenesis and compaction for the dewatering of the pelites, and the development of chemical interfaces in groundwater for the formation of the ore deposits.

Hydrologic systems and diagenesis: With the accumulation of the pelites of the Brushy Basin Member over the Westwater Canyon sandstone, a regime of two juxtaposed groundwaters of different chemistry evolved. The waters of the Westwater Canyon sandstone, particularly the deeper portions, were locally oxidizing and locally reducing, depending upon the distribution and influence of indigenous organic debris. In general, however, the groundwater flowing through the Westwater Canyon was more of oxidizing than of reducing nature but it was not strongly oxidizing because ilmenite and magnetite have only thin hematite coatings. These waters destroyed most of the fine organic debris in the

sands, leaving only silicified and carbonized larger fragments. This concept assumes a continuous flow of groundwater within the Westwater Canyon beginning with the time of its deposition.

With the sedimentation of the overlying Brushy Basin Member the groundwater within the Westwater Canyon Member was confronted with solutions of a markedly different composition derived from the pelitic Brushy Basin strata. These sediments consisted of 40 to 60% solids by weight, the remainder being porewaters. With increasing thicknesses of the Brushy Basin sediments, the contained water began to be expelled. The chemistry of the mobilized solutions was strongly influenced by their contact with altering volcanic material. The solutions became alkaline and hence capable of dissolving the fine organic debris dispersed within the Brushy Basin.

The organic-enriched alkaline and reducing solutions imposed the typical grayish-green to green reduction colors upon the Brushy Basin pelites before they were released from the Brushy Basin down into the Westwater Canyon sandstone. Here they altered the detrital ilmenite, magnetite, and feldspar. The alterations are strongest at the top of the Westwater Canyon, which is compatible with such an interpretation. Since the reducing Brushy Basin fluids were in distinct chemical contrast to the oxidizing or very mildly reducing groundwaters flowing in the Westwater Canyon, a chemical interface and gradient must have developed. It is postulated that along this interface the primary uranium-humate mineralization of the Grants Uranium Region most probably precipitated.

The configuration and position of the front between the two groundwater regimes was probably controlled by the rate of flow of the Westwater Canyon groundwater and the volume and lateral changes in flow rates across the Brushy Basin-Westwater Canyon interface. Stratigraphic-lithologic relations suggest that in the vicinity of presentday ore districts of the Grants Uranium Region the Westwater Canyon Member thickens unusually at the expense of the overlying Brushy Basin Member, and upper sands of the Westwater Canyon laterally interfinger with the Brushy Basin sediments. This lithologic interrelationship provides a unique geometry for the discharge and concentration of greater volumes of reducing solution from the Brushy Basin Member laterally and vertically into these zones of overthickened Westwater Canyon sands.

Ore formation: The hypothesized mixing of the two solutions outlined above provided a fairly simple mechanism for the formation of the peneconcordant uraniferous humate deposits.

Where the Brushy Basin waters mixed with the Westwater Canyon groundwaters, a decrease in pH occurred, leading to the precipitation of the organic material, which is notably less soluble in more acid solutions. Depending upon the hydrodynamics, the interface between the two water regimes supposedly has fluctuated vertically, leading to the deposition of a vertical series of stacked organic-rich lenses and to numerous local complexities in alteration, ore distribution, and mineral paragenesis. The fixation of the humate in tabular lenses that locally transform into S-shaped rolls may have been the simplest minerochemical response to the redox interface between the two water regimes. Once precipitated, the humic matter may have allowed the initiation of other alteration processes. Silica, alumina, and alkali and alkali-earth cations originally complexed on the organic material were released. The liberation of these ions partly resulted in the formation of authigenic clay rims on detrital clasts through changes in the chemical environment around the organic material and partly through its degradation. Furthermore, the alteration and replacement of feldspars within the reduced zones must also have been associated with the removal and mobilization of considerable amounts of alumina and silica a process which was probably also influenced by the dissolved organic substance.

It may also be postulated that once the humic material had been precipitated as gel-like masses in the form of tabular zones in the sandstone, the continued percolation of groundwater and the hydrodynamic setting would have modified the organic distribution into those shapes that have been recognized in the deposits of the Ambrosia Lake district (Squyres 1970). The solutions migrating through and past the humic zones, furthermore, are thought to have introduced small amounts of uranium in solution, particularly as the solutions were mildly oxidizing Westwater Canyon groundwaters proper.

With time, the expulsion of Brushy Basin waters into the Westwater Canyon sands probably diminished and ultimately ceased. This permitted the deeper more oxidizing water system to increasingly encroach upon the shallower reduced groundwater regime. Such a groundwater flow

could continuously contribute uranium to the deposits, ultimately producing the high grades now characteristic of the ore in the Grants Uranium Region. The solutions are required to have been not sufficiently oxidizing, however, to completely destroy the mineralization.

Once the groundwater regime became more stagnant at the end of the Jurassic depositional period, it changed to mildly reducing due to the influence of the residual detrital and epigenetic carbonaceous material. This last process created the widespread characteristic drab color of the sandstones now seen in the subsurface. A similar metallogenetic evolution may be envisioned to have operated between the Brushy Basin pelites and the Jackpile sandstones following their deposition.

Model II of Adams and Saucier (1981).
Prerequisites to this hypothesis are: (a) All the humic material and most of the uranium derived from a *Westwater Canyon sandstone source* and not from the Brushy Basin mudstones. (b) Sufficient organic debris was buried with the sediments creating an anaerobic environment below the static water table (Jensen 1958). (c) Bacterogenic H_2S and carbon dioxide, methane and hydrogen gas from fermentation of the vegetal material cause a drop in pH, as proposed by Rackley (1976). (d) Iron in the groundwater and in iron-bearing detrital grains may react with the H_2S to form monosulfides, and eventually, stable pyrite.

This organic-chemical reduction of the sands can develop very early and at shallow depths.

Hydrologic systems and diagenesis: The surface and shallow groundwaters in late Jurassic time are assumed to have been oxidizing and alkaline with a probable pH of about 7.5 to 8 due to the hydrolysis of the volcanic ash in the sediments. Humic acids leached from plant debris by the alkaline solutions in the upper oxidizing portions of the channel sediments could have migrated down to a more static water table. At this position they encountered a pH environment sufficiently low for flocculation of the humic substances to occur. Granger (1968) hypothesizes that the precipitation took place along the interface between the stream underflow and the deeper, slower-moving groundwaters. Flocculation of the humic material will definitely occur at a pH of 5, but may begin at a higher pH value if the humic acids contain metallic ions. Precipitation of uranyl humate complexes at a pH of 6.5 are reported by Schmidt-Collerus (1969).

The humate will be distributed in the form of broad, tabular, semi-horizontal masses in the channel sands, perhaps as shallow as 5 m below the stream bed. As soon as the channel deposit is buried, the humate lense is protected by the development of an acidic reducing environment, and by the continued adsorption of cations. Once adequate younger sediments cover the channel deposit, the sequence can be repeated over again at a higher stratigraphic level, as in the Jackpile sandstone, if organic material is contained in the overlying sediments.

Ore formation: The surface and shallow groundwaters may have contained in the order of 50 to 300 ppb U. The uranium was probably transported by both uranyl carbonate complexes, as suggested by Gruner (1958), and organic acid complexes, as proposed by Schmidt-Collerus (1979). Precipitation of the uranyl humate complexes could have occurred directly as a result of the drop in pH across the subhorizontal redox interface. In some contrast, the uranyl carbonate complexes were probably broken up by the deeper acid solutions, and the liberated uranium became available for the enrichment of the uraniferous humate. Hydrogen sulfide generated in the humate gel by bacteria is assumed by Adams and Saucier (1981) to be the cause for the precipitation of Fe, Mo, Se, and As as sulfides. The molybdenum apparently precipitated in a negative colloidal sulfide which was repelled by the negative humic colloids. This is considered to be the reason why the jordisite mineralization is almost never in direct contact with humate.

With ongoing time the tabular humate impregnation matured and hardened into a brittle material coating grains and filling interstices in the sandstone. During the maturation, which was accompanied by oxidation, microbial attack, aging, and radiation, the organic molecules broke down and much of the complexed uranium and vanadium was released. The uranium associated with silicate to form coffinite, and the vanadium entered the lattice of authigenic chlorite. The grade and magnitude of any ore body formed by Adams and Saucier's (1981) Model II processes require as salient parameters: (a) an initial concentration of humic substances, (b) a uranium-bearing water, and (c) a permeability of the host sands which steered the rate of exposure of the uranium to the organic particles. All of these

parameters had a maximum coincidence immediately after the deposition of the host sandstones.

Turner-Peterson and coworkers (1986), based on their studies particularly on the distribution of altered Fe-Ti-oxides, feldspars, and authigenic clay minerals, relate the favorable site for ore formation to a distinct sedimentary facies, the *mudflat facies* of the Brushy Basin Member. Diagenetic processes within this facies produced the solutions which were directly or indirectly essential for the formation of the peneconcordant primary ore.

In their *Lacustrine-Humate Model*, which corresponds in principle with Adams and Saucier's (1981) Model I, Turner-Peterson and Fishman (1986) derive both the solubilizing fluids and the humic acids from the mudflat facies of the Brushy Basin Member.

In their *Internal Source Model*, which corresponds to some extent with Adams and Saucier's Model II, the solubilizing fluids also originated from pore waters of the mudflat facies. But it was in the adjacent sandstones into which the fluids were expelled that they dissolved the organic debris to form the humic acids required for the formation of the uraniferous humate.

References and Further Reading for Chapter 5.4.1
(for details of publication see Bibliography)

Adams SS, pers. commun.; Adams et al. 1974, 1978; Adams and Saucier 1981; Austin 1963, 1980; Baird et al. 1980; Bell 1986; Birdseye 1957; Brookins 1975, 1979, 1980a, 1980b; Brookins et al. 1977; Cadigan 1967; Chapman et al. 1979; Chenoweth 1953, 1977; Chenoweth WL person. commun.; Chenoweth and Holen 1980; Chenoweth and Stehle 1957; Clark 1980; Clark and Havenstrite 1963; Coffin 1921; Condon and Peterson 1986; Corbett 1964; Craig et al. 1955; Crawley 1983; Crawley, Holen and Chenoweth 1985; Cronk 1963; Dooley et al. 1966; Ethridge et al. 1980; Falkowski 1980; Fishman et al. 1984; Fishman and Reynolds 1986; Fitch 1980; Forhan 1977; Foster and Quintanar 1980; Gabelman et al. 1956; Galloway 1978, 1980; Gould et al. 1963; Granger 1962, 1963, 1968; Granger et al. 1961; Granger and Santos 1982, 1986; Green 1980; Hafen et al. 1976; Haji-Vassiliou and Kerr 1973; Hanshaw and Dahl 1956; Hansley 1984, 1986a, 1986b; Harmon and Taylor 1963; Hatcher et al. 1986; Hazlett and Kreek 1963; Hicks et al. 1980; Hilpert 1963, 1969; Hilpert and Moench 1960; Holen 1982; Huffman and Lupe 1977; Jacobsen 1980; Jenkins and Cunningham 1980; Jensen 1963; Jobin 1962; Kelley 1955, 1963; Kelly et al. 1968; Kendall 1971; Kirk and Condon 1986; Kirk et al. 1986; Kittel 1963; Kittel et al. 1967; Knox and Gruner 1957; Kozusko and Saucier 1980; Lease 1980; Lee 1976; Lee and Brookins 1978, 1980; Leventhal 1980; Leventhal and Threlkeld 1978; Livingston 1980; Ludwig 1980; Ludwig et al. 1977, 1982, 1984; MacRae 1963; Martinez 1979; Mathewson 1953; McCammon et al. 1986; McLemore 1983; Megrue and Kerr 1965; Melvin 1976; Miller and Kulp 1963; Moench 1962, 1963; Moench and Schlee 1967; Moore and Lavery 1980; Nash 1967, 1968; Nash and Kerr 1966; Peterson 1980; Pierson and Green 1980; Rapaport 1952, 1963; Rautman 1980; Rawson 1980; Reimer 1969; Reynolds et al. 1986; Ridgley 1980; Ridgley et al. 1978; Riese 1977, 1979; Riese and Brookins 1977, 1980, 1984; Ristorcelli 1980; Roeber 1972; Sachdev 1980; Santos 1963, 1970, 1975; Santos and Turner-Peterson 1986; Saucier 1974, 1976, 1980; Saucier AE person. commun.; Sayala and Ward 1983; Schlee 1963; Schlee and Moench 1961; Schmidt-Collerus 1979; Sears et al. 1974; Sharp 1955; Smith and Peterson 1980; Spirakis and Pierson 1986; Squyres 1963, 1970, 1974, 1980; Steele 1984; Thaden and Zech 1986; Turner-Peterson 1981, 1985, 1986; Turner-Peterson et al. 1980, 1986; US AEC 1959; Webster 1983; Weege 1963; Wentworth et al. 1980; Whitney 1986; Whitney and Northrop 1984; Wylie 1963; Young 1960; Young and Delicate 1965; Young and Ealy 1956; Zitting et al. 1957.

5.4.2 Vanadium-Uranium Deposits in Phanerozoic Sandstones, Colorado Plateau, USA

Eleven mining districts distributed through the north central part of the Colorado Plateau have produced uranium and vanadium from the Salt Wash Member of the Jurassic Morrison Formation. Total production amounts to about 55 000 mt U_3O_8, approximately 42 000 mt U_3O_8 of which and about five times as much vanadium have been delivered from the Uravan Mineral Belt, the oldest uranium-mining district in the USA. The average grade of ore mined in most districts ranged from ca. 0.15 to 0.25% U_3O_8 and ca. 1.25 to 1.5% V_2O_5. (Chenoweth W.L. pers. commun.)

Due to the vanadium-uranium composition of the ore emplaced as more or less peneconcordant lenses in Jurassic channel sandstones this mineralization has been classified as Phanerozoic tabular/peneconcordant vanadium-uranium deposits (class 4.1.2 Chap. 4).

Abundant information on Salt Wash Member uranium deposits has been published by numerous authors. Thamm et al.'s (1981) present a comprehensive synopsis of the regional setting and local characteristics of the deposits, as well as a hypothesis on ore formation. The following description has drawn extensively from Thamm et al.'s (1981) report and in many cases their text has been used in the form of quotations abbre-

viated and modified and therefore not set in quotation marks.

Data of more recent research work, particularly by Northrop (1982) who studied V-U mineralizations in the Henry Mountains, Utah, amend the text.

Geological Setting of Mineralization

The V-U hosting *Salt Wash Member* of the Late Jurassic Morrison Formation consists of continental *fluvial sediments* in composition very similar to the host rocks of the other major sandstone uranium districts in the western United States.

The Salt Wash Member is overlain by the Brushy Basin Member and underlain by the Tidwell Member of the Upper and Lower Morrison Formation respectively. Thamm et al. (1981) classify the Salt Wash Member sandstones as orthoquartzites to feldspathic orthoquartzites. They were deposited as braided and meandering stream and floodplain deposits in an *alluvial fan system* during a semi-arid climate which supported abundant vegetation along the water

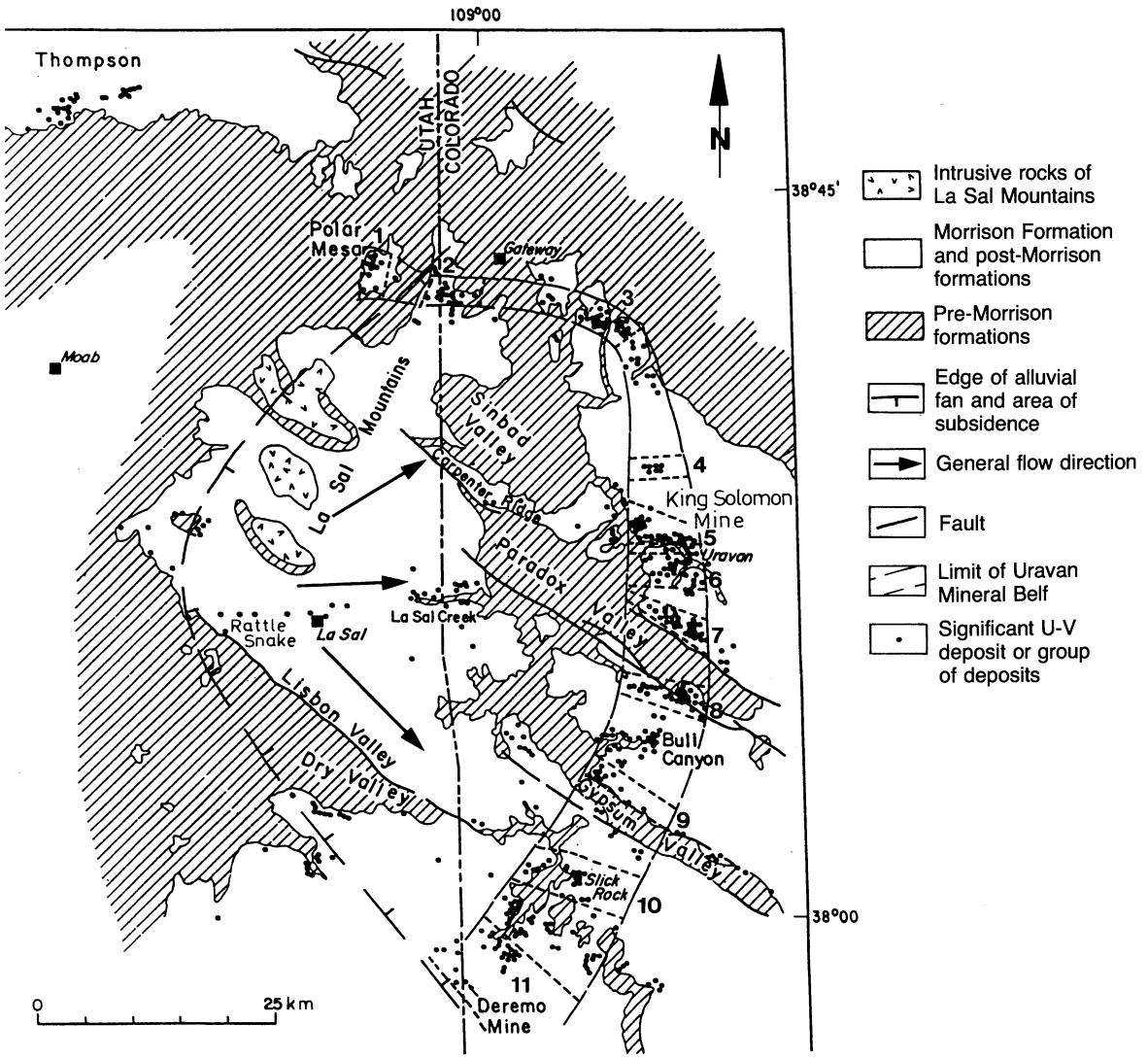

Fig. 5.68. Uravan Mineral Belt, generalized geological map displaying the outline of the belt with position of significant U-V deposits or groups of deposits at the toe of an alluvial fan of the Salt Wash Member of the Morrison Formation. Deposits often cluster in "cross-trends" (numbered *1* to *11*). Mineralized cross trends: *1* Polar Mesa; *2* Beaver Mesa; *3* Outlaw Mesa; *4* Long Mesa; *5* Atkinson Mesa; *6* Club Mesa; *7* Long Park; *8* Monogram Channel; *9* Radium MT; *10* Slick Rock-Burro Canyon; *11* Deremo. (After Butler and Fisher 1978; Motica 1968)

courses. Clay lenses rich in *volcanic debris* were deposited locally as basal muds in shallow ponds or lakes.

Proximal facies of the Salt Wash alluvial fan system are characterized by high sandstone to mudstone ratios and braided stream deposits. The proximal facies consist of thick, massive sandstone units containing only a few thin interbeds of clay.

In the *intermediate distal facies*, e.g., farther to the east, in the Uravan area (Fig. 5.68), a much lower sandstone to mudstone ratio prevails in the meandering stream deposits of that area. A great part of the channel sediments of this alluvial fan section subsided early below the water table, preserving accumulations of detrital plant debris which subsequently contributed to the formation of the carbon-facies sandstones. Adjacent overbank muds were oxidized above the water table and are now represented by the hematitic sediments that bound many ore zones.

The *distal facies* of the alluvial fan system were deposited under conditions of low energy flow as discrete channel sandstones and floodplain clays. Still farther to the east, the sedimentology changes to lacustrine facies.

The *Brushy Basin Member* consists of predominantly oxidized fluvial sediments presumably deposited in a floodplain environment. Large volumes of acid volcanic ash are incorporated in these sediments.

Brushy Basin deposition was followed by a cycle of erosion, then by deposition of the Burro Canyon and Dakota sandstones and the thick black shales of the Mancos Shale.

Host Rock Alterations

Oxidation and reduction are the most prominent alteration features observed in the ore-hosting Salt Wash sediments. Associated processes which may or may not be related to mineralization include silicification, calcitization, pyritization, destruction of opaque minerals particularly magnetite and ilmenite, and hematitization of certain facies.

Shawe (1976a) distinguishes three redox facies of the Salt Wash sediments based on studies in the Slick Rock district, Uravan Mineral Belt, which are more or less typical also for other Salt Wash districts: an *oxidized (hematitic) red bed facies*, a *reduced carbon facies* (rich in carbonaceous matter) and a *reduced altered facies* (the main ore host).

Mineralogically and chemically, the rocks of the three facies are similar except for the redox state, the relative abundance of heavy minerals and the black opaque minerals fraction thereof and the abundance of pyrite, which apparently reflect the kind and degree of alteration.

The heavy mineral contents and the black opaque fractions thereof are in the oxidized, reduced carbon and reduced altered facies 0.31% (59% thereof black opaques), 0.16% (42%), and 0.12% (2%) respectively. The amount of black opaques present in carbon facies rocks is therefore about two-thirds of that in red bed facies rocks, and almost zero in altered facies rocks due to their almost complete destruction. Pyrite is absent in red bed facies rocks, sparse in carbon facies rocks, and moderately abundant in altered facies rocks. Small, but perhaps important, differences in the amounts of trace elements in the three facies have been noticed.

Principal Characteristics of Mineralization

Mineralization occurs in various degrees of oxidation, depending largely upon their proximity to the surface and their position with respect to the water table. Three types of mineralization may be distinguished (Thamm et al. 1981):

- Unoxidized mineralization referred to as primary or black ore,
- partially oxidized mineralization or blue-black ore,
- oxidized mineralization or yellow carnotite ore.

Unoxidized mineralization contains as main ore minerals pitchblende and coffinite, montroseite, and vanadium alumino-silicates. Associated minerals are predominantly pyrite and marcasite. In minor to trace amounts occur various Cu, Fe, Pb, Zn, Mo, Se, Ni, Co, Ag, Cr, and As-bearing minerals.

Pitchblende and coffinite are commonly intimately associated with carbonaceous debris. Pitchblende may replace plant material, in particular the cell walls of fossil wood, iron sulfides, and quartz grains near vegetal debris.

Vanadium of low-valent state occurs in the form of oxide minerals, mainly montroseite, and in a suite of alumino-silicates including vanadium bearing chlorites and hydromicas. The minerals

occupy pore spaces and replace quartz grains and fossil wood in the sandstone.

Calcite, dolomite, and baryte are present within and close to mineralization as cement in the sandstone. Total carbonate contained in most Salt Wash ore is less than 6%. The unoxidized mineralization constitutes the majority of the deposits. The preservation of this dark gray to black mineralization is due to its position below the water table.

Partially oxidized blue-black ore is intermediate between the unoxidized black ore and the fully oxidized yellow carnotite ore. It contains as principal uranium mineral the uranyl vanadate rauvite, and as predominant vanadium (IV) and (V) minerals doloresite and hewettite. The blue-black mineralization shows a strong affiliation with accumulations of carbonaceous matter, as does the carnotite ore, presumably reflecting areas of greatest resistance to intense oxidation and destruction.

Completely oxidized yellow ore contains uranyl vanadates, primarily tyuyamunite and carnotite and a series of vanadates including hewettite, pascoite, hummerite and, rarely, navajoite. The color of the ore can be brown, red, orange, and yellow.

There appears virtually to be no loss of uranium and change in the uranium-vanadium ratios of the ore during the oxidation processes, only a change of mineralogy.

Table 5.27. Deremo mine, concentrations of selected elements in samples collected across an oxidation-reduction boundary (see Fig. 5.69 for sample locations). (Thamm et al. 1981, based on Union Carbide Corp. data)

Element (concentration in ppm)	Sample number				
	1	2	3	4	5
U	803	878	1013	113	371
V	17807	38037	52939	280	250
Se	365	520	470	255	115
Mo	20	25	5	<5	<5
Cu	78	170	502	302	40
Pb	<5	<5	15	190	10
Zn	19	38	62	13	9
As	63	38	68	20	25
S	635	1012	736	220	230
Cr	8	14	13	5	5
Fe^{3+}/Fe^{2+}	2.5	1.9	2.8	4.1	9.8

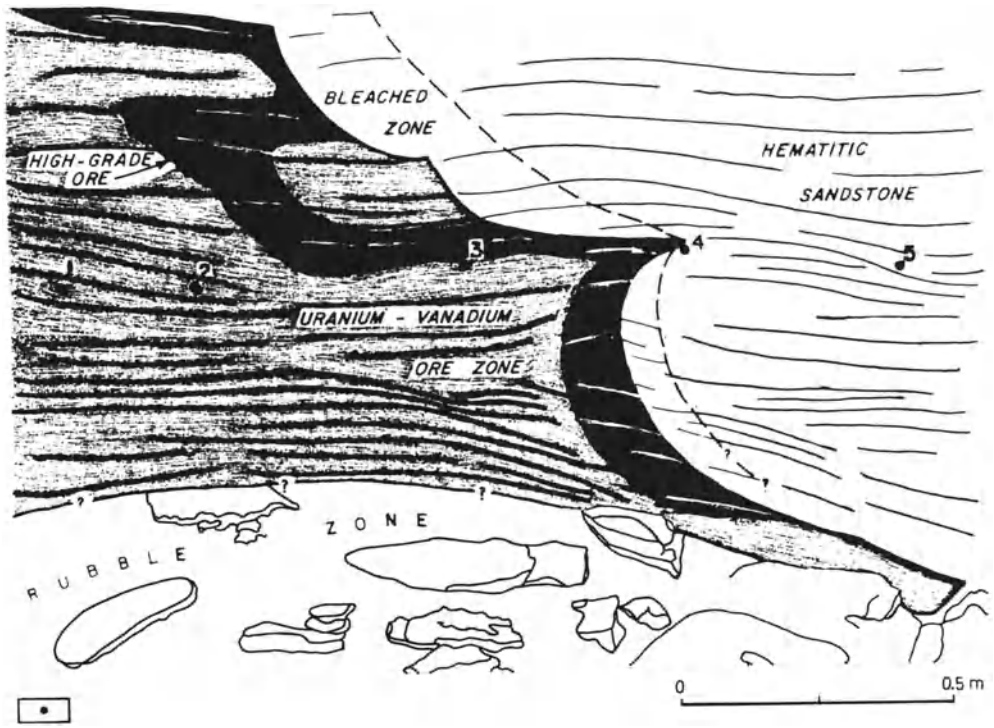

Fig. 5.69. Uravan Mineral Belt, Deremo mine, diagrammatic cross-section of a redox boundary entirely within a Salt Wash sandstone horizon and distribution of U-V mineralization. (*Numbers* refer to samples given in Table 5.27) (Thamm et al. 1981, based on Union Carbide Corporation)

The partial oxidation alters the primary uranium and vanadium oxides, pitchblende, coffinite, montroseite, first, for example, to rauvite, and subsequently by complete oxidation to carnotite. Vanadium fixes all of the available hexavalent uranium in the form of uranyl vanadates thereby protecting it against removal. Excess vanadium crystallizes to the vanadates mentioned above. In contrast, the vanadium aluminosilicates of the unoxidized ore remain relatively stable during the oxidation processes.

Zoning of ore and ore-related elements similar to that of the Wyoming rollfronts, in particular of Se, V, U, and Mo is evident across roll and tabular deposits of the Salt Wash Member (Figs. 5.69, 5.70, Tables 5.27, 5.28). The orientation and sequence of the Se-V-U-Mo zoning differs, however, between ore shapes and between deposits. Rolls or C-shaped configurations almost always display zones with selenium on the concave side of the uranium-vanadium zone, whereas calcite has commonly crystallized at the convex side. Tabular deposits tend to show more variation, with selenium concentrated at the top or bottom, or at the top and bottom of the ore lenses, although in general, selenium was most commonly precipitated at the top of a tabular ore zone. In contrast to this scheme, Brooks and Campbell (1976) describe from the La Sal Mine, Utah, a systematic zoning of Se-V-U-Mo from the bottom to the top of ore lenses. An inverted ore-forming system or irregularities in the ore horizons are thought to be the reason for the inverted element zoning.

Mineralization forms two geometric *configurations* of ore bodies which can be transitional into each other: Tabular ore bodies concordant to the bedding and elongated to the sedimentary trends (Fig. 5.71) and roll-shaped ore bodies that discordantly transect the bedding (Figs. 5.69, 5.70, 5.71).

The *tabular ore bodies* typically are elongated parallel to sedimentary trends and concordant to bedding (Fig. 5.72a). Their horizontal extensions generally are small, in the order of some meters to tens of meters. The ore averages about 1 to 1.5 m thick, but in a few places ore thicknesses approach 10 m. Although individual ore bodies may locally be connected by weak mineralization, more commonly the ore terminates abruptly against barren rock. Ore lenses generally have a sharp upper and a more diffuse lover boundary. Figure 5.72 illustrates the typically erratic distribution of this style of ore body and the relatively small size of individual ore shoots.

Table 5.28. Virgin No. 3. mine, concentration of selected elements in samples collected across vanadium-uranium rolls. (Thamm et al. 1981, based on Shawe 1966) (see Fig. 5.70 for sample locations)

Element / Sample no.		eU %	U %	V %	As ppm	Se ppm
Figure a	1	0.004	–	0.3	20	10
	2	0.005	0.006	0.2	50	20
	3	0.003	–	0.3	40	20
	4	0.003	–	0.2	10	200
	5	0.065	0.068	1.5	40	70
	6	0.11	0.12	2.5	40	15
	7	0.073	0.12	2.5	60	7
	8	0.016	0.021	2.5	20	10
	9	0.041	0.051	2.5	40	10
	10	0.13	0.15	2.5	90	15
Figure b	1	0.009	0.011	0.09	40	20
	2	0.008	0.009	0.09	10	10
	3	0.030	0.027	0.2	20	50
	4	0.22	0.34	1.2	100	150
	5	0.26	0.40	1.5	150	20
	6	0.39	0.61	1.2	150	1500
Figure c	1	0.008	0.012	0.09	10	40
	2	0.10	0.15	0.2	20	1500
	3	0.17	0.17	>6.0	40	30

The *roll-shaped ore bodies* in plan view are generally narrow, not more than a few decimeters to about 1 m wide. They are sinuous and elongated parallel to local sedimentological features, major channels, or axes of good permeability. Most rolls are C- or S-shaped in cross-section. The upper and lower surfaces are commonly bounded against clayey beds. The concave boundary of rolls is usually sharp whereas the convex side is diffuse.

Ore bodies tend to be clustered within elongated favorable trends a few kilometers long by several hundred to thousand meters wide (Fig. 5.68). But in these trends, the *distribution* of vanadium-uranium mineralization is rather erratic and unpredictable (Fig. 5.73) as compared with other types of sandstone uranium deposits. Although the mineralization is widespread, it is generally thin. Only locally does it become sufficiently thick and high grade to be economic. Even within deposits, the shapes, orientations, and *dimensions* of ore pods are often highly unpredictable.

Average production from these elongated favorable areas has ranged from a few hundred to

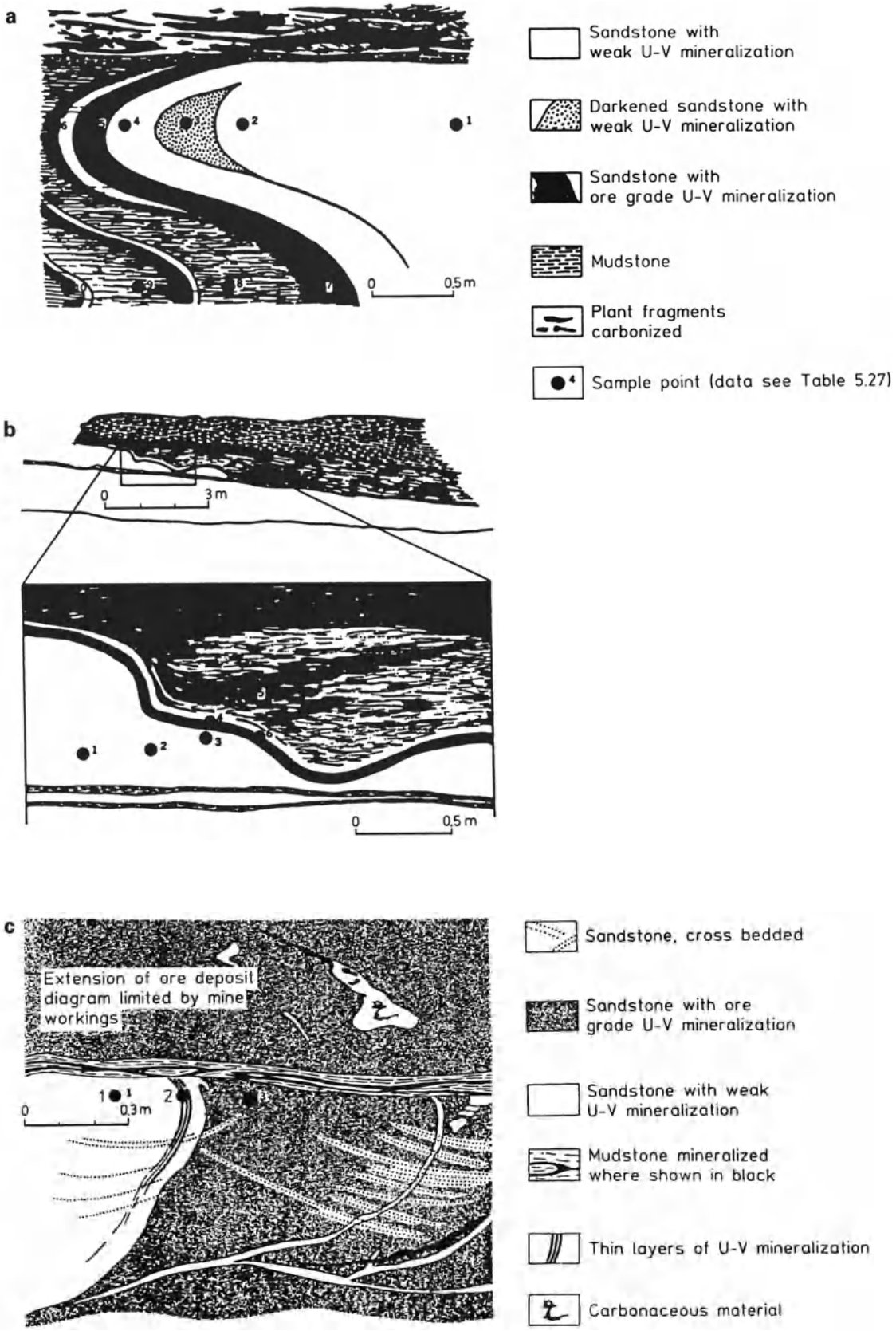

Fig. 5.70. Central Uravan Mineral Belt, Virgin No. 3 mine, cross-sections of U-V rolls and content of U, V, As, and Se in the various parts of the rolls. (*Numbers* refer to samples given in Table 5.28) (Thamm et al. 1981, based on Shawe, 1966)

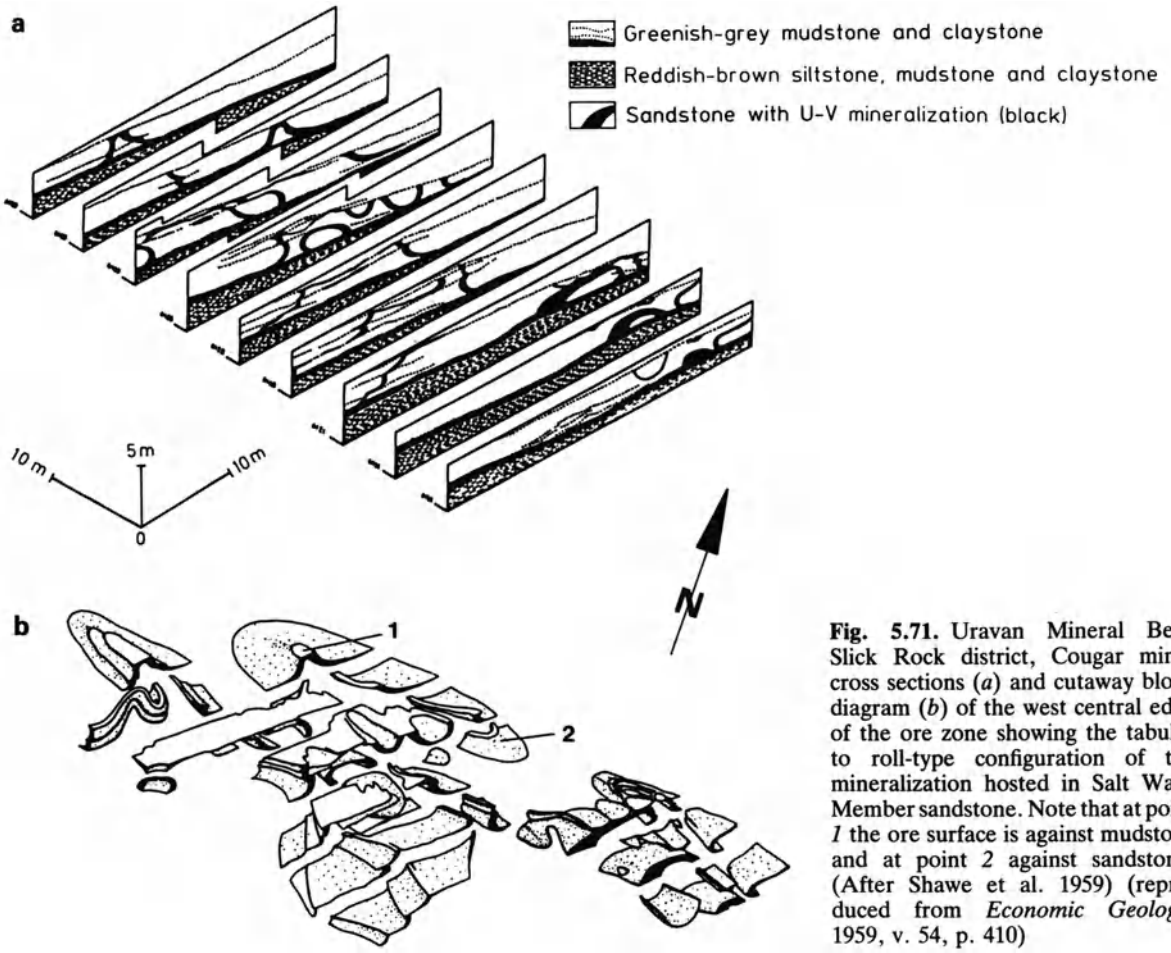

Fig. 5.71. Uravan Mineral Belt, Slick Rock district, Cougar mine, cross sections (*a*) and cutaway block diagram (*b*) of the west central edge of the ore zone showing the tabular to roll-type configuration of the mineralization hosted in Salt Wash Member sandstone. Note that at point *1* the ore surface is against mudstone and at point *2* against sandstone. (After Shawe et al. 1959) (reproduced from *Economic Geology*, 1959, v. 54, p. 410)

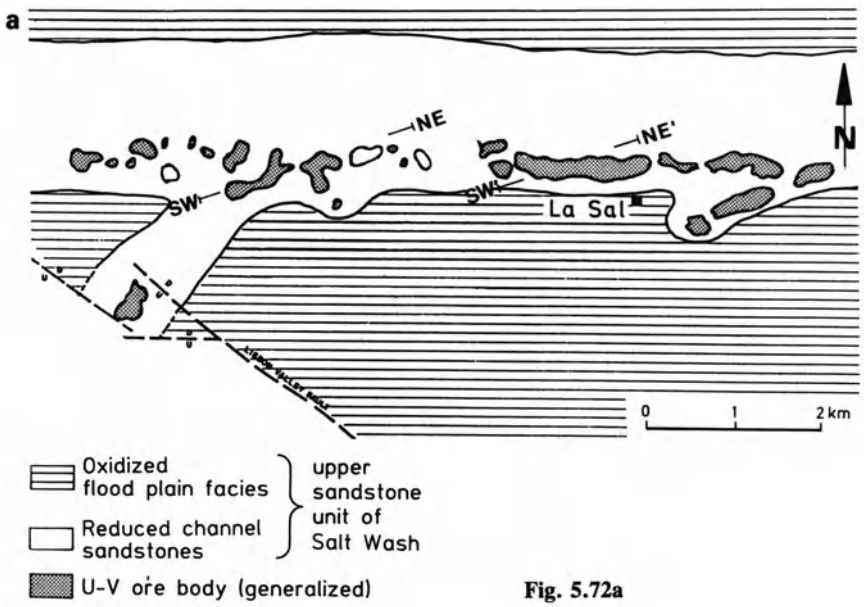

Fig. 5.72a

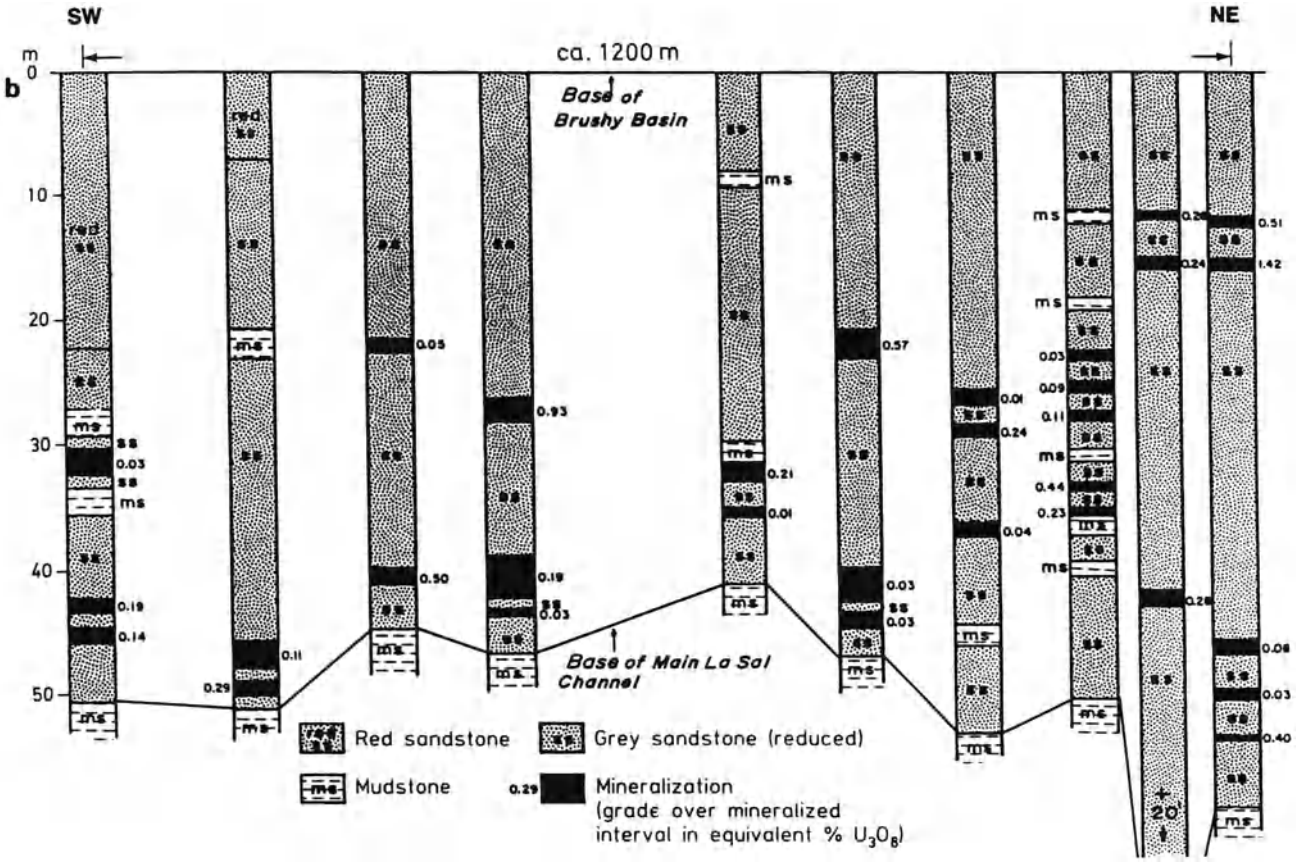

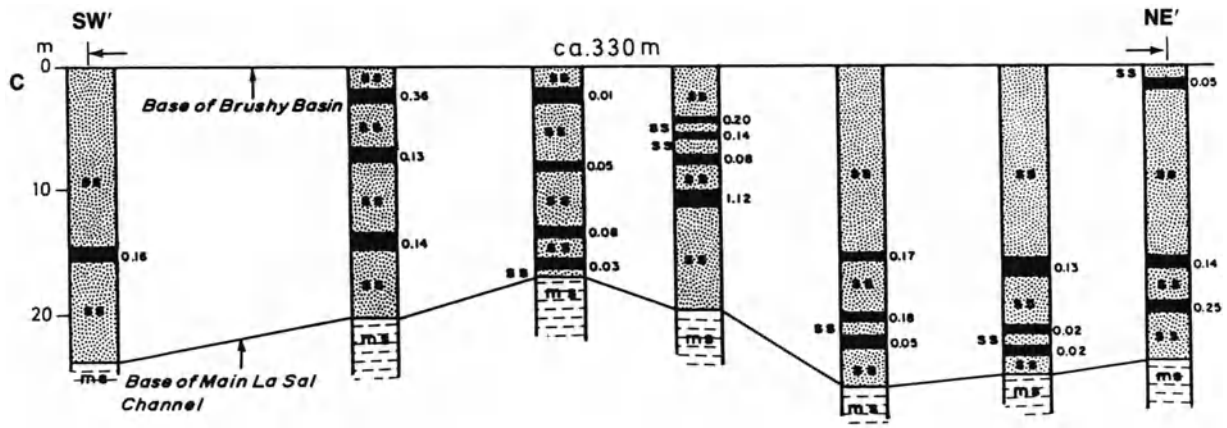

Fig. 5.72. La Sal district. **a** Generalized map of distribution of reduced channel sand facies and oxidized flood plain sediments of the upper sandstone unit of the Salt Wash Member. All ore is in the reduced channel facies where it occurs at several levels as shown in the cross-sections. **b** Western part of La Sal district. **c** La Sal mine. (After **a** Thamm et al. 1981; **b**, **c** Kovschak and Nylund 1981)

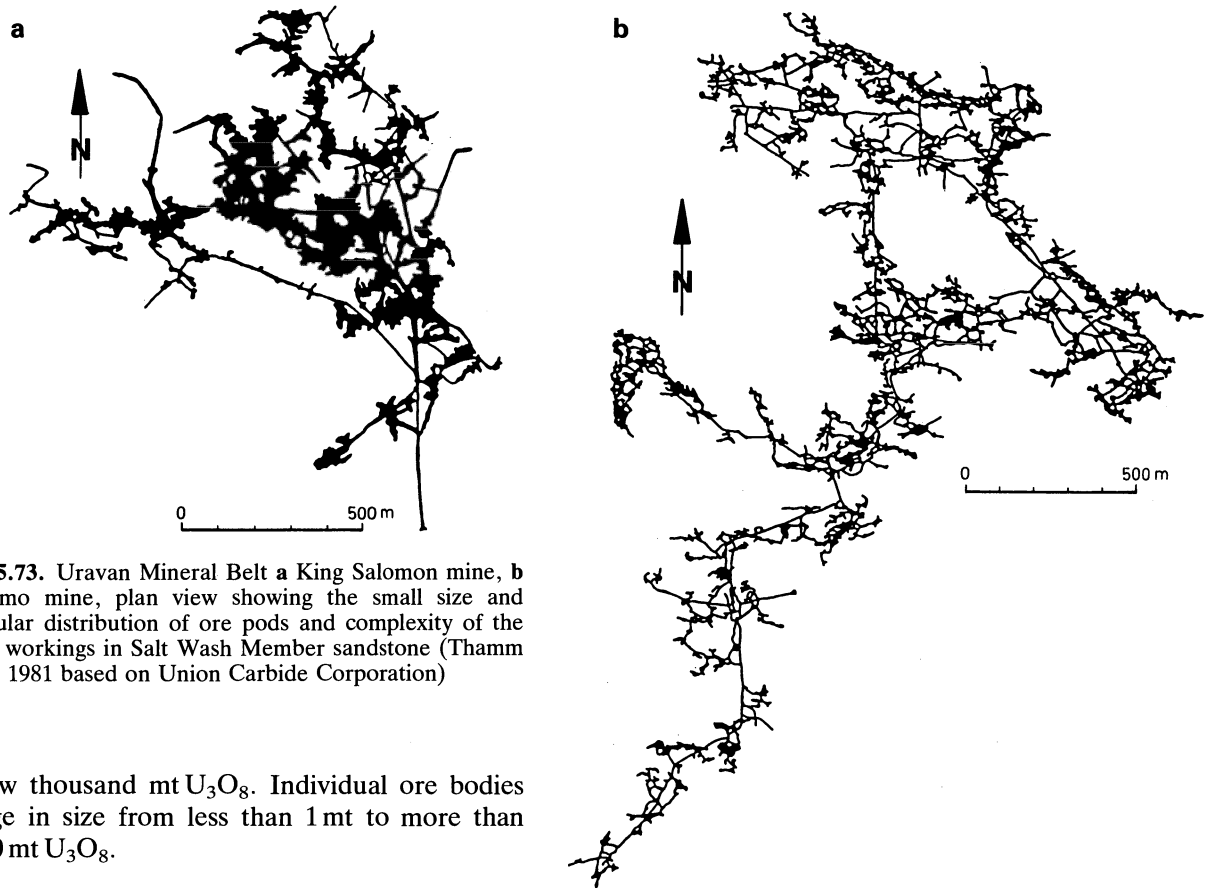

Fig. 5.73. Uravan Mineral Belt **a** King Salomon mine, **b** Deremo mine, plan view showing the small size and irregular distribution of ore pods and complexity of the mine workings in Salt Wash Member sandstone (Thamm et al. 1981 based on Union Carbide Corporation)

a few thousand mt U_3O_8. Individual ore bodies range in size from less than 1 mt to more than 1000 mt U_3O_8.

Potential Sources of Uranium and Vanadium

The origin of the *uranium* is still open to debate. Salt Wash deposits and other uranium deposits of the Colorado Plateau, as for example, those in Chinle sediments (Chap. 5.4.3) occur within a province of uraniferous Precambrian basement. Thamm et al. (1981) suggest that the uranium-enriched Precambrian rocks, or younger uraniferous igneous or volcanic rocks constitute potential sources for much of the uranium now found in the sandstone deposits of the Colorado Plateau. Particularly the tuffaceous material incorporated within the Salt Wash host sandstones and the overlying Brushy Basin pelites are considered to have contained anomalous amounts of uranium which provided an adequate source for the Salt Wash mineralization. This idea, however, is based more on the presence of tuffaceous constituents in the various V-U districts than on any geochemical documentation.

The source of the *vanadium* is likewise unknown. Favorite hypotheses consider vanadium to be derived from either decomposition of detrital magnetite and ilmenite within the host sediments, diagenetic introduction from the overlying Cretaceous sediments, and/or leaching and erosion of Paleozoic sediments located to the west of the Colorado Plateau.

All of these hypotheses are, to some extent, plausible, but remain as yet speculations.

Ore Controls and Recognition Criteria

Essential ore controlling or recognition criteria of Salt Wash type vanadium-uranium deposits as listed by Thamm et al. (1981) include:

Host Environment

- A sequence of continental clastic sediments interbedded with tuffaceous layers contains the ore deposits.
- The dominant host rock is an altered-facies sandstone of fluvial provenance characterized by megascopically buff to gray, highly cross-bedded channel sands, relative high permeabil-

ity, some combination of detrital plant debris with minor redistributed humates and iron sulfides, detrital ilmenite, and magnetite grains largely or completely altered, and interbedded gray clay layers.
- The ore hosting Salt Wash Member is overlain by mainly pelitic sediments of the Brushy Basin Member, Morrison Formation, which are largely, if not dominantly, oxidized in the general region of the Salt Wash deposits.
- Sedimentological peculiarities influenced the localization of ore districts and ore bodies on a regional and local scale.
- Regional scale parameters are reflected by the restriction of larger deposits to major transmissive sandstones which can be either major sandstone channels deposited in the intermediate distal facies of an alluvial fan system, as in the Uravan Mineral Belt, or thicker alluvial sand accumulations, as in the Henry Mountains.
- Local scale parameters controlling the position of ore include a relatively thick reduced sandstone bed interbedded with gray mudstones or mudstone conglomerates/clay gall zones, cross-bedding, abundant carbonaceous material and scour surfaces.
- A control by sedimentary facies is indicated in the Uravan Mineral Belt by the concentration of highest grade ore predominantly in point bar sediments, a kind of transitional facies between meandering and braided stream deposited sandstones (Tyler and Ethridge 1981). A similar relationship between certain sand facies and the V-U grade also characterizes the deposits in the Henry Mountains (Northrop 1982).

Alteration

- Significant alterations are related to redox processes.
- Two different types of lithologically controlled oxidation-reduction boundaries are distinguished:
- The first type is entirely within sandstone and seems to occur typically within major channel systems. In this setting, oxidized sands are generally located in the upstream direction, i.e., from where the sediments were derived. Minor redistribution and enrichment of the mineralization appear to have taken place at this redox interface.
- The second type is between predominantly sandstone and predominantly mudstone sections. Processes generating this redox boundary apparently influenced also the mineralization as reflected by the position and concentration of ore bodies.

Mineralization

- Mineralization of the Salt Wash Member sandstone type is of vanadium-uranium composition.
- Within ore lenses, the V-U minerals are concentrated along cross-bedding planes, adjacent to scour surfaces and in clay gall zones.
- Ore bodies are generally of small size occurring within broader zones or trends in the form of commonly thin, discontinuous, and rather erratic mineralization.
- Ore bodies are predominantly tabular, elongate, and lenticular, mostly peneconcordant with the bedding of the host rocks. Occasionally, mineralization crosses the bedding at a sharp angle in the form of a roll. No apparent genetic difference, however, appears to have caused the tabular and roll shape configurations, as indicated by a similar zonal distribution of U, V and Se across both types (Shawe 1966, 1976a). Consequently, the
- Salt Wash rolls are not true roll-type deposits comparable to those in the Wyoming Basins.
- Ore lenses occur suspended within a particular level in the host sandstone rarely touching either the upper or the lower contact of the host sandstone unit (Fig. 5.72b,c). No property of the host beds has been established as a control for this tendency.
- Although the long axes of many individual ore bodies is subparallel to the major trend axes, those of other ore bodies strike at oblique angles to them.
- Individual deposits or lenses of mineralization commonly terminate against shale horizons, channel margins, and any other sedimentological feature that creates changes in permeability.
- Clusters or trends of deposits emplaced within major sedimentary channels tend to be aligned along their margins (Fig. 5.72a). Most of the ore trends are oriented parallel to the paleocurrent directions, suggestive of an affinity to a broader hydrologic system.

- Ore bodies (a) occur in reduced channel sands adjacent to oxidized overbank deposits and (b) are commonly larger and more numerous near the redox interface than in reduced sands more distant from such contacts.
- The highest grade ore in any deposit occurs proximal to the oxidation-reduction boundary (Fig. 5.69). Where narrow zones of gray, reduced sandstone extend into red, oxidized sands, both the grade and the continuity of the ore substantially increase. These zones, bounded above and below by red sediments, do not make major ore bodies in themselves, but constitute high-grade pods within larger deposits.
- Although all major Salt Wash deposits occur in some proximity to oxidized sediments (red bed overbank deposits or oxidized sandstone), the mineralization itself is generally emplaced entirely within reduced sandstone, without adjacent tongues of oxidized sandstone. This suggests that the ore did not originate by the mechanism that forms roll-type deposits of the Wyoming Basins type. The mineralization is, in this respect, more like that of the deposits of the Grants Uranium Region, which similarly occur within reduced sandstones.

Metallogenetic Concepts

Genetic models for the Salt Wash vanadium-uranium deposits vary widely from synsedimentary to hydrothermal ore-forming processes. All salient features, however, are more suggestive for a formation from groundwaters at low temperatures than for either a hypogene hydrothermal or synsedimentary origin. More recent concepts by Nash et al. (1981) and Northrop (1982) (details see later), which were already proposed as early as 1947 by Fischer, consider epigenetic ore formation along a solution interface existing within the host sandstone between a saline fluid and meteoric water.

Thamm et al. (1981) visualize the ore-forming process, in summary, as follows:

The *gray Salt Wash sandstones and mudstones* filling channels were deposited under conditions permitting the formation of a *reducing environment*, as reflected by the presence of pyrite and carbonaceous material. Otherwise these two components would have been destroyed. When individual small channels within major channel systems were abandoned, the trapped porewater in the sands became stagnant and reducing from the decay of buried vegetal organic material. Reduced zones could have been small to large, depending on the size of the abandoned channels and the amount of organic debris within them.

Larger channels with abundant carbonaceous debris underwent more intense reduction, leading to the destruction of magnetite and ilmenite. This type of alteration, represented by the altered facies described by Shawe (1976a), corresponds to the alteration associated with the deposits of the Grants Uranium Region (see Chap. 5.4.1).

The more intensely reduced portions of the channel sands tend to occur near the base of thicker sandstone units along one margin of a major channel system.

The predominantly *red Salt Wash floodplain sediments* achieved presumably their color as a result of oxidation of magnetite and ilmenite to hematite under alternating wet and dry conditions of deposition. This oxidation also destroyed any carbonaceous debris which had accumulated in the floodplain environment. These red bed facies sandstones and mudstones do not contain uranium deposits and rarely contain uranium occurrences.

After the channel-sandstone systems of the Salt Wash Member were covered by the predominantly oxidized, tuff-interbedded pelites of the Brushy Basin Member, *diagenesis* caused the expulsion of oxidizing porewaters from the Brushy Basin sediments into the Salt Wash channel-sandstone aquifers. These waters are considered to have contained significant amounts of uranium leached from the tuffaceous material.

The *chemical conditions* for the ore-forming processes, as suggested by Thamm et al. (1981), include a partial decomposition of plant trash in the deeper channel sands, contributing humic acids to the groundwater. As a result, a reducing environment developed, forcing the decomposition of ilmenite and magnetite, with associated liberation of iron and vanadium. The hydrolysis of volcanic material liberated silica and alumina and produced a rise in pH, which further promoted the decomposition of plant material. The contact of these reducing solutions with the more oxygenated, uranium(VI)-bearing solutions, expelled from adjacent Salt Wash red beds, overlying Brushy Basin sediments and recharge areas up the hydrologic gradient, was the site of ore formation.

The dominant *groundwater movement* followed the sedimentological gradient. The oxidizing water which was under hydrologic head from the compacting pelites above and marginal to the channel axes migrated tangential to and into the reduced sands. In more uraniferous, thicker sand units as found in the Henry Mountains region, the redox contact assumed a simple tabular configuration and produced the more consistent, tabular orebodies of the Tony M/Shootering Canyon and adjacent deposits. Where the sediments consisted of complex sand-shale alternations, the solution interface became contorted between shale interbeds leading to mineralization of mixed tabular-roll patterns.

The *precipitation of ore elements* at the interface between an overlying oxidizing and an underlying reducing water system produced an element zoning that proceeded from selenium and vanadium at the top, through uranium to molybdenum at the bottom of the mineralized section. Although this is the element pattern most commonly observed ore rolls also display inverted element distribution on their overturned limbs.

The vanadium-uranium mineralization predominantly occurs within altered-facies sandstones commonly adjacent to carbon-facies sandstones, both of which contain carbonaceous material. There is, however, no evidence of the type of oxidized sandstone tongues that are typically associated with Wyoming type rollfront uranium deposits. It appears, therefore, that the uraniferous solutions were balanced in their oxidation capacity, namely strong enough to carry uranium in the hexavalent state but sufficiently low to leave the majority of the carbonaceous debris unaltered. The absence of redistributed humates within the vanadium-uranium mineralization suggests that the pH of the two mixing solutions was sufficiently similar to prevent the precipitation of humates.

Once deposited, the V-U mineralization remained essentially at the site of its precipitation. The majority of the U of the original ore minerals, especially in those ores of high vanadium content, that became oxidized remained in situ due to the fixation of the uranium in insoluble secondary V-U minerals (Thamm et al. 1981).

The mechanisms of ore mineral precipitation include the hypothesis of Granger and Warren (1981), who suggest that the reduction of U^{6+} by V^{3+} led to the precipitation of insoluble U^{4+} and V^{4+} minerals. The two authors point out, however, that such a redox regime required a groundwater composition other than that derived from the Morrison sediments. They propose that the solution possibly originated from underlying strata containing evaporites, and that the solution carried uranium and sufficient magnesium to displace complexed vanadium and aluminum contained in soluble humates. The coupled precipitation of uranium, vanadium, and aluminum as hydroxide gels co-precipitated Mg^{2+} and K^{+}, which subsequently aged to form the clay-bearing assemblages characteristic of the mineralization.

Breit and Goldhaber (1983) studied authigenic minerals in the Salt Wash Member in the Dolores anticline, Gypsum Valley anticline, and the intervening Disappointment Valley syncline. Their results indicate a multi-stage geochemical history with implications for the genesis of the vanadium-uranium and the copper deposits of the region. The authigenic minerals consist of dolomite, calcite, kaolinite, chlorite, baryte, pyrite, and albite. Some of them, in particular dolomite and chlorite, imply the presence of saline fluids. These *saline fluids* are believed by the authors to have influenced the formation of the vanadium-uranium deposits. Potential sources for these brines include the Paradox Formation evaporites (Pennsylvanian), which occupy the cores of the anticlines, and the paleoformation waters of the Morrison Formation.

Northrop (1982) studied Salt Wash mineralization in the Henry structural basin (Henry Mountains). The author proposes a model in which the uranium precipitation occurred at an *interface of brine and meteoric waters*. This concept is based on the chemical and isotopic compositions and the stratigraphic distribution of authigenic/diagenetic mineral phases, in particular those phases which are more or less cogenetic with the vanadium-uranium mineralization. Northrop's arguments are as follows:

The ore-related tabular-planar layers of authigenic dolomite cement, the $\delta^{18}O$, $\delta^{13}C$ values of these dolomites, and the $\delta^{34}S$ values of the disulfide phases suggest a high Mg : Ca ratio of greater than 1 : 1, enrichment in dissolved sulfate and carbonate, and probably also an abundance of Na for brines derived from the Tidwell Unit which underlies the Salt Wash Member. The brines or other fluids did not deplete any ore and ore-related elements (Se, Mo, Co, Ni, Cr) of the Tidwell Unit and the author concludes that these brines, unlike the ore fluids, were confined within

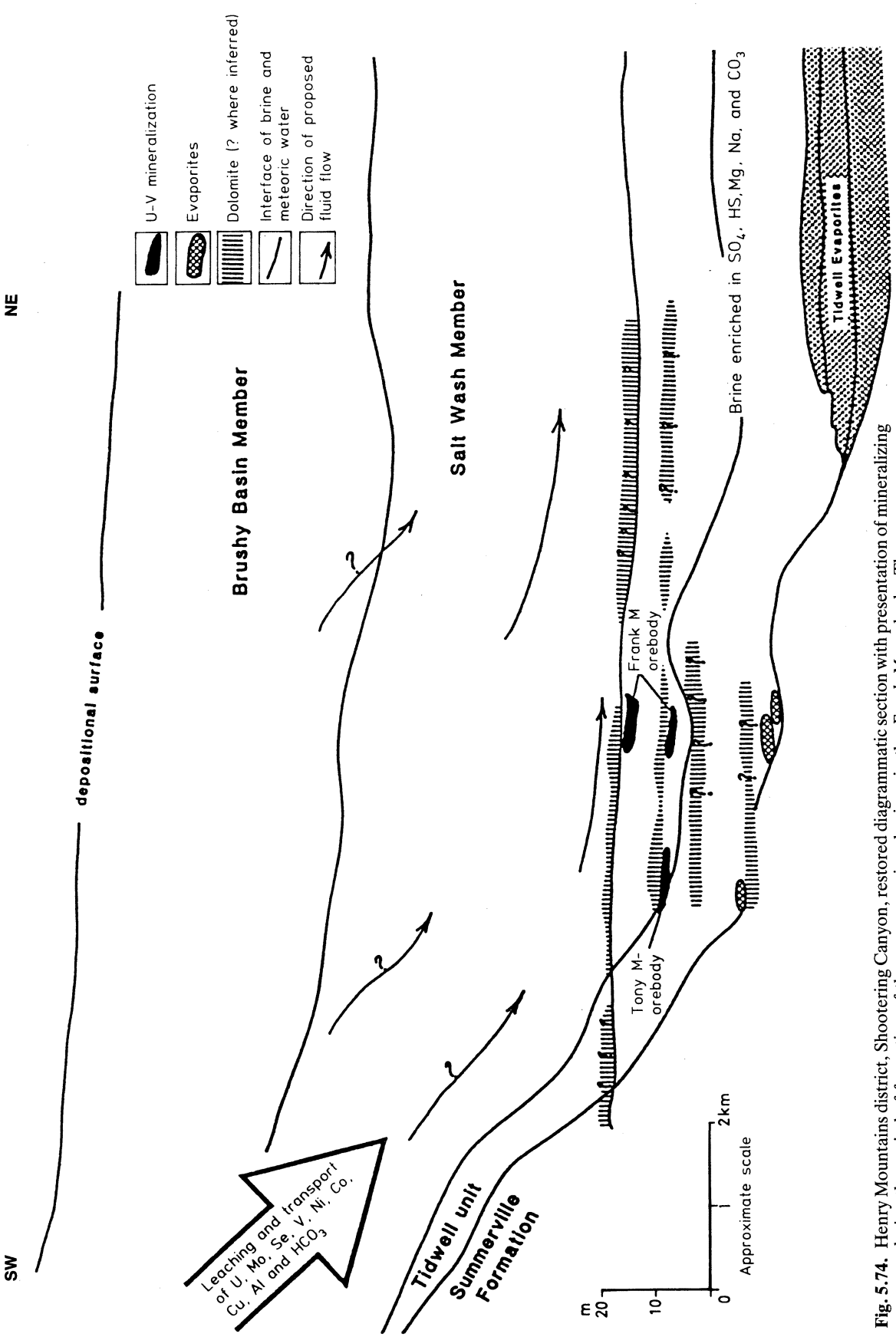

Fig. 5.74. Henry Mountains district, Shootering Canyon, restored diagrammatic section with presentation of mineralizing processes during the period of formation of the upper uranium horizon in the *Frank M* ore body. The ore zones were originally horizontal but are now tilted at ca. 2° SW. (After Northrop 1982)

the Henry Basin. In contrast, uranium and vanadium have been mobilized from the two higher Morrison members, Salt Wash, and Brushy Basin, and were transported by meteoric fluids to the sites of ore formation in the Henry Basin.

Northrop (1982) identified four stratigraphic positions of a stable brine-meteoric water interface in the Henry Basin. Dolomite maxima that are superjacent to each interface position identify the general position of an interface, whereas the mineralogy and composition of clay minerals establish the exact position of an interface. Chlorite and/or chlorite-smectite, enriched in vanadium and magnesium, occur only at the brine-meteoric water interface positions, which in turn also control the position of the vanadium-uranium ore.

The mineralization is restricted to *intrabasinal synclines* in which it is confined to those sites where the brine-meteoric water interface intersects sandstone horizons containing anomalous concentrations of organic matter. Where the sandstone does not contain detrital organic debris, Mg- and V-enriched chlorites still occur. These lateral extensions of ore-related gangue (?) minerals also contain anomalous uranium above the normal background values of the Salt Wash sandstone.

The authigenic clay mineral in the upper part of the mineralized interval in the Tony M ore body is a vanadium-bearing chlorite. It derived apparently from a precursor smectite and detrital illite-smectite. The clays in the mineralized zones and in their unmineralized lateral extensions show an asymmetric distribution of magnesium and vanadium into the interlayer octahedral sheets in the ore-clays, with Mg generally more abundant than Fe in the chlorites.

The destruction of pre-mineralization clay minerals and also of quartz generated a siliceous-rich environment which probably caused the silicification as observed in zones of quartz overgrowths positioned both above and below the vanadium-uranium ore horizons. The prevalence of coffinite may be likewise the result of abundant availability of silica. Provision of silica is further indicated by the close spatial relationship between coffinite and vanadium chlorite (Goldhaber, unpublished data in Northrop 1982).

Northrop (1982) concludes from his data that the formation of the Salt Wash Member hosted vanadium-uranium mineralization in the Henry structural basin/Henry Mountains is the result of distinct geological features associated with integrated processes (Fig. 5.74) namely:

1. The appropriate setting and the kind of sedimentation within the Henry Basin provided (a) an *evaporite horizon* in the Tidwell Member of the Morrison Formation, (b) sandstones containing abundant, preserved, *detrital organic matter* and (c) an available *source of uranium and vanadium* in the overlying Salt Wash and Brushy Basin members.
2. Diagenesis generated a *saline fluid* from the Tidwell Member evaporites but unlike the vanadium-uranium transporting fluids the brines remained confined within the Henry Basin.
3. *Oxygenated meteoric waters* moving downward into the basin leached uranium and vanadium from the overlying Salt Wash and Brushy Basin members.
4. Deposition of the ore elements occurred at a *stable interface* between the reducing saline and oxidizing meteoric fluids.

References and Further Reading for Chapter 5.4.2

(for details of publications see Bibliography

Botinelly and Weeks 1957; Boutwell 1905; Boyer 1956; Bowers and Shawe 1961; Breit 1986; Breit and Goldhaber 1989; Brooks and Campbell 1976; Brooks et al. 1978; Burwell 1920; Butler and Fischer 1978; Butler et al. 1920; Carter and Gualtieri 1965; Chenoweth 1975, 1978, 1980, 1981, 1983; Chenoweth WL, pers. commun.; Chenoweth and Malan 1969, 1973; Coffin 1921; Crawley 1983; Doelling 1969; Ethridge et al. 1980; Finch 1967; Fischer 1947, 1950, 1957, 1959, 1960, 1968, 1970, 1974; Fischer and Hilpert 1952; Fischer and Stewart 1960, 1961; Fleck and Haldane 1907; Galloway 1978; Garrels 1953, 1955, 1957; Garrels and Larsen 1959; Goldhaber et al. 1983; Granger and Finch 1988; Granger et al. 1985; Gruner 1954; Hess 1914; Heyl 1957; Hillebrand and Ransome 1900, 1905; Hintze et al. 1967; Huff and Lesure 1962, 1965; Huffman and Lupe 1977; Huffman et al. 1980; Isachsen 1955; Jobin 1962; Johnson 1959; Johnson and Thordarson 1966; Keller 1959; Kerr 1958; Koeberlin 1938; Kovschak and Nylund 1981; LaPoint and Markos 1977; McLemore 1983; Meunier 1984, 1989; Meunier and Breit 1987; Meunier et al. 1987; Miesch 1962, 1963; Miller and Kulp 1963; Motica 1968; Nestler and Chenoweth 1958; Newman 1962; Newman and Elston 1959; Nash et al. 1981; Noble 1960; Northrop 1982; Northrop et al. 1982; Peirce et al. 1970; Peterson 1977, 1978, 1980a, 1980b; Peterson and Turner-Peterson 1980; Phoenix 1958; Pitman 1958; Plateau Resources Ltd. 1983; Rackley 1976, 1980; Ridgley et al. 1978; Scarborough 1981; Scott 1961; Shawe 1956a, 1956b, 1962, 1966, 1976a, 1976b; Shawe et al. 1959; Silver et al. 1980; Spirakis 1977; Stokes 1953a, 1953b, 1953c, 1954a, 1954b, 1954c, 1954d, 1967a, 1967b; Stokes and Mobley 1954; Thamm JK, pers. commun.; Thamm,

Kovschak and Adams 1981; Trimble and Doelling 1978; Tyler 1983; Tyler and Ethridge 1981; US-AEC 1959; Wanty 1986; Weeks 1951; Weeks et al. 1957, 1959; Wright 1955; Young 1978; Young et al. 1957

5.4.3 Channel/Basal Uranium Deposits in Phanerozoic Sandstones: Monument Valley-White Canyon Districts, USA

Eight principal mining districts distributed through the Colorado Plateau have produced in excess of

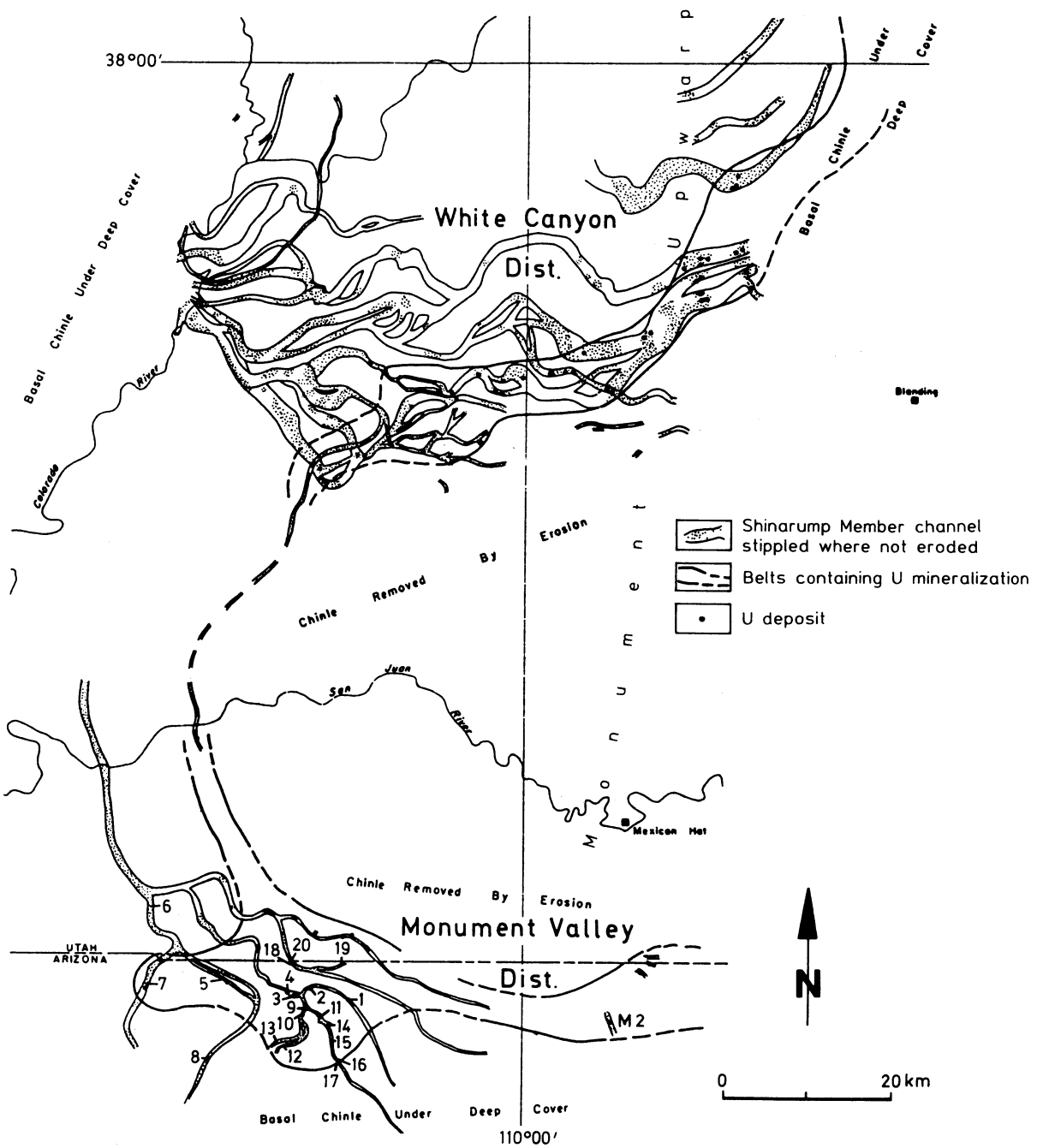

Fig. 5.75. Monument Valley and White Canyon districts, map of the Shinarump channel systems and location of uranium deposits. *Numbers* refer to former mines *1* Monument-Mitten 2; *2* Moonlight; *3* Daylight; *4* Starlight; *5* Tract 11; *6* Tract 14; *7* Tract 17; *8* Tract 2a; *9* Sunlight; *10* Big Four; *11* Big Chief; *12* Boot Jack; *13* Joe Rock; *14* Naschoy; *15* Alma-Seggin; *16* Black Rock; *17* Sally; *18* Fern; *19* Harvey Black 2; *20* Radium Hill. (After Malan 1968)

50 000 mt U_3O_8 from the Triassic Chinle Formation. The most typical channel/basal uranium deposits are found in the Monument Valley-White Canyon districts at the southeastern border line of Utah. (Fig. 5.75). They produced ca. 3900 mt U_3O_8 and 4500 mt V_2O_5 at average grades of 0.32 and 0.26% U_3O_8 and 0.23 and 0.94% V_2O_5 respectively (Chenoweth, WL, pers. commun.)

All major deposits consist of more or less lenticular ore pods located within distinct Triassic sandstone channels and generally in the lower part thereof. They are therefore classified as Phanerozoic tabular/peneconcordant channel/basal uranium deposits (class 4.1.3, Chap. 4).

Malan (1968), Wood (1968), Stewart et al. (1972) Chenoweth (1975) and Chenoweth and Malan (1973) published comprehensive studies of the various districts with Chinle mineralization including the Monument Valley-White Canyon districts. They are used as the main base for the following descriptions amended by data of the other authors mentioned.

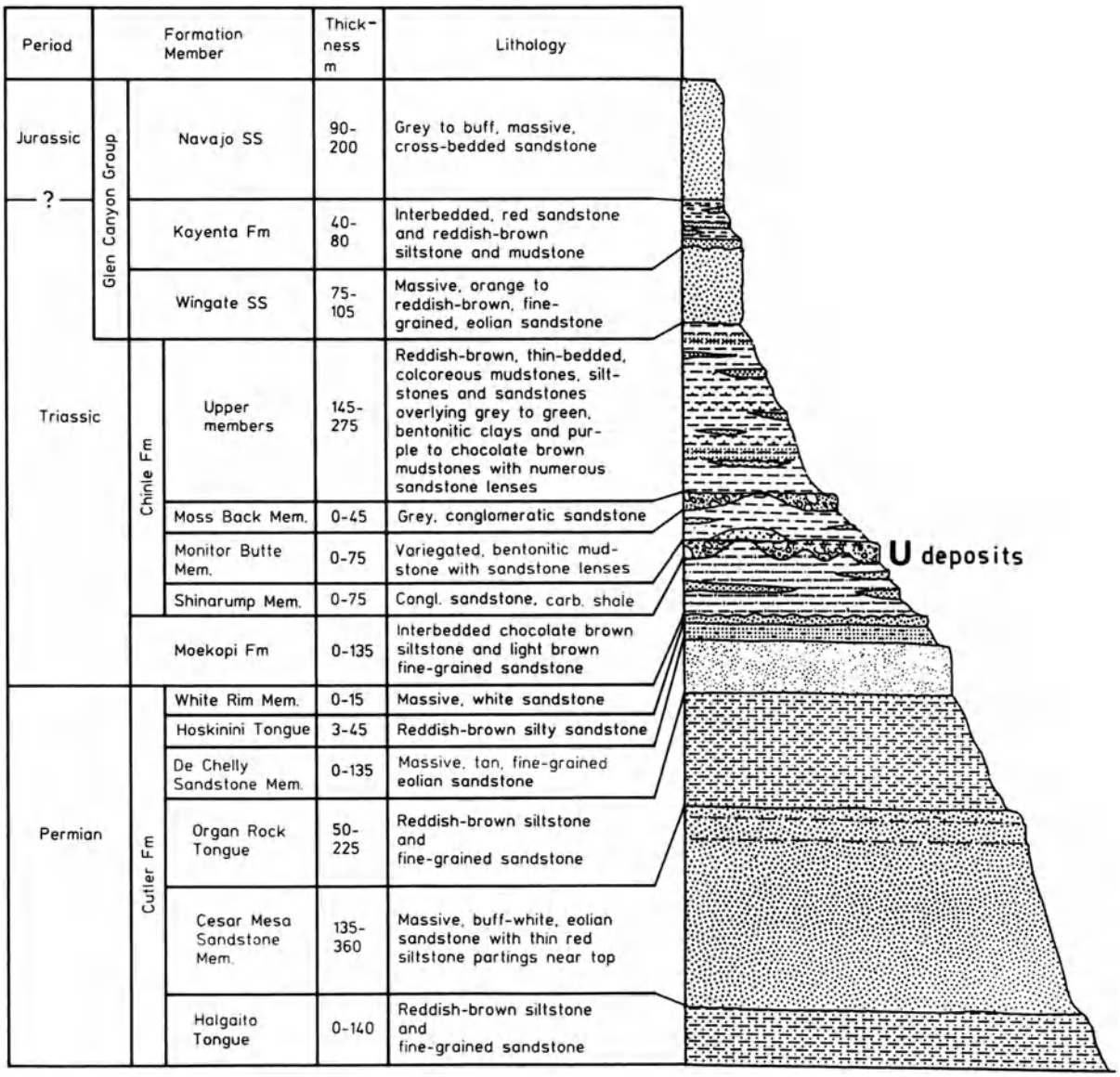

Fig. 5.76. Monument Valley and White Canyon area, generalized litho-stratigraphic column showing the stratigraphic position of U deposits in Shinarump Member channels and the lithologies of the Permian-Triassic-Jurassic units. (After Malan 1968)

Geological Setting of Mineralization

Ore host is the 50 to 600 m thick *Chinle Formation* of late Triassic age. It consists of *fluvial sediments* deposited on an extensive alluvial plain in braided and meandering channels, temporary lakes, and mud flats. The dominant sediments are red to vari-colored mudstones and siltstones, and generally light-colored sandstones and conglomeratic sandstones. *Volcanic material* was incorporated in the fluvial sediments, as was abundant carbonaceous debris. The Chinle Formation is subdivided into seven members. Three of the lower members (Fig. 5.76), from bottom to top, the Shinarump, Monitor Butte and Moss Back members, contain uranium deposits whereever any one of them forms locally the basal unit of the Chinle Formation (Fig. 5.77a).

The following description focusses on the Shinarump Member which is in the Monument Valley-White Canyon districts the basal Chinle unit and the host to the uranium deposits.

The Shinarump Member rests unconformably on the Middle Triassic *Moenkopi Formation* (Fig. 5.76) composed of continental sandy and silty red beds interfingering with minor marine calcareous sediments.

The *Shinarump Member* consists of light gray feldspathic sandstones and conglomerates with rare lenses of mudstone. The clastic deposits contain volcanic components and locally abundant carbonized and silicified plant fragments and logs. The sediments are cemented variably by calcite and silica. Thickness is generally between 10 and 30 m, but locally attains 100 m and more.

The Shinarump Member forms commonly a fairly extensive and uniform conglomeratic blanket but locally also distinct narrow channels incised into the underlying red Moenkopi siltstone as in the Monument Valley which are filled with mainly cross-bedded coarse psammites and psephites, partly of granitic provenance, and some pelites (Fig. 5.77c).

Local subsidence caused the abandonment of segments of the Shinarump channels (Fig. 5.75) and their subsequent preservation as valley-fill deposits. Reducing conditions prevailed in certain areas where groundwater tables were probably high.

The Shinarump sediments grade upward and intertongue laterally with the younger members of the Chinle Formation.

The most pronounced structural feature in the region is the Monument Upwarp. The Monument Valley is located on the southern flank and the White Canyon district on the western flank of the uplift.

Host Rock Alterations

Oxidation and reduction affected the Shinarump sediments apparently repeatedly. Most prominent reduction feature is bleaching around uranium mineralization. The bleaching extends locally into the underlying red Moenkopi sediments for a quarter of a meter or more particularly under mineralized scour and fill of paleochannels. Calcitization and silicification cemented to some extent the host rocks.

Principal Characteristics of Mineralization

Principal ore minerals in the *reduced zone* include pitchblende, coffinite, montroseite, locally doloresite, vanadium-bearing mica, -chlorite and -clay. Associated minerals may include sulfides of Cu, Fe, Mo, Pb, Zn, and trace minerals containing Se, Cr, Ni, Co, Ag, Cd, Sr.

The *oxidized zone* contains hexavalent uranium minerals, uranyl vanadates, higher-valent vanadium oxides, and hydro-mica; copper carbonates, native copper, etc.

The ore minerals impregnate sandstone voids, replace quartz grains, clay particles, and abundant fossil plant debris, and fill vertical fractures which extend beneath the scour base.

Calcium carbonate (1–10%) is present in ore mostly as cementing material of the sandstone host rock.

Meander loops and channels with deep scours appear to be the most favorable sites for the *location of mineralization*. In the Monument Valley ore bodies are primarily restricted to scours in the basal part of the Shinarump Member. Commonly there is only one ore-bearing scour, but not all scours of the paleochannels contain uranium mineralization. In a few mines, ore extended downward as much as 5 m from the Shinarump channel into the underlying beds.

Most of the deposits are linear in plan view with some deposits having a curvilinear to non-linear *shape*, e.g., the Happy Jack deposit of the White Canyon district. The ore bodies are usually composed of lenticular mineralized pods also referred to as rods (Fig. 5.77c,d) that are subparallel to the bedding and closely spaced.

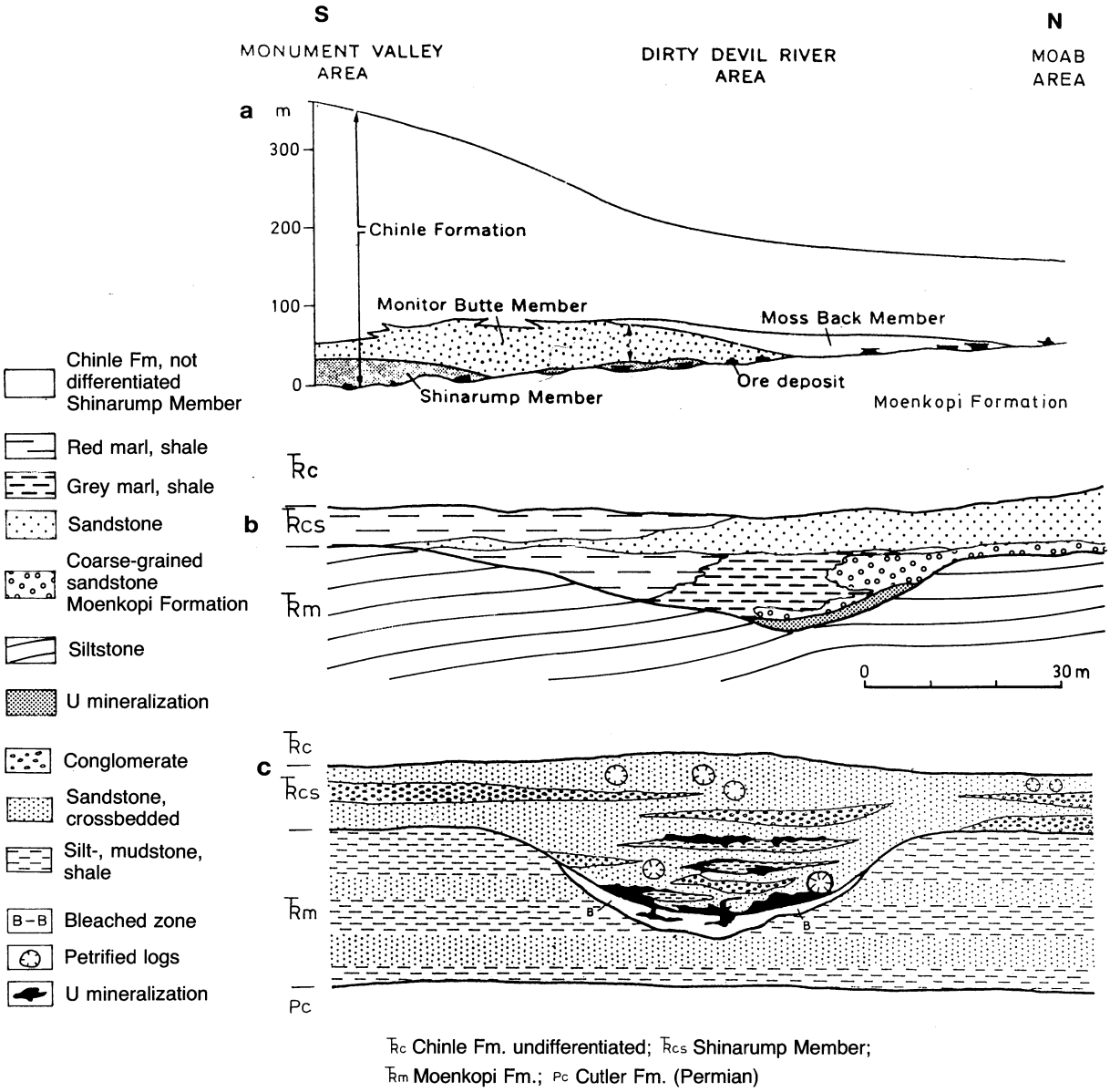

Fig. 5.77. North central Colorado Plateau, diagrammatic sections illustrating the position and lithologic environment of uranium deposits hosted in basal fluvial channels of the Chinle Formation. **a** Regional geological S-N section from Monument Valley to the south and Moab to the north showing the distribution of the basal members of the Chinle Formation and the position of uranium deposits. *b.c.*d Details of mineralization and ore distribution in Shinarump Member channels. **b** *White Canyon* district. **c** *Monument Valley* district. **d** Rod ore bodies in the *Monument No. 2* mine. (After **a** Johnson and Thordarson 1966 based on Stewart et al. 1959; **b** Miller 1955; **c** Mitcham and Evensen 1955; **d** Witkind 1956b) (**b** and **c** reproduced from *Economic Geology*, 1955, v. 50, p. 156ff, 170ff resp.)

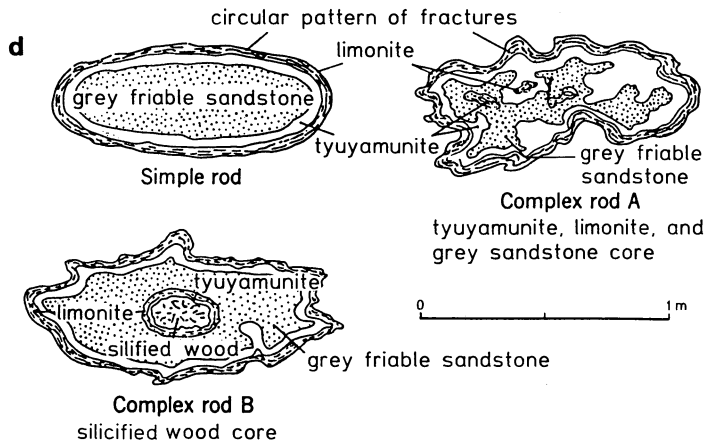

Dimensions of individual ore pods range from 0.3 to 3 m high, 0.3 to 3 m wide, and a few meters to 100 m in length. Deposits range in size from a few to rarely >2000 mt U_3O_8. About half of the deposits are smaller than 5 mt U_3O_8 and all but a few are smaller than 150 mt U_3O_8.

The largest deposit in the Monument Valley, *Monument No. 2*, (2400 mt U_3O_8, 0.34% U_3O_8, 1.42% V_2O_5) is emplaced in a Shinarump paleochannel scour extending for at least 3 km in a north-south direction within a wider depression or scour about 15 m deep cut into underlying Moenkopi and DeChelly units (Figs. 5.78, 5.77c). A narrow, inner scour is another 10 m deep and 200 m wide. The ore-bearing scour is eroded to the north and south. Best ores are in typical cigar or rod-shaped concentrations as much as 2.5 m in diameter and 30 m long. (Chenoweth, WL, pers. commun.; Malan 1968).

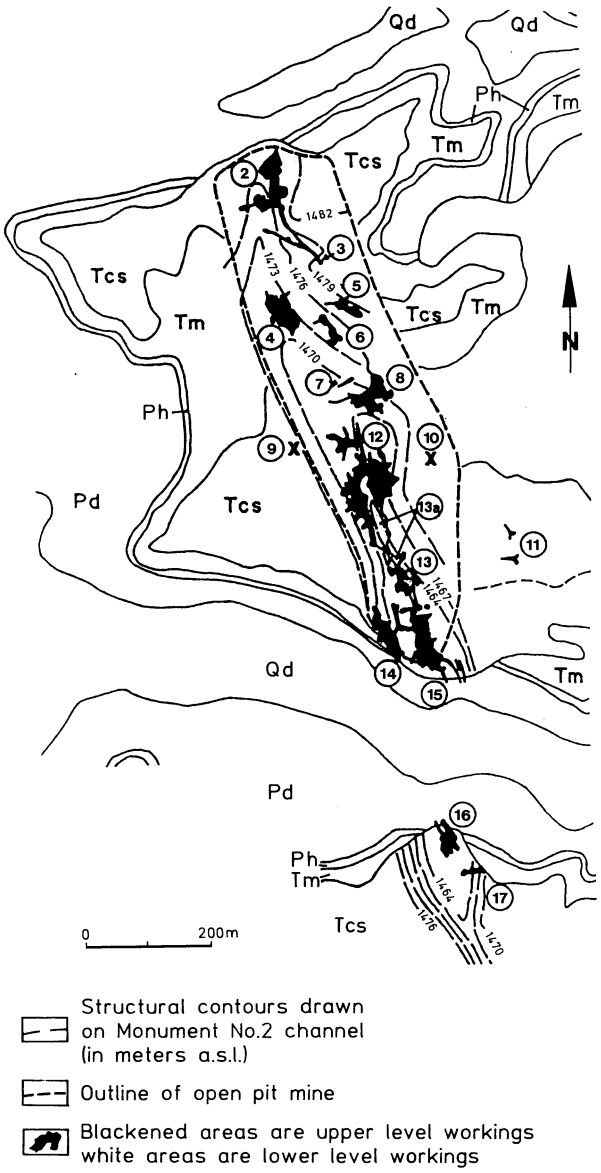

Fig. 5.78. Monument Valley district, Monument No. 2 deposit, geological map with outline of uranium ore bodies and mines in a Shinarump channel segment. *Numbers* refer to former mines. For a generalized cross-section see Fig. 5.77c. (After Witkind and Thaden 1963; US AEC 1959)

Potential Sources of Uranium

No valid source of the uranium has been established to date. Potential sources are speculated to have been uraniferous volcanic ash preserved in the form of bentonitic clays in the lower Chinle sediments or uranium-enriched granites which supplied the arkosic ore-hosting sands or these clastics themselves, or a combination of these sources. (see also Chap. 5.4.2)

Ore Controls and Recognition Criteria

Essential ore controlling or recognition criteria of the uranium deposits hosted in channels of the Shinarump Member, Chinle Formation, in the Monument Valley-White Canyon districts include:

Host Environment

- Host rocks are reduced, buff to gray feldspathic sandstones and conglomerates of continental fluvial origin filling channel systems scoured into pelitic-psammitic sediments.
- The arenaceous sediments have a relatively high permeability.
- Tuffacous material is incorporated in the sediments.
- Carbonaceous debris is abundant in the channel and overbank facies.

Alteration

- Significant alterations are related to redox processes reflected by color changes of the host and country rocks. Most prominent is bleaching around uranium mineralization.
- Calcitization and silicification cemented the host rocks to some extent.

Mineralization

- Principal ore minerals are pitchblende and coffinite associated with vanadium minerals, and sulfides of a number of other metals, most of them in trace amounts.
- Uranium mineralization commonly occurs associated with or near accumulations of detrital plant debris, redistributed humate, and iron sulfides.
- Uranium occurs disseminated in reduced sandstone but also replaces quartz grains, clay particles, and particularly plant fragments. Locally it extends as fissure filling into the underlying mud/siltstones.
- Deposits consist of a number of closely spaced small ore pods of medium grade commonly located in the lower part of a channel.
- Ore pods are mostly lenticular in shape more or less concordant with the bedding.
- Uranium occurs in a wide distribution of small, low-grade occurrences within reduced sediments but larger economic deposits are restricted to distinct sandstone channels.
- Preferential sites of deposits are relatively narrow channels, where these channels converge, and where the permeable channel sands gradually change into impervious carbonaceous mudstone.

Metallogenetic Concepts

Although a magmatic origin by hypogene fluids was formerly proposed for the Chinle uranium deposits, the most convincing model envisages supergene ore forming processes through *multiple migration-accretion* as presented by Malan (1968) for the Monument Valley-White Canyon districts and later in modified form for the Lisbon Valley district by Huber (1980).

Fluvial deposition of the arkosic Chinle sediments occurred into channel systems within a basin adjacent to a granitic highland. The exposed granitic rocks provided the detritus and a possible source of uranium as well.

The *river systems* which deposited the clastics of the Shinarump Member in the Monument Valley-White Canyon area were of degrading nature and scoured into the bedrock. Volcanic material was incorporated in the fluvial sediments, as was abundant carbonaceous debris as found in the channel sands and associated overbank deposits.

Mineralizing processes were probably initiated soon after the sedimentation of the fluvial sequence. Surface and groundwaters containing small amounts of U, V, and Cu migrated down the hydrologic gradient along the Shinarump channel systems during or soon after the deposition of the channel sands. Circumstantial evidence suggests that the metals may have been leached from granitic rocks, arkosic sandstones, and tuff beds affected by active erosion in the source areas of the sediments.

Wherever the dissolved uranium encountered accumulations of organic debris along the course of the river bed, it was extracted from the waters and fixed by reduction as colloid or adsorption on organic fragments forming minor and dispersed concentrations, a kind of *protore*, of U, V, and Cu. The *reducing agent* was either the organic debris itself or H_2S produced from the carbonaceous matter by activity of anaerobic bacteria.

Subsequent to the Shinarump sedimentation, renewed upwarp of large areas took place north and southeast of the Monument Valley and east of the White Canyon district. The dispersed protore uranium occurrences deposited initially in the Shinarump sands were *remobilized* during the erosion of channels from the higher parts of the uplifted areas and the partial destruction of numerous large channels in the adjacent lowland. Groundwaters transported the liberated uranium into reducing environments in the channels that survived along the lower flanks of the rejuvenated uplifts and formed the ore bodies as they are found today. In the Monument Valley, the most favorable sites for uranium *precipitation* were the heterogenous channel sands that were laid down where anastomosing streams converged (Fig. 5.75). In the White Canyon area, preferential sites for ore formation were in the transition zone between the upland and lowland which is characterized by a gradual change from permeable sands in the channels on the flanks of the uplifts to impervious carbonaceous mudstone in the same channels in the lowlands (Fig. 5.77b) (Malan 1968).

References and Further Reading for Chapter 5.4.3

(for details of publications see Bibliography)

Bohn 1977; Butler and Fisher 1978; Chenoweth 1975; Chenoweth WL pers. commun.; Chenoweth and Magleby

1971; Chenoweth and Malan 1969, 1973; Corey 1959; Crawley 1983; Davidson 1967; Dix 1953; Doelling 1969; Droullard and Jones 1955; Dubiel 1983; Elevatorski 1978; Finch 1959; Finnell et al. 1963; Fischer 1968; Gross 1956; Gruner et al. 1954; Hawley et al. 1968; Hintze et al. 1967; Huber 1980; Isachsen 1954; Isachsen and Evensen 1956; Jennings 1976; Johnson and Thordarson 1966; Koch et al. 1964; Lekas and Dahl 1956; Lewis and Campbell 1965; Lewis and Trimble 1959; Loring 1958; Lupe 1976; McRae and Grubaugh 1957; Malan 1968; Miesch 1963; Miller and Kulp 1963; Pilmore pers. commun.; Purvance 1980; Rackley 1976; Scarborough 1981; Schmitt 1968; Spirakis 1980; Stewart et al. 1972; Stokes 1967a, 1967b; Thaden et al. 1964; Thomson 1967; US-AEC 1959; Weir 1960; Witkind and Thaden 1963; Wood 1968; Young 1964, 1978

5.4.4 Roll-Type Detrital Carbon-Uranium Deposits in Phanerozoic Continental Basin Sandstones: Wyoming Basins, USA

Major uranium districts occur in four Tertiary basins in Wyoming, in the Windriver, Shirley, Powder River, and Great Divide basins. Minor districts are in the Maybell-Baggs area, and the Washaki-Sand Wash Basin, Wyoming-Colorado.

The Wyoming Basins constitute a prominent uranium province, second in magnitude in the USA after the Colorado Plateau. Total resources including ca. 75 000 mt U_3O_8 production until 1990 amount to more than 250 000 mt U_3O_8 in the \$80/kg U production category. The average grade of ore mined ranges from 0.05 to 0.25% U_3O_8. Individual deposits range in size from few 100 to several 1000 mt U_3O_8.

Uranium occurs in the form of rollfront or roll-type mineralization emplaced at a redox front in continental sandstone containing detrital carbonaceous debris. As such the Wyoming deposits represent a distinctive class of the Phanerozoic sandstone-type uranium deposits classified as roll-type detrital carbon-uranium deposits (class 4.2.1, Chap. 4.).

The following compilation is essentially based on Harshman and Adams (1981), who have elaborated in great detail on the Wyoming uranium deposits, amended by data of other authors listed.

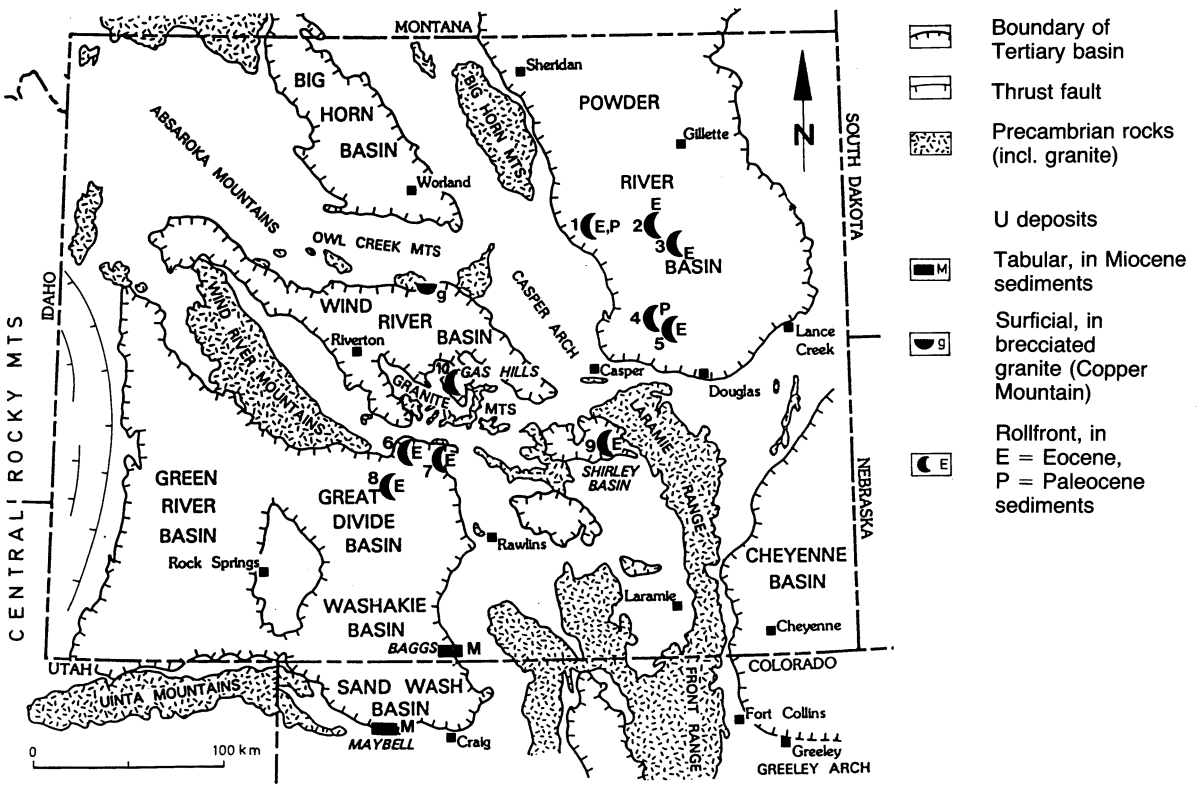

Fig. 5.79. Wyoming, generalized structural map of Tertiary Basins, Precambrian uplifts and location of uranium districts. The Precambrian rocks include uraniferous granites of Archean to Lower Proterozoic age. Districts with rollfront uranium deposits include *1* Kaycee; *2* Pumpkin Buttes; *3* Turnercrest; *4* Monument Hill; *5* Highland-Box Creek; *6* Crooks Gap; *7* Green Mountain; *8* Sweetwater-Red Desert; *9* Shirley Basin; *10* Gas Hills. (After Harshman 1970; Bailey and Childers 1974)

Geological Setting of Mineralization

The major rollfront uranium deposits occur in *intermontane Tertiary basins* ranging in size from a few hundred (Shirley Basin) to several thousand square kilometers (Powder River Basin). Crystalline rocks including uraniferous granites of Archean to Proterozoic age surround most of the basins (Fig. 5.79).

The basins are predominantly filled with *continental sediments* of Paleocene to Quaternary age. The younger formations contain *acid volcanic* interbeds with elevated uranium background values. Subsidence, uplift, and displacement along faults at the margins of some basins continued through most of the Tertiary, but in most cases later tectonism did not greatly affect the basin fill and its uranium deposits.

Significant rollfront uranium deposits have formed in the early *Eocene Wasatch, Wind River, and Battle Spring formations*, and to a lesser extent in the *Paleocene Fort Union Formation*.

The most favorable *host rocks* are friable fine- to coarse-grained or pebbly, arkosic sandstones containing considerable pyrite and carbonaceous substance, and occasional iron-stained mudstone clasts and tabular mudstone splits. Sand or silt-filled channels with cross-bedding are universally present.

Calcite cement or concretions are sparingly present in, but not characteristic of host sandstones. Calcite content of favorable sandstones, unaffected by the mineralization processes, is generally less than 1%. Calcite accumulations, however, occur associated with ore bodies.

Carbonaceous material is dispersed through the host sandstones with somewhat greater concentration on cross-stratification beds. This organic debris is generally fragments of leaves and twigs, but occasionally also humic material coating sand grains. A few large sections of tree trunks and branches, some silicified and others carbonized, are present in the Shirley Basin host rocks. The organic carbon content of the host rocks ranges widely from place to place but probably averages 0.5% or less.

Detrital heavy minerals constitute between 1 and 5% of the ore-hosting sandstones.

Below the water table, and where not altered by the ore-forming solutions, the host sandstones are generally light gray or greenish gray.

The fine-grained rocks interbedded with the sandstones range from mudstones or claystones to compact but somewhat friable siltstones. They are brown to tan, greenish-gray, dark gray, and almost black when high in organic material.

These lithologies, favorable for ore deposition, are found principally in the *central part of the fluvial system* in the basins, in large fans that range in length from a few km or tens of km as in the Wind River and Shirley basins, to more than 100 km in the Powder River Basin (Figs. 5.80, 5.81).

Individual sandstone beds within the fans have only a limited lateral continuity. Thicknesses range from a few to several tens of meters.

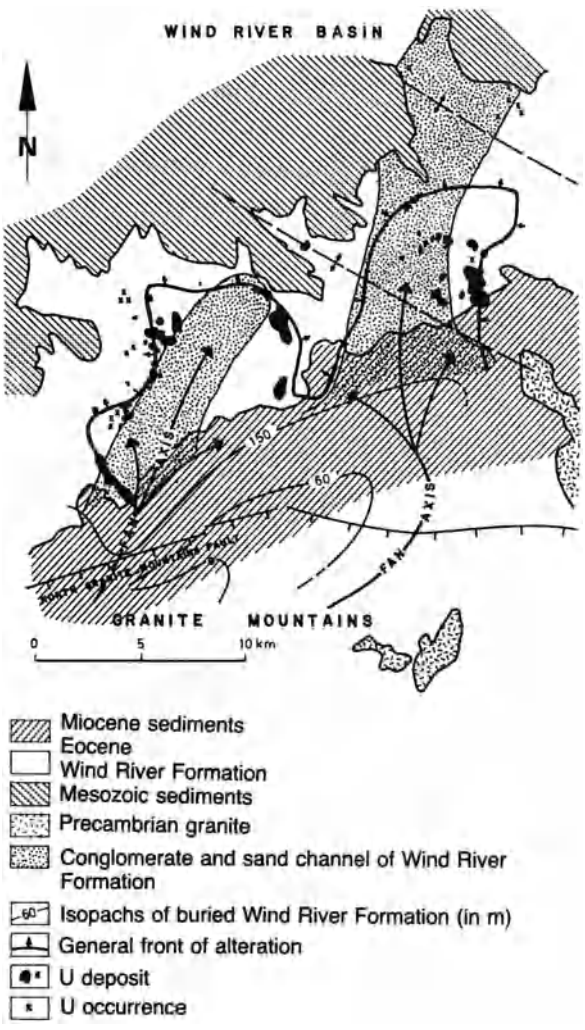

Fig. 5.80. Wind River Basin, Gas Hills, sedimentary patterns and distribution of alteration front in the Wind River Formation moving northward from the Precambrian Granite Mountains. Uranium deposits are dominantly localized along the main solution front. (After Galloway 1979b; Harshman and Adams 1981)

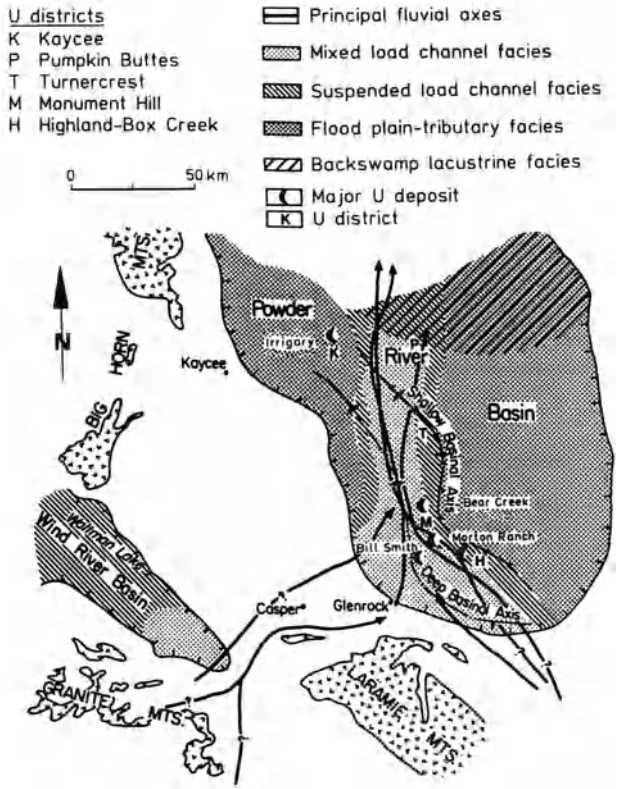

Fig. 5.81. Southern Powder River Basin, regional flow patterns and facies distribution of the upper Fort Union-lower Wasatch (?) fluvial systems and position of uranium deposits. (After Galloway 1979b)

Although widespread, favorable sandstone units contribute only a limited fraction of the total volume of the sediments in the basins.

According to Galloway (1979b), the sediments were deposited under coarse bed-load conditions or on the distal parts of *wet alluvial fans* in two major Paleocene-early Eocene drainage systems.

Host Rock Alterations

Diagenetic and particularly oxidation processes caused distinct alterations of the ore-hosting clastic strata. Although there are certain differences in character and extension of alteration of the host rocks in the various Wyoming Basins, there are some distinct similarities caused by *oxidation* of the sandstones in the major districts. Harshman and Adams (1981) list for altered sandstones:

- a distinctive change in color from the normal gray of unaltered sand,
- a selenium content considerably higher than in unaltered sand,
- an eU/U ratio generally higher than in unaltered sand,
- calcium carbonate, organic carbon, and sulfate contents much lower than in unaltered sand,
- partial or complete destruction of some or most of the heavy minerals, particularly pyrite and magnetite.

Figure 5.82a,b shows the different alteration and mineralization zones, related authigenic minerals and (Fig. 5.83) chemical reactions involved.

The *oxidative alteration* penetrates the host formations in a *tongue-like* fashion. Tongues may range considerably in size and shape. They can have lateral extensions of several hundreds of square kilometers and thicknesses of as much as a few tens of meters. In most districts there are several altered tongues and associated mineralizations within a generally favorable sequence of beds, each separated from the other by an interval of fine-grained impervious sediment. In some instances superimposed tongues of oxidized sandstone are connected by altered sand filling a depositional breach in the bounding impermeable sediments. Although altered tongues frequently overlap, their edges are rarely superimposed. Tongues of oxidized sandstone may or may not completely fill the sandy interval in which they are confined. Incompletely filled intervals occur most frequently at the ends of the oxidation tongues.

Principal Characteristics of Mineralization

Uranium has accumulated in a roll-shaped form at the edge of oxidized sandstone tongues (Figs. 5.80, 5.84) the features of which are displayed in Figs. 5.82a,b and 5.83.

The principal *ore minerals* are pitchblende and coffinite. They occur as coatings on sand grains, as void fillings in the sandstones and possibly as replacements of organic matter.

Uranium is accompanied by a number of elements which have been deposited in or adjacent to the altered tongues forming the rollfront (Figs. 5.82b, 5.83, 5.85). Selenium occurs as native selenium and ferroselite on the concave side of the rollfront, and as native Se in the unaltered mineralized rocks. Molybdenum (jordisite, MoS_2) and calcite are present on the convex side. Further on exist arsenic, phosphorus, and copper.

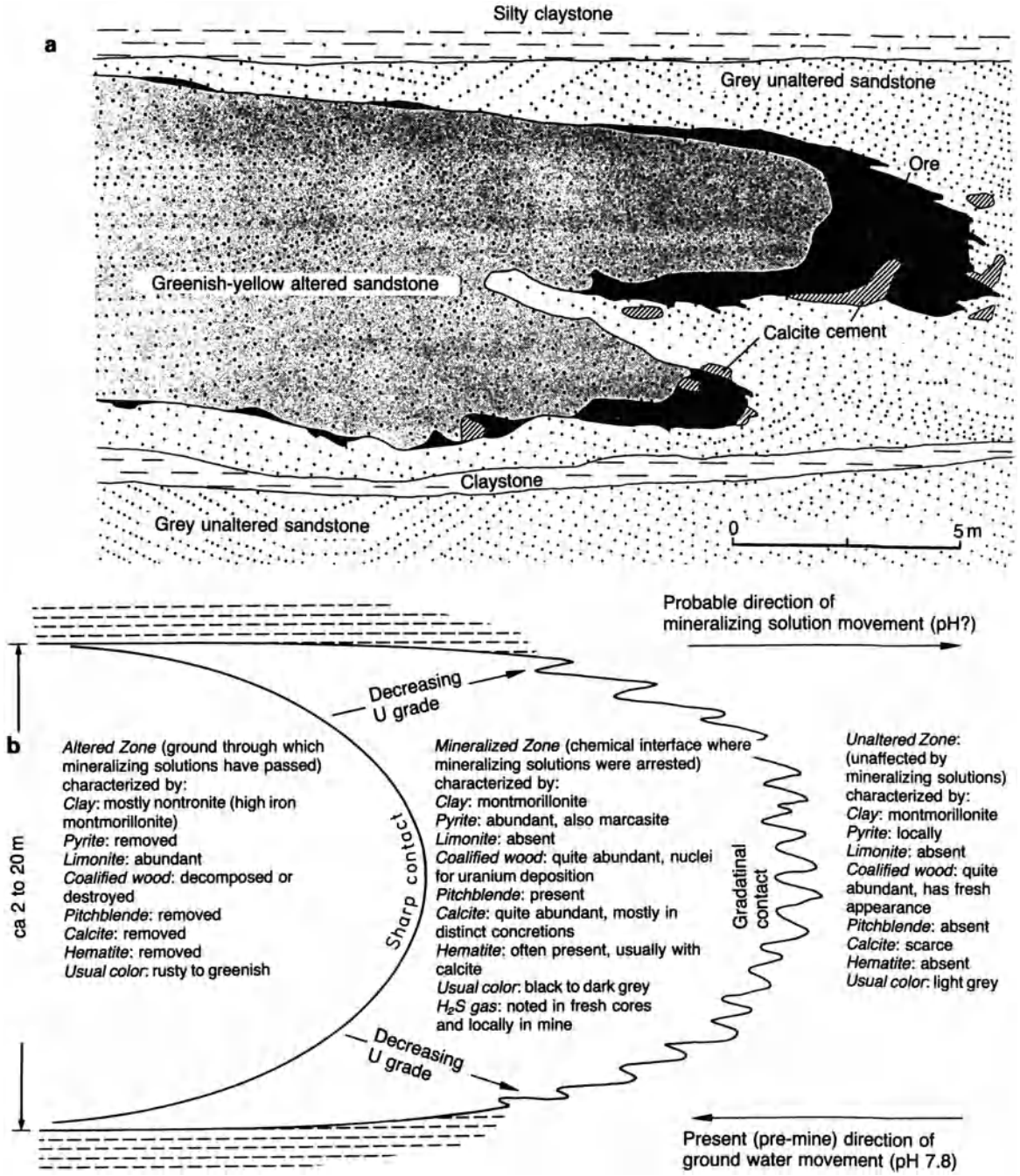

Fig. 5.82. Wyoming Basins, cross-sections with characteristics of roll-type uranium deposits. **a** Typical position and shape. **b** Schematic presentation of characteristic authigenic and allogenic minerals related to alteration zones (Shirley Basin). (After **a** Harshman 1974; **b** Bailey 1965)

Ludwig (1978), for his geochronologic studies, subdivided the uranium ore in the Shirley Basin into three types: disseminated pitchblende ore, calcite-cemented ore, and massive pitchblende ore, a division that can be, somewhat generalized, applied to most of the deposits in the Wyoming Basins.

Disseminated pitchblende ore is found in water-saturated, essentially unconsolidated, texturally and mineralogically immature, coarse-grained arkose. One of the samples with 9% U_3O_8 contained abundant charcoal-like organic material. Such fossil carbonaceous trash is moderately common in the unaltered arkose, in many cases

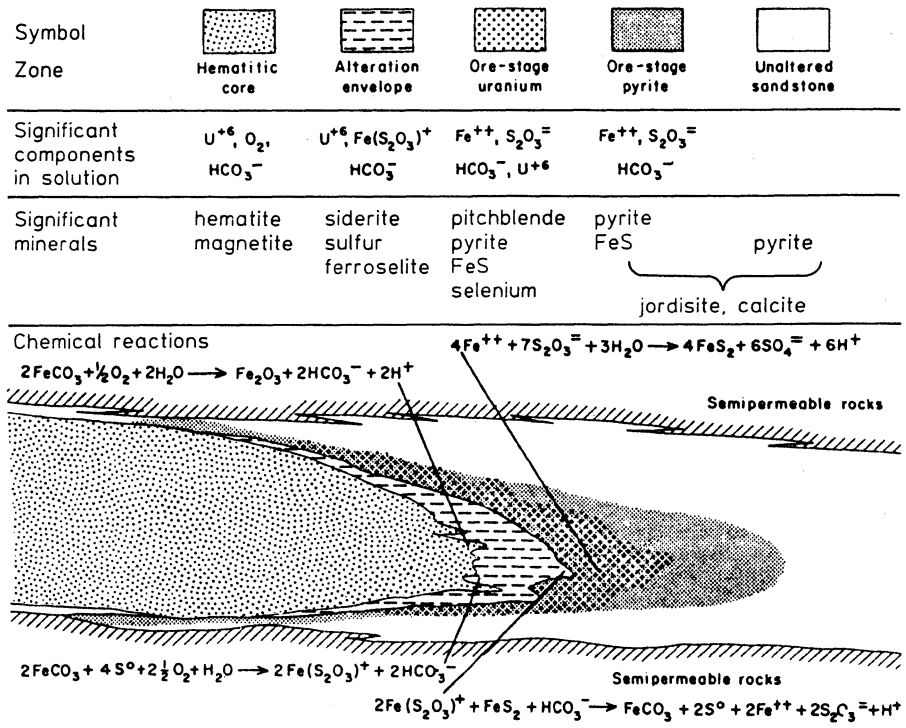

Fig. 5.83. Wyoming Basins, idealized scheme of a rollfront system with alteration zones, related mineral components, solution components and summary reactions in the Fe-S-O-CO_2 aqueous system during formation of a rollfront deposit. (After Granger and Warren 1974)

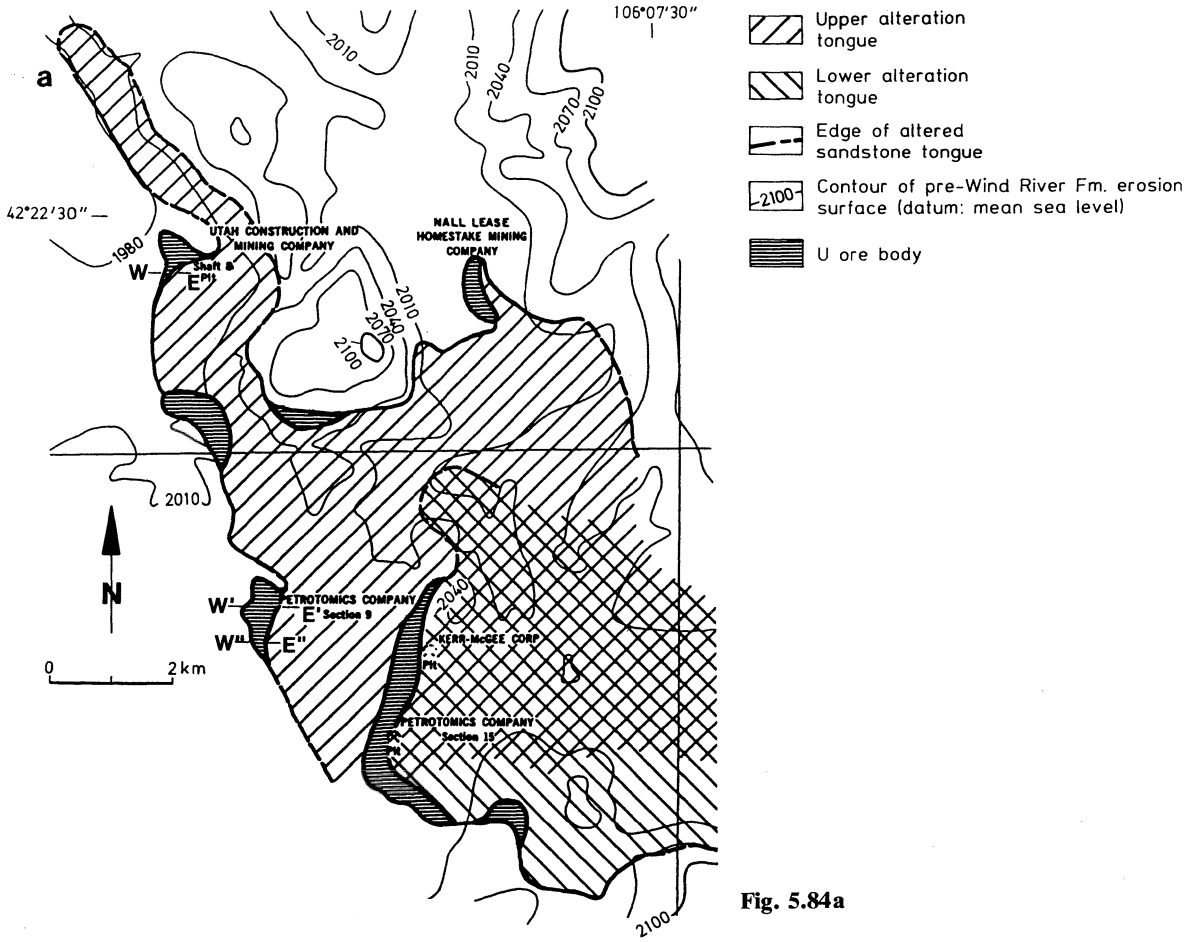

Fig. 5.84a

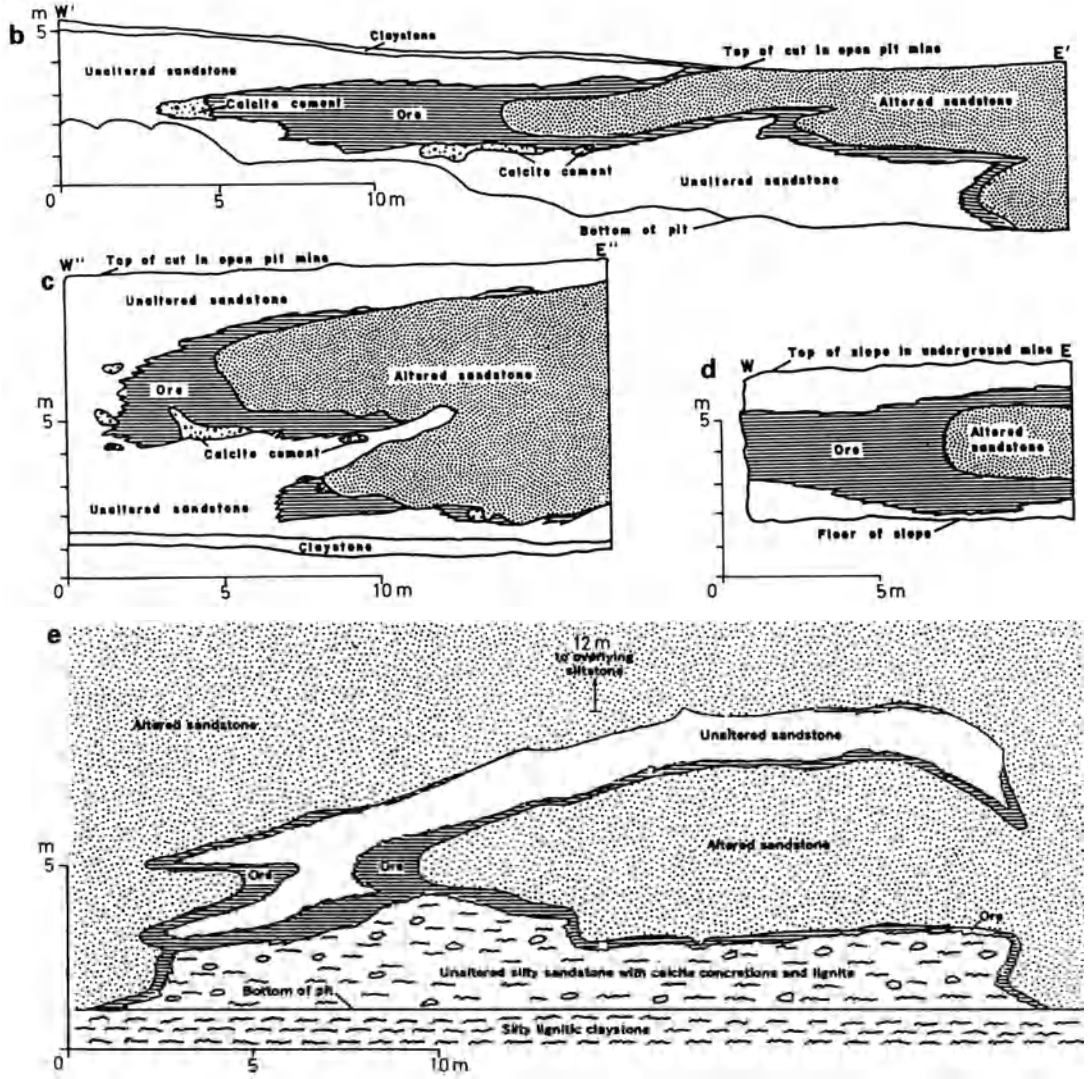

Fig. 5.84. Shirley Basin. **a** Distribution of an upper and lower altered sandstone tongue in the Wind River Formation and position of mineralization. **b**, **c**, and **d** Cross-sections at the western edge of the upper altered sandstone tongue. **e** Cross-section of small ore pods along the bottom of the altered sandstone tongue ca. 360 m backwards from the edge of the tongue in Petrotomics Section 9 pit. (After **a** Harshman and Adams 1981; **b**, **c**, **d**, and **e** Harshman 1972)

with well-preserved log- or limb-like forms. Pitchblende, pyrite-marcasite, and rare baryte were the only nondetrital minerals recognized in the ores. Pyrite occurs in three varieties including framboid habits which perhaps formed during early diagenesis. The pitchblende appeared quite pure with pyrite being the only visible contaminant.

Calcite-cemented ore is unusual both in its high grade (12.3% U_3O_8) and its texture. Calcite forms a pervasive matrix for the detrital grains of mostly quartz and feldspar, with a few heavy minerals. Calcite also corrodes the feldspar. Pyrite-marcasite (ratio: 20–50/1) and pitchblende are intimately associated. These minerals occur both as incomplete replacements of the detrital grains and as rims around them.

Massive pitchblende ore (65–72% U_3O_8) consists almost entirely of pitchblende, with very minor quartz and pyrite. No oxidation products of pitchblende were observed.

Harshman (1974) investigated in much detail the *distribution of the ore and associated elements and minerals* in ore bodies within and adjacent to the redox fronts in the various Wyoming Basins. One of his striking results is the great similarity of

the chemical distribution in most of the deposits. The essential elements and minerals reveal in summary, the following patterns (Fig. 5.85).

Uranium has been added to reduced sandstone in zones close to or in contact with the edges of altered sandstone tongues. The redox-interface for uranium coincides with that for iron in some of the deposits; in others the uranium interface is separated from the iron interface by as much as 5 m of pyrite-bearing reduced sandstone. The

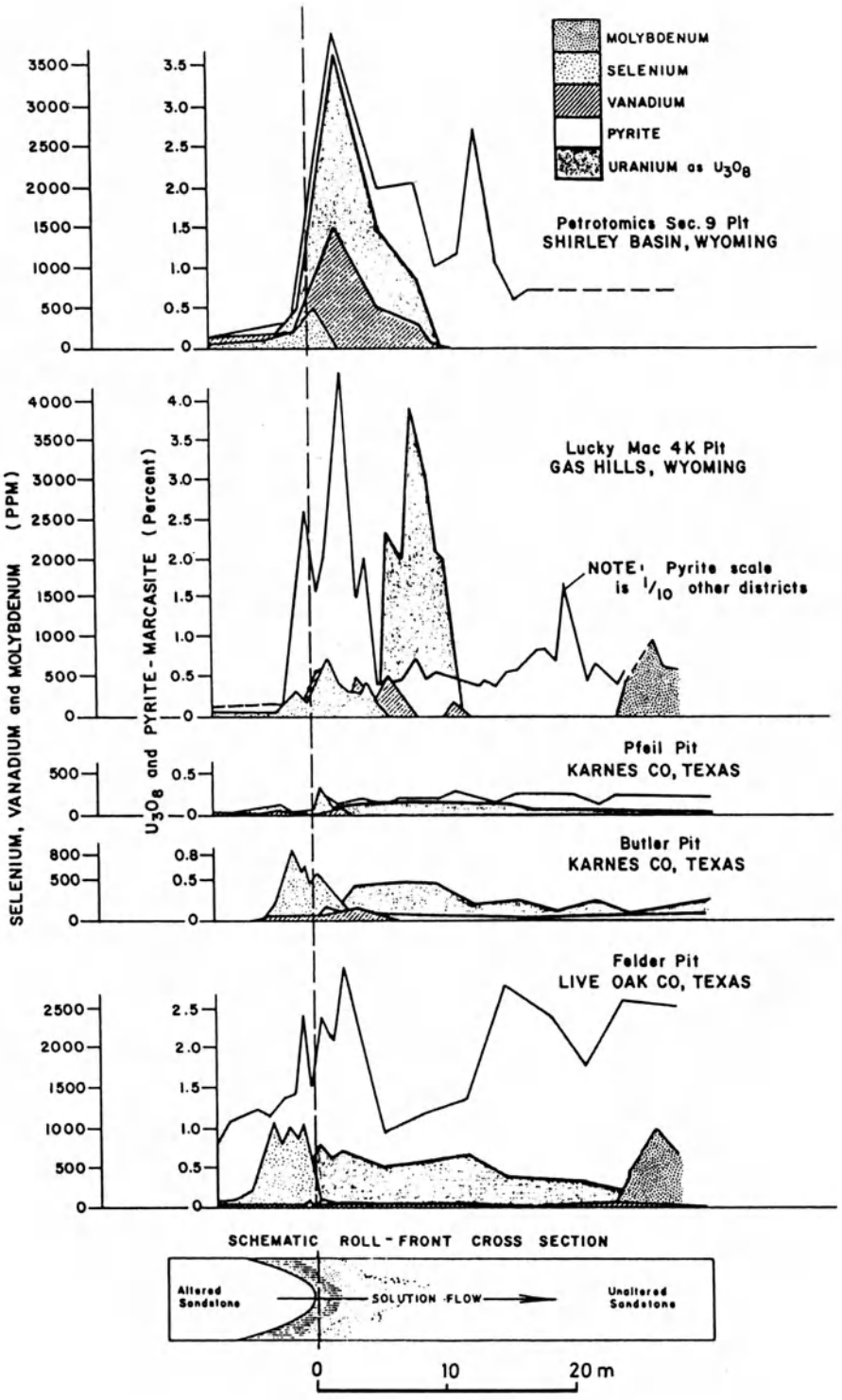

Fig. 5.85. Roll-type uranium deposits, graphic summary of the distribution of U, Se, V, Mo and pyrite across a rollfront in the *Wyoming Basins* (*Shirley* Basin, *Gas Hills/Windriver* Basin), and *South Texas Coastal Plain* (*Karnes* County, *Live Oak* County). (Harshman 1974)

uranium content of altered sandstone is slightly greater (6 ppm) than that of unmineralized reduced sandstone (2 to 4 ppm), at least within 300 m of the rollfront.

Iron, principally as pyrite and to a lesser extent as marcasite, has been added to reduced sandstone at the edges of the altered sandstone tongues. Pyrite gradually decreases in amount away from the edges toward unaltered sandstone. In most deposits it extends beyond the uranium mineralization. Pyrite has been destroyed, generally but not always totally, in most of the altered oxidized tongues. Marcasite occurs together with pyrite and is most abundant in mineralized reduced sandstone at and adjacent to the edges of the altered tongues.

Selenium has been deposited in narrow zones at the edges of the altered tongues, astride the edges, or in reduced mineralized sandstone close to the edges. Selenium in the altered sandstones may be present as ferroselite ($FeSe_2$) or native selenium, but in the reduced sandstones it is generally present as native selenium.

Molybdenum contents range from a few tens of ppm to several percent. It is concentrated at the distal, downdip edge of the mineralized zone. Although molybdenum is present in many deposits, the amounts vary strongly in the different basins.

Vanadium occurs in amounts of a few hundred ppm in most of the deposits. It has been deposited on the convex side of the rollfront where it overlaps the zones of ferroselite, pyrite, and uranium.

Arsenic is present in amounts of <50 ppm to ca. 1%, varying from basin to basin.

Beryllium ranges from 1.5 to 5.5 ppm. It is associated with uranium in the ore and is below 1.5 ppm in altered and unaltered sandstone.

Copper tenors are 10 to 20 ppm. It has not been deposited with any of the other ore minerals.

Organic carbon has generally a rather erratic distribution. Contents range from <0.05 to 2%. Similar ranges are obtained from *mineral carbon*, principally calcite. No consistent direct correlation between the organic carbon and uranium contents of mineralized sandstones could be established.

Sulfate sulfur occurs in amounts of 1% or more in mineralized sandstone. It has been removed from the altered sandstone where it was originally present as gypsum.

Phosphate is present in many deposits. High amounts (up to 1% P_2O_5) can be related to high uranium contents. Uranium/phosphate ratios range from 0.02 to ca. 30, so the phosphate-uranium relationship is not a direct one.

The *quantitative distribution* of the above-mentioned elements on both sides of the rollfront shows that contents of Se, V, and As are greater in altered oxidized sandstones whereas Fe, Mo, and organic carbon are higher in unaltered reduced sandstone.

In its simple form, the *shape* of an ore body resembles a crescent in cross-section, in plan view it is like that of an irregularly laid pipe following the edges of the altered sandstone tongues (Figs. 5.80, 5.84). Ore boundaries generally transect the stratification of the host sandstones at sharp angles, although the tails of the crescent or roll may be peneconcordant with the bedding (Figs. 5.82a, 5.84). The inner contacts of ore and altered sandstones, i.e., the concave side or trailing edge of a roll, are generally sharp, whereas the convex side is gradational. Simple crescent-shaped ore bodies are rare. Most of the ore bodies are complex and consist of several interconnected rolls.

Ore is also not continuous in their lateral direction along the edges of the altered tongues. Small ore bodies are found on the top and bottom surfaces of the altered tongues and are associated with small bodies of residual unaltered sandstone enveloped by the tongues (Figs. 5.80, 5.84).

Dimensions of rollfront type ore bodies are up to 15 m (typically a few tens of centimeters to 10 m) thick in the apex zone. Their widths perpendicular to the redox front range between a few centimeters and several hundred meters. The strike lengths extend up to several kilometers.

Most uranium ore in the rollfronts is in *radiometric disequilibrium*. Chemical U values are higher on the convex side of the roll and radiometric U values are higher on the concave side.

Although the radiometric disequilibrium hampers a precise U/Pb dating of the ore, Dooley et al. (1974) and Ludwig (1978, 1979) could establish apparent *ages* scattering between 22 to 35 m.y., suggesting that mineralization started at least in the Oligocene. Mineralizing or uranium redistribution processes continued over a large time span probably to the present. This may be inferred from studies by Dooley et al. (1964) and Rosholt et al. (1964, 1965a,b). Their data indicate that significant migration within the ore bodies of both ^{234}U and total U occurred within the last 100 000 years.

Potential Sources of Uranium

The two most probable sources for the uranium are uraniferous granitic rocks of Lower Proterozoic to Archean age that crop out in the ranges which surround the uranium bearing basins in Wyoming, and uraniferous tuffs and bentonitic volcaniclastic sediments of Eocene and younger age that overlie or once overlaid the basins.

Granitic rocks as found in the Laramie and Shirley Mountains, and considered to be the sources of the arkose of the Shirley Basin, and partly of the Powder River Basin, contain 0.5 to 7 ppm of leachable uranium (Harshman 1972). Granites of the Sweetwater Uplift, that furnished much of the arkosic host sediment for the Shirley Basin, Gas Hills, and Crooks Gap-Great Divide Basin contain up to 30 ppm U and locally more. These granites lost an estimated 70 to 75% of their original uranium endowment over the past 40 m.y., as deduced from the existing radiogenic lead amounts (Rosholt et al. 1973; Stuckless and Nkomo 1978).

Tuffaceous sediments are anomalous in their uranium content and experienced a loss of the uranium as documented by Zielinski (1980). Zielinski reports 250 ppm U in chalcedony collected from and directly beneath accumulations of rhyolite ash in the White River Formation in the Shirley Basin. He postulates that uranium and silica were leached from the ash by downward percolating groundwater and were precipitated as a uraniferous silica gel directly above the relatively impervious claystone underlying the silicified material. A minimum age of 20 m.y. was obtained for the uraniferous silica and 32.4 ± 2.6 m.y. for the overlying rhyolite tuff. These investigations show that uranium was being leached from ash and carried by groundwater at the time the Shirley Basin deposits are thought to have formed between 20 and 35 m.y. ago.

Spring waters in both granitic and tuffaceous (White River Fm.) terrains contain anomalous uranium contents of up to 8 and 52 ppb respectively (Harshman 1972), supporting any hypothesis deriving the uranium for ore formation from either one of these sources.

Ore Controls and Recognition Criteria

Significant ore controlling or recognition criteria of the rollfront uranium deposits in the Wyoming Basins as listed by Harshman and Adams (1981) are as follows.

Host Environment

- Most favorable host sediments are permeable medium- to coarse-grained carbonaceous, pyrite-bearing (<1 to 3%), arkosic sandstones of fluvial provenance interbedded with impermeable pelitic sediments of late Paleocene to early Eocene age.
- Favorable lithologic settings are found along Paleocene-early Miocene drainage systems in Wyoming, and principally in the central part of the fluvial systems, where stream gradients are moderate and permeable carbonaceous channel sands with considerable longitudinal continuity, interbedded with fine-grained sediments, are deposited in shallow but wide stream channels.
- The rock constituents derived largely from granitic highlands that surrounded the downwarping basins.
- Detrital organic debris present in the sediments was supplied by abundant vegetation.
- Reducing conditions reflected by diagenetic pyrite prevailed in the lower parts of the basins where water tables were high.
- The early Eocene host rocks are covered by fine-grained clastic sediments admixed with volcanic debris which were deposited during the middle Eocene (White River Fm.) to Pliocene interrupted by periods of erosion. This burial protected the early Eocene arkosic rocks and most of their uranium deposits from Pleistocene and recent erosion and oxidation.

Mineralization and Alteration

- Uranium occurs in roll-shaped ore bodies in the marginal zone of oxidized sandstone tongues, i.e., in or immediately adjacent to the redox front that separates oxidized from unoxidized sandstones and that is regarded as the furthest downdip or outer penetration front of oxidizing groundwater.

- A characteristic elemental zoning of U, Fe, Mo, Se, V, and As has developed across the redox interface (Fig. 5.85).
- Uranium accretion apparently is highest
  - at the convex side of the redox-interface at the outer edge of an altered tongue,
  - in gently, generally <5° dipping beds of arkosic sandstone which are interbedded with continuous impermeable beds,
  - where zones of mineralization narrow down,
  - where larger amounts of carbonaceous debris and/or pyrite is present in the rollfront,
  - at changes of permeability partly caused by gradation of coarse arkosic sandstone into more pelitic beds,
  - at changes in strike of the rollfront.
- Deposits range from narrow and high-grade (Shirley Basin, Gas Hills) to wide and relatively low-grade (Great Divide Basin), and there appears to be an inverse relation of grade to width. The lower-grade, wider deposits frequently occur in sandstones with small amounts of carbonaceous plant remains and/or small amounts of pyrite in the unaltered host rock. This contrasts with larger amounts of carbonaceous debris and/or pyrite associated with the higher-grade relatively narrow deposits.
- The edge of the oxidized tongue is not everywhere uniformly mineralized, and ore bodies are dispersed at irregular intervals along it. The best ore bodies seem to be where there are changes in strike of the tongue's edge and where the direction of flow of the solutions was nearly perpendicular to the edge of the tongue. Local concentrations of carbonaceous material and/or pyrite may additionally produce very reducing conditions in local areas and thus cause increased deposition in those areas.

Metallogenetic Concepts

A variety of models have been put forward to explain the formation of the Wyoming roll-type uranium deposits.

Harshman and Adams (1981) have comprehensively analyzed all information on the formation of this type of uranium deposits in Wyoming and elsewhere. The following is an

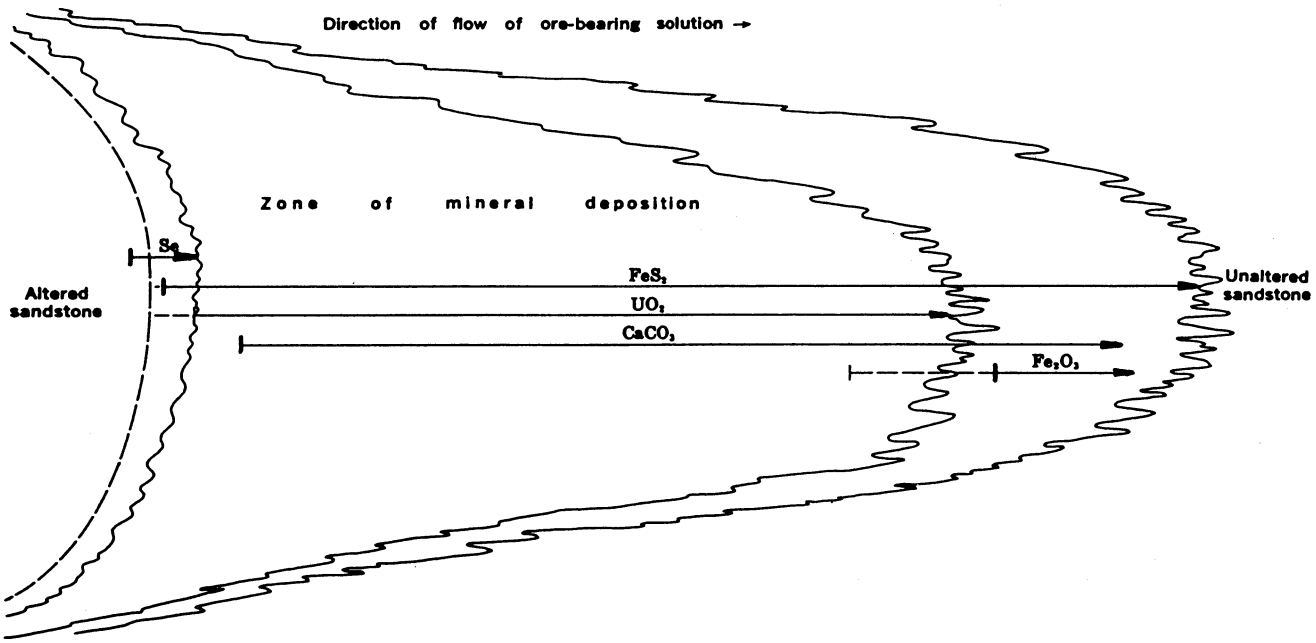

Fig. 5.86. Shirley Basin, graphic summary of epigenetic mineral deposition. *Length of arrows* indicates relative positions and widths of zones through which minerals were deposited; *dashed lines* show intervals of possible deviations from normal conditions. In a general way, the *tails of the arrows* at the left side of the figure indicate the points at which the various elements or compounds began to deposit as a unit of ore-bearing solution flowed toward the right from the altered sandstone tongue to the left. The *arrow heads* show the points at which deposition stopped for the particular position of the rollfront shown. As the rollfront advanced to the right, so also did the zone of precipitation for each element or compound. (Harshman 1972; Harshman and Adams 1981)

excerpt largely based on their findings and conclusions, unless otherwise cited.

Uranium deposits as found in the Wyoming Basins are related to roll or *redox fronts* that are the frontal edges of an altered sandstone tongue in permeable arkosic sandstone interbedded with less or impermeable strata.

A rollfront is a dynamic feature migrating down a hydrologic gradient, generally basinward, by oxidation and solution on its updip side and reduction and deposition on its downdip side. In sensu stricto, the redox front is an oxidation-reduction interface for iron. This interface may, but mostly does not, coincide with the redox interfaces of other elements (Fig. 5.86). Nevertheless, there is a striking similarity in the distribution of elements and minerals along the redox fronts in all of the roll-type uranium deposits in the Wyoming Basins and in other districts as well, e.g., Black Hills or Texas Coastal Plains. Neither the size of the deposit nor the geological environment in which it is found seem to have had much effect on this distribution, a fact that suggests that similar genetic processes were responsible for all rollfront uranium deposits.

Uranium ore formation began in Wyoming after the deposition of the White River and younger formations, i.e., at about Oligocene time when *oxygenated groundwater* started to enter the exposed or truncated edges of the early Eocene sediments in the Wyoming Basins. This water originated in the granitic, metamorphic, and sedimentary rocks of the mountains updip from the host rock outcrops and moved down the flanks of the basins.

There is general agreement that this groundwater flow was the mechanism for the alteration in the host rocks and the formation of the deposits associated with them.

Furthermore, all of the elements in the deposits and the character of the alteration associated with them can be related to the geochemistry of groundwater under the environmental conditions extant in the Wyoming Basins at the time the deposits are thought to have formed.

The *physico-chemical mechanism* for dissolution, migration, and precipitation of the various elements in rollfront type deposits is to a major extent a function of changes of the oxidation potential (Eh) and of the grade of acidity (pH) of the mineralizing fluids.

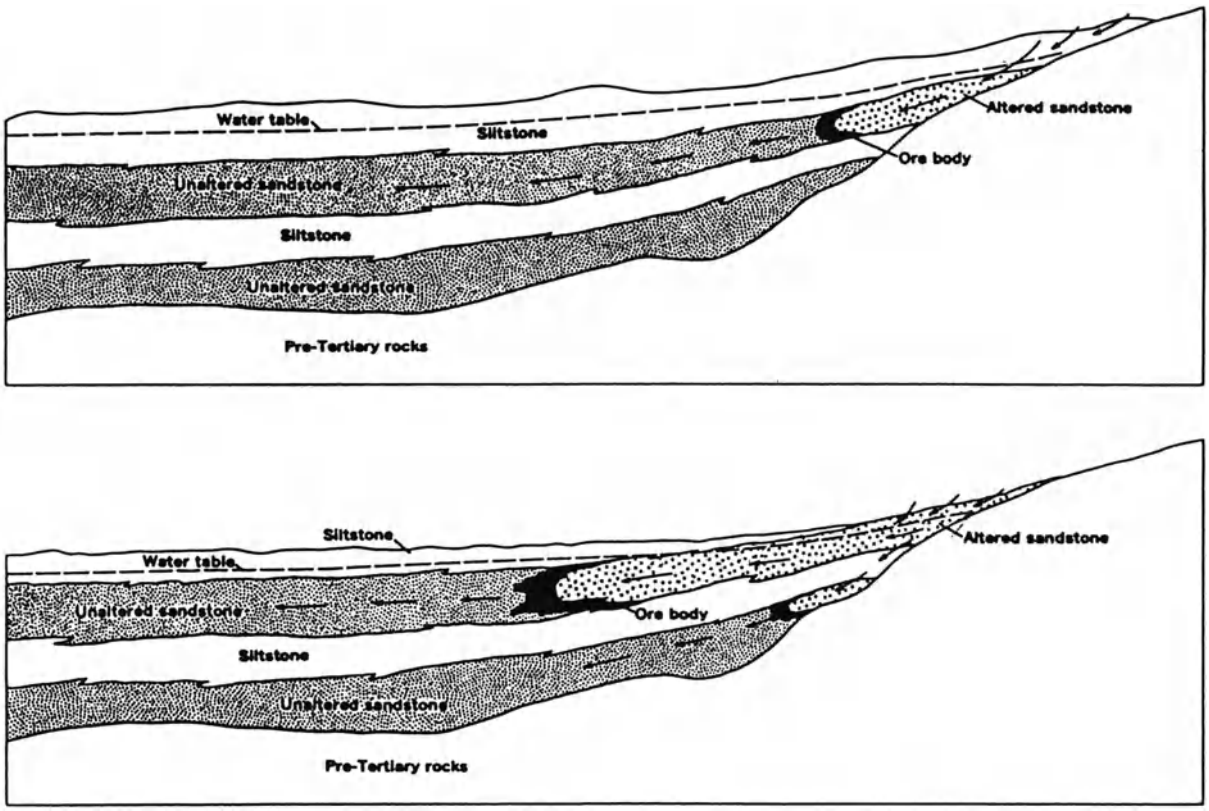

Fig. 5.87. Wyoming Basins, general scheme of flow paths for mineralizing fluids. (Harshman 1972)

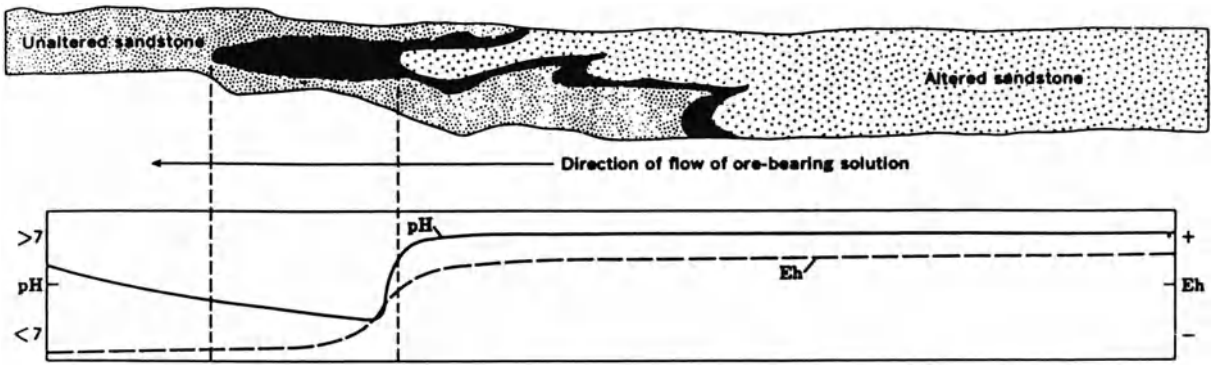

Fig. 5.88. Wyoming Basins, postulated Eh and pH conditions for groundwaters during transportation and deposition of uranium and other elements. (Harshman 1970)

Uranium was probably transported in the hexavalent state as a uranyl-ion. Somewhat generalized, it can be said with respect to alkalinity that, in the presence of phosphorous, uranyl-ions form predominantly (more than 50%) complexes with phosphate between pH 4.5–7.5. In the absence of phosphate, uranyl carbonate complexes predominate above pH 4.5, but in the presence of $UO_2(HPO_4)_2$, they predominate only above pH 7.5.

Vanadium, selenium, arsenic, and *molybdenum* all form oxygenated anionic complexes and can be carried in those forms by solutions of pH near 8 and Eh above −200 mV, conditions extant in ground waters of the Wyoming Basins. Other elements in the ore are probably carried in solution as simple cations.

Figure 5.87 shows the postulated paths of *alteration and ore-forming solutions* and Figure 5.88 the presumed path of a unit of solution, within an Eh-pH diagram, as the solution moves from the oxidizing environment of the altered sandstone through the rollfront and into the unaltered sandstone. The postulated decrease in Eh downdip away from the redox front for iron would cause elements requiring the lowest Eh for this reduction to be deposited the furthest advanced from the edge of the iron redox interface. Figure 5.89 is a composite Eh-pH diagram showing the equilibrium boundaries between

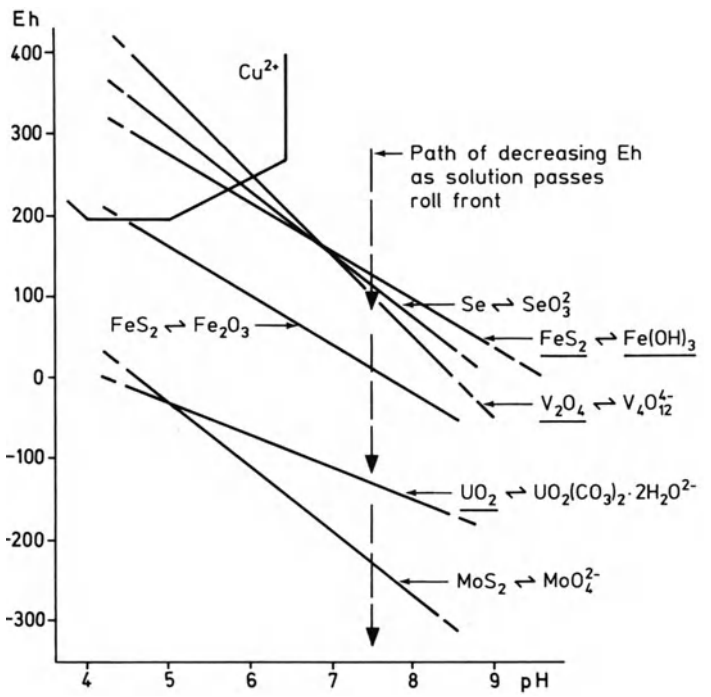

Fig. 5.89. Roll-type uranium deposits, composite Eh-pH diagram for the mobility and stability of the principal elements. Solid phases are underlined. (Harshman and Adams 1981 based on Harshman 1974, with data from Garrels 1960; Garrels and Christ 1965; Hansuld 1966; Hostetler and Garrels 1962; Lakin 1961; Lisitsin 1969)

the relatively soluble and insoluble forms of selenium, vanadium, uranium, and molybdenum and between pyrite and two ferric iron compounds, expressed for conditions of temperature, pressure, and solution composition, and concentration that approximate the likely but somewhat simplified conditions in the mineral-bearing solutions. If one assumes a starting solution pH of 7.5, then decreases its Eh from +300 to −300 mV near the rollfront, at constant pH, the diagram predicts the path of solution Eh will intersect the element boundaries in the same order that they are actually found in rolltype deposits (Fig. 5.85). The diagram also shows that a one- or two-unit decrease in pH concurrent with decreasing Eh will not change the sequence of deposition.

Investigations by Lisitsin and Kuznetsova (1967) on groundwater collected below the permanent water table along traverses extending from altered sandstone through ore and into unaltered sandstone in a sedimentary basin in the USSR confirmed Eh and pH conditions almost identical with those of the Wyoming Basins and shown in Fig. 5.88.

Although there is wide agreement on the concept of a migrating redox front responsible for the ore formation, there remains some disagreement on the processes involved. Two *alternative geochemical systems* are paramount, biogenic-biochemical processes, and chemical processes. Perhaps a combination of both might have accomplished the oxidation, migration and reduction environments necessary for the ore formation as summarized by Harshman and Adams (1981) in the following.

Biochemical system: Rackley (1972) states that an all-biogenic system involves two species of bacteria functioning in two very restricted environments of different Eh and pH zones, sharply separated from one another by the redox front. On the reduced side of the front (Fig. 5.90) anaerobic bacteria of the genus *Desulfovibrio* predominate. They are sulfate reducers, derive their energy from organic matter in the sandstone or in solution, and produce H_2S. Other bacteria may assist in breaking down cellulose into products usable by *Desulfovibrio* in its life process. These bacteria are strict anaerobes and create an environment of pH 7.8 to 8.4 and an Eh of −200 mV or less.

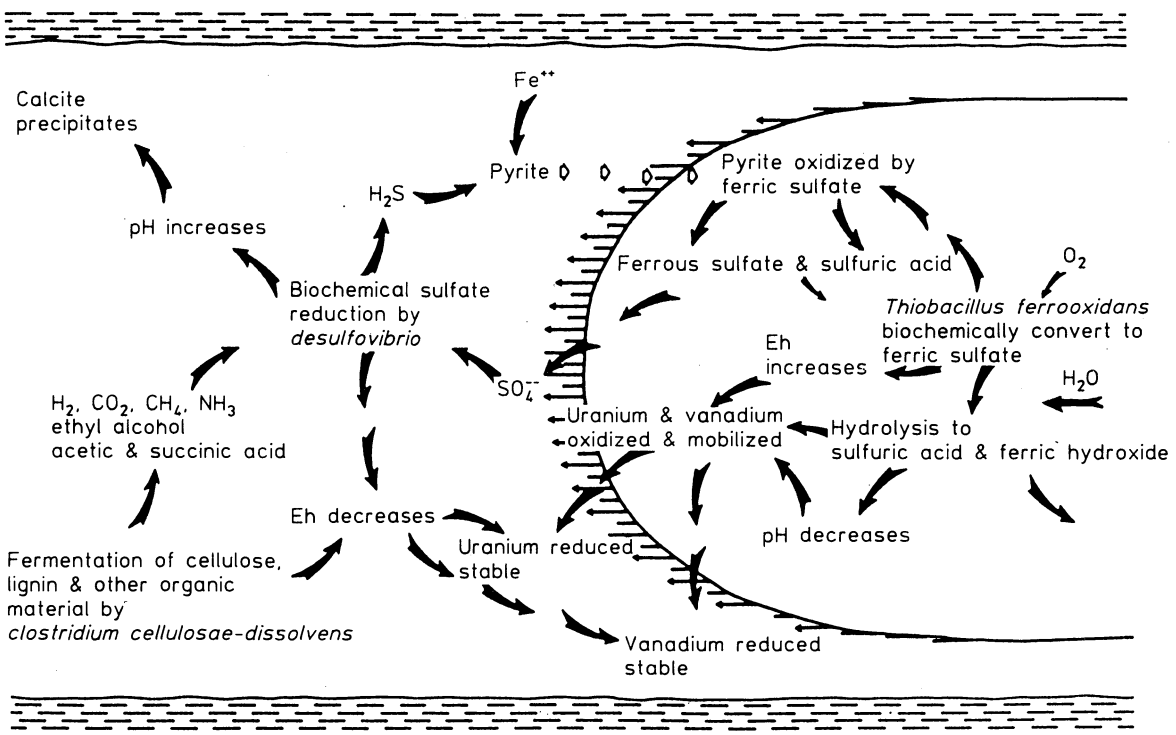

Fig. 5.90. Wyoming Basins, possible chemical reactions in a host sand bed (*white*) involved in the formation of and across a rollfront due to activity of bacteria. *H_2O arrow* indicates flow direction of solution. (After Rackley 1972) (reprinted by permission of AAPG)

On the oxidized or altered side of the front, *Thiobacillus ferrooxidans* and related bacteria predominate. They are strictly aerobic, derive their carbon from CO_2, their energy from nitrogen and sulfur compounds, hydrogen, and iron, and they are capable of producing pH as low as 1.8, although the optimum pH for maximum activity is from 2 to 4. In addition to producing a low pH, they are capable of producing Eh values as high as +760 mV although such high values are unlikely in a natural environment. *Thiobacillus* is thought to act as an intermediate agent in the conversion of pyrite to iron hydroxide and eventually to goethite, hematite, or high iron montmorillonite. The first step is the reaction of pyrite, ferric sulfate and water to produce ferrous sulfate and sulfuric acid; the second step, the biochemical oxidation (by *Thiobacillus*) of ferrous sulfate and sulfuric acid to ferric sulfate and water, and finally the hydrolysis of ferric sulfate to ferric hydroxide and sulfuric acid. Excess sulfate in the system is carried across the front into the reducing environment of *Desulfovibrio*, where it is reduced to H_2S.

The biogenic system is almost self-perpetuating and needs only oxygen, pyrite, CO_2, and organic matter to complete the oxidation, migration, and reduction cycle required by a dynamic system of deposition. The needs of the system can be met by constituents of the host sandstones (pyrite, organic matter, CO_2) and the ore-bearing solution (oxygen and CO_2).

With respect to the need of pyrite, Austin (written commun. in Harshman and Adams 1981) points out that there is no need for sulfide to initiate the process as long as there is a supply of sulfate in the groundwater. However, it is likely that once the process is started, at least part of the sulfate will be provided by oxidation of pyrite or other sulfides, and if the sulfide is pyrite, oxidizing bacteria can, and most likely will, speed up the process and provide the continuous system described. If the sulfide is a less stable species, such as marcasite, or other metal sulfides, the process has much less need of oxidizing bacteria. The biogenic system requires no sulfur more reduced than sulfate for initiation, whereas the inorganic system requires more reduced phases such as sulfide.

Studies by Thode et al. (1951) on the role played by sulfate-reducing bacteria reveal that the bacteria selectively reduce the lighter ^{32}S. Cheney and Jensen (1966) report that sulfur isotope analyses from the Gas Hills, from both diagenetic pyrite in unaltered sandstone and pyrite in the ore bodies, have the wide isotopic spread in the $^{32}S/^{34}S$ ratios and the relative enrichment in ^{32}S that is characteristic of H_2S of biogenic origin. Reynolds and Goldhaber (1983) arrive at a similar conclusion, based on their sulfur isotope studies, for pre-ore-stage pyrite.

Some support is given the biogenic system by the investigations of Lisitsyn and Kuznetsova (1967). They sampled waters from wells and mine openings in and near roll-type deposits in an artesian basin at an undisclosed location in the USSR. From the limited geological data given, one can conclude that the deposit (or deposits) is similar in all major aspects to those found in the Wyoming Basins, and that it was forming at the time of their investigation. The host rocks are permeable Cretaceous sandstones, and the waters flowing in the mineralized zone have a pH of about 7.5, and an Eh of about −200 mV. The authors conclude that (a) the negative Eh results from the anaerobic activity of microflora that produce H_2S and H_2, and (b) the character and distribution of elements within the deposit depend on the relative amounts of the various products of microbiological activity.

Lisitsyn and Kuznetsova's (1967) data are difficult to analyze, but they seem to confirm the presence of H_2- and H_2S-forming bacteria in the water on the reduced and mineralized side of the oxidation-reduction interface, but the presence of *Thio*-bacteria in the oxidized sandstone near the interface is open to serious question.

The chemical-biochemical concept postulates that mineral-bearing solutions are alkaline and oxyenated when they approach the redox interface. Without the aid of bacteria, the solutions oxidize pyrite to sulfuric acid and ferrous sulfate. The oxidation process will be slow if pyrite is the only sulfide, but much faster if marcasite or other sulfur-deficient species are present. These products are carried downdip into the reduced mineralized zone, where sulfate-reducing bacteria convert the sulfate to H_2S and the sulfuric acid is converted to gypsum by the alkaline environment of the slightly calcareous arkose.

Chemical system: Granger and Warren (1969, 1974, Fig. 5.83) have shown that solution, migration, and redeposition of the elements along a rollfront can be accomplished by inorganic chemical reactions and without the intervention

of bacteria. They recognize the probability that the widely disseminated pyrite in the unaltered ground and that destroyed in the altered tongue is of biogenic origin and formed shortly after deposition of the host sediments. Their thesis is that oxidation of pyrite at the rollfront is accomplished by the ore-bearing solution, but that the amount of oxygen in that solution is limited. This results in the formation of soluble, metastable, partly oxidized sulfur species which are carried downdip by the ore-bearing solution until they spontaneously undergo disproportionation; that is, they divide into equivalent amounts of more reduced species such as H_2S, and more oxidized species such as sulfate $(SO_4)^{2-}$. Sulfate is kinetically inert to further reduction or oxidation reactions and this leaves the more reactive reduced metastable sulfur species and H_2S to control the environment. Chemical theory and laboratory experiments support the above considerations and show that isotopic fractionation of sulfur, similar to that caused by biochemical reactions, can result from inorganic chemical reactions. It appears therefore, that a pyrite-bearing sandstone is completely capable of establishing and maintaining a rollfront, once oxygenated waters are introduced, without the participation of any organic components whatsoever.

Two other reductants have been proposed because of their spatial relation to the deposits, vegetal material and H_2S.

Coalified woody material: Coalified woody material, or humates derived from such material, are present in all of the host rocks of the Wyoming deposits. For this reason, as well as for the fact that some ore contains as much as 0.5 to 1% organic carbon, some investigators suggest that organic carbon is the direct reductant of uranium and associated elements.

However, the correlation between uranium and organic carbon within the roll-type system is neither simple nor consistent, hence the precipitation of uranium by organic material may not be the only important mechanism. Studies by Schmidt-Collerus (1969, 1979), Kochenov et al. (1965), and others, suggest that the organic matter may initially complex uranium from solution to subsequently be reduced by the oxidation of some combination of carbon and sulfide, and perhaps other elements.

Hydrogen sulfide: The close spatial relationship between the uranium deposits in the Wyoming Basins and oil- and gas-producing Cretaceous formations suggests a possible genetic relationship between uranium deposition and H_2S from sour gas. Grutt (1957) concluded that H_2S derived from sour gas was the precipitant for the ore minerals in the Gas Hills area. He pointed out that producing oil and gas wells are adjacent to the area, that the gas from the wells contains as much as 2% H_2S, that there are gas seeps in the area, and that exploration drilling encountered H_2S in the Wind River Formation. He proposed that sour gas ascended along the faults that border the district on the south, entered the unconformity at the base of the Wind River Formation, and entered the host sandstone where it rested on the unconformity.

The above presented documentations make it difficult to decide what kind of chemical processes were ultimately responsible for the ore-forming chemical environment in and adjacent to rollfronts. More recent work by Goldhaber and Reynolds (1979 and 1983) may shed some light on this problem. Their experimental work and studies on marcasite of Texas and Wyoming uranium deposits, and on geochemical environments analagous to those governing the formation of rollfront deposits, indicate that relatively low pH and the presence of elemental sulfur favor marcasite, whereas higher pH and the presence of polysulfide ions favor pyrite, i.e., a dominant factor in the formation of marcasite or pyrite as ore-stage minerals is the complex interrelationship of pH and sulfur species that are the precursors of iron-disulfide minerals.

Conditions that favor marcasite as the dominant ore-stage iron disulfide are most likely to arise in noncarbonaceous rocks. In rocks with considerable organic matter, the presence of polysulfide ions and pH buffering by anaerobic bacterial metabolic processes apparently led to the formation of ore-stage pyrite. Since in the Wyoming Basins most of the ore-stage iron sulfide is in pyrite, this can be regarded as a clear implication that biochemical activity was responsible for the reduction along the redox front.

In summary, Harshman and Adams (1981) view the actual *ore-forming processes* as follows:

Oxygenated groundwater that carried uranium and associated elements was probably derived in part from the basin flanking Precambrian granitic massifs and in part from the tuffaceous White River Formation. Where these solutions reached equilibrium with the host rocks by the oxidation of the rock components, particularly pyrite and

carbonaceous debris, an interface, the rollfront, was established between oxidizing conditions in the updip part of the host and reducing conditions in the downdip part. Across this interface, deposition of U, Fe, Se, Mo, V, and other elements carried in solution has been most pronounced at the respective redox boundary for each element, and decreased rapidly as the solution moved beyond that interface into the reduced zone.

Any mineralized zone established at any time in the cycle would migrate generally in the downdip direction of the groundwater flow by oxidation and solution on the updip side of the mineralized zone and reduction and redeposition on the downdip side. A continuous extrinsic supply of uranium and associated elements in the mineralizing solution passing through the zone of deposition would cause the mineralized zone to increase in both grade and magnitude and eventually to reach, particularly in gently dipping beds, the size of the presentday deposits.

The processes described above continued downdip in the host rocks for distances of 8 to 20 km and to depths of several tens to several hundreds of meters below the ground surface. As long as oxygen and slightly mineral-bearing water is supplied to the redox interface, mineralization will accumulate at a rate governed by the supply of oxygen, amount of pyrite and/or carbonaceous material, biological or abiological reduction of sulfur, rate of flow of the mineral-bearing solution, and possibly the length of the altered tongue. The process stops when either the hydrologic system changes, the reduced zone is destroyed by oxidation, or the oxygenated water entering the host sandstone at or near the outcrop or paleo-outcrop becomes diluted by reducing water entering the host from overlying sediments.

Some of the deposits, particularly those associated with limonite-bearing altered tongues (e.g., in the Powder River Basin) may have undergone recent remobilization, migration, and redeposition of elements in the original deposits.

In case of a reversal of the groundwater flow, for example by tilting of the area, as indicated by Harshman (1972) for the Shirley Basin, previous deposits could even be turned into a stage of destruction.

References and Further Reading for Chapter 5.4.4
(for details of publications see Bibliography)

Adler 1974; Adler and Sharp 1967; Anderson 1969; Armstrong 1970; Austin 1970; Baily 1965, 1969, 1980; Cheney and Jensen 1966; Chenoweth 1980; Childers 1970, 1974; Crawley 1983; Curry 1976; Dahl and Hagmaier 1976; Davis 1969; Denson and Chisolm 1971; Files 1970; Fischer 1970; Gabelman 1970; Gabelman and Krusiewski 1964; Galloway 1979a, 1979b; Goldhaber and Reynolds 1979; Granger and Warren 1969, 1978, 1979; Gruner 1956; Grutt 1957, 1972; Harris 1984; Harshman 1962, 1966, 1968, 1970, 1972, 1974; Harshman EN pers. commun.; Harshman and Adams 1981; Houston 1969; Jensen 1958; Klingmüler 1989; Keefer 1970; King and Austin 1966; Lange and Kidwell 1974; Ludwig 1978, 1979; Ludwig and Grauch 1980; Masursky 1962; Melin 1964, 1969; Rackley 1968, 1972, 1976; Reade 1976; Santos 1981; Santos and Ludwig 1983; Seeland 1976; Sharp and Gibbons 1964; Sharp et al. 1964; Sherborne et al. 1980; Sheridan et al. 1961; Stephens 1964; Van Houten 1964; Vickers 1957; Vine and Tourtelot 1970; Warren 1971, 1972

5.4.5 Roll-Type Extrinsic Sulfide-Uranium Deposits in Phanerozoic Coast Plain Sandstones: South Texas Coastal Plain, USA

The Texas Coastal Plain, also referred to as the South Texas Uranium Region or South Texas Mineral Belt, contains sandstone type uranium deposits in a 20 to 45 km wide curvilinear belt which approximately parallels the coast of the Gulf of Mexico about 130 km inland. The mineral belt is almost 400 km long in a NE to SSW direction, extending from eastern-central Texas to the Mexican border, and probably continues into Mexico. Some hundred properties have been mined principally in Karnes, Live Oak, McMullen, and Duval counties, but also in some other counties (Fig. 5.91a).

Total reserves in the south Texas region are estimated at between 45 000 and 80 000 mt U_3O_8, with average ore grades running around 0.1% U_3O_8.

The south Texas uranium deposits are roll-type mineralizations to some extent similar to those in the Wyoming Basins. But in contrast to the latter, the reduction of the host rocks resulted from the influx of reductants such as H_2S, and the deposits occur in a marginal marine environment. Therefore, the south Texas uranium deposits are classified as roll-type extrinsic sulfide-uranium deposits in coast plains (class 4.2.2, Chap. 4).

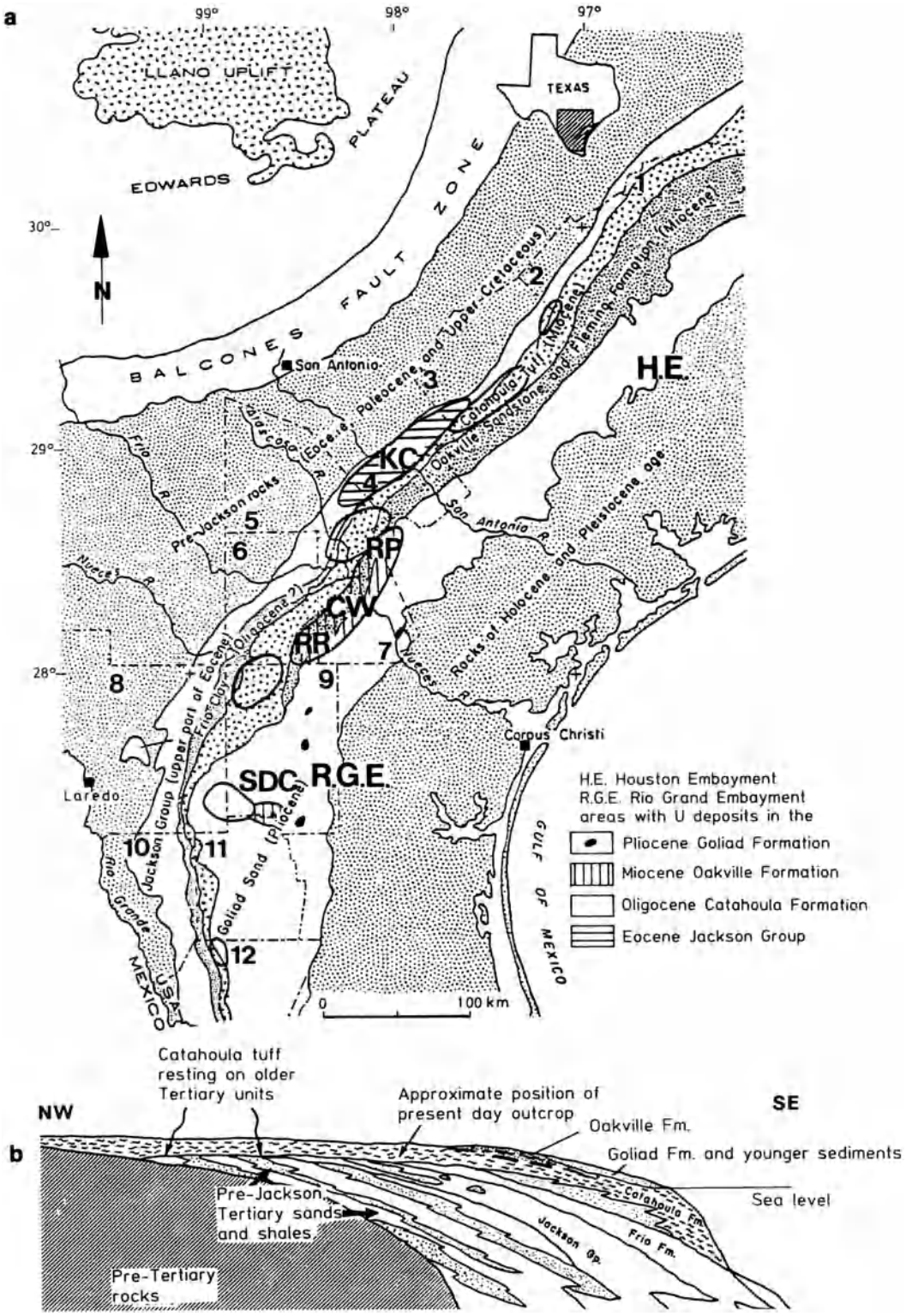

Fig. 5.91. South Texas, generalized geological map (**a**) and NW-SE cross-section (**b**) of the coastal plain and location of areas containing major uranium deposits. Host units for deposits are fluvial-marginal marine sediments of the Eocene Jackson Group, Oligocene Catahoula, Miocene Oakville and Pliocene Goliad formations. Counties containing U deposits: *1* Washington; *2* Fayette; *3* Gonzales; *4* Karnes; *5* Atascosa; *6* McMullen; *7* Live Oak; *8* Webb; *9* Duval; *10* Zapata; *11* Jim Hogg; *12* Starr. Uranium districts: *K.C.* Karnes County; *R.P.* Ray Point; *C.W.* Clay West-Burns; *R.R.* Rhodes Ranch area; *S.D.C.* South Duval County Mineral Trend. (After **a** Crawley et al. 1983 based on Eargle et al. 1975; **b** Adams and Smith 1981) (**a** reprinted by permission of AAPG)

The following description is largely based on Adams and Smith (1981), who have published a concise compilation of the south Texas uranium deposits which incorporates information from many authors, particularly from Eargle, Fisher, Galloway, Weeks, and their coworkers.

Geological Setting of Mineralization

The Texas Coastal Plain is underlain by more than 15000 m of flat-lying interbedded marine and nonmarine sediments of Tertiary age which rest on Jurassic and Cretaceous sediments (Figs. 5.91a,b). The *Tertiary sediments* were deposited on coastal plains by major river systems and intervening marine transgressions. Instabilities due to the constant loading of sediments into the subsiding gulf led to local faulting particularly to *growth faults* that become younger toward the coast. The principal faults and fault systems form a general arcuate pattern around the basin of sedimentation. *Acid volcanism*, synchronous with part of the subsidence, provided volcaniclastic-rich sediments to a portion of the Tertiary sedimentary sequence.

Associated with the sediments and the contemporaneous growth faults are occurrences of oil and gas, lignite, geothermal resources and uranium. Oil and gas occurrences are controlled regionally by depositional facies and locally by structures which in many cases place sands and shales in juxtaposition, forming ideal traps for hydrocarbon accumulation. Galloway (1977) has estimated that one third of the South Texas Coastal Plain is underlain by closely spaced hydrocarbon reservoirs that are largely fault-controlled.

Host sediments of the known uranium occurrences are sandstones deposited between middle Eocene and early Pliocene (Figs. 5.91a,b, 5.92). Stratigraphic units containing major deposits are particularly the late Eocene *Jackson Group*, late Oligocene *Catahoula Formation*, early Miocene *Oakville Formation*, and the late Miocene-early Pliocene *Goliad Formation*. Deposits of modest size also occur in other formations. Very young uranium was discovered in the Pleistocene *Lissie Formation*. In spite of this wide stratigraphic range, the uranium deposits are restricted to a belt (Fig. 5.91a), the boundaries of which do not entirely correspond with regional geological boundaries. Although the trend does reflect important geological features, such as the strike of the formations and positions of the favorable lithologic facies in some of the host sediments, some geological features cross the trend. Of particular interest are persistent fluvial depositional zones forming *mega-channels*. These mega-channels appear to provide environments important to the location of ore bodies.

In principle, the ore-hosting sequences are flat-lying, dipping about 1° SE and strike around NE-SW almost parallel to the Gulf coast. They are of continental fluvial and marginal marine deltaic, lagoonal, and littoral provenance.

The prominent uranium *host rocks* are permeable, fine-grained, tuffaceous, pyrite-bearing, arkosic sandstones, containing only locally, as in the Jackson Group, carbonaceous plant material. The sands are interbedded with tuffaceous, zeolitic, and bentonitic mudstones, and lignite seams. The volcanics are of rhyolitic, trachytic, and trachyandesitic composition.

Host Rock Alterations

Principal alterations of the host rocks resulted from diagenetic and repeated pre-, syn- and post-ore oxidation and reduction processes. Alterations related directly or indirectly to ore formation resulted in the situation that some deposits are associated with a classical geochemical interface at the edge of an oxidized sandstone tongue whereas other deposits are emplaced in entirely reduced sands. For example, deposits in the Jackson Group are associated with *geochemical rollfronts* located at the edges of altered sandstone tongues. Their host rocks exhibit the general mineralogic and geochemical characteristics of the unaltered downdip and altered, oxidized updip sands similar to those of the rollfront deposits in the Wyoming Basins (see Sect. 5.4.4 for more details on alteration, mineralogy, and chemistry).

In addition to the normal alteration characteristics of a rollfront, some of the south Texas rolls exhibit peculiarities. Adams and Smith (1981) describe, for example, the setting and mineralogy of a roll-type deposit in the South Duval County Mineral Trend. Here, *two alteration zones* exist within the oxidized tongue (Fig. 5.93). The first is well updip from the rollfront and contains Fe-Ti-oxides that are in various states of oxidation. The second extends for a

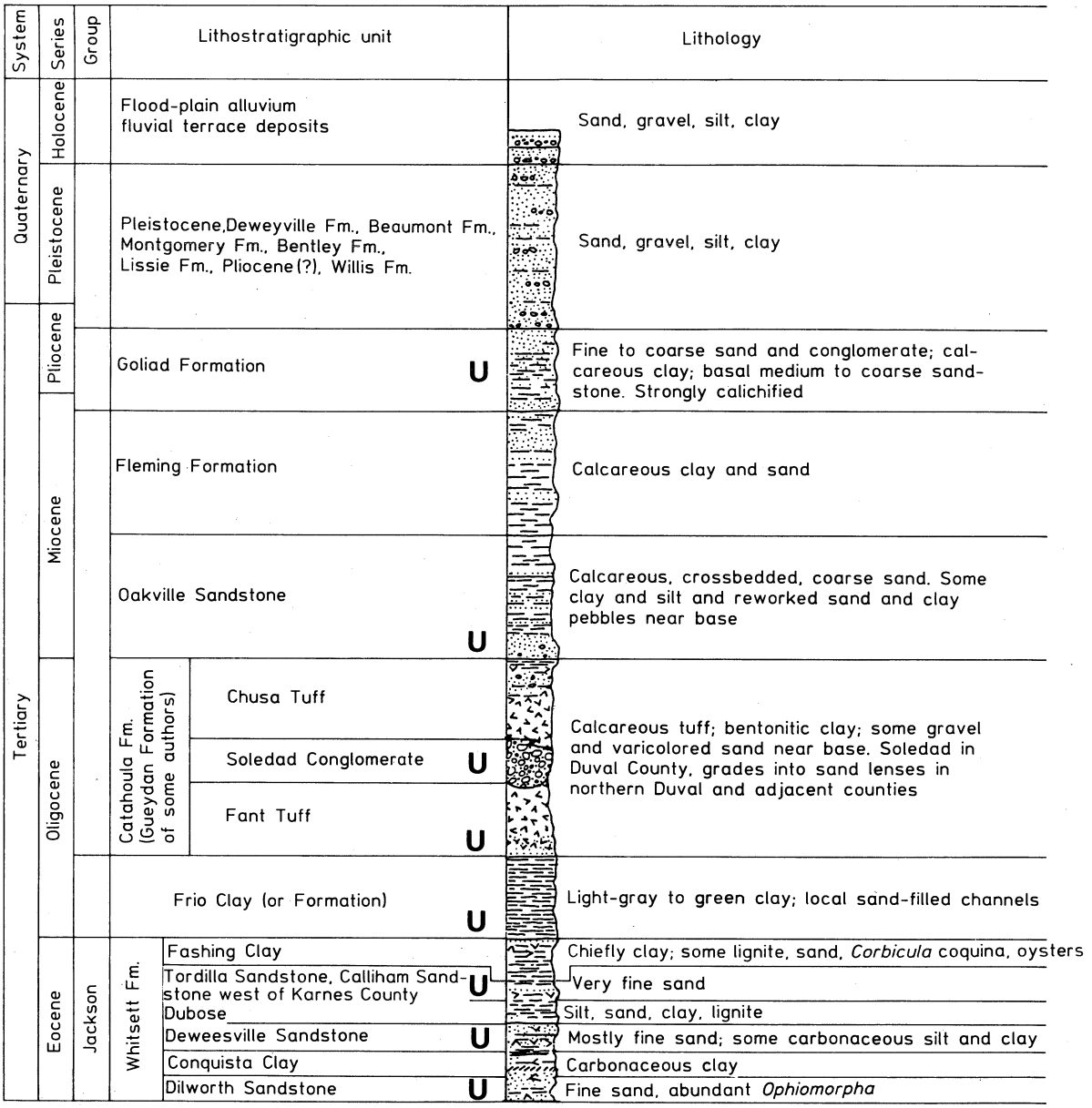

Fig. 5.92. South Texas, litho-stratigraphic column showing the principal uranium bearing units in the Rio Grande Embayment. (After Galloway 1979b)

variable distance back updip from the geochemical interface and contains vestiges of ilmenite and magnetite. In the reduced sands downdip from the rollfront, Fe-Ti-oxides have also been completely destroyed, in part through replacement by pyrite. A subsequent introduction of oxidizing solutions into these sulfide-bearing sands oxidized the pyrite and produced the geometric relations as they are observed today.

At other locations, some roll-shaped deposits occur *entirely* within *reduced, sulfide-bearing sandstone*.

Research by Goldhaber and coworkers supports earlier suggestions that the distribution and

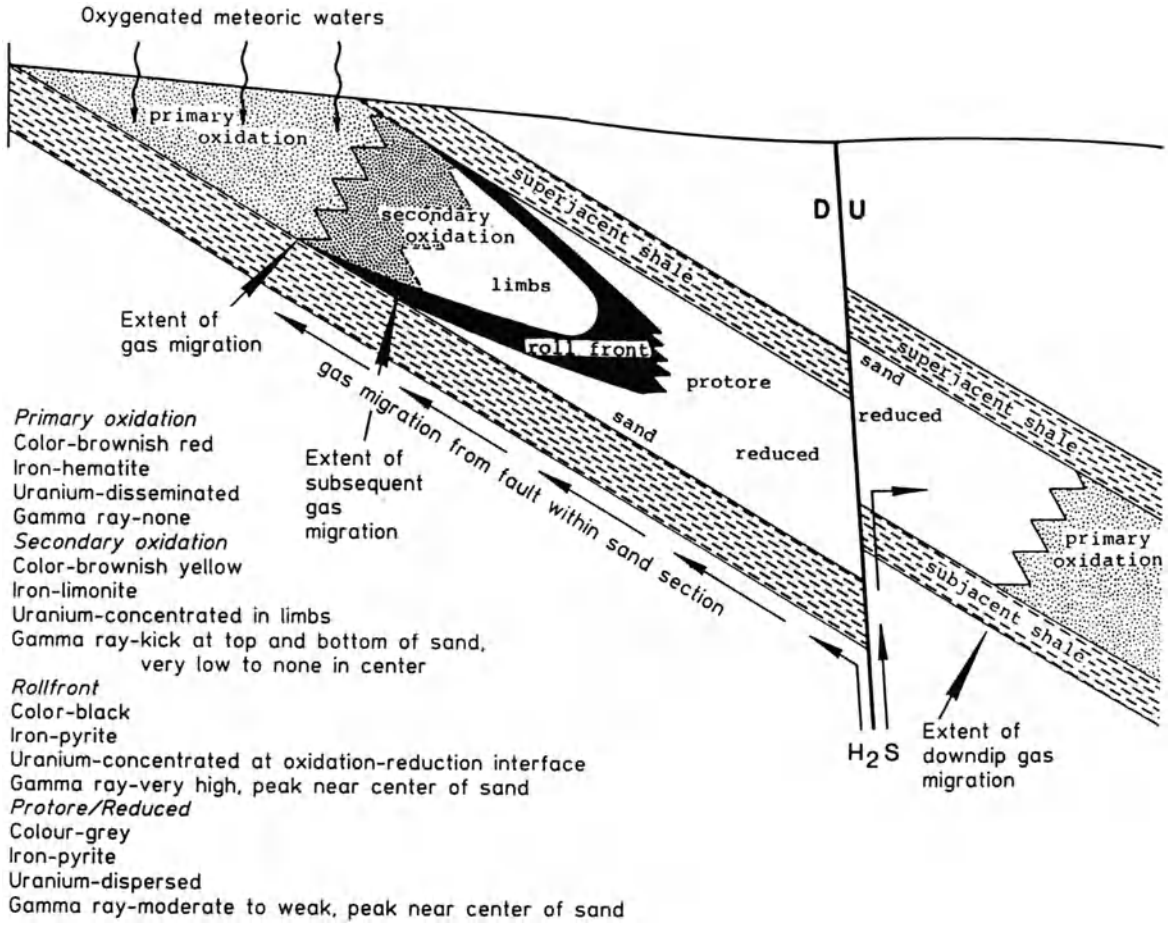

Fig. 5.93. South Texas, diagrammatic section across a rollfront illustrating the relations for fault-controlled influx of reducing media (H_2S, hydrocarbon) leading to secondary reduction followed by partial re-oxidation of the alteration tongue. (Adams and Smith 1981)

abundance of pyrite within the host sands of these deposits probably reflects the *introduction of H_2S* up along faults from various hydrocarbon reservoirs within the Mesozoic-Tertiary sediment pile. Such pre-ore introductions prepared the sands for rollfront development, whereas post-ore H_2S influx produced re-reduction of portions of the altered tongue, leaving the deposit suspended in reduced sandstone. The deposits are, therefore, only a variant of the normal roll-type deposit. Deposits in the Catahoula and Oakville formations contain marcasite in a broad zone downdip from the rollfronts. This marcasite has been interpreted to have formed during ore formation by the oxydative destruction of pre-ore stage pyrite in sulfide-rich, carbonaceous-poor systems (Adams and Smith 1981).

Principal Characteristics of Mineralization

In *unoxidized ore*, the dominant uranium minerals are pitchblende/sooty pitchblende and coffinite. Associated minerals and elements include pyrite, marcasite, calcite; Se, Mo, and locally clinoptilolite, authigenic feldspar, opal, and montmorillonite. Pyrite and marcasite occur in several pre-, syn-, and post-ore stages.

Oxidized ore contains hexavalent uranium minerals, chiefly uranyl phosphates (autunite), -vanadates (tyuyamunite, more rarely carnotite) and -silicates.

The south Texas deposits occur in four principal *geological settings*: (1) In beach sandstones and related sediments; (2) in sandstones along the margins of major fluvial channel systems; (3) in sandstones close to faults along which hydrogen sulfide could be introduced into the aquifer; and

(4) in sandstones above salt domes. The various deposit settings may overlap or be superimposed upon one another.

Within these environments, uranium has formed ore bodies of roll-type and nonroll-type shape (Figs. 5.93, 5.94, 5.95).

Many of the deposits are of the classical *roll-front type* emplaced at the margins of alteration tongues in sandstone. They display the characteristic uranium disequilibrium patterns, elemental zoning, and mineral distributions of the Wyoming roll-type deposits (Fig. 5.85).

The shape of these ore bodies is commonly cuspate or C-shaped when they occur in uniform sands that are bounded by impervious shales or siltstones. Many deposits exhibit a complex geometry, however, due to the often complex interrelations between sand units of variable permeability and pelitic units of very low permeability. Indigenous and introduced reductants exerted an additional influence on the distribution and habit of uranium rolls.

Other deposits do not resemble classical roll-type mineralization in that their geochemical environment is strikingly dissimilar from the roll-fronts of the Wyoming Basins. The important differences of the *nonroll-type* deposits include: (1) the mineralization does not occur at the margin of altered sandstone tongues but rather occurs entirely within reduced, pyrite-bearing practically hematite- and limonite-free sandstone; and (2) the host sands contain essentially no carbonaceous plant material, only abundant disseminated pyrite.

Although anomalous uranium concentrations are widespread in the uranium belt of the Texas Coastal Plain, Adams and Smith (1981) suggest that all noteworthy uranium occurrences appear to be grouped in fluvial *mega-channel systems* which formed and were maintained practically over the entire time span from the early Eocene Wilcox Group to the Pleistocene Lissie Formation. Most of the deposits occur in clusters more or less along the fluvial trends in either one of these mega-channels. An example, the South Duval County Mineral Trend, is given in Fig. 5.96. The exception to this are those deposits in the Jackson Group which formed in littoral environments such as beach sands.

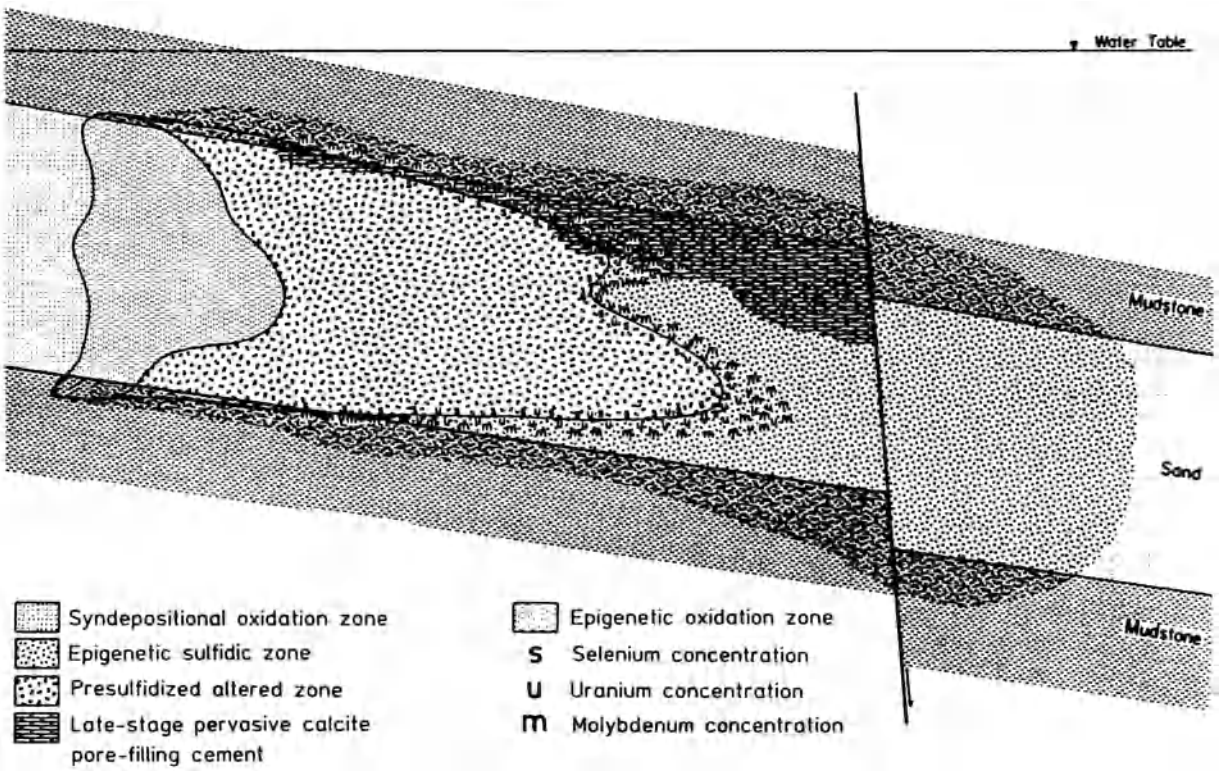

Fig. 5.94. South Texas, diagrammatic section across a roll-shaped ore body illustrating the typical association with a fault zone, and metal and alteration zonation characteristic of Catahoula and younger uranium host aquifers. Multiple epigenetic alteration stages include pre- and post-mineralization sulfidization, ore-stage epigenetic oxidation and modern oxidation. U, Se, and Mo minerals precipitated and are zoned across the front of mineralization. (Galloway 1985)

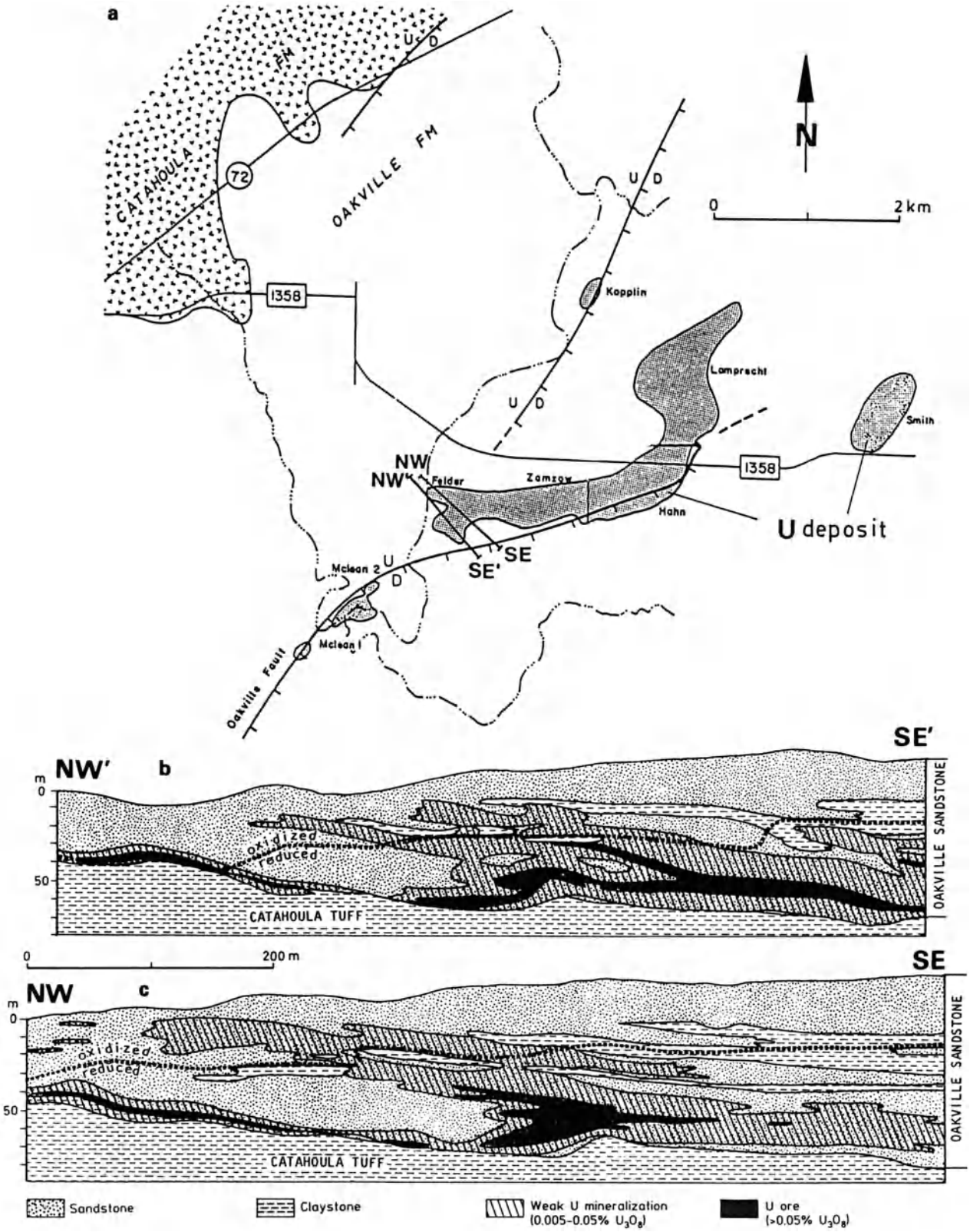

Fig. 5.95. Live Oak County, Ray Point district, Felder-Zamzow-Lamprecht deposit. **a** Map of outline of the Oakville Sandstone hosted deposit. **b** *and* **c** NW-SE sections through the Felder mine with U grade distribution. (After **a** Galloway 1979a; **b** and **c** Klohn and Pickens 1970, modified by Eargle et al. 1975) (see also Fig. 5.97)

A number of mining districts are known within the mega-channel systems (see Table 5.29 and Fig. 5.91a).

Of the listed stratigraphic units, the Catahoula and Oakville formations furnish the most productive uranium hosts. They combine more than 60% of the known uranium reserves in south Texas.

In general, the *dimensions* of south Texas ore bodies tend to be smaller and of lower grade than the roll-type deposits in the Wyoming Basins. They are generally thin, seldom exceeding 5 m in thickness, and rarely occur as stacked or multiple-front deposits, such as are common in some deposits in Wyoming. The average deposit contains only about 5000 mt U_3O_8, and the largest deposits known to date are estimated to contain about 14 000 mt U_3O_8. The average grade is in the order of 0.1% U_3O_8.

Table 5.29. South Texas, the most important mining districts in the mega-channel systems

District	Main ore-hosting formation
Karnes County District	Jackson Group
Ray Point District, Live Oak County	Oakville Fm.
Clay West-Burns Dist., Live Oak County	Oakville Fm.
Rhode Ranch District, McMullen County	Oakville Fm.
South Duval County Mineral Trend	Catahoula, Oakville, Goliad Fms.

Reductants

Two kinds of reducing agents appear to be critical for the south Texas deposits: Hydrocarbons-H_2S in the pyritic fluvial sands of the Catahoula, Oakville, and Goliad formations, and detrital vegetal organic matter in the littoral sands of the Jackson Group.

Hydrocarbons-H_2S: Most of the non-Jackson deposits contain none or negligible quantities of carbonaceous matter, which may be due to oxidation at or shortly after burial, essentially destroying any indigenous carbonaceous material. If this was the case, then the introduction of hydrocarbons-H_2S must have been here a critical factor in the ore-forming process.

The assumption that H_2S introduction occurred into the aquifers probably along faults and presumably from hydrocarbon reservoirs at depth is largely based on the following observations: (a) the spatial distribution of sands containing finely dispersed pyrite with respect to faults, (b) sulfur isotope data, (c) the occurrence of some reduced sandstones entirely within oxidized sandstone, and (d) the virtual absence of carbonaceous material.

Goldhaber et al. (1979) and Reynolds and Goldhaber (1983) established at least four periods

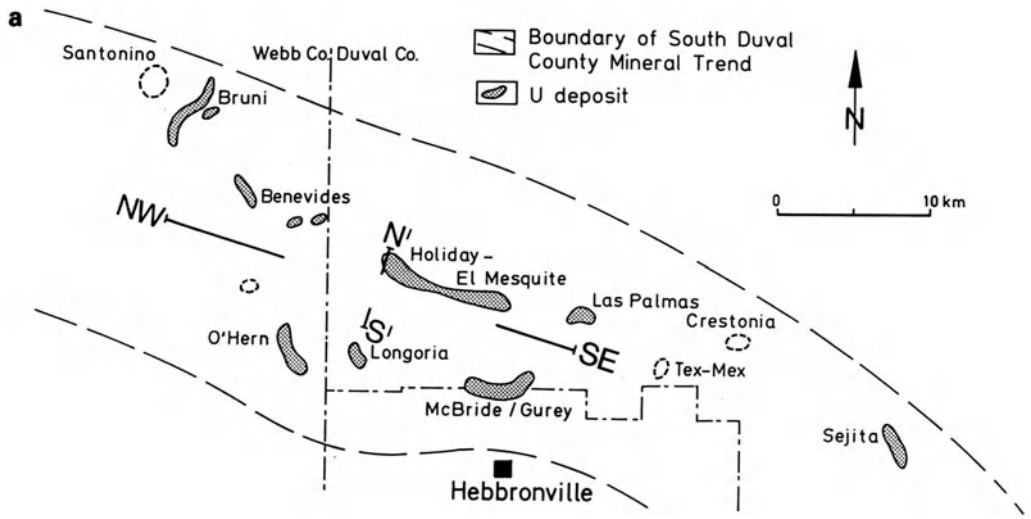

Fig. 5.96. South Duval County Mineral Trend. **a** Map with outline of uranium deposits, **b** NW-SE section. **c** N-S section through the mineral trend showing the stratigraphic position of the U deposits hosted in the Soledad Member of the Oligocene Catahoula Formation in the northwestern part, and of minor deposits in the Miocene Oakville Sandstone in the southeastern part of the belt. Sandstone units are indicated by *patterns* in Sections. (After Adams and Smith 1981)

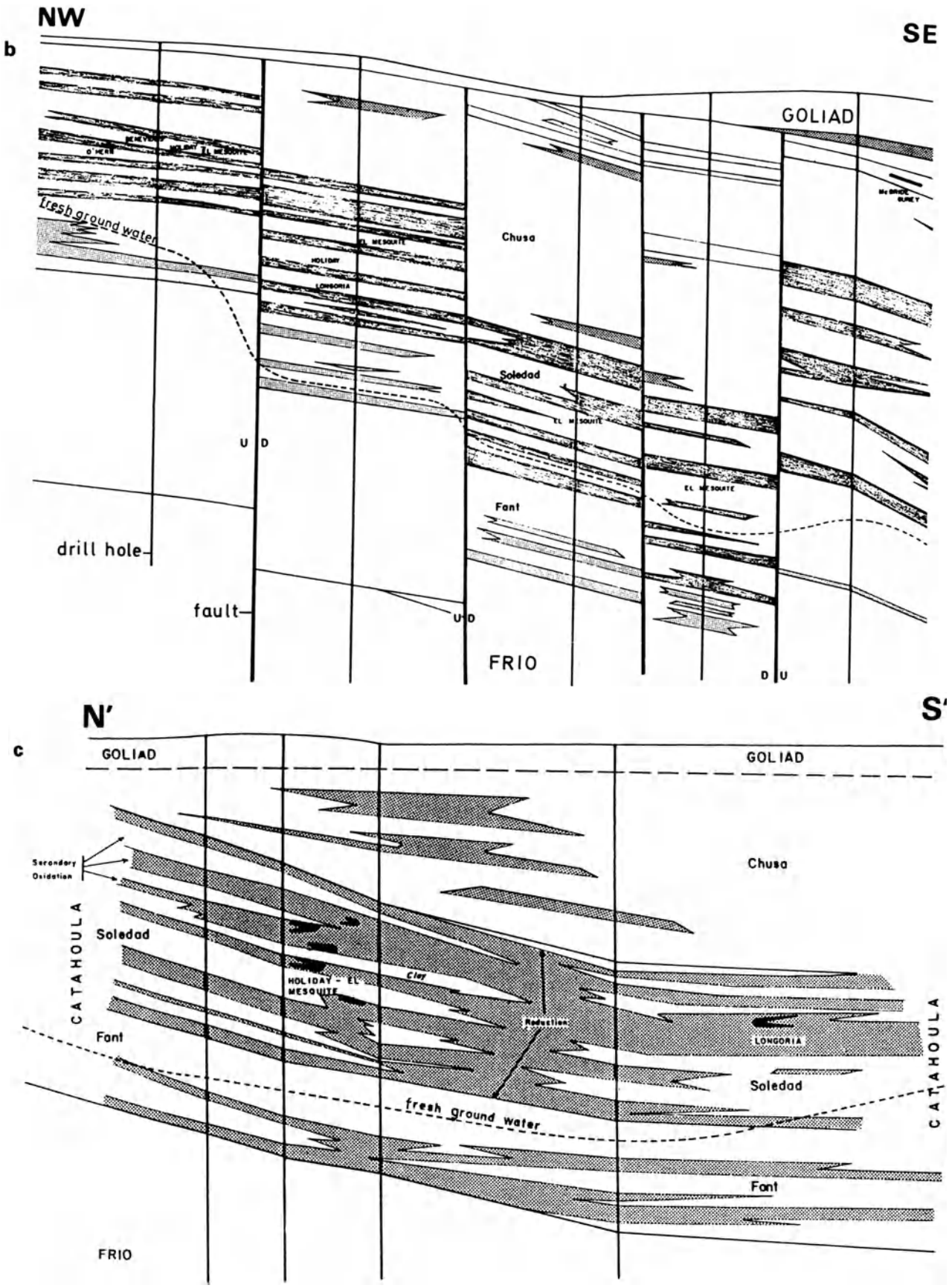
b
NW
SE
GOLIAD
fresh ground water
Chusa
HOLIDAY
LONGORIA
EL MESQUITE
Soledad
U D
Fant
drill hole
fault
U D
FRIO
D U
N'
S
c
GOLIAD
GOLIAD
Secondary Oxidation
Chusa
CATAHOULA
Soledad
HOLIDAY - EL MESQUITE
Clay
Reduction
Fant
LONGORIA
Soledad
fresh ground water
CATAHOULA
Fant
FRIO

of probable H_2S introduction, and the presence of two different sulfur isotopes in the sulfides of Oakville host sandstones: Isotopically heavy sulfur which has been proposed as being derived from the deep Edwards Limestone oil and gas fields and isotopically light sulfur as being derived from shallower horizons. The light sulfur isotopes may have originated by bacterial sulfate reduction in shallow aquifers promoted by the seepage of organic matter from Tertiary hydrocarbon deposits.

Detrital carbonaceous matter: Only sediments of the Jackson Group and possibly of the Carrizo Sand contain abundant plant material which visibly exerted a strong influence on a rollfront formation. Compared with the host rocks of deposits in other Tertiary sequences in south Texas, those of the Jackson Group are of beach sand provenance.

Potential Sources of Uranium

Uraniferous *volcaniclastics* are the most favored source of uranium. This hypothesis is supported by geochemical and geological data provided by Dickinson (1976b), Eargle and Weeks (1973), Galloway (1977), Adams and Smith (1981), etc. The deposits may have derived their uranium either intraformationally from interbedded volcaniclastics, as found in the Catahoula, Jackson, and Oakville formations, or extraformationally from the (former) superposition of the Catahoula or similar fertile tuffs above an unconformity.

Ore Controls and Recognition Criteria

Significant ore controlling or recognition criteria of the south Texas uranium deposits as listed by Adams and Smith (1981) are as follows.

Host Environment

- The uranium deposits occur within or in proximity to permeable sandstones which range in composition from littoral quartz arenites to fluvial arkoses. Metallogenetically, the sandstones appear to be of primary importance as aquifers for migrating uraniferous

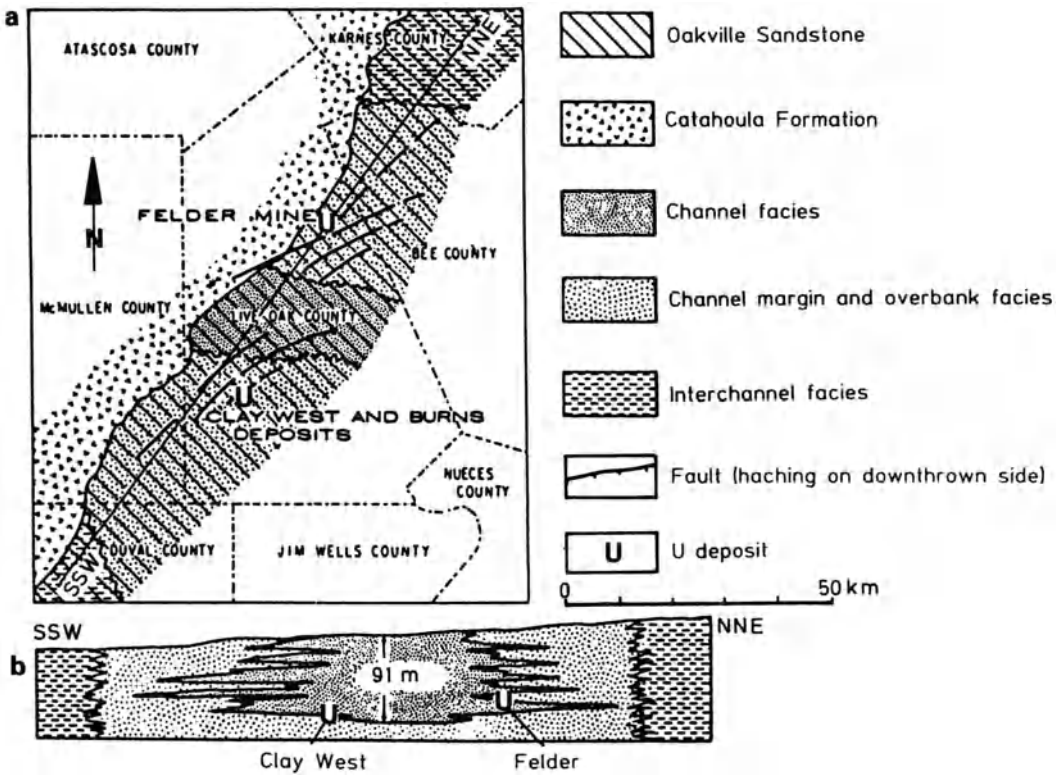

Fig. 5.97. Live Oak County, Ray Point and Clay West districts. **a** Generalized geological map. **b** SSW-NNE section showing location of major uranium deposits in, and their relation to depositional facies of the Miocene Oakville Sandstone. (After Eargle et al. 1975 based on Klohn and Pickens 1970)

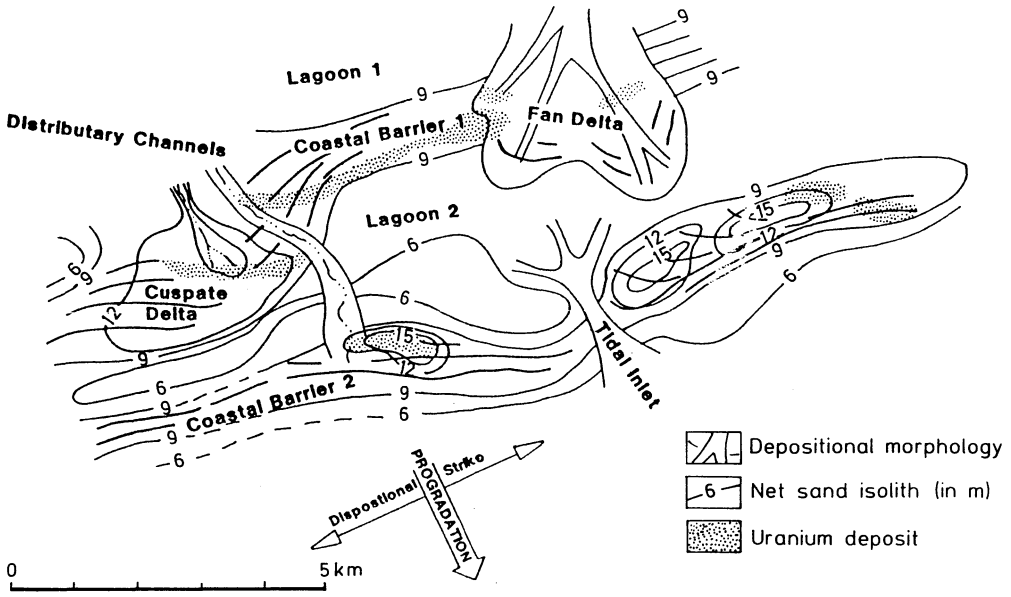

Fig. 5.98. Southwestern Karnes County, schematic map of relations between uranium deposits and littoral depositional environments and net-sand isoliths for the Tordilla Sandstone Member of the upper Jackson Group. (After Bonner et al. 1982 based on Galloway 1979a)

groundwaters, whereas the composition and provenance of the sandstones seem to be of no or only minor importance for the emplacement of ore provided most clasts are resistant to alteration.

- Favorable sand facies susceptible for mineralization include point bars, lateral bars, and crevasse splays associated with fluvial channel systems (Fig. 5.97), and barrier bars and offshore bars deposited in littoral domains (Fig. 5.98). Relations between these permeable and adjacent nonpermeable sediments vary both laterally and vertically.
- The positions of the fluvial channels in the various formations tend to be superimposed and stacked in the form of mega-channels.
- Growth faults cut the multi-stratigraphic sediment pile, thus interconnect more or less the various permeable sand units. These faults acted as pathways for oxydizing groundwaters and migrating reductants such as H_2S and thereby controlled the development of reduced, pyrit-bearing sandstones, and finally the uranium emplacement (Figs. 5.93, 5.99).
- Broad-scale sedimentary features such as mega-channel systems combined with the above-listed parameters control the distribution and configuration of major uranium deposits and ore trends. For example, most of the deposits occur in mega-channel systems. Ore trends are dip-orientated in these systems as, for example, in the South Duval County Mineral Trend, and deposits are developed in successively younger formations in a downdip direction. The strike-oriented rollfronts in the beach sands of the Jackson Group reflect a different broad-scale sedimentary feature. They do not occur in continental fluvial channel sands but rather in littoral sands.

Mineralization and Alteration

- Principal ore minerals are pitchblende/sooty pitchblende and coffinite associated with mainly Fe-sulfides and minor Mo, Se and V minerals.
- The major south Texas uranium deposits occur in two principal configurations related to two different geochemical environments:
  - At the redox boundary on the downdip margin of tongues of oxidized sandstone in the form of classical rollfront deposits, e.g., in the Jackson Group and the Catahoula Formation.
  - Entirely within reduced sandstone as non-rollfront associated deposits, e.g., in the Catahoula, Oakville and Goliad Formations.
- Rollfront deposits exhibit in cross-section in many cases the typical C-shaped form and element zoning (Fig. 5.85) that reflects the

direction of groundwater flow and the propagation of the redox front. The oxidized sands show the typical mineralogic effects of exposure to oxidizing solutions, in particular the oxidation of pyrite (Fig. 5.93). At other places these ore bodies do not display the crescentic roll shape, and this seems to be due to the presence of interbedded argillaceous material which disrupts the groundwater flow and prevents the development of the classical deposit shape.

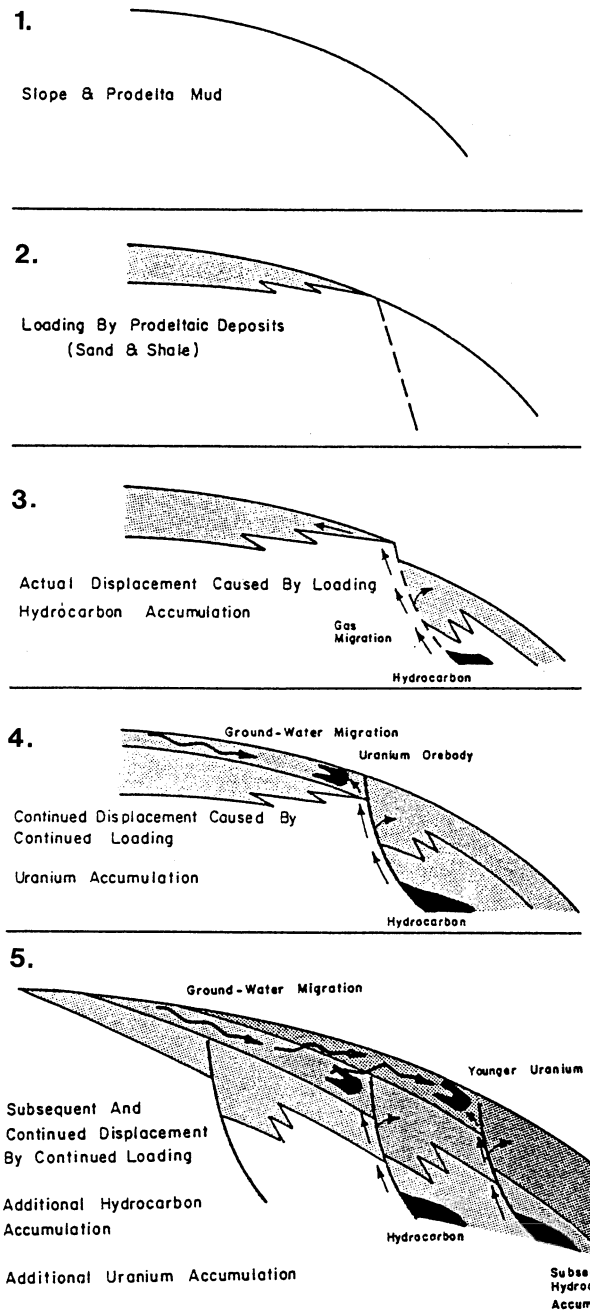

Fig. 5.99. South Texas, diagrammatic sections illustrating the sequence of geological events involved in the genesis of roll-type uranium deposits related to fault-derived H_2S. The ingress of H_2S probably preceded and followed the formation of the rollfront but was not synchronous. (Adams and Smith 1981)

- Non-rollfront deposits occur entirely within pyrite-bearing sandstone. Some of these deposits display almost the classic crescentic shape such as many of the Oakville deposits, e.g., Felder, Clay West, Rhode Ranch, etc. They are classic rollfronts in shape but are enveloped in later stages of reduction (Figs. 5.94, 5.95b,c).
- Other deposits, for example the Holiday-El Mesquite deposit in the South Duval County Mineral Trend, are elongate parallel to the axis of groundwater movement and occur at the lateral boundary between oxidized sandstone and H_2S-reduced sandstone (Figs. 5.96). The orientation of the deposit parallel to, rather than perpendicular to, the direction of groundwater flow suggests that large volumes of uraniferous water flowed tangentially past reduced sandstone rather than directly through the rollfront leading to the deposition of considerable uranium within and along the contact with pyrite-rich sandstone. The reduced and subsequently oxidized sands in proximity to these deposits do not contain either Fe-Ti oxides or their oxidation products.
- Most deposits are of low grade ($\pm 0.1\%$ U_3O_8) and low tonnage (<5000 mt U_3O_8).

Metallogenetic Concepts

Models on ore formation have been presented by a number of geoscientists including Eargle, Galloway, Goldhaber, Reynolds, and their coworkers. Adams and Smith (1981) provide a concise concept in which the Texas uranium province appears to be unique among well-described rollfront regions because the deposits are developed within a *complex heterogeneous sedimentologic sequence* ranging from littoral-marine to fluvial-continental provenance. The geometry of the sand bodies and the resulting groundwater regimes are vastly more complicated

than those of the braided fluvial systems, such as in the Wyoming Basins. The distribution and characteristics of the uranium deposits depend, therefore, on the local mode of sedimentation, and the relations between the sediments of the diverse depositional environments, in addition to the normal geochemical and physico-chemical conditions required for uranium transport and precipitation.

Adams and Smith (1981) summarize the sequence of metallogenetically essential processes which led to the formation of the south Texas uranium ore bodies as follows (Fig. 5.99):

Sedimentation

1. The ore-hosting *Tertiary sediments* of south Texas were deposited in highly variable continental fluvial to marginal marine environments. As a result, the stratigraphic lithologic situation and the related hydrologic regimes are rather variable and complex. The transmissivity and hydrology of the sediments can range from simple in the mega-channels to more contorted and complicated in crevasse splays and barrier bars.

2. *Early oxidation* affected the mega-channels either during the sedimentation or during early diagenesis. This inferred early oxidation does not seem to have been related to, and therefore is probably not essential for the formation of the uranium deposits.

Formation of Wyoming-Type Rollfront Uranium Deposits

3. *Uranium mobilization* occurred in an early stage from interbedded uraniferous tuffaceous layers within the Catahoula and adjacent Jackson Group sequences. This can be deduced from the findings of Galloway et al. (1979), which indicate an effective release of uranium directly associated with pedogenic processes. Hence, the uranium release must have occurred immediately after the sedimentation of the respective formation.

4. The uranium was *transported by groundwaters*, for example (Fig. 5.100), from the Catahoula source down into the underlying permeable horizons. Where the penetrated horizons contained reductants, e.g., in the form of *plant debris*, the oxygenated uranium-bearing waters lost their oxidation potential. As a result, redox fronts developed along which uranium and other elements were precipitated.

The *roll-type ore bodies* in the carbonaceous-rich beach sands of the Jackson Group are the examples of deposits of this type. Their uranium was probably infiltrated dip-oriented along fluvial channels which extended from the Catahoula unconformity down to the Jackson beach sand environment.

With minor exceptions related to the nature of the sediments, the deposits in the Jackson Group, therefore, are similar in terms of ore-forming processes to some of the classical rollfront districts, particularly in the Black Hills, Wyoming-South Dakota, and Weld County, Colorado.

Formation of Texas Roll-Type Uranium Deposits

5. With continued sedimentation from the Catahoula into Oakville time, many of the sands subsequently involved in ore formation were buried. *Connate waters* derived from the compaction of adjacent and overlying shales probably moved into these permeable sand systems. This was the period of greatest uranium availability, and it is likely that all important deposits in the Catahoula and Oakville formations gained their initial uranium endowment during this very early diagenetic period.

6. Early after the deposition of the sediments, *hydrogen sulfide/hydrocarbon* was introduced locally along structures into the sands of the Catahoula and Oakville formations and caused the crystallization of finely dispersed *authigenic pyrite* in the potential ore sands. The H_2S apparently emanated into the sands along growth faults (Fig. 5.93) that formed contemporaneously with and intermittently after sedimentation. Reduction of the sands may have occurred locally even during sedimentation where the H_2S reached the surface and permeated the sandstone adjacent to the structures. The local preservation of carbonaceous trash and highly sulfidic sediments tends to confirm this. The source of some of the H_2S is believed to have been, on the basis of geological relations and sulfur isotope data, the Cretaceous Edwards Formation (Goldhaber et al. 1979), whereas other sulfur sources are in the Tertiary sediments. Reynolds and Goldhaber's (1983) investigations suggest that H_2S introduction was predominantly pre- and post-ore and apparently only limited during the ore formation.

7. In consequence of the above described lithologic and physico-chemical circumstances, *rollfronts* within the Catahoula and Oakville

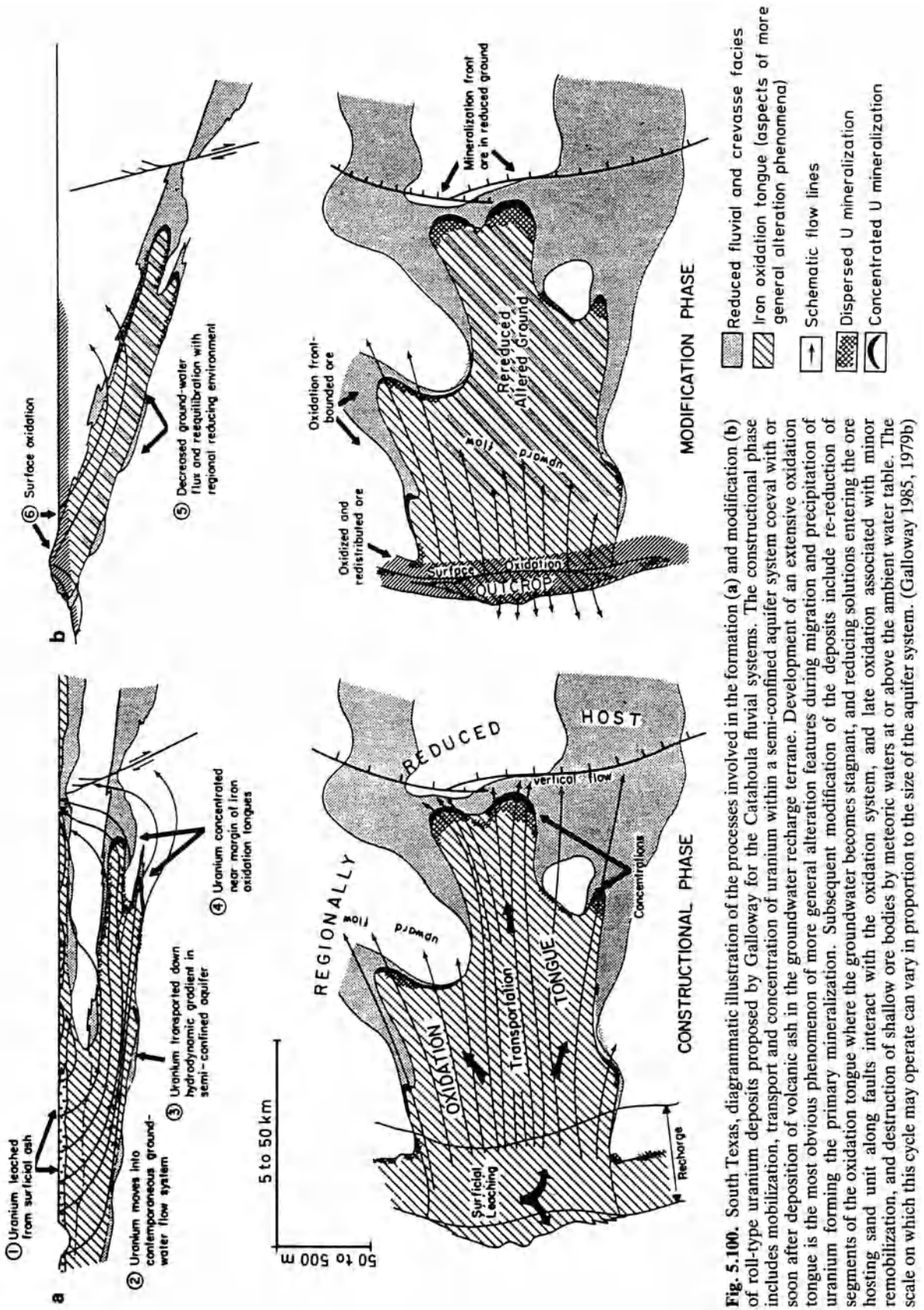

Fig. 5.100. South Texas, diagrammatic illustration of the processes involved in the formation (**a**) and modification (**b**) of roll-type uranium deposits proposed by Galloway for the Catahoula fluvial systems. The constructional phase includes mobilization, transport and concentration of uranium within a semi-confined aquifer system coeval with or soon after deposition of volcanic ash in the groundwater recharge terrane. Development of an extensive oxidation tongue is the most obvious phenomenon of more general alteration features during migration and precipitation of uranium forming the primary mineralization. Subsequent modification of the deposits include re-reduction of segments of the oxidation tongue where the groundwater becomes stagnant, and reducing solutions entering the ore hosting sand unit along faults interact with the oxidation system, and late oxidation associated with minor remobilization, and destruction of shallow ore bodies by meteoric waters at or above the ambient water table. The scale on which this cycle may operate can vary in proportion to the size of the aquifer system. (Galloway 1985, 1979b)

formations very probably formed by the introduction of oxygenated uraniferous waters into the sulfidized, pyrite-bearing sandstones. The ore-forming process was similar to the formation of roll-type deposits elsewhere, except that in the virtual absence of carbonaceous matter in the ore-bearing sands, *H_2S-derived pyrite* was essentially the only reductant available to establish the oxidation-reduction boundary.

Modification Events

8. Subsequent to the ore formation in some of the sandstones, several phases of *re-reduction and partial re-oxidation* (Figs. 5.93, 5.94, 5.100) affected the ore-hosting sediments. Renewed introduction, probably of H_2S, resulted in a re-reduction of portions of the altered sandstone tongues and arrested the ore formation and the propagation of the rollfront. Oxidizing groundwaters may have again moved down the sand horizons to form a second rollfront at a new updip redox boundary. But they may also have proceeded to and joined the original front or may have gone beyond the first front, leaving only relict or ghost deposits with the main ore formed as a downdip rollfront deposit. The progress of the younger front, however, might also have been interrupted by the interference of renewed introduction of H_2S.

9. The formation of uranium deposits in *younger formations*, such as the Goliad, may be the results of continued movement of oxygenated groundwaters, particularly in the mega-channels. The oxidizing fluids probably destroyed some early mineralization in older formations and moved the uranium into younger formations. The apparent presence of both oxidized sandstones and uranium mineralization in younger formations, e.g., in the Goliad sands, well down some mega-channel systems suggests that the two are related.

References and Further Reading for Chapter 5.4.5
(for details of publications see Bibliography)

Adams S.S. pers. commun.; Adams and Smith 1981; Baker 1979; Boenig 1970; Bomber et al.1980, 1986; Bonner et al.1982; Bowman et al.1981; Brewton 1970; Bunker and MacKallor 1973; Busche et al.1981; Craig 1980; Dickinson 1976a, 1976b, 1976c; Dickinson and Duval 1977; Dickinson and Sullivan 1976; Duex 1971; Eargle 1968, 1972; Eargle et al.1971, 1975; Eargle and Snider 1957; Eargle and Weeks 1961, 1973; Fisher et al.1970; Galloway 1979, 1982, 1985; Galloway and Kaiser 1979, 1980; Galloway et al.1979a, 1979b, 1982; Garner et al. 1979; Goldhaber and Reynolds 1979; Goldhaber et al. 1978, 1979; Harshman 1974; Henry et al. 1982; Hoel 1982; Huang 1978; Johnston 1977; Klohn and Pickens 1970; Ludwig et al. 1982; McBride et al. 1968; McKnight 1972; Quick et al. 1977; Renick 1926; Reynolds and Goldhaber 1978, 1979; Reynolds et al.1980, 1982; Ricoy and Brown 1977; Smith 1977, 1979; Smith R.B., pers. commun.; Walton et al. 1981; Weeks and Eargle 1960, 1963; Wilbert and Templain 1978

5.4.6 Uranium Deposits in Proterozoic Sandstones: Franceville Basin, Gabon

The Franceville Basin is located about 500 km SE of Libreville, Gabon. All deposits found to date cluster in two groups, 30 km apart, along the southwestern edge of the basin adjacent to the Massif du Chaillu. The northwestern group includes all major deposits, Boyindzi, Mounana, Oklo, and Okelobondo; the southwestern group contains Mikouloungou and Kaya-Kaya.

Total reserves including production amount to ca. 42 000 mt U_3O_8 (NEA/IAEA, 1986). The grade is about 0.2 to 0.4% U_3O_8.

The uranium deposits of the Franceville Basin (type 4b, Chap. 4) occurring as they do in unmetamorphosed sandstone, are similar in many respects to the tabular and tectonic-lithologic sandstone-type uranium deposits of Phanerozoic age except that they occur in Proterozoic arenites and that, therefore, the organic material is supposedly derived from marine flora (e.g., algae) and not, as in the Phanerozoic deposits, of land plant origin.

The deposits may represent a precursor type of uranium mineralization which may have been present in the middle to upper Lower Proterozoic sediments in Australia and Canada prior to their metamorphism. The deposits of Gabon may provide, therefore, a link in the evolution of subunconformity-epimetamorphic type uranium deposits (type 2, Chap. 4).

The subsequent description is largely based on the papers by Chauvet (1975), Diouly-Osso and Chauvet (1979) and Pfiffelmann (1975) amended by data of the other authors listed.

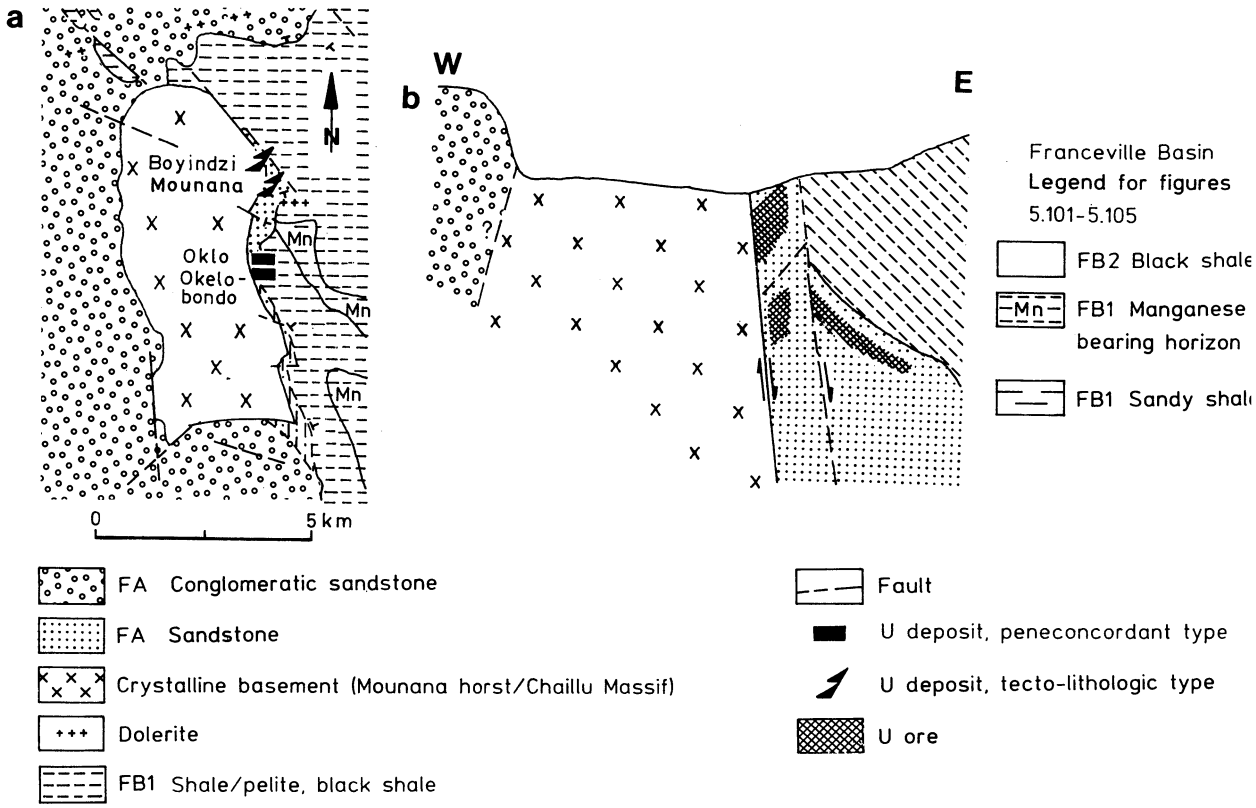

Fig. 5.101. Franceville Basin Mounana-Oklo area. **a** Simplified geological map displaying the position of the sandstone hosted uranium deposits of (from N to S) Boyindzi, Mounana, Oklo and Okelobondo. The first two are tectonic-lithologically controlled while the latter two exhibit a tabular stratabound nature. **b** Simplified geological W-E cross-section illustrating diagrammatically the localization of the different deposits. (After Chauvet 1975)

Geological Setting of Mineralization

The Franceville Basin was formed as an *intracratonic* structural depression during the late Lower to early Middle Proterozoic. It is surrounded by Archean-Lower Proterozoic crystalline complexes. The contact between sediments and crystalline horsts is commonly faulted.

The *crystalline basement* consists predominantly of granites and gneisses, which were dated about 2600 m.y. in the Massif du Chaillu.

The age of the *Franceville sediments* is dated at 1740 ± 20 m.y. (Weber and Bonhomme 1975), but U/Pb dates for the Oklo ore yield ages of up to 2000 m.y.

The sediments transgressed the crystalline basement in two major psammitepelite sedimentary cycles.

The *lower cycle* comprises the FA Formation and the overlying FB 1 Formation.

The *FA* consists of fluvial and fluvio-deltaic (arkosic) sandstones. Its thickness is about 50 m along the edge of the basin and increases to 1000 m towards the center. The basal part consists of quartz pebble conglomerates and coarse-grained arkosic (microcline) sandstones, which grade progressively upwards into medium- to coarse-grained sandstones with dolomitic matrix. They in turn are succeeded by a succession of alternating fine-, medium-, and coarse-grained sandstones, with occasional intercalations of conglomeratic lenses. The matrix of these younger, feldspar-poor sandstones consists of silica or organic material. The individual sandstone layers exhibit cross-bedding and rapid lateral facies change. All uranium deposits occur in this upper sandstone of the FA Formation.

The FA Formation is transgressed by the *FB 1* Formation which consists of up to 600 m thick pelitic sediments containing organic material.

The *upper cycle* is composed of the *FB 2a to FE* formations consisting of psammites and organic bearing pelites intercalated with minor cherty beds, dolomites, and tuffs.

Deformation resulted in slight folding along NW-SE axes, and fault systems trending N-S and NW-SE. Along the latter are the NE-blocks generally downfaulted relative to the SW-blocks. A third set of faults trends E to NE. Dolerite dikes dated ca. 870, 730 to 715 and 545 to 530 m.y. (Weber and Bonhomme 1975) follow this E to NE system.

The northwestern group of deposits which contains all major ore bodies is immediately adjacent to the granite-gneiss *horst of Mounana*, a tectonic outlier of the Chaillu Massif. The eastern edge of the horst comprises a zone of predominantly N-S-trending 70 to 80°E dipping fractures. They separate the granites and gneisses from the FA and FB 1 sediments. The faults produced displacements of up to several hundred meters. The development of the various segments caused tilting of the sedimentary strata towards the east, forming a monoclinelike structure which dips 45°E (Fig. 5.101).

Mineralization, Ore Controls and Recognition Criteria

In the *reduced ores*, the principal minerals are pitchblende and coffinite. In the area of the natural reactor at Oklo, pitchblende is recrystallized to uraninite. Associated and gangue minerals include karelianite, montroseite, roscoelite and minor pyrite, galena, sphalerite, chalcopyrite, marcasite, melnikovite, baryte, and calcite as fissure fillings. In the *oxidized ores*, the principal minerals are francevillite, vanuralite, uranocircite, autunite, torbernite and renardite. Associated minerals include vanadinite, chervetite and brackebuschite.

All uranium deposits display a lithological control and most show some structural control. Based on local geologic features, Pfiffelmann (1975) identified three *types of deposits*: stratiform (e.g., Oklo), veinlike (e.g., Mounana, Boyindzi), and mixed stratiform-tectonic deposits (e.g., Mikouloungou). Characteristics of mineralization and geologic setting of these deposits are briefly reviewed below based on descriptions particularly by Chauvet (1975), Diouly-Osso and Chauvet (1979), and Pfiffelmann (1975).

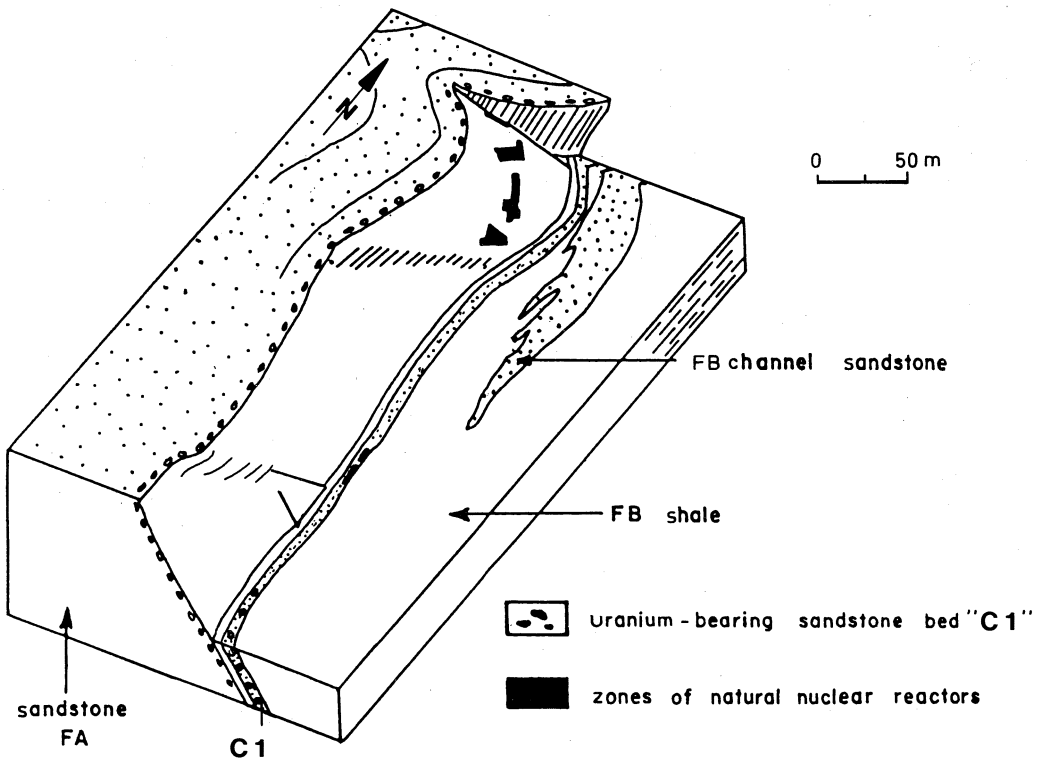

Fig. 5.102. Oklo deposit, schematic block diagram showing the folded nature of the U mineralized C1 horizon and the location of natural reactors which were active between 2000 and 1700 m.y. ago. (After Gauthier-Lafaye et al. 1980)

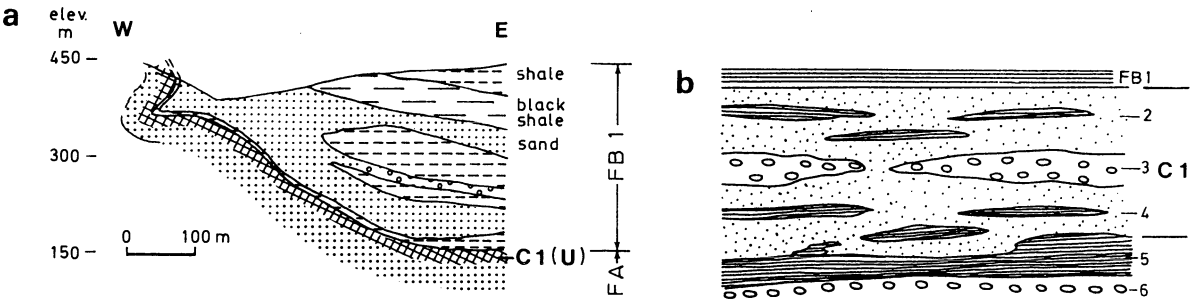

Fig. 5.103. Oklo deposit. **a** Geological-lithologic W-E section. **b** Lithologic details of the mineralized C1 horizon. *1* FB 1 shale; *2–4* C1; *2* sandstone; *3* intercalated conglomerate; *4* intercalated fine-grained sandstone; *5* footwall fine-grained sandstone; *6* footwall conglomerate. (After Chauvet 1975; Diouly-Osso and Chauvet 1979)

Oklo (reserves including production ca. 18000 mt U_3O_8, grade ca. 0.5% U_3O_8)

Mineralization is concentrated in the upper 5 to 10 m of the FA Formation which is subdivided into two units. The lower n + 3 unit (<30 m thick) contains the weakly and irregularly mineralized C2 horizon. The overlying n + 4 unit (4 to 10 m thick) contains the main ore horizon (C1) (Figs. 5.102, 5.103). Both units grade from fine-grained, in part pelitic, sandstone upwards into coarse-grained sandstones and conglomerates. Green- and black-banded pelites of the FB 1 Formation rest slightly unconformable on the n + 4 unit.

The main ore horizon (*C1*) consists of a series of lenses of cross-bedded fluvial sandstones with a conglomeratic interbed. The C1 was deposited immediately above the upper conglomerate and a fine-grained pelitic bed of the unit n + 3. Uranium is concentrated predominantly in sandy zones in the form of microcrystalline pitchblende within organic matrix. Mineralization appears to avoid pelitic horizons. In contrast to Mounana (see below), no vanadium is associated with uranium at Oklo. The ore horizon plunges between 15 and 60°E and flattens at depth. Maximum depth is 300 m. N-S length of the deposit is 900 m and maximum E-W width 600 m.

The *natural reactors* of Oklo (Boyer et al. 1975) are a unique phenomenon among uranium deposits of the world. They are characterized by a depletion of ^{235}U from 0.72% to between 0.62% and 0.296%. Six reactors have been found which occupied a total area of 3500 to 4000 m^2 (1.5% of the total mineralized area). Individual reactors extend laterally from a few meters up to 20 m, at ore thicknesses of up to 1 m. At each locality, uranium was enriched to more than 50 times the normal concentration with extreme values up to 70% U_3O_8. The reactors are located at places where the overlying pelites are cut by sand-filled paleochannels (Fig. 5.102). About 800 t of natural uranium was destroyed by the reactors. Alteration minerals generated by the reactor processes are presented in Table 5.30. Ages of ore from the nuclear reaction zones are dated at 2000 m.y. by Devillers et al. (1975) and 1700 to 1900 m.y. by Cowan et al. (1975), which predates the isotopic age of 1740 m.y. of the host sediments. The period of criticality lasted at least 200000 years. At the time the reactors were active, ^{235}U amounted to almost 3% of the total uranium (compared with 0.7% today).

The Oklo mineralization shows a strong lithologic *ore control*. Within the fluvial-deltaic sandstones of the C1 zone, uranium seems to be

Table 5.30. Oklo deposit, alteration products of the natural reactor zone (Gauthier-Lafaye et al. 1980)

	Sandstone	Clay of transition zone	Chlorite fringe	Clay of reactor zone	Reactor zone facies
Dominant clay minerals	Illite 1 M	Illite 2 M	Mg-chlorite	Illite 1 Md + chlorite	
Other constituents	— Quartz —				
	Pitchblende	Heavy minerals		Hematite, leucoxene	Uraninite

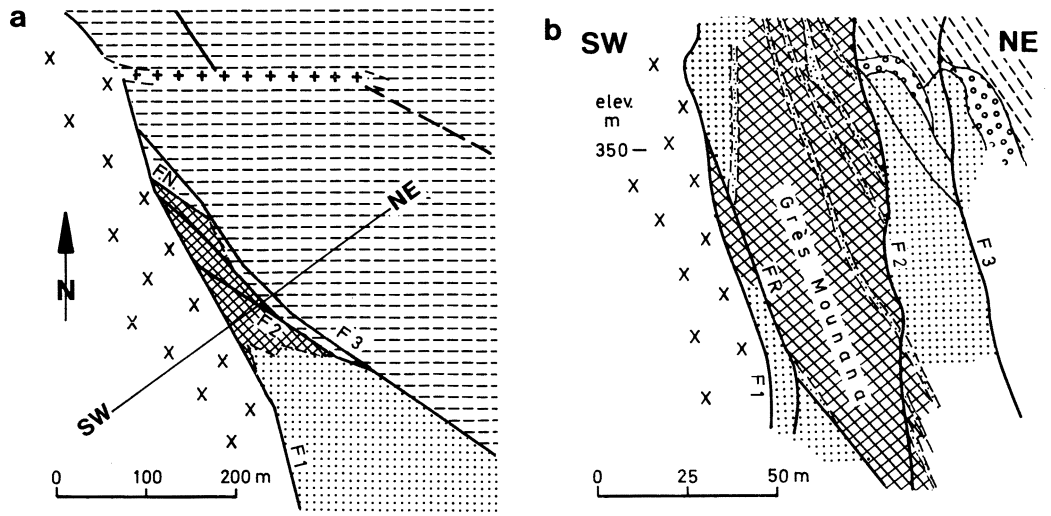

Fig. 5.104. Mounana deposit. **a** Geological plan map for the 350 m level. **b** Geological SW-NE section (grès Mounana = Mounana sandstone; *FN*, *F1* etc. denote faults). (**Legend** see Fig. 5.101) (After Pfiffelmann 1975)

concentrated on the flanks or rims of paleochannels or where intermediate thicknesses of sandstone are combined with high concentrations of organics and moderate interbedding. The mineralization decreases in zones of thick sandstone and/or low concentrations of organic material. There also seems to be some relationship to the dip. Best ore occurs in sediments dipping about 30°. A regional ore control may be related to the western bounding fault of the Franceville Basin and the crystalline Massif du Chaillu less than 1000 m to the west of the deposit.

Mounana (reserves [depleted] 6800 mt U_3O_8, grade 0.58% U_3O_8)

Mineralization occurs in the same C1 horizon and regional structural setting as Oklo. Mounana lies immediately east of the fault separating the crystalline wedge of the Massif du Chaillu from the Franceville sediments (Fig. 5.104). Another fault zone borders the ore body to the east.

The ore-hosting sandstones dip steeply, possibly due to drag on the faults and are heavily fractured. Quartz and microcline constitute 90% of the sandstone. The matrix contains organic material and is silicified. The ore body was about 100 m long, 40 m wide, and extended to a depth of 120 m.

In the oxidized upper 40 m of the deposit, the ore consisted of uranyl vanadates. Primary mineralization then occurred down to a depth of 120 m.

The *ore control* is structural as well as lithological. Mineralization is restricted to the FA sandstones where organic material is abundant. An assumed control is the apparent occurrence of the ore body on the west flank of a paleochannel that is scoured into the upper FA Formation. Later tectonics, however, have strongly overprinted this feature. Structural control is reflected by marginal faults and fractures that separate ore from nonmineralized rocks and by structures within the deposit that separate rich from poor mineralization.

Mikouloungou (estimated reserves: 6000 to 12000 mt U_3O_8, grade: 0.2 to 0.25% U_3O_8)

Mikouloungou and the nearby Kaya-Kaya deposit are within the Franceville Basin, several kilometers distant from a crystalline horst.

The Mikouloungou *mineralization* extends for more than 1500 m along an E-W-striking overthrust that dips 45°N and persists for more than 250 m deep. N-dipping FB 1 pelites in the upper plate of the thrust overlie horizontal to gently SW-dipping FA sandstones in the lower plate (Fig. 5.105).

The FA Formation (>500 m thick) is subdivided into four sequences of fine- and coarse-grained sandstones. Uranium is restricted to sequence 2 which is 175 m thick and comprises 21 beds each of alternating fine- and coarse-grained, feldspathic sandstones. Near the overthrust, the host rocks are shattered by micro-fractures, and

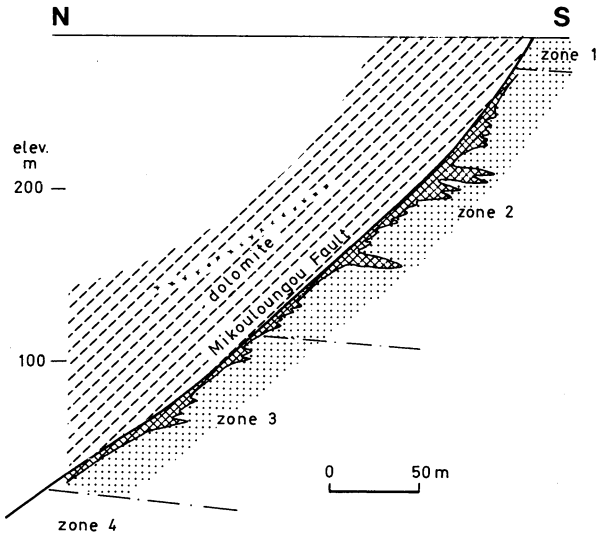

Fig. 5.105. Mikouloungou deposit, schematic N-S cross-section displaying the tectonic-lithologic control of the uranium mineralization. Uranium penetrates tongue-like from the Mikouloungou Fault along coarser sandstone beds into the FA sandstone unit. (**Legend** see Fig. 5.101) (After Pfiffelmann 1975)

feldspars are kaolinized. The sandstones are variably silicified. Sequence 2 is overlain by 75 m of fine-grained sandstones of sequence 1.

Mineralization occurs (a) along the footwall of the thrust zone independent of the lithology and (b) extending as tonguelike projections for 5 to 20 m from the thrust into the coarse-grained sandstone horizons. In plan, the ore tongues show irregular, amoeba-like shapes.

The ore consists of a mixture of pitchblende and clay minerals accompanied by pyrite and, in fissures and joints, calcite.

The *ore controls* are structural and lithologic. Mineralization is sharply separated from the adjacent pelites by the overthrust. It occurs only on the footwall side of the fault and within coarse-grained kaolinized sandstones where joints with gouge partly control the mineralization. A change in alteration is observed within the host rocks from a barren, fresh feldspathic sandstone to a sandstone impregnated with pitchblende and clay minerals close to the fault.

A lithochemical control was possibly provided by the overthrusted pelites. Their organic material may have produced a reducing environment supporting the precipitation of uranium. Silicification also appears to have influenced the distribution of the uranium.

References and Further Reading for Chapter 5.4.6
(for details of publication see Bibliography)

Baud 1967; Bernazeaud 1959; Bonhomme et al. 1965; Bonhomme and Weber 1969; Bourrel and Pfiffelmann 1972; Boyer et al. 1975; Branche et al. 1975; Chauvet 1975; Cortial 1985; Cowan et al. 1975; Devillers et al. 1975; Diouly-Osso and Chauvet 1979; Donnot and Weber 1969; Drozd et al. 1974; Faure-Mercuret 1965; Gangloff 1970; Gauthier-LaFaye 1977; Gauthier-LaFaye et al. 1975, 1980; Geffroy 1975; Geffroy et al. 1964; LeCoq et al. 1958; Molina and Besombes 1975; Morin and Tardieu 1972; Naudet et al. 1975; Openshaw et al. 1978; Pfiffelmann 1975; Rouzaud 1979; Ruhland and Gauthier-Lafaye 1978; Weber and Bonhomme and 1975.

5.5 Examples of Collapse Breccia Pipe-Type Uranium Deposits (Type 5, Chap. 4): Arizona Strip Area, USA

The uranium district is located in the Arizona Strip area, to the north and south of the Grand Canyon, northwestern Arizona. Numerous solution collapse breccia pipes crop out on the plateaus and in the canyons. Some contain economic Cu, Pb, Zn, Ag, and/or U mineralization. Minable deposits, classified as collapse breccia pipe-type uranium deposits (Type 5, Chap. 4), contain uranium reserves in a range from a few hundreds to about 2500 mt U_3O_8. Total reserves discovered so far are in the order of about 14 000 mt U_3O_8 contained in at least 11 pipes (Fig. 5.106). Production grades are high averaging from 0.4 to 0.8% U_3O_8 and locally more. Ag, Cu, and V are recoverable from some of the lodes.

Geological Setting of Mineralization

The regional geological setting is the classical one of the Grand Canyon region with its well established stratigraphy and evolution. (Billingsley 1978; Breed and Roat 1978; Four Corners Geol. Soc. 1969; Karlstrom et al., 1974). The rock sequence ranges in age from Precambrian (>2 b.y.) to Permian (approx. 200 m.y.) and locally Triassic. These rocks are intruded and capped in places by Miocene to late Pleistocene volcanics. Figure 5.107 displays schematically the stratigraphy and lithology of the various formations in the Grand Canyon region.

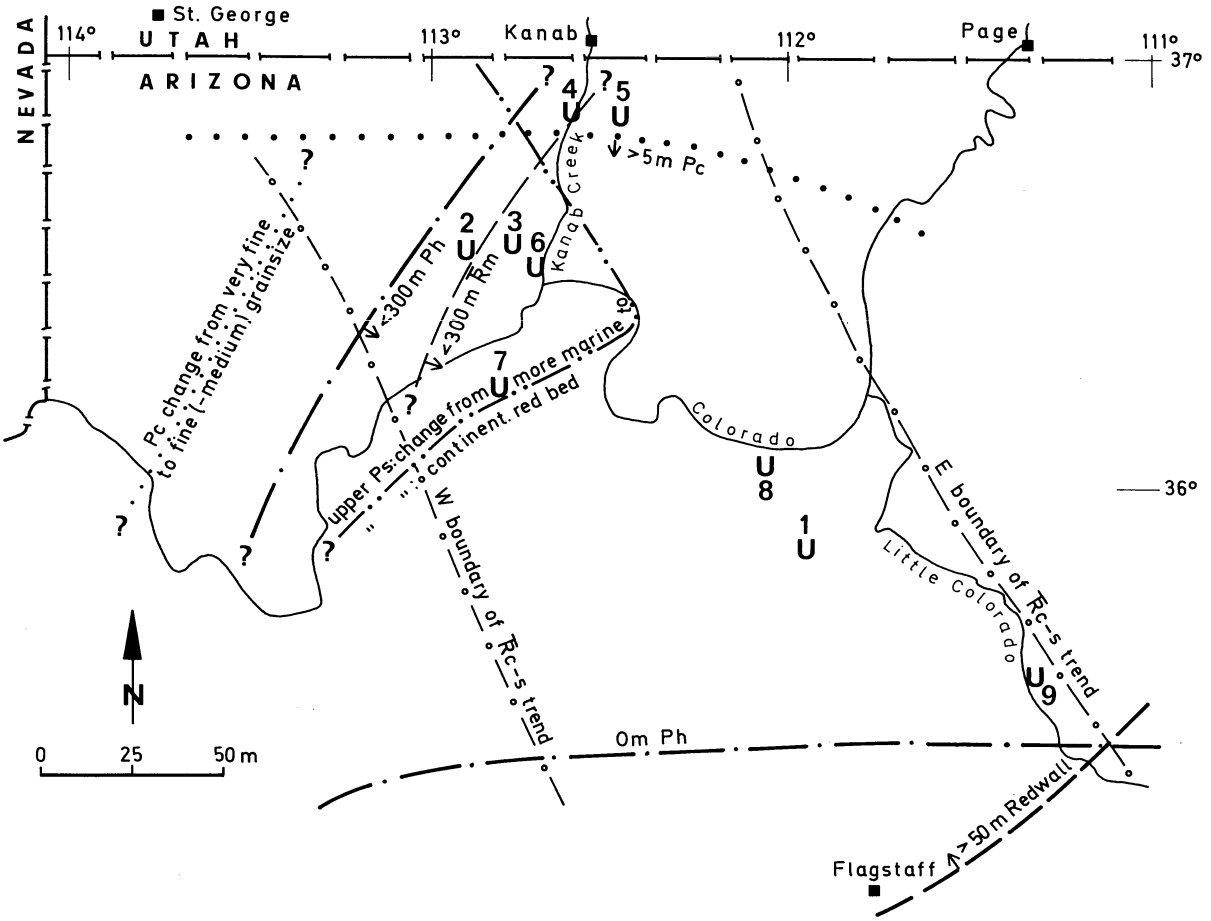

Fig. 5.106. Arizona Strip area, inferred distribution and thickness of Mississippian Redwall to Permian Coconino and Triassic Moenkopi and Chinle/Shinarump formations and location of principal uranium ore bearing breccia pipes. *Arrows* at isoliths indicate direction of increasing thickness. *Tc-s* Chinle Fm/Shinarump; *Tm* Moenkopi Fm; *Pc* Coconino Sandstone; *Ph* Hermit Fm; *Ps* Supai Fm/ Esplanade; ore bearing pipes *1* Canyon; *2* EZ-2; *3* Hack Canyon 1, 2 and 3; *4* Kanab North; *5* Pigeon; *6* Pinenut; *7* Union Pacific; *8* Orphan Lode; *9* Riverview. (Karlstrom et al. 1974, McGee and Gutschick 1969; Mallory et al. 1972 and other unpublished sources)

The breccia pipe hosting *Mississippian to Lower Triassic* stratigraphic units consist of almost horizontally bedded marine to marginal continental limestones, mudstones, and sandy to silty sediments (McGee 1974).

Major *tectonic features* of the Arizona Strip area include block-faulting with associated warping (e.g., Kaibab Uplift), N- to NNE-trending lineaments (e.g., Toroweap Fault), and NNW- and NE-striking fault systems.

Numerous collapse structures called "*collapse or solution breccia pipes*" or simply "breccia pipes" have been found in the Arizona Strip area in formations younger than the Mississippian. The pipes are of combined solution and tectonic origin and should not be confused with diatreme pipes generated by volcanic gaseous explosion. A pipe may crop out on the surface or may be blind (Fig. 5.107).

Roof collapse of caverns (paleokarst) in the carbonate strata of the Mississippian Redwall Limestone initiated the formation of a pipe. The generally circular collapse transgressed chimney-like upwards into the overlying, essentially flat-bedded sediments, from the Redwall Limestone as much as about 1200 m into the Permian Kaibab Limestone, and locally into the overlying Lower Triassic Moenkopi Formation or Upper Triassic Chinle Formation. A breccia pipe consists of a throat ranging in diameter from about 15 to 100 m and more. Pipes stoped upward to surface exhibit a surface expression in form of a collapse cone that may have a diameter of up to 750 m. The cone results from dissolution of gypsum and other

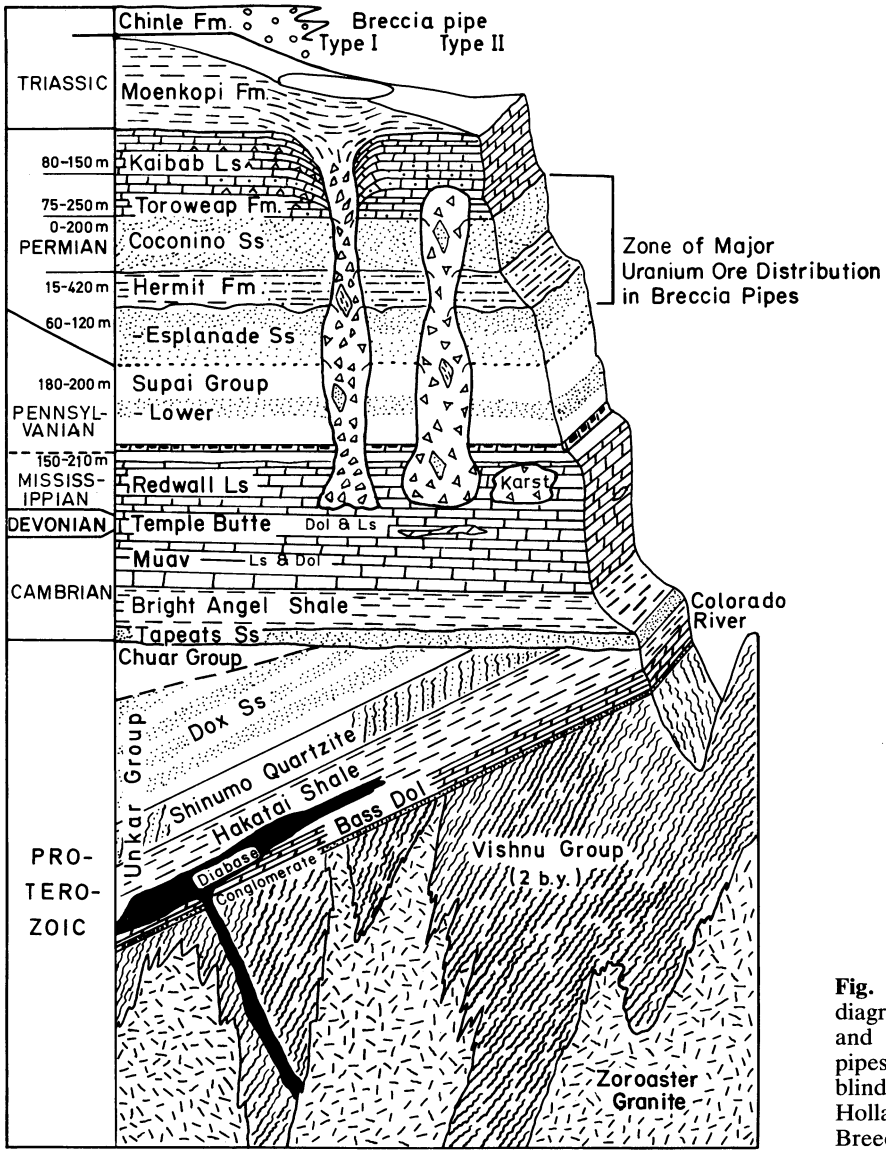

Fig. 5.107. Arizona Strip area, diagrammatic stratigraphic section and position of collapse breccia pipes. *Type I* out-cropping, *Type II* blind. (After drawing by R.F. Holland unpubl.; stratigraphy after Breed and Roat 1976)

leachable material of the Kaibab and Toroweap formations, causing a gradual thinning of the affected strata towards the pipe throat. In contrast, a pipe which does not outcrop has no solution cone.

A breccia pipe is filled with clasts of highly variable size up to several meters in diameter which are embedded in matrix. Fragments and matrix are made up of downward displaced material of the stoped sediments.

Host Rock Alterations

A variety of alterations affected either both or separately the pipe infill and the strata peripheral to the pipe. Principal alterations include pyritization, dolomitization, calcitization, silicification, desilicification, Mg-depletion (dedolomitization), gypsum/anhydrite formation, and bleaching. It is not established, however, which of these processes were related to mineralization and which developed during the pipe formation itself. Most alteration processes tend to have been very mild although some produced striking color changes. Figure 5.108 displays the distribution of the various alteration features within and outside a pipe.

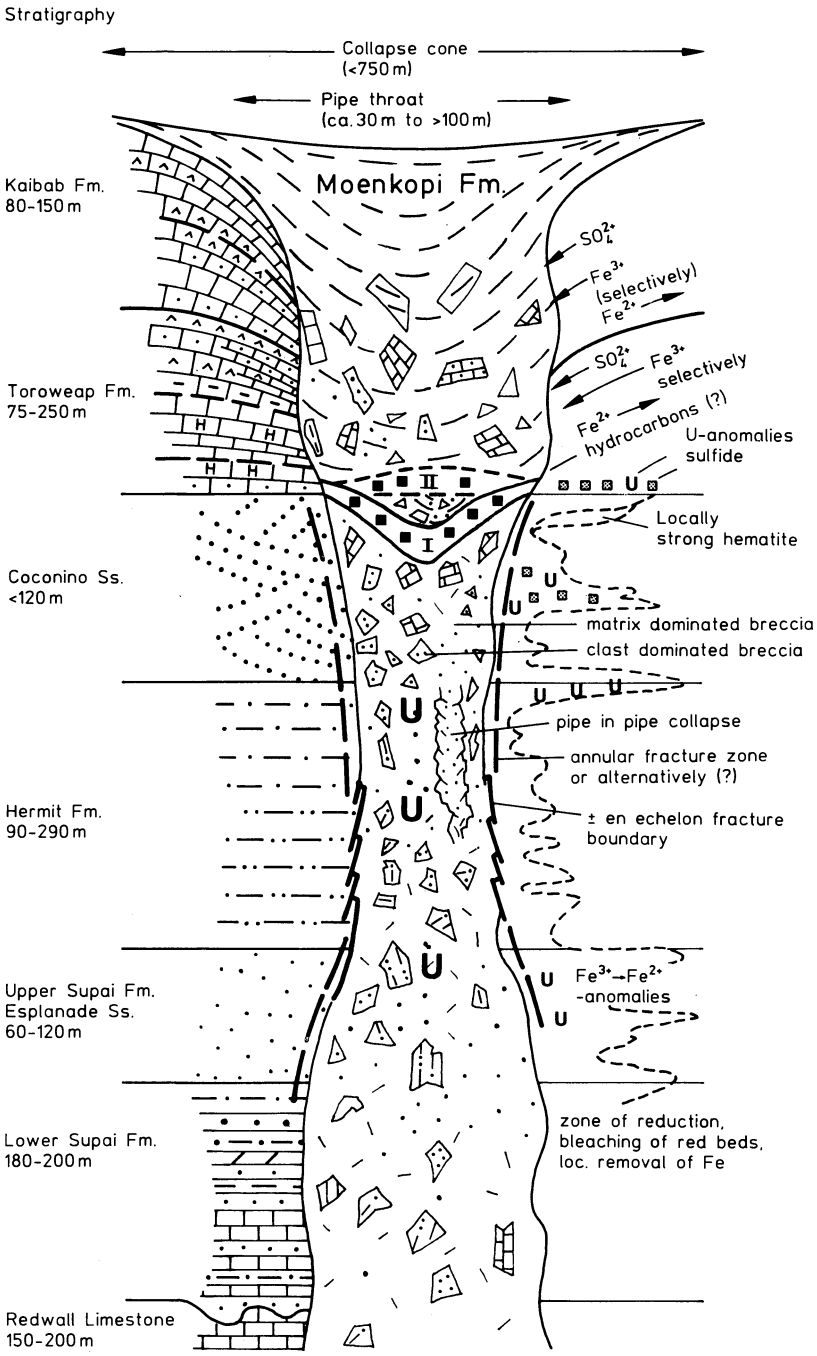

Pipe internal alteration/mineralization
-sulfide cap
-±total reduct/bleaching of red fragments in well mineralized pipes
-calcitization, dolomitization, silicification
-mineralization see Table.....

Alteration
Mineralization
Pipe external

1. *Collapse cone/surface expression*
concentric collapse, breccia, arcuate fractures, anomalous limonite pseudomorphic after pyrite

2. *Kaibab Fm.*
-dissolution of evaporites, carbonate
-removal of SO_4, Fe
-thinning
-deformation
-strata-selective reduction/ sulfidization with gradational increase toward pipe

3. *Toroweap Fm.*
-as in Kaibab Fm.
-removal of hydrocarbons (?)
-dissem. sulfidiz. in basal Toroweap
-Kaolinization

in pipe:
±massive sulfide cap
I in outcropping pipe
II in blind pipe (?)

4. *Coconino Ss.*
-disaggregation with thinning
-reduction particularly in upper and lower portions
-locally sulfidization
-locally U, or Pb, Zn, As anomalies
-locally strong hematit. near upper cont
-kaolinization

5. *Hermit Fm.*
-bleaching
-local. Fe-removal
-local. anomal. U at top

6. *Supai Fm.*
-bleaching
-local. Fe and CO_3 removal
-local. anomal. U

7. *Redwall Ls.*
-karst development
-local. Pb, Zn mineralization

Fig. 5.108. Arizona Strip area, diagrammatic section of an outcropping uranium ore-bearing breccia pipe with types of alteration and mineralization which may or may not be present.

Principal Characteristics of Mineralization

The ore mineralogy of the collapse breccia pipes is quite heterogenous. The most common *uranium mineral* is pitchblende, locally coffinite. A series of *associated minerals* but not necessarily paragenetic ones are present in variable amounts (Table 5.31, Fig. 5.109). They include sulfides, arsenides, sulfoarsenides, locally oxides, carbonates, and sulfates of Fe, Cu, Ni, Co, Mo, Pb, Zn, and Ag. Traces of Au, Cd, Mo, Sb, Se, and V are also present. *Gangue minerals* which may or may not be related to mineralization are calcite, dolomite, siderite, baryte, collophane, chalcedony, quartz, anhydrite, and gypsum. A black glassy bitumen is locally abundant but only in some pipes.

The mineral assemblages vary from pipe to pipe. The Orphan Lode and Hack pipes for example (Table 5.31), display a large variety of metallic minerals whereas the Pigeon pipe has a more simple mineralogy (Rasmussen J.D. and Gautier A., pers. commun.). In general, three principal paragenetic stages of mineralization may be distinguished succeeded by a fourth, supergene stage (Fig. 5.109).

Table 5.31. Arizona Strip area, selected ore minerals of breccia pipes

Mineral	Hack	Pigeon	Orphan	Canyon
Arsenopyrite	x		?	
Bornite		x	x	x
Bravoite	x	x	x	x
Chalcocite	x		x	x
Chalcopyrite	x	x	x	
Cinnabar			x	
Clausthalite	x		x	
Cobaltite			x	
Coffinite			x	
Covellite	x	x	x	
Digenite			x	x
Enargite (Luzonite)	x	x		
Galena	x	x	x	x
Gersdorffite	x	x	x	
Hematite	x		x	
Ilsemannite	x			
Jordisite	x			
Marcasite	x	x	x	
Millerite	x			
Pitchblende	x	x	x	x
Proustite			x	
Pyrite	x	x	x	x
Rammelsbergite			x	
Siegenite	x		x	
Skutterudite			x	
Sphalerite	x	x	x	
Stibnite			x	
Violarite		x		
Tennantite-tetrahedrite	x	x	x	

(Ref. Orphan Lode: Gornitz and Kerr 1970; Kofford 1969; Hack, Pigeon, Canyon: Rasmussen J.D. and Gautier A.M., pers. commun.)

Uranium forms irregular *ore shoots* distributed intermittently over a vertical pipe interval of as much as 200 m from the Coconino stratigraphic level downward. Ore grade mineralization is generally concentrated in sections filled with not or partially cemented sand and silt. These particular lithologic sections are located predominantly (a) at and just below the Coconino-Hermit contact in the stratigraphic wall rock pile, (b) within the Hermit interval, and/or (c) immediately below the Hermit-Supai boundary (Fig. 5.108).

The *pitchblende distribution* within these intervals is in form of (a) veinlets and stringers both within the pipe and in an annular ring closely surrounding the pipe, (b) pseudo-stratiform mineralization in permeable sandstone blocks, and predominantly (c) dissemination in irregular masses, disseminated in mainly sandy-silty matrix within the reduced brecciated interior of the pipe.

Sulfides occur disseminated in variable amounts within the whole pipe. Particular concentrations of sulfide containing up to 80% pyrite and marcasite form a 3 to 15 m thick *sulfide cap* above the uranium ore, at an elevation corresponding to the stratigraphic Toroweap-Coconino contact (Fig. 5.108).

Uranium – lead isotope dating of pitchblende from various pipes yield four groups of apparent *ages*: ca. 260 m.y. (Ludwig, K., pers. commun.), ca. 220 to 200 m.y. (Ludwig et al. 1986), ca. 184 to 165 m.y. (Krewedl and Carisey 1986) and ca. 141 m.y. (minimum age, Miller and Kulp 1963).

Stable Isotopes and Fluid Inclusions

Sulfides in breccia pipes give $\delta^{34}S$ values of -3 to $-20‰$ and in nonmineralized Kaibab and Toroweap sediments of $+12$ to $+14‰$ (Adamek P., pers. commun.).

Galena with nonradiogenic lead has $^{206}Pb/^{204}Pb$ ratios of >19 and $^{208}Pb/^{204}Pb$ ratios of >38 comparable to Mississippi Valley type mineralization. Assumed source of the lead is ca. 1.8 b.y. old basement (Ludwig K.R., pers. common.).

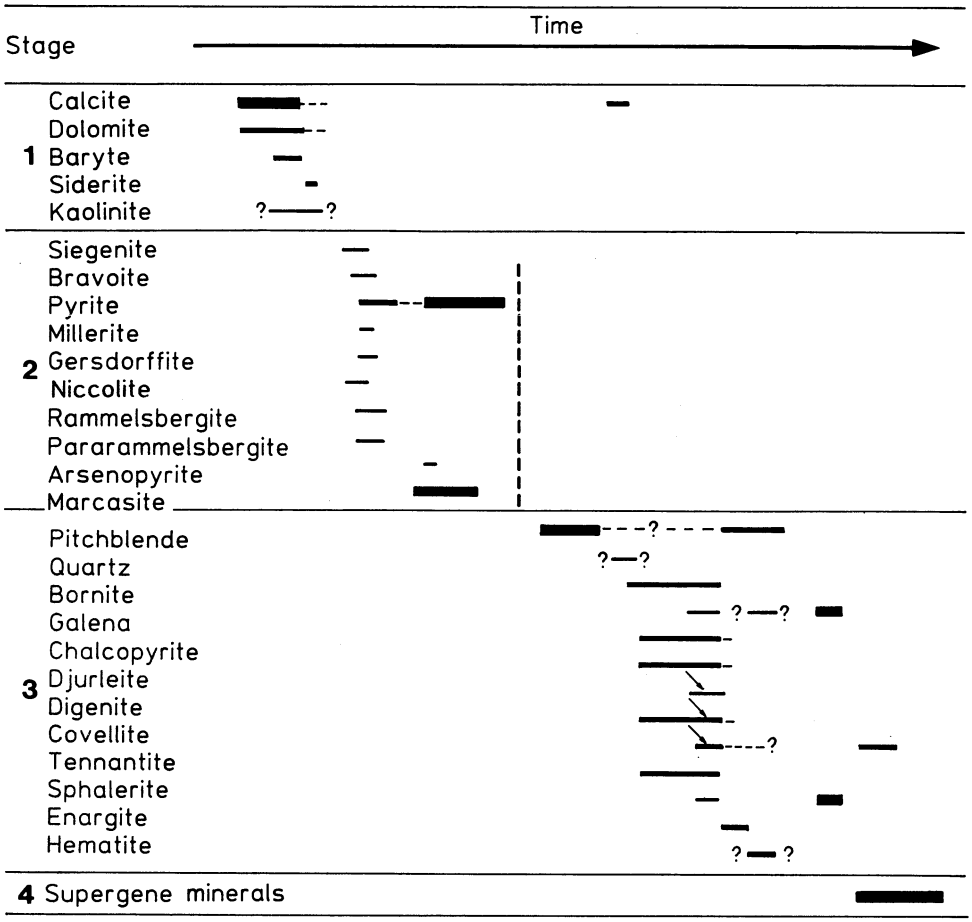

Fig. 5.109. Arizona Strip area, Orphan Lode, paragenetic sequence for minerals in the breccia pipes. (*hatched vertical line* indicates fracturing of pyrite). (After Wenrich and Sutphin 1987; J.D. Rasmussen and A. Gautier pers. commun.)

Fluid inclusion studies from various pipes yield in summary the following homogenization temperatures and salinities. Gypsum, anhydrite, calcite, sphalerite: 54 to 125°C (average 90°C) (Landais in Krewedl and Carisey 1986); calcite, dolomite, sphalerite: 80 to 173°C (salinities >9 wt. % eq. NaCl with most common values >18 wt. % eq. NaCl), primary inclusions of which in sphalerite measure filling temperatures of 80 to 100°C and secondary inclusions 103 to 173°C (Wenrich and Sutphin 1989); sphalerite from Hack 1 and 2: 93 to 115°C (salinity 9.9 to 16.4 wt. % eq. NaCl) (Rasmussen et al. 1986).

Potential Sources of Uranium

No definite uranium source could be established to date. Speculative uranium sources include the crystalline Proterozoic basement underlying the Arizona Strip area, crystalline Proterozoic rocks that were already exposed in Triassic time in the Mogollon Highland at the southern margin of the Colorado Plateau, fluvial channel sediments of the lower Chinle Formation of Triassic age, which covered as a NW-SE belt part of the Arizona Strip area, fluvial sediments of the Jurassic Morrison Formation distributed to the E and NE of the Arizona Strip area, and altered volcanics forming the bentonites in the Petrified Forest Member of the Chinle Formation.

Ore Controls and Recognition Criteria

Ore bearing breccia pipes display the following ore controls and recognition criteria (Figs. 5.107, 5.108).

Host Environment

- Breccia pipes occur in flat lying sediments extending over a stratigraphic interval from the Mississippian Redwall Limestone through Pennsylvanian and Permian sediments into the Permian Kaibab Formation, locally into the Lower Triassic Moenkopi and rarely into the Upper Triassic Chinle Formation.
- A breccia pipe is a vertical to steeply inclined sometimes slightly curved structure with a pipe or hourglas shape, circular to oval in planview, and as much as 1200 deep.
- Surface expression of pipes persistant up into the Moenkopi Formation, is a circular depression up to 750 m in diameter, and as much as 100 m deep filled by downdropped Moenkopi sediments.
- Strata above the Coconino Sandstone dip pipeward due to concentric removal of evaporitic and calcareous constituents in the Toroweap and Kaibab formations.
- Pipes are bordered by concentric fractures (annular ring fractures) (e.g., Orphan Lode) or by steeply outward inclined sets of fractures interconnected by flat inward dipping fractures (e.g., Pigeon).
- Intrapipe breccia consists of angular to rounded rock fragments ranging in size from a few millimeters to several meters, embedded in a matrix derived both from the host strata and overlying formations.
- Clasts in the mineralized sections of most pipes consist of more or less silicified or carbonate cemented and reduced Coconino, Hermit, minor Toroweap, and Esplanade/Supai material (e.g., Hack 1, 2, 3, EZ-2, Orphan, Canyon). Those in the northern segment of the Arizona Strip, where the Coconino Sandstone pinches out, are chiefly derived from the Hermit, Toroweap and Fossil Mountain Member/Kaibab formations with very minor Coconino Sandstone (Pigeon, Kanab North).
- Mineralized matrix ranges from reduced Coconino or Esplanade derived sand and Hermit or Toroweap derived silt/sand, loosely to strongly cemented by clay, sericite, calcite, dolomite, gypsum and/or anhydrite.
- Altered hydrocarbons (pyrobitumen etc.) occur in all ore-bearing pipes, although in highly variable quantities. The highest concentrations commonly are found at the lower Toroweap to upper Hermit stratigraphic invervals.
- Pipe infill may be a structurally simple though heterogenous assemblage of downfaulted material or it may display a more complex structural zoning of material repeatedly displaced by selected internal subsidence forming "pipe in pipes" (Fig. 5.108).

Alteration

Alteration features include bleaching (common at all pipes), pyritization (common), dolomitization (common but variable intense), calcitization (variable), gypsum/anhydrite formation (variable, locally none), silicification (minor), desilicification (common), Mg-depletion (dedolomitization) (locally in ore zones).

Mineralization

- Principal uranium minerals are pitchblende and minor coffinite.
- Associated minerals include sulfides, arsenides, sulfoarsenides, locally oxides and sulfates of Fe, Cu, Ni, Co, Mo, Pb, and locally Ag, and traces of Au, As, Sb and V.
- Principal gangue minerals are Ca-, Mg-, Fe-carbonates, Ba- and Ca-sulfates, phosphates and Si-oxides.
- Distribution and quantity of above elements/minerals is highly variable from pipe to pipe (Table 5.31).
- An almost characteristic phenomenon in ore bearing pipes is a massive sulfide (pyrite) cap located at and below the Toroweap-Coconino formational contact.
- Uranium ore persists intermittently in irregular ore bodies over a vertical interval of as much as 200 m from the Coconino stratigraphic level downward into the middle Supai level.
- Ore grade mineralization occurs in lithologic zones of favorable permeability, that are a function of pipe fill material and structure. Favorable hosts are loosely packed matrix material of dominantly sandy composition, porous sandy or vuggy silty-sandy, rarely calcareous clasts, fractures, joints or fissures within the pipe breccia or along the annular ring. Near such structures, uranium may impregnate tongue-like into permeable wall rock.

- Most favorable host for disseminated mineralization is non- or partially cemented, medium- to fine-grained sand derived from the Coconino Sandstone, the Esplanade Sandstone, and, to a minor degree, sand-siltstone from the Hermit and lower Toroweap formations. In the latter case, however, mineralization is more fracture-hosted than in purer sands.
- Uranium ore concentrations within the pipe are particularly at and below the stratigraphic Coconino-Hermit contact (e.g., Hack, Kanab North, EZ-2, and Canyon), within the Hermit interval (Pigeon, Kanab North, Pinenut, Hack, EZ-2, Orphan), at and below the Hermit-Esplanade/Supai contact (Orphan, Pigeon, Kanab North) (Fig. 5.108).

Metallogenetic Concepts

A collapse breccia pipe containing economic uranium ore bodies is a unique feature generated by the superimposition of multiple geologic and metallotectic processes. Critical parameters required for these processes and hence constrain any genetic modeling include

- a thick sequence of flat-lying sediments which include interbedded arenaceous units,
- presence of a basal limestone which underwent extensive karst development to form large caverns,
- collapse of the caverns associated with discriminative stoping through the superjacent sediments to create a chimney-like breccia pipe. Certain structural systems such as sets of joints or shears are very probably required for the karst and pipe development,
- arenaceous lithologies providing a porous and transmissive pipe infill in volume and physicochemical properties adeqate to host ore bodies,
- presence of chemical constituents in the system to supply the essential elements for the creation of a reducing environment, like H_2S, SO_2, Fe^{2+}, hydrocarbons, etc.,
- transmissive systems to permit mineralizing and other chemical fluids needed for ore formation to migrate to a pipe and within a pipe to optimum sites for ore emplacement,
- a uranium source capable of supplying the quantities required for economic ore grades and reserves,
- distinct epeirogenic, geohydrologic, and climate-related conditions to generate the necessary processes for leaching, transport, and concentration of the elements involved in ore formation,
- a long-lasting cratonic stability that continued until the present and prevented the deposits from destruction.

Impact of Lithologic-Stratigraphic Units on Formation of Breccia Pipes and Mineralization

The individual stratigraphic units of the Arizona Strip area may have contributed in a positive or negative way to the above criteria, and as such delineated an area favorable for ore formation as follows (Fig. 5.106):

Redwall Limestone:
- Sufficient thickness of carbonatic unit is required for formation of karst caverns large enough to initiate stoping of pipes of adequate size: estimated minimum thickness of karst unit in Redwall: ca. 25 m, which is present throughout Arizona Strip area;
- zones affected by strong karst development [according to Wenrich and Sutphin (1989), controlled by pre-Supai fracture sets oriented NW-SE and NE-SW];
- Redwall sediments contain Pb, Zn and other metal mineralizations, and may have provided these elements to the pipe mineralization.

Upper Supai Formation/Esplanade Sandstone:
- Arenaceous red bed strata with minor siltstone-mudstone beds may provide both favorable pipe infilling, and host rocks for annular ring ore;
- red beds constitute a potential source of Fe required for Fe-sulfide formation in the pipe;
- distribution of favorable lithology: to the E of a line trending about NNW-SSE on the N side of Grand Canyon and running somewhere between Kanab Creek and the Hurricane Fault; S of Grand Canyon the line turns into SW direction along about Peach Springs Canyon. Westwards of this line, the Esplanade grades into the marine Pakoon Limestone.

Hermit Formation:
- The dominantly ferrugenous siltstones are commonly unfavorable hosts for disseminated

mineralization unless they become more sandy, which appears to be the case in some of the northern segments of the Arizona Strip area, or where they are jointed and fractured. The annular ring and other pipe-bounding faults within the Hermit interval are good ore hosts,
- where too thick and too fine-grained, the silts may more or less seal breccia pipes, particularly those with small diameters, hence hampering circulation of mineralizing fluids,
- the unit represents a potential source of Fe,
- distribution: the Hermit thickens from an 0 isopach near Flagstaff to the N and W with a thickness of 120 m at the south rim of Grand Canyon, ca. 200 m at Pigeon and EZ-2 and ca. 300 m at Andrus Canyon.

Coconino Sandstone:
- The fine- and locally medium-grained quartzose sandstone provides in many pipes the most important host for disseminated mineralization,
- minimum thickness for providing sufficient host material for ore-bearing pipe fill is estimated to be 5 to 10 m,
- zones of limited consolidation at time of pipe formation would have permitted the flow of larger amounts of sands into the pipe (indicated sometimes by concentric thinning around pipes),
- noncemented zones could have served as conduit for mineralizing fluids,
- distribution: northern limit of the Coconino is along a more or less E-W-trending 0 isopach running about 10 to 30 km S of the Arizona-Utah state line, turning SE on the Paria Plateau. The Coconino thickens southward to about 25 m in the Hack Canyon area, 75 m at the Orphan Lode and 120 to 150 m in the Red Butte area. The grain size apparently decreases in the western part of the Arizona Strip along a transition zone which is more indicative for a marginal marine than continental environment of deposition.

Toroweap and Kaibab Formations:
- Much of the soluble material of the two formations has been leached concentrically around breccia pipes and parts thereof certainly entered the pipe,
- interbedded arenaceous facies, which become more abundant from about Kanab Creek eastward, may have been the source for ore hosting sand and silt pipe infill (e.g., in Pigeon and Kanab North),
- evaporitic gypsiferous beds are a potential source for sulfur (all sulfide caps in pipes are at the lower Toroweap interval),
- hydrocarbons are abundant in the two lower Toroweap members and are considered candidates for reducing agents in breccia pipes; also two oilfields in southwestern Utah produce from the Kaibab Formation,
- distribution: both formations occur throughout the Arizona Strip area, with typical marine sediments to the W and some littoral influence to the E.

Moenkopi Formation:
- The pelitic to semi-psammitic, partly calcareous sediments, 100 to 500 m thick from the E to the W of the Arizona Strip area, probably formed a rather impermeable cover over most of the Permian and older rocks of the Arizona Strip, particularly in its western section, hampering downward migration of solutions;
- distribution: originally (now largely eroded) throughout the Arizona Strip area, thickening from about 120 m near Marble Canyon in the E and Red Butte in the SE to 300–350 m in the Kanab area to the N and in excess of 500 m near Grand Wash Cliffs to the W.

Chinle Formation:
- The channel-filling fluvial arenites of the Shinarump Member are host to minable uranium deposits (e.g., Cameron at the eastern edge of the Arizona Strip area). The uranium has formed coeval with the 220 to 200 m.y. uranium generation in breccia pipes. This opens the possibility that uranium of both hosts derived from the same source and/or uranium has been transported from the Chinle channels through structural pathways into the pipes, perhaps via a permeable intermediary conduit like Coconino or Supai sandstones;
- distribution: originally (now largely eroded) in a NW-SE-oriented belt, 80 to 130 km wide, coming from the Petrified Forest National Park area in the far SE through Cameron to Kanab-Colorado City in the NW and further beyond. Flow direction was from SE to NW.

Proposed Model for Ore Formation

Ore formation was apparently not a single event but the result of several pulses of mineralization as indicated by the paragenetic interrelationship of ore and gangue minerals. The time frame for the metallogenesis is given by the following criteria. The time of formation of the breccia pipes in the Arizona Strip area started in late Mississippian time (Billingsley 1986) and continued intermittently into late Triassic Chinle time. Time constraints on the episode of the original mineralization are provided by the stratigraphic sequence involved in the collapse and the radiometric pitchblende ages. The stratigraphically bracketed period of ore formation is thereby comprised within the late Permian and the Triassic, and that of *earliest uranium introduction* by the oldest host rock, viz. the Permian Esplanade Sandstone. Consequently, the first uranium introduction cannot be older than the Esplanade what appears to be consistent with the 260 m.y. U-Pb pitchblende age, and almost certainly not younger than Triassic. Further on, initial ore introduction into the pipes must have occurred prior to the final cementation of the ore hosting sand pipe fill.

Mineralogical, isotope, and fluid inclusion data provide certain evidence on the *processes involved in ore formation*. The presence of calcite suggests that uranium was probably transported as a uranyl carbonate complex. Deposition of pitchblende and other minerals as well may have occurred when the mineralizing fluids entered the more open spaces in a solution pipe. Effervescence of CO_2 with associated *Pressure release* in breccia zones, fissures (annular ring structures etc.) and porous sands are considered a significant factor in the break-up of uranyl compounds. Invading hydrocarbons or H_2S derived from the pipe surrounding sediments may have been the agent for the required *reduction* of the U^{6+} ions but dissolution of early sulfides such as pyrite may have likewise created a reducing environment. A coeval oxidation of some pyrite to hematite associated with the pitchblende deposition could possibly explain the local coexistence of these minerals and may support the latter hypothesis.

Fluid inclusion studies suggest that the ore forming solutions, at least those which deposited calcite, dolomite and sphalerite but not necessarily pitchblende had temperatures ranging from about 80 to 170°C and salinities of always >9 and commonly >19 wt.% eq.NaCl (Wenrich and Sutphin 1989).

Sulfur isotope studies yield $\delta^{34}S$ values of −3 to −20% (Adamek P., pers. commun.) a spread similar to common sandstone-type uranium deposits on the Colorado Plateau but in contrast to the narrow range of isotopic ratios in magmatic hydrothermal deposits.

Nonradioactive lead isotope systematics of galenas give ratios comparable to Mississippi Valley type mineralization (Ludwig K.R., pers. commun.).

In summary, fluid inclusion and stable isotope data compare to some extent with those of Mississippi Valley type mineralization, hence they support a metallogenetic synthesis involving *brines* derived from connate or supergene sources in ore formation but reject a magmatic origin of the mineralizing fluids. A not magmatic origin is also consistent with the geological evolution of the Grand Canyon region because there are no igneous intrusions contemporaneous with the presumed time of ore formation. *Conduits* for the uranium mineralizing fluids are speculated to be either sandy horizons or structures. A conduit horizon favored by many geologists is the Coconino Sandstone. But any metallogenetic model involving this lithologically fairly uniform horizon of eolean clastics faces the problem of explaining the discriminative ore formation in different pipes that occur adjacent to each other in the same area and in the same facies of strata instead of a mutual ore emplacement in all these pipes. A more selective pathway for the solutions could more easily explain this phenomenon, for example, more restricted conduits such as faults or cataclastic zones through which fluids could migrate from uranium mineralized Chinle sandstone channels locally into the Coconino horizon and then downdip along the unit into a nearby breccia pipe if not directly into a pipe. Other potential conduits include channel-hosted arenaceous sediments as found in the Esplanade Sandstone or perhaps silty-sandy channels in the Toroweap Formation.

The *source of the uranium* is still enigmatic. Considering the different age determinations for pitchblende, a speculated source can include uraniferous sandstones of Permian, Triassic, and even Jurassic age, which elsewhere on the Colorado Plateau gave rise to extensive uranium mining. These formations are now largely eroded in the Grand Canyon region but remnants testify the

former presence at least of the Triassic Chinle Formation. Last but not least the Proterozoic basement may be considered a potential source either in the Mogollon Highland exposed to the S and SE, or immediately underlying the Arizona Strip area.

References and Further Reading
(for details of publication see Bibliography)

Adamek P pers. commun.; Barrington and Kerr 1963; Baillieul and Zollinger 1982; Billingsley et al. 1986; Bowles 1965, 1977; Boyden 1978; Chenoweth 1986; Chenoweth and Malan 1969; Energy Fuels Personnel, pers. commun.; Finch 1967; Gautier A pers. commun.; Gornitz 1969; Gornitz and Kerr 1970; Granger and Raup 1962; Hoffman 1977; Holland R pers. commun.; Jensen et al. 1960; Kofford 1969; Krewedl and Carisey 1986; Landais et al. 1987; Ludwig et al. 1986; Magleby 1961; Mathews 1978b; Mathisen IW, pers. commun.; Miller 1954a, 1954b; Miller and Kulp 1963; O'Neill et al. 1981; Peirce et al. 1970; Rasmussen et al. 1986; Rasmussen JD pers. commun.; Scarborough 1981; Sutphin 1986; Wenrich 1985, 1986, 1989; Wenrich and Sutphin 1989; Watkins 1976

5.6 Examples of Surficial-Type Uranium Deposits (Type 6, Chap. 4): Surficial Uranium Deposits in Duricrusted Sediments: Yilgarn Block, Australia

The Archean Yilgarn Block in Western Australia hosts in its northern part surficial-type uranium occurrences (Fig. 5.110). Almost all occurrences are of small size (few tens to <5000 mt U_3O_8) and low grade (0.025 to 0.09% U_3O_8) except Yeelirrie which contains 52 500 mt U_3O_8 at a grade of 0.15% U_3O_8. Total known resources of the district are 68 300 mt U_3O_8 (Battey et al. 1987).

Mineralization is confined to surficial duricrusted valley and playa sediments. The occurrences are therefore classified as surficial-type uranium deposits in duricrusted sediments (subtype 6.1, Chap. 4). They are sometimes also referred to as calcrete U deposits.

The following synopsis is essentially based on publications by the authors listed in section References unless otherwise stated.

Geological Setting of Mineralization

Noteworthy surficial uranium occurrences are associated with nonpedogenic calcrete or dolocrete within *intracratonic Tertiary to Quaternary drainage systems*. The shallow (dry) lakes and valleys are incised into Archean granites and greenstones, and filled with clastic material from the basement and evaporitic products. *Nonpedogenic calcretes*, also referred to as valley calcretes developed only north of the *Menzies Line* (roughly parallel to latitude 29°S, Fig. 5.110) whereas south of it pedogenic calcretes have formed. Butt et al. (1977, 1984) refer to the Menzies Line as a boundary separating different surface related *geochemical environments*. North of the line neutral to acid soils prevail composed of red, noncalcareous earths, sands and lithosols, more or less compacted by extensive hardpans. Calcretes are common in valley fills and locally in playas. The hydrochemistry of groundwaters is neutral to alkaline and less saline, particularly in calcrete terrane. South of the Menzies Line, groundwaters are neutral to acid and tend to be saline. Soils are predominantly neutral to acid and are comprised of orange to pink earthy sands, noncalcareous earths and calcareous and saline loams with kankar development.

Butt et al. (1984) note the importance of another morphologic-geochemical line, the *Meckering Line*. The line trends curvilinear in N-S direction and is the eastern boundary to all active streams dewatering to the Indian Ocean. No uranium occurrences are found in the Yilgarn Block west of this line.

Host Rock Alterations

Principal alteration of the host rocks is surface to subsurface hydrology related *Ca-, Mg-, Si-, and CO_2-metasomatism* leading selectively to the formation of calcrete, dolocrete, and other duricrust facies by gradual replacement of clay-sand material within the upper 10 m of the alluvial host sediments.

Valley sediments consist of varying amounts of quartz and kaolinite, with minor illite, montmorillonite, and feldspar. Calcrete and dolocrete formation resulted by the partial to complete replacement of kaolinite and quartz by carbonates (dolomite, calcite) and montmorillonite. Vugs within the calcrete may be filled with sepiolite or other Mg-clays.

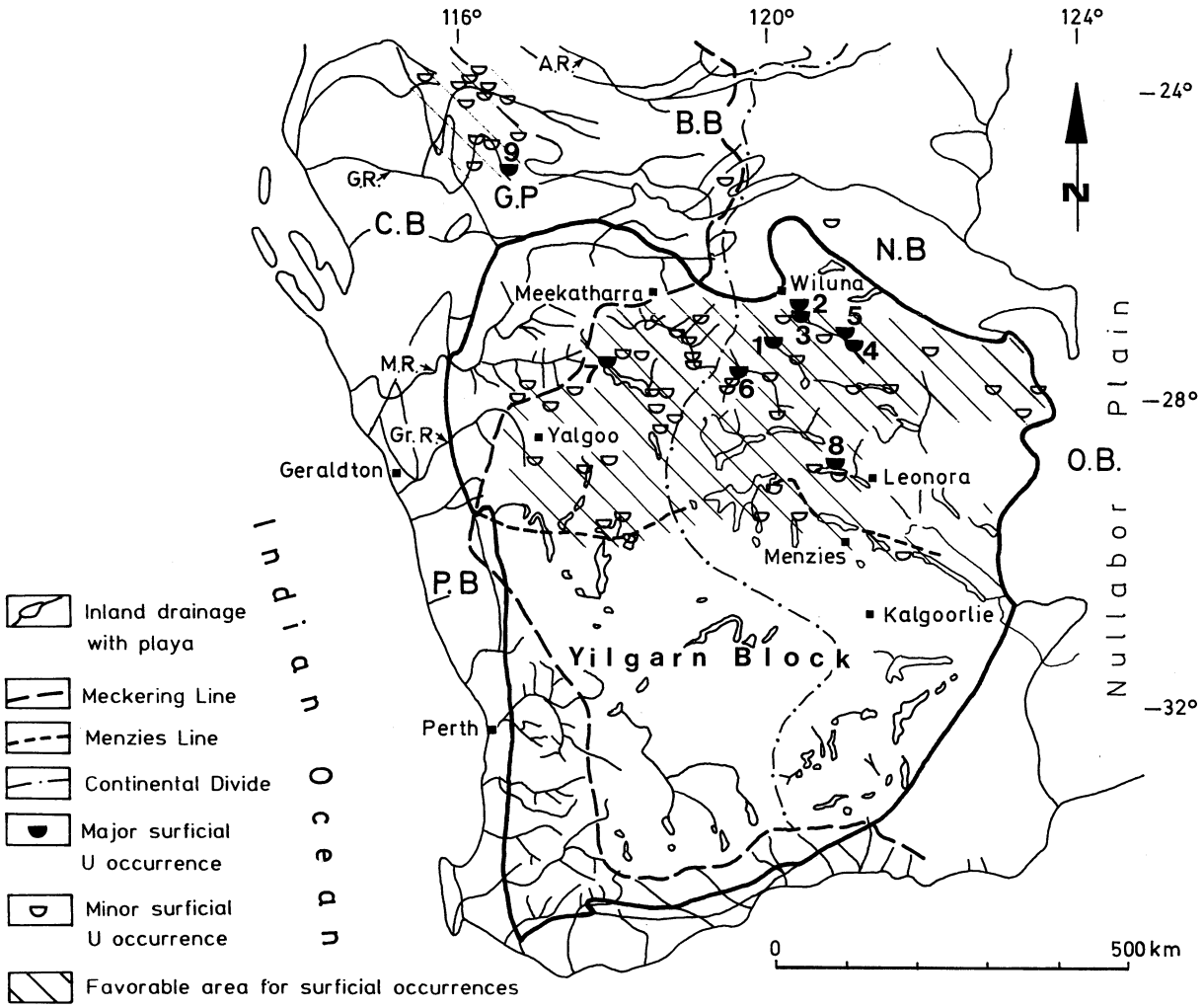

Fig. 5.110. Yilgarn Block, distribution of surficial uranium occurrences in relation to drainage systems and geomorphological features. All significant U occurrences within the Yilgarn Block are restricted to the section north of the Menzies Line and east of the Meckering Line. Minor U occurrences are found in the northerly adjacent Gascoyne Province. U occurrences: *1* Yeelirrie; *2* Lake Way; *3* Hinkler-Centipede; *4* Lake Maitland; *5* Mount Joel; *6* Lake Mason; *7* Lake Austin; *8* Lake Raeside; *9* Minindi Creek. Geotectonic units: *B.B.* Bangemall Basin; *C.B.* Carnarvon Basin; *G.P.* Gascoyne Province; *N.B.* Nabberu Basin; *O.B.* Officer Basin; *P.B.* Perth Basin. Major rivers: *A.R.* Ashburton River; *G.R.* Gascoyne River; *Gr.R.* Greenough River; *M.R.* Murchison River. (After Butt et al. 1984)

Gypsum and celestite may occur locally in larger amounts. Gypsum was preferentially precipitated in the upper part of a channel profile and is concentrated particularly in overburden. Celestite is found mainly in the clay-sand unit both as crystals and as fine bands.

The *replacement processes* were associated with an increase in rock volume provoking small-scale folds, faults, ubiquitous slickensides and, locally, diapiric structures or mounds bounded by faults. Karst development, another feature common to calcretes, was accompanied by caving and slumping (Mann and Horwitz 1979).

Host rock alteration in calcreted *playas* is in principle similar to that in valleys but often the calcrete development is not as well pronounced.

Principal Characteristics of Mineralization

Principal uranium mineral is *carnotite*. It occurs disseminated throughout earthy calcrete and in quartz-clay facies, fills small fissures and voids, replaces the argillaceous matrix of the host rock, and coats calcite, dolomite, silica and/or sepiolite, pore spaces in porcellaneous calcrete, and sand

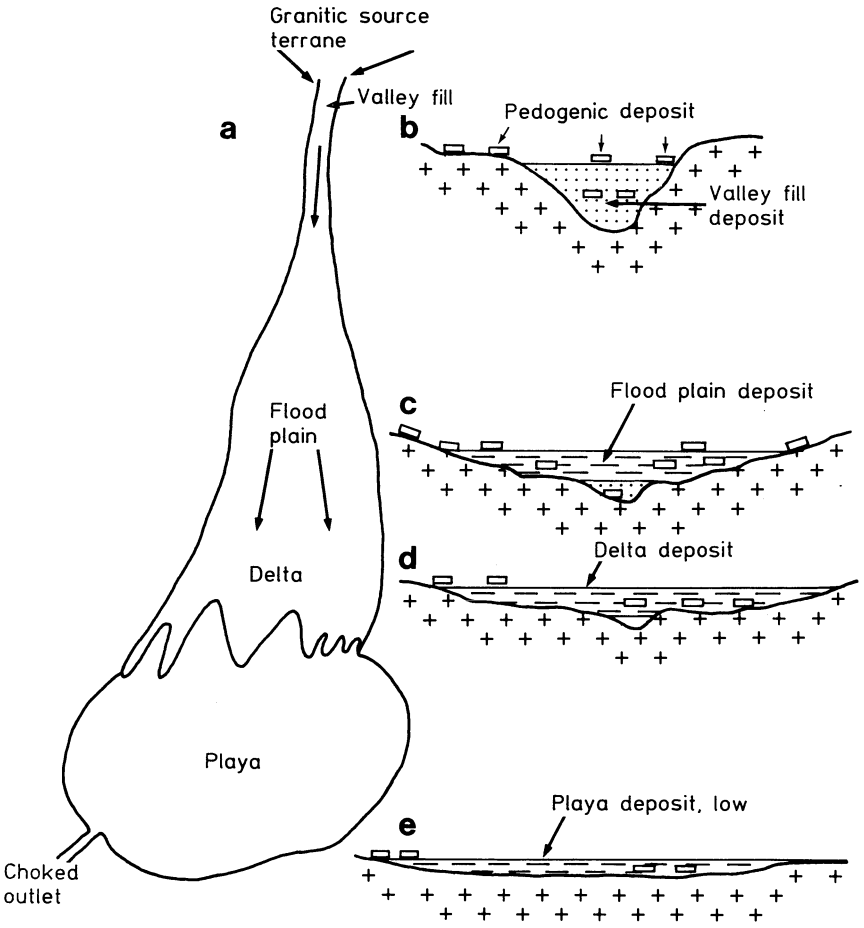

Fig. 5.111. Scheme of distribution of surficial uranium mineralizations located in valley-fill, flood plain, delta, and playa environments within a drainage system. Interspersed pedogenic formations representing periods of quiescence occur, as indicated, throughout the sediments. (After Toens and Hambleton-Jones 1984)

grains of clay-sand units. Some uranium in concentrations of up to 400 ppm occurs within thin veinlets of highly fluorescent opaline silica.

Two principal types of geomorphologic-lithologic uranium distribution, valley-fill and playa hosted mineralization prevail in the Yilgarn Block (Fig. 5.111). Butt et al. (1984) furnish the following characteristics of the two types.

Valley-fill deposits are hosted by calcrete or dolocrete and associated underlying sediments in the central channels of major drainage systems [for example Yeelirrie (Fig. 5.112), Hinkler Well] and in deltaic platforms transitional with these channels at playa margins [e.g., Lake Way (Fig. 5.113), Lake Raeside, Centipede].

Playa deposits [e.g., Lake Maitland (Fig. 5.114), Lake Austin] are hosted by near surface (a few meters deep), locally developed thin calcrete horizons and/or alluvial and evaporitic sediments composed of orange to red and brown saline and gypsiferous clays and muds commonly less than 2 m thick. They frequently rest on sandy and silty clays that may contain calcareous nodules.

Uraniferous playas are interconnected with valley calcrete drainages which themselves contain at least some uranium either in the main channel or the chemical delta (e.g., Lake Austin).

The *dimension* of uranium accumulations is often very large, in valleys up to some hundred meters wide, several kilometers long and 1 to 5 m thick in average. Playa mineralization can extend over a few square kilometers at a thickness of <1 to 5 m. Grades are mostly low, in the order of some 100 ppm U (Table 5.32). Ore grade pods (above ca. 0.1% U_3O_8) are rare exhibiting a patchy distribution within the anomalous zone.

Best uranium concentrations formed along the water table in calcrete which constitutes the principal aquifer. At several localities, however, as in the chemical delta type North Lake Way occurrence, uranium concentrated predominantly in subcalcrete clays and clay-quartz layers.

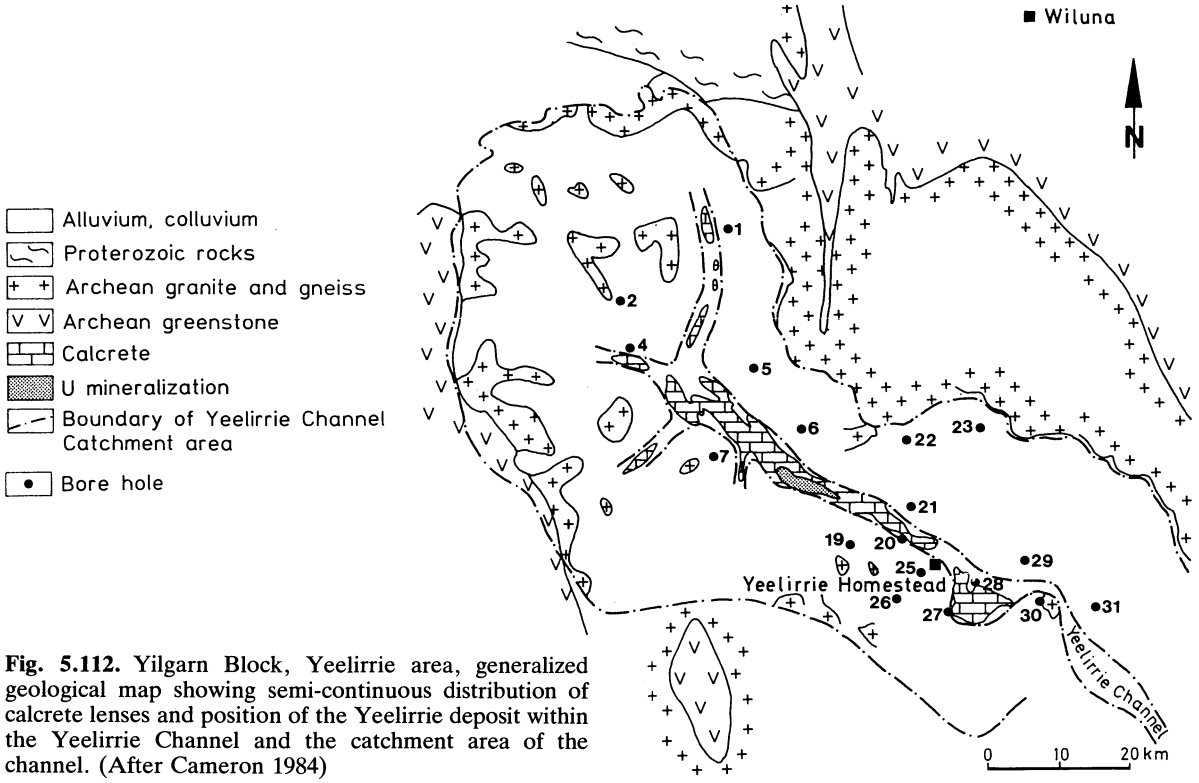

Fig. 5.112. Yilgarn Block, Yeelirrie area, generalized geological map showing semi-continuous distribution of calcrete lenses and position of the Yeelirrie deposit within the Yeelirrie Channel and the catchment area of the channel. (After Cameron 1984)

Potential Sources of Uranium

The spatial relationship of uranium occurrences with *granitic rocks*, anomalous in U content, strongly suggests that these rocks also served as the source for U, K and probably V to form carnotite. Fresh granites commonly contain 3 to 8 ppm U but range up to 80 ppm U (Gamble 1984). Since they are deeply weathered down to 250 m, the uranium has become accessible to leaching. Vanadium is probably derived from mafic minerals in the granitic rocks or perhaps from greenstones. (Butt et al. 1984).

Ore Controls and Recognition Criteria

Criteria that may have had a direct or indirect influence on the metallogenesis include:

Host Environment and Alteration

- Hot arid climate with occasional summer-only rainfall, and evaporation (±3500 mm/y) exceeding precipitation (±200 mm/y) by more than 15 to 1.
- Former humid climate reflected by intense lateritic weathering profiles in granite extending about 250 m deep (Oversby 1975).
- Very stable ancient block.
- Mature morphology with low relief.
- Drainage systems composed of linear depressions discharging into closed basins less than 100 m deep.
- Very low drainage gradient (ca. 0.001).
- Large catchment area in a terrane dominated by deeply weathered granitic rocks, many appreciably anomalous in uranium (av. 8–10 ppm with maxima of 80 ppm U, Gamble 1984) and greenstone belts considered a potential source for vanadium additional to the mafic minerals in granite.
- Absence of soils capable of fixing liberated U (pedogenic calcrete, ferricrete etc.).
- Depression fill of predominantly fine-clastic (clay-silt) fluvial, alluvial and lacustrine-evaporitic material.
- Absence of organic material in soil and depression fills.
- Epigenetic replacement of near surface sediments (within upper 10 m) by nonpedogenic calcrete, dolocrete, gypcrete and silcrete causing variable induration.

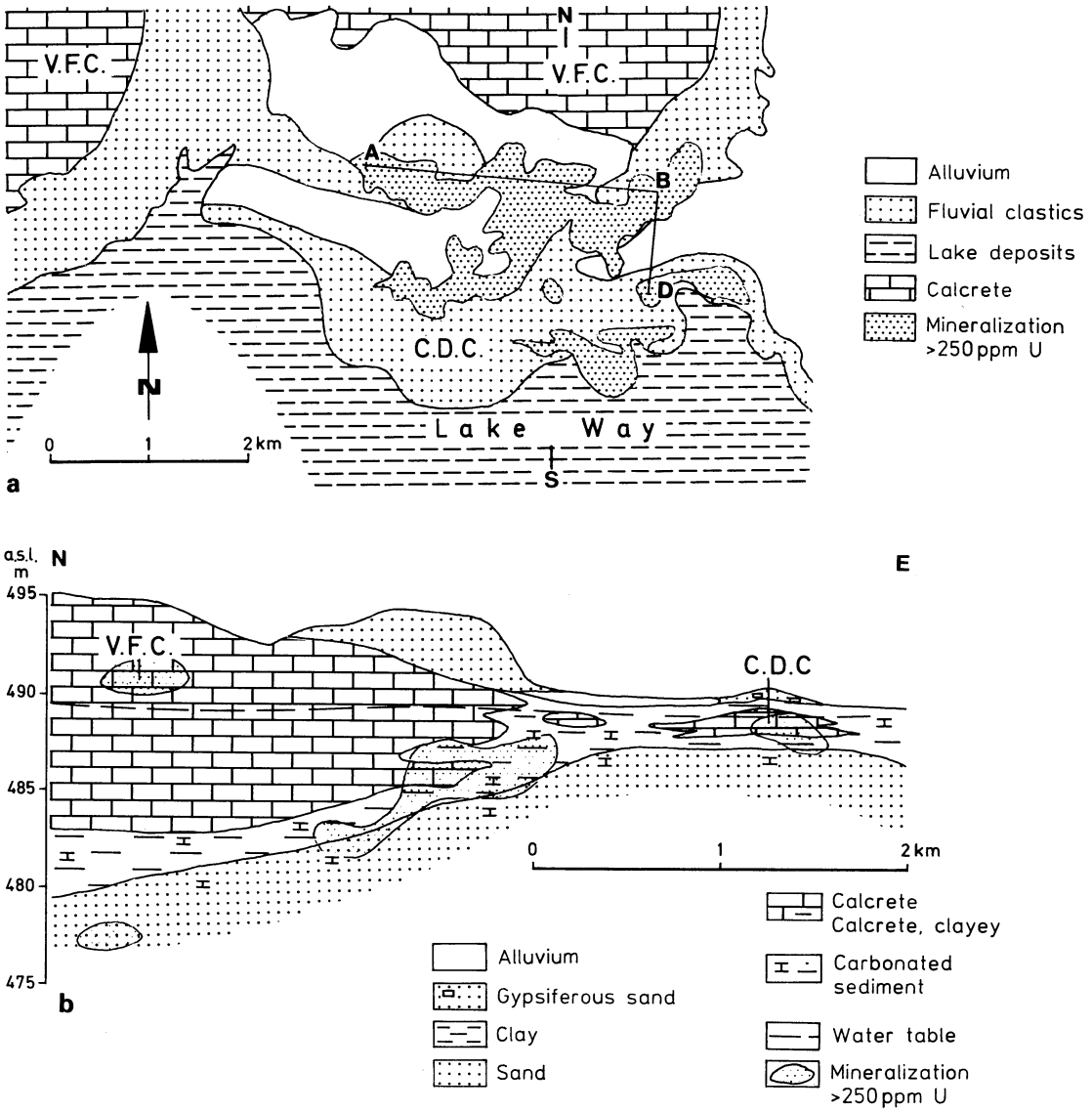

Fig. 5.113. Yilgarn Block, Lake Way. **a** Map of surficial geology with distribution of uranium mineralization in valley fill-delta environment. **b** Lithological N-S section through the uranium mineralized zone. **c** Lithological columns with distribution and grades of uranium (bulk samples) from three locations shown in **a**. Calcrete types: *V.F.C.* valley fill calcrete, light to dark gray; *C.D.C.* chemical delta calcrete (younger than V.F.C.), more massive, dolomitic, distinct brown *I* carbonate zone; *II* transition zone. (After French and Allen 1984)

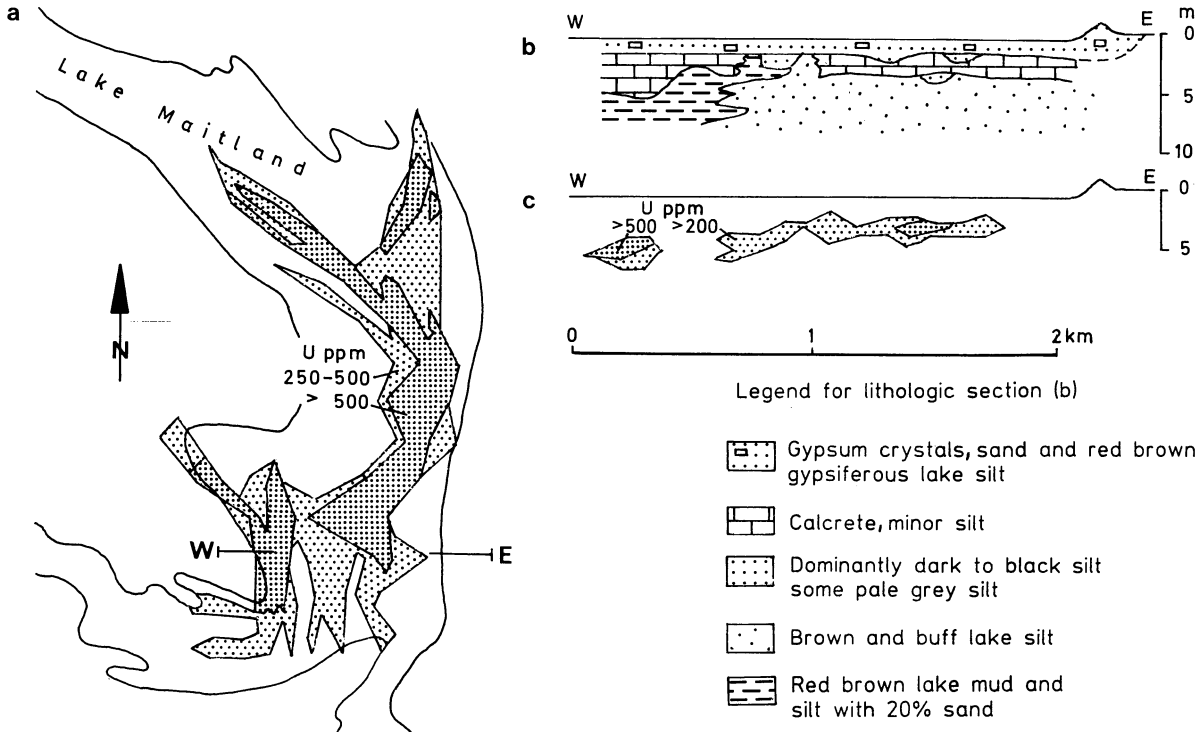

Fig. 5.114. Yilgarn Block, Lake Maitland. **a** Map of distribution and grade of uranium mineralization in playa environment. **b** Lithological W-E section. **c** Distribution and grade of uranium mineralization within the given lithological section. (After Cavanay 1984)

- Authigenic formation of silica hardpan cementing permeable, reddish acidic soils devoid of calcrete/dolocrete in headwater areas and valley flanks by opaline or chalcedonic silica; distribution of this type of hardpan coincides with the zone of non-pedogenic calcrete (Carlisle 1984).
- Distribution of calcrete/dolocrete mainly in axial segments of large channels becoming less well developed at playa margins (deltas) where the -cretes occur in irregular thin layers (up to 2 m thick).
- Thickest and most continuous calcrete/dolocrete development in the vadose and uppermost phreatic section above a shallow groundwater table in valleys.
- Distinct morphologies, structures, textures of calcrete/dolocrete (fault bound mounds, collapse structures, karst-solution cavities) with large-scale downdrainage variations of evaporative authigenic minerals, e.g., increasing dolomitization.
- Calcrete/dolocrete being the main and excellent aquifer.
- Very slow lateral movement of groundwater.
- Constrictions of channels by bedrock barriers resulting in a decreased flow rate and upward migration of groundwater to the evaporative surface.
- Similar effects as above by argillaceous horizons and hypersaline waters in salt lakes.
- Hydrochemistry of valley groundwater enriched in dissolved U, V, Ca, Mg, K, Na, CO_3, SO_4, and Cl, with U largely present as uranyl carbonate complex ions,
- Disproportionate down-drainage increase of ionic species, pH and TDS (total dissolved solids) except CO_3^{2-}, by approximately an order of magnitude between catchment area and mineralized zones supposedly due to evaporitic enrichment.
- Between lower valleys and salt lakes further increase of Ca, Na, K, Cl, SO_4, and TDS by about another order of magnitude or more at

Table 5.32. Yilgarn Block, summary of characteristics and dimensions of surficial uranium occurrences. (VF = valley fill, P = playa, D = delta/chemical delta, T = terrace type). (Data from Battey et al. 1987; Toens (ed.) (IAEA 1984) (for localities see Fig. 5.110)

U occurrence	Type of mineraliz.	Geological setting of mineralization	Dimension m	Grade % U_3O_8	Resource mt U_3O_8
1. Yeelirrie	VF	Calcrete in Tertiary drainage, intense dolomitization and development of sepiolite; mineral, parallel to channel	l: 9000 w: 750 th: 3–7	0.15	52500
2. Lake Way	VF	Calcrete in drainage channel entering Lake Way, in carbonatized fluvial clastics and in chemical delta carbonatic sed.	4 areas th: few cm to 5 m	0.09	3300
3. Hinkler Well-Centipede	VF	Calcrete in drainage channel, partly eroded, composed of calcite, chalcedony with minor dolomite, gypsum, sepiolite; chemical delta sediments; few better grade pods in very low grade U zone	l: 15000 w: <2000 th: 1–5 (very low grade zone) pods in 1 × 3 km^2	0.0001 –0.2	?
4. Lake Maitland	P	Discontinuous calcrete rich in dolomite, sand, sandy clays, silt; 2 zones	a) l: 6000 w: 300–500 th: 1–2	a) <0.07 b) <0.06	a) 3500 b) 500
5. Mount Joel	VF(?) D(?)	Channel calcrete bordering salt lake system	l: >5200 w: 550	?	?
6. Lake Mason	VF(?)	Calcrete zone	l: 4900 w: 250–750 th: <1	0.035	2700
7. Lake Austin	P	Calcrete (calcite, dolomite) with chalcedony in silicified zones, sandy clays, carbonate-rich, with kaolinite/smectite	l: 1500 w: 50 th: 1–5	>0.045	?
8. Lake Raeside	D	Calcareous clay, clayey grit in low-lying peninsula	l: 5600 w: 100–800 th: 1–2	0.025	1700
9. Minindi Creek	T (VF?)	Calcrete and calcareous alluvial, colluvial material on river valley terraces	?	0.0125	470
10. Thatcher Soak	D(?) VF(?)	Calcrete bordering salt lake system	l: 7500 w: 100–200 th: <2 m	0.03	4100

indifferent behavior of U, V, and Mg partly due to ore precipitation and its remobilization (Carlisle 1982).

Mineralization

- Principal ore mineral is carnotite precipitated in patchy ore grade accumulation within both the main calcrete/dolocrete lenses and immediately below it in ± carbonate-rich alluvium.
- Irregular distribution of mineralization both in grade and configuration.
- Commonly low grade and small tonnage ore bodies (<0.05% U_3O_8, rarely up to 5000 mt U_3O_8) in form of thin lenses (<1 to <5 m thick), Yeelirrie being the only exception.

Metallogenetic Concepts

Models for the formation of calcrete-related carnotite mineralization have been developed by a number of workers. The uranium source does not create a serious problem. More dubious is the

actual source of vanadium. The principal points of controversy are, however, (a) the composition and down-stream evolution of fertile solutions, which on the one hand require an oxygenated fluid to transport hexavalent uranium, on the other hand a reduced fluid to carry tetravalent vanadium, and (b) mechanisms to precipitate carnotite and to prevent it from remobilization in order to form ore.

Precipitation of carnotite may have theoretically occurred under a variety of conditions. Mann (1974) and Mann and Deutscher (1978a) consider seven possibilities

- separate U and V groundwater aquifers,
- variation of carnotite solubility with change of pH,
- dissociation of uranyl carbonate complexes,
- local rise in K activity,
- change in partial pressure of CO_2,
- redox-controlled deposition,
- evaporation of groundwater.

Butt et al. (1984) arrive at the conclusion that carnotite precipitates where concentrations of U and K have been increased by evaporation and where V^{4+} is oxidized to the pentavalent state. This may be at a site where V has migrated upwards along a redox gradient from a saturated zone at depth or where a subsurface bedrock barrier has forced upwelling of such vanadiferous groundwaters into a relatively oxidizing environment, places also characterized by mounding and lateral spread of calcrete.

Briot and Fuchs (1984) suggest the following evolution of carnotite deposits. Alluvial and calcareous lacustrine sediments were deposited during earlier wet periods. Subsequent drier, semi-arid conditions led to epigenetic alterations accompanied by mineralization. Limited precipitation and surface water flow contributed only minor recharge to the groundwater. As a result, semi-stagnant groundwater conditions evolved particularly in regimes where the hydraulic gradient was low (ca. 0.001 in the Yeelirrie channel) and/or where the waters ponded in front of a natural barrier such as a basement rise cutting a channel. Retardment of the waters was accompanied by a hydrochemical change to weakly oxidizing conditions and oversaturation of dissolved elements. These hydrologic and hydrochemical conditions implemented the epigenetic modification of lacustrine limestone by dolomitization and carnotite deposition in playas. In channel systems, such as the Yeelirrie channel, limited down-drainage recharge of the groundwater initiated slightly oxidizing conditions that acted as a geochemical barrier where dissolved V^{4+} was oxidized to V^{5+}, thereby providing the conditions required for carnotite precipitation by reaction of V^{5+} with already available $(UO_2)^{2+}$ and K^+ in solution. Concomitantly, Mg activity provoked partial dolomitization of the calcitic rock. This led to an increase in volume and related mound uplifting followed by sepiolite deposition in voids and fractures. In a subsequent interval of greater aridity, the epigenetic dolomitization process was interrupted. It was succeeded by silicification expressed by the development of opaline silica. The silica partly covered the carnotite, thereby protecting it against significant leaching.

Carlisle et al. (1978) believe that silica hardpan, valley calcrete and carnotite formation are closely related to the same arid climate prevailing in Western Australia for the past 25 000 years. All three phenomena are restricted to the same region north of the Menzies Line and east of the Meckering Line. The soil-moisture regime, resulting from evaporation significantly exceeding precipitation, is a critical factor in this scheme. In this climatic environment, opaline or chalcedonic hardpans devoid of calcrete are common in headwater areas and on valley flanks.

Within depressions, calcrete developed best and is most likely mineralized where chemically fertile groundwaters migrate laterally at a very low rate and approach or are forced toward the surface where they are exposed to evaporation.

The evaporation promotes an increase in the dissolved calcrete and ore-forming elements by about an order of magnitude between the headwaters and the site of calcrete and carnotite deposition.

Carlisle (1980, 1983) addresses the hydrochemical aspects of calcrete and carnotite precipitation and conservation. Groundwaters in most of the drainage systems, except in the headwaters, are neutral to alkaline, carbonated, and oxygenated. This composition makes a transport of uranium as uranyl carbonate complex ions most likely. Precipitation of calcrete from these solutions can be initiated by

- evaporative concentration of Ca^{2+} and Mg^{2+} down the drainage system,

- common-ion precipitation where waters enriched in Ca/Mg-carbonate intersect Ca/Mg-chloride or sulfate brines as in salt lakes,
- removal of CO_2 and concurrent increase in pH and the ratio CO_3^{2-} / HCO_3^-.

The first two mechanisms are prerequisites for the carnotite precipitation and preservation since they provoke crystallization of calcite or dolomite with continuous decrease of CO_3^{2-}. Other essential factors required for carnotite crystallization include the availability and concentration of U, V, and K.

Simple evaporative enrichment of U, V, and K ions improves the conditions of carnotite formation which precipitates where U- and V-bearing waters react with K-enriched hypersaline waters as in playas. Another critical factor for localizing carnotite is the oxidation of V to the pentavalent state. Processes proposed by Mann and Deutscher (1978) and mentioned earlier may be instrumental here.

The influence of CO_3^{2-} activity is as follows. Simple extraction of CO_2 and associated carbonate precipitation is insufficient for the fixation of carnotite. CO_2 extraction in fact decreases the solubility of $CaCO_3$, but it simultaneously increases the pH and the CO_3^{2-}/HCO_3^- ratio. In this environment and influenced by other factors, the solubility of carnotite is likely to increase and not to drop. Therefore, calcrete formation by simple removal of CO_2 from groundwater is not a satisfactory mechanism for fixing carnotite. On the other hand, combined evaporation and common-ion extraction associated with the deposition of carbonate removes CO_3^{2-} directly from the groundwater and thereby it makes carnotite less soluble.

Other mechanisms of U mineralization such as adsorption on clays, deposition of carnotite in

Table 5.33. Yilgarn Block, summary of geological criteria and processes involved in the formation of surficial carnotite deposits in inland drainage systems, (Arakel 1988)

Control	Influence
Tectonic stability	Development of subdued weathering topography and subsurface morphology
Arid to semi-arid climatic conditions	Development of phreatic carbonate and gypsite facies in axial sections of paleodrainage channels Development of vadose carbonate and gypsite facies overprinting the phreatic lithofacies Evaporative concentration of ionic species (including Ca, Mg, U, V, and K ions) in groundwater flowing down the drainages
Development of internal drainage systems	Relatively large catchment areas Source terrains variably anomalous in U content and rich in V, K, and Mg Relatively low drainage gradients Subsurface flow of groundwater in aquifers with different hydraulic characteristics and storage capacities
Carnotite precipitation	Destabilization of uranyl carbonate complexes by lowered $a_{CO_3^{2-}}$ Evaporative concentration of U, V, and/or K Oxidation processes Common ion precipitation of carbonates Absorption and surface catalysis
Ponding	Physical constriction Chemical barrier development
Postdepositional changes	Reconcentration due to continuous dissolution and reprecipitation of carnotite Removal of carnotite due to rejuvenated groundwater flow Relocation of carnotite due to the redistribution of hydrologic zones Redistribution of carnotite due to localized mobilization of vadose calcretes Complete preservation of carnotite due to a complete shift in groundwater flow patterns

response to a pH change toward neutral or by introduction of V from independent sources have been discussed but not substantiated as significant contributions to calcrete type ore formation.

Finally, preservation of carnotite mineralization demands tectonic and climatic stability to protect it from dissolution and/or erosion.

Table 5.33 provides in summary the criteria and processes involved in the formation of surficial carnotite deposits.

References and Further Reading for Chapter 5.6
(for details of publication see Bibliography)

Arakel 1988; Arriens 1971; Battey et al. 1987; Bettenay et al. 1976; Briot 1978, 1982, 1983; Butt 1988; Butt et al. 1977, 1984; Cameron 1976, 1984; Cameron et al. 1980; Cameron E, pers. commun.; Carlisle 1984; Carlisle et al. 1978; Carter 1981; Deutscher et al. 1980; Dickson 1984; Gaskin et al. 1981; Gee 1976; Heath et al. 1980, 1984; IAEA 1984; Johnstone et al. 1973; Jutson 1950; Mann and Deutscher 1978a, 1978b; Morgan 1965; Stuckless et al. 1981; Thomas WN, pers. commun.; Vels B, pers. commun.; Western Mining Corp 1976, 1978

5.7 Examples of Quartz-Pebble Conglomerate-Type Uranium Deposits (Type 7, Chap. 4)

5.7.1 Uranium-Rare Earth Elements Deposits in Quartz-Pebble Conglomerate: Blind River – Elliot Lake, Canada

The Blind River-Elliot Lake district is located in southern Ontario to the north of Lake Huron (Fig. 5.115). The district encloses three major ore trends. They are from N to S:

1. The Quirke trend in the Quirke Lake area with the active mines (1991) of Quirke, Denison and Panel, and abandoned mines Spanish-American, Stanrock and Can-Met (Fig. 5.116).
2. The Nordic trend in the Elliot Lake area with the Stanleigh mine and the former mines of Milliken Lake, Lacnor, Nordic, and Buckles.
3. The Pronto trend in the Blind River area.

A small deposit, Agnew Lake, is located ca. 100 km E of the district.

Production to 1990 amounts to more than 150 000 mt U_3O_8. Minor amounts of Th and Y were additionally produced.

The mining grade varied between 0.06 and 0.13% U_3O_8 averaging 0.108% U_3O_8. More recently mined ore had an average grade of less than 0.095% U_3O_8. Remaining reserves are about 300 000 to 350 000 mt U_3O_8, recoverable at costs of up to \$120/lb. U_3O_8 (Robertson 1987).

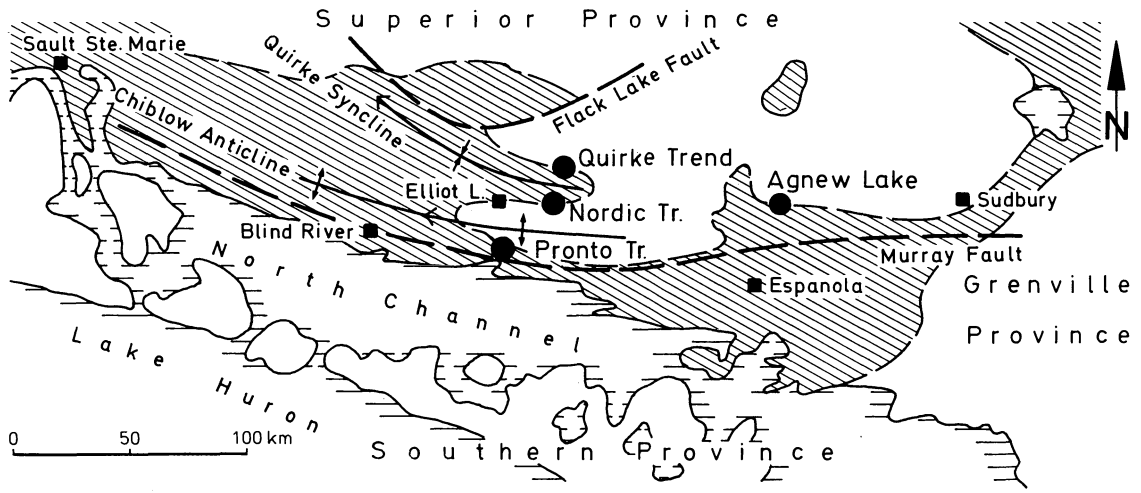

Fig. 5.115. Blind River-Elliot Lake-Agnew Lake area, distribution of the Huronian Supergroup (*hatched*) and position of uranium production centers (*black circle*). (After D.S. Robertson 1974)

Minable mineralization consists of uranium and REE minerals emplaced in a distinct oligomictic paleoconglomerate facies. The deposits are therefore classified as U-REE quartz-pebble conglomerate-type deposits of Lower Proterozoic age (subtype 7.1, Chap. 4).

The subsequent presentation is largely based on the comprehensive papers by J.A. Robertson (1978 to 1989), Roscoe (1969), and Theis (1979) unless otherwise stated.

Geological Setting of Mineralization

The Blind River–Elliot Lake district lies at the southern margin of the Canadian Shield. The area is underlain by three principal stratigraphic–petrographic units of early Precambrian age: The Archean basement, the Lower Proterozoic Huronian Supergroup, and post-Huronian intrusives. Paleozoic sediments and Pleistocene to Recent glacial deposits rest on the Precambrian.

The *Archean* includes (a) older metavolcanics, metasediments, and granitic and gabbroic intrusions and (b) late Archean/Kenoran quartz-monzonite (Algoman Granite). The quartz-monzonite contains anomalous contents of uranium in the area to the north and northwest of Elliot Lake (Richardson et al. 1975).

The *Huronian Supergroup* is a thick clastic sequence with minor tholeiitic basalts. Rocks of the Archean craton located to the northwest of Elliot Lake provided the sediments. Four groups constitute the supergroup. They are from bottom to top:

The *Elliot Lake Group* which consists of initial eugeosynclinal psammites, psephites, and volcanics and includes the uraniferous quartz-pebble conglomerate-arkose bearing Matinenda Formation (formerly named Lower Mississagi/ Bruce Group).

The *Hough Lake* and *Quirke Lake groups*. Each displays a sedimentary cycle starting with polymictic para-conglomerates interpreted as tillite and followed by clastics coarsening upward, in the Quirke Lake Group with intervening calcareous and dolomitic beds.

The *Cobalt Group* consists of three glacial to fluvial cycles ending with an upper coastal beach facies.

The *evolution of the Huronian Supergroup* strata is reflected in the lower Huronian section by the presence of sulfides, dominantly pyrite, associated with uranium in the near-shore clastic units such as the ore-bearing greenish-gray colored Matinenda Formation. In contrast, the upper Huronian contains thorium and abundant

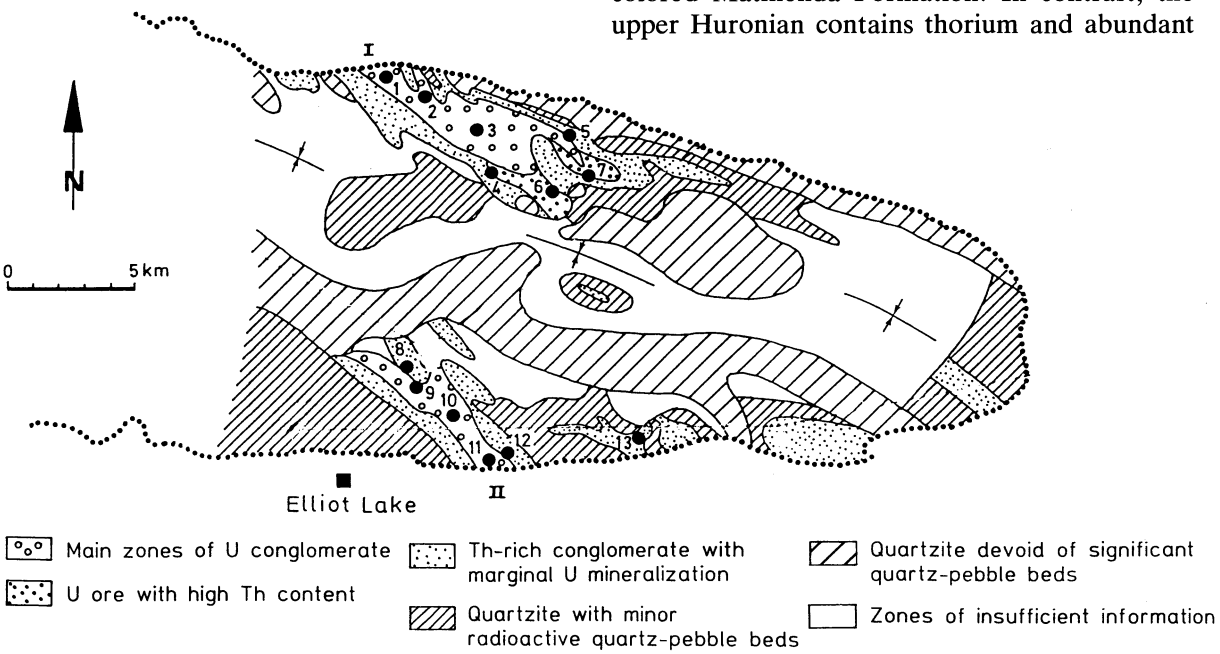

Fig. 5.116. Blind River-Elliot Lake, Quirke Syncline, distribution of uraniferous and other radioactive conglomerates within the Matinenda Formation. Mineralized trends and mines: I Quirke trend; *1* Quirke 1; *2* Quirke 2; *3* Denison; *4* Spanish American; *5* Panel; *6* Stanrock; *7* Can-Met; II Nordic trend: *8* Stanleigh; *9* Milliken; *10* Lacnor; *11* Buckles; *12* Nordic; *13* Pardee/Pardee trend. [After Roscoe in Douglas (ed.) 1970]

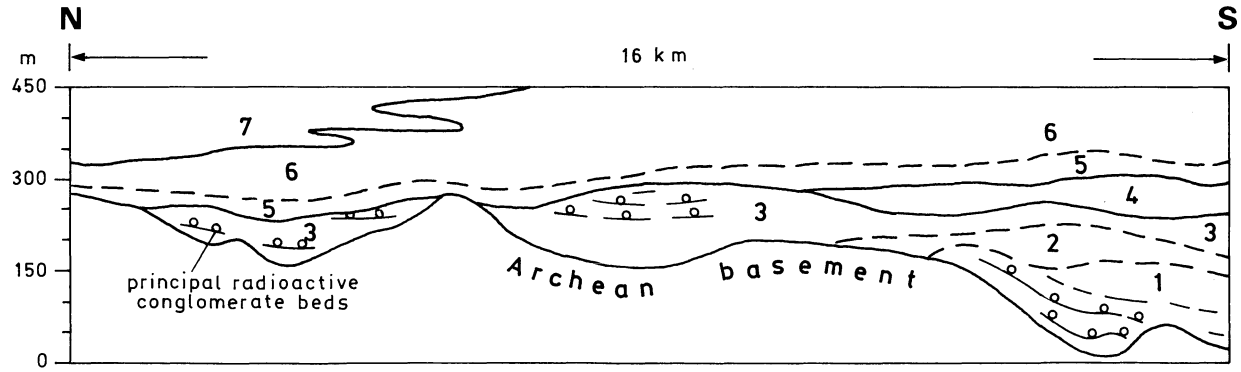

Fig. 5.117. Blind River-Elliot Lake, Quirke Syncline, restored stratigraphic section prior to Hudsonian folding. *1* Matinenda Formation, Ryan Member: greenish subarkose with radioactive quartz-pebble conglomerate. *2* Matinenda Formation, Stinson Member: various sorted conglomerates including beds rich in quartz pebbles. *3* Matinenda Formation, Manfred Member: white subarkose and greenish subarkose with beds of radioactive quartz-pebble conglomerate. *4* McKim Formation: fine-grained subgreywacke, subarkose, siltstone and argillite, grading northward into white and greenish subarkose. *5* Ramsay Lake Formation: conglomeratic greywacke. *6* Pecors Formation: argillite, siltstone and subgreywacke. *7* Mississagi Formation: medium-grained, well-sorted white subarkose at base and coarse-grained, poorly sorted greenish subarkose above. [After Roscoe in Douglas (ed.) 1970]

hematite that imposes a pink hue on certain rocks from the Gowganda Formation upwards. The variation is considered due to an increase of atmospheric oxygen during the period of the Huronian Supergroup deposition.

The Matinenda Formation, the basal unit of the early Lower Proterozoic Elliot Lake Group is the host to the uranium deposits. The psephitic and psammitic sediments of the Matinenda Formation were deposited in regressive cycles, resulting in several superimposed quartz-pebble conglomerate horizons interbedded with arkose and sandstone within depressions of the Archean basement (Fig. 5.117).

Pienaar (1963) and Fralick and Miall (1982) document a high energy, braided fluvial environment with a S to SE-directed stream flow for the deposition of the Matinenda Formation.

During the Blezardian (ca. 2100 m.y.) and Penokean (Hudsonian) (ca. 1900–1750 m.y.) orogenies the sediments were mildly metamorphosed and gently folded. The main fold axes trend WNW-ESE in the western part of the belt and E-W to ENE-WSW in the eastern part.

Diabase (Nipissing Diabase) intruded about 115 m.y. ago (Stockwell 1982).

Structures consist of steeply dipping, mainly NW-SE-striking faults with minor displacements. A regional structure in the uranium region is the *Murray Fault*, a high angle reverse fault which trends about E-W, parallel to the main axes of the fold belt. To the north of the Murray Fault (Fig. 5.115), the Huronian rocks are developed relatively uniform over a width of about 25 km and a thickness of 1200 m. All economic uranium deposits are located in this northern section. To the south of the Murray Fault, the thickness of the Huronian suite increases associated with facies changes.

In the Blind River-Elliot Lake district, i.e., on the northern side of the Murray Fault, the Huronian sediments are folded into a WNW-ESE-oriented syncline, the *Quirke Syncline* (Fig. 5.116), paralleled to the south by the Chiblow Anticline, which is formed in its eastern part by Archean granitic rocks.

Host Rock Alterations

No major alteration related to the initial uranium emplacement has affected the host rocks. *Post-depositional modifications* as reported by Robinson and Spooner (1984) include (a) pressure solution of quartz reflected by slight impression of adjacent quartz-pebbles into each other and formation of irregular quartz masses, (b) growth of secondary quartz, (c) sericitization in different degrees of K-feldspars and (d) pyritization with more than about 90% of the pyrite present being of post-depositional origin.

Remobilization of the uraninite was accompanied by certain mineral transformations and recrystallization of some authigenic minerals, particularly involving Ti-minerals and hydrocarbons.

Intrusion of Nipissing Diabase dikes and sills caused locally albitization, chloritization, and carbonatization of the wall rocks but affected generally only on a very minor scale pre-existing uranium mineralization (Robertson 1968, 1978). An exception to this is at the Pronto mine, where a larger part of the deposit has been modified partly into albitic-chloritic-carbonatic host rocks (Heinrich 1958, 1982).

Alteration related to *paleoweathering* of the Archean basement is best preserved on granitic rocks, where it produced a paleosol composed of quartz, microcline, and sericite with a conserved granitic texture grading into fresh granite (Robertson 1978, 1986; Pienaar 1963).

The chemical character of the paleosol, particularly the presence of uranium and ferrous iron, suggests the weathering processes operated under reducing conditions. (for more details on the paleosol see Gay and Grandstaff 1980; Goddard 1987; Kimberley et al. 1984).

Principal Characteristics of Mineralization

Principal *ore minerals* are uraninite, U-Ti-phases ("brannerite"), and monazite, constituting up to 5 wt. % of the ore mined. Coffinite, uraniferous kerogen (formerly listed as thucholite), uranothorianite, uranothorite, xenotime, and gummite occur in subordinate to trace quantities. The in-situ U/Th ratios range within the various ore bodies from 5 to 0.3 and in ore milled from 2 to 3.

Dominant *associated mineral* is pyrite (5 to 20 wt. %). In minor to trace amounts occur zircon, ilmenite, chromite, cassiterite, ilmenomagnetite, allanite, rutile, garnet, spinel, tourmaline, titanite, apatite, pyroxene, and perthitic microcline. Gold is very rare.

Uraninite is the important ore mineral in some ore zones, whereas in others U-Ti-phases predominate with uraninite second.

Uraninite grains are up to 0.2 rarely 1 mm in diameter and contain 48–69% (av. 65%) UO_2, 4–10% (av. 6.5%) ThO_2, 1.5–4.5% (av. 2.5%) Y_2O_3, ca. 0.9% Ce_2O_3 and ca. 18% PbO. Further rare earth elements are in order of relative abundance Nd, Dy, Gd, Sm, Er, Pr, and La, totalling 3–8% rare earth oxides (Grandstaff 1980; Roscoe 1969; Robertson 1978; Theis 1979).

Uraninite occurs (a) as small clusters of grains between pebbles, (b) in 0.5 to 1 cm thick, almost monomineralic subparallel bands of well-sorted angular grains, (c) concentrated proximal to the base of small-scale depositional units within conglomerates and (d) in a notable positive correlation with maximum apparent quartz-pebble diameter (r = 0.47) (Theis 1979; Roscoe 1969).

Ruzicka and Steacy (1976) describe ribbons 0.3 to 1 cm thick composed of uraninite fragments cemented by sulfur-rich filamentous *hydrocarbon* and associated with subrounded grains of brannerite, monazite, and fractured pyrite below the bands. Small quartz pebbles depress the top of the band. The feature is interpreted by the authors as reflecting a hydraulic separation of the ore constituents and that the hydrocarbons originally accumulated as an oily material on the top of that depositional sequence, possibly capable of acting as a collector for the uraninite.

"*Thucholite*", also referred to as uraniferous hydrocarbon or kerogen, is present in only minor quantities. It occurs (a) as ribbons on the top of ore reefs as mentioned above, (b) as disseminations within ore beds and (c) in post-ore fractures associated with post-ore sulfides. Willingham et al. (1985) identified the hydrocarbon as kerogen probably derived from algal mats.

"*Brannerite*" (amorphous U-Ti-oxide mixtures) is considered to be the reaction product of uranium with titanium oxides within the conglomerates after their deposition. It occurs as minute grains filling pores with sizes ranging up to 1.5 mm. Theis (1979) noticed three varieties of "brannerite" which may contain 8–41% U_3O_8, 0–2% ThO_2, up to >5% CaO and 20–37% TiO_2 with wide variations in the U_3O_8/TiO_2 and U_3O_8/ThO_2 ratios.

Pyrite is the most common associated mineral. It occurs as 0.5 to 3 mm grains of various shapes, composition, and generations dispersed throughout the matrix of the uraniferous conglomerates and, to a lesser extent, the intervening quartzite beds. Individual grains range from rounded ("buckshot" pyrite) to euhedral, and some are spongy.

For more detailed mineralogical descriptions the reader is referred to Roscoe (1969) and Theis (1979).

Economic uranium mineralization has been found in *three ore trends* corresponding to three NW-SE-oriented fluvial systems of the Matinenda Formation: (1) the *Quirke trend* on the northern and (2) the *Nordic trend* on the southern limb of the Quirke Syncline located to the north of the Chiblow Anticline, and (3) the

Pronto trend located on the southern slope of the Chiblow Anticline (Figs. 5.115, 5.116).

Uranium mineralization is confined to *several horizons* of oligomictic quartz-pebble conglomerate (Figs. 5.117, 5.118) rich in pyrite which were deposited in braided and interfingering stream channels or as lenticular, sheetlike beds. The conglomerates are interbedded with weakly mineralized or unmineralized, poorly sorted and coarse-grained quartzites or arkoses with greenish colored sericitic matrix.

The *uraniferous conglomerates* consist of well-rounded and well-sorted quartz (>95% of the pebble fraction) and chert pebbles (diameter 2–10 cm) which are often smokey, and a matrix of quartz, feldspar, sericite and pyrite, the latter constituting 5–20 wt. %. Heavy minerals including the ore specimen occur in the matrix. Clay- and silt-size particles are almost absent. The conglomerates display a gradational sedimentary, and mineralogic and geochemical zoning in the direction of transport. (Fralick and Miall 1982; Pienaar 1958, 1963; Robertson 1968; Roscoe 1969; Theis 1979). Characteristics of this zoning are listed in section Ore Control and Recognition Criteria, p. 350.

The major and presently (1991) mined ore bodies occur in the *Quirke Syncline*. Dimensions of the syncline are up to 15 km wide, more than 50 km long, and slightly more than 1000 m thick in its mineralized portion. The axis of the Quirke Syncline trends WNW-ESE and plunges to the WNW at a low angle (Fig. 5.116). Uranium mineralization occurs in a basal stratigraphic zone which is up to 150 m thick but does not necessarily lie directly on the Archean basement (Figs. 5.117, 5.118). It crops out locally at surface and extends downdip to a depth of 1000 m.

Two economic ore trends are recognized in the Quirke Syncline (Fig. 5.116) but it should be noted that uranium mineralization is not restricted to these two. The *Quirke trend*, the main ore producer, has a length of almost 10 km in WNW-ESE direction and a width of 1.8 to 2.7 km. The Quirke trend covers an area of about 20 km^2. Up to eight mineralized conglomeratic horizons, referred to as reefs, are developed within a 50 m thick sequence of the Manfred Member near the base of the Matinenda Formation. The strata dip to the south at angles of 15 to 25° (Table 5.34, Fig. 5.118).

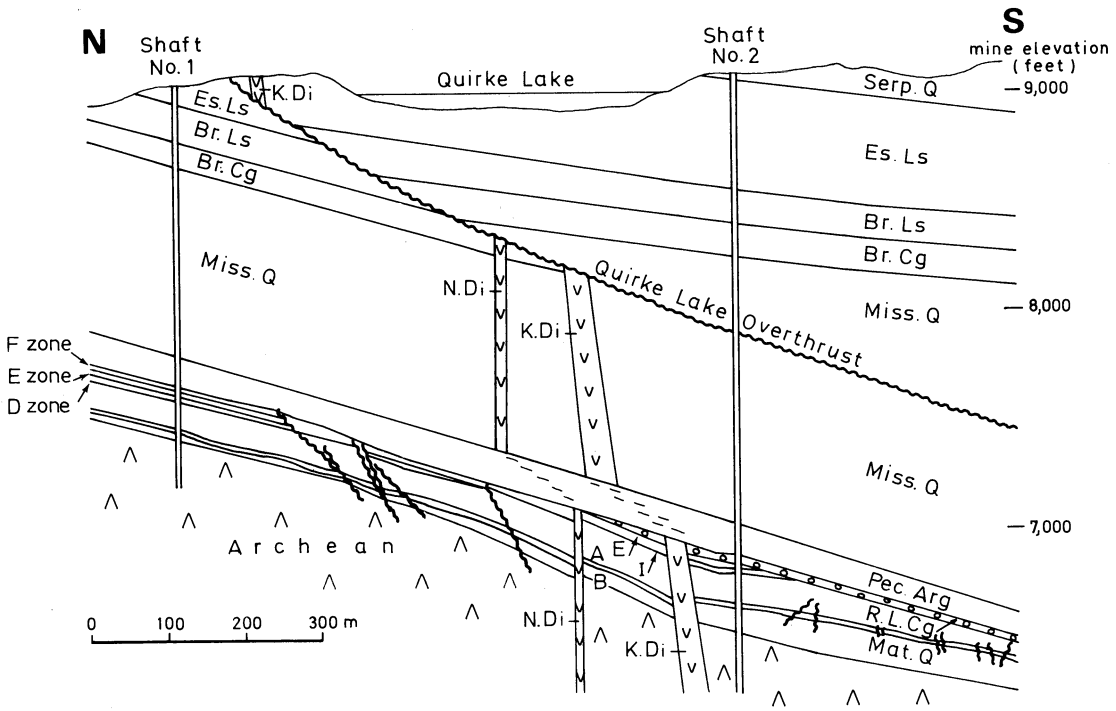

Fig. 5.118. Blind River-Elliot Lake, Denison mine, geological N-S section showing position and attitude of the uraniferous conglomerate horizons (A to F zones) *Serp. Q* Serpent Quartzite; *Es. Ls* Espanola Limestone; *Br. Ls* Bruce Limestone; *Br. Cg* Bruce Conglomerate; *Miss. Q* Mississagi Quartzite; *Pec. Arg* Pecors Argillite; *R. L. Cg* Ramsay Lake Conglomerate; *Mat. Q* Matinenda Quartzite; *K. Di* Keyes Dike (diabase); *N. Di* Negri Dike (diabase), *Archean*: undifferentiated, essentially greenstone. (After J.A. Robertson 1989, based on Denison Mines Ltd.)

Table 5.34. Blind River-Elliot Lake, Quirke Trend, stratigraphic position and correlation and thickness of uraniferous quartz-pebble conglomerates in the *Denison* and *Quirke* mining areas. Minable conglomerate beds/zones are printed in italics. (Based on data from Gunning in Robertson J.A. 1966 and Little et al. 1972) (for location see Fig. 5.116)

Denison Mine		New Quirke Mine
Post-Matinenda cover		
300 to 900 m		115 to 700 m
Matinenda Formation		
Dip of strata: 20° S Strike of strata: ±E–W Plunge of ore zones: 5° SE		Dip of strata: 0 to 50° S, av. 23° S Strike of strata: ESE–WNW
Quartzite: 15 m		Quartzite + thin conglomerates: 0 to 9 m
F-zone: 1.2 to 2.7 m, av. 1.8 m Quartzite: 6 m		Upper upper zone: av. 1.5 m Quartzite + thin conglomerates: 7.5 m *Upper zone*: av. 1.5 m Quartzite + thin conglomerates: 2.4 to 3.6 m
E-zone: 1.5 to 2.7 m, av. 2.1 m Quartzite: 6 m	=	*A (Quirke 1)-zone*: av. 2.7 m Quartzite: 3.6 to 5.1 m
D-zone: 1.5 to 2.4 m, av. 1.8 m Quartzite: 33 m	=	B-zone: av. 2.25 m Quartzite + thin conglomerates: 19.5 to 25.5 m
		CL-zone: av. 3 m Quartzite: 2.4 to 6 m
A1 + A2-zone: 1.8 to 3.6 m, av. 2.4 m Intercalated quartzites: 1 to 2 m		
		C (Quirke 2)-zone: av. 3.3 m
B-zone: 1.2 to 3 m, av. 2.4 m Quartzite: 0 to 55 m		C-Footwall zone: 0 to 12 m, av. 9 m Quartzite, basal conglomerate: 0 to 27.6 m
Archean basement		

Individual mineralized conglomerate sheets vary in thickness from 1.5 to 3.6 m. They are separated by quartzitic arenites 6 to 33 m thick. Robertson (1962) notes the conglomerate banks have relatively abrupt up-channel terminations and long fingering down-channel ends. They wedge out against Archean highs to the NW and W and are truncated to the N by unconformably transgressed Ramsay Lake sediments. The eastern and southern boundaries are associated with the thinning of the conglomerates, the thickening of intervening quartzites and decrease in the uranium grade.

The *Nordic trend* is located near Elliot Lake, about 12 km to the south of the Quirke trend. It has a NW-SE length of almost 6 km and a width of 1.3 to 1.8 km.

The Nordic trend contains three uraniferous conglomerate horizons in the lower 50 m of the Ryan Member of the Matinenda Formation, which dips about 15° N. Thickness (Robertson 1987) and grade of the conglomerates from top to bottom are 1.2–3.9 m with 0.115% U_3O_8 in the upper Pardee horizon, which extends from the Nordic mine into the Pardee and Pecors zones, 1.5–5.4 m with 0.125% U_3O_8 in the middle main (Nordic) horizon, and 1.5–7.5 m with 0.1% U_3O_8 in the lower Lacnor horizon. All three horizons extend downdip into the Stanleigh mine. The conglomerates are truncated in up-channel direction by the younger Stinson conglomerate or by facies changes within the Matinenda Formation or against Archean basement.

The *Pronto trend*, located some 25 km S of the Quirke Syncline, has an extension of about 1 × 1 km. It contains one mineralized conglomeratic bed which has a thickness of 2.0 to 2.5 m in the average and which dips 15 to 20° S. The Pronto ore trend is truncated at its southern end at a depth of about 300 m by the Pronto overthrust, a structure associated with the Murray Fault. The northern end of the Pronto trend is eroded.

Uranium mineralization occurs not only in the conglomerate but also in structures.

Dating of heavy minerals in the Matinenda conglomerates yields *ages* of 2550 ± 50 m.y. for uraninite (Meddaugh and Holland 1981), 2500 m.y. for monazite and 2450 m.y. for zircon (Mair et al. 1960). These data are compatible with a primary age of an Archean source.

Potential Sources of Uranium

The primary ore-forming mineral assemblages attest to a detrital origin of *granitic provenance*. The uraninite contains amounts of ThO_2 (up to about 9%) and rare earth oxides (up to 8%) which are typical for pyrogenetic uraninites of granites and particularly of pegmatites, e.g., as found in the Bancroft district and a number of other occurrences of uraninite in Archean rocks as outlined by J.A. Robertson. The apparent age of ca. 2550 ± 50 m.y. of detrital uraninite grains (Meddaugh and Holland 1981) attest a pre-Huronian origin. Similar ages were obtained for monazite and zircon. These data reflect a source of Archean age. Depositional trends indicate a source to the N and NW of the ore district, where predominantly granites and minor greenstones of Archean age outcrop.

Ore Control and Recognition Criteria

Essential ore controlling or recognition criteria include:

Host Environment

- Host rock is a pyritiferous oligomictic quartz-pebble conglomerate deposited in Lower Proterozoic time prior to the oxyatmoversion of the earth atmosphere.
- The uraniferous conglomerates were laid down in alternation with arenaceous sediments by rivers flowing from NW to SE as reflected by regional variations in pebble size and relative pebble packing and heavy mineral zonal distribution.
- Provenance of the conglomerates was largely from granitic terrane.
- Deposition occurred immediately above the Archean-Lower Proterozoic unconformity in paleovalleys or braided fan deltas (Fig. 5.117).
- Heavy minerals are particularly concentrated on the lee-side of Archean basement highs (Fig. 5.119).

With respect to the Quirke trend, the following features are listed by Theis (1979) (Fig. 5.120):

- Conglomerate development within the ore horizon is more variable to the NW and more persistant and continuous to the SE.

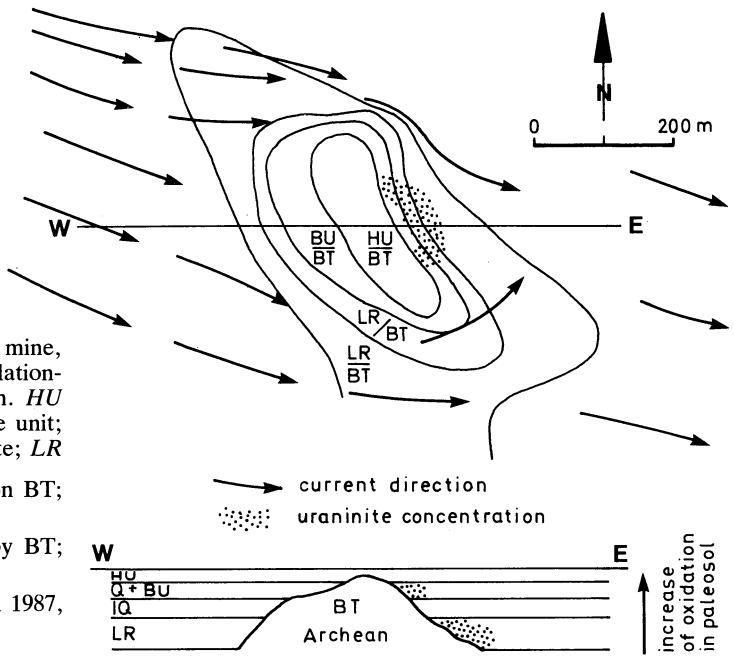

Fig. 5.119. Blind River-Elliot Lake, Denison mine, stratigraphic, spatial and fluvial dynamic relationship of ore reefs and a local basement high. *HU* Hanging wall (upper reef); *Q* Thin quartzite unit; *BU* Basal upper reef; *IQ* Interstitial quartzite; *LR* Lower reef; *BT* Basement. $\frac{HU}{BT}$ HU rests on BT; $\frac{BU}{BT}$ Bu rests on BT; LR/BT LR cut off by BT; $\frac{LR}{BT}$ LR rests on BT. (After J.A. Robertson 1987, based on Goddard 1987 and Theis 1979)

- Well-packed conglomerate is commonly more abundant to the NW and less abundant to the SE.
- Poorly packed conglomerate and quartzite within the ore horizon increase to the SE.
- Pebbles decrease in size from NW to SE and within a vertical section from bottom to top.

Alteration

- There is no alteration associated with the deposition of the detrital ore-forming minerals.
- Postdepositional modifications include intense pyritization, some silicification, minor sericitization of feldspar, destruction and neoformation of Ti-minerals, and hydrocarbons.
- Intrusion of diabase dikes and sills resulted locally in albitization, chloritization, and carbonatization of the wall rocks.
- Paleoweathering of the Archean paleosurface was essentially of physical nature.

Mineralization

- Original ore minerals are detrital uraninite, uranothorianite, uranothorite, xenotime, and monazite deposited synsedimentary with the enclosing conglomerate.
- Post-depositional modification of the ore produced U-Ti-phases (brannerite), coffinite, and uraniferous kerogen (thucholite).
- A *sedimentological control* of the mineralization is indicated by lithologic, mineralogical, and geochemical zonation. The zoning is expressed by changes in the relative abundance of specific heavy minerals related to variations in the depositional facies as reflected by the size and packing density of quartz pebbles. Salient criteria of this sort in the Quirke trend are as follows (Fig. 5.120) (similar characteristics are known from the Nordic trend except that here the U/Th ratios are lower):
  - Association of ore minerals with well-sorted oligomictic quartz and minor chert pebbles.
  - Downslope decrease of pebble diameter from ca. 10 cm near the source to about 2 cm several kilometers away, correlates with a transition from uranium-rich to thorium-rich and finally to titanium-zirconium-enriched zones. (uraninite is associated with coarse pebbles while it is scarce or absent in facies with pebbles of less than 3 cm in size).
  - A downslope increase of the Th/U ratio, over a distance of about 8 km from 0.27 in the Old Quirke mine to 0.4–0.5 in the Denison mine and to 0.8 in the Panel and Stanrock mines. Chemical data of hand-specimen (Theis 1979) attest to a corresponding quantitative distribution of U. Samples contain ca. 1% in the NW part of the Quirke trend decreasing to ca. 300 ppm U_3O_8 in the SE part. In contrast, Ce, La, Th, Ti, Y, and Zr increase down the paleoflow direction. Th shows a less clear pattern than the others due to its incorporation (a) in uraninite, which is dominant in the coarser upstream fraction, and (b) in thoriferous minerals, which prevail further downstream.
  - A certain correlation, but not as a rule, of high content of pyrite (5–20 wt. %) with uranium accumulations.
- The mineral assemblages and lithology attest to a *sedimentary differentiation* of the heavy minerals during the fluvial transport due to different specific gravities:
- Trapping of the more dense uranium minerals occurred in a high energy environment, while the less dense thorium, zirconium etc. minerals were transported further into a distal zone of lower energy.
- Heavy minerals of a restricted range of grain size such as uraninite (0.05–0.2 mm), monazite (0.2–0.4 mm) and zircon (0.075–0.2 mm) reflect variations in the depositional energy conditions by variations in their concentrations, while minerals with a large range in grain size, such as pyrite (0.5 to 2.9 mm), reflect changes in the depositional energy spectrum by corresponding changes in their grain size. Pyrite grain size and quartz pebble size give a correlation coefficient of 0.93, suggesting that the control of deposition of most of the pyrite was exerted by the same mechanism as that of the quartz pebbles (Theis 1979).

Metallogenetic Concepts

The most favored metallogenetic hypothesis is the *modified placer model* that includes a synsedimentary placer deposit modified by postdepositional processes generated by diagenesis or mild metamorphism (Table 5.35).

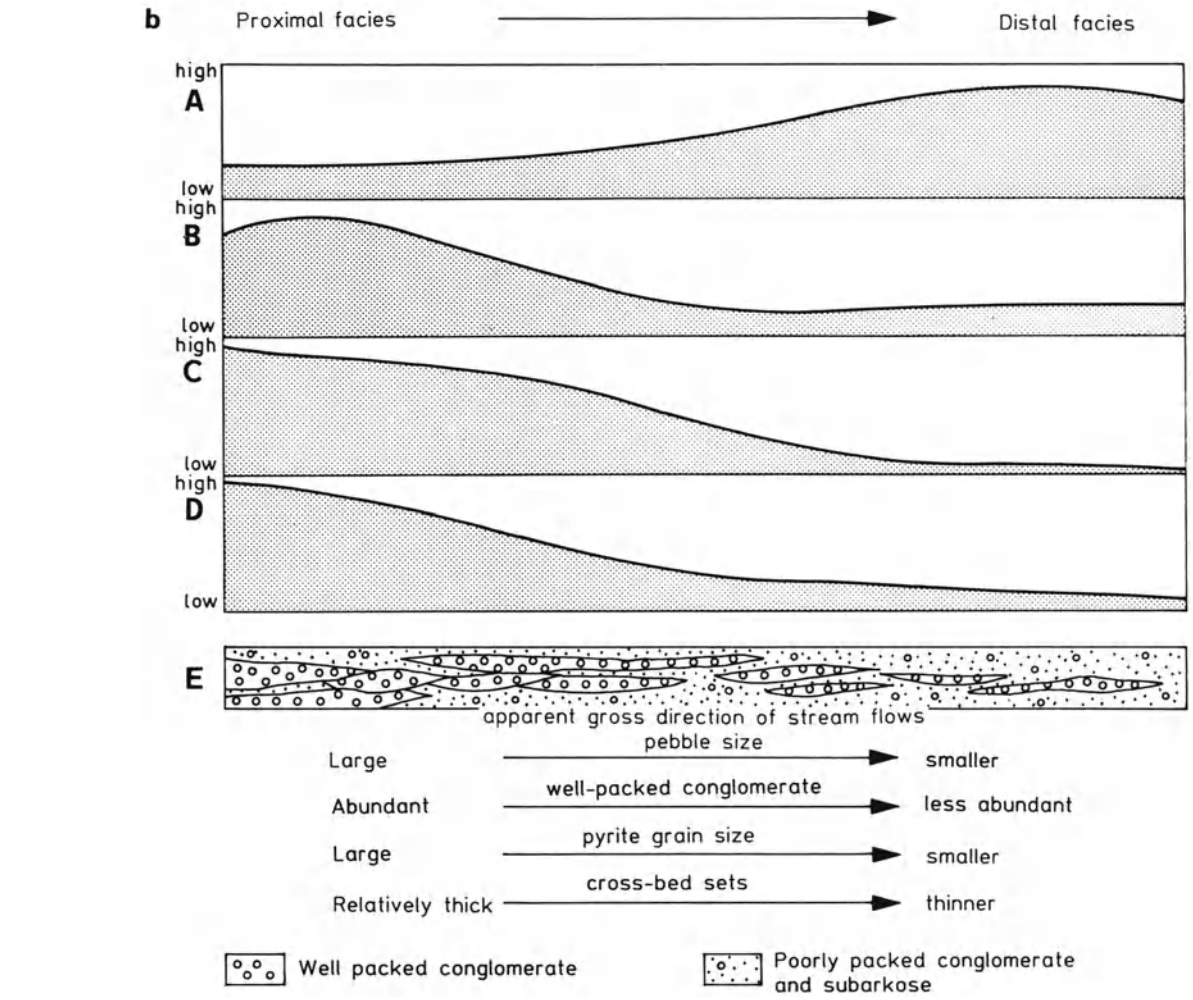

Fig. 5.120. Blind River-Elliot Lake, lithologic-mineralogical characteristics of a mineralized Matinenda conglomerate sheet **a** Planview of a typical shape of a mineralized conglomerate sheet with relatively blunt up-channel boundary and long, fingering down-channel limit. The *arrow* indicates the apparent gross direction of stream flows, **b** Schematic diagrams displaying down-channel variations in a Matinenda Formation ore body. *A* Abundance of monazite, zircon, and rutile aggregates after ilmenite/ilmeno-magnetite; *B* abundance of uraninite; *C* U/Th ratio; *D* abundance of brannerite in rutile aggregates. *E* Lithologic changes. (After **a** D.S. Robertson 1962; **b** Button and Adams 1981 compiled from information in Theis 1979) (**a** reproduced from *Economic Geology*, 1962, v. 57, p. 1176)

There can be little doubt that uraninite of the conglomerates of the Matinenda Formation was derived from an igneous parent rock as outlined earlier. The uraninite grains are rounded in a way that is best explained by fluvial transport and abrasion. Hence it is assumed that they were liberated by physical weathering under oxygen-deficient conditions from granites and pegmatites.

During the time of deposition in the early Proterozoic, there was still a sufficiently *oxygen-deficient atmosphere*, as well documented worldwide by Schidlowski and others. During this episode, physical weathering with very limited chemical disintegration was predominant, as reflected by the composition of the paleosol developed on the Archean surface. This environment prohibited or at least minimized meteoric chemical dissolution of uranium from its igneous source rocks. Instead, uraninite and other minerals could be *transported as detrital grains* over distances of several kilometers from their place of origin into the conglomeratic host rock. The

Table 5.35. Blind River-Elliot Lake, metallogenetic model presented by Robertson J.A. (1989) based on various papers by Ruzicka

1. Source	
Uraniferous granitic rocks + pegmatite 2600 m.y.	Radioactive anomalies, U showings in pegmatite
↓	
2. Weathering	
Disintegration & weathering, formation of uraninite-bearing detritus, little or no oxidation or solution	Regolith at Archean-Proterozoic contact
↓	
3. Transportation	
Rapid transportation by SE-flowing streams and rivers of quartz pebbles, feldspar, uraninite and resistates, little or no oxidation or solution	Huronian sedimentation directions (SE), no red beds
↓	
4. Deposition	
Rapid deposition and burial of quartz-pebble conglomerate with uraninite, iron oxide (?), pyrite, monazite and zircon in shallow fluvial/littoral environment. Little or no exposure to oxygen. Algal mats in quiescent areas trap uraninite grains	Scour and fill structures, Cross-bedding, thick arkose sequences, fining upwards cycles, basement valleys (magnetic expression). Embayments in Archean contact. Radiometric anomalies. QPC lenses and beds + radioactivity, pyrite, kerogen
↓	
5. Diagenesis and modification	
Compaction and consolidation, migration of pore fluids. Clay minerals form from feldspar debris, "brannerite" by migration of U from uraninite to titaniferous aggregates, sulfur of authigenic pyrite possibly derived from volcanism	Yellow green color. No magnetite
Hydrothermal/contact-metamorphic alteration near Nipissing diabase (2115 m.y.), little U remobilization	Albite (red), chlorite (green), carbonate near diabase contacts. Post-ore veins and joint coatings of sulfides
↓	
6. Preservation	
Lack of exposure to oxygen, little or no post-depositional solution, no erosion of unconsolidated materials, no destruction by later metamorphism, erosion	

ore minerals were transported by streams, and redeposited syngenetically in placers within a braided fluvial system.

Deposition of uraninite and other heavy minerals was governed by the hydraulic energy gradient of the transporting stream system and by paleomorphology. The result is a zonal distribution of the heavy minerals, uraninite being deposited most proximal to the source terrane.

After the primary sedimentation there has been some *recycling* of uraninite. At sites where uraninite-bearing conglomerate of the Matinenda Formation is truncated and eroded by a younger conglomerate, as for example the Ramsay Lake conglomerate, the latter is uraniferous (Robertson 1987).

A different post-depositional *modification* occurred by mobilization of uranium and other elements and redeposition as authigenic and replacement minerals due to diagenesis-related processes. Robinson and Spooner (1984a) established three stages of alteration:

1st stage: Complete fluid-mediated leaching of Fe from detrital ilmeno-magnetite and mobilization of U, Th, REE, Y, PO_4^{2-}, and SiO_2. During this stage (a) uraninite was replaced by coffinite and quartz, (b) monazite was corroded and slightly altered, (c) U reacted with TiO_2 liberated from titaniferous heavy minerals to form composite aggregates of brannerite and other U and Ti-bearing alteration phases and (d) coffinite formed together with a Y-REE-U phosphate.

2nd stage: Precipitation of authigenic pyrite.

3rd stage: Sealing of the conglomerate by pressure solution associated with additional alteration of microcline; impression of margins of the quartz pebbles and filling of interstices with quartz and sericite.

The most likely Eh-pH ranges for the *solutions* governing the post-depositional alterations are given by the two authors as (a) a low to moderate Eh of ca. −1 to +0.2 V (field of $H_2SO_4^- - SO_4^{2-}$ predominance) and slightly acid pH of ca. 3 to 6 for the ilmeno-magnetite leaching and (b) a low Eh of ca. <-0.1 V (field of H_2S dominance) and a slightly acid to neutral pH of ca. 5 to 8 for the precipitation of authigenic pyrite. Both fields of inferred Eh-pH values fall within the range of thermodynamic stability of uraninite and coffinite where solubility of U is low to extremely low. Phosphate leached from apatite and monazite may have improved the uranium solubility at the higher inferred Eh values.

Ferris and Ruud (1971) address the lack of magnetite and hematite and state that these minerals and also ilmenite were converted to pyrite by *sulfurization*. Sulfur isotope studies indicate sulfur of magmatic (volcanic ?) origin rather than of biogenic fractionation. Therefore, sulfurization of ilmenite and magnetite produced a reduced environment, stabilizing detrital uraninite which had been previously affected by partial leaching.

A different type of alteration is represented by a pronounced *post-Nipissing metasomatism* which affected the western part of the Pronto mine, the southernmost deposit of the Blind River-Elliot Lake district. Similar but less intense alteration is seen locally at Elliot Lake mines, where it is more clearly linked to diabase intrusives (Robertson 1968, 1986).

Heinrich (1958, 1982) documents for the *Pronto mine* intense and extensive Na-, Ca-, and Mg-, and minor Ba-metasomatism associated with marked modification of the originally detrital mineralization resulting in the redistribution of about 25% of ore grade uranium. The general alteration sequence is albitization-chloritization (±biotite)–dolomitization/calcitization (locally with abundant baryte)–sericitization. Sulfidization occurred in a postmetasomatic stage. Sulfur isotope ratios (M.L. Jensen in Heinrich 1982) give for authigenic and detrital pyrite a range of $\delta^{34}S$ ‰ of −1.3 to +0.4 and for chalcopyrite, pyrrhotite, galena, and sphalerite −2.7 to +3.1, which indicates a magmatic origin.

These data suggest that the altered zone of the Pronto deposit resulted from a magmatic-derived metasomatic overprint of the original Lower Proterozoic uraniferous conglomerates and as such the altered deposit represents a special type of an albitite deposit.

References and Further Reading for Chapter 5.7.1
(for details of publication see Bibliography)

Armstrong (ed.) 1981; Bottrill 1971; Boyle 1979; Button and Adams 1981; Derry 1960; Ellsworth 1928; Fairbairn 1965; Ferris and Ruud 1971; Frarey and Roscoe 1970; Fralick and Miall 1982; Free B, pers. commun.; Griffith and Roscoe 1964; Griffith 1967; Heinrich 1958, 1982; Holmes 1957; Joubin 1960; Kimberley et al. 1980, 1984; Lang et al. 1976; Little et al. 1972; Mossman and Harron 1983; Nuffield 1954; Patchett 1960; Pienaar 1958, 1963; Pretorius 1981; Ramdohr 1957, 1980; Rice 1958; Robertson, D.S. 1962, 1974; Robertson, D.S. et al. 1978; Robertson, D.S. and Steenland 1960; Robertson, J.A. 1978, 1981, 1986, 1987, 1989; Robertson J.A. and Gould 1981, 1983; Robertson J.A. pers. commun.; Robinson and Spooner 1982, 1984a; Roscoe 1959, 1960, 1969, 1973, 1981; Roscoe and Steacy 1958; Ross 1981; Ruzicka 1979, 1981; Ruzicka and Le Cheminant 1984; Ruzicka and Steacy 1976; Saager and Stupp 1983; Saint Martin 1983; Sims et al. 1980, 1981; Theis 1973, 1976, 1978, 1979; Thorpe 1963; Traill 1954; Willingham et al. 1985

5.7.2 Gold-Uranium Deposits in Quartz-Pebble Conglomerates: Witwatersrand Basin, South Africa

The Witwatersrand Basin is located along the border between the Orange Free State and Transvaal. The various ore horizons crop out in a discontinuous band approximately 450 km long on the western and northern sides of the basin. The band includes the Virginia-Welkom/Orange Freestate, Klerksdorp, Carletonville, West-Rand, Central-Rand, East-Rand, and Evander Gold Fields (Fig. 5.121).

The Witwatersrand Basin is the largest gold-uranium province in the world.

Since the uranium grade of in-situ ore is generally very low, ranging from 0.016% to 0.07% U_3O_8, more than 80% of the uranium reserves are economically recoverable only as a by-product of gold mining. Former production amounts to ca. 150 000 mt U_3O_8. Remaining reserves, recoverable at less than $30/lb U_3O_8 are ca. 320 000 mt U_3O_8 (Brynard et al. 1988).

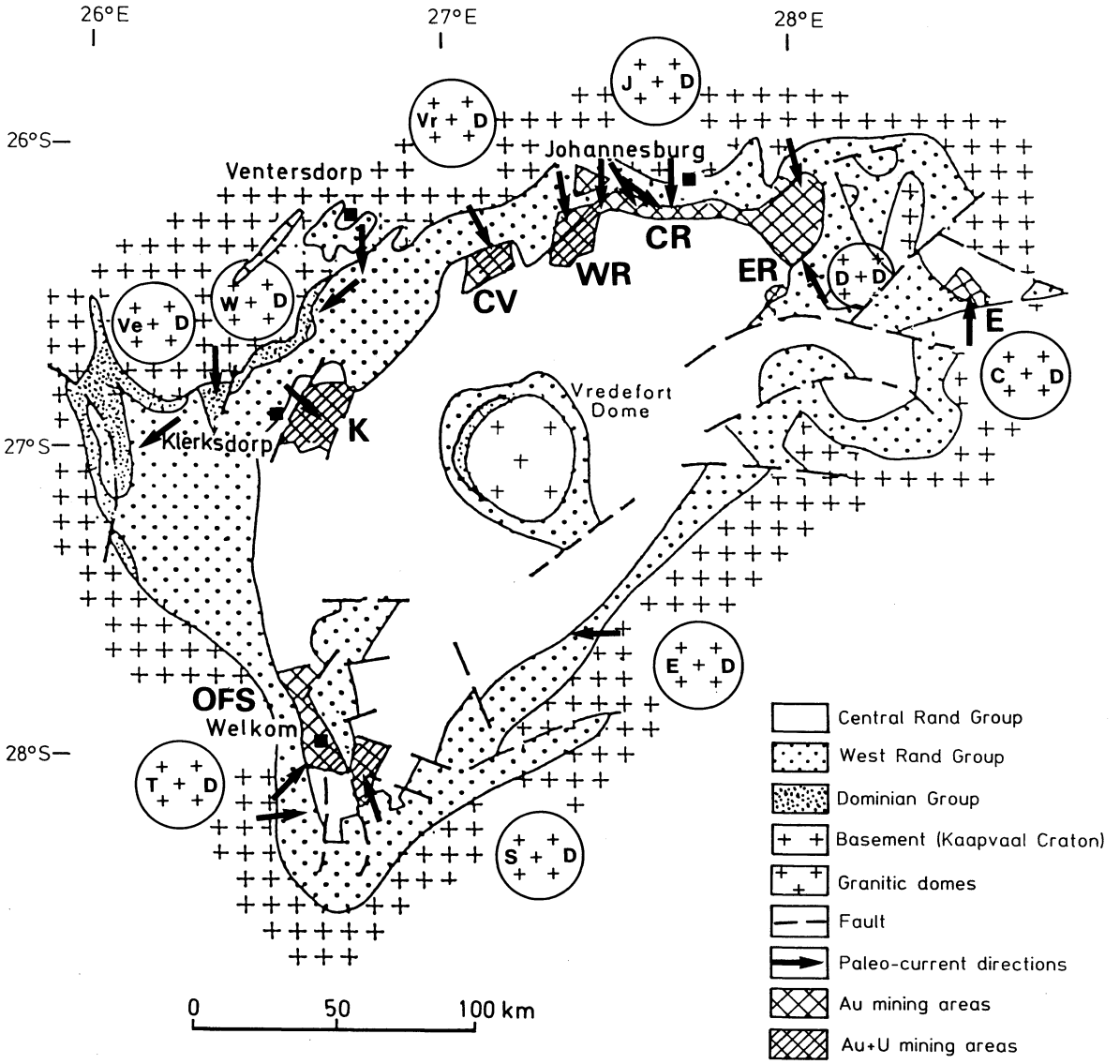

Fig. 5.121. Witwatersrand Basin, generalized geological map showing the distribution of the Lower Proterozoic Dominion, West Rand and Central Rand groups, granite domes adjacent to the basin, and the location of the major U and Au mining districts/goldfields which are identical with the major fluvial fans. Mining districts/Goldfields from E to SW: *E* Evander; *ER* East Rand; *CR* Central Rand; *WR* West Rand; *CV* Carletonville or Far West Rand; *K* Klerksdorp; *OFS* Orange Free State or Welkom Goldfield. Granite domes, clockwise from E: *CD* Cedarmont; *ED* Edenville; *SD* Steynsrus; *TD* Theunissen; *VeD* Vermaas; *WD* Westerdam; *VrD* Vreysrus; *JD* Johannesburg; *DD* Devon Dome. (After Andreoli et al. 1988; Brynard et al. 1988; IAEA 1986a; Buck and Minter 1987)

Minable mineralization consists primarily of gold and uranium emplaced in a distinct oligomictic paleoconglomerate facies. The deposits are therefore classified as gold-uranium quartz-pebble conglomerate-type deposits of Lower Proterozoic age (subtype 7.2, Chap. 4).

Geology, lithology, mineralogy, and origin of the gold-uranium conglomerates of the Witwatersrand have attracted a great number of geoscientists. Comprehensive summaries have been published by Pretorius (1974, 1975, 1976), Feather and Koen (1975), Liebenberg (1955) and Whiteside (1970). Their data, supplemented by more recent information on selected subjects, published by the authors listed, provided the base for the subsequent compilation. (see also papers on individual deposits in Anhaeusser and Maske, eds. 1986).

Geological Setting of Mineralization

The Witwatersrand Basin (Fig. 5.121) covers an area of almost 50 000 km^2, of which approximately 30 000 km^2 are underlain by more than 8000 m thick, slightly metamorphosed strata of the Dominion Group and Witwatersrand Supergroup, which host the ore-bearing quartz-pebble conglomerates, and the Ventersdorp Supergroup, which is only minor mineralized. All three units combined are referred to as the *Witwatersrand Triad*. The Transvaal Sequence rests unconformably on the Triad.

The Lower Proterozoic sediments rest unconformably upon granitic gneisses, ultramafics, and metasediments of the Swaziland Supergroup, a unit of the Archean *Kaapvaal Craton*. Prior to the deposition of the arenites, a paleosol had developed by predominantly physical weathering (Grandstaff et al. 1986).

The lowermost sediment unit is the *Dominion Group* (age approximately 2.8 b.y.). The basal sequence is 40 to 100 m thick and consists of conglomerates, arkoses, and quartzites capped by lavas, tuffs, and shale with a composite thickness of almost 2700 m. Uranium occurs within the basal section in two oligomictic quartz-pebble conglomerates, the Lower Reef and the Upper Reef. The *Lower Reef* forms narrow lenses within paleo-valleys incised into the Archean basement. The *Upper Reef*, in contrast, is laterally more persistent. It was deposited on an intraformational erosion surface.

The overlying *Witwatersrand Supergroup* (Fig. 5.122) (age approximately 2.8 to 2.6 b.y.) is divided into a lower division, the West Rand Group, about 4500 m thick, and an upper division, the Central Rand Group, about 2500 m thick.

The *West Rand Group* includes shales/slates, quartzites, occasional conglomerates, and andesitic lavas. Notable quantities of uranium occur in only one zone of conglomerates within the Government Subgroup.

The *Central Rand Group* contains predominantly medium to coarse-grained quartzites and conglomerates with minor amounts of interbedded slates and andesitic lavas deposited in a fluvial fan environment.

Pretorius (1975) identified six major fluvial fans along the northern, northwestern and southern margin of the Witwatersrand Basin (Fig. 5.121). They are identical with the major mining areas and in a number of conglomerate horizons contain Au-U ore.

Although the main Au-U producer, the percentage of conglomerate in the Witwatersrand Supergroup is relatively small. Pretorius (1976a) estimates that only 8% of the clastic column is composed of conglomerate on the NW or proximal to source side of the basin and this amount decreases to ca. 1% on the distal SE side.

The *Ventersdorp Supergroup* (age approximately 2.6 b.y.) unconformably overlies the Witwatersrand sediments. Mainly andesitic and some acid porphyritic lavas with thin interbedded quartzites and conglomerates are the constituents. The supergroup was originally at least 5000 m thick.

The *Transvaal Sequence* (age approximately 2.2 b.y.) transgressed over a distinct unconformity over the Ventersdorp strata. It contains slates, quartzites, conglomerates, dolomitic limestones, and diabase sills. Some uranium and gold is found in the basal part of the Black Reef conglomerate, which fills erosion channels, cut into the older systems.

All sedimentary units have experienced structural disturbances. A considerable number of *faults* cut and displace the strata with offsets in the mineralized horizons from several meters up to tens of meters.

Host Rock Alterations

No major alteration related to the initial syn-sedimentary uranium deposition has affected the host rocks. Diagenetic and/or mild metamorphic processes and locally intrusion of sills and dikes caused a certain remobilization of the ore-forming elements under reducing conditions as reflected by crystallization of abundant pyrite.

Principal Characteristics of Mineralization

Minable mineral assemblages, which can vary from reef to reef and within the same horizon, commonly contain as principal *ore minerals* uraninite, native gold, osmiridium, locally uranothorite, brannerite or other U-Ti-phases (leucoxene), thucholite, coffinite, and minor amounts of hexavalent uranium minerals.

Paragenetic or *associated minerals*, some of them in several generations, include pyrite,

euxenite, xenotime, monazite, zircon, columbite, chromite, ilmenite, magnetite, cassiterite, arsenopyrite, pyrrhotite, cobaltite, gersdorffite, galena, corundum, diamond, rutile, tourmaline, apatite, and garnet.

Monazite, euxenite, zircon, allanite, xenotime, and rarely kerogen contain minor amounts of uranium. Phyllosilicates may have significant U contents (>500 ppm, Feather and Glatthaar 1987).

Remobilization by erosional redistribution (Minter et al. 1987) and diagenetic or mild metamorphic processes (Thiel et al. 1979) resulted in *modification* and neo-formation of uranium ore and associated minerals. The diagenetically most affected minerals were sulfides, uraninite, native gold, and titaniferous minerals.

Mobilized uranium and titanium led to the formation of brannerite and other U-Ti-phases such as uraniferous leucoxene (Smits 1981; Saager and Strupp 1983). Other authigenic alteration products include uranothorite, coffinite, and orangite (Feather and Glatthaar 1987) and cobaltite, gersdorffite, millerite, pentlandite, tucekite, and breithauptite. These authigenic arsenosulfides have Co/Ni ratios <1 compared to detrital arsenosulfides which have a Co/Ni ratio of >1 (Saager and Oberthür 1984).

Pyrite is the most abundant sulfide. It is present in several varieties and generations.

Uraninite grains contain an average of 62.7% UO_2, 3.9% ThO_2 and 23.6% PbO_2. The ThO_2/UO_2 ratio is highly variable ranging from ca. 6 to 47 (Feather 1976, 1981). Individual grains are up to ca. 0.2 mm in diameter.

Feather and Koen (1976) have described the mineral assemblages in much detail and established a *mineral paragenesis* as presented in Fig. 5.123. Button and Adams (1981) give a comprehensive synopsis on the various detrital and authigenic minerals of the Witwatersrand reefs and compare them with those found in other Lower Proterozic conglomerate-type deposits (Blind River-Elliot Lake, Serra de Jacobina, etc.). The reader is referred to these papers and to more recent works by Saager and coworkers, Schidlowski (1981), Hallbauer (1986), Feather and Glatthaar (1987) and the classical works by Ramdohr (1955) and Liebenberg (1955), which also provide extensive coverage of references for detailed information on the ore and associated minerals.

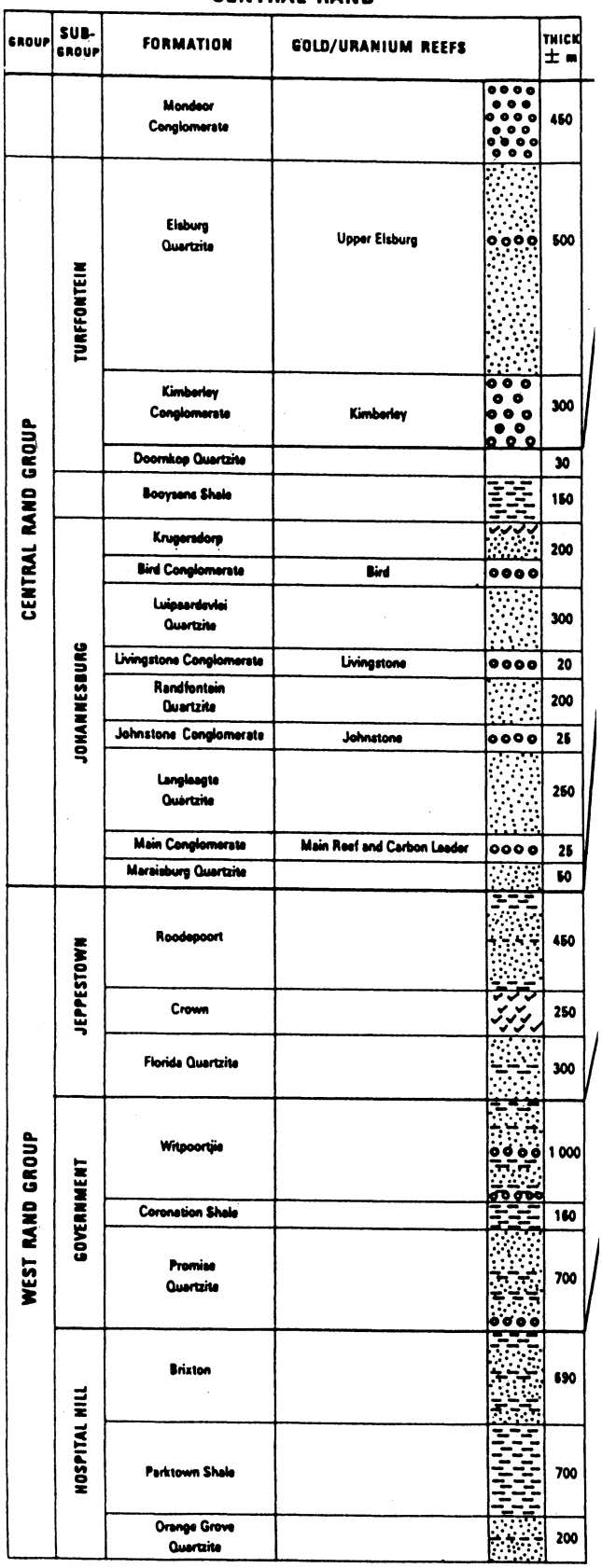

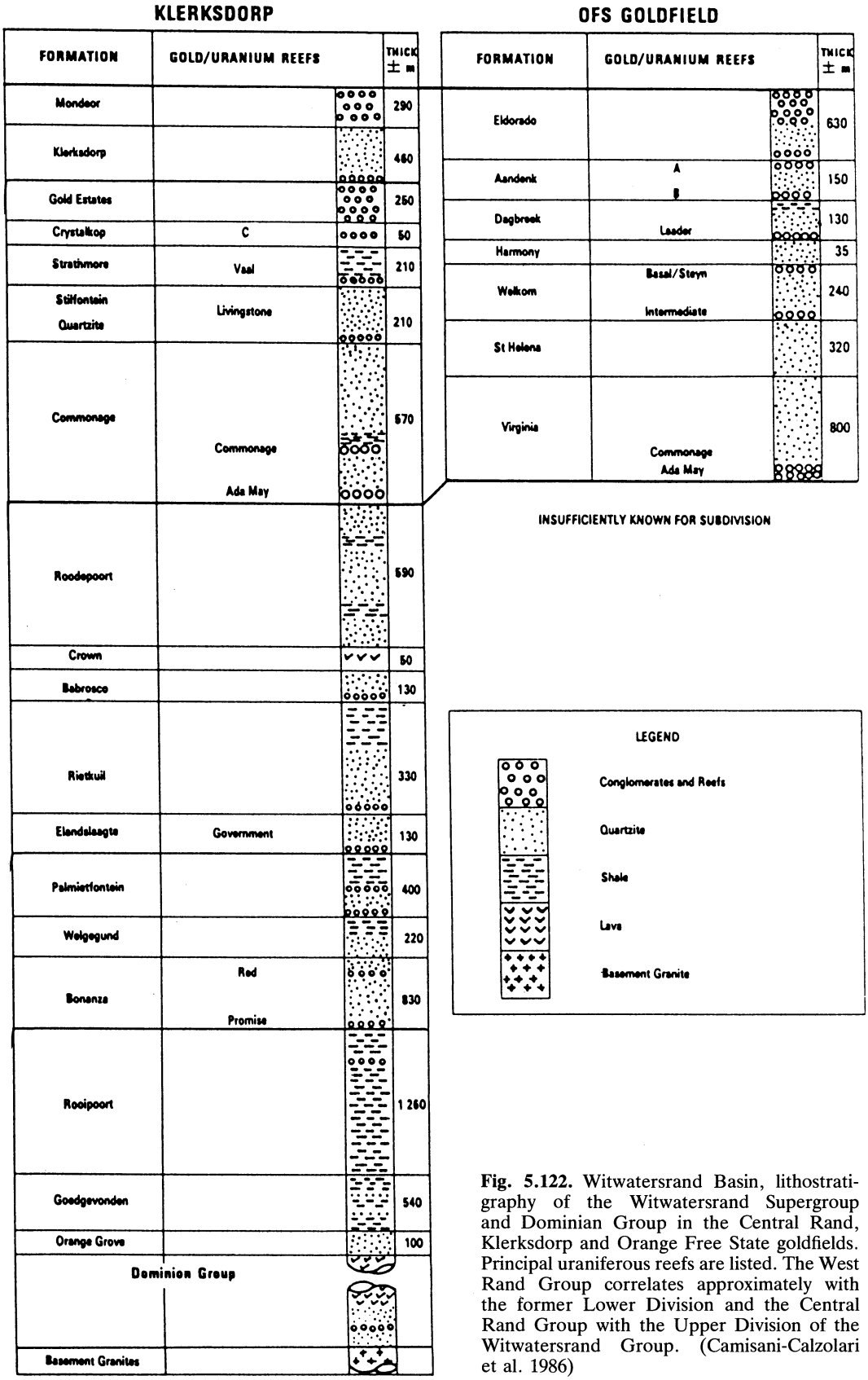

Fig. 5.122. Witwatersrand Basin, lithostratigraphy of the Witwatersrand Supergroup and Dominian Group in the Central Rand, Klerksdorp and Orange Free State goldfields. Principal uraniferous reefs are listed. The West Rand Group correlates approximately with the former Lower Division and the Central Rand Group with the Upper Division of the Witwatersrand Group. (Camisani-Calzolari et al. 1986)

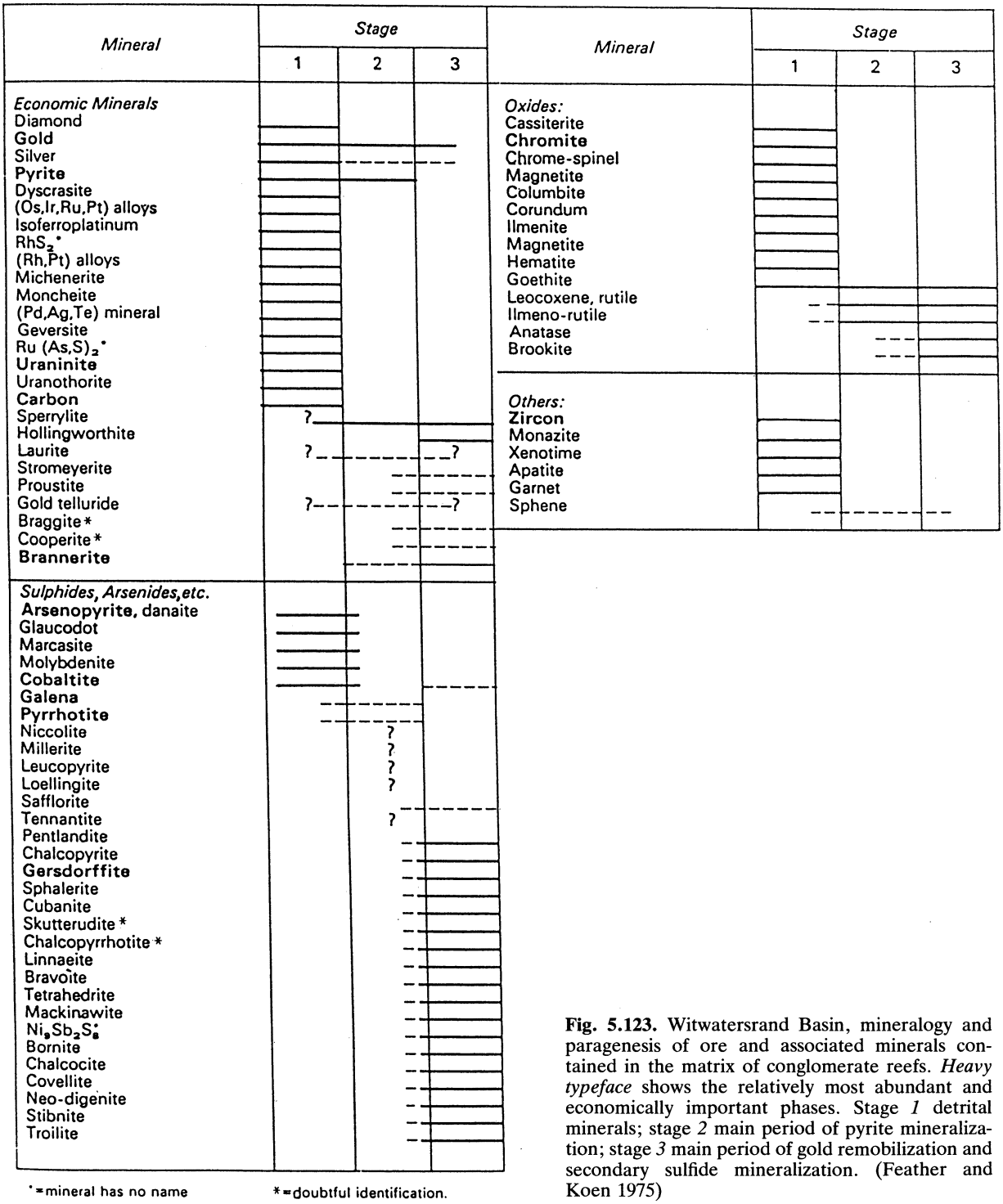

Fig. 5.123. Witwatersrand Basin, mineralogy and paragenesis of ore and associated minerals contained in the matrix of conglomerate reefs. *Heavy typeface* shows the relatively most abundant and economically important phases. Stage *1* detrital minerals; stage *2* main period of pyrite mineralization; stage *3* main period of gold remobilization and secondary sulfide mineralization. (Feather and Koen 1975)

Four principal *modes of uranium mineralization*, based on U ore mineralogy, may be distinguished consisting of (a) detrital grains of dominantly uraninite associated with minor amounts of uranium-bearing monazite, euxenite, zircon, allanite, and/or xenotime, (b) uraniferous phyllosilicates in concretionary pyrite nodules and in lenticles of clay minerals (Simpson and Bowles 1977), (c) authigenic minerals of dominantly complex U-Ti-phases ranging from

brannerite to uraniferous leucoxene, and locally some uranothorite, and coffinite, (d) uraniferous carbonaceous matter composed of either polymerized hydrocarbons or columnar "thucholite" containing entrapped uraninite grains or of granular ("fly-speck") carbon buttons associated with pitchblende/uraninite and pyrite (Robb and Meyer 1985).

Lithology-related uranium distribution is differentiated into five types by Pretorius (1974). Uranium accumulated (a) as matrix constituent in conglomerates composed of dominantly quartz pebbles with a matrix of mainly quartz, sericite, chlorite, pyrophyllite and chloritoid, (b) in pyritic sands that filled shallow erosion channels during successive cycles of sedimentation, (c) in quartzites along unconformity surfaces, (d) in shales along unconformity surfaces, and (e) in carbonaceous bands on or adjacent to unconformity surfaces often present as continuous mineralized seams, ca. 1 mm to 2 cm thick.

The last three ore types were formed in the terminal stages of one cycle of sedimentation and the two first types in the initial stages of a sedimentation cycle.

The *stratigraphic distribution* of the Au-U reefs in the Witwatersrand Supergroup is shown in Fig. 5.122. The Central Rand Group hosts the most important uraniferous reefs particularly within the Johannesburg Subgroup. More than 80% of the uranium production of the Witwatersrand has come from this subgroup.

Other uraniferous reefs are within the basal section of the Dominion Group (Lower and Upper Reef), the Government Subgroup/West Rand Group, the Ventersdorp Contact Reef/Ventersdorp Supergroup, and the Black Reef/Transvaal Sequence. Most of these mineralized conglomerates are subeconomic with respect to uranium.

Typical *features of a mineralized reef* in the more than 800 m thick Johannesburg Subgroup may be demonstrated by the Vaal Reef as found in the Stilfontain Mine, Klerksdorp district (Hahn 1974).

In general, the *Vaal Reef* is defined by numerous transport channels and local deltas which cover an area of approximately 260 km^2 (Winter 1964) (Table 5.36). The Vaal Reef is considered to be the product of a meandering stream system on a broad coalescent flood plain. The direction of transport was to the southeast. In total view, the Vaal Reef dips to the southeast from 12 to 60° and has a maximum thickness of 100 cm. It overlies a carbonaceous (coaly) and frequently thucholite-bearing horizon. Faulting caused downdip displacements and occasionally overthrusts, which resulted locally in tectonic superposition (doubling) of the ore horizon.

The Vaal Reef is composed of well-sorted and well-rounded pebbles of milky to dark quartz and occasionally chert in a matrix of silica and carbonate. Larger pebbles are normally concentrated at the base of the reef. The matrix contains gold (average 13 ppm), the uranium minerals (500 ppm U_3O_8), pyrite (3%) and accessory minerals of silver, copper, lead, nickel, and cobalt. Fossil hydrocarbon occurs disseminated as fine specks, in a seam approximately 5 cm thick at the base of the reef. Uraninite is the main uranium mineral. Its degree of roundness is equivalent to that of monazite and other heavy minerals. Uranium is distributed over the whole reef. About 20% of the uraninite, however, has accumulated at the base of the reef with 80% of the gold. The total uranium content increases with reef thickness.

In the Stilfontain Mine itself the Vaal Reef consists mainly of one bed, which bifurcates occasionally into two. The thickness ranges from

Table 5.36. Witwatersrand Basin, Central Rand Group, dimensions of selected Au-U-bearing reefs. [After Button and Adams 1981, based on (1) Minter 1978; (2) areas given by Minter 1978, for the placer sheet as a whole, including some unpay intervals, (3) approximate figures calculated by Button and Adams 1981, (4) Pretorius 1976b, (5) Whiteside et al. 1976]

Dimension / Reef	Long dimension[a] (km)	Short dimension (km)	Approximate area (km^2)	Thickness range (m)	Ore tonnage (mt × 10^6)	Grade U_3O_8 (ppm)	Grade Au (ppm)
Vaal	20[1]	3–8[1]	260[2]	0–1[1]	200[3]	258[4]	13[4]
Basal/Steyn	22[1]	4–8[1]	400[2]	0–4[1]	500[3]	196[4]	15[4]
Carbon Leader	25[5]	ca. 5[5]	125[3]	0–0.3	45[3]	248[4]	21[4]

[a] indicates long axis perpendicular to mean sediment transport direction

1 to 90 cm and averages 24 cm. The average metal content is 510 ppm U_3O_8, 10 ppm Au, 2% pyrite. The mineralized conglomerate overlies a layer with a matrix containing carbonaceous matter and uranium, the latter often as thucholite.

In the past, uranium has also been recovered from *other reefs* of the Central Rand Group. The mines at Carletonville (Far West Rand) exploited conglomerates of the Main Conglomerate Formation (grade: 0.015 to 0.017% U_3O_8). In the Kinross area, uranium was extracted from the Kimberley Conglomerate Formation (grade: 0.02 to 0.025% U_3O_8). Conglomerate beds of the Elsburg Quartzite Formation contain only minor amounts of uranium, which have not yet been recovered.

On a regional basis, Au-U-bearing beds are found within *six major fluvial fans* constituting from SW to NE the gold fields of the Orange Free State or Welkom, Klerksdorp, Far West Rand or Carletonville, West Rand, East Rand, and Evander (Fig. 5.121).

The original Central Rand represents the coalescence of the eastern part of the West Rand fan and the western part of the East Rand fan.

The fans have lateral *dimensions* of up to several tens of kilometers (Fig. 5.124). The largest of the fans is that which contains the East Rand gold and uranium field. It measures 40 km in length along the fan center, 50 km in width across the midfan section and 90 km in width across the fan base. The western margin of this fan is 45 km long and the eastern flank 60 km.

A fan may contain several oligomictic conglomerate beds (reefs) with uranium and gold contents of economic interest. The thickness of individual reefs ranges from about 5 to 200 cm and locally to about 400 cm. Lateral extensions of pay-streaks can reach several hundreds to several thousands of meters parallel to the paleo-stream. Across simple paleo-channels the deposits are several meters to tens of meters wide, and across coalescent channels up to several hundreds of meters.

The uranium grades are variable but generally very low. During the peak period of U production, the in-situ grade of ore mined in 1982 ranged from 0.016 (Harmony) to 0.077% U_3O_8 (Beisa). Approximately 50 to 70% of the in-situ content is recoverable.

For comparison, dimensions, grades, U/Au ratios and pebble composition of selected reefs are given in Tables 5.36 and 5.37. Figure 5.125 shows the lithologic features and position and Fig. 5.126 the distribution and spatial relationship of U and Au in a selected reef.

Uraninite grains from Witwatersrand ores yield apparent U/Pb *ages* of 3065 ± 100 m.y., which is compatible with that of granites in the surrounding of Witwatersrand Basin and a rejuvenation age of 2040 m.y. that is coeval with the emplacement of the Bushveld Complex (Allsopp and Welke 1986).

Potential Sources of Uranium

Uraninite grains have up to ca. 10% ThO_2 which is typical for uraninites from *granites and pegmatites*. The apparent age of ca. 3065 m.y. of

Table 5.37. Witwatersrand Basin, Central Rand Group, thickness, composition and U/Au ratios of selected reef horizons. (After Pretorius 1974)

Reef group	Reef horizon	Gold-field	TN	SZ	QU	CT	QT	OS	U/Au
Bird	Zone 2	West Rand	62	21	77	7	16	–	769
Bird	Monarch	West Rand	99	18	82	6	11	–	435
Bird	White	West Rand	35	12	85	8	3	4	40
Bird	Vaal	Klerksdorp	15	22	85	12	3	–	11
Bird	Basal	Welkom/OFS	36	20	60	23	5	12	18
Main	Livingstone	West Rand	50	35	–	–	–	–	11
Main	South	West Rand	10	17	86	7	7	–	14
Main	Main	West Rand	110	37	84	6	10	–	9
Main	North	West Rand	50	30	83	6	11	–	–

TN : Average thickness (cm)
SZ : Average size of 10 largest pebbles (mm)
QU : Percentage vein quartz pebbles
CT : Percentage chert pebbles
QT : Percentage quartzite pebbles
OS : Percentage other types of pebbles
U/Au : Ratio of uranium content to gold content

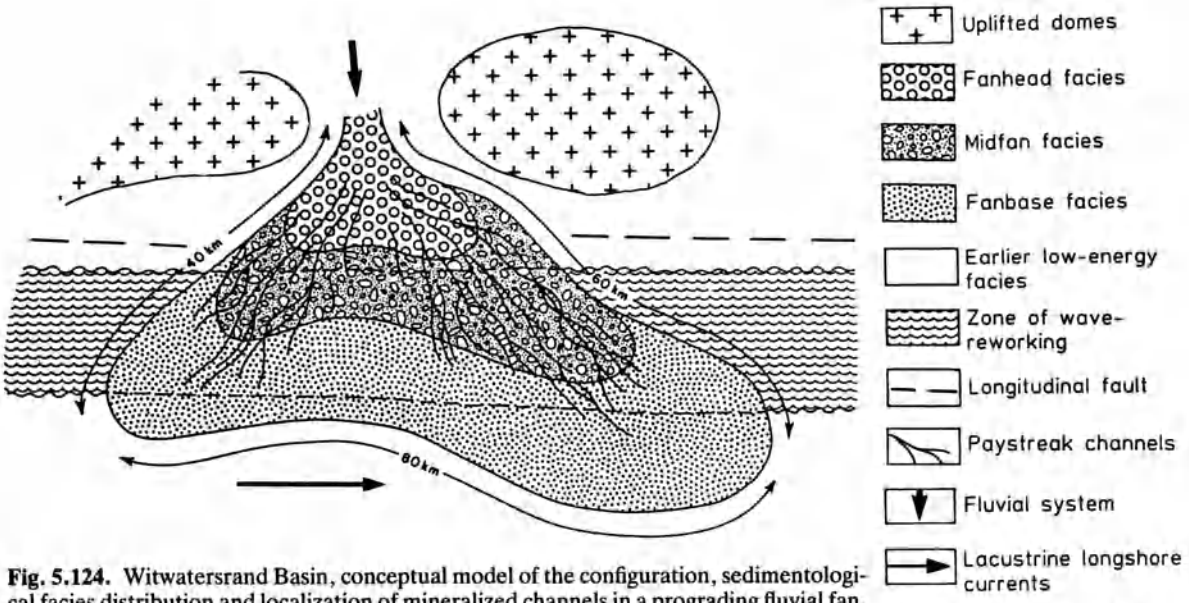

Fig. 5.124. Witwatersrand Basin, conceptual model of the configuration, sedimentological facies distribution and localization of mineralized channels in a prograding fluvial fan. The fan developed at the mouth of a fluvial system dewatering from between uplifted granite domes. Clockwise flow direction of long-shore currents in the lake caused the asymmetrical shape of the lobe. (After Pretorius 1974, 1981) (in part reproduced from *Economic Geology*, 1981, Spec. Vol., p. 134)

uraninite (Allsopp and Welke 1986) attests to a source of Archean age. Granitic domes of Archean age are mapped in the vicinity of the Witwatersrand Basin. They include granitic facies enriched in uranium. For example, the Vredefort dome contains relics of a "HHP-type" (high heat production) granite affected by hydrothermal alteration. The altered granite has uranium contents of up to 30 ppm and 70 ppm Th. Part of the uranium is bound in uraninite. (Andreoli et al. 1988; Robb and Meyer 1985). These data suggest that these kinds of granites provided a potential source for the uraninite found in the conglomerates.

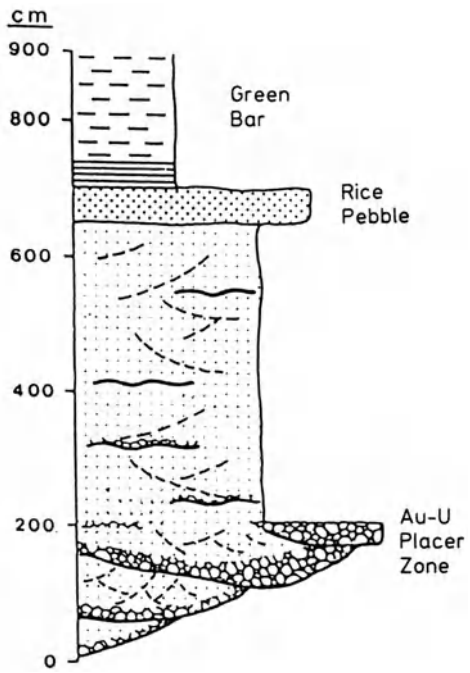

Fig. 5.125. Witwatersrand Basin, Carletonville Goldfield, lithologic section of the Carbon Leader Formation, Johannesburg Subgroup, showing the position of mineralized conglomerate beds. (Buck and Minter 1987)

Ore Control and Recognition Criteria

Essential ore controlling or recognition criteria include:

Host Environment

- Host rock is a pyritiferous oligomictic quartz-pebble conglomerate deposited in Lower Proterozoic time prior to the oxyatmoversion of the earth atmosphere.
- Favorable conglomerates alternating with dominantly arenaceous horizons were deposited in several cycles separated by major and intraformational unconformities.
- The conglomerates were laid down in fluvial-deltaic fans in an intracontinental basin.

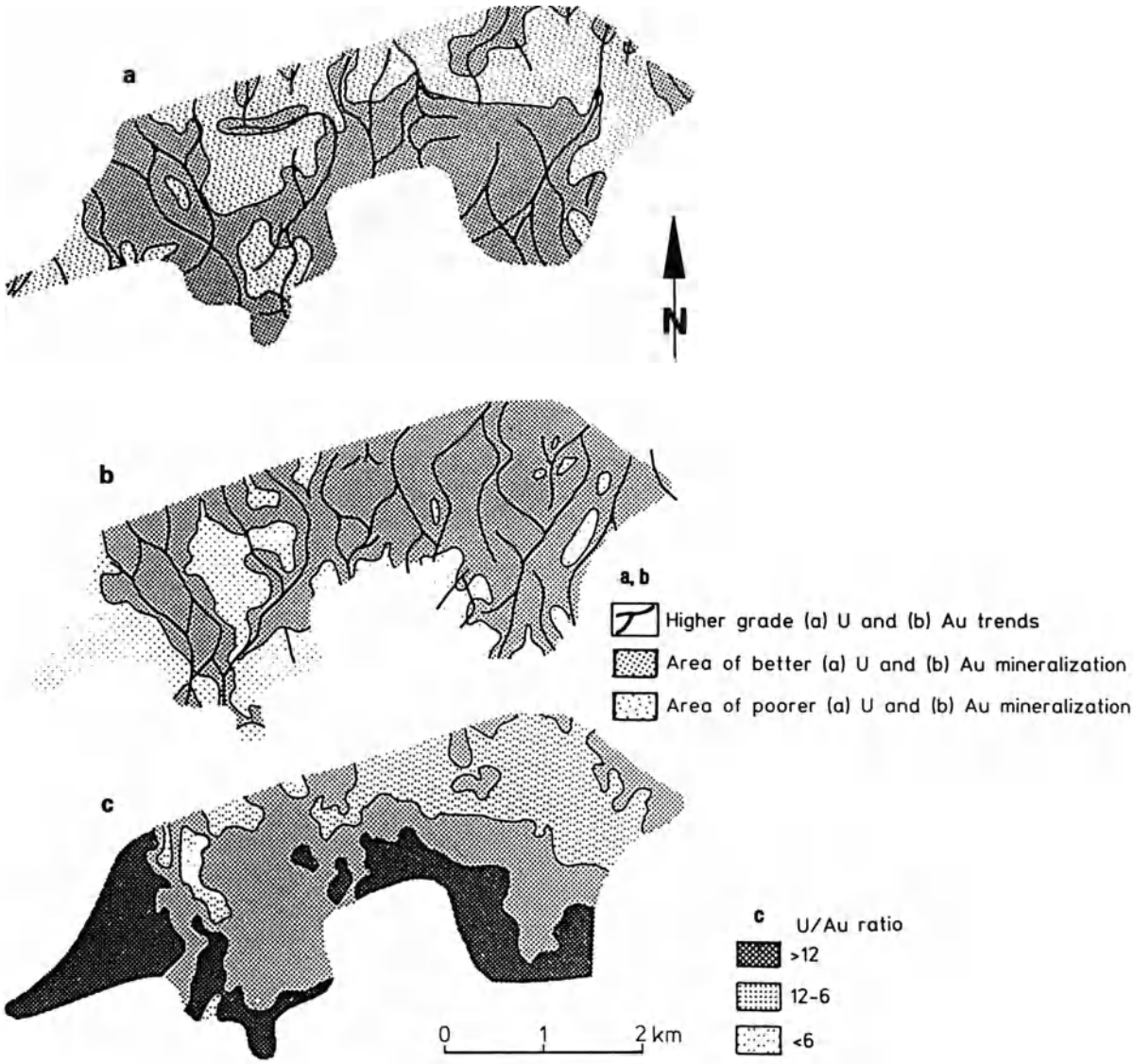

Fig. 5.126. Witwatersrand Basin, Carletonville Goldfield, surface plan of the Carbon Leader reef with distribution of **a** relative uranium contents, **b** relative gold contents, and **c** U/Au ratios showing the downstream oriented relative enrichment of uranium. (Buck and Minter 1987)

- Provenance of the conglomerates was from a variety of Archean rocks including uraniferous granites.
- Younger conglomerates derived partly by reworking of those deposited earlier.

Alteration

- There is no alteration associated with the deposition of the detrital ore forming minerals.
- Post-depositional modifications resulted particularly in intense pyritization and partial remobilization of the ore forming minerals (see below).
- Paleoweathering of the Archean surface and the intraformational erosion planes in the Witwatersrand Basin fill was predominantly of physical nature.

Mineralization

- Original uranium minerals are detrital uraninite and uranothorite associated with gold and other heavy minerals (Fig. 5.123).

- Ore minerals produced by postdepositional processes include U-Ti-phases, coffinite, arsenosulfides, and sulfides.
- The distribution of the Au-U ore reflects a predominant sedimentological control and is characterized by the following features (von Backström 1975, 1976; Pretorius 1974, 1975, 1976b):
- Uranium and gold are concentrated in a quantitative ratio of 5–>500 U to 1 Au (Fig. 5.126, Tables 5.36, 5.37) in conglomerates adjacent to the edge of a continental structural basin.
- Recoverable uranium and gold mineralization occurs particularly in fluvial-deltaic fans in the Central Rand Group of the Witwatersrand Supergroup which are distributed in a belt running parallel to the original western and northern coastline (Fig. 5.121).
- Important concentrations of ore are found only in distinct narrow stratigraphic-lithologic zones which occupy approximately 2% of the total Central Rand Group.
- A tight correlation exists between concentration of ore and sedimentary features. Enrichments are commonly found
  - in the midfan facies of the fluvial fans (Fig. 5.124),
  - near the base of conglomerates along distinct argillaceous/shaly footwall boundaries,
  - in conglomeratic beds less than 30 cm thick,
  - in pay-streaks running generally subparallel to each other (Figs. 5.124, 5.126) and that are characterized by densely packed well-rounded and well-sorted pebbles of predominantly quartz and by larger accumulations of heavy minerals.
- Uranium and gold tend to be enriched immediately above stratigraphic and intraformational, local unconformities, in particular where conglomerates fill depressions or excavations in the footwall rocks, or where conglomerates abut a slight rise or swell in the underlying formations (Fig. 5.125). (Some important uranium- and gold-bearing conglomerates, however, also occur within the stratigraphic sequence independent of unconformities).
- The distribution of uranium and gold within a transgressive reef, suprajacent to an unconformity, is clearly influenced by the degree of denudation or depth of erosion of the underlying sediments.
- In shallow depressions with gentle slopes, normally well-developed conglomerates with high metal grades prevail. In deep depressions with steep slopes the conglomerates are poorly developed in the center but the peripheral zones consist of well-developed, densely packed conglomerates with generally high values of uranium and gold.
- The uranium and gold mineralizations rarely extend into the adjacent arenaceous sediments, except where redistribution by erosion and redeposition of older ore beds occurred.
- Most reefs contain carbon/kerogen often forming continuous mineralized seams as much as 5 cm thick.

Metallogenetic Concepts

The most favored metallogenetic hypothesis is the *modified placer model* that includes a synsedimentary detrital ore mineral deposition succeeded by post-depositional modifications through both erosional redistribution into younger conglomerates and diagenetic-mild metamorphic processes. Other genetic models put forward range from hypogene hydrothermal (e.g. Davidson 1957) to supergene rollfront (Clemmy 1981) forming processes. In the early days of uranium mining in the 1950's Davidson (1957) vehemently defended a hypogene hydrothermal genesis against the "placerists" Ramdohr (1955) and Liebenberg (1955).

From the areal geometry of the different ore-bearing horizons the pattern of facies variations, the trends in the grain-size change of the host rock, the pattern of the paleo-current directions, the nature of the depositional environment, and the distribution of heavy minerals, it appears that gold and uranium minerals accumulated within a *fluvial fan system* or a *fan delta* where the river system was discharged into a large lake, which means that the uranium and gold accumulations constituted an integral part of a short, high-energy fluvial transfer system from the source to the depository.

Pretorius (1974) elaborates in detail on this hypothesis and arrives, in summary, at the following conclusion. The older Witwatersrand sediments were deposited in a fluvial-deltaic environment within an intermontane/intracratonic, yoked basin. The basin was fault-bounded on the northwestern edge and downwarped on the

southeastern boundary. Transport of the sediments was by high-energy transfer systems from the source in the northwest to the depository. Fluvial fan systems or fan deltas were formed where the river systems were discharged into a large lake via a canyon. After emerging from the canyons, the rivers flowed short distances over a piedmont plain and were then dispersed through a braided-stream system into the basin (Fig. 5.124). The fluvial fans were restricted to the northwestern margin of the depository. Some of them coalesced in their more distal parts, creating extensive sheets of uniform gravel (Fig. 5.121).

A *typical fluvial fan* of this kind had two main lobes in which a large number of braided-stream channels developed (Fig. 5.124), thicker and coarser clastic sediments deposited and higher concentrations of detrital gold and uranium accumulated. The material laid down between the lobes was predominantly psammites and pelites, similar to the sediments accumulated on the fan margins and on its base. Conditions under these lower-energy regimes between the lobes, which existed also at the end of certain cycles of sedimentation on the fans of the major rivers, at times provided a favorable environment for the growth of thin algal or lichen colonies.

Transport of gold and uranium was as detrital minerals, and the gold also in solution perhaps as chloride and cyanide complexes.

Concentration of Au and U took place (a) physically through gravity settling and subsequent winnowing by wave and current action and (b) biochemically through interaction between Au and U, and algal or lichen mats.

The gold was supposedly of too small grain size to precipitate in the fanhead facies. Instead, the highest gold settlement took place in the midfan lobes, whereas the peak of the uranium deposition occurred a little farther down-slope (Figs. 5.124, 5.126). Further downstream, the fluvial energy level dropped rapidly below the transport capability for detrital gold and uranium, hence these heavy minerals could not be transported to the fanbase section. Only the gold and uranium in solution were transported beyond the energy threshold until they encountered and interacted with the biogenic material in the low-energy environment.

End-of-cycle winnowing by the waters of the streams and the lake led to a greater concentration of residual heavy minerals on the erosion surface.

At the start of the sedimentation of the next cycle, *reworking* of this depositional pediment destroyed the thin streaks of lag gold and uranium at the unconformity plane. These minerals were then redistributed into the younger gravels by pickup from the footwall rocks and downward infiltration during the sand deposition that followed the deposition of the pebble phase.

During this stage and after burial, uraninite was destabilized to various degrees by physical and chemical action including break-up by lichen growth, as documented by Pretorius (1974), and Smits (1981).

Minter et al. (1987) established the mineralogical changes at the Eldorado paleosurface at the Welkom Goldfield, where the pediment represents the last major period of erosion at the end of the deposition of the Witwatersrand sequence. The suite of *reworked ore minerals* identified in fluvial bedload concentrates within shallow paleochannels and conglomeratic diamictites resembles that present in the suboutcropping conglomerates except for the virtual lack of uraninite. The dominant uranium minerals are brannerite and uraniferous leucoxene, which occur associated with detrital pyrite and other heavy minerals. Pyrite is present in three varieties, all of which display abrasional rounding. One type of pyrite corresponds to that originally formed as authigenic mineral in the older placers and therefore suggests that it represents a reworked accumulate. This interpretation is supported by the rounded nature of kerogen particles which appear to have originated by erosion from fragmented columnar kerogen. The kerogen granules contain uraninite largely altered to brannerite. The alteration of uraninite to brannerite is attributed by the authors to weathering in both the source and depositional area rather than to selective modification processes after burial. The almost complete removal of uraninite may reflect an increasing content of oxygen in the atmosphere at the end of the Witwatersrand period.

Hallbauer and von Gehlen (1983) address the impact of regional and thermal *metamorphism* on the Witwatersrand mineralization. Regional metamorphism was weak (lower greenschist facies) and essentially isochemical, i.e., without extrinsic admissions. Temperatures ranged between 157 and 250°C, as deduced from inversion of marcasite into pyrite and decrepitation temperatures of secondary fluid inclusions in quartz pebbles and ore mineral compositions. The upper

limit of 250°C is further supported by as much as 17% volatiles contained in the carbonaceous matter, which would have been expelled at temperatures in excess of 250°C.

These findings are supported by Saager and Oberthür (1984). Based on their studies on authigenic Ni-Co minerals, the two authors assume a low-grade metamorphic overprint at temperatures commonly below 250°C.

Intrusion of *volcanic dikes and sills* caused a certain mineral redistribution within a spatially restricted halo. Particularly large quantities of authigenic pyrite recrystallized, and pyrite, galena, sphalerite, and chalcopyrite, but rarely gold were redeposited in veinlets (Hallbauer and von Gehlen 1983).

In summary, the above-listed sedimentological, mineralogical, and minerochemical parameters of the auriferous and uraniferous conglomerate reefs of the Dominion Group and Witwatersrand Supergroup are largely consistent with the modified placer model favored by most investigators, though not unanimously.

The suggested *succession of events* leading to the formation of uraniferous reefs begins with

- anomalous uranium concentrations in form of uraninite and other ore-forming heavy

Table 5.38. South Africa, late Archean–early Lower Proterozoic events in the Kaapvaal Craton. (Andreoli et al. 1988, based on references listed there)

Cycle	Geological event	U-related process	Age (b.y.)
VIII	Ventersdorp Supergroup deposition: rifting; basaltic and bimodal volcanism; arenaceous sediments	Minor brannerite/uraninite in gold-bearing basal placer	?
VII	Central Rand Group deposition: repeated uplifting of the hinterland causes reworking of older strata, intensified basement erosion and development of quartz-pebble conglomerates in intra-group unconformities	Deposition of economically important uraninite – kerogen-U-Ti-oxides – gold-bearing conglomerates. Rare monazite and other Th-bearing phases	?
VI	West Rand Group deposition: prevalence of shale in marine shelf and tidal environment	Minor development of conglomerates with minor U (and Th)-bearing phases	?
V	Widespread hydrothermal activity affects basement and Dominion Group cover in the hinterland of the Witwatersrand Basin. Tectonic activity, hydraulic fracturing, brecciation	H_2O, CO_2, F, B, S, -bearing fluids introduce pyrite, uranium and gold	Wide range of ages may apply
IV	Dominion Group deposition: minor clastic sedimentation and volcanism	(Th-) Uraninite, monazite-rich gold-bearing basal conglomerate; kerogen rare	2.72 ± 0.07 $\leqslant 2.74$
III	Late Archaean granite intrusions in the Schweizer – Reneke Dome. Major tectonothermal event results in the formation of the Vredefort discontinuity; granulite facies metamorphism at depth	Migration of uranium at higher crustal level (?) Depletion of uranium from rocks below the Vredefort discontinuity	$\geqslant 2.74$ ± 2.78
II	Mozaan Group deposition in the Eastern Transyaal	Brannerite and minor uraninite in Mozaan conglomerates	± 2.9
I	Metamorphism and extensive U, Th, fluxing through a Barberton Mountain Land-type terrain as evident in the vertical Vredefort profile. High level HHP granite in the Vredefort structure	Distribution of U and Th according to an exponential vertical profile Preferential U enrichment at high crustal level	± 3.05

minerals in certain hydrothermally altered granitic and/or pegmatitic-granitic complexes integrated in the Archean granite-greenstone belt, located northwesterly of the Witwatersrand Basin.
- Liberation of the detrital minerals by predominantly physical weathering as reflected by the paleosol topping the crystalline basement (Grandstaff et al. 1986).
- Transport and redeposition governed by fluvial systems as documented by Pretorius (1974). Schidlowski et al. (1975) provided convincing evidence that the atmosphere was oxygen-deficient during this time interval (see Chap. 3).
- Destabilization of uraninite to various degrees by physical and chemical processes during deposition and after burial. Post-burial mobilization of uranium together with alteration and recrystallization of other minerals occurred during and/or subsequent to regional metamorphism, locally associated with volcanic intrusions.
- Preservation of the ore by a thick cover of sediments and cratonic stabilization, i.e., lack of major intrusive and tectonic events.

A summary of events active in the Kaapvaal Craton and leading to the Au-U mineralization in the Witwatersrand Basin has been compiled by Andreoli et al. (1988) and is presented in Table 5.38.

References and Further Reading for Chapter 5.7.2
(for details of publication see Bibliography)

Andreoli et al. 1988; Anhaeusser 1973, 1975, 1976; Anhaeusser et al. 1969; Antrobus 1986; Antrobus et al. 1986; Antrobus and Whiteside 1964; Armstrong 1968; Bourret 1975; Bowles 1977; Brynard, HJ, pers. commun.; Brynard et al. 1988; Buck 1983; Buck and Minter 1987; Burger and Coertze 1973; Burger et al. 1962; Burke et al. 1986; Button 1968, 1973, 1976; Button and Adams 1981; Button and Tyler 1979; Camisani-Calzolari et al. 1985; Chamber of Mines of S.A. and A.E.B. of S.A. 1985; Clemmey 1981; Coetzee 1965; Corner et al. 1986; Cousins 1960, 1965, 1973; Davidson 1953, 1957; De Kock 1964; De Waal and Herzberg 1969; Dimroth 1979; Du Toit 1954; Feather 1976, 1981; Feather and Glatthaar 1987; Feather and Koen 1975, 1981; Feather and Snegg 1978; Frey 1981; Frey et al. 1987; Fuller 1958; Glatthaar and Feather 1984; Grandstaff 1974b 1980; Hahn 1974; Hallbauer 1975, 1977, 1980, 1983, 1986; Hallbauer et al. 1977; Hallbauer and Joughin 1973; Hallbauer and Kable 1982; Hallbauer and Utter 1977; Hallbauer and van Warmelo 1974; Hallbauer and von Gehlen 1983; Herzberg W, pers. commun.; Hiemstra 1968a, 1968b; Hirdes 1979, 1984; Hirdes and Saager 1983; Hutchison 1975; Jacob 1966; Knowles 1966; Koen 1961, 1962; Köppel and Saager 1974; Krapez 1980; Liebenberg 1955, 1973; Malan 1959; McKinney et al. 1964; McLachlan 1968; Meyer et al. 1987; Minter 1970, 1972, 1976, 1978, 1979; Minter et al. 1986, 1987; Nicolaysen et al. 1962; Oberthür 1983, 1985, 1987; Ortlepp 1962; Papenfus 1964; Pretorius 1964a, 1964b, 1974, 1975, 1976a, 1976b, 1981, 1986a, 1986b; Ramdohr 1955, 1958, 1980; Reimer 1975; Reinecke 1927; Rundle and Snelling 1977; Saager 1968, 1969, 1970, 1973; Saager et al. 1982, 1983; Saager and Esselaar 1969; Saager and Mihálik 1967; Saager and Muff 1978; Saager and Oberthür 1984; Schidlowski 1966a,b,c,d,e,f, 1967b, 1969, 1970, 1981; Shepherd 1977; Simpson and Bowles 1977, 1981; Sims 1969; Smith and Minter 1980; Smits 1981, 1984, 1987; Snyman 1965; Steyn 1977; Taylor et al. 1962; Thiel et al. 1979; Toens and Griffiths 1964; Toens and le Roux 1978; Toens et al. 1980; Tweedie 1968, 1978, 1986; Tucker and Viljoen 1986; Utter 1977; Viljoen 1964, 1967, 1968; von Backström 1975, 1976; von Rahden 1970; von Rahden and Hiemstra 1967; Whiteside 1970; Winter 1964; Zumberge et al. 1978, 1981.

5.8 Examples of Intrusive-Type Uranium Deposits (Type 9, Chap. 4) Alaskite Uranium Deposits: Rössing, Damara Orogenic Belt, Namibia

Rössing is located in the Namib desert approximately 65 km NE of Swakopmund in western central Namibia. Total reserves in the \$30/lb. U_3O_8 RAR category are estimated at approximately 130 000 mt U_3O_8 (OECD/NEA 1986) of which about 55 000 mt U_3O_8 have been recovered from a large open pit until 1991. The average grade is approximately 0.03 to 0.04% U_3O_8.

The uranium mineralization is disseminated, indigenous in an intrusive leucogranite/alaskite and is therefore classified as intrusive alaskite – type uranium deposit (subtype 9.1, Chap. 4).

The subsequent deposit description is largely based on Berning et al. (1976), Berning (1986), and Toens and Corner (1980) supplemented by data of the other authors cited. The regional geology has been summarized mainly from Brynard and Andreoli (1988).

Geological Setting of Mineralization

The Upper Proterozoic *Damara orogenic belt* is 400 to 500 km wide and extends in northeasterly direction from the Atlantic Ocean in the SW across southwestern Africa before submerging

beneath the post-Paleozoic Kalahari Basin. Further north it eventually links up with the Lufilian belt of similar age in Zambia-Zaïre.

The Damara branch in Namibia has been subdivided into four main structural zones (from NW to SE): The Northern, Transition, Central or Core, and the Southern Zone.

All known uranium alaskite occurrences occur within the *Central Zone*. This zone is constituted by a broadly uplifted block of metasediments and intrusions, and displays domal antiforms, commonly NE-SW elongated, and synforms. The metasediments were subjected to amphibolite grade metamorphism (estimated peak T 555 to 645°C, P 2.6 to 3.4 kbar) with polyphase deformation accompanied by the intrusion of pre-, syn- and post-tectonic granites.

Five principal varieties/generations of granitic rocks intruded into the metasediments of the Damara belt (Table 5.39) including alaskites. The intruded metasediments include several stratigraphic units those in the Rössing area are presented in Table 5.40 with their corresponding lithologies.

Certain *alaskitic granites* (for petrographic description see next paragraph) are of interest for uranium mineralization. Although granitic intrusives are widespread and may contain anomalous concentrations of uranium, they rarely carry ore grade concentrations. The alaskitic granites, sterile as well as mineralized, intruded concordantly and disconcordantly along bedding and schistosity planes into the steeply dipping metasediments. The geometric forms are generally of irregular shape and extension. They occur as simple pegmatitic appearing dikes, apophyses, or lenses, and batholithic bodies of considerable size. The batholithic bodies contain numerous xenoliths of metasediments several tens of meters to more than 100 m in diameter. Country rocks intruded by alaskitic granites are biotite gneisses of the Etusis Formation, pyroxene-amphibole-biotite gneisses and schists, and marbles of the Khan and Rössing formations. Quartzites and similar rock types were mostly avoided.

Where alaskites were emplaced into Rössing metasediments, metablastesis of feldspar affected adjacent biotite-cordierite schists. Contact-metamorphism is also noted as skarn developed several meters into marbles.

Dolerite dikes of post-Karoo (Triassic) age cut all the Precambrian suites.

The regional *tectonic grain* is characterized by dense, almost vertical to slightly overturned, NE-SW-trending folds. Steeply inclined cleavages and joints within alaskitic bodies and metasediments exhibit a pronounced NNW-SSE strike and a less distinct NE-SW strike.

Rössing is located on the southern flank of a regional oval NE-SW trending dome. Fracturing created in the zone of the deposit transverse, steeply dipping faults with small scale vertical displacements, but with strike-slip movements of more than 50 m.

Table 5.39. Damara Orogen, types, average contents of U, Th, K, Th/U ratios and ages of the main granite generations (Brynard and Andreoli 1988, based on Haack et al. 1983 and (1) Toens et al. 1979; ages from (2) Marlow 1983 (3) Kröner and Hawkesworth 1977) *n = number of samples.*

Rock type	n	U (ppm) min-max	Th (ppm) min-max	K (%) min-max	Th/U min-max	Age m.y.
Salem-type granite (granodiorite, granite, adamellite emplaced well below level of Karibib Fm.)	78	5.8 1–14	36.8 12–104	5.1 3–7	7.5 2–21	601 ± 79 (2)
Red granite (domes, dikes, lit-par-lit intrusions emplaced below level of Karibib Fm.)	26	7.6 2–42	79.0 13–273	5.7 1–9	12.8 2–26	516 ± 23 (2)
Leucogranite (diapirs, plugs)	36	3.7 1–15	12.4 0.1–34	4.7 2–7	3.7 0.1–13	484 ± 25 (2)
Mineralized alaskite[1] (domes, dikes, anastomosing veins emplaced at Khan and Rössing Fm. level)	12	319.0 38–1120	39.0 2–98	5.1 2–8	0.3 0.02–2	468 ± 25 (3) (Rössing)
Unmineralized alaskite[1]	10	6 1–17	30 1–101	5.2 1–7	4.3 1–20	542 ± 33 (2) (Swakop River)

Table 5.40. Rössing area, lithostratigraphy of metasediments. (After Berning 1986, based on South African Committee on Stratigraphic Nomenclature)

Sequence	Group	Subgroup	Formation	Local lithostratigraphic units	Thickness (m)	
Damara (Upper Proterozoic)	Swakop	Khomas	Kuiseb	Quartz-biotite schist	3000	Stratigraphic position of Rössing uraniferous pegmatitic granite/ alaskite (late to post Damaran tectogenesis)
			Karibib	Marble and quartz-biotite schist	350	
			Chuos	Tillite	300	
		Ugab	Rössing	Feldspathic quartzite	50	
				Upper biotite-cordierite gneiss	50	
				Upper marble	60	
				Conglomerate	5	
				Lower biotite-cordierite gneiss	40	
				Lower marble	40	
			Khan	Biotite-amphibole schist	15	
				Upper pyroxene-hornblende gneiss	90	
	Nosib		Etusis	Lower pyroxene-hornblende gneiss	110	
				Upper biotite gneiss	260	
				Marker quartzite	5	
				Lower biotite gneiss	180	
				Feldspathic quartzite	200	
				Unconformity		
	Abbabis Complex (early Precambrian)					

Principal Characteristics of Mineralization

Principal *ore minerals* are uraninite, betafite, and hexavalent uranium minerals, primarily beta-uranophane. *Associated minerals* are monazite, zircon, apatite, titanite, occasionally pyrite, chalcopyrite, bornite, molybdenite, arsenopyrite, magnetite, hematite, ilmenite, and fluorite.

The ore minerals are of minute size. *Uraninite* has a diameter of a few microns to 0.3 mm, with a frequency in the 0.05 to 0.1 mm fraction. It occurs as inclusions in quartz, feldspar, and biotite, in intergranular spaces or interstices and in microfractures within the mentioned minerals, and reveals a particular affinity to biotite and zircon. It encloses or is intergrown with the latter. *Betafite* occurs predominantly as inclusions in quartz and feldspar.

The *hexavalent uranium minerals* are apparently of secondary origin. Beta-uranophane, and others, replace the primary uraninite and partly the betafite in situ. They also occur as fine films or rarely as crystals in cleavages and fissures. Their presence is not restricted to alaskite, but extends locally into adjacent metasediments.

Mineralogical *distribution of uranium* in crude ore is approximately 55% in uraninite, 5% in betafite, and 40% in hexavalent U minerals.

The uranium-bearing *host rock* is generally described as *alaskite* or alaskitic-granite (Berning et al. 1976) intruded into the Damara Sequence (Table 5.40, Figs. 5.127, 5.128). The main rock constituents are quartz, microcline, and mirocline-perthite. Biotite occurs in subordinate quantity, although local enrichments exist. Fluorite is present in accessorial amount. According to other investigations (Adloff pers. commun.), there are rock facies with more than 20% plagioclase, which would classify the investigated samples as aplite-granite according to Tröger (1969). The grain size averages 1 to 5 mm, but can be as much as several centimeters. Textures are variable, corresponding to those of aplite, granite, and pegmatite. The latter is prevailing. Graphic fabric occurs locally.

Chemistry and mineral composition are rather uniform and constant both in plan and vertical view. Primary uranium minerals occur disseminated throughout the alaskitic body, but are

locally concentrated in bands or clusters of biotite causing an irregular distribution of the ore.

The Rössing deposit has *dimensions* of a NW-SE width of approximately 500 to 600 m and a slightly longer NE-SW length. Minable ore is proven to a depth of approximately 300 m (lowest level of open pit) but drilling intersected ore grades to a depth of at least 700 m. The average ore grade is 0.03 to 0.04% U_3O_8 but there are strong variations with local grades of up to 1% U_3O_8.

The ore occurs in two main zones, a northern and central zone, separated by a wide wedge of barren upper pyroxene-hornblendegneiss of the Khan Formation. Toward the east, the barren track pinches out and the two mineralized zones, although thinned, conjugate. All the metasediments strike about NE-SW and dip steeply SE (Fig. 5.127, 5.128). At the western end of both ore zones exist a near surface accumulation of ore that lacks depth. The enrichment plunges progressively deeper towards the east until it is lost in blind ore shoots in depth.

The *age* of the Rössing alaskite is given as 468 ± 8 m.y. (Kröner and Hawkesworth 1977 in Berning 1986).

Ore Control and Recognition Criteria

Principal ore controls and recognition criteria include:

Host Environment and Mineralization

Jacob et al. (1986) report the following recognition criteria for uraniferous alaskites in the Damara mobile belt in Namibia including Rössing:

- Occurrence restricted to the Central Zone of the belt.
- Confinement to areas of highest metamorphic grade.
- Situation along the Abbabis Swell.
- Preferential occurrence in and around anticlinal and dome structures.
- Association with the older red granite-gneiss suite.
- Intrusion levels in basement: Nosib Group and lower Swakop Group, mainly below the prominent marbles of the Karibib Formation and with apparent preference to the Khan and Rössing formations.
- Intrusion after early migmatization.
- Syn- and post-tectonic emplacement.
- Larger and better mineralized alaskites are post-tectonic.
- Petrographic composition corresponds to alkali-feldspar granites with potassium dominance.
- Rapidly changing grain size between 1 mm and 20 cm.
- No textural or mineral zonation.
- Considerable variations in U content in individual bodies and among adjacent bodies.
- Completely barren and economically mineralized intrusives of apparently similar mineralogy and texture are positioned close together.
- Mineralized intrusives are usually biotite-bearing and microcline rich, contain smoky quartz and weather reddish-brown.
- Intrusives characterized by presence of muscovite, garnet or major amounts of plagioclase are less likely to be mineralized.
- Th/U ratios in mineralized alaskites range from 0.03 to 0.5 but commonly fall within the lower end of this range for better mineralized varieties.

Berning (1986) hints at the complex nature of the Rössing ore zone reflected by:

- Mixture of uraniferous alaskite and barren metasediments.
- Size of alaskite bodies ranges from large masses to narrow bodies interbanded with barren metasediments.

Berning et al. (1976) list the following parameters controlling uranium concentrations within the Rössing alaskite:

- Alaskite bodies intruded into metasediments along axial planes.
- Alaskites replacing amphibolite.
- Locations where wide bodies of alaskite become abruptly constricted and merge into apophyses or dikes.
- Zones in alaskite rich in biotite.
- The bulk of mineralization is contained at the level of the pyroxene-garnet gneiss/amphibole-biotite schist/lower marble, lower cordierite-biotite gneiss units.

Because the position, size, and uranium content of the alaskitic intrusions are spatially close to the *lower marble band* in the Swakop Group,

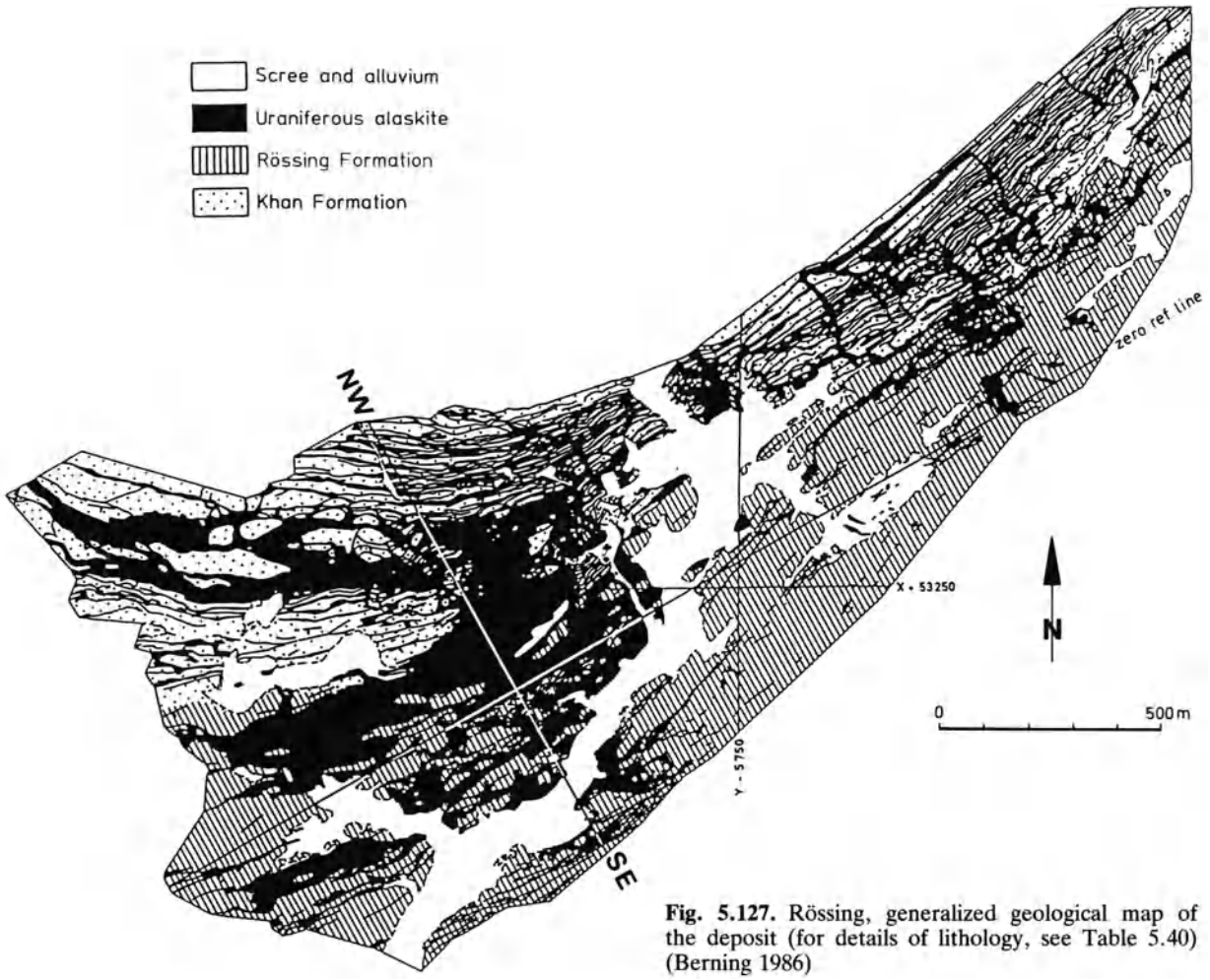

Fig. 5.127. Rössing, generalized geological map of the deposit (for details of lithology, see Table 5.40) (Berning 1986)

some authors think that the marble band has exerted a control on this setting. Jacob (1974b) suggests that the band acted as a trap for the intruding alaskitic granites, while Cuney (1980) considers it a geochemical reaction barrier (see below).

Metallogenetic Concepts

A number of theories on the origin and evolution of the uraniferous alaskites have been put forward. Brynard and Andreoli (1988) present the most recent review and discuss most models. In essence they state that none of the various models proposed to date adequately explains the observed petrological features. Some concepts presented arrive at the following metallogenetic conclusions.

Smith (1965) interprets the composition of, and the close spatial relationship between the uraniferous alaskites and their emplacement level at the disconformity between the Khan and Rössing formations as being suggestive of an alaskite origin during amphibolite grade metamorphism associated with *pegmatite* (alaskite) formation from uraniferous protosediments. Intrusion of the pegmatites occurred when declining metamorphism permitted brittle deformation.

Von Backström and Jacobs (1979) and Toens et al. (1980) propose that the generation of Rössing-type uranium mineralization involves *partial melting* of uraniferous rocks of the Abbabis Complex and overlying metasediments of the Nosib Group. Enrichment of uranium in the anatectic melt resulted from fractional crystallization. The final intrusive product was a fluid-rich pegmatitic granite.

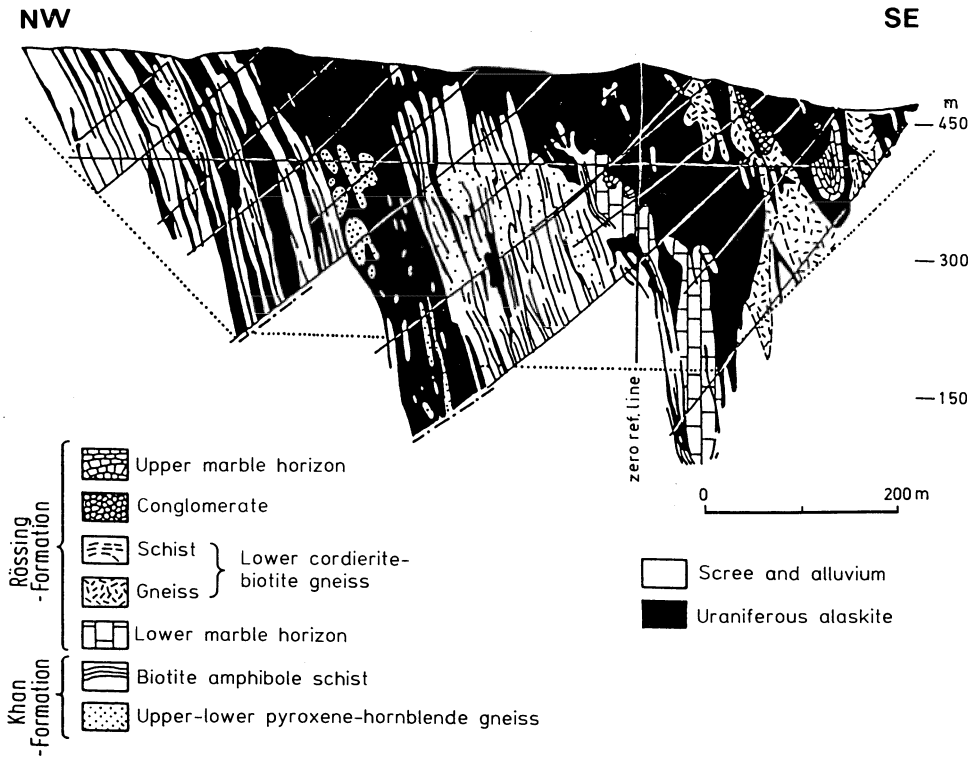

Fig. 5.128. Rössing, NW-SE cross-section through the uranium mineralized zone showing the unpredictable distribution and irregular shapes of uraniferous alaskite. The *open pit outline* (**dotted**) indicates the lateral extent of minable mineralization. (Berning et al. 1976) (reproduced from *Economic Geology*, 1976, v. 71, p. 354)

Winkler (1983) applies phase relationships in the system Qz-Ab-Or-An-H_2O, and concludes that no origin other than *anatexis* of metasediments tends to be feasible. A singular long-lasting episode of magma generation by anatexis for a variety of metasediments provided the source to a variety of dioritic and granitic magmas which then intruded at different levels of the overlying stratigraphic succession.

Cuney (1980) studied geochemistry and fluid inclusions in the uraniferous alaskites and presents in summary this hypothesis. The intruding *alaskitic magma* reacted with the marbles of the Rössing Formation which acted as a geochemical reaction barrier. *Reaction with the marble* caused boiling of the magma by an increase in CO_2 partial pressure and crystallization. An immiscibility between a CO_2-rich and a dense saline fluid supposedly existed contemporaneously or immediately after the fluid saturation of the magma. Uranium mineralization possibly originated during *deuteric alteration* of the alaskite. Part of the uraninite crystallized at the magmatic stage and another part from magmatic fluids in the biotite-rich selvages of the alaskite or in the uraninite-fluorite veins. Crystallization of uraninite is predominantly controlled by the oxygen fugacity that prevailed in the magma and the surrounding rocks.

Critical parameters that contradict the above concepts and other models mentioned below are given by Brynard and Andreoli (1988) as follows:

a) Any concept deriving uraniferous alaskite by anatexis of sediments has to consider the fact that the minerals constituting the alaskite are those with the lowest melting points and should therefore be the first to melt. This would imply the alaskite to be the oldest intrusives and not the youngest, as is mostly the case.

b) Isotope age dating shows that crystallization of diorites and granites predates that of the alaskites and intrusion of uraniferous alaskites occurred at a late to posttectonic stage. These are features which lack explanation in the models

proposed by Smith (1965) and von Backstöm and Jacob (1979)/Toens et al. (1980). The latter model assumes that uranium and volatiles remained in the parent metasediments during the main tectonic events. Their escape occurred only during the posttectonic anatectic episode. This would require a storage system for uranium and volatiles in an environment with high pressure and temperature conditions. But, given a suite of uraniferous hydrous (evaporitic) sediments, one would expect that volatiles and uranium should have been depleted already during the early stages of anatexis under prograde metamorphism.

c) Although mineralization patterns in the Rössing deposit show that the bulk of the uranium concentration occurs at certain lithologic levels near the lower marble band some mineralization occurs well below this level particularly in the eastern part of the deposit where better grades occur at greater depth. Brynard and Andreoli (1988) therefore conclude that most of the uranium must have been present within the magma at the time of intrusion at the levels and that the effects of the marbles could not have affected the magma as suggested by Cuney (1980).

d) If uranium is considered to be indigenous to the parent metasediments of the alaskite, the lack of mineralization in the early alaskite leucosomes requires an explanation. The occurrence of these alaskites at stratigraphic levels from the older Nosib Group to the younger Rössing Formation may indicate a source at a level of the Khan Formation or the underlying unit.

e) Uraniferous alaskites do not occur throughout the Central Zone but are confined to the wider Rössing area. This raises the question why adequate P-T conditions for alaskite-forming anatexis prevailed in this restricted region and not elsewhere and what was their nature? Haack et al. (1983) infer a high potential of heat generation in the Damaran granites (9.5–9.8 HGU) which may be partly due to the high crustal radioactivity in the high grade zones. They calculated that at the level of depth exposed at the present surface, metamorphic temperatures have increased by 100 to 150°C per 5 HGU of heat generation in the Central Zone, which implies a thermal gradient of the order of 10°C/km higher than in adjacent zones.

f) Another possibility, addressed by Brynard and Andreoli (1988), considers a derivation of the alaskite by remelting of high heat-generating granites (e.g., red granites) which were intruded during an earlier stage of the Damara Orogeny. The remelting may have occurred during the peak of the orogeny when temperatures were highest in the Central Zone. Since the alaskites have a much lower density than the metasediments in the stratigraphic column, they could have invaded the present level by diapiric uprise in a suitable field of temperature, accompanied by a high volatile component as noted by Barnes and Hambleton-Jones (1978). Upward migration of the alaskite may have been associated by fractionation of the volatile phase to produce a residual potassium-rich facies from which uranium crystallized.

g) An alternative source rock was provided by Barnes and Hambleton-Jones (1978). They report orbicular-like gray granite schlierens in the alaskite which appear to have been derived from melting of the Khan Formation. The schlierens are frequently mineralized even if the host alaskite is barren. Otherwise, nonuraniferous schlierens occur in mineralized alaskite. The gray granite schlierens display a remanent paleomagnetic orientation different from that of the enveloping granite, which permits the assumption that the Khan metasediments were mineralized in place.

In summary, Brynard and Andreoli (1988) conclude that available data do not satisfy either of the above presented concepts. The authors hint at the possibility that other processes may have been involved in the formation of the uraniferous alaskites. The position of most of the significant occurrences along the Welwitschia Lineament may possibly provide additional clues.

References and Further Reading for Chapter 5.8

(for details of publication see bibliography)

Barnes and Hambleton-Jones 1978; Brynard and Andreoli 1988; Berning 1986; Berning et al.1976; Brynard HJ, pers. commun.; Cuney 1980; Jacob et al.1986; Mouillac et al. 1986; Robb 1986; Robb et al.1986; Robb and Schoch 1985; Toens and Corner 1980; Toens et al.1980; von Backström 1970; von Backström and Jacob 1979.

Appendix

Uranium Minerals (based on Smith 1984), for reference lists see Dahlkamp 1979 and Smith 1984

Mineral	Formula	System	
U^{4+} minerals			
Brannerite/U-Ti phases	$(U,Ca,Ce)(Ti,Fe)_2O_6$	Mono.	
Coffinite	$U(SiO_4)_{1-x}(OH)_{4x}$	Tetra.	
Ishikawaite	$(U,Fe,Y,Ca)(Nb,Ta)O_4$		
Lermontovite	$(U,Ca,Ce)PO_4(OH)\cdot H_2O$		
Mourite	$UMo_5O_{12}(OH)_{10}$	Mono.	
Ningyoite	$(U,Ca,Ce)_2(PO_4)_2\cdot 1-2H_2O$	Orth.	
Petscheckite	$UFe(Nb,Ta)_2O_8$	Hex.	
Sedovite	$U(MoO_4)_2$	Orth.	
Uranmicrolite	$(U,Ca,Ce)_2(Nb,Ta)_2O_6(OH,F)$	Cubic	
Uranpyrochlore	$(U,Ca,Ce)_2(Ta,Nb)_2O_6(OH,F)$	Cubic	
$U^{4+} - U^{6+}$ minerals			
Uraninite	$UO_{2+x}(X <$ ca. 0.3)($\pm$Th,REE,Pb a.o.)	Cubic	
Pitchblende	$UO_{2+x}(X <$ ca. 0.67)($\pm$Ca,Si,Ti,Pb a.o.)	Cubic	
Sooty/earthy pitchbl.	$UO_{3-x}(X <$ ca. 0.3)($\pm H_2O$ a.o)	Amorphous	
Ianthinite	$U(UO_2)_5(OH)_{14}\cdot 3H_2O$	Orth.	
Liandratite	$U(Nb,Ta)_2O_8$	Hex.	
Moluranite	$H_4U(UO_2)_3(MoO_4)_7\cdot 18H_2O$	Amorphous	
Orthobrannerite	$UTi_4O_{12}(OH)_2$	Orth.	
Unnamed	α-U_3O_7	Tetr.	
Wyartite	$Ca_3U(UO_2)_6(CO_3)_2(OH)_{18}\cdot 3-5H_2O$	Orth.	
Uranyl oxide hydrates (gummite minerals)			
Ianthinite	$UO_2\cdot 5UO_3\cdot 10H_2O$	Orth.	
Metaschoepite	$UO_3\cdot 2H_2O$	Orth.	
Paraschoepite	$UO_3\cdot 2H_2O$	Orth.	
Schoepite	$UO_3\cdot 2H_2O$	Orth.	
Studtite	$UO_4\cdot 4H_2O$	Mono.	
Metastudtite	$UO_4\cdot 2H_2O$	Orth.	
Alkali and alkaline-earth uranyl oxide hydrates			Sobry Formula
Agrinierite	$(K_2Ca,Sr)U_3O_{10}$	Orth.	
Bauranoite	$BaU_2O_7\cdot 4-5H_2O$		
Becquerelite	$Ca(UO_2)_6O_4(OH)_6\cdot H_2O$	Orth.	
Billietite	$Ba(UO_2)_6O_4(OH)_6\cdot 8H_2O$	Orth.	$X(H_3O)_5[(UO_2)_6O_7(OH)_5]$
Calciouranoite	$(Ca,Ba,Pb)U_2O_7\cdot 5H_2O$	Metamict	$X(H_3O)[(UO_2)_2O_3(OH)]\cdot 3H_2O$
Clarkeite	$(Na,Ca,Pb)_2U_2(O,OH)_7$		
Compreignacite	$K_2(UO_2)_6O_4(OH)_6\cdot 8H_2O$	Orth.	
Curite	$Pb_2U_5O_{17}\cdot 4H_2O$	Orth.	$Pb_4(H_3O)_6[(UO_2)_{10}O_{14}(OH)_6]$
Fourmarierite	$PbU_4O_{13}\cdot 6H_2O$	Orth.	$Pb(H_3O)_3[(UO_2)_4O_5(OH)_3]$
Masuyite	$Pb_3U_8O_{27}\cdot 10H_2O$	Orth.	$Pb_3(H_3O)_5[(UO_2)_8O_5(OH)_5]$
Metacalciouranoite	$(Ca,Na,Ba)U_2O_7\cdot 2H_2O$	Metamict	$X(H_3O)[(UO_2)_2O_3(OH)]$
Metavandend-riesscheite	$PbU_7O_{22}\cdot nH_2O(n < 12)$		$Pb(H_3O)_6[(UO_2)_7O_8(OH)_6]$
Rameauite	$K_2CaU_6O_{20}\cdot 9H_2O$	Mono.	

Mineral	Formula	System	
Alkali and alkaline-earth uranyl oxide hydrates			Sobry Formula
Richetite	Pb-U oxide		
Roubaultite	$Cu_2(UO_2)_3(OH)_{10}\cdot 5H_2O$	Tricl.	
Sayrite	$Pb_2(UO_2)_5O_6(OH)_2\cdot 4H_2O$		
Uranosphaerite	$Bi_2U_2O_9\cdot 3H_2O$		
Vandenbrandeite	$Cu(UO_2)(OH)_4$	Tricl.	
Vandendriesscheite	$PbU_7O_{22}\cdot 22H_2O$	Orth.	$Pb(H_3O)_6[(UO_2)_7O_8(OH)_6]\cdot 10H_2O$
Wolsendorfite	$(Pb,Ca)U_2O_7\cdot 2H_2O$	Orth.	$Pb(H_3O)[(UO_2)_2O_3(OH)]$
Uranyl carbonates			
Wyartite	$Ca_3U(UO_2)_6(CO_3)_2(OH)_{18}\cdot 3\text{–}5H_2O$	Orth.	
Joliotite	$(UO_2)(CO_3)\cdot 1.5\text{–}2H_2O$	Orth.	
Rutherfordine	$(UO_2)(CO_3)$	Orth.	
Sharpite	$(UO_2)(CO_3)\cdot H_2O$	Orth.	
Metazellerite	$Ca(UO_2)(CO_3)_2\cdot 3H_2O$	Orth.	
Zellerite	$Ca(UO_2)(CO_3)_2\cdot 5H_2O$	Orth.	
Andersonite	$Na_2Ca(UO_2)(CO_3)_3\cdot 6H_2O$	Hex.	
Bayleyite	$Mg_2(UO_2)(CO_3)_3\cdot 18H_2O$	Mono.	
Grimselite	$K_3Na(UO_2)(CO_3)_3\cdot H_2O$	Hex.	
Liebigite	$Ca_2(UO_2)(CO_3)_3\cdot 11H_2O$	Orth.	
Rabbittite	$Ca_3Mg_3(UO_2)_2(CO_3)_6(OH)_4\cdot 18H_2O$	Mono.	
Schroeckingerite	$NaCa_3(UO_2)(CO_3)_3SO_4F\cdot 10H_2O$	Tricl.	
Swartzite	$CaMg(UO_2)(CO_3)_3\cdot 12H_2O$	Mono.	
Widenmannite	$Pb_2(UO_2)(CO_3)_3$	Orth.	
Voglite	$Ca_2Cu(UO_2)(CO_3)_4\cdot 6H_2O$	Mono.	
Mckelveyite	$Ca_3Na(Ca,U)Y(CO_3)_6\cdot 3H_2O$	Hex.	
Bijvoetite	$(RE)_2(UO_2)_4(CO_3)_4(OH)_6$		
Lepersonnite	$Ca(RE)_2U_{24}(CO_3)_8Si_{4.2}O_{76}\cdot 60H_2O$		
Uranyl molybdates			
Calcurmolite	$Ca(UO_2)_3(MoO_4)_3(OH)_2\cdot 11H_2O$		
Cousinite	$Mg(UO_2)_2(MoO_4)_2(OH)_2\cdot 5H_2O$		
Iriginite	$(UO_2)Mo_2O_7\cdot 3H_2O$	Orth.	
Moluranite	$H_4U(UO_2)_3(MoO_4)_7$		
Mourite	$UMo_5O_{12}(OH)_{10}$	Mono.	
Sedovite	$U(MoO_4)_2$		
Umohoite	$(UO_2)(MoO_2)(OH)_4\cdot 2H_2O$	Mono.	
Uranyl phosphates and arsenates			
Arsenuranylite	$Ca(UO_2)_4(AsO_4)_2(OH)_4\cdot 6H_2O$ possibly $Ca_2(UO_2)_3(AsO_4)_2(OH)_4\cdot 6H_2O$	Orth.	
Bergenite	$Ba(UO_2)_4(PO_4)_2(OH)_4\cdot 8H_2O$ possibly $Ba_2(UO_2)_3(PO_4)_2(OH)_4\cdot 8H_2O$	Orth.	
Kivuite	$(Th,Ca,Pb)(H_3O)_2(UO_2)_4(PO_4)_2(OH)_8\cdot 5H_2O$ possibly $(Th,Ca,Pb)(H_3O)_2(UO_2)_3(PO_4)_2(OH)_6\cdot 5H_2O$	Orth.	
Renardite	$Pb(UO_2)_4(PO_4)_2(OH)_4\cdot 7H_2O$ possibly $Pb_2(UO_2)_3(PO_4)_2(OH)_4\cdot 7H_2O$	Orth.	
Dumontite	$Pb_2(UO_2)_3(PO_4)_2(OH)_4\cdot 3H_2O$	Mono.	
Huegelite	$Pb_2(UO_2)_3(AsO_4)_2(OH)_4\cdot 3H_2O$	Similar to dumontite	
Phosphuranulite	$(H_3O)_2Ca(UO_2)_3(PO_4)_2(OH)_4\cdot 4H_2O$	Orth.	
Phurcalite	$Ca_2(UO_2)_3(PO_4)_2(OH)_4\cdot 4H_2O$	Orth.	

Mineral	Formula	System
Uranyl phosphates and arsenates		
Phuralumite	$Al_2(UO_2)_3(PO_4)_2(OH)_6 \cdot 10H_2O$	Mono.
Upalite	$Al(UO_2)_3(PO_4)_2(OH)_3$	Orth.
Vanmeersscheite	$U(UO_2)_3(PO_4)_2(OH)_6 \cdot 4H_2O$	Orth.
Metavanmeerss-cheite	$U(UO_2)_3(PO_4)_2(OH)_4 \cdot 2H_2O$	Orth.
Autunite family	$R_{1-2}(UO_2)_2(TO_4)_2 \cdot 8-12H_2O$	see extra table
Dewindtite	$Pb(UO_2)_2(PO_4)_2 \cdot 3H_2O$	= renardite?
Meta-autunite I family	$R_{1-2}(UO_2)_2(TO_4)_2 \cdot 6-8H_2O$	see extra table
Coconinoite	$Fe_2Al_2(UO_2)_2(PO_4)_2(SO_4)(OH)_2 \cdot 20H_2O$	Mono.
Furongite	$Al_2(UO_2)(PO_4)_2(OH)_2 \cdot 8H_2O$	Tricl.
Hallimondite	$Pb(UO_2)(AsO_4)_2 \cdot nH_2O$	Tricl.
Parsonsite	$Pb(UO_2)(PO_4)_2 \cdot nH_2O$	Tricl.
Pseudo-autunite	$(H_3O)_4Ca_2(UO_2)_2(PO_4)_4 \cdot 5H_2O$	Orth.
Walpurgite	$(BiO)_4(UO_2)_2(AsO_4)_4 \cdot 6H_2O$	Tricl.
Walpurgite-(P)	$(BiO)_4(UO_2)_2(PO_4)_4 \cdot 6H_2O$	Tricl.
Uranyl phosphates of the autunite family		
Arsenuranospathite	$HAl(UO_2)_4(AsO_4)_4 \cdot 40H_2O$	Tetr.
Autunite	$Ca(UO_2)_2(PO_4)_2 \cdot 8-12H_2O$	Tetr.
Fritzcheite	$Mn(UO_2)_2(VO_4)_2 \cdot 10H_2O$	
Heinrichite	$Ba(UO_2)_2(AsO_4)_2 \cdot 10-12H_2O$	Tetr.
Kahlerite	$Fe(UO_2)_2(AsO_4)_2 \cdot 10-12H_2O$	Tetr.
Novacekite	$Mg(UO_2)_2(AsO_4)_2 \cdot 12H_2O$	Tetr.
Sabugalite	$HAl(UO_2)_4(PO_4)_4 \cdot 16H_2O$	Tetr.
Saleeite	$Mg(UO_2)_2(PO_4)_2 \cdot 10H_2O$	Tetr.
Threadgoldite	$Al(UO_2)_2(PO_4)_2(OH) \cdot 8H_2O$	Mono.
Torbernite	$Cu(UO_2)_2(PO_4)_2 \cdot 8-12H_2O$	Tetr.
Uranocircite	$Ba(UO_2)_2(PO_4)_2 \cdot 12H_2O$	Tetr.
Uranospathite	$HAl(UO_2)_4(PO_4)_4 \cdot 40H_2O$	Tetr.
Uranospinite	$Ca(UO_2)_2(AsO_4)_2 \cdot 10H_2O$	Tetr.
Xiangjiangite	$(Fe,Al)(UO_2)_4(PO_4)_2(SO_4)_2(OH) \cdot 22H_2O$	Orth.
Zeunerite	$Cu(UO_2)_2(PO_4)_2 \cdot 40H_2O$	Tetr.
Uranyl phosphates of the meta-autunite family		
Abernathyite	$K_2(UO_2)_2(AsO_4)_2 \cdot 8H_2O$	Tetr.
Bassettite	$Fe(UO_2)_2(PO_4)_2 \cdot 8H_2O$	Mono.
Meta-ankoleite	$K_2(UO_2)_2(PO_4)_2 \cdot 6H_2O$	Tetr.
Meta-autunite	$Ca(UO_2)_2(PO_4)_2 \cdot 6H_2O$	Tetr.
Meta-autunite II	$Ca(UO_2)_2(PO_4)_2 \cdot 4-6H_2O$	Orth.
Metaheinrichite	$Ba(UO_2)_2(AsO_4)_2 \cdot 8H_2O$	Tetr.
Metakahlerite	$Fe(UO_2)_2(AsO_4)_2 \cdot 8H_2O$	Tetr.
Metakirchheimer-ite	$Co(UO_2)_2(AsO_4)_2 \cdot 8H_2O$	Tetr.
Metalodevite	$Zn(UO_2)(AsO_4)_2 \cdot 10H_2O$	Tetr.
Metanovacekite	$Mg(UO_2)_2(AsO_4)_2 \cdot 4-8H_2O$	Tetr.
Metatorbernite	$Cu(UO_2)_2(PO_4)_2 \cdot 8H_2O$	Tetr.
Meta-uranocircite	$Ba(UO_2)_2(PO_4)_2 \cdot 8H_2O$	Tetr.
Meta-uranocircite II	$Ba(UO_2)_2(PO_4)_2 \cdot 6H_2O$	Mono.
Meta-uranospinite	$Ca(UO_2)_2(AsO_4)_2 \cdot 8H_2O$	Tetr.
Metazeunerite	$Cu(UO_2)_2(AsO_4)_2 \cdot 8H_2O$	Tetr.
Przhevalskite	$Pb(UO_2)_2(PO_4)_2 \cdot 2H_2O$	Orth.
Ranunculite	$(H_3O)Al(UO_2)(PO_4)(OH)_3 \cdot 3H_2O$	Mono.
Sodium meta-autunite	$(Na_2,Ca)(UO_2)_2(PO_4)_2 \cdot 8H_2O$	Tetr.

Mineral	Formula	System
Uranyl phosphates of the meta-autunite family		
Sodium uranospinite	$(Na_2,Ca)(UO_2)_2(AsO_4)_2 \cdot 5H_2O$	Tetr.
Triangulite	$Al_3(UO_2)_4(PO_4)_4(OH)_5 \cdot 5H_2O$	
Trögerite	$UO_2(UO_2)_2(AsO_4)_2 \cdot 8H_2O$	Tetr.
Trögerite-(P)	$UO_2(UO_2)_2(PO_4)_2 \cdot 8H_2O$	Tetr.
Uramphite	$(NH_4)_2(UO_2)_2(PO_4)_2 \cdot 4\text{–}6H_2O$	Tetr.
Uranyl selenates and tellurates		
Guilleminite	$Ba(UO_2)_3(SeO_3)_2(OH)_4 \cdot 3H_2O$	Orth.
Marthozite	$Cu(UO_2)_3(SeO_3)_3(OH)_2 \cdot 7H_2O$	Orth.
Schmitterite	UO_2TeO_3	Orth.
Derriksite	$Cu_4(UO_2)(SeO_3)_2(OH)_6 \cdot H_2O$	Orth.
Moctezumite	$Pb(UO_2)(TeO_3)_2$	Mono.
Cliffordite	$UO_2Te_3O_7$	Cub.
Demesmaekerite	$Pb_2Cu_5(UO_2)_2(SeO_3)_6(OH)_6 \cdot 2H_2O$	Tricl.
Uranyl silicates		
Soddyite	$(UO_2)_2SiO_4 \cdot 2H_2O$	Orth.
Oursinite	$(CO,Mg)(UO_2)_2Si_2O_7 \cdot 6H_2O$	
Beta-uranophane	$(H_3O)_2Ca(UO_2)_2(SiO_4)_2 \cdot 3H_2O$	Mono.
Boltwoodite	$K_2(UO_2)_2(SiO_3OH)_2 \cdot 5H_2O$	Mono.
Cuprosklodowskite	$(H_3O)_2Cu(UO_2)_2(SiO_4)_2 \cdot 4H_2O$	Tricl.
Kasolite	$Pb_2(UO_2)_2(SiO_4)_2 \cdot 2H_2O$	Mono.
Sklodowskite	$(H_3O)_2Mg(UO_2)_2(SiO_4)_2 \cdot 4H_2O$	Mono.
Sodium boltwoodite	$(H_3O)_2(Na,K)_2(UO_2)_2(SiO_4)_2 \cdot 2H_2O$	Orth.
Uranophane	$(H_3O)_2Ca(UO_2)_2(SiO_4)_2 \cdot 3H_2O$	Mono.
Swamboite	$Vo_3H_2(UO_2)_2(SiO_4)_2 \cdot 10H_2O$	
Haiweeite	$Ca(UO_2)_2Si_6O_{15} \cdot 5H_2O$	Mono.
Weeksite	$K_2(UO_2)_2Si_6O_{15} \cdot 4H_2O$	Orth.
Haiweeite-(Mg)	$Mg(UO_2)_2Si_6O_{15} \cdot 9H_2O$	
Uranosilite	$U^{6+}Si_7O_{17}$	
Uranyl sulfates		
Meta-uranopilite	$(UO_2)_6(SO_4)(OH)_{10} \cdot 5H_2O$	
Uranopilite	$(UO_2)_6(SO_4)(OH)_{10} \cdot 12H_2O$	Mono.
Cobalt zippeite	$Co_2(UO_2)_6(SO_4)_3(OH)_{10} \cdot 16H_2O$	Orth.
Magnesium zippeite	$Mg_2(UO_2)_6(SO_4)_3(OH)_{10} \cdot 16H_2O$	Orth.
Nickel zippeite	$Ni_2(UO_2)_6(SO_4)_3(OH)_{10} \cdot 16H_2O$	Orth.
Sodium zippeite	$Na_4(UO_2)_6(SO_4)_3(OH)_{10} \cdot 16H_2O$	Orth.
Zinc zippeite	$Zn_2(UO_2)_4(SO_4)_3(OH)_{10} \cdot 16H_2O$	Orth.
Zippeite	$K_4(UO_2)_6(SO_4)_3(OH)_{10} \cdot 16H_2O$	Orth.
Johannite	$Cu(UO_2)_2(SO_4)_2(OH)_2 \cdot 8H_2O$	Tricl.
Coconinoite	$Fe_2Al_2(UO_2)_2(PO_4)_2SO_4(OH)_2 \cdot 20H_2O$	Mono.
Schroeckingerite	$NaCa_3(UO_2)_2(CO_3)_3SO_4F \cdot 10H_2O$	Tricl.
Uranyl vanadates		
Carnotite group		
Carnotite	$K_2(UO_2)_2V_2O_8 \cdot 3H_2O$	Mono.
Curienite	$Pb(UO_2)_2V_2O_8 \cdot 5H_2O$	Orth.
Francevillite	$Ba(UO_2)_2V_2O_8 \cdot 5H_2O$	Orth.
Fritzcheite	$Mn(UO_2)_2V_2O_8 \cdot 10H_2O$	Orth.
Margaritasite	$Cs(UO_2)_2V_2O_8 \cdot 1.5H_2O$	Mono.
Metatyuyamunite	$Ca(UO_2)_2V_2O_8 \cdot 3\text{–}5H_2O$	Orth.
Metavanuralite	$Al(UO_2)_2V_2O_8(OH) \cdot 8H_2O$	Tricl.
Sengierite	$Cu_2(UO_2)_2V_2O_8(OH)_2 \cdot 6H_2O$	Mono.
Strelkinite	$Na_2(UO_2)_2V_2O_8 \cdot 6H_2O$	Orth.

Mineral	Formula	System
Uranyl vanadates		
Tyuyamunite	$Ca(UO_2)_2V_2O_8 \cdot 8H_2O$	Orth.
Vanuralite	$Al(UO_2)_2V_2O_8(OH) \cdot 11H_2O$	Mono.
Vanuranylite	$(H_3O)_2(UO_2)_2V_2O_8 \cdot 4H_2O$	Mono.
Unclassified		
Ferghanite	$(UO_2)_3V_2O_8 \cdot 6H_2O$	
Rauvite	$Ca(UO_2)_2V_{10}O_{28} \cdot 16H_2O$	
Unnamed	$Ca\text{-}U\text{-}V\text{-}O\text{-}H_2O$	
Unnamed	$Pb\text{-}U\text{-}V\text{-}O\text{-}H_2O$	
Uvanite	$(UO_2)_2V_6O_{17} \cdot 15H_2O$	

Uranium niobates, tantalates and titanates (U substitutional but not dominant ion)

	Formula	Structure type	System
Ashanite	$(Nb,Ta,U,Fe,Mn)_4O_8$	Ixiolite	Orth.
Betafite	$(Ca,Na,U)(Ti,Nb,Ta)_2O_6(OH)$	Pyrochlore	Cubic
Davidite	$(Fe,La,U,Ca)_6(Ti,Fe)_{15}(O,OH)_{36}$	Crichtonite	Hex.
Euxenite	$(Y,Ca,Ce,U,Th)(Nb,Ta,Ti)_2O_6$	Columbite	Orth.
Kobeite	$(Y,U)(Ti,Nb)_2(O,OH)_6$	Columbite	
Pisekite	$(As,Ca,U)(Nb,Ta,Ti)O_4$		
Plumbobetafite	$(Pb,U,Ca)(Nb,Ti)_2O_6(OH,F)$	Pyrochlore	
Plumbomicrolite	$(Pb,Ca,U)Ta_2O_6(OH)$	Pyrochlore	
Plumbopyrochlore	$(Pb,Y,U,Ca)_{2-x}Nb_2O_6(OH)$	Pyrochlore	Cubic
Polycrase	$(Y,Ca,Ce,U,Th)(Ti,Nb,Ta)_2O_6$	Columbite	
Samarskite	$(Y,Ce,U,Ca,Pb)(Nb,Ta,Ti,Sn)_2O_6$	Columbite	
Tanteuxenite	$(U,Fe,V)(Ti,Sn)_2O_6$	Columbite	
Thorutite	$(Th,U,Ca)Ti_2(O,OH)_6$	Brannerite	
Yttrobetafite	$(Y,U,Ce)_2(Ti,Nb,Ta)_2O_6(OH)$	Pyrochlore	
Yttrocolumbite	$(Y,U,Fe)(Nb,Ta)O_4$	Stannocolumbite?	
Yttrocrasite	$(Y,Th,Ca,U)(Ti,Fe)_2(O,OH)$	Columbite	
Yttromicrolite (hjelmite)	$(Y,Ca,U)_2(Ta,Nb)_2O_6(OH)$	Pyrochlore	
Yttropyrochlore	$(Y,Na,Ca,U)_{1-2}(Nb,Ta,Ti)_2O_6(OH)$	Pyrochlore	Cubic

Minerals with traces of uranium

Aeschynite	$(Ce,Ca\ldots)(Ti,Nb)_2(O,OH)_6$	Aeschynite
Allanite	$(Ce,Ca,Y,U)(Al,Fe)_3(SiO_4)_3(OH)$	Epidote
Belovite	$(Sr,Ce,Na,Ca)_5(PO_4)_3(OH)$	Apatite
Britholite	$(Ce,Ca)_5([Si,P]O_4)_3(OH,F)$	Apatite
Cerianite	$(Ce,U)O_2$	Fluorite
Cheralite	$(Ca,Ce,Th)(P,Si)O_4$	Monazite
Ekanite	$(Th,U)(Ca,Fe,Pb)_2Si_8O_{20}$	Ekanite
Ewaldite	$Ba(Ca,RE)(CO_3)_2$	Ewaldite
Fergusonite	$YNbO_4$	Fergusonite
Formanite	$YTaO_4$	Fergusonite
Iimoriite	$(Y,Ca,Zr)_{15}(Mg,Fe,Al)(Si,Al,P)_9O_{34}(OH)_{16}$	Apatite
Iraqite	$(La,Ce,Th,U)_2(K,Y)_2(Ca,La,Ce,Na)_4(Si,Al)_{16}O_{40}$	Ekanite
Melanocerite	$(Ce,Ca)_5(Si,B)_3O_{12}(OH,F) \cdot nH_2O$	Apatite
Monazite	$(Ce,Th,Ca,U)PO_4$	Monazite
Niobo-aeschynite	$(Ce,Ca,Th)(Nb,Ti)_2(O,OH)_6$	Aeschynite
Rhabdophane	$(Y,\ldots)PO_4 \cdot H_2O$	Rhabdophane
Thorianite	$(Th,U)O_2$	Fluorite
Thorite	$(Th,U)SiO_4$	Zircon
Umbozerite	$(Na,K)_3(Sr,Ba)_4(Th,U,Fe)_3O_{24}$	Umbozerite

Bibliography

Adamek PM, Wilson MR (1977) Recognition of a new uranium province from the Precambrian of Sweden, *in*: Recognition and evaluation of uraniferous areas, IAEA, Vienna, pp 199–214

Adamek PM, Wilson MR (1979) The evolution of a uranium province in northern Sweden, Proc Royal Soc, London, 291, pp 355–368

Adams JAS (1954) Uranium content of Wisconsin rivers and their use in geochemical prospecting, Bull Geol Soc Amer, v 65, no. 12, pt. 2, p 1225

Adams JAS, Lowder WM, eds. (1964) The natural radiation environment, Univ Chicago Press, 1069 p

Adams JAS, Osmond JK, Rogers JJW (1959) The geochemistry of thorium and uranium, *in*: Ahrens, LH et al., eds., Physics and chemistry of the earth, v 3, Pergamon Press, New York, pp 298–348

Adams JAS, Richardson KA (1960) Thorium, uranium and zirconium concentrations in bauxite, Econ Geol, v 55, pp 1653–1675

Adams, JW, Stugard Jr F (1956) Wall-rock control of certain pitchblende deposits in Golden Gate Canyon, Jefferson County, Colorado, US Geol Surv Bull 1030-G, pp 187–209

Adams SS, Saucier AE (1981) Geology and recognition criteria for uraniferous humate deposits, Grants mineral region, New Mexico, US-DOE, GJBX-2(81), 225 p

Adams SS, Smith RB (1981) Geology and recognition criteria for sandstone uranium deposits in mixed fluvial-shallow marine sedimentary sequences, south Texas, Final report, US-DOE, GJBX-4(81), 145 p

Adams SS, Curtis, HS, Hafen, PL (1974) Alteration of detrital magnetite-ilmenite in continental sandstones of the Morrison Formation, New Mexico, *in*: Formation of uranium deposits, IAEA, Vienna, pp 219–253

Adams SS, Curtis HS, Hafen PL Salek-Nejad H (1978) Interpretation of post-depositional processes related to the formation and destruction of the Jackpile-Paguate uranium deposit, northwest New Mexico, Econ Geol, v 73, pp 1635–1654

Adamson DW (1983) Uranium and thorium abundances in high-grade rocks from the western Saskatchewan shield, unpubl MSc thesis, Univ Regina, 224 p

Adamson DW, Parslow GR (1985) Granulite facies depletion of uranium: reality or not; *in*: Les Mécanismes de Concentration de l'Uranium dans les Environnements Géologiques, Programme et Resumés, Nancy, pp 87–90

Adler HH (1974) Concepts of uranium-ore formation in reducing environments in sandstones and other sediments, *in*: Formation of uranium ore deposits, IAEA, Vienna, pp 141–168

Adler HH (1977) Geochemical factors contributing to uranium concentration in alkalic igneous rocks, *in*: Recognition and evaluation of uraniferous areas, IAEA, Vienna, pp 35–46

Adler HH, Sharp BJ (1967) Uranium ore rolls-occurrence, genesis, and physical and chemical characteristics, Utah Geol Soc Guidebook, no. 21, pp 53–77

Ahmad R, Wilson CJL (1981) Uranium and boron distributions related to metamorphic microstructures evidence for metamorphic fluids activity, Contrib. Miner Petrol, v 76, pp 24–32

Ahrens LH (1965a) The comparative geochemistry of potassium, rubidium, calcium, argon, strontium, uranium, thorium, and lead, *in*: Applied geochronology, Hamilton El, ed., Academic Press, London and New York, 267 p

Äikäs O, Sarikkola R (1987) Uranium in Lower Proterozoic conglomerates of the Koli Area, eastern Finland, *in*: Uranium deposits in Proterozoic quartz-pebble conglomerates, TECDOC-427, IAEA, Vienna, pp 189–234

Aiken MJ (1981) Mineralogy and geochemistry of a lacustrine uranium occurrence, Anderson Ranch, Brewster County, Texas, Masters thesis, Univ Texas, El Paso, 162 p

Akin H, Gatzweiler R (1985) Exploration und Bewertung der Lagerstaette Key Lake – Status und Rueckblick am Beginn der Produktion (I), Erzmetall, 38, Nr. 1, pp 11–17, Nr. 2, pp 78–82

Albarede F, Michard A, Cuney M (1985) Les chronomètres uranium – thorium – plomb. Extrait de: Roth E, Poty B, eds., Méthodes de datation par les phénomènes nucléaires naturels – Applications, Masson, pp 123–173

Alcock FJ (1936) Geology of the Lake Athabasca region, Saskatchewan, Geol Surv Can Mem 196, 41 p

Alekseyev VA, Ananyeva LA Rafalsky RP (1981) Effects of composition on lattice parameter of UO_{2+X}, Intern Geol Rev, v 23, 10, pp 1229–1236

Alexander RL (1986) Geology of Madawaska Mines Limited, Bancroft, Ontario, *in*: Evans, EL, ed., Uranium deposits of Canada, CIM Spec Vol. 33, pp 62–69

Allman-Ward P (1985) Distribution of uranium and thorium in the western lobe of the St. Austell granite and the effects of alteration processes, *in*: Halls C, ed., High heat production granites, hydrothermal circulation and ore genesis, IMM, London, pp 437–458

Allsopp HL (1964) Rubidium/strontium ages from the western Transvaal, Nature, v 204, pp 361–363

Allsopp HL, Welke HJ (1986) Age limits to the Witwatersrand Supergroup, *in*: Anhaeusser CR, Maske S, Mineral deposits of southern Africa, Geol Soc S Afr, v 1, pp 495–496

Allsopp HL, Roberts HR, Schreiner GDL, Hunter DR (1962) Rb-Sr age measurements on various Swaziland granites, J Geophys Res, v 67, pp 5307–5313

Altschuler ZS (1980a) The geochemistry of trace elements in marine phosphorites: I. Characteristic abundances and enrichment, Soc Econ Paleont Miner Spec Pub 29, pp 19–30

Altschuler ZS (1980b) The bearing of geochemistry on the recovery of uranium and rare earths in phosphorites, Internat Cong Phosphorus Compounds, 2nd, Boston, April 1980, Proc, pp 605–625

Altschuler ZS Clarke RS, Jr, Young EJ (1958) Geochemistry of uranium in apatite and phosphorite, US Geol Surv Prof Paper 314-D, pp 45–90

Amstutz GC (1974) Spilites and spilitic rocks. Springer, Berlin, 482 p

Anderson DC (1969) Uranium deposits of the Gas Hills, Wyoming Univ Contributions to Geology, v 8, pp 93–103

Andrade N (1989) The Eagle Point uranium deposits, northern Saskatchewan, Canada, *in*: Uranium resources and geology of North America, TECDOC-500, IAEA, Vienna, pp 455–490

Andreoli MAG, Robb LJ, Meyer M, Ainslie LC, Hart RJ (1985) Granitoids of the pre-Witwatersrand basement; clues to the source of uranium placer mineralization, *in*: Recognition of uranium provinces, IAEA, Vienna, pp 213–234

Andreyev PF, Chumachenko AP (1964) Reduction of uranium by natural organic substances, Geochem Intern, v 1, pp 3–7

Angeiras AG, Netto AM, de Campos M (1981) Phosphoro-uraniferous mineralization associated with sodium episyenites in the Ceara Precambrian (Brazil), *in*: Uranium deposits in Latin America: geology and exploration, IAEA, Vienna, pp 555–577

Anhaeusser CR (1973) The evolution of the early Precambrian crust of southern Africa, Phil Trans Royal Soc, London, A273, pp 359–388

Anhaeusser CR (1975) Precambrian tectonic environments, Annual Rev Earth Planet Sci, v 3, pp 31–53

Anhaeusser CR (1976) The nature and distribution of Archaean gold mineralization in southern Africa, Miner Sci Eng, v 8, pp 46–84

Anhaeusser CR, Maske S, eds. (1986) Mineral deposits of southern Africa, Geol Soc S Afr, v 1 and 2, 2340 p

Anhaeusser CR, Mason R, Viljoen MJ, and Viljoen RP (1969) A reappraisal of some aspects of Precambrian shield geology, Geol Soc Am Bull, v 80, pp 2175–2200

Aniel B (1983) Les gisements d'uranium associés au volcanisme acide tertiaire de la Sierra de Peña Blanca (Chihuahua, Mexique), Géol Géochim Uranium, Mém Nancy, no. 2, 291 p

Anthony PJ (1975) Nabarlek uranium deposit, *in*: Knight CL, ed., Economic geology of Australia and Papua New Guinea, 1. Metals, AIMM Monograph 5, pp 304–307

Antrobus ESA (1986) The South Rand Goldfield, *in*: Anhaeusser CR, Maske S, Mineral deposits of southern Africa, Geol Soc S Afr, v 1, pp 689–704

Antrobus ESA, Whiteside HCM (1964) The geology of certain mines in the East Rand, *in*: Haughton SH, ed., The geology of some ore deposits in southern Africa, Geol Soc S Afr, v 1, pp 125–159

Antrobus ESA, Brink WCJ, Brink HC, Caulkin J, Hutchinson RI, Thomas DE, Van Graan JA, Viljoen JJ (1986) The Klerksdorp Goldfield, *in*: Anhaeusser CR, Maske S, Mineral deposits of southern Africa, Geol Soc S Afr, v 1, pp 549–598

Antropov PYa, Yevseyeva LS, Poluarshinov GP (1978) Uranium deposits in sedimentary rocks of depressions. Intern Geol Review, v 20, no. 9, pp 1067–1071

Appleyard EC (1981) Calc-silicate rocks and associated metasomatites of the Wollaston Group, *in*: Summ Invest 1981, Sask Geol Surv Misc Rept 81–4, pp 44–46

Appleyard EC (1984) The origin of plagioclasite in the vicinity of the Rabbit Lake uranium deposit, *in*: Summ Invest 1984, Sask Geol Surv Misc Rep pp 84–4

Arakel AV (1988) Carnotite mineralization in inland drainage areas of Australia, *in*: Gabelman JW, ed., Unconventional uranium deposits. Ore Geol Rev, 3, pp 289–311

Armands G (1972) Geochemical studies of U, Mo, and V in a Swedish Alum Shale, Stockholm Contributions in Geology, Acta Univ Stockholm, v 27, no. 1, 148 p

Armstrong GC, (1968) Sedimentological control of gold mineralization in the Kimberley Reefs of the East Rand Goldfield, Univ Witwatersrand, Johannesburg, Econ Geol Res Unit Inform Circ 47, 24 p

Armstrong FC (1970) Geologic factors controlling uranium resources in the Gas Hills district, Wyoming, Wyoming Geol Ass, 22nd Field Conf Guidebook, pp 31–44

Armstrong FC, ed. (1981) Genesis of uranium and gold-bearing Precambrian quartz-pebble conglomerates, Proc Workshop 1975, Golden Colorado, US Geol Surv 1161-A-BB

Armstrong RL, Ramaekers P, (1985) Sr isotope study of Helikian sediment and diabase dikes in the Athabasca Basin, northern Saskatchewan, Can J Earth Sci, v 22, pp 399–407

Arribas A (1962) Mineralogia y metalogenia de los yacimientos españoles de uranio: las pizarras uraniferas de la provincia de Salamanca, Est Geol 18, pp 155–172

Arribas A (1970) Las pizarras uraniferas de la provincia de Salamanca, Stud Geol, 1, pp 69–100

Arribas A (1975) Caracteres geologicos de los yacimientos españoles de uranio, Stud Geol, 9, pp 7–63

Arribas A (1978) Mineral paragenesis in the Variscan metallogeny of Spain, Stud Geol, 14, pp 223–260

Arribas A (1986) Sobre el origen de los yacimientos filonianos de uranio en rocas metasedimentarias: el caso de Mina Fé, Salamanca (España), *in*: Vein-type uranium deposits, TECDOC-361, IAEA, Vienna, pp 211–232

Arribas A, Martin-Izard A, Montes J (1983) Las mineralizaciones de uranio de la zona de Alameda de Gardón y su posición en el contexto geotectónico de las pizarras del Oeste de la provincia de Salamanca, VIII Reun Geol Oest Penins, Stud Geol, manusc

Arribas A, Martin-Izard A, Montes J (1984) Distribución geoquímica del uranio en los metasedimentos del CXG del Oeste de la provincia de Sala-manca, VII Congr Int Min Met, Barcelona, I, pp 353–357

Artru P, Berville M, Moreau M, Tona F (1986) Geological Environment of the vein-type deposits in the Aphebian basement of the Carswell structure on the Athabasca Plateau (Northern Saskatchewan) – comparison with other deposits of the same type, *in*: Vein-type uranium deposits, TECDOC-361, IAEA, Vienna, pp 57–76

Ashley PM (1984) Sodic granitoids and felsic gneisses associated with uranium-thorium mineralisation, Crockers Well, South Australia, Mineral Deposita, v 19, pp 7–18

Aubrey WM (1986) The nature of the Dakota-Morrison boundary, southeastern San Juan basin, *in*: Turner-Peterson CE, Santos ES, Fishman NS, eds., A basin analysis case study – the Morrison Formation, Grants Uranium Region, New Mexico, Amer Ass Petrol Geol, Studies in Geology, no. 22, pp 93–104

Aumento F (1979) Distribution and evolution of uranium in the oceanic lithosphere, Philos Trans Royal Soc, London, A291, pp 423–431

Austin SR (1963) Alteration of Morrison sandstone, *in*: Kelley VC, ed., Geology and technology of the Grants Uranium Region, New Mex Bur Mines Mineral Res Mem 15, pp 38–44

Austin SR (1970) Some patterns of sulfur isotope distribution in uranium deposits, Wyoming Geol Ass, Earth Sci Bull, v 3, no. 2, pp 5–22

Austin SR (1980) Dissolution and authigenesis of feldspars, *in*: Rautman CA, ed., Geology and mineral technology of the Grants Uranium Region 1979, New Mex Bur Mines Mineral Res Mem 38, pp 107–115

Austin SR D'Andrea RF, Jr (1978) Sandstone-type uranium deposits, *in*: Mickle DG, Mathews GW, eds., Geologic characteristics of environments favorable for uranium deposits, US-DOE, GJBX-67(78), pp 87–120

Autran A, Guillot PL (1974) L'évolution orogénique et métamorphique du Limousin (Massif Central français) au Paléozoïque: relation entre les cycles calédoniens et varisques, *in*: La chaîne varisque d'Europe Moyenne et Occidentale, CNRS, Rennes, pp 211–226

Autran A, Lameyre J (1980) Les granitoïdes de France, *in*: Autran A, Dercourt J, ed., scientif, Evolutions géologiques de la France, Mém BRGM, no. 107

Avital Y, Starinsky A, Kolodny Y (1983) Uranium geochemistry and fission-track mapping of phosphorites, Zefa Field, Israel, Econ Geol, v 78, pp 121–131

Avrashov A (1980) Albitized uranium deposits: Six articles translated from Russian literature, US-DOE, GJBX-193(80), 114 p

Ayres DE, Eadington PJ (1975) Uranium mineralization in the South Alligator River Valley, Mineral Deposita, 10, pp 27–42

Baadsgaard H, Cumming GL, Worden JM (1984) U-Pb geochronology of minerals from Midwest uranium deposit, northern Saskatchewan, Can J Earth Sci, v 21, pp 642–648

Babanek F (1884) Über die Erzführung der Joachimsthaler Gänge, Öster Zeitschr f Berg- und Hüttenwesen, Jg XXXII, no. 1, pp 21–24 and 61–62

Bailey JC, Larsen LM, Sørensen H, eds. (1981) The Ilímaussaq intrusion, South Greenland. A progress report on geology, mineralogy, geochemistry and economic geology, Geol Surv Greenl, Copenhagen, Rep 103, pp 1–130

Bailey JC, Rose-Hansen J, Løvborg L, Sørensen H, (1981) Evolution of Th and U whole-rock contents in the Ilímaussaq intrusion, Rapp Grønlands geol Unders 103, 87 p

Bailey RV (1965) Applied geology in the Shirley Basin uranium district, Wyoming, Wyoming Univ, Contribut Geology, v 4, pp 27–35

Bailey RV (1969) Uranium deposits in the Great Divide Basin-Crooks Gap area, Fremont and Sweetwater Counties, Wyoming, Wyoming Univ, Contrib Geology, v 8, pp 105–120

Bailey RV (1980) Comments on Shirley Basin uranium deposits and on the ages of all Wyoming uranium deposits in Eocene host rocks, *in*: Third annual uranium seminar, New York, Amer Inst Min Metal Petrol Eng, pp 41–59

Bailey RV, Childers MO (1977) Applied mineral exploration with special reference to uranium, Westview Press, Golden, 542 p

Baillieul TA, Zollinger RC (1982) National uranium resource evaluation, Grand Canyon quadrangle, Arizona, PGJ-020, 41 p

Baird CW, Martin KW, Lowy RM, (1980) Comparison of the braided stream depositional environment and uranium deposits at the Saint Anthony underground mine, New Mex Bur Mines Mineral Res Mem 38, pp 292–298

Baker ET, Jr (1979) Stratigraphic and hydrogeologic framework of part of the coastal plain of Texas, Texas Dep Water Res Rep 236, 43 p

Ball TK, Basham IR (1979) Radioactive accessory minerals in granites from South West England, Proc Usher Soc, 44(Part 3), pp 437–448

Ballhorn RK, Thakur VK, Da Fonte JEC, Suckav V (1981) Geology of the Espinharas uranium deposit, Brazil, *in*: Uranium deposits in Latin America; geology and exploration, IAEA, Vienna, pp 521–532

Banaś M, Mochnacka K (1986) The two uranium deposits in the Polish part of the Sudeten Mountains, *in*: Vein-type uranium Deposits, TECDOC-361, IAEA, Vienna, pp 335–358

Banaś M, Mochnacka K (1989) Genetic types of uranium mineralization of Poland and their metallogenic relationships, *in*: Metallogenesis of uranium deposits, IAEA, Vienna, pp 187–200

Barbey P, Cuney M (1982) K, Rb, Sr, Ba, U and Th geochemistry of the Lapland granulites (Fennoscandia). LILE fractionation controlling factors, Contrib Miner Petrol 81, pp. 304–316

Barbier J (1974) Continental weathering as a possible origin of vein-type uranium deposits, Mineral Deposita, 9, pp 271–288

Barbier J, Baubron JC, Bosch B, Briot P, Jacob C (1980) Données préliminaires sur les isotopes du soufre dans les calcrétes uranifères, un exemple dans la Province de Mudugh (Somalie), CR Acad Sci Paris, D, 290, pp 1047–1050

Barbier J, Carrat HG, Ranchin G (1967) Presence d'uraninite en tant que mineral accessoire usuel dans les granites à deux micas uranifères du Limousin et de la Vendée, CR Acad Sci Paris Ser D, v 264, pp 2436–2439

Barbier J, Ranchin G (1969a) Zonalité pétrographique et géochimique dans le massif granitique de St. Sylvestre, *in*: Géologie de l'uranium dans le massif granitique de St. Sylvestre (Limousin/Massif Central français), Sci Terre, Mem 15, pp 59–113

Barbier J, Ranchin G (1969b) Geochimie de l'uranium dans le massif de Saint-Sylvestre (Limousin, Massif Central francais); occurrences de l'uranium geochimique primaire et processus de remaniements, Sci Terre, Mem 15, pp 115–157

Barbier J, Ranchin G (1969c) Influence de l'altération météorique sur l'uranium à l'état de traces dans le granite à deux micas de St. Sylvestre, Geochim Cosmochim Acta, 33, pp 39–47

Barretto PMC (1985) Sedimentary and tectonic environments for uranium mineralization in the Paraná Basin, Brazil, *in*: Geological environments of sandstone-type uranium deposits, TECDOC-328, IAEA, Vienna, pp 173–195

Barretto P (1988) The identification of uranium provinces in Brazil, *in*: Recognition of uranium provinces, IAEA, Vienna, pp 371–401

Barrington J, Kerr PF (1963) Collapse features and silica plugs near Cameron, Arizona, Geol Soc Am Bull, v 74, pp 1237–1258

Barros RF (1966) O jazigo da Senhora das Fontes, Com Serv Geol Portugal 50, pp 110–129

Barthel FH (1974) Review of U occurrences in Permian

sediments in Europe with special reference to U mineralization in Permian sandstone, *in*: Formation of uranium ore deposits, IAEA, Vienna, pp 277–290
Barthel F, Dahlkamp FJ, Fuchs H, Gatzweiler R (1986) Kernenergierohstoffe, *in*: Bender F, ed., Angewandte Geowissenschaften, Ferd Enke Verlag, Stuttgart, pp 268–298
Barthel F, Hahn L (1985) Sedimentary uranium occurrences in Eastern Europe with special reference to sandstone formations, *in*: Geological environments of sandstone-type uranium deposits, TECDOC-328, IAEA, Vienna, pp 51–68
Barthel F, Mehnert KR (1970) Die Verteilung von Uran und Thorium im Malsburger Granit, NJb Miner, Abh 114, pp 18–47
Basham IR, Ball TK, Beddoe-Stephens B, Michie, UMcL (1982a) Uranium-bearing accessory minerals and granite fertility: II Studies of granites from the British Isles, *in*: Uranium exploration methods, OECD-NEA, Paris, pp 385–413
Basham IR, Bowles JFW, Atkin D, Bland DJ (1982b) Mineralogy of uranium distribution in samples of unaltered and sericitized granite from Urgeiriça, Portugal, in relation to mineralization processes, *in*: Vein-type and similar uranium deposits in rocks younger than Proterozoic, IAEA, Vienna, pp 299–309
Basham IR, Vairinho MMB, Bowles JFW (1982c) Uranium-bearing accessory minerals in the Sao Pedro do Sul Granite, Portugal, *in*: Vein-type and similar uranium deposits in rocks younger than Proterozoic, IAEA, Vienna, pp 279–298
Basham IR, Matos Dias JM (1986) Uranium veins in Portugal, *in*: Vein type uranium deposits, TECDOC-361, IAEA, Vienna, pp 181–192
Batashov BG, Onoprienko ME, Kudlaev AR (1984) The Zheltorechenskoe uranium deposit, 27th, Intern Geol Congr, Abstracts, Vol. IX, Part 1, Moscow, pp 330–332
Battey GC, Miezitis Y, McKay AD (1987) Australian uranium resources, BMR, Geology and Geophysics, Resource Rep 1, Canberra, 69 p
Baud L (1967) Carte des minéralisations de la République Gabonaise, Feuille Franceville-Ouest: Libreville, unpublished map
Baumann L (1967) Zur Frage der varistischen und postvaristischen Mineralisation im sächsischen Erzgebirge, Freiberger Forschungshefte, C 209, pp 15–38
Baumann L, Krs M (1966) Paläomagnetische Altersbestimmungen an einigen Mineralparagenesen des Freiberger Lagerstättenbezirkes, Geologie H. 6
Baur ME (1978) Thermodynamics of heterogeneous iron-carbon systems: Implications for the terrestrial primitive reducing atmosphere, Chem Geol, v 22, pp 189–206
Beck LS (1969) Uranium deposits of the Athabasca region, Saskatchewan, Sask Dep Miner Resour Rep 126, 139 p
Beck LS (1970) Genesis of uranium in the Athabasca region and its signification in exploration, CIM Trans, v 73, pp 59–69
Beck LS (1986) General geology and uranium deposits of the Beaverlodge district, *in*: Evans EL, ed., Uranium deposits of Canada, CIM Spec Vol. 33, pp 85–96
Beeson R (1978) The geochemistry of surface uranium mineralization in the south west Karoo basin, S Afr Geol Surv Rep 75, 12 p
Bejenaru C, Bobe M, (1991) Some aspects regarding the uranium geological survey in Romania: Technical committee meeting on new developments in uranium exploration, resources, production and demand, August 1991, IAEA, Vienna, manuscript 4 p
Belevtsev YN (1980) Endogenic uranium deposits of Precambrian shields: environment of formation, *in*: Albitized uranium deposits, six articles translated from Russian literature, US-DOE, GJBX-193(80), pp 55–80
Belevtsev YN, Batashov BG, Koval VB (1984a) The Zholtye Vody uranium deposit and the iron ore deposits of Krivoi Rog, 27th Intern Geol Congr, Guidebook, Excursion 108, Moscow, pp 21–32
Belevtsev YN, Koval VB, Stryghin AI (1984b) Genetic pattern for the deposits of uranium-albitite formation, (Symposium: Metallogenesis and Uranium Deposits) 27th Intern Geol Congr, Abstracts, Vol. IX, Part 1, Moscow, pp 332–333
Bell KG (1963) Uranium in carbonate rocks. US Geol Surv Paper 474-A, 29 p
Bell, K (1981) A review of the geochronology of the Precambrian of Saskatchewan – some clues to uranium mineralization, Miner Mag, v 44, pp 371–378
Bell K (1985) Geochronology of the Carswell area, Northern Saskatchewan, *in*: Lainé R, Alonso D, Svab M, eds., The Carswell structure uranium deposits, Saskatchewan, Geol Ass Can Spec Paper 29, pp 33–46
Bell K, Blenkinsop J (1980) Saskatchewan geochronology project, *in*: Summary of investigations 1980, Sask Geol Surv Misc Rep 80–4, p 18
Bell K, Blenkinsop J (1982) Saskatchewan shield geochronology project, *in*: Summary of investigations 1982, Sask Geol Surv Misc Rep 82–4, p 16
Bell K, Macdonald R (1982) Geochronological calibration of the Precambrian shield in Saskatchewan, *in*: Summary of investigations 1982, Sask Geol Surv Misc Rep 82–4, pp 17–22
Bell RT (1970) The Hurwitz Group – a prototype for deposition on metastable cratons, Geol Surv Can Paper 70–40, pp 159–168
Bell RT (1978) Uranium in black shales: a review; *in*: Kimberley MM, ed., Short course in uranium deposits: their mineralogy and origin, Miner Ass Can, Short Course Handbook no. 3, pp 207–329
Bell RT (1985) Overview of uranium in volcanic rocks of the Canadian Cordillera, *in*: Uranium deposits in volcanic rocks, IAEA, Vienna, pp 319–336
Bell RT (1987) A conceptual model for development of megabreccias and associated mineral deposits in Wernecke Mountains, Canada, Copperbelt, Zaire and Flinders Range, Australia, *in*: Uranium resources and geology of North America, TECDOC-500, IAEA, Vienna, pp 149–170
Bell TE (1986) Deposition and diagenesis in the Brushy Basin Member and upper part of the Westwater Canyon Member of the Morrison Formation, San Juan basin, New Mexico, *in*: Turner-Peterson CE, Santos, ES, Fishman NS, (eds.), A basin analysis case study – the Morrison Formation, Grants Uranium Region, New Mexico, Amer Ass Petrol Geol, Studies in Geology, no. 22, pp 77–91
Bellière J (1961) Manifestations metamorphiques dans la region d'Elisabethville, Pub Etat d'Elisabethville, Katanga, pp 175–179
Bellon H, Devillers C, Hagemann R, Touray J-C (1976) Dater les Minéralisations, Mém Soc Géol France, no. 7, pp 265–268
Berezina LA, Goleva RV, Zheleznova EI (1976) Content

and distribution of uranium in minerals from an ultrametamorphic complex and from uraniferous sodium metasomatites, Geochem Intern, 13, no. 6, pp 41–50; Geokhimiya, no. 11, pp 1673–1682

Berggren WA, Van Couvering JA (1974) The late Neogene: Biostratigraphy, geochronology and paleoclimatology of the last 15 million years in marine and continental sequences, Palaeogeography, Palaeoclimatology, Palaeoecology, v 16, no. 1/2, 216 p

Berkman DA (1968) The geology of the Rum Jungle uranium deposits, *in*: Uranium in Australia, AIMM Symposium, pp 12–31

Berkman DA, Fraser WJ (1980) The Mount Fitch copper and uranium deposits, Rum Jungle Uranium Field, NT Australia, *in*: Ferguson J, Goleby AB, eds., Uranium in the Pine Creek Geosyncline, IAEA, Vienna, pp 343–350

Berman ER (1955) Unit cell dimensions of uraninite, Amer Miner, v 40, pp 925–927

Berman RM (1957) The role of lead and excess oxygen in uraninite, Amer Miner, v 42, pp 705–731

Bernard JH et al. (1967) Hydrothermal ore deposits of the Bohemian massif, *in*: Guide to excursion, 23rd Intern Congr (1968), Prague

Bernard JH, Dudek A (1967) Sur le magmatisme et les mineralisations hydrothermales du Massif de Bohème, Mineral Deposita, v 2, pp 63–79

Bernard-Griffiths J, Peucat JJ, Sheppard SMF, Vidal Ph (1985) Petrogenesis of Hercynian leucogranites from the Southern Armorican massif: Contribution of REE and isotopic (Sr, Nd, Pb and O) geochemical data to the study of source rocks characteristics and ages, Earth Planet Sci Lett, 74, pp 235–250

Bernazeaud J (1959) Premières données sur le gisement d'uranium de Mounana, Chron Mines Outre-Mer Rech Minière, v 27, pp 315–318

Berning J (1986) The Rössing uranium deposit, South West Africa/Namibia, *in*: Anhaeusser CR, Maske S, Mineral deposits of Southern Africa, Geol Soc S Afr, v 2, pp 1819–1832

Berning J, Cooke R, Hiemstra SA (1976) The Rössing uranium deposit, SWA, Econ Geol, v 71, pp 351–368

Berthelin J, Munier-Lamy C (1983) Microbial mobilization and preconcentration of uranium from various rock materials by Fungi, *in*: Hallberg R, ed., Environmental biogeochemistry, Ecol Bull (Stockholm) 35, pp 395–401

Berthelin J, Gueniot B, Munier-Lamy C, Poty B, Souchier B, Guillet G (1984) Distribution et sites de fixation de l'uranium dans les sols: application à la prospection, Documents BRGM, no. 79, pp 127–147

Berzina IG, et al. (1967) Determining the concentration of uranium and its manner of distribution in minerals and rocks, Sov Atomic Energy (Trans). v 23, pp 1288–1297

Berzina IG, Korpova MI, Kharitonova RS (1976) Uranium distribution in nodular platform phosphorites, Lithol Miner Res, v 11, no. 2, pp 215–222

Berzina IG, Yeliseyeva OP, Popenko DP (1974) Distribution relationships of uranium in intrusive rocks of northern Kazakhstan, Intern Geol Rev, v 16, pp 1191–1204

Betekhtin AG (1959) Exogenic processes of formation of uranium deposits: Geologiya Rudn Mestorozh, no. 6, pp 5–26/Econ Geol, v 56, pp 1156–1157

Bettenay E, Smith RE, Butt CRM (1976) Physical features of the Yilgarn Block, *in*: Excursion guide No.-41C, 25th Intern Geol Congr, pp 5–11

Beus AA, Zalashkova NY (1964) Post-magmatic high temperature metasomatic processes in granitic rocks, Intern Geol Rev, v 6, no. 4, pp 668–680

Bickford ME, Van Schmus WR, MacDonald R, Lewry JF, Pearson JG (1986) U-Pb zircon geochronology project for the Trans-Hudson Orogen: current sampling and recent results, *in*: Summary of investigations, 1986, Sask Geol Surv, pp 101–107

Billingsley GH (1978) A synopsis of stratigraphy in the Western Grand Canyon, Museum Northern Arizona, Res Paper 16, 26 p

Billingsley GH, Wenrich KJ, Huntoon PW (1986) Breccia pipe and geologic map of the southeastern Hualapai Indian Reservation and vicinity, Arizona, US Geol Surv Rep 86–458B, 26 p

Binns RA, Ayres DE, Wilmshurst JR, Ramsden AR (1980a) Petrology and geochemistry of alteration association with uranium mineralization at Jabiluka NT, Australia, *in*: Ferguson J, Goleby AB eds., Uranium in the Pine Creek Geosyncline, IAEA, Vienna, pp 417–438

Binns R, McAndrew J, Sun S-S (1980b) Origin of uranium mineralization at Jabiluka, *in*: Ferguson J, Goleby A, eds., Uranium in the Pine Creek Geosyncline, IAEA, Vienna, pp 543–562

Bird AG (1958) The petrology and ore deposits of the Schwartzwalder uranium mine, Jefferson County, Colorado, Univ Colorado, Boulder unpubl Master's thesis

Bird AG (1979) An epigenetic model for the formation of the Schwartzwalder uranium deposit – a discussion, Econ Geol, v 74, pp 947–948

Birdseye HS (1957) The relation of the Ambrosia Lake uranium deposits to a pre-existing oil pool, *in*: Geology of Southwestern San Juan basin. Four Corners Geol Soc, Second Field Conf, pp 26–29

Blaise JR, Koning E (1985) Mineralogical and structural aspects of the Dominique-Peter uranium deposit, *in*: Lainé R, Alonso D, Svab M, eds., The Carswell structure uranium deposits, Saskatchewan, Geol Ass Can Spec Paper 29, pp 139–152

Blenkinsop J, Bell K (1981) Saskatchewan shield geochronology project, *in*: Summary of investigations (1981) Sask Geol Surv Misc Rep 81–4, pp 25–44

Boenig CM (1970) Deltaic and coastal interdeltaic environments of the Carrizo Formation (Eocene), Milam County, Texas, Texas A&M Univ Master's thesis, 104 p

Boguslavsky JS, Kalenov AD, Egel LY (1966) Metasomatic albitites found for the first time in the MPR, Doklady Akad Nauk SSSR, 168, 5, pp 1154–1157

Bohn RT (1977) A subsurface correlation of Permian-Triassic strata in Lisbon Valley, Utah, Brigham Young Univ Geol Studies, v 24, part 2, pp 103–116

Bohse H, Rose-Hansen J, Sørensen H, Steenfelt A, Løvborg L, Kunzendorf H (1974) On the behaviour of uranium during crystallization of magmas – with special emphasis on alkaline magmas, *in*: Formation of uranium ore deposits, IAEA, Vienna, pp 49–60

Boitsov EV (1966) Association of pitchblende and selenides in ore of hydrothermal uranium deposits, Atomnaya Energiga 20, pp 46–50

Boitsov VE, Legierski Y (1977) Sequence and time of mineralization on certain hydrothermal uranium deposits, Geologiya rudnykh mestorozhdenij, v XIX, no. 1, pp 39–50 (in Russian)

Bomber BJ, Ledger EB, Tieh TT (1980) Textural study of

a sedimentary uranium deposit in south Texas, Geol Soc Am Annual Meeting, Atlanta, Georgia, Abstracts with programs, p 389
Bomber BJ, Ledger EB, Tieh TT (1986) Ore petrography of a sedimentary uranium deposit, Live Oak County, Texas, Econ Geol, v 81, pp 131–142
Bone Y (1983) Interpretation of magnesite at Rum Jungle, NT, using fluid inclusions, J Geol Soc Australia, v 30, pp 375–381
Bonhomme M, Weber F (1969) Compléments à la géochronologie du Bassin de Franceville et de son environnement (République Gabonaise), Annales Faculté Sci Univ Clermont-Ferrand, no. 41, pt. 19, pp 85–88
Bonhomme M, Weber F, Favre-Mercuret R (1965) Âge par la méthode rubidium-strontium des sédiments du Bassin de Franceville (République Gabonaise), Bull Serv Carte Géol Alsace-Lorraine, no. 18, pp 243–252
Bonin B (1982) Les granites des complexes annulaires, BRGM Manuals et Methodes, v 4, 183 p
Bonner JA, Herold CE, Nibbelink KA (1982) Uranium in the marginal marine depositional system, 111 AIME Annual Meeting, Dallas, Tx, manuscript, 9 p
Borodin LS, Pavlenko AS (1974) The role of metasomatic processes in the formation of alkaline rocks, *in*: Sörensen H, ed., The alkaline rocks, Wiley, London, pp 515–534
Bostock HH (1987) Geology of the south half of the Taltson Lake map area, District of MacKenzie, *in*: Current research, Part A, Geol Surv Can Paper 87-1A, pp 443–450
Botinelly T, Weeks AD (1957) Mineralogic classification of uranium-vanadium deposits of the Colorado Plateau, US Geol Surv Bull 1074-A, pp 1–5
Bottrill TJ (1971) Uraniferous conglomerates of the Canadian Shield, *in*: Report of activities, Geol Surv Can Paper 71-1, pt. A, pp 77–83
Bouchez JL (1989) Fine scale structures and discontinuities in granitoid rocks: their potential importance for primary concentration of uranium, *in*: Metallogenesis of uranium deposits, IAEA, Vienna, pp 115–117
Bourrel J, Pfiffelmann J-P (1972) La province uranifère du Bassin de Franceville (République Gabonaise), Mineral Deposita, 7, pp 323–336
Bourret W (1975) Investigation of Witwatersrand uranium bearing quartz-pebble conglomerates in 1944–45, Armstrong FC, ed., Genesis of uranium- and gold-bearing Precambrian quartz-pebble conglomerates, US Geol Surv Prof Paper 1161-A-BB, pp A1–17
Boutwell JM (1905) Vanadium and uranium in southeastern Utah, US Geol Surv Bull 260
Bowers HE, Shawe DR (1961) Heavy minerals as guides to uranium-vanadium ore deposits in the Slick Rock district, Colorado, US Geol Surv Bull 1107-B, pp 169–218
Bowie SHU (1977) Uranium distribution and availability, *in*: Geol min extr process uranium, IMM, London, pp 76–82
Bowie SHU (1979) The mode of occurrence and distribution of uranium deposits, Royal Soc London, pp 35–46
Bowie SHU, Davis M, Ostle D, eds. (1972) Uranium prospecting handbook, IMM, London, 346 p
Bowles CG (1965) Uranium-bearing pipe formed by solution and collapse of limestone, US Geol Surv Prof Paper 525-A, pp 25–27
Bowles CG (1977) Economic implications of a new hypothesis of origin of uranium- and copper-bearing breccia pipes, Grand Canyon, Arizona, *in*: Campbell J, ed., Short papers of the US geol surv uranium and thorium symposium, US Geol Surv Circ 753, pp 25–27
Bowman EC, Cygan NE, Alief MH (1981) Exploration of the Pana Maria uranium mine, Karnes County, Texas, USA, *in*: Uranium exploration case histories, IAEA, Vienna, pp 311–327
Boyden T (1978) Uranium occurrences in breccia pipes, NUEXCO, Rep 123, pp 2.0–2.2
Boyer WH (1956) Geologic reconnaissance of the northwest White River US-AEC, RME-90, 46 p
Boyer RL, Naudet R, Pfiffelmann J-P (1975) Exploration des foyers de réaction, *in*: The Oklo phenomenon, IAEA, Vienna, pp 67–81
Boyle DR (1982b) The formation of basal-type uranium deposits in south central British Columbia, Econ Geol, v 77, pp 1176–1209
Boyle DR (1984) The genesis of surficial uranium deposits, *in*: Surficial uranium deposits, TECDOC-322, IAEA, Vienna, pp 45–52
Boyle DR (1985) Geologic environments for basal-type uranium deposits in sedimentary host rocks, *in*: Geological environments of sandstone-type uranium deposits, TECDOC-328, IAEA, Vienna, pp 363–382
Boyle DR (1986) Basal type uranium deposits in south central British Columbia, *in*: Evans EL, ed., Uranium deposits of Canada, CIM Spec Vol. 33, pp 309–320
Boyle DR (1989) The formation of infiltration-type uranium deposits associated with granitic and metamorphic basement complexes: exploration guidelines, (abstr), *in*: Uranium resources and geology of North America, TECDOC-500, IAEA, Vienna, p 171
Boyle RW (1979) The geochemistry of gold and its deposits. Geol Surv Can Bull 280, 584 p
Boyle RW (1982a) Geochemical prospecting for thorium and uranium deposits, Elsevier-Scientific Publ Co, Amsterdam-Oxford-New York, 498 p
Branche G, Chantret F, Guillemaut A, Pouget R (1975) Données chimiques et minéralogiques sur le gisement d'Oklo, *in*: The Oklo phenomenon, IAEA, Vienna, pp 119–131
Braun R (1974) Etude des hamadas de la dorsale Reguibat Région d'Ain Ben Tili (Rep Mauritanie), Rapport DEA Faculté St Jérome-Marseille, 67 p
Bray CJ, Spooner ETC, Golightly JP, Saracoglu N (1982) Carbon and sulphur isotope geochemistry of unconformity-related uranium mineralization, McClean Lake deposit, N Saskatchewan, Canada: Geol Soc Am, Abstracts with Program, v 14, p 451
Bray CJ, Spooner ETC, Longstaffe F (1984) Oxygen and hydrogen isotope geochemistry of unconformity-related uranium mineralization, McClean deposits, N Saskatchewan, Canada, Geol Ass Can, Miner Ass Can, Program with Abstracts, v 9, p 48
Bray CJ, Spooner ETC, Hall CM, York D, Bills TM, Krueger HW (1987) Laser probe $^{40}Ar/^{39}Ar$ and conventional K/Ar dating of illites associated with the McClean unconformity-related uranium deposits, north Saskatchewan, Canada, Can J Earth Sci, v 24, pp 10–23
Bray CJ, Spooner ETC, Longstaffe F (1988) Unconformity-related uranium mineralization, McClean deposits, north Saskatchewan, Canada: Hydrogen and oxygen isotope geochemistry, Can Miner, v 26, Pt. 2, pp 249–282
Breed WJ, Roat EC, eds. (1976) Geology of the Grand Canyon, Museum Northern Arizona, 186 p

Breger IA (1974) The role of organic matter in the accumulation of uranium: The organic geochemistry of the coal-uranium association, *in*: Formation of uranium ore deposits, IAEA, Vienna, pp 99–124

Breit GN, Goldhaber M (1983) Relationship of authigenic minerals to the V-U and Cu mineralization of the Salt Wash Member of the Morrison Formation, San Miguel County, Colorado; Geol Soc Amer, Rocky Mtns Cordilleran Sections, Abstract with Program, p 399

Breit GN, Goldhaber MB (1989) Hematite-cemented sandstones and chromium-rich clays – clues to the origin of vanadium-uranium deposits in the Morrison Formation, southwest Colorado and southeast Utah, United States, *in*: Uranium resources and geology of North America, TECDOC-500, IAEA, Vienna, pp 201–225

Brewton JL (1970) Heavy mineral distribution in the Carrizo Formation (Eocene), east Texas, Univ Texas, Austin, PhD diss, 167 p

Briot P (1978) Phénomènes de concentration de l'uranium dans les environs évaporitiques intercontinentaux: les calcrétes de l'Yilgarn Australien. Essai de comparaison avec les calcrétes de Mauritanie et de Namibie, Thèse Orsay, 167 p

Briot P (1982) Sur la genèse de certaines gîtes uranifères, Mineral Deposita, v 17, pp 151–157

Briot P (1983) Géologie et géochimie des gisements d'uranium liés aux milieux pré-évaporitiques intracontinentaux: les calcrétes uranifères, Thèse d'Etat, Paris, France, 216 p

Briot P, Fuchs Y (1984) Processus de minéralisation uranifères des calcrétes: une hypothèse non pédologique, *in*: Surficial uranium deposits, TECDOC-322 IAEA, Vienna, pp 15–24

Briqueu L, Lancelot JR, Valois JP, Walgenwitz F (1980) Géochronologie U-Pb et genèse d'un type de minéralisation uranifère: les alaskites de Goanikontes (Namibie) et leur encaissant, Bull Cent Rech Explor Prod Elf-Aquitaine 4, pp 759–811

Brock BB, Pretorius DA (1964) Rand Basin sedimentation and tectonics, *in*: Haughton SH, ed., The geology of some ore deposits in southern Africa, Geol Soc S Afr, v 1, pp 549–600

Brögger WC (1920) Die Eruptivgesteine des Kristianiagebietes IV, Das Fengebiet in Telemark, Vid Selsk Skr Math -nat Kl 9, pp 150–167

Brooker EJ, Nuffield EW (1952) Studies of radioactive compounds: IV – Pitchblende from Lake Athabasca, Amer Min, v 37, pp 363–385

Brookins DG (1975) Coffinite-uraninite stability relations in Grants Mineral Belt, New Mexico, (abst.), Amer Ass Petrol Geol Bull, v 59, no. 5, p 905

Brookins DG (1976) Position of uraninite and/or coffinite accumulations to the hematite-pyrite interface in sandstone-type deposits, Econ Geol, v 71, pp 944–948

Brookins DG (1979) Uranium deposits of the Grants, New Mexico mineral belt (II) US-DOE GJBX-141(79), 411 p

Brookins DG (1980a) Geochemical and clay mineralogical studies, Grants mineral belt (abstract), *in*: Rautman CA, ed., Geology and mineral technology of the Grants Uranium Region 1979, New Mex Bur Mines Mineral Res Mem 38, p 396

Brookins DG (1980b) Geochronologic studies in the Grants Mineral Belt, *in*: Rautman CA, ed., Geology and mineral technology of the Grants Uranium Region 1979, New Mex Bur Mines Mineral Res Mem. 38, pp 52–58

Brookins DG, Lee MJ, Riese WC (1977) Trace elements as possible prospecting tools for uranium in the southern San Juan Basin, New Mex Geol Soc, Guidebook, 28th Field Conf, San Juan Basin III, pp 263–269

Brooks RA, Campbell JA (1976) Preliminary investigation of the elemental variation and diagenesis of a tabular uranium deposit, La Sal mine, San Juan County, Utah. US Geol Surv Rep 76–287, 30 p

Brooks RA, Perry RV, Rackley RI (1978) New model for some Colorado Plateau uranium deposits (abstr), Am Ass Petrol Geol Bull, v 62, no. 6, pp 1091–1092

Bryant B, Naeser CW (1980) The significance of fission-track ages of apatite in relation to the tectonic history of the Front and Sawatch Ranges, Colorado, Geol Soc Amer Bull, v 91, pp 156–164

Brynard HJ, Andreoli MAG (1988) The overview of the regional, geological and structural setting of the uraniferous granites of the Damara Orogen, Namibia, *in*: Recognition of uranium provinces, IAEA, Vienna, pp 195–212

Brynard HJ, Ainslie LC, van der Merwe PJ (1988) Uranium in South Africa-1987, AEC South Africa, Pretoria, 28 p

Buck SG (1983) The Saaiplaas Quartzite Member: a braided system of gold- and uranium-bearing channel placers within the Proterozoic Witwatersrand Supergroup of South Africa, *in*: Collinson JD, Lewin J, eds., Modern and ancient fluvial systems, Spec Pub Int Ass Sediment. 6, pp 549–562

Buck SG, Minter WEL (1985) Placer formation by fluvial degradation of an alluvial fan sequence: the Proterozoic Carbon Leader placer, Witwatersrand Supergroup, South Africa, J Geol Soc, London, v 142, pp 757–764

Buck SG, Minter WEL (1987) Paleocurrent and lithological facies control of uranium and gold mineralization in the Witwatersrand carbon leader placer, Carletonville Goldfield, South Africa, *in*: Uranium deposits in Proterozoic quartz-pebble conglomerates, TECDOC-427, IAEA, Vienna, pp 335–353

Bunker CM, MacKallor JA (1973) Geology of the oxidized uranium ore deposits of the Tordilla Hill-Deweesville area, Karnes County, Texas; a study of a district before mining, US Geol Surv Prof Paper 765, 37 p

Burger AJ, Coertze FJ (1973) Radiometric age measurements on rocks from southern Africa to the end of 1971, Rep S Afr, Geol Surv Bull 58, 46 p

Burger AJ, Nicolaysen LO, De Villiers JWL (1962) Lead isotopic compositions of galenas from the Witwatersrand and Orange Free State, and their relation to the Witwatersrand and Dominion Reef uraninites, Geochim Cosmochim Acta, v 26, pp 25–59

Burgess JW, Alieff MH, Winsor DK, Lewis LE (1987) Mount Taylor uranium project, unpubl manuscript, 18 p

Burke K, Kidd WSF, Kuskey TM (1986) Archean foreland basin tectonics in the Witwatersrand, South Africa, Tectonics, v 5, no. 3, pp 429–456

Burnol L (1973) Géochimie du béryllium et types de concentration dans les leucogranites du Massif Central français, Mém. BRGM, Paris, no. 85, 168 p

Burt DM, Sheridan MF (1980) A model for the formation of uranium/lithophile element deposits in fluorine-enriched volcanic rocks. *In*: Burt DM, Sheridan MF,

eds., Uranium mineralization in fluorine-enriched volcanic rocks, US-DOE, GJBX-225(80), pp 1–36
Burt DM, Sheridan MF (1985) Relation of topaz rhyolite volcanism to uranium mineralization in the western United States of America, *in*: Uranium deposits in volcanic rocks, IAEA, Vienna, pp 337–344
Burwash RA, Cumming GL (1976) Uranium and thorium in the Precambrian basement of western Canada. I. Abundance and distribution, Can J Earth Sci, v 13, pp 284–293. II Petrologic and tectonic controls, ibid v 16, pp 472–483
Burwash RA, Baadsgaard H, Peterman ZE (1962) Precambrian K-Ar Dates from the Western Canada Sedimentary Basin, J Geophys Res 67–4, pp 1617–1625
Burwash RA, Krupicka J, Basu AR, Wagner PA (1985) Resetting of Nd and Sr whole-rock isochrons from polymetamorphic granulites, northeastern Alberta, Can J Earth Sci, v 22, no. 7, pp 992–1000
Burwell B (1920) Carnotite mining in southwestern Colorado, Eng Min J,v 110, no. 16, pp 755–758
Busche FD, Goldhaber MB, Reynolds RL (1981) Fault leaked H_2S and the origin of south Texas uranium deposits: Implications of sulfur isotopic studies, (abstr), Geol Soc Am, Abstracts with Programs, v 13, p 234
Butler AP (1975) U and Th in rocks of White Mountains plutonic series, New Hampshire, and chemical analyses of selected samples, US Geol Surv Rep 75–59, 15 p
Butler AP, Jr, Fischer RP (1978) Uranium and vanadium resources in the Moab 1° × 2° Quadrangle, Utah and Colorado, US Geol Surv Prof Paper 988-B, pp B1–B22
Butler BS, Loughlin GF, Heikes VC (1920) The ore deposits of Utah, US Geol Surv Prof Paper 111, 672 p
Butt CRM (1988) Major uranium provinces: Yilgarn Block and Gascoyne Province, Western Australia, *in*: Recognition of uranium provinces, IAEA, Vienna, pp 273–304
Butt CRM, Cole MJ (1984) Helium determinations in mineral exploration. Aust Dep Resources Energy Rep NERDDP/EG/84/271, 351 p
Butt CRM, Mann AW (1984) Surficial uranium deposits in Australia, *in*: Surficial uranium deposits, TECDOC-322, IAEA, Vienna, p 119
Butt CRM, Horwitz RC, Mann AW (1977) Uranium occurrences in calcrete and associated sediments in Western Australia. CSIRO Res Lab Rep FP16, 67 p
Butt CRM, Mann AW, Horwitz RC (1984) Regional setting, distribution and genesis of surficial uranium deposits in calcretes and associated sediments in Western Australia, *in*: Surficial uranium deposits, TECDOC-322, IAEA, Vienna, pp 121–127
Butt KA (1989a) Uranium occurrences in magmatic and metamorphic rocks of northern Pakistan, *in*: Uranium deposits in magmatic and metamorphic rocks, IAEA, Vienna, pp 131–154
Butt KA (1989b) Release of uranium through cataclastic deformation of Manehra granite gneiss and its precipitation in the overlying intramountain basin in northern Pakistan, *in*: Uranium deposits in magmatic and metamorphic rocks, IAEA, Vienna, pp 155–166
Button A (1968) Subsurface stratigraphic analysis of the Witwatersrand and Transvaal sequences in the Irene-Delmas-Devon area, Transvaal. Univ Witwatersrand, Johannesburg, unpubl MSc thesis, 120 p
Button A (1973) A regional study of the stratigraphy and development of the Transvaal Basin in the eastern and northeastern Transvaal, Univ Witwatersrand, Johannesburg, unpubl PhD diss 352 p
Button A (1976) Transvaal and Hamersley Basins – review of basin development and mineral deposits, Miner Sci Eng, v 8, pp 262–293
Button A, Adams SS (1981) Geology and recognition criteria for uranium deposits of the quartz-pebble conglomerate type, US-DOE, GJBX-3(81), 390 p
Button A, Tyler N (1979) Precambrian paleoweathering and erosion surfaces in southern Africa: Review of their character and economic significance, Univ Witwatersrand, Johannesburg, Econ. Geol Res Unit, Inform Circ 135, 37 p
Byers VP (1978) Principal uranium deposits of the world, US Geol Surv Rep 78-1008, 308 p
Byers VP, Finch WI (1979) Preliminary map of the uranium provinces in the conterminous United States, US Geol Surv Rep 79-756-V
Cadel G (1986) Geology and uranium mineralization of the Collio basin (central southern Alps, Italy), Uranium, 2, 215–240
Cadigan RA (1963) Tuffaceous sandstone in the Triassic Chinle Formation, Colorado Plateau, US Geol Surv Prof Paper 475-B, B48–B51
Cadigan RA (1967) Petrology of the Morrison Formation in the Colorado Plateau region, US Geol Surv Prof Paper 556, 113 p
Cahen L (1970) Etat actuel de la géochronologie du Katangien, Mus Royal Afrique Centre, Annales, Ser in 80, Sci Geol 65, pp 7–14
Cahen L (1974) Geological background to the copper-bearing strata of southern Shaba (Zaïre), *in*: Bartholomé P, ed., Gisements stratiformes et provinces cuprifères, Liège, Soc Géol Belgigue, pp 57–77
Cahen L, Pasteels P, Ledent D, Bourguillot R, Van Wambeke L, Eberhardt P (1961) Recherches sur l'âge absolu des minéralisations uranifères du Katanga et de Rodesie du Nord, Mus Royal Afrique Centre Annales, 41, pp 1–54
Cahen L, Francois A, Ledent D (1971) Sur l'âge des uraninites de Kambove ouest et de Kamoto principal et révision des connaissances relatives aux minéralisations uranifères du Katanga et du Copperbelt de Zambia, Soc Géol Belgique Annales, 94, pp 185–198
Cahen L, Snelling NJ, Delhal, J, Vail JR (1984) The geochronology and evolution of Africa, Oxford, Clarendon Press, 512 p
Calas G (1979) Étude expérimentale du comportement de l'uranium dans les magmas: efat d'oxydation et coordinance, Geochim Cosmochim Acta, 43, pp 1521–1531
Cameron E (1976) Uranium in a calcrete environment, Western Australia. 47th ANZAAS Congr, Hobart. Tasmania, (manuscript)
Cameron E (1984) The Yeelirrie calcrete uranium deposit, Western Australia, *in*: Surficial uranium deposits, TECDOC-322, IAEA, Vienna, pp 157–165
Cameron E, Fletcher CI (1976) Yeelirrie, *in*: Smith RE, Butt CRM, Bettenay E, eds., Superficial mineral deposits and exploration geochemistry, Yilgarn block, Western Australia, 25th Intern, Geol Congr Excursion Guide no. 41C, Sydney, pp 41–45
Cameron E, Mazzucchelli RH, Robbins TW (1980) Yeelirrie calcrete uranium deposit, Murchison Region, Western Australia, J Geochem Explor, 12, pp 350–353
Cameron EM, Garrels RM (1980) Geochemical composit-

ions of some Precambrian shales from the Canadian Shield, Chem Geol, v 28, pp 181–197
Cameron J (1959) Structure and origin of some uranium-bearing veins in Portugal, Tech Paper no. 22. JEN, Lisbon, 56 p
Cameron J (1970) The Alio Ghelle radioactive mineral occurrence in the Bur region of the Republic of Somalia, *in*: Uranium exploration geology, IAEA, Vienna, pp 169–175
Cameron J (1982a) Geomorphology and the uranium vein deposits of the Beira region of Portugal, *in*: Vein-type and similar uranium deposits in rocks younger than Proterozoic, IAEA, Vienna, pp 237–278
Cameron J (1982b) Mineralogical aspects and origin of the uranium in vein deposits of Portugal, *in*: Vein-type and similar uranium deposits in rocks younger than Proterozoic, IAEA, Vienna, pp 349–372
Cameron J, McKillen T, Wilpolt R,/IUREP (1980) International uranium resources evaluation project; Portugal, OECD-NEA, Paris, 116 p
Cameron-Schiman M (1978) Electron microprobe study of uranium minerals and its application to some Canadian deposits, PhD Thesis, Univ Alberta, 343 p
Camisani-Calzolari FAGM, Ainslie LC, Van Der Merwe PJ (1986) Uranium in South Africa (1985) AEC-S Afr, Pretoria, 27 p
Canada Wide Mines Ltd (1981) The Midwest uranium deposit, CIM, Geol Div Uranium Field Excursion Guidebook, pp 37–42
Capdevilar R, Corretge G, Floor P (1973) Les granitoïdes varisques de la Meseta Ibérique, Bull Soc géol Fr, XV, 3–4, pp 209–228
Card KD, Church WR, Franklin JM, Frarey MJ, Robertson JA, West, GF, Young GM (1972) The Southern Province, *in*: Price RA, Douglas RJW, eds., Variation in tectonic styles in Canada, Geol Ass Can Spec Paper 11, pp 335–380
Cariou P (1964) Les gites et indices uranifères des regions medianes et sud du Massif Central français, *in*: Roubault M, ed., Les minerals uranifères français, III PUF ed., Paris, pp 1–162
Carl C, Höhndorf AV, Pechmann E, Strnad JG, Ruhrmann G (1988) Geochronology of the Key Lake uranium deposit, Saskatchewan, Canada, Chem Geol, v 70, no. 1/2 p 133
Carlisle D (1980) Possible variations on the calcrete-gypcrete uranium model, US-DOE, GJBX-53(80), 38 p
Carlisle D (1983) Concentration of uranium and vanadium in calcretes and gypcretes, *in*: Wilson RCL, ed., Residual deposits: surface related weathering processes and materials, Geol Soc, London, pp 185–196
Carlisle D (1984) Surficial uranium occurrences in relation to climate and physical setting, *in*: Surficial uranium deposits, TECDOC-322, IAEA, Vienna, pp 25–35
Carlisle D, Merifield PM, Orme RR, Kohl MS, Kolker O (1978) The distribution of calcretes and gypcretes in southwestern United States and their uranium favourability based on a study of deposits in Western Australia and South West Africa (Namibia), US-DOE, GJBX-29(78), 274 p
Carlsson, D, Nojd LA (1977) Uranium production from Low-grade Swedish shale, Paper (IAEA-CN 36/277) pres to Intern Conf Nuclear Power and its Fuel Cycle, Salzburg, 12 p
Carpenter DJ (1980) Elemental, isotopic and mineralogic distributions within a tabular-type uranium-vanadium deposit, Henry Mountains mineral belt, Garfield County, Utah; unpub MS thesis, Colorado School Mines, Golden, 156 p
Carpenter RH, Gallagher JRL, Huber GG (1979) Modes of uranium occurrences in Colorado Front Range, Colo Sch Mines Quart, v 74, no. 3, 76 p
Carrat HG (1974) Tectonique tardihercynienne, magmatisme basique et mise en place des filons d'uranium dans le Massif Central francais. *In*: Réunion annuelle, sci terre (Pont à Mousson): programme et resumés, Soc Geol France, Paris p 99
Carter JD (1981) Uranium exploration in Western Australia, West Aust Geol Surv Rec 1981/6, 68 p (unpubl)
Carter WD, Gualtieri JL (1965) Geology and uranium-vanadium deposits of the La Sal quadrangle, San Juan County, Utah and Montrose County, Colorado, US Geol Surv Prof Paper 508, 82 p
Cathelineau M (1981a) Les gisements d'uranium liés spatialement aux leucogranites Sud Armoricains et à leur encaissant métamorphique, Sci Terre Mém, Nancy, no. 42, 475 p
Cathelineau M (1981b) Les gisements uranifères de la presqu'ile Guerandaise (Sud Bretagne), Approche structurale et metallogenique, Mineral Deposita, 16, pp 227–240
Cathelineau M (1982a) Les mécanismes de type 'roll-front' dans les granites, un modèle de remobilisation dans les gisements hydrothermaux d'uranium, CR Acad Sci Fr 294 II, pp 865–868
Cathelineau M (1982b) Signification de la fluoruine dans les gisements d'uranium de la chaine hercynienne, Bull BRGM II 4, pp 407–413
Cathelineau M (1983a) Potassic alteration in French hydrothermal uranium deposits, Mineral Deposita, 18, pp 89–97
Cathelineau M (1983b) Les minéraux phylliteux dans les gisements hydrothermaux d'uranium. I Distribution et évolution cristallochimique des illites interstratifiés, smectites et chlorites, Bull Miner 103, pp 553–569
Cathelineau M (1984) Uranium veins in western France, mineralogy and geochemistry of uranium deposition, *in*: Proceedings of ICAM 84 Congress, Los Angeles, TMS AIME, pp 1083–1094
Cathelineau M (1985) Minéralogie – Episyénitisation ou déquartzification hydrothermale: une typologie basée sur les successions minérales et sur le comportement différentiel le Si, Na et K, CRAS, t. 300, Série II, no. 14, pp 677–680
Cathelineau M (1986) The hydrothermal alkali metasomatism effects on granitic rocks: quartz dissolution and related subsolidus changes, J Petrol, v 27, Part 4, pp 945–965
Cathelineau M (1987) U, Th, REE mobility during albitization and quartz dissolution in granitoids: evidence from south-east French Massif Central, Bull Minér, v 110, pp 249–260
Cathelineau M, Leroy, J (1981) Reactions between uranium veins and their host rocks in Vendée and Limousin (France), Min Mag, 44, pp 417–423
Cathelineau M, Nieva D (1985) A chlorite solid solution geothermometer. The Los Azufres (Mexico) geothermal system, Contrib Mineral Petrol, 91, pp 235–244
Cathelineau M, Poty B (1989) U-Th-REE mobility in granitic environments at the hydrothermal stage, *in*:

Metallogenesis of uranium deposits, IAEA, Vienna, pp 63–78
Cathelineau M, Cuney M, Leroy J, Lhote F, Nguyen Trung C, Pagel M, Poty B (1982) Caractères minéralogiques des pechblendes de la province hercynienne d'Europe – Comparaison avec les oxydes d'uranium du protérozoique de différents gisements d'Amérique du Nord, d'Afrique et d'Australie. *in*: Vein-type and similar uranium deposits in rocks younger than Proterozoic, IAEA, Vienna, pp 159–177
Cathelineau M, Oliver R, Nieva D (1987) Geochemistry of volcanic series of the Los Azufres geothermal field (Mexico), Geol Interp, v 26, no. 2, pp 273–290
Cathelineau M, Oliver R, Nieva D, Garfias A (1985) Mineralogy and distribution of hydrothermal mineral zones in Los Azufres (Mexico) geothermal field, Geothermics, v 14, no. 1, pp 49–57
Cavaney RJ (1984) Lake Maitland uranium deposit, *in*: Surficial uranium deposits, TECDOC-322, IAEA, Vienna, pp 137–140
Cazoulat M (1985) Geologic environment of the uranium deposits in the Carboniferous and Jurassic sandstones of the western margin of the Aïr Mountains in the Republic of Niger, *in*: Geological environments of sandstone-type uranium deposits, TECDOC-328, IAEA, Vienna, pp 247–264
CEA (commissariat à l'énergie atomic) (1969) The French uranium mining industry, CEA, Paris, 123 p
Cerveira A (1956) Notas sobre as pecheblendas francesas de portuguesas, Bol Soc Geol Portugal 12, 129 p
Cevales G (1960) Erzmikroskopische Untersuchungen von zehn Uranvorkommen des italienischen Perms der West- und Ostalpen, N Jb Miner, Abh, Bd 94, pp 735–758
Cevales G (1961) Metamorphe Mobilisationsvorgäuge in der Uranlagerstätte des Preittals (Cottische Alpen), N Jb Miner, Abh, Bd 96, pp 112–123
Chapman, Wood, Griswold, Inc (1979) Geologic map of the Grants Uranium Region, New Mex, Bur Mines Mineral Res, Geol Map 31, revised, 3 sheets, scale 1 inch = 2 miles. Text on sheet no. 3
Chapot CG (1979) L'essai du tunnelier Bouygues à Cogéma Crouzille, Industrie Minérale, Férrier 1979, pp 1–6
Charbonneau BW (1982) Radiometric study of three radioactive granites in the Canadian Shield: Elliot Lake, Ontario; Fort Smith, and Fury and Hecla, NWT, *in*: Maurice YT, ed., Uranium in granites, Geol Surv Can Paper 81-23, pp 91–99
Chatterjee AK, Strong DF (1984) Discriminant and factor analysis of geochemical data from granitoid rocks hosting the Millet Brook uranium mineralization, South Mountain Batholith, Nova Scotia, Uranium, 1, pp 289–305
Chatterjee AK, Strong DF (1985) Geochemical characteristics of the polymetallic tin domain, southwestern Nova Scotia, Canada. *in*: Taylor RP, Strong DF eds., Granite-related mineral deposits, CIM, Geol Div, Halifax, NS, pp 41–52
Chauvet RJ (1975) Description du gisement d'uranium d'Oklo, *in*: The Oklo phenomenon, IAEA, Vienna, pp 53–65
Chen Zhaobo (1981) "Double mixing" genetic model of uranium deposits in volcanic rocks and the relationship between China's Mesozoic vein-type uranium deposits and Pacific plate tectonics, Proc 26th Int Geol Congr on Metallogenesis of Uranium (1980), Geoinstitut, Beograd, pp 65–97
Chen Zhaobo (1985) Some basic metallogenetic aspects on Phanerozoic vein-type uranium deposits, Uranium Geology, Beijing, 1, 1, p 1–
Chen Zhaobo et al. (1982) Uranium deposits in Mesozoic volcanics in Southeast China, Acta Geologica Sinica, 56, 3, p 235–
Chen Zhaobo, Fang Xiheng (1985) Main characteristics and genesis of Phanerozoic vein-type uranium deposits, *in*: Uranium deposits in volcanic rocks, IAEA, Vienna, pp 69–82
Chen Zuyi et al. (1983) The stages of the development of fault-block movement and continental red beds with respect to the regional uranium mineralization in South China, Acta Geologica Sinica, 57, 3, p 294– (in Chinese)
Chenevoy M (1958) Contribution à l'étude des schistes cristallins de la partie nord-ouest du Massif Central français, Mém Serv Carte géol Fr, 428 p
Cheney ES, Jensen ML (1966) Stable isotopic geology of the Gas Hills, Wyoming, uranium district, Econ Geol, v 61, pp 44–71
Chenoweth WL (1953) The variegated member of the Morrison Formation in the southeastern part of the San Juan Basin, Valencia County, New Mexico, Univ Masters thesis, 86 p
Chenoweth WL (1975) Uranium deposits of the Canyonlands area, Four Corners Geol Soc, 8th Field Conf Guidebook, pp 253–260
Chenoweth WL (1977) Uranium in the San Juan Basin – an overview, New Mex Geol Soc Guidebook, 28th Field Conf, San Juan Basin III, pp 257–262
Chenoweth WL (1978) Uranium in western Colorado, Mountain Geologist, v 15, no. 3, pp 89–96
Chenoweth WL (1980) Uranium-vanadium deposits of the Henry Mountains, Utah, *in*: Henry Mountains Symposium, Utah Geol Ass, pp 299–304
Chenoweth WL (1981) The uranium-vanadium deposits of the Uravan Mineral Belt and adjacent areas, Colorado and Utah, New Mexico Geol Soc Guidebook, 32nd Field Conf, Western Slope Colorado, pp 165–170
Chenoweth WL (1983) Uranium-vanadium deposits on the west flank of the La Sal Mountains, Grand and San Juan Counties, Utah, Grand Junction Geol Soc-1983 Field Trip, pp 41–43
Chenoweth WL (1986) The Orphan Lode Mine, Grand Canyon, Arizona, a case history of a mineralized, collapse-breccia pipe, US Geol Surv Rep 86–510, 126 p
Chenoweth WL, Holen HK (1980) Exploration in the Grants Uranium Region since Memoir 15, *in*: Rautman CA, ed., Geology and mineral technology of the Grants uranium region 1979, New Mex. Bur Mines Mineral Res Mem. 38, pp 17–21
Chenoweth WL, Magleby DN (1971) Mine location map, Cameron uranium area, Coconino County, Arizona, US-AEC, Prelim. Map 20
Chenoweth WL, Malan RC (1969) Significant geologic types of uranium deposits – United States and Canada, Remarks at US-AEC Uranium Workshop, Grand Junction, Colorado, Paper 5, 50 p
Chenoweth WL, Malan RC (1973) The uranium deposits of northeastern Arizona, in Monument Valley and vicinity, Arizona and Utah, New Mexico Geol Soc, Guidebook, 24th Field Conf, pp 139–149

Chenoweth WL, Stehle FT (1957) Reconnaissance for uranium in parts of the San Juan Basin, New Mexico and Colorado USA, US-AEC, TM-114, 19 p

Chernokov AA (1982) Typomorphism of uranium minerals and its practical significance, Inter Geol Rev, v 24, 5, pp 567–576

Chiaranzelli JR, Macdonald R (1986) A U-Pb zircon date for the Ennadai Group, *in*: Summary of investigations, 1986, Sask Geol Surv, pp 112–113

Childers MO (1970) Uranium geology of the Kaycee area, Johnson County, Wyoming, Wyoming Geol Ass, 22nd Field Conf Guidebook, pp 13–20

Childers MO (1974) Uranium occurrences in Upper Cretaceous and Tertiary strata of Wyoming and northern Colorado, Mountain Geologist, v 11, no. 4, pp 131–147

Christie AM (1953) Goldfields Martin-Lake map area, Geol Surv Can Mem 269, 126 p

Christie AM, Kesten SN (1949) Pitchblende occurrences of the Goldfields Area, Saskatchewan. CIM Bull, v 42, pp 285–293

Civetta L, Gasparini, P (1972) A review of U and Th distributions in recent volcanics from southern Italy: magmatological and geophysical implications, *in*: Adams JAS, Lowder WM, Gesell TS, eds., The natural radiation environment II, Rice Univ Dep Geol, Houston, Texas pp 483–516

Clark DS (1980) Uranium ore rolls in the Westwater Canyon Sandstone, San Juan Basin, New Mexico, *in*: Rautman, CA, ed., Geology and mineral technology of the Grants Uranium Region 1979, New Mex Bur Mines Mineral Res Mem 38, pp 195–201

Clark DS, Havenstrite SR (1963) Geology and ore deposits of the Cliffside Mine, Ambrosia Lake area, *in*: Kelley VC, ed., Geology and technology of the Grants Uranium Region, New Nex Bur Mines Mineral Res Mem 15, pp 108–116

Clark RJM, Homeniuk LA, Bonnar R (1982a) Uranium geology in the Athabasca and a comparison with other Canadian Proterozoic basins, CIM Bull, v 75, no. 840, pp 91–98

Clark RJM, Homeniuk LA, Bonnar R (1982b) The Fond du Lac uranium deposits, CIM Bull, v 75, no. 841, pp 84–89

Clark SP, Jr et al. (1966) Abundances of U, Th, and K, *in*: Handbook of physical constants, Geol Soc Amer Mem 97, pp 521–541

Clarke PJ and Fogwill WD (1986) Geology of the Dawn Lake Uranium deposits, northern Saskatchewan, *in*: Evans, EL, ed., Uranium deposits of Canada, CIM Spec Vol. 33, pp 184–192

Clary TA, Mobley CM, Moulton GF Jr (1963) Geologic setting of an anomalous ore deposit in the Section 30 Mine, Ambrosia Lake area, *in*: Kelley VC, ed., Geology and technology of the Grants Uranium Region, New Mex Bur Mines Mineral Res Mem 15, pp 72–79

Clemmey H (1981) Some aspects of the genesis of heavy mineral assemblages in Lower Proterozoic uranium-gold conglomerates, Min Mag, 44, pp 399–408

Cluzel D (1985) Géologie et metallogénie de la Série des mines au Shaba (Ex-Katanga) meridional (Zaïre). Métaévaporites et reprises hydrothermales, CR Acad Sc Paris, 301, II, 16, pp 1209–1212

Cluzel D (1986) Contribution à l'étude du metamorphisme des gisements cupro-cobaltifères stratiformes du Sud-Shaba, Zaïre. Le district minier de Lwishia, J African Earth Sci, 5, 6, pp 557–574

Coetzee CB (1960) The geology of the Orange Free State goldfield, S Afr Geol Surv Mem 49, 198 p

Coetzee F (1965) Distribution and grain-size of gold, uraninite, pyrite and certain other heavy minerals in gold-bearing reefs of the Witwatersrand Basin, Trans Geol Soc S Africa, v 68, pp 61–88

Coffin RC (1921) Radium, uranium, and vanadium deposits of southwestern Colorado, Colorado Geol Surv Bull 16, 231 p

Collot B (1981) Le granite albitique hyperalcalin de Bokan Mountain (SE Alaska) et ses minéralisations U-Th. Sa place dans la Cordillère Canadienne, 3° cycle thesis, USTL, Montpellier, 238 p

Coma F (1983) Litología, tectónica y mineralización del yacimiento Fé, Saelices el Chico (Salamanca), VIII Reun Geol Oest Penin, Stud Geol (manuscr)

Compston W, Arriens, PA (1968) The Precambrian geochronology of Australia, Can J Earth Sci, 5, pp 561–583

Condon MA, Walpole BP (1955) Sedimentary environment as a control of uranium mineralization in the Katherine-Darwin Region, Northern Territory, BMR, Canberra, Rep 24, 14 p

Condon SM, Peterson F (1986) Stratigraphy of Middle and Upper Jurassic rocks of the San Juan basin: Historical perspective, current ideas, and remaining problems, *in*: Turner-Peterson CE, Santos ES, Fishman NS, eds., A basin analysis case study – the Morrison Formation, Grants Uranium Region, New Mexico, Amer Ass Petrol Geol, Studies in Geology, no. 22, pp 7–26

Coppens R, Bernard A (1978) Déplacements de l'uranium dans les roches cristallines: Application à la prospection des dépôts uranifères, Mineral Deposita, v 13, pp 165–182

Coppens R, Kosztolanyi C, Dottin H (1969) Etude géochronologique de la mine du Brugeaud, Mém Sci Terre, no. 15, pp 195–213

Corbett RG (1964) The geology and mineralogy of Section 22 Mine, Ambrosia Lake uranium district, New Mexico, unpubl PhD Diss, Univ Michigan, 161 p

Cordfunke EH (1969) The chemistry of uranium, Elsevier Publishing Co, New York, 250 p

Corey AS (1959) Mineralogy and petrology of the uranium deposits of Cane Springs Canyon, San Juan and Grand counties, Utah, US-AEC, RME-128

Corner B, Durrheim RJ, Nicolaysen LO (1986) The structural framework of the Witwatersrand Basin as revealed by gravity and aeromagnetic data, Extended abstracts, 21st Biennial congress, Geol Soc S Afr, Johannesburg, pp 27–30

Corretge G, Lopez Plaza M (1976), Geologia del area granitica y metamorfica al oeste de Cuidad Rodrigo (Salamanca). I: El complejo esquisto-grauvaquico, Stud Geol, 11, pp 121–161

Cortial F (1985) Les bitumes du Francevillien et leurs kérogènes. Relations avec les minéralisations uranifères, Thèse doct, Strasbourg

Cortini M (1984) Uranium in mantle processes, *in*: De Vivo B, Ippolito F, Capaldi G, Simpson PR, eds., Uranium geochemistry, mineralogy, exploration and resources, IMM, London, pp 4–11

Cousins CA (1965) Disconformities in the Main Reef Zone of the Witwatersrand System, and their bearing on reef correlation, with particular reference to the

East, Central and West Witwatersrand, Trans Geol Soc S Africa, v 68, pp 121–142
Cousins CA (1973) Platinoids in the Witwatersrand System, JS Afr Inst Min Metal, v 73, pp 184–199
Cowan GA, Bryant EA, Daniels WR, Maeck WJ (1975) Some United States studies of the Oklo phenomenon, *in*: The Oklo phenomenon, IAEA, Vienna, pp 341–356
Crabb D, Dudley R, Mann AW (1984) Hinkler Well – Centipede deposits, *in*: Surficial uranium deposits, TECDOC-322, IAEA, Vienna, pp 133–36
Craig RM (1980) Geochemical and sedimentologic problems of uranium deposits of Texas Gulf coastal plain: discussion, Amer Assoc Petrol Geol Bull, 64, p 583
Craig LC, Holmes CN, Cadigan RA, Freeman VL, Mullens TE, Weir GW (1955) Stratigraphy of the Morrison and related formations, Colorado Plateau region – a preliminary report, US Geol Surv Bull 1009-E, pp 125–168
Cramer JJ, Vilks P (1989) Hydrogeochemistry and uranium fixation in the Cigar Lake uranium deposit, northern Saskatchewan, *in*: Uranium resources and geology of North America, (abstr) TECDOC-500, IAEA, Vienna, p 359
Crawley RA (1983) Sandstone uranium deposits in the United States: a review of the history, distribution, genesis, mining areas, and outlook, US-DOE, GJBX-15(83), 57 p
Crawley RA, Holen HK, Chenoweth WL (1985) Geology and application of geologic concepts, Morrison Formation, Grants Uranium Region, New Mexico, USA, *in*: Geological environments of sandstone-type uranium deposits, TECDOC-328, IAEA, Vienna, pp 199–214
Crew ME (1981) NURE Uranium deposit model studies, *in*: Uranium industry seminar proceedings, US-DOE, GJO-108(81).
Crick IH, Muir MD (1980) Evaporites and uranium mineralisation in the Pine Creek Geosyncline. *in*: Ferguson J, Goleby AB, eds., Uranium in the Pine Creek Geosyncline, IAEA, Vienna, pp 531–542
Crick IH, Muir MD, Needham RS, Roarty MJ (1980) The geology and mineralisation of the South Alligator Uranium Field, *in*: Ferguson J, Goleby AB, eds., Uranium in the Pine Creek Geosyncline, IAEA, Vienna, pp 273–286
Cronk RJ (1963) Geology of the Dysart no. 1 Mine, Ambrosia Lake area, *in*: Kelley VC, ed., Geology and technology of the Grants Uranium Region, New Mex Bur Mines Mineral Res Mem 15, pp 60–65
Culbert RR, Boyle DR, Levinson AA (1984) Surficial uranium deposits in Canada, *in*: Surficial uranium deposits, TECDOC-322, IAEA, Vienna, pp 179–192
Cumming GL, Rimsaite J (1979) Isotopic studies of lead-depleted pitchblende, secondary radioactive minerals and sulfides from the Rabbit Lake uranium deposit, Saskatchewan, Can J Earth Sci, v 16, pp 1702–1715
Cumming GL, Krstic D, Wilson JA (1987) Age of the Athabasca Group, northern Alberta, *in*: Program with abstracts, joint annual meeting Geol Ass Can, Miner Ass Can, v 12, p 35
Cuney M (1978) Geologic environment, mineralogy and fluid inclusions of the "Bois Noirs-Limouzat" uranium vein, Forez, France, Econ Geol, v 73, pp 1567–1610
Cuney M (1980) Preliminary results on the petrology and fluid inclusions of the Rössing uraniferous alakites, Trans Geol Soc S Afr, 83, pp 39–45
Cuney M (1981) Comportment de l'uranium et du thorium au cours du métamorphisme – Rôle de l'anatexie dans la genèse des magmas riches en radioéléments, thesis, INPL (Inst Natl Polytech Lorraine), Nancy, unpubl
Cuney M (1982) Processus de concentration de l'uranium et du thorium au cours de la fusion partielle et de la cristallisation des magmas granitiques, *in*: Les méthodes de prospection de l'uranium, OCDE, Paris, pp 277–292
Cuney M (1985) Chemical and crystallochemical controls on U and Th rich accessory minerals paragenesis in granitic rocks, (abstr), *in*: Intern Meeting, Nancy, Concentration mechanisms of uranium in geological environments, pp 117–120
Cuney M, Friedrich M (1987) Physicochemical and crystal-chemical controls on accessory mineral paragenesis in granitoïds: implications for uranium metallogenesis, Bull Minér 110, pp 235–247
Cuney M, Peyrel JY (1984) Origine des granitoïdes fertiles, conséquences sur la définition de leurs caractéristiques spécifiques, unpubl CEE report, Contrat EXU028F (G), 123 p
Cuney M, Leroy J, Pagel M (1979) Comportement de l'uranium et du thorium dans les granites uranifères français, Sci Terre, Série 'Informatique Géologique', Nancy, 13, pp 56–63
Cuney M, Friedrich M, Poty B (1984a) Pétrologie et géochimie des radioéléments dans les granites et dans les leucogranites en particulier – Conséquences génétiques et applications à la prospection, Doc BRGM Paris, Mo 79, pp 91–125
Cuney M, Le Fort P, Wang ZX (1984b) Uranium and thorium geochemistry and mineralogy in the Manaslu leucogranite (Nepal, Himalaya), *in*: Geology of granites and their metallogenetic relations. Symp Nanjing, 1982, University Press, Beijing, pp 853–873
Cuney M, Friedrich M, Drin N (1985a) Traitement par l'analyse statistique de données multivariables sur le complexe de Brâme, St Sylvestre, St Goussaud – Differenciation magmatique et polygénisme, Sci Terre, Sér Info Géol, Nancy, 23, pp 1–25
Cuney M, Autran A, Burnol L (1985b) Premiers résultats apportés par le sondage GPF de 900 m réalisé sur le granite sodo-lithique et fluoré à minéralisation disséminée de Beauvoir (complexe granitique d'Echassières, Massif Central, France), Chron Rech Min, no. 481, pp 59–63
Cuney M, Leroy J, Valdiviezo PA, Daziano C, Gamba M, Zarco AJ, Morello O, Ninci C, Molina P (1989) Geochemistry of the uranium mineralized Achala granitic complex (Argentina): comparison with Hercynian peraluminous leucogranites of western Europe, *in*: Metallogenesis of uranium deposits, IAEA, Vienna, pp 211–232
Cuney M, von Pechmann E, Rimsaite J, Simova F, Sørensen H, Augustithis SS, eds. (1989) Primary radioactive minerals, Theophrastus Publications SA, Athens, 406 p
Cunningham LJ (1977) Origin of Elliot Lake uranium deposits still open to debate, Northern Miner, March 3
Curry DL (1976) Evaluation of uranium resources in the Powder River Basin, Wyoming, Wyoming Geol Ass, 28th Field Conf, Guidebook, pp 235–242
Curtis L (1985) Post-Kombolgie alteration at Jabiluka II and its significance with regards to the Athabasca-Alligator Rivers comparison, *in*: Sibbald T II, Petruk W, ed., Geology of uranium deposits, CIM Spec Vol. 32, pp 231–245

Dahl AR, Hagmaier JL (1974) Genesis and characteristics of the southern Powder River Basin uranium deposits, Wyoming, USA, *in*: Formation of uranium ore deposits, IAEA, Vienna, pp 201–216

Dahl AR, Hagmaier JL (1976) Genesis and characteristics of the southern Powder River Basin uranium deposits, Wyoming, Wyoming, Geol Ass, 28th Field Conf, Guidebook, pp 243–252

Dahlkamp FJ (1977) Geochronological-metallogenetic correlation of uranium mineralization, *in*: Recognition and evaluation of uraniferous areas, IAEA, Vienna, pp 131–148

Dahlkamp FJ (1978a) Classification of uranium deposits, Mineral Deposita, 13, pp 83–104

Dahlkamp FJ (1978b) Geologic appraisal of the Key Lake U-Ni deposits, northern Saskatchewan. Econ Geol, v 73, pp 1430–1449

Dahlkamp FJ (1979) Uranlagerstätten, Gmelin Handbuch. Springer, Berlin Heidelberg New York, 280 p

Dahlkamp FJ (1980) Typology and geographic/geotectonic distribution of uranium deposits, *in*: Burollet PF, Ziegler V, eds., Energy resources (Paris: Edition Technip), (26th Int Geol Congr, Colloque C2), pp 499–536

Dahlkamp FJ (1982) Genesis of uranium deposits. An appraisal of the present state of knowledge, *in*: Amstutz et al., eds., Ore genesis, The state of the art, Springer, Berlin, Heidelberg, New York, pp 644–654

Dahlkamp FJ (1984) Characteristics and problematics of the metallogenesis of Proterozoic veinlike-type uranium deposits, *in*: Wauschkuhn et al., eds, Syngenesis and epigenesis in the formation of mineral deposits, Springer, Berlin, Heidelberg, New York, Tokyo, pp 183–192

Dahlkamp FJ (1989) Classification scheme of uranium deposits, *in*: Metallogenesis of uranium deposits, IAEA, Vienna, pp 1–31

Dahlkamp FJ, Adams SS (1981) Geology and recognition criteria for veinlike uranium deposits of the Lower to Middle Proterozoic unconformity- and strata-related types, US-DOE, GJBX-5(81), 254 p

Dahlkamp FJ, Scivetti N (1981) IUREP/International uranium resources evaluation project: Austria, OECD-NEA, Paris, 87 p

Dahlkamp FJ, Tan B (1977) Geology and mineralogy of the Key Lake U-Ni deposits, northern Saskatchewan, Canada, *in*: Jones MJ, ed., Geology, mining and extractive processing of uranium, IMM, London, pp 145–157

Dall'aglio M, Gragnani R, Locardi E (1974) Geochemical factors controlling the formation of secondary minerals of uranium, *in*: Formation of uranium ore deposits, IAEA, Vienna, pp 33–48

Danchev VI, Strelyanov NP (1973) Uranium-coal deposits and their principal genetic types, Geologiya Rudn Mestorozh, no. 3, pp 66–81

Danchev VI, Strelyanov NP (1978) Stages in ore deposition and classification of exogenic uranium deposits, Intern Geol Rev, v 20, no. 1, pp 81–92

D'arcy G (1949) Mineralogy of uranium and thorium bearing minerals, US-AEC, RMO-563, Washington, 198 p

Dardel J, Peinardor Fernandes A, Jamet P, Le Caignec R, Moreau M, Serrano JR, Ziegler V (1979) Gisements d'uranium dans les schistes péribatholitiques (type ibérique) et dans les leucogranites (type Limousin) (Portugal, Espagne, France), livret guide d'excursion, Sci Terre, Nancy XXIII, 47 p

Darnley AG (1961) Pitchblende from Carrasca, Portugal, Geol Surv Great Britain, Atom Energy Div, Age Determination Rep no. 17, 5 p

Darnley AG (1981) The relationship between uranium distribution and some major crustal features in Canada, Miner Mag, 44, pp 425–436

Darnley AG, Charbonneau BW, Richardson KA (1977) Distribution of uranium in rocks as a guide to the recognition of uraniferous regions, *in*: Recognition and evaluation of uraniferous areas, IAEA, Vienna, pp 55–86

Davidson CF (1953) The gold-uranium ores of the Witwatersrand, Min Mag, 88, pp 73–85

Davidson CF (1957) On the occurrence of uranium in ancient conglomerates, Econ Geol, v 52, pp 668–693

Davidson CF, Cosgrove ME (1955) On the impersistence of uraninite as a detrital mineral, Bull Geol Surv Ct Brit, no. 10, pp 74–80

Davidson CF, Ponsford DRA (1954) On the occurrence of uranium in coals, Min Mag, 91, no. 5, pp 265–273

Davidson ES (1967) Geology of the Circle Cliffs area, Garfield and Kane Counties, Utah, US Geol Surv Bull 1229, 140 p

Davies RD, Allsopp HL, Erlank AJ, Manton WT (1969), Sr-isotopic studies on various layered mafic intrusions in southern Africa, Geol Soc S Afr Spec Publ 1, pp 576–593

Davis JF (1969) Uranium deposits in the Powder River Basin, Wyoming Univ Contrib Geology, v 8, pp 131–147

Davydova RI, Shaposhnikov GH (1966) The geological conditions of davidite formation in an area of the USSR, Zap Vses Mineralogy. Obshck, 95, pp 467–474 (in Russian)

Dawson KR (1951) A petrographic description of the well-rocks and alteration products associated with the pitchblende-bearing veins in the Goldfields Region, Saskatchewan, Geol Surv Can Paper 51–24, 83 p

Dawson KR (1956) Petrology and red coloration of wall-rocks, radioactive deposits, Goldfields Region, Saskatchewan, Geol Surv Can Bull 33, 46 p

Dayvault RD, Castor SB, Berry MR (1985) Uranium associated with volcanic rocks of the McDermitt Caldera, Nevada and Oregon, *in*: Uranium deposits in volcanic rocks, IAEA, Vienna, pp 379–410

de Carle AL (1986) Geology of the Key Lake deposits, *in*: Evans EL, ed., Uranium deposits of Canada, CIM Spec Vol. 33, pp 170–177

de Fraipont P (1982) Approche multiscalaire de la fracturation du massif granitique de Saint Sylvestre. Télédétection et analyse tectonique appliquées aux gisements d'uranium de la division minière de la Couzille (Cogema) – Limousin, Massif Central Français, Thèse 3e cycle, Univ Strasbourg, 201 p

de Fraipont P, Marquaire CH, Sierak JP, Horrenberg JCC, Ruhland M (1982) Réseau de fractures et répartition des corps tectoniques élémentaires de fracturation: Recherche sur le contrôle tectonique de la minéralisation uranifère du Secteur de Pény (La Crouzille, France), *in*: Vein-type and similar uranium deposits in rocks younger than Proterozoic, IAEA, Vienna, pp 87–102

De Jager FSJ (1964) The Witwatersrand System in the Springs-Nigel-Heidelberg section of the East Rand Basin, *in*: Haughton SH, ed., The geology of some

ore deposits in southern Africa, Geol Soc S Afr, v 1, pp 161–189
Dekkers MJ, Vriend SP, Van Diest Ph, Van der Weijden CH, Oosterom MG (1983a) Geochemical controls of transport and deposition of uranium from solution. Case study: São Pedro do Sul (Portugal), Extern Rep, Inst Earth Sci, State Univ Utrecht, 54 p
Dekkers MJ, Vriend SP, Walen CG, Van der Weijden CH (1983b) Geochemical controls of transport and deposition of uranium from solution. Case study: Nisa (Portugal), Extern Rep, Inst Earth Sci, State Univ Utrecht, 87 p
De Kock WP (1964) The geology and economic significance of the West Wits Line, *in*: Haughton SH, ed., The geology of some ore deposits in southern Africa, Geol Soc S Afr, v 1, pp 323–386
de Kun N (1965) The mineral resources of Africa, Elsevier, Amsterdam, London, New York
Deliens M (1977) Associations de mineraux secondaires d'uranium à Shinkolobwe (region du Shaba, Zaïre), Bull Soc francaise Miner, Crist, v 100, no. 1, pp 32–38
Deliens M (1979) Die Uranlagerstätte von Shinkolobwe, Shaba/Zaïre, Lapis, Jg 4, Nr 7/8, pp 33–35
Deliens M, Piret P (1981) Uranyl and aluminum phosphates from Kobokobo V Mundite, a new mineral, Bull Minèr, v 104, 669–
De Luna RJ, Freitas F (1954) Metallogeny of the uranium deposits of the Muvudzi Valley, Tete, Mozambique, Congr Geol Intern Compt Rend 19e, Algiers 1952, II, pp 293–307
de Magnee I, François A (1985) Genesis of the Kipushi (Cu, Zn, etc...) and the Shinkolobwe (U, Ni, Co) deposits (Shaba, Zaïre) in direct relation with Proterozoic salt diapirs, (abst), Fortschr Miner, v 63, Beiheft 1, I–II, Stuttgart, p 140
Denson NM, Chisholm WA (1971) Summary of mineralogic and lithologic characteristics of Tertiary sedimentary rocks in the middle Rocky Mountains and the northern Great Plains, US Geol Surv Prof Paper 750-C, pp C117–C126
Denson NM, Gill JR (1965) Uranium-bearing lignite and carbonaceous shale in the southwestern part of the Williston basin, US Geol Surv Prof Paper 463, 75 p
Derrick GM (1977) Metasomatic history and origin of uranium mineralization at Mary Kathleen, northwest Queensland, BMR, J Austral, v 2, pp 123–130
Derriks JJ, Oosterbosch R (1958) The Swambo and Kalongwe deposits compared to Shinkolobwe: Contribution to the study of Katanga uranium, *in*: UN, Internat Conf Peaceful Uses of Atomic Energy, 2nd, Geneva, Proc, v 2. Survey raw material resources, pp 663–695
Derriks JJ, Vaes JF (1956) The Shinkolobwe uranium deposit. Current status of our geologic and metallogenic knowledge, *in*: UN, Intern Conf Peaceful Uses of Atomic Energy, 1st, Geneva, Proc, v 6, Geology of uranium and thorium, pp 94–128
Derry DR (1960) Evidence of the origin of the Blind River uranium deposits, Econ Geol, v 55, pp 906–927
Deutscher RL, Mann AW, Butt CRM (1980) Model for calcrete uranium mineralization, J geochem Explor, 12, 2–3, pp 158–161
Deutscher RC, Mann AW, Giblin AM (1980) Groundwater geochemistry in the vicinity of the Jabiluka deposits, *in*: Ferguson J, Goleby AB, eds., Uranium in the Pine Creek Geosyncline, IAEA, Vienna, pp 477–486
Devillers C, Ruffenach J-C, Menes J, Lucas M, Hagemann R, Nief G (1975) Âge de la minéralisation de l'uranium et date de la réaction neucléaire, *in*: The Oklo phenomenon, IAEA, Vienna, pp 293–302
De Vivo B, Ippolito F, Capaldi G, Simpson PR, eds. (1984) Uranium geochemistry, mineralogy, exploration and resources, IMM, London, 201 p
De Voto RH (1978) Uranium geology and exploration: lecture notes and references, Colorado School Mines, Golden, 396 p
De Voto RH, Paschis JA (1980) Geology of uranium vein deposits (including Schwartzwalder Mine) in Proterozoic metamorphic rocks, Front Range, Colorado, *in*: Ferguson J, Goleby AB, eds., Uranium in the Pine Creek Geosyncline, IAEA, Vienna, pp 683–692
De Voto RH, Stevens DN, eds. (1979) Uraniferous phosphate resources and technology and economics of uranium recovery from phosphate resources, United States and the free world, US-DOE, GJBX-110(79), v 1, 686 p, v 2, 606 p
De Waal SA, Herzberg W (1969) Uranium and gold mineralization of the Black Reef Series in the Kaapsehoop area, Nelspruit district, eastern Transvaal Annals, Rep S Afr, Geol Surv, v 7, pp 111–124
Dibobol Kitmut, Malu Wa Kaleriga (1979) Les gisements d'uranium du Zaïre, *in*: Uranium deposits in Africa: geology and exploration, IAEA, Vienna, pp 123–148
Dickinson KA (1976a) Sedimentary depositional environments of uranium and petroleum host rocks of the Jackson Group, south Texas, US Geol Surv J Res, v 4, no. 5, pp 615–629
Dickinson KA (1976b) Uranium potential of the Texas coastal plain, US Geol Surv Rep 76–879, 7 p
Dickinson KA (1976c) Geologic controls of uranium deposition, Karnes County, Texas, US Geol Surv Rep 76–331, 16 p
Dickinson KA, Duval JS (1977) Trend areas and exploration techniques, *in*: Campbell MD, ed., Geology of alternate energy resources in the south-central United States, Houston Geol Soc, pp 45–66
Dickinson KA, Sullivan MW (1976) Geology of the Brysch uranium mine, Karnes County, Texas, US Geol Surv J Res, v 4, no. 4, pp 397–404
Dickson BL (1984) Uranium series disequilibrium in the carnotite deposits of Western Australia, *in*: Surficial uranium deposits, TECDOC-322, IAEA, Vienna, pp 165–170
Dickson FW, Rye RO, Radtke AS (1979) The Carlin gold deposit as a product of rock-water interactions, Nevada Bur Mines Geol Rep 33, pp 101–108
Dill H (1980) Neue Ergebnisse zur Mineralogie der primären Uranträger auf den Gruben Höhensteinweg/Poppenreuth und Wäldel/Mähring in Nordostbayern mit besonderer Berücksichtigung der Uran-Titan- und Phosphor-Kohlenstoffverbindungen, Geol Jb, D 42, pp 3–39
Dill H (1983a) Vein and metasedimentary-hosted carbonaceous matter and phosphorus from NE Bavaria (FR Germany) and their implication on syngenetic and epigenetic uranium concentration, N Jb Min, Abh 148, pp 1–21
Dill H (1983b) Plutonic mobilization, sodium metasomatism, propylitic wall-rock alteration and element partitioning from Höhensteinweg uranium occurrence (Northeast Bavaria, FRG), Uranium 1, pp 139–166
Dill H (1985) Granite-related and granite-induced ore

mineralization on the western edge of the Bohemian Massif, *in*: HHP granites, hydrothermal circulation and ore genesis, Conf IMM, St Austell, Cornwall, pp 55–70
Dimanche F, Bartholomé P (1976) The alteration of ilmenite in sediments, Miner Sci Eng, v 8, pp 187–201
Dimroth E (1979) Significance of diagenesis for the origin of Witwatersrand-type uraniferous conglomerates, Phil Trans Royal Soc, London, A291, pp 277–287
Dimroth E, Kimberley MM (1976) Precambrian atmospheric oxygen; evidence in the sedimentary distributions of carbon, sulfur, uranium, and iron, Can J Earth Sci, 13, pp 1161–1185
Diouly-Osso P, Chauvet RJ (1979) Les gisements d'uranium de la région de Franceville (Gabon), *in*: Uranium deposits in Africa, geology and exploration, IAEA, Vienna, pp 123–148
Dix GP, Jr, (1953) Reconnaissance of the uranium deposits of the Lockhart Canyon-Indian Creek area, San Juan County, Utah, US-AEC, RME-4038, Tech Inf Service, Oak Ridge, Tenn
Dodson RG (1972) Some environments of formation of uranium deposits, *in*: Bowie SHU, Davis M, Ostle D, eds., Uranium prospecting handbook, IMM, London, pp 33–44
Dodson RG, Prichard CE (1975) Uranium in the Pine Creek Geosyncline, *in*: Knight CL, ed., Economic geology of Australia and Papua New Guinea, AIMM, Monograph Series, no. 5, 1. Metals, pp 281–284
Dodson RG, Needham RS, Wilkes PG, Page RW, Smart PG, Watchman AL (1974) Uranium mineralization in the Rum Jungle – Alligator Rivers Province, Northern Territory, Australia, *in*: Formation of uranium ore deposits, IAEA, Vienna, pp 551–568
Doelling HH (1969) Mineral resources, San Juan County, Utah, and adjacent areas, Part II: Uranium and other metals in sedimentary host rocks, Utah Geol Miner Surv Spec Studies 24(II), 64 p
Doi K, Hirono S, Sakamari Y (1975) Uranium mineralization by groundwater in sedimentary rocks, Japan, Econ Geol, v 70, pp 628–646
Donnelly TH, Ferguson J (1980) A stable isotope study of three deposits in the Alligator Rivers Uranium Field, *in*: Ferguson J, Goleby AB, eds., Uranium in the Pine Creek Geosyncline, IAEA, Vienna, pp 387–406
Donnot M, Weber F (1969) Carte géologique de reconnaissance au 1/500 000 Franceville Ouest avec notice explicative, BRGM, Paris
Dooley JR, Tatsumoto M, Rosholt JN (1964) Radioactive disequilibrium studies of roll features, Shirley Basin, Wyoming, Econ Geol, v 59, pp 586–595
Dooley JR, Granger HC, Rosholt JN (1966) Uranium 234 fractionation in the sandstone-type uranium deposits of the Ambrosia Lake district, New Mexico, Econ Geol, v 61, pp 1362–1382
Dooley JR, Jr, Harshman EN, Rosholt JN (1974) Uranium-lead ages of the uranium deposits of the Gas Hills and Shirley Basin, Wyoming, Econ Geol, v 69, pp 527–531
Dostal J, Capedri S (1978) Uranium in metamorphic rocks, Contr Miner Petrol, v 66, pp 409–414
Douglas RJW, ed. (1968) Geology and economic minerals of Canada, Geol Surv Can Econ Geol Rep no. 1, 838 p
Downs GR, Bird AG (1965) The Schwartzwalder uranium mine, Jefferson County, Colorado, Mountain Geologist, v 2, pp 183–191
Drin N, Friedrich M, Cuney M (1986) Influence d'intrusions sepcialisées sur la fertilité uranifère de massifs granitiques polygéniques (abstr) 11e RST (Réun Sci Terre), Clermont-Ferrand, Soc Géol Fr, Paris, p 55
Droullard RF, Jones EE (1955) Geology of the Seven Mile – Canyon uranium deposits, Grand County, Utah, US-AEC, RME-4066, Tech Inf Service, Oak Ridge, Tenn
Drozd RJ, Hohenberg CM, Morgan CJ (1974) Heavy rare gases from Rabbit Lake (Canada) and the Oklo mine (Gabon): Natural spontaneous chain reactions in old uranium deposits, Earth Planet Sci Lett, v 23, pp 28–33
Dubessy J, Ramboz C, Nguyen Trung C, Cathelineau M, Charoy B, Cuney M, Leroy J, Poty B, Weisbrod A (1987) Physical and chemical controls (fO_2, T, pH) of the opposite behaviour of U and Sn-W as examplified by hydrothermal deposits in France, Great Britain, and by solubility data, Bull Miner, 110, no. 2, pp 261–281
Dubessy J, Landais P, Wang A (1989) Graphite disordering during the gneissic basement alteration in the Saskatchewan uranium deposits (Canada), *in*: Uranium resources and geology of North America, IAEA, Vienna, pp 345–356
Dubiel RF (1983) Sedimentology of the lower part of the Upper Triassic, Chinle Formation and its relationship to uranium deposits, White Canyon area, southeastern Utah, US Geol Surv Rep 83–459, 49 p
Dubinchuk VT, Siderenko GA (1978) On the mode of occurrence of lead in natural uranium oxides, Geochem Int, 15, 1, pp 61–65
Dubinchuk VT, Siderenko GA (1980) The position of U(VI) in natural oxides, Scripta Publishing Co 144–151. Transl from Geochimiya 1979, 12, pp 1850–1858
Duex TW (1971) K/Ar dates and U, K geochemistry of the Gueydan (Catahoula) Formation, *in*: Adams JAS, ed., Final report, US-AEC, Res Contract AT (05-1)-935, pt. 7, pp 101–145
Duex TW, Henry CD (1985) Uranium mobility in late magmatic and hydrothermal processes: Evidence from fluorite deposits, Texas and Mexico, *in*: Uranium deposits in volcanic rocks, IAEA, Vienna, pp 365–378
Dukovsky AA (1980) Geophysical characteristics of greisen deposits, Intern Geol Rev, 24, 1, pp 44–52
Du Letian (1982) Geological regularities and model of granite-type uranium deposits in China. Collection of granite-type uranium deposits, Atomic Energy press, Beijing, p 1–
Du Letian (1986) Granite-type uranium deposits of China, *in*: Vein type uranium deposits, TECDOC-361, IAEA, Vienna, pp 377–394
Dunn PR (1962) Alligator River, NT: Explanatory notes, sheet D/53–1, 1:250 000 geological series, BMR, Canberra, 22 p
Durak B (1983) Le Gisement de Jabiluka, *in*: Pagel M, ed., Géologie et Géochemie de L'Uranium, Mem. Centre de Recherches sur la Geologie de l'Uranium, 1, pp 57–93
Durak B, Pagel M, Poty B (1983) Températures et salinités des fluides au cours des silicifications diagénétiques d'une formation gréseuse surmontant un gisement d'uranium du socle: l'exemple des grès Kombolgie (Australie), CR Acad Sc Paris, Sér II, 296, pp 571–574
Duthou JL (1977) Chronologie Rb-Sr et géochimie des granitoïdes d'un segment de la chaine varisque. Relations avec le métamorphisme. Le Nord Limousin (Massif Central français), Ann Fac Sci Univ Clermont, no. 63, 250 p
Duthou JL, Cantagrel JM, Didier J, Vialette Y (1984)

Paleozoic granitoids of the French Massif Central: age and origin studied by ^{87}Rb-^{87}Sr system, Phys Earth Planet Inter, 35, pp 131–144

Du Toit AL (1954) The geology of South Africa (3d ed) Hafner Publishing Co, New York, 611 p

Dybeck J (1962) Zur Geochemie und Lagerstättenkunde des Urans, Clausth Hefte z Lagerstättenkunde und Geochemie mineral Rohstoffe, 1, 162 p

Dyck W (1978) The mobility and concentration of uranium and its decay products in temperate surficial environments, *in*: Kimberley MM, ed., Uranium deposits; their mineralogy and origin, Miner Ass Can, pp 57–100

Dyck W, Tan B (1978) Seasonal variations of helium, radon, and uranium in lake waters near the Key Lake uranium deposit, Saskatchewan, J Geochem Explor, v 10, pp 153–167

Dymkov YM (1960) Zur Genese des Nasturans, Transl from Geochimiya 7, 10 p

Dymkov YM (1961) Uranmineralisation des Erzgebirges, Ubers aus dem Russ, BTJdSDAG Wismut, Sonderdr Nr 1 (als Manuskr gedr)

Eargle DH (1968) Nomenclature of formations of the Claiborne Group, Middle Eocene coastal plain of Texas, US Geol Surv Bull 1251-D, 25 p

Eargle DH (1972) Revised classification and nomenclature of the Jackson Group (Eocene), south-central Texas, Amer Ass Petrol Geol Bull, v 56, no. 3, pp 561–566

Eargle DH, Snider JL (1957) A preliminary report on the stratigraphy of the uranium-bearing rocks of the Karnes County area, south-central Texas, Univ Texas, Austin, Bur Econ Geol Rep Invest 30, 30 p

Eargle DH, Weeks AMD (1961) Possible relation between hydrogen sulfide-bearing hydrocarbons in fault-line oil fields and uranium deposits in the southeast Texas coastal plain, US Geol Surv Prof Paper 424-D, pp 7–9

Eargle DH, Weeks AMD (1973) Geologic relations among uranium deposits, south Texas coastal plain region, USA, *in*: Amstutz GC, Union Geol Sci Series A, no. 3, pp 101–113

Eargle DH, Dickinson KA, Davis BO (1975) South Texas uranium deposits, Amer Ass Petrol Geol Bull, v 59, no. 5, pp 766–779

Earle SAM, Sopuck VJ (1989a) Regional lithogeochemistry of the eastern part of the Athabasca Basin uranium province, Saskatchewan, Canada, *in*: Uranium resources and geology of North America, TECDOC-500, pp 263–296

Earle SAM, Sopuck VJ (1989b) Alteration halo characteristics of uranium deposits in the Athabasca Basin, northern Saskatchewan (abstr), *in*: Uranium resources and geology of North America, TECDOC-500, IAEA, Vienna, p 343

Eldorado Staff (1964) Uranium in Canada, Ottawa, Eldorado Mining and Refining Ltd, 134 p

Eldorado Resources Ltd (1986) (updated 1987) The Eagle Point uranium deposits, northern Saskatchewan, manuscript, 56 p

Elevatorski EA (1978) Uranium guidebook for the Paradox Basin, Utah and Colorado, Minobras, 95 p

Elisejewa OP, Omelyanenko BJ (1978) Die lokale Uranverbreitung in Gesteinen und Mineralen als petrogenetischer Indikator, Z angewandte Geol, 24, 9, pp 386–387

Ellsworth HV (1928) Thucholite, a remarkable primary carbon mineral from the vicinity of Parry Sound, Ontario, Amer Miner, 13, pp 419–441

Ellsworth HV (1930) Four stages in the alteration of Villeneuve uraninite, Amer Miner, 16, pp 455–460

Engelbrecht GJ, Baumbach GWS, Matthysen JL, Fletcher P (1986) The West Wits Line, *in*: Anhaeusser CR, Maske S, Mineral deposits of southern Africa, Geol Soc S Afr, v 1, pp 599–648

Ethridge FG, Ortiz NV, Sunada DK, Tyler N (1980) Laboratory, field and computer flow study of the origin of Colorado Plateau-type uranium deposits, US Geol Surv Rep 80–805, 81 p

Eulry M, Vargas JM (1980) Le rôle des altérations anté-Liasiques dans la métallogenèse de la périphérie du Mont Lozère (France), Cas de L'Uranium, *in*: Palaeosurfaces et Leur métallogenèse, Mem BRGM 104, Orléans, pp 15–175

Eupene GS (1980) Stratigraphic structural and temporal control of mineralization in the Alligator Rivers uranium province, NT, Australia, Proceed. Fifth Quadrennial IAGOD Symp, E. Schweizerbart'sche Verlagsbuchhandlumg, Stuttgart, pp 347–376

Eupene GS, Fee PH, Colville RG (1975) The Ranger One uranium deposits, *in*: Knight CL, ed., Economic geology of Australia and Papua New Guinea, AIMM, Monograph Series no. 5, 1. Metals, pp 308–317

Evans EL ed. (1986) Uranium deposits of Canada, CIM Spec Vol. 33, 323 p

Everhart DL (1985) Tectonic setting of the world's sandstone-type uranium deposits, *in*: Geological environments of sandstone-type uranium deposits, TECDOC-328, IAEA, Vienna, pp 21–46

Everhart DL, Wright RJ (1953) The geologic character of typical pitchblende veins, Econ Geol, v 48, pp 77–96

Ewers GR, Higgins NC (1985) Geochemistry of the Early Proterozoic metasediments of the Alligator Rivers region, Northern Territory, Australia, Precamb, Res, 29, pp 331–357

Ewers GR, Ferguson J (1980) Mineralogy of the Jabiluka, Ranger, Koongara uranium deposits, *in*: Ferguson J, Goleby AB eds., Uranium in the Pine Creek Geosyncline, IAEA, Vienna, pp 363–374

Ewers GR, Ferguson J, Donnelly TH (1983) The Nabarlek uranium deposit – petrology, geochemistry, and some constraints on genesis, Econ Geol, v 78, pp 823–837

Ewers GR, Ferguson J, Needham RS, Donnelly TH (1984) – Pine Creek Geosyncline NT, *in*: Proterozoic unconformity and stratabound uranium deposits, TECDOC-315, IAEA, Vienna, pp 135–206

Ewers GR, Needham RS, Stuart-Smith PG, Crick IH (1985) Geochemistry of the low-grade Early Proterozoic sedimentary sequence in the Pine Creek Geosyncline, Northern Territory, Aust J Earth Sci, 32, pp 137–154

Ey F, Lillié F, Gauthier-Lafaye F, Weber F (1985) A uranium unconformity deposit: the geological setting of the D orebody (Saskatchewan-Canada), *in*: Lainé R, Alonso D, Svab M, eds., The Carswell structure uranium deposits, Saskatchewan, Geol Ass Can Spec Paper 29, pp 121–138

Evoy EF (1961) Geology of the Gunnar uranium deposit, Beaverlodge area, Saskatchewan, Univ Wisconsin, unpubl PhD dissertation, 62 p

Evoy EF (1986) The Gunnar uranium deposit, *in*: Evans EL, ed., Uranium deposits of Canada, CIM Spec Vol. 33, pp 250–260

Fahrig WF (1961) The geology of the Athabasca Formation, Geol Surv Can Bull 68, 41 p

Fahrig WF, Jones DL (1969) Paleomagnetic evidence for

the extent of Mackenzie igneous events, Can J Earth Sci, v 6, pp 679–688

Fahrig WF, Loveridge WD (1981) Rb-Sr isochron age of weathered Pre-Athabasca Formation basement gneiss, Northern Saskatchewan: Rb-Sr and U-Pb Isotopic Age Studies, Report 4: *in* Current research, Part C, Geol Surv Can, Paper 81–1C, pp 127–129

Fahrig WF, Christie KW, Freda G (1978) The paleolatitude and paleomagnetic age of the Athabasca Formation, northern Saskatchewan, Geol Surv Can Paper 78–1C, pp 1–6

Fairbairn HW (1965) Re-examination of Rb-Sr whole rock ages at Sudbury-Blind River, Ontario, Massachusetts Inst Technology, Dep Geol Geophys, 13th Annual Rep, 1381–13, p 107

Fairbairn HW, Hurley PM, Card KD, Knight CJ (1969) Correlation of radiometric ages of Nipissing Diabase and Huronian metasediments with Proterozoic orogenic events in Ontario, Can J Earth Sci, v. 6, pp 489–497

Falkowski SK (1980) Geology and ore deposits of the Johnny M Mine, Ambrosia Lake district, New Mexico, *in*: Rautman CA, Geology and mineral technology of the Grants Uranium Region 1979, New Mex Bur Mines Mineral Res Mem 38, pp 230–239

Farstad J, Ayers DE (1986) Geology of the Midwest uranium deposit, northern Saskatchewan, *in*: Evans EL (ed), Uranium deposits of Canada, CIM Spec Vol. 33, pp 178–183

Faure-Mercuret R (1965) Contribution à l'étude sédimentologique et géochimique du bassin de Franceville, République Gabonaise, Univ Strasbourg, diss, 127 p

Favorskaya M (1977) Metallogeny of deep lineaments and new global tectonics, Mineral Deposita, 12, pp 163–169

Feather CE (1976) Studies on the mineralogy and geochemistry of the Witwatersrand Super-Group, PhD Thesis, Univ Cape Town, (unpubl)

Feather CE (1981) Some aspects of Witwatersrand mineralization with special reference to uranium minerals, *in*: Genesis of uranim- and gold-bearing Precambrian quartz-pebble conglomerates, US Geol Surv Prof Papers 1161-A-BB, Q1–Q23

Feather CE, Glatthaar CW (1987) A review of uranium-bearing minerals in the Dominion and Witwatersrand placers, *in*: Uranium deposits in Proterozoic quartz-pebble conglomerates, TECDOC-427, IAEA, Vienna, pp 355–386

Feather CE, Snegg JA (1987) The role of brannerite in the recovery of uranium from Witwatersrand reefs, Trans Geol Soc S Afr, v 81, pp 255–260

Feather CE, Koen GM (1975) The mineralogy of the Witwatersrand reefs, Miner Sci Eng, v 7, pp 189–224

Fehn U, Cathles LM, Holland HD (1978) Hydrothermal convection and uranium deposits in abnormally radioactive plutons, Econ Geol, v 73, pp 1556–1566

Ferguson J (1980) Metamorphism in the Pine Creek Geosyncline and its bearing on stratigraphic correlations, *in*: Ferguson J, Goleby AB, eds., Uranium in the Pine Creek Geosyncline, IAEA, Vienna, pp 91–100

Ferguson J ed. (1984a) Proterozoic unconformity and stratabound uranium deposits, TECDOC-315, IAEA, Vienna, 338 p

Ferguson J (1984b) Epilogue *in*: Ferguson J, ed., Proterozoic unconformity and stratabound uranium deposits, TECDOC-315, IAEA, *Vienna*, pp 325–338

Ferguson J (1987) The distribution of uranium in space and time, Uranium, v 3, pp 131–144

Ferguson J (1988) The uranium cycle, *in*: Recognition of uranium provinces, IAEA, Vienna, pp 3–16

Ferguson J, Goleby AB eds., (1980) Uranium in the Pine Creek Geosyncline, IAEA, Vienna, 760 p

Ferguson J, Rowntree JC (1980) Vein-type uranium deposits in Proterozoic rocks, Rev Inst Français Pétrole 35, pp 485–496

Ferguson J, Winer P (1980) Pine Creek Geosyncline, statistical treatment of whole rock chemical data, *in*: Ferguson J, Goleby AB, eds., Uranium in the Pine Creek Geosyncline, IAEA, Vienna, pp 191–208

Ferguson J, Ewers GR, Donnelly TH (1980b) Model for the development of economic uranium mineralization in the Alligator Rivers Uranium Field, *in*: Ferguson J, Goleby AB, eds., Uranium in the Pine Creek Geosyncline, IAEA, Vienna, pp 563–574

Ferguson J, Chappell BW, Goleby AB (1980a) Granitoids in the Pine Creek Geosyncline, *in*: Ferguson J, Goleby AB, eds., Uranium in the Pine Creek Geosyncline, IAEA, Vienna, pp 73–90

Fernandez Polo JA (1970) Genesis de los yacimientos uraniferos en metasedimentos de Salamanca (España), *in*: Uranium exploration geology, IAEA, Vienna, pp 242–252

Ferris CS, Ruud CO (1971) Brannerite: Its occurrences and recognition by microprobe, Colorado School Mines Quarterly, v 66, pp 1–35

Fiebiger W (1976) Präkambrische Itabirite und Uran-Gold-Konglomerate als geochemische Zeitmarken in der Erdrevolution, Geol Rundsch, Bd 65, pp 1035–1055

Files FG (1970) Geology and alteration associated with Wyoming uranium deposits, Univ California, Berkeley, PhD diss, 113 p

Finch WI (1959) Geology of uranium deposits in Triassic rocks of the Colorado Plateau region, US Geol Surv Bull 1074-D, 164 p

Finch WI (1967) Geology of epigenetic uranium deposits in sandstone in the United States, US Geol Surv Prof Paper 538, 121 p

Finch WI, ed. (1985a) Geological environments of sandstone-type uranium deposits, TECDOC-328, IAEA, Vienna, 408 p

Finch WI (1985b) Sandstone-type uranium deposits – summary and conclusions, *in*: Geological environments of sandstone-type uranium deposits, TECDOC-328, IAEA, Vienna, pp 401–408

Finch WI (1987) A synthesis of genetic models for major types of uranium deposits in the United States, (abstr) Technical Committee Meeting on Uranium Resources and Geology of North America, IAEA Meeting, Saskatoon, 2 p

Finch WI, Davis JF (1985) Sandstone-type uranium deposits – an introduction, *in*: Geological environments of sandstone-type uranium deposits, TECDOC-328, IAEA, Vienna, pp 11–20

Finch WI, Granger HC, Lupe RD, McCammon RB, (1980) Research on interactive genetic-geologic models to evaluate favorability for undiscovered uranium resources, *in*: Uranium evaluation and mining techniques, IAEA, Vienna, pp 447–462

Finnell TL, Franks PC, Hubbard HA (1963) Geology, ore deposits, and exploration drilling in the Deer Flats area, White Canyon district, San Juan County, Utah, US Geol Surv Bull 1132

Fischer RP (1947) Deposits of vanadium-bearing sandstone, *in*: Vanderwilt JW, ed., Mineral resources of Colorado, Denver, State Colorado Miner Res Board, pp 451–456

Fischer RP (1950) Uranium-bearing sandstone deposits of the Colorado Plateau, Econ Geol, v 45, pp 1–11

Fischer RP (1957) Localization and origin of the vanadium-uranium deposits on the Colorado Plateau, US-AEC, TEI-690, pp 383–389

Fischer RP (1959) Vanadium and uranium in rocks and ore deposits, *in*: Garrels RM, Larsen ES, III, Compilers, Geochemistry and mineralogy of the Colorado Plateau uranium ores, US Geol Surv Prof Paper 320, pp 219–230

Fischer RP (1960) Vanadium-uranium deposits of the Rifle Creek area, Garfield County, Colorado, US Geol Surv Bull 1101, 52 p

Fischer RP (1968) The uranium and vanadium deposits of the Colorado Plateau region, *in*: Ridge JD, ed., Ore deposits of the United States, 1933–1967 (Graton-Sales volume), Amer Inst Min Met Petrol Eng, v 1, pp 735–746

Fischer RP (1970) Similarities, differences and some genetic problems of the Wyoming and Colorado Plateau types of uranium deposits in sandstone, Econ Geol, v 65, pp 778–784

Fischer RP (1974) Exploration guides to new uranium districts and belts, Econ Geol, v 69, pp 362–376

Fischer RP, Hilpert LS (1952) Geology of the Uravan mineral belt, US Geol Surv Bull 988-A, pp 1–13

Fischer RP, Stewart JH (1960) Distribution and lithologic characteristics of sandstone beds that contain deposits of copper, vanadium, and uranium, *in*: Geological Survey research 1960, US Geol Surv Prof Paper 400-B, pp 42–44

Fischer RP, Stewart JH (1961) Copper, vanadium, and uranium deposits in sandstone – their distribution and geochemical cycles, Econ Geol, v 56, pp 509–520

Fisher JC (1976) Remote sensing applied to exploration for vein-type uranium deposits, Front Range, Colorado, Colorado School Mines, Remote Sensing Rep 76–2, 157 p

Fisher WI, Proctor CV, Jr, Galloway WE, Nagle JS (1970) Depositional systems in the Jackson Group of Texas – their relationship to oil, gas and uranium, Gulf Coast Ass Geol Soc Trans, v 20, pp 234–261

Fishman NS, Reynolds RL (1986) Origin of the Mariano Lake uranium deposit, McKinley County, New Mexico, *in*: Turner-Peterson CE, Santos ES, Fishman NS, eds., A basin analysis case study – The Morrison Formation, Grants Uranium Region New Mexico, Amer Ass Petrol Geol, Studies in Geology, no. 22, pp 211–226

Fishman NS, Turner-Peterson CE, Reynolds RL (1984) Alteration of magnetite and ilmenite in Upper Jurassic Morrison Formation, San Juan basin, New Mexico: Relationship to facies and primary uranium mineralization, Amer Ass Petrol Geol Bull, v 68, p 936

Fitch DC (1980) Exploration for uranium deposits, Grants mineral belt, *in*: Rautman CA, ed., Geology and mineral technology of the Grants Uranium Region 1979, New Mex Bur Mines Mineral Res Mem 38, pp 40–51

Flageollet JC (1976) Formations superficielles et reliefs d'érosion différentielle dans les massifs anciens cristallins: l'exemple du Limousin et de la Vendée du Nord-Ouest, Sci Terre Mém, Fr, 35, 461 p

Flageollet JC, Magne R (1969) Observations géomorphologiques dans un massif uranifère (St Sylvestre, Limousin, France), Sci Terre, 14, pp 383–409

Fleck H, Haldane WG (1907) A study of the uranium and vanadium belts of southern Colorado, Colorado Bur Mines Twelfth Biennial Rep, 47 p

Flehoc C, Palacin P, Villemant B, Semet M (1989) Uranium enrichment processes in the petrogenesis of Vico volcanites; fission track, uranium isotope, disequilibrium and halogene concentration study, *in*: Metallogenesis of uranium deposits, IAEA, Vienna, pp 153–168

Fogwill WD (1985) Canadian and Saskatchewan uranium deposits: compilation, metallogeny, models, exploration, *in*: Sibbald, TII, Petruk W, eds., Geology of uranium deposits, CIM Spec Vol. 32, pp 3–19

Forhan R (1977) Grade control in underground mines, Grants mineral belt, New Mexico, *in*: Kim YS, ed., Uranium mining technology, Univ Nevada, Reno, 46 p

Forman JMA, Angeiras AG (1981) Poços de Caldas and Itataia: two case histories of uranium exploration in Brazil, *in*: Uranium exploration case histories, IAEA, Vienna, pp 99–140

Foster JF, Quintanar RJ (1980) An anomalous ore body within the Ambrosia Lake trend at the Sandstone Mine, *in*: Rautman CA, ed., Geology and mineral technology of the Grants Uranium Region 1979, New Mex Bur Mines Mineral Res Mem 38, pp 240–243

Fouques JR, Fowler M, Knipping HD, Schimann K (1986a) The Cigar Lake uranium deposit: discovery and general characteristics, *in*: Evans EL, ed., Uranium deposits of Canada, CIM Spec Vol. 33, pp 218–229

Fouques JP, Fowler M, Knipping HD, Schimann K (1986b) Le gisement d'uranium de Cigar Lake: découverte et caractéristiques générales, CIM Bull, v 79, no. 886, pp 70–82

Four Corners Geological Society (1969) Geology and natural history of the Grand Canyon region, Ninth Field Conf, Guidebook, Powell Centennial River Expedition, 212 p

Fourel E, Lancelot JR, Allegre CJ, Dupre B (1988) Isotopic analyses of uraniferous minerals by both U-Pb and Sm-Nd methods, (abstr), Chem Geol, Spec Issue, v 70, no. 1/2, p 134

Fowler AD, Doig R (1979) Origin of uraniferous granitoids, Grenville Province, Quebec and Ontario, (abstr), Ann Mtg Geol Ass Can, Miner Ass Can, v 4, p 50

Foy MF, Pedersen CP (1975) The Koongarra uranium deposit, *in*: Knight, CL, ed., Economic geology of Australia and Papua New Guinea, 1. Metals, AIMM Monograph 5, pp 317–321

Fralick PW, Miall AD (1982) Sedimentology of Huronian deposits, including uranium-bearing rocks, Ont, Geol Surv OFR ep. 5375, 28 p

François A (1974) Stratigraphie tectonique et minéralisations dans l'arc cuprifères du Shaba, *in*: Bartholomé P, ed., Gisements stratiformes et provinces cuprifères, Centenaire Soc Géol Belgique, pp 79–101

Frarey MJ, Roscoe SM (1970) Symposium on basins and geosynclines of the Canadian Shield, Geol Surv Can Pap 70–40, pp 151–153

Fraser JA (1954) Crackingstone, Saskatchewan; Geol Surv Can Paper 54–8

Fraser JA, Robinson SC (1954) Preliminary description of the geology and mineralogy of the Gunnar deposit, Saskatchewan, Can Min J, v 75, pp 59–62

Fraser JA, Donaldson JA, Fahrig WF, Tremblay LP (1970) Helikian basins and geosynclines of the northwestern Canadian Shield, *in*: Symposium on basins and geosynclines of the Canadian Shield, Geol Surv Can Paper 70–40, pp 213–238

Fraser WJ (1980) Geology and exploration of the Rum Jungle Uranium Field, *in*: Ferguson J, Goleby AB, eds., Uranium in the Pine Creek Geosyncline, IAEA, Vienna, pp 287–298

French RR, Allen JH (1984) Lake Way uranium deposit, Wiluna, Western Australia, *in*: Surficial uranium deposits, TECDOC-322, IAEA, Vienna, pp 149–156

Frey M (1981) Lagerstättenkundliche Untersuchungen an einigen Profilen der Intermediate Reefs der Witwatersrand Supergruppe, Welkom Goldfeld, Südafrika, unpubl diploma thesis, Univ Köln, 114 p

Frey M, Saager R, Buck S (1987) 'Heavy mineral distribution and geochemistry related to sedimentary facies variation within the uraniferous intermediate reefs placers, Witwatersrand Supergroup, South Africa, *in*: Uranium deposits in Proterozoic quartz-pebble conglomerates, TECDOC-427, IAEA, Vienna, pp 313–334

Friedrich M (1981) Pétrographie et géochimie des granites de St Jouvent et de la Brâme – Relations avec la distribution de l'uraninite, Massif de St Sylvestre, France, CREGU (Cent Rech Géol Uranium), Vandoeuvre-lès-Nancy, Rep no. 81–2, 50 p

Friedrich M (1984) Le complexe granitique hyperalumineux de St Sylvestre (Nord-Ouest du Massif Central Français), Géol Géochim Uranium, Mém Nancy, no. 5, 361 p

Friedrich M, Cuney M (1983) Cristallisation de l'uraninite et polygénisme dans le complexe granitique de St Jouvent, Brâme, St Sylvestre (Limousin), CR Acad, Sci, Paris, 296, pp 1249–1252

Friedrich M, Cuney M (1989) Uranium enrichment processes in peraluminous magmatism, *in*: Uranium deposits in magmatic and metamorphic rocks, IAEA, Vienna, pp 11–36

Friedrich M, Cuney M, Poty B (1987) Uranium geochemistry in peraluminous leucogranites, *in*: Concentration mechanisms of uranium in geological environments – a conference report, Uranium, v 3, pp 353–385

Fritsche R (1986) Natrium-Metasomatose und Urananreicherung am Beispiel Kitongo-Granit/Kamerun und vergleichbare Uranvorkommen, unveröffentlichte Dissertation, Univ Heidelberg, 190 p

Fritsche R, Amstutz GC, Dahlkamp FJ (1988) Primäre Uranerzminerale und ihre lagerstättengenetische Stellung, Deutsche Forschungsgemeinschaft, final report, DFG Project Am 23/65, 212 p

Fritsche R, Dahlkamp FJ, Amstutz GC Composition of uranium oxide phases and related genetic implications, in press

Frondel JW et al. (1967) Glossary of uranium- and thorium-bearing minerals, 4th edition, US Geol Suiv Bull 1250, 69 p

Frondel C (1958) Systematic mineralogy of uranium and thorium, US Geol Surv Bull 1064, 400 p

Fryer BJ (1977) Geochemistry of Early Proterozoic paleosols, north of Lake Huron, Ontario, Geological Abstracts and Proceedings, 25th annual meeting, Lake Superior Conf

Fryer BJ, Taylor RP (1984) Sm/Nd direct dating of the Collins Bay hydrothermal uranium deposit, Saskatchewan, Geology, v 12, pp 479–482

Fuchs HD, Hilger W (1989) Kiggavik (Lone Gull): an unconformity related uranium deposit in the Thelon Basin, Northwest Territories, Canada, *in*: Uranium resources and geology of North America, TECDOC-500, IAEA, Vienna, pp 429–454

Fuchs HD, da Fonte J, Suckau V, Thakur V (1981) The Espinharas uranium occurrence, Brazil, *in*: Uranium exploration case histories, IAEA, Vienna, pp 3–13

Fuchs YA (1989) Hydrothermal alteration at the Novazza volcanic field; Relation to the U-Mo-Zn Novazza deposit, northern Italy, *in*: Metallogenesis of uranium deposits, IAEA, Vienna, pp 137–152

Fuller AO (1958) A contribution to the petrology of the Witwatersrand System, Trans Geol Soc S Africa, v 61, pp 19–45

Fuzikawa K (1982) Fluid inclusion and oxygen isotope studies of the Nabarlek uranium deposit, Northern Territory, Australia, PhD thesis, Adelaide Univ, (unpubl), 226 p

Fyfe WS (1979) The geochemical cycle of uranium, Phil Trans Royal Soc, A 291, pp 433–445

Gabelman JW (1970a) Metallotectonic control over uranium distribution, *in*: Uranium exploration geology, IAEA, Vienna, pp 187–204

Gabelman JW (1970b) Speculations on the uranium ore fluid, *in*: Uranium exploration geology, IAEA, Vienna, pp 315–330

Gabelman JW (1977a) Migration of uranium and thorium-exploration significance, Amer Ass Petrol Geolog, 168 p

Gabelman JW (1977b) Orogenic and taphrogenic uranium concentration, *in*: Recognition and evaluation of uraniferous areas, IAEA, Vienna, pp 109–121

Gabelman JW (1984) Magmatic rocks vs rest fluids as source of uranium fluids, *in*: Wauschkuhn A, Kluth C, Zimmermann RA, eds., Syngenesis and epigenesis in the formation of mineral deposits, Springer, Berlin, pp 519–536

Gabelman JW, Krusiewski SV (1964) Zonal distribution of uranium deposits in Wyoming, USA, 22nd Intern Geol Congr, New Delhi, India, pt. 5, pp 661–672

Gabelman JW, Young RC, Ealy GK (1956) Uranium-Ambrosla Lake-New Mexico's newest bonanza, Mines Mag, v 46, no. 3, pp 58–64

Galer SJG, O'Nions RK (1985) Residence time of thorium, uranium and lead in the mantle with implications for mantle convection, Nature, 316, pp 778–782

Galloway WE (1977) Catahoula Formation of the Texas coastal plain: Depositional systems, composition, structural development, groundwater flow history, and uranium distribution, Univ Texas, Austin, Bur Econ Geol Rep 87, 59 p

Galloway WE (1978) Morrison Formation – Colorado Plateau, *in*: Galloway WE, Kreitler CW, McGowen JH, eds., Depositional and ground-water flow systems in the exploration for uranium, Univ Texas, Austin, Bur Econ Geol, pp 214–228

Galloway WE (1979) Jackson and Catahoula systems of the Texas Gulf coastal plain, *in*: Depositional and groundwater flow systems in the exploration for uranium, Univ Texas, Austin, Bur Econ Geol, pp 181–213

Galloway WE (1979a) Fluvial depositional systems, *in*: Depositional and ground-water flow systems in the exploration for uranium, Univ Texas, Austin, Bur Econ Geol, pp 13–42

Galloway WE (1979b) Early Tertiary-Wyoming intermontane basins, *in*: Depositional and ground-water flow systems in the exploration for uranium, Univ Texas, Austin, Bur Econ Geol, pp 197–213

Galloway WE (1979c) Morrison Formation of the Colorado Plateau, *in*: Galloway WE, Kreitler CW, McGowen JH, Depositional and ground-water flow systems in the exploration for uranium, Univ Texas, Austin, Bur Econ Geol, pp 214–228

Galloway WE (1980) Deposition and early hydrologic evolution of the Westwater Canyon wet alluvial fan system, *in*: Rautman CA, ed., Geology and mineral technology of the Grants Uranium Region 1979, New Mex Bur Mines Mineral Res Mem 38, pp 59–69

Galloway WE (1982) Epigenetic zonation and fluid flow history of uranium-bearing fluvial aquifer systems, south Texas uranium province, Univ Texas, Austin, Bur Econ Geol Rep Invest no. 119, 31 p

Galloway WE (1985) The depositional and hydrogeologic environment of Tertiary uranium deposits, south Texas uranium province, *in*: Geological environments of sandstone type uranium deposits, TECDOC-328, IAEA, Vienna, pp 215–228

Galloway WE, Kaiser WR (1979) Catahoula Formation of the Texas coastal plain: origin, geochemical evolution and characteristics of uranium deposits, US-DOE, GJBX-131(79), 139 p

Galloway WE, Kaiser WR (1980) Catahoula Formation of the Texas coastal plain: origin, geochemical evolution, and characteristics of uranium deposits, Univ Texas, Austin, Bur Econ Geol Rep Invest no. 100, 81 p

Galloway WE, Finley RJ, Henry CD (1979a) South Texas uranium province geologic perspective, Univ Texas, Austin, Bur Econ Geol Guidebook 18, 81 p

Galloway, WE, Kreitler CW, McGowen JH (1979b) Depositional and ground-water flow systems in the exploration for uranium – a research colloquium, Univ Texas, Austin, Bur Econ Geol, 267 p

Galloway WE, Henry CD, Smith GE (1982) Depositional framework, hydrostratigraphy, and uranium mineralization of the Oakville Sandstone (Miocene), Texas coastal plain, Univ Texas, Austin, Bur Econ Geol Rep Invest no. 113, 51 p

Gamble D (1984) The Lake Raeside uranium deposit, *in*: Surficial uranium deposits, TECDOC-322, IAEA, Vienna, pp 141–148

Gancarz AJ (1979) Chronology of the Cluff Lake uranium deposit, Intern Uranium Symp Pine Creek Geosyncline, Sydney, Australia, Extended Abstracts, pp 91–94

Gandhi SS (1983) Age and origin of pitchblende from the Gunnar deposit, Saskatchewan, *in*: Current research, Part B, Geol Surv Can Paper 83–1B, pp 291–297

Gandhi SS (1986) Uranium in Early Proterozoic Aillik Group, Labrador, *in*: Evans EL, ed., Uranium deposits of Canada, CIM Spec Vol. 33, pp 70–82

Gangloff A (1970) Notes sommaires sur la géologie des principaux districts uranifères étudiés par le CEA, *in*: Uranium exploration geology, IAEA, Vienna, pp 77–105

Garner LE, St. Clair AE, and Evans TJ (1979) Mineral resources of Texas, Univ Texas, Austin, Bur Econ Geol, scale 1:1,000,000

Garrels RM (1955) Some thermodynamic relations among the uranium oxides and their relation to the oxidation states of the uranium ores of the Colorado Plateau, Amer Miner, v 40, no. 11–12, pp 1004–1021

Garrels RM (1957) Geochemistry of "sandstone-type" uranium deposits, *in*: Advances in nuclear engineering, Pergamon Press, New York, v 2, pp 288–293

Garrels RM (1960) Mineral equilibria, Harper and Brothers, New York, 254 p

Garrels RM, Christ CL (1959) Behavior of uranium minerals during oxidation, US Geol Surv Prof Paper 320, pp 81–89

Garrels RM, Christ CL (1965) Solutions, minerals, and equilibria, Harper and Row, New York, 450 p

Garrels RM, Larsen ES, III (1959) Geochemistry and mineralogy of the Colorado Plateau uranium ores, US Geol Surv Prof Paper 320, 236 p

Gashnig J (1980) Development of uranium exploration models for the prospector consultant system: Menlo Park, California, SRI Intern Proj 7856, 603 p

Gaskin AJ, Butt CRM, Deutscher RL, Horwitz RC, Mann AW (1981) Hydrology of uranium deposits in calcretes of Western Australia, *in*: Halbouty MT, ed., Energy resources of the Pacific region, Amer Ass Petrol Geol, Studies in Geology 12, pp 311–316

Gatzweiler R, Lehnert-Thiel K, Clasen D, Tan B, Voultsidis V, Strnad JG, Rich J (1979) The Key Lake uranium-nickel deposits, CIM Bull, v 72, pp 73–79

Gauthier-Lafaye F (1977) Oklo et les gisements d'uranium du Franceville: Aspects tectonique et métallogénique Univ Strasbourg doctoral dissertation, 92 p

Gauthier-Lafaye F, Ruhland M, Weber F (1975) Analyse tectonique du gisement d'Oklo, *in*: The Oklo phenomenon, IAEA, Vienna, pp 103–118

Gauthier-Lafaye F, Weber F, Naudet R, Pfiffelmann JP, Chauvet R, Michel B, Reboul JC (1980) Le gisement d'Oklo et ses réacteurs de fission naturels, *in*: Ferguson J, Goleby AB, eds., Uranium in the Pine Creek Geosyncline, IAEA, Vienna, pp 663–673

Gay AL, Grandstaff DE (1980) Chemistry and mineralogy of Precambrian paleosols at Elliot Lake, Ontario, Canada, Precamb Res, 12, pp 349–373

Geddes WP (1983) The uranium and nuclear industries in China, Resources Policy, Dec, pp 235–251

Gee, RD (1976) Tectonic divisions of the Yilgarn Block, *in*: Smith RE, Butt CRM, Bettenay E, eds., Superficial mineral deposits and exploration geochemistry, Yilgarn Block, Western Australia, Excursion Guide No. 41C, 25th Intern Geol Congr, Sydney, Australia, pp 1–5

Geoffroy J (1973) Les gites uranifères dans le Massif Central français, *in*: Géologie, géomorphologie et structure profonde du Massif Central français, Symposium J. Jung, 1971, Plein Air Service Edit., Clermont-Ferrand, pp 541–579

Geffroy J (1975) Étude microscopique des minerais uranifères d'Oklo, *in*: The Oklo phenomenon, IAEA, Vienna, pp 133–151

Geffroy J, Sarcia JA (1955) Contribution à l'étude des pechblendes françaises, Rapport CEA no. 380, 157 p, (Sci. Terre, 2, 1954 157 p)

Geffroy J, Sarcia JA (1958) La notion de gite epithermal uranifère et les problems qu'elle pose, Bull Soc Geol France, 6 e serie VIII, pp 173–190

Geffroy J, Sarcia JA (1960) Les minerais noirs, *in*: Roubault M, ed., Les minerais uraniferes français, v. 1, PUF Ed., Paris, pp 1–68

Geffroy J, Cesbron F, Lafforgue P (1964) Donnée préliminaire sur les constituants profonds des minerais uranifères et vanadifères de Mounana (République Gabonaise), Comité National Français de Géodesie et Géophysique, Comptes Rendus, v. 259, pp 601–603

Gentry RV, Christie W, Smith D, Emery J, Reynolds S, Christy S, Gentry P (1976) Radiohalos in coalified wood: New evidence relating to time of uranium introduction and coalification, Science, v 198, pp 315–317

George E (1985) Les minéralisations uranifères jurassiques liées spatialement à une discordance hercynienne. Pétrographie, minéralogie, et géochimie des gisements du Rouergue (Aveyron, France), Géol Géochim Uranium, Mém, Nancy, no. 9, 219 p

George E, Pagel M, Dusausoy Y, Gauthier JM (1986) Formation conditions of a tetragonal uranium oxide: αU_3O_7 in the Brousse Broquiès basin (Aveyron France), Uranium, 3, pp 69–89

George-Aniel B, Leroy J, Poty B (1985) Uranium deposits of the Sierra Peña Blanca: Three examples of mechanisms of ore deposit formation in a volcanic environment, *in*: Uranium deposits in volcanic rocks, IAEA, Vienna, pp 175–186

Gerasimovsky VI (1956) Mineralogical characteristics of uranium deposition in the oxidized zone of the Shinkolobwe ore deposits, Geochem, no. 7, pp 722–727

Gerasimovskiy VI (1957) Occurrence of uranium in different rocks, Sov Atom Energy, v 3, pp 525–529

Getseva RV, (1963) Some data on behavior of uranium during metamorphism, *in*: Problems of applied radiogeology, Moscow, pp 208–227

Giblin AM, Snelling AA (1983) Application of hydrogeochemistry to uranium exploration in the Pine Creek Geosyncline, Northern Territory, Australia, J Geochem Explor, 19, pp 33–55

Giere R (1986) Zirconolite, allanite and hoegbomite in a marble skarn from the Bergell contact aureole: implications for mobility of Ti, Zr, and REE, Contrib Miner Petrol, 93, pp 459–470

Giese P (1983) Die Europäische Geotraverse (EGT), Mitt XIII Geokommission, pp 29–50

Gilboy CF (1977) Reconnaissance geology: Cree Lake south area. (Part of NTS area 74G), *in*: Christopher JE, Macdonald J, eds., Summary of investigations 1977, Sask Geol Surv, pp 21–29

Gilboy CF (1982) Geology of an area around Rottenstone and Dobbin Lakes, Part of NTS area 74A, Rep 193, Sask Miner Res, Regina

Gilboy CF, Lewry JF, Ray GE, Sibbald TII (1976) Rb/Sr dating of rocks from the Wollaston Lake Belt, Saskatchewan: Discussion, Can J Earth Sci, v 13, pp 1643–1645

Glatthaar CW, Feather CE (1984) Predicting the hydrometallurgical recovery of uranium by mineralogical mass balance study of the uranium-bearing minerals in Dominion Reef, South Africa, Intern Conf Appl Miner (ICAM84), Los Angeles, (manuscript)

Goddard CC (1987) Geology of paleosols at the lower Huronian Archean unconformity – Elliot Lake, Ontario, unpubl BSc Thesis, Mt Allison Univ, Sackville NB, 128 p

Goddard CC, Mossman DJ (1988) Geology of Precambrian paleosols at the base of the Huronian Supergroup, Elliot Lake, Ontario, Canada, (manuscript 36 p)

Goldhaber MB (1983) Experimental study of metastable sulfur oxy-anion formation during pyrite oxidation at pH 6–9 and 30°C, Am J Sci, v 283, pp 193–217

Goldhaber MB, Reynolds RL (1979) Origin of marcasite and its implications regarding the genesis of roll-front uranium deposits, US Geol Surv Rep 79–1696, 38 p

Goldhaber MB, Reynolds RL, Rye RO (1978) Origin of a south Texas roll-type uranium deposit: II. Sulfide petrology and sulfur isotope studies, Econ Geol, v 73, pp 1690–1705

Goldhaber MB, Reynolds RL, Rye RO (1979) Formation and resulfidization of a south Texas roll-type uranium deposit, US Geol Surv Rep 79–1651, 41 p

Goldhaber MB, Reynolds RL, Campbell JA, Wanty RB, Grauch RI, Northrop HR (1983?) Genesis of the Tony M tabular-type vanadium-uranium deposit, Henry structural basin, Utah: Mechanisms of ore and gangue mineral formation at the interface between brine and meteoric water (manuscript)

Goldhaber MB, Hemingway BS, Mohagheghi A, Reynolds RL (1987) Origin of coffinite in sedimentary rocks by a sequential adsorption-reduction mechanism, Bull Miner, v 110, pp 131–144

Goldschmidt VM (1911) Die Kontaktmetasomatose im Kristianiagebiet, Krist Vidensk Skr I, Math-nat, Kl 1, pp 193–224

Goldschmidt VM (1914) Uber einen Fall von Natriumzufuhr bei Kontaktmetasomatose, N Jb Miner, Bl-Bd 39, pp 193–224

Gomez P, Josa J, Membrillera J, Otero J, Serrano J (1977) Mining and processing of uranium deposits in Salamanca (Spain), *in*: Geology, mining and extractive processing of uranium, IMM, London, pp 103–108

Goodell PC (1985a) Classification and model of uranium deposits in volcanic environments, *in*: Uranium deposits in volcanic rocks, IAEA, Vienna, pp 1–16

Goodell PC (1985b) Chihuahua City uranium province, Chihuahua, Mexico, *in*: Uranium deposits in volcanic rocks, IAEA Vienna, pp 97–124

Goodell PC, Trentham RC (1980) Experimental leaching of uranium from tuffaceous rocks, US-DOE, GJBX-148(80), 144 p

Goodell PC, Waters AC eds., (1981) Uranium in volcanic and volcanoclastic rocks, Amer Ass Petrol Geol, Studies in Geology no. 13

Goodell PC, Trentham R, Carraway K (1979) Geologic setting of the Peña Blanca uranium deposits, Chihuahua, Mexico: Chap. IX, *in*: Henry CD, Walton AW, eds., Formation of uranium ores by diagenesis of volcanic sediments, US-DOE, GJBX-22(79), 38 p

Goodwin AM, Ambrose JW, Ayers LD, Clifford PM, Curie KL, Ermanovics IM, Fahrig WF, Gibb RA, Hall DH, Innes MJS, Irvine TN, Maclaren AS, Norris AW, Pettijohn FJ (1972) The Superior Province, *in*: Price RA, Douglas RJW, eds. Variations in tectonic styles in Canada, Geol Ass Can Spec Paper 11, pp 527–623

Gorbunova LM (1974) Uranium in metamorphic rocks in the northwestern part of the Kola Peninsula, J Leningrad Min Inst, v 44, no. 2, pp 97–104

Gornitz VM (1969) Mineralization, alteration, and mechanism of emplacement, Orphan ore deposit, Grand Canyon, Arizona, New York, Columbia Univ, PhD diss, 186 p

Gornitz VM, Kerr PF (1970) Uranium mineralization and alteration, Orphan mine, Grand Canyon, Arizona, Econ Geol, v 65, pp 751–768

Gosnold WD (1976) A model for uranium and thorium assimilation by intrusive magmas and crystallizing plutons through interaction with crustal fluids, PhD thesis, Southern Methodist Univ, 131 p

Gotman YaD, Zubrev IN (1965) Genetic classification of uranium deposits, Intern Geol Rev, v 7, no. 3, pp 518–525

Gould W, Smith RB, Metzger SP, Melancon PE (1963) Geology of the Homestake-Sapin uranium deposits, Ambrosia Lake area, *in*: Kelley, VC, ed., Geology and technology of the Grants Uranium Region, New Mex Bur Mines Mineral Res Mem 15, pp 66–71

Goulevitch J (1980) Stratigraphy of the Kapalga Formation in the Pine Creek Area and its relationship to base metal mineralization, *in*: Ferguson J, Goleby AB, eds, Uranium in the Pine Creek Geosyncline, IAEA, Vienna, pp 307–318

Grandstaff DR (1973) Kinetics of uraninite oxidation: implications for the Precambrian atmosphere, Princeton Univ, PhD thesis, 153 p

Grandstaff DE (1974a) Uraninite oxidation and the Precambrian atmosphere (abstr), Trans Amer Geophys Union, v 55, p 457

Grandstaff DE (1974b) Microprobe analyses of uranium and thorium in uraninite from the Witwatersrand, South Africa, and Blind River, Ontario, Canada, Trans Geol Soc S Afr, v 77, pp 291–294

Grandstaff DE (1976) A kinetic study of the dissolution of uraninite, Econ Geol, v 71, pp 1493–1505

Grandstaff DE (1980) Origin of uraniferous conglomerates at Elliot Lake, Canada and Witwatersrand, South Africa: Implications for oxygen in Precambrian atmosphere, Precamb Res, v 13, pp 1–26

Grandstaff DE, Edelman MJ, Foster RW, Zbinden E, Kimberley MM (1986) Chemistry and mineralogy of Precambrian paleosols at the base of the Dominion and Pongola Groups (Transvaal, South Africa), Precamb Res, v 32, pp 97–131

Granger HC (1963) Mineralogy, *in*: Kelley VC, ed., Geology and technology of the Grants Uranium Region, New Mex Bur Mines Mineral Res Mem 15, pp 21–37

Granger HC (1968) Localization and control of uranium deposits in the southern San Juan Basin Mineral Belt, New Mexico – an hypothesis, US Geol Surv Prof Paper 600-B, pp 60–70

Granger HC (1976) Fluid flow and ionic diffusion and their roles in the genesis of sandstone-type uranium ore bodies, US Geol Surv Rep 76–454, 26 p

Granger HC, Finch WI (1988) The Colorado Plateau uranium province, (with contributions by Bromfield CS, Duval JS, Grauch VJS, Green MW, Hills FA, Peterson F, Pierson CT, Sanford RF, Spirakis CS, Wahl RR, *in*: Recognition of uranium provinces, IAEA, Vienna, pp 157–193

Granger HC, Raup RB (1962) Reconnaissance study of uranium deposits in Arizona, US Geol Surv Bull 1147-A, pp 7–12, 18–21

Granger HC, Santos ES (1982) Geology and ore deposits of the Section 23 Mine, Ambrosia Lake district, New Mexico, US Geol Surv Rep OF-82-0207, 74 p

Granger HC, Santos ES (1986) Geology and ore deposits of the Section 23 mine, Ambrosia Lake district, New Mexico, *in*: Turner-Peterson CE, Santos ES, Fishman NS, eds., A basin analysis case study – the Morrison Formation, Grants Uranium Region, New Mexico, Amer Ass Petrol Geol, Studies in Geology no. 22, pp 185–210

Granger HC, Warren CG (1969) Unstable sulfur compounds and the origin of roll-type uranium deposits, Econ Geol, v 64, pp 160–171

Granger HC, Warren CG (1974) Zoning in the altered tongue associated with roll-type uranium deposits, *in*: Formation of uranium ore deposits, IAEA, Vienna, pp 185–199

Granger HC, Warren CG (1978) Some speculations on the genetic geochemistry and hydrology of roll-type uranium deposits, Wyoming Geol Ass, 30th Field Conf Guidebook, pp 349–361

Granger HC, Warren CG (1979) The importance of dissolved free oxygen during formation of sandstone-type uranium deposits, US Geol Surv Rep 79–1603, 21 p

Granger HC, Warren CG (1981) Genetic implications of the geochemistry of vanadium-uranium deposits in the Colorado Plateau region, Amer Ass Petrol Geol, Regional Meeting, Albuquerque, New Mexico, Abstracts with Programs

Granger HC, Santos ES, Dean BG, Moore FB (1961) Sandstone-type uranium deposits at Ambrosia Lake, New Mexico – an interim report, Econ Geol, v 56, pp 1179–1210

Grauch RI (1978) Geology of the uranium prospect at Camp Smith, New York, with a model for the formation of uranium deposits in metamorphosed submarine volcanogenic rocks, US Geol Surv Rep 78–949, 29 p

Grauch RI (1984) Mineralogy and petrology of gold occurrences within the Jabiluka Deposit, NT, Australia, *in*: Abstracts, v IX, Part 1, Intern Geol Congr, Moscow, p 351

Grauch RI (1985) Precambrian submarine volcanogenic uranium deposits: An example from southeastern New York, United States of America, *in*: Uranium deposits in volcanic rocks, IAEA, Vienna, pp 363–364

Grauch RI, Zarinski K (1976) Generalized descriptions of uranium-bearing veins, pegmatites, and disseminations in non-sedimentary rocks, eastern US, US Geol Surv Rep 76–582, 114 p

Grauch RI, Leventhal JS, Harper CT (1984) Organic material from the Cluff Lake (Canada) uranium district, its nature and paragenetic implications of the included mineral assemblages, *in*: Abstracts, v IX, Part 1, 27th Intern Geol Congr, Moscow, pp 351–352

Green MW (1980) Disconformities in the Grants mineral belt and their relationship to uranium deposits, *in*: Rautman CA, ed., Geology and mineral technology of the Grants uranium region 1979, New Mex Bur Mines Mineral Res Mem 38, pp 70–74

Griffith JW (1967) The uranium industry – its history, technology and prospects, Can Dep Energy, Mines, Resources, Mineral Rep 12, 335 p

Griffith JW (1986) Uranium deposits of the Bancroft area, Ontario, *in*: Evans EL, ed., Uranium deposits in Canada, CIM Spec Vol. 33, pp 57–61

Griffith JW, Roscoe SM (1964) Canadian resources of uranium and thorium, Can Dep Mines Techn Surv, MR 77

Gross EB (1956) Mineralogy and paragenesis of the uranium ore, Mi Vida mine, San Juan County, Utah, Econ Geol, v 51, pp 632–648

Group A (1970) Uranium deposits of unusual occurrence, *in*: Uranium exploration geology, IAEA, Vienna, pp 369–374

Gruner JW (1956) Concentration of uranium in sediments by multiple migration-accretion, Econ Geol, v 51, pp 495–520

Gruner JW, et al. (1954) The mineralogy of the "Mi Vida" uranium ore deposits of the Utex Exploration

Company in the Indian Wash area, Utah, US-AEC, Rme-3094, pp 15–27
Grutt EW (1957) Environment of some Wyoming uranium deposits: Advances in nuclear engineering, 2nd Nuclear Eng Sci Conf, Philadelphia, Pennsylvania, v 2, pp 313–323
Grutt EW, Jr (1972) Prospecting criteria for sandstone-type uranium deposits, *in*: Bowie SHU, Davis M, Ostle D, eds., Uranium prospecting handbook, IMM, London, pp 47–77
Gruzdev BI, Rubtsov DM (1972) Accumulation of thorium, uranium and radium by plants and organic horizons of soils, *in*: Verkhovskaya IN, ed., Radio-ecological investigations in the biosphere, Nauka Press, Moscow, pp 112–123
GSA (Geol Soc Amer) Rocky Mountain Section, (Wenrich and Billingsley, eds.) (1986) Abstracts with Programs, v 18, 39th Annual Meeting, Northern Arizona Univ, Flagstaff
Gueniot B (1983) Distribution et modes de fixation de l'uranium dans les grands types de pédogenèses climatiques et stationnelles sur roches cristallines, Géol Géochim Uranium, Mém Nancy, no. 3, 259 p
Guevara EH, Garcia R (1972) Depositional systems and oil-gas reservoirs in the Queen City Formation (Eocene), Texas, Gulf Goast Ass Geol Soc Trans, v 22, pp 1–22
Guineberteau B (1986) Le massif granitique de Mortagne sur Sèvre (Vendée). Structure, gravimétrie, mise en place; distribution de U-Th-K, Géol Géochim Uranium, Mém Nancy, no. 11, 218 p
Gulson BL, Mizon KJ (1980) Lead isotope studies at Jabiluka, *in*: J Ferguson, J Goleby AB, ed., Uranium in the Pine Creek Geosyncline. IAEA, Vienna, pp 439–456
Gupta RK, Perumal NVAS, Sagar S, Upadhyaya LD, Verma HM (1989) Uranium mineralization in some typical igneous-metamorphic environments of India, *in*: Uranium deposits in magmatic and metamorphic rocks, IAEA, Vienna, pp 113–130
Gustafson B (1981) Uranium exploration in the N. Västerbotten – S. Norrbotten province, northern Sweden, *in*: Uranium exploration case histories, IAEA, Vienna, pp 333–352
Gustafsson B, Minell H (1977) Prospecting in areas of glaciated terrain, IMM, London, pp 72–79
Gustafson LB, Curtis LW (1983) Post-Kombolgie metasomatism at Jabiluka, Northern Territory, Australia, and its significance in the formation of high grade uranium mineralization in Lower Proterozoic rocks, Econ Geol, v 78, pp 26–56
Guzman M, Hålenius U, Smellie JAT (1980) Selected uranium mineralizations in the Arjeplog-Arvidsjaur-Sorsele area, Geol För Stockh Förh 102, pp 288–290
Haack U (1983) On the content and vertical distribution of K, Th and U in the continental crust, Earth Planet Sci Lett 62, pp 360–366
Haack U, Gohn E, Hartmann O (1983) Radiogenic heat generation in Damaran rocks, *in*: Miller RMcG, Evolution of the Damara Orogen of South West Africa/Namibia, Geol Soc S Afr Spec Publ II, pp 225–232
Hafen PL, Adams SS, Secor GB (1976), Application of magnetic susceptibility measurements to uranium exploration in sandstones, *in*: Exploration for uranium ore deposits, IAEA, Vienna, pp 367–378
Hahn L (1974) Bericht über eine Reise nach Süd- und Südwest-Afrika im Rahmen des wissenschaftlichen Erfahrungsaustausches der Bundesanstalt für Bodenforschung sowie der Weiterbildung einzelner Mitarbeiter im Hinblick auf die Gutachtertätigkeit bei der Uranprospektion, Bundesanstalt für Bodenforschung, 37 p
Haji-Vassiliou A, Kerr PF (1973) Analytic data on nature of urano-organic deposits, Amer Ass Petrol Geol Bull, v 57, no. 7, pp 1291–1296
Hålenius U, Smellie JAT (1983) Mineralizations of the Arjeplog-Arvidsjaur-Sorsele uranium province, Mineralogical studies of selected uranium occurrences, N Jb Miner, Ab 147.3, pp 229–252
Hålenius U, Smellie JAT, Wilson MR (1986) Uranium genesis within the Arjeplog-Arvidsjaur-Sorsele uranium province, northern Sweden, *in*: Vein type uranium deposits, IAEA, Vienna, TECDOC-361, pp 21–42
Halladay CR (1989) The Swanson uranium deposit, Virginia: a structurally-controlled, albitite deposit, (abstr), *in*: Uranium resources and geology of North America, TECDOC-500, IAEA, Vienna, p 519
Hallbauer DK (1975) The plant origin of the Witwatersrand "carbon", Miner Sci Eng, v 7, pp 111–131
Hallbauer DK (1977) Morphology and microtexture of minerals from fossil gold and uranium placers, Chamber Mines S Afr, Res Rev 1976/77, pp 36–50
Hallbauer DK (1980) Geochemistry and morphology of mineral components from the fossil gold and uranium placers of the Witwatersrand, US Geol Surv Prof Paper 1161-M
Hallbauer DK (1983) Geochemistry and fluid inclusions in detrital minerals as guides to their provenance and distribution, Geol Soc S Afr Spec Publ 7, pp 39–57
Hallbauer DK (1986) The mineralogy and geochemistry of Witwatersrand pyrite, gold, uranium, and carbonaceous matter, *in*: Anhaeusser CR, Maske S, Mineral Deposits of Southern Africa, Geol Soc S Afr, v 1, pp 731–752
Hallbauer DK, Jahns HM, Beltmann HA (1977) Morphological and anatomical observations on some Precambrian plants from the Witwatersrand, South Africa, Geol Rundsch, Bd 66, pp 477–491
Hallbauer DK, Joughin NC (1973) The size distribution and morphology of gold particles in Witwatersrand reefs and their crushed products, J African Inst Min Metal, v 73, pp 395–405
Hallbauer DK, Kable EJD (1982) Fluid inclusions and trace element content of quartz and pyrite pebbles from Witwatersrand conglomerates: their significance with respect to the genesis of primary deposits, *in*: Amstutz et al., eds., Ore Genesis, The state of the art, Springer, Berlin, Heidelberg, New York, pp 742–752
Hallbauer DK, Utter T (1977) Geochemical and morphological characteristics of gold particles from recent river deposits and the fossil placers of the Witwatersrand, Mineral Deposita, 12, pp 293–306
Hallbauer DK, von Warmelo KT (1974) Fossilized plants in thucholite from Precambrian rocks of the Witwatersrand, South Africa, Precamb Res, v 1, pp 199–212
Hallbauer DK, von Gehlen K (1983) The Witwatersrand pyrites and metamorphism, Miner Mag, 47, pp 473–479
Hallbauer DK, Utter T, Hirdes W (1978) Size and com-

position of gold, pyrite, and other sulphides in some Witwatersrand conglomerates, Coal Gold Base Miner SA, v 26, pp 65–79
Halter G, Pagel M, Sheppard MF, Weber F (1989) Alterations in the Carswell structure (Saskatchewan-Canada): petrology, mineralogy and stable isotopes geochemistry, (abstr), *in*: Uranium resources and geology of North America, IAEA, Vienna, pp 357–358
Hambleton-Jones BB (1976) The geology and geochemistry of some epigenetic uranium deposits near the Swakop River, South West Africa, Univ Pretoria, DSc Thesis (unpubl) 306 p
Hambleton-Jones BB (1978) The geology and geochemistry of calcrete-gypcrete uranium deposits in duricrust: Namib desert, Southwest Africa, Econ Geol, 73, pp 1407–1408
Hambleton-Jones BB (1984a) Surficial uranium deposits in Namibia, *in*: Surficial uranium deposits, TECDOC-322, IAEA, Vienna, pp 205–216
Hambleton-Jones BB (1984b) Surficial uranium deposits in South Africa, *in*: Surficial uranium deposits, TECDOC-322, IAEA, Vienna, pp 221–230
Hambleton-Jones BB, Smit MCB (1984) Calculation of the carnotite solubility index, *in*: Surficial uranium deposits, TECDOC-322, IAEA, Vienna, pp 81–86
Hamilton PJ (1976) Isotope and trace element studies of the Great Dyke and Bushveld mafic phase and their relation to early Proterozoic magma genesis in southern Africa, J Petrol, v 12, pp 24–52
Hansen DA (1980) Radiometrics, *in*: Van Blaricom R (compilor), Practical geophysics, Northwest Mining Ass, pp 1–38
Hanshaw BB, Dahl HM (1956) Preliminary fracture study, Smith Lake area, McKinley County, New Mexico, US-AEC, TM-128, 4 p
Hansink JD (1976) Equilibrium analysis of a sandstone roll-front uranium deposit, *in*: Exploration for uranium ore deposits, IAEA, Vienna, pp 683–692
Hansley PL (1984) Feldspar alteration patterns in the Upper Jurassic Morrison Formation, northwestern New Mexico, SEPM, First National Midyear Meeting, Technical Program, p 37
Hansley PL (1986a) Relationship of detrital, nonopaque heavy minerals to diagenesis and provenance of the Morrison Formation, southwestern San Juan Basin, New Mexico, *in*: Turner-Peterson CE, et al., eds., A basin analyses case study: the Morrison Formation, Grants Uranium Region, New Mexico, Amer Ass Petrol Geol, Studies in Geology no. 22, pp 257–276
Hansley PL (1986b) Regional diagenetic trends and uranium mineralization in the Morrison Formation across the Grants Uranium Region, *in*, as 1986a, pp 277–302
Hansuld JA (1966) Behavior of molybdenum in secondary dispersion media, Min Eng, v 18, no. 12, p 75
Han Zheaong, Rong Jiashu, Wang Yanting, Feng Mingyue, Sheng Zhuyong (1985) A possible origin of uranium deposits in granites with special reference to the formation of SL deposit, Geochem, 4, 2, pp 127–140
Hargraves RB (1962) Cross-bedding and ripple-marking in the Main-Bird Series of the Witwatersrand System in the East Rand area, Trans Geol Soc S Afr, v 65, pp 263–275
Hargraves RB (1963) Silver-gold ratios in some Witwatersrand conglomerates, Econ Geol, v 58, pp 952–970
Harlass E, Schützel H (1965) Zur paragenetischen Stellung der Uranpechblende in den hydrothermalen Lagerstätten des westlichen Erzgebirges, Z Angew Geol, v 11, no. 11, pp 569–582
Harmon GF, Taylor PS (1963) Geology and ore deposits of the Sandstone Mine, southeastern Ambrosia Lake area, *in*: Kelley VC, ed., Geology and technology of the Grants Uranium Region, New Mex Bur Mines Mineral Res Mem 15, pp 102–107
Harper CT (1978) Uranium metallogenic studies: Maurice Bay, *in*: Christopher JE, Macdonald R, eds., Summary of investigations 1978, Sask Geol Surv Misc Rep 78–10, pp 74–83
Harper CT, Taylor RP, Fryer BJ (1986) Geology and lithochemistry of the Maurice Bay uranium deposit, northern Saskatchewan, *in*: Evans EL, ed., Uranium deposits of Canada, CIM Spec Vol. 33, pp 241–249
Harris RE (1984) Alteration and mineralization associated with sandstone uranium occurrences, Morton Ranch area, Wyoming, Geol Surv Wyoming, Rep Invest no. 25, 29 p
Harshman EN (1962) Alteration as a guide to uranium ore, Shirley Basin, Wyoming, US Geol Surv Prof Paper 450-D, pp D8–D10
Harshman EN (1966) Genetic implications of some elements associated with uranium deposits, Shirley Basin, Wyoming, US Geol Surv Prof Paper 550-C, pp C167–C173
Harshman EN (1968) Uranium deposits of Wyoming and South Dakota, *in*: Ridge JD, ed., Ore deposits of the United States, 1933–1967 (Graton-Sales volume), Amer Inst Min Metal Petrol Eng, v 1, pp 815–831
Harshman EN (1970) Uranium ore rolls in the United States, *in*: Uranium exploration geology, IAEA, Vienna, pp 219–232
Harshman EN (1972) Geology and uranium deposits, Shirley Basin area, Wyoming, US Geol Surv Prof Paper 745, 82 p
Harshman EN (1974) Distribution of elements in some roll-type uranium deposits, *in*: Formation of uranium ore deposits, IAEA, Vienna, pp 169–183
Harshman EN, Adams SS (1981) Geology and recognition criteria for roll-type uranium deposits in continental sandstones, US-DOE, GJBX-1(81), 185 p
Hatcher PG, Spiker EC, Orem WH, Romankiw LA, Szeverenyi NM, Maciel GE (1986) Organic geochemical studies of uranium-associated organic matter from the San Juan basin: A new approach using solid-state ^{13}C nuclear magnetic resonance, *in*: Turner-Peterson CE, Santos ES, Fishman NS, eds., A basin analysis case study – the Morrison Formation, Grants Uranium Region, New Mexico, Amer Ass Petrol Geol, Studies in Geology no. 22, pp 171–184
Hattori K, Campbell FA, Krouse HR (1981) Stable isotope study on uraniferous conglomerate in Elliot Lake (abstr), Geol Ass Can, Miner Ass Can, Can Geophys Union, Joint Annual Meeting, Calgary, p A24
Hauptman CM (1956) Uranium in the Pryor Mountains area of southern Montana and northern Wyoming, Uranium and Modern Mining, v 3, no. 11, pp 14–21
Hawkesworth CJ, Kramers JD, Miller RMcG (1981) Old model Nd ages in Namibian Pan-African rocks: Nature, London, 289, pp 278–282

Hawley CC, Robeck RC, Dyer HB (1968) Geology, altered rocks, and ore deposits of the San Rafael Swell, Emery County, Utah, US Geol Surv Bull 1239, 115 p

Hazlett GW, Kreek J (1963) Geology and ore deposits of the south-eastern part of the Ambrosia Lake area, *in*: Kelley, VC, ed., Geology and technology of the Grants Uranium Region, New Mex Bur Mines Mineral Res Mem 15, pp 82–89

Heath AG, Deutscher RL, Butt CRM (1980) Lake Austin prospect, Murchison Region, WA, *in*: Butt CRM, Smith RE, eds., Conceptual models in exploration geochemistry, Australia, J Geochem Explor, 12, pp 257–259

Heath AG, Deutscher RL, Butt CRM (1984) Lake Austin uranium deposit, Western Australia, *in*: Surficial uranium deposits, TECDOC-322, IAEA, Vienna, pp 129–132

Hedges MM, Wall VJ, Bloom MS (1984) Hydrothermal transport and deposition of uranium modelling and implications, (abstr), Geol Soc Aust, no. 12, pp 226–227

Hegge MR (1977) Geologic setting and relevant exploration features of the Jabiluka uranium deposits, AIMM Proc 264, pp 19–32

Hegge MR, Rowntree JC (1978) Geologic setting and concepts on the origin of uranium deposits in the East Alligator River region, NT, Australia, Econ Geol, v 73, pp 1420–1429

Hegge MR, Mosher DV, Eupene GS, Anthony PJ (1980) Geologic setting of the East Alligator uranium deposits and prospects, *in*: Ferguson J, Goleby AB, eds., Uranium in the Pine Creek Geosyncline, IAEA, Vienna, pp 259–272

Heier KS (1962a) A note on the U, Th, and K contents in the nepheline syenite and carbonatite on Stjernoy, North Norway, Norsk Geol Tidsskr, 42, pp 287 ff

Heier KS (1962b) Spectrometric uranium and thorium determinations on some high-grade metamorphic rocks on Langöy, Northern Norway, Norsk Geol Tidsskr 42, pp 143 ff

Heier KS (1963) Uranium, thorium, and potassium in eclogitic rocks, Geochim Cosmochim Acta, 27, pp 849 ff

Heier KS (1978) The distribution and re-distribution of heat producing elements in the continents, Philos Trans Royal Soc, London, A288, pp 393–400

Heier KS (1979) The movement of uranium during higher grade metamorphic processes, Phil Trans Royal Soc, London, A291, pp 413–421

Heier KS, Adams JAS (1965) Concentration of radioactive elements in deep crustal material, Geochim Cosmochim Acta, 29, pp 53–61

Heier KS, Carter JL (1964) Uranium, thorium, and potassium contents in basic rocks and their bearing on the nature of the upper mantle, *in*: Adams JAS and Lowder WM eds., The natural radiation environment, Chicago, Chicago Univ Press, pp 75 ff

Heier KS, Rhodes JM (1966) Thorium, uranium and potassium concentrations in granites and gneisses of the Rum Jungle Complex, Northern Territory, Australia, Econ Geol, v 61, pp 563–571

Heier KS, McDougall I, Rogers JJW (1963) Radiometric determination of thorium, uranium and potassium in basalts and in two magmatic differentiation series, Geochim Cosmochim Acta, 27, pp 137 ff

Heier KS, McDougall I, Adams JAS (1964) Th, U and K in Hawaiian lavas, Nature, 201, pp 254 ff

Heine TH (1981) The Rabbit Lake deposit and the Collins Bay deposits, *in*: CIM Geol Div Uranium Field Excursion Guidebook, pp 87–102

Heine TH (1986) The geology of the Rabbit Lake uranium deposit, Saskatchewan, *in*: Evans EL, ed., Uranium deposits of Canada, CIM Spec Vol. 33, pp 134–143

Heinrich EW (1958) Mineralogy and geology of radioactive raw materials, McGraw Hill, New York-Toronto-London, 654 p

Heinrich EW (1982) Hydrothermal alterations of conglomeratic uranium ores at Elliot Lake, Ontario, Canada, *in*: Amstutz et al., eds., Ore genesis, the state of the art, Springer Verlag Berlin, Heidelberg, New York, pp 16–24

Hendry HE, Wheatley KL (1985) The Carswell Formation, Northern Saskatchewan: Stratigraphy sedimentology, and structure, *in*: Lainé R, Alonso D, Svab M, eds., The Carswell Structure uranium deposits (Saskatchewan), Geol Ass Can Spec Paper 29, pp 87–104

Henry CD, Duex TW (1981) Uranium in diagenesis of the Pruett, Duff and Tascotal Formations, Trans Pecos Texas, *in*: Goodell PC, Waters AC, eds., Uranium in volcanic and volcaniclastic rocks, Amer Ass Pet Geol, Stud Geol 13, pp 167–181

Henry CD, Galloway WE, Smith GE, Ho CL, Morton JP, Gluck JK (1982) Geochemistry of ground water in the Oakville Sandstone, a major aquifer and uranium host of the Texas coastal plain, Univ Texas, Austin, Bur Econ Rep Invest no. 118, 63 p

Herring BG (1976) The metamorphism and alteration of the basement rocks in the Carswell circular structure, Saskatchewan, unpubl MSc thesis, Univ British Columbia, Vancouver, 136 p

Herzberg A (1977) Zur Greisenbildung im Zinngranit des Fichtelgebirges, Fortschr Miner, 55, Bh 1, 46–49

Hess FJ (1914) A hypothesis for the origin of the carnotites of Colorado and Utah, Econ Geol, v 9, pp 675–688

Hess FJ, Wells RC (1920), Brannerite, a new uranium mineral, J Frankline Inst, 189, pp 225–237, 779–789

Heyl AV (1957) Zoning of the Bitter Creek vanadium-uranium deposit near Uravan, Colorado, US Geol Surv Bull 1042-F, pp 187–201

Heyse JV (1972) Mineralogy and paragenesis of the Schwartzwalder Mine uranium ore, Jefferson County, Colorado, US-AEC, GJO-912-1, 87 p

Hicks RT, Lowy RM, Della Valle RS, Brookins DG (1980) Petrology and geochemistry of Westwater Canyon Member, Morrison Formation, northern San Juan Basin – Similarities and differences with Grants mineral belt, *in*: Rautman CA, ed., Geology and mineral technology of the Grants Uranium Region 1979, New Mex Bur Mines Mineral Res Mem 38, pp 208–214

Hiemstra SA (1968a) The mineralogy and petrology of the uraniferous conglomerate of the Dominion Reefs mine, Klerksdorp area, Trans Geol Soc S Afr, v 71, pp 1–65

Hiemstra SA (1968b) The geochemistry of the uraniferous conglomerate of the Dominion Reefs mine, Klerksdorp area, Trans Geol Soc S Afr, v 71, pp 67–100

Hillebrand WF, Ransome FL (1900) On carnotite and associated vanadiferous minerals in western Colorado, Amer J Sci, 4th series, v 10, no. 56, pp 120–144

Hillebrand WF, Ransome FL (1905) On carnotite and

associated vanadiferous minerals in western Colorado, *in*: Clarke FW, et al., Contributions to mineralogy from the United States Geological Survey, US Geol Surv Bull 262, pp 9–31

Hills JH, Richards JR (1972) The age of uranium mineralization in northern Australia, Search, 3(10), pp 382–386

Hills JH, Richards JR (1973) Radiogenic lead in north Australian galenas, Nature, Phys Sci, 241, pp 18–19

Hills JH, Richards JR (1976) Pitchblende and galena ages in the Alligator Rivers region, Northern Territory, Australia, Mineral Deposita, 11, pp 133–154

Hilpert LS (1963) Regional and local stratigraphy of uranium-bearing rocks. New Mex Bur Min Res Mem 15, pp 6–18

Hilpert LS (1969) Uranium resources of northwestern New Mexico, US Geol Surv Prof Pap 603, 166 p

Hilpert LS, Moench RH (1960) Uranium deposits of the southern part of the San Juan Basin, New Mexico, Econ Geol, v 55, pp 429–464

Hintze LF, ed (1967) Uranium districts of southeastern Utah, Utah Geol Soc Guidebook to the Geology of Utah no. 21

Hirdes W (1979) The Proterozoic gold-uranium Kimberley Reef placers in the Evander- and East Rand Goldfields/ Witwatersrand/South Africa: different facies and their source-area aspects, PhD thesis, Univ Heidelberg, 199 p

Hirdes W (1984) Different populations of gold particles as outlined by their silver content: a regional investigation in the Precambrian Kimberley Reef placer of the East Rand Goldfield/Witwatersrand/South Africa, *in*: Wauschkuhn A, et al., eds., Syngenesis and epigenesis in the formation of mineral deposits, Springer Verlag, Berlin, New York, Heidelberg, Tokyo, pp 247–259

Hirdes W, Saager R (1983) The Proterozoic Kimberley Reef placer in the Evander Goldfield, Witwatersrand, South Africa, Monograph Series Min Deposits, 20, 101 p

Hochman MB (1980) Geochemical investigations in the Mt Bundy area, Northern Territory, *in*: Ferguson J, Goleby AB, eds., Uranium in the Pine Creek Geosyncline, IAEA, Vienna, pp 335–342

Hoefs J, Schidlowski M (1967) Carbon isotope composition of carbonaceous matter from the Precambrian of the Witwatersrand System, Science, v 155, pp 1096–1097

Hoefs J, Nielsen H, Schidlowski M (1968) Sulfur isotope abundances in pyrite from the Witwatersrand conglomerates, Econ Geol, v 63, pp 975–977

Höhndorf A, Carl C (1987) Zeitliche Abfolge der Uranmineralisation in diskordanzgebundenen proterozoischen Uranlagerstätten am Beispiel des Athabasca Beckens, Bundesanstalt für Geowissenschaften und Rohstoffe, 1. Zwischenbericht, Projekt UR 1945–5

Höhndorf A, Lenz H, v Pechmann E, Voultsidis V, Wendt I (1985b) Radiometric age determinations on samples of Key Lake uranium deposits, *in*: Sibbald TII, Petruck W, eds., Geology of uranium deposits, CIM Spec Vol. 32, pp 48–53

Höhndorf A, Voultsidis V, v Pechmann E (1985a) U/Pb isotopic investigations of the Maurice Bay uranium deposit, *in*: Sibbald, ITT, Petruk W, eds., Geology of uranium deposits, CIM Spec Vol. 32, pp 151–154

Höhndorf A, Strnad JG, Carl C (1989) Age determination of basement units in the Key Lake uranium deposit area, Saskatchewan, Canada, *in*: Uranium resources and geology of North America, TECDOC-500, IAEA, Vienna, pp 381–410

Hoel HD (1982) Goliad Formation of the South Texas Gulf Coastal Plain: regional genetic stratigraphy and uranium mineralization, Univ Texas, Austin, Master's thesis, 173 p

Hoeve J (1977) Uranium metallogenetic studies, II, Rabbit Lake: Mineralogy and geochemistry, *in*: Christopher JE, Macdonald R, eds., Summary of investigations 1977, Sask Geol Surv Misc Rep 77–10, pp 124–135

Hoeve J (1982a) Perspective on uranium mineralization Beaverlodge, Sask Res Publ no. G-745-1-E-82, 23 p

Hoeve J (1982b), Host rock alteration and its application as an ore guide at the Midwest uranium deposit, northern Saskatchewan, Sask Res Counc Publ, pp 1–44

Hoeve J (1984) Host rock alteration and its application as an ore guide at the Midwest Lake uranium deposit, northern Saskatchewan, CIM Bull, v 77, no. 868, pp 63–72

Hoeve J, Quirt D (1984) Uranium mineralization and host-rock alteration in relation to clay mineral diagenesis and evolution of the Middle Proterozoic Athabasca Basin, northern Saskatchewan, Sask Res Counc Tech Rep no. 187, 187 p

Hoeve J, Quirt D (1986) A common diagenetic-hydrothermal origin for unconformity-type uranium and stratiform copper deposits, Sask Res Counc Publ no. R-855-5-A-86, 50 p

Hoeve J, Quirt D (1987) A stationary redox front as a critical factor in the formation of high grade unconformity-type uranium ores in the Athabasca Basin, Saskatchewan, Canada, Bull Minér, v 110, pp 157–171

Hoeve J, Sibbald TII (1978) On the genesis of Rabbit Lake and other unconformity-type uranium deposits in northern Saskatchewan, Canada, Econ Geol, v 73, pp 1450–1473

Hoeve J, Sibbald TII, Ramaekers P, and Lewry JF (1980) Athabasca Basin unconformity-type uranium deposits: A special class of sandstone-type deposits, *in*: Ferguson J, Goleby A, eds., Uranium in the Pine Creek Geosyneline, IAEA, Vienna, pp 575–594

Hoeve J, Cumming GL, Baadsgaard H, Morton RD (1981) Geochronology of uranium metallogenesis in Saskatchewan, CIM Uranium Symp, Saskatoon, 1981, Abstract Volume, pp 11–12

Hoeve J, Rawsthorn K, Quirt D (1981a) Uranium metallogenetic studies: Collins Bay B Zone, II. Clay mineralogy, *in*: Summary of investigations 1981, Sask Surv Misc Rep 81–4, pp 73–75

Hoeve J, Rawsthorn K, Quirt D (1981b) Uranium metallogenetic studies: clay mineral stratigraphy and diagenesis in the Athabasca Group, *in*: Summary of investigations 1981, Sask Geol Surv Misc Rep 81–4, pp 76–89

Hoeve J, Quirt D, Alonso D (1985) Clay mineral stratigraphy of the Athabasca Group: Correlation inside and outside the Carswell Structure, *in*: Laine R, et al., eds., The Carswell Structure uranium deposits, Saskatchewan, Geol Ass Can Spec Paper 29, pp 19–32

Hoffmann J (1943a) Bioelement Uran im Pflanzen- und Tierreich sowie im menschlichen Organismus, Biochem Z, 313, pp 377–387

Hoffman J (1943b) A further contribution to the distribution of uranium in plant material, Bodenk u Pfl Ernähr, 32, pp 295–306

Hoffman ME (1977) Origin and mineralization of breccia

pipes, Grand Canyon district, Arizona, Univ Laramie, Wyoming, MSc thesis, 47 p
Holliger P (1987) U-Pb age of some French uranium ore deposits: chronological relationships with the host rocks, manuscript
Holliger P, Cathelineau M (1986) Le chronomètre U-Pb en milieu uranifère: application aux gisements hydrothermaux d'uranium liés spatialement au batholite de Mortagne (Vendée, France), Chron Rech Min, no. 485, pp 33–43
Holliger P, Cuney M, Friedrich M, Turpin L (1986) Géochimie et géochronologie isotopiques – Age carbonifère de l'unité de Brâme du complexe granitique peralumineux de St Sylvestre (NO Massif Central) défini par les données isotopiques. U-Pb sur zircon et monazite, CRAS, Paris, t 303, Série II, no. 14, pp 1309–1314
Holen HK (1982) A summary of uranium geology in the Grants mineral belt, New Mexico, US-DOE, TM-311, 3 p
Holmes A (1928) The nomenclature of petrology, Th Murby & Co., London, 284 p
Holmes SW (1957) Pronto Mine, *in*: Structural geology of Canadian ore deposits, v 2, CIM Congr, pp 324–339
Homeniuk LA, Clark RJ (1986) North Rim Deposits Athabasca Basin, *in*: Sibbalt, TII, Petruck W, eds., Geology of uranium deposits, CIM Spec Vol. 33, pp 230–240
Horne JET (1960) Age of pitchblende from Lenteiros, Reboleiro, Portugal, JEN Tech Paper no. 27, pp 7–10
Hostetler PB, Garrels RM (1962) Transportations and precipitation of uranium and vanadium at low temperatures, with special reference to sandstone-type uranium deposits, Econ Geol, v 57, pp 139–167
Hounslow AW (1976) Mineralogy of uranium and thorium, Colorado School Mines, 1 Table
Houston RS (1969) Aspects of the geologic history of Wyoming related to the formation of uranium deposits, Wyoming Univ Contr Geol, v 8, pp 67–79
Hsi, Ching-Kuo D, Langmuir D (1985) Adsorption of uranyl onto ferric oxyhydroxides: Application of the surface complexation site-binding model, Geochim Cosmochim Acta, v 49, pp 1931–1941
Huber GC (1980) Stratigraphy and uranium deposits, Lisbon Valley district, San Juan County, Utah, Colorado School Mines Quarterly, v 75, no 2, 44 p
Hubregtse JJ, Sopuck V (1989) Alteration paragenesis of the Helikian sandstone and the Aphebian basement of the Key Lake mine and other uranium deposits in the eastern Athabasca Basin (Saskatchewan, Canada), (abstr), *in*: Uranium resources and geology of North America, IAEA, Vienna, p 379
Huff LC, Lesure FG (1962) Diffusion features of uranium-vanadium deposits in Montezuma Canyon, Utah, Econ Geol, v 57, pp 226–237
Huff LC, Lesure FG (1965) Geology and uranium deposits of Montezuma Canyon area, San Juan County, Utah, US Geol Surv Bull 1190, 102 p
Huffman CA Jr, Lupe RD (1977) Influences of structure on Jurassic depositional patterns and uranium occurrences, northwestern New Mexico, *in*: New Mex Geol Soc Guidebook, 28th Field Conf, San Juan Basin III, pp 277–283
Huffman CA Jr, Kirk AR, Corken RJ (1980) Depositional environments as ore controls in Salt Wash Member, Morrison Formation (Upper Jurassic), Carrizo Mountains area, Arizona and New Mexico, *in*: Rautman CA, ed., Geology and mineral technology of the Grants Uranium Region 1979, New Mex Bur Mines Mineral Res Mem 38, pp 122–129
Hunter DR (1957) The geology, petrology and classification of the Swaziland granites and gneisses, Trans Geol Soc S Afr, v 60, pp 85–120
Hunter DR (1974) Crustal development in the Kaapvaal Craton, Precamb Res, v 1, pp 259–326
Hunter J, Michie UMcL (1988) Uranium provinces and the exploration industry, *in*: Recognition of uranium provinces, IAEA, Vienna, pp 405–427
Hurley PM, Fisher NH, Pinson WH, Fairbairn HW (1961) Geochronology of Proterozoic granites in Northern Territory, Australia, Part 1: K-Ar and Rb-Sr age determinations, Geol Soc Am Bull 72, pp 653–662
Husmann O (1956) Bestimmungen des Thorium- und Uran-Gehaltes an Gneissen und magmatischen Gesteinen des mittleren Schwarzwaldes mittels der Koinzidenz-Methode, N Jb Miner, Monatsh 108
Hutchinson RW, Blackwell JD (1984) Time, crustal evolution and generation of uranium deposits, *in*: de Vivo, Ippolito, Capaldi, Simpson, eds., Uranium geochemistry, mineralogy, geology, exploration and resources, IMM, London, p. 89–100
Hutchison RI (1975) The Witwatersrand System as a model of sedimentation in an intracratonic basin, unpubl DSc thesis, Univ Orange Free State, Bloemfontein, 255 p
IAEA (1979) Uranium deposits in Africa: geology and exploration, IAEA, Vienna, 262 p
IAEA (1980) Uranium in the Pine Creek Geosyncline, IAEA, Vienna, 760 p
IAEA (1981) Yacimientos de Uranio en América Latina: Geología y Exploratión, IAEA, Vienna, 625 p
IAEA (1982) Vein-type and similar uranium deposits in rocks younger than Proterozoic, IAEA, Vienna, 391 p
IAEA (1983a) Uranium exploration in wet tropical environments, IAEA, Vienna, 162 p
IAEA (1983b) Age, sedimentary environments, and other aspects of sandstone and related host rocks for uranium deposits, Tech Rep Series no. 231, IAEA, Vienna, 62 p
IAEA (1984a) Geología y Metalogénesis de los Depósitos y Manifestaciones Uraníferos de Sudamerica, IAEA, Vienna, 275 p
IAEA (Ferguson J ed.) (1984b) Proterozoic unconformity and stratabound uranium deposits, TECDOC-315, IAEA, Vienna, 338 p
IAEA (Toens D ed.) (1984c) Surficial uranium deposits, TECDOC-322, IAEA, Vienna, 252 p
IAEA (1985a) Uranium deposits in volcanic rocks, IAEA, Vienna, 468 p
IAEA (Finch W ed.) (1985b) Geological environments of sandstone-type uranium deposits, TECDOC-328, IAEA, Vienna, 408 p
IAEA (1986a) Correlation of uranium geology between South America and Africa, IAEA, Vienna, 475 p
IAEA (1986b) (INTURGEO) US-DOE National Uranium Resource Evaluation Program (NURE), Uranium occurrence reports: database compiled by the IAEA from Appendix C of the NURE Quadrangle Reports series PGJ/F- and GJQ- published from 1978 through 1982, (Available on magnetic media) 5000 p
IAEA (Fuchs H ed.) (1986c) Vein-type uranium deposits, TECDOC-361, IAEA, Vienna, 423 p
IAEA (Pretorius D ed.) (1987) Uranium deposits in

Proterozoic quartz-pebble conglomerates, TECDOC-427, IAEA, Vienna, 459 p
IAEA (1988a) Recognition of uranium provinces, IAEA, Vienna, 459 p
IAEA (1988b) Uranium deposits in Asia and the Pacific: geology and exploration, IAEA, Vienna, 341 p
IAEA (1988c) INTURGEO: The International Uranium Geology Information System, a world atlas of uranium occurrences and deposits, TECDOC-471, IAEA, Vienna, 493 p
IAEA (1989a) Uranium deposits in magmatic and metamorphic rocks, IAEA, Vienna, 253 p
IAEA (1989b) Uranium resources and geology of North America, TECDOC-500, IAEA, Vienna, 529 p
Ibrahim HJ, Woo HF (1985) Geochemical and mineralogical alteration at the Midwest uranium-nickel deposit, *in*: Sibbald TII. Petruck W, eds., Geology of uranium deposits, CIM Spec Vol. 32, pp 73–84
Ingram JA (1974) Uranium deposit Austral BMR, Miner Res Rep 6, 52 p
Isachsen YW (1954) Ore deposits of the Big Indian Wash-Lisbon Valley area, uranium deposits and general geology of southeastern Utah, Utah Geol Soc Guidebook, 9, pp 95–107
Isachsen YW (1955) Uranium deposits in the Skull Creek and Uranium Peak districts, northwestern Colorado, Intermountain Ass Petrol Geol, 6th Annual Field Conf, Salt Lake City, Utah, pp 124–125
Isachsen YW, Evensen CG (1956) Geology of uranium deposits of the Shinarump and Chinle Formations on the Colorado Palteau, US Geol Surv Prof Paper no. 302, pp 263–280
Ishihara S (1977) The magnetite series and ilmenite series granitic rocks, Min Geol, 27, pp 293–305
Jacob RE (1966) The geology of the Vaal Reefs mine Rhodes Univ, Grahamstown, unpubl MSc thesis
Jacob RE (1974a) Geology and metamorphic petrology of part of the Damara Orogen along the lower Swakop River, South West Africa, Bull Precamb Res Unit, Univ Cape Town, 17, 185 p
Jacob RE (1974b) The radioactive mineralization in part of the central Damara belt, South West Africa, and its possible origin, S Afr Atomic Energy Board Rep PIN 234(B/R), 17 p
Jakob RE, Corner B, Brynard HJ (1986), The regional geological and structural setting of the uraniferous granitic provinces of southern Africa, *in*: Anhaeusser CR, Maske S, eds., Mineral deposits of southern Africa, Geol Soc S Afr, v 2, pp 1807–1818
Jacobsen LC (1980) Sedimentary controls on uranium ore at L-Bar deposits, Laguna district, New Mexico, *in*: Rautman CA, ed. Geology and mineral technology of the Grants Uranium Region, 1979, New Mex Bur Mines Mineral Res Mem 38, pp 284–291
Jenkins JT, Jr, Cunningham SB (1980) Depositional environment of the Poison Canyon Sandstone, Morrison Formation, in the Gulf Mariano Lake mine, McKinley County, New Mexico, *in*: Rautman CA, ed., Geology and mineral technology of the Grants Uranium Region 1979, New Mex Bur Mines Mineral Res Mem 38, pp 153–161
Jennings JK (1976) Interaction of uranium with naturally occurring organic substances, Colorado School Mines, MSc thesis, 71 p
Jennings JK, Leventhal JS (1977) A new structural model for humic material which shows sites for attachment of oxidized uranium species, *in*: Campbell, JA ed., Short papers of the US Geol Surv uranium-thorium symp 1977, US Geol Surv Circ 753, pp 10–11
Jensen ML (1958) Sulphur isotopes and the origin of sandstone-type uranium deposits, Econ Geol, v 53, pp 598–616
Jensen ML (1963) Sulfur isotopes and biogenic origin of uraniferous deposits of the Grants and Laguna districts, *in*: Kelley VC, ed., Geology and technology of the Grants Uranium Region, New Mex Bur Mines Mineral Res Mem 15, pp 182–190
Jensen ML, Field CW, Nakai, Nobuyuki (1960) Sulfur isotopes and the origin of sandstone-type uranium deposits, Biennial Progress Report for 1959–1960, US-AEC AT (30-1)-2261, 281 p
Jiaron Z, Zhitian G, (1984), The Liangshanguan uranium deposit, northeast China: Some petrological and geochemical constraints on genesis, *in*: Proterozoic unconformity and stratabound uranium deposits, TECDOC-315, IAEA, Vienna, pp 115–134
Jiashu R, Zehong H (1984) Form of uranium occurrence and its distribution in uraniferous granites, *in*: Geology of granites and their metallogenetic relations, Proc Symp Nanjing, 1982, Univ Press, Beijing, pp 621–635
Jiashu Rong, Zehong Han, Yuliang Xia (1989) Uranium metallogenesis of coarse-grained granite in Area H, China, *in*: Uranium deposits in magmatic and metamorphic rocks, IAEA, Vienna, pp 93–112
Jobin DA, (1962), Relation of the transmissive character of the sedimentary rocks of the Colorado Plateau to the distribution of uranium deposits, US Geol Surv Bull 1124, 151 p
John EC (1978) Mineral zones in the Utah Copper orebody, Econ Geol, v 73, pp 1250–1259
Johnson HS, Jr (1957) Uranium resources of the San Rafael district, Emery County, Utah – a regional synthesis, US Geol Surv Bull 1046-D, pp 37–54
Johnson HS, Jr (1959) Uranium resources of the Green River and Henry Mountains districts, Utah – a regional synthesis, US Geol Surv Bull 1087C, 104 p
Johnson HS, Jr, Thordarson W (1966) Uranium deposits of the Moab, Monticello, White Canyon and Monument Valley districts, Utah and Arizona, US Geol Surv Bull 122-H, pp H1–H53
Johnson SY, Otton JK, Macke DL (1987) Geology of the Holocene surficial uranium deposit of the north fork of Flodelle Creek, northeastern Washington, Geol Soc AM Bull, v 98, no. 1, pp 77–85
Johnston DJ (1984) Structural evolution of the Pine Creek inlier and mineralization therein, Northern Territory, Australia, PhD thesis, Monash Univ, 335 p (unpubl)
Johnston JE (1977) Depositional systems in the Wilcox Group and the Carrizo Formation (Eocene) of central and south Texas and their relationship to lignite, Master's thesis, Univ Texas, Austin, 113 p
Johnstone MH, Lowry DC, Quilty PG (1973) The geology of southwestern Australia – a review, J Soc West Aust, v 56, pp 5–15
Jolliffe AW, Evoy EF (1957) Gunnar Mine, *in* Gilbert G, ed., Structural geology of Canadian ore deposits, CIM, v 2, pp 240–246
Jones BE (1980) The geology of the Collins Bay uranium deposit, Saskatchewan, CIM Bull, v 83, June, pp 84–90
Jones CA (1978a) A classification of uranium deposits in sedimentary rocks, *in*: Mickle DG, ed., Preliminary classification of uranium deposits, US-DOE, GJBX-63 (78), pp 1–15
Jones CA (1978b) Uranium occurrences in sedimentary

rocks exclusive of sandstone, *in*: Mickle DG, Mathews GW, eds., Geologic characteristics of environments favorable for uranium deposits, US-DOE, GJBX-67(78), pp 1–86

Joubin FR (1960) Comments regarding the Blind River (Algoma) uranium ores and their origin, Econ Geol, v 55, pp 1751–1756

Jurain G, Renard JP (1970a) Remarques générales sur les caractères geochimiques des granites encaissant les principaux districts uranifères français, Sci Terre, Nancy, Tome XV, n°2, pp 195–205

Jurain G, Renard JP (1970b) Géochimie de l'uranium dans les minéraux phylliteux et les roches du massif granitique de Mortagne sur Sevre (Vendée – France), Mineral Deposita, 5, pp 354–364

Jutson JT (1950) The physiography of Western Australia, West Aust Geol Surv Bull 95 (3rd Ed), 366 p

Ju Yejun, et al., (1985) On the sedimentary environments of the Late Sinian and Early Cambrian carbonaceus formation in South China and their relations with uranium mineralization. Scientific Papers on Geology for International Exchange, Beijing, 5, pp 181 ff

Kaiman S, Borwood JL (1976) An unusual "Thucholite" from Elliot Lake, Ontario, Can Min, 14, pp 422–428

Kalliokoski J, Langford FF, Ojakangas RW (1978) Criteria for uranium occurrences in Saskatchewan and Australia as guides to favorability for similar deposits in the United States, US-DOE, GJBX-114(78), 480 p

Kalyaev GI (1980) Mode of albite distribution in zones of the Ukrainian Shield, *in*: Avrashov A, Abov-Zied S, Kerns G, eds., Albitized uranium deposits, six articles translated from Russian literature, US-DOE, GJBX-193(80), pp 1–13

Karlson R, Krokosz M (1983) Brecciation and associated mineralization at the Schwartzwalder Mine, Jefferson County, Colorado, *in*: Symposium brecciation and mineralization, geologic occurrence and genesis, (abstr), Colorado Springs, 1 p

Karlstrom TNV, Swann GA, Eastwood RL, eds. (1974). Geology of northern Arizona, with notes on archeology and paleoclimate; Part I, Regional studies; Part II, Area studies and field guides, Guidebook Geol Soc Amer, Rocky Mountain Section Meeting, Flagstaff, Arizona, 805 p

Kashirtseva MF (1964) Mineral and geochemical zonation of infiltration uranium ores, Soviet Geology, v 10, pp 51–65

Kashirtseva MF, Sidelnikova VD (1973) Distribution of selenium, uranium and molybdenum during infiltration mineralization, Geologiia Rudnykh Mestorozhdenii, v 15, pp 82–92 (in Russian)

Kaspar J, Hejl V (1970) Thermodynamic conditions of the origin of uraninites, *in*: Uranium exploration geology, IAEA, Vienna, pp 301–314

Katayama N, Kamiyama T (1977) Favourable conditions for the formation of basal type uranium deposits, Min Geol (Japan), v 27, pp 1–8

Katayama N, Kubo K, Hirono S (1974) Genesis of uranium deposits of the Tono Mine, Japan, *in*: Formation of uranium ore deposits, IAEA, Vienna, pp 437–452

Katz JJ, Rabinovitch E (1951) The chemistry of uranium, Part I, National nuclear energy series, McGraw Hill, 609 p

Kazansky VI, et al. (1967) Geologic position of hydrothermal uranium ore fields in uranium-bearing provinces of different types, *in*: Geology of hydrothermal uranium-bearing deposits, Izd-vo Nauka, Moscow

Kazansky VI, Krupenikov VA, Omel' Yanenko BI, Pruss AK (1968) Structural and petrological conditions of the formation of uraniferous albitites, Geol Rudn Mestorozhd, Dokl Akad, SSSR, 10, pp 3–16 (in Russian)

Kazansky VI, Laverov NP, Tugarinov AI (1975) Sources of ore material in endogenic uranium deposits, Intern Geol Rev, v 19(3), pp 283–294

Kazansky VI, Laverov NP, Tugarinov AI (1976) Die Herkunft der Erzsubstanzen endogener Uranlagerstätten, Z angew Geol, 22, H 10, pp 448–454

Kazansky VI, Laverov NP (1977) Deposits of uranium, *in*: Smirnov VI, ed., Ore deposits of the USSR – Vol. II, Pitman Publ, London-San Francisco-Melbourne, pp 349–424

Kazansky VI, Laverov NP, Tugarinov AI (1978) Evolution of uranium deposits, Atomizad, Moscow, 208 p

Kazansky VL, Laverov NP, Tugarinov AI, 1978b Lagerstätten der Gebiete der Protoaktivierung; Uranführende Natrium-Metasomatite; German translation from: Evoljucija uranovogo rudoobrozovabija (Evolution of uranium ore formation), Moskau, pp 58–72, BGR Hannover, 21 p

Kazhdan AB (1978) Associational assignment of commercial types of uranium deposits, Intern Geol Rev, v 20, no. 12, pp 1389–1401

Keefer WR (1970) Structural geology of the Wind River Basin, Wyoming, US Geol Surv Prof Paper 495-D, 35 p

Keller WD (1959) Clay minerals in the mudstones of the ore-bearing formation, *in*: Garrels RM, Larsen ES, III, compilers, Geochemistry and mineralogy of the Colorado Plateau uranium ores, US Geol Surv Prof Paper 320, pp 113–119

Kelley VC (1951) Tectonics of the San Juan Basin, *in*: Guidebook of the south and west sides of the San Juan Basin, New Mexico and Arizona, Second Field Conf New Mex Geol Soc, pp 124–131

Kelley VC (1955) Influence of regional structure and tectonic history upon the origin and distribution of uranium on the Colorado Plateau, US Geol Surv Prof Paper 300, pp 171–178

Kelley VC, ed. (1963a) Geology and technology of the Grants Uranium Region, New Mex Bur Mines Mineral Res Mem 15, 277 p

Kelley VC (1963b) Tectonic setting, *in*: Geology and technology of the Grants Uranium Region, New Mex, Bur Mines Mineral Res Mem 15, pp 19–20

Kent LE (1961) Note on chloritoid in the Witwatersrand System, Trans Geol Soc S Afr, v 64, pp 91–96

Kerr PF (1945) Cattierite and vaesite: new Co-Ni minerals from the Belgian Congo, Am Miner, 30, pp 483–497

Kerr PF (1958) Uranium emplacement in the Colorado Plateau, Geol Soc Amer Bull, v 69, no. 9, pp 1075–1111

Kettner R (1926) Geologie Příbramska (Geology of the Příbram area), Sbor Stát geol ústavu, v Prague, pp 1–52

Kim JH (1988) Uranium geology of the Republic of Korea, *in*: Uranium deposits in Asia and the Pacific: geology and exploration, IAEA, Vienna, pp 141–154

Kimberley MM (1978a) Short course in uranium deposits: their mineralogy and origin, Miner Ass Can, v 3, Univ Toronto Press, Toronto, 521 p

Kimberley MM (1978b) Origin of stratiform uranium deposits in sandstone, conglomerate, and pyroclastic

rock, *in*: Kimberley MM, ed., Short course in uranium deposits: their mineralogy and origin, Miner Ass Can, v 3, pp 339–381
Kimberley MM, Grandstaff DE, Tanaka RT (1984) Topographic control on Precambrian weathering in the Elliot Lake Uranium District, Canada, J Geol Soc, London, 141, pp 229–233
Kimberley MM, Tanaka RT, Farr MR (1980) Composition of Middle Precambrian uraniferous conglomerate in the Elliot Lake-Agnew Lake area of Canada, Precamb Res, 12, pp 375–392
King JW, Austin SR (1966) Some characteristics of roll-type uranium deposits at Gas Hills, Wyoming, Min Eng, v 18, no. 5, pp 73–80
Kirchheimer F (1963) Das Uran und seine Geschichte, Stuttgart, 372 p
Kirchner G, Lehnert-Thiel K, Rich J, Strnad JG (1980), The Key Lake U-Ni deposits: A model for Lower Proterozoic uranium deposition, *in*: Ferguson J, Goleby AB, eds., Uranium in the Pine Creek Geosyncline, IAEA, Vienna, pp 617–629
Kirk AR, Condon M (1986) Structural control of sedimentation patterns and the distribution of uranium deposits in the Westwater Canyon Member of the Morrison Formation, northwestern New Mexico – A subsurface study, *in*: Turner-Peterson CE, Santos ES, Fishman NS, eds., A basin analysis case study – the Morrison Formation, Grants Uranium Region, New Mexico, Amer Ass Petrol Geol, Studies in Geology, no. 22, pp 105–143
Kirk AR, Huffman Jr, HC, Zech RS (1986) Design and results of the Mariano Lake-Lake Valley drilling project, northwestern New Mexico, *in*: Turner-Peterson CE, Santos ES, Fishman NS, eds., A basin analysis case study – the Morrison Formation, Grants Uranium Region, New Mexico, Amer Ass Petrol Geol, Studies in Geology no. 22, pp 227–240
Kittel DF (1963) Geology of the Jackpile Mine area, *in*: Kelley VC, ed., Geology and technology of the Grants Uranium Region, New Mex Bur Mines Mineral Res Mem 15, pp 167–176
Kittel DF, Kelley VC, Melancon PE (1967) Uranium deposits of the Grants region, *in*: New Mexico Geol Soc 18th Field Conf Guidebook, Defiance-Zuni-Mt Taylor Region, pp 173–183
Klemd R, Hallbauer DK (1987) Hydrothermally altered peraluminous Archaean granites as a provenance model for Witwatersrand sediments, Mineral Deposita, 22, pp 227–235
Klepper MR, Wyant DG (1957) Notes on the geology of uranium, US Geol Surv Bull 1046-F, 148 p
Klingmuller LML (1989) The Green Mountain uranium district, central Wyoming: type locality of solution front limb deposits, *in*: Uranium resources and geology of North America, TECDOC-500, IAEA, Vienna, pp 173–190
Klohn ML, Pickens WR (1970) Geology of the Felder uranium deposit, Live Oak County, Texas, Soc Min Eng, Amer Inst Min Metal Petrol Eng, preprint, no. 70-1-38, 19 p
Knipping HD (1974) The concepts of supergene versus hypogene emplacement of uranium at Rabbit Lake, Saskatchewan, Canada, *in*: Formation of uranium ore deposits, IAEA, Vienna, pp 531–548
Knowles AG (1966) A palaeocurrent study of the Ventersdorp Contact Reef at Western Deep Levels, Limited, on the Far West Rand, Univ Witwatersrand, Johannesburg, unpubl M Sc thesis, 125 p
Knox JW, Gruner JW (1957) Mineralogy of the Ambrosia Lake uranium deposits in McKinley County, New Mexico, *in*: Annual report for April 1, 1956 to March 31, 1957, US-AEC, RME-3148, pp 5–28
Koch GS, et al. (1964) Statistical interpretation of sample assay data from the Mi Vida uranium mine, Big Indian district, San Juan County, Utah, US Bur Mines Rep Inv 6550, 40 p
Kochenov AV, Chernikov AA (1976) The character of surface uranium concentrations in arid regions, Lith Min Res, 11, pp 110–116
Kochenov AV, Korolev KG, Dubinchuk VT, Medvedev YL (1978) Experimental data on the conditions of precipitation of uranium from aqueous solutions, Geochem Intern, v 14, pp 82–87
Kochenov AV, Zinevyev VV, Lovaleva SA (1965) Some features of the accumulation of uranium in peat bogs, Geochem Intern, v 2, n 1, pp 65–70
Koczy FF (1963) The natural radioactive series in organic material, *in*: Schultz V, Klement AW, eds., Radioecology, New York, Am Inst Biolog Sci, Reinholt Publ Co, 611 p
Koczy FF, Tomic E, Hecht F (1957) Zur Geochemie des Urans im Ostseebecken, Geochim Cosmochim Acta, 11, p 86
Koeberlin FR (1938) Sedimentary copper, vanadium-uranium, and silver in southwestern United States, Econ Geol, v 33, pp 458–461
Koen GM (1958) The attrition of uraninite, Trans Geol Soc S Afr, v 61, pp 183–191
Koen GM (1961) The genetic significance of the size distribution of uraninite in Witwatersrand bankets, Trans Geol Soc S Afr, v 64, pp 23–46
Koen GM (1962) Note on chlorite pseudomorphs after detrital amphibole in Witwatersrand banket, Trans Geol Soc S Afr, v 65, pp 57–58
Köppel V (1968) Age and history of the uranium mineralization of the Beaverlodge area, Saskatchewan, Geol Surv Can Paper 67–31, 111 p
Köppel VH, Saager R (1974) Lead isotope evidence on the detrital origin of Witwatersrand pyrites and its bearing on the provenance of Witwatersrand gold, Econ Geol, v 69, pp 318–331
Kofford ME (1969) The Orphan mine, *in*: Geology and natural history of the Grand Canyon region, Four Corners Geol Soc Guidebook, 5th Annual Field Conf, Powell Centennial River Expedition, pp 190–194
Kohl E (1954) Uran: Die metallischen Rohstoffe, Heft 10, Ferdinand Enke Verlag, Stuttgart, 234 p
Kolektiv (ČSSR), (1984), Czechoslovakian uranium deposits, Nakl technické literatury, Prague, 365 p (in Czech)
Komarov AN, Shukolyukov YuA (1966) Forms of uranium occurrence in micas, Geokhimiya, no. 11, pp 1322–1330
Komínek J, Veselý T (1986) Uranium deposit of Jáchimov, CSSR, *in*: Vein type uranium deposits, TECDOC-361, IAEA, Vienna, pp 293–306
Korolev KG, Rumyantseva GV (1976) Conditions of formation of collomorphic uranotitanates and brannerite, Intern Geol Rev, v 18, p 167–171
Korshinsky DS (1965) Abriß der metasomatischen Prozesse, Akademie Verlag, Berlin, 195 p
Kostov I (1977) Crystallochemical differentiation and

localization of uranium ore deposits in the earth's crust, *in*: Recognition and evaluation of uraniferous areas, IAEA, Vienna, pp 15–33
Kotlyar VN (1961) Geology of uranium deposits, Gosteoltekhizdat, Moscow
Koul S, Wall VJ, Johnston JD (1984) Fission-track studies of the East Alligator River uranium field (Northern Territory, Australia) and their implications, (abstr), Geol Soc Aust, no. 12, pp 311–313
Koul S, Wilde AR, Tickoo AW (1987) A thermal history of the Proterozoic East Alligator River terrain, Northern Territory, Australia: a fission track study, Tectonophysics, v 145
Kovschak AA, Jr, Nylund RL (1981) General geology of uranium-vanadium deposits of Salt Wash sandstones, La Sal area, San Juan County, Utah, New Mex Geol Soc Guidebook, 32nd Field Conference, Western Slope, Colorado, pp 171–175
Kozlova PS, Gurvich MYu (1979) The behavior of uranium in post-magmatic alteration of potassic alkali-rocks, Geochem Intern, pp 109–117
Kozusko RG, Saucier AE (1980) The Bernabe Montano uranium deposit, Sandoval County, New Mexico, *in*: Rautman CA, ed., Geology and mineral technology of the Grants Uranium Region 1979, New Mex Bur Mines Mineral Res Mem 38, pp 262–268
Krapez B (1980) A sedimentological study of the Ventersdorp Contact Reef at East Driefontein Gold Mine, Carletonville, South Africa, Univ Witwatersrand, Johannesburg, unpubl M Sc thesis, 237 p
Kraus M (1916) Das staatliche Uranpecherzbergbaurevier bei St Joachimsthal in Böhmen, Bergbau u Hütte, pp 1–10
Krauskopf KB (1979) Introduction to geochemistry (2d ed), McGraw-Hill Book Co, New York, 617 p
Kreitler CW (1979) Ground-water hydrology of depositional systems, *in*: Depositional and ground-water flow systems in exploration for uranium, Univ Texas, Austin, Bur Econ Geol, pp 118–176
Krendelev FP, Pavlov AL (1972) The causes of the joint occurrence of gold and uranium in ore provinces, *in*: Radioaktivnye elementy v gornykh porodakh, pt 2, Novosibirsk, pp 22–23
Krewedl DA, Carisey JC (1986) Contributions to the geology of uranium mineralized breccia pipes in northern Arizona, Arizona Geol Soc Digest, v XVI, pp 179–186
Krogh TE, Clark LA (1987) Zircon dating of sub-Athabasca granitoid rocks, Saskatchewan, *in*: program with abstracts, Joint annual meeting Geol Ass Can, Miner Ass Can, v 12, p 64
Kröner A, Anhaeusser CR, Vajner V (1973) Neue Ergebnisse zur Evolution der präkambrischen Kruste im südlichen Afrika, Geol Rundsch, v 62, pp 281–309
Kröner A, Hawkesworth C (1977) Late Pan-African emplacement ages for Rössing alaskites granite (Damara belt) and R Lepel bostonite (Gariep belt) in Namibia and their significance for the timing of metamorphic events, Res Inst afr Geol, Univ Leeds, 20th ann Rep, pp 14–16
Krupicka J, Sassano GP (1972) Multiple deformation of crystalline rocks in the Tazin Group, Eldorado Fay mine, NW Saskatchewan, Can J Earth Sci, 9, pp 422–433
Krupp R (1984) The Nahe Caldera – a resurgent caldera in the Permo-Carboniferous Saar-Nahe Basin, SW Germany, Geol Rundsch, v 73, pp 981–1005
Krylov AY (1958) Radioactivity in various rock complexes of the Terskei Ala-Tau Mountains, Geochemistry (USSR) (English Transl), pp 240 ff
Krylov AY (1963) The evolution of radioactivity and general chemical composition, North Tien-Shan Rocks, Radiokhimiya, 5, pp 173 ff [in Russian]
Krylov AY, Atrashenok LY (1959) The mode of occurence of uranium in granites, Geochem, no. 3, pp 307–313
Kunzendorf H, Nyegaard P, Nielsen BL (1982) Distribution of characteristic elements in the radioactive rocks of the northern part of Kvanefjeld, Ilímaussaq Intrusion, South Greenland, Geol Surv Greenl, Copenhagen, Rep 109, pp 1–32
Kuznetsov VA, Zhuravlev RS, Osipov DK, eds., (1975) Radioactive elements in rocks, "Nauka" Siberian Branch, Novosibirsk, 296 p
Kyser TK, Wilson MR, Ruhrmann G (1989) Graphite, a prerequisite for unconformity-type uranium deposits? – stable isotope constraints, manusc
Lainé R (1985) Conclusion: the Carswell uranium deposits – an example of not so unique unconformity-related uranium mineralization, *in*: Lainé R, Alonso D, Svab M, eds., The Carswell Structure uranium deposits (Saskatchewan), Geol Ass Can Spec Paper 29, pp 225–230
Lainé R (1986) Uranium deposits of the Carswell Structure, *in*: Evans EL, ed. Uranium deposits of Canada CIM Spec Vol. 33, pp 155–169
Laine R, Alonso D, Svab M, eds. (1985) The Carswell Structure uranium deposits, Saskatchewan, Geol Ass Can Spec Paper 29, 240 p
Lakin HW (1961) Geochemistry of selenium in relation to agriculture, *in*: Selenium in agriculture, US Dep Agricult, Handbook 200, pp 3–12
Lambert RStJ, Chamberlain VE, Holland JG (1976) Geochemistry of Archean rocks, *in*: Windley BF, ed., The early history of the earth, John Wiley and Sons, New York, pp 377–403
Lambert IB, Heier KS (1967) The vertical distribution of uranium, thorium and potassium in the continental crust, Geochim Cosmochim Acta, 31, pp 377–390
Lambert IB, Heier KS (1968a) Geochemical investigation of deep-seated rocks in the Australian Shield, Lithos, v 1, pp 30–53
Lambert IB, Heier KS (1968b) Estimates of the crustal abundances of thorium, uranium and potassium, Chem Geol, v 3, pp 233–238
Lameyre J (1966) Leucogranites et muscovitisation dans le Massif Central français, Ann Fac Sci Univ Clermont, 29, 263 p
Lancelot J, Vella V (1989) Datation U-Pb Liassic de la pechblende de Rabejac. Mise en evidence d'un pre-concentration uranifère Permienne dans le Basin de Lodève (Herault), Bull Soc Geol France, vB, no. 2, pp 309–315
Lancelot J, de Saint André B, de la Boisse H (1984) Systematique U-Pb et evolution du gisement d'uranium de Lodève (France), Mineral Deposita, 19, 44–53
Landais P (1986) Geochemical analyses of the organic matter associated with the breccia pipes in the Grand Canyon area, *in*: Geol Soc Amer, Rocky Mountain Section, Abstracts with Programs, p 389
Landais P (1989) Oil biodegradation in uranium deposits,

in: Metallogenesis of uranium deposits, IAEA, Vienna, pp 43–62

Landais P, Dereppe JM (1985) A chemical study of the carbonaceous material from the Carswell Structure, *in*: Laine R, Alonso D, Svab M, eds., The Carswell Structure uranium deposits, Saskatchewan, Geol Ass Can Spec Paper 29, pp 165–174

Landais P, Connan J, Dereppe JM, George E, Meunier JD, Monthioux M, Pagel M, Pironon J, Poty B (1987) Alterations of the organic matter, a clue for uranium ore genesis reconstruction, Uranium, v 3, pp 307–342

Landais P, Meyer A, Carisey JC, Krewedl DA, Brosse E, Forbes P (1989) Geothermal analyses of the breccia pipes (Arizona) – Organic matter, fluid inclusions, fission tracks and computerized modeling, (abstr), *in*: Uranium resources and geology of North America, IAEA, Vienna, p 239

Lang AH, Goodwin AM, Mulligan R, Whitmore DRE, Gross GA, Boyle RW, Johnson AG, Chamberlain JA, Rose ER (1976) Economic minerals of the Canadian Shield, *in*: Douglas RJW, ed., Geology and economic minerals of Canada, Geol Surv Can Econ Geol Rep Part A, pp 151–226

Lang AH, Griffith JW, Steacy HR (1962) Canadian deposits of uranium and thorium, Geol Surv Can Econ Geol Series no. 16, 324 p

Lange G, Freyhoff G (1991) Geologie und Bergbau in der Uranlagerstätte Ronneburg/Thüringen, Erzmetall 44, Nr 5, pp 264–269

Lange G, Mühlstedt P, Freyhoff G, Schröder B (1991) Der Uranerzbergbau in Thüringen und Sachsen – ein geologisch-bergmännischer Überblick, Erzmetall 44, Nr 3, pp 162–171

Langen RE, Kidwell AL, (1974), Geology and geochemistry of the Highland uranium deposit, Converse County, Wyoming, Mountain Geologist, v 11, no. 2, pp 85–93

Langford FF (1977) Surficial origin of North American pitchblende and related uranium deposits, Amer Ass Petrol Geol Bull, v 61, pp 28–42

Langford FF (1978) Origin of unconformity-type pitchblende deposits in the Athabasca Basin of Saskatchewan, *in*: Kimberley MM, ed., Short course in uranium deposits: their mineralogy and origin, Miner Ass Can, v 3, pp 485–499

Langford FF (1981) The Martin Group in the greater Beaverlodge area, *in*: Summary of investigations 1981, Sask Geol Surv Sask Miner Resour Misc Rep 81–4, pp 38–43

Langford FF (1986) Geology of the Athabasca Basin, *in*: Evans EL, ed, Uranium deposits of Canada, CIM Spec Vol. 33, pp 123–133

Langmuir D (1978) Uranium solution-mineral equilibria at low temperatures with applications to sedimentary ore deposits, *in*: Kimberley MM, ed., Short course in uranium deposits: their mineralogy and origin, Miner Ass Can, v 3, pp 17–55

Langmuir D, Applin K (1977) Refinement of the thermodynamic properties of uranium minerals and dissolved species, with application to the chemistry of ground waters in sandstone-type uranium deposits, *in*: Campbell JA, ed., Short papers of the US Geol Surv Uranium-Thorium Symp 1977, US Geol Surv Circ 753, pp 57–60

Langmuir D, Herman JS (1982) The mobility of thorium in natural waters at low temperatures, Geochim Cosmochim Acta, 44, pp 1753–1766

Lanier G, John EC, Swensen AJ, Reid J, Bard CE, Caddey SW, Wilson JC (1978) General geology of the Bingham mine, Bingham Canyon, Utah, Econ Geol, v 73, pp 1228–1241

LaPoint DJ, Markos G (1977) Geochemical interpretation of ore zonation at the Rifle vanadium mine, Colorado, *in*: Campbell JA, ed., Short papers of the US Geol Surv Uranium-Thorium Symp 1977, US Geol Surv Circ 753, pp 53–55

La Roche H, de Stussi JM, Chauris L (1980) Les granites à deux micas hercyniens français, essais de cartographie et de correlations géochimiques appuyés sur une banque de données, implications pétrologiques et métallogéniques, Sci Terre, Fr XXIV, pp 5–121

Larsen ES, Jr (1954) Geologic investigation of radioactive deposits. Semi-Annual Progress Report, June through November, 1954, US Geol Surv TEI 490, 255 p

Larsen ES, Jr, Gottfried D (1960) Uranium and thorium in selected suites of igneous rocks, Am J Sci, 258-A, pp 151 ff

Larsen ES, Jr, Gottfried D (1961) Distribution of uranium in rocks and minerals of Mesozoic batholiths in Western United States, US Geol Surv Bull 1070-C, 63 p

Larsen ES, Jr, Phair G (1954) The distribution of uranium and thorium in igneous rocks, *in*: Faul H, ed., Nuclear geology, John Wiley and Sons, Inc, New York, pp 75–89

Larsen ES, Jr, Phair G, Gottfried D, Smith WL (1956) Uranium in magmatic differentation, US Geol Surv Prof Paper 300, pp 65–74

Larsen ES, Jr, Gottfried D, Molloy M (1958) Distribution of uranium in the volcanic rocks of the San Juan Mountains, southwestern Colorado, UN Second Intern Conf Peaceful Uses Atomic Energy, Geneva, 2, pp 509–514

Laverov NP, Velichkin VI, Vetrov VI, Krotkov VV, Lapin AL, Naumov SS, Pelminev MD, Shumilin MV (1991) USSR uranium raw material resources: Technical Committee Meeting on New Developments in Uranium Exploration, Resources, Production and Demand, August 1991, IAEA, Vienna, manuscript, 18p+Figs+Tables

Le VT (1975) Géochimie de l'uranium et du thorium dans les granitoïdes et formations associées de la Montagne Bourbonnaise (Massif Central français), Thesis, INPL (Inst Natl Polytech Lorraine), Nancy (unpubl)

Lease LW (1980) Geologic report on East Chaco drilling project, McKinley and San Juan Counties, New Mexico, US-DOE, GJBX-98(80), 62 p

Lee MJ (1976) Geochemistry of the sedimentary uranium deposits of the Grants mineral belt, southern San Juan Basin, New Mexico, unpubl PhD diss, Univ New Mexico, Albuquerque, 241 p

Lee MJ, Brookins DG (1980) Rubidium-strontium minimum ages of sedimentation, uranium mineralization, and provenance, Morrison Formation (Upper Jurassic), Grants mineral belt, New Mexico – Reply, Amer Ass Petrol Geol Bull, v 64, p 1719

Lefebvre JJ, Tshauka T (1986) Alterations associées à la mineralisation uranifère de Mososhe (Shaba-Zaïre), Musée Royal de l'Afrique Centrale – Tervuren, Belg Ann Ser 8 Sci Gèol 92, 63 p

Le Fort P (1981) Manaslu leucogranite: a collision signature of the Himalaya – a model for its genesis and emplacement, J Geophys Res, 86, pp 10545–10568

Legierski J (1966) Některé nové poznatky o metalogenezi

Českého masivu získané metodou izotopů obyčejného olova (Some new disclosures on the metallogeny of the Bohemian Nucleus obtained using the Pb-isotopes method) Ústřední ústav geol., Prague, Zprávy o geol výzk. 1964, v. 1, pp 18–82

Legierski J (1967) Využití izotopického složení olova v galenitech pro řešení metalogenetických problemů českého masivu (Solution of problems in metallogeny of the Bohemian Massif using the isotopic composition of lead in galenas), Sbornik I geochemické konference, Ostrava

Legierski J, Sattran V (1967) Blei-Isotope in Galeniten des Böhmischen Massivs, Freiberger Forschungshefte C 209, pp 73–80

Lehnert-Thiel K (1987) Exploration for high-grade uranium deposits in the Athabasca Basin, Canada, manuscript (paper given at Bergmannstag, Leoben, Austria, 17 p

Lehnert-Thiel K, Kretschmar W, Petura J (1981) The geology of the Maurice Bay uranium deposit, *in*: CIM, Geol Div, Uranium Field Excursion Guidebook, pp 103–108

Lekas MA, Dahl HM (1956) The geology and uranium deposits of the Lisbon Valley anticline, Utah, *in*: Peterson JA, ed., Geology and economic deposits of east-central Utah, 7th Field Conf IAPG, Salt Lake City, pp 161–168

Lemoine A (1975) Contribution à l'étude du comportement de UO_2 en milieu aqueux à haute température et haute pression, Doctoral thesis (unpubl), Univ Nancy, 111 p

Lenthall DH (1970) A micro-sedimentological study of the upper Witwatersrand sequence in the East Rand-Delmas area, Transvaal, Univ Witwatersrand, Johannesburg, unpubl MSc thesis, 105 p

Leonova LL (1962) Distribution of thorium in minerals of the granites of the Susamyr Batholith (Central Tien Shan), Geochem (USSR) (English Transl), pp 571 ff

Leonova LL (1964) Uranium and thorium in the Variscan alkaline intrusives of Southern Tien Shan (Matcha and Turpi Massifs), Geochem (USSR) (English Transl), pp 925 ff

Leonova LL, Pogiblova LS (1961) Uranium in minerals of the intrusive rocks of the Kyzyl-Ompul Mountains (northern Kirgiziya), Geochem (USSR) (English Transl), pp 999 ff

Leonova LL, Renne OS (1964) Distribution of uranium, thorium, and potassium in homogeneous granites, Geochem (USSR) (English Transl), pp 775 ff

Leonova LL, Tauson LV (1958) The distribution of uranium in the minerals of the Caledonian granitoids of the Susamyr Batholith (central Tien Shan), Geochem (USSR) (English Transl), pp 815 ff

Le Roux JP (1985) Palaeochannels and uranium mineralization in the main Karoo basin of South Africa, PhD thesis (unpubl), Univ Stellenbosch

Le Roux JP, Smits H, Toens PD, Uiterwijk BH (1979) A review of the uranium occurrences in the Karoo [extended abs], Geol Soc S Afr, Geokongres 79, Karoo Basin Symposium, Port Elizabeth, Pt 2, pp 32–37

Leroy J (1971) Les épisyénites non minéralisées dans le massif de granite à deux micas de St Sylvestre (Limousin, France), Equilibres entre minéraux et solutions, unpubl, thesis, Univ Nancy I, 87 p

Leroy J (1978a) Métallogénèse des gisements d'uranium de la Division de la Crouzille (COGEMA – Nord Limousin – France), Sci Terre, Nancy, Mém no. 36, 276 p

Leroy J (1978b) The Margnac and Fanay uranium deposits of the La Crouzille district (western Massif Central, France): geologic and fluid inclusion studies, Econ Geol, v 73, pp 1611–1634

Leroy J (1982) Le gisement du Bernardan, Etudes minéralogiques chimiques et des inclusions fluides de l'épisyénitisation, Rapport CREGU 82-01, 93 p

Leroy J (1984) Episyénitisation dans le gisement d'uranium du Bernardan (Marche), Comparaison avec des gisements similaires du Nord Ouest du Massif Central français, Mineral Deposita, 19, pp 26–35

Leroy J, Cathelineau M (1982) Les minéraux phylliteux dans les gisements hydrothermaux d'uranium I. Christallochimie des micas hérités et néoformés, Bull Minér, v 105, pp 99–109

Leroy J, Holliger P (1984) Mineralogical, chemical and isotopic (U-Pb method) studies of Hercynian uraniferous mineralizations (Margnac and Fanay mines, Limousin, France), Chem Geol, 45, pp 121–134

Leroy J, Poty B (1969) Recherches préliminaires sur les fluides associés à la genèse des minéralisations en uranium du Limousin (France), Mineral Deposita, 4, pp 395–400

Leroy J, Sonet J (1976) Contribution à l'étude géochronologique des filons de lamprophyres recoupant le granite à deux micas de St Sylvestre (Limousin Massif Central français), CR Acad Sci Fr 283, pp 1477–1480

Leroy J, George-Aniel B, Pardo-Leyton E (1985) Deposits and radioactive anomalies in the Sevaruyo region (Bolivia), *in*: Uranium deposits in volcanic rocks, IAEA, Vienna, pp 289–300

Leroy J, Aniel B, Poty B (1987) The Sierra Peña Blanca (Mexico) and the Meseta Los Frailes (Bolivia): The uranium concentration mechanisms in volcanic environment during hydrothermal processes, Uranium, 3, pp 211–234

Lespinasse M (1984) Contexte structural des gisements d'uranium de la Marche Occidentale, Fracturation, circulations fluides, propagation de l'épisyénitisation, Géol Géochim Uranium, Mém, Nancy, 8, 200 p

Lespinasse M (1989) Microfracturing and regional stress field: relation with fluid chronology and hydrothermal quartz leaching (episyenitization), *in*: Uranium deposits in magmatic and metamorphic rocks, IAEA, Vienna, pp 57–76

Lespinasse M, Pecher A (1985) Microfissuration and regional stress field: a study of the preferred orientation of fluid inclusion planes in a granite from the Massif Central, France, (submitted to Journal of Structural Geology) (manusc)

Leutwein F (1957) Alter und paragenetische Stellung der Pechblende erzgebirgischer Lagerstätten, Geologie 6, H 8, pp 797–805

Leventhal JC, Granger HC (1977) Conceptual-mathmatical models of uranium ore formation in sandstone-type deposits, *in*: Campbell JA, ed., Short papers of the US Geol Surv Uranium-Thorium Symp 1977, US Geol Surv Circ, p 753

Leventhal JS (1980) Organic geochemistry and uranium in the Grants mineral belt, *in*: Rautman CA, ed., Geology and mineral technology of the Grants Uranium Region 1979, New Mex Bur Mines Mineral Res Mem 38, pp 75–84

Leventhal JS, Threlkeld CN (1978) Carbon-13/Carbon-12 fractionation of organic matter associated with uranium

ores induced by alpha irradiation, Science, v 202, pp 430–432
Leventhal J, Daws T, Frye J (1986) Organic geochemical analysis of sedimentary organic matter associated with uranium, Appl Geochem, v 1, pp 241–247
Leventhal JS, Grauch RI, Threlkeld CN, Lichte FE, Harper CT (1987) Unusual organic matter associated with uranium from the Claude deposit, Cluff Lake, Canada, Econ Geol, v 82, pp 1169–1176
Levinson AA (1980) Introduction to exploration geochemistry, 2nd Ed, The 1980 supplement, Applied Publishing, Ltd, Wilmette, III, pp 615–924
Levinson AA, Bland CJ (1978) Examples of the variability of disequilibrium and the emanation factor in some uraniferous materials, Can J Earth Sci, v 15, pp 1867–1871
Lewis RQ, Sr, Campbell RH (1965) Geology and uranium deposits of Elk Ridge and vicinity, San Juan County, Utah, US Geol Surv Prof Paper 474-B
Lewis RQ, Sr, Trimble DE (1959) Geology and uranium deposits of Monument Valley, San Juan County, Utah, US Geol Surv Bull 1087-D, pp 105–131
Lewry JF, Sibbald TII (1977) Variation in lithology and tectonometamorphic relationships in the Precambrian basement of northern Saskatchewan, Can J Earth Sci, v 14, pp 1453–1467
Lewry JF, Sibbald TII (1979) A review of pre-Athabasca basement geology in northern Saskatchewan, *in*: Parslow GR, ed., Uranium exploration techniques, Geol Soc Sask Spec Publ 4, pp 19–58
Lewry JF, Sibbald TII (1980) Thermotectonic evolution of the Churchill Province in northern Saskatchewan, Tectonophysics, 68, pp 45–82
Lewry JF, Sibbald TII, Rees CJ (1978) Metamorphic patterns and their relation to tectonism and plutonism in the Churchill Province in northern Saskatchewan, *in*: Metamorphism in the Canadian Shield, Geol Surv Can Paper 78–10, pp 139–154
Li WC, Victor DM, Chakrabarti CL (1980) Effect of pH and uranium concentration on interaction of uranium (VI) and uranium (IV) with organic ligands in aqueous solutions, Anal Chem, v 52, pp 520–523
Li T, Huang Z (1986) Vein uranium deposits in granites of the Ziazhung ore field, *in*: Vein type uranium deposits, TECDOC-361, IAEA, Vienna, pp 359–376
Li YH (1972) Geochemical mass balance among lithosphere, hydrosphere, and atmosphere, Amer J Sci, v 272, pp 119–137
Liebenberg WR (1955) The occurrence and origin of gold and radioactive minerals in the Witwatersrand System, the Dominion Reef, the Ventersdorp Contact Reef and the Black Reef, Trans Geol Soc S Afr, v 58, pp 101–254
Liebenberg WR (1973) Mineralogical features of gold ores in South Africa, *in*: Adamson RJ, ed., Gold metallurgy in South Africa, Chamber Mines S Afr, Johannesburg, pp 352–446
Limpo de Faria F (1966) Gites d'uranium portugais dans des formations metasedimentaires, Com Serv Geol Portugal 50, pp 9–50
Lindroos H, Smellie JAT (1979) A stratabound uranium occurrence within Middle Precambrian ignimbrites at Duobblon, northern Sweden, Econ Geol, v 74, pp 1118–1130
Lisitsyn AK (1969) Conditions of molybdenum and selenium deposition in exogenous epigenetic uranium deposits, Lith Miner Res, (translated from Russian) v 5, pp 542 ff
Lisitsyn AK, Kuznetsova EC (1967) Role of microorganisms in development of geochemical reduction barriers where limonitization bedded zones wedge-out, Intern Geol Review, v 9, no. 9, pp 1180–1191
Li Tiangang, Huang Zhizhang (1986) Vein uranium deposits in deposits of Xiazhuang ore field, *in*: Vein type uranium deposits, TECDOC-361, IAEA, Vienna, pp 359–376
Little HW (1957) Geology of the Kettle River (east half) area, British Columbia, Geol Surv Can Map 6-1957
Little HW (1961) Geology of the Kettle River (west half) Area, British Columbia, Geol Surv Can Map 15-1961
Little HW (1970) Distribution of types of uranium deposits and favourable environments for uranium exploration, *in*: Uranium exploration geology, IAEA, Vienna, pp 35–48
Little HW (1974) Uranium in Canada, *in*: Report of activities, Part A; Geol Surv Can Pap 74-1A, pp 137–139
Little HW, Smith EEN, Barnes FQ (1972) Uranium deposits of Canada, 24th Intern Geol Cong, Montreal 1972, Guidebook to Field Excursion C67, 64 p.
Liu Xingzhong (1982) The types of uranium deposits and characteristics of geological mineralization in China, Chinese J Nuclear Sci Eng, v 2, 1, 81 p
Lobato LM, Forman JMA, Fyfe WS, Kerrik R, Barnett RL (1983) Uranium enrichment in Archean crustal basement associated with overthrusting, Nature, 303, pp 235–237
Locardi E (1977) Recent volcanoes and uranium mineralizations, *in*: Recognition and evaluation of uraniferous areas, IAEA, Vienna, pp 229–240
Locardi E (1985) Uranium in acidic volcanic environments, *in*: Uranium deposits in volcanic rocks, IAEA, Vienna, pp 17–28
Locardi E (1988) Uranium provinces and mantle anomalies, *in*: Recognition of uranium provinces, IAEA, Vienna, pp 33–44
Lopatkina AP (1964) Characteristics of migration of uranium in the natural waters of humid regions and their use in the determination of the geochemical background for uranium, Geochem Intern, pp 788–795
Loring WB (1958) Geology and ore deposits of the northern part of the Big Indian district, San Juan County, Utah, Univ Arizona, PhD thesis
Loskorin BN, Metalnikov SS, Terentiev AS (1958) Extraction of uranium from natural water, UN Intern Conf Peaceful Uses Atomic Energy, 2nd, Geneva, v 3, pp 211–215
Louw JD (1954) Geological age determinations on Witwatersrand uraninites using the lead isotope method, Trans Geol Soc S Afr, v 57, pp 209–227
Louw JD (1955) Geological ages of Witwatersrand uraninites, Nature, v 175, p 349
Love JD (1970) Cenozoic geology of the Granite Mountains area, central Wyoming, US Geol Surv Prof Paper 495-C, pp C1–C154
Lovering JF, Morgan JW (1963) Uranium and thorium in possible upper mantle materials, Nature, 197, pp 138 ff
Lovering JF, Morgan JW (1964) Uranium and thorium abundances in stony meteorites, 1. The chondritic meteorites, J Geophys Res, 69, pp 1979 ff
Lowdon JA, ed. (1961) Age determinations by the Geo-

logical Survey of Canada, Geol Surv Can Rep 2, Isotopic ages, Paper 61–17
Lowdon JA, Stockwell CH, Tipper HW, Wanless RK (1963) Age determinations and geological studies, Geol Surv Can Paper 62–17
Ludwig KR (1978) Uranium-daughter migration and U-Pb isotope apparent ages of uranium ores, Shirley Basin, Wyoming, Econ Geol, v 73, pp 29–49
Ludwig KR (1979) Age of uranium mineralization in the Gas Hills and Crooks Gap districts, Wyoming, as indicated by U-Pb isotope apparent ages, Econ Geol, v 74, pp 1654–1668
Ludwig KR (1980) Rubidium-strontium minimum ages of sedimentation, uranium mineralization, and provenance, Morrison Formation (Upper Jurassic), Grants mineral belt, New Mexico: Discussion, Amer Ass Petrol Geol, v 64, pp 1718–1719
Ludwig KR, Grauch RI (1980) Coexisting coffinite and uraninite in some sandstone-host uranium ores of Wyoming, Econ Geol, v 75, pp 296–302
Ludwig KR, Goldhaber MB, Reynolds RL, Simmons KR (1982) Uranium-lead isochron age and preliminary sulfur isotope systematics of the Felder uranium deposit, south Texas, Econ Geol, v 77, pp 557–563
Ludwig KR, Young EJ (1975) Absolute age of disseminated uraninite in Wheeler Basin, Grand County, Colorado, US Geol Surv J Res, v 3, no. 6, pp 747–751
Ludwig KR, Szabo BN, Granger HC (1977) Pleistocene apparent ages by U-Pb isotope and U-series methods for uranium ore in Dakota Sandstone near Gallup, New Mexico, US Geol Surv J Res, v 5, no. 6, pp 669–672
Ludwig KR, Rubin B, Fishman NS, Reynolds RL (1982) U-Pb ages of uranium ores in the Church Rock uranium district, New Mexico, Econ Geol, v 77, pp 1942–1945
Ludwig KR, Simmons KR, Webster JD (1984) U-Pb isotope systematics and apparent ages of uranium ores, Ambrosia Lake and Smith Lake districts, Grants mineral belt, New Mexico, Econ Geol, v 79, pp 322–337
Ludwig KR, Wallace AR, Simmons KR (1985) The Schwartzwalder uranium deposit, II: Age of mineralization and lead isotope constraints on source areas, Econ Geol, v 80, pp 1858–1871
Ludwig KR, Rasmussen JD, Simmons KR (1986) Age of uranium ores in collapse-breccia pipes in the Grand Canyon area, northern Arizona, Geol Soc Amer Bull 18, 5, p 392
Lupe R (1976) Deposition environments as a guide to uranium mineralization in the Chinle Formation, San Rafael Swell, Utah, US Geol Surv Rep 76–283, 18 p
Lyons JB (1961) Uranium and thorium in the older plutonic rocks of New Hampshire, Art 32 US Geol Surv Prof Paper 424-B, B 69
Lyons JB (1964) Distribution of thorium and uranium in three early Paleozoic Plutonic Series of New Hampshire, US Geol Surv Bull 1144-F, 43 p
Maas R (1989) Nd-Sr isotope constraints on the age and origin of unconformity-type uranium deposits in the Alligator Rivers Uranium Field, Northern Territory, Australia, Econ Geol, v 84, pp 64–90
MacDonald CC (1980) Mineralogy and geochemistry of a Precambrian regolith in the Athabasca Basin, unpubl MSc thesis, Univ Saskatchewan, 151 p
Macdonald CC (1985) Mineralogy and geochemistry of the sub-Athabasca regolith near Wollaston Lake, *in*: Sibbald, TII, Petruk, W, eds., Geology of uranium deposits, CIM Spec Vol. 32, pp 155–163
Mackin JH, Schmidt DL (1955) Uranium and thorium-bearing minerals in placer deposits in Idaho, *in*: Contributions to the geology of uranium and thorium by the USGS and AEC, UN Intern Conf Peaceful Uses Atomic Energy, Geneva, pp 375–380
MacRae ME (1963) Geology of the Black Jack No. 1 mine, Smith Lake area, *in*: Kelley VC, ed., Geology and technology of the Grants Uranium Region, New Mex Bur Mines Mineral Res Mem 15, pp 45–48
Magleby DN (1961) Orphan Lode uranium mine, Grand Canyon, Arizona, US-AEC Techn Memo TM-134, 8 p
Mahadevan TM (1988) The Singhbhum uranium province, India, *in*: Recognition of uranium provinces, IAEA, Vienna, pp 337–400
Mahon WAJ, McDowell GD, Finlayson JB (1980) Carbon dioxide: Its role in geothermal systems, New Zealand J Sci, v 23, pp 133–148
Mahood GA (1983) Review of uranium in volcanic and volcanoclastic rocks, *in*: P Goodell P, A Waters A, eds., (1981) Econ Geol, v 78, pp 546–551
Mair JA, Maynes AD, Patchett JE, Russel RD (1960) Isotopic evidence on the origin and age of the Blind River uranium deposits, J Geophys Res, v 65, pp 341–348
Makarov ES, Lipova IM, Dolmanova IF, Melik'jan AA (1960) Crystal constitution of uraninites and pitchblendes, Transl from Geochim 3, 40 p
Malan RC (1968) The uranium industry and geology of the Monument Valley and White Canyon districts, Arizona and Utah, *in*: Ore deposits of the United States, 1933–1967, v 1, Amer Inst Min Met Petrol Eng, pp 790–803
Malan RC (1972) Summary report – distribution of uranium and thorium in the Precambrian of the western United States, US-AEC, AEC-RD-12, 59 p
Malan RC (1980) Volcanogenic uranium-molybdenum deposits in Russia and China, Country File, CN-14
Malan SP (1959) The petrology and mineralogy of the rocks of the Dominion Reef System near Klerksdorp, unpubl MSc thesis, Univ Witwatersrand, Johannesburg
Mallory WW, et al., eds. (1972) Geologic atlas of the Rocky Mountain region, Rocky Mountain Ass Geol, Denver, Colorado, 331 p
Mangas J, Arribas A (1984) Caracteristicas fisico-quimicas de los fluidos asociados con las mineralizaciones de uranio de mina Fé (Salamanca), VII Congr. Intern Min Met, Barcelona, I, pp 435–451
Mann AW, Deutscher RL (1978a) Genesis principles for the precipitation of carnotite in calcrete drainages in Western Australia, Econ Geol, v 731 pp 1724–1737
Mann AW, Deutscher RL (1978b) Hydrogeochemistry of a calcrete-containing aquifer near Lake Way, Western Australia, J Hydrol, 38, pp 357–377
Mann AW, Horwitz R (1979) Groundwater calcrete deposits in Australia: some observations from Western Australia, J Geol Soc Aust, 26, pp 293–303
Manning DAC (1982) An experimental study of the effects of fluorine on the crystallization of granitic melts, *in*: Evans AM, ed., Metallization associated with acid magmatism, Wiley, Chichester, pp 191–209
Marignac Ch, Leroy J (1979) Données nouvelles sur les rapports entre les massifs granitiques de la Brâme et de Saint Sylvestre (Nord Limousin, Massif Central, France), Implications, Bull BRGM 1, pp 3–26
Marjaniemi DK, Basler AL (1972) Geochemical investigations of plutonic rocks in the western United States

for the purpose of determing favorability for vein-type uranium deposits, US-AEC, GJO-912-16, 134 p
Marlow AG (1983) Geology and Rb-Sr geochronology of mineralized and radioactive granites and alaskites, Namibia, *in*: Miller R McG, ed., Evolution of the Damara Orogen of South West Africa/Namibia, Geol Soc S Afr Spec Publ no. II, pp 289–298
Marquaire C, Moreau M (1969) Esquisse géologique du Nord Limousin et répartition des minéralisations uranifères, Rapport CEA R 3684, pp 7–40
Martin S (1981) Episyénitisation et minéralisation dans le leucogranite d'Hyverneresse (Nord Millevaches, MCF), unpubl thesis, Univ Clermont II, 222 p
Martinez R (1979) Provenance study of the Westwater Canyon and Brushy Basin Members of the Morrison Formation between Gallup and Laguna, New Mexico, unpubl PhD diss, Univ New Mexico, Albuquerque, 79 p
Maruejol P, Cuney M (1985) Xihuashan tungsten-bearing granites (Jiangxi, China): mineralogical controls on REE, Y, Th, U mobility during magmatic evolution and hydrothermal alteration, (abstr), K 54, EUG III, Strasbourg
Marvin RF, Dobson SW (1979) Radiometric ages, compilation B, US Geol Surv Isochron West no. 25
Masek J (1981) Contribution to the geology of the Proterozoic of the SE limb of the Barrandian Basin (in Czech, Engl res), *in*: Pouba Z, ed., Correlation of the Proterozoic and Palaeozoic stratiform deposits, VI, UUG Prague, pp 14–28
Maslyn RM (1978) An epigenetic model for the formation of the Schwartzwalder uranium deposit, Econ Geol, v 73, pp 552–557
Masursky H (1962) Uranium-bearing coal in the eastern part of the Red Desert area, Wyoming, US Geol Surv Bull 1099-B, pp B1–B152
Mathews GW (1978a) Uranium occurrences in and related to plutonic igneous rocks, *in*: Mickle DG, Mathews GW, eds., Geologic characteristics of environments favorable for uranium deposits, US-DOE, GJBX-67(78), pp 121–180
Mathews GW (1978b) Uranium occurrences of uncertain genesis, *in*: Mickle DG, and Mathews GW, eds., Geologic characteristics of environments favorable for uranium deposits, US-DOE, GJBX-67(78), pp 221–250
Mathews GW, Jones CA, Pilcher RC, D'Andrea RF, Jr (1979) Preliminary recognition criteria for uranium occurrences: a field guide, US-DOE, GJBX-32(79), 41 p
Mathewson DE (1953a) Geology of the Poison Canyon mine, Valencia County, Sec 19, T 13 N, R 9 W, near Grants, New Mexico, US-AEC, TM-24, 7 p
Matos Dias JM, Soares de Andrade AA (1970) Uranium deposits in Portugal, *in*: Uranium exploration geology, IAEA, Vienna, pp 129–252
Matolin M, Pluskal O, Rene M (1981) Uranium mineralization in the Bohemian Massif and its exploration, *in*: Uranium exploration case histories, IAEA, Vienna, pp 389–398
Matte P (1974) Raccord des segments iberiques d'Europe sud-occidentale, Franz Kossmat Symp, Nova Acta Leopoldina, 224, pp 239–262
Matte P (1986) Tectonics and plate tectonics model for the Variscan belt of Europe, Tectonophysics, 126, pp 329–374
Matthews PE, Scharrer RH (1968) A graded unconformity at the base of the Early Precambrian Pongola System, Trans Geol Soc S Afr, v 71, pp 257–271
Maucher A (1962) Die Lagerstätten des Urans, Vieweg Verlag, Braunschweig, 162 p
Maurice YT, ed. (1982) Uranium in granites, Geol Surv Canada P 29 81–23, 173 p
Mazimhaka PK, Hendry HE (1987) The Martin Group: Middle Proterozoic terrigenous clastic cover rocks associated with "unconformity-type pitchblende" deposits in the Martin Lake Basin area, northern Saskatchewan, Canada, (abstr) IAEA meeting, Saskatoon, Canada, 1 p
Mazimhaka PK, Hendry HE (1989) Uranium deposits in the Beaverlodge area, northern Saskatchewan: their relationship to the Martin Group (Proterozoic) and the underlying basement, *in*: Uranium resources and geology of North America, TECDOC-500, IAEA, Vienna, pp 297–320
McAndrew J, Finlay CJ (1980) The nature and significance of the occurrence of uranium in the Nanambu Complex of the Pine Creek Geosyncline, *in*: Ferguson J, Goleby AB, eds., Uranium in the Pine Creek Geosyncline, IAEA, Vienna, pp 357–362
McBride EF, Lindemann WL, Freeman PS (1968) Lithology and petrology of the Gueydan (Catahoula) Formation in south Texas, Univ Texas, Austin, Bur Econ Geol Rep Invest 63, 122 p
McCammon RB, Finch WI, Kork JO, Bridges NJ (1986) Estimation of uranium endowment in the Westwater Canyon Member, Morrison Formation, San Juan Basin, using a data-directed numerical method, *in*: Turner-Peterson CE, Santos EC, Fishman NS, eds., A basin analysis case study – The Morrison Formation, Grants Uranium Region, New Mexico, Amer Ass Petrol Geol, Studies in Geology no. 22, pp 331–355
McDowell JP (1957) The sedimentary petrology of the Mississagi Quartzite in the Blind River area, Ontario Dep Mines Geol Circ 6, 31 p
McKee ED (1978) Paleozoic rocks of the Grand Canyon, *in*: Breed WJ, Roat E, eds., Geology of the Grand Canyon (3rd ed), Museum Northern Arizona and Grand Canyon Natural History Ass, pp 42–64
McKee ED (1982) The Supai Group of Grand Canyon, US Geol Surv Prof Paper 1173
McKee ED, Gutschick RC (1969) History of the Redwall Limestone of northern Arizona, Geol Soc Amer Mem 114, 726 p
McKelvey VE, Carswell LD (1956) Uranium in the Phosphoria Formation, US Geol Surv Prof Pap 300, pp 483–487
McKelvey VE, Everhart DL, Garrels RM (1955) Origin of uranium deposits, Econ Geol 50th Anniversary Vol., pp 474–492
McKelvey VE, William JS, Sheldon RP, Cressman ER, Cheney TM, Swanson RW (1956) Summary descriptions of Phosphoria, Park City, and Shedhorn Formations in western phosphate field, Amer Assoc Petrol Geol Bull, v 40, pp 2326–2863
McKinney JS et al. (1964) Geology of the Anglo American Group mines in the Welkom area, Orange Free State Goldfield, *in*: Haughton SH, ed., The geology of some ore deposits in southern Africa, Geol Soc S Afr, v 1, pp 451–506
McKnight WM, Jr (1972) A review of South Texas

uranium geology, Gulf Coast Ass Geol Soc Trans, v 22, pp 97–103
McLachlan C (1968) A grain study of zircon and chromite in the Vaal Reef of the Klerksdorp Goldfield, Transvaal, Univ Witwatersrand, Johannesburg, unpubl MSc thesis
McLemore VT (1983) Uranium and thorium occurrences in New Mexico, New Mex Bur Mines Mineral Res Rep no 183, 180 p
McLennan SM, Scott M, Taylor SR, (1980) Th and U in sedimentary rocks: crustal evolution and sedimentary recycling, Nature, v 285, pp 621–624
McLennan SM, Taylor SR (1979) Rare earth element mobility associated with uranium mineralization, Nature, v 282, pp 247–249
McLennan SM, Taylor SR (1980) Rare earth elements in sedimentary rocks, granites and uranium deposits of the Pine Greek Geosyncline, *in*: Ferguson J, Goleby AB, eds., Uranium in the Pine Creek Geosyncline, IAEA, Vienna, pp 175–190
McMillan RH (1977a) Metallogenesis of Canadian uranium deposits: a review, *in*: Jones MJ, ed., Geology, mining and extractive processing of uranium, IMM, London, pp 43–55
McMillan RH (1977b) Uranium in Canada, Bull Can Petrol Geol, v 25, pp 1222–1249
McRae OM, Grubaugh PL (1957) Geology of uranium deposits in the Inter-River area, Grand and San Juan Counties, Utah, US-AEC, RME-112
Meddaugh WS, Holland HD (1981) Age and origin of uraninite in the Elliot Lake, Ontario, uranium deposits, Geol Soc Amer, Abstr with Prog 13, p 509
Megrue GH, Kerr PF (1965) Alteration of sandstone pipes, Laguna, New Mexico, Geol Soc Amer Bull, v 76, no. 12, pp 1347–1360
Mehnert KR (1960) Zur Geochemie der Alkalien im tiefen Grundgebirge, Beitr Miner Petr, 7, pp 318–339
Melgunov SV, Mitropolsky AS, Kulik NA (1975) Uranium and thorium in the process of rock formation in zonal metamorphic complexes, *in*: Kuznetsov VA, ed., Radioactive elements in rocks, Nauka, Novosibirsk, USSR, pp 146–151
Melin RE (1969) Uranium deposits in Shirley Basin, Wyoming, Wyoming Univ Contr Geology, v 8, pp 143–149
Melin RE (1964) Description and origin of uranium deposits in Shirley Basin, Wyoming, Econ Geol, v 59, pp 835–849
Mellinger M (1980) Uranium metallogenic studies: Maurice Bay deposit, *in*: Christopher JE, McDonald R, eds., Summary of investigations, 1980, Regina, Sask Geol Surv, pp 89–92
Mellinger M (1985) The Maurice Bay uranium deposit (Saskatchewan): geology, host-rock alteration and genesis, *in*: Sibbald TII, Petruk W, eds., Geology of uranium deposits, CIM Spec Vol. 32, pp 140–150
Mellinger M, Quirt D, Hoeve J (1987) Geochemical signatures of uranium deposition in the Athabasca Basin of Saskatchewan, Canada, Uranium, 3, pp 187–209
Mel'nikov IV, Berzina IG (1973) Some characteristic features of the behaviour of uranium in the formation of uranium-molybdenum deposits, Soviet Atomic Energy, v 35, no. 1, pp 615–621 (Trans Consultants Bureau)
Melvin JW (1976) Systematic distribution of large uranium deposits in the Grants Uranium Region, New Mexico, *in*: Tectonics and mineral resources of south-western North America, New Mex Geol Ass Spec Publ no. 6, pp 144–150
Membrillera Membrillera J, Josa J, Delgado, E (1964) El uranio en España, UN Intern Conf Peaceful Uses of Atomic Energy, Sess 2.11, Geneva, pp 73–80
Meneghel L (1979) Uranium occurrence in the Katanga System of north-western Zambia, *in*: Uranium deposits in Africa, geology and exploration, IAEA, Vienna, pp 97–122
Meneghel L (1981a) The occurrence of uranium in the Katanga system of northwestern Zambia, Econ Geol, v 76, pp 56–68
Meneghel L (1981b) Methodology and history of discovery of uranium mineralization in North-Western Province of Zambia, *in*: Uranium exploration case histories, IAEA, Vienna, pp 75–97
Meneghel L (1984) Proterozoic stratabound uranium deposits of Zambia and Zaïre, *in*: Proterozoic unconformity and stratabound uranium deposits, TECDOC-315, IAEA, Vienna, pp 7–34
Meunier JD (1984) Les phénomènes d'oxydo-réduction dans un gisement urano-vanadifère de type tabulaire: les grès du Salt-Wash (Jurassique Supérieur), district miner de Cottonwood-Wash (Utah, Etats-Unis), Géol Géochim Uranium, Mém Nancy, no. 4, 214 p
Meunier JD (1989) Diagenesis and ore deposition in sandstone-hosted uranium-vanadium deposits in the Colorado Plateau: evidence from fluid inclusions, *in*: Uranium resources and geology of North America, TECDOC-500, IAEA, Vienna, pp 227–238
Meunier JD, Breit GN (1987) Fluid inclusion studies in calcite associated with sandstone-hosted uranium-vanadium deposits of the Colorado Plateau, (abstr), IAEA Meeting, Saskatoon, 1 p
Meunier JD, Landais P, Monthioux M, Pagel M (1987) Oxidation – reduction processes in the genesis of the uranium – vanadium tabular deposits of the Cottonwood Wash mining area (Utah, USA): evidence from petrological study and organic matter analysis, Bull Minér, 110, pp 145–156
Meyer M, Saager R, Koeppel V (1987) Uranium distribution and redistribution in a suite of fresh and weathered pre- Witwatersrand and Witwatersrand conglomerates from South Africa, *in*: Uranium deposits in Proterozoic quartz-pebble conglomerates, TECDOC-427, IAEA, Vienna, pp 255–273
Miall AD (1977) A review of the braided river depositional environment, Earth Sci Rev, v 13, pp 1–62
Michel JJ (1983) Episyénite et concentrations uranifères associées dans le massif de St. Sulpice-Les-Feuilles (Hte Vienne), unpubl thesis, INPL, 461 p
Mickle DG, Mathews GW (1978) Geologic characteristics of environments favorable for uranium deposits; US-DOE, GJBX-67(78), 250 p
Miesch AT (1963) Distribution of elements in Colorado Plateau uranium deposits – a preliminary report, US Geol Surv Bull 1147-E, pp E1-E57
Miesch AT (1962) Composition of sandstone host rocks of uranium deposits, Amer Inst Min Metal Petrol Eng Trans, v 223, pp 178–184
Miller DS, Kulp JL (1963) Isotopic evidence on the origin of the Colorado Plateau uranium ores, Geol Soc Amer Bull, v 74, pp 609–630
Miller LJ (1955) Uranium ore deposits of the Happy Jack

deposit, White Canyon, San Juan County, Utah, Econ Geol, v 50, pp 156–169
Miller RD (1954) Copper-uranium deposit at the Ridenour mine, Hualapai Indian Reservation, Coconino County, Arizona, Part I, US-AEC, RME-2014, pp 3–18
Miller RMcG (1983) The Pan-African Damara Orogen of South West Africa/Namibia, *in*: Miller RMcG, ed., Evolution of the Damara Orogen of South West Africa/Namibia, Geol Soc S Afr Spec Publ no. II, pp 431–515
Mineeva IG (1984) Mineralogisch-geochemische Aspekte der Bildung uranführender Albitite, 27th Inter Geol Congress, Moscow, manuscript, 15 p
Mineeva IG, Tarkhanova GA (1964) Behaviour of uranium and thorium during the postmagmatic process of potassic alkaline rocks, Geol rud mestorozh, v 6, no. 4, pp 3–14 (Econ Geol, v 60, p 1543)
Minter WEL (1970) Gold distribution related to sedimentology of a Precambrian Witwatersrand conglomerate, South Africa, as outlined by moving-average analysis, Econ Geol, v 65, pp 963–969
Minter WEL (1972) Sedimentology of the Vaal Reef in the Klerksdorp area, Univ Witwatersrand, Johannesburg, unpubl PhD diss, 170 p
Minter WEL (1976) Detrital gold, uranium, and pyrite concentrations related to sedimentology in the Precambrian Vaal Reef placer, Witwatersrand, South Africa, Econ Geol, v 71, pp 157–176
Minter WEL (1978) A sedimentological synthesis of placer gold, uranium and pyrite concentrations in Proterozoic Witwatersrand sediments, *in*: Miall AD, ed., Fluvial sedimentology, Can Soc Petrol Geol Mem 5, pp 801–829
Minter WEL (1979) Hydraulic equivalence of gold and pyrtie grains in the Carbon Leader Reef, Blyvooruitzicht, Carletonville Goldfield, Anglo American Corporation, Welkom Office, Rep 11/000/366/79/1146, 4 p
Minter WEL (1981a) The crossbedded nature of Proterozoic Witwatersrand placers in distal environments and a paleocurrent analysis of the Vaal Reef placer, *in*: Genesis of uranium and gold-bearing Precambrian quartz-pebble conglomerates, US Geol Surv Prof Paper 1161-A-BB, pp G1–G9
Minter WEL (1981b) Preliminary notes concerning the uranium-gold ratio and the gradient of heavy-mineral size distribution as factors of transport distance down the paleoslope of the Proterozoic Steyn Reef placer deposit, Orange Free State Goldfield, Witwatersrand, South Africa, *in*: Armstrong, CF, ed., Genesis of uranium- and gold-bearing Precambrian quartz-pebble conglomerates, US Geol Surv Prof Paper 1161-K, pp K1–K3
Minter WEL (1981c) The distribution and sedimentary arrangement of carbon in South African Proterozoic placer deposits, *in*: Armstrong, CF, ed., Genesis of uranium- and gold-bearing Precambrian quartz-pebble conglomerates, US Geol Surv Prof Paper 1161-P, pp P1–P4
Minter WEL, Feather CE, Glatthaar CW (1987) Mineralogical changes in Witwatersrand placer uranium during Proterozoic weathering, Welkom Goldfield, South Africa, *in*: Uranium deposits in Proterozoic quartz-pebble conglomerates, TECDOC-427 IAEA, Vienna, pp 275–291
Minter WEL, Hill WCN, Kidger RJ, Kingsley CS, Snowden PA (1986) The Welkom Goldfield, *in*: Annhaeusser, CR, Maske S, eds., Mineral deposits of southern Africa, Marshalltown, Geol Soc S. Afr, v 1, pp 497–539
Mitcham TW, Evensen CG (1955) Uranium ore guides, Monument Valley district, Arizona, Econ Geol, v 50, no. 2, pp 170–176
Modnikov IS, Chesnokov LV, Lebedev-Zinov'yev AA, Khaldey AY, Frolov GI (1978) Distribution patterns of uranium–molybdenum mineralization in volcanic-tectonic complexes of regions of continental volcanism, Intern Geol Rev, 21(1), pp 11–24
Moench RH (1962) Properties and paragenesis of coffinite from the Woodrow mine, New Mexico, Amer Miner, v 47, no. 1, pp 26–33
Moench RH (1963) Geologic limitations on the age of uranium deposits in the Laguna district, *in*: Kelley VC, ed., Geology and technology of the Grants Uranium Region, New Mex Bur Mines Mineral Res Mem 15, pp 157–166
Moench RH, Schlee JS (1967) Geology and uranium deposits of the Laguna district, New Mexico, US Geol Surv Prof Paper 519, 117 p
Moine B, Rakotondratsima C, Cuney M (1985) Les pyroxénites à urano-thorianite du Sud Est de Madagascar: conditions physico-chimiques de la métasomatose, Bull Minér, 108, pp 325–340
Molina P, Besombes JC (1975) Place du Francevillien dans le contexte géologique de l'Afrique, *in*: The Oklo phenomenon, IAEA, Vienna, pp 3–14
Mollier B (1984) Le granite de Brâme-St Sylvestre-St Goussaud – Ses structures magmatiques – Une étude de la distribution de l'uranium à l'échelle du grain, Geol Geochim Uranium, Mém Nancy, no. 7, 148 p
Mollier B, Bouchez JL (1982) Structuration magmatique du complexe granitique de Brâme, St Sylvestre, St Goussaud (Limousin, Massif Central français), CR Acad Sci Fr 294, pp 1329–1334
Mollier B, Bouchez JL, Cuney M, Friedrich M (1985) Magmatic and late-magmatic structure of the St Sylvestre peraluminous granitic complex (Limousin, France) – Implication on uranium metallogenesis, (abstr) Terra Cognita, 5(2–3), p 256
Money PL (1968) The Wollaston Lake fold-belt system, Saskatchewan-Manitoba, Can J Earth Sci, 5, pp 1489–1504
Money PL, Baer AJ, Scott BP, Wallis RH (1970) The Wollaston Lake belt, Saskatchewan, Manitoba, Northwest Territories, *in*: Baer AJ, ed., Basins and geosynclines of the Canadian Shield, Geol Surv Can Paper 70–40, pp 171–200
Monster J, Appel PWV, Thode HG, Schidlowski M, Carmichael CM, Bridgwater D (1979) Sulfur isotope studies in early Archean sediments from Isua, west Greenland: Implications of the antiquity of bacterial sulfate reduction, Geochim Cosmochim Acta, v 43, pp 405–413
Moorbath S, O'Nions RK, Pankhurst RJ (1973) Early Archean age for the Isua iron formation, west Greenland, Nature, v 245, pp 138–139
Moore GW (1954) Extraction of uranium from aqueous solution by coal and some other materials, Econ Geol, v 49, pp 652–658
Moore SC, Lavery NG (1980) Magnitude and variability of disequilibrium in San Antonio Valley uranium deposit, *in*: Rautman, CA, ed., Geology and mineral technology of the Grants Uranium Region 1979, New Mex Bur Mines Mineral Res Mem 38, pp 276–283

Moore WS (1967) Amazon and Mississippi River concentrations of uranium, thorium, and radium isotopes, Earth Planet Sci Lett, v 2, pp 231–234

Moreau M (1977) L'uranium et les granitoïdes: essai d'interprétation, *in*: Jones MJ, ed., Geology, mining and extractive processing of uranium, IMM, London, pp 83–102

Moreau M, Ranchin G (1971) Altérations hydrothermales et contrôles tectoniques dans les gites filoniens d'uranium intragranitiques du Massif Central français, *in*: Les roches plutoniques dans leurs rapports avec les gites minéraux, Symp E Raguin, Paris, pp 77–100

Moreau M, Poughon A, Puybaraud Y, Sanselme H (1966), L'uranium et les granites, Chron Mines Rech minière, 350, pp 47–50

Morgan BD (1965) Uranium ore deposit of Pandanus Creek, *in*: McAndrew J, ed., Geology of Australian ore deposits, Eighth Commonwealth Mining & Metallurgy Congress, 1, pp 210–211

Morin N, Tardieu Y (1972) Le gisement d'uranium de Mounana, République Gabonaise, Rev l'Indust Minér, v 54, pp 21–32

Morosenko NK (1965) Metallogenic epochs of uranium, Intern Geol Rev, v 8, no. 5, pp 608–620

Morton RD (1977) The western and northern Australia uranium deposits – Exploration guides or exploration deterrents for Saskatchewan, *in*: Dunn CE, ed., Uranium in Saskatchewan, Sask Geol Soc Spec Publ no. 3, pp 211–255

Morton RD, Beck LS (1978) The origins of the uranium deposits of the Athabasca region, Saskatchewan, Canada (abstr), Econ Geol, v 73, p 1408

Morton RD, Sassano GP (1972) Reflectance and microindentation hardness vs chemical composition in some Canadian uraninites, N Jb Miner, Mh 8, pp 350–360

Mossman DJ, Harron GA (1983) Origin and distribution of gold in the Huronian Supergroup, Canada – the case for Witwatersrand-type paleoplacers, Precamb Res, 20, pp 543–583

Motica JE (1968) Geology and uranium-vanadium deposits in the Uravan Mineral Belt, southwestern Colorado, *in*: Ridge JD, ed., Ore deposits of the United States, 1933–1967 (Graton-Sales volume), Amer Inst Min Metal Petrol Eng, v 1, pp 805–814

Mouillac JL, Valois J-P, Walgenwitz (1986) The Goanikontes uranium occurrence in South West Africa/Namibia, *in*: Anhaeusser CR, Maske S, Mineral deposits of Southern Africa, Geol Soc S Afr, v 2, pp 1833–1844

Moxham RM (1964) Radioelement dispersion in a sedimentary environment and its effect on uranium exploration, Econ Geol, v 59, pp 309–321

Mrak VA (1968) Uranium deposits in the Eocene sandstones of the Powder River Basin, Wyoming, *in*: Ridge JD, ed., Ore deposits of the United States, 1933–1967 (Graton-Sales volume), Amer Inst Min Metal Petrol Eng, v 1, pp 838–848

Mrňa F (1963a) Polyascendent and monoascendent zoning in the Jáchymov ore veins (Krusné hory mts, Czechoslovakia), *in*: Symposium problems of postmagmatic ore deposition, Prag, v I, pp 207–211

Mrňa F (1963b) On the genesis of ore veins in Jáchymov, *in*: Symposium problems of postmagmatic ore deposition, Prag, v I, pp 446–449

Mrňa F (1967) Zum Alter der Bi-Co-Ni-U-Ag-Formation in Jáchymov, Freiberger Forschungshefte, C 209, pp 81–86

Mrňa F, Pavlů D (1958) Několik poznámek k teorii rudodarných roztoků na podkladě studie Ag-Bi-Co-Ni formace v Jáchymove (Some remarks on the theory of ore solutions based on the studies of Ag-Bi-Co-Ni formation in Jáchymov), Věstnik Ústř ústavu geol, Prague, v 33, pp 235–244

Mrňa F, Pavlů D (1961) Některé problémy hydrothermalního zrudnění v území východně od karlovarského plutonu na české straně Krušných hor (Some problems of the hydrothermal mineralization in the area east from Karlovy Vary pluton on the Bohemian part of Krušné hory (Erzgebirge)), Sbornik Ústř ústavu geol, Prague, v 28, pp 523–579

Mrňa F, Pavlů D (1967) Ložiska Ag-Bi-Co-Ni-As formace v Českém masivu (Deposits of Ag-Bi-Co-Ni-As formation in the Bohemian Massif), Sbornik geol. věd, Prague, řada LG, v 9, pp 7–104

MSR&D/Mountain States Research and Development (1978) Engineering assessment and feasibility study of the Chattanooga Shale as a future source of uranium, US-DOE, GJBX-4(79), v 1, 257 p, v 2, 365 p, v 3, 216 p

Mullens TE, Freeman VL (1957) Lithofacies of the Salt Wash Member of the Morrison Formation, Colorado Plateau, Geol Soc Amer Bull, v 68, no. 4, p 505–526

Munday RJ (1979) Uranium mineralization in northern Saskatchewan, CIM Bull, v 72, no. 804, pp 102–111

Murphy M et al. (1978) Uranium in alkaline rocks, US-DOE, GJBX-78(78), 185 p

Murphy R (1948) Eldorado mine – structural geology of Canadian ore deposits, Trans CIM Symp 48, pp 259–268

Mursky G (1973) Geology of the Port Radium map area, District of Mackenzie, Geol Surv Can Mem 374, 40 p

Mutschler PH, Hill JJ, Williams BB (1976) Uranium from the Chattanooga Shale, US Bur Mines Inform Circ 8700, 85 p

Naeser CW (1978) Fission track dating, US Geol Surv Rep 76–190

Nakashima S, Disnar JR, Perruchot A, Trichet J (1984) Experimental study of mechanisms of fixation and reduction of uranium by sedimentary organic matter under diagenetic or hydrothermal conditions, Geochim Cosmochim Acta, 48, pp 2321–2329

Nakashima S, Disnar JR, Perruchot A (1985) Etude expérimentale des mécanismes de concentration de l'uranium par une matière organique sédimentaire dans des conditions de diagenèse croissante, premiers résultats, CR Acad Sc Paris, t 296, Série II, pp 1425–1428

Nakoman E (1979) Geology of radioactive deposits, Maden Tetik ve Arama Enst Vayinl, Egit Ser no. 20, 575 p, Ankara, (in Turkish)

Nash JT (1967) Geology and uranium deposits of the Jackpile mine area, Laguna, New Mexico, unpubl PhD diss, Columbia Univ, New York, 216 p

Nash JT (1968) Uranium deposits in the Jackpile sandstone, New Mexico, Econ Geol, v 63, pp 737–750

Nash JT, Frishman D (1981) Progress report on geologic studies of the Ranger orebodies, Northern Territory, Australia, *in*: Sibbald TII, Petruk W, eds., Geology of uranium deposits, CIM Spec Vol. 32, pp 205–215

Nash JT, Frishman D (1982) Progress report on geologic studies of the Ranger orebodies, Northern Territory, Australia, US Geol Surv Rep 82–936, 49 p

Nash JT, Frishman D (1983) Chemical data and statistical interpretations for rocks and ores from the Ranger

uranium mine, NT, Australia, US Geol Surv Rep 83–239, 135 p
Nash JT, Kerr PF (1966) Geologic limitations on the age of uranium deposits in the Jackpile sandstone, New Mexico, Econ Geol, v 61, pp 1283–1287
Nash JT, Granger HC, Adams SS (1981) Geology and concepts of genesis of important types of uranium deposits, Econ Geol, 75th Anniversary Volume, pp 63–116
Nations D, Stump (1981) Geology of Arizona, Kendall/Hunt Publ, Dubuque, lowa, 221 p
Naudet R, Filip A, Renson C (1975) Distribution detaillée de l'uranium à l'intérieur des amas, *in*: The Oklo phenomenon, IAEA, Vienna, pp 83–101
Naumov GB (1959) On the transport of uranium in carbonate hydrothermal solutions, Geokhim, no. 1, pp 6–19
Naumov GB (1961) Some physicochemical characteristics of the behavior of uranium in hydrothermal solutions, Geochem, no. 2, pp 127–147
Naumov GB (1973) The behavior of the radioactive components in hydrothermal processes, *in*: Radioactive elements in rocks, Izd-vo Nauka SO AN SSSR, Novosibirsk
Naumov GB (1978) Principles of physicochemical modelling of uranium ore formation, Atomizdat, Moscow, 213 p
Naumov GB, Mironova OF (1965) The migration of uranium in hydrothermal carbonate solutions, *in*: Prob Geochymii Isd Nauka
Naumov GB, Mironova OF (1969a) Migration of uranium in hydrothermal carbonate solutions (according to physicochemical data), *in*: Khitarov NI, ed., Problems of geochemistry, pp 166–175
Naumov GB, Mironova OF (1969b) Das Verhalten der Kohlensäure in hydrothermalen Lösungen bei der Bildung der Quarz-Nasturan-Kalzit-Gänge des Erzgebirges, Z Angew Geol, v 15, no. 5, pp 240–241
Naumov GB, Motorina ZM, Naumov VB (1971) Conditions of formation of carbonates in veins of the lead-cobalt-nickel-silver-uranium type, Geochem Intern, v 6, pp 590–598
Needham RS (1979) Solid geology of the Pine Creek Geosyncline, Northern Territory, Austral BMR, scale 1:500000
Needham RS (1981) A tabulated presentation of metallic mine and prospect data for the Pine Creek Geosyncline, NT, BMR, Canberra, 1981/39
Needham RS (1982) Geology of the Nabarlek region, Northern Territory, 1:100000 geological map and commentary, sheet 5573 and 5572, BMR, Canberra, 33 p
Needham RS (1984) Alligator Rivers, Northern Territory: Explanatory notes to the 1:250000 Geol Series, BMR, Canberra, 41 p
Needham RS (1985) A review of the distribution and controls of uranium mineralization in the Alligator Rivers Uranium Field, Northern Territory, Australia, *in*: Sibbald TII, Petruk W, eds., Geology of uranium deposits, CIM Spec Vol. 32, pp 216–230
Needham RS, Roarty MJ (1980) An overview of metallic mineralization in the Pine Creek Geocyncline, *in*: Ferguson J, Goleby AB, eds., Uranium in the Pine Creek Geosyncline, IAEA, Vienna, pp 157–173
Needham RS, Stuart-Smith PG (1976) The Cahill Formation – host to uranium deposits in the Alligator Rivers Uranium Field, Australia, BMR J, 1, pp 321–334
Needham RS, Stuart-Smith PG (1980) Geology of the Alligator Rivers Uranium Field, *in*: Ferguson J, Goleby AB, eds., Uranium in the Pine Creek Geosyncline, IAEA, Vienna, pp 233–258
Needham RS, Stuart-Smith PG (1984) The relationship between mineralization and depositional environment in Early Proterozoic metasediments of the Pine Creek Geosyncline, AIMM Conf Series 13, pp 201–212
Needham RS, Stuart-Smith PG (1985) Geology and mineralization of the South Alligator Valley Uranium Field. 1:75000 special map. Preliminary Edition, BMR, Canberra
Needham RS, Ferguson J, Prichard CE (1979) Excursion guide, Intern Uranium Symp Pine Creek Geosyncline, Sydney, Australia, 37 p
Needham RS, Crick HI, Stuart-Smith PG (1980) Regional geology of the Pine Creek Geosyncline, *in*: Ferguson J, Goleby AB, eds., Uranium in the Pine Creek Geosyncline, IAEA, Vienna, pp 1–22
Needham RS, Ewers GR, Ferguson J (1988) Pine Creek Geosyncline, *in*: Recognition of uranium provinces, IAEA, Vienna, pp 235–262
Negga HS, Sheppard SMF, Rosenbaum JM, Cuney M (1986) Late Hercynian U-vein mineralization in the Alps: fluid inclusion and C, O, H isotopic evidence for mixing between two externally derived fluids, Contrib Miner Petrol, 93, pp 179–186
Nekrasova ZA (1958) The origin of uranium mineralization in coal, *in*: The geology of uranium, Suppl no. 6, Sov Jour Atomic Energy, Trans Consultants Bureau, New York, pp 29–42
Nelson CE, Gallagher JRL (1982) Proterozoic origins of uranium mineralization in the Colorado Front Range, Econ Geol, v 77, pp 1221–1225
Nestler RK, Chenoweth, WL (1958) Geology of the uranium deposits of the Lukachukai Mountains, Apache County, Arizona, US-AEC, RME-118, 64 p
Nevskiy VA, Filonenko YD (1976) Fractured structures and screens of uranium deposits in calderas of subsidence, Intern Geol Rev, 20(10), pp 1221–1229
Nevskiy VA, Laverov NP, Tolkunov AY (1976) Structural-geological features of uranium deposits in calderas of subsidence, Atomnaya Energiya, v 40, vyp 2
Newman WL (1962) Distribution of elements in sedimentary rocks of the Colorado Plateau – a preliminary report, US Geol Surv Bull 1107-F, pp 337–445
Newman WL, Elston DP (1959) Distribution of chemical elements in the Salt Wash Member of the Morrison Formation, Jo Dandy area, Montrose County, Colorado, US Geol Surv Bull 1084-E, pp 117–150
Ngongo-Kashisha (1975) Sur la similitude entre les gisements uranifères (type Shinkolobwe) et les gisements cuprifères (type Kamoto) au Shaba, Zaïre, Ann Soc Gèol Belg, 98, pp 449–462
Nguyen-Trung C (1985) Géochimie théorique et expérimentale des oxydes d'uranium dans les solutions aqueuses de 25 à 700°C sous une pression de 1 à 6000 bars – Synthèses hydrothermale de certains minéraux d'U^6, et d'U^4, Thesis, INPL (Inst Natl Polytech Lorraine), Nancy, 479 p
Nicolaysen LO (1962) Stratigraphic interpretation of age measurements in southern Africa, *in*: Engel AEJ, Leonard BF, eds., Petrologic studies, a volume in honour of AF Buddington, Geol Soc Amer, pp 569–598
Nicolaysen LO, Burger AJ, Liebenberg WR (1962) Evidence for the extreme age of certain minerals from the

Dominion Reef conglomerates and the underlying granite in the western Transvaal, Geochim Cosmochim Acta, v 26, pp 15–23
Nininger RD (1977) Recognition of uranium districts, *in*: Recognition and evaluation of uraniferous areas, IAEA, Vienna, pp 1–11
Nishimori RK, Powell JD (1980) Uranium in carbonatites, USA, US-DOE, GJBX-147-80, 180 p
Nishimori RK et al. (1977) Uranium deposits in granitic rocks, US-DOE, GJBX-13(77), 298 p
Noble EA (1960) Genesis of uranium belts of the Colorado Plateau, Proc Intern Geol Congr, 21st Session, Copenhagen, pt 15, pp 26–39
Northrop HR (1982) Origin of the tabular-type vanadium-uranium deposits in the Henry structural basin, Utah, PhD thesis, Colorado School Mines, Golden, 194 p
Nuffield EW (1954) Brannerite from Ontario, Canada, Amer Miner, v 39, pp 520–522
Nyegaard P, Armour-Brown A, Steenfelt A (1986) Vein type uranium mineral occurrences in South Greenland, *in*: Vein type uranium deposits, TECDOC-361, IAEA, Vienna, pp 43–56
Oberthür T (1983) Metallogenetische Überlegungen zur Bildung des Carbon Leader Reef, Carletonville Goldfeld, Witwatersrand, Südafrika, unpubl PhD thesis, Univ Köln, 241 p
Oberthür T (1987) Mineralogy and geochemistry of phosphate minerals and brannerite from the Proterozoic Carbon Leader Reef gold and uranium deposit, Witwatersrand, South Africa, Gebrüder Borntraeger, Berlin-Stuttgart, Mon Ser Mineral Deposits, v 27, pp 129–142
Obradovich JD, Cobban WA (1975) A time scale for the Late Cretaceous of the western interior of North America, Geol Ass Can Spec Paper 13, 54 p
OECD(NEA)/IAEA (1970 to 1988) Uranium resources, production and demand, Paris (biannual joint reports)
OECD-NEA (1989) Nuclear energy data, ("brown book") OECD-NEA, Paris, 41 p
Oelsner O (1958) Die erzgebirgischen Granite, ihre Vererzung und die Stellung der Bi-Co-Ni-Formation innerhalb dieser Vererzung, Geologie, 7, H 3–6, pp 682–701
Offield TW, Miller GB, Pettersson BA (1982) Regional setting and uranium occurrence, Olden-Hotagen district of Sweden and adjacent Norway: Preliminary Landsat interpretation, *in*: Uranium exploration methods, OECD-NEA, Paris, pp 67–69
Ojakangas RW (1986) Sedimentology of the basal Kombolgie Formation, Northern Territory, Australia: A Proterozoic fluvial quartzose sequence, (abstr), 12th Intern Sed Congress Sediments Down Under, Canberra, Australia, p 231
Ojakangas RW (1987) The search for Elliot Lake-type uraniferous quartz-pebble conglomerates, southern Lake Superior region, USA, *in*: Uranium deposits in Proterozoic quartz-pebble conglomerates, TECDOC-427, IAEA, Vienna, pp 59–74
Olivier HJ (1965) The tectonics of the Upper Division of the Witwatersrand System in the Loraine area of the Orange Free State Goldfield, Trans Geol Soc S Afr, v 68, pp 143–175
Olson JC (1988) Geology and uranium deposits of the Cochetopa and Marshall Pass districts, Saguache and Gunnison Counties, Colorado, US Geol Surv Rep, 44 p
Omel'yanenko BI (1984) The types of uraniferous wall rock metasomatism, Symp Metallogenesis and Uranium Deposits, Moscow, pp 363–365
Omel'yanenko BI, Mineeva IG (1979) A vertical zoning of Precambrian uraniferous sodium metasomatites, Izv Akad Nauk SSSR, Ser Geol, no. 9, pp 96–106
Omel'yanenko BI, Mineeva IG (1982) Pre- and syn-ore vertical zonation in Precambrian uraniferous sodic metasomatites, Intern Geol Rev, 14, pp 422–430
Omel'yanenko BI et al. (1973) Behaviour of uranium during the wall rock alteration of rocks, Geol rud mestorozhd, v 15, no. 5, pp 60–65
O'Neill AJ, Nystrom RJ, Thiede DS (1981) National uranium resource evaluation, Williams quadrangle, Arizona, US-DOE, GJQ-009(81), 56 p
Openshaw R, Pagel M, Poty B (1978) Phases fluides contemporaines de la diagénèse des grès, des mouvements tectoniques et du fonctionnement des réacteurs nucléaires d'Oklo (Gabon), *in*: Les réacteurs de fission naturels, IAEA, Vienna, pp 267–296
Oosterbosch R (1962) Les minéralisations dans le système de Roan au Katanga *in*: Lombard J, Nicolini P, eds, Gisements Stratiformes de Cuivre en Afrique, Symposium, lre Partie, Assoc Services Géol Africains, pp 71–136
Oosterbosch R (1970) La prospection de l'uranium à Katanga, Peaceful Uses of Atomic Energy in Africa, Proc Symp, Kinshasa, 1969, IAEA, Vienna
Oosthuyzen EJ (1970) The geochronology of a suite of rocks from granitic terrain surrounding the Barberton Mountain Land, Univ Witwatersrand, Johannesburg, unpubl diss
Oosthuyzen EJ, Burger AJ (1964) Radiometric dating of intrusives associated with the Waterberg System, Annals, Rep S Afr Geol Surv, v 3, pp 87–106
Orajaka IP (1981) Mineralogy and uranium geochemistry of selected volcaniclastic sediments in the western United States – an exploration model, DGSc diss, Univ Texas, El Paso, 365 p
Ortlepp RJ (1962) On the occurrence of uranothorite in the Dominion Reef, Trans Geol Soc S Afr, v 65, pp 197–202
Ostle D (1982) Recognition of uranium provinces, *in*: Uranium exploration methods, OECD-NEA, Paris, pp 953–954
O'Sullivan RB, MacLachlan ME (1975) Triassic rocks of the Moab-White Canyon area, southeastern Utah, Canyonlands country guidebook, Four Corners Geol Soc, pp 129–142
Otton JK (1986) Geological environment of uranium in lacustrine host rocks in the western United States, *in*: Geological environments of sandstone-type uranium deposits, TECDOC-328, IAEA, Vienna, pp 229–241
Otton JK, Zielinski RA (1985) Movement and concentration of uranium in young, organic-rich sediments, Stevens County, Washington, *in*: Les Mécanismes de Concentration de l'Uranium dans les Environments Géologiques, Soc Franç Miner Cristall and CREGU, Nancy, pp 49–52
Otton JK, Zielinski RA (1987) The Flodelle Creek, young, organic, surficial uranium deposit, Stevens County, Washington, USA, (abstr), IAEA Meeting, Saskatoon, 1 p
Otton JK, Zielinski RA, Johnson SY (1989) The Flodelle Creek surficial uranium deposit, Stevens County, Washington, USA, *in*: Uranium resources and geology of North America, TECDOC-500, IAEA, Vienna, pp 241–262
Ouddou D (1984) Le massif de Guérande Le Croisic

(Loire Atlantique), Caractérisations géochimiques et minéralogiques de l'évolution magmatique, Implications métallogéniques, unpubl thesis, INPL Nancy, 306 p

Oversby YM (1975) Lead isotope systematics and ages of Archaean intrusives in the Kalgoorlie-Norseman area, Western Australia, Geochim Cosmochim Acta, 39, pp 1107–1125

Paar W, Köppel V (1978) Die Uranknollenparagenese von Mitterberg, Salzburg, Österreich, N Jb Miner, Abh 131, pp 254–271

Pacquet A, McNamara S (1985) The study of the basal Athabasca succession in the D, E, L, F, and S areas of the Carswell Structure, *in*: Lainé R, Alonso D, Svab M, eds, The Carswell Structure uranium deposits, (Saskatchewan), Geol Ass Can Spec Paper 29, pp 81–86

Page RW (1976) Geochronology of Archaean and Lower Proterozoic rocks in the Rum Jungle-Alligator Rivers area, Northern Territory, Australia, (abstr), 25th Intern Geol Congr, Section 1A

Page RW (1983) Chronology of magmatism, skarn formation, and uranium mineralization, Mary Kathleen, Queensland, Australia, Econ Geol, v 78, pp 838–853

Page RW, Compston W, Needham RS (1980) Geochronology and evolution of the Late Archaean basement and Proterozoic rocks in the Alligator Rivers Uranium Field, Northern Territory, Australia, *in*: Ferguson J, Goleby AB, eds, Uranium in the Pine Creek Geosyncline, IAEA, Vienna, pp 39–68

Pagel HO, Borshoff J, Coles R (1984) Veinlike uranium deposits in the Rum Jungle area – geological setting and relevant exploration features, Proc AIMM, pp 225–234

Pagel M (1975a) Cadre géologique des gisements d'uranium dans la structure Carswell (Saskatchewan-Canada), "Étude des Phases Fluides", Univ Nancy, diss, 156 p

Pagel M (1975b) La diagénèse des grès et les gisements d'uranium du Bassin Athabasca (Canada), *in*: Rapport d'activité 1975, Nancy, Équipe de Recherches sur les Équilibres entre Fluides et Minéraux, pp 50–52

Pagel M (1975c) Determinations des conditions physiochemiques de la silicification diagenetic des gres Athabasca (Canada) au moyen des inclusions fluides, Acad Sci [Paris] Comptes Rendus, v 280, ser D, pp 2301–2304

Pagel M (1976) Conditions de dépôt des quartz et dolomites automorphes du gisement uranifère de Rabbit Lake, Canada, Soc Géol France, 4th Réunion, Annales, 1 p

Pagel M (1977) Microthermometry and chemical analysis of fluid inclusions from the Rabbit Lake uranium deposit, Saskatchewan, Canada, (abstr), Trans IMM, London, v 86, B 157

Pagel M (1979) Particularités géochimiques uranium, thorium dans les complexes subalcalins potassiques: exemple du massif des Ballons (Vosges méridionales), CR Acad Sc Paris, t 289, Série D, pp 53–56

Pagel M (1981) Facteurs de distribution et de concentration de l'uranium et du thorium dans quelques granites de la chaine hercynienne d'Europe, Thesis, Inst Nat Polytech Lorraine, 566 p

Pagel M (1982a) Successions paragénétiques et teneurs en uranium des minéraux accessoires dans les roches granitiques, guides pour la recherche des granites favorables à la présence d'uranium, *in*: Uranium exploration methods, OECD-NEA, Paris, pp 445–456

Pagel M (1982b) The mineralogy and geochemistry of uranium, thorium, and rare-earth elements in two radioactive granites of the Vosges, France, Miner Mag, 46(339), pp 151–163

Pagel M (1982c) Granites et gisements d'uranium du Portugal, typologie, alterations et minéralisations, *in*: Vein-type and similar uranium deposits in rocks younger than Proterozoic, IAEA, Vienna, pp 323–347

Pagel M (1983) Les gisements d'uranium liés spatialement aux discordances, Géol Géochim Uranium, Mém Nancy, no. 1, 380 p

Pagel M (1984) Petrology, mineralogy and geochemistry of surficial uranium deposits, *in*: Surficial uranium deposits, TECDOC-322, IAEA, Vienna, pp 37–44

Pagel M (1989) Similarities and differences between unconformity-spatially related uranium deposits from Aveyron (France) and Saskatchewan, (abstract), *in*: Uranium resources and geology of North America, IAEA-TECDOC-500, Vienna, p 339

Pagel M, Jaffrezic H (1977) Analyses chimiques des saumures des inclusions de quartz et de la dolomite du gisement d'uranium de Rabbit Lake (Canada) – aspect méthodologique et importance génétique, CR l'Académie Sci, Paris, Série D, 284, pp 113–116

Pagel M, Pironon J (1986) Un modèle de formation de gisements d'uranium dans les shales noirs continentaux, Sci Géol Bull, 39, pp 277–292

Pagel M, Ruhlmann F (1985) Chemistry of uranium minerals in deposits and showings of the Carswell Structure (Saskatchewan-Canada), *in*: Lainé R, Alonso D, Svab M, eds., The Carswell Structure uranium deposits, Saskatchewan, Geol Ass Can Spec Paper 29, pp 153–164

Pagel M, Svab M (1985) Petrographic and geochemical variations within the Carswell Structure metamorphic core and their implications with respect to uranium mineralization, *in*: Lainé R, Alonso D, Svab M, eds; The Carswell Structure uranium deposits, Saskatchewan, Geol Ass Can Spec Paper 29, pp 55–70

Pagel M, Poty B, Sheppard SMF (1980) Contribution to some Saskatchewan uranium deposits mainly from fluid inclusion and isotopic data, *in*: Ferguson J, Goleby AB, eds, Uranium in the Pine Creek Geosyncline, IAEA, Vienna, pp 639–654

Pagel M, Pinte G, Rotach-Toulhoat N (1985) Rare earth elements in natural uranium oxides, (abstr) Fortschr Miner, 63, 1, p 174

Papenfus JA (1964) The Black Reef Series within the Witwatersrand Basin with special reference to its occurrence at government gold mining areas, *in*: Haughton, SH, ed., The geology of some ore deposits in southern Africa, Geol Soc S Afr, v 1, pp 189–218

Pardo-Leyton E (1985) Uranio en rocas ígneas: Intrusivas sub-efusivas y piroclásticas del Orogeno Andino boliviano, *in*: Uranium deposits in volcanic rocks, IAEA, Vienna, pp 255–274

Parslow GR (1989) Basement geochemistry and possible links between "Beaverlodge" and "Athabasca" type uranium mineralization, *in*: Uranium resources and geology of North America, TECDOC-500, IAEA, Vienna, p 321 (abstr)

Parslow GR, Adamson D (1982) Preliminary data on U and Th values in the basement rocks of the W Saskatchewan Shield, *in*: Uranium exploration methods, OECD-NEA, Paris, pp 219–234

Parslow GR, Thomas DJ (1982) Uranium occurrences in

the Cree Lake zone, Saskatchewan, Canada, Miner Mag, 46, pp 163–171
Paschis JA (1979) Mining and geologic developments at Cotter Corporations's Schwartzwalder uranium mine, Jefferson County, Colorado, Colo Min Ass, 1979 Mining Yearbook, pp 123–129
Patchett JE (1960) A study of the radioactive minerals of the uraniferous conglomerate, Blind River area, Univ Toronto, unpubl PhD diss, 220 p
Paterson J, von Pechmann E, Borshoff J (1984) Nature of uranium mineralization and associated wall rock alteration in the White's East area of the Embayment, Rum Jungle, Northern Territory, Proc AIMM, pp 235–248
Pearce JA, Harris NBW, Tindle AG (1984) Trace element discrimination diagrams for the tectonic interpretation of granitic rocks, J Petrol, 25(4), pp 956–983
Pecher A, Lespinasse M, Leroy J (1985) Relation between fluid inclusion trails and regional stress field: a tool for fluid chronology, Example of an intragranitic uranium ore deposit, north-west French Massif Central, Lithos, 18, pp 229–237
Pertlik F, et al. (1969) Uranium, *in*: Wedepohl KH, ed., Handbook of geochemistry, II-5, Springer, Berlin, Heidelberg, New York, 50 p
Peterman ZE, Hedge CE (1968) Chronology of Precambrian events in the Front Range, Colorado, Can J Earth Sci, v 5, pp 749–756
Peterson F (1977) Uranium deposits related to depositional environments in the Morrison Formation (Upper Jurassic), Henry Mountains mineral belt of southern Utah, *in*: Campbell JA, ed., Short papers of the US Geol Surv Uranium-Thorium Symp 1977, US Geol Surv Circ 753, pp 45–47
Peterson F (1978) Measured sections of the lower member in Salt Wash Member of the Morrison Formation (Upper Jurassic) in the Henry Mountains mineral belt of southern Utah, US Geol Surv Rep 78–1094, 97 p
Peterson F (1980a) Sedimentology of the uranium-bearing Salt Wash Member and Tidwell Unit of the Morrison Formation in the Henry and Kaiparowits basins, Utah, *in*: Picard MD, ed., Henry Mountains symposium, Utah Geol Ass Publ 8, pp 305–322
Peterson F (1980b) Sedimentology as a strategy for uranium exploration: concepts gained from analysis of a uranium-bearing depositional sequence in the Morrison Formation of south-central Utah. *in*: Turner-Peterson CE, ed., Uranium in sedimentary rocks: application of the facies concept to exploration, Soc Econ Paleontol Miner, Rocky Mountain Section, Short Course Notes, pp 65–126
Peterson F, Turner-Peterson CE (1980) Lacustrine-humate model: sedimentologic and geochemical model for tabular sandstone uranium deposits in the Morrison Formation, Utah, and application to uranium exploration, US Geol Surv Rep 80–319, 43 p
Peterson RJ (1980) Geology of a pre-Dakota uranium geochemical cell on Section 13, T 16 N, R 17 W, Churchrock area, McKinley County, New Mexico, *in*: Rautman CA, ed., Geology and mineral technology of the Grants Uranium Region 1979, New Mex Bur Mines Mineral Res Mem 38, pp 131–138
Petrascheck W and WE (1950) Lagerstättenlehre, Springer Verlag, Wien, 410 p
Petroš R, Prokeš S, Komínek J (1986) Uranium deposits of Příbram, CSSR, *in*: Vein type uranium deposits, TECDOC-361, IAEA, Vienna, pp 307–318
Petrosyan EV (1961) Characteristic features of the geological structure and composition of ores in a certain ore occurrence of the U-Ti-formation, Sovetsk, Geol, Coll, 11, pp 64–72 (in Russian)
Petrov BV, Krendelev FP, Bobrov VA, Tsimbalist VG (1972) Behaviour of radioelements and gold during metamorphism of sedimentary rocks in the Patom Uplands, Geochem Intern, v 9, no. 4, pp 647–655
Pettijohn FJ (1975) Sedimentary rocks (3d ed), Harper and Row, New York, 628 p
Peyrou E (1981) Pétrographie et géochimie du leucogranite de Grandrieu (Margeride, Massif Central), CREGU (Cent Rech Géol Uranium), Rep 81–3 (unpubl)
Pflffelmann, J-P (1975) L'uranium dans le bassin de Franceville, *in*: The Oklo phenomenon, IAEA, Vienna, pp 37–51
Phair G (1952) Radioactive Tertiary porphyries in the Central City district, Colorado, and their bearing upon pitchblende deposition, USGS TEI-247, US-AEC, Tech Inf Service, Oak Ridge, Tenn
Phair G (1955) Geologic investigations of radioactive deposits. Semiannual Progress Report, Dec 1954 to May 1955, US Geol Surv TEI 540, p 237
Phair G (1956) Geologic investigations of radioactive deposits. Semiannual Progress Report, Dec 1955 to May 1956, US Geol Surv TEI 620, p 310
Phair G (1975) Uranium, thorium, and lead in igneous rocks and veins, Colorado, US Geol Surv Rep 75–595, 34 p
Phair G (1979) Interpretation of lead-uranium ages of pitchblende deposits in the central Front Range, Colorado, Geol Soc Amer Bull, v 90, pp 858–870
Phair G, Gottfried D (1964) The Colorado Front Range, Colorado, USA, as a uranium and thorium province, *in*: Adams JAS, Lowder WM, eds., The natural radiation environment, Univ Chicago Press, pp 7–38
Phelps WT, Zech RS, Huffman AC, Jr (1986) Seismic studies in the Church Rock uranium district, southwest San Juan Basin, New Mexico, *in*: Turner-Peterson CE, Santos ES, Fishman NS, eds., A basin analysis case study – the Morrison Formation, Grants Uranium Region, New Mexico, Amer Ass Petrol Geol, Studies in Geology no. 22, pp 145–159
Philippe S, Lancelot J (1988) U-Pb Geochronological investigation of the Cigar Lake U ore deposit, Saskatchewan, (abstr), Chem Geol, v 70, no. 1/2, p 135
Phoenix DA (1958) Uranium deposits under conglomeratic sandstone of the Morrison Formation, Colorado and Utah, Geol Soc Amer Bull, v 69, no. 4, pp 403–417
Pierce HW, Keith SB, Wilt JC (1970) Coal, oil, natural gas, helium, and uranium in Arizona, Arizona Bur Mines Bull 182, 289 p
Pienaar PJ (1958) Stratigraphy, petrography and genesis of the Elliot Group including the uraniferous conglomerates, Quirke Lake Syncline, Blind River area, Ontario, unpubl PhD thesis, Queens Univ
Pienaar PJ (1963) Stratigraphy, petrology, and genesis of the Elliot Group, Blind River, Ontario, including the uraniferous conglomerate, Geol Surv Can Bull 83, 140 p
Pierson CT, Green MW (1980) Factors that localized uranium deposition in the Dakota Sandstone, Gallup and Ambrosia Lake mining districts, McKinley County, New Mexico, US Geol Surv Bull 1485, 31 p

Pierson CT, Spirakis CS, Robertson JF (1983) Comparison of abundances of chemical elements in mineralized and unmineralized sandstone of the Brushy Basin Member of the Morrison Formation, Smith Lake district, Grants Uranium Region, New Mexico, US Geol Surv Rep 83–818, 45 p

Piestrzyński A (1988a) Uranium and thorium in the Lubin polymetallic ore deposits, Fore-Sudetic Monocline, SW Poland, Miner Polon, 20, 1, pp 41–57

Piestrzyński A (1988b) Thucholite from Lubin polymetallic deposit, new data, N Jb Miner Abh, 160, pp 57–60

Piirainen T (1968) Die Petrologie und die Uranlager stätten des Koli-Kaltimogebietes im finnischen Nordkarelien, Bull Comm Géol Finlande, 237, pp 1–99

Pilar L (1966a) Condiçoes de formaçao do jazigo uranifero de Nisa, Com Serv Geol Portugal, 50, pp 51–83

Pilar L (1966b) Petrografia das rochas metamorficas e dos granitos de contacto da regiào de Nisa, Port Serv Geol Comun, 50, pp 51–83

Pilcher RC (1978) Volcanogenic uranium occurrences, *in*: Mickle DG, Mathews GW, eds., Geologic characteristics of environments favorable for uranium deposits, US-DOE, GJBX-67(78), pp 181–219

Piper JDA (1976) Paleomagnetic evidence for a Proterozoic supercontinent, Phil Trans Royal Soc, London, A 280, pp 469–490

Pironon J (1986) Zonalités géochimiques et minéralogiques dans les bassins continentaux uranifères. Exemples de St Hippolyte (Massif Vosgien), Müllenbach (Forêt Noire, RFA), Salamanière (Massif Central français), Géol Géochim, Mém Nancy, 13, 296 p

Pitman RK (1958) Uranium-vanadium deposits of the Cottonwood Wash mining area, San Juan County, Utah, US-AEC, RME-109 (Rev)

Plateau Resources Ltd (1983) Summary of the Shootaring Canyon project, Garfield County, Utah, AIME field trip, manuscipt, 18 p

Pliler R (1956) The distribution of thorium and uranium in sedimentary rocks and the oxygen content of the pre-Cambrian atmosphere, MA thesis, Rice Inst

Pliler R, Adams JAS (1962a) The distribution of thorium, uranium, and potassium in the Mancos shale, Geochim Cosmochim Acta, 26, p 1115

Pliler R, Adams JAS (1962b) The distribution of thorium and uranium in a Pennsylvanian weathering profile, Geochim Cosmochim Acta, 26, pp 1137–1146

Plumb KA, Derrick GM (1975) Geology of the Proterozoic of the Kimberley to Mount Isa region, *in*: Knight CL, ed., Economic geology of Australia and Papua New Guinea. 1. Metals, AIMM Monograph 5, pp 217–252

Pluskal O, René M (1976) Fundamental problems of uranium metallogeny in European Variscan belt, Internal Rep, Faculty of Science, Charles Univ, Prague, 108 p (in Czech)

Portugal Ferreira M, Matos Dias JM (1982) Uranium mineralization and episyenites. A case study in Portugal, *in*: Vein-type and similar uranium deposits in rocks younger than Proterozoic, IAEA, Vienna, pp 311–321

Posey-Dowty J, Axtmann E, Crerar D, Borcsik M, Ronk A, Woods W (1987) Dissolution rate of uraninite and uranium roll-front ores, Econ Geol, v 82, pp 184–194

Poty B, Leroy J, Cathelineau M, Cuney M, Friedrich M, Lespinasse M, Turpin L (1986) Uranium deposits spatially related to granites in the French part of the Hercynian Orogen, *in*: Vein type uranium deposits, TECDOC-361, IAEA, Vienna, pp 215–246

Poty B, Leroy J, Cuney M (1974) Les inclusions fluides dans les minerais des gisements d'uranium intragranitiques du Limousin et du Forez (Massif Central, France), *in*: Formation of uranium ore deposits, IAEA, Vienna, pp 569–582

Prashnowsky AA, Schidlowski M (1967) Investigation of Precambrian thucholite, Nature, v 216, pp 560–563

Premoli C (1979) Metallogeny of radioactive raw materials of Madagascar, *in*: Uranium deposits in Africa: geology and exploration, IAEA, Vienna, pp 41–68

Pretorius DA (1964a) The geology of the Central Rand Goldfield, *in*: Haughton SH, ed., The geology of some ore deposits in southern Africa, Geol Soc S Afr, v 1, pp 63–108

Pretorius DA (1964b) The geology of the South Rand Goldfield, *in*: Haughton SH, ed., The geology of some ore deposits in southern Africa, Geol Soc S Afr, v 1, pp 219–282

Pretorius DA (1974) The nature of the Witwatersrand gold-uranium deposits, Econ Geol Research Unit, Univ Witwatersrand, Info Circ no. 86, 50 p

Pretorius DA (1975) The depositional environment of the Witwatersrand goldfields: A chronological review of speculations and observations, Miner Sci Eng, v 7, pp 18–47

Pretorius DA (1976a) Gold in the Proterozoic sediments of South Africa: Systems, paradigms and models, *in*: Wolf KH, ed., Handbook of strata-bound and stratiform ore deposits, v 7, Elsevier, Amsterdam, pp 1–27

Pretorius DA (1976b) The nature of the Witwatersrand gold-uranium deposits, *in*: Wolf KH, ed., Handbook of strata-bound and stratiform ore deposits, v 7, Elsevier, Amsterdam, pp 29–88

Pretorius DA (1979) The crustal architecture of southern Africa, Geol Soc S Afr, 13th Alex du Toit Memorial Lecture, 60 p

Pretorius DA (1981) Gold and uranium in quartz-pebble conglomerates, Econ Geol, 75th Anniversary Volume, pp 117–138

Pretorius DA (1986a) The Goldfields of the Witwatersrand Basin, *in*: Anhaeusser CR, Maske S, eds., Mineral deposits of southern Africa, Geol Soc S Afr, v 1, pp 489–494

Pretorius DA (1986b) The geometry of the Witwatersrand Basin and its structural setting in the Kaapvaal Craton, Ext abstr, 21st Biennial congress, Johannesburg, Geol Soc S Afr, pp 47–52

Pluskal O (1991) The present state and future of the Czechoslovakian uranium industry: Technical Committee Meeting on New Developments in Uranium Exploration, Resources, Production and Demand, August 1991, IAEA, Vienna, manuscript 8 p

Purvance D (1980) Lisbon mine geology, Rio Algom Corp hand out, 6 p

Quenardel JM (1987) Super imposed deformations and magmatic intrusions in French western Massif Central and southeastern Brittany, manusc

Quick JV, Thomas NG, Brogdon LD, Jones CA, Martin TS (1977) Uranium favorability of Late Eocene through Pliocene rocks of the south Texas coastal plain, US-DOE, GJBX-7(77), 48 p

Quirt DH (1985) Lithogeochemistry of the Athabasca sandstone, Saskatchewan, Sask Res Council Publ no. R-855-3-B-85

Rackley RI (1972) Environment of Wyoming Tertiary

uranium deposits, Amer Ass Petrol Geol Bull, v 56, no. 4, pp 755–774
Rackley RI (1976) Origin of western-states type uranium mineralization, *in*: Wolf KH, ed., Handbook of stratabound and stratiform ore deposits, Elsevier, Amsterdam, pp 89–156
Rackley RI (1980) A prospect-scale "western-states" sandstone uranium model, *in*: Gaschnig J, ed., Development of uranium exploration models for the prospector consultant system, Menlo Park, California, SRI Intern Proj 7856, pp 15–62
Rafal'skiy RP (1958) The experimental investigation of the conditions of uranium transport and deposition by hydrothermal solutions, *in*: Proc UN, 2nd Internat Conf Peaceful Uses of Atomic Energy, v 2, Survey of raw material resources, Geneva, pp 432–444
Rafal'skiy RP (1963) On the transport and deposition of uranium by hydrothermal solutions and the role of complexing in these processes, Geochem (Trans), no. 5, pp 540–543
Rafal'skiy RP (1979) Thermodynamic analysis of equilibria in geochemistry and uranium deposition conditions in the supergenesis zone, Intern Geol Rev, v 21, no. 6, pp 672–686
Rafal'skiy RP, Osipov BS (1967) Equilibria in systems containing uranium and sulfides of heavy metals at 200° to 360°C, Geochem Intern, v 4, pp 202–213
Rafal'skiy RP, Alekseyev VA, Anan'yeva LA (1979) Phase compositions of natural and synthetic uranium oxides, Geochem Intern, v 16, no. 6, pp 13–26
Ragland PC, Rogers JJW (1980) Favourable tectonic belts for granitic uranium deposits: Pan-Africa and the southern Appalachians, J Geochem Explor, 13, pp 181–199
Rakotondratsimba Ch (1983) Les pyroxénites à uranothorianite du Sud-Est de Madagascar. Etude pétrographique, minéralogique et géochimique. Conséquences métallogéniques, unpub thesis, Lyon Univ, 215 p
Rakotondratsimba Ch, Cuney M (1984) The metasomatic origin of the uranothorianite-bearing pyroxenites, granulite facies, Geochroniques, 10, 34, Résumés 27 GCI
Ramaekers P (1979a) Stratigraphy of the Athabasca Basin, *in*: Summary of investigations 1979, Sask Geol Surv, Sask Miner Resour Misc Rep 79-10, pp 254–160
Ramaekers P (1979b) The paleolatitude and paleomagnetic age of the Athabasca Formation, northern Saskatchewan – discussion, Geol Surv Can Pap 79-10, pp 117–119
Ramaekers P (1980a) Stratigraphy and tectonic history of the Athabasca Group (Helikian) of northern Saskatchewan, *in*: Summary of investigations 1980, Sask Geol Surv, Sask Miner Res Misc Rep 80–4, pp 99–106
Ramaekers P (1980b) The paleolatitude and paleomagnetic age of the Athabasca Formation, northern Saskatchewan – further discussion, Geol Surv Can Pap 80-1B, pp 297–299
Ramaekers P (1981) Hudsonian and Helikian basins of the Athabasca region, northern Saskatchewan, *in*: Campbell FHA, ed., Proterozoic basins of Canada, Geol Surv Can Paper 81-10, pp 219–233
Ramaekers P (1983) Geology of the Athabasca Group, NEA/IAEA Athabasca test area, *in*: Cameron EM, ed., Uranium exploration in Athabasca Basin, Saskatchewan, Canada, Geol Surv Can Paper 82-11, pp 15–25
Ramaekers P, Dunn CE (1977) Geology and geochemistry of the eastern margin of the Athabasca Basin, *in*: Dunn CE, ed., Uranium in Saskatchewan, Sask Geol Soc Spec Publ 3, pp 297–332
Ramaekers PP, Hartling AA (1978) Structural geology and intrusive events of the Athabasca Basin and their bearing on uranium mineralization, *in*: Parslow GR, ed., Uranium exploration techniques, Geol Soc Sask Spec Publ 4, pp 221–234
Ramdohr P (1955) Neue Beobachtungen an Erzen des Witwatersrands in Südafrika und ihre genetische Bedeutung, Abh Dtsch Akad Wiss, Berlin, Kl Math Allg Naturwiss, 5, pp 1–43
Ramdohr P (1957a) Die "Pronto-Reaktion", N Jb Miner, Monatshefte, v 10–11, pp 217–222
Ramdohr P (1957b) Neue Beobachtung über radioaktive Höfe und über radioaktive Sprengungen, Abh dtsch Akad Wiss, Berlin, 2, 17 p
Ramdohr P (1958a) Die Uran- and Goldlagerstätten Witwatersand-Blind River District-Dominion Reef-Serra de Jacobina, Abh Deutsch Akad Wiss, Berlin, Klasse Chem Geol Biolog, no. 3, pp 1–35
Ramdohr P (1958b) New observations on the ores of the Witwatersrand in South Africa, Geol Soc S Afr, v 71, pp 67–100
Ramdohr P (1961) Das Vorkommen von Coffinit in hydrothermalen Uranerzgängen, besonders yom Co-Ni-Bi-Typ, N Jb Miner Abh, 95, pp 313–324
Ramdohr P (1980) The ore minerals and their intergrowths, Pergamon Press, 1207 p
Ramdohr P (1986) Die Metamorphose in der Uraninitfamilie, Bull Geol Soc Finland, 58, Part 1, pp 263–269
Ranchin G (1968) Contribution à l'étude de la répartition de l'uranium à l'état de traces dans les roches granitiques saines – Les granites à teneur élevée de massif de Saint Sylvestre, Sci Terre, Nancy, 13(2), pp 159–205
Ranchin G (1971) La géochimie de l'uranium et la différenciation granitique dans la province uranifère du Nord-Limousin, Sci Terre, Mém Fr 19, 394 p
Rapaport I (1952) Interim report on the ore deposits of the Grants district, New Mexico, US-AEC, RMO-1031, 19 p
Rapaport I (1963) Uranium deposits of the Poison Canyon ore trend, Grants district, *in*: Kelley VC, ed., Geology and technology of the Grants Uranium Region, New Mex Bur Mines Mineral Res Mem 15, pp 122–135
Rasmussen JD, Cunningham CG, Gautier AM (1986) Primary fluid inclusions in sphalerite from the Hack 1 and 2 mines, Mohave County, Arizona, (abstr), Geol Soc Amer, Rocky Mountain Section, Abstracts with Programs, p 394
Rautman CA, ed. (1980) Geology and mineral technology of the Grants Uranium Region 1979, New Mex Bur Mines Mineral Res Mem 38, 400 p
Rawson RR (1980) Uranium in Toldilto Limestone (Jurassic) of New Mexico – example of a sabkha-like deposit, *in*: Rautmann CA, ed., Geology and mineral technology of the Grants Uranium Region 1979, New Mex Bur Mines Mineral Res Mem 38, pp 304–312
Ray GE (1977) The geology of the Highrock Lake-Key Lake vicinity, Saskatchewan, Sask Dep Miner Res Rep 197, 36 p
Ray GE (1979) Reconnaissance bedrock geology: Wollaston Lake East (NTS 64L), *in*: Summary of

investigations 1979, Sask Geol Surv Misc Rep 79-10, pp 19–28
Ray GE (1980a) Compilation bedrock geology: Geikie River area (NTS 74H) *in*: Summary of investigations 1980, Sask Geol Surv Misc Rep 80–4, pp 10–12
Ray GE, Wanless RD (1980) The age and geological history of the Wollaston, Peter Lake and Rottenstone domains in northern Saskatchewan, Can J Earth Sci, v 17, pp 333–347
Reade HJ, Jr (1976) Grover uranium deposit: a case history of uranium exploration in the Denver Basin, Colorado, Mountain Geologist, v 13, no. 1, pp 21–31
Reed GW, Hamaguchi H, Turkevich A (1958) The uranium contents of iron meteorites, Geochim, Cosmochim Acta, v 13, p 248
Reed GW, Kigoshi K, Turkevich A (1960) Determinations of concentrations of heavy elements in meteorites by activation analysis, Geochim Cosmochim Acta, v 20, p 122
Reimer LR (1969) Stratigraphy, paleohydrology and uranium deposits of Church Rock Quadrangle, McKinley County, New Mexico, MS thesis, Colorado School Mines, Golden, 254 p
Reineck HE, Singh IB (1973) Depositional sedimentary environments, Springer, New York, 439 p
Reinecke L (1927) The location of payable ore-bodies in the gold-bearing reefs of the Witwatersrand, Trans Geol Soc S Afr, v 30, pp 89–119
Renard JP (1970) Géochimie de l'uranium de surface dans les massifs granitiques vendéens. Cas particulier du massif de Mortagne sur-Sèvre, Sci Terre, tome 15, no. 2, pp 167–194
Renard JP (1974) Étude pétrographique et géochimique des granites du district uranifère de Vendée – Liaison entre l'évolution minéralogique et le comportement de l'uranium, Sci Terre, Mém Nancy, no. 30, 214 p
Renick BC (1926) The Jackson Group and the Catahoula and Oakville Formations in a part of the Texas Gulf coastal plain, Univ Texas, Austin, Bull 2645, 187 p
Respaut JP (1984) Géochronologie et géochimie isotopique U-Pb de la minéralisation uranifère de la mine des Pierres Plantées (Lozère) et de son encaissant: le massif granitique de la Margeride, unpubl thesis, US TL Montpellier, 122 p
Reynolds RL, Goldhaber MB (1978) Origin of a south Texas roll-type uranium deposit: I. Alteration of iron-titanium oxide minerals, Econ Geol, v 73, pp 1677–1689
Reynolds RL, Goldhaber MB (1979) Iron disulfide minerals and the origin of roll-type uranium deposits, Geol Soc Amer, Annual Meeting, San Diego, California, Abstracts with programs
Reynolds RL, Goldhaber MB (1983) Iron disulfide minerals and the genesis of roll-type uranium deposits, Econ Geol, v 78, pp 105–120
Reynolds RL, Goldhaber MB, Grauch RI (1977) Uranium associated with iron-titanium oxide minerals and their alteration products in a south Texas roll-type deposit, US Geol Surv Circ 753, pp 37–39
Reynolds RL, Goldhaber MB, Rye RO, Fishman NS, Ludwig KR, Grauch RI (1980) History of sulfidization of the Felder uranium deposit, south Texas, US Geol Surv Rep 80–1096, 23 p
Reynolds RL, Goldhaber MB, Carpenter DJ (1982) Biogenic and nonbiogenic ore-forming processes in the south Texas uranium district: evidence from the Panna Maria deposit, Econ Geol, v 77, pp 541–556
Reynolds RL, Fishman NS, Scott JH, Hudson MR (1986) Iron-titanium oxide minerals and magnetic susceptibility anomalies in the Mariano Lake-Lake Valley cores – Constraints on conditions of uranium mineralization in the Morrison Formation, San Juan Basin, New Mexico, *in*: Turner-Peterson CE, Santos ES, Fishman NS, eds., A basin analysis case study – the Morrison Formation, Grants Uranium Region, New Mexico, Amer Ass Petrol, Geol Studies in Geology no. 22, pp 303–313
Rhett DW (1980) Heavy mineral criteria for subsurface uranium exploration, San Juan Basin, New Mexico, *in*: Rautman CA, ed., Geology and technology of the Grants Uranium Region 1979, New Mex Bur Mines Mineral Resources Mem 38, pp 202–207
Rice CM, Lux DR, Macintyre RM (1982) Timing of mineralization and related intrusive activity near Central City, Colorado, Econ Geol, v 77, pp 1655–1666
Rice R (1958) Geology and ore deposits of the Elliot Lake district, Ontario, unpubl PhD diss, Emmanuel College
Rich RA, Barabas AH (1982) Genetic implications of preliminary mineralogic, paragenetic, and fluid inclusion data for the Schwartzwalder uranium mine, Colorado, USA, *in*: Vein-type and similar uranium deposits, IAEA, Vienna, pp 181–193
Rich RA, Holland HD, Petersen U (1977) Hydrothermal uranium deposits, Elsevier Scientific Publ Co, Amsterdam-Oxford-New York, 264 p
Richards JR, Ruxton BP, Rhodes JM (1977) Isotopic dating of the leucocratic granite, Rum Jungle, Australia, Proc AIMM, 264, pp 33–43
Richards TE (1986) Geological characteristics of rare-metal pegmatites of the Uis type in the Damara Orogen, South West Africa/Namibia, *in*: Anhaeusser CR, Maske S, eds., Mineral deposits of southern Africa, Geol Soc S Afr, v 2, pp 1845–1862
Richardson KA (1964) Thorium, uranium, and potassium in the Conway granite, New Hampshire, USA, *in*: Adams JAS, Lowder WM, eds., The natural radiation environment, Chicago Univ Press, p 47
Richardson KA, Killen PG, Charbonneau BW (1975) Results of a reconnaissance type airborne gamma-ray spectrometer survey of the Blind River-Elliot Lake area, Geol Surv Can Paper 75-1A, pp 133–135
Ricoy JU, Brown LF, Jr (1977) Depositional systems in the Sparta Formation (Eocene) Gulf Coast Basin of Texas, Gulf Coast Ass Geol Soc Trans, v 27, pp 139–154
Ridgley JL (1980) Geology and characteristics of uranium mineralization in the Morrison Formation at the Dennison-Bunn claim, Sandoval County, New Mexico, *in*: Rautman CA, ed., Geology and mineral technology of the Grants Uranium Region 1979, New Mex Bur Mines Mineral Res Mem 38, pp 299–303
Ridgley JL, Goldhaber MB, Green MW, Pierson CT, Finch WI, Lupe RD (1978) Summary of the geology and resources of uranium in the San Juan Basin and adjacent region, New Mexico, Arizona, Utah, and Colorado, US Geol Surv Rep 78–964, 107 p
Riese WC (1977) Geology and geochemistry of the Mt Taylor uranium deposit, Valencia County, New Mexico, unpubl MS thesis, Univ New Mexico, Albuquerque, 146 p
Riese WC (1979) The Mount Taylor uranium deposit of the Grants Mineral Belt, New Mexico, PhD diss, Univ New Mexico, Albuquerque
Riese WC, Brookins DG (1984) The Mount Taylor

uranium deposit, San Mateo, New Mexico, USA, Uranium, v 1, pp 189–209
Riese WC, Brookins DG, Della Valle RS (1980) Scanning-electron-microscope investigation of paragenesis of uranium deposits, Mount Taylor and elsewhere, Grants mineral belt, *in*: Rautman CA, ed., Geology and mineral technology of the Grants Uranium Region 1979, New Mex Bur Mines Mineral Res Mem 38, pp 244–251
Riley GH (1980) Granite ages in the Pine Creek Geosyncline, *in*: Ferguson J, Goleby AB, eds., Uranium in the Pine Creek Geosyncline, IAEA, Vienna, pp 69–72
Riley GH, Binns RA, Craven SJ (1980) Rb-Sr chronology of mines at Jabiluka, *in*: Ferguson J, Goleby AV, eds., Uranium in the Pine Creek Geosyncline, IAEA, Vienna, pp 457–468
Rimsaite JYH (1977) Mineral assemblage at the Rabbit Lake uranium deposit, Saskatchewan, A preliminary report, *in*: Report of activities, Part B, Geol Surv Can Paper 77-1B, pp 235–246
Rimsaite JYH (1979) Petrology of basement rocks at the Rabbit Lake deposit and progressive alteration of pitchblende in an oxidation zone of uranium deposits in Saskatchewan, *in*: Current research, Part B, Geol Surv Can Paper 79-1B, pp 281–299
Rimsaite JYH (1989) Genetic significance of inclusions and fracture fillings in magmatic and metamorphic rocks from selected Canadian uranium occurrences, *in*: Uranium deposits in magmatic and metamorphic rocks, IAEA, Vienna, pp 167–188
Ristorcelli SJ (1980) Geology of the eastern Smith Lake ore trend, Grants mineral belt, New Mexico, *in*: Rautman CA, ed., Geology and mineral technology of the Grants Uranium Region 1979, New Mex Bur Mines Mineral Res Mem 38, pp 145–152
Robb LJ (1978) A general geological description of the Archaean granitic terrane between Nelspruit and Bushbuckridge, eastern Transvaal, Trans Geol Soc S Afr, v 81, pp 331–338
Robb LJ (1979) The distribution of granitophile elements in Archean granites of the eastern Transvaal and their bearing on geomorphological and geological features of the area, Trans Geol Soc S Afr, v 82, pp 169–178
Robb LJ (1986) Uraniferous leucogranites from the Namaqualand Metamorphic Complex: Part I – Geology, geochemistry and petrogenesis, *in*: Anhaeusser CR, Maske S, eds., Mineral deposits of southern Africa, Vol. I & II, Geol Soc S Afr, pp 1609–1628
Robb LJ, Meyer M (1985) The nature of the Witwatersrand hinterland: conjectures on the source-area problems, Information Circ no. 178, Econ Geol Res Unit, Univ Witwatersrand, 25 p
Robb LJ, Schoch AE (1985) Deuteric alteration and uranium mineralization processes in leucogranite intrusions from the Namaqualand Metamorphic Complex, South Africa, Proc Conf High Heat Production (HHP) Granites, Hydrothermal Circulation and Ore Genesis, IMM, London, pp 301–314
Robb LJ, Thiel K, Vorwerk R (1986) Uraniferous leucogranites from the Namaqualand Metamorphic Complex: Part II – Uranium distribution and mineralization processes, *in*: Anhaeusser CR, Maske S, eds., Mineral deposits of southern Africa, Geol Soc S Afr, v 2, pp 1629–1650
Roberts DE (1988) The Olympic Dam copper-uranium-gold deposit, *in*: Recognition of uranium provinces, IAEA, Vienna, pp 263–272
Roberts DE, Hudson GRT (1984) The Olympic Dam copper-uranium-gold deposit, Roxby Downs, South Australia, *in*: Proterozoic unconformity and strata-bound uranium deposits, TECDOC-315, IAEA, Vienna, pp 69–94
Robertson DS (1962) Thorium and uranium variations in the Blind River ores, Econ Geol, v 57, pp 1175–1184
Robertson DS (1974) Basal Proterozoic unit as fossil time markers and their use in uranium prospection, *in*: Formation of uranium ore deposits, IAEA, Vienna, pp 495–512
Robertson DS, Steenland NC (1960) The Blind River uranium ores and their origin, Econ Geol, v 55, pp 659–694
Robertson DS, Tilsley JE, Hogg GM (1978) The time-bound character of uranium deposits, Econ Geol, v 73, pp 1409–1419
Robertson JA (1966) The relationship of mineralization to stratigraphy in the Blind River area, Ontario, Geol Ass Can Spec Paper 3, pp 121–136
Robertson JA (1968) Geology of Townships 149 and 150 District of Algoma, Ont Dept Mines GR57, 162 p
Roberston JA (1976) The Blind River uranium deposits: the ores and their setting, Ontario Div Mines Misc Paper 65
Robertson JA (1978) Uranium deposits in Ontario, *in*: Kimberley MM, ed., Short course in uranium deposits: their mineralogy and origin, Miner Ass Can, v 3, pp 229–280
Robertson JA (1983) Uranium and thorium deposits of Northern Ontario, Ont Geol Surv Mineral Deposits Circ 25, 152 p
Robertson JA (1986) Huronian geology and the Blind River (Elliot Lake) uranium deposits, *in*: Evans EL, ed., Uranium deposits of Canada, CIM Spec Vol. 33, pp 7–31
Robertson JA (1989) The Blind River (Elliot Lake) uranium deposits, *in*: Uranium resources and geology of North America, TECDOC-500, IAEA, Vienna, pp 111–147
Robertson JA, Gould KL (1981) Uranium and thorium deposits of Ontario, East Central Sheet, Ont Geol Surv Map P 2426, Mineral Deposits Series, 1 inch to 16 miles
Robertson JA, Gould KL (1983) Uranium and thorium deposits of northern Ontario, Ont Geol Surv MDC 25, 152 p
Robinson A, Spooner TC (1982) Source of the detrital components of uraniferous conglomerates, Quirke ore zone, Elliot Lake, Ontario, Canada, Nature, 299, pp 622–624
Robinson A, Spooner TC (1984a) Postdepositional modification of uraninite-bearing quartz-pebble conglomerates from the Quirke ore zone, Elliot Lake, Canada, Econ Geol, v 79, pp 297–321
Robinson A, Spooner TC (1984b) Can the Elliot Lake uraninite-bearing quartz pebble conglomerates be used to place limits on the oxygen content of the Early Proterozoic atmosphere? J Geol Soc, London, 141, pp 221–228
Robinson SC (1955a) Genesis of uranium in the Athabasca region and its significance in exploration, CIM Bull, v 48, pp 367–377
Robinson SC (1955b) Mineralogy of uranium deposits, Goldfields, Saskatchewan, Geol Surv Can Bull 31, 128 p

Robinson SC, Sabina AP (1955) Uraninite und thorianite from Ontario and Quebec, Amer Miner, 40, pp 624–633

Rodrigo F, Belluco AE (1981) Discovery of the Sierra Pintada uranium district, Mendoza Province, Argentina, *in*: Uranium exploration case histories, IAEA, Vienna, pp 23–57

Roeber MM, Jr (1972) Possible mechanics of lateral enrichment and physical positioning of uranium deposits Ambrosia Lake area, New Mexico, Supplement to New Mex Bur Mines Mineral Res Circ 118, 16 p

Rogers AF (1947) Uraninite and pitchblende, Amer Miner, 32, pp 90–91

Rogers JJW (1964) Statistical tests of the homogeneity of the radioactive components of granitic rocks, *in*: Adams JAS, Lowder WM, eds., The natural radiation environment, Chicago University Press, pp 51 ff

Rogers JJW, Adams JAS (1969a) Geochemistry of uranium, *in*: Wedepohl KH, ed., Handbook of geochemistry, Sect. II, 5, Springer, Berlin, pp 92E1–92E5

Rogers JJW, Adams JAS (1969b) Uranium, *in*: Wedepohl KH, ed., Handbook of geochemistry, v 2, no. 4, Springer, Berlin, pp 92-B–92-O

Rogers JJW, Donnelly TW (1966) Radiometric evidence for the origin of eugeosynclinal materials, Tulane Studies in Geology 4, 133 p

Rogers JJW, Ragland PC (1961) Variation of thorium and uranium in selected granitic rocks, Geochim Cosmochim Acta, 25, pp 99 ff

Rogers JJW, Richardson KA (1964) Thorium and uranium contents of some sandstones, Geochim Cosmochim Acta, 28, pp 2005–2011

Rogers JJW, Adams JAS, Gatlin B (1965) Distribution of thorium, uranium, and potassium concentrations in three cores from the Conway granite, New Hampshire, USA, Amer J Sci, 263, pp 817 ff

Rogers JJW, Ragland PC, Nishimori RK, Greenberg JK, Hauck SA (1978) Varieties of granitic uranium deposits and favourable exploration areas in the eastern United States, Econ Geol, v 73, pp 1539–1555

Romberger SB (1984) Transport and deposition of uranium in hydrothermal systems at temperatures up to 300°C: geological implications, *in*: De Vivo B et al., eds., Uranium geochemistry, mineralogy, geology, exploration and resources, IMM, London, pp 12–17

Roscoe SM (1959) On thorium-uranium ratios in conglomerate and associated rocks near Blind River, Ontario, Econ Geol, v 54, pp 511–512

Roscoe SM (1969) Huronian rocks and uraniferous conglomerates in the Canadian Shield, Geol Surv Can Paper 68-40, 205 p

Roscoe SM (1973) The Huronian Supergroup, a Paleoaphebian succession showing evidence of atmosphere evolution, *in*: Young GM, ed., Huronian stratigraphy and sedimentation, Geol Assoc Can Spec Vol. 12, pp 31–48

Roscoe SM (1981) Temporal and other factors affecting deposition of uraniferous conglomerates, *in*: Armstrong FC, ed., Genesis of uranium- and gold-bearing Precambrian quartz-pebble conglomerates, US Geol Surv Prof Paper 1161-A-BB, pp W1–W17

Roscoe SM, Steacy HR (1958) On the geology and radioactive deposits of Blind River region, UN 2nd Intern Conf Peaceful Uses Atomic Energy, Geneva, Proc, v 2, 222, pp 473–483

Rosenberg PE, Hooper RL (1981) Fission track dating of sandstone-type uranium deposits (abstr), Geol Soc Amer, Abstracts with Programs, v 13, p 541

Rosenberg PE, Hooper RL (1982) Fission-track dating of sandstone-type uranium deposits, Geology, v 10, pp 481–485

Rosholt JN (1983) Isotopic composition of uranium and thorium in crystalline rocks, J Geophys Res, 88(B9) pp 7315–7330

Rosholt JN, Bartel AJ (1969) Uranium, thorium and lead systematics in the Granite Mountains, Wyoming, Earth Planet Sci Lett, 7, pp 141–147

Rosholt JN, Harshman EN, Shields WR, Garner EL (1964) Isotopic fractionation of uranium related to roll features in sandstone, Shirely Basin, Wyoming, Econ Geol, v 59, pp 570–585

Rosholt JN, Butler AP, Garner EL, Shields WR (1965a) Isotopic fractionation of uranium in sandstone, Powder River Basin, Wyoming, and Slick Rock district, Colorado, Econ Geol, v 60, pp 199–213

Rosholt JN, Tatsumoto M, Dooley JR, Jr (1965b) Radioactive disequilibrium studies in sandstone, Powder River Basin, Wyoming, and Slick Rock district, Colorado, Econ Geol, v 60, pp 477–484

Rosholt JN, Prijana, Noble DC (1971) Mobility of uranium and thorium in glassy and crystallized silicic volcanic rocks, Econ Geol, v 66, pp 1061–1069

Rosholt JN, Zartman RE, Nkomo IT (1973) Lead isotope systematics and uranium depletion in the Granite Mountains, Wyoming, Geol Soc Am Bull, v 84, pp 989–1002

Ross DI (1981) The distribution of gold and other elements in the uranium conglomerates of Elliot Lake, Ontario, unpubl, M Sc thesis, McMaster Univ, Hamilton, Ontario, 103 p

Rossiter AG, Ferguson J (1980) A Proterozoic tectonic model for northern Australia and its economic implications, *in*: Ferguson J, Golbey AB, eds., Uranium in the Pine Creek Geosyncline, IAEA, Vienna, pp 209–232

Roubault M (1958) Géologie de l'Uranium, Masson et Cie, Editeurs, Paris, 462 p

Roubault M, Coppens R (1955) Sur les relations entre certains gites filoniens d'uranium et la présence d'inclusions radioactives dans les roches encaissantes, CR Acad Sci Fr 240, pp 214–216

Roubault M, Coppens R (1958) Observation de déplacements de l'uranium dans les roches cristallines, relations possibles de ce phénomène avec la genèse de certains gisements, UN 2nd Intern Conf Peaceful Uses Atomic Energy, Proc, v 2, Genève, pp 335–337

Roubault M, Coppens R (1960) Etude radiogéologique d'une partie du Massif de Mortagne (Vendée), *in*: 21st Intern Geol Congr, part XV, Copenhague, pp 78–97

Roubault M et al. (1969) La geologie de l'uranium dans le massif granitique de Saint-Sylvestre (Limousin, Massif Central Francais), Sci Terre, Mem No. 15, 213 p

Rouzaud JN (1979) Étude structurale de matières carbonées associées à de minéralisations uranifères, doctoral diss, Orléans

Rouzaud J, Oberlin A, Trichet J (1981) Interaction of uranium and organic matter in uraniferous sediments, Adv Organic Geochem, v 1979, pp 505–516

Rozhkova EV, Rasumnaza EG, Serebryakova MB, Shcherbak DV (1958) The role of sorption in the process of uranium concentration in sedimentary rocks, UN 2nd Intern Conf Peaceful Uses of Atomic Energy, Proc, v 2, Geneva, pp 420–431

Rubin B (1970) Uranium roll-front zonation in the southern Powder River Basin, Wyoming, Earth Sci Bull, v 3, no. 4, pp 5–12

Ruhland M, Gauthier-Lafaye F (1978) Organisation des gisements d'uranium de la boutonnière de Mounana (Gabon), *in*: Les réacteurs de fission naturels, IAEA, Vienne, pp 25–34

Ruhlmann F (1980) Quelques examples de relation uranium-titane, Bull Minér, 103, pp 240–244

Ruhlmann F (1985) Mineralogy and metallogeny of uraniferous occurrence in the Carswell Structure, *in*: Lainé R et al., The Carswell Structure uranium deposits, Saskatchewan, Geol Ass Can Spec Paper 29, pp 105–120

Ruhrmann G (1987) The Gaertner uranium orebody at Key Lake (northern Saskatchewan, Canada) after three years of mining: an update of the geology, *in*: Gilboy CF, Vigrass LW, eds., Economic minerals of Saskatchewan, Sask Geol Soc Spec Publ no. 8, pp 120–137

Ruhrmann G, von Pechmann E (1989) Structural and hydrothermal modification of the Gaertner uranium deposit. Key Lake, Saskatchewan, Canada, *in*: Uranium resources and geology of North America, TECDOC-500, IAEA, Vienna, pp 363–378

Ruhrmann G , DeCarle AL, Gay F, Singer G (1987) Ore types and ore distribution in the Gaertner uranium deposit at Key Lake, northern Saskatchewan, Canada, (abstr), Joint Annual Meeting, Geol Ass Can, Miner Ass Can, Saskatoon

Rundkwist DW, Nesheskij IA (1977) Die Zonalität endogener Erzlagerstätten, Z angew Geologie, Bd 23, H 12, pp 642–645

Rundle CC, Snelling NJ (1977) The geochronology of uraniferous minerals in the Witwatersrand triad; an interpretation of new and existing U-Pb age data on rocks and minerals from the Dominion Reef, Witwatersrand and Ventersdorp Supergroups, Phil Trans Royal Soc, London, A286, pp 567–583

Ruzicka V (1971) Geological comparison between East European and Canadian uranium deposits, Geol Surv Can Paper 70-48, 196 p

Ruzicka V (1979) Uranium and thorium in Canada , 1978, *in*: Current research, Part A, Geol Surv Can Paper 79-1A, pp 139–155

Ruzicka V (1981) Some metallogenic features of the Huronian and Post-Huronian uraniferous conglomerates, *in*: Genesis of uranium- and gold-bearing Precambrian quartz-pebble conglomerates, US Geol Surv Prof Paper 1161-V, pp V1–V8

Ruzicka V (1984) Unconformity-related uranium deposits in the Athabasca Basin region, Saskatchewan, *in*: Proterozoic unconformity and stratabound uranium deposits, TECDOC-315, IAEA, Vienna, pp 219–267

Ruzicka V (1986) Uranium deposits in the Rabbit Lake-Collins Bay area, Saskatchewan, *in*: Evans EL, ed., Uranium deposits in Canada, CIM Spec Vol. 33, pp 144–154

Ruzicka V (1988) Geology and genesis of uranium deposits in the Early Proterozoic Blind River-Elliot Lake Basin, Ontario, Canada, *in*: Recognition of uranium provinces, IAEA, Vienna, pp 107–130

Ruzicka V (1989) Conceptual genetic models for important types of uranium deposits and areas favourable for their occurrence in Canada, *in*: Uranium resources and geology of North America, TECDOC-500, IAEA, Vienna, pp 49–79

Ruzicka V, LeCheminant GM (1984) Uranium deposit research 1983, *in*: Curr Res Part A, Geol Surv Can Paper 84-1A, pp 39–51

Ruzicka V, LeCheminant GM (1986) Developments in uranium geology in Canada, 1985, *in*: Curr Res Part A, Geol Surv Can Paper 86-1A, pp 531–540

Ruzicka V, LeCheminant GM (1987) Uranium investigations in Canada, 1986, *in*: Curr Res Part A, Geol Surv Can Paper 87-1A, pp 249–262

Ruzicka V, Littlejohn AL (1982) Notes on mineralogy of various types of uranium deposits and genetic implication, *in*: Curr Res Part A, Geol Surv Can Paper 81-1A, pp 341–349

Ruzicka V, Steacy HR (1976) Some sedimentary features of conglomeratic uranium ore from Elliot Lake, Ontario, Geol Surv Can Paper 76-1A, pp 343–346

Ryall WR, Binns RA (1980) Mercury distribution in the Jabiluka 2 orebody and its host rocks, *in*: Ferguson J, Goleby A, eds., Uranium in the Pine Creek Geosyncline, IAEA, Vienna, pp 469–478

Ryan GR (1977) Uranium in Australia, *in*: Jones MJ, ed., Geology mining and extractive processing of uranium, IMM, London, pp 24–42

Rytuba JJ, Glanzman RK (1978) Relation of mercury, uranium and lithium deposits to the McDermitt Caldera complex, Nevada–Oregon, US Geol Surv Rep 78–926, pp 1–19

Saager R (1968) Newly observed ore-minerals from the Basal Reef in the Orange Free State Goldfield in South Africa, Econ Geol, v 63, pp 116–123

Saager R (1969) The relationship of silver and gold in the Basal Reef of the Witwatersrand System, South Africa, Mineral Deposita, 4, pp 93–113

Saager R (1970) Structures in pyrite from the Basal Reef in the Orange Free State Goldfield, Trans Geol Soc S Afr, v 73, pp 29–46

Saager R (1973) Geologische und geochemische Untersuchungen an primären und sekundären Goldvorkommen im frühen Präkambrium Südafrikas. Ein Beitrag zur Deutung der primären Herkunft des Goldes in der Witwatersrand-Lagerstätte, Habil Schrift, Univ Heidelberg, 150 p

Saager R (1976) Geochemical aspects of the origin of detrital pyrite in Witwatersrand conglomerates, Univ Witwatersrand, Johannesburg, Econ Geol Res Unit Inform Circ 105, 21 p

Saager R, Esselaar PA (1969) Factor analysis of geochemical data from the Basal Reef, Orange Free State Goldfield, South Africa Econ Geol, v 64, pp 445–451

Saager R, Mihálik P (1967) Two varieties of pyrite from the Basal Reef of the Witwatersrand System, Econ Geol, v 62, pp 719–731

Saager R, Muff R (1978) Petrographic and mineragraphic investigations of the Archean gold placers at Mount Robert in the Pietersburg greenstone belt, northern Transvaal, Univ Witwatersrand, Johannesburg, Econ Geol Res Unit Inform Circ 114, 10 p

Sagger R, Oberthür T (1984) Nickel-cobalt sulfides in Precambrian gold and uranium-bearing quartz-pebble conglomerates of South Africa, *in*: Wauschkuhn A et al., eds., Syngenesis and epigenesis in the formation of mineral deposits, Springer Verlag, Berlin, Heidelberg, New York, Tokyo, pp 237–246

Saager R, Strupp HD (1983) U-Ti phases from

Precambrian quartz-pebble conglomerates of the Elliot Lake area, Canada, and the Pongola Basin, South Africa, Tschermaks Min Petr Mitt, 31, pp 83–102

Saager R, Thiel K, Hennig GJ, Bangert U (1981) Uranium redistribution in weathered conglomerates of the early Precambrian Pongola Supergroup, South Africa – Inferences from a study by alpha spectrometry and fission track micromapping, J Geoch Expl, 15, pp 233–249

Saager R, Utter T, Meyer M (1982) Pre-Witwatersrand and Witwatersrand conglomerates in South Africa: A mineralogical comparison and bearings on the genesis of gold-uranium placers, *in*: Amstutz et al., eds., Ore genesis – the state of the art, Springer, Berlin, Heidelberg, New York, Tokyo, pp 38–56

Sachdev SC (1980) Mineralogical variations across Mariano Lake roll-type uranium deposit, McKinley County, *in*: Rautman CA, ed., Geology and mineral technology of the Grants Uranium Region 1979, New Mex Bur Mines Mineral Res Mem 38, pp 162–171

Saima Deposit Research Group (1976) Uranium deposits in the Saima Alkaline Massif, northeast China, Peking Inst Uranium Geol, pp 1–18

Saint-Martin M (1983) The petrology and geochemistry of uraniferous chloritized rocks at Panel mine, Ellio Lake, Ontario, unpubl BSc thesis, Univ Ottawa

Salop LJ (1977) Precambrian of the northern hemisphere, Elsevier, New York, 378 p

Samama JC (1984) Uranium in lateritic terranes, *in*: Surficial uranium deposits, TECDOC-322, IAEA, Vienna, pp 53–59

Sanford RF (1982) Preliminary model of regional Mesozoic groundwater flow and uranium deposition in the Colorado Plateau, Geology, v 10, pp 348–352

Santana Pérez D (1958) Uranium mining in Spain, UN 2nd Intern Conf Peaceful Uses of Atomic Energy, Proc, v 2, Geneva, pp 43–49

Santos ES (1963) Relation of ore deposits to the stratigraphy of the Ambrosia Lake area, *in*: Kelley VC, ed., Geology and technology of the Grants Uranium Region, New Mex Bur Mines Mineral Res Mem 15, pp 53–59

Santos ES (1970) Stratigraphy of the Morrison Formation and structure of the Ambrosia Lake District, New Mexico, US Geol Surv Bull 1272-E, 30 p

Santos ES (1975) Lithology and uranium potential of Jurassic formations in the San Ysidro-Cuba and Majors Ranch areas, northwestern New Mexico, US Geol Surv Bull 1329, 22 p

Santos ES, Ludwig KR (1983) Age of uranium mineralization at the Highland mine, Powder River Basin, Wyoming, as indicated by U-Pb isotope analyses, Econ Geol, v 78, pp 498–501

Santos ES, Turner-Peterson CE (1986) Tectonic setting of the San Juan Basin in the Jurassic, *in*: Turner-Peterson CE, Santos ES, Fishman NS, eds., A basin analysis case study – the Morrison Formation, Grants Uranium Region, New Mexico, Amer Ass Petrol Geol, Studies in Geology no. 22, pp 27–33

Saraswat AC, Mahadevan TM (1989) On the genetic aspects of uranium mineralization in Himalaya, *in*: Metallogenesis of uranium deposits, IAEA, Vienna, pp 369–398

Sarcia JA (1958) La Province uranifère de Nord-Limousin: ses trois principaux gisements, UN, 2e Conf Int pour les applications pacif Energ atom, Genève, pp 578–591

Sarcia JA (1980) L'uranium des albitites, XXVIième Congrès Geol Intern, Paris, Sec 12, t 2.02, Resumés 3, pp 57–60

Sarcia JA, Carrat HG, Poughon A, Sanselme H (1958) Géologie des gites uranifères filoniens en France, UN, 2e Conf Int pour les applications pacif Energ atom, v 2, Genève, pp 280–300

Sarcia J, Sarcia JA (1956) Les gites d'uranium du Nord Limousin, Sci Terre, Mém 4, pp 239–306

Sarcia J, Sarcia JA (1962) Gites et gisements du Limousin, *in*: Les minerais uranifères français, II, PUF ed., pp 185–292

Sarkar SC (1982) Uranium (nickel-cobalt-molybdenum) mineralization along the Singhbhum copper belt, India, and the problem of ore genesis, Mineral Deposita, 17, pp 257–278

Sarkar SC (1984) Geology and ore mineralization of the Singhbhum copper-uranium belt, eastern India, Jadavpur Univ, Calcutta, 263 p

Sarkar SC (1986) The problem of uranium mineralization in Precambrian metamorphic shear tectonites – with particular reference to the Singhbhum copper-uranium belt, eastern India, *in*: Vein-type uranium deposits, TECDOC-361, IAEA, Vienna, pp 9–20

Sassano GP (1972) The nature and origin of the uranium mineralization at the Fay mine, Eldorado, Saskatchewan, Canada, unpubl diss, Univ Alberta, Edmonton

Sassano GP, Baadsgaard H, Burwash RA (1974) Rb-Sr age of a late kinematic phase of the Hudsonian Orogeny in the Beaverlodge area, Saskatchewan, Can J Earth Sci, v 11, pp 643–649

Sassano GP, Baadsgaard H, Morton RD (1972a) Rb-Sr isotopic systematics of the Foot Bay gneiss, Donaldson Lake gneiss, and pegmatitic dikes from the Fay Mine, NW Saskatchewan, Can J Earth Sci, v 9, pp 1368–1381

Sassano GP, Fritz P, Morton RD (1972b) Paragenesis and isotopic composition of some gangue minerals from the uranium deposits of Eldorado, Saskatchewan, Can J Earth Sci, v 9, pp 141–157

Saucier AE (1967) The Morrison and related formations in the Gallup region, Albuquerque, Univ New Mexico unpubl MS thesis, 106 p

Saucier AE (1974) Stratigraphy and uranium potential of the Burro Canyon Formation in the southern Chama Basin, New Mexico, *in*: New Mex Geol Soc Guidebook, Ghost Ranch, 25th Anniversary Volume, pp 211–217

Saucier AE (1976) Tectonic influence on uraniferous trends in the Late Jurassic Morrison Formation, *in*: Tectonics and mineral resources of southwestern North America, New Mex Geol Soc Spec Publ no. 6, pp 151–157

Saucier AE (1980) Tertiary oxidation in the Westwater Canyon Member of the Morrison Formation, *in*: Rautman CA, ed., Geology and mineral technology of the Grants Uranium Region 1979, New Mex Bur Mines Mineral Res Mem 38, pp 151–157

Sayala D, Ward DL (1983) Multidisciplinary studies of a uranium deposit in the San Juan Basin, New Mexico, US-DOE, GJBX-2(83), 220 p

Scarborough RB (1981) Radioactive occurrences and uranium production in Arizona, US-DOE, GJBX 79-374E, 297 p

Schidlowski M (1966a) Mineralbestand und Gefügebilder in Faseraggregaten von kohliger Substanz ("Thucholith")

aus den Witwatersrand-Konglomeraten, Contrib Miner Petrol, v 12, pp 365–380
Schidlowski M (1966b) Zellular strukturierte Elemente aus dem Präkambrium des Witwatersrand-Systems (Südafrika), Zeitsch Deutsch Geol Ges, v 115, pp 783–786
Schidlowski M (1966c) Beiträge zur Kenntnis der radioaktiven Bestandteile der Witwatersrand-Konglomerate. I. Uranpecherz in den Konglomeraten des OranjeFreistaat-Goldfeldes, N Jb Miner Abh, v 105, pp 183–202
Schidlowski M (1966d) Beiträge zur Kenntnis der radioaktiven Bestandteile der Witwatersrand-Konglomerate. II. Brannerit und "Uranpecherzgeister," N Jb Miner Abh, v 105, pp 310–324
Schidlowski M (1966e) Beiträge zur Kenntnis der radioaktiven Bestandteile der Witwatersrand-Konglomerate. III. Kohlige Substanz ("Thucholith"), N Jb Miner Abh, v 106, pp 55–71
Schidlowski M (1966f) Some observations on radioactive blasting haloes and radioactive corrosion phenomena in conglomerates from the Orange Free State Goldfield, Trans Geol Soc S Afr, v 69, pp 155–159
Schidlowski M (1967a) A composite detrital grain from the Witwatersrand conglomerates (South Africa), J Sed Petrol, v 37, pp 227–228
Schidlowski M (1967b) Note on graphite in the Witwatersrand conglomerates, Trans Geol Soc S Afr, v 70, pp 65–66
Schidlowski M (1968) The gold fraction of the Witwatersrand conglomerates from the Orange Free State Goldfield (South Africa), Mineral Deposita, 3, pp 334–363
Schidlowski M (1969) Critical remarks on a postulated genetic relationship between Precambrian thucholite and boghead coal, *in*: Schenck PA, Havenaar I, eds., Advances in organic geochemistry, Pergamon Press, Oxford, pp 579–592
Schidlowski M (1970) Untersuchungen zur Metallogenese im südwestlichen Witwatersrand-Becken, Beih Geol Jahrb 85, 80 p
Schidlowski M (1976) Archaean atmosphere and evolution of the terrestrial oxygen budget, *in*: Windley BF ed., The early history of the earth, Wiley, New York, pp 525–535
Schidlowski M (1981) Uraniferous constituents of the Witwatersrand conglomerates: Ore-microscopic observations and implications for the Witwatersrand metallogeny, US Geol Surv Prof Paper 1161-N, 29 p
Schidlowski M, Junge C (1973) Die Evolution der Erdatmosphäre, Phys Bl, 29, pp 203–212
Schidlowski M, Ottemann J (1966) Mackinawite from the Witwatersrand conglomerates, Amer Miner, v 51, pp 1535–1541
Schidlowski M, Trurnit P (1966) Drucklösungserscheinungen an Geröllpyriten aus den Witwatersrand-Konglomeraten. Ein Beitrag zur Frage des diagenetischen Verhaltens von Sulfiden, Schweiz Miner Petrogr Mitt, v 46, pp 337–351
Schidlowski M, Eichmann R, Junge CE (1974) Evolution des irdischen Sauerstoffbudgets und Entwicklung der Erdatmosphäre, Umschau, 74, H 22, pp 703–707
Schidlowski M, Eichmann R, Junge CE (1975) Precambrian sedimentary carbonates: Carbon and oxygen isotope geochemistry and implications for the terrestrial oxygen budget, Precamb Res, v 2, pp 1–69
Schieferdecker AAG, ed. (1959) Geological nomenclature, Royal Geol and Min Soc Netherlands, Gorinchem, 523 p
Schlee JS (1963) Sandstone pipes of the Laguna area, New Mexico, J Sed Petrol, v 33, no. 1, pp 112–123
Schlee JS, Moench RH (1961) Properties and genesis of "Jackpile" sandstone, Laguna, New Mexico, *in*: Geometry of sandstone bodies, Amer Ass Petrol Geol, pp 134–150
Schmidt-Collerus JJ (1969) Part II, Experimental investigations, *in*: Investigations of the relationship between organic matter and uranium deposits, US-AEC, GJO-933-2, 192 p
Schmidt-Collerus JJ (1979) Investigation of the relationship between organic matter and uranium deposits, US-DOE, GJBX-130(79), 281 p
Schmitt JM (1986) Albitisation Triassique, hydrothermalisme Jurassique et altération supergène récente: Métallogenie des gisements uranifères du Rouergue, Thèse de doctorat d'Etat, Univ Strasbourg, 243 p
Schmitt JM, Clement JY (1989) Triassic regolithization: a major stage of pre-enrichment in the formation of unconformity related deposits in southern France, *in*: Metallogenesis of uranium deposits, IAEA, Vienna, pp 93–114
Schmitt JM, Baubron JC, Bonhomme MG (1984) Pétrographie et datations K-Ar des transformations minérales affectant le gîte uranifère de Bertholène (Aveyron-France), Mineral Deposita, 19, no. 2, pp 123–131
Schmitt LJ (1968) Uranium and copper mineralization in the Big Indian Wash-Lisbon Valley mining district, southeast Utah, PhD thesis, Columbia Univ, 173 p
Schoep A (1930) Ann Mus Congo Belge, AII, 2, p 18
Schumacher, F (1933) Die erzgebirgische Metallprovinz und ihre Genesis, Metall und Erz, 30, H 9, pp 1–6
Schumm SA (1977) The fluvial system, Wiley-Interscience, New York, 338 p
Schweigart H, von Rahden H (1964) Oolithische Strukturen in Pyriten des Ventersdorp-Contact-Reefs, Südafrika, Geol Rundsch, v 54, pp 1143–1148
Scott AK, Scott AG (1985) Geology and genesis of uranium-rare-earth deposits at Mary Kathleen, northwest Queensland, AIMM Proc, 290, pp 79–89
Scott RA (1961) Fossil woods associated with uranium on the Colorado Plateau, *in*: Short papers in the geologic and hydrologic sciences, US Geol Surv Prof Paper 424-B, pp B130–B132
Scott RC, Barker FB (1962) Data on uranium and radium in ground water in the United States, 1954 to 1957, US Geol Surv Prof Paper 426, 115 p
Scott Meddaugh W, Holland HD, Shimizu N (1982) The isotopic composition of lead in galenas in the uranium ores at Elliot Lake, Ontario, Canada, *in*: Amstutz GC et al., eds., Ore genesis – the state of the art, Springer, Berlin, Heidelberg, New York, Tokyo, pp 25–37
Sears RS, Marjaniemi DK, Blomquist JT (1974) A study of the Morrison Formation in the San Juan Basin, New Mexico and Colorado, US-AEC, GJO-912-20, 102 p
Seeland DA (1976) Relationship between early Tertiary sedimentation patterns and uranium mineralization in the Powder River Basin, Wyoming, *in*: Geology and energy resources of the Powder River, Wyoming, Geol Ass Guidebook, 28th Annual Field Conf, pp 53–64
Sellards EH, Adkins WS, Plummer RB (1932) The

geology of Texas, v 1, Stratigraphy, Univ Texas, Austin, Bull 3232, 1007 p
Senecal J (1969) Monographie du gisement du Brugeaud, Sci Terre, Mem 15, pp 161–193
Sergeyeva EI, Nikitin AA, Khodakovsky IL, Naumov GB (1972) Experimental investigation of equilibria in the system UO_3-CO_2-H_2O in 25°–200°C temperature interval, Geochem. Intern, v 9, pp 900–910
Seyfert CA, Sirkin LA (1973) Earth history and plate tectonics, Harper and Row, New York, 257 p
Sharp JWA (1955) Uranium deposits in the Morrison Formation, Church Rock area, McKinley County, New Mexico, US-AEC, RME-79, 19 p
Sharp WN, Gibbons AB (1964) Geology and uranium deposits of the southern part of the Powder River Basin, Wyoming, US Geol Surv Bull 1147-D, pp D1–D60
Sharp WN, McKay EJ, McKeown FA, White AM (1964) Geology and uranium deposits of the Pumpkin Buttes area of the Powder River Basin, Wyoming, US Geol Surv Bull 1107-H, pp 541–638
Shatkov GA, Shatkov LN, Gushchin, YeN (1970) The distribution of uranium, thorium, fluorine, molybdenum and niobium in liparites and acid volcanic glasses, Geochem Intern, v 7, pp 1051–1063
Shawe DR (1956a) Significance of roll ore bodies in genesis of uranium-vanadium deposits on the Colorado Plateau, *in*: Page LR, Stocking HE, Smith HB, Compilers, Contributions to the geology of uranium and thorium by the United States Geological Survey and Atomic Energy Commission, UN, Intern Conf Peaceful Uses Atomic Energy, Geneva, 1955, US Geol Surv Prof Paper 300, pp 239–241
Shawe DR (1956b) Alteration related to Colorado Plateau ore deposits (abstr), Geol Soc Amer Bull, v 67, no. 12, pt. 2, pp 1732–1733
Shawe DR (1962) Localization of the Uravan Mineral Belt by sedimentation, US Geol Surv Prof Paper 450-C, pp C6–C8
Shawe DR (1966) Zonal distribution of elements in some uranium-vanadium roll and tabular ore bodies on the Colorado Plateau, *in*: Geol Surv Res 1966, Chapter B, US Geol Surv Prof Paper 550-B, pp B169–B175
Shawe DR (1976a) Sedimentary rock alteration in the Slick Rock district, San Miguel and Dolores Counties, Colorado, US Geol Surv Prof Paper 576-D, pp D1–D51
Shawe DR (1976b) Geologic history of the Slick Rock district and vicinity, San Miguel and Dolores Counties, Colorado, US Geol Surv Prof Paper 576-E, 19 p
Shawe DR, Archbold NL, Simmons GC (1959) Geology and uranium-vanadium deposits of the Slick Rock district, San Miguel and Dolores Counties, Colorado, Econ Geol, v 54, pp 395–415
Shegelski R (1980) Archean red beds in the Lake Shebandowan area and their implications for Archean oxygen levels, Paper presented at the joint meeting Intern Geol Correl Program, proj 157 and 160 working groups, Santa Barbara, California
Shepherd TJ (1977) Fluid inclusion study of the Witwatersrand gold-uranium ores, Phil Trans Royal Soc, London, A286, pp 549–565
Sherborne JE, Jr, Buckovic WA, Dewitt DB, Hellinger TS, Pavlak SJ (1979) Major uranium discovery in vulcaniclastic sediments, basin and range province, Yavapai County, Arizona, Amer Ass Petrol Geol Bull, v 63/4, pp 621–645
Sherborne JE, Jr, Pavlak SJ, Peterson CH, Buckovic WA (1980) Uranium deposits of the Sweetwater Mine area, Great Divide Basin Wyoming, *in*: Third Annual Uranium Seminar, New York, Amer Inst Min Metal Petrol Eng, pp 27–37
Sheridan DM, Maxwell CH, Collier JT (1961) Geology of the Lost Creek Schroeckingerite deposits, Sweetwater County, Wyoming, US Geol Surv Bull 1087-J, pp 391–478
Sheridan DM, Maxwell CH, Albee AL (1967) Geology and uranium deposits of the Ralston Buttes District, Jefferson County, Colorado, US Geol Surv Prof Paper 520, 121 p
Shiqing YU (1989) Characteristics and regional geological environments of uranium deposits in Mesozoic volcanics in east China, *in*: Uranium deposits in magmatic and metamorphic rocks, IAEA, Vienna, pp 77–92
Shirvington PJ (1983) Fixation of radionuclides in the ^{238}U decay series in the vicinity of mineralized zones: 1. The Austatom uranium prospect, Northern Territory, Australia, Geochim Cosmochim Acta, v 47, pp 403–412
Shoemaker EM, Miesch AT, Newman WL (1959) Elemental composition of the sandstone-type deposits, *in*: Garrels RM, Larsen ES, III, compilers, Geochemistry and mineralogy of the Colorado Plateau uranium ores, US Geol Surv Prof Paper 320, pp 25–54
Shtshurov VP, Timofeiev EV (1965) Quelques types de contrôle structural de la minéralisation dans les gisements uranifères hydrothermaux, Geol Rud Mestorozhd, 4, pp 34–44 (abbrev translation from Russian by V Ziegler for IAEA, Vienna)
Sibbald TII (1977) Uranium metallogenic studies: I, Rabbit Lake, geology, *in*: Christopher JE, Macdonald R, eds., Summary of investigations 1977, Sask Geol Surv Misc Rep 77–10, pp 111–123
Sibbald TII (1983) Geology of the crystalline basement, NEA/IAEA Athabasca test area, *in*: Cameron EM, ed., Uranium exploration in Athabasca Basin, Geol Surv Can Pap 81-11, pp 11–14
Sibbald TII (1985) Geology and genesis of the Athabasca Basin uranium deposits, *in*: Summary of investigations 1985, Sask Geol Surv Misc Rep 85-4, pp 133–155
Sibbald TI (1988) Geology and genesis of the Athabasca uranium deposits, *in*: Recognition of uranium provinces, IAEA, Vienna, pp 61–106
Sibbald TII, Petruk W, eds. (1985) Geology of uranium deposits, CIM Spec Vol. 32, 268 p
Sibbald TII, Quirt D (1987) Uranium deposits of the Athabasca Basin, Sask Res Council Publ no. R-855-1-G-87, 72 p
Sibbald TII, Munday RJC, Lewry JR (1976) The geological setting of uranium mineralization in northern Saskatchewan, *in*: Uranium in Saskatchewan, Sask Geol Soc Spec Publ 3, pp 51–98
Sibbald TII, Hoeve J, Ramaekers P, Lewry JF (1981) Saskatchewan uranium field trip guide, *in*: Field guides to geology and mineral deposits, Calgary 81 Ann Mtg Geol Ass Can, pp 121–142
Sibson RH, McM.Moore J, Rankin AH (1975) Seismic pumping. A hydrothermal fluid transport mechanism, J Geol Soc, 131, pp 653–659
Siderenko GA (1958) X-ray investigations of natural oxides of uranium, Geochem, 1, pp 26–50
Silver LT, Williams IS, Woodhead JA (1980a) Uranium in granites from the southwestern United States: Actinide

parent-daugher systems, sites and mobilization – First year report, US-DOE, GJBX-45(81), 380 p
Silver LT, Williams IS, Woodhead JA (1980b) Uranium and thorium endowment, distribution and mobilization in a uraniferous Precambrian granite, Geol Soc Amer Abstracts with Programs, 1980 Annual Meeting, p 522
Silver LT, Woodhead JA, Williams IS (1982) Primary mineral distribution and secondary mobilization of uranium and thorium in radioactive granites, *in*: Uranium exploration methods, OECD-NEA, Paris, pp 355–367
Simov SD (1979) Uranium epochs, *in*: Uranium deposits in Africa: geology and exploration, IAEA, Vienna, pp 191–204
Simov SD (1986) Uranium deposits in foothills of a granitic massif in the southeastern Alps, *in*: Uranium deposits in magmatic and metamorphic rocks IAEA, Vienna, pp 1–10
Simov SD (1988) Formation of uranium deposits, *in*: Recognition of uranium provinces, IAEA, Vienna, pp 17–32
Simov SD (1989) Migration of uranium, *in*: Metallogenesis of uranium deposits, IAEA, Vienna, pp 33–42
Simov SD, Boijkov IB (1991) Case histories and new areas for uranium exploration in Bulgaria: Technical Committee Meeting on New Developments in Uranium Exploration, Resources, Production and Demand, August 1991, IAEA, Vienna, manuscript 7p + Figs + Tables
Simpson PR, Bowles JFW (1977) Uranium mineralization of the Witwatersrand and Dominion Reef systems, Phil Trans Royal Soc, London, A286, p. 527–548
Simpson PR, Bowles JFW (1981a) Uranium mineralization of the Witwatersrand and Dominion Reef systems, *in*: Armstrong FC, ed., Genesis of uranium and gold-bearing Precambrian quartz-pebble conglomerates, US Geol Surv Prof Paper 1161-A-33, pp R1–R26
Simpson PR, Bowles JFW (1981b) Detrital uraninite and pyrite: Are they evidence for a reducing atmosphere? *in*: Armstrong FC, ed., Genesis of uranium and gold-bearing Precambrian quartz-pebble conglomerates, US Geol Surv 1161-A-BB, Paper 5, 9 p
Simpson PR, Hurdley J (1985) Relationship between metalliferous mineralization and Sn-U-F rich mildly alkaline High Heat Production (HHP) granites in the Bushveld Complex, South Africa, *in*: Proceedings of a meeting on high heat production (HHP) granites, hydrothermal circulation and ore genesis, IMM, London, pp 365–382
Simpson PR, Hurdley J (1988) Granites as indicators of uranium provinces, *in*: Recognition of uranium provinces, IAEA, Vienna, pp 45–58
Simpson PR, Plant J (1984) Role of high heat production granites in uranium province formation, *in*: De Vivo B, et al., Uranium geochemistry, mineralogy, geology, exploration and resources, IMM, London, 167–178
Simpson PR, Shiqing Yu (1989) Uranium metallogeny, magmatism and structure in southeast China, *in*: Metallogenesis of uranium deposits, IAEA, Vienna, pp 357–368
Simpson PR, Plant J, Cope MJ (1977) Uranium abundance and distribution in some granites from northern Scotland and southwest England as indicators of uranium provinces, *in*: Jones MJ, ed., Geology, mining and extractive processing of uranium, IMM, London, pp 126–139
Simpson PR, Brown GC, Plant J, Ostle D (1979) Uranium mineralization and granite magmatism in the British Isles, Phil Trans Royal Soc, London, Ser A, v 291, pp 385–412
Simpson PR, Plant JA, Watson JV, Green PM, Fowler MB (1982a) The role of metalliferous and mineralized uranium granites in the formation of uranium provinces, in: Uranium exploration methods, OECD-NEA, pp 157–170
Simpson PR, Plant JA, Brown GC, eds. (1982b) Uranium 81, Miner Soc, London, 216 p
Sims JF (1969) The stratigraphy and paleocurrent history of the upper division of the Witwatersrand System on President Steyn mine and adjacent areas in the Orange Free State Goldfield, with specific reference to the origin of the auriferous reefs, unpubl PhD diss, Univ Witwatersrand, Johannesburg, 181 p
Sims PK (1976) Precambrian tectonics and mineral deposits, Lake Superior region, Econ Geol, v 71, pp 1092–1127
Sims PK, Sheridan DM (1964) Geology of uranium deposits in the Front Range, Colorado, US Geol Surv Bull 1159, 116 p
Sims PK, Card KD, Lumbers SB (1981) Evolution of early Proterozoic basins of the Great Lakes region, *in*: Cammpbell FHA, ed., Proterozoic basins of Canada, Geol Surv Can Paper 81-10, pp 379–397
Sims PK, Card KD, Morey GB, Peterman ZE (1980) The Great Lakes tectonic zone – a major crustal structure in central North America, Geol Soc Amer, v 91, pp 690–698
Skinner BJ (1981) Thoughts about uranium-bearing quartz-pebble conglomerates: a summary of ideas presented at the Workshop, *in*: Armstrong FC, ed., Genesis of uranium- and gold-bearing Precambrian quartz-pebble conglomerates, US Geol Surv Prof Paper 1161-A-BB, BB1–BB5
Smart PG, Wilkes PG, Needham RS, Watchman AL (1975) Geology and geophysics of the Alligator Rivers Region, *in*: Knight CL, ed., Economic geology of Australia and Papua New Guinea, AIMM, Monograph 5, v 1, pp 285–310
Smellie JAT (1982) The mineralogy and genesis of uranium in rhyolitic ignimbrites of Precambrian age from Dubblon, Sweden, Miner Mag, 46, pp 187–199
Smellie JAT, Laurikko J (1984) Skuppesavon, northern Sweden, a uranium mineralization associated with alkali metasomatism, Mineral Deposita, 19, pp 183–192
Smellie JAT, Coggrer N, Herrington J (1978) Standards for quantitative microprobe determination of uranium and thorium with additional information on the chemical formulae of davidite and euxenite, Chem Geol, 22, pp 1–10
Smirnov VL (1970) Geologie der Lagerstätten mineralischer Rohstoffe, VEB-Verlag f Grundstoffindustrie, Leipzig, 503 p
Smirnov VI (1977) Ore deposits of the USSR, Pitman, London, 1258 p
Smith DAM (1965) The geology of the area around the Khan and Swakop Rivers in South West Africa, Mem Geol Surv S Afr, 3 (SWA Series), 113 p
Smith DA, Peterson RJ (1980) Geology and recognition of a relict uranium deposit in Section 28, T 14 N, R 10 W, southwest Ambrosia Lake area, McKinley County, New Mexico, *in*: Rautman CA, ed., Geology and mineral technology of the Grants Uranium Region

1979, New Mex Bur Mines Mineral Res Mem 38, pp 215–225
Smith DK (1984) Uranium mineralogy, *in*: de Vivo F et al., eds., Uranium geochemistry, mineralogy, geology, exploration and resources, IMM, London, pp 43–88
Smith DK, Scheetz BE, Anderson CAF, Smith KL (1982) Phase relations in the uranium–oxygen–water system and its significance on the stability of nuclear waste forms, Uranium, 1, pp 79–110
Smith EEN (1974) Review of current concepts regarding vein deposits of uranium, *in*: Formation of uranium ore deposits, IAEA, Vienna, pp 515–529
Smith EEN (1986) Geology of the Beaverlodge operation Eldorado Nuclear, *in*: Evans EL (ed), Uranium deposits of Canada, CIM Spec Vol. 33, pp 95–109
Smith ND, Minter WEL (1980) Sedimentological controls of gold and uranium in two Witwatersrand paleoplacers, Econ Geol, v 75, pp 1–14
Smith RB (1977) The theory of multiple oxidation and reduction of uranium deposits in south Texas, South Texas Uranium Seminar, Corpus Christi, Texas
Smith RB (1979) Geology of south Texas uranium deposits, *in*: South Texas Uranium Seminar, Denver, Colorado, Amer Inst Min Met Petrol Eng, pp 45–46
Smits G (1981) The occurrence of uranium in the Witwatersrand Basin, S Afr Atomic Energy Board Tech Note 300, 103 p
Smits G (1984) Some aspects of the uranium mineralization of Witwatersrand sediments of the early Proterozoic, Precamb Res, v 25, no. 1–3, pp 37–59
Smyslov A (1974) Uranium and thorium in the earth's crust, Izd-vo Nedra, Leningrad, 232 p
Synman CP (1965) Possible biogenetic structures in Witwatersrand thucholite, Trans Geol Soc S Afr, v 68, pp 225–235
Soboleva MV, Pudovkina IA (1957) Mineraly urana: Spranvochnik (Uranium minerals: a reference book) Gosgeoltekhizdat, Moscow, 408 p (Russian text); Mineralog Abstr, 14, 1959–60, 13–14; US-AEC Translation Series 4487, 1961, 433 p
Sokolova NT, Acheyev BN (1972) Causes of localization of uranium mineralization in contact metamorphism aureoles of granitoids, Géochem Intern, 1, pp 1067–1077
Sopuck VJ, De Carle A, Wray EM, Cooper B (1983) Application of lithogeochemistry to the search for unconformity-type uranium deposits in the Athabasca Basin, *in*: Cameron EM, ed., Uranium exploration in Athabasca Basin, Geol Surv Can Paper 82-11, pp 192–205
Sørensen H (1970) Occurrence of uranium in alkaline igneous rocks, *in*: Uranium exploration geology, IAEA, Vienna, pp 161–168
Sørensen H, ed. (1974) The alkaline rocks, Wiley, London, 622 p
Sørensen H, Rose-Hansen J, Nielsen BL, Løvborg L, Sørensen E, Lundgaard T (1974) The uranium deposit at Kvanefjeld, Ilímaussaq intrusion, South Greenland, Rapp Grønlands geol Unders 60, 54 p
South African Committee for Stratigraphy (SACS) (1980) Stratigraphy of South Africa. Part I (Comp LE Kent). Lithostratigraphy of the Republic of South Africa, South-West Africa/Namibia, and the Republics of Bophuthatswana, Transkei and Nenda, Department of Mineral and Energy Affairs, Geol Surv, Handb Geol Surv S Afr, 8, 690 p
Spirakis CS (1977) A theory for the origin of the Rifle-Garfield vanadium-uranium deposit, *in*: Campbell JA, ed., Short Papers of the US Geol Surv Uranium-Thorium Symp (1977), US Geol Surv Circ 753, pp 8–10
Spirakis CS (1980) Possible relationship between subsidence and uranium in Petrified Forest Member, Chinle Fm in Cameron – Holbrook – St Johns areas, Atizona, US Geol Surv Rep 80–808
Spirakis CS (1981) The possible role of sulfate reduction kinetics in the formation of hydrothermal uranium deposits, Econ Geol, v 76, pp 2236–2239
Spirakis CS, Pierson CT (1986) Some aspects of the genesis of uranium deposits of the Morrison Formation in the Grants Uranium Region, New Mexico, inferred from chemical characteristics of the deposits, *in*: Turner-Peterson CE, Santos ES, Fishman NS, eds., A basin analysis case study – The Morrison Formation, Grants Uranium Region New Mexico, Amer Ass Petrol Geol, Studies in Geology no. 22, pp 161–169
Spirakis CS, Pierson CT, Granger HC (1981) Comparison of the chemical composition of mineralized and unmineralized (barren) samples of the Morrison Formation in the Ambrosia Lake uranium area, New Mexico, US Geol Surv Rep 81–508, 43 p
Spirakis CS, Pierson CT, Peterson F (1984) Chemical characteristics of the uranium-vanadium deposits of the Henry Mountains mineral belt, Utah, US Geol Surv Rep 84–367, 11 p
Spirakis CS, Pierson CT, Santos ES, Fishman NS (1983) Statistical treatment and preliminary interpretation of chemical data from a uranium deposit in the northeast part of the Church Rock area, Gallup mining district, New Mexico, US Geol Surv Rep 83–379, 44 p
Squyres JB (1963) Geology and ore deposits of the Ann Lee mine, Ambrosia Lake area, *in*: Kelley VC, ed., Geology and technology of the Grants Uranium Region, New Mex Bur Mines Mineral Res Mem 15, pp 90–101
Squyres JB (1970) Origin and depositional environment of uranium deposits of the Grants region, New Mexico, unpubl PhD diss, Stanford Univ, 228 p
Squyres JB (1974) Uranium deposits of the south San Juan Basin, New Mexico, Paper presented at Amer. Inst Min Eng Annual Meeting, Dallas, Texas, preprint no. 74-5-13, 20 p
Squyres JB (1980) Origin and significance of organic matter in uranium deposits of Morrison Formation, San Juan Basin, New Mexico, *in*: Rautman CA, ed., Geology and mineral technology of the Grants Uranium Region 1979, New Mex Bur Mines Mineral Res Mem 38, pp 86–97
Starinsky A, Katz A, Klodny Y (1982) The incorporation of uranium into diagenetic phosphorite, Geochim Cosmochim Acta, 46, pp 1365–1374
Steacy HR, Kaiman S (1978) Uranium minerals in Canada: Their description, identification and field guides, *in*: Kimberley, MM, ed., Short course in uranium deposits: their mineralogy and origin, Miner Ass Can, pp 107–140
Steele BA (1984) Preliminary report on the petrography of the Upper Jurassic Morrison Formation, Mariano Lake-Lake Valley drilling project, McKinley County, New Mexico, US Geol Surv Res 84–170, 43 p
Steenfelt A, Armour-Brown A (1988) Characteristics of the south Greenland uranium province, *in*: Recognition of uranium provinces, IAEA, Vienna, pp 305–336

Step J, Becke F (1904) Das Vorkommen des Uranpecherzes zu St Joachimsthal, Akad Wiss, Wien, Sitzber Math-Naturw Kl 113 (Abt. I), pp 1–34

Stephens JG (1964) Geology and uranium deposits at Crooks Gap, Fremont County, Wyoming, US Geol Surv Bull 1147-F, pp F1–F82

Steven TA, Cunningham CG, Machette MN (1981) Integrated uranium systems in the Marysvale volcanic field, west-central Utah, US Geol Surv Rep 80–524, 39 p

Stevens RD, Delabio RN, Lachance GR (1982) Age determinations and geological studies: K-Ar isotopic ages, Rep 15, Geol Surv Can Pap 81–2, 35 p

Stewart JH et al. (1959) Stratigraphy of the Triassic and associated formations in part of the Colorado Plateau region, US Geol Surv Bull 1046-Q, pp 487–576

Stewart JH, Poole FG, Wilson RF (1972) Stratigraphy and origin of the Chinle Formation and related Triassic strata in the Colorado Plateau region, US Geol Surv Prof Paper 690, 336 p

Stewart JR (1965) Middle Proterozoic volcanic rocks in the Katherine-Darwin area, Northern Territory, Rep BMR, Canberra, 90 p

Steyn LS (1964) The sedimentology and gold distribution pattern of the Livingstone Reefs on the West Rand, unpubl MSc thesis, Univ Witwatersrand, 132 p

Steyn P (1977) The occurrence of gold in banded "buckshot" pyrite from the Witwatersrand auriferous conglomerates, Abstracts of Papers, 17th Congress, Geol Soc S Afr, pp 103–104

Stieff LR, Stern TW (1960) Age study of uraninites from the Urgeiriça and Lenteiro mines, Portugal, JEN Tech Paper no. 27, pp 11–17

Stockwell CH (1982) Proposals for time classification and correlation of Precambrian rocks and events in Canada and adjacent areas of the Canadian Shield, Part 1: a time classification of Precambrian rocks and events, Geol Surv Can Paper 80–19, 135 p

Stokes WL (1953a) Preliminary sedimentary trend indicators as applied to ore findings in the Carrizo Mountains, Arizona and New Mexico, US–AEC, RME-3043 (Part 1), 48 p

Stokes WL (1953b) Progress report on relation of sedimentary features of the Salt Wash sandstone to tectonic elements and uranium mineralization (Colorado Plateau), US–AEC, RME-3058, 5 p

Stokes WL (1953c) Sedimentary patterns and uranium mineralization in the Morrison Formation of the Colorado Plateau (abstr), Geol Soc Amer Bull, v 64, no. 12, p 1516

Stokes WL (1954a) Cyclical deposition of fluvial sediments (Colorado Plateau) (abstr), Geol Soc Amer Bull, v 65, no. 12, pt. 2, p 1309

Stokes WL (1954b) Some stratigraphic, sedimentary, and structural relations in uranium deposits in the Salt Wash sandstone, final report – April 1, 1952 to June 30, 1954, US–AEC, RME-3102

Stokes WL (1954c)) Stratigraphy of the southeastern Utah uranium region, *in*: Stokes WL, ed., Uranium deposits and general geology of southeastern Utah, Utah Geol Soc Guidebook no. 9, pp 16–47

Stokes WL (1954d) Relation of sedimentary trends, tectonic features, and ore deposits in the Blanding district, San Juan County, Utah, US–AEC, RME-3093 (Part 1), 40 p

Stokes WL (1967) A survey of southeastern Utah uranium districts, *in*: Uranium districts of southeastern Utah, Utah Geol Soc Guidebook no. 21, pp 1–11

Stokes WL, Mobley CM (1954) Geology and uranium deposits of the Thompson area, Grand County, Utah, *in*: Stokes WL, ed., Uranium deposits and general geology of southeastern Utah, Utah Geol Soc Guidebook no. 9, pp 78–94

Strnad J (1986) Contribution to the problems on Pre-Variscan precursors of uranium vein deposits in the Bohemian Massif, *in*: Vein type uranium deposits, TECDOC-361, IAEA, Vienna, pp 319–334

Strnad J (1989) Global metallotects and regional basement controls of unconformity-type uranium deposits of the Athabasca Basin (Canada), *in*: Uranium deposits in magmatic and metamorphic rocks, IAEA, Vienna, pp 189–211

Strunz H (1962) Die Uranfunde in Bayern von 1804–1962, Acta Albertina Ratisbonensia, Bd. 24, pp 1–92

Stuart-Smith PG, Wills K, Crick IH, Needham RS (1980) Evolution of the Pine Creek Geosyncline, *in*: Ferguson J, Goleby AB, eds., Uranium in the Pine Creek Geosyncline, IAEA, Vienna,pp 23–28

Stuckless JS (1979) Uranium and thorium concentrations in Precambrian granites as indicators of a uranium province in central Wyoming, Univ Wyoming Contrib Geology, v 17, pp 173–178

Stuckless JS (1987) A review of applications of U-Th-Pb isotope systematics to investigations of uranium source rocks, Uranium, v 3, no. 2–4, pp 235–244

Stuckless JS, Ferreira CC (1976) Labile uranium in granitic rocks, *in*: Exploration of uranium ore deposits, IAEA, Vienna, pp 717–730

Stuckless JS, Nkomo IT (1978) Uranium-lead isotope systematics in uraniferous alkali-rich granites from the Granite Mountains, Wyoming: Implications for uranium source rocks, Econ Geol, v 73, pp 427–441

Stuckless JS, Troëng B (1984) Uranium mineralization in response to regional metamorphism at Lilljuthatten, Sweden, Econ Geol, v 79, pp 509–528

Stuckless JS, van Trump G (1982) A compilation of radioelement concentrations in granitic rocks of the contiguous United States, *in*: Uranium exploration methods, OECD–NEA, Paris, pp 191–208

Stuckless JS, Bunker CM, Nkomo IT (1975) Uranium mobility in a uraniferous granite from the Granite Mountains, Wyoming (abstr), Geol Soc Amer, Abstracts with Programs, v 7, pp 1286–1287

Stuckless JS, Bunker CM, Bush CA, Doering WP, Scott JH (1977a) Geochemical and petrological studies of a uraniferous granite from the Granite Mountains, Wyoming, J Res US Geol Surv, v 5, no. 1, pp 61–81

Stuckless JS, Bunting JA, Nkomo IT (1981b) U-Th-Pb systematics of some granitoids from the northeastern Yilgarn Block, Western Australia and implication for uranium source rock potential, J Geol Soc Aust, v 28, pp 365–375

Stuckless JS, Nkomo IT, Doe BR (1981a) U-Th-Pb systematics in hydrothermally altered granites from the Granite Mountains, Wyoming, Geochim Cosmochim Acta, v 45, pp 635–645

Stuckless JS, Troëng B, Hedge CE, Nkomo IT, Simmons KR (1982) Age of uranium mineralization at Lilljuthatten in Sweden and constraints on ore genesis, Sveriges Geol Undersökning, ser C, no. 789, 49 p

Stussi JM (1985) Magmatic control of granite related

mineralization in the French Variscan Chain, (abstr) Fortschr Miner, BA63, p 229
Stussi JM, De La Roche H (1984) Le magmatisme orogénique granitique de la chaine varisque française. Typologie chimique et répartition spatiale, CR Acad Sc, Paris, t 298, Série II, no. 2, pp 43–48
Sullivan CJ (1957) The classification of metalliferous provinces and deposits, CIM Bull, v 50, pp 599–601
Sutphin HB (1986) Occurrence and structural control of collapse features on the southern Marble Plateau, Coconino County, Arizona, MSc thesis, Northern Arizona Univ, 139 p
Svoboda J, et al. (1966) Regional geology of Czechoslovakia, Part 1, The Bohemian Massif, Prague, 668 p
Swanson VE (1960) Oil yield and uranium content of black shales, US Geol Surv Prof Paper 356A, pp 1–44
Swanson VE (1961) Geology and geochemistry of uranium in marine black shales, a review, US Geol Surv Prof Paper 356-C, pp 67–112
Symons DTA, O'Leary RJ (1978) Huronian polar wander and paleomagnetism of the Thessalon Volcanics, Can J Earth Sci, v 15, pp 1141–1150
Szalay A (1964) Cation exchange properties of humic acids and their importance in the geochemical enrichment of UO_2^{++} and other cations, Geochim Cosmochim Acta, v 28, pp 1605–1614
Szalay S, Samsoni Z (1969) Investigation of the leaching of uranium from crushed magmatic rocks, Geochem Intern, v 6, pp 613–623
Tankard AJ, Jackson MPA, Eriksson KA, Hobday DK, Hunter DR, Minter WEL (1982) Crustal evolution of southern Africa, Springer-Verlag, Berlin, 523 p
Tapaninen K (1975) Geology and metallogenesis of the Carswell area uranium deposits, CIM Annual Western Meeting, Edmonton, Alberta
Tapaninen K (1976) Cluff Lake area. Geol Ass Can, Miner Ass Can Annual Meeting, Edmonton, Field-Trip Manual A-1, pp 50–71
Tarkhanov AV, Poluarshinov GP (1989) Spatio-chronological position of the Precambrian uranium deposits, *in*: Metallogenesis of uranium deposits, IAEA, Vienna, pp 201–210
Tauson LV (1954) Geochemistry of uranium in granitoids of the Chernovinsky Massif (Altai Mountain), Geochem. no. 3, pp 236–245
Taylor HP Jr, (1979) Oxygen and hydrogen isotope relationships in hydrothermal mineral deposits, *in*: Barnes HL, ed., Geochemistry of hydrothermal ore deposits, (2nd ed). John Wiley & Sons, New York, pp 236–277
Taylor K, Bowie SHU, Horne JET (1962) Radioactive minerals in the Dominion Reef, Min Mag, v 107, pp 329–332
Taylor SR (1964) Abundance of chemical elements in the continental crust: a new table, Geochim Cosmochim Acta, v 28, pp 1273–1285
Thaden RE, Trites AF Jr, Finnell TL (1964) Geology and ore deposits of the White Canyon area, San Juan and Garfield counties, Utah, US Geol Surv Bull 1125
Thaden RE, Zech RS (1986) Structure contour map of the San Juan Basin and vicinity, *in*: Turner-Peterson CE, Santos ES, Fishman NS, eds., A basin analysis case study – The Morrison Formation, Grants Uranium Region, New Mexico, Amer Ass Petrol Geol, Studies in Geology no 22, pp 35–45
Thamm JK, Kovschak AA, Adams SS (1981) Geology and recognition criteria for sandstone uranium deposits of the Salt Wash type, Colorado Plateau province, US-DOE, GJBX-6(81), 136 p
The Saskatchewan Geological Survey (1987) Saskatchewan's mineral industry: past and present, CIM Directory, pp 67–115
Theis NJ (1973) Comparative mineralogy of the Quirke No. 1 and New Quirke mines, Rio Algom Mines Limited, Elliot Lake, Ontario, MSc thesis, Queens Univ, Kingston, Ontario, 61 p (unpubl)
Theis NJ (1976) Uranium-bearing and associated minerals in their geochemical and sedimentological context, Elliot Lake, Ontario, PhD thesis, Queens Univ, Kingston, Ontario, 148 p (unpubl)
Theis NJ (1978) Mineralogy and setting of Elliot Lake deposits, *in*: Kimberley MM, ed., Short course in uranium deposits: their mineralogy and origin, Miner Ass Can, pp 331–338
Theis NJ (1979) Uranium-bearing and associated minerals in their geochemical and sedimentological context, Elliot Lake, Ontario, Geol Surv Can Bull 304, 50 p
Thiel K, Saager R, Muff R (1979) Distribution of uranium in early Precambrian gold-bearing conglomerates of the Kaapvaal Craton, South Africa: A review of a case study for the application of fission track micromapping of uranium, Min Sci Eng, v 11, pp 225–245
Thode HG, Kleerekoper H, McElcheren D (1951) Isotopic fractionation in the bacterial reduction of sulfate, Research (London), v 4, pp 581–582
Thomas D (1979) Uranium metallogenic studies: "Pegmatite" prospect geology, *in*: Christopher JE, Macdonald R, eds., Summary of investigations 1979, Sask Geol Surv Misc Rep 79–10, pp 86–95
Thomas D (1980) Uranium metallogenic studies: Uraniferous pegmatite prospect geology, *in*: Christopher JE, Macdonald R, eds., Summary of investigations 1980, Sask Geol Surv Misc Rep 80–4, pp 49–53
Thomas D (1982) Compilation geological map of the Tazin Lake Sheet (74N), Sask Geol Surv, unpubl map, scale 1:250 000
Thomas D (1983) Distribution, geological controls and genesis of uraniferous pegmatites in the Cree Lake zone of northern Saskatchewan, unpub MSc thesis, Univ Regina, 213 p
Thomas WN (1976) Notes on the Yeelirrie uranium deposit, WA, unpubl rep, 13 p
Thompson TB, Lyttle T, Pierson JR (1980) Genesis of the Bokan Mountain, Alaska, uranium thorium deposits, US-DOE, 80–38, 237 p
Thompson TB, Pierson JR, Lyttle T (1982) Petrology and petrogenesis of Bokan granite complex, southeastern Alaska, Geol Soc Amer Bull, 93, pp 898–908
Thomson KC (1967) Structural features of southeast Utah and their relations to uranium deposits, *in*: Uranium districts of southeast Utah, Guidebook 21, Utah Geol Soc, pp 23–31
Thoreau J, du Trieu de Terdonck R (1933) Le gîte d'uranium de Shinkolobwe-Kasolo (Katanga), Extrait Mem. Inst Colonial Belge, v 1, pp 18–64
Thoreau J, du Trieu de Terdonck R (1936) Concentrations uranifères du Katanga (Congo Belge), 16th Intern Geol Congr, Washington DC, v 2, pp 1099–1101
Thorpe RI (1963) The radioactive mineralogy of the ore conglomerate at Panel mine, Blind River, Ontario, unpubl MSc thesis, Queens Univ, Kingston, Ontario, 148 p
Tilsley JE (1980a) Continental weathering and develop-

ment of paleosurface-related uranium deposits: some genetic considerations, *in*: Ferguson J, Goleby AB, eds., Uranium in the Pine Creek Geosyncline, IAEA, Vienna, pp 721–732

Tilsley JE (1980b) Genetic considerations relating to some uranium ore deposits, Geosci Can, v 7, pp 143–148

Titov VK, Bilibina TV, Kochkin GB (1975) Uranium and thorium in processes of regional metamorphism, *in*: Radioactive elements in rocks, "Nauka" Siberian Branch, Novosibirsk, pp 151–154

Toens PD (1980) The uranium geology and tectonic correlation between the African and Latin American continents, S Afr Atomic Energy Board Rep PER-58, 80 p

Toens PD (1981) Uranium provinces and their time-bound characteristic, Trans Geol Soc S Afr, v 84, pp 293–312

Toens PD, Andrews-Speed CP (1984) The time-bound character of uranium mineralizing processes, with special reference to the Proterozoic of Gondwana, Precamb Res, v 25, pp 13–36

Toens PD, Corner B (1980) Uraniferous alaskitic granites with special reference to the Damara orogenic belt, S Afr Atomic Energy Board Res PER 55, 18 p

Toens PD, Griffiths GH (1964) The geology of the West Rand, *in*: Haughton SH, ed., The geology of some ore deposits in southern Africa, Geol Soc S Afr, v 1, pp 283–321

Toens PD, Hambleton-Jones BB (1980) Uraniferous surficial deposits, S Afr Atomic Energy Board Rep PER 57, 16 p

Toens PD, Hambleton-Jones BB, (1984) Definition and classification of surficial uranium deposits, *in*: Surficial uranium deposits, TECDOC-322, IAEA, Vienna, pp 9–14

Toens PD, Le Roux JP (1978) The Permo-Triassic uranium deposits of southern Africa within the Gondwana framework, S Afr Atomic Energy Board Rep VB-579, 26 p

Toens PD, Le Roux, JP, Hartnady CJH, Van Biljon, WJ (1980) The uranium geology and tectonic correlation between the African and Latin American continents, S Afr Atomic Energy Board Rep PER 58, 80 p

Toens PD, Oosthuyzen EJ, Jacob RE, Brits RIN, Hambleton-Jones BB, Smit MCB (1979) A mineralogical, petrological and geochemical study of a suite of rocks from the Damara orogenic belt, South West Africa, S Afr Atomic Energy Board Rep PEL 269, 31 p

Tona F, Alonso D, Svab M (1985) Geology and mineralization in the Carswell Structure – a general approach, *in*: Lainé R, Alonso D, Svab M, eds., The Carswell Structure uranium deposits (Saskatchewan), Geol Ass Can Spec Paper 29, pp 1–18

Tooker EW (1983) Correlation of metal occurrence and terrane attributes in the northwestern conterminous United States, Can J Earth Sci, v 20, pp 1030–1039

Tortosa DJJ, Langford FF (1986) The geology of the Cenex uranium deposit, Beaverlodge, Saskatchewan, *in*: Evans EL ed., Uranium deposits of Canada, CIM Spec Vol 33, pp 110–119

Toulhoat P, Bigot S, Chupeau J (1989) In-situ study of compared fixation of U, Ca, Na, and K by pumping through multi-layered aquifers in sandstone-clay sequential successions, *in*: Metallogenesis of uranium deposits, IAEA, Vienna, pp 79–92

Traill RJ (1954) A preliminary account of the mineralogy of radioactive conglomerates in the Blind River region, Ontario, Can Min J, v 75, pp 63–68

Tremblay LP (1958a) Geology and uranium deposits of Beaverlodge region, Saskatchewan, UN Second Intern Conf Peaceful Uses Atomic Energy, Geneva, Proc, v 2, pp 491–497

Tremblay LP (1958b) Uranium City, Saskatchewan, Geol Surv Can, Map 25–1957

Tremblay LP (1970) The significance of uranium in quartzite in the Beaverlodge area, Saskatchewan, Can J Earth Sci, v 7, pp 280–305

Tremblay LP (1972) Geology of the Beaverlodge mining area, Saskatchewan, Geol Surv Can Mem 367, 265 p

Tremblay LP (1978a) Geological setting of the Beaverlodge type of vein-uranium deposits and its comparison to that of the unconformity type, *in*: Kimberley MM, Short course in uranium deposits: their mineralogy and origin, Miner Ass Can, v 3, pp 431–456

Tremblay LP (1978b) Uranium subprovinces and types of uranium deposits in the Precambrian rocks of Saskatchewan, Geol Surv Can Paper 78-1A, pp 427–435

Tremblay LP (1978c) Notes on possibilities for additional uranium deposits in Saskatchewan, Geol Surv Can Paper 78-1A, pp 437–439

Tremblay LP (1982) Geology of the uranium deposits related to the sub-Athabasca unconformity, Saskatchewan, Geol Surv Can Paper 81–20, 56 p

Tremblay LP (1983) Some chemical aspects of the regolithic and hydrothermal alterations associated with the uranium mineralization in the Athabasca Basin, Saskatchewan, *in*: Current research, Part A, Geol Surv Can Paper 83-1A, pp 1–14

Tremblay LP, Loveridge WD, Sullivan RW (1981) U-Pb ages of zircons from the Foot Bay Gneiss, Beaverlodge area, northern Saskatchewan, Geol Surv Can Paper 81-1C, pp 123–126

Trentham RC (1981) Leaching of uranium from felsic volcanics and volcaniclastics; model, experimental studies and analysis of sites, DGSc diss, Univ Texas, El Paso, 204 p

Treuil M (1985) A global geochemical model of uranium distribution and concentration in volcanic rock series, *in*: Uranium deposits in volcanic rocks, IAEA, Vienna, pp 53–68

Trimble LM, Doelling HH (1978) The geology and uranium-vanadium deposits of the San Rafael River mining area, Emery County, Utah, Utah Geol Miner Surv Bull 113, 122 p

Trocki LK, Curtis DB, Gancarz AJ, Banar JC (1984) Ages of major uranium mineralization and lead loss in the Key Lake uranium deposit, northern Saskatchewan, Canada, Econ Geol, v 79, pp 1378–1386

Tröger WE (1969) Spezielle Petrographie der Eruptivgesteine; ein Nomenklaturkompendium mit 1. Nachtrag Eruptivgesteinsnamen, (Nachdruck) Stuttgart, 360 + 50 p

Troëng B (1982) Uranium-rich granites in the Olden window, Sweden, Miner Mag, v 46, pp 219–228

Troëng B, Wilson MR (1982) Geological setting of uranium mineralizations in the Hotagen area, central Swedish Caledonides, *in*: Vein-type and similar uranium deposits in rocks younger than Proterozoic, IAEA, Vienna, pp 65–85

Trow J (1977) Uraniferous quartz-pebble conglomerates and their chemical relation to CO_2-deficient atmospheres synchronous with glaciations of almost any age (abstr), Geol Soc Am, Abstract with Programs, v 9, pp 1205–1206

Trueman T, Fortuna PA (1976) Dubyna Lake uranium deposit (31 zone), Eldorado, Saskatchewan, Geol Soc Sask Spec Publ 3, pp 355–382

Tucker DH, Stuart DC, Hone IG, Sampath N (1980) The characteristics and interpretation of regional gravity, magnetic and radiometric surveys in the Pine Creek Geosyncline, *in*: Ferguson J, Goleby AB, eds., Uranium in the Pine Creek Geosyncline, IAEA, Vienna, pp 101–140

Tucker RF, Viljoen RR (1986) The geology of the West Rand Goldfield, with special reference to the southern limb, *in*: Anhaeusser CR, Maske S, eds., Mineral deposits of southern Africa, Geol Soc S Afr, v 1, pp 649–688

Tugarinow AI, (1963) Uran in metasomatischen Prozessen, *in*: Grundzüge der Geochemie des Urans, Moskau

Tugarinov AI (1975) Origin of uranium deposits, *in*: Tugarinov AI, ed., Recent contributions to geochemistry and analytical chemistry, Wiley, New York, pp 293–302

Tugarinov AI, Naumov GB (1969) Thermobaric conditions of formation of hydrothermal uranium deposits, Geochem Intern, v 6, pp 89–103

Tugarinov AI, Naumov GB (1974) Die Migrations- und Absatzverhältnisse des Urans bei der endogenen Erzbildung, Z Angew Geol, v 20, pp 410–413

Tugarinov AI, Smejenkowa AW (1961) Die Herkunft der Erzsubstanz bei der endogenen Lagerstättenbildung, Z angewandte Geol, v 3, pp 109–113

Tugarinov AI, Bibikova EV, Zykov SI (1964) Metamorphism of uranium deposits and individual uranium minerals, Sov Atomic Energy, v 16, no. 4, pp 404–415

Turek A (1965) Geology of the Lake Cinch mine, Uranium City, Saskatchewan, CIM Trans, v 68, pp 80–86

Turekian KK, Wedepohl KH (1961) Distribution of the elements in some major units of the earth's crust, Geol Soc Amer Bull, 72, pp 175–191

Turner, PA (1979) The planar auriferous Witwatersrand conglomerates: Pediment mantles of the Proterozoic, unpubl Rep, 18th Congr Geol Soc S Afr, 10 p

Turner-Peterson CE (1981) Application of lacustrine-humate model to New Mexico Grants mineral belt and relation between ore types and hydrologic history of San Juan Basin, Am Ass Petrol Geol Bull, v 65, pp 571–572

Turner-Peterson CE (1985) Lacustrine-humate model for primary uranium ore deposits, Grants Uranium Region, New Mexico, Amer Ass Petrol Geol Bull, v 69, pp 1999–2020

Turner-Peterson CE (1986) Fluvial sedimentology of a major uranium host sandstone – a study of the Westwater Canyon Member of the Morrison Formation, San Juan Basin, New Mexico, *in*: Turner-Peterson CE, Santos ES, Fishman NS, eds., A basin analysis case study – the Morrison Formation, Grants Uranium Region, New Mexico, Amer Ass Petrol Geol, Studies in Geology no. 22, pp 47–75

Turner-Peterson CE, Fishman NS (1986) Geologic synthesis and genetic models for uranium mineralization in the Morrison Formation, Grants Uranium Region, New Mexico, *in*: Turner-Peterson CE, Santos ES, Fishman NS, eds., A basin analysis case study: the Morrison Formation, Grants Uranium Region, New Mexico, Amer Ass Petrol Geol, Studies in Geology no. 22, pp 357–388

Turner-Peterson CE, Peterson F (1978) Uranium in sedimentary rocks, with emphasis on facies control in sandstone-type deposits, US Geol Surv Rep 78–359, 15 p

Turner-Peterson CE, Santos ES, Fishman NS, (1986) eds., A basin analysis case study: the Morrison Formation, Grants Uranium Region, New Mexico, Amer Ass Petrol Geol, Studies in Geology no. 22, 391 p

Turner-Peterson CE, Gundersen LC, Francis DS, Aubrey WM (1980) Fluvio-lacustrine sequences in the Upper Jurassic Morrison Formation and the relationship of facies to tabular uranium ore deposits in the Poison Canyon area, Grants mineral belt, New Mexico, *in*: Turner-Peterson CE, ed., Uranium in sedimentary rocks – application of the facies concept to exploration, Soc Econ Paleont Miner, Rocky Mountain Section, Short Course Notes, pp 177–211

Turpin L (1984) Altérations hydrothermales et caractérisation isotopique (OHC) des minéraux et des fluides dans le massif uranifère de St Sylvestre. Extension à d'autres gisements intragranitiques français, Géol Géochim Uranium, Mém. 6, Nancy, 190 p

Turpin L (1985) Rb-Sr dating of hydrothermal alteration in the St Sylvestre leucogranite (French Massif Central), 3rd EUG Meeting Strasbourg, (abstr K 37)

Turpin L, Sheppard SMF (1983) Stable isotope studies on Saint Sylvestre granitic complex and associated uranium mineralizations (Limousin, Massif Central français), 2nd EUG Meeting Strasbourg, (abstr HB 21)

Turpin L, Respaut JP, Cathelineau M, Leroy J (1987) Application of Sr and Nb isotope geochemistry to uranium metallogenesis in granitic environments, manusc

Tweedie EB (1978) History, geology and value distribution of Evander Goldfield, eastern Transvaal, South Africa, IMM, Eleventh Commonwealth Mining and Metallurgical Congress, Hong Kong, Paper 23, 8 p

Tweedie EB (1986) The Evander Goldfield, *in*: Anhaeusser CR, Maske S, eds., Mineral deposits of southern Africa, Geol Soc S Afr, v 1, pp 705–730

Tweedie JR, (1979) Origin of uranium and other metal enrichments in the Helmsdale Granite, eastern Sutherland, Scotland, Trans IMM, London, Sec B, v 88, pp B145–B153

Tweedie KAM (1968) The stratigraphy and sedimentary structures of the Kimberley Shales in the Evander Goldfield, eastern Transvaal, South Africa, Trans Geol Soc S Afr, v 71, pp 235–256

Tweto O (1975) Laramide (late Cretaceous-early Tertiary) Orogeny in the southern Rocky Mountains, Geol Soc Amer Mem 144, pp 1–44

Tweto O (1977) Nomenclature of Precambrian rocks in Colorado, US Geol Surv Bull 1422-D, 22 p

Tweto O (1979) Geologic map of Colorado, US Geol Surv, scale 1:500 000

Tweto O, Sims PK (1963) Precambrian ancestry of the Colorado Mineral Belt, Geol Soc Amer Bull, v 74, pp 991–1014

Tyler N, Ethridge FG (1981) A re-evaluation of depositional environments of the uraniferous Salt Wash Member of the Morrison Formation, Uravan Mineral Belt, southwest Colorado, (abstr), Amer Ass Petrol Geol, Regional Meeting, Abstracts with Programs

Unrug R (1988) Mineralization controls and source of metals in the Lufilian Fold Belt, Shaba (Zaïre), Zambia, and Angola, Econ Geol, v 83, pp 1247–1258

US–AEC (1959) Guidebook to uranium deposits of the western United States, US–AEC, Grand Junction, Colorado, 1–1 to 7–14 p

Utter T (1977) Morphology and geochemistry of pyrites from the Upper Witwatersrand System of the Klerksdorp Goldfield, Chamber Mines, Johannesburg, Res Rep 8/77, 48 p

Utter T (1978a) Morphology and geochemistry of different pyrite types from the Upper Witwatersrand System of the Klerksdorp Goldfield, South Africa, Geol Rundsch, 67(2), pp 774–804

Utter T (1978b) The origin of chromites from the Klerksdrop Goldfield, Witwatersrand, South Africa, N Jb Miner Abh, 133(2), pp 191–209

Utter T (1979) The morphology and silver content of gold from the Upper Witwatersrand and Ventersdorp System of the Klerksdorp Goldfield, South Africa, Econ Geol, v 74, pp 27–44

Vail PR, Mitchum RM Jr, Thompson S III, (1977) Global cycles of relative changes of sea level, Amer Ass Petrol Geol Mem 26, pp 83–97

Valdiviezo PA (1987) Geochemistry of the uranium mineralized Achala granitic complex, Argentina: comparison with Hercynian peraluminous leucogranites of western Europe, manusc

Van Blaricom R (1980) Practical geophysics for the exploration geologist, Northwest Min Ass, Spokane, 303 p

Van Breemen O, Thompson PH, Bostock HH, Loveridge WD (1987) Timing of plutonism in the northern Thelon tectonic zone and the Taltson magmatic zone, *in*: Program with Abstracts of the Joint Annual Meeting, Geol Ass Can, Miner Ass Can, v 12, p 98

Van Houten FB (1964) Tertiary geology of the Beaver Rim area, Fremont and Natrona Counties, Wyoming, US Geol Surv Bull 1164, 99 p

Van Niekerk CB, Burger AJ (1964) The age of the Ventersdorp System, Annals, Rep S Afr, Geol Surv, v 3, pp 75–86

Van Niekerk CB, Burger AJ (1978) A new age for the Ventersdorp acidic lavas, Trans Geol Soc S Afr, v 81, pp 155–163

Van Schmus WR (1965) The geochronology of the Blind River-Bruce mines area, Ontario, Canada, J Geol, v 73, pp 755–780

Van Schmus WR (1976) Early and middle Proterozoic history of the Great Lakes area, North America, Phil Trans Royal Soc, London, A280, pp 605–628

Van Schmus WR, Bickford ME, Lewry JF, Macdonald R (1987) U-Pb geochronology in the Trans-Hudson Orogen, northern Saskatchewan, Canada, Can J Earth Sci, 24, pp 407–424

Van Schmus WR, Persons SS, Macdonald R, Sibbald TII (1986) Preliminary results from U-Pb zircon geochronology of the Uranium City region, *in*: Summary of investigations, 1986, Sask Geol Surv, pp 108–111

Van Valkenburgh T (1979) Petrology of the pre-2800 m.y. old paleosol below the Dominion Reef Group, South Africa, Campbell Univ, North Carolina, student res proj, 7 p

Veizer J, Hoefs J (1976) The nature of O^{18}/O^{16} and C^{13}/C^{12} secular trends in sedimentary carbonate rocks, Geochim Cosmochim Acta 40, pp 1387–1395

Vickers RC (1957) Alteration of sandstone as a guide to uranium deposits and their origin, northern Black Hills, South Dakota, Econ Geol, v 52, pp 599–611

Vidal Ph, Bernard-Griffiths J, Cocherie A, Le Fort P, Peucat JJ, Sheppard SMF (1984) Geochemical comparison between Himalayan and Hercynian leucogranites, Phys Earth Planet Inter, 35, pp 179–190

Viljoen RP (1963) Petrographic and mineragraphic aspects of the Main Reef and Main Reef Leader of the Main Bird Series, Witwatersrand System, M Sc thesis, Univ Witwatersrand, Johannesburg, 196 p

Viljoen RP (1967) The composition of the Main Reef and Main Reef Leader conglomerate horizons in the north-eastern part of the Witwatersrand Basin, Univ Witwatersrand, Johannesburg, Econ Geol Res Unit Inform Circ 40, 54 p

Viljoen RP (1968) The quantitative mineralogical properties of the Main Reef and Main Reef Leader of the Witwatersrand System, Univ Witwatersrand, Johannesburg, Econ Geol Res Unit Inform Circ 41, 63 p

Viljoen RP, Saager R, Viljoen MJ (1970) Some thoughts on the origin and processes responsible for the concentration of gold in the early Precambrian of southern Africa, Mineral Deposita, 5, pp 164–180

Vine JD, Tourtelot EB (1970a) Geochemistry of the black shale deposits – a summary report, Econ Geol, v 65, pp 253–272

Vine JD, Tourtelot EB (1970b) Preliminary geochemical and petrographic analysis of Lower Eocene fluvial sandstones in the Rocky Mountain region, Wyoming Geol Ass 22nd Field Conf Guidebook, pp 251–263

Vinogradov AP, ed. (1963) The essential features of the geochemistry of uranium, Izd Akad Nauk SSSR, Moscow, 352 p (in Russian)

Vinogradov AP, Tugarinow AI, Zirova VV, Zykov SI, Knorre KG, Lebedev VI (1959) Über das Alter der Granite und Erzvorkommen in Sachsen, Freiberger Forschungshefte, C 57, pp 73–85

Virag K, Vincze J (1967) Specific features of the formation of the uranium ore occurrence, Mecsek Mountains, Hungary, Foeldt Koezlem, Budapest, v 97, no. 1, pp 39–59

Vol'fson FI, Ishtshukova LP, Vishniakov VE, Palshine IG, Schleider VA, Dronov IV (1967) Conditions de la mise en place de la minéralisation uranifère hydrothermale dans les formations stratifiées de l'étage structural supérieur, Izv Akad Nauk SSSR, Ser Geol, 11: 114–134 [abbrev translation from Russian by V Ziegler for IAEA, Vienna)

Von Backström JW (1970) The Rössing uranium deposit near Swakopmund, South West Africa. A preliminary report, *in*: Uranium exploration geology, IAEA, Vienna, pp 143–150

Von Backström JW (1975) Uranium and the generation of power, South Africa perspective, Trans Geol Soc S Africa, v 78, pp 275–292

Von Backström JW (1976) Uranium, *in*: Coetzee CB, ed., Mineral resources of the Republic of South Africa, Rep S Afr Geol Surv, p 233–239

Von Backström JW, Jacob RE (1979) Uranium in South Africa and South West Africa (Namibia), Phil Trans Royal Soc, Lond, A291, pp 307–319

von Borstel D (1984) Bindungsformen von Uran in kohligen Ablagerungen von Sedimenten unterschiedlichen Diagenesegrades, Diss TU Clausthal, 156 p

von Borstel D, Halbach P (1982) Polarographic and spectrophotometric determination of the oxidation state of uranium in rocks and ores containing pitch-

blende, Fres Z Anal Chem, 310, pp 431–432
von Pechmann E (1985) Mineralogy of the Key Lake U-Ni orebodies, Saskatchewan, Canada: Evidence for their formation by hypogene hydrothermal processes, *in*: Sibbald TII, Petruk W, eds., Geology of uranium deposits, CIM Spec Vol. 32, pp 27–37
von Pechmann E, Huerter H (1988) Mikrochemische Untersuchungen an anisotropen Uraniniten, (Athabasca-Becken, Saskatchewan, Kanada und Pine Creek-Geosynklinale, NT, Australien), *in*: Referate der Vorträge und Poster, 66. Jahrestagung der Deutsch. Miner Ges, Bonn, Fortschr Miner, Bd 66, Beih 1, p 118
von Rahden HVR, Hiemstra SA (1967) The mineralogy of uranium in Western Area ores, NIM Res Rep 237, 13 p
Voultsidis V, Clasen D (1978) Probleme und Grenzbereiche der Uranmineralogie, Erzmetall, 31, pp 8–13
Voultsidis V, von Pechmann E, Classen D (1982) Petrography, mineralogy and genesis of the U-Ni deposits, Key Lake, Saskatchewan, Canada, *in*: Amstutz et al., eds., Ore genesis – the state of the art, Springer Verlag Berlin, Heidelberg, New York, pp 469–490
Vredenburgh LD, Cheney ES (1971) Sulfur and carbon isotopic investigation of petroleum, Wind River Basin, Wyoming, Amer Ass Petrol Geol Bull, v 55, no. 11, pp 1954–1975
Walker GW, Adams JW, Osterwald FW (1963) Geology of uranium-bearing veins in the conterminous United States, US Geol Surv Prof Paper 455-A,B,C,D,E,F, 120 p
Walker JCG (1980) Oxygen content of the early atmosphere resulting from abiotic photochemical processes, (abstr), joint meeting of Intern Geol Corr Program project 157 and 160 working groups, Santa Barbara, California, April 1980
Wall VJ, Johnston JD, Koul SL (1985) The plumbing systems of unconformity-related uranium deposits, *in*: Concentration mechanisms of uranium in geological environments, Soc Franç Miner Crist and GREGU, Nancy, France, pp 225–230
Wallace AR (1983a) Alteration and vein mineralization, Schwartzwalder uranium deposit, Front Range, Colorado, US Geol Surv Rep 83–417, 172 p
Wallace AR (1983b) Analytical data from host rocks and ores, Schwartzwalder uranium deposit, Front Range, Colorado, US Geol Surv Rep 83–364, 2 p, 15 tables
Wallace AR (1986) Geology and origin of the Schwartzwalder uranium deposit, Front Range, Colorado, USA, *in*: Vein-type uranium deposits, TECDOC-361, IAEA, Vienna, pp 159–168
Wallace AR, Karlson RC (1982) Alteration and vein mineralization, Schwartzwalder uranium mine, Jefferson County, Colorado, Geol Soc Amer, Abstr with Programs, v 14, no. 6, p 353
Wallace AR, Whelan JF (1986) The Schwartzwalder uranium deposit, III: Alteration, vein mineralization, light stable isotopes and genesis of the deposit, Econ Geol, v 81, pp 872–888
Wallace AR, Ludwig KR, Whelan JF (1983) The age and origin of the Schwartzwalder uranium deposit, Front Range, Colorado, Amer Ass Petrol Geol, Rocky Mtn Cordilleran Sect, abstr w progr, p 399
Wallis RH, Saracoglu N, Brummer JJ, Golightly JP (1985) The geology of the McClean uranium deposits, northern Saskatchewan, *in*: Sibbald TII, Petruck W, Geology of uranium deposits, CIM Spec Vol. 32, pp 101–131
Wallis RH, Saracoglu N, Brummer JJ, Golightly JP (1986) The geology of the McClean uranium deposits, northern Saskatchewan, *in*: Evans EL, ed., Uranium deposits of Canada, CIM Spec Vol. 33, pp 193–217
Walpole BP, Crohn PW (1965) Katherine-Darwin metalliferous province, *in*: McAndrew J, ed., Geology of Australian ore deposits, AIMM, v 1, pp 168–175
Walpole BP, Crohn PW, Dunn PR, Randal MA (1968) Geology of the Katherine-Darwin region, Northern Territory, Australia, BMR, Canberra, Bull 82, 304 p
Walton AW (1978) Release of uranium during alteration of volcanic glass, *in*: Formation of uranium ores by diagenesis of volcanic sediments, US-DOE, GJBX-22(79), Sect VI, pp 1–51
Walton AW, Galloway WE, Henry CD (1981) Release of uranium from volcanic glass in sedimentary sequences: an analysis of two systems, Econ Geol, v 76, pp 69–88
Wang A, Dubessy J, Landais P (1987) Graphite disordering during the gneissic basement alteration in the Saskatchewan uranium deposits (Canada), (abstr), IAEA Technical Committee Meeting on Uranium Resources and Geology of North America, Saskatoon, 1 p
Wang C, Youxin E (1980) The uranium deposits in Shengyuan volcanic basin, south China, The Beijing Uranium Geol Res Inst, 93 p
Wang Xuezheng, Yao Zhenkai (1985) Some characterictics of uranium mineralization in the Hunan-Guangxi region, Geotectonica et Metallogenia, China, v 9, 1, 47 p
Wanless RK, Traill RJ (1956) Age of uraninites from Blind River, Ontario, Nature, v 178, pp 249–250
Wanless RK, Stevens RD, Lachance GR, Rimsaite RYH (1965) Age determinations and geological studies: isotopic ages, Rep 5, Geol Surv Can Paper 64–17, 126 p
Wanless RK, Stevens RD, Lachance GR, Rimsaite RYH (1966) Age determinations and geological studies: K-Ar isotopic ages, Rep 6, Geol Surv Can Paper 65–17, 101 p
Wanless RK, Stevens RD, Lachance GR, Edmonds CM (1967) Age determinations and geological studies, K-Ar isotopic ages, Rep 7, Geol Surv Can Paper 66–17, 77 p
Wanless RK, Stevens RD, Lachance GR, Edmonds CM (1968) Age determinations and geological studies, K-Ar isotopic ages, Report 8 Geol Surv Can Paper 67–2, 141 p
Wanless RK, Stevens RD, Lachance GR, Delabio RN (1979) Age determinations and geological studies, K-Ar isotopic ages, Geol Surv Can Paper 79–2, 67 p
Wanty RB, Chatham JR, Langmuir D (1987) The solubilities of some major and minor element minerals in ground waters associated with a sandstone-hosted uranium deposit, Bull Miner, v 110, pp 209–226
Ward DM (1984) Uranium geology, Beaverlodge area, *in*: Proterozoic unconformity and stratabound uranium deposits, TECDOC-315, IAEA, Vienna, pp 269–284
Warren CG (1971) A method of discriminating between biogenic and chemical origins of the ore-stage pyrite in a roll-type uranium deposit, Econ Geol, v 66, pp 919–928
Warren CG (1972) Sulfur isotopes as a clue to the genetic geochemistry of a roll-type uranium deposit, Econ Geol, v 67, pp 759–767

Watchorn MB (1981) Continental sedimentation and volcanism in the Dominion Group of the Western Transvaal: a review, Trans Geol Soc S Afr, v 84, pp 67–73

Waters AC, Granger HC (1953) Volcanic debris in uraniferous sandstones, and its possible bearing on the origin and precipitation of uranium, US Geol Surv Circ 224, 26 p

Watkins TA (1975) The geology of the Copper House, Copper Mountain, and Parashant breccia pipes, western Grand Canyon, Mohave County, Arizona, MSc thesis, Colorado School Mines, Golden, 83 p

Watson JV, Plant J (1979) Regional geochemistry of uranium as a guide to deposit formation, Phil Trans Royal Soc, London, A, v 291, pp 321–338

Watson JV, et al. (1982) Uranium provinces in relation to metamorphic grade and regional geochemistry, *in*: Uranium exploration techniques, OECD-NEA, Paris, pp 235–248

Weber C, Barbey P, Cuney M, Martin H (1985) Trace element behaviour during migmatization – evidence for a complex melt-residuum-fluid interaction in the St Malo migmatitic dome (France), Contrib Miner Petrol, 90, pp 52–62

Weber F, Bonhomme M (1975) Données radiochronologiques nouvelles sur le Francevillien et son environnement, *in*: The Oklo phenomenon, IAEA, Vienna, pp 17–35

Webster JD (1983) Petrography of some Ambrosia Lake, New Mexico, prefault uranium ores, and implications for their genesis, US Geol Surv Rep 83–8, 72 p

Wedepohl KH, ed. (1969–1974) Handbook of geochemistry, Springer, Berlin, Heidelberg, New York, 92A, 1–3

Weege RJ (1963) Geology of the Marquez mine, Ambrosia Lake, *in*: Kelley VC, ed., Geology and technology of the Grants Uranium Region, New Mex Bur Mines Mineral Res Mem 15, pp 117–121

Weeks AD (1951) Red and gray clay underlying ore-bearing sandstone of the Morrison Formation in western Colorado, US-AEC, TEM-251, 19 p

Weeks AD, Eargle DH (1960) Uranium at Palagana salt dome, Duval County, Texas, *in*: Short papers in the geological sciences, US Geol Surv Prof Paper 400-B, pp B48–B52

Weeks AD, Eargle DH (1963) Relation of diagenetic alterations and soil-forming processes to the uranium deposits of the southeast Texas coastal plain, *in*: Clays and clay minerals, v 10, 10th National Conf on Clays and Clay Minerals, 1961, Macmillan Co, New York, pp 23–41

Weeks AD, Thompson ME (1954) Identification and occurrence of uranium and vanadium minerals from the Colorado Plateau, US Geol Surv Bull 1009B, pp 13–62

Weeks AD, Truesdale AH, Haffty J (1957) Nature of the ore boundary and its relation to diagenesis and mineralization, Uravan district, Colorado, (abstr), Geol Soc Amer Bull, v 68, no. 12, pt. 2, pp 1810–1811

Weeks AD, Coleman RG, Thompson ME (1959) Summary of the ore mineralogy, *in*: Garrels RM, Larsen ES, III, compilers, Geochemistry and mineralogy of the Colorado Plateau uranium ores, US Geol Surv Prof Paper 320, pp 65–79

Weir GW, Puffet WP (1960) Similarities of uranium-vanadium and copper deposits in the Lisbon Valley area, Utah-Colorado, Intern Geol Congr Rep 21st Sess Norden, Copenhagen, Tl 15, p 133

Wenrich KJ (1985) Mineralization of breccia pipes in northern Arizona, Econ Geol, v 80, pp 1722–1735

Wenrich KJ (1986) Uranium mineralization of collapse breccia pipes in northern Arizona, western United States, *in*: Vein-type uranium deposits, TECDOC-361, IAEA, Vienna, pp 395–414

Wenrich KJ, Sutphin HB (1989) Lithotectonic setting necessary for formation of uranium-rich solution-collapse breccia-pipe province, Grand Canyon region, Arizona, *in*: Metallogenesis of uranium deposits, IAEA, Vienna, pp 307–344

Wentworth DW, Porter DA, Jensen HN (1980) Geology of the Crownpoint Section 29 uranium deposit, McKinley County, New Mexico, *in*: Rautman CA, ed., Geology and mineral technology of the Grants Uranium Region 1979, New Mex Mines Mineral Res, Mem 38, pp 139–144

Western Mining Corporation Ltd. (1975) A general account of the Yeelirrie uranium deposit, 13 p

Western Mining Corporation Ltd. (1978) Draft environmental statement and environmental review and management program

Westrum EF, Grønvold F (1962) Triuranium heptaoxides: heat capacity and thermodynamic properties of α and β U_3O_7 from 5 to 450 K, J Chem Solids, v 23, pp 39–53

White MVW, Martin RF (1980) The metasomatic changes that accompany uranium mineralization in the non-orogenic rhyolites of the upper Aillik Group, Labrador, Can Miner, v 18, pp 459–479

Whiteside HCM (1970) Uraniferous Precambrian conglomerates of South Africa, with discussion, *in*: Uranium exploration geology, IAEA, Vienna, pp 49–75

Whiteside HCM, Glasspool KR, Hiemstra SA, Pretorius DA, Antrobus ESA (1976) Gold in the Witwatersrand Triad, *in*: Coetze CB, ed., Mineral resources of South Africa, Handbook 7, Pretoria, p 39–73

Whitfield JM, Rogers JJW, Adams JAS (1959) The relationship between petrology and the thorium and uranium contents of some granitic rocks, Geochim Cosmochim Acta, v 17, p 248

Whitney CG (1986) Petrology of clay minerals in the subsurface Morrison Formation near Crownpoint, southern San Juan Basin, New Mexico: An interim report, *in*: Turner-Peterson CE, Santos ES, Fishman NS, eds., A basin analysis case study – the Morrison Formation, Grants Uranium Region, New Mexico, Amer Ass Petrol Geol, Studies in Geology no. 22, pp 315–329

Wilbert WP, and Templain CJ (1978) Preliminary study of uranium favorability of the Wilcox and Claiborne Groups (Eocene) in Texas, US-DOE, GJBX-7(78), 30 p

Wilde AR, Wall VJ (1987) Geology of the Nabarlek uranium deposit, Northern Territory, Australia, Econ Geol, v 82, pp 1152–1168

Wilde AR, Wall VJ, Bloom MS (1985) Wall-rock alteration associated with unconformity-related uranium deposits, Northern Territory, Australia: Implications for uranium transport and depositional mechanisms, *in*: Concentration mechanisms of uranium in geol environments, Soc Franç Miner Crist and GREGU, Nancy, pp 231–239

Wilde AR, Mernagh TP, Bloom MS, Hoffmann CF (1988) Evidence from fluid inclusions on the origin of some Australian unconformity-related uranium deposits (manuscript 19 p)

Williams-Jones AE, Sawiuk MJ (1985) The Karpinka Lake uranium prospect, Saskatchewan: a possible metamorphosed Middle Precambrian sandstone-type uranium deposit, Econ Geol, v 80, pp 1927–1941

Willingham TO, Nagy B, Nagy L, Krinsly D, Mossman O (1985) Uranium bearing stratiform organic matter in paleo-placers, Elliot Lake-Blind River, Canada, Can J Earth Sci, v 22, pp 1930–1944

Wilson MR (1987) Petrogenesis of fluids associated with unconformity-type uranium deposits in Saskatchewan, and with the Zortman-Landusky Au-Ag deposits in Montana, PhD thesis, Univ Saskatchewan, Saskatoon

Wilson MR, Åkerblom GV (1982) Geological setting and geochemistry of uranium-rich granites in the Proterozoic of Sweden, Miner Mag, v 46, pp 235–247

Wilson MR, Fallick AE (1982) The relationship between uranium-enriched granites and hydrothermal mineralization in northern Sweden, *in*: Uranium exploration methods, OECD-NEA, Paris, pp 293–306

Wilson MR, Kyser TK (1987) The stable isotope geochemistry of alteration associated with the Key Lake uranium deposit, Canada, Econ Geol, v 82, pp 1540–1557

Wilson MR, Sundin NO (1979) Isotopic age determinations on rocks and minerals from Sweden 1960–1978, Sveriges Geol Undersökning Rap och Medd, v 16, 41 p

Wilson MR, Hamilton PJ, Fallick AE, Aftalion M, Michard A (1985) Granites and early Proterozoic crustal evolution in Sweden, evidence from Sm-Nd, U-Pb and O isotope systematics, Earth Planet Sci Lett, v 72, pp 376–388

Wilson MR, Kyser TK, Mehnert H, Hoeve J (1987) Changes in the H-O-Ar isotope composition of clays during retrograde alteration, Geochim et Cosmochim Acta, v 51, no. 4, pp 869–878

Windley BF (1977) The evolving continents, John Wiley and Sons, New York, 385 p

Winkler HGF (1983) *in*: Martin H, Eder FW, eds., Intracontinental fold belts, Springer, Berlin, Heidelberg, New York, Tokyo, 945 p

Winter H, de la Rey (1964) The geology of the Virginia section of the Orange Free State Goldfield, *in*: Haughton SH, ed., The geology of some ore deposits in southern Africa: Marshalltown, Geol Soc S Afr, v 1, pp 507–548

Witkind IJ (1956) Uranium deposits at the base of the Shinarump Conglomerate, Monument Valley, Arizona, US Geol Surv Bull 1030-C, pp 99–130

Witkind IJ, Thaden RE (1963) Geology and uranium-vanadium deposits of the Monument Valley area, Apache and Navajo Counties, Arizona, US Geol. Surv Bull 1103, 171 p

Wood HB (1968) Geology and exploitation of uranium deposits in the Lisbon Valley area, Utah, *in*: Ridge JD, ed., Ore deposits of the United States, 1933–1967, Am Inst Min Metal Petrol Eng, v 1, pp 770–789

Woodmansee WC (1976) Uranium, *in*: Mineral facts and problems, 1975 edition, US Bur Mines Bull 667, pp 1177–1200

Worden, JM, Cumming GL, Baadgsaard H (1985) Geochronology of host rocks and mineralization of the Midwest uranium deposit, northern Saskatchewan, *in*: Sibbald TII, Petruk W, eds., Geology of uranium deposits, CIM Spec Vol. 32, pp 67–72

Wray EM, Ayers DE, Ibrahim HJ (1985) Geology of the Midwest uranium deposit, northern Saskatchewan, *in*: Sibbald, TII, Petruk W, eds., Geology of uranium deposits, CIM Spec Vol. 32, pp 54–66

Wright JH (1980) Economic geology of the Schwartzwalder mine, *in*: Uranium resource technology, v III, Golden, Colo Sch Mines Press, pp 73–92

Wright JH, Wallace AR, Karlson RC (1981) New studies at the Schwartzwalder mine, Jefferson County, Colorado, CIM, Geol Div, Uranium Symposium and Field Tours, pp 25–26

Wright RJ (1955) Ore controls in sandstone uranium deposits of the Colorado Plateau, Econ Geol, v 50 pp 135–155

Wrucke CT, Sheridan DM (1968) Precambrian rocks penetrated by the deep disposal well at the Rocky Mountain Arsenal, Adams County, Colorado, US Geol Surv Prof Paper 600-B, pp 852–859

Wyatt BA (1976) The geology and geochemistry of the Klipriviersberg volcanics, Ventersdorp Supergroup, south of Johannesburg, unpubl MSc thesis, Univ Witwatersrand, Johannesburg, 178 p

Wylie ET (1963) Geology of the Woodrow breccia pipe, *in*: Kelley VC, ed., Geology and technology of the Grants Uranium Region, New Mex Bur Mines Mineral Res em 15, pp 177–181

Wyllie PJ (1979) Magma and volatile components, Am Miner, v 64, pp 469–500

Xu G, Wang A, Gu Q, Zhang J, Zhang Z, Huang Y (1981) Some characteristics of uranium oxides in China, Bull Minér, 104, pp 565–574

Yao Zhenkai (1983a) The geotectonic types and their main character of uranium deposits in China, Geotectonica et Metallogenia, China, v 7, 1, pp 117 ff

Yao Zhenkai (1983b) The distribution and geological characteristics of stratabound uranium deposits in Diwa regions of China, Mineral Deposits, Beijing, 1, pp 83 ff

Yao Zhenkai (1984a) Geological-geochemical condition of mineralization of stratabound carbonate uranium deposits in China, Acta Sedimentologica Sinica, China, v 2, 1, pp 65 ff

Yao Zhenkai (1984b) Tectonic-geochemical manifestation of uranium mineralization in carbonate rocks, Geotectonica et Metallogenia, China, v 8, 3, pp 261 ff

Yao Zhenkai (1986) The application of Diwa theory in the search for uranium and metallogeny of uranium, Geotectonica et Metallogenia, China, v 10, 4, pp 323 ff

Yao Zhenkai, et al. (1984) The metallotectonic features of a stratabound uranium deposit formed by Diwa metallogenesis, Bull Changsha Inst Geot Acad Sinica, 1, pp 103 ff

Yao Zhenkai, et al. (1986) Types and characteristics of karst uranium deposits, Carsologica Sinica, v 5, 2, pp 79 ff

Yao Z, Liu Y, Zhu R, Yang S, Li D (1989) Uranium metallogenesis in southeast China, *in*: Metallogenesis of uranium deposits, IAEA, Vienna, pp 345–356

Yeliseyeva OP (1977) Content and distribution of uranium, thorium, yttium, and the rare earths in accessory minerals in granitoids, Geochem Intern, v 14, pp 37–49

Yeliseyeva OP, Omel'yanenko VI (1976) Local distribution of uranium in rocks and minerals as an indicator of petrogenetic processes, Sov Geol, no. 1, pp 76–91

Yerle JJ (1978) Albitisations et minéralisations uranifères dans le socle et les sédiments permo-houillers du bassin de Brousse Broquiès (Aveyron, France), Thèse de Docteur – Ingénieur, Paris ENSM, 142 p

Yerle JJ, Thiry M (1979) Albitisations et minéralisations

uranifères dans le socle et dans les sédiments permo-houillers du bassin de Brousse-Broquiès, Bull BRGM, 2ème Sér, Sect II, 2, pp 275–290
Yermolayev NP (1971) Processes of redistribution and extraction of uranium in progressive metamorphism, Geochem Intern, v 8, pp 599–609
Yermolayev NP (1973) Uranium and thorium in regional and contact metamorphism, Geochem Intern, v 10, pp 418–423
Yermolayev NP (1975) Physicochemical principles governing the redistribution of radioactive elements during progressive rock metamorphism, *in*: Kuznetsov VA, ed., Radioactive elements in rocks, Nauka, Novosibirsk, USSR, pp 140–146
Yermolayev NP, Zhidikova AP (1966) Behaviour of uranium in progressive metamorphism and ultrametamorphism as observed in the western part of the Aldan Shield, Geochem Intern, v 3, pp 716–731
Yermolayev NP, Zhidikova AP, Zarinskiy VA (1965) Transport of uranium in aqueous solutions in the form of complex silicate ions, Geochem Intern, v 2, pp 629–641
Yes'hova EM, Mineyev DA, Mineyeva IG (1962) Uranium and thorium in the alkalic rocks of the Urals, Geochem (USSR) (English Transl) p 885
Yevseyeva LS, et al. (1967) Conditions of formation and classification of exogenic epigenetic uranium deposits, *in*: Problems of applied radiogeology, vyp 2, Atomizdat, Moscow, pp 326–367
Yevseyeva LS, Perel'man AL, Ivanov K Ye (1974) Geochemistry of uranium in the supergene zone, (2nd Ed.), Atomizdat, Moscow, 280 p
Yevstrakhin VA (1967) Uranium ore depositional epochs Izv Akad Nauk SSSR, Ser Geol, no. 3, pp 13–27
Young EJ (1977) Geologic, radiometric, and mineralogic maps and underground workings of the Schwartzwalder uranium mine and area, Jefferson County, Colorado, US Geol Surv Rep 77–725, 38 p
Young EJ (1979a) Analytical data on the Schwartzwalder uranium deposit, Jefferson County, Colorado, US Geol Surv Rep 79–968, 34 p
Young EJ (1979b) Genesis of the Schwartzwalder uranium deposit, Jefferson County, Colorado, Contrib Geol, Univ Wyoming, v 17, no, 2, pp 179–186
Young EJ (1985) Summary of the geology, economic aspects, and geochemistry of the Schwartzwalder uranium-bearing area, Ralston Buttes district, Jefferson County, Colorado, US Geol Surv Bull 1555, 32 p
Young EJ, Hauff PL (1975) An occurrence of disseminated uraninite in Wheeler Basin, Grand County, Colorado, J Res U S Geol Surv, v. 3, no. 3, pp 305–311
Young RG (1960) Uranium deposits of the southern San Juan mineral belt, New Mexico, US-AEC, TM-170, 48 p
Young RG (1964) Distribution of uranium deposits in the White Canyon-Monument Valley district, Utah-Arizona, Econ Geol, v, 59, pp 850–873
Young RG (1978) Depositional systems and dispersal patterns in uraniferous sandstones of the Colorado Plateau, Utah, Geology, v 5, pp 85–102
Young RG, Ealy GK (1956) Uranium occurrences in the Ambrosia Lake area, McKinley County, New Mexico, US-AEC, RME-86, 15 p
Young RG, Million I, Hausen DM (1957) Geology of the San Rafael River Desert mining district, Emery and Grand Counties, Utah, US-AEC, RME-98, 100 p
Young WE, Delicate DT (1965) Mining methods and costs at Section 23 uranium mine, Homestake-Sapin Partners, McKinley County, New Mexico, US Bur Mines Inform Circ 8280, 48 p
Ypma PJM, Fuzikawa K (1980) Fluid inclusion and oxygen isotope studies of the Nabarlek and Jabiluka deposits, Northern Territory, Australia, *in*: Ferguson J, Goleby AB, eds., Uranium in the Pine Creek Geosyncline IAEA, Vienna, pp 375–395
Yu S (1989) Characteristics and regional geological environments of uranium deposits in Mesozoic volcanics in east China, *in*: Uranium deposits in magmatic and metamorphic rocks, IAEA, Vienna, pp 77–92
Zagruzina IA, Smyslov AA (1978) Uranium and thorium in rocks of the Soviet Northeast, Intern Geol Rev, v 20, no. 10, pp 1230–1238
Zhou Weixun, Xia Yuliang (1984) A study of the U-Pb isotopic systematics and its application in uranium geology, Geochem, Beijing, v 3, 2, pp 142 ff
Zhukova AM, Bergman IA, Zhukov GV (1975) Distribution of uranium in the geological formations of the Ukrainian Shield, Geochem Intern, v 12, pp 103–116
Zhukova VY (1980) Mineralogy and primary zoning of hydrothermal metasomatic uranium deposits in Precambrian iron formations, *in*: Avrashov A, translater, Albitized uranium deposits: six articles translated from Russian literature, US-DOE, GJBX-193(80), pp 91–114
Zhuravleva LN, Berezina LA, Gulin Y (1976) Geochemistry of rare and radioactive elements in apatite-magnetite ores in alkali-ultrabasic complexes, Geochem Intern, v 13, pp 145–166
Ziegler V (1974) Essai de classification metallotectonique des gisements d'uranium, *in*: Formation of uranium ore deposits, IAEA, Vienna, pp 661–677
Ziegler V (1978) Relation of metallogenic, tectonic and zoning factors to the origin of uranium deposits: Introductory remarks; *in*: Discussions of the uranium geology working groups, Intern Geol Congr, Sydney, Tech Rept Series, no. 183, IAEA, Vienna, pp 73–79
Ziegler V, Dardel J (1984) Uranium deposits in Europe, *in*: de Vivo F, et al., eds., Uranium geochemistry, mineralogy, geology, exploration and resources, IMM, London, pp 140–161
Zielinski, RA (1978) Uranium abundances and distribution in associated glassy and crystalline rhyolites of the western United States, Geol Soc Amer Bull, 89, pp 409–414
Zielinski RA (1979) Uranium mobility during interaction of rhyolitic obsidian, perlite and felsite with alkaline carbonate solutions, Chem Geol, v 27, pp 47–63
Zielinski RA (1980) Uranium in secondary silica: a possible exploration guide, Econ Geol, v 75, pp 592–602
Zielinski RA (1982) The mobility of uranium and other elements during alteration of rhyolitic ash to montmorillonite: A case study in the Troublesome Formation, Colorado, USA, Chem Geol, v 35, p 185
Zielinski RA (1985) Volcanic rocks as sources of uranium: Current perspective and future directions, *in*: Uranium deposits in volcanic rocks, IAEA, Vienna, pp 83–97
Zielinski RA, Johnson SY, Otton JK (1987) The geologic setting of a surficial uranium deposit, northeastern Washington, IAEA meeting, Saskatoon, Canada, manuscript, 22 p
Zielinski RA, Lindsey DA, Rosholt JN (1980) The dis-

tribution and mobility of uranium in glassy and zeolitized tuff, Keg Mountain area, Utah, USA, Chem Geol, v 29, pp 139–162

Zielinski RA, Lipman PW, Millard HT Jr (1977) Minor element abundances in obsidian, perlite and felsite of calc-alkalic rhyolites, Amer Miner, v 62, 426–437

Zimmer P (1986) Etude expérimentale, à haute température et haute pression, du système ternaire UO_2-ThO_2-SiO_2 en présence d'une phase fluide. Comparaison avec les systèmes ZrO_2-ThO_2-SiO_2 et UO_2-ZrO_2-SiO_2. Implications géologiques, Mém CREGU, no. 12, Nancy, 227 p

Zitting RT, Masters JA, Groth FA, Webb MD (1957) Geology of the Ambrosia Lake area uranium deposits, McKinley County, New Mexico, Min Mag, v 47, no. 3, pp 53–58

Zubov AI (1960) The uraniferous solid bitumens, Geol rud mestorozh, v 2, no. 5, pp 6–24 (Econ Geol, v 57, pp 641–642)

Zubov AI, Kotel'nikov GN (1968) Vein asphaltites in a uranium deposit, Sov Atomic Energy, v 24, pp 637–641

Zückert R (1926) Die Paragenesen von gediegen Silber und Wismut mit Co-Ni-Kiesen zu St. Joachimsthal in Böhmen, Mitt d Abt Erz-, Salz- u Gesteinsmikroskopie, H 1, pp 69–126

Zumberge JE, Nagy B, Nagy LA (1981) Some aspects of Vaal Reef uranium-gold carbon seams, Witwatersrand Sequence, US Geol Surv Prof Paper 1161-0, pp 1–7

Zumberge JE, Sigleo AC, Nagy B (1978) Molecular and elemental analyses of the carbonaceous matter in the gold- and uranium-bearing Vaal Reef carbon seams, Witwatersrand Sequence, Miner Sci Eng, v 10, pp 223–246

For comprehensive listings of bibliography published prior to 1966, see IAEA, Geology of Uranium and Thorium, bibliographical series no. 4, 1962, 130 p and no. 31, 1968, 102 p

Locality Index

(bold type indicates selected deposits or districts described in more detail)

ABC, Canada 192
Abertamy, ČSFR 224, 230
Abikwaskolk, South Africa 102
Abokan (Siberia), Russia 8
Ace, Canada 53, 191, 192, 193, 194, 195, 196, 199
Acropolis, Australia 110
Adelaide River, Australia 169
Agades Basin, Niger 35, 38, 51, 54, 88
Agnew Lake, Canada 106, 343
Ain Ben Tili, Mauritania 101
Aïr Massif, Niger 35, 51
Akbakay, Kazakhstan 113
Akouta, Niger 51, 88
Aksuyek, Kazakhstan 113
Alameda, Spain 232, 233, 234
Alberode-Niederschlema, Germany 81
Albuquerque, Spain 232
Aldan Shield, Russia 31
Alio Ghelle, Somalia 125
Aljão, Portugal 232
Alligator Rivers (Uranium Field), Australia 7, 38, 42, 43, 46, 58, 70, **168ff.**
Alm Bos, Italy 82
Altai Mts., Russia 54
Altiplano, Bolivia 98
Alto Alentejo, Portugal 43, 59, 74, 79, 84, 232, 233, 237
Amadeus Basin, Australia 7, 35, 54, 87
Ambindrakemba, Madagascar 8, 129
Ambrosia Lake (Trend), USA 88, 251, 254, 258, 260, 261, 262, 263, 266
Amer Lake, Canada 129
Anderson, USA 88
Angela, Australia 87
Antsirabe Basin, Madagascar 88
Apuseni Mts., Romania 7, 83, 88, 120
Aqitaine Basin, France 88, 89
Araxa, Brazil 14, 114
Arnhem Land, Australia 168
Archontovouni, Greece 104
Arizona Strip, USA 7, 38, 42, 61, 94, 96, **324ff.**
Arjeplog-Arvidsjaur, Sweden 7, 36, 83
Arlit, Niger 51, 88
Armorican Massif, France 7, 36, 79, 80
Arunta Block, Australia 7, 35
Arvidsjaur, Sweden (see Arjeplog)
Ascension Mine, USA 83, 238
Athabasca Basin, Canada 7, 35, 42, 46, 53, 58, 65, **137ff.**
Aubrey, USA 238
Augères, France 202, 203
Aurora, USA 47, 63, 119, 121
Aussinanis, Namibia 101
Autun, France 5
Aveyron, France 68, 69
Azelik, Niger 88
Azere, Portugal 232, 233, 236, 237

Baggs, USA 290
Baghal Chur, Pakistan 35
Baker Lake, Canada 35
Bakouma, Central African Republic 8, 42, 54, 103, 117
Balkan Mts., Bulgaria 7, 36, 87, 120
Balyanghe, China 7, 120
Banat, Romania 88
Bancroft, Canada 7, 35, 41, 53, 63, 114
Bangemall Basin, Australia 335
Bankers Lode, USA 238
Beaufort-West, South Afrika 7, 88, 89
Beaverdell, Canada 35, 42, 45, 73
Beaverlodge, Canada 7, 38, 43, 46, 48, 53, 58, 67, 70, 71, 73, 74, 125, 155, 156, 199ff. (see also Uranium City)
Beiras, Portugal 8, 79, 82, 232, 233, 235, 237
Beisa, South Africa 360
Bellezane, France 202, 203
Benavides, USA 93, 312f.
Bendada, Portugal 232
Ben Lomond, Australia 7, 121
Bennac, France 68
Bertholène, France 65, 68
Beshkak, Uzbekistan 88
Beverly, Australia 61, 88, 93
Bica, Portugal 232, 235
Bigrlyi, Australia 90
Bílá Voda, ČSFR 81
Billiken, USA 238
Billingen, Sweden 5, 38
Bingham, USA 42, 46, 63, 107, 112
Black Forest, Germany 7, 36, 51, 79, 81, 87
Black Hawk, USA 81
Black Hills, USA 7, 52, 88, 93, 106
Black Jack, USA 267
Black Knight, USA 238
Blind River, Canada 7, 53, 62, 105, 127, **343ff.** (see also Elliot Lake)
Blizzard, Canada 7, 92
Blue Jay, USA 238
Bohemian Massif, ČSFR 7, 36, 47, 54
Bois Noirs, France 80
Bokan Mountain, USA 35, 123, 125
Bolger, Canada 53, 74, 192, 195, 200
Bolivian Basin, Argentina 87
Bondon, France 99
Bone Valley, USA 8, 30, 117, 118 (see also Florida)
Borrega, Portugal 232
Boyindzi, Gabon 319, 321
Bratrství, ČSFR 224
Brazilian belt, Brazil 53
Březinka, ČSFR 80
Brousse-Broquiès, France 68, 125
Brulkolk, South Africa 101
Bruni, USA 312
Buckles, Canada 343f.
Bukinay, Uzbekistan 88
Burgos Basin, Mexico 7, 35, 88
Bushmanland Plateau, South Africa 101, 102
Bytíz, ČSFR 218

Cabinda, Angola 30
Caceres, Spain 232
Cameron, USA 331
Campbell Island, Canada 115
Canadian Shield, Canada 137ff., 344ff.
Can-Met, Canada 343f.
Canyon, USA 96, 325, 328, 331
Cape Province, South Africa 7, 101, 102, 103
Caridad, Spain 232, 233
Carletonville Goldfield, South Afrika 353f., 360, 361, 362
Carnarvon Basin, Australia 88, 92, 93, 335
Carpathian Mts., Romania 7, 83
Caroll, USA 238
Carrizo, USA 90
Carswell Structure (district), Canada 31, 137, 138, 141, 149, 150, 151, 152, 153, 154, 155, 156, 157, 159, 161, 164, 166
Casillas, Spain 232
Catalão, Brazil 114
Central Bohemian Pluton, ČSFR 218ff.
Central City, USA 5, 26, 238
Central Rand Goldfield, South Afrika 353, 356, 360
Central-Transbaikalsky, Russia 8
Cerilly Basin, France 88

Chaco Slope, USA 251
Chanziping, China 8, 134
Charlebois Lake, Canada 112
Chatanooga, USA 8, 38, 64, 131, 132
Chengxian, China 8, 134
Chiblow Anticline, Canada 345, 346 ff.
Chienxinan, China 8, 134
Chita, Russia 8
Chubut, Argentina 87
Chuquicamata, Chile 113
Chupa, Russia 8, 115
Churchill Structural Province, Canada 193 ff.
Church Rock, USA 251, 265, 267
Cigar Lake, Canada 46, 53, 58, 65, 67, 143, 145, 150, 151, 152, 158, 159, 160, 161Ciudad Rodrigo, Spain 82, 232, 233, 234 f.237
Claude, Canada 143, 150, 157, 166
Clay West-Burns, USA 306, 312, 314, 316
Cluff Lake, Canada 68
– D (orebody) 143, 151, 152, 153, 161
– N (orebody) 143, 150, 151
– OP (orebody) 143, 150, 151, 152
Coles Hill, USA 7
Collins Bay, Canada 68, 143, 149, 150, 151, 152, 153, 159, 161
Colorado Mineral Belt, USA 82, 244
Colorado Plateau, USA 7, 42, 59, 88, 89, 90, 92, 251 ff., 270 ff., 284 ff., 324 ff.
Colorado Plateau, Salt Wash districts, USA 270 ff.
Conway/White Mountain, USA 26
Copper Mountain, USA 104, 290
Cornwall, Great Britain 5, 36, 81
Coronation Hill, Australia 169
Cosquin, Argentina 90
Cotaje, Bolivia 7, 42, 47, 63, 96, 99, 100, 104, 119, 121
Cottonwood, USA 63, 121
Cougar Mine, USA 276
Coutras, France 7, 88
Cree Lake Mobile Belt/Zone, Canada 53, 139, 153, 154, 155, 156
Crockers Well, Australia 113
Crooks Gap, USA 290, 298
Crow Butte, USA 7, 61, 88, 94
Crown Point, USA 251
Cuddapah Basin, India 8
Cunha Beixa, Portugal 232, 235

Daladi, China 7, 87
Damara belt, Namibia 35, 51, 53, 112, 366 ff.
Damětice, ČSFR 80
Danfeng-Zhuyangguan-Shangnan area, China 7
Date Creek Basin, USA 63, 88, 122
Dawn Lake, Canada 68, 143, 149, 151, 161, 165
Daybreak Mine, USA 42, 47, 62, 96, 99, 100, 103
Dekalb County, USA 132
Denison Mine, Canada 343 f., 347, 348, 349
Denver-Julesburg Basin, USA 93
Dera Ghazi Khan, Pakistan 7, 88
Deremo Mine, USA 271, 273, 278
Dirkskop, South Africa 102
Dominique-Janine, Canada 67, 143, 151
Dominique-Peter, Canada 67, 143, 150, 151, 152, 157
Don Benito, Spain 82
Donna, Canada 152
Duobblon, Sweden 8, 122
Drummond Basin, Australia 87
Dubyna, Canada 197
Duddridge Lake, Canada 129, 153
Dusa Mareb-El Bur, Somalia 7, 101
Duval County, USA 94, 305 ff.
Dyleň, ČSFR 83
Dzhantuar, Uzbekistan 8, 134

Eagle, Canada 192
Eagle Point, Canada 58, 65, 66, 67, 141, 143, 144, 148, 149, 150, 151, 152, 157, 163
East Athabasca district, Canada 137, 138, 141, 142, 147, 148, 149, 150, 151, 152, 153, 158, 161
East Calhoun, USA 238
East Rand Goldfield, South Afrika 353 f., 360
Easy-1, USA 96
Ebala, Niger 88
Echo Bay, Canada 81
Eibenstock Massif (= Karlovy Vary Massif), Germany-ČSFR 80, 225
Elbsandsteingebirge, Germany 7, 87
Eleshnitza, Bulgaria 7, 87
Elliot Lake, Canada 7, 42, 53, 106, **343 ff.**
El Sherana, Australia 169
Erzgebirge, Germany 5, 7, 31, 54, 59, 81, 224 ff.
Esperanza, Spain 232, 233, 234
Espinharas, Brazil 5, 7, 54, 63, 125, 127
Evander Goldfield, South Afrika 353 f.360
Eva-Barbora, ČSFR 224
EZ-2, USA 325, 330, 331, 332

Fanay, France 59, 74, 77, 202, 203, 204
Far East (Siberia), Russia 8
Fair Day, USA 238
Far West Rand Goldfield, South Afrika 354, 360
Fay, Canada 53, 58, 70, 191, 192, 193, 194, 195, 196, 199
Felder, USA 311, 314, 316
Fe, Mina, Spain 232, 233, 234
Ferghana Basin, Uzbekistan 7, 103
Fichtelgebirge, Germany 79
Figuera, Brazil 7, 87
Fleur de Lys, Australia 169
Flodell Creek, USA 100, 102 (see also Stevens Couny)
Florida, USA 5, 8, 30, 42, 46, 54, 63, 115, 118
Fond du Lac, Canada 143, 151, 152, 156
Foothills, USA 238
Forez, France 80
Forstau, Austria 43, 46, 51, 53, 63, 127
Fort Dauphin, Madagascar 129
Franceville Basin, Gabon 7, 35, 42, 47, 51, 53, 61, 87, 88, 90, **319 ff.**
Freital, Germany 8, 130
Freixiosa, Portugal 232
Front Range, USA 7, 83, 238 ff.

Gan-Hang belt, China 7, 8, 120
Ganntour-Bahira, Morocco 117
Gaoligang, China 7, 87
Gascoyne, Australia 335
Gas Hills, USA 51, 93, 290, 291, 296, 298, 299, 304
George Creek, Australia 169
Georgetown Inlier, Australia 35
Georg Wagsfort Mine, Germany 5
Glatzer Schneeberg (Snieznik Klodzki), Poland 81
Goanikontes, Namibia 112
Goldfields, Canada 125
Grandrieu, France 213, 215
Granite Mts., USA 27, 51, 290, 291
Grand Canyon, USA 324 ff.
Grants Uranium Region, USA 7, 42, 47, 60, 61, 84, 88, **250 ff.**, 280
Grapevine, USA 238
Great Bear Lake, Canada 35, 81
Great Divide Basin, USA 290, 298, 299
Great Plains, USA 94
Green Mountain, USA 290
Green River, USA 117
Grosschloppen, Germany 79
Guangxi-Hunan-N.Guangdong, China 8, 134
Guarda, Portugal 232
Guérande Peninsula, France 80, 213, 215
Guizhou, China 8, 35, 134
Gunnar, Canada 70, 73, 79, 125, 126, 155, 191, 194, 197

Hab, Canada 74
Hack Canyon, USA 94, 325, 328, 330, 331
Hammadas, Mauritania 101
Hamr, ČSFR 65, 87
Harmony, South Africa 360
Henkries, South Africa 103
Henriette, France 78, 203, 205
Henry Basin, USA 281ff.
Henry Mts., USA 90, 279, 281f.
Highland-Box Creek, USA 290, 292
Hinkler-Centipede, Australia 101, 335, 336, 340
Höhenstein, Germany 129
Hoggar, Algeria 7, 35, 83
Holiday-El Mesquite, USA 312f., 316
Honeymoon, Australia 93
Horseshoe, Canada 67, 149, 151
Hotagen, Sweden 36

Iberian Meseta, Spain-Portugal 7, 36, 47, 59, **232ff.**
Ida Dome, Namibia 112
Idaho, USA 30, 54, 63, 115
Igaliko Fjord, Greenland 7, 80
Illimaussaq, Greenland 7, 26, 27, 42, 46, 53, 114, 125 (see also Kvanefjeld)
Imouraren, Niger 88
Itataia, Brazil 7, 54, 79

Jabiluka, Australia 70, 72, 168, 169, 176, 177, 178, 179, 180, 182, 183, 186, 187, 188, 191
Jáchymov (= St. Joachimsthal), ČSFR 5, 53, 74, 80, **224ff.**
Jaduguda, India 7
Javorník, ČSFR 81
JEB, Canada 149
Jenissei (= Yeniseisky), Russia 8, 37
Jeruzalém, ČSFR 218
Jianchang, China 7, 87
Jiangnan Block, China 8, 35, 132
Jiangxi belt, China 7
Jingan Basin, China 7, 38, 87
Joachimsthal, Sankt (= Jáchymov), ČSFR
Johan Beetz, Canada 112
Johanngeorgenstadt, Germany 5, 81
Jos Plateau, Nigeria 26
Jujuy-Bolivian Basin, Argentina 87

Kaapvaal-Kalahari Craton, South Africa 35, 36, 354f., 365
Kaipokok Bay, Canada 38
Kalahari Basin, Namibia 367
Kalongwe, Zaïre 83, 250
Kamenná, ČSFR 218
Kanab North, USA 96, 325, 330, 331
Kanimekh, Uzbekistan 88
Kannikwa, South Africa 103
Karamazarsky, Uzbekistan 8, 36, 120
Karin Lake, Canada 153
Karlovy Vary Massif (= Eibenstock Massif), ČSFR-Germany 80
Karnataka, India 106
Karnes County, USA 94, 296, 305ff.
Karoo, South Africa 88, 89, 130
Kashi, China 7, 87
Katanga belt/Copper Province, Zaïre-Zambia 7, 35, 53, 83, 246ff.
Kaya-Kaya, Gabon 319
Kaycee, USA 290, 292
Keberovsk (Siberia), Russia 8
Kelowna, Canada 35
Kem, Russia 8, 115
Ketilidian belt, Greenland 36
Kettle Falls, USA 129
Key Lake, Canada 53, 58, 67, 143, 144, 147, 150, 151, 153, 155, 158, 159, 160, 161, 162, 165, 168
Khouribga, Morocco 8, 117
Kiggavik, Canada 7, 67
King Solomon Mine, USA 271, 278
Kinross, South Afrika 360
Kintyre, Australia 7, 67, 73
Kirk, USA 238
Kirovogradsky, Ukraine 7 (see also Krivoj Rog)
Kislovodsky, Russia 88
Kitongo, Cameroun 7, 32, 125, 126
Kitts, Canada 8, 43, 53, 129
Kiyakhty, Kazakhstan 113
Kladno, ČSFR 8
Klerksdorp Goldfield, South Afrika 353f., 356, 359, 360
Kletno, Poland 81
Königstein, Germany 54, 87
Kokchetavsky, Kazakhstan 7, 35
Koktas, Uzbekistan 113
Koongara, Australia 70, 72 168, 169, 176, 177, 178, 179, 180, 182, 183, 186, 187, 188, 191
Kouvervaara, Finland 127
Koscheka, Uzbekistan 8, 134
Kotili Basin, Greece 130
Kowary (= Schmiedeberg), Poland 81, 82
Krivoj Rog, Ukraine 32, 36, 38, 63 (see also Krivorozhsky)
Krivorozhsky, Ukraine 7, 36, 123, 126 (see also Krivoj Rog)
Krušné Hori (see Erzgebirge)
Kuusamo belt, Finland 127
Kvanefjeld, Greenland 7, 41, 53, 63, 110, 114 (see also Illimaussaq)
Kyzylkumsky, Uzbekistan 7, 8, 36, 88, 134

Labe Lineament Region, ČSFR 59
Lachlan belt, Australia 35
Lacnor, Canada 343f.
La Commanderie, France 78
La Crouzille, France 201ff.
La Dorgissière, France 80
Ladwig, USA 238
Lagõa Real, Brazil 7, 54, 126
Laguna, USA 251, 254, 256
Lake Austin, Australia 102, 335, 336, 340
Lake Baykal, Russia 8, 83
Lake Cinch, Canada 74
Lake Frome, Australia 7, 35, 38, 51, 61, 88, 92, 93
Lake Maitland, Australia 47, 62, 96, 102, 335, 336, 339, 340
Lake Mason, Australia 335, 340
Lake Onega, Russia 132
Lake Raeside, Australia 101, 335, 336, 340
Lakeview, USA 121
Lake Way, Australia 101, 335, 336, 338, 340
Lama Kara, Togo 129
Lampinsaari, Finland 129
Lamprecht, USA 311
Land Pebble district, USA 8, 45, 115, 116, 118 (see also Florida)
Langer Heinrich, Namibia 99, 101
Langshan, China 7, 8, 87, 120
Laramie Mts., USA 298
La Sal, USA 90, 271, 274
La Sal Creek, USA 90
La Sierrita, Mexico 35, 88
Las Palmas, USA 312
Laure, Canada 153
Le Brugeaud, France 202, 208, 209
Le Fraisse, France 202, 203
Lermontovsky, Russia 88
Le Roube, France 68
Le Rousset, France 80
Lešetice-Brod, ČSFR 218, 220
Les Sagnes, France 203
Lianshanguan, China 7
Limousin, France 42, 59, 79, 201ff.
Lisbon Valley, USA 52, 92, 289
Little Man Mine, USA 43, 82
Little Mts., USA (see Pryor Mts.)
Live Oak County, USA 94, 296, 305ff.
Lodève Basin, France 7, 51, 54, 88, 89
Lolodorf, Cameroun 114
Lombre, France 7, 88
Longoria, USA 312f.
Longshoushan belt, China 7
Los Colorados, Argentina 87
Los Ratones, Spain 79, 232
Lower Yangzi belt, China 7
Lukachukai-Carrizo, USA 90
Lucky Lass Mine, USA 121

Lufilian belt, Namibia 367
Lyavlyakan, Uzbekistan 88

Macusani, Peru 7, 121
Madaouela, Niger 88
Madawaska, Canada 7, 42, 63, 110, 114 (see also Bancroft)
Makkovik, Canada 8, 129
Malargue, Argentina 7, 87
Malbooma, Australia 87
Manyingee, Australia 7, 87, 88, 92, 93
Marche, France 79
Margaritas, Mexico 42, 47, 63, 119, 122
Margeride, France 59, 79, 217
Margnac, France 202, 203, 207, 209, 214, 217
Mariano Lake, USA 251, 266
Marshall Pass, USA 83
Martin Lake, Canada 192
Mary Kathleen, Australia 8, 129
Marysvale, USA 121
Mas Lavayre, France 88
Massif Central, France 5, 7, 27, 36, 47, 59, 92, 201
Massif de Chaillu, Gabon 35, 51, 319, 320, 321, 323
Materie Neuve, France 80
Maureen, Australia 7, 120, 122
Maurice Bay, Canada 68, 143, 151, 152, 156, 159, 165
Maybell, USA 290
Mazarete, Spain 7, 88
McArthur Basin, Australia 169, 189
McBride/Gury, USA 312
McClean, Canada 68, 143, 145, 149, 151, 152, 153, 156, 158, 159, 160, 161, 165
McDermitt, USA 8, 27, 42, 47, 63, 120, 121
Meckering Line, Australia 334, 335
McMullen County, USA 305 ff.
Mecsek Mts., Hungary 7, 88
Medicine Bow-Sierra Madre, USA 106
Melovoye Peninsula, Kazakhstan 8
Mena, USA 83, 238
Menzenschwand, Germany 79
Mengqiguer, China 7, 87
Menzies Line, Australia 334, 335, 341
Michelin, Canada 122
Middle Lake, Canada 152
Midnite Mine, USA 7, 80
Midwest (Lake), Canada 68, 134, 149, 150, 151, 152, 155, 156, 158, 159, 160, 161, 165
Mikouloungou, Gabon 84, 88, 90, 319 f., 323 f.
Millet Brook, Canada 79
Millevaches, France 79
Milliken Lake, Canada 343 f.
Mina Fe, Spain 232, 233, 234
Mindola, Zambia 54
Minindi Creek, Australia 335, 340, 341
Mohawk, USA 96
Mogollon Highland, USA 89, 254, 329, 334
Momino, Bulgaria 7
Montpelier, USA 45, 115, 117
Montrose County, USA 5
Montulat, France 202
Monument Hill, USA 290, 292
Monument Valley, USA 52, 60, 84, 91, **284 ff.**
Monument No. 2 Mine, USA 287, 288
Moonlight, USA 63, 120
Mont Laurier, Canada 129
Mortagne, France 27
Morvan, France 78, 79
Mosquito Gulch, Canada 32, 127
Motzfeld Center, Greenland 114
Mounana, Gabon 51, 53, 84, 88, 90, 319 ff.
Mounana Horst, Gabon 320 f.
Mount Isa Geosyncline, Australia 35
Mount Joel, Australia 335, 340
Mount Painter, Australia 51
Mount Spokane, USA 35
Mount Taylor, USA 253, 263
Mudugh, Somalia 54, 101
Müllenbach, Germany 51, 87
Mulga Rock, Australia 87, 92

Nabarlek, Australia 67, 168, 169, 170, 175, 178, 180, 182, 183, 184, 186, 187, 188
Namib Desert, Namibia 7, 54, 61, 98, 101
Nanambuh Complex, Australia 170, 174, 178, 183, 185, 191
Nanling belt, China 7
Navoi region, Uzbekistan 7, 88, 134
Nchanga, Zambia 250
Nesbitt Labin, Canada 192
Neuquén Basin, Argentina 87
Ngalia Basin, Australia 7, 35, 54, 90
Niamtougou, Togo 129
Nicholson, Canada 73
Nimbuwah Complex, Australia 170, 173, 185
Ningyo-Toge, Japan 7, 35, 60, 92
Nisa, Portugal 232, 233, 237
Nkana, Zambia 250
Nonacho, Canada 127
Nopal I, Mexico 42, 47, 63, 119, 120
Nordic, Canada 343 f.
Nordic Trend, Canada 107, 343 ff.
Norgai, China 8, 134
Noril'sk (Siberia), Russia 106
North Bohemian Basin, ČSFR 7, 38, 54, 87
North Guangxi, China 134
North Hebei, China 7
North Qilian belt, China 7
North Rim Athabasca district, Canada 137, 138, 151, 152
North Star, USA 238
Northwest Rim Athabasca district, Canada 137, 138
Novazza, Italy 122
Novogodneye (Transbaikal), Russia 122
Novogorny, Russia 8, 114
Novoveská Huta-Muráň, ČSFR 121
Numac, Canada 152
Nuottijärvi, Finland 129

Oberpfalz, Germany 5
Officer Basin, Australia 87, 92, 335
Ogcheon, South Korea 132
O'Hern, USA 312 f.
Ohman, USA 238
Okanagan region, Canada 7, 92, 103
Okelobondo, Gabon 319 f.
Oklo, Gabon 51, 53, 87, 90, 319 ff.
Okrouhlá Radouň, ČSFR 83
Olary, Australia 113
Olden Window, Sweden 36
Old Glory Mine, USA 103
Olší, ČSFR 83
Olympic Dam, Australia 7, 9, 42, 45, 47, 62, 108
Onezhsky, Russia 8, 115
Orange Freestate Goldfield, South Afrika 353 f., 356, 360
Orient, USA 129
Orphan Lode, USA 94, 325, 328, 329, 330, 331
Orranovo-Simitli Basin, Bulgaria 7, 87
Osamu Utsumi, Brazil 120
Oulad Abdoun, Morocco 117

P-2 North (McArthur River), Canada 68, 151
Paganzo Basin, Argentina 87
Paguate Mine, USA 265
Palette, Australia 169
Palheuros de Tolosa, Portugal 233
Palmottu, Finland 115
Pandanus Creek, Australia 35, 91
Panel, Canada 343 f.
Panna Maria, USA 93
Panorama, ČSFR 224
Paradox Valley, USA 5
Paraná Basin, Brazil 7, 35, 38, 87
Pardee, Canada 344
Pecs, Hungary 88
Peña Blanca, Mexico (see Sierra de Peña Blanca)

Pennaran, France 80
Peny, France 202, 203
Phalaborwa (Palabora), South Africa 7, 14, 26, 42, 46, 54, 63, 110, 113
Phantom Lake, USA 106
Pichiñan, Argentina 7, 87
Pierre du Cantal, France 7
Pierres Plantées, France 59, 74, 77, 217
Pigeon, USA 96, 325, 328, 330, 331, 332
Pilanesberg, South Africa 114
Pine Creek Geosyncline, Australia 35, 38, 53, 72, **168ff.**
Pine Nut, USA 96, 325, 331
Pinhal do Souta, Portugal 232
Pitch Mine, USA 83
Plavno, ČSFR 224
Pleutajokk, Sweden 125
Poços de Caldas, Brazil 7, 26, 54, 120, 125
Pöhla Tellerhäuser, Germany 81
Poison Canyon Trend, USA 258, 262
Port Radium, Canada 6, 7, 81
Powder River Basin, USA 52, 93, 290, 291, 292, 298
Prairie Flats, Canada 103
Pribalkhasky, Kazakhstan 8, 35, 121
Příbram, ČSFR 59, 74, 79, **218ff.**
Pronto Mine, Canada 127, 346, 353
Pronto Trend, Canada 343, 347, 348
Pryor Mts., USA 7, 42, 47, 62, 96, 103
Puissagtaq, Greenland 80
Pukuitang, China 8, 134
Pumpkin Buttes, USA 290, 292
Pyatigorsk, Russia 88

Qilian-Qinling, China 7, 8, 35, 87
Quadrilatero Ferrifero, Brazil 7, 37, 106
Quinta do Bispo, Portugal 232
Quinlong-Daxing'anling, China 7, 8, 87, 120
Quirke Mine, Canada 343f., 348
Quirke Lake, Canada 35, 343ff. (see also Elliot Lake)
Quirke Syncline, Canada 343ff.
Quirke Trend, Canada 107, 343ff.

Rabbit Lake, Canada 58, 65, 66, 67, 143, 148, 149, 151, 153, 157, 161, 162
Radium Hill, Australia 6, 7, 42, 126
Ranger, Australia 48, 53, 58, 70, 72, 168, 169, 178, 180, 181, 182, 183, 185, 186, 191
Ranstad, Sweden 8, 29, 38, 42, 45, 46, 54, 64, 131, 132 (see also Billingen)
Raven, Canada 67, 149, 151
Ray Point, USA 306, 311, 312, 314
Razès, France 202
Rebolero, Portugal 232
Red Desert, USA 93, 290
Red Tree, Australia 88
Retail, France 83
Rexspar, Canada 7, 121
Rhodes Ranch, USA 306, 312, 316
Rhodope Mts., Bulgaria 7, 120
Riesengebirge, Poland 81
Riverview, USA 325
Rio Grande Embayment, USA 94
Ritord, France 203
Rockhole, Australia 169
Rodolfo, Argentina 90
Rössing, Namibia 7, 41, 42, 46, 53, 62, 110, 112 366ff.
Ronneburg, Germany 8, 29, 38, 54, 133
Roraima, Guyana-Venezuela, 67
Ross Adams, USA 7, 42, 46, 54, 63, 123, 125, 126 (see also Bokan Mountain)
Rovnost-Eliáš, ČSFR 224
Rožná, ČSFR 83
Ruby Mines, USA 266
Ruijin, China 79
Rum Jungle (Uranium Field), Australia 7, 38, 72, 169, 170, 188
Rychlebské Hory, ČSFR 81

Sabatini, Italy 122
Saima Massif, China 7, 114, 125
Saint Goussoud, France 202
Saint Pierre du Cantal, France 92
Saint Stephan, Great Britain 5
Saint Sylvestre, France 26, 27, 201ff.
Sakami Lake, Canada 106
Sand Wash Basin, USA 290
San Juan Basin, USA 52, 88, 251ff.
San Juan Mts., USA 26
Sankt Joachimsthal (see Jáchymov)
São Francisco Craton, Brazil 36
Saskatchewan, Canada 35, 66, 67, 69, 125, 137ff., 191ff.
San Juan Basin, USA 52
San Rafael Basin, Argentina 87
Saxonian Ore Mountains (see Erzgebirge)
Schlagintweit, Argentina 7, 104
Schmiedeberg (= Kowary), Poland
Schneeberg, Germany 81
Schwartzwalder Mine, USA 47, 59, 74, 75, 77, 82, **237**
Schwarzwald, Germany (see Black Forest)
Seal Lake, Canada 35, 125
Searles Lake, USA 33
Sejita, USA 312
Semizbay, Kazakhstan 7
Senhora das Fontes, Portugal 232, 233
Serra de Jacobina, Brazil 7, 37
Serres Basin, Greece 130
Serro do Corrego, Brazil 106
Sevathur, India 114
Seven Devils, USA 238
Shaba, Zaïre 83, 246
Sherwood, USA 7, 88
Shinkolobwe, Zaïre 6, 7, 54, 59, 74, 75, 83, **246ff.**
Shirley Basin, USA 52, 93, 290, 291, 293, 294f., 296, 298, 299
Shirley Mts., USA 298
Shootering Canyon, USA 281
Sierra de Peña Blanca, Mexico 8, 27, 35, 42, 47, 63, 104, 120, 122
Sierra Pintada, Argentina 7, 54, 87
Silord, France 203
Simitli, Bulgaria 7
Singhbhum belt, India 35, 38
SJ Claims, Namibia 112
Skalka-Obořiště, ČSFR 218
Sleisbeck, Australia 169
Slick Rock, USA 271, 272, 275, 276f.
Slim Buttes, USA 130
Smith Lake, USA 251, 266, 267
Snieznik Klodski (= Glatzer Schneeberg) 81
Sokli, Finland 14, 114
Sokolov Basin, ČSFR 8, 130
Sophie, Canada 153, 155
Sorsele, Sweden 36
South Alligator Valley (Uranium Field), Australia 7, 73, 169, 170, 188
South Duval County Mineral Trend 306, 307, 310, 312, 315, 316
Southeast Athabasca district, Canada 137, 138, 151, 152
Southeast China 7, 8
South Jiangxi-North Guangdong belt, China 7, 8, 120
South Lancang, China 7, 87
South Qinling, China 134
South Terras, Great Britain 5
South Texas, USA 7, 47, 54, 61, 84, 88, 93, 94, 296, 300, **305ff.**
Spanish American, Canada 343f.
Springbok Flats, South Africa 130
Stanleigh, Canada 343f.
Stanrock, Canada 343f.
Stavropol, Russia 7, 88
Stevens County, USA 7, 42, 47, 54, 62, 96, 130
Steward Island, Canada 143, 152
Stilfontein, South Afrika 359
Stockheim, Germany 8, 130
Stráž, ČSFR 87
Streltsovsky (Transbaikal), Russia 8, 36, 121, 122
Stuart Shelf, Australia 35

Superior Structural Province, Canada 36
Svornost, ČSFR 224, 231
Swambo, Zaïre 83, 250
Swanson (Coles Hill), USA 7
Sweetwater, USA 291
Sweetwater Uplift, USA 298

Tallahassee Creek, USA 88
Tarabau, Portugal 232, 233
Tarkait, Niger 88
Tasmurun, Kazakhstan 8
Taybagar, Kazakhstan 8
Tazin belt, Canada 53, 193
Temakskoye, Kazakhstan 8
Tenelles, France 203
Tennessee, USA 132
Tete district, Mozambique 7, 83
Texas Coastal Plains, USA (see South Texas)
Thatcher Soak, Australia 340
Thelon Basin, Canada 35, 67
Tien Shan, CIS 54
Tim Mersoï Basin, Niger 7 (see also Agades Basin)
Todilto Mines, USA 258
Tolosa, Portugal 232
Tonco-Amblayo, Argentina 7, 87
Tono, Japan 7, 35, 92
Tracian Basin, Bulgaria 7, 88
Trancoso, Portugal 232
Trekkopje, Namibia 112
Trutnov, ČSFR 8, 130
Tumas, Namibia 101
Tunling, China 7, 87
Turnercrest, USA 290, 292
Twin Buttes, USA 113
Tyee, Canada 92
Tyuya Muyun, Uzbekistan 6, 7, 15, 103

Uchkuduk, Uzbekistan 88
Union Pacific (pipe), USA 325
Union Pacific Shaft, USA 238
Uranium City, Canada 7, 35, 73, 139, **191ff.** (see also Beaverlodge)
Uravan Mineral Belt, USA 52, 60, 84, 89, 90, **270ff.**
Urgeiriça, Portugal 232

Val Seriana, Italy 122
Vendée, France 27, 54, 79
Vénachat, France 203
Verna, Canada 53, 58, 70, 73, 191, 192, 193, 194, 195, 196, 198
Vikhorevka (Siberia), Russia 8, 83
Vincou, France 214
Virgin No.3 Mine, USA 274, 275, 276f.
Virgin River (Shear Zone), Canada 155
Vishnevogorsk, Russia 8, 114
Vitimsky (Siberia), Russia 8
Vredefort Dome, South Africa 354, 361
Vulsini, Italy 122

Washaki-Sand Wash Basin, USA 290
Way Lake, Canada 153, 155
Webb County, USA 94, 312
Weld County, USA 88, 93
Welkom Goldfield, South Africa 353f., 360, 364
West American Cordillera, Canada-USA 54
West Bear, Canada 151
Western Craton, Canada 31, 154, 155, 193
Westmoreland, Australia 7, 35, 87, 88, 91
West Rand Goldfield, South Africa 353f., 360
West Yunnan, China 7, 35
White Canyon, USA 92, **284ff.**
White King Mine, USA 121
Williston Basin, USA 8, 42, 46, 64, 129, 130, 131
Willyama Block, Australia 51, 126
Windriver Basin, USA 5, 290, 291, 296
Witwatersrand, South Africa 7, 35, 42, 46, 62, 105, 107, **353ff.**
Wittichen, Germany 5, 81
Wollaston belt/domain 147, 153
Wood, USA 238
Wood Mine, Great Britain 5
Woodrow Pipe, USA 259
Wudang-Huaiyong Massif, China 7, 87
Wyoming Basins, USA 7, 42, 47, 54, 61, 84, 88, 92, **290ff.**

Xi'an, China 7, 79
Xiangshan, China 8
Xiazhuang, China 79
Xuefong-Jiuling, China 8

Yarramba, Australia 92
Yeelirrie, Australia 42, 45, 47, 51, 61, 96, 99, 100, 101, 334, 335, 336, 337, 340
Yeniseisky (= Jenissei) (Siberia), Russia 8, 37
Yerington, USA 113
Yilgarn Block, Australia 7, 35, 36, 47, 51, 54, 61, 98, 101, 102, **334ff.**
Yinshan-Liaohe, China 7, 8, 35, 87
Yingtan, China 8
Youssoufia, Morocco 8, 117
Yubileynoye (Transbaikal), Russia 122
Yunnan, China 87
Yurchison Lake, Canada 153

Zadní Chodov, ČSFR 83
Zamzow, USA 311
Zakaspiyisky, Kazakhstan 8
Zauralsky-Chelyebinsk, Russia 8
Zefa, Israel 8, 117
Železne Hory, ČSFR 80
Zheltorechenskoe, Ukraine 127
Zheltye Vody, Ukraine 123
Zhungel-Tianshan, China 7, 8, 35, 87
Zimmer Lake, Canada 155
Zirovski Vrh, Slovenia 7, 88
Zuni Uplift, USA 251, 254, 266

Subject Index

Absorption/adsorption (see Uranium)
Alaskite, alaskitic 24, 42, 44, 46, 62, 110, 111, 112, 366ff.
– uranium content 25, 112, 369
(see also Types of U deposits, -intrusive)
Albitite 31ff., 122, 123, 124, 125
– deposit 123, 125
– uraniferous 32f.
– uranium content 25, 32
(see also Types of U deposits, -metasomatite)
Alteration/metasomatism (for characteristics of deposit types see Types of U deposits)
– albitization 31ff., 48, 63, 66, 68, 70, 73, 76, 78, 80, 88, 111, 125, 126, 139, 154, 194, 197, 206, 212, 226, 255, 264, 353 (see also -Na-metasomatism)
– Al-metasomatism 164
– argillitization 66, 68, 70, 72, 76, 90, 92, 93, 94, 113, 119, 120, 121, 122, 123, 126, 140ff., 206, 233, 255
– Ba-metasomatism 353
– bleaching 61, 91, 93, 95, 121, 133, 140ff., 239, 259, 273, 286, 326f.
– B-metasomatism 70, 72, 164
– calcitization 80, 88, 90, 91, 94, 121, 255, 272, 286, 2993, 326f., 334, 353
– Ca-metasomatism 334, 353
– carbonatization 67, 68, 70, 72, 73, 76, 79, 82, 95, 123, 124, 127, 133, 140ff., 174ff., 194, 197, 219, 226, 240, 334
– chloritization 66, 68, 72, 73, 76, 78, 79, 80, 81, 88, 113, 121, 133, 140ff., 174ff., 194, 197, 206, 213, 219, 226, 233, 247, 255, 264, 353
– decomposition, destruction, corrosion of rock constituents 60, 67, 88, 90, 92, 93, 94, 87, 107, 142ff., 174ff., 227, 240, 255, 264, 272, 286, 293, 295, 307ff., 325ff.
– desilicification 70, 72, 124, 126, 174ff., 194, 206, 213, 326f.
– devitrification 119, 120, 122, 253
– dolomitization 66, 80, 133, 154, 157, 226, 247, 326f., 334, 353
– epidotization 73, 113, 194, 197
– episyenitization 76, 78, 194, 206, 213, 214, 216
– Fe-Mg-metasomatism 127
– greisenization 206, 213, 226
– hematitization 61, 66, 68, 70, 72, 73, 76, 78, 80, 81, 82, 88, 93, 115, 119, 122, 123, 126, 133, 140ff., 174ff., 194, 197, 206, 219, 226, 233, 240, 255, 272, 293, 309, 322 (see also -oxidation)
– illitization 67, 140ff., 174ff., 219
– kaolinitization 88, 120, 121, 140ff., 213, 226, 255 (see also -argillitization)
– K-feldspatization 76, 77, 78, 80, 82, 119, 206, 226, 240, 255, 264
– K-metasomatism 32, 113, 206, 217
– Li-metasomatism 70, 72
– limonitization 88, 93, 255, 259, 293, 309 (see also -oxidation)
– marcasitization 94, 257, 297, 309
– Mg-metasomatism 70, 72, 83, 113, 154, 157, 164, 187, 247, 334, 353
– montmorillonitization 78, 88, 92, 93, 94, 120, 121, 206, 255, 293, 334
– muscovitization 76, 77, 78, 81, 206, 212f., 217, 226
– Na-metasomatism 46, 63, 70, 73, 122, 123, 124, 126, 127, 139, 150, 154, 157, 191ff., 353 (see also -albitization)
– non-pedogenic duricrust related alteration 101, 102, 334ff.
– oxidation 88, 94, 133, 254ff., 272ff., 286ff., 292ff., 307ff.
– phlogopitization 80
– pyritization 68, 78, 80, 90, 94, 121, 206, 226, 255, 272, 293, 308, 337, 326, 345, 362, 365
– reduction 88, 89, 91, 94, 254ff., 272ff., 286ff., 307ff., 324
– sericitization 66, 70, 72, 79, 81, 82, 113, 174ff., 219, 226, 233, 345, 353
– sideritization 68
– sulfidization 67, 70, 88, 95, 106, 133, 140ff., 181, 310, 353
– silicification 67, 68, 70, 72, 73, 76, 78, 79, 88, 94, 95, 119, 120, 121, 122, 127, 133, 140ff., 174ff., 194, 206, 206, 226, 233, 247, 255, 264, 272, 286, 326f., 334, 339, 345
– Si-metasomatism 334
– tourmalinization 67, 70, 140ff., 233
– zeolitization 119, 120, 121
Alteration halo (see Halo)
Alum shale 38, 131, 132, 133
– uranium content 133 (see also Black shale)
Anatectic (environment, processes) 23ff., 36, 38, 41, 42, 45, 48, 53, 54, 71, 72, 73, 110, 111, 138, 136, 371f.
Annular ring (fracture) 94, 327, 328
Apatite 22, 27, 29, 30, 63, 112, 115, 116, 117, 118, 120, 123, 124, 126, 127, 188, 209ff., 236, 346, 356, 358
– uranium content 22, 116, 117
Aquiclude 98
Aquifer/solution conduit 98, 102, 309, 310, 314, 318, 333, 339, 342,
Associated elements, minerals (see Mineral assemblages, Types of U deposits, and Uranium deposits/mineralization)
Atmosphere
– anoxic/oxygen deficient 36, 45, 53, 106, 351
– oxygenated 36, 45, 53, 345, 364
– oxyatmoversion 105, 106, 349
Auto-/selfoxidation 18

Bacteriogenetic (bacterial, biogenic) 21, 86, 99, 187, 269, 289, 302f., 314
Basins
– Aphebian 38
– Cenozoic (Tertiary) 87f., 290ff.
– continental, intermontane, intracratonic 23, 36, 37, 45, 53, 84, 85, 88, 92, 98, 102, 105, 137ff., 252ff., 290ff., 320ff., 337, 353ff.
– Early Proterozoic 36f., 344ff., 353ff.
– epicontinental 132
– euxenic 38
– limnic 129, 130
– Mesozoic 87f., 252ff.
– Middle Proterozoic (Carpentarian, Helikian) 65, 69, 137ff., 169ff., 193ff., 320ff.
– Paleozoic 68, 87f.
– paralic 129, 130
– Precambrian 87f.
Bituminous shale (see Black shale)
Bentonite, bentonitic 30, 86, 88, 92, 93 (see also Tuff)
Black shale 14, 24, 29, 38, 42, 115, 116, 131ff., 133
– bituminous-sapropelic 29, 64, 131, 132

– deposits (see Types of U deposits)
– humic/kolm 29, 64, 131, 132 f.
– uranium content 28, 29, 132, 133
Bog (see Organic material)
Bone, fish bone 8, 117
Breccia(s) (see Shape of deposits, -breccia fill)
Breccia complex deposits (see Types of U deposits)
Breccia pipe (see Types of U deposits, -collapse breccia pipe)

Calcrete (deposits) (see Types of U deposits, -surficial duricrusted sediments)
Carbonaceous (see Organic material, and Sandstone)
Carbonatite 14, 23, 26, 42, 44, 46, 63, 110, 113 f.
– uranium content 25, 26, 114
(see also Types of U deposits, -intrusive)
Channel, paleochannel (fluvial) 60, 84, 85, 89, 90, 91, 92, 94, 87, 98, 99, 101, 105, 106, 263, 270 ff., 284 ff., 291, 307 ff., 322 f., 335 ff., 347, 355 ff.
Classes of uranium deposits 58 ff. (see also Types of U deposits, -subtypes)
Classification of uranium deposits 57, 58 ff. (see also Types of U deposits)
Climate (see Uranium)
Closed system 23, 30, 45 f., 54, 71, 111, 128
Coal (see Organic material)
Collapse breccia pipe deposits (see Types of U deposits)
Complexing agents/elements (see Uranium)
Conglomerate, oligomictic, Proterozoic (see Types of U deposits, -quartz-pebble conglomerate)
Contact-metamorphic 43, 59, 74, 75, 81, 223, 225, 232 ff., 352, 367
Copper porphyry 42, 46, 63, 110

Deuteric 76, 208, 371
Diabase/dolerite 65, 70, 73, 139, 154, 156, 162, 164, 166, 170, 174, 184, 185, 190, 193, 197, 199, 219, 220, 321, 345, 346, 350, 367
Diagenesis, diagenetic 66, 71, 139, 254, 256, 265, 269, 280, 283, 292, 295, 307, 317, 350, 352, 355, 356, 363 (see also Hydrogenic)
Disequilibrium (radioactive) 297, 310
Duricrust, duricrusted
– nonpedogenic 42, 47, 61, 96, 98, 101, 334 ff.
– – calcrete (groundwater-, valley-) 42, 97, 98, 101, 102, 334 ff.
– – dolocrete 97, 98, 102, 334 ff.
– – gypcrete 97, 98, 101, 334 ff.
– – silcrete 97, 98, 101, 334 ff.
– pedogenic 62, 96, 100, 103, 334
– – calcrete 97, 103
– – ferricrete 97, 103
– – gypcrete 97, 103
– – laterite 97, 103
– uranium content 30, 101, 336

Effusive/extrusive rocks (see Uranium content)
Elements, associated with uranium mineralization (see Types of U deposits, and Uranium deposits/mineralization)
Endogenic/endogenetic 21, 42
Epigenetic deposits (see Uranium deposits)
Episyenite 59, 74, 75, 78, 202, 206 ff., 213 f. (see also Alteration)
Eugeosynclinal 70, 72, 73, 344
Evaporation 99, 341 f.
Evaporite, evaporitic, evaporative 97, 138, 139, 162, 166, 185, 189, 190, 281, 282, 283, 330, 334, 336 ff., 372
Exogenic/exogenetic 42, 44
Extrinsic/introduced elements 84, 85, 87, 88, 93, 94, 251, 264, 310

Faults, lineaments, structures (see Types of U deposits, -host environments)
Fluid inclusions (see Types of U deposits)
Fossil bone, wood, plant debris (see Organic material)

Gangue minerals (see Mineral assemblages, and Types of U deposits, -mineralogy)
Gas (natural) 86, 92, 94, 304, 307, 309
Geochemistry (see Uranium)
Geochronological (age) data
– Alligator Rivers/Pine Creek Geosyncline 178, 184 ff.
– Arizona Strip area 328, 333
– Athabasca Basin region 152, 154, 155 f.
– Blind River-Elliot Lake 349, 352
– Colorado Plateau (U-V Saltwash deposits) 271
– Franceville Basin 320, 322
– Grants Uranium Region 255, 260, 265, 267
– Iberian Meseta 233, 237
– Joachimsthal/Jáchymov district 225 f., 228
– Limousin/La Crouzille district 216
– Monument Valley-White Canyon 286
– Příbram district 219, 222
– Rössing 367, 371
– Schwartzwalder Mine 242, 243, 244
– Shinkolobwe 249, 250
– South Texas Coastal Plain 307
– Uranium City region/Beaverlodge 193, 197
– Witwatersrand 355, 360, 365
– Wyoming Basins 297, 298
Glass, glassy
– exoterrestrial 34
– volcanic 24, 28, 119, 120, 267
Grade (of uranium deposits) 3
– deposit types 9, 58 ff.
– payability 18
(see also Types of U deposits)
Granite
– albite-riebekite 26
– alkali 25, 26, 27, 108, 123, 126, 368
– calc-alkaline 26, 209, 236
– leucocratic 25, 27, 78, 80, 209, 226, 235 f., 367
– metasomatized 27, 123 ff.
– peraluminous (leucocratic, two-mica) 23, 27, 28, 59, 74, 76, 78, 111, 201 ff., 208 ff.
– subalkaline 209
– uranium content 24, 25, 26, 27, 32, 108, 209 ff., 226, 235, 298, 337, 361, 367
Graphite, graphitic 30, 31, 58, 65, 68, 72, 73, 80, 127, 138, 142, 146, 149, 154, 156, 157, 165, 178, 181, 193
Groundwater (see Hydrogenic, -supergene)
Groundwater table 97, 100, 101, 104, 120, 208, 269, 272, 286, 298, 336, 338 f.
Growth faults 307 ff.
Guano 12, 117

Halo/aureole
– contact-metamorphic 80, 81, 111, 225, 233, 367
– wall rock alteration 67, 68, 70, 72, 73, 76, 78, 79, 80, 82, 95, 120, 133, 141 ff., 175, , 187, 189, 197, 206, 220, 225, 229, 233, 240 f., 256 f., 259, 260, 273, 286, 292 ff., 307 ff., 327, 365
Host environments, -rocks (see Types of U deposits)
Humate, humic (see Organic material)
Hydrocarbon(s) 29, 85, 93, 94, 99, 100, 156, 216, 217, 307, 312, 317, 327, 333, 346, 350, 359
Hydrogen sulfide 29, 61, 85, 86, 93, 94, 99, 100, 181, 216, 217, 245, 266, 269, 289, 302 ff., 305, 309, 312 ff., 333

Hydrogenic/hydrothermal solutions/systems (see also Types of U deposits, -metallogenesis, and Uranium, -hydrochemistry)
– brines 33, 164, 180, 189, 190, 250, 281 ff., 333, 342
– connate 77, 215, 244, 317, 333
– convective 236, 250
– diagenetic 44, 46, 48, 53, 66, 86, 140, 154, 156, 161 f., 190, 256, 265 ff. (see also Diagenesis)
– hypogene 18, 42, 47, 48, 120, 162, 212, 217, 237
– hypogene convective 47, 77, 191, 215, 244 f.
– lateral-secretionary 77, 236
– magmatic 23, 250, 371
– metamorphic 23, 44, 45, 46, 48, 53, 71, 124, 185, 198 ff.
– metasomatic 46, 71, 124, 353
– mixed connate-meteoric 77
– springs (thermal) 33, 298
– supergene, meteoric water, groundwater 33, 38, 45, 47, 86 f., 97 ff., 100, 101, 104, 120, 130, 134, 162, 183, 185, 188, 190, 200, 208, 212, 213, 215 ff., 237, 245, 262, 266 ff., 280 ff., 289, 300 ff., 314 f., 333, 339, 341 ff.
– volcanic 45, 47, 120

Igneous rocks (see Uranium contents)
Impermeable, impervious 292, 298 (see also Permeability)
Intergranular, interstitial (see Uranium)
Intrusive deposits (see Types of U deposits)
Intrusive rocks (see below, and Uranium contents)
Intrusive granitic, magmatic, anatectic units/complexes
– Achala batholith 7, 104
– Aïr Massif 35, 51
– Algoman granite 344
– Bokan Mountain granite 126
– Boulder Creek granodiorite 243
– Central Bohemian pluton 79, 218 ff.
– Conway/White Mountain granite 26
– Damara granites, alaskites 367
– Eibenstock Massif 80, 225
– Erzgebirgsgranit 225 f.
– Gebirgsgranit 225 f.
– Grandrieu granite 213, 215
– Granite Mountains 27, 51, 290
– Guérande granite 213, 215
– Jiangxi granite belt 7
– Jos Plateau 26
– Kaapvaal Craton, Witwaterrand region granite domes 354
– Karlovy Vary (= Eibenstock) Massif
– Longshoushan belts 7
– Massif de Chaillu 35, 51, 320, 321, 323
– Mogollon Highland 89
– Mortagne Massif 27
– Mount Painter Block 51
– Nanambuh Complex 169, 170, 174, 1178, 183, 185, 191
– Nanling granite belt 7
– Nimbuwah Complex 169, 170, 173, 185
– Nisa-Tolosa-Castelo de Vide batholith 236
– Phillips Lake granodiorite 100, 102
– Rössing alaskite 367 ff.
– Rum Jungle Complex 169, 170
– Saima Massif 7, 114, 125
– Saint Sylvestre granite massif 26, 27, **201 ff.**
– São Pedro do Sul pluton 235
– Silver Plume granite 243
– Waterhouse Complex 169, 170
– Willyama Block 51, 126
– Yangzi granite belt 7
Isotopes (see Types of U deposits, and Uranium)

Karst (cavern) 47, 62, 94, 96, 97, 98, 100, 103, 331, 335
Kolm (see Organic material)

Lacustrine (see Sediments)
Lagoon, lagoonal (see Sediments)
Lamprophyre 76, 78, 79, 80, 111, 134, 206, 208, 212, 215, 216, 217
– uranium content 25
Land plant evolution (see Uranium)
Laterite, lateritic 97, 103, 163
– uranium content 28, 30, 163
Lignite (see Organic material, and Types of U deposits)
Lineaments (see Types of U deposits, -host environments)
Lujavrite 26, 27, 115
– uranium content 26, 27

Magmatic (igneous) environment, processes 20, 21, 23 ff., 36, 38, 41, 42, 48, 54, 110, 125, 208 ff., 225 f., 371 f.
Magmatic differentiation 25, 111, 208 ff.
Marine life forms/evolution (Proterozoic) (see Uranium)
Mega-channel 93, 307 ff.
Metallogenesis (see Types of U deposits)
Metamict minerals 22, 23, 212
Metamorphic environment 20, 21, 30 f., 45 f., 127 ff., 163, 198 ff., 225, 233, 238 f., 367
– amphibolite grade 2, 30, 31, 45, 53, 66, 69, 70, 71, 72, 82, 123, 138, 154, 170, 185, 193, 238, 367
– epi-, mesozonal/low, medium grade 2, 30, 45, 345, 355, 356, 363
– granulite grade 31, 53, 66, 70, 71, 72, 138, 154, 193
– greenschist grade 45, 69, 70, 105, 127, 138, 154, 170, 184, 193, 223, 233, 364
– ultrametamorphic grade 111, 124
Metasomatic environment, processes 31 ff., 45, 48, 122 ff., 353
Metasomatic alteration (see Alteration, and Types of U deposits)
Metasomatite deposits (see Types of U deposits)
Methane 92, 93, 94, 269
Migmatite, migmatitic, migmatization 32, 66, 69, 70, 71, 72, 73, 112, 138, 150, 154, 185, 196, 370
Mineral assemblages (ore, gangue, associated minerals)
– Alligator Rivers/Pine Creek Geosyncline 177 ff.
– Arizona Strip area 328 ff.
– Athabasca Basin region 141 ff.
– Blind River-Elliot Lake 346 ff.
– Colorado Plateau (U-V Saltwash deposits) 272 ff.
– Franceville Basin 321 ff.
– Grants Uranium Region 257 ff.
– Iberian Meseta 233 ff.
– Joachimsthal/Jáchymov district 226 ff.
– Limousin/La Crouzille district 206 ff.
– Monument Valley-White Canyon 286 ff.
– Příbram district 220 ff.
– Rössing 368 ff.
– Schwartzwalder Mine 241 ff.
– Shinkolobwe 248 ff.
– South Texas Coastal Plain 309 ff.
– Uranium City region/Beaverlodge 194 ff.
– Witwatersrand 355 ff.
– Wyoming Basins 292 ff.
– Yilgarn Block 335 ff.
(see also Types of U deposits, -mineralogy)
Mining dilution 14
Miogeosynclinal 138
Monazite 22, 29, 107, 112, 114, 123, 126, 209 ff., 236, 351, 356, 358, 368
– uranium content 22, 211
Monometallic (see Uranium deposits/mineralization)

Nasturan 18
Natural nuclear reactors 321 f.

Oil 307 (see also Petroleum)
Open system 23, 48, 54, 71

Ore and associated elements, minerals (see Mineral assemblages, Types of U deposits, and Uranium deposits/mineralization, -ore composition)
Ore controls (see Types of U deposits)
Organic material
– bitumen, bituminous 34, 65, 67, 131, 132, 156, 159, 166, 222, 328
– bog, marshes, muskeg, paludal, peat, swamp 29, 34, 42, 47, 62, 96, 98, 102, 129, 130
– bones, fish bones (fossil, phosphatic) 8, 28, 117
– carbonaceous 29, 30, 37, 38, 60, 61, 69, 71, 83, 85, 92, 98, 99, 108, 116, 117, 122, 127, 130, 131, 133, 138, 188, 193, 234, 236, 246, 251 ff., 272 ff., 286 ff., 307 ff., 359, 365
– coal, coaly, coalified 29, 34, 86, 129, 130, 131, 293
– humate, humic 29, 30, 60, 85, 88, 89, 99, 129, 130, 131, 132, 250 ff., 264, 265 ff., 279, 289, 291
– kerogen 346, 350, 356, 363, 364
– kolm 64, 131, 132, 133
– lignite 29, 34, 42, 44, 46, 129 ff., 307, 308
– marine microorganisms (algae, lichens, Proterozoic) 36, 37, 38, 84, 86, 90, 132, 319 ff., 346, 364
– organic (not differentiated) 21, 28, 30, 34, 53, 87, 89, 95, 98, 100, 131, 133, 160, 162, 165, 181 ff., 187, 320 ff.
– plant, detrital carbon, vegetal debris/trash 29, 34, 36, 37, 38, 54, 60, 61, 84, 85, 86, 87, 89, 90, 91, 93, 97, 102, 129, 130, 132, 253 ff., 271 ff., 286 ff., 291 ff., 307, 312, 314, 317
– tree logs/trunks 89, 90, 91, 286, 291
Orogenies, orogenic -belts, -zones
– Alpidic 54, 230, 237
– Appalachian 54
– Blezardian 163, 345
– Brazilian 53
– Caledonian 54
– Central Iberian Zone 233 ff.
– Damara 53, 98, 112, 366
– Damara, Central Zone 366 ff.
– Elsonian 54
– Grenville 115, 166
– Hercynian (= Variscan) 38, 49, 54, 76, 77, 134, 201 ff., 225 ff., 232 ff.
– Hudsonian 53, 67, 74, 139, 163, 193, 199, 200
– Katanga 53, 246 ff.
– Laramide 49, 54, 77, 82, 88, 244, 253, 265
– Lufilian 83, 246 ff., 367
– Moldanubian Zone 201 ff., 218 ff., 228, 233
– Pan African 53, 54, 112
– Saxo-Thuringian Zone 225 ff.
Oxidized deposits (see Uranium deposits/mineralization)

Paragenetic mineral assemblages (see Types of U deposits, -mineralogy)
Peat (see Organic material)
Pechblende (= pitchblende) 5
Pegmatite, pegmatitic 23, 25, 26, 42, 44, 46, 63, 66, 73, 76, 78, 79, 80, 111, 114 f., 138, 139, 150, 179, 193, 196, 200, 201, 212, 226, 238, 360, 368, 371
– uranium content 25, 115
Peralkaline (nepheline) syenite 8, 24, 42, 46, 53, 63, 111, 114
– uranium content 25, 114
Permeabiliy, transmissivity 85, 86, 94, 130, 212, 245, 267, 278 f., 288, 294, 298, 299, 310, 314 f., 317, 330, 342
Petroleum 85, 94
Phosphorite, phosphate
– continental 30, 42
– deposits (see Types of U deposits)
– marine 14, 28, 30, 42, 44, 46, 63, 115 ff.
– residual 117
– phosphatic bones, fish bones 8, 117
– phosphorous dolomite 8
– uranium content 14, 28, 30, 116, 117, 140
Pitchblende 2 f., 5, 18, 20, 22, 23, 29, 30, 48 (for occurrence in deposits see Types of deposits, -mineralogy)
Placer, paleoplacer deposits
– alluvial/fluvial 23, 29, 42, 45, 345 ff., 355 ff.
– fossil (= Paleoplacer) 345 ff., 355 ff.
– littoral/beach 23
– modified 105, 106, 350, 363
– uranium content 29, 107, 348, 353, 359 f.
Playa (see Sediments)
Pneumatolytic 26
Polygenetic, polyphase, polymetallic (see Uranium deposits/mineralization)
Potassium
– in uranium bearing rocks 24
– in uraniferous minerals 22
Precipitation (deposition) of uranium (see Uranium)
Province, uranium 34 ff.
Pyroclastic rocks (see Uranium contents, -volcanic rocks)

Quartz-bostonite 25, 26
– uranium content 25, 26
Quartz-monzonite 24, 42, 46, 110, 112 f.
– uranium content 24, 113
Quartz-pebble conglomerate deposits (see Types of U deposits)

Radium 15
Recognition criteria (see Types of U deposits)
Red bed environment, rocks 37, 58, 60, 65, 66, 67, 138, 162, 164, 193, 238
Redox conditions, reduction-oxidation interfaces 21, 45, 54, 61, 68, 87, 93, 99, 167, 188, 231, 265, 266, 268, 272, 279, 280, 292 ff., 300 ff., 315 ff., 341
Reducing agents (see Uranium)
Regolith (paleosol) 3, 44, 67, 99, 139 ff., 163 ff., 238
Reserves/Resources (of uranium)
– byproduct 9, 13, 14
– contained cumulatively in deposit types 9
– conventional 13 f.
– coproduct 9, 13
– cost categories 11, 13, 14
– definitions, categories 3, 12 f.
– deposit types (see Types of U deposits)
– estimated additional (EAR) 12
– former Eastern Block countries 10, 14
– geochronologic-stratigraphic distribution 50 f.
– reasonably assured (RAR) 12
– recoverable 13
– unconventional 14 f.
– WOCA 10, 11, 14
– world distribution 10 f.
Resistate/refractory uraniferous minerals 23, 28, 29, 30, 111, 114 (see also Uranium deposits/mineralization, -detrital)
Rhyolite, rhyolitic 54, 63, 98, 100, 104, 119, 120, 121, 122, 128, 129, 130, 298
– uranium content 24, 25, 26, 27
Rollfront, roll-type (see Uranium deposits/mineralization)

Sabkha 190
Salt domes/diapirs 89, 94, 310
Sand/Sandstone (arkose, arkosic, feldsphathic)
– carbonaceous (organic bearing) 85, 92, 253 ff., 271 ff., 284 ff., 291 ff., 307 ff., 320 ff.
– continental, fluvial-alluvial 42, 59 ff., 65, 72, 73, 84, 85, 86, 88, 89, 91, 92, 253 ff., 271 ff., 284 ff., 290 ff., 320 ff., 334 ff.
– deposits (see Types of U deposits)

– marginal marine, fluvial, littoral 61, 84, 93, 105, 306ff.
– permeability, transmissivity 85, 86, 267, 278f., 288, 294, 298, 299, 310, 314f., 317
– Proterozoic 58, 59, 65, 69, 84, 86, 320ff.
– red bed 58, 65, 65, 66, 67, 138, 164, 187
– sandstone/mudsone (shale) ratio 60, 88, 92, 264, 272, 315
– tuffaceous, tuff/acid volcanic interbeds 24, 59, 253ff., 272, 286, 291, 298, 307f.
– uranium content 24, 28, 164, 254
Saprolite, saprolitic 3, 187 (see also Regolith)
Sediments, sedimentary environments 23, 28ff., 42, 45, 84ff., 105ff.
– continental 42, 65, 70, 138f., 253ff., 271ff., 290ff., 320ff., 354ff.
– delta, fluvial 97, 106, 108, 345ff., 354ff.
– delta, chemical 336, 338, 340
– epicontinental 131ff.
– eugeosynclinal 70, 72, 73, 344
– fluvial, alluvial 84ff., 97, 101, 105, 106, 253ff., 271ff., 284ff., 290ff., 307, 334ff., 345ff., 354ff.
– lacustrine 47, 60, 62, 67, 70, 72, 73, 96, 97, 121, 122, 165, 337, 341
– lagoonal 138, 162, 166
– limnic 130
– marginal marine 61, 84, 93, 105, 306ff.
– marine 42, 115ff.
– marine, continental shelf margin 115ff.
– miogeosynclinal 138
– paralic 130
– playa 47, 62, 96, 99, 102, 253, 254, 256, 334ff.
– shallow marine near-shore platform 115ff.
– volcanogenic 119, 121, 122
Shape of ore bodies/shoots, style of uranium (mineral) distribution 58ff.
– accretionary 79, 299
– breccia fill 58, 61, 67, 72, 73, 78, 80, 83, 94f., 108f., 121, 157, 178ff., 194, 206, 248, 259, 327f.
– coatings 89, 90, 92, 93, 101, 102, 103, 120, 122, 141ff., 178ff., 257ff., 292ff., 335
– clusters 220ff., 225ff., 274, 279, 310, 369
– disseminated, dispersed, impregnated 23, 31, 60, 61, 62, 63, 64, 67, 68, 70, 73, 74, 77, 78, 81, 89, 90, 95, 101, 102, 103, 105, 107, 109, 112, 113, 114, 115, 117, 118, 119, 120, 121, 122, 123, 126, 127, 128, 133, 141ff., 182, 194, 206, 233, 248, 257ff., 286, 293f., 309, 318, 328, 335, 346, 359, 368f.
– fracture, fissure fill, stringers, veinlets 58, 63, 64, 67, 68, 70, 73, 74, 79, 81, 92, 95, 96, 97, 100, 103, 104, 112, 120, 121, 122, 123, 126, 133, 141ff., 178ff., 184, 194, 230, 233, 241, 248, 251, 286, 327f., 335
– horsetail 82, 223, 229, 239ff.
– intergranular, interstitial 22, 28, 257, 368
– lense, lenticular 60, 63, 78, 79, 89, 92, 101, 127, 128, 223, 257ff., 274, 286
– linear (vein) 59, 72, 73, 74, 78, 79, 80, 82, 83, 121, 194ff., 204ff., 221ff., 225ff., 240ff.
– massive 67, 68, 70, 73, 141ff., 182, 194, 248
– pipe-like 59, 68, 70, 78, 120, 206, 259, 327f.
– pocket, pod 63, 79, 90, 92, 104, 111, 115, 128, 142ff., 223, 274, 278, 286, 328
– reef, seam, sheet (conglomerate) 347ff., 356ff.
– stockwork 42, 58, 59, 72, 73, 74, 78, 83, 133, 246ff.
– strata-transgressive 108, 109
– tabular, blanket, trend 47, 58, 60, 85, 89, 90, 91, 94, 251ff., 270ff., 285
Soil 30 (see also Duricrust, -pedogenic)
Stable isotopes (see Types of U deposits)
Strata controlled – structure-bound deposits (see Types of U deposits)
Stratigraphy
– Alligator Rivers/Pine Creek Geosyncline 170ff.
– Arizona Strip area 325f.
– Athabasca Basin region 139, 140
– Blind River-Elliot Lake 344f.
– Colorado Plateau (U-V Saltwash deposits) 271, 282
– Franceville Basin 320
– Grants Uranium Region 252ff.
– Iberian Meseta 232f.
– Joachimsthal/Jáchymov district 225
– Monument Valley-White Canyon 285f.
– Příbram district 218f.
– Rössing 367f.
– Schwartzwalder Mine 239
– Shinkolobwe 246f.
– South Texas Coastal Plain 306ff.
– Uranium City region/Beaverlodge 193
– Witwatersrand 354f.
– Wyoming Basins 291
Stratigraphic units (Cgl = Conglomerate, Fm = Formation, Gp = Group, Ls = Limestone, Mbr = Member, Sh = Shale, Ss = Sandstone)
– Abbabis Complex 368, 371
– Aillik Gp 38
– Amer Lake Gp 38
– Athabasca Gp 137, 139, **140,** 145, 151, 156, 160, 162, 164, 166, 168, 199
– Aurora Lava 27
– Barbora Series 225ff.
– Basal/Steyn Reef 359, 360
– Battle Springs Fm 291ff.
– Bird Reef Stage 107, 360
– Black Reef 359
– Bone Valley Fm 116, 118
– Bruce Gp 344, 345
– Brushy Basin Mbr 252ff., 271ff.
– Cahill Fm 170, 174, 178, 181, 185, 186, 190
– Carbon Leader Reef/Fm 359, 361, 362
– Carrizo Sand 314
– Catahoula Fm 306ff.
– Central Rand Gp 354ff.
– Chattanooga Shale 38, 132
– Chinle Fm 91, 285ff., 325, 326, 329, 330, 332, 333f.
– Chontes Fm 27
– Clu ff. Breccias 156
– Cobalt Gp 344
– Coconino Ss 325ff.
– Cow Springs Ss 252
– Cutler Fm 285
– Dakota Ss 252, 253, 258
– Damara Sequence 368ff.
– Deweesville Ss 308
– Dilworth Ss 308
– Dominion Gp (Lower, Upper Reef) 354ff.
– Donaldson Lake Gneiss 155, 192, 193
– Earl River Complex 155, 157
– Edith River Volcanics 170, 185
– Edwards Ls/Fm 314, 317
– Elliot Lake Gp 344ff.
– Elsburg Quartzite Fm 360
– El Sherana Gp 170, 172
– Escuadra Fm 27
– Esplanade Ss 325ff.
– Etusis Fm 267ff.
– Fant Tuff 308
– Fay Complex 155, 193, 200
– Finniss River Gp 170, 173
– Foot Bay Gneiss 155, 192, 193
– Fort Union Fm 291
– Franceville Sequence (FA, FB etc) 320ff.

– Frio Clay/Fm 308
– Gassaway Mbr 132
– Goliad Fm 306ff.
– Government Subgroup 359
– Grand Conglomerate System 246, 247
– Graptolitenschiefer (Graptolite Sh) 29, 133, 134
– Gueydan Fm 308
– Hermit Sh/Fm 325ff.
– Hidden Bay Assemblage 139
– Hough Lake Gp 344
– Huronian Supergroup 344
– Hurwitz Gp 38
– Idaho Springs Fm (equivalent to) 238ff.
– Inyan Kara Gp
– Jáchymov Series 225ff.
– Jackpile Ss 252, 265
– Jackson Gp 306ff.
– Jatulian Gp 38
– Johannesburg Subgroup 359, 361
– Kaibab Ls 325ff.
– Kakadu Gp 170, 174, 185
– Karibib Fm 368, 370
– Katanga Gp 246
– Katherine River Gp 170, 172, 174
– Khan Fm 367ff.
– Khoman Subgroup 368
– Kibara Gp 246
– Kimberley Conglomerate Fm 360
– Kombolgie Fm 170, 174, 176, 179, 180, 184, 186, 187, 188, 190, 191
– "K"Shale 252, 263
– Kundelungu System 246, 247
– Kupferschiefer (Copper Sh) 28, 42
– La Mesa Fm 27
– Lederschiefer (Leather Sh) 133
– Lissie Fm 307, 308, 310
– Madison Ls 100, 103
– Main Conglomerate Fm 360
– Main Reef 360
– Mancos Sh 28, 252, 253, 258
– Manfred Mbr 345, 347
– Manitou Falls Fm 140, 156, 166, 168
– Martin Fm 138, 156, 192, 193, 194, 195, 196, 197, 199
– Matinenda Fm 344ff.
– Mead Peak Phosphatic Shale Mbr 117
– Meta-Arkosic Unit 139
– Meta-Pelitic Unit 139
– Mica Schist Fm 225ff.
– Mines Series 54, 146ff.
– Mississagi Fm, Lower (now Matinenda Fm) 344, 345
– Moenkopi Fm 91, 285ff., 325, 326, 327, 330
– Monitor Butte Mbr 285f.
– Morrison Fm 88, 89, 252ff., 271ff., 329
– Moss Back Mbr 285f.
– Mount Partridge Gp 170, 173
– Mozaan Gp 365
– Murmac Bay Gp 155, 192, 193
– Mwashya Series 246, 247
– Myra Falls Metamorphics 170, 172, 178
– Namuna Gp 170, 173
– Nippissing Diabase 345, 346, 352
– Nopal Fm 27
– North Park Fm
– Nourlangie Schist 170, 172, 185
– Nosib Gp 368, 371, 372
– Nullagine Cgl 37
– Oakville Ss/Fm 306ff.
– Ockerkalk 133
– Oenpelli Dolerite 170, 172, 183, 185, 188
– Olympic Dam Fm 108
– Palimba Cgl 37
– Paradox Fm 281
– Peña Blanca Fm 27
– Peter River Series 154, 155, 163
– Petit Conglomerate System 247
– Phosphoria Fm 116, 117
– Poison Canyon Ss 252ff.
– Quirke Lake Gp 344
– Recapture Mbr 252
– Redwall Ls 325ff.
– Roan Gp 246, 247
– Rössing Fm 367ff.
– Ryan Mbr 345, 348
– Salt Wash Mbr 89
– San Rafael Gp 252
– Schist-greywacke Complex 81, 232ff.
– Série des Mines (= Mines Series) 54, 146ff.
– Shale-Dolomite System 146
– Shinarump Mbr 91, 284ff., 325, 332
– Soledad Cgl 308
– South Alligator Gp 170, 173
– Spilite Series 218ff.
– Stinson Mbr 345
– Summerville Fm (now Beclabito Mbr) 252, 282
– Supai Fm 325ff.
– Swakop Gp 368ff.
– Swaziland Supergroup 355
– Tazin Gp 155, 192, 193, 194, 195, 196, 197, 199
– Tentaculitenschiefer (Tentaculite Sh) 134
– Tidwell Mbr 271, 281ff.
– Todilto Limestone Mbr 252, 258
– Tordilla Ss 308, 315
– Toroweap Fm 326, 327, 328, 330, 331
– Transvaal Sequence 355, 359
– Ugap Subgroup 368
– Vaal Reef 359
– Ventersdorp Contact Reef 359
– Ventersdorp Supergroup 355, 359
– Wanaka Fm 252
– Wasatch Fm 291ff.
– West Rand Gp 354ff.
– Westwater Canyon Mbr 88, 252ff.
– White River Fm 298, 300, 304
– Whitsett Fm 308
– Wilcox Gp 310
– Wind River Fm 291ff.
– Witwatersrand Supergroup 355ff.
– Witwatersrand System, Upper (now Central Rand Group/Witwatersrand Supergroup) 107
– Wollaston Gp 154, 155, 163
– Wolverine Point Fm 140, 156
– Zamu Dolerite 170, 173, 185
Structures, faults, lineaments (see Types of U deposits, -host environments)
Subtypes of uranium deposits 58ff. (see also Types of U deposits)
Subunconformity (see Types of U deposits)
Supergene (see Hydrogenic, and Uranium deposits/mineralization)
Surficial
– deposits (see Types of U deposits)
– environment 29, 96ff., 334ff.
Syngenetic (see Uranium deposits/mineralization)
Synmetamorphic deposits (see Types of U deposits)

Thorium (in uraniferous rocks and minerals)
– alaskite 370
– carbonatite 113
– intrusive rocks 24, 111
– Lower Proterozoic quartz-pebble conglomerate 105, 107, 346ff., 355ff.
– metamorphic rocks 24
– metasomatite 123f.
– pegmatite 115
– peralkaline syenite 24, 114
– leucogranite 209ff.
– sedimentary rocks 24
– uranium bearing minerals 19, 22, 111, 112, 114, 115, 122, 123, 124.126, 209ff., 346, 356
– volcanic rocks 121
Transmissivity (see Permeability)
Tuff, tuffaceous units 27, 30, 59, 61, 85, 86, 89, 92, 93, 121, 122, 129, 264, 266, 267, 278, 280, 288, 298, 307, 314, 320
Types (of uranium deposits) (bold type in headings refers to sections in Chap. 4 and 5, and in

subheadings to principal descriptions in Chap. 5)
– black shale 8, 42, 44, 64, **131 ff.**
– – age/geochronologic distribution 54, 132
– – alteration 132
– – associated elements, minerals 132, 133
– – definition 131
– – dimensions 132, 133
– – examples 8, 131, 132
– – geographic distribution 6, 8
– – grades 132, 133
– – host environments, -rocks 46, 131, 132
– – metallogenesis/mode of origin 42, 45, 46, 132
– – mineralogy/mineralization 131, 132, 133 (see also Uranium deposits/mineralization)
– – recognition criteria 64, 131 f.
– – resources 132, 133
– – subtypes
bituminous/sapropelic 64, 131, **132**
humic/kolm in alum shale 64, 131, **132 f.**
– breccia complex 7, 42, 44, 62, **108 ff.**
– – age/geochronologic distribution 49, 110
– – alteration 108 f.
– – associated elements, minerals 109
– – definition 108
– – dimensions 110
– – examples 7
– – geographic distribution 6, 7
– – grades 110
– – host environments, -rocks 47, 108
– – metallogenesis/mode of origin 42, 45, 47, 110
– – mineralogy/mineralization 109
– – recognition criteria 62, 108 f.
– – resources 110
– – sources of uranium 110
– – structures 108
– collapse breccia pipe 7, 42, 44, 61, **94 ff., 324 ff.**
– – age/geochronologic distribution 49, 95, 328, 333
– – alteration 95, **326 f.,** 330
– – alteration halo 95, **327**
– – associated elements, minerals 95, 324, **328,** 329
– – definition 94
– – dimensions 96, 325, 327, 328
– – examples 7, 94, 96
– – fluid inclusions 329, 333
– – formational temperatures 329, 333
– – geographic distribution **6,** 7, 325
– – grades 96, **324**
– – host environments, -rocks 47, 94, **324 ff.,** 330, 331 f.
– – metallogenesis/mode of origin 42, 47, 48, 95, **331 ff.**
– – mineralogy/mineralization 95, **328 f.**
– – recognition criteria, ore controls 61, 94 f., **329 ff.**
– – resources (including production) 96, **324**
– – sources of uranium 329, 333 f.
– – stable isotopes 328, 333
– – structures 96, 325
– intrusive 7, 42, 44, 55, 62 f., **110 ff., 366 ff.**
– – age/geochronologic distribution 49, 53, 54, 111, 112, 113, 114, 115, 367, 371
– – alteration/metasomatism 111, 113, 115
– – alteration halo (contact-metamorphic) 111
– – associated elements, minerals 111, 113, 114, 368
– – definition 110
– – dimensions 112, 113, 114, 115, **369**
– – examples 7, 110, 112, 113, 114, 115, 196
– – fluid inclusions 371
– – formational temperatures 372
– – geographic distribution 6, 7
– – grades 112, 113, 114, 115, 366, **369**
– – host environments, -rocks 46, 111, 112, 113, 114, **366 ff.**
– – metallogenesis/mode of origin 41, 42, 46, 111 f., **371 ff.**
– – mineralogy/mineralization 111, 112, 113, 114, 115, **368 ff.**
– – recognition criteria, ore controls 62 f., 111, **369 ff.**
– – resources (including production) 112, 113, 114, 115, **366**
– – sources of uranium 112, 371, 372
– – structures 113, 115, 367, 370
– – subtypes
alaskite 53, 62, 110, **112**
carbonatite 54, 63, 110, **113**
pegmatite 53, 63, 110, 111, **114 f.**
peralkaline syenite 53, 63, 110, 111, **114**
quartz-monzonite 63, 110, **112**
– lignite 8, 42, 44, 64, **129 ff.**
– – age/geochronologic distribution 129 f.
– – associated elements, minerals 130, 132
– – definition 129
– – dimensions 130
– – examples 8, 130
– – host environments, -rocks 46, 129, 130, 131
– – geographic distribution 6, 8
– – grades 130, 131
– – metallogenesis/mode of origin 42, 46, 130
– – mineralogy/mineralization 129, 130, 131
– – recognition criteria 64, 129 f.
– – resources 130
– – sources of uranium 129, 130
– – structures 130
– – subtypes
joint-fracture-related 64, 129, **130**
stratiform 64, 129, **131**
– metasomatite 7, 8, 42, 44, 63, **122 ff.**
– – age/geochronologic distribution 54, 126, 127
– – alteration/metasomatism 123, 126, 127
– – associated elements 124, 127
– – definition 122
– – dimensions 126, 127
– – examples 7, 8, 123, 126, 127, 191
– – formational temperatures 124
– – geographic distribution 6, 7, 8
– – grades 33, 125, 126
– – host environments, -rocks 46, 123, 126 f.
– – metallogenesis/mode of origin 33, 42, 45, 46, 124
– – mineralogy/mineralization 123, 126, 127
– – recognition criteria 63, 123
– – resources 126, 127
– – sources of uranium 124
– – structures 123, 126, 127
– – subtypes
metasomatized granite 63, 123, **125 f.**
metasomatized metasediments 63, 123, **126 f.**
– phosphorite 8, 63, **115 ff.**
– – age/geochronologic distribution 49, 54
– – alteration 117, 118
– – definition 115
– – dimensions 117, 118
– – examples 8, 115, 117, 118
– – geographic distribution 6, 8
– – grades 117, 118
– – host environments, -rocks 46, 115, 117, 118
– – metallogenesis/mode of origin 41, 42, 45, 46, 116 f.
– – mineralogy/mineralization 115 f., 117, 118
– – recognition criteria 63, 115 f.
– – resources 117, 118
– – subtypes
land pebble 63, 115, **118**
phosphoria 63, 115, **117**
– quartz-pebble conglomerate 7, 42, 44, 62, **104 ff., 343 ff.**

– – age/geochronologic distribution 49, 53, 55, 106, 107, 108, 349, 352, 355, 360, 365
– – alteration 196
– – alteration/metasomatism 196, **345f.,** 350, 352, 355, 362, **365**
– – alteration halo 346, 365
– – associated elements, minerals 105, 107, **346f., 355f.**
– – definition 105
– – dimensions 105, 107, 108, **347f., 359f.**
– – examples 7, 105, 106, 107
– – fluid inclusions 364
– – formational temperatures 364
– – geographic distribution **6,** 7, 343, 344, 354
– – grades 105, 107, 108, **343,** 348, **353,** 359f.
– – host environments, -rocks 46, 105, 106, 107, **344f,** 349, **355,** 361
– – lithology related U distribution 347, 349, **350, 359,** 361, 363
– – metallogenesis/mode of origin 41, 42, 45, 46, 106, **350ff., 363ff.**
– – mineralogy/mineralization 105, 107f., **48ff.,** 350, **355ff.,** 362f.
– – recognition criteria, ore controls 62, 105f., **349f., 361ff.**
– – resources (including production) 107, 108, **343, 353,** 359
– – sources of uranium 106, **349, 360f.**
– – stable isotopes 353
– – structures 343, **345,** 347, 355, **359**
– – subtypes
Au>U-dominant 62, 105, **107f., 353ff.**
U-dominant with REE 62, 105, **106f., 343ff.**
– sandstone 7, 42, 44, 55, 59ff., **84ff., 250ff.**
– – age/geochronologic distribution 49, 53, 54, 55, 86, 91, 255, 260, 265, 267, 271, 286, 297, 298, 307, 320, 322
– – alteration 88, 89, 91, 93, 94, **254ff.,** 264, **272,** 279, **286, 292ff.,** 298f., **307ff.,** 315f., **321ff.**
– – alteration halo **256f.,** 259, 260, **273, 286, 292ff., 307ff.**
– – associated elements, minerals 89, 90, 91, 93, 94, **257,** 265, **272ff., 286, 292ff.,** 309, **315, 321**
– – classes (see -subtypes)
– – definition 84f.
– – dimensions 89, 90, 91, 92, 93, 94, **257ff., 274ff., 288, 297, 312, 322ff.**
– – examples 7, 84, 87f., 89, 90, 91, 92, 93, 94
– – geographic distribution **6,** 7, 251, 271, 284, 290, 306, 320
– – grades 87, 89, 90, 91, 92, 93, 94, **250,** 259, 260, **270, 285, 290,** 299, **305,** 311, **319,** 322, 323
– – host environments, -rocks 47, 85, 88, 89, 90, 91, 92, 93f., **251ff.,** 264, **271ff.,** 278f., **286,** 288, **21ff.,** 298, **306ff.,** 314, **320ff.**
– – metallogenesis/mode of origin 41, 42, 45, 47, 86f., **265ff., 280ff., 287, 299ff., 316ff.**
– – mineralogy/mineralization 85, 89, 990, 91f., 93, 94, **257ff.,** 265, **272ff.,** 279, **286ff.,** 287, **292ff.,** 298f., **309ff.,** 315f., **321ff.**
– – recognition criteria, ore controls 59ff., 85f., **264f., 278ff., 288f., 298f., 314ff., 321ff.**
– – resources (including production) 89, 90, 91, 92, 93, 94, **250,** 260, **270, 285, 290, 305,** 312, **319,** 322, 323
– – sources of uranium 86, 87, 88, **262, 278, 288, 298, 314**
– – stable isotopes 281, 303, 314, 317
– – structures 85, 88, 89, 90, 91, 92, 94, **253,** 259, 265, **287,** 307, 309, 310, **315,** 316, 318
– – subtypes/classes
Phanerozoic, rollfront, continental basin ass.with detrital carbon 54, 61, 84, **92f., 290ff.**
Phanerozoic, rollfront, mixed fluvial marine ass.with extrinsic sulfide 61, 84, **93f., 305ff.**
Phanerozoic, tabular, basal channel 60, 84, **91f., 284ff.**
Phanerozoic, tabular, extrinsic carbon (humate-uranium) 54, 60, 84, **88f., 250ff.**
Phanerozoic, tabular, vanadium-uranium 54, 60, 84, **89f., 270ff.**
Phanerozoic, tectonic-lithologic 61, 84, 85, **259**
Proterozoic 53, 84, **90f., 319ff.**
– strata controlled – structure-bound 8, **133f.**
– – age/geochronologic distribution 134
– – alteration 133
– – alteration halo 133
– – associated elements, minerals 133
– – definition 133
– – dimensions 134
– – examples 8, 133, 134
– – geographic distribution 6, 8
– – grades 134
– – host environments, -rocks 133
– – metallogenesis/mode of origin 134
– – mineralogy/mineralization 133
– – recognition criteria 133f.
– – resources (including production) 134
– – sources of uranium 134
– – structures 113
– subunconformity-epimetamorphic 7, 42, 43, 44, 58, **69ff., 168ff.**
– – age/geochronologic distribution 49, 53, 55, 71, 72, 73, 178, **183ff.,** 194, **197,** 200
– – alteration/metasomatism 70, 72, 73, **174ff.,** 187, **193f.,** 197
– – alteration halo 72, 73, **175ff.,** 187, **197**
– – associated elements, minerals 71, **175ff.,** 188, 191, **194**
– – definition 69
– – dimensions **73,** 74, **175, 179, 180, 181, 194f.**
– – examples 7, 69, 70, 72, 73, 74
– – fluid inclusions **180, 200**
– – formational temperatures 180, 183, **87,** 189, 190, **200**
– – geographic distribution **6,** 7, 169, 192
– – grades **182, 191**
– – host environments, -rocks 47, 70, 72, 73, **170ff.,** 186f., **193,** 196f.
– – metallogenesis/mode of origin 42, 43, 47, 48, 71, **187ff., 198ff.**
– – mineralogy/mineralization 70, 71, 72, 73, **177ff.,** 187, **194ff.,** 197f.
– – recognition criteria, ore controls 58, 70f., **186f, 196ff.**
– – resources (including production) 72, 73, 74, **182, 191**
– – sources of uranium 183, 196
– – stable isotopes 181
– – structures 70, 72, 73, 175, 179, 180, **184f.,** 192, **193,** 195f.
– – subtypes
albitized metasediments 58, 69ff., **73f., 191ff.**
not albitized metasediments 58, 69ff., **72f., 168ff.**
– surficial 7, 42, 44, 61, **96ff., 334**
– – age/geochronologic distribution 49, 54, 55, 97
– – alteration 101, 102, 103, 104, 334f., **337ff.**
– – associated elements 98, 102
– – classes (see -subtypes)
– – definition 96
– – dimensions 101, 102, 103, 104, 336ff., **340**

– – examples 96f., 100, 101, 102, 103, 104, 184, 335, **340**
– – geographic distribution **6,** 7, 335
– – grades 101, 102, 103, 104, 334, 336, 338f., **340**
– – host environments, -rocks 47, 97, 101, 102, 103, 334, **337ff.**
– – metallogenesis/mode of origin 41, 42, 45, 47, 97ff., **340ff.**
– – mineralogy/mineralization 97, 101, 102, 103, 104, **335f.,** 340
– – recognition criteria, ore controls 61f., 97, **337ff.**
– – resources 101, 102, 103, 104, **340**
– – sources of uranium 97f., **337**
– – structures 104, **335**
– – subtypes/classes
duricrusted sediments, fluvial/valley-fill 54, 61, 96, **100f., 334ff.**
duricrusted sediments, lacustrine/playa 62, 96, **102, 334ff.**
peat-bog 54, 62, 96, **102f.**
karst-cavern 62, 96, **103**
surficial pedogenic and structure fill 62, 96, 97, **103f.**
– synmetamorphic 8, 43, 44, 63, **127ff.**
– – age/geochronologic distribution 53, 128
– – alteration 128
– – associated elements, minerals 128
– – definition 127
– – dimensions 128
– – examples 8, 127, 129, 153
– – geographic distribution 6, 8
– – grades 128
– – host environments, -rocks 46, 127f.
– – metallogenesis/mode of origin 43, 46, 128
– – mineralogy/mineralization 128
– – recognition criteria 63, 127f.
– – resources 128
– – sources of uranium 128
– – structures
– unconformity-contact 7, 42, 44, 57, 58, **65ff., 137ff.**
– – age/geochronologic distribution 49, 53, 54, 66, 67, 68, 152, 154
– – alteration/metasomatism 65, 66, 67, 68, **139ff.,** 154ff., 158ff.
– – alteration halo 141ff.
– – associated elements, minerals **142ff.**
– – classes (see -subtypes)
– – definition 57
– – dimensions 67, 68, 69, **151**
– – examples 7, 65, 66, 68
– – fluid inclusions 153
– – formational temperatures **153,** 164, 166, 167, 168
– – geographic distribution **6,** 7, 138, 149
– – grades 67, 68, 69, 137, 141, **151**
– – host environments, -rocks 47, 65, 66, 67, 68, **137ff.,** 154
– – metallogenesis/mode of origin 42, 47, 66, **161ff.**
– – mineralogy/mineralization 66, 67, 68, **141ff.,** 156ff.
– – recognition criteria, ore controls 58, 65f., **154ff.**
– – resources (including production) 67, 68, 69, 137, **151**
– – sources of uranium 153
– – stable isotopes **153,** 164, 168
– – structures 65, 66, 67, 68, **139,** 141, 142, 146, 149, 158f.
– – subtypes/classes
Proterozoic unconformity, clay-bound 58, 65, **67f., 138ff.**
Proterozoic unconformity, fracture-bound 58, 65, **66f., 138ff.**
Phanerozoic unconformity 58, **68f.**
– vein 7, 42, 44, 58f., **74ff., 201ff.**
– – age/geochronologic distribution 49, 53, 54, 55, 76, 83, 216, 219, 222, 225f., 228, 233, 237, 238, 242, 243, 244, 249, 250
– – alteration/metasomatism 76, 77, 78, 79, 80, 81, 82, 83, 206, **212ff., 219f.,** 223, **226,** 228, **233,** 236, **239ff., 247,** 249
– – alteration halo 76, 78, 79, 80, 82, **206, 220, 226, 229, 233, 240f.**
– – associated elements 76, 79, 80, 82, 83, **206, 220ff., 226ff., 233ff., 241f., 248f.**
– – classes (see -subtypes)
– – definition 74
– – degree of vein occupancy by ore 76, **207,** 220, **223, 230,** 231, **240, 248**
– – dimensions 78, 80, 81, 82, 83, **207f., 221f.,** 223, **228,** 230, **233, 241f., 249**
– – examples 7, 74, 77, 79, 80, 81, 82, 83
– – fluid inclusions **217, 243,** 245
– – formational temperatures **216f., 231, 236f., 243**
– – geographic distribution 6, 7, 202, 218, 224, 232, 238
– – grades 78f., 80, 81, 82, 83, 201, 207, **208, 219,** 224, **226, 230,** 231, **233, 237, 246**
– – host environments, -rocks 47, 76, 78, 79, 80, 81, 82, 83, **201ff.,** 208, **219,** 220f., **225f.,** 228, **233,** 236, **238f.,** 243, **246f.,** 249
– – metallogenesis/mode of origin 41, 42, 45, 47, 48, 76f., **208ff., 223f., 230ff., 236f., 244f., 250**
– – mineralogy/mineralization 76, 78, 79, 80, 81, 82, 83, **206ff., 220ff., 226ff., 229ff., 233ff., 244ff., 248ff.**
– – recognition criteria, ore controls 58f., 76, **208, 222f., 228ff., 236, 243f., 249f.**
– – resources (including production) 78, 80, 81, 82, 83, **201, 219, 224, 233,** 235, **237, 246**
– – sources of uranium **211, 223, 231, 235f., 242, 249**
– – stable isotopes **211,** 217, **223, 242**
– – structures 76, 78, 79, 80, 81, 82, 83, **203ff., 218ff., 225ff., 233, 238ff., 247ff.**
– – subtypes/classes
granite-related, disseminations in episyenite 59, 74, 75, **77ff., 206ff.**
granite-related, intragranitic veins 41, 59, 74, 75, **77ff., 201ff.**
perigranitic, in contact-metamorphics 59, 74, 75, **81f., 232ff.**
perigranitic, in (meta)-sediments, monometallic 59, 74, 75, **79f., 218ff.**
perigranitic, in metasediments, polymetallic 59, 74, 75, **80f., 224ff.**
not granite-related, in metamorphic rocks 59, 74, 75, **82f., 237ff.**
not granite-related, in sediments (polymetallic) 59, 74, 75, **83, 246ff.**
– volcanic 7, 8, 42, 44, 63, **118ff.**
– – age/geochronologic distribution 49, 54
– – alteration/metasomatism 119, 120, 121, 122
– – alteration halo 120
– – associated elements, minerals 119, 120, 121, 122
– – classes (see -subtypes)
– – definition 119
– – dimensions 120, 121, 122
– – examples 7, 8, 77, 79, 80, 81, 82, 83
– – geographic distribution 6, 7, 8
– – grades 120, 121, 122
– – host environments, -rocks 47, 119, 120, 121, 122
– – metallogenesis/mode of origin 42, 47, 48, 119f.
– – mineralogy/mineralization 119, 120, 121, 122
– – recognition criteria 63, 119

– – resources 120, 121, 122
– – sources of uranium 119 f.
– – structures
– – subtypes/classes
strata-bound, exocaldera 63, 119, **122**
strata-bound, intracaldera 63, 119, **121 f.**
structure-bound, intrusive veins 63, 119, **120 f.**
structure-bound, surficial vein-like 63, 119, **121**

Unconformity, paleounconformity
– intraformational 105, 107, 121, 129, 130, 355, 361, 363
– deposits (see Types of U deposits)
– Phanerozoic 49, 58, 65, 68 f.
– Proterozoic 53, 58, 65, 66, 67, 69
– – Early Proterozoic/Archean 105, 107
– – Middle Proterozoic/Carpentarian 168, 174, 176, 179, 187 f.
– – Middle Proterozoic/Meso-Helikian 139, 141 ff., 157, 158, 163 f.
– – Middle Proterozoic/Paleo-Helikian 193, 194, 197, 199
Uraninite 2 f., 18, 20, 21, 23, 27, 28, 29, 30, 36, 48, 53, 209 ff., 346, 356
– detrital 21, 36, 53, 106, 346, 356 (for occurrence in deposits see Types of U deposits, -mineralogy)
Uranium
– absorption, adsorption 18, 20 f., 29, 30, 61, 62, 97, 99, 100, 102, 132, 255, 342
– ab-, adsorbing agents 18, 20 f., 28, 30, 117, 119, 129, 130, 131, 132, 133
– abundance 17 ff.
– atmosphere, related to (see Atmosphere)
– auto-/selfoxidation 18
– chemical behavior in natural environments 21, 23 f., 28 f., 30 f.
– cleavage-bound 128, 368
– climate, related to 28, 29, 30, 45, 51, 55, 67, 97, 98, 134, 162, 163 f., 267, 271, 337, 341, 343
– complexing agents/elements 86, 99, 265, 269, 274, 281
– coordination number 17, 18
– coprecipitation with hydrous phases 29
– crustal evolution, related to 36 ff.
– deposits (see Types of deposits, and Uranium deposits/mineralization)
– deposition/fixing/precipitation 21, 28 f., 45 f., 54, 77, 85, 86, 98, 99, 100, 120, 163 ff., 184 ff., 198 ff., 223, 231, 236 f., 245, 268 ff., 281 ff., 289, 300 ff., 316 ff., 333, 341 ff., 350 ff., 364 ff.
– diagenesis of overlying sediments, related to 48, 164 ff., 188 ff., 199
– disequilibrium (radioactive) 297, 310
– district(s) 35
– epeirogenic movements, related to 48, 166, 191, 199, 331
– geochemistry 17 ff.
– geothermal (volcanic) system, related to 45
– half life 17
– hexavalent (U^{6+}) ion 17, 18, 19 f., 21
– history 5 ff., 225, 246, 270
– hydro(geo)chemistry 18, 19, 21, 28, 86 f., 99 f., 120, 124, 161, 164 ff., 180 ff., 188 ff., 198, 212, 216 f., 231, 244 f., 265 ff., 280 ff., 294 ff., 300 ff., 327, 333, 334, 339 ff.
– ionic radii 17, 18
– isotopes 17
– land plants, related to 36, 37, 38, 54
– lattice incorporated 21, 128
– magmatic (igneous)/anatectic environment 20, 21, 23 ff., 36, 38, 41, 42, 48, 54, 110, 125
– magmatic differentiation 25, 201 ff., 208 ff.
– marine (Proterozoic) microorganisms (algae) related to 36 f., 53
– metallogenesis 41 ff., 46 f. (see also Types of U deposits)
– metallogenetic cycle 21, 41 ff.
– metamorphic environment 2, 20, 21, 30 f., 45 f., 127, 163, 198 ff.
– metasomatic environment 31 ff., 122 ff.
– mineralization (see Shape of deposits, and Types of U deposits)
– minerochemistry 18 ff.
– minerogenic distribution 21 ff.
– mobile belts, related to 45
– mobilization, mobility 21, 28 f., 36 ff., 45, 54, 97, 98, 163 ff., 184 ff., 212, 216 f., 266, 280 ff., 300 ff., 316 ff., 352
– oxidation, oxidizing conditions 17, 21, 165, 212, 301, 317 ff., 341
– oxidation states 17, 18
– petrogenic distribution 21
– pH, related to 21, 99, 100, 190, 223, 231, 243, 245, 266, 268, 269, 280 f., 293, 300 ff., 334, 339, 341 ff.
– physico-chemical properties 17
– plate tectonics, related to 45
– production 5, 10, 15
– protocrust (Archean) 36
– provinces 34 ff.
– redistribution, recrystallization (see Uranium deposits/mineralization)
– reducing agents 29, 85, 86, 87, 165 ff., 188, 217, 231, 245, 289, 302 ff., 310, 312 ff.
– reduction 18, 21, 28, 29, 85, 86, 87, 97, 166 ff., 188, 190, 245, 289, 302, 317 ff., 333
– replacement 21, 89, 90, 92, 109, 223, 272, 286, 292, 335, 352
– resources (see Resources, and Types of U deposits)
– sedimentary environment 23, 28 ff., 42, 45, 84 ff., 105 ff., 115 ff., 129 f., 131 f., 138, 162, 165 f., 253 ff., 271 ff., 284 ff., 290 ff., 306 ff., 320 ff., 345 ff. (see also Sediments)
– source (rocks) 28, 34 f., 35, 36, 38, 54, 55, 86, 87, 88, 97 f., 112, 119, 124, 128, 134, 153, 183, 196, 211, 223, 231, 235 f., 242, 249, 262, 278, 288, 298, 314, 333 f., 337, 349, 360 f., 371 f.
– substitution 19, 21, 22, 29, 115
– substituting elements 19, 22
– surficial environment 29, 96 ff., 334 ff.
– taphrogenic tectonics, related to 45
– tetravalent (uranous) ion (U^{4+}) 17, 18 f., 21
– transport 21, 29, 37, 45, 54, 97, 98, 120, 130, 165 ff., 184 ff., 198 ff., 216, 223, 236 f., 244 f., 250, 266, 280 ff., 289, 300 ff., 316 ff., 333, 341 ff., 350 ff., 364 ff.
– valencies 17
– weathering, related to (see Weathering)
Uranium contents
– alaskite 25, 112, 369
– albitite 25, 32 f.
– alkaline igneous rocks 25, 26
– alum shale 133
– anorogenic alkaline intrusions 26
– apatite 22, 116, 117
– arenites, rudites 24, 28, 105, 164, 254, 348, 359 f.
– asphalt(ite) 29, 34
– basic rocks (see mafic rocks)
– bauxites 28, 30
– bentonites 28, 30
– bitumens 34
– black shale 28, 29, 132, 133
– brines 33
– calc-alkaline igneous rocks 26
– carbonates 28
– carbonatite 25, 26, 114
– coals 29, 34, 133
– continental crust 17 f.
– duricrusts 30, 101, 336

– effusive/extrusive rocks 24, 25, 26, 27
– evaporites 28
– exoterrestrial material 24, 34
– felsic/leucocratic) igneous rocks 24, 27 (see also below -granite)
– fluvial sediments 29
– fossil bones 28
– glass, exoterrestrial 34
– glass, volcanic 24
– granite 24, 25, 26, 27, 32, 108, 209 ff., 226, 235, 298, 337, 361, 367
– guano 28
– igneous rocks 23 ff.
– intermediate igneous rocks 24, 25
– intrusive rocks 24, 25
– island arc andesite 25
– kolm 133
– laterite 28, 30, 163
– lignite 29, 34, 130, 131
– living organisms 33 f.
– lutites 28
– magmatic/anatectic rocks 23 ff.
– mafic igneous rocks 24, 25, 27
– manganese nodules 28
– mantle 26
– marine sediments 28 ff.
– melanocratic igneous rocks 26
– metamorphic rocks 24, 30 f., 128, 196, 243
– metasomatic rocks 32 ff., 126
– meteorites 34
– minerals 19, 21
– oceanic crust 25
– organic material 29, 30, 33 f. (see also Urano-organic complexes)
– pegmatite 25, 115
– pelites 28
– peralkaline (nepheline) syenite 25, 114
– petroleum 34
– phosphorites 14, 28 f., 30, 116, 117, 140
– placers 29, 107, 348, 353, 359 f.
– sediments 24, 28 f.
– soils 30, 163
– tectites 34
– ultrabasic/ultramafic igneous rocks 24, 25, 27
– volcanic rocks 24, 25, 26, 27, 122, 298
– waters 33, 100, 298

Uranium deposits/mineralization (general)
– associated elements, minerals (see Types of U deposits)
– calcrete associated (see Types of U deposits, -surficial, duricrusted
– classes 57, 58 ff. (see also Types of U deposits)
– classification 57, 58 ff. (see also Types of U deposits)
– clay-bound 58, 65, 67 f., 137 ff.
– detrital 46, 53, 105, 106, 107, 349 ff., 356 ff.
– dynamic processes, related to 87, 300 ff., 316 ff.
– economic ranking 8
– endogenetic 42
– epigenetic 23.28, 42 f., 45, 46 f.
– exogenetic 42
– generations 51 ff.
– geochronologic distribution 49 ff.
– grades of deposit types 9, 58 ff. (see also Types of U deposits)
– geographic distribution 6 ff., 10
– host environment/rocks 42 f., 46 f., 58 ff. (see also Types of U deposits)
– hypogene 48 (see also Hydrogenic)
– magmatic 42, 46, 111, 112
– metallogenesis/mode of origin 41 ff., 46 f. (see also Types of U deposits)
– metamorphic 43, 46, 127 ff., 153, 163
– metasomatic 46, 122 ff., 191, 353
– mineralogy (see Types of U deposits)
– mixed/transitional category 48
– modified 105, 106, 110, 188, 189, 350, 356, 363 (see also below -redistributed)
– monometallic (or simple) 3, 58, 59, 65, 66, 67, 70, 72, 73, 74, 79, 105, 141 ff., 177 ff., 191 ff., 218 ff., 227 f., 236
– ore composition by potentially economic metals
– – U, Ag, Co, Ni, Bi 59, 74, 80, 224 ff.
– – U, Au 62, 70, 72, 105, 107, 353 ff.
– – U, Cu 91, 113
– – U, Cu, Au, Ag, REE 62, 108 f.
– – U, Cu, Mo 9, 112 f.
– – U, Cu, Pb, Zn 70, 328
– – U, Cu, Zr 113 f.
– – U, Mo 118
– – U, Ni, Co 68, 83, 141 ff., 246 ff.
– – U, REE 62, 63, 105, 106, 113, 343 ff.
– – U, V 9, 89 ff., 91 f., 271 ff., 285, 323, 335
– oxidized 81, 84, 90, 91, 120, 121, 206 ff., 233 ff., 248, 257, 272 ff., 286, 309, 321 ff.
– peneconcordant 46, 58, 60, 63, 70, 72, 73, 84, 85, 88, 89, 251 ff., 270 ff., 285 ff., 297
– placer, paleoplacer (see Placer)
– polymetallic (or complex) 3, 58, 59, 65, 70, 72, 73, 74, 80, 83, 105, 141 ff., 224 ff., 246 ff., 270 ff., 286, 328 f., 353 ff.
– polygenetic/polyphase/multistage 41, 42, 46, 48, 53, 66, 71, 80, 134, 161, 162 ff., 191 ff., 230 ff., 317 ff.
– primary category 41 ff.
– recognition criteria (principal) 57, 58 ff. (see also Types of U deposits)
– redistributed, recrystallized, remobilized, reworked 30, 48, 53, 61, 66, 70, 71, 73, 77, 87, 88, 89, 106, 107, 108, 124, 137, 154, 157, 167, 186, 188, 199 ff., 208, 217, 226, 237, 244, 249, 289, 319, 342, 346, 352 f., 356, 364, 365
– reduced (environment, zone) 84, 85, 90, 91, 257 ff., 272 ff., 286, 309 f., 316 ff., 321 ff., 349 ff., 356, 363 ff.
– regional setting 44
– resources (see Reserves/resources, and Types of U deposits)
– rollfront, roll-type 47, 60 f., 85, 89, 90, 92, 93, 94, 257, 274, 275, 279, 290 ff., 296, 305 ff.
– rollfront, South Texas type 305, 317 f.
– rollfront, Wyoming type 290, 317
– secondary category 42, 45
– sedimentological control 85 ff., 98, 105 ff., 115 ff., 264 ff., 271 ff., 287 ff., 298 ff., 322 ff., 331 ff., 347, 349 ff., 359, 361, 363
– shape, configuration (see Shape of ore bodies, and Types of U deposits, -mineralogy/mineralization)
– stack, stacked 85, 88, 89, 257 ff.
– stationary processes, related to 86
– strata-bound, -controlled 23, 31, 46, 47, 53, 63, 64, 70, 72, 96, 105, 109, 115, 118, 119, 127, 129, 131, 132, 243, 253 ff., 270 ff., 285 ff., 291 ff., 309 f., 321 ff., 34, 343 ff., 353 ff.
– strata-structure-bound, -controlled 46, 61, 69, 70, 130, 133 f., 191, 321, 323 f.
– structure (fracture)-bound, -controlled 46, 47, 58 f., 63, 64, 66 f., 70, 72, 76, 96, 118, 119, 129, 130, 137 ff., 141 ff., 178 ff., 201 ff., 219 ff., 224 ff., 236, 241 ff., 248 ff., 259
– subtypes 58 ff. (see also Types of U deposits)
– supergene 42, 47 (see also Hydrogenic)
– surficial 42, 47, 49, 61 f., 96 ff.
– syngenetic 23, 28, 42 f., 45, 46, 106, 115, 116, 127, 128, 129, 130, 132, 133, 153, 352, 363

– tectonic/lithologic (petrographic) control 47, 61, 77f., 79, 80, 81, 82, 84, 85, 87, 91, 96, 108f., 120f., 123, 157f., 204ff., 223, 228f., 233, 236, 239, 243f., 259, 329
– tertiary category 43, 45
– types 6ff., 8, 46f., 58ff. (for details see Types of U deposits)
– uncommon and uncertain types 6, 8
– uranium (mineral) distribution (see Shape of ore bodies)
– world distribution 6ff.
Uranium (bearing) minerals 18f., 22f (see also Appendix)
– accessory minerals 19, 21, 22, 27, 209ff.
– complex ore minerals 22f.
– hexavalent 3, 19, 23 (see also Uranyl -ion, -complexes)
– ore minerals 22, 23 (see also Types of U deposits, -mineralogy
– refractory 23, 28, 29, 30, 111, 114
– rock forming minerals 21, 22
– secondary 3
Urano-organic complexes 21, 102, 129, 130, 131, 132, 133, 272 (for occurrence in deposits see Types of U deposits, -mineralogy)
– anthraxolite 220, 222
– asphalt(ite) 29, 34
– humate 60, 89, 129, 130, 131, 250ff., 264, 265ff., 279
– kerogen 346, 350, 356
– ucholite 34
– thucholite 34, 105, 187
Uranium oxide phases 2f., 18ff., 23, 144f. (see also Pitchblende, Uraninite)
– composition 20
– correlation oxidation degree-lattice constant 19
– ionic radii 18
– lattice constants 18, 19
U-Al compounds/phases 29, 30
U-phosphatic compounds/phases 29, 297, 352
U-Ti compounds/phases 18, 29, 30, 99, 105, 106, 110, 120, 123, 215, 322, 345, 346, 352, 355ff.
U-Zr compounds/phases 18, 29, 30
Uranpecherz 18
Uranyl ion, complexes, minerals 19f., 21, 23, 28, 29, 38, 53, 61, 62, 77, 86, 97, 99, 119, 120, 121, 129, 130, 131 (for occurrence in deposits see Types of U deposits, -mineralogy)

Vanadium (see Uranium deposits/mineralization, -U-V)
Vegetal matter (see Organic material)
Vein (see Types of U deposits, and Shape of ore bodies, -linear)
Volcanic, volcanite 63, 118ff.
– deposits (see Types of U deposits)
– endocaldera 118, 119
– exocaldera 118, 119
– uranium content 24, 25, 26, 27, 122, 298

Wall rock alteration (see Alteration, Halo, -wall rock, and Type of deposits, -alteration)
Weathering/paleoweathering 23, 42, 58, 65, 69, 70, 107, 118, 117, 174, 346, 364
– chemical 28f., 41, 45, 57, 67, 97, 99, 100, 134, 139, 154, 162, 163f., 187, 199, 215, 236, 337
– physical 29, 45, 70, 105, 106, 193, 199, 351, 355, 362, 366
WOCA 4, 10, 11, 14

Xenolith 111, 200, 201, 233, 367

Zircon 22, 29, 112, 115, 123, 126, 127, 209ff., 236, 351, 356, 368
– uranium content 22
Zoning/zonation 81, 93, 109, 113, 123, 124, 157, 159f., 225ff., 249, 256f., 274, 281, 294ff., 310, 315, 347, 350